

# Proceedings

**5<sup>th</sup> Stochastic Modeling Techniques and  
Data Analysis International Conference with  
Demographics Workshop**

# SMTDA2018

*Editor*

**Christos H Skiadas**

**12 - 15 June 2018**

**Cultural Centre of Chania, Crete, Greece**



**Imprint**

**Proceedings of the 5<sup>th</sup> Stochastic Modeling Techniques and Data  
Analysis International Conference with Demographics Workshop  
Chania, Crete, Greece: 12-15 June, 2018**

Published by: ISAST: International Society for the Advancement of  
Science and Technology.

Editor: Christos H Skiadas

© Copyright 2018 by ISAST: International Society for the Advancement of  
Science and Technology.

*All rights reserved. No part of this publication may be reproduced, stored,  
retrieved or transmitted, in any form or by any means, without the written  
permission of the publisher, nor be otherwise circulated in any form of binding  
or cover.*

## Preface

It is our pleasure to welcome the guests, participants and contributors to the International Conference (SMTDA 2018) on Stochastic Modeling Techniques and Data Analysis and (DEMOGRAPHICS2018) Demographic Analysis and Research Workshop.

The main goal of the conference is to promote new methods and techniques for analyzing data, in fields like stochastic modeling, optimization techniques, statistical methods and inference, data mining and knowledge systems, computing-aided decision supports, neural networks, chaotic data analysis, demography and life table data analysis.

SMTDA Conference and DEMOGRAPHICS Workshop aim at bringing together people from both stochastic, data analysis and demography areas. Special attention is given to applications or to new theoretical results having potential of solving real life problems.

SMTDA 2018 and DEMOGRAPHICS 2018 focus in expanding the development of the theories, the methods and the empirical data and computer techniques, and the best theoretical achievements of the Stochastic Modeling Techniques and Data Analysis field, bringing together various working groups for exchanging views and reporting research findings.

We thank all the contributors to the success of these events and especially the authors of this Book of Proceedings. Special thanks to the Plenary, Keynote and Invited Speakers, the Session Organisers, the Scientific Committee, the ISAST Committee, Yiannis Dimotikalis, the Conference Secretary Mary Karadima and all the members of the Secretariat.

November 2018

Christos H. Skiadas  
Conference Co-Chair

## SCIENTIFIC COMMITTEE

Jacques Janssen, Honorary Professor of Universite' Libre de Bruxelles, Honorary Chair  
 Alejandro Aguirre, El Colegio de México, México  
 Alexander Andronov, Transport and Telecom. Institute, Riga, Latvia  
 Vladimir Anisimov, Statistical Consultant & Honorary Professor, University of Glasgow, UK  
 Dimitrios Antzoulakos, University of Piraeus, Greece  
 Soren Asmussen, University of Aarhus, Denmark  
 Robert G. Aykroyd, University of Leeds, UK  
 Narayanaswamy Balakrishnan, McMaster University, Canada  
 Helena Bacelar-Nicolau, University of Lisbon, Portugal  
 Paolo Baldi, University of Rome "Tor Vergata", Italy  
 Vlad Stefan Barbu, University of Rouen, France  
 S. Bersimis, University of Piraeus, Greece  
 Henry W. Block, Department of Statistics, University of Pittsburgh, USA  
 James R. Bozeman, American University of Malta, Malta  
 Mark Brown, Department of Statistics, Columbia University, New York, NY  
 Ekaterina Bulinskaya, Moscow State University, Russia  
 Jorge Caiado, Centre Appl. Math., Econ., Techn. Univ. of Lisbon, Portugal  
 Enrico Canuto, Dipart. di Automatica e Informatica, Politec. di Torino, Italy  
 Mark Anthony Caruana, University of Malta, Valletta, Malta  
 Erhan Çinlar, Princeton University, USA  
 Maria Mercè Claramunt, Barcelona University, Spain  
 Marco Dall'Aglio, LUISS Rome, Italy  
 Guglielmo D'Amico, University of Chieti and Pescara, Italy  
 Pierre Devolder, Université Catholique de Louvaine, Belgium  
 Giuseppe Di Biase, University of Chieti and Pescara, Italy  
 Yiannis Dimotikalis, Technological Educational Institute of Crete, Greece  
 Robert Elliott, Haskayne School of Business, University of Calgary, and University of South  
 Australia, Adelaide, Australia  
 Dimitris Emiris, University of Piraeus, Greece  
 N. Farmakis, Aristotle University of Thessaloniki, Greece  
 Lidia Z. Filus, Dept. of Mathematics, Northeastern Illinois University, USA  
 Jerzy K. Filus, Dept. of Math. and Computer Science, Oakton Community College, USA  
 •Ilia Frenkel, Sami Shamon College of Engineering, Israel  
 Leonid Gavrilov, Center on Aging, NORC at the University of Chicago, USA  
 Natalia Gavrilova, Center on Aging, NORC at the University of Chicago, USA  
 A. Giovanis, Technological Educational Institute of Athens, Greece  
 Valerie Girardin, Université de Caen Basse Normandie, France  
 Joseph Glaz, University of Connecticut, USA  
 Maria Ivette Gomes, Lisbon University and CEAUL, Lisboa, Portugal  
 Gerard Govaert, Université de Technologie de Compiègne, France  
 Alain Guenoche, University of Marseille, France  
 Y. Guermeur, LORIA-CNRS, France  
 Montserrat Guillen University of Barcelona, Spain  
 Steven Haberman, Cass Business School, City University, London, UK  
 Diem Ho, IBM Company  
 Emilia Di Lorenzo, University of Naples, Italy  
 Aglaia Kalamatianou, Panteion Univ. of Political Sciences, Athens, Greece  
 Udo Kamps, Inst. für Stat. und Wirtschaftsmath., RWTH Aachen, Germany  
 Alex Karagrigoriou, Department of Mathematics, University of the Aegean, Greece

A. Katsirikou, University of Piraeus, Greece  
 Włodzimierz Klonowski, Lab. Biosign. An. Fund., Polish Acad of Sci, Poland  
 A. Kohatsu-Higa, Osaka University, Osaka, Japan  
 Tõnu Kollo, Institute of Mathematical Statistics, Tartu, Estonia  
 Krzysztof Kolowrocki, Depart. of Math., Gdynia Maritime Univ., Poland  
 Dimitrios G. Konstantinides, Dept. Stat. & Act. Sci., Univ. Aegean, Greece  
 Volodymyr Koroliuk, University of Kiev, Ukraine  
 Markos Koutras, University of Piraeus, Greece  
 Raman Kumar Agrawalla, Tata Consultancy Services, India  
 Yury A. Kutoyants, Lab. de Statistique et Processus, du Maine University, Le Mans, France  
 Stéphane Lallich, University of Lyon, France  
 Ludovic Lebart, CNRS and Telecom France  
 Claude Lefevre, Université Libre de Bruxelles, Belgium  
 Mei-Ling Ting Lee, University of Maryland, USA  
 Philippe Lenca, Telecom Bretagne, France  
 Nikolaos Limnios, Université de Technologie de Compiègne, France  
 Bo H. Lindqvist, Norwegian Institute of Technology, Norway  
 Brunero Liseo, University of Rome, Italy  
 Fabio Maccheroni, Università Bocconi, Italy  
 Claudio Macci, University of Rome "Tor Vergata", Italy  
 P. Mahanti, Dept. of Comp. Sci. and Appl. Statistics, Univ. of New Brunswick, Canada  
 Raimondo Manca, University of Rome "La Sapienza", Italy  
 Domenico Marinucci, University of Rome "Tor Vergata", Italy  
 Laszlo Markus, Eötvös Loránd University – Budapest, Hungary  
 Sally McClean, University of Ulster  
 Gilbert MacKenzie, University of Limerick, Ireland  
 Terry Mills, Bendigo La Trobe University and Deakin University, Australia  
 Leda Minkova, Dept. of Prob., Oper. Res. and Stat. Univ. of Sofia, Bulgaria  
 Ilya Molchanov, University of Berne, Switzerland  
 Karl Mosler, University of Koeln, Germany  
 Amílcar Oliveira, UAb-Open University in Lisbon, Dept. of Sciences and Technology and  
 CEAUL-University of Lisbon, Portugal  
 Teresa A Oliveira, UAb-Open University in Lisbon, Dept. of Sciences and Technology and  
 CEAUL-University of Lisbon, Portugal  
 Annamaria Olivieri, University of Parma, Italy  
 Enzo Orsingher, University of Rome "La Sapienza", Italy  
 T. Papaioannou, Universities of Piraeus and Ioannina, Greece  
 Valentin Patilea, ENSAI, France  
 Mauro Piccioni, University of Rome "La Sapienza", Italy  
 Ermanno Pitacco, University of Trieste, Italy  
 Flavio Pressacco University of Udine, Italy  
 Pere Puig, Dept of Math., Group of Math. Stat., Universitat Autònoma de Barcelona, Spain  
 Yosi Rinott, The Hebrew University of Jerusalem, Israel  
 Jean-Marie Robine, Head of the res. team Biodemography of Longevity and Vitality,  
 INSERM U710, Montpellier, France  
 Fabrizio Ruggeri, CNR IMATI, Milano, Italy  
 Leonidas Sakalauskas, Inst. of Math. and Informatics, Vilnius, Lithuania  
 Werner Sandmann, Dept. of Math., Clausthal Univ. of Tech., Germany  
 Gilbert Saporta, Conservatoire National des Arts et Métiers, Paris, France  
 W. Sandmann, Dept. of Mathematics, Clausthal University of Technology, Germany  
 Lino Sant, University of Malta, Valletta, Malta  
 José M. Sarabia, Department of Economics, University of Cantabria, Spain

Sergio Scarlatti, University of Rome "Tor Vergata", Italy  
Hanspeter Schmidli, University of Cologne, Germany  
Dmitrii Silvestrov, University of Stockholm, Sweden  
P. Sirirangsi, Chulalongkorn University, Thailand  
Christos H. Skiadas, Technical University of Crete, Greece (Co-Chair)  
Charilaos Skiadas, Hanover College, Indiana, USA  
Dimitrios Sotiropoulos, Techn. Univ. of Crete, Chania, Greece  
Fabio Spizzichino, University of Rome "La Sapienza", Italy  
Gabriele Stabile, University of Rome "La Sapienza", Italy  
Valeri Stefanov, The University of Western Australia  
Anatoly Swishchuk, University of Calgary, Canada  
R. Szekli, University of Wroclaw, Poland  
T. Takine, Osaka University, Japan  
Andrea Tancredi, University of Rome "La Sapienza", Italy  
P. Taylor, University of Melbourne, Australia  
Cleon Tsimbos, University of Piraeus, Greece  
Mariano Valderrama, University of Granada, Spain  
Panos Vassiliou, Department of Statistical Sciences, University College London, UK  
Beatrice Venturi, University of Cagliari, Italy  
Larry Wasserman, Carnegie Mellon University, USA  
Wolfgang Wefelmeyer, Math. Institute, University of Cologne, Germany  
Shelly Zacks, Binghamton University, State University of New York, USA  
Vladimir Zaiats, Universitat de Vic, Spain  
K. Zografos, Department of Mathematics, University of Ioannina, Greece

## Plenary/Keynote Talks

In celebration of Raimondo Manca's 70th birthday and in honour of his contributions to Applied Statistics, Stochastic Modeling and Data Analysis and his support to ASMDA and SMTDA activities

### **Raimondo Manca**

Department of Methods and Models for Economics, Territory and Finance  
University of Rome "La Sapienza"  
Rome, Italy

### **N. Balakrishnan**

Department of Mathematics and Statistics  
McMaster University  
Hamilton, Ontario  
Canada

### **Mark Brown**

Department of Statistics  
Columbia University  
USA

### **Robert J. Elliott**

Haskayne School of Business,  
University of Calgary, Canada and  
Centre for Applied Financial Studies,  
University of South Australia, Adelaide, Australia

### **Olympia Hadjiliadis**

Department of Mathematics and Statistics at  
Hunter College of the City University of New York, USA

### **Markos Koutras**

Department of Statistics and Insurance Science, University of Piraeus, Greece

### **Nikolaos Linnios**

Sorbonne University, Université de technologie de Compiègne  
Applied Mathematics Lab of Compiègne (LMAC), France

### **Erol Pekoz**

Center for Information & Systems Engineering  
Boston University, USA

### **Jean-Marie Robine**

MMDN, INSERM U1198, EPHE/PSL & University of Montpellier,  
France

**Dmitrii Silvestrov**

Department of Mathematics  
Stockholm University, Stockholm, Sweden

**Nozer Singpurwalla**

Department of Systems Engineering and Engineering Management and  
Department of Management Science City University of Hong Kong and  
George Washington University, Washington, D.C., USA

**Anatoliy Swishchuk**

Department of Mathematics and Statistics  
University of Calgary, Canada

**P.-C.G. VASSILIOU**

Department of Statistical Sciences, University College London, UK,  
Mathematics Department AUTH, Greece

**Elena Yarovaya**

Lomonosov Moscow State University  
Faculty of Mechanics and Mathematics, Department of Probability Theory,  
Moscow, Russia

<b>Contents</b>	<b>Page</b>
Preface	iii
Scientific Committee	iv
Plenary/Keynote Talks	vii
Papers	1



# Selection of proximity measures for a Topological Correspondence Analysis

Rafik Abdesselam

COACTIS-ISH Management Sciences Laboratory - Human Sciences Institute,  
University of Lyon, Lumière Lyon 2  
Campus Berges du Rhône, 69635 Lyon Cedex 07, France  
(E-mail: [rafik.abdesselam@univ-lyon2.fr](mailto:rafik.abdesselam@univ-lyon2.fr))  
(<http://perso.univ-lyon2.fr/~rabdesse/fr/>)

**Abstract.** In this paper, we propose a new approach which compares and classifies proximity measures in a topological structure to select the "best" one for a Topological Correspondence Analysis.

Similarity measures play an important role in many domains of data analysis. The results of any investigation into whether association exists between variables or any operation of clustering or classification of objects are strongly dependent on the proximity measure chosen. The user has to select one measure among many existing ones. Yet, according to the notion of topological equivalence chosen, some measures are more or less equivalent. The concept of topological equivalence uses the basic notion of local neighborhood. We define the topological equivalence between two proximity measures, in the context of association between two qualitative variables, through the topological structure induced by each measure.

We compare proximity measures and propose a topological criterion for choosing the "best" association measure, adapted to the data considered, among some of the most used proximity measures for qualitative data. The principle of the proposed approach is illustrated using a real data set with conventional proximity measures of literature for qualitative variables.

**Keywords:** Proximity measure; topological structure; neighborhood graph; adjacency matrix; topological equivalence; topological independence index..

## 1 Introduction

In order to understand and act on situations that are represented by a set of objects, very often we are required to compare them. Humans perform this comparison subconsciously using the brain. In the context of artificial intelligence, however, we should be able to describe how the machine might perform this comparison. In this context, one of the basic elements that must be specified is the proximity measure between objects.

Certainly, application context, prior knowledge, data type and many other factors can help in identifying the appropriate measure. For instance, if the objects to be compared are described by boolean vectors, we can restrict our

---

*5<sup>th</sup> SMTDA Conference Proceedings, 12-15 June 2018, Chania, Crete, Greece*

© 2018 ISAST



comparisons to a class of measures specifically devoted to this type of data. However, the number of candidate measures may still remain quite large. Can we consider that all those measures remaining are equivalent and just pick one of them at random? Or are there some that are equivalent and, if so, to what extent? This information might interest a user when seeking a specific measure. For instance, in information retrieval, choosing a given proximity measure is an important issue. We effectively know that the result of a query depends on the measure used. For this reason, users may wonder which one is more useful? Very often, users try many of them, randomly or sequentially, seeking a "suitable" measure. If we could provide a framework that allows the user to compare proximity measures and therefore identify those that are similar, they would no longer need to try out all measures.

The present study proposes a new framework for comparing proximity measures in order to choose the best one in a context of association between two qualitative variables.

We deliberately ignore the issue of the appropriateness of the proximity measure as it is still an open and challenging question currently being studied. The comparison of proximity measures can be analyzed from different angles.

The comparison of objects, situations or ideas is an essential task to assess a situation, to rank preferences, to structure a set of tangible or abstract elements, and so on. In a word, to understand and act, we have to compare. These comparisons that the brain naturally performs, however, must be clarified if we want them to be done by a machine. For this purpose, we use proximity measures. A proximity measure is a function which measures the similarity or dissimilarity between two objects within a set. These proximity measures have mathematical properties and specific axioms. But are such measures equivalent? Can they be used in practice in an undifferentiated way? Do they produce the same learning database that will serve to find the membership class of a new object? If we know that the answer is negative, then, how to decide which one to use? Of course, the context of the study and the type of data being considered can help in selecting a few possible proximity measures but which one to choose from this selection as the best measure for summarizing the association?

We find this problematic in the context of correspondence analysis. The eventual links or associations between modalities of two qualitative variables partly depends on the learning database being used. The results of the correspondence analysis can change according to the selected proximity measure. Here we are interested to in characterizing a topological equivalence index of independence between two qualitative variables. The greater this topological index is, the more independent the variables are, according to the proximity measure  $u_i$  chosen.

Several studies on topological equivalence of proximity measures have been proposed, [2] [11] [3] [8] [18], but none of these propositions has an association objective.

Therefore, this article focuses on how to construct the "best" adjacency matrix [1] induced by a proximity measure, taking into account the indepen-

dence between two qualitative variables. A criterion for statistically selecting the "best" correspondence proximity measure is defined below.

This paper is organized as follows. In section 2, after recalling the basic notions of structure, graph and topological equivalence, we present the proposed approach. How to build the adjacency matrix for no association between two qualitative variables, the choice of a measure of the degree of topological equivalence between two proximity measures, and the selection criterion for picking the "best" association measure are discussed in this Section. Section 3 presents an illustrative example with using qualitative economic data. A conclusion and some perspectives of this work are given in section 4.

**Table 1.** Some proximity measures.

Measures	Similarity	Dissimilarity
Jaccard	$s_1 = \frac{a}{a+b+c}$	$u_1 = 1 - s_1$
Dice, Czekanowski	$s_2 = \frac{2a}{2a+b+c}$	$u_2 = 1 - s_2$
Kulczynski	$s_3 = \frac{1}{2} \left( \frac{a}{a+b} + \frac{a}{a+c} \right)$	$u_3 = 1 - s_3$
Driver, Kroeber and Ochiai	$s_4 = \frac{a}{\sqrt{(a+b)(a+c)}}$	$u_4 = 1 - s_4$
Sokal and Sneath 2	$s_5 = \frac{a}{a+2(b+c)}$	$u_5 = 1 - s_5$
Braun-Blanquet	$s_6 = \frac{a}{\max(a+b, a+c)}$	$u_6 = 1 - s_6$
Simpson	$s_7 = \frac{a}{\min(a+b, a+c)}$	$u_7 = 1 - s_7$
Kendall, Sokal-Michener	$s_8 = \frac{a+d}{a+b+c+d}$	$u_8 = 1 - s_8$
Russel and Rao	$s_9 = \frac{a}{a+b+c+d}$	$u_9 = 1 - s_9$
Rogers and Tanimoto	$s_{10} = \frac{a+d}{a+2(b+c)+d}$	$u_{10} = 1 - s_{10}$
Pearson $\phi$	$s_{11} = \frac{ad-bc}{\sqrt{(a+b)(a+c)(d+b)(d+c)}}$	$u_{11} = \frac{1-s_{11}}{2}$
Hamann	$s_{12} = \frac{a+d-b-c}{a+b+c+d}$	$u_{12} = \frac{1-s_{12}}{2}$
bc		$u_{13} = \frac{4bc}{(a+b+c+d)^2}$
Sokal and Sneath 5	$s_{14} = \frac{ad}{\sqrt{(a+b)(a+c)(d+b)(d+c)}}$	$u_{14} = 1 - s_{14}$
Michael	$s_{15} = \frac{4(ad-bc)}{(a+d)^2 + (b+c)^2}$	$u_{15} = \frac{1-s_{15}}{2}$
Baroni, Urbani and Buser	$s_{16} = \frac{a+\sqrt{ad}}{a+b+c+\sqrt{ad}}$	$u_{16} = 1 - s_{16}$
Yule Q	$s_{17} = \frac{ad-bc}{ad+bc}$	$u_{17} = \frac{1-s_{17}}{2}$
Yule Y	$s_{18} = \frac{\sqrt{ad}-\sqrt{bc}}{\sqrt{ad}+\sqrt{bc}}$	$u_{18} = \frac{1-s_{18}}{2}$
Sokal and Sneath 4	$s_{19} = \frac{1}{4} \left( \frac{a}{a+b} + \frac{a}{a+c} + \frac{d}{d+b} + \frac{d}{d+c} \right)$	$u_{19} = 1 - s_{19}$
Sokal and Sneath 3		$u_{20} = \frac{b+c}{a+d}$
Gower and Legendre	$s_{21} = \frac{a+d}{a+\frac{(b+c)}{2}+d}$	$u_{21} = 1 - s_{21}$
Sokal and Sneath 1	$s_{22} = \frac{2(a+d)}{2(a+d)+b+c}$	$u_{SS1} = 1 - s_{22}$

Table 1 shows some classic proximity measures used for binary data [17], we give on  $\{0, 1\}^n$  the definition of 22 of them.

$\{x^j; j = 1, \dots, p\}$  and  $\{y^k; k = 1, \dots, q\}$  are sets of two qualitative variables, partition of  $n = \sum_{j=1}^p n_j = \sum_{k=1}^q n_k$  individuals-objects into  $p$  and

$q$  modalities-subgroups. The interest lies in whether there is a topological association between these two variables. Let us denote:

- $X_{(n,p)}$  the data matrix associated to the  $p$  dummy variables  $\{x^j; j = 1, p\}$ , of a qualitative variable  $x$  with  $n$  rows-objects and  $p$  columns-variables,
- $Y_{(n,q)}$  the data matrix associated to the  $q$  dummy variables  $\{y^k; k = 1, q\}$  of a qualitative variable  $y$  with  $n$  rows-objects and  $q$  columns-variables,
- $Z_{(n,r)} = [X | Y] = [z^1 = x^1, \dots, z^j = x^j, \dots, z^p = x^p | z^{p+1} = y^1, \dots, z^k = y^k, \dots, z^r = y^q]$  the full binary table, juxtaposition of X and Y binary tables, with  $n$  rows-objects and  $r = p + q$  columns-modalities,
- $K_{(p,q)} = {}^t X Y$  the contingency table,
- $M_{B(r,r)} = {}^t Z Z = \left( \begin{array}{c|c} {}^t X X & {}^t X Y \\ \hline {}^t Y X & {}^t Y Y \end{array} \right) = \left( \begin{array}{c|c} {}^t X X & K \\ \hline {}^t K & {}^t Y Y \end{array} \right)$  the symmetric Burt matrix of the two-way cross-tabulations of the two variables. The diagonal are the cross-tabulations of each variable with itself,
- $W_{(r,r)} = \text{Diag}[M_B] = \left( \begin{array}{c|c} {}^t X X & 0 \\ \hline 0 & {}^t Y Y \end{array} \right) = \left( \begin{array}{c|c} W_p & 0 \\ \hline 0 & W_q \end{array} \right)$  the diagonal matrix of  $r = p + q$  frequencies. The diagonal terms are the frequencies of the modalities of  $x$  and  $y$ , totals rows and columns of contingency table K.
- $U = 1_r {}^t 1_r$  is the  $r \times r$  matrix of 1s,  $I_r$  the  $r \times r$  identity matrix where  $1_r$  denotes the  $r$  vector of 1s and  $1_n$  the  $n$  vector of 1s.

The dissimilarity matrices associated with proximity measures are computed from data given by the contingency table K. The attributes of any two points' modalities'  $z^j$  and  $z^k$  in  $\{0, 1\}^n$  of the proximity measures can be easily written and calculated from the following matrices. Computational complexity is thus considerably reduced.

- $A_{(r,r)} = (a_{jk}) = M_B$

Whose element,  $a_{jk} = |Z^j \cap Z^k| = \sum_{i=1}^n z_i^j z_i^k$  is the number of attributes common to both points  $z^j$  and  $z^k$ ,

- $B_{(r,r)} = (b_{jk}) = {}^t Z (1_n {}^t 1_r - Z) = {}^t Z 1_n {}^t 1_r - {}^t Z Z$   
 $= W 1_r {}^t 1_r - A = W U - A$

Whose element,  $b_{jk} = |Z^j - Z^k| = |Z^j \cap \overline{Z^k}| = \sum_{i=1}^n z_i^j (1 - z_i^k)$  is the number of attributes present in  $z^j$  but not in  $z^k$ ,

- $C_{(r,r)} = (c_{jk}) = {}^t (1_n {}^t 1_r - Z) Z = {}^t (1_n {}^t 1_r) Z - {}^t Z Z$   
 $= 1_r {}^t 1_n Z - {}^t Z Z = U W - A$

Whose element,  $c_{jk} = |Z^k - Z^j| = |Z^k \cap \overline{Z^j}| = \sum_{i=1}^n z_i^k (1 - z_i^j)$  is the number of attributes present in  $z^k$  but not in  $z^j$ .

- $D_{(r,r)} = (d_{jk}) = {}^t (1_n {}^t 1_r - Z) (1_n {}^t 1_r - Z)$   
 $= 1_r {}^t 1_n 1_n {}^t 1_r - 1_r {}^t 1_n Z - {}^t Z 1_n {}^t 1_r + {}^t Z Z$   
 $= n 1_r {}^t 1_r - U W - W U + A = n U - U W - W U + A$   
 $= n U - (A + B + C)$

Whose element,  $d_{jk} = |\overline{Z^j} \cap \overline{Z^k}| = \sum_{i=1}^n (1 - z_i^j)(1 - z_i^k)$  is the number of attributes in neither  $z^j$  or  $z^k$ .

$Z^j = \{i/z_i^j = 1\}$  and  $Z^k = \{i/z_i^k = 1\}$  are the sets of attributes present in data point-modality  $z^j$  and  $z^k$  respectively, and  $|\cdot|$  the cardinality of a set.

The attributes are linked by the relation:

$$\forall j = 1, p; \forall k = 1, q \quad a_{jk} + b_{jk} + c_{jk} + d_{jk} = n.$$

Together, the four dependent quantities  $a_{jk}, b_{jk}, c_{jk}$  and  $d_{jk}$  can be presented in the following table 2, where the information can be summarized by an index of similarity (affinity, resemblance, association, coexistence).

**Table 2.** The  $2 \times 2$  contingency table between modalities  $z^j$  and  $z^k$

	$z^k = 1$	$z^k = 0$	Total
$z^j = 1$	$a_{jk}$	$b_{jk}$	$a_{jk} + b_{jk}$
$z^j = 0$	$c_{jk}$	$d_{jk}$	$c_{jk} + d_{jk}$
Total	$a_{jk} + c_{jk}$	$b_{jk} + d_{jk}$	n

## 2 Topological Correspondence

Topological equivalence is based on the concept of topological graph also referred to as the neighborhood graph. The basic idea is actually quite simple: two proximity measures are equivalent if the corresponding topological graphs induced on the set of objects remain identical. Measuring the similarity between proximity measures consists of comparing the neighborhood graphs and measuring their similarity. We will first define more precisely what a topological graph is and how to build it. Then, we propose a measure of proximity between topological graphs that will subsequently be used to compare the proximity measures.

Consider a set  $E = \{z^1 = x^1, \dots, z^p = x^p, z^{p+1} = y^1, \dots, z^r = y^q\}$  of  $r = |E|$  modalities in  $\{0, 1\}^n$ , associated with the variables  $x$  and  $y$ . We can, by means of a proximity measure  $u$ , define a neighborhood relationship  $V_u$  to be a binary relationship on  $E \times E$ . There are many possibilities for building this neighborhood binary relationship.

Thus, for a given proximity measure  $u$ , we can build a neighborhood graph on a set of objects-modalities, where the vertices are the modalities and the edges are defined by a property of the neighborhood relationship.

Many definitions are possible to build this binary neighborhood relationship. One can choose the Minimal Spanning Tree (MST) [7], the Gabriel Graph (GG) [10] or, as is the case here, the Relative Neighborhood Graph (RNG) [14] [6].

For any given proximity measure  $u$ , we construct the associated adjacency binary symmetric matrix  $V_u$  of order  $r = p + q$ , where, all pairs of neighboring modalities  $(z^j, z^k)$  satisfy the following RNG property.

*Property 1.* Relative Neighborhood Graph (RNG)

$$\begin{cases} V_u(z^j, z^k) = 1 & \text{if } u(z^j, z^k) \leq \max[u(z^j, z^l), u(z^l, z^k)]; \forall z^j, z^k, z^l \in E, z^l \neq z^j \text{ and } z^l \neq z^k \\ V_u(z^j, z^k) = 0 & \text{otherwise} \end{cases}$$

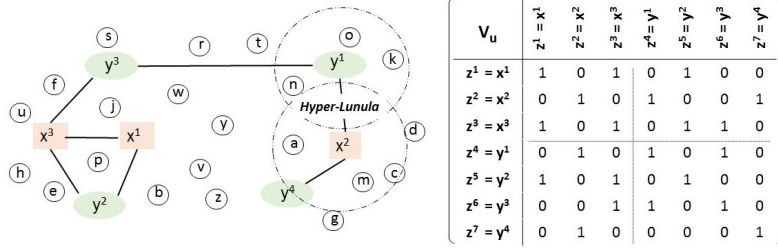


**Fig. 1.** RNG example with seven groups-modalities - Associated adjacency matrix

This means that if two modalities  $z^j$  and  $z^k$  which verify the RNG property are connected by an edge, the vertices  $z^j$  and  $z^k$  are neighbors.

Thus, for any proximity measure given,  $u$ , we can associate an adjacency matrix  $V_u$ , binary and symmetrical of order  $r = p + q$ . Figure 1 illustrates a set of  $n$  object-individuals around seven modalities associated with two qualitative variables  $x$  and  $y$  respectively with three and four modalities.

For example, if  $V_u(z^2 = x^2, z^4 = y^1) = 1$  it means that on the geometrical plane, the hyper-Lunula (intersection between the two hyperspheres centered on the two modalities  $x^2$  and  $y^1$ ) is empty.

For a given neighborhood property (MST, GG or RNG), each measure  $u$  generates a topological structure on the objects in  $E$  which are totally described by the adjacency binary matrix  $V_u$ . In this paper, we chose to use the Relative Neighbors Graph (GNR) [14].

## 2.1 Comparison and selection of proximity measures

First we compare different proximity measures according to their topological similarity in order to regroup them and to better visualize their resemblances.

To measure the topological equivalence between two proximity measures  $u_i$  and  $u_j$ , we propose to test if the associated adjacency matrices  $V_{u_i}$  and  $V_{u_j}$  are different or not. The degree of topological equivalence between two proximity measures is measured by the following property of concordance.

*Property 2.* Topological equivalence index between two adjacency matrices

$$S(V_{u_i}, V_{u_j}) = \frac{\sum_{k=1}^r \sum_{l=1}^r \delta_{kl}(z^k, z^l)}{r^2} \quad \text{with} \quad \delta_{kl}(z^k, z^l) = \begin{cases} 1 & \text{if } V_{u_i}(z^k, z^l) = V_{u_j}(z^k, z^l) \\ 0 & \text{otherwise.} \end{cases}$$

Then, in our case, we want to compare these different proximity measures according to their topological equivalence in a context of association. So we define a criterion for measuring the spacing from the independence or no association position.

The contingency table is one of the most common ways to summarize categorical data. Generally, interest lies in whether there is an association between the row variable and the column variable that produce the table; sometimes there is further interest in describing the strength of that association. The data can arise from several different sampling frameworks, and the interpretation of

the hypothesis of no association depends on the framework. The question of interest is whether there is an association between the two variables.

We note  $V_{u_*} = I_r$ , the  $r = p + q$  identity matrix. It is a perfect adjacency matrix, which corresponds to the null hypothesis  $H_0$  of independence: no association between the two variables.

$$V_{u_*} = \left( \begin{array}{c|c} I_p & 0 \\ \hline 0 & I_q \end{array} \right) = I_r$$

This adjacency diagonal reference matrix is associated with an unknown proximity measure denoted  $u_*$ .

Thus, with this reference proximity measure we can establish the Topological Independence Index  $TII_i = S(V_{u_i}, V_{u_*})$  - the degree of topological equivalence of no association between the two variables - by measuring the percentage of similarity between the adjacency matrix  $V_{u_i}$  and the reference adjacency matrix  $V_{u_*}$ . The greater this topological index is and tends to 1, the more independent the variables are, according to the proximity measure  $u_i$  chosen.

In order to visualize the similarities between all the twenty-two proximity measures considered, a Principal Component Analysis (PCA) followed by a Hierarchical Ascendant Classification (HAC) were performed upon the twenty-two-component dissimilarity matrix defined by  $[D]_{ij} = D(V_{u_i}, V_{u_j}) = 1 - S(V_{u_i}, V_{u_j})$  to partition them into homogeneous groups and to view their similarities in order to see which measures are close to one another.

We can use any classic visualization techniques to achieve this. For example, we can build a dendrogram of hierarchical clustering of the proximity measures. We can also use multidimensional scaling or any other technique, such as Laplacian projection, to map the twenty-two proximity measures into a two dimensional space.

Finally, in order to evaluate and select the no association proximity measures, we project the reference measure  $u_*$  as supplementary element into the methodological chain of data analysis methods (PCA and HAC), positioned by the dissimilarity vector with twenty-two components  $[D]_{*i} = 1 - S(V_{u_*}, V_{u_i})$ .

## 2.2 Statistical comparisons between two proximity measures

In a metric framework, there are several ways of testing the null hypothesis,  $H_0$ , of no association between two variables, and many of the tests are based on the chi-square statistic.

In this paragraph, we use Cohen's kappa coefficient to test statistically the degree of topological equivalence between two proximity measures. This non-parametric test compares these measures based on their associated adjacency matrices.

The comparison between indices of proximity measures has also been studied by [12], [13] and [5] from a statistical perspective. The authors proposed an approach that compares similarity matrices obtained by each proximity measure, using Mantel's test [9], in a pairwise manner.

Cohen's nonparametric Kappa test [4] is the statistical test best suited to our problem, it as makes it possible in this context to measure the agreement or the concordance of binary values of two adjacency matrices associated with two measures of proximity, unlike the coefficients of Kendall or Spearman, for example, who evaluate the degree of concordance between quantitative values. The Kappa concordance rate between two adjacency matrices is estimated to evaluate the degree of topological equivalence between their proximity measures.

Let  $V_{u_i}$  and  $V_{u_j}$  be adjacency matrices associated with two proximity measures  $u_i$  and  $u_j$ . To compare the degree of topological equivalence between these two measures, we propose to test if the associated adjacency matrices are statistically different or not, using a non-parametric test of paired data. These binary and symmetric matrices of order  $r$ , are unfolded in two vector-matched components, consisting of  $\frac{r(r+1)}{2}$  values: the  $r$  diagonal values and the  $\frac{r(r-1)}{2}$  values above or below the diagonal.

The degree of topological equivalence between two proximity measures is estimated from the Kappa coefficient of concordance, computed on the a  $2 \times 2$  contingency table  $N = (n_{kl})_{k,l=0,1}$  formed by the two binary vectors, using the following relation :

$$\kappa = \kappa(V_{u_i}, V_{u_j}) = \frac{P_o - P_e}{1 - P_e}$$

where,

$$P_o = \frac{2}{r(r+1)} \sum_{k=0}^1 n_{kk} \quad \text{is the observed proportion of concordance,}$$

$P_e = \frac{4}{r^2(r+1)^2} \sum_{k=0}^1 n_{k.} \cdot n_{.k}$  represents the expected proportion of concordance under the assumption of independence.

The Kappa coefficient is a real number, without dimension, between -1 and 1. The concordance will be even higher when the value of Kappa is close to 1 and the maximum concordance is reached ( $\kappa = 1$ ) when  $P_o = 1$  and  $P_e = 0.5$ . When there is perfect independence,  $\kappa = 0$  with  $P_o = P_e$ , and in the case of total mismatch,  $\kappa = -1$  with  $P_o = 0$  and  $P_e = 0.5$ .

The true value of the Kappa coefficient in the population is a random variable that approximately follows a Gaussian law of mean  $\kappa$  and variance  $Var(\kappa)$ . The null hypothesis  $H_0$  is  $\kappa = 0$  against the alternative hypothesis  $H_1 : \kappa > 0$ . We formulate the null hypothesis  $H_0 : \kappa = 0$  independence of agreement or concordance. The concordance is even higher when its value tends to 1, or a perfect maximum if  $\kappa = 1$ . It is equal to  $-1$  in the case of a perfect discordance.

We also test each proximity measure  $u_i$  with the perfect measure  $u_*$  by comparing adjacency matrices  $V_{u_i}$  and  $V_{u_*}$  to estimate the degree of topological equivalence of independence of each measure.

### 3 Illustrative example and Empirical results

The data displayed in Table 3 are from an INSEE study concerning the 554,000 enterprise births in France 2016 [15]. The question was whether there was any association between the type of enterprise and the sector of activity of the enterprise's operation.

**Table 3.** Contingency table - Enterprise births in France 2016 (in thousands)

Activity sector	Type of enterprise			Total
	Company	Traditional Individual Enterprise	Micro Entrepreneur	
Industry	8,6	7,7	8,3	24,6
Construction	26,5	18,6	16,5	61,6
Trade, Transport, Accommodation and Restoration	64	48,7	48,7	161,5
Information and communication	11,1	2,1	14,5	27,6
Financial and insurance activities	12,6	1,3	2	15,8
Real estate activities	11,3	5,1	2,5	18,9
Specialized, scientific and technical activities	27,6	11,9	51	90,6
Education and Health	6,5	26,4	36,4	69,4
Service activities	20,6	20,6	42,9	84
Total	188,8	142,4	222,8	554

In a metric context, the null hypothesis of the chi-square independence test is clearly rejected with a risk of error  $\alpha \leq 5\%$ . So there is a strong association between the type of enterprise and the activity sector. One can also perform a factorial Correspondence Analysis to locate and visualize any significant links between all the modalities of these two variables.

In a topological context, the main results of the proposed approach are presented in the following tables and graphs that allow visualization of the proximity measures that are close to each other in a context of no association between the type of enterprise and the activity sector.

Table 4 summarizes the similarities and Kappa statistic values between the reference measure  $u_*$  and each of the 22 proximity measures in a topological framework.

The proximity measures are given in ascending order of the topological independence index  $S(V_{u_i}, V_{u_*})$ . So, greater this index is, further we getting closer the independence position, and more the null hypothesis will be rejected. All the 22 proximity measures considered reject the null hypothesis  $H_0 : \kappa = 0$  (no concordance, independence), so they all conclude that there is a link between the type of enterprise and the activity sector.

The results of similarities and statistical Kappa tests between all pairs of proximity measures are given in the Appendix, Table 7. The values below

**Table 4.** Topological Index of Independence & Kappa test

Measure	$TII_i$	$\hat{\kappa}(V_{u_j}, V_{u_*})$	$p - value$
Jaccard	0.625	0.308	< .0001
Dice, Czekanowski	0.625	0.308	< .0001
Kulczynski	0.625	0.308	< .0001
Driver, Kroeber and Ochiai	0.625	0.308	< .0001
Sokal-Sneath-2	0.625	0.308	< .0001
Braun and Blanquet	0.625	0.308	< .0001
Simpson	0.625	0.308	< .0001
Russel and Rao	0.625	0.308	< .0001
Sokal and Sneath 5	0.625	0.308	< .0001
Baroni, Urbani and Buser	0.625	0.308	< .0001
Q-Yule	0.625	0.308	< .0001
Y-Yule	0.625	0.308	< .0001
Sokal and Sneath 4	0.708	0.397	< .0001
Pearson	0.736	0.432	< .0001
Michael	0.736	0.432	< .0001
Simple Matching	0.847	0.606	< .0001
Rogers and Tanimoto	0.847	0.606	< .0001
Hamann	0.847	0.606	< .0001
BC	0.847	0.606	< .0001
Sokal and Sneath 3	0.847	0.606	< .0001
Gower and Legendre	0.847	0.606	< .0001
Sokal and Sneath 1	0.847	0.606	< .0001

the diagonal correspond to the similarities  $S(V_{u_i}, V_{u_j})$  and the values above the diagonal are the Kappa coefficients  $\hat{\kappa}(V_{u_i}, V_{u_j})$ . All Kappa statistical tests are significant with  $\alpha \leq 5\%$  level of significance. The similarities in pairs between the twenty-two proximity measures differ somewhat: some are closer than others. Note in Table 4, that proximity measures with the same letter are in perfect topological equivalence  $S(V_{u_i}, V_{u_j}) = 1$  with a perfect concordance  $\hat{\kappa}(V_{u_i}, V_{u_j}) = 1$ .

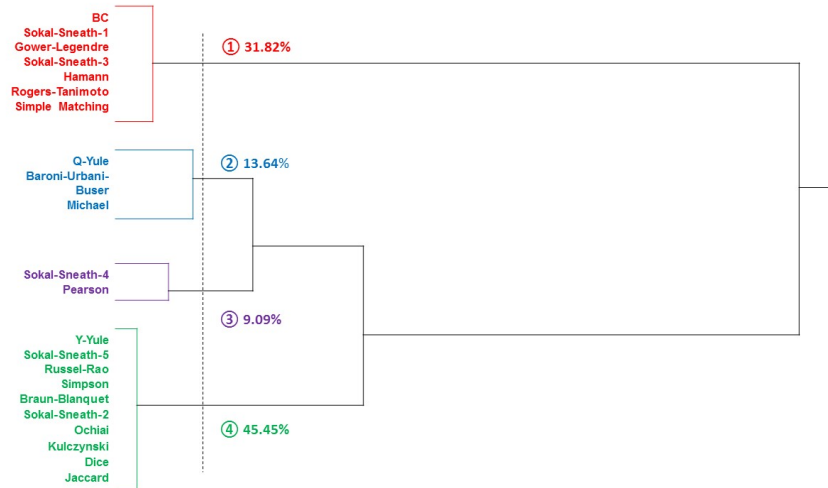


**Fig. 2.** Hierarchical tree of the proximity measures

**Table 5.** Assignment of the reference measure

Number Frequency	Class 1 7	Class 2 3	Class 3 2	Class 4 10
Proximity measures	$u_{Simple-Matching}$	$u_{Michael}$	$u_{Pearson}$	$u_{Jaccard}$
	$u_{Rogers-Tanimoto}$	$u_{Baroni-Urbani-Buser}$	$u_{Sokal-Sneath-4}$	$u_{Dice}$
	$u_{Hamann}$	$u_{Q-Yule}$		$u_{Kulczynski}$
	$u_{BC}$			$u_{Ochiai}$
	$u_{Sokal-Sneath-3}$			$u_{Sokal-Sneath-2}$
	$u_{Gower-Legendre}$			$u_{Braun-Blanquet}$
	$u_{Sokal-Sneath-1}$			$u_{Simpson}$
				$u_{Russel-Rao}$
				$u_{Sokal-Sneath-5}$
				$u_{Y-Yule}$
Reference	$u_*$			

An HAC algorithm based on the Ward criterion [16] was used in order to characterize classes of proximity measures relatively to their similarities. The reference measure  $u_*$  is projected as supplementary element. The dendrogram of Figure 2 represents the hierarchical tree of the twenty two proximity measures considered.

Table 5 summarizes the main results of the chosen partition into four homogeneous classes of proximity measures, obtained from the cut of the hierarchical tree of Figure 2.

Moreover, in view of the results in Table 5, the reference measure  $u_*$  is closer to the measures of the first class, measures for which there is a weak association between the two variables among the twenty two proximity measures considered. We will have a stronger association between the type of enterprise and the activity sector if we choose one proximity measure among those of class 4.

It was shown in [1] and [18], by means of a series of experiments, that the choice of proximity measure has an impact on the results of a supervised or unsupervised classification.

For any proximity measure given in Table 1, we will show how to build and apply the Kappa test in order to compare two adjacency matrices to measure and test their topological equivalence  $\kappa(V_{u_i}, V_{u_j})$  and their degree of independence  $\kappa(V_{u_i}, V_{u_*})$ .

Let  $V_{u_*}$  and  $V_{Jaccard}$ , the reference and Jaccard adjacency matrices, be  $n \times n$  binary symmetric matrices with lower similarity  $S(V_{u_*}, V_{Jaccard}) = 0.625$ . These matrices are unfolded to two vectors comprising the  $r(r+1)/2 = 78$  diagonal and upper-diagonal values. These two binary vectors are two dummy variables represented in the same sample size of 78 pairs of objects. We then formulated the null hypothesis,  $H_0 : \kappa = 0$  (independence), that there is no association between the two variables.

---

Aggregation based on the criterion of the loss of minimal inertia.

Table 6 shows the contingency table observed between the two binary vectors associated to the reference and Jaccard proximity measures. Thus, for this example, the calculated Kappa value  $\hat{\kappa} = 0.3077$  corresponds to a p-value of less than 0.01%. Since this probability is lower than a pre-specified significance level of 5%, the null hypothesis of independence is rejected. We can therefore conclude that the Jaccard measure and reference measure are not independent.

**Table 6.** The  $2 \times 2$  contingency table - Reference and Jaccard measures

	$V_{Jaccard} = 0$	$V_{Jaccard} = 1$	Total
$V_{u^*} = 0$	39	27	66
$V_{u^*} = 1$	0	12	12
Total	39	39	78

$\hat{\kappa} = 0.3077$  ; p-value < 0.01%

## 4 Conclusion and perspectives

The choice of a proximity measure is very subjective; it is often based on habits or on criteria such as the interpretation of the *a posteriori* results.

This work proposes a new approach to select the best proximity measure in a context of topological independence between two qualitative variables, for the purpose of performing a Topological Correspondence Analysis (TCA). The proposed approach is based on the concept of neighborhood graphs induced by a proximity measure in the case of qualitative data. Results obtained from a real dataset highlight the effectiveness of selecting the best proximity measure(s).

Future research will focus on developing TCAs with the best proximity measure selected and on extending this approach to analyze associations between more than two categorical variables, called Topological Multiple Correspondence Analysis (TMCA).

# Appendix

**Table 7.** Similarities  $S(V_{u_i}, V_{u_j})$  & Kappa coefficient  $\hat{\kappa}(V_{u_i}, V_{u_j})$

Measure	Jaccard	Dice	Kulczynski	Ochiai	Sokal-Sneath-2	Braun-Blanquet	Simpson	Simple Matching	Russel-Rao	Rogers-Tanimoto	Pearson	Hamann	BC	Sokal-Sneath-5	Michael	Baroni-Urbani-Buser	Q-Yule	Y-Yule	Sokal-Sneath-4	Sokal-Sneath-3	Gower-Legendre	Sokal-Sneath-1
Jaccard	1	1	1	1	1	1	1	0.18	1	0.18	0.74	0.18	0.18	1	0.64	1	1	1	0.79	0.18	0.18	0.18
Dice	1	1	1	1	1	1	1	0.18	1	0.18	0.74	0.18	0.18	1	0.64	1	1	1	0.79	0.18	0.18	0.18
Kulczynski	1	1	1	1	1	1	1	0.18	1	0.18	0.74	0.18	0.18	1	0.64	1	1	1	0.79	0.18	0.18	0.18
Ochiai	1	1	1	1	1	1	1	0.18	1	0.18	0.74	0.18	0.18	1	0.64	1	1	1	0.79	0.18	0.18	0.18
Sokal-Sneath-2	1	1	1	1	1	1	1	0.18	1	0.18	0.74	0.18	0.18	1	0.64	1	1	1	0.79	0.18	0.18	0.18
Braun-Blanquet	1	1	1	1	1	1	1	0.18	1	0.18	0.74	0.18	0.18	1	0.64	1	1	1	0.79	0.18	0.18	0.18
Simpson	1	1	1	1	1	1	1	0.18	1	0.18	0.74	0.18	0.18	1	0.64	1	1	1	0.79	0.18	0.18	0.18
Simple Matching	0.56	0.56	0.56	0.56	0.56	0.56	0.56	0.18	1	0.18	0.74	0.18	0.18	1	0.64	1	1	1	0.79	0.18	0.18	0.18
Russel-Rao	0.56	0.56	0.56	0.56	0.56	0.56	0.56	0.18	1	0.18	0.74	0.18	0.18	1	0.64	1	1	1	0.79	0.18	0.18	0.18
Rogers-Tanimoto	0.56	0.56	0.56	0.56	0.56	0.56	0.56	0.18	1	0.18	0.74	0.18	0.18	1	0.64	1	1	1	0.79	0.18	0.18	0.18
Pearson	0.86	0.86	0.86	0.86	0.86	0.86	0.86	0.69	0.69	0.38	0.38	0.38	0.38	0.74	0.74	0.74	0.74	0.74	0.95	0.38	0.38	0.38
Hamann	0.56	0.56	0.56	0.56	0.56	0.56	0.56	0.18	1	0.18	0.74	0.18	0.18	1	0.64	1	1	1	0.79	0.18	0.18	0.18
Sokal-Sneath-5	0.56	0.56	0.56	0.56	0.56	0.56	0.56	0.18	1	0.18	0.74	0.18	0.18	1	0.64	1	1	1	0.79	0.18	0.18	0.18
Michael	0.81	0.81	0.81	0.81	0.81	0.81	0.81	0.75	0.81	0.75	0.94	0.75	0.75	0.81	0.64	0.64	0.64	0.64	0.84	0.50	0.50	0.50
Baroni-Urbani-Buser	1	1	1	1	1	1	1	0.56	1	0.56	1	1	1	1	0.81	0.81	0.81	0.81	0.79	0.18	0.18	0.18
Q-Yule	1	1	1	1	1	1	1	0.56	1	0.56	1	1	1	1	0.81	0.81	0.81	0.81	0.79	0.18	0.18	0.18
Y-Yule	1	1	1	1	1	1	1	0.56	1	0.56	1	1	1	1	0.81	0.81	0.81	0.81	0.79	0.18	0.18	0.18
Sokal-Sneath-4	0.89	0.89	0.89	0.89	0.89	0.89	0.89	0.67	0.89	0.67	0.67	0.67	0.67	0.67	0.56	0.56	0.56	0.56	0.56	0.67	0.34	0.34
Sokal-Sneath-3	0.56	0.56	0.56	0.56	0.56	0.56	0.56	0.18	1	0.18	0.69	1	1	1	0.56	0.56	0.56	0.56	0.56	0.67	1	1
Gower-Legendre	0.56	0.56	0.56	0.56	0.56	0.56	0.56	0.18	1	0.18	0.69	1	1	1	0.56	0.56	0.56	0.56	0.56	0.67	1	1
Sokal-Sneath-1	0.56	0.56	0.56	0.56	0.56	0.56	0.56	0.18	1	0.18	0.69	1	1	1	0.56	0.56	0.56	0.56	0.56	0.67	1	1

All Kappa statistical tests are significant with  $\alpha \geq 5\%$  level of Significance.

Example :  $S(u_{Simple\ matching}, u_{Jaccard}) = 0.56$   
 $\hat{\kappa}(u_{Jaccard}, u_{Simple\ matching}) = 0.18$  ;  $p - value = 0.0411$

## References

1. Abdesselam, R.: Proximity measures in topological structure for discrimination. *In a Book Series SMTDA-2014*, 3rd Stochastic Modeling Techniques and Data Analysis, International Conference, Lisbon, Portugal, C.H. Skiadas (Ed), ISAST, 599–606, 2014.
2. Batagelj, V., Bren, M.: Comparing resemblance measures. In Proc. International Meeting on Distance Analysis (Distancia'92), 1992.
3. Batagelj, V., Bren, M.: Comparing resemblance measures. *In Journal of classification*, 12, 73–90, 1995.
4. Cohen, J.: A coefficient of agreement for nominal scales. *Educ Psychol Meas*, Vol 20, 27–46, 1960.
5. Demsar, J.: Statistical comparisons of classifiers over multiple data sets. *The journal of Machine Learning Research*, Vol. 7, 1–30, 2006.
6. Jaromczyk, J.-W. and Toussaint, G.-T.: Relative neighborhood graphs and their relatives. *Proceedings of IEEE*, 80, 9, 1502–1517, 1992.
7. Kim, J.H. and Lee, S.: Tail bound for the minimal spanning tree of a complete graph. *In Statistics & Probability Letters*, 4, 64, 425–430, 2003.
8. Lesot, M. J., Rifqi, M. and Benhadda, H.: Similarity measures for binary and numerical data: a survey. *In IJKESDP*, 1, 1, 63–84, 2009.
9. Mantel, N.: A technique of disease clustering and a generalized regression approach. *In Cancer Research*, 27, 209–220, 1967.
10. Park, J. C., Shin, H. and Choi, B. K.: Elliptic Gabriel graph for finding neighbors in a point set and its application to normal vector estimation. *In Computer-Aided Design Elsevier*, 38, 6, 619–626, 2006.
11. Rifqi, M., Detyniecki, M. and Bouchon-Meunier, B.: Discrimination power of measures of resemblance. *IFSA'03 Citeseer*, 2003.
12. Schneider, J. W. and Borlund, P.: Matrix comparison, Part 1: Motivation and important issues for measuring the resemblance between proximity measures or ordination results. *In Journal of the American Society for Information Science and Technology*, 58, 11, 1586–1595, 2007.
13. Schneider, J. W. and Borlund, P.: Matrix comparison, Part 2: Measuring the resemblance between proximity measures or ordination results by use of the Mantel and Procrustes statistics. *In Journal of the American Society for Information Science and Technology*, 11, 58, 1596–1609, 2007.
14. Toussaint, G. T.: The relative neighbourhood graph of a finite planar set. *In Pattern recognition*, 12, 4, 261–268, 1980.
15. INSEE 2016, <https://www.insee.fr/fr/statistiques/2562977>.
16. Ward, J. R.: Hierarchical grouping to optimize an objective function. *In Journal of the American statistical association JSTOR*, 58, 301, 236–244, 1963.
17. Warrens, M. J.: Bounds of resemblance measures for binary (presence/absence) variables. *In Journal of Classification*, Springer, 25, 2, 195–208, 2008.
18. Zighed, D., Abdesselam, R., and Hadgu, A.: Topological comparisons of proximity measures. *In the 16th PAKDD 2012 Conference*. In P.-N. Tan et al., Eds. Part I, LNAI 7301, Springer-Verlag Berlin Heidelberg, 379–391, 2012.

# Updating of PageRank in Evolving Tree graphs

Benard Abola<sup>2</sup>, Pitos Seleka Biganda<sup>1,2</sup>, Christopher Engström<sup>2</sup>, John Mango Magero<sup>3</sup>, Godwin Kakuba<sup>3</sup>, and Sergei Silvestrov<sup>2</sup>

<sup>1</sup> Department of Mathematics, College of Natural and Applied Sciences, University of Dar es Salaam, Box 35062 Dar es Salaam, Tanzania  
(E-mail: [pitos.biganda@mdh.se](mailto:pitos.biganda@mdh.se))

<sup>2</sup> Division of Applied Mathematics, School of Education, Culture and Communication (UKK), Mälardalen University, Box 883, 721 23, Västerås, Sweden  
(E-mails: [benard.abola@mdh.se](mailto:benard.abola@mdh.se), [christopher.engstrom@mdh.se](mailto:christopher.engstrom@mdh.se), [sergei.silvestrov@mdh.se](mailto:sergei.silvestrov@mdh.se))

<sup>3</sup> Department of Mathematics, School of Physical Sciences, Makerere University, Box 7062, Kampala, Uganda  
(E-mails: [mango@cns.mak.ac.ug](mailto:mango@cns.mak.ac.ug), [godwin.a.kakuba@gmail.com](mailto:godwin.a.kakuba@gmail.com))

**Abstract.** Updating PageRank refers the process of computing new PageRank values after change(s) has occurred in a graph. The main goal of the updating is to avoid re-calculating the values from scratch. It is known from literature that handling PageRank's update is problematic, in particular when it involves both link and page updates. In this paper we focus on updating PageRank of evolving tree graph when vertex and edge are added sequentially. We describe how to maintain level structures when a cycle is created, and also investigate the practical and theoretical efficiency to update PageRanks for an evolving graph with many cycles. Our experimental result demonstrates that applying power method to stochastic complement of Google matrix when feedback vertex set partitioning strategy is used has quite good convergence. Particularly when ones encounter cyclic components in a evolving network.

**Keywords:** PageRank, Feedback vertex set, graph, link-update, stochastic complement..

## 1 Introduction

The field in which graphs are proving to be natural modelling abstraction in real life are many. For instance, biology, transportation system, internet, communication data and many others. The challenges posed by processing huge graphs include storage and keeping up with changes in the graph. Numerous research effort have been devoted to the study of dynamic graph problems, [9] and [8].

In [8], dynamic algorithms for maintaining a breadth-first search tree in a directed graph was studied. The study reveals that such algorithm requires  $\mathcal{O}(E + V)$  and insertion or deletion edges needs about  $\mathcal{O}(E \min(E, V))$ . Baswana *et al* [9] looks at how to maintain a depth first search tree when edges are added or deleted from a directed graph. In fact, graph transverse using depth-first search (DFS) can be used in many practical situations like finding connected components, topological sorting and cycles or strongly connected



components, [9]. In their case maintaining a DFS tree in a evolving directed acyclic graph(DAG) was the key problem. It was observed that the algorithm takes about  $\mathcal{O}(EV \log V)$  time to process any online sequence of edge deletions arbitrarily. The important point to note here is that DFS can be used to structure the vertices of the graph and in-turn provides an intrinsic partition of static and dynamic graph. Hence, provides a way to speed up calculations of PageRank by handling certain vertices in the graph separately [6].

In PageRank problem, where one is want to answer queries like are the top ranked vertices still in the top list after several changes?. It is possible that the rank of sub-components of the graph can be evaluated when edges are added or deleted?. Finding PageRank of evolving networks, effort that geared towards determining ranks of a graph where a evolving tree graph is far from being conclusive. In this paper we will extent the PageRank method we proposed in [7] and show how a partition of the network into cyclic components can be used together with the old PageRank to calculate the new PageRank after certain changes on the graph. In particular we will first have a look at how cycles are maintained in a network and secondly, how would PageRank be re-calculated when we have many cycles. It is known that a cycle is a deadlock, hence its existence in evolving network is problematic from computational point of view.

According to [4], DFS can transverse a graph in linear time and also it is able to find whether a graph is connected or has cycle. It important to point out that when the graph is dense, that is the number of edges is high as compared to the number of vertices, then the process time increase drastically. This is one of bottle neck of in computing PageRank, essentially when using Power method. Poor asymptotic convergence of the method is encountered when there is cyclic component(s). Thus, we describe how one can speed-up PageRank update by partition of vertices into unchange, feedback vertex set and non-feedback vertex set.

We emphasize that PageRank can be computed as the stationary distribution of a random walk on a directed graph using weighted adjacency matrix or its modified version (Google matrix).

This article is structured as follows: the first section has review of known facts, key notations and basic concepts necessary for the article. Section 2 deals with maintaining cyclic components. In Section 3, we describe how to compute PageRank of tree graph when one or more cycles are formed. Finally a conclusion is given in section 4.

## 1.1 Abbreviations and Definitions

The following abbreviations will be used throughout this article

- *CC*: cyclic component.
- *DAG*: directed acyclic graph.
- *DFS*: depth first search.

**Definition 1.** Given a simple graph  $G = (V, E)$ , where  $V$  and  $E$  are set of vertices and edges respectively. A path is a sequence of  $v_1, v_2, \dots, v_n$  such that between any consecutive vertices  $v_i, v_{i+1}$  in the sequence there is  $(v_i, v_{i+1})$  edge.

A path in a directed graph where the order of the vertices in the  $(v_i, v_{i+1})$  edge is important is also called a directed path.

**Definition 2.** A directed graph  $G = (V, E)$  is strongly connected if there is a path  $u \rightarrow v$  from  $u$  to  $v$  and  $v \rightarrow u$ , for  $u, v \in V$  or if a subgraph  $G^\dagger$  is connected in a way that there is a path from each node to all other nodes.

- The level  $L_C$  of component  $C$  is equal to the longest path in the underlying DAG starting in  $C$ .
- The level  $L_{v_i}$  of some vertex  $v_i$  is defined as the level of the component for which  $v_i$  belongs ( $L_{v_i} \equiv L_C$ , if  $v_i \in C$ ). In short, we denote  $L_{v_i}$  as  $L_i$ .
- $P_{ts}(\bar{c})$  is the probability to reach vertex  $v_s$  starting at  $v_t$  without passing through  $v_c$ .
- Denote  $P_{\rightarrow s} = w_s + \sum_{v_i \neq v_s} w_i P_{is}$  and  $R_s = \frac{P_{\rightarrow s}}{1 - P_{ss}}$ .

On account of [5], we give an example of a partition of graph as in Fig.1.

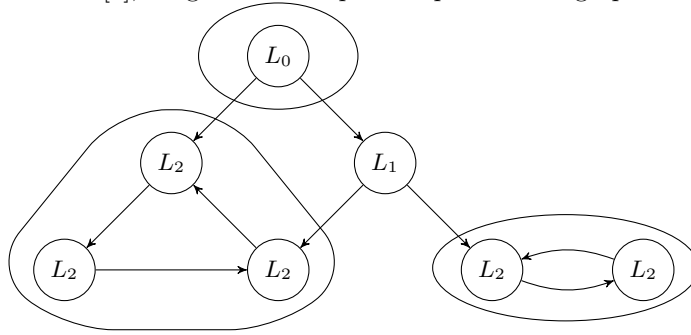


**Fig. 1.** A directed graph and corresponding components.  $L_i$  denotes the  $i$ th label of a vertex.

## 1.2 Component finding

This section presents technique of finding component, where the graph is partitioned into CAC and cyclic,  $CC$ . Although, taking into account  $CC$  in the graph might be looked at as overhead work, it is necessary to find them because they are important when calculating PageRank for each cycle. The purpose is to isolate the vertices that form part of different components as well as keep track of every vertices in the partitions. Also, their levels are found using a depth first search.

**Isolation of vertices in the graph:** Since the vertices that form back edge is known from the previous algorithm, DFS algorithm can be deployed starting from one of such vertices in order to find  $CC$  and its vertices. For instance, in the previous step, a cycle is detected together with back edge  $(v_i, v_j)$  where  $v_i$  is an ancestor of  $v_j$  before a cycle was formed. To detect the vertices that form

$CC$ , we keep track of every vertices visited by DFS in stack and if we reach a vertex that is already in updated stack, then there is cycle in the graph whose vertices are in the stack. Once, this is found a vertex  $v \in V$  that does not belong to  $C$  must be in  $CAC$ .

Denote the component the vertex  $v$  is part of by  $v.comp$  such that

$$v.comp = \begin{cases} 1 & \text{if } v \in CC \\ 0 & \text{if } v \in CAC \end{cases}$$

**Keeping track of every vertex in the components:** For further computation, we keep record of every vertex as follows

- $v.comp$ : as defined previously.
- $v.index$ : the order in which the vertex was discovered in DFS
- $v.level$ : indicates the level of  $v$ . For thee case of component  $CC$ , the vertices will have the same level.
- $v.parent$ : indicates the parent(s) of  $v$ .
- $v.levelcomp$ : indicates the level of  $CAC$  or  $CC$  which  $v$  belongs. Here we are more interested in the level of  $CC$ .

Next, we have discovery step, values are initialised and vertices in the graph are stacked. The detailed algorithms will not be presented here, it will appear in the elsewhere.

## 2 Maintaining the level of cycles

In this section, steps essential to maintain level of dynamic graph with cycle is described. For such a case one is able to update the level of connected components previously in the system or as they are created during the evolution. This kind of algorithm can address information flow in evolving strongly connected components. We focus on sequential addition of a vertex and edge only. We believe that the idea can be extended to vertex addition/deletion as well as edge. In view [6], addition of outgoing edges to a vertex with no previous outgoing edges can be seen as adding a single vertex to the graph. In particular, adding a vertex to a graph with no incoming edges and outgoing can be seen as first adding the vertex and then adding edge(s). It is also assumed that once a cycle is formed, it must be maintained.

An overview of the algorithm that support maintaining cyclic components. Assume that we started with a tree graph, where the level of all vertices were determined using Tarjan depth first search (DFS).

1. *Vertex addition*:
  - Add a vertex sequentially and give them level accordingly.
2. *Edge addition*:
  - Add an edge randomly.

- Run DFS from the target vertex and see if there is path to the source.
- Cases that may occur:-
- if **No cycle** is formed, update the level of target vertex as  $\max(\mathbf{prev}, \mathbf{source} + 1)$ .
  - if a **Cycle** is formed, create cyclic component and identify all its vertices.
  - update all the level of vertices of the cycle to the level of target vertex.

It is known that directed graph has a topological order if and only if it is acyclic, therefore detecting cycles and maintaining their levels fits in link-update or page-update problem in PageRank. In the next section we consider updating PageRank as a cycle is form. We demonstrate the idea with an example.

### 3 Calculating PageRank

First let state a well known result in [6], that is.,

**Lemma 1.** *Let  $v_t$  be the source vertex to vertex  $v_s$  such that adding a back-edge  $v_t \rightarrow v_s$  forms a cycle, then the PageRank of  $v_s$  can be expressed as*

$$\mathbf{R}_s = \frac{\mathbf{P}_{\rightarrow s}}{1 - \mathbf{P}_{ss}} + \frac{\mathbf{R}_t \mathbf{P}_{st}(\bar{t})}{1 - \mathbf{P}_{ss}(\bar{t})}.$$

*Proof.* The first term to the right gives the expected number of visits to  $v_s$  without passing through  $v_t$ . this is correspond to the Pagerank before the cycle was formed. The second, correspond to the number of visits to  $v_t$  at least once.

To proof Lemma 1, let  $r_i$  be the expected number of visits to  $v_t$  after the  $i^{\text{th}}$  visit to  $i + 1^{\text{th}}$ . Then,

$$\begin{aligned} \mathbf{R}_s &= r_0 + r_1 + r_2 + \dots \\ &= \frac{\mathbf{P}_{\rightarrow s}}{1 - \mathbf{P}_{ss}} + \frac{\mathbf{P}_{\rightarrow s} \mathbf{P}_{ts}(\bar{t})}{1 - \mathbf{P}_{ss}(\bar{t})} + \frac{\mathbf{P}_{\rightarrow s} \mathbf{P}_{tt} \mathbf{P}_{ts}(\bar{t})}{1 - \mathbf{P}_{ss}(\bar{t})} + \dots, \\ &= \frac{\mathbf{P}_{\rightarrow s}}{1 - \mathbf{P}_{ss}} + \frac{\mathbf{P}_{\rightarrow s} \mathbf{P}_{ts}(\bar{t})}{1 - \mathbf{P}_{ss}(\bar{t})} [1 + \mathbf{P}_{tt} + \mathbf{P}_{tt} + \dots], \\ &= \frac{\mathbf{P}_{\rightarrow s}}{1 - \mathbf{P}_{ss}} + \frac{\mathbf{P}_{\rightarrow t}}{1 - \mathbf{P}_{tt}} \cdot \frac{\mathbf{P}_{\rightarrow s}}{1 - \mathbf{P}_{ss}}, \\ &= \frac{\mathbf{P}_{\rightarrow s}}{1 - \mathbf{P}_{ss}} + \frac{\mathbf{R}_t \mathbf{P}_{st}(\bar{t})}{1 - \mathbf{P}_{ss}(\bar{t})}. \end{aligned}$$

In lemma 1, we are able to handle simple setting as in tree graph.

Another case that we will have a look at is where the vertex  $v_t$  have at least one outgoing edge but non is linked to a cycle. Denote  $\varpi_{1,t}$  and  $\varpi_{2,t}$  as weight of  $v_t$  before and after the change respectively, (see Fig.2). We seek to update the PageRank of the target vertex  $v_s$  when a back-edge  $v_t \rightarrow v_s$  is added. The next theorem details how to update ranks within the cycle components.

**Theorem 1.** Consider a graph  $G = [V, E]$  with PageRank  $\mathbf{R}^1$ , after adding a back-edge  $v_t \rightarrow v_s$  the new PageRank  $\mathbf{R}_s^2$  are expressed as

$$\mathbf{R}_s^2 = \mathbf{R}_s^1 + \left( \frac{\mathbf{R}_t^2}{\mathbf{R}_t^1} - \frac{\varpi_{1,t}}{\varpi_{2,t}} \right) \frac{\varpi_{2,t} \mathbf{R}_t^1 P_{ts}^1(\bar{t})}{\varpi_{1,t} (1 - P_{ss}^1(\bar{t}))}, \quad (1)$$

*Proof.* The proof follows similar from argument in [4].

### 3.1 PageRank of tree with a cycle after addition an edge

Consider a directed connected graph  $G$  as in Figure 2, where vertex  $v_s$  denotes the root and a cyclic component of graph consist of the following vertices  $v_j, \dots, v_{j+3}$ . The edge  $v_{j+3} \rightarrow v_j$  correspond to back-edge. Throughout this paper, it is assumed that  $G$  is ordered as depth first search-tree type graph. Also, it is essential to note that the previous ranks were known before a cycle was formed.

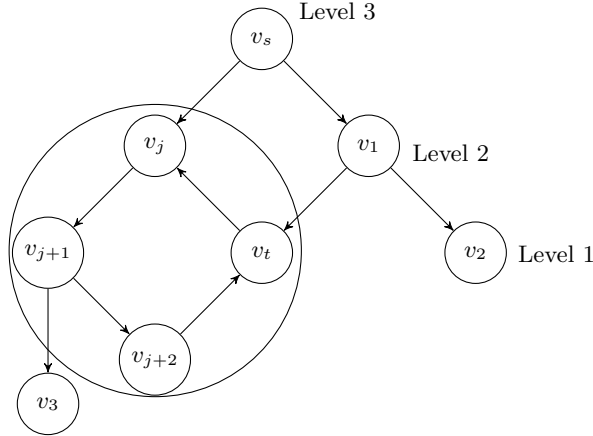


**Fig. 2.** Example of a graph and corresponding a component from the SCC partitioning of the graph with vertices  $v_j, \dots, v_t$ . Edge  $v_t \rightarrow v_j$  is considered as back-edge.

The basic idea in Lemma 2 is to update PageRank of target vertex belonging to a cyclic component while Lemma 1 characterises the updating process when the vertex(ices) belongs to tree graph.

**Lemma 2.** Suppose  $\mathbf{R}^{(1)}$  and  $\mathbf{R}^{(2)}$  denote PageRank of vertex  $v \in G/CAC$  before and after addition of and edge from  $v_t \rightarrow v_j$  (backward edge). So that  $v_t, v_j \in G/CAC$ , then the PageRank of vertex in the cyclic sub-graph after the change is expressed as

$$\mathbf{R}_j^{(2)} = \mathbf{R}_j^{(1)} + P_{v_t \rightarrow v_t} \mathbf{R}_t^{(1)} \sum_{k=0}^{\infty} P_{jj}^k, \quad (2)$$

where  $P_{jj}$  represent the transition probability from  $v_j \rightarrow v_j$  multiple times and including through the vertices in the cyclic component.

*Proof.* The first term on the right is expected to visit  $v_j$  without reaching  $v_t$ . For the second last term, It is expected number of visits to  $v_j$  through  $v_t$  at least once after  $m$  steps. (It is essential to note that if there is a cycle in a subgraph, then there is a path of infinite step). Hence, applying lemma 2 in [4], we can write the PageRank of  $R_j^2$  as

$$\mathbf{R}_j^{(2)} = \mathbf{R}_j^{(1)} + P_{v_t \rightarrow v_j} \mathbf{R}_t^{(1)} P_{jj} + P_{v_t \rightarrow v_j} \mathbf{R}_t^{(1)} P_{jj}^2 + \dots \quad (3)$$

$$= \mathbf{R}_j^{(1)} + P_{v_t \rightarrow v_j} \mathbf{R}_t^{(1)} \sum_{k=0}^{\infty} P_{jj}^k. \quad (4)$$

*Example 1.* Let demonstrate Lemma 2 using simple network in Figure 2. Note that  $R_v^1$  presents, rank of vertex  $v$  before a cycle was formed. Here, we write PageRank of vertex  $\{v_j, v_{j+1}, \dots, v_t\}$  before formation of a loop as

$$\left[1 + \frac{1}{2}c, 1 + cR_j^1, 1 + \frac{1}{2}cR_{j+1}^1, 1 + c + \frac{1}{2}c^2 + cR_{j+2}^1\right].$$

Then we obtain

$$\begin{aligned} R_j^2 &= R_j^1 + cR_t^1 \sum_{k=0}^{\infty} (c^4)^k, \\ &= 1 + \frac{1}{2}c + c\left(1 + c + \frac{1}{2}c^2 + cR_{j+2}^1\right)[1 + c^4 + c^8 + \dots], \\ &= 1 + \frac{1}{2}c + \frac{c\left(1 + c + \frac{1}{2}c^2 + cR_{j+2}^1\right)}{1 - c^4}. \end{aligned}$$

Assume that  $v_t \rightarrow v_j$  is deleted after the transition, therefore the subsequent PageRank of  $v_{j+1}$  is  $R_{j+1}^2 = R_{j+1}^1 + cR_j^2$ .

Looking at computing PageRank this way allows for the use of different methods for different components. However, if network has at least one cycle well known Power method or Power series method might not give accurate ranks values [2]. The subsection that follows is devoted to address a case when a hyperlink matrix  $\mathbf{A}^\top$  has neither a dominant eigenvalue which is simple nor eigenvalue which is real and k-multiple ( that is,  $\lambda_1 = \lambda_2 = \dots = \lambda_k > \lambda_{k+1} \geq \dots \geq \lambda_n$ ).

### 3.2 Updating PageRank of evolving graphs consist of many cycles

In this section we describe a method of re-calculating PageRank of a graph when one or more cycles are formed as the graph evolved. We will make the following assumptions **A**:

- A vertex of the graph has no self-loop.
- The matrix  $\mathbf{A}^\top$  contains  $k \geq 1$  feedback vertex set.

Without loss of generality we observe that assumptions  $\mathbf{A}$  has similarity with assumption 1 in [7]. Hence, one of the problem is to compute the PageRank  $\mathbf{R}^2$  of  $M$  when a stochastic matrix  $A$  satisfies those conditions. In such case, asymptotic convergence of power method is worse than iterative aggregation/disaggregation method. Moreover, it is not trivial to aggregate the set of vertices  $V$  so that stochastic complement  $S_M$  satisfies the property that the second dominant eigenvalue  $\lambda_2(S_M) \leq \lambda_2(M)$ .

We adopt the approach in [1] and [7], the only different being that we focus on partitioning discrete phase spaces of stochastic matrix  $A$  into feedback vertex set and non-feedback vertex set rather than partitioning states by those which are likely to change as mentioned in[1]. In a directed graph, a feedback vertex set is a set of vertices which, if removed, the resultant graph becomes acyclic. This has several advantages, namely:- it ensures irreducibility and aperiodicity of Markov chain. It known that finding FVS is an NP-problem, however a simple heuristic approach is just to consider vertices with maximum sum of incoming and outgoing degree or maximum multiplication of the number of incoming and outgoing links of vertices in cyclic components. In the subsection that follows, we briefly describe aggregation/disaggregation method, interested reader is referred to [3]. We further, claim that partition with FVS speed up the updating of PageRank because FVS has simmilar property as essential vertex set in [7].

### 3.3 Aggregation-disaggregation methods of stochastic matrices

Let  $M$  be Google transition matrix after a change (addition of edges for example) such that the number of cycles increases. We partition the matrix into 3-class of states, namely:-1) States that will not be affected by change of links and it's denoted by  $X_1$ , 2) Set of states that cause break down of cyclic components and denoted by  $X_2$ . 3) Set of states  $X_3$  that are likely to change but their removal will not break the cyclic components. Assume that  $X \in \mathbb{R}^{n \times n}$  has the following partition

$$M = \begin{matrix} & X_1 & X_2 & X_3 \\ \begin{matrix} X_1 \\ X_2 \\ X_3 \end{matrix} & \begin{pmatrix} M_{11} & M_{12} & M_{13} \\ M_{21} & M_{22} & M_{23} \\ M_{31} & M_{32} & M_{33} \end{pmatrix} \end{matrix},$$

where all  $M_{ii}$ , for  $i = 1, 2, 3$  are square matrices of size  $n_i \times n_i$  such that  $n_1 + n_2 + n_3 = n$ . Suppose the corresponding stationary distribution (normalized PageRank vector) of  $M$  is  $[R_1, R_2, R_3]$ . Since, in aggregation algorithm one aims to compute smaller components of matrices called stochastic complements, thus this matrix matrix associated to  $M_{ii}$  can be expressed as

$$S_{ii} = M_{ii} + M_{i\circ} (\mathbf{I} - \mathbf{M}_i)^{-1} M_{\circ i}, \quad (5)$$

where  $\mathbf{M}_i$  is the principal block submatrix of  $M$  obtained by deleting the  $i^{\text{th}}$  row and column of  $M$ .  $M_{i\circ}$  and  $M_{\circ i}$  are  $i^{\text{th}}$  row and column removed respectively. It worthy mentioning that  $\mathbf{M}_i$  does not contain any recurrent class,

then  $(\mathbf{I} - \mathbf{M}_i)^{-1} = \sum_{k=0}^{\infty} \mathbf{M}_i^k$  exist for finite  $k$ . Hence, choosing such  $M_i$  has computational advantage as it comes to inverse of matrix  $\mathbf{I} - \mathbf{M}_i$ . Accordingly, let  $r_i$  be stationary distribution of  $S_{ii}$  and handling to the fact that we are dealing with  $(i, j)^{\text{th}}$  entry of  $3 \times 3$  aggregation matrix  $\mathbf{B} = (b_{ij})$  for  $i, j \in (1, 2, 3)$ , then

$$b_{ij} = r_i^\top \mathbf{M}_{ij} \mathbf{I}_{n_j}, \quad (6)$$

where  $r_i = [r_i, \dots, r_{n_i}]$  is normalized PageRank vector of  $S_{ii}$ . It is essential to point out that the distribution vector of  $\mathbf{B}$  is  $[\alpha_1, \alpha_2, \alpha_3]$  from which the stationary distribution of  $\mathbf{M}$  can be explicitly expressed as  $[\alpha_1 r_1, \alpha_2 r_2, \alpha_3 r_3]$ .

We now state a theorem that guarantee  $\lambda_2(S_M) \leq \lambda_2(\mathbf{M})$ .

**Theorem 2.** Let Google matrix  $\mathbf{M} = c\mathbf{A}^\top + (1 - c)\frac{\mathbf{\Pi}^\top}{n}$ , where damping parameter  $c \in (0, 1)$ ,  $\mathbf{I}_{n \times 1}$  is column vector of ones and  $\mathbf{A}^\top$  is stochastic matrix that satisfies assumption **A**, Then

$$|\lambda_2(S_M)| < |\lambda_2(\mathbf{M})|. \quad (7)$$

*Proof.* The proof of (7) is similar to Theorem 9.1 in [7], thus we will not repeat the arguments.

In the next subsection, an experiment is performed with the modified (that is, FVS) partition. The example is motivated by our previous work in investigating changes in small graphs. More specifically, if changes in small network effect almost all previous rank of vertices. We accept that the example is artificial but there are areas such as social networks, advertisement and telecommunications systems that seem to reveal these set-up.

### 3.4 Numerical experiment 1

The problem considered is  $9 \times 9$  adjacency matrix with 2-cycle and it has one vertex  $v_s$ , when removed the graph becomes acyclic, Figure 3.

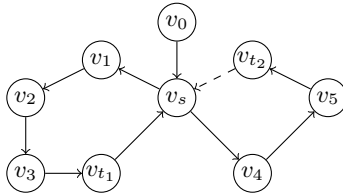


**Fig. 3.**  $\{v_s\}$  is a feedback vertex set

It is assumed that addition of an edge  $v_{t_2} \rightarrow v_s$  effect almost all vertices, hence only two partitions were made, that is,  $X_2 = [v_s]$  and  $X_3 =$

$[v_0, v_1, v_2, v_3, v_{t_1}, v_4, v_5, v_{t_2}]$  such that

$$M = \begin{matrix} & X_2 & X_3 \\ \begin{matrix} X_2 \\ X_3 \end{matrix} & \begin{pmatrix} M_{22} & M_{23} \\ M_{32} & M_{33} \end{pmatrix} \end{matrix}, \quad \mathbf{r} = [r_2, r_3]$$

Define  $r_3^\top S_{33} = r_3^\top$  and  $r_2^\top = r_3^\top M_{32} (\mathbf{I} - \mathbf{M}_{22})^{-1}$ , where

$$S_{33} = M_{33} + M_{32} (\mathbf{I} - \mathbf{M}_{22})^{-1} M_{23}.$$

Since  $\mathbf{M}_{22} = [*]_{1 \times 1}$ , we have  $S_{33} = M_{33} + M_{32} M_{23}$ . Consider the hyperlink matrix of network in Figure, as

$$A = \begin{matrix} & v_s & v_0 & v_1 & v_2 & v_3 & v_{t_1} & v_4 & v_5 & v_{t_2} \\ \begin{matrix} v_s \\ v_0 \\ v_1 \\ v_2 \\ v_3 \\ v_{t_1} \\ v_4 \\ v_5 \\ v_{t_2} \end{matrix} & \begin{pmatrix} 0 & 0 & 0.5 & 0 & 0 & 0 & 0.5 & 0 & 0 \\ 1 & 0 & 0 & 0 & 0 & 0 & 0 & 0 & 0 \\ 0 & 0 & 0 & 1 & 0 & 0 & 0 & 0 & 0 \\ 0 & 0 & 0 & 0 & 1 & 0 & 0 & 0 & 0 \\ 0 & 0 & 0 & 0 & 0 & 1 & 0 & 0 & 0 \\ 1 & 0 & 0 & 0 & 0 & 0 & 0 & 0 & 0 \\ 0 & 0 & 0 & 0 & 0 & 0 & 0 & 1 & 0 \\ 0 & 0 & 0 & 0 & 0 & 0 & 0 & 0 & 1 \\ 1 & 0 & 0 & 0 & 0 & 0 & 0 & 0 & 0 \end{pmatrix} \end{matrix}$$

such that the Google matrix  $M = cA^\top + (1-c)\frac{\mathbf{1}\mathbf{1}^\top}{n}$ , where damping parameter  $c = 0.85$  and  $\mathbf{1}_{n \times 1}$  is column vector of ones. The aim of experiment one was to verify whether the FVS partition yields better convergency for power method to compute PageRank scores in a evolving graph with many cycles. We observed that FVS partitioning strategy seem to out performed both a partition where one focuses on vertices that are likely to change and when rank vector is computed from the scratch as shown in Fig.4. The key to realizing an improvement in the iterative aggregation over aggregation by considering the possible nodes that are likely to be effected depend on finding FVS. We also observed that the corresponding the second subdominant eigenvalue,  $\lambda_2(S_{33})$  is smaller as compared to partition the graph into states which are most likely to change without paying much attention to periodicity of the states. We suggest that this approach seem to fit in framework of updating PageRank when there are many cyclic components a network. It may be beneficial to giant component as well which encounter significant amount of changes most often.

### 3.5 Procedure to compute PageRank

1. Partition the graph into cyclic components and find their corresponding levels.
2. For each level (starting at the lowest, that is,. the level of the root):
  - Calculate PageRank for each component on current level (can be done in parallel). If the network has cyclic component, partition the vertices of component into FVS and non-FVS. Then use aggregation-disaggregation method to find PageRank
  - Adjust weight vector for all higher level components.

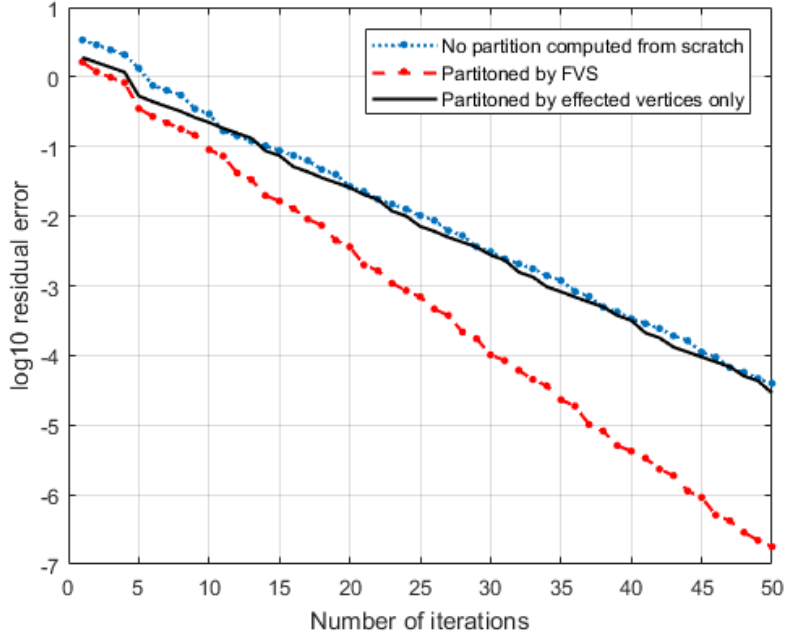


**Fig. 4.** A comparison of convergence of PageRank vector computed by power method in an evolving graph with cycles.

## 4 Conclusion

In this paper we have shown how it is possible to update PageRank in an evolving network given sequential addition of vertex and edge. First we showed how to maintain cyclic component when it is formed.

Secondly we showed how the partition by feedback vertex set improves asymptotic convergence of power method in updating PageRank in a network with cyclic components.

In the future we would like to take a look at optimal algorithm for feedback vertex set identification so that updating ranks in a system with cyclic components have minimum rounding error, that is, when computing  $(I - M_i)^{-1}$ .

**Acknowledgements** This research was supported by the Swedish International Development Cooperation Agency (Sida), International Science Programme (ISP) in Mathematical Sciences (IPMS), Sida Bilateral Research Program (Makerere University and University of Dar-es-Salaam). We are also grateful to the research environment Mathematics and Applied Mathematics (MAM), Division of Applied Mathematics, Mälardålen University for providing an excellent and inspiring environment for research education and research.

## References

1. A. N. Langville and C. D. Meyer. *Google's PageRank and Beyond: The science of search engine rankings*. Princeton University Press, 2011.
2. A. Xie and P. A. Beerel. Accelerating markovian analysis of asynchronous systems using string-based state compression. In *Advanced Research in Asynchronous Circuits and Systems, 1998. Proceedings. 1998 Fourth International Symposium on* (pp. 247-260). IEEE, 1998.
3. C. D. Meyer. Stochastic complementation, uncoupling Markov chains, and the theory of nearly reducible systems. *SIAM review*, 31(2), 240-272, 1989
4. C. Engström and S. Silvestrov. A componentwise pagerank algorithm. In *16th Applied Stochastic Models and Data Analysis International Conference (ASMDA2015) with Demographics 2015 Workshop, 30 June–4 July 2015, University of Piraeus, Greece* (pp. 185-198). ISAST: International Society for the Advancement of Science and Technology.
5. C. Engström and S. Silvestrov. Graph partitioning and a componentwise PageRank algorithm. *arXiv preprint arXiv:1609.09068.*, 2016.
6. C. Engström and S. Silvestrov. Using graph partitioning to calculate PageRank in a changing network. In *4th Stochastic Modeling Techniques and Data Analysis International Conference with Demographics Workshop* (pp. 155-164), 2016
7. I. C. Ipsen and S. Kirkland. Convergence analysis of a PageRank updating algorithm by Langville and Meyer. *SIAM journal on matrix analysis and applications*, 27(4), 952-967, 2006
8. P. G. Franciosa, D. Frigioni and R. Giaccio. Semi-dynamic breadth-first search in digraphs. *Theoretical Computer Science*, 250(1-2), 201-217, 2001.
9. S. Baswana and K. Choudhary. On dynamic DFS tree in directed graphs. In *International Symposium on Mathematical Foundations of Computer Science* (pp. 102-114). Springer, Berlin, Heidelberg, 2015.
10. S. Brin and L. Page. The anatomy of a large-scale hypertextual web search engine. *Computer networks and ISDN systems*, Elsevier, 30(1-7), 107–117, 1998.

# Methods for assessing critical states of complex systems

Valery Antonov

Department of Mathematics, Peter the Great St.Petersburg Polytechnic University, Polytechnicheskaja str., 29, 195251, Russia  
(E-mail [antonovvi@mail.ru](mailto:antonovvi@mail.ru))

**Abstract.** In the study of a complex system (for example, the human body), a large number of characteristics are required to assess the current state and forecast their development. Often this measurement is impossible due to lack of time and equipment. Therefore, it becomes necessary to assess the state and short-term dynamics of a change in the system, using characteristic signals that can be obtained in real time.

It is assumed that the system measures the periodic character  $R_T$ , which is a discrete sequence of intervals  $r_i$ . Under these conditions, the investigation of complex system is reduced to analyzing the time series. This paper presents overview existing research methods. Particular attention is paid to the methods of nonlinear dynamics and chaotic behavior of systems.

**Keywords:** complex system, critical state, time series, nonlinear dynamics

## 1. Introduction

We will consider the human body as an example of complex system. In some situations, it is necessary to determine, whether the system is in a stable state or it undergoes substantial changes. It is equally important to recognize the transition of the system to a critical condition. For example, such a problem is faced by physicians conducting an operation under general anesthesia. It should be noted that in emergency cases, the decision time must not exceed five minutes. Otherwise, irreversible changes can occur in the patient's body in a state of clinical death. Therefore, it becomes necessary to assess the state and short-term dynamics of a change in the system, using characteristic signals that can be obtained in real time.

Mathematical transformations are applied to the signal in order to get additional information about it. Most of the signals encountered in practice are represented in the time domain, that is, the signal is a function of time. Thus, we obtain an amplitude-time representation of the signal. However, in many cases the most significant information is hidden in the frequency domain of the signal. The frequency spectrum is a collection of frequency (spectral) components; it displays the presence of certain frequencies in the signal.

It is assumed that the system measures the periodic character  $R_T$ , which is a discrete sequence of intervals  $r_i$ . Under these conditions, the investigation of

---

5<sup>th</sup> SMTDA Conference Proceedings, 12-15 June 2018, Chania, Crete, Greece

© 2018 ISAST



complex system is reduced to analyzing the time series. The problem appearing in this case connected with the search of indicators describing relations between heart rate regulatory systems, has been directed for usage and development the theory of determined chaos. An important aim of this article is to demonstrate the development of the mentioned methodology using the example of heart rate variability (HRV) and researches being performed by our scientist group (Antonov and Zagainov [1]). The main emphasis is on analyzing state of the human body. However, the developed methods can be successfully applied to analyze the functioning of other, in particular, technical objects. This paper presents an overview existing research method.

## 2. Hart rate variability

The recommendations for physiological interpretation of successive intervals between the electrocardiogram QRS-complexes given in 1996 by the European Society of Cardiology and the North American Society of Pacing and Electrophysiology (M. Malik et al. [2]), make such time-series the most perspective ones in the non-invasive diagnostics used in the modern scientific researches. The problem appearing in this case connected with the search of indicators describing connections between the systems of heart rate regulation.

The main tendency of the problem appearing in this case connected with the search of indicators of connections between the systems of heart rate regulation. It has been directed for development the theory of determined chaos fundamental concept which is connected with concepts of heart rate variability (HRV). Heart rate variability (HRV) is the physiological phenomenon of variation in the time interval between heartbeats. It is measured by the variation in the “RR interval” (where R is a point corresponding to the peak of the QRS complex of the ECG wave, and RR is the interval between successive Rs). As an object of study, a time series is considered, as a result of the treatment of an electrocardiogram

$$R_T = \{r_i(t_i)\}_{i=1}^K, t_i = \sum_{j=1}^i r_j, T = t_K$$

The numerical approach proposes the transition from the time-series (signal) itself to a certain object formed in the phase space of finite dimensionality, which is called as a restored attractor. Various measures can be used for characterizing the restored attractor, and the most fundamental of them is probably its fractal dimensionality (Gudkov [3]).

It should be noted that in order to determine the transition of an organism to a critical state, one must learn to distinguish real threats from variations associated with the daily changes in cardiac rhythm taking into account possible cardiac pathologies. All this requires careful verification of the mathematical models being developed for their adequacy.

Figures 1.2 give examples illustrating the concept of heart rate variability.

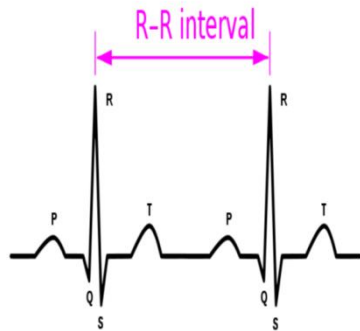


Fig.1. Hart rate

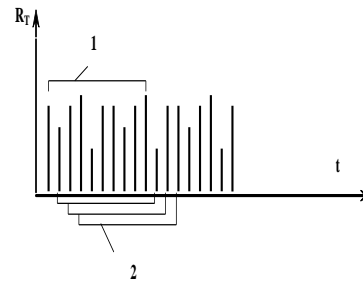


Fig.2. Hart rate variability

### 3. Time series processing methods

Figure 3 shows a diagram of methods for investigating time series.

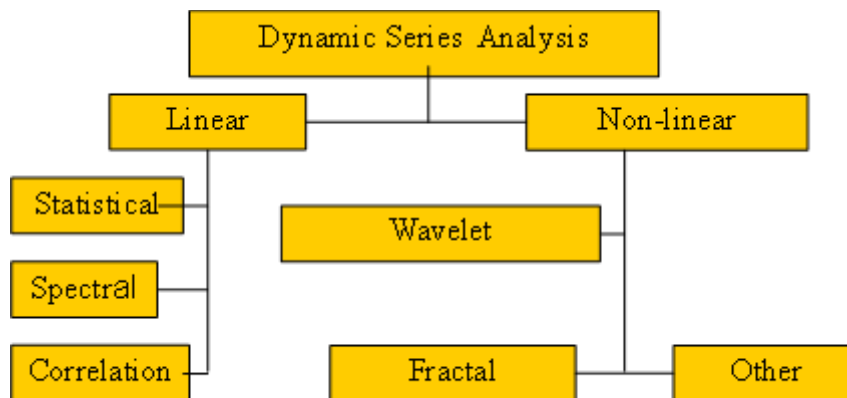


Fig.3. Dynamic series analysis

**Statistical methods** are used to directly quantify the signal in the time interval under study (dispersion, coefficient of variation, etc.)

**Time analysis** consists in studying the law of intervals distribution as random variables. In this case, a histogram is constructed and its main characteristics are determined:

- $M_o$  - the most frequent value of the interval in this dynamic series;
- $AM_o$  - number of intervals corresponding to the value of the mode, in % to the sample size;

- TINN - variation range. It is calculated from the difference between the maximum (Mx) and the minimum (Mn) values of the intervals and is sometimes denoted as MxDMn;

**Autocorrelation analysis** makes it possible to recognize the latent periodicity in  $R_T$ . (Fig.4):

- $C_1$  - the value of the correlation coefficient after the first shift;
- $C_0$  - the number of shifts, as a result of which the correlation coefficient value becomes negative.

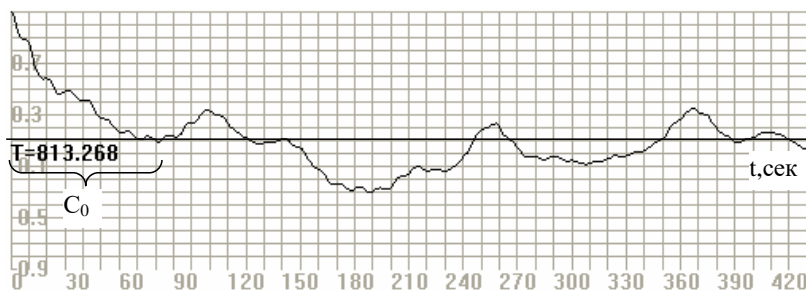


Fig.4. Autocorrelation function

**Frequency analysis.** Analysis of the oscillations spectral power density provides information on the power distribution as a function of frequency. The use of spectral analysis allows quantifying the effect on the heart work of various regulatory systems. High frequency (HF), low frequency (LF) and Very Low Frequency (VLF) components are selected that are used for short-term ECG recording. The HF component is associated with respiratory movements and reflects the effect on the work of the heart of the vagus nerve. LF component characterizes the influence on the heart rhythm of both sympathetic and parasympathetic. VLF and ULF components reflect the effect of various factors, which include, for example, vascular tone, thermoregulation system, etc. (Fig.5).

There are parametric and nonparametric methods of spectral analysis. The first relates to autoregressive analysis, the second – to the fast Fourier transform (FFT) and period gram analysis. There are three main spectral components that correspond to fluctuations in the rhythm of the heart of different periodicity. Both these groups of methods give comparable results. In the spectral analysis, calculate:

- absolute total and mean spectrum power;
- maximum harmonic value;
- centralization index  $IC=(HF+LF)/VLF$

The spectrum is calculated by means of the Fourier transform:

$$F(\{r_n, n = 0, \dots, N\}, f) = \sum_{n=0}^N r_n \cos\left(2\pi f \frac{nT}{N+1}\right)$$

This transform has a disadvantage. It does not indicate the time when the frequencies components occur.

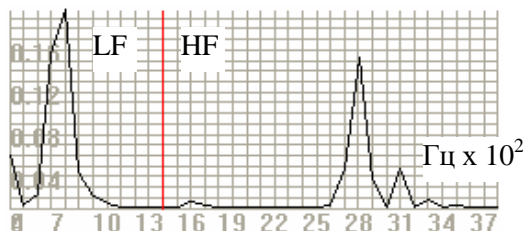


Fig.5. High-frequency and low-frequency parts of the spectrum

In addition to the Fourier transform, there are many other frequently used transformations of the signal. Examples are the Hilbert transform, windowed PF, Wigner distribution, Walsh transform, wavelet transform, and many others. For each transformation, you can specify the most suitable area of application, advantages and disadvantages.

**Correlation rhythm graph.** The method consists in graphically displaying successive pairs of intervals (the previous and the following) in the two-dimensional coordinate plane. When constructing a scatter gram, a set of points is formed, the center of which is located on the bisector of the first quarter of the coordinate plane. The distance from the center to the origin of the coordinate axes corresponds to the most expected duration of the interval (Mo). The point deviation shows how far this interval is shorter than the previous one; to the right of the bisector - how much longer than the previous one (Fig.6).

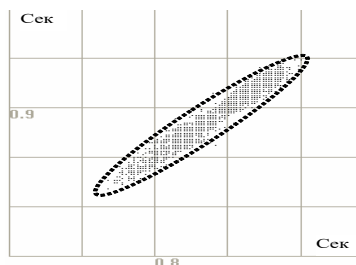


Fig.6. Scatter gram

The above analysis methods have a serious drawback. With their help it is difficult to determine at which point in time the system undergoes significant changes. This fact makes them inadequate for operational diagnostics.

At present, methods of non-linear dynamics and fractal analysis, as well as wavelet transforms, which allow determining the moment of serious changes in the behavior of the system, are increasingly used.

**Fractal analysis** assesses fractal characteristics of data (Alligood., Sauer, and Yorke, [4]). From the point of view of nonlinear analysis, the processes under investigation contain deterministic chaos, and from the point of view of linear

processes these processes are stochastic (Mandelbrot [5]). For an exhaustive description of the system state, a lot of variables are needed, combined into a vector from the phase space of states  $Q(t)=(q_1(t),q_2(t),\dots,q_n(t))$ . Phase portraits of systems with chaotic behavior, regardless of the initial conditions, comes to a certain area of the phase space - the attractor of the system. It should be noted that the phase portrait of a nonlinear system is a multifractal. A **multifractal system** is a generalization of a fractal system in which a single exponent or fractal dimensions not enough to describe its dynamics; instead, a continuous (singularity) spectrum of exponents is needed.

A numerical characteristic that determines the chaotic state of a system can be its entropy. To quickly diagnose transient states in the behavior of a system, the Renyi entropy is usually chosen:

$$H_q(p) = \frac{1}{1-q} \log \sum_{i=1}^N p_i^q$$

It tends to Shannon entropy

$$H(p) = -k \sum_{i=1}^N p_i \ln p_i \text{ as } q \rightarrow 1.$$

At  $q=0$  this is dimension of Kolmogorov – Hausdorff.

The principle is to weight the probability of the most often visited cubes according to the order of the dimension. Embedding process has to precede any estimation of fractals from a data series. The main practical task consists in the choice of the embedding variable and embedding delay. The right embedding delay can be estimated by the first zero crossing of the autocorrelation function or, better, by the first local minimum of the mutual information

However, the probability of finding a point on the attractor is necessary. Usually for this purpose informational dimension and related informational entropy is used, as well as correlation dimension and correlation entropy. Theoretically, according to the Takens theorem, any state variable can be used to calculate the invariants of the dynamics (Takens [6]). But practically, it is not a calculation that is made, but only estimation. This raises the problem of convergence and it is related to the good conditioning of the information into the variables.

If the measurement variable at time  $t$  is defined by  $x(t)$ , an  $(n+1)$  - dimensional embedding is defined by:  $[x(t), x(t+\tau), \dots, x(t+n\tau)]$ .

A detailed exposition of the method allowing carrying out operational diagnostics on the basis of calculating the fractal dimension of the system attractor is presented in the work (Antonov, Zagainov and Kovalenko [7]). Also, there is a description of our software for rapid diagnosis of a body state. Some calculated results of the attractor's correlation dimension are shown in Fig. (7.8).

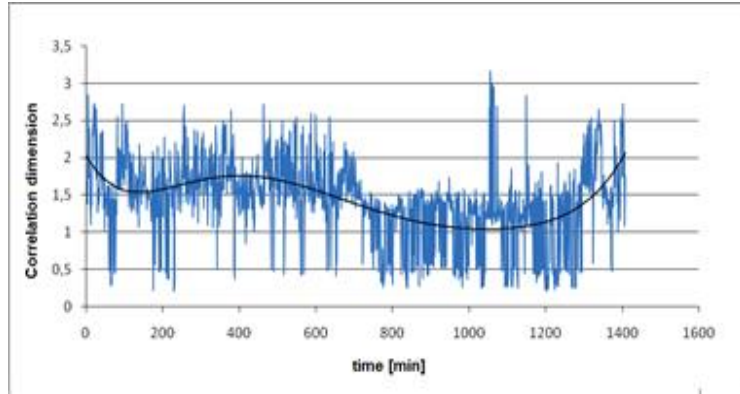


Fig.7. Trend of correlation dimension. Pneumonia

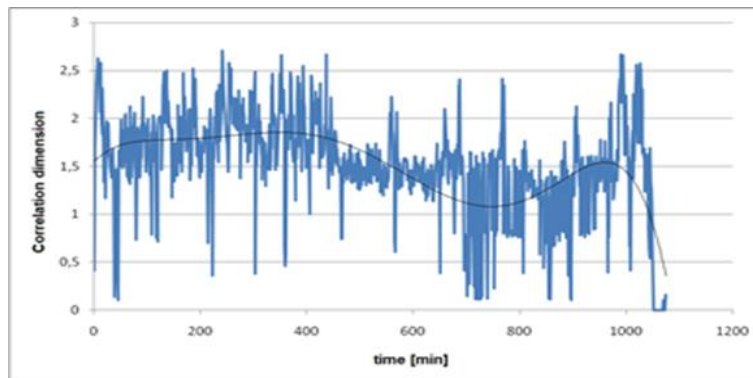


Fig.8. Severe pneumonia

In the severe pneumonia the trend of correlation dimension reach approximately 2 during the day. Finally, in the near-death state for a period of time the trend stays permanent. However, further on, sharp fluctuations start, followed by a rapid dropping down to zero (case of death). This dropping down is observed for several minutes. However, due to the sharp leap after a long period of system calm-condition, the prediction of the trend dropping down can be made.

**Wavelet analysis** provides important information about the mathematical morphology of a signal (Daubechies [8]). In our software package we use the Wavelet Transform Modulus Maxima (WTMM)-method (Mallat and Hwang [9]). The WTMM-formalism is suitable for analyzing multi-dimensional patterns, but the complexity increases fast when dimensions are added. In our work we consider multifractals constructed using time series. As a result, the processing can be determined "scaling exponent", which studies the properties of multi fractal in the aggregate. Automated software, which includes a number of functionalities, has been created.

**Wavelet transforms modulus maxima (WTMM)** is a method for detecting the fractal dimension of a signal. It uses plotting of the local maximum line of wavelet transform and gives the possibility of partitioning the time and scale domain of a signal into fractal dimension regions.

$$W_\psi(t, a) = \frac{1}{a} \int_{-\infty}^{\infty} f(x) \psi\left(\frac{x-t}{a}\right) dx,$$

where the initial signal  $f(x)$  is divided using the function  $\psi(x)$  generated from the soliton-like one with special features by its scale measurements and shifts [9]. In the simplest variant (Holder's exponent  $h$ ) the scaling of one of the lines (for example, the maximum one) is researched:

$$|W_\psi(t_i, s)| \propto s^{h(t_i)}$$

**Holder exponent**, a measure of the degree to which a signal is differentiable, is used to detect the presence of damage and when that damage occurred.

The more complicated approach to plotting the scaling is based on analysing all lines by introducing the partial function with the weight degree of all wavelet transform maximums:

$$P_q(s) = \sum_i [W_\psi(t_i, s)]^q,$$

and plotting the scaling using the scaling function  $k(q)$ :  $P_q(s) \propto s^{k(q)}$ .

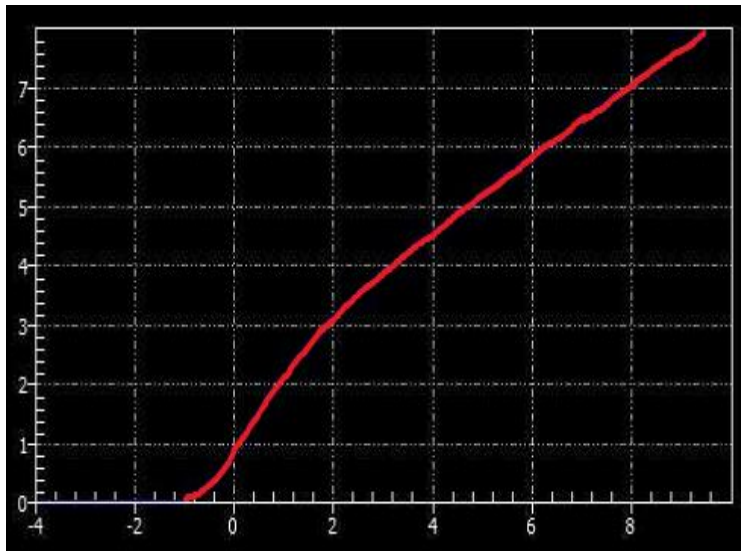


Fig.7. Scaling function

## Conclusions

The paper presents an overview of methods for analyzing the state of complex systems. These methods are divided into two large groups: linear and not linear. It is shown that the traditional approaches to signal analysis based on the methods of mathematical statistics and Fourier transforms give unsatisfactory results in the presence of non-stationarity in the initial processes. As a result, it was found that for nonstationary processes the most suitable are multifractal analysis and wavelet transform. These methods make it possible to monitor the status of the system in real time.

To implement the methods of multifractal analysis, a special software package has been developed. It includes:

- A mathematical model for evaluating the state of the body, based on fractal analysis of variation of heart rate in real time.
- The program complex, allowing carrying out a study of time series in static and dynamic modes.
- The evaluation of software tools designed using the classic examples of attractors.
- The analysis of real processes in healthy and sick people. With some confidence we can assert that the analysis of data allows determining the estimated time of systems transition in a critical condition.

## References

1. V. Antonov, A. Zagaynov. Software Package for Calculating the Fractal and Cross Spectral Parameters of Cerebral Hemodynamic in a Real Time Mode. *New Trends in Stochastic Modeling and Data Analysis. ISAST.* 440. 339{345}. 2015.
2. M.Malik, J.T.Bigger, A.J.Camm, R.E.Kleiger, A.Malliani, A.J.Moss and P.J.Schwartz. Heart rate variability. Standards of measurement, physiological interpretation and clinical use. *European Heart Journal.* 17. 354{381}. 1996.
3. Gudkov,G.V.: The role of deterministic chaos in the structure of the fetal heart rate variability, *Modern problems of science and education, Moscow., Krasnodar, .* 1 413{423}. 2008.
4. Alligood, K.T., Sauer, T., Yorke, J.A.: *Chaos: an introduction to dynamical systems*, Springer-Verlag. ISBN 0-387-94677-2. 1997
5. Mandelbrot B. *Fractals: Form, Chance, Dimension.* Freeman, San-Francisco, 1977.
6. Takens F. Detecting strange attractors in turbulence. In: *Dynamical Systems and Turbulence. Lecture Notes in Mathematics*, edited by D.A.Rand L.S.Young. Heidelberg: Springer-Verlag. 366{381}. 1981.
7. V. Antonov, A. Zagainov and A. Kovalenko. Stochastic Models in Society. *Fractal Analysis of Biological Signals in a Real Time Mode. Global and Stochastic Analysis GSA.* 3. 2.. 75{84}. 2016.
8. I. Daubechies. *Ten lectures on wavelets.* CBMS-NSF Regional Conference Series in Applied Mathematics, 1992.
9. S. Mallat and W.L. Hwang. Singularity detection and processing with wavelets. *IEEE Transactions on Information Theory*, 38 .2, 1992.



# Support Vector Machines: A Review and Applications in Statistical Process Monitoring

A. Apsemidis<sup>1</sup> and S. Psarakis<sup>2</sup>

<sup>1</sup> Department of Statistics, Athens University of Economics and Business, Athens, Greece

(E-mail: [apsemidis@gmail.com](mailto:apsemidis@gmail.com))

<sup>2</sup> Department of Statistics, Athens University of Economics and Business, Athens, Greece

(E-mail: [psarakis@aueb.gr](mailto:psarakis@aueb.gr))

**Abstract.** The modern industrial problems become more and more complex and classical process monitoring techniques do not suffice in order to solve them. That is why Statistical Learning methodologies are nowadays really popular in this area. In this article, we examine a specific statistical learning technique named Support Vector Machines, which is a most powerful algorithm used in different fields of statistics and computer science. We present a review of the literature concerning support vector machines in the process monitoring field, we test one of the mentioned works on a real data set and, finally, we present an alternative approach which is able to yield better results.

**Keywords:** Support vector machines, statistical process monitoring, multivariate control charts, review.

## 1 Introduction

The term Statistical Process Control refers to a wide variety of statistical tools used to improve the performance of a process and ensure the good quality of the products produced. The main use of Statistical Process Control takes place in industrial environments, but this is not always the case, since many techniques are used in financial or other kinds of problems. In practice, the way that Statistics is used in Quality Control is through the construction of Control Charts (see, for example, M. R. Reynolds et al., 1990 [1], D. M. Hawkins and K. D. Zamba, 2005 [2]).

In order that a statistician can check whether the process is in or out of control, a statistic is calculated using samples taken from the process and, if it takes a value outside of some specified Control Limits, then the process is out of control and corrective actions must be taken. However, a value outside of the control limits of a chart is not the only case, when a problem might have occurred in a process. These cases are referred in the bibliography as Control Chart Pattern Recognition (CCPR) problems. They occur when the plotting statistic presents a pattern and the process must then be stopped, even if the

---

<sup>5</sup>*th* SMTDA Conference Proceedings, 12-15 June 2018, Chania, Crete, Greece



statistic is still between the control limits (see for instance J.-H. Yang and M.-S. Yang, 2005 [3]). There are eight basic patterns that might occur in a process: normal, upward trend, downward trend, upward shift, downward shift, systematic, cyclic and stratification. All except of the first one (“normal”) are considered out-of-control situations.

In statistics, when we do not know something, we estimate it. That is what “learning” means: estimation. G. James et al. (2013) [4] explain Statistical Learning as a vast set of tools for understanding data. Among the many choices someone has, we selected the Support Vector Machines (SVM) algorithm, which can be used for both regression and classification and produces impressive results.

Suppose we have data belonging to two classes and we want to separate them. The main idea of SVM is: Draw a line in between, so that the distance of that line from the data is as long as possible. Let  $\mathbf{x}_i \in \mathbb{R}^p$  be our  $i$ th observation and  $y_i \in \{-1, 1\}$  its class label,  $\forall i = 1, \dots, n$ . The linear boundary of the support vector classifier can be found solving the optimization problem

$$\begin{aligned} \min_{\beta, \beta_0, \xi} & \left( \frac{1}{2} \|\beta\|^2 + C \sum_{i=1}^n \xi_i \right) \\ \text{subject to} & \quad \xi_i \geq 0, \forall i = 1, \dots, n \\ & \quad y_i(\langle \mathbf{x}_i, \beta \rangle + \beta_0) \geq 1 - \xi_i, \forall i = 1, \dots, n \end{aligned}$$

where  $C \in \mathbb{R}$ ,  $\xi \in \mathbb{R}^n$ ,  $\beta \in \mathbb{R}^n$  and  $\beta_0 \in \mathbb{R}$ . The  $C$  is the *cost* parameter, which describes our tolerance in misclassifications. A large  $C$  gives few errors. The  $\xi$  is a vector of slack variables responsible for the violations to the margin. Because of them, some observations are allowed to lie on the wrong side of the margin and the wrong side of the hyperplane. Finally,  $\beta$  and  $\beta_0$  are the parameters that define the hyperplane  $\langle \mathbf{x}, \beta \rangle + \beta_0 = 0$  used as the decision boundary.

In order for the above problem to be solved, one can re-express it as the Lagrangian dual problem

$$\begin{aligned} \max_{\alpha} & \left( \sum_{i=1}^n \alpha_i - \frac{1}{2} \sum_{i=1}^n \sum_{j=1}^n \alpha_i \alpha_j y_i y_j \langle \mathbf{x}_i, \mathbf{x}_j \rangle \right) \\ \text{subject to} & \quad \sum_{i=1}^n \alpha_i y_i = 0 \\ & \quad 0 \leq \alpha_i \leq C, \forall i = 1, \dots, n \end{aligned}$$

Therefore, in order to be able to produce non-linear boundaries, all we need to do is to replace the standard inner product of  $\mathbf{x}_i$ ,  $\mathbf{x}_j$  with the inner product of some transformation  $h(\cdot)$  of these vectors, i.e.  $\langle h(\mathbf{x}_i), h(\mathbf{x}_j) \rangle$ . Thus, the Lagrange dual objective function takes the form

$$\sum_{i=1}^n \alpha_i - \frac{1}{2} \sum_{i=1}^n \sum_{j=1}^n \alpha_i \alpha_j y_i y_j \langle h(\mathbf{x}_i), h(\mathbf{x}_j) \rangle$$

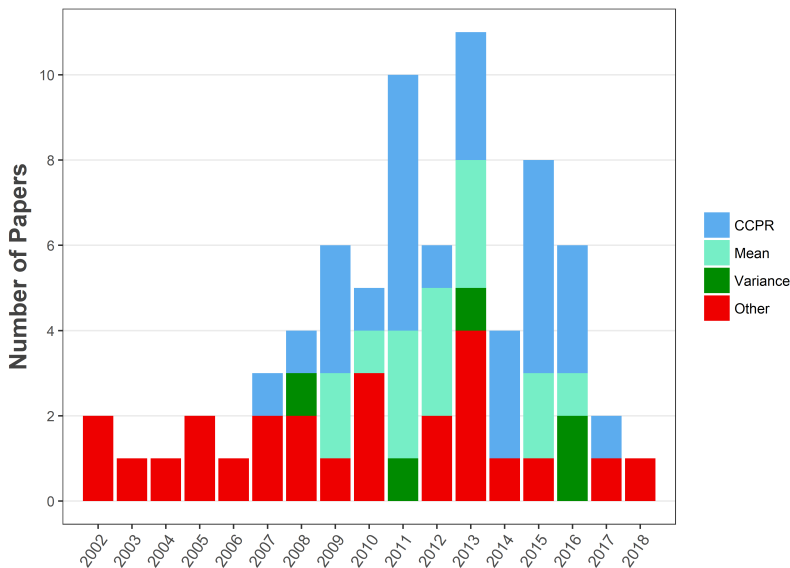


**Fig. 1.** A stacked barplot for our four categories and publication year of the articles.

and the decision boundary now becomes  $\langle h(\mathbf{x}), \boldsymbol{\beta} \rangle + \beta_0 = 0$ . The observations  $\mathbf{x}_i$  for which it holds that  $\alpha_i > 0$  are the support vectors. In the above formulation, we do not even need to specify the transformation  $h(\cdot)$ , but only use a kernel function  $K(\mathbf{x}_i, \mathbf{x}_j) = \langle h(\mathbf{x}_i), h(\mathbf{x}_j) \rangle$ . Then, the decision function can be written as

$$\text{sgn} \left( \sum_{i=1}^n \alpha_i y_i K(\mathbf{x}, \mathbf{x}_i) + \beta_0 \right)$$

One of the most frequently used kernels and the one that will be of interest to us is the (Gaussian) radial basis function (RBF), defined as

$$K(\mathbf{x}_i, \mathbf{x}_j) = \exp(-\gamma \|\mathbf{x}_i - \mathbf{x}_j\|^2), \gamma > 0$$

The rest of the paper is organised as follows: In the second section, we present a review of the literature of Statistical Process Monitoring articles, which are based on SVM models. In the third section we apply the D-SVM chart of S. He et al. (2018) [5] on a real data set and also propose a new method that gives better results.

## 2 Review of the Literature

We now present a review of the role of support vector machines in the SPC context, providing some information about 73 papers from 2002 to 2018. The four groups which we built to categorise the articles, as well as their publication years are shown in Figure 1. The CCPR category contains the articles about the pattern recognition problem, the Mean and Variance categories contain the

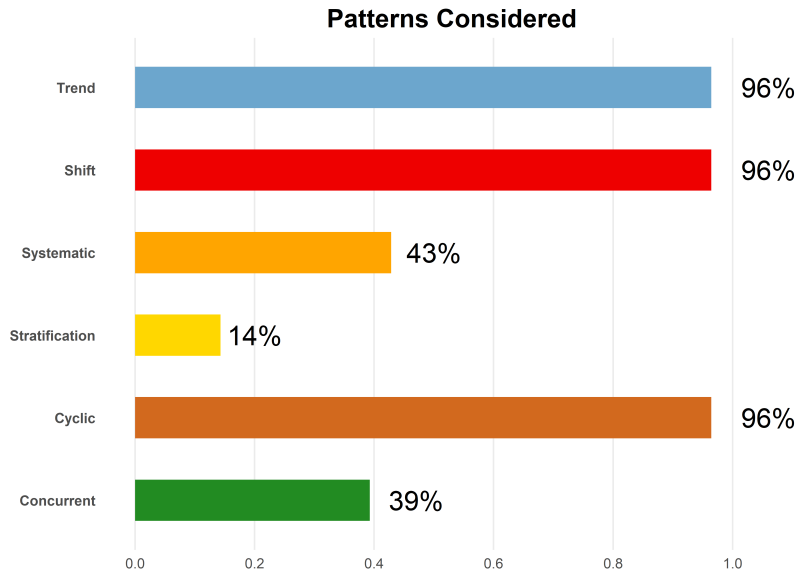


**Fig. 2.** As we can see in the barplot, 96% of the CCPR papers try to handle cases with trends, shifts and cyclic patterns, 43% deal with systematic patterns, 14% deal with stratification patterns and 39% tackle with concurrent patterns.

articles concerning the mean and variance of a process respectively and the last category contains everything else, which can be either something that does not fit in the previous ones or a combination of them. For instance, when an author builds an approach for mean shifts, this does not belong to the CCPR category, since it can only work for a case of a shift.

We can see that, after 2007, many authors use SVM for process monitoring problems and, especially CCPR problems. Specifically, someone can observe in the left-hand side of Figure 3, that 38% of the published works is about control chart pattern recognition, which is a pretty big percentage. The patterns that the authors deal with in most cases (96%) are trend, shift and cyclic patterns. Last but not least, let us mention that the vast majority of the research is conducted not taking into account autocorrelated data. A lot of authors deal with correlated variables, but only a few about autocorrelated ones (right-hand side of Figure 3), although this is something very usual in the real world.

Testing the proposed method on a real dataset is really important, in order to validate that it actually works in the real world. However, 55% of the authors have used only simulated data in their research and 45% have used real (or both real and simulated) data. This is shown in the left-hand side of Figure 4. When building a new method, the authors use either the raw data or features of the data to feed their models. When someone uses features of the data, they always conclude that their method works better this way, than using the other approach. However, it is almost 50-50 the percentages for the two approaches (right-hand side of Figure 4). The features that are used are either statistical like the mean, the standard deviation, the skewness etc., or

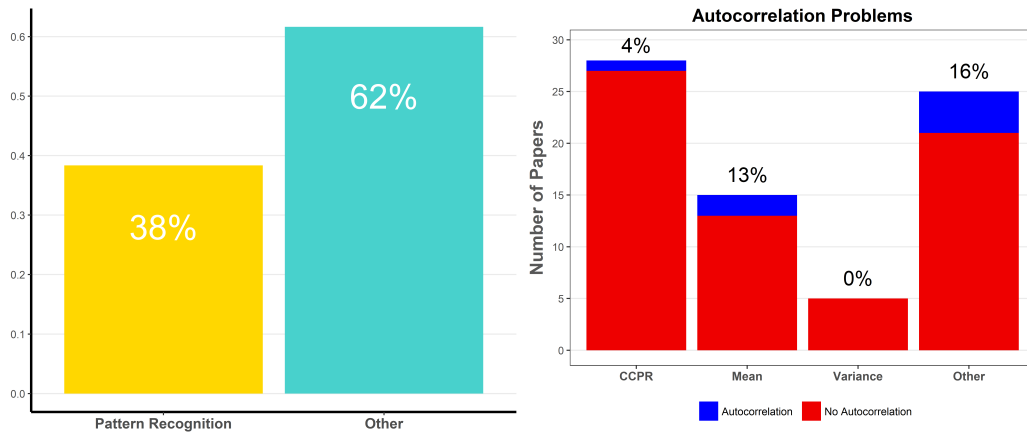


**Fig. 3.** Left: 38% of the published works belongs to our first category (CCPR problems), while 62% belongs to the rest of them. Right: Autocorrelation problems considered in a research. Only 4% of the CCPR problems deal with autocorrelation. The percentages for the *Mean*, *Variance* and *Other* categories are 13%, 0% and 16% respectively.

shape features like the area between the pattern and the mean line, or the area between the pattern and its least square line.

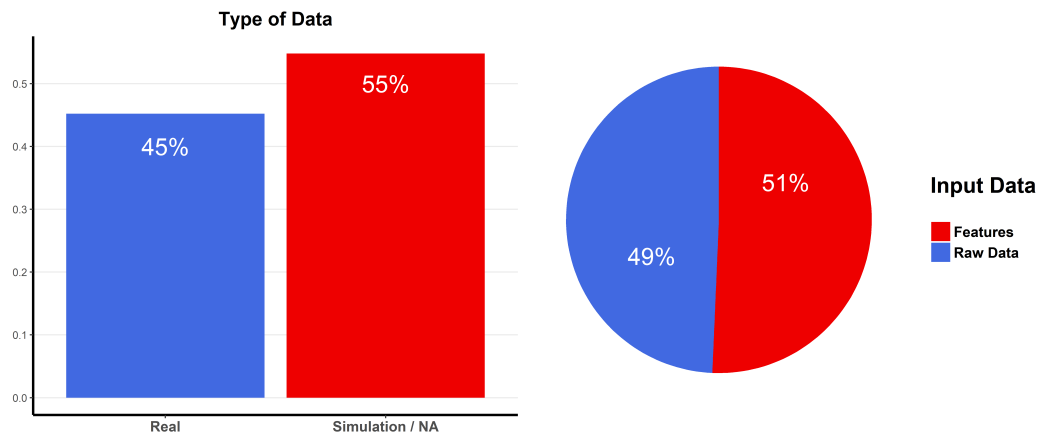


**Fig. 4.** Left: The type of data that are used to test the proposed method. Right: The type of the data that are used as inputs for the SVM model considered.

Although the SVM algorithm provides great flexibility thanks to the different kernels that can be used to replace the simple dot product, the vast majority (71%) of the models constructed use the RBF one, as we can see in the left-hand side of Figure 5. 7% use a hybrid one, which is a combination of two kernels that can take advantage of the benefits each one provides. Finally, 22% of the papers use a different kernel, which usually is a polynomial one, or they

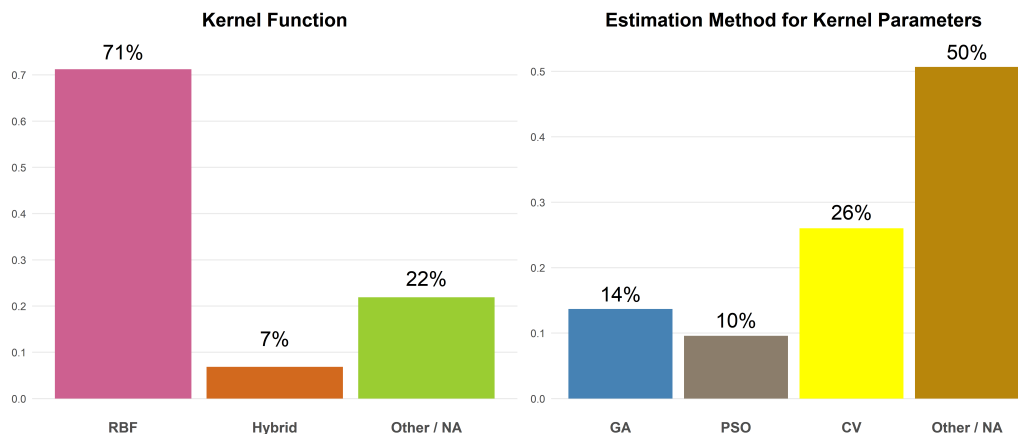


**Fig. 5.** Left: The kernel functions used for the SVM models. Right: The algorithms used to optimise the kernel parameters. 14% of the methods are genetic algorithms, 10% of the times the parameters are set by particle swarm optimisation and 26% by cross-validation. 50% of the times the authors either do not mention how they selected the parameters, or they use some other technique.

do not mention the type of kernel at all. When we use a kernel to replace the simple dot product, we actually search for a hyperplane in a high dimensional space. Thus, we need to carefully select the parameters of the kernel function, so that the optimal performance is achieved. Many authors in the review take under consideration the article of C.-W. Hsu et al. (2003) [6] in order to do that. However, this is far from a trivial issue, since there are no general rules on how to select the best parameters. Luckily for all, there are algorithms that are able to deal with this problem, such as genetic algorithms (GA), particle swarm optimisation (PSO), cross-validation (CV), bees algorithm and other. The right-hand side of Figure 5 provides information about the frequency of the most used methods.

The original SVM algorithm was designed for two-class classification problems. In order to tackle multi-classification ones, one has to choose among a variety of methods, such as one-against-one (OAO), one-against-all (OAA), binary tree (BT) and directed acyclic graph (DAG). Figure 6 provides information about the frequency of these methods in the literature.

In order to achieve high classification performance and reduce the complexity of a problem, the authors use a variety of data preprocessing techniques, instead of just extracting statistical and shape features. These techniques include: Principal Components Analysis (8% of the times), Independent Components Analysis (10% of the times), Singular Spectrum Analysis (1% of the times), Wavelet Analysis (7% of the times), Supervised Locally Linear Embedding (1% of the times), Logistic Regression (1% of the times), Multivariate Adaptive Regression Splines (1% of the times), High/Low Pass Filtering (1% of the times). In 70% of the papers, the authors do not mention any data-preprocessing technique, or they just do a normalisation or scaling, or they

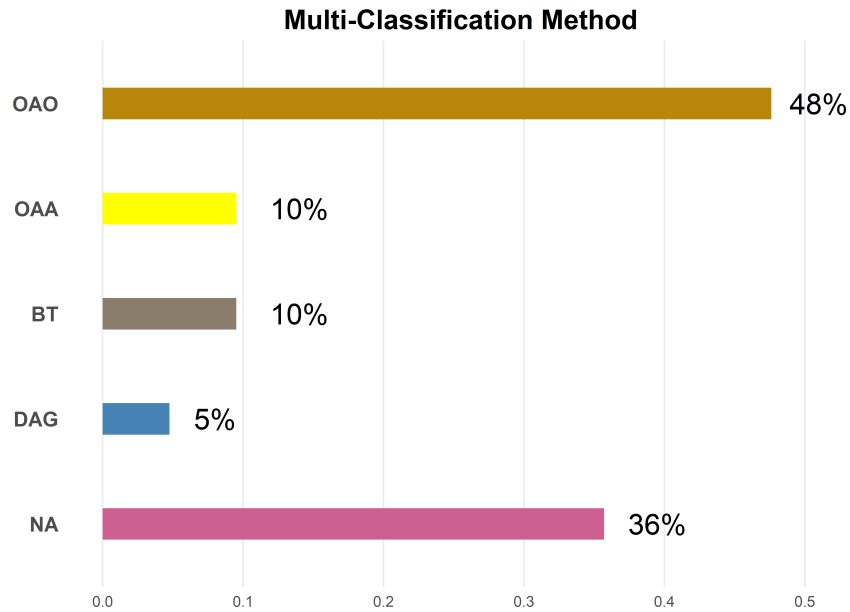


**Fig. 6.** The One-Against-One method is used 48% of the times, the One-Against-All and the Binary Tree are used for 10% of the problems and the Directed Acyclic Graph is preferred for only 5% of the times. 36% of the cases do not mention the way the multi-classification is conducted. The percentages do not sum to 100%, because some authors use more than one method and do not conclude which one is better, or should be preferred.

extract the statistical and shape features we have already talked about. The results are shown in Figure 7.

Let us now present some results about the role of the SVM model in the proposed methods (left-hand side of Figure 8), i.e. what the SVM algorithm is used for. 40% of the times the SVM is used to recognise a pattern (this time we even counted the cases that consider only one pattern). In 16% of the articles, the SVM is used for detecting which variable caused a problem, in 40% of the articles it is used for identifying a faulty process and 4% of the times it is used for other purposes, like helping in the determination of some control bands.

We can clearly see that SVM methods have gained a place in the SPC context, since they are able to produce impressive results and be competitive against other state-of-the-art methods. The majority of comparisons is made among SVM and ANN methods and it seems that the structural risk minimisation of SVMs benefits their performance, in contrast with the empirical risk minimisation of ANNs, which creates problems (see C. J. C. Burges, 1998 [7]). While ANNs try to minimise the training error, the SVMs minimise the upper bound of the error, something that enables them to generalise easier even when the dataset is small. Furthermore, SVMs find a global solution and cannot get stuck in local minima, in contrast with the ANNs. In the right-hand side of Figure 8 we can see that 51% of the papers concerning the support vector

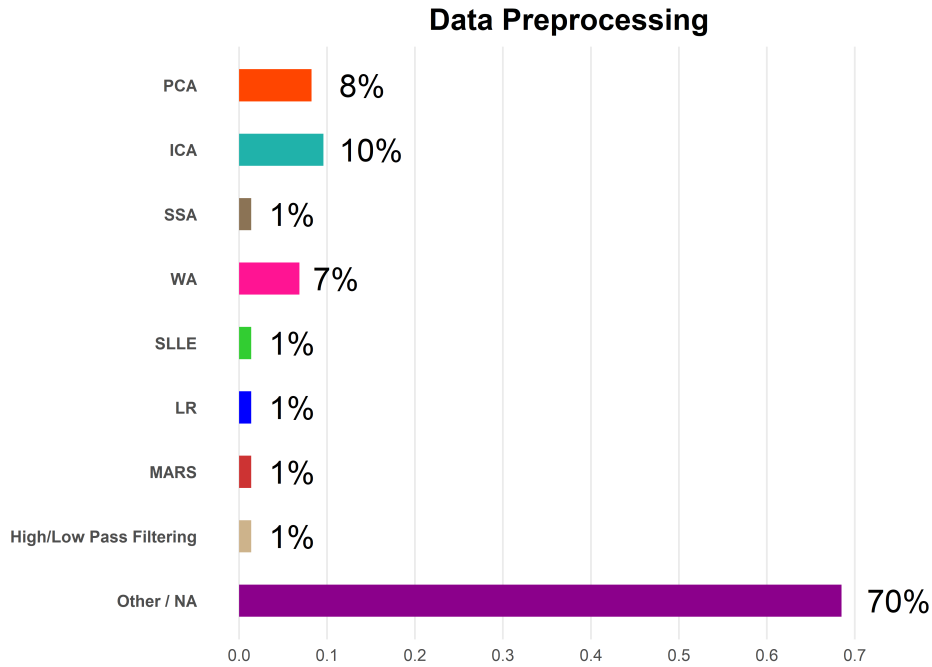


**Fig. 7.** The data preprocessing procedures that are mentioned in the review. From top to bottom, the abbreviations mean: principal components analysis, independent component analysis, singular spectrum analysis, wavelet analysis, supervised locally linear embedding, logistic regression and multivariate adaptive regression splines.

machines do mention a neural network algorithm as well. In 7% of the cases the SVM and ANN model work together in the proposed method, while in 44% of the cases we find a comparison between an SVM and an ANN algorithm, the majority of which is detected in the CCPR problems.

### 3 Application

In this section, we present the D-SVM chart introduced by S. He et al. (2018). Specifically, we test its performance on a real data set, downloaded from UCI Machine Learning Repository. We choose to test this particular chart, because it has some very nice properties. First of all, it is able to detect both mean and variance changes and also both big and small changes. In addition, it can work using only a small amount of in-control data, which may follow any arbitrary distribution, in contrast with other alternatives. Last but not least, its performance has been tested in high dimensional cases and it seems to produce good results. The data set is about the Vinho Verde white wine and includes 12 variables that describe the quality of it, using a sample of size 4898. Further information can be found in the article of P. Cortes et al. (2009) [8].

The 12th variable (named “quality”) of the data set is the score that each wine is characterised with, according to specialists in a scale of 1 (not good) to

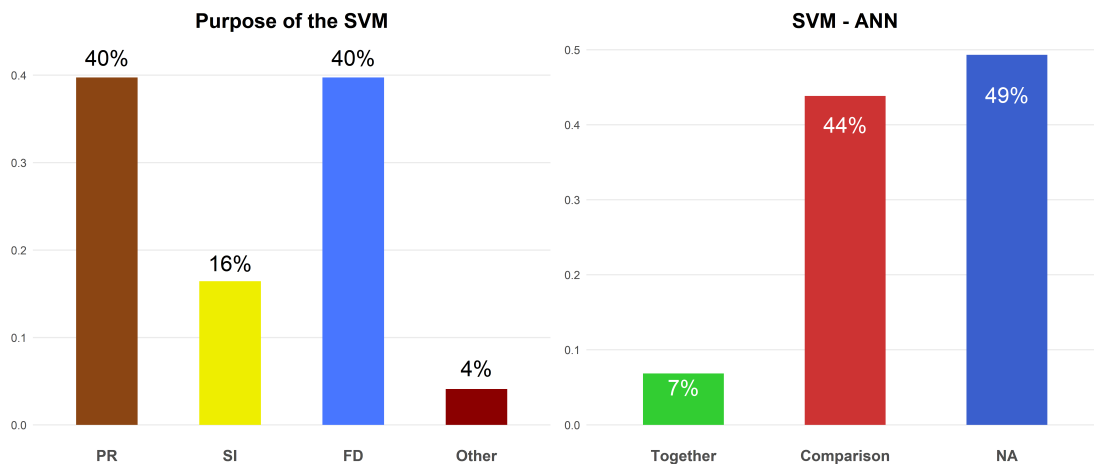


**Fig. 8.** Left: The purpose of the SVM model in the proposed methods. PR stands for Pattern Recognition, SI stands for Source Identification and FD stands for Fault Diagnosis. Right: A barplot for the cases that an SVM and an ANN model can be found in the same paper.

10 (good). Thus, we take the wines with quality level 7 and 8 as the normal state of the process and build the D-SVM chart in order to detect an out-of-control situation, which is the quality level 5 and 6. The only difference is that we use another formulation of SVM models, which uses the  $\nu$  parameter, instead of the  $C$  (that He et al. use). We did this because, the  $\nu$  parameter has a nicer interpretation, which is the upper bound of errors and lower bound of support vectors.

The size of the reference data set  $S_0$  is selected to be  $N_0 = 300$  and the moving window size is selected to be  $N_w = 10$ . We actually tested the performance of the chart with  $N_0$  being 100 as well, but the results are not good, so we stick to the option of 300. A bigger reference data set would be able to exploit much more information, so it might be able to give better results. However, S. He et al. notice that this is not always the case. The effect of the moving window size is as follows: when the shift is small, we should choose a large window and, when the shift is large, we should choose a small window. S. Jang et al. (2017) [9], who also use a moving window analysis for their RTC-RF chart, mention that, if the shift size is not known, a good choice for the moving window would be having a size of 10. Thus, we stick to the choice of 10, since we do not have any idea, whether the change from levels 7-8 to levels 5-6 is a small or a big one (although we gave it a try with  $N_w = 15$  as well).

S. He et al. follow the tactic of keeping the cost parameter constant at the value of 1 and change only the gamma parameter of the RBF kernel in such a way that they have a small error rate in the in-control set. However, they reach to that decision based on a simulated five-dimensional Gaussian process. There are no general guidelines in the literature on how to specify the SVM parameters. Thus, in this application, we just provide some results based on different combinations of the parameters and select the best one among them.

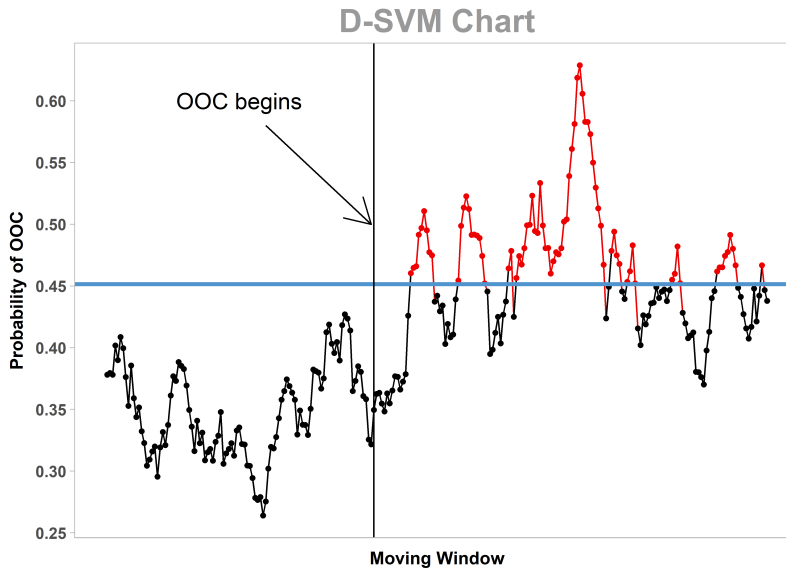


**Fig. 9.** The D-SVM chart applied on the white wine dataset produces 11 false alarms and gives a signal after 15 faulty observations. The black points are in-control data, while red points are out-of-control ones. (The Figure shows only the data close to the changing point.)

The values for  $\nu$  and  $\gamma$  tested are 0.001, 0.005, 0.01, 0.05 and 0.1. Values that are bigger than 1 in either of the two parameters give poor performance for the chart, while others between the five selected (like 0.002, 0.003, etc.) give similar results. The best solution to our problem is setting both the  $\nu$  and  $\gamma$  parameters equal to 0.05, in which case the out-of-control state is detected after 15 out-of-control observations and having produced a false alarm 11 times. We also conduct a small sensitivity analysis of the parameters around the value of 0.05, but the results show that we should stick to our initial decision of  $\nu = 0.05$  and  $\gamma = 0.05$ . If we set the control limit to be 0.4515, then we get  $ARL_0 = 200$  with standard error 6.68. A nice feature of this chart is that, when the process gets out-of-control, it produces many signals for a long time, i.e. the monitoring statistic does not return under the control limit, after an out-of-control situation occurs. The D-SVM chart is shown in Figure 9.

Finally, we present an alternative approach, which is very similar with the D-SVM chart and yields better results in this particular example. The only difference is that we do not use only in-control data in the reference set, but also out-of-control ones. Since we are considering a case of wines that some specialists have already rated, we consider the scenario that some of the bottles that didn't do so well in the tests are available to us before the on-line monitoring. Specifically, we use 300 in-control wines and 300 out-of-control ones in order to build the SVM boundary. Therefore, our  $D_a$ -SVM chart ( $D_{\text{alternative-SVM}}$  chart) actually deals with a two-class classification scenario, rather than a one-class classification, as the original D-SVM does.

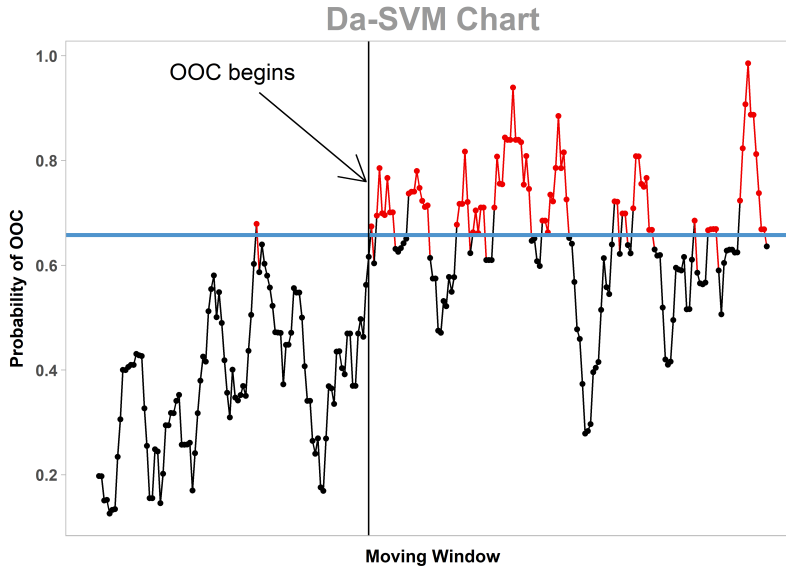


**Fig. 10.** The proposed  $D_a$ -SVM chart is a better approach for the particular problem, since it finds the error after 2 moves of the moving window and having produced 8 false alarms. The black points are in-control data, while red points are out-of-control ones. (The Figure shows only the data close to the changing point.)

Another modification is that we actually optimise the parameters used in the SVM model by a grid search with 5-fold cross validation or a GA. As far as the grid search is concerned, we first conduct it in the  $(0, 0.1)$  interval for both  $\nu$  and  $\gamma$ , then extend the interval of the  $\gamma$  parameter to  $(0, 0.5)$  and finally extend both intervals of  $\gamma$  and  $\nu$  to  $(0, 2)$  and  $(0, 0.15)$  respectively. In every case we test 200 values for each parameter, i.e. 40000 models in each grid search. The three chosen set of parameters produce equally good results in terms of classification error, so we select the one that makes the fewer support vectors in the SVM model. Since we have a supervised problem in our hands, we also build a logistic regression model to optimise the sigmoid curve, which produces the probabilities. When using this approach for the particular problem, we are able to detect the change more quickly and with fewer false alarms (see Figure 10).

## 4 Conclusion

The scope of this article is to present the importance and continuous development of the Support Vector Machines algorithm in the process monitoring field. We give a review of the work that has been done in a span of 16 years concerning process monitoring methods using support vector machines and select one of them to test it with real data. Based on that chart (D-SVM chart), we build a new one ( $D_a$ -SVM chart), which uses a two-class SVM model and it is shown to outperform the original one in the case under study. As far as the

D-SVM chart is concerned, it needs a way of optimisation for its parameters and maybe some method to better project the decision values to probabilities of out-of-control.

## 5 Acknowledgement

This work was supported by the “Statistical Methodology Lab” of the Department of Statistics of the Athens University of Economics & Business and the project “EP-2207-03” of the GSRT.

## References

1. Marion R Reynolds, Raid W Amin, and Jesse C Arnold. Cusum charts with variable sampling intervals. *Technometrics*, 32(4):371–384, 1990.
2. Douglas M Hawkins and KD Zamba. Statistical process control for shifts in mean or variance using a changepoint formulation. *Technometrics*, 47(2):164–173, 2005.
3. Jenn-Hwai Yang and Miin-Shen Yang. A control chart pattern recognition system using a statistical correlation coefficient method. *Computers & Industrial Engineering*, 48(2):205–221, 2005.
4. Gareth James, Daniela Witten, Trevor Hastie, and Robert Tibshirani. *An introduction to statistical learning*, volume 112. Springer, 2013.
5. Shuguang He, Wei Jiang, and Houtao Deng. A distance-based control chart for monitoring multivariate processes using support vector machines. *Annals of Operations Research*, 263(1-2):191–207, 2018.
6. Chih-Wei Hsu, Chih-Chung Chang, Chih-Jen Lin, et al. A practical guide to support vector classification. 2003.
7. Christopher JC Burges. A tutorial on support vector machines for pattern recognition. *Data mining and knowledge discovery*, 2(2):121–167, 1998.
8. Paulo Cortez, António Cerdeira, Fernando Almeida, Telmo Matos, and José Reis. Modeling wine preferences by data mining from physicochemical properties. *Decision Support Systems*, 47(4):547–553, 2009.
9. Seongwon Jang, Seung Hwan Park, and Jun-Geol Baek. Real-time contrasts control chart using random forests with weighted voting. *Expert Systems with Applications*, 71:358 – 369, 2017.

# Calculation Methods for Binary Classification based on Discrete Data. An Application on Synthetic and Real Data.

Fragkiskos G. Bersimis<sup>1</sup>, Iraklis Varlamis<sup>1</sup>, Malvina Vamvakari<sup>1</sup>

and Demosthenes B. Panagiotakos<sup>2</sup>

<sup>1</sup> Department of Informatics and Telematics, Harokopio University, 9 Omirou Str., Athens, Greece;

<sup>2</sup>Department of Nutrition Science - Dietetics, Harokopio University, 70 Eleftheriou Venizelou Str., Athens, Greece

## ARTICLE HISTORY

Compiled July 17, 2018

## ABSTRACT

**Objective:** This work explores the performance of popular classification methods and multivariate indices on binary classification tasks, for datasets that comprise discrete valued features. This is directly applicable in the evaluation of the diagnostic accuracy of composite health related indices or screening tests, which combine multiple discrete-valued attributes (variables), usually using a weighted sum. **Methodology:** Several classification methods (e.g. logistic regression, classification trees, neural networks, support vector machines, ensemble classifiers etc) and multivariate indices that combine feature weighting techniques, are evaluated in this study using both simulated and actual medical-dietary data collected from the “*ATTICA study*” in Greece. A variety of scenarios that modify the discrete values’ distribution parameters of the variables, and the number of variables as well as, are tested. All methods were assessed as to their classification performance by using a set of classification validity criteria such as: area under the ROC curve, true positive and true negative rates, positive and negative predictive value. The predictability of methods and the statistical significance of the results are evaluated using Monte-Carlo cross validation. **Results:** Results indicate that specific classification methods outperform all others in almost all the validity criteria and they also perform better than multivariate indices in certain cases, with regards to the data distribution, the number of features used and the number of their possible values. However, multivariate indices demonstrate a better performance when the number of features is small and the number of possible values in these features is also small. **Conclusion:** This work’s findings propose a methodology for selecting more suitable techniques for predicting the clinical status of a person in the case of general or specific populations, depending on the data nature.

## KEYWORDS

Binary Classification; Discrete Variables; Ordinal Features; ROC; AUC; Logistic Regression; Classification Trees; Neural Networks; Support Vector Machines, Classifier Ensemble

## 1. Introduction

The binary classification of living beings (e.g. to health or unhealthy), based on characteristics measured on a discrete scale, is an objective of many different scientific fields,

---

CONTACT F. G. Bersimis. Email: fbersim@hua.gr

*5<sup>th</sup> SMTDA Conference Proceedings, 12-15 June 2018, Chania, Crete, Greece*

© 2018 ISAST



such as medicine, psychometry, dietetics, etc (Carlsson, 1983; Jackson, 1970; Kant, 1996). This dichotomous classification was traditionally performed in health sciences with the aid of health indices (Bach et al., 2006; Beck et al., 1961; McDowell, 2006). Health related indices are quantitative variables that holistically assess a person’s clinical condition by converting information usually from a variety of different attributes into a single-dimensional vector.

Discrete health indices are produced by the sum of discrete component variables that may be derived from discrete or continuous scale variables. An example of a discrete-scale variable is the number of cardiovascular events experienced by a patient and an example of a continuous-scale variable is the body mass index, which for convenience is appropriately categorized as "fat", "normal", "overweight" and "obese" with corresponding limits proposed by official health organizations, creating a hierarchical variable. Because of the ease of evaluating a feature in a discrete way, discrete scales are widely used (e.g., it is difficult for a person to accurately measure his training intensity per day, while it is easier to describe as mild, moderate or intense) although they provide less valid results than the continuous scales (Likert, 1952).

Although data mining is almost at the end of its third decade of research, and it has become popular in various fields during the last two decades, it is only recently that health scientists have invested on it (Tomar and Agarwal, 2013; Yoo et al., 2012). This is probably because supervised data mining techniques, such as classification and regression, need a lot of data to be trained and achieve a comparable performance to existing health indices, so they apply only on large cohort studies (Austin et al., 2013; Boucekine et al., 2013), or data from medical registries (Delen et al., 2005; Varlamis et al., 2017). It is also because of the limited interpretability of certain data mining based models, which in turns limits their applicability in certain cases. Classification and regression, are the two techniques that have been mostly applied on medical data in order to classify cases (Tang et al., 2005) or predict risks (Bottle et al., 2006), whereas clustering (Khanmohammadi et al., 2017; Yelipe et al., 2018) and association rules (Doddi, 2001; Sanida and Varlamis, 2017) are applied more rarely and mainly for their descriptive capabilities, that let researchers better understand or pre-process the dataset in hand.

The aim of the current study is to evaluate the performance of health related indices and classification algorithms under various dataset setups, given that they comprise only discrete valued features. For this, we comparatively examine classification methods and health related indices in terms of their classification accuracy on general population datasets, which comprising patients and non-patients. The research question is whether data mining (classification) methods can improve the sensitivity and specificity of existing health related indices (Kourlaba and Panagiotakos, 2009), in what extend and under which conditions. Synthetic and real data are used to study the aforementioned research question.

Since health indices are constructed specifically for each specific health case and dataset, in this work, we introduce a methodology for the data driven creation of composite indices. Their performance is compared against some well-known classification methods such as logistic regression, classification (decision) trees, random forests, artificial neural networks, support vector machine techniques and nearest neighbors classifiers as well as an ensemble classifier (meta-classifier) that combines all the previous methods.

In summary, the main contributions of this work are:

- a generic methodology for the construction of composite health indices for the

- classification of datasets with discrete valued features,
- the evaluation of classification ensemble methods that combines more than one classifiers in order to improve individual classifiers performance,
- the evaluation of plain and ensemble classification methods and composite health related indices on synthetic and real datasets, with varying features.
- an open source software solution for the generation and evaluation of synthetic datasets that comprise discrete valued features, which can be used by future researchers to validate and extent the results of our study.

In section 2 that follows some related work is provided in order to identify similarities and differences with previous efforts in the recent literature. In section 3 the weighting process for the multivariate indices and the classification methods employed in the study are briefly described. Section 4 explains how the synthetic data were generated, how the “ATTICA study” data were collected and what evaluation criteria have been used in this study. Section 5 presents the results on synthetic data by providing the performance of the classification algorithms and indices for a varying number of discrete values and features, for a varying population size and ratio between diseased and healthy, as well as for different distribution parameters used. In section 6 the results of our work are discussed and an interpretation from a methodological perspective is attempted and section 7 summarizes our findings and concludes with directions for future work.

## 2. Related Work

Most of health related indices are combinations of individual attributes designed to measure specific medical and behavioral characteristics that are ambiguous or, in some cases, even impossible to be quantified directly and objectively (Bansal and Sullivan Pepe, 2013). There is a variety of clinical situations that cannot be measured with absolute precision, such as depression, anxiety, pain sensation of a patient, and the quality of eating habits (Huskisson, 1974; Trichopoulou et al., 2003; Zung, 1965). For clinical features such as the aforementioned there is a need of appropriate methods/tools to be discovered that quantify them on a discrete scale in order to classify individuals of a general population as patients or healthy. Even when the clinical features can be accurately measured with the appropriate measurement tools, such as hematological and biochemical markers, discretization contributes in the reduction of noise from the original readings (Ding and Peng, 2005).

Composite indices measure specific clinical features by using a suitable cut-off point (e.g., optimal separation point (Youden, 1950)). A health related index is usually synthesized by the sum of  $m$  component variables (features), where each of these features  $X_i, i = 1, 2, \dots, m$  expresses a particular aspect relative to the individual’s clinical status. The scores of the  $m$  components are summed, with or without weighting, to provide an overall score. In the case of a composite health index  $T_m$ , the variables  $X_i, i = 1, 2, \dots, m$  can be either discrete or continuous. According to the index’s value, the respective subjects examined are classified as either healthy or unhealthy, in terms of the appropriate diagnostic threshold for a particular disease (McDowell, 2006). In recent literature, several methods have been proposed to improve sensitivity, specificity and precision of these tools (Bersimis et al., 2013). More specifically, a health indice’s diagnostic ability is improved by increasing the support of the component variables (Bersimis et al., 2017a) as well as by assigning weights to them (Bersimis et al., 2017b).

Composite health indices have been widely used in the medical field. For example, for predicting risk from cardiovascular disease by using mathematical/statistical models, explanatory variables such as age, gender, smoking, nutritional habits etc are associated with the existence of a chronic disease. Such indices have been used in prospective epidemiological studies (e.g. Framingham Heart) (Wang et al., 2003; Wilson et al., 1998), where the aggregation of the component variables provides the final index's score for the 10-year risk of a cardiovascular event (Dagostino et al., 2008). In the field of psychometry for the assessment of depression, there are a number of indices in the literature, such as the Hamilton Rating Scale for Depression (Hamilton, 1960) and the BDI (Beck Depression Inventory) (Beck et al., 1961). The aggregation of variable components provides the final index's score for depression estimation. The scoring of the above-mentioned indices is conducted by assigning high values in attitudes consistent with the condition of depression when they correspond to a high frequency and vice versa (Radloff, 1977). In the field of dietetics, a variety of indices have been constructed for evaluating the consumption's frequency and variety of food groups, such as the Diet Quality Index (DQI) (Patterson et al., 1994) and the Healthy Eating Index (HEI) (Kennedy et al., 1995).

For the classification of persons to patients and healthy, apart from the use of health indices that provide a univariate usually segregation approach, there are some well-known statistical multivariate methods. In particular, several statistical classification methods such as Logistic Regression (LR) (Vittinghoff et al., 2011), Classification and Regression Trees (CART) (Breiman et al., 1984), Neural Networks (NN) (Haykin, 1994) and data mining elements such as machine learning and Support Vector Machines (SVM) (Kruppa et al., 2014) aiming at distinguishing two or more different groups in data sets that have a specific feature or not. The above methods have been developed mainly in the last decades when the application of Informatics' methods became an irreplaceable part of the medical research, resulting in the creation of Bioinformatics, which is a very wide interdisciplinary branch, aiming at studying and interpreting various biological phenomena. In addition, Biostatistics is the specialized scientific branch of Statistics that deals with the application of statistical methods, such as the management and analysis of numerical data, in the wider field of medicine and biological research.

Our work can be compared to (Maroco et al., 2011) since it extensively evaluates the performance of classification methods in terms of accuracy, sensitivity and specificity using a real dataset. In addition to this, we perform an extensive evaluation on synthetic data and provide the tool to future researchers for reproducing or extending our study. The current work extends previous works on the same dataset (the ATTICA study), which apply classification methods for risk prediction (Kastorini et al., 2013; Panaretos et al., 2018). However, in this study, it is the first time that an ensemble classification method that combines the merits of multiple classifiers is applied on the dataset.

### 3. Materials and methods

The main objective of this work is to evaluate the predictive performance of classification methods and health indices in the case of classifying a binary outcome variable based on discrete input variables. This section briefly presents the proposed health index construction methods, which apply to any dataset comprising discrete input variables and a binary output (Section 3.1), highlights the classification methods em-

ployed in our study (Section 3.2), and concludes with the proposed classifier ensemble method (Section 3.2.6), which considers all the available classifiers in tandem, in order to perform the binary prediction.

### 3.1. Data driven health index construction

This study proposes a data driven composite indices' construction methodology, which targets on deriving the corresponding weighting formulas from logistic regression. More specifically, four discrete weighting methods  $w_{ij}, i = 1, 2, \dots, m, j = 1, 2, \dots, 4$  for each component are proposed developed by using the odds ratios (OR) of univariate and multivariate logistic regression, as well as, by using the deviance statistic as modifying factor. These produced weighted indices  $(T_1, T_2, T_3, T_4)$  are tested in simulated and real data. Moreover, weighted index  $T_1$  is constructed by using the odds ratios of each component obtained from univariate logistic regression model ( $OR_{ULR}$ ), whereas weighted index  $T_2$  is constructed by using the odds ratios of each component obtained from multivariate logistic regression model ( $OR_{MLR}$ ). Weighted indices  $T_3$  and  $T_4$  are constructed by using the aforementioned odds ratios in combination with the deviance statistic (DS) obtained from the corresponding logistic regressions. The deviance statistic (DS) i.e. the deviation between the theoretical model and the estimated model, is used for amplifying weights for the component variables that corresponds to lower deviation scores. Therefore, the weighted indices are defined by Equation 1:

$$T_j = \sum_{i=1}^m w_{ij} X_i, i = 1, 2, \dots, m, j = 1, 2, \dots, 4 \quad (1)$$

where each  $w_{ij}$  depending on the weighting method is given by the equations that follow:

$$w_{i1} = \frac{(OR_{ULR})_i}{\sum_{i=1}^m (OR_{ULR})_i}, w_{i2} = \frac{(OR_{MLR})_i}{\sum_{i=1}^m (OR_{MLR})_i}, \quad (2)$$

$$w_{i3} = \frac{(OR_{ULR}/DS)_i}{\sum_{i=1}^m (OR_{ULR}/DS)_i}, w_{i4} = \frac{(OR_{MLR}/DS)_i}{\sum_{i=1}^m (OR_{MLR}/DS)_i}, \quad (3)$$

$$(4)$$

where  $i = 1, 2, \dots, m$  corresponds to the components variables' multitude (Bersimis et al., 2017b).

### 3.2. Classification methods for discrete data

#### 3.2.1. Logistic Regression

The logistic regression model is a non-linear regression model applied in classification problems, where the dependent response variable  $Y$  is categorical (not quantitative) with two or more categories. In the present study, a Binary Logistic Regression (where for example  $Y=1$  means presence of a health risk and  $Y=0$  means risk absence in a medical dataset) is applied. The simple logistic model is given by the following relation

(Vittinghoff et al., 2011):

$$P(Y = 1|X_j) = \frac{e^{\alpha+\beta X_j}}{1 + e^{\alpha+\beta X_j}} = \left(1 + e^{-(\alpha+\beta X_j)}\right)^{-1}, j = 1, 2, \dots, m \quad (5)$$

where  $P(Y = 1|X_j)$  express the conditional probability of a diseased individual.

### 3.2.2. Classification tree analysis

Classification (decision) trees (Quinlan, 1986) constitute a highly interpretable machine learning technique, which uses a set of instances with known input and output variables to train a model, which can then be used to classify unknown instances. The learned models are represented using suitable graphs (tree form), which can also be interpreted as sets of rules (one rule for each path from root to the tree leafs) and can as well operate as decision models. As a prediction tool, classification trees are intended for problems that aim in predicting the right class for an unknown instance, choosing from one or more possible classes. During the training phase, they optimize the division of the known instances (training samples) to the tree leafs so that each leaf contains samples from the same class. The information gain (or KullbackLeibler divergence (Kullback and Leibler, 1951)) is one of the criteria employed to decide on the best split at each step. During the operation phase, the unknown instance is classified using the classification rules of the same tree and the label of the leaf defines its predicted class. Classification trees can work both with discrete and continuous data, although they usually discretize continuous feature in their pre-processing phase.

In this work, several input variables that correspond to discrete-valued dietary features are used in the real dataset and the output variable is also discrete and binary (the aim is to classify individuals as patients or not). However, when the input and output variables are continuous in nature, then it is possible to use regression tree analysis methods (e.g. CART (Breiman, 2017)) and learn the discretization limits of the output variable ((Bersimis et al., 2017b)).

Another limitation of decision tree methods is that they poorly operate in high-dimensional dataset, that comprise many features. Since the trees are usually shallow, they employ only a few of the features in their decision model with the risk to loose useful information from other features. For this reason, several multi-tree models, also known as *forests*, have been introduced in the literature and applied in classification problems, outperforming simple decision trees (see Random Forest (Liaw et al., 2002) and Rotation Forest (Rodriguez et al., 2006) algorithms). Such methods, are also known as classifier ensemble methods, since they combine more than one classifier in order to reach a decision. However, the classifiers in such ensembles are all of the same type (trees), whereas in this work, we experiment with a proposed mixed classified ensemble.

### 3.2.3. Bayesian (probabilistic) classifiers

Probabilistic classifiers assume generative models, in form of product distributions over the original attribute space (as in naive Bayes) or more involved spaces (as in general Bayesian networks) (Kononenko, 2001). They output a probability for each unknown instance to belong to each of the classes and have been shown experimentally successful on real world applications (Pattekari and Parveen, 2012), despite the many simplified probabilistic assumptions. The Bayesian classifiers rely on Bayes' theorem,

which mainly assumes a strong (naive) independence between the input features.

Given an unknown instance to be classified, which is represented by a vector  $x = (x_1, \dots, x_n)$  in the space of  $n$  features (independent variables), the classifier assigns to this instance probabilities:  $p(C_k | x_1, \dots, x_n)$  for each of  $k$  possible outcomes or classes  $C_k$ .

For a large number of features ( $n$ ), or for features with many discrete values the model based on probabilities is infeasible, since it will require too many instances to train (to learn probabilities). However, using Bayes' theorem, the conditional probability can be expressed proportionally to the product of all conditional probabilities of the classes given the feature values of the unknown instance.

$$p(C_k | x_1, \dots, x_n) \propto p(C_k) \prod_{i=1}^n p(x_i | C_k) \quad (6)$$

As a result, the unknown instance  $x$  is classified to the class  $C_k$  that has the highest conditional probability according to equation 6.

#### 3.2.4. Artificial neural networks

Artificial neural networks (ANN) are applied in a variety of scientific fields such as medical diagnosis, speech & pattern recognition etc (Cho et al., 2014; Nigam and Graupe, 2004). ANN is a computing scheme representing partly the biological neural networks existing in human or animal brains, expressed by connected nodes (artificial neurons) organized properly in layers. All artificial neurons are connected and able to transmit signals, usually real numbers, through their connections (synapses) resulting to an output calculated suitably by a non-linear function according the initial inputs based on specific weights assigned to all neurons. ANN's greatest advantage is expressed by its ability to improve its performance by learning continuously by past procedures (Sutton et al., 1998).

#### 3.2.5. Support Vector Machines

Support vector machines are a supervised classification method, which is preferred for binary classification problems with high dimensionality (i.e. a large number of features) (Cortes and Vapnik, 1995). An SVM uses the training data, in order to build a model that correctly classifies instances with a non-probabilistic procedure. First, the space of the input samples, is mapped onto a high dimensional feature space so that the instances are better linearly separated. This transforms SVM learning into a quadratic optimization problem, which has one global solution. The optimal separating hyper plane in this new space must have the maximum possible margin from the training instances it separates from the two classes and the resulting formulation, instead of minimizing the training error seeks to minimize an upper bound of the generalization error. SVMs use non-linear kernel functions to overcome the curse of dimensionality (Azar and El-Said, 2014; Ding and Peng, 2005). They can handle both discrete and continuous variables as long as all are scaled or normalized. The ability of SVMs to handle datasets of large dimensionality (many features) made them very popular for medical data classification tasks. They are usually employed as is in binary classification tasks, but there is ongoing work on optimizations that can further improve SVM classifiers performance (Shen et al., 2016; Weng et al., 2016).

### 3.2.6. Meta-classifier ensemble

Ensemble classification methods are learning algorithms that construct a set of classifiers and then classify new data points by taking a (weighted) vote of their predictions (Dietterich (2000)). Voting is the simplest form of a classifier ensemble. The main idea behind Voting is to use the majority vote or the average predicted probabilities given from conceptually different machine learning classifiers to predict the class labels. Such a classifier can be useful for a set of equally well performing model in order to balance out their individual weaknesses. Random and Rotation Forest algorithms are also considered ensemble methods, but they combine more classifiers of the same type (decision trees). Gradient Boosting (Friedman, 2001) is a meta-classifier that builds an additive model in a forward stage-wise fashion, which allows for the optimization of arbitrary differentiable loss functions. In each stage the algorithm trains a set of binary regression trees on the negative gradient of the binomial or multinomial deviance loss function. Gradient Tree Boosting (Hastie et al., 2001) or Gradient Boosted Regression Trees (GBRT) is a generalization of boosting to arbitrary differentiable loss functions. They have good predictive power and robustness to outliers in output space, but have increased complexity and phase scalability restrictions.

## 4. Experimental evaluation

This paragraph includes the methodology for the generation of synthetic data (section 4.1), the data collection method and the details of the ATTICA study dataset (section 4.2), as well as, the proposed methods accuracy evaluation measures (section 4.3). The code for generating the synthetic dataset and running the classification algorithms is available at BitBucket<sup>1</sup>.

### 4.1. Synthetic data generation

In order to evaluate the performance of composite indices and classifiers, we perform multiple tests, using various scenarios with regards to the input features, such as the distribution of each input variable and the number of their partitions, the number of samples in the population and the number of input variables in the dataset. For this reason, we developed a Python script for generating synthetic datasets, using several parameters, as explaining in the following.

First, we parametrized the variables' partitioning ( $k$ ) (i.e. the possible values an input variable can take, ranging from 1 to  $k$ ), which for simplicity was the same for all variables in our experiments<sup>2</sup>.

Second, we employed a skewed discrete uniform distribution in all variables, with different mean ( $meanpos, meanneg$ ) and deviation ( $stdevpos, stdevneg$ ) for the distribution of diseased (positive) and non-diseased (negative) individuals. In our experiments we use the same shift of the mean (higher than the normal mean for positive samples and lower than the normal mean for negative samples), which however is proportional to  $k$  ( $meanshift = \frac{k+1}{2} + \lambda * (\frac{k+1}{2} - 1)$ , where  $\lambda$  defines the ratio of the shift). For example, the distribution of values (for positive and negative samples) in an attribute of the generated dataset for  $k=5$ ,  $stdevpos = stdevneg = 1$  and respectively

---

<sup>1</sup><https://bitbucket.org/varlamis/discretedatagenerator>

<sup>2</sup>The code can be easily expanded to support the use of a vector or  $k_i$  values, where  $i$  is the number of input variables, instead of a single  $k$

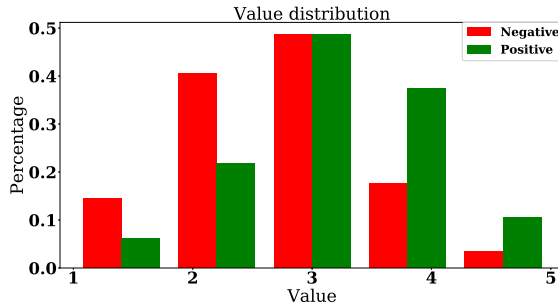


Figure 1.: Value distribution between positive and negative samples for  $k=5$ .

$mean_{pos} = 3.4$  and  $mean_{neg} = 2.6$  is similar to that depicted in Figure 1.

Third, we varied the hypothetical population ratio between diseased and healthy individuals ( $pos, neg$  respectively). Finally, we parametrized the population size ( $samples$ ) and the number of input variables ( $features$ ).

Modifying the aforementioned parameters leads to a dataset that simulates the dataset perspective of a real survey.

#### 4.2. ATTICA study - Dietary data collection

All methods and indices are also evaluated on real data, more specifically on data from the ATTICA epidemiologic study that took place in the Greek region of Attica within 2001 and 2002 (Pitsavos et al., 2003). At the beginning of the study, all participants were found healthy, free of any cardiovascular disease and during the study period, the consumption frequency of food groups was measured for the following food groups: cereals, fruits, nuts, vegetables, potatoes, legumes, eggs, fish, red meat, poultry, full fat dairy products, sweets and alcohol (measured in times/week consumed). From all participants in the ten-year follow up of the ATTICA study, we excluded those having missing values in any of the food groups, in order to avoid any missing values issues. From the 700 individuals that finally used in our study, 78 have reported a cardiovascular disease in the 10-years and 622 were categorized as healthy. This resulted in an unbalanced real dataset with the ratio of healthy to diseased being approximately 1:8.

The food consumption information was the only information used for classifying individuals to be healthy or non-healthy, with regards to the risk of occurrence of a cardiovascular disease within the 10-years period. More specifically, all variables corresponding to the aforementioned food groups were measured on a continuous scale, by counting portions per week. Then data were standardized using z-score and discretized by dividing the range of values into fixed-width intervals, depending on the desired number of partitions ( $k$ ). This way, discrete data were produced with 3, 5, 7, 9 and 11 partitions each.

#### 4.3. Evaluation of classification performance

The diagnostic ability of a classification procedure is evaluated usually by using: i) accuracy (True Rate - TR) and the area (AUC) under the receiver operating characteristic curve (ROC), which is produced by mapping two-dimensionally the conditional probabilities Sensitivity (True Positive Rate - TPR) and 1- Specificity (True Negative

Rate - TNR), and ii) the Positive Predicted Value (PPV) and Negative Predicted value (NPV), in a specific cut off point. The value of Youdens J statistic (Youden, 1950) is a criterion for selecting the optimized cut off point of a diagnostic test, by maximizing the sum of sensitivity and specificity.

If we assume a random sample of diseased and non-diseased persons, who are classified by using a suitable discriminating method, four outcomes may occur that are presented in a 2x2 contingency table that includes:

- True characterized cases: the true positive cases (a) and the true negative cases (d).
- False characterized cases: the false positive cases (b) and the false negative cases (c).

Table 1.: 2x2 Contingency table for binary classification health cases. Green and red color indicates correct and incorrect classification, correspondingly.

		True Clinical Status		
		Positive (Y=1)	Negative (Y=0)	
Predicted Clinical Status by the diagnostic test	Positive (Diseased)	(a) True Positive Cases (TP)	(b) False Positive Cases (FP)	a+b
	Negative (Healthy)	(c) False Negative Cases (FN)	(d) True Negative Cases (TN)	c+d
		a+c	b+d	a+b+c+d=N

A test's sensitivity expresses the conditional probability of positives cases that are correctly identified as such, whereas specificity expresses the conditional probability of negative cases that are correctly identified as such. In addition, a test's positive predicted value expresses the conditional probability that a person with a positive examination is truly ill, and, negative predicted value expresses the conditional probability that a person with a negative examination is truly healthy (Daniel and Holcomb, 1995). Finally, accuracy expresses the conditional probability of positives or negative cases that are correctly identified as such (Daniel and Holcomb, 1995). The prediction accuracy was evaluated by using cross validation methods, such as 10-fold or Monte Carlo with a large number of repetitions and a randomized split (e.g. with 70:30 training/test ratio). More specifically, the prediction performance was evaluated for each method by separating initial synthetic data into training set and test set by using each partitioning technique. The process was performed 100 times and AUC average values are presented, along with their confidence intervals.

For evaluation purposes, we added two parameters that concern the train/test split ratio (*testpercentage*) and the number of repetitive (Monte Carlo) cross validations (*iterations*).

## 5. Results

### 5.1. Results on synthetic data

The aim of the first experiment is to evaluate the performance of the different classification algorithms and multivariate indices, using several criteria. For this purpose, we use the dataset generator with specific parameters that simulate a typical case of a real world dataset with discrete valued attribute. We choose the number of possible

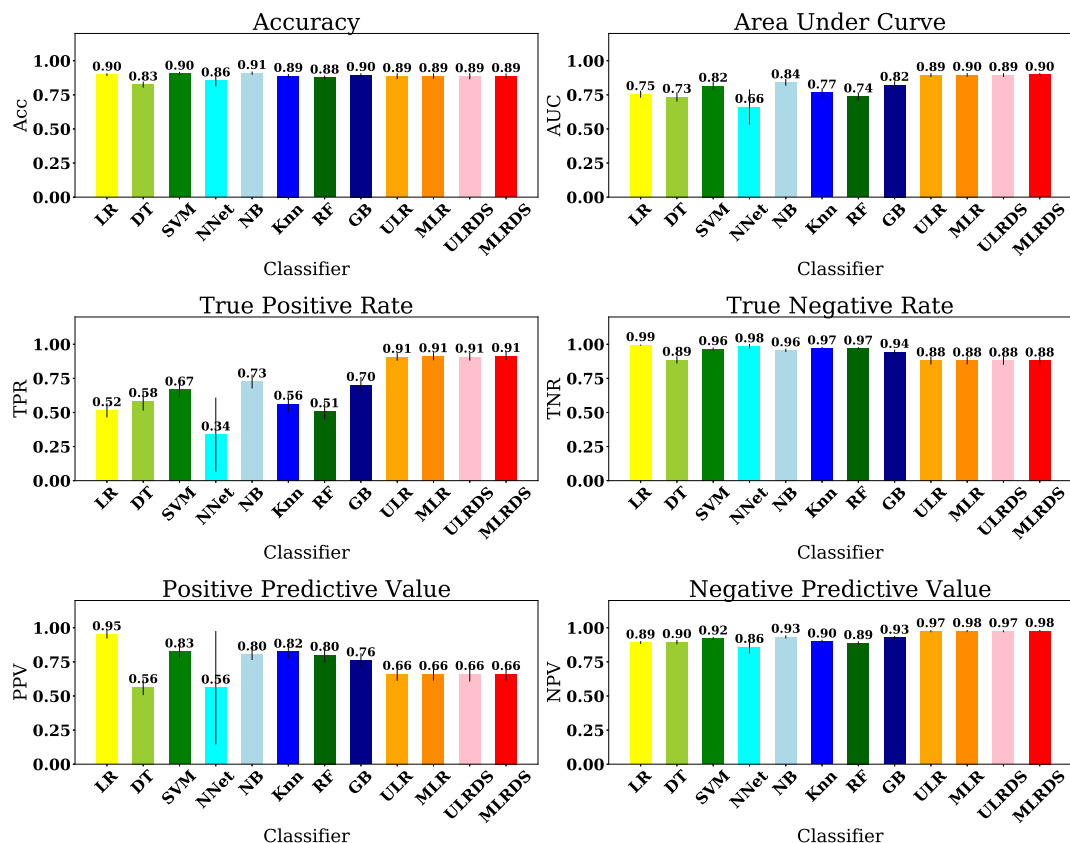


Figure 2.: The performance of the classification algorithms and indices.

values (we call them partitions) for all attributes to be from 1 to 5 (i.e.  $k=5$ ), used a value of  $\lambda = 0.2$  which results to  $meanpos = 3.4$  and  $meanneg = 2.6$  and the same standard deviation for positive and negative samples ( $stdevpos = stdevneg=1$ ). The distribution of randomly generated values in the 10 features ( $feat=10$ ) resembles that of Figure 1. We assumed a variety of samples with 1000 hypothetical individuals and a 1:4 positive to negative ratio (i.e. 200 patients and 800 healthy).

In the dataset that we generated, we repeated a random 70:30 train/test split 100 times and report the average values (and standard deviation). The results are summarized in the plots of Figure 2 that contain the six evaluation metrics (accuracy, AUC, sensitivity - TPR, true negative ratio - TNR, positive predictive value - PPV and negative predictive value - NPV) for each of the classification algorithms (logistic regression LR, Decision trees - DT, Support Vector Machines -SVM, Multi Layer Perceptron neural network -NN, Gaussian Naive Bayes classifier - NB, k-nearest neighbors classifier - Knn, Random Forests - RF, Gradient Boost classifier - GB) and the multivariate indices (ULR, MLR, ULRDS and MLRDS). The default parameters have been employed for all classifiers<sup>3</sup> in order to avoid biasing the results, with parameter tuning.

The results of Figure 2 show a good accuracy performance for all methods (0.81-0.89), with Naive Bayes (NB) having the highest accuracy from all methods and SVM

<sup>3</sup>We encourage reader to refer to the Sci-kit learn API documentation for more details on the default value parameters for each algorithm <http://scikit-learn.org/stable/modules/classes.html>

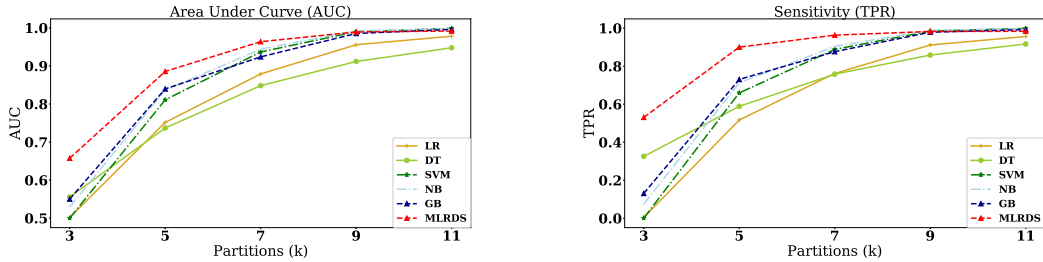


Figure 3.: AUC and Sensitivity for different  $k$  values.

and Gradient Boost ensemble classifiers to follow. However, Naive Bayes suffers from low sensitivity, compared to other methods. On the contrary, the multivariate indices have a high sensitivity and high AUC values (the best among all methods), which is very important when searching for the minority of positives in a population. The multivariate indices suffer from low positive predictive values, which are probably due to the number of false positives they introduce.

In the second experiment, we keep all other values constant and modify the number of partitions ( $k$  in the discretization step, or assuming that the discrete variables take values that range from 1 to  $k$ ). Although we test all the algorithms, in Figure 3 we focus on the algorithms that performed better in the first experiment. From the results in Figure 3 it is obvious that as the number of partitions ( $k$ ) increases, the AUC and sensitivity performance of the classifiers increase respectively. This was expected, since with more partitions (i.e. possible values for a discrete variable) the problem of class separation becomes easier. This finding is in agreement with earlier work by Bersimis (Bersimis et al., 2013) where it was proved that partition's increase corresponds to sensitivity increase. However, some algorithms always perform worse than others (e.g. decision trees and logistic regression perform worse than Gradient Boosting ensemble classifier, SVMs or Naive Bayes). Data driven indices such as *MLRDS*, which was constructed from the multivariate logistic regression model perform better than all other algorithms, even than Naive Bayes or SVM, although, for higher  $k$  values there are no significant differences in their performance. In this particular set of experiments on synthetic data, the performance of the very simple method of Naive Bayes is extremely good. This happens because Naive Bayes is based on the naive assumption that the features are orthogonal (non correlated) to each other, which normally is not valid in a real dataset. The way we generated the synthetic dataset results in this orthogonality of features and justifies the high performance of Naive Bayes.

The third experiment examines the effect of the number of features ( $feat$ ) in the classifiers' performance. For this purpose we repeat the experiments of datasets with 5, 10, 15, 20 and 50 features, using five discrete values ( $k=5$ ) in all cases. From the results in Figures 4 we notice that decision trees cannot handle the high dimensionality of the dataset, which is a known restriction from the literature. Similarly, logistic regression demonstrates a low performance, which improves, but slightly, when the number of features increases. Ensemble classifiers such as Random Forests (not in the plots) and Gradient Boost manage to cover the high dimensionality by training more than one models with a subset of the dimensions each time, but still perform worse than SVMs. Finally, the performance of Naive Bayes (with the assumption of orthogonality) and SVM improves in high dimensions and outperforms that of multivariate regression indices. The latter are ideal for datasets with a few discrete valued features but reach

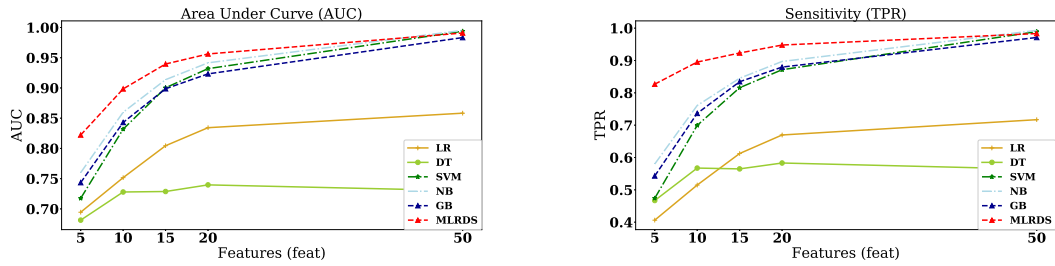


Figure 4.: AUC and Sensitivity for a varying features number.

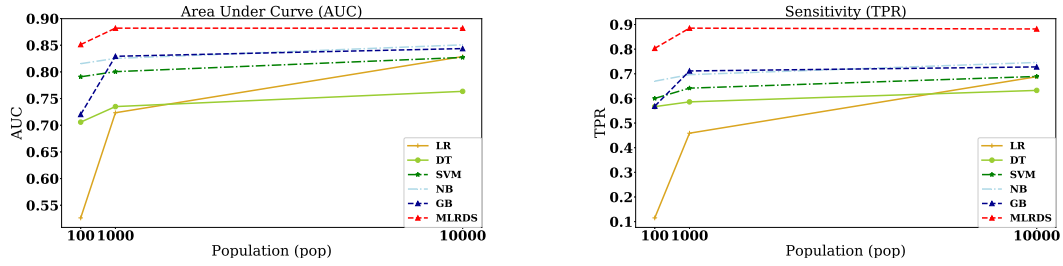


Figure 5.: AUC and Sensitivity for a varying population size.

a performance upper bound above 20 features.

The aim of the fourth experiment was to examine the effect of the population size to the performance of the different classification methods. Using the same configuration as in the first experiment but with a population varying from 100 to 10,000 instances we get the results depicted in Figure 5. The results show a significantly better performance for the MLRDS classifier, but all classifiers tend to improve their performance as the population size increases. The logistic regression method improves the most by this increase in the population size, which probably means that it needs more data to be trained than other methods. However, it is far from the performance of MLRDS.

The fifth experiment examines the effect of the ratio between healthy and patient samples in the dataset. It is very unusual in medical datasets to have a balance in the number of patient and healthy instances, and this adds restrictions to several classification methods. In this experiment, we keep the same configuration as in the first experiment but we modify the ratio of patient:healthy in the following values: 1 : 1 (balanced), 1 : 2, 1 : 4, 1 : 9. The results in Figure 6 show a drop in the performance of

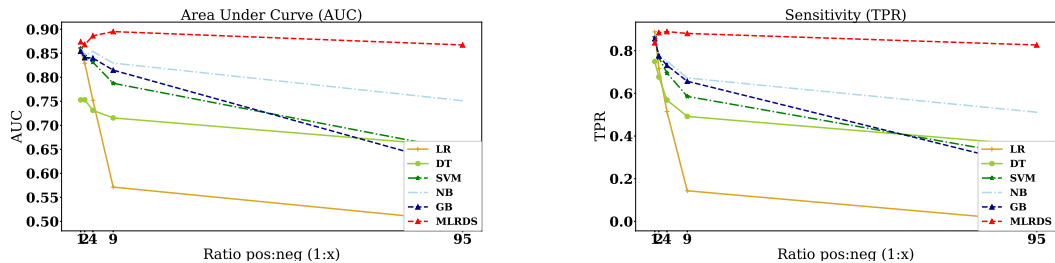


Figure 6.: AUC and Sensitivity for a varying positive:negative ratio.

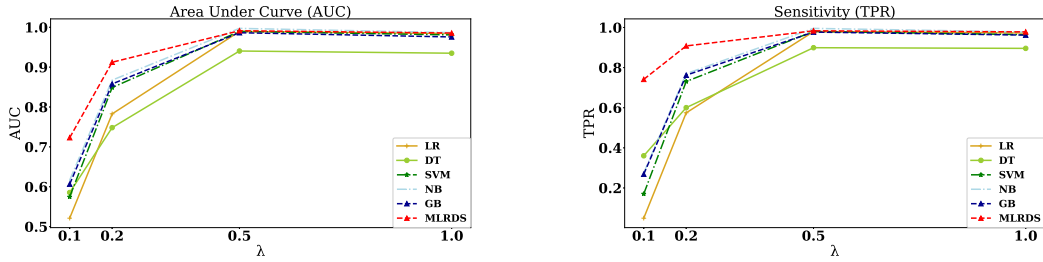


Figure 7.: AUC and Sensitivity for varying  $\lambda$  values.

all algorithms for ratios lower than 1 : 4 (25% patients in the dataset). It is interesting to note the increase in performance of MLRDS for the 1 : 4 ratio (10% patients in the dataset) and its significantly better performance for highly unbalanced datasets (ratios 1 : 9 or 1 : 95).

The last experiment on synthetic datasets examines the effect of the separation of the distribution of feature values between positive and negative instances as determined by the  $\lambda$  parameter. Once again, we keep the same configuration as in the first experiment, but modify  $\lambda$  from 0.1 to 1. The results in Figure 7 show the poor performance of Logistic regression and Decision Trees for small  $\lambda$  values, where the separation problem is harder. They also show that Multivariate indices achieve the best performance. We expect the classifiers' performance to improve, since the problem is easier when the distributions of values for positive and negative samples are well separated, and this happens for all methods. However, results show that Decision Trees perform worse than other methods for higher  $\lambda$  values. This bad performance is probably due to the use of default parameters for the decision tree algorithm and can be possibly improved with the proper parameter tuning, which however is outside the scope of this work.

## 5.2. Results on real data

The results of the evaluation of all algorithms on the ATTICA study data, are depicted in Figure 8.

Although the accuracy of data mining algorithms is higher than that of the multivariate indices, this is mainly due to their high true negative ratio (TNR). The performance of multivariate indices is more stable in all metrics and they demonstrate slightly higher AUC values than the data mining algorithms. More specifically, data mining algorithms seems to fail in the criterion of true positive ratio (TPR), whereas, achieve slightly greater values in negative predicted value (NPR). A more careful examination of the TPR subplot shows that Decision Tree classifier and Naive Bayes, which usually work better with discrete data, outperform all other data mining techniques in TPR and rank after the multivariate indices techniques in AUC.

Further experiments with less and more fine-grain discretization ( $k$  from 5 to 51) shows that the sensitivity (TPR) of the multivariate indices<sup>4</sup> is in average much higher than that of the other classifiers, even of the Decision Trees classifier, that comes second. In terms of AUC, the MLRDS index and the Gradient Boost classifier ensemble are slightly better, but not significantly, than other methods, and have small fluctuations (in the third decimal) for higher  $k$  values.

<sup>4</sup>only the MLRDS index is depicted in Figure 9, but all other indices behave similarly.

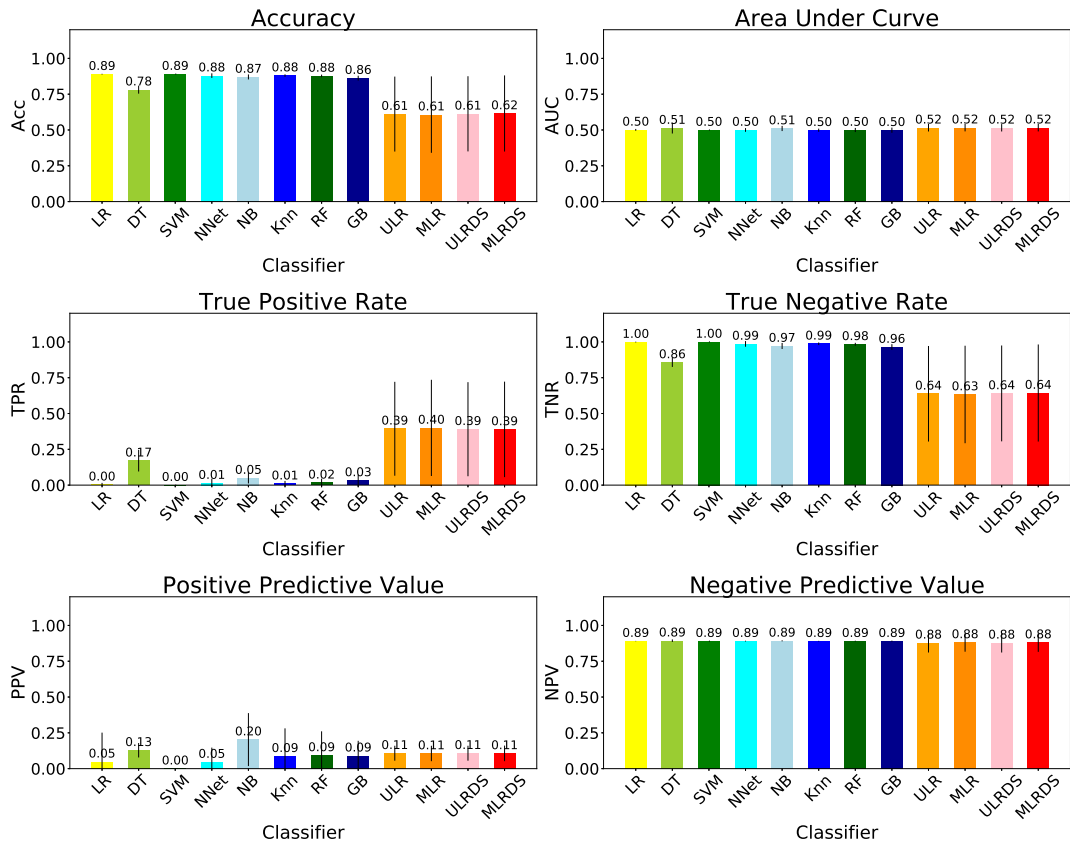


Figure 8.: The performance of the classification algorithms and indices on the data of the ATTICA study ( $k=7$ ).

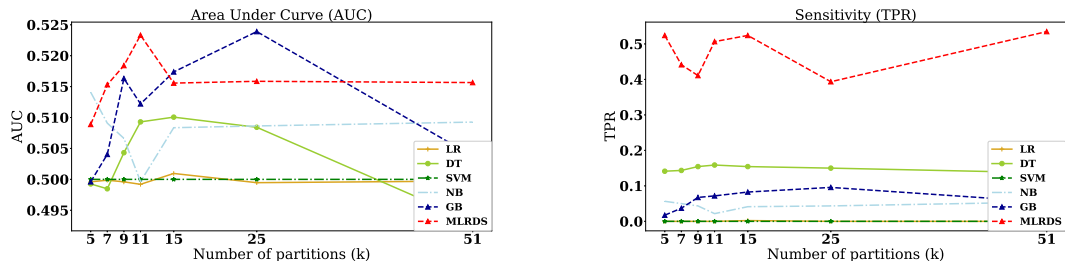


Figure 9.: AUC and Sensitivity for different discretization levels ( $k$ ).

## 6. Discussion

Health indices are extensively used in health research fields such as cardiovascular risk prediction (Wang et al., 2003), depression evaluation (Zung, 1965) and nutritional assessment (Patterson et al., 1994) by measuring diseases' specific aspects and calculating a total score for classifying an individual as high or low risk etc. Classification methods are also used lately in health fields such as cardiovascular and cancer risk prediction by using data mining techniques Varlamis et al. (2017); Weng et al. (2016). Both tools aim to evaluate, classify and predict health conditions aiming to assist medical community to understand and interpret the mechanisms of various diseases. In this work, classification methods and composite indices are compared in order to construct a methodological framework, which could assist any researcher aiming to conduct a classification procedure in medical data. The simulations' results by various scenarios performed in this work, showed differences in evaluation criteria for classification methods and indices used. More specifically, Naive Bayes (NB) classifier achieved the greatest value in accuracy, whereas the greatest value of the area under the receiver characteristic curve (AUC) and true positive ratio was achieved by the weighted indices. This shows an efficient performance of weighted indices in classification problems, when applied on data with similar characteristics as the simulated data of our study (equal value distribution and scale for all features, zero correlation between features, and imbalance between the two classes. The greatest value of true negative ratio was achieved by logistic regression and neural networks, therefore these methods could be conducted in special populations where high specificity is needed. The greatest value of positive predictive value was achieved by logistic regression and support vector machine. In contrary, the greatest value of negative predictive value was achieved by the weighted indices.

The simulations results revealed a significant increase in AUC and sensitivity of classification methods and weighted indices when the number of partitions increase above 7. For small values of  $k$  ( $k < 7$ ), weighted indices seems to outperform classification methods, whereas for great values of  $k$  ( $k > 7$ ) classification methods like SVM achieve greater scores in criteria AUC and sensitivity. This shows that classification methods can better handle features with many discrete values, which resemble to continuous features. Even among the classification methods, there exist many differences. For example, decision trees and logistic regression perform worse than Gradient Boosting Ensemble classifier, SVMs or Naive Bayes.

In addition, increase of the features' multitude led to the AUC increase except the method of decision trees in which the increase in the components seems to confuse the discretion of this method, which is noted in the literature ((Zekić-Sušac et al., 2014)). The results of our study in low and high dimensional spaces are in agreement with the related literature: i) we observe that for a small number of features, the weighted indices perform better than the classification methods, whereas when the number of features significantly increases, support vector machines (SVM) and Naive Bayes (NB) performed better (Bolivar-Cime and Marron, 2013), and ii) in all cases the increase rate is smaller for a larger number of features (Bersimis et al., 2017b).

Increasing the size of the population leads to an increase in the values achieved by many classification methods in the AUC and sensitivity evaluation criteria and, at the same time, to a reduction in the values achieved by the weighted indices in the same criteria. The highest increase rate is recorded by logistic regression, while weighted indices achieve higher values than classification methods, at any sample size. Therefore, the increase in the size of the population seems to have a more pronounced impact on

some classification methods.

A lower ratio of patients to healthy individuals results in a drop in performance for all methods. Thus, for highly unbalanced sets the classifiers performance is worst, i.e. the rarer a disease is, the more difficult it is to detect it. Indices show greater diagnostic ability in cases of very rare diseases, such as 1:95, and they also showed an increase in 1:4 case, in contrast to other methods.

When the distance between the theoretical *population means* of health and diseased individuals is relatively small, i.e. small  $\lambda$  values, then the diagnostic ability of the weighted indices is low, but higher than the one of the classification methods, measured by AUC and sensitivity criteria. When the separation between diseased and non-diseased becomes easier, i.e. higher  $\lambda$  values, the classification methods outperform weighted indices.

The better performance of composite indices in some of the setups in the artificial (synthetic) data is validated with the real data of ATTICA study. For example the composite indices have a larger AUC area and sensitivity than classification methods. However, the overall accuracy of classification methods is higher, and this is mainly because classification methods tend to produce more negatives (i.e. their Negative Predictive Value is close to 1).

The combination of a variety of medical (clinical, biological or behavioral) features, measured on a discrete scale, for classifying individuals of a general population as diseased or not, is an important process for establishing effective prevention strategies in various health areas, such as cardiovascular and cancer risk, metabolic disorders, malnutrition, risk of infant mortality, etc.

Conclusively, this work propose methods for the selection of an effective diagnostic method by using suitable classification methods or weighted indices in relation to the health data nature such as derived from psychological diseases or nutritional adequacy, etc. (McCullough et al., 2000). Moreover, the use of classification methods or weighted indices should be suggested for diagnostic procedures due to the fact that sensitivity and/or specificity increase in many cases shown as it is shown in previous paragraphs. In addition, further research is needed in this area because the classification method's accuracy and weighted indices' diagnostic ability have not been adequately studied.

## 7. Conclusions

Composite indices derived from multivariate methods seem to be sufficient solutions for classifying individuals in the case of discrete features with small partition number, since they perform better than classification algorithms. However, the latter are better for higher numbers of partitions  $k$ . Classification methods such as SVMs are preferable for high dimensional spaces i.e. for datasets with a big number of features/variables. In addition, in the case of orthogonal feature spaces, i.e. non-correlated variables, Naive Bayes classifier is a fast alternative that outperforms all other methods. In the case of available large training datasets, logistic regression is a well performing and fast alternative that competes other methods in evaluation criteria. For highly imbalanced datasets it is preferable to use multivariate indices than simple regressions methods or SVMs. Ensemble methods are also a good solution, since they combine multiple classifiers. Finally, for high  $\lambda$  values, i.e. easy separable problems, SVMs and ensemble methods perform better than multivariate indices.

The next steps of our work in this field are to experiment with more real datasets, especially datasets that are inherently discrete. Also we plan to extend our synthetic

dataset generator to allow for different scales for each feature, different distributions and combinations of discrete and continuous features. Thus we will better simulate real datasets and will allow researchers to experiment with synthetic data of any size that resemble their real data. Finally, we will add more classification methods and optimization strategies, e.g. feature selection and parameter tuning in order to compile a powerful experimentation platform.

## 8. Acknowledgements

\* The ATTICA study was supported by research grants from the Hellenic Cardiological Society (HCS2002) and the Hellenic Atherosclerosis Society (HAS2003).

## References

- P. C. Austin, J. V. Tu, J. E. Ho, D. Levy, and D. S. Lee. Using methods from the data-mining and machine-learning literature for disease classification and prediction: a case study examining classification of heart failure subtypes. *Journal of clinical epidemiology*, 66(4): 398–407, 2013.
- A. T. Azar and S. A. El-Said. Performance analysis of support vector machines classifiers in breast cancer mammography recognition. *Neural Computing and Applications*, 24(5): 1163–1177, 2014.
- A. Bach, L. Serra-Majem, J. L. Carrasco, B. Roman, J. Ngo, I. Bertomeu, and B. Obrador. The use of indexes evaluating the adherence to the mediterranean diet in epidemiological studies: a review. *Public health nutrition*, 9(1a):132–146, 2006.
- A. Bansal and M. Sullivan Pepe. When does combining markers improve classification performance and what are implications for practice? *Statistics in medicine*, 32(11):1877–1892, 2013.
- A. T. Beck, C. H. Ward, M. Mendelson, J. Mock, and J. Erbaugh. An inventory for measuring depression. *Archives of general psychiatry*, 4(6):561–571, 1961.
- F. Bersimis, D. Panagiotakos, and M. Vamvakari. Sensitivity of health related indices is a non-decreasing function of their partitions. *Journal of Statistics Applications & Probability*, 2(3):183, 2013.
- F. Bersimis, D. Panagiotakos, and M. Vamvakari. Investigating the sensitivity function’s monotony of a health-related index. *Journal of Applied Statistics*, 44(9):1680–1706, 2017a.
- F. G. Bersimis, D. Panagiotakos, and M. Vamvakari. The use of components weights improves the diagnostic accuracy of a health-related index. *Communications in Statistics-Theory and Methods*, pages 1–24, 2017b.
- A. Bolivar-Cime and J. Marron. Comparison of binary discrimination methods for high dimension low sample size data. *Journal of Multivariate Analysis*, 115:108–121, 2013.
- A. Bottle, P. Aylin, and A. Majeed. Identifying patients at high risk of emergency hospital admissions: a logistic regression analysis. *Journal of the Royal Society of Medicine*, 99(8): 406–414, 2006.
- M. Boucekine, A. Loundou, K. Baumstarck, P. Minaya-Flores, J. Pelletier, B. Ghattas, and P. Auquier. Using the random forest method to detect a response shift in the quality of life of multiple sclerosis patients: a cohort study. *BMC medical research methodology*, 13(1):20, 2013.
- L. Breiman. *Classification and regression trees*. Routledge, 2017.
- L. Breiman, J. Friedman, R. Olshen, and C. Stone. Classification and regression trees, chapman & hall. *New York, NY, USA*, 1984.
- A. M. Carlsson. Assessment of chronic pain. i. aspects of the reliability and validity of the visual analogue scale. *Pain*, 16(1):87–101, 1983.

- K. Cho, B. Van Merriënboer, C. Gulcehre, D. Bahdanau, F. Bougares, H. Schwenk, and Y. Bengio. Learning phrase representations using rnn encoder-decoder for statistical machine translation. *arXiv preprint arXiv:1406.1078*, 2014.
- C. Cortes and V. Vapnik. Support-vector networks. *Machine learning*, 20(3):273–297, 1995.
- W. W. Daniel and J. J. Holcomb. Biostatistics: a foundation for analysis in the health sciences. 1995.
- D. Delen, G. Walker, and A. Kadam. Predicting breast cancer survivability: a comparison of three data mining methods. *Artificial intelligence in medicine*, 34(2):113–127, 2005.
- T. G. Dietterich. Ensemble methods in machine learning. In *International workshop on multiple classifier systems*, pages 1–15. Springer, 2000.
- C. Ding and H. Peng. Minimum redundancy feature selection from microarray gene expression data. *Journal of bioinformatics and computational biology*, 3(02):185–205, 2005.
- S. R. D. C. T. S. Doddi, Achla Marathe. Discovery of association rules in medical data. *Medical informatics and the Internet in medicine*, 26(1):25–33, 2001.
- R. B. D'Agostino, R. S. Vasan, M. J. Pencina, P. A. Wolf, M. Cobain, J. M. Massaro, and W. B. Kannel. General cardiovascular risk profile for use in primary care: the framingham heart study. *Circulation*, 117(6):743–753, 2008.
- J. H. Friedman. Greedy function approximation: a gradient boosting machine. *Annals of statistics*, pages 1189–1232, 2001.
- M. Hamilton. A rating scale for depression. *Journal of neurology, neurosurgery, and psychiatry*, 23(1):56, 1960.
- T. Hastie, J. Friedman, and R. Tibshirani. Boosting and additive trees. In *The Elements of Statistical Learning*, pages 299–345. Springer, 2001.
- S. Haykin. *Neural networks: a comprehensive foundation*. Prentice Hall PTR, 1994.
- E. Huskisson. Measurement of pain. *The lancet*, 304(7889):1127–1131, 1974.
- D. N. Jackson. A sequential system for personality scale development. In *Current topics in clinical and community psychology*, volume 2, pages 61–96. Elsevier, 1970.
- A. K. Kant. Indexes of overall diet quality: a review. *Journal of the American Dietetic Association*, 96(8):785–791, 1996.
- C.-M. Kastorini, G. Papadakis, H. J. Milionis, K. Kalantzi, P.-E. Puddu, V. Nikolaou, K. N. Vemmos, J. A. Goudevenos, and D. B. Panagiotakos. Comparative analysis of a-priori and a-posteriori dietary patterns using state-of-the-art classification algorithms: a case/control study. *Artificial intelligence in medicine*, 59(3):175–183, 2013.
- E. Kennedy, J. Ohls, S. Carlson, and K. Fleming. The healthy eating index: design and applications. *Journal of the American Dietetic Association*, 95(10):1103–1108, 1995.
- S. Khanmohammadi, N. Adibeig, and S. Shanehbandy. An improved overlapping k-means clustering method for medical applications. *Expert Systems with Applications*, 67:12–18, 2017.
- I. Kononenko. Machine learning for medical diagnosis: history, state of the art and perspective. *Artificial Intelligence in medicine*, 23(1):89–109, 2001.
- G. Kourlaba and D. Panagiotakos. The number of index components affects the diagnostic accuracy of a diet quality index: the role of intracorrelation and intercorrelation structure of the components. *Annals of epidemiology*, 19(10):692–700, 2009.
- J. Kruppa, Y. Liu, G. Biau, M. Kohler, I. R. König, J. D. Malley, and A. Ziegler. Probability estimation with machine learning methods for dichotomous and multicategory outcome: Theory. *Biometrical Journal*, 56(4):534–563, 2014.
- S. Kullback and R. A. Leibler. On information and sufficiency. *The annals of mathematical statistics*, 22(1):79–86, 1951.
- A. Liaw, M. Wiener, et al. Classification and regression by randomforest. *R news*, 2(3):18–22, 2002.
- R. Likert. A technique for the development of attitude scales. *Educational and psychological measurement*, 12:313–315, 1952.
- J. Maroco, D. Silva, A. Rodrigues, M. Guerreiro, I. Santana, and A. de Mendonça. Data mining methods in the prediction of dementia: A real-data comparison of the accuracy, sensitivity

- and specificity of linear discriminant analysis, logistic regression, neural networks, support vector machines, classification trees and random forests. *BMC research notes*, 4(1):299, 2011.
- M. L. McCullough, D. Feskanich, E. B. Rimm, E. L. Giovannucci, A. Ascherio, J. N. Variyam, D. Spiegelman, M. J. Stampfer, and W. C. Willett. Adherence to the dietary guidelines for americans and risk of major chronic disease in men-. *The American journal of clinical nutrition*, 72(5):1223–1231, 2000.
- I. McDowell. *Measuring health: a guide to rating scales and questionnaires*. Oxford University Press, USA, 2006.
- V. P. Nigam and D. Graupe. A neural-network-based detection of epilepsy. *Neurological Research*, 26(1):55–60, 2004.
- D. Panaretos, E. Koloverou, A. C. Dimopoulos, G.-M. Kouli, M. Vamvakari, G. Tzavelas, C. Pitsavos, and D. B. Panagiotakos. A comparison of statistical and machine-learning techniques in evaluating the association between dietary patterns and 10-year cardiometabolic risk (2002–2012): the attica study. *British Journal of Nutrition*, pages 1–9, 2018.
- S. A. Pattekari and A. Parveen. Prediction system for heart disease using naïve bayes. *International Journal of Advanced Computer and Mathematical Sciences*, 3(3):290–294, 2012.
- R. E. Patterson, P. S. Haines, and B. M. Popkin. Diet quality index: capturing a multidimensional behavior. *Journal of the American Dietetic Association*, 94(1):57–64, 1994.
- C. Pitsavos, D. B. Panagiotakos, C. Chrysohoou, and C. Stefanadis. Epidemiology of cardiovascular risk factors in greece: aims, design and baseline characteristics of the attica study. *BMC public health*, 3(1):32, 2003.
- J. R. Quinlan. Induction of decision trees. *Machine learning*, 1(1):81–106, 1986.
- L. S. Radloff. The ces-d scale: A self-report depression scale for research in the general population. *Applied psychological measurement*, 1(3):385–401, 1977.
- J. J. Rodriguez, L. I. Kuncheva, and C. J. Alonso. Rotation forest: A new classifier ensemble method. *IEEE transactions on pattern analysis and machine intelligence*, 28(10):1619–1630, 2006.
- T. Sanida and I. Varlamis. Application of affinity analysis techniques on diagnosis and prescription data. In *Computer-Based Medical Systems (CBMS), 2017 IEEE 30th International Symposium on*, pages 403–408. IEEE, 2017.
- L. Shen, H. Chen, Z. Yu, W. Kang, B. Zhang, H. Li, B. Yang, and D. Liu. Evolving support vector machines using fruit fly optimization for medical data classification. *Knowledge-Based Systems*, 96:61–75, 2016.
- R. S. Sutton, A. G. Barto, et al. *Reinforcement learning: An introduction*. MIT press, 1998.
- T.-I. Tang, G. Zheng, Y. Huang, G. Shu, and P. Wang. A comparative study of medical data classification methods based on decision tree and system reconstruction analysis. *Industrial Engineering and Management Systems*, 4(1):102–108, 2005.
- D. Tomar and S. Agarwal. A survey on data mining approaches for healthcare. *International Journal of Bio-Science and Bio-Technology*, 5(5):241–266, 2013.
- A. Trichopoulou, T. Costacou, C. Bamia, and D. Trichopoulos. Adherence to a mediterranean diet and survival in a greek population. *New England Journal of Medicine*, 348(26):2599–2608, 2003.
- I. Varlamis, I. Apostolakis, D. Sifaki-Pistolla, N. Dey, V. Georgoulas, and C. Lionis. Application of data mining techniques and data analysis methods to measure cancer morbidity and mortality data in a regional cancer registry: The case of the island of crete, greece. *Computer methods and programs in biomedicine*, 145:73–83, 2017.
- E. Vittinghoff, D. V. Glidden, S. C. Shiboski, and C. E. McCulloch. *Regression methods in biostatistics: linear, logistic, survival, and repeated measures models*. Springer Science & Business Media, 2011.
- T. J. Wang, J. M. Massaro, D. Levy, R. S. Vasan, P. A. Wolf, R. B. D’agostino, M. G. Larson, W. B. Kannel, and E. J. Benjamin. A risk score for predicting stroke or death in individuals with new-onset atrial fibrillation in the community: the framingham heart study. *Jama*, 290(8):1049–1056, 2003.

- Y. Weng, C. Wu, Q. Jiang, W. Guo, and C. Wang. Application of support vector machines in medical data. In *Cloud Computing and Intelligence Systems (CCIS), 2016 4th International Conference on*, pages 200–204. IEEE, 2016.
- P. W. Wilson, R. B. DAgostino, D. Levy, A. M. Belanger, H. Silbershatz, and W. B. Kannel. Prediction of coronary heart disease using risk factor categories. *Circulation*, 97(18):1837–1847, 1998.
- U. Yelipe, S. Porika, and M. Golla. An efficient approach for imputation and classification of medical data values using class-based clustering of medical records. *Computers & Electrical Engineering*, 66:487–504, 2018.
- I. Yoo, P. Alafaireet, M. Marinov, K. Pena-Hernandez, R. Gopidi, J.-F. Chang, and L. Hua. Data mining in healthcare and biomedicine: a survey of the literature. *Journal of medical systems*, 36(4):2431–2448, 2012.
- W. J. Youden. Index for rating diagnostic tests. *Cancer*, 3(1):32–35, 1950.
- M. Zekić-Sušac, S. Pfeifer, and N. Šarlija. A comparison of machine learning methods in a high-dimensional classification problem. *Business Systems Research Journal*, 5(3):82–96, 2014.
- W. W. Zung. A self-rating depression scale. *Archives of general psychiatry*, 12(1):63–70, 1965.



# Exploring the relationship between ordinary PageRank, lazy PageRank and random walk with backstep PageRank for different graph structures

Pitos Seleka Biganda<sup>1,2</sup>, Benard Abola<sup>2</sup>, Christopher Engström<sup>2</sup>, John Mango Magero<sup>3</sup>, Godwin Kakuba<sup>3</sup>, and Sergei Silvestrov<sup>2</sup>

<sup>1</sup> Department of Mathematics, College of Natural and Applied Sciences, University of Dar es Salaam, Box 35062 Dar es Salaam, Tanzania  
(E-mail: [pitos.biganda@mdh.se](mailto:pitos.biganda@mdh.se))

<sup>2</sup> Division of Applied Mathematics, School of Education, Culture and Communication (UKK), Mälardalen University, Box 883, 721 23, Västerås, Sweden  
(E-mails: [benard.abola@mdh.se](mailto:benard.abola@mdh.se), [christopher.engstrom@mdh.se](mailto:christopher.engstrom@mdh.se), [sergei.silvestrov@mdh.se](mailto:sergei.silvestrov@mdh.se))

<sup>3</sup> Department of Mathematics, School of Physical Sciences, Makerere University, Box 7062, Kampala, Uganda  
(E-mails: [mango@cns.mak.ac.ug](mailto:mango@cns.mak.ac.ug), [godwin.a.kakuba@gmail.com](mailto:godwin.a.kakuba@gmail.com))

**Abstract.** Ordinary PageRank, introduced by Brin and Page, may be considered as the probability that an internet surfer hits a given webpage in a type of random walk. That is, being at a particular webpage, the surfer visits the next page with uniform probability. There are two other random walks in PageRank problem, these are, lazy random walk and random walk with backstep. The corresponding PageRank is lazy PageRank and random walk with backstep PageRank, respectively. The three walks reveal different behaviour of the surfer in graph structures. However, the relationship between ordinary PageRank, lazy PageRank and random walk with backstep PageRank is not well understood. In this article, we have shown how the three variants of PageRank depend on hyperlink matrices and the damping factor  $c$ . We have also shown that ordinary PageRank can be formulated from lazy PageRank and random walk with backstep PageRank, by some proportionality relationships. The computational behaviour of these variants of PageRank is also discussed.

**Keywords:** Graph, lazy PageRank, random walk with backstep.

## 1 Introduction

PageRank is the algorithm for ranking of Web pages that was founded by Larry Page and Sergey Brin at Stanford University [10,5]. It is the first and best known Webgraph-based algorithm in Google search engine[2]. The algorithm is simple, robust and reliable to measure the importance of Web pages [4].

---

*5<sup>th</sup> SMTDA Conference Proceedings, 12-15 June 2018, Chania, Crete, Greece*

© 2018 ISAST



The idea of PageRank can be described by considering a random surfer that starts from a random page  $v_i$ , and at every time clicks the next page  $v_j$  uniformly at random among the links present in the current page with uniform (transition) probability  $p_{ij}$ , otherwise, with a fixed uniform probability, he gets bored and jumps to any Web page [6,9]. This kind of random walk (or surf) gives the so called ordinary PageRank, which can be thought of as the rank of a page as the fraction of time that the surfer spends on that page on the average [9].

Following the random surf described above, if the move of the surfer from one page to another is decided by first tossing a coin, then the surf is called lazy random surf [3], and the PageRank is called lazy PageRank, which differs from ordinary PageRank in that the surfer has a 50% probability of staying at page  $v_i$  and 50% probability of leaving to the next page  $v_j$  provided the tossing of coin is fair, otherwise the surfer leaves the page with probability  $1 - \lambda$  and stays at the very same page with probability  $\lambda$ , where  $\lambda$  is called laziness degree [6].

Another kind of random surf is that which allows back clicks of the browser. This results into a PageRank called random walk with backstep PageRank. As opposed to ordinary PageRank, here the random surfer clicks the back button of the browser with probability  $\beta$ , otherwise he behaves similarly to ordinary random surfer [6].

The above three walks reveal different behaviour of a surfer in graph structures. However, the relationship between ordinary PageRank, lazy PageRank and random walk with backstep PageRank is not well understood. In this paper, we will show how the three variants of PageRank depend on hyper-link matrices and the damping factor  $c$ . We will also describe how the ordinary PageRank can be formulated from lazy PageRank and random walk with backstep PageRank. A geometric convergence of these variants is also presented.

This article is structured as follows: the next section outlines key notations and basic concepts necessary for the article. This is followed by description of the variants of PageRank in section 3 and a discussion on their convergence rates is given in Section 4. Using some specific graph structures, a comparison of the variants of PageRank is discussed in section 5. Finally a conclusion is given in section 6.

## 2 Notations and basic concepts

Below are some important notations and key concepts necessary throughout this work.

- $n_G$ : The number of nodes in the graph  $G$ .
- $A_G$ : A link matrix of size  $n_G \times n_G$ , where an element  $a_{ij} = 0$  means there is no link from node  $i$  to node  $j$ . If the link exists, then  $a_{ij} = 1/r_i$ , where  $r_i$  is the number of links from node  $i$ .
- $\mathbf{u}_G$ : Non-negative weight vector of size  $n_G \times 1$ , usually with sum of its elements equal to 1.
- $c$ : A parameter  $0 < c < 1$  for calculating PageRank. Usually  $c = 0.85$ .

- $\varepsilon$ : A boring factor  $0 < \varepsilon < 1$  for a random walk on a graph. Usually  $\varepsilon = 1 - c$ . Consequently, we will denote the boring factor corresponding to ordinary, lazy and random walk with backstep PageRanks by  $\varepsilon^{(t)}$ ,  $\varepsilon^{(l)}$  and  $\varepsilon^{(b)}$ , respectively.
- $\mathbf{g}_G$ : A vector of size  $n_G \times 1$ ; with elements equal to 1 for nodes with zero out-links and 0 otherwise in the graph.
- $M_G$ : Modified link matrix, also called Google matrix,  $M_G = (1 - \varepsilon)(A_G + \mathbf{g}_G \mathbf{u}_G^\top)^\top + \varepsilon \mathbf{u}_G \mathbf{e}^\top$ , used to calculate PageRank  $\mathbf{R}$  of the graph.  $\mathbf{e}$  is the vector of size  $n_G \times 1$  whose elements are 1's. In most cases we write

$$M_G = (1 - \varepsilon)P + \varepsilon \mathbf{u}_G \mathbf{e}^\top,$$

where  $P = (A_G + \mathbf{g}_G \mathbf{u}_G^\top)^\top$  is a stochastic matrix. Hence  $P$  is the transition probability matrix of a Markov chain. Note that  $M_G$  is stochastic too.

- $\mathbf{R}_i$ : PageRank of node  $i$  in the graph.
- $\lambda$ : Laziness degree for a generalized lazy PageRank  $\mathbf{R}^{(g)}$ , where  $0 < \lambda < 1$ . For a lazy PageRank  $\mathbf{R}^{(l)}$ ,  $\lambda = 0.5$ .
- $\beta$ : Backstep parameter for a random walk with backstep PageRank  $\mathbf{R}^{(b)}$ , usually  $0 < \beta < 1$ .

### 3 Mathematical relationships between variants of PageRank

In this section we describe three variants of PageRank, that is ordinary, lazy and random walk with backstep, in terms of their dependence on hyperlink matrix  $P$  and parameters  $c$ ,  $\lambda$  and  $\beta$ . We declare here that the mathematics presented in this section were originally given by Kłopotek *et al.*[6], ours is to comprehend them. In later sections, our interest will be to use the relationships between the variants of PageRank to analyze their computational behaviours.

#### 3.1 Ordinary PageRank $\mathbf{R}^{(t)}$

The PageRank problem is stated as the eigenvector problem  $\mathbf{R} = M_G \mathbf{R}$  with eigenvalue 1 [1]. That is, PageRank is the normalized eigenvector of the modified link matrix  $M_G$  associated with the dominant eigenvalue 1, with the normalization equation  $\mathbf{e}^\top \mathbf{R} = 1$ . It follows that

$$\mathbf{R}^{(t)} = M_G \mathbf{R}^{(t)} = \left( (1 - \varepsilon^{(t)})P + \varepsilon^{(t)} \mathbf{u}_G \mathbf{e}^\top \right) \mathbf{R}^{(t)}$$

or

$$\mathbf{R}^{(t)} = (1 - \varepsilon^{(t)})P \mathbf{R}^{(t)} + \varepsilon^{(t)} \mathbf{u}_G. \quad (1)$$

As in [6], the solution to the equation (1) is  $\mathbf{R}^{(t)}(P, \mathbf{u}_G, \varepsilon^{(t)})$ , a function which depends on hyperlink matrix  $P$ , weight vector  $\mathbf{u}_G$  and the boring factor  $\varepsilon^{(t)}$ .

In terms of the damping parameter  $c^{(t)}$ , the function (1) can be written as

$$\mathbf{R}^{(t)} = c^{(t)}P \mathbf{R}^{(t)} + (1 - c^{(t)}) \mathbf{u}_G, \quad (2)$$

or, in Power series formulation, as

$$\mathbf{R}^{(t)} = (1 - c^{(t)}) \sum_{k=0}^{\infty} (c^{(t)}P)^k \mathbf{u}_G. \quad (3)$$

### 3.2 Generalized Lazy PageRank $\mathbf{R}^{(g)}$

For the generalized lazy PageRank, the eigenvector problem is expressed as

$$\mathbf{R}^{(g)} = (1 - \varepsilon^{(g)}) (\lambda I + (1 - \lambda)P) \mathbf{R}^{(g)} + \varepsilon^{(g)} \mathbf{u}_G, \quad (4)$$

where  $I$  is the identity matrix,  $\varepsilon^{(g)}$  is the boring factor and  $\lambda$  is the laziness degree in the lazy random walk on graphs. Its solution is denoted  $\mathbf{R}^{(g)}(P, \mathbf{u}_G, \varepsilon^{(g)}, \lambda)$  [6]. Further transformation of (4) gives

$$\mathbf{R}^{(g)} = \frac{(1 - \varepsilon^{(g)})(1 - \lambda)}{1 - \lambda + \varepsilon^{(g)}\lambda} P \mathbf{R}^{(g)} + \frac{\varepsilon^{(g)}}{1 - \lambda + \varepsilon^{(g)}\lambda} \mathbf{u}_G. \quad (5)$$

It follows from (1) that  $\varepsilon^{(t)}$  and  $\varepsilon^{(g)}$  are related as follows:

$$\varepsilon^{(t)} = \frac{\varepsilon^{(g)}}{1 - \lambda + \varepsilon^{(g)}\lambda} \Leftrightarrow \varepsilon^{(g)} = \frac{\varepsilon^{(t)}(1 - \lambda)}{1 - \varepsilon^{(t)}\lambda}. \quad (6)$$

Assume that  $\lambda = 0.5$ , then equation (5) reduces to

$$\mathbf{R}^{(l)} = \frac{1 - \varepsilon^{(l)}}{1 + \varepsilon^{(l)}} P \mathbf{R}^{(l)} + \frac{2\varepsilon^{(l)}}{1 + \varepsilon^{(l)}} \mathbf{u}_G. \quad (7)$$

This is a lazy PageRank, which is then related to ordinary PageRank by

$$\mathbf{R}^{(l)}(P, \mathbf{u}_G, \varepsilon^{(l)}) = \mathbf{R}^{(t)}\left(P, \mathbf{u}_G, \frac{2\varepsilon^{(l)}}{1 + \varepsilon^{(l)}}\right).$$

Suppose we want to express equation (4) as a power series formulation, then this result follows.

**Corollary 1.** *The lazy PageRank  $\mathbf{R}^{(l)}$  is proportional to ordinary PageRank and can be expressed as*

$$\mathbf{R}^{(l)} = \left(\frac{2 - \varepsilon^{(t)}}{\varepsilon^{(t)}}\right) (1 - c^{(t)}) \sum_{k=0}^{\infty} (c^{(t)}P)^k \mathbf{u}_G. \quad (8)$$

*Proof.* Define two matrices,  $D$  and  $B$ , as

$$D = (1 - \varepsilon^{(g)})\lambda I \quad \text{and} \quad B = (1 - \varepsilon^{(g)})(1 - \lambda)P.$$

Then equation (4) can be rewritten as

$$\mathbf{R}^{(g)} = \sum_{k=0}^{\infty} (D + B)^k \mathbf{u}_G. \quad (9)$$

Let  $d = (1 - \varepsilon^{(g)})\lambda$ , so that  $D = dI$ , a diagonal matrix with all its main diagonal entries equal to  $d$ . Since  $d \in (0, 1)$ , the power series (9) becomes

$$\begin{aligned} \mathbf{R}^{(g)} &= \frac{1}{1 - d} \mathbf{u}_G + \frac{1}{(1 - d)^2} B \mathbf{u}_G + \frac{1}{(1 - d)^3} B^2 \mathbf{u}_G + \dots \\ &= \frac{1}{1 - d} \sum_{k=0}^{\infty} \left(\frac{B}{1 - d}\right)^k \mathbf{u}_G. \end{aligned} \quad (10)$$

Note that  $\frac{1}{1-d} = \frac{1}{1-\lambda+\varepsilon^{(g)}\lambda}$ . By substituting the actual expression for  $B$ , equation (10) becomes

$$\mathbf{R}^{(g)} = \frac{1}{1-\lambda+\varepsilon^{(g)}\lambda} \sum_{k=0}^{\infty} \left( \frac{(1-\varepsilon^{(g)})(1-\lambda)P}{1-\lambda+\varepsilon^{(g)}\lambda} \right)^k \mathbf{u}_G. \quad (11)$$

Now substituting  $\varepsilon^{(g)} = \frac{\varepsilon^{(t)}(1-\lambda)}{1-\varepsilon^{(t)}\lambda}$  into (11) we obtain

$$\mathbf{R}^{(g)} = \frac{1-\varepsilon^{(t)}\lambda}{1-\lambda} \sum_{k=0}^{\infty} ((1-\varepsilon^{(t)})P)^k \mathbf{u}_G. \quad (12)$$

Moreover,  $\frac{1-\varepsilon^{(t)}\lambda}{1-\lambda} = \frac{\varepsilon^{(t)}}{\varepsilon^{(g)}}$  and  $1-\varepsilon^{(t)} = c^{(t)}$ , thus

$$\mathbf{R}^{(g)} = \frac{1}{\varepsilon^{(g)}} (1-c^{(t)}) \sum_{k=0}^{\infty} (c^{(t)}P)^k \mathbf{u}_G. \quad (13)$$

By comparing (3) and (13) we see that  $\mathbf{R}^{(g)}$  is proportional to  $\mathbf{R}^{(t)}$ , with proportionality constant equal to  $\frac{1}{\varepsilon^{(g)}}$ . It follows that, for a lazy PageRank ( $\lambda = 1/2$ ), equation (13) becomes

$$\mathbf{R}^{(l)} = \left( \frac{2-\varepsilon^{(t)}}{\varepsilon^{(t)}} \right) (1-c^{(t)}) \sum_{k=0}^{\infty} (c^{(t)}P)^k \mathbf{u}_G,$$

which also proves that  $\mathbf{R}^{(l)} \propto \mathbf{R}^{(t)}$ .  $\square$

### 3.3 Random walk with backstep PageRank $\mathbf{R}^{(b)}$

Sydow [7,8] introduced a new variant of PageRank named as random walk with backstep PageRank. In contrast to ordinary PageRank, the author coins the behaviour of a random walker in such a way that with probability  $\beta$ , the walker chooses to jump backward. Otherwise, that is, with some probability  $\varepsilon^{(b)}$ , the walker gets bored and jumps to any page and with the remaining probability  $1-\beta$  uniformly chooses the child of the page. Hence, a probabilistic approximation model for computing ranks of web pages that accounts for a backstep can be derived. The model is believed to have fast computation and produces ranking different from ordinary PageRank [8].

In this subsection we will review a PageRank model presented by Kłopotek *et al.*[6]. For simplicity, we will restrict our discussion on a single backstep only. However, both single backstep and multiple backsteps models developed in [6] produce similar ranking behaviours, so that looking at one of them is still valid for the intention of our study.

Let  $p_j$  and  $c_j$  be the authority from the parent  $p$  and child  $c$  of vertex  $v_j$  as shown in Fig. 1. Then the possible voters for  $v_j$  are the parents and children. Hence  $R_j^{(b)} = p_j + c_j$ . If a move has to occur from the vertex  $v_j$ , then it will give

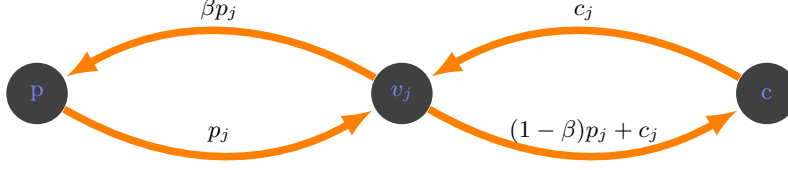


**Fig. 1.** Random walk with back-step at vertex  $v_j$ :  $p$  is a parent and  $c$  a child.

away  $\beta p_j$  to the parents by backstep jump and  $(1 - \beta)p_j + c_j$  to the children. To this end, the children give back  $\beta((1 - \beta)p_j + c_j)$ . At steady state,

$$c_j = \beta((1 - \beta)p_j + c_j) \Rightarrow c_j = \beta p_j.$$

Therefore

$$R_j^{(b)} = p_j + c_j = p_j + \beta p_j = (1 + \beta)p_j.$$

It turns out that

$$p_j = \frac{1}{1 + \beta} R_j^{(b)} \quad \text{and} \quad c_j = \frac{\beta}{1 + \beta} R_j^{(b)}.$$

It follows that the children receives from  $v_j$  same votes as  $v_j$  receives from the parents. That is

$$(1 - \beta)p_j + c_j = (1 - \beta)p_j + \beta p_j = p_j = \frac{1}{1 + \beta} R_j^{(b)}.$$

Note that the proportion  $\varepsilon^{(b)} R_j^{(b)}$  of these votes is distributed over all vertices in the network by boring jump. The remaining  $p_j - \varepsilon R_j^{(b)}$  authority is the one that the real children will get due to follow-link flow. That is

$$p_j - \varepsilon^{(b)} R_j^{(b)} = \left( \frac{1}{1 + \beta} - \varepsilon^{(b)} \right) R_j^{(b)}.$$

Hence

$$\mathbf{p} = \left( \frac{1}{1 + \beta} - \varepsilon^{(b)} \right) P \mathbf{R}^{(b)} + \varepsilon^{(b)} \mathbf{u}_G \quad \text{and} \quad \mathbf{c} = \frac{\beta}{1 + \beta} \mathbf{R}^{(b)}.$$

It follows that

$$\begin{aligned} \mathbf{R}^{(b)} &= \mathbf{c} + \mathbf{p} \\ &= \frac{\beta}{1 + \beta} \mathbf{R}^{(b)} + \left( \frac{1}{1 + \beta} - \varepsilon^{(b)} \right) P \mathbf{R}^{(b)} + \varepsilon^{(b)} \mathbf{u}_G, \end{aligned} \quad (14)$$

or

$$\mathbf{R}^{(b)} = \left( 1 - \varepsilon^{(b)}(1 + \beta) \right) P \mathbf{R}^{(b)} + \varepsilon^{(b)}(1 + \beta) \mathbf{u}_G. \quad (15)$$

Comparing with (1), equation (15) reveals that  $\mathbf{R}^{(b)}$  for a boring factor  $\varepsilon^{(b)}$  is equivalent to  $\mathbf{R}^{(t)}$  for  $\varepsilon^{(t)} = \varepsilon^{(b)}(1 + \beta)$ , formally

$$\mathbf{R}^{(b)} \left( P, \mathbf{u}_G, \varepsilon^{(b)}, \beta \right) = \mathbf{R}^{(t)} \left( P, \mathbf{u}_G, \varepsilon^{(b)}(1 + \beta) \right),$$

where  $0 < \varepsilon^{(b)}(1 + \beta) < 1$ .

Another way of re-writing equation (14) is as follows.

$$\mathbf{R}^{(b)} = (1 - \varepsilon^{(b)}) \left( \frac{\beta}{(1 + \beta)(1 - \varepsilon^{(b)})} I + \frac{1 - \varepsilon^{(b)}(1 + \beta)}{(1 + \beta)(1 - \varepsilon^{(b)})} P \right) \mathbf{R}^{(b)} + \varepsilon^{(b)} \mathbf{u}_G, \quad (16)$$

where  $I$  is the identity matrix. This equation indicates that a random walk with backstep PageRank is also related to generalized lazy PageRank in the following way.

$$\mathbf{R}^{(b)} \left( P, \mathbf{u}_G, \varepsilon^{(b)}, \beta \right) = \mathbf{R}^{(g)} \left( P, \mathbf{u}_G, \varepsilon^{(b)}, \frac{\beta}{(1 + \beta)(1 - \varepsilon^{(b)})} \right). \quad (17)$$

**Proposition 1.** *The random walk with backstep PageRank  $\mathbf{R}^{(b)}$  is also proportional to ordinary PageRank and the relationship is expressed as*

$$\mathbf{R}^{(b)} = \frac{1 + \beta}{\varepsilon^{(t)}} (1 - c^{(t)}) \sum_{k=0}^{\infty} (c^{(t)} P)^k \mathbf{u}_G. \quad (18)$$

*Proof.* From (17), the laziness parameter  $\lambda$  for  $\mathbf{R}^{(g)}$  is a function of  $\beta$  and  $\varepsilon^{(b)}$ , i.e.

$$\lambda = \frac{\beta}{(1 + \beta)(1 - \varepsilon^{(b)})}. \quad (19)$$

It follows that (16) can be expressed analogously to (13), which is a consequence of (4), by substituting

$$\varepsilon^{(g)} = \frac{\varepsilon^{(t)}(1 - \lambda)}{1 - \varepsilon^{(t)}\lambda} = \frac{\varepsilon^{(t)}}{1 + \beta}$$

into (13). Note that the latter expression is obtained as a result of substituting  $\lambda$  given by (19) into the expression for  $\varepsilon^{(g)}$ . Thus (16) can be expressed as

$$\mathbf{R}^{(b)} = \frac{1 + \beta}{\varepsilon^{(t)}} (1 - c^{(t)}) \sum_{k=0}^{\infty} (c^{(t)} P)^k \mathbf{u}_G, \quad (20)$$

which proves that  $\mathbf{R}^{(b)} \propto \mathbf{R}^{(t)}$ , with proportionality constant  $\frac{1 + \beta}{\varepsilon^{(t)}}$ .  $\square$

## 4 Convergence Rates of the Variants of PageRank

In this section we discuss the computational behaviour of the three variants of PageRank described in the previous section. In particular, we will compare their convergence rates by using infinity norm  $\|\cdot\|_{\infty}$ .

Recall that for a  $n$ -square matrix  $A = (a_{ij})$  the norm  $\|\cdot\|_\infty$  is defined as  $\|A\|_\infty = \max_{1 \leq i \leq n} \sum_{j=1}^n |a_{ij}|$  and for a row vector  $\mathbf{x}$  it is defined as  $\|\mathbf{x}\|_\infty = \max_{1 \leq i \leq n} |x_i|$ .

Also recall that, given  $\alpha$  as the probability to follow a link in a random walk, PageRank is the normalized eigenvector of the Google matrix  $M_G(\alpha) = \alpha P + (1 - \alpha)\mathbf{e}\mathbf{v}^\top$  associated with the eigenvalue 1 [1]. Note that  $P$  is the transition probability matrix of an irreducible Markov chain. Using Lemma 1 in [9] we write

$$\begin{aligned} (M_G(\alpha))^k &= (\alpha P + (1 - \alpha)\mathbf{e}\mathbf{v}^\top)^k \\ &= \alpha^k P^k + (1 - \alpha) \sum_{j=0}^{k-1} \alpha^j \mathbf{e}\mathbf{v}^\top P^j. \end{aligned} \quad (21)$$

Let  $\mathbf{v}$  be the personalized distribution with  $\sum_i v_i = 1$ , then the  $k^{\text{th}}$  step distribution of the Markov chain (21) is expressed as

$$\begin{aligned} \mathbf{v}^\top (M_G(\alpha))^k &= \alpha^k \mathbf{v}^\top P^k + (1 - \alpha) \mathbf{v}^\top \sum_{j=0}^{k-1} \alpha^j \mathbf{e}\mathbf{v}^\top P^j \\ &= \alpha^k \mathbf{v}^\top P^k + (1 - \alpha) \sum_{j=0}^{k-1} \alpha^j \mathbf{v}^\top \mathbf{e}\mathbf{v}^\top P^j \\ &= \alpha^k \mathbf{v}^\top P^k + (1 - \alpha) \sum_{j=0}^{k-1} \alpha^j \mathbf{v}^\top P^j. \end{aligned} \quad (22)$$

At stationary state, the probability distribution (22) converges to the PageRank  $\mathbf{R}(\alpha)^\top$ ; and the convergence rate is expressed as

$$\begin{aligned} \|\mathbf{R}(\alpha)^\top - \mathbf{v}^\top (M_G(\alpha))^k\|_\infty &= \|\alpha^k \mathbf{v}^\top P^k + (1 - \alpha) \sum_{j=0}^{\infty} \alpha^j \mathbf{v}^\top P^j - \alpha^k \mathbf{v}^\top P^k \\ &\quad - (1 - \alpha) \sum_{j=0}^{k-1} \alpha^j \mathbf{v}^\top P^j\|_\infty \\ &= \|(1 - \alpha) \sum_{j=k}^{\infty} \alpha^j \mathbf{v}^\top P^j\|_\infty \\ &\leq (1 - \alpha) \|\mathbf{v}^\top \sum_{j=k}^{\infty} \alpha^j P^j\|_\infty \end{aligned}$$

$$\begin{aligned}
\|\mathbf{R}(\alpha)^\top - \mathbf{v}^\top (M_G(\alpha))^k\|_\infty &\leq (1-\alpha)\|\mathbf{v}^\top (\alpha^k P^k + \alpha^{k+1} P^{k+1} + \dots)\|_\infty \\
&= (1-\alpha)\|\alpha^k \mathbf{v}^\top P^k (I + \alpha P + (\alpha P)^2 + \dots)\|_\infty \\
&= (1-\alpha)\|\alpha^k \mathbf{v}^\top P^k \sum_{j=0}^{\infty} (\alpha P)^j\|_\infty \\
&\leq (1-\alpha)\alpha^k \|\mathbf{v}^\top P^k\|_\infty \sum_{j=0}^{\infty} (\alpha P)^j \|I\|_\infty \\
&= (1-\alpha)\alpha^k \|\mathbf{v}^\top P^k\|_\infty \|(I - \alpha P)^{-1}\|_\infty \\
&< (1-\alpha)\alpha^k \cdot \hat{\alpha} \cdot \frac{1}{1-\alpha} \\
&= \hat{\alpha} \alpha^k
\end{aligned} \tag{23}$$

where  $\hat{\alpha} = \|\mathbf{v}^\top P^k\|_\infty < \infty$ . It follows that

**Lemma 1.** *The convergence rates of ordinary PageRank, lazy PageRank and random walk with backstep PageRank are, respectively*

$$\begin{aligned}
(a) \quad &\|\mathbf{R}^{(t)}(c)^\top - \mathbf{v}^\top (M_G(c))^k\|_\infty < \hat{c} c^k, \\
(b) \quad &\|\mathbf{R}^{(l)}(c)^\top - \mathbf{v}^\top (M_G(c))^k\|_\infty < \hat{c} \left(\frac{c}{2-c}\right)^k \text{ and} \\
(c) \quad &\|\mathbf{R}^{(b)}(c, \beta)^\top - \mathbf{v}^\top (M_G(c, \beta))^k\|_\infty < \hat{c} (c + \beta(1-c))^k.
\end{aligned}$$

*Proof.* Referring to equation (1), (7) and (15), the probability to follow the link is  $c$  for ordinary PageRank,  $c/(2-c)$  for lazy PageRank and  $c + \beta(1-c)$  for random walk with backstep PageRank, respectively, where  $c = 1 - \varepsilon$ . Substituting these probabilities for  $\alpha$  in (23) we obtain the desired results.  $\square$

Using Lemma 1 it is true that for the same value of  $c$ , the lazy PageRank converges faster than the other two variants. It is noted also that the random walk with backstep has faster convergence than ordinary PageRank, but their convergence is the same if  $\beta = 0$  (see Fig. 2). Further, in Fig. 2 we also observe that the three variants are parallel to each other. In fact, this observation reflects the proportionality relationships that exist between the variants of PageRank as discussed in section 3.

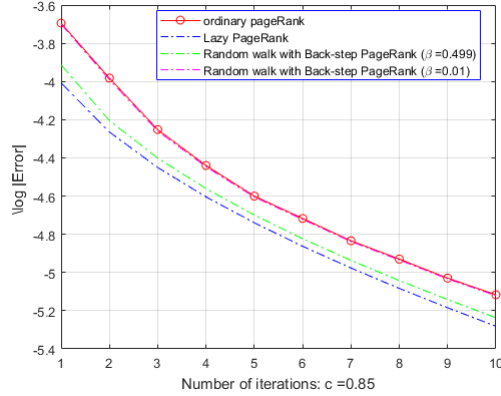


Fig. 2. Geometric convergence of the variants of PageRanks

## 5 Comparison of ranking behaviours for the variants of PageRank

In this section, we investigate whether the PageRank variants have the same or different PageRank values for small networks, like a simple line graph (Fig. 3) and the simple line connected with a complete graph as in Fig. 5. We use normalized PageRank in our comparisons. In addition, we compare the ranks (ordering of top ten vertices) for the variants in a large network.

### 5.1 Comparing PageRank of simple networks

Following equations (1), (7) and (15), we first compared the variants of PageRank basing on their scores in a simple line graph as given by Fig. 3.

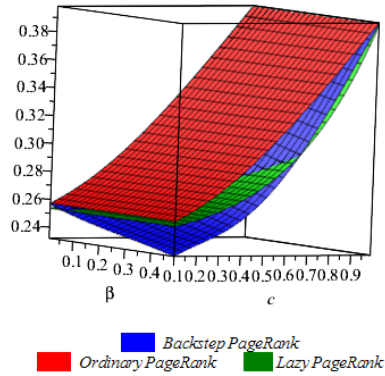


Fig. 3. A simple line graph  $V = \{v_1, v_2, v_3, v_4\}$

Considering vertex  $v_1$ , the corresponding normalised ordinary PageRank, lazy PageRank and random walk with baskstep PageRank are expressed as

$$\begin{aligned}
 R_1^{(t)} &= \frac{(1+c)(1+c^2)}{4+3c+2c^2+c^3}, \\
 R_1^{(l)} &= \frac{4-4c+2c^2}{16-18c+8c^2-c^3}, \\
 R_1^{(b)} &= \frac{(1+c+\beta(c-1))(1+c^2+2c\beta(c-1)+\beta^2(c-1)^2)}{4+3c+2c^2+c^3+\beta(3c^3+c^2-c-3)+\beta^2(3c^3-4c^2-c-2)+\beta^3(c-1)^3}.
 \end{aligned}$$

Findings indicate that ordinary PageRank gives higher scores for a line graph as compared to the other two variants. Also it can be seen that the random walk with backstep PageRank has higher scores than lazy PageRank except for high values of  $\beta$  where lazy PageRank ranks higher (see Fig. 4).



**Fig. 4.** Comparison of the variants of PageRanks for  $v_1$ .

Secondly, we consider a simple line with one vertex linked to a complete graph as in Fig. 5. It would be of interest to know the ranking behaviour of two vertices in the complete graph: one which is directly linked by the simple line and any other vertex in the complete graph.

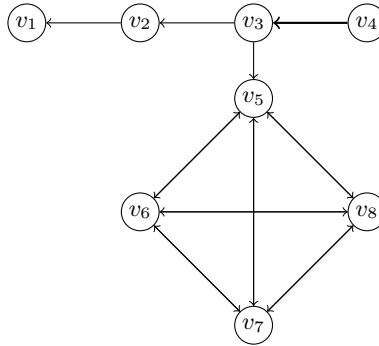


**Fig. 5.** A simple line graph and a complete graph

Let consider the nodes  $v_5$  and  $v_7$ . Explicit formulae of normalized PageRank of the three variants are given by equations (24), (25) and (26) for  $v_5$ , and (27), (28) and (29) for  $v_7$ . Similar to the previous case (simple line graph), ordinary

PageRank has the highest scores in both vertices (see Fig. 6).

$$\mathbf{R}_5^{(t)} = \frac{2c^3 - c^2 - 5c - 6}{(c^4 + c^3 + 2c^2 + 2c - 16)(c + 3)} \quad (24)$$

$$\mathbf{R}_5^{(l)} = \frac{(c - 2)^2 (2c^3 - 9c^2 + 26c - 24)}{(16c^4 - 134c^3 + 400c^2 - 528c + 256)(c - 3)} \quad (25)$$

$$\mathbf{R}_5^{(b)} = \frac{k_1 + k_2}{(k_3 + k_4)k_5} \quad (26)$$

where

$$\begin{aligned} k_1 &= 2\beta^3(c - 1)^3 + \beta^2(6c^3 - 13c^2 + 8c - 1), \\ k_2 &= \beta(6c^3 - 8c^2 - 3c + 5) + 2c^3 - c^2 - 5c - 6, \\ k_3 &= \beta^4(c - 1)^4 + \beta^3(4c + 1)(c - 1)^3 + \beta^2(6c^4 - 9c^3 + 2c^2 - c + 2), \\ k_4 &= \beta(4c^4 - c^3 + c^2 - 2c - 2) + c^4 + c^3 + 2c^2 - 16, \quad \text{and} \\ k_5 &= \beta(c - 1) + c + 3. \end{aligned}$$

$$\mathbf{R}_7^{(t)} = \frac{c^3 + c^2 + 2c + 6}{(16 - 2c - 2c^2 - c^3 - c^4)(3 + c)} \quad (27)$$

$$\mathbf{R}_7^{(l)} = \frac{(c - 2)^2 (2c^3 - 15c^2 + 32c - 24)}{(16c^4 - 134c^3 + 400c^2 - 528c + 256)(c - 3)} \quad (28)$$

$$\mathbf{R}_7^{(b)} = \frac{h_1}{(h_2 + h_3)h_4} \quad (29)$$

where

$$\begin{aligned} h_1 &= -\beta^3(c - 1)^3 + \beta^2(-3c^3 + 5c^2 - c - 1) + \beta(-3c^3 + c^2 + 2) - (c^3 + c^2 + 2c + 6), \\ h_2 &= k_3, \quad h_3 = k_4 \quad \text{and} \quad h_4 = k_5. \end{aligned}$$

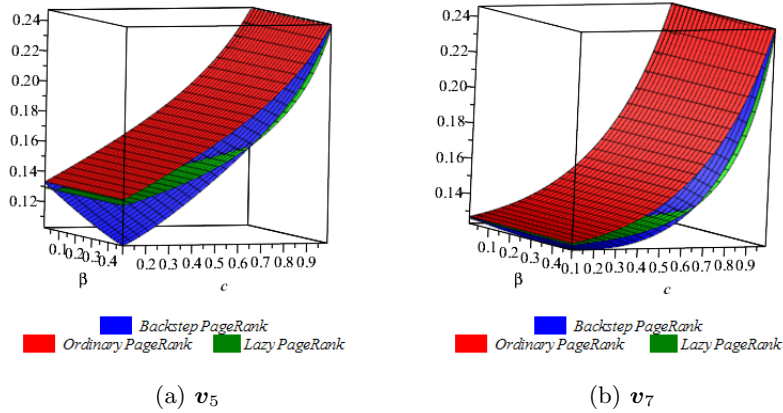


**Fig. 6.** Comparison of the variants of PageRanks for nodes  $v_5$  and  $v_7$

## 5.2 Numerical experiments for large network

Next, we look further at the comparison by using an example of a network with 434,818 vertices and 3,419,124 edges. The interest is to see the top ten vertices picked by each of the variants of PageRank when a Power method is used but with varying  $c$  and  $\beta$  values as shown in Tables 1 - 4, where the abbreviations LPR, OPR and RBS in the tables stand for lazy PageRank, ordinary PageRank and random walk with backstep PageRank, respectively. We carried out 30 iterations in all experiments.

We see that, with small values of  $c$  and  $\beta$  (see Table 1), 50% of the vertices picked by ordinary PageRank and random walk with backstep are the same. If  $c$  is increased to 0.85 but keeping low value of  $\beta$ , 70% of the top ten vertices picked by the three variants of PageRank are the same and 100% are the same for ordinary and random walk with backstep PageRanks (see Table 2).

Rank	1	2	3	4	5	6	7	8	9	10
LPR	32574	73303	<b>130750</b>	154860	168136	194686	<b>196645</b>	257029	<b>257771</b>	270913
OPR	73303	320622	32574	270913	286632	257029	194686	329575	168136	154860
RBS	32574	73303	270913	286632	320622	257029	194686	329575	168136	154860

**Table 1.** Top 10 vertices picked by the variants of PageRank when  $\beta = 0.01$  and  $c = 0.25$

Rank	1	2	3	4	5	6	7	8	9	10
LPR	73303	320622	32574	270913	286632	257029	194686	329575	168136	154860
OPR	73303	320622	32574	270913	286632	257029	194686	290	12962	30312
RBS	73303	320622	32574	270913	286632	257029	194686	290	12962	30312

**Table 2.** Top 10 vertices picked by the variants of PageRank when  $\beta = 0.01$  and  $c = 0.85$

Rank	1	2	3	4	5	6	7	8	9	10
LPR	32574	73303	130750	154860	168136	194686	196645	257029	257771	270913
OPR	32574	73303	130750	154860	168136	194686	196645	257029	257771	270913
RBS	<b>237059</b>	<b>268696</b>	<b>133010</b>	<b>280965</b>	<b>8600</b>	<b>197937</b>	<b>238961</b>	<b>386354</b>	<b>290440</b>	<b>46317</b>

**Table 3.** Top 10 vertices picked by the variants of PageRank when  $\beta = 0.499$  and  $c = 0.25$

In the case where  $\beta$  is increased and  $c$  is kept relatively small, LPR and OPR ranks the same vertices whereas RBS picks completely different top ten vertices

Rank	1	2	3	4	5	6	7	8	9	10
LPR	73303	320622	32574	270913	286632	257029	194686	329575	168136	154860
OPR	73303	320622	32574	270913	286632	257029	194686	290	12962	30312
RBS	73303	320622	32574	270913	286632	257029	194686	329575	168136	254358

**Table 4.** Top 10 vertices picked by the variants of PageRank when  $\beta = 0.499$  and  $c = 0.85$

(see Table 3). When both parameters are increased as shown in Table 4, the situation is similar as in Table 2 where 70% of top ten vertices are picked by all three variants. Note that we decided to use  $\beta < 0.5$  as the threshold value as suggested in [6] and  $c \leq 0.85$  as the optimal value as in [5].

One general remark on the four cases presented in Tables 1 - 4 above is that, except for the top ten vertices picked by RBS in Table 3, most of the vertices appear in all the cases with either same or different rank position from one table to another. The reason is that if  $\beta$  is increased a random walk with backstep jumps randomly more frequently than the other two variants of random walks such that it is difficult to trap the walker in the network. This leads for RBS to have different ranks as suggested in [6].

## 6 Conclusion

We have considered an exploratory study on the relationships between three variants of PageRank, namely ordinary PageRank, lazy PageRank and random walk with backstep PageRank. We have shown, mathematically, that both lazy PageRank and random walk with backstep PageRank are proportional to ordinary PageRank. This kind of relationship suggests that the three variants of PageRank can be computed by using one algorithm, except that one need to adjust the damping factor. This kind of conclusion was also suggested by Kłopotek *et al.*[6]. We have also noted that there is no improvement on the convergence speed of the Power method in the computation of any of the three variants of PageRank. Using same damping parameter value  $c = 0.85$ , the three variants of PageRank have parallel convergence speeds, which was expected because of proportionality relationships existing between the variants of PageRank.

**Acknowledgements** This research was supported by the Swedish International Development Cooperation Agency (Sida), International Science Programme (ISP) in Mathematical Sciences (IPMS), Sida Bilateral Research Program (Makerere University and University of Dar-es-Salaam). We are also grateful to the research environment Mathematics and Applied Mathematics (MAM), Division of Applied Mathematics, Mälardålen University for providing an excellent and inspiring environment for research education and research.

## References

1. A. N. Langville and C. D. Meyer. *Google's PageRank and beyond: The science of search engine rankings*. Princeton University Press, 2011.

2. D. Sullivan. What Is Google PageRank? A Guide For Searchers & Webmasters. *Search Engine Land*, 2007. [Online]. Available: <https://searchengineland.com/what-is-google-pagerank-a-guide-for-searchers-webmasters-11068> (Accessed 2018-04-15).
3. F. Chung and W. Zhao. PageRank and random walks on graphs. In *Fete of combinatorics and computer science* (pp. 43–62). Springer, Berlin, Heidelberg, 2008.
4. J. Kleinberg & D. Gibson. Hypersearching the Web. *Scientific American*, 280(6), 1999.
5. L. Page, S. Brin, R. Motwani and T. Winograd. *The PageRank citation ranking: Bringing order to the web*. Stanford InfoLab, 1999.
6. M. A. Kłopotek, S. T. Wierzchoń, K. Ciesielski, D. Czerski, and M. Dramiński. Lazy Walks Versus Walks with Backstep: Flavor of PageRank. In *Proceedings of the 2014 IEEE/WIC/ACM International Joint Conferences on Web Intelligence (WI) and Intelligent Agent Technologies (IAT)-Volume 01*, pp. 262-265. IEEE Computer Society, 2014.
7. M. Sydow. Link analysis of the web graph. measurements, models and algorithms for web information retrieval. (Ph.D. dissertation) *Institute of Computer Science, Polish Academy of Sciences*, Warsaw, Poland, 2004.
8. M. Sydow. Random surfer with back step. *Fundamenta Informaticae*, 68, 4, 379–398, 2005.
9. P. Boldi, M. Santini and S. Vigna. PageRank as a function of the damping factor. In *Proceedings of the 14th international conference on World Wide Web*, pp. 557-566. ACM, 2005.
10. S. Brin and L. Page. The anatomy of a large-scale hypertextual web search engine. *Computer networks and ISDN systems*, Elsevier, 30(1-7), 107–117, 1998.



# Semi-supervised Learning Based on Distributionally Robust Optimization

Jose Blanchet<sup>1</sup> and Yang Kang<sup>2</sup>

<sup>1</sup> Management Science and Engineering, Stanford University, Stanford, CA, U.S.A.  
(E-mail: [jblanche@stanford.edu](mailto:jblanche@stanford.edu))

<sup>2</sup> Department of Statistics, Columbia University, New York, NY., U.S.A.  
(E-mail: [yang.kang@columbia.edu](mailto:yang.kang@columbia.edu))

**Abstract.** We propose a novel method for semi-supervised learning (SSL) based on data-driven distributionally robust optimization (DRO) using optimal transport metrics. Our proposed method enhances generalization error by using the non-labeled data to restrict the support of the worst case distribution in our DRO formulation. We enable the implementation of our DRO formulation by proposing a stochastic gradient descent algorithm which allows to easily implement the training procedure. We demonstrate that our Semi-supervised DRO method is able to improve the generalization error over natural supervised procedures and state-of-the-art SSL estimators. Finally, we include a discussion on the large sample behavior of the optimal uncertainty region in the DRO formulation. Our discussion exposes important aspects such as the role of dimension reduction in SSL.

**Keywords:** Distributionally Robust Optimization, Semi-supervised Learning, Stochastic Gradient Descent..

## 1 Introduction

We propose a novel method for semi-supervised learning (SSL) based on data-driven distributionally robust optimization (DRO) using an optimal transport metric – also known as earth-moving distance (see [19]).

Our approach enhances generalization error by using the unlabeled data to restrict the support of the models which lie in the region of distributional uncertainty. The intuition is that our mechanism for fitting the underlying model is automatically tuned to generalize beyond the training set, but only over potential instances which are relevant. The expectation is that predictive variables often lie in lower dimensional manifolds embedded in the underlying ambient space; thus, the shape of this manifold is informed by the unlabeled data set (see Figure 1 for an illustration of this intuition).

To enable the implementation of the DRO formulation we propose a stochastic gradient descent (SGD) algorithm which allows to implement the training procedure at ease. Our SGD construction includes a procedure of independent interest which, we believe, can be used in more general stochastic optimization problems.

---

<sup>5</sup>*th* SMTDA Conference Proceedings, 12-15 June 2018, Chania, Creete, Greece



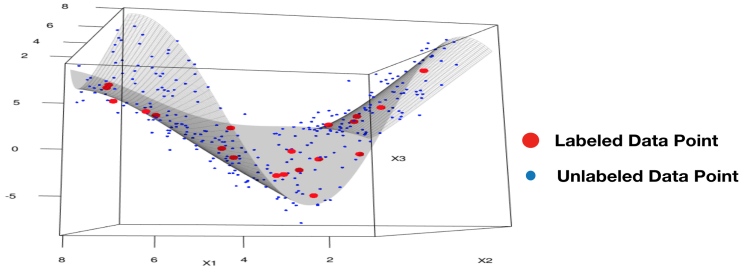


**Fig. 1.** Idealization of the way in which the unlabeled predictive variables provide a proxy for an underlying lower dimensional manifold. Large red dots represent labeled instances and small blue dots represent unlabeled instances.

We focus our discussion on semi-supervised classification but the modeling and computational approach that we propose can be applied more broadly as we shall illustrate in Section 4.

We now explain briefly the formulation of our learning procedure. Suppose that the training set is given by  $\mathcal{D}_n = \{(Y_i, X_i)\}_{i=1}^n$ , where  $Y_i \in \{-1, 1\}$  is the label of the  $i$ -th observation and we assume that the predictive variable,  $X_i$ , takes values in  $\mathbb{R}^d$ . We use  $n$  to denote the number of labeled data points.

In addition, we consider a set of unlabeled observations,  $\{X_i\}_{i=n+1}^N$ . We build the set  $\mathcal{E}_{N-n} = \{(1, X_i)\}_{i=n+1}^N \cup \{(-1, X_i)\}_{i=n+1}^N$ . That is, we replicate each unlabeled data point twice, recognizing that the missing label could be any of the two available alternatives. We assume that the data must be labeled either -1 or 1.

We then construct the set  $\mathcal{X}_N = \mathcal{D}_n \cup \mathcal{E}_{N-n}$  which, in simple words, is obtained by just combining both the labeled data and the unlabeled data with all the possible labels that can be assigned. The cardinality of  $\mathcal{X}_N$ , denoted as  $|\mathcal{X}_N|$ , is equal to  $2(N - n) + n$  (for simplicity we assume that all of the data points and the unlabeled observations are distinct).

Let us define  $\mathcal{P}(\mathcal{X}_N)$  to be the space of probability measures whose support is contained in  $\mathcal{X}_N$ . We use  $P_n$  to denote the empirical measure supported on the set  $\mathcal{D}_n$ , so  $P_n \in \mathcal{P}(\mathcal{X}_N)$ . In addition, we write  $E_P(\cdot)$  to denote the expectation associated with a given probability measure  $P$ .

Let us assume that we are interested in fitting a classification model by minimizing a given expected loss function  $l(X, Y, \beta)$ , where  $\beta$  is a parameter which uniquely characterizes the underlying model. We shall assume that  $l(X, Y, \cdot)$  is a convex function for each fixed  $(X, Y)$ . The empirical risk associated to the parameter  $\beta$  is

$$E_{P_n}(l(X, Y, \beta)) = \frac{1}{n} \sum_{i=1}^n l(X_i, Y_i, \beta).$$

In this paper, we propose to estimate  $\beta$  by solving the DRO problem

$$\min_{\beta} \max_{P \in \mathcal{P}(\mathcal{X}_N): D_c(P, P_n) \leq \delta^*} E_P[l(X, Y, \beta)], \quad (1)$$

where  $D_c(\cdot)$  is a suitably defined discrepancy between  $P_n$  and any probability measure  $P \in \mathcal{P}(\mathcal{X}_N)$  which is within a certain tolerance measured by  $\delta^*$ .

So, intuitively, (1) represents the value of a game in which the outer player (we) will choose  $\beta$  and the adversary player (nature) will rearrange the support and the mass of  $P_n$  within a budget measured by  $\delta^*$ . We then wish to minimize the expected risk regardless of the way in which the adversary might corrupt (within the prescribed budget) the existing evidence. In formulation (1), the adversary is crucial to ensure that we endow our mechanism for selecting  $\beta$  with the ability to cope with the risk impact of out-of-sample (i.e. out of the training set) scenarios. We denote the formulation in (1) as semi-supervised distributionally robust optimization (SSL-DRO).

The criterion that we use to define  $D_c(\cdot)$  is based on the theory of optimal transport and it is closely related to the concept of Wasserstein distance, see Section 3. The choice of  $D_c(\cdot)$  is motivated by recent results which show that popular estimators such as regularized logistic regression, Support Vector Machines (SVMs) and square-root Lasso (SR-Lasso) admit a DRO representation *exactly equal to* (1) in which the support  $\mathcal{X}_N$  is replaced by  $\mathbb{R}^{d+1}$  (see [6] and also equation (9) in this paper.)

In view of these representation results for supervised learning algorithms, the inclusion of  $\mathcal{X}_N$  in our DRO formulation (1) provides a natural SSL approach in the context of classification and regression. The goal of this paper is to enable the use of the distributionally robust training framework (1) as a SSL technique. We will show that estimating  $\beta$  via (1) may result in a significant improvement in generalization relative to natural supervised learning counterparts (such as regularized logistic regression and SR-Lasso). The potential improvement is illustrated in Section 4. Moreover, we show via numerical experiments in Section 5, that our method is able to improve upon state-of-the-art SSL algorithms.

As a contribution of independent interest, we construct a stochastic gradient descent algorithm to approximate the optimal selection,  $\beta_N^*$ , minimizing (1).

An important parameter when applying (1) is the size of the uncertainty region, which is parameterized by  $\delta^*$ . We apply cross-validation to calibrate  $\delta^*$ , but we also discuss the non-parametric behavior of an optimal selection of  $\delta^*$  (according to a suitably defined optimality criterion explained in Section 6) as  $n, N \rightarrow \infty$ .

In Section 2, we provide a broad overview of alternative procedures in the SSL literature, including recent approaches which are related to robust optimization. A key role in our formulation is played by  $\delta^*$ , which can be seen as a regularization parameter. This identification is highlighted in the form of (1) and the DRO representation of regularized logistic regression which we recall in (9). The optimal choice of  $\delta^*$  ensures statistical consistency as  $n, N \rightarrow \infty$ .

Similar robust optimization formulations to (1) for machine learning have been investigated in the literature recently. For example, connections between robust optimization and machine learning procedures such as Lasso and SVMs have been studied in the literature, see [23]. In contrast to this literature, the use of distributionally robust uncertainty allows to discuss the optimal size of the uncertainty region as the sample size increases (as we shall explain in Section 6). The work of [20] is among the first to study DRO representations

based on optimal transport, they do not study the implications of these types of DRO formulations in SSL as we do here.

We close this Introduction with a few important notes. First, our SSL-DRO is not a robustifying procedure for a given SSL algorithm. Instead, our contribution is in showing how to use unlabeled information on top of DRO to enhance traditional supervised learning methods. In addition, our SSL-DRO formulation, as stated in (1), is not restricted to logistic regression, instead DRO counterpart could be formulated for general supervised learning methods with various choice of loss function.

## 2 Alternative Semi-Supervised Learning Procedures

We shall briefly discuss alternative procedures which are known in the SSL literature, which are quite substantial. We refer the reader to the excellent survey of [24] for a general overview of the area. Our goal here is to expose the similarities and connections between our approach and some of the methods that have been adopted in the community.

For example, broadly speaking graph-based methods [7] and [9] attempt to construct a graph which represents a sketch of a lower dimensional manifold in which the predictive variables lie. Once the graph is constructed, a regularization procedure is performed, which seeks to enhance generalization error along the manifold while ensuring continuity in the prediction regarding an intrinsic metric. Our approach bypasses the construction of the graph, which we see as a significant advantage of our procedure. However, we believe that the construction of the graph can be used to inform the choice of cost function  $c(\cdot)$  which should reflect high transportation costs for moving mass away from the manifold sketched by the graph.

Some recent SSL estimators are based on robust optimization, such as the work of [1]. The difference between data-driven DRO and robust optimization is that the inner maximization in (1) for robust optimization is not over probability models which are variations of the empirical distribution. Instead, in robust optimization, one attempts to minimize the risk of the worst case performance of potential outcomes inside a given uncertainty set.

In [1], the robust uncertainty set is defined in terms of constraints obtained from the testing set. The problem with the approach in [1] is that there is no clear mechanism which informs an optimal size of the uncertainty set (which in our case is parameterized by  $\delta^*$ ). In fact, in the last paragraph of Section 2.3, [1] point out that the size of the uncertainty could have a significant detrimental impact in practical performance.

We conclude with a short discussion on the work of [14], which is related to our approach. In the context of linear discriminant analysis, [14] also proposes a distributionally robust optimization estimator, although completely different from the one we propose here. More importantly, we provide a way (both in theory and practice) to study the optimal size of the distributional uncertainty (i.e.  $\delta^*$ ), which allows us to achieve asymptotic consistency of our estimator.

### 3 Semi-supervised Learning based on DRO

This section is divided into two parts. First, we provide the elements of our DRO formulation. Then we will explain how to solve the SSL-DRO problem, i.e. find optimal  $\beta$  in (1).

#### 3.1 Defining the optimal transport discrepancy:

Assume that the cost function  $c : \mathbb{R}^{d+1} \times \mathbb{R}^{d+1} \rightarrow [0, \infty]$  is lower semi-continuous. As mentioned in the Introduction, we also assume that  $c(u, v) = 0$  if and only if  $u = v$ .

Now, given two distributions  $P$  and  $Q$ , with supports  $\mathcal{S}_P \subseteq \mathcal{X}_N$  and  $\mathcal{S}_Q \subseteq \mathcal{X}_N$ , respectively, we define the optimal transport discrepancy,  $D_c$ , via

$$D_c(P, Q) = \inf\{E_\pi[c(U, V)] : \pi \in \mathcal{P}(\mathcal{S}_P \times \mathcal{S}_Q), \pi_U = P, \pi_V = Q\}, \quad (2)$$

where  $\mathcal{P}(\mathcal{S}_P \times \mathcal{S}_Q)$  is the set of probability distributions  $\pi$  supported on  $\mathcal{S}_P \times \mathcal{S}_Q$ , and  $\pi_U$  and  $\pi_V$  denote the marginals of  $U$  and  $V$  under  $\pi$ , respectively.

If, in addition,  $c(\cdot)$  is symmetric (i.e.  $c(u, v) = c(v, u)$ ), and there exists  $\varrho \geq 1$  such that  $c^{1/\varrho}(u, w) \leq c^{1/\varrho}(u, v) + c^{1/\varrho}(v, w)$  (i.e.  $c^{1/\varrho}(\cdot)$  satisfies the triangle inequality), it can be easily verified (see [22]) that  $D_c^{1/\varrho}(P, Q)$  is a metric. For example, if  $c(u, v) = \|u - v\|_q^\varrho$  for  $q \geq 1$  (where  $\|u - v\|_q$  denotes the  $l_q$  norm in  $\mathbb{R}^{d+1}$ ) then  $D_c(\cdot)$  is known as the Wasserstein distance of order  $\varrho$ .

Observe that (2) is obtained by solving a linear programming problem. For example, suppose that  $Q = P_n$ , and let  $P \in \mathcal{P}(\mathcal{X}_N)$  then, using  $U = (X, Y)$ , we have that  $D_c(P, P_n)$  is obtained by computing

$$\begin{aligned} \min_{\pi} \{ & \sum_{u \in \mathcal{X}_N} \sum_{v \in \mathcal{D}_n} c(u, v) \pi(u, v) : \text{s.t.} \sum_{u \in \mathcal{X}_N} \pi(u, v) = \frac{1}{n} \forall v \in \mathcal{D}_n, \\ & \sum_{v \in \mathcal{D}_N} \pi(u, v) = P(\{u\}) \forall u \in \mathcal{X}_N, \pi(u, v) \geq 0 \forall (u, v) \in \mathcal{X}_N \times \mathcal{D}_n \} \end{aligned} \quad (3)$$

We shall discuss, for instance, how the choice of  $c(\cdot)$  in formulations such as (1) can be used to recover popular machine learning algorithms.

#### 3.2 Solving the SSL-DRO formulation:

A direct approach to solve (1) would involve alternating between minimization over  $\beta$ , which can be performed by, for example, stochastic gradient descent and maximization which is performed by solving a linear program similar to (3). Unfortunately, the large scale of the linear programming problem, which has  $O(N)$  variables and  $O(n)$  constraints, makes this direct approach rather difficult to apply in practice.

So, our goal here is to develop a direct stochastic gradient descent approach which can be used to approximate the solution to (1).

First, it is useful to apply linear programming duality to simplify (1). Note

that, given  $\beta$ , the inner maximization in (1) is simply

$$\begin{aligned} \max_{\pi} \{ & \sum_{u \in \mathcal{X}_N} \sum_{v \in \mathcal{D}_N} l(u, \beta) \pi(u, v) : \text{s.t. } \sum_{u \in \mathcal{X}_N} \pi(u, v) = \frac{1}{n} \forall v \in \mathcal{D}_n \quad (4) \\ & \sum_{u \in \mathcal{X}_N} \sum_{v \in \mathcal{D}_n} c(u, v) \pi(u, v) \leq \delta, \pi(u, v) \geq 0 \forall (u, v) \in \mathcal{X}_N \times \mathcal{D}_n \}. \end{aligned}$$

Of course, the feasible region in this linear program is always non-empty because the probability distribution  $\pi(u, v) = I(u = v) I(v \in \mathcal{D}_n) / n$  is a feasible choice. Also, the feasible region is clearly compact, so the dual problem is always feasible and by strong duality its optimal value coincides with that of the primal problem, see [2,3],blanchet2016robust. The dual problem associated to (4) is given by

$$\begin{aligned} \min \{ & \sum_{v \in \mathcal{D}_N} \gamma(v) / n + \lambda \delta \text{ s.t. } \gamma(v) \in \mathbb{R} \forall v \in \mathcal{D}_n, \lambda \geq 0, \quad (5) \\ & \gamma(v) \geq l(u, \beta) - \lambda c(u, v) \forall (u, v) \in \mathcal{X}_N \times \mathcal{D}_n. \} \end{aligned}$$

Maximizing over  $u \in \mathcal{X}_N$  in the inequality constraint, for each  $v$ , and using the fact that we are minimizing the objective function, we obtain that (5) can be simplified to

$$E_{P_n} [\max_{u \in \mathcal{X}_N} \{l(u, \beta) - \lambda c(u, (X, Y)) + \lambda \delta^*\}].$$

Consequently, defining  $\phi(X, Y, \beta, \lambda) = \max_{u \in \mathcal{X}_N} \{l(u, \beta) - \lambda c(u, (X, Y)) + \lambda \delta^*\}$ , we have that (1) is equivalent to

$$\min_{\lambda \geq 0, \beta} E_{P_n} [\phi(X, Y, \beta, \lambda)]. \quad (6)$$

Moreover, if we assume that  $l(u, \cdot)$  is a convex function, then we have that the mapping  $(\beta, \lambda) \mapsto l(u, \beta) - \lambda c(u, (X, Y)) + \lambda \delta^*$  is convex for each  $u$  and therefore,  $(\beta, \lambda) \mapsto \phi(X, Y, \beta, \lambda)$ , being the maximum of convex mappings is also convex.

A natural approach consists in directly applying stochastic sub-gradient descent (see [8] and [17]). Unfortunately, this would involve performing the maximization over all  $u \in \mathcal{X}_N$  in each iteration. This approach could be prohibitively expensive in typical machine learning applications where  $N$  is large.

So, instead, we perform a standard smoothing technique, namely, we introduce  $\epsilon > 0$  and define

$$\phi_{\epsilon}(X, Y, \beta, \lambda) = \lambda \delta^* + \epsilon \log \left( \sum_{u \in \mathcal{X}_N} \exp(\{l(u, \beta) - \lambda c(u, (X, Y))\} / \epsilon) \right).$$

It is easy to verify (using Hölder inequality) that  $\phi_{\epsilon}(X, Y, \cdot)$  is convex and it also follows that

$$\phi(X, Y, \beta, \lambda) \leq \phi_{\epsilon}(X, Y, \beta, \lambda) \leq \phi(X, Y, \beta, \lambda) + \log(|\mathcal{X}_N|)\epsilon.$$

Hence, we can choose  $\epsilon = O(1/\log N)$  in order to control the bias incurred by replacing  $\phi$  by  $\phi_{\epsilon}$ . Then, defining

$$\tau_{\epsilon}(X, Y, \beta, \lambda, u) = \exp(\{l(u, \beta) - \lambda c(u, (X, Y))\} / \epsilon),$$

we have (assuming differentiability of  $l(u, \beta)$ ) that

$$\begin{aligned}\nabla_{\beta}\phi_{\epsilon}(X, Y, \beta, \lambda) &= \frac{\sum_{u \in \mathcal{X}_N} \tau_{\epsilon}(X, Y, \beta, \lambda, u) \nabla_{\beta} l(u, \beta)}{\sum_{v \in \mathcal{X}_N} \tau_{\epsilon}(X, Y, \beta, \lambda, v)}, \\ \frac{\partial \phi_{\epsilon}(X, Y, \beta, \lambda)}{\partial \lambda} &= \delta^* - \frac{\sum_{u \in \mathcal{X}_N} \tau_{\epsilon}(X, Y, \beta, \lambda, u) c(u, (X, Y))}{\sum_{v \in \mathcal{X}_N} \tau_{\epsilon}(X, Y, \beta, \lambda, v)}.\end{aligned}\quad (7)$$

In order to make use of the gradient representations (7) for the construction of a stochastic gradient descent algorithm, we must construct unbiased estimators for  $\nabla_{\beta}\phi_{\epsilon}(X, Y, \beta, \lambda)$  and  $\partial\phi_{\epsilon}(X, Y, \beta, \lambda)/\partial\lambda$ , given  $(X, Y)$ . This can be easily done if we assume that one can simulate directly  $u \in \mathcal{X}_N$  with probability proportional to  $\tau(X, Y, \beta, \lambda, u)$ . Because of the potential size of  $\mathcal{X}_N$  and especially because such distribution depends on  $(X, Y)$  sampling with probability proportional to  $\tau_{\epsilon}(X, Y, \beta, \lambda, u)$  can be very time-consuming.

So, instead, we apply a strategy discussed in [4] and explained in Section 2.2.1. The proposed method produces random variables  $A(X, Y, \beta, \lambda)$  and  $\Gamma(X, Y, \beta, \lambda)$ , which can be simulated easily by drawing i.i.d. samples from the uniform distribution over  $\mathcal{X}_N$ , and such that

$$\begin{aligned}E(A(X, Y, \beta, \lambda) | X, Y) &= \partial_{\lambda}\phi_{\epsilon}(X, Y, \beta, \lambda), \\ E(\Gamma(X, Y, \beta, \lambda) | X, Y) &= \nabla_{\beta}\phi_{\epsilon}(X, Y, \beta, \lambda).\end{aligned}$$

Using this pair of random variables, then we apply the stochastic gradient descent recursion

$$\begin{aligned}\beta_{k+1} &= \beta_k - \alpha_{k+1}\Gamma(X_{k+1}, Y_{k+1}, \beta_k, \lambda_k), \\ \lambda_{k+1} &= (\lambda_k - \alpha_{k+1}A(X_{k+1}, Y_{k+1}, \beta_k, \lambda_k))^+, \end{aligned}\quad (8)$$

where learning sequence,  $\alpha_k > 0$  satisfies the standard conditions, namely,  $\sum_{k=1}^{\infty} \alpha_k = \infty$  and  $\sum_{k=1}^{\infty} \alpha_k^2 < \infty$ , see [21].

We apply a technique from [4] to construct the random variables  $A$  and  $\Gamma$ , which originates from Multilevel Monte Carlo introduced in [10], and associated randomization methods [16],[18].

First, define  $\bar{P}_N$  to be the uniform measure on  $\mathcal{X}_N$  and let  $W$  be a random variable with distribution  $\bar{P}_N$ . Note that, given  $(X, Y)$ ,

$$\begin{aligned}\nabla_{\beta}\phi_{\epsilon}(X, Y, \beta, \lambda) &= \frac{E_{\bar{P}_N}(\tau_{\epsilon}(X, Y, \beta, \lambda, W) \nabla_{\beta} l(W, \beta) | X, Y)}{E_{\bar{P}_N}(\tau_{\epsilon}(X, Y, \beta, \lambda, W) | X, Y)}, \\ \partial_{\lambda}\phi_{\epsilon}(X, Y, \beta, \lambda) &= \delta^* - \frac{E_{\bar{P}_N}(\tau_{\epsilon}(X, Y, \beta, \lambda, W) c(W, (X, Y)) | X, Y)}{E_{\bar{P}_N}(\tau_{\epsilon}(X, Y, \beta, \lambda, W) | X, Y)}.\end{aligned}$$

Note that both gradients can be written in terms of the ratios of two expectations. The following results from [4] can be used to construct unbiased estimators of functions of expectations. The function of interest in our case is the ratio of expectations.

Let us define:  $h_0(W) = \tau_\epsilon(X, Y, \beta, \lambda, W)$ ,  $h_1(W) = h_0(W) c(W, (X, Y))$ , and  $h_2(W) = h_0(W) \nabla_\beta l(W, \beta)$ , Then, we can write the gradient estimator as

$$\begin{aligned} \partial_\lambda \phi_\epsilon(X, Y, \beta, \lambda) &= \frac{E_{\bar{P}_N}(h_1(W) \mid X, Y)}{E_{\bar{P}_N}(h_0(W) \mid X, Y)}, \\ \text{and } \nabla_\beta \phi_\epsilon(X, Y, \beta, \lambda) &= \frac{E_{\bar{P}_N}(h_2(W) \mid X, Y)}{E_{\bar{P}_N}(h_0(W) \mid X, Y)}. \end{aligned}$$

The procedure developed in [4] proceeds as follows. First, define for a given  $h(W)$ , and  $n \geq 0$ , the average over odd and even labels to be

$$\bar{S}_{2^n}^E(h) = \frac{1}{2^n} \sum_{i=1}^{2^n} h(W_{2i}), \quad \bar{S}_{2^n}^O(h) = \frac{1}{2^n} \sum_{i=1}^{2^n} h(W_{2i-1}),$$

and the total average to be  $\bar{S}_{2^{n+1}}(h) = \frac{1}{2} (\bar{S}_{2^n}^E(h) + \bar{S}_{2^n}^O(h))$ . We then state the following algorithm for sampling unbiased estimators of  $\partial_\lambda \phi_\epsilon(X, Y, \beta, \lambda)$  and  $\nabla_\beta \phi_\epsilon(X, Y, \beta, \lambda)$  in Algorithm 1.

---

**Algorithm 1** Unbiased Gradient

---

- 1: Given  $(X, Y, \beta)$  the function outputs  $(\Lambda, \Gamma)$  such that  $E(\Lambda) = \partial_\lambda \phi_\epsilon(X, Y, \beta, \lambda)$  and  $E(\Gamma) = \nabla_\beta \phi_\epsilon(X, Y, \beta, \lambda)$ .
- 2: **Step1:** Sample  $G$  from geometric distribution with success parameter  $p_G = 1 - 2^{-3/2}$ .
- 3: **Step2:** Sample  $W_0, W_1, \dots, W_{2^{G+1}}$  i.i.d. copies of  $W$  independent of  $G$ .
- 4: **Step3:** Compute

$$\begin{aligned} \Delta^\lambda &= \frac{\bar{S}_{2^{G+1}}(h_1)}{\bar{S}_{2^{G+1}}(h_0)} - \frac{1}{2} \left( \frac{\bar{S}_{2^{G+1}}^O(h_1)}{\bar{S}_{2^{G+1}}^O(h_0)} + \frac{\bar{S}_{2^G}^E(h_1)}{\bar{S}_{2^G}^E(h_0)} \right), \\ \Delta^\beta &= \frac{\bar{S}_{2^{G+1}}(h_2)}{\bar{S}_{2^{G+1}}(h_0)} - \frac{1}{2} \left( \frac{\bar{S}_{2^{G+1}}^O(h_2)}{\bar{S}_{2^{G+1}}^O(h_0)} + \frac{\bar{S}_{2^G}^E(h_2)}{\bar{S}_{2^G}^E(h_0)} \right). \end{aligned}$$

5: **Output:**

---


$$\Lambda = \delta^* - \frac{\Delta^\lambda}{p_G(1-p_G)^G} - \frac{h_1(W_0)}{h_0(W_0)}, \quad \Gamma = \frac{\Delta^\beta}{p_G(1-p_G)^G} + \frac{h_2(W_0)}{h_0(W_0)}.$$


---

## 4 Error Improvement of Our SSL-DRO Formulation

Our goal in this section is to intuitively discuss why, owing to the inclusion of the constraint  $P \in \mathcal{P}(\mathcal{X}_N)$ , we expect desirable generalization properties of the SSL-DRO formulation (1). Moreover, our intuition suggests strongly why our SSL-DRO formulation should possess better generalization performance than natural supervised counterparts. We restrict the discussion for logistic regression due to the simple form of regularization connection we will make in (9), however, the error improvement discussion should also apply to general supervised learning setting.

As discussed in the Introduction using the game-theoretic interpretation of (1), by introducing  $\mathcal{P}(\mathcal{X}_N)$ , the SSL-DRO formulation provides a mechanism

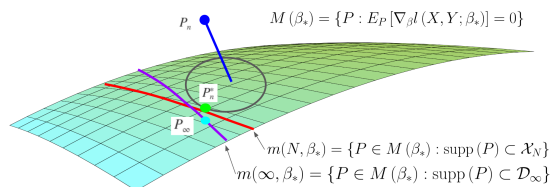
for choosing  $\beta$  which focuses on potential out-of-sample scenarios which are more relevant based on available evidence.

Suppose that the constraint  $P \in \mathcal{P}(\mathcal{X}_N)$  was not present in the formulation. So, the inner maximization in (1) is performed over all probability measures  $\mathcal{P}(\mathbb{R}^{d+1})$  (supported on some subset of  $\mathbb{R}^{d+1}$ ). As indicated earlier, we assume that  $l(X, Y; \cdot)$  is strictly convex and differentiable, so the first order optimality condition  $E_P(\nabla_{\beta} l(X, Y; \beta)) = 0$  characterizes the optimal choice of  $\beta$  assuming the validity of the probabilistic model  $P$ . It is natural to assume that there exists an actual model underlying the generation of the training data, which we denote as  $P_{\infty}$ . Moreover, we may also assume that there exists a unique  $\beta^*$  such that  $E_{P_{\infty}}(\nabla_{\beta} l(X, Y; \beta^*)) = 0$ .

The set  $\mathcal{M}(\beta_*) = \{P \in \mathcal{P}(\mathbb{R}^{d+1}) : E_P(\nabla_{\beta} l(X, Y; \beta^*)) = 0\}$  corresponds to the family of all probability models which correctly estimate  $\beta^*$ . Clearly,  $P_{\infty} \in \mathcal{M}(\beta_*)$ , whereas, typically,  $P_n \notin \mathcal{M}(\beta_*)$ . Moreover, if we write  $\mathcal{X}_{\infty} = \text{supp}(P_{\infty})$  we have that

$$P_{\infty} \in m(N, \beta^*) := \{P \in \mathcal{P}(\mathcal{X}_{\infty}) : E_P(\nabla_{\beta} l(X, Y; \beta^*)) = 0\} \subset \mathcal{M}(\beta_*).$$

Since  $\mathcal{X}_N$  provides a sketch of  $\mathcal{X}_{\infty}$ , then we expect to have that the extremal (i.e. worst case) measure, denoted by  $P_N^*$ , will be in some sense a better description of  $P_{\infty}$ .



0.2in

**Fig. 2.** Pictorial representation of the role that the support constraint plays in the SSL-DRO approach and how its presence enhances the out-of-sample performance.

Figure 2 provides a pictorial representation of the previous discussion. In the absence of the constraint  $P \in \mathcal{P}(\mathcal{X}_N)$ , the extremal measure chosen by nature can be interpreted as a projection of  $P_n$  onto  $\mathcal{M}(\beta_*)$ . In the presence of the constraint  $P \in \mathcal{P}(\mathcal{X}_N)$ , we can see that  $P_N^*$  may bring the learning procedure closer to  $P_{\infty}$ . Of course, if  $N$  is not large enough, the schematic may not be valid because one may actually have  $m(N, \beta^*) = \emptyset$ .

The previous discussion is useful to argue that our SSL-DRO formulation should be superior to the DRO formulation which is not informed by the unlabeled data. But this comparison may not directly apply to alternative supervised procedures that are mainstream in machine learning, which should be considered as the natural benchmark to compare with. Fortunately, replacing the constraint that  $P \in \mathcal{P}(\mathcal{X}_N)$  by  $P \in \mathcal{P}(\mathbb{R}^{d+1})$  in the DRO formulation recovers exactly supervised learning algorithms such as regularized logistic regression.

Recall from [6] that if  $l(x, y, \beta) = \log(1 + \exp(-y \cdot \beta^T x))$  and if we define

$$c((x, y), (x', y')) = \|x - x'\|_q I(y = y') + \infty I(y \neq y'),$$

for  $q \geq 1$  then, according to Theorem 3 in [6], we have that

$$\min_{\beta} \max_{D_c(P, P_n) \leq \bar{\delta}} E_P[l(X, Y, \beta)] = \min_{\beta \in \mathbb{R}^d} \left\{ E_{P_n}[l(X, Y, \beta)] + \bar{\delta} \|\beta\|_p \right\}, \quad (9)$$

where  $q$  satisfies  $1/p + 1/q = 1$ . Formulation (1) is, therefore, the natural SSL extension of the standard regularized logistic regression estimator.

We conclude that, for logistic regression, SSL-DRO as formulated in (1), is a natural SSL extension of the standard regularized logistic regression estimator, which would typically induce superior generalization abilities over its supervised counterparts, and similar discussion should apply to most supervised learning methods.

## 5 Numerical Experiments

We proceed to numerical experiments to verify the performance of our SSL-DRO method empirically using six binary classification real data sets from UCI machine learning data base [13].

We consider our SSL-DRO formulation based on logistic regression and compare with other state-of-the-art logistic regression based SSL algorithms, entropy regularized logistic regression with  $L_1$  regulation (ERLRL1) [11] and regularized logistic regression based self-training (STLRL1) [12]. In addition, we also compare with its supervised counterpart, which is regularized logistic regression (LRL1). For each iteration of a data set, we randomly split the data into labeled training, unlabeled training and testing set, we train the models on training sets and evaluate the testing error and accuracy with testing set. We report the mean and standard deviation for training and testing error using log-exponential loss and the average testing accuracy, which are calculated via 200 independent experiments for each data set. We summarize the detailed results, the basic information of the data sets, and our data split setting in Table 5.

We can observe that our SSL-DRO method has the potential to improve upon these state-of-the-art SSL algorithms.

## 6 Discussion on the Size of the Uncertainty Set

One of the advantages of DRO formulations such as (1) and (9) is that they lead to a natural criterion for the optimal choice of the parameter  $\delta^*$  or, in the case of (9), the choice of  $\bar{\delta}$  (which incidentally corresponds to the regularization parameter). The optimality criterion that we use to select the size of  $\delta^*$  is motivated by Figure 2.

First, interpret the uncertainty set

$$\mathcal{U}_{\delta}(P_n, \mathcal{X}_N) = \{P \in \mathcal{P}(\mathcal{X}_N) : D_c(P, P_n) \leq \delta\}$$

as the set of plausible models which are consistent with the empirical evidence encoded in  $P_n$  and  $\mathcal{X}_N$ . Then, for every plausible model  $P$ , we can compute

		Breast Cancer	qsar	Magic	Minibone	Spambase
LRL1	Train	.185 ± .123	.614 ± .038	.548 ± .087	.401 ± .167	.470 ± .040
	Test	.428 ± .338	.755 ± .019	.610 ± .050	.910 ± .131	.588 ± .141
	Accur	.929 ± .023	.646 ± .036	.665 ± .045	.717 ± .041	.811 ± .034
ERLRL1	Train	.019 ± .010	.249 ± .050	2.37 ± .987	.726 ± .353	.008 ± .028
	Test	.265 ± .146	.720 ± .029	4.28 ± 1.51	1.98 ± .678	.505 ± .108
	Accur	.944 ± .018	.731 ± .026	.721 ± .056	.708 ± .071	.883 ± .018
STLRL1	Train	.089 ± .019	.498 ± .120	3.05 ± .987	1.50 ± .706	.370 ± .082
	Test	.672 ± .034	2.37 ± .860	8.03 ± 1.51	4.81 ± .732	1.47 ± .316
	Accur	.955 ± .023	.694 ± .038	.692 ± .056	.704 ± .033	.843 ± .023
DROSSL	Train	.045 ± .023	.402 ± .039	.420 ± .075	.287 ± .047	.221 ± .028
	Test	.120 ± .029	.555 ± .025	.561 ± .039	.609 ± .054	.333 ± .012
	Accur	.956 ± .016	.734 ± .025	.733 ± .034	.710 ± .032	.892 ± .009
Num Predictors	30	30	10	20	56	
Labeled Size	40	80	30	30	150	
Unlabeled Size	200	500	9000	5000	1500	
Testing Size	329	475	9990	125034	2951	

**Table 1.** Numerical experiments for real data sets.

$\beta(P) = \arg \min_{\beta} E_P[l(X, Y, \beta)]$ , and therefore the set  $A_{\delta}(P_n, \mathcal{X}_N) = \{\beta(P) = \arg \min E_P[l(X, Y, \beta)] : P \in \mathcal{U}_{\delta}(P_n, \mathcal{X}_N)\}$  can be interpreted as a confidence region. It is then natural to select a confidence level  $\alpha \in (0, 1)$  and compute  $\delta^* := \delta_{N,n}^*$  by solving

$$\min\{\delta : P(\beta^* \in A_{\delta}(P_n, \mathcal{X}_N)) \geq 1 - \alpha\}. \quad (10)$$

Similarly, for the supervised version, we can select  $\bar{\delta} = \bar{\delta}_n$  by solving

$$\min\{\delta : P(\beta^* \in A_{\delta}(P_n, \mathbb{R}^{d+1})) \geq 1 - \alpha\}. \quad (11)$$

It is easy to see that  $\bar{\delta}_n \leq \delta_{N,n}^*$ . Now, we let  $N = \gamma n$  for some  $\gamma > 0$  and consider  $\delta_{N,n}^*, \bar{\delta}_n$  as  $n \rightarrow \infty$ . This analysis is relevant because we are attempting to sketch  $\text{supp}(P_{\infty})$  using the set  $\mathcal{X}_N$ , while considering large enough plausible variations to be able to cover  $\beta^*$  with  $1 - \alpha$  confidence.

More precisely, following the discussion in [6] for the supervised case in finding  $\bar{\delta}_n$  in (10) using Robust Wasserstein Profile (RWP) function, solving (11) for  $\delta_{N,n}^*$  is equivalent to finding the  $1 - \alpha$  quantile of the asymptotic distribution of the RWP function, defined as

$$R_n(\beta) = \min_{\pi} \left\{ \sum_{u \in \mathcal{X}_n} \sum_{v \in \mathcal{D}_n} c(u, v) \pi(u, v), \sum_{u \in \mathcal{X}_n} \pi(u, v) = \frac{1}{n}, \forall v \in \mathcal{D}_n, \right. \quad (12)$$

$$\left. \pi \subset \mathcal{P}(\mathcal{X}_n \times \mathcal{D}_n), \sum_{u \in \mathcal{X}_n} \sum_{v \in \mathcal{D}_n} \nabla_{\beta} l(u; \beta) \pi(u, v) = 0 \right\}.$$

The RWP function is the distance, measured by the optimal transport cost function, between the empirical distribution and the manifold of probability measures for which  $\beta_*$  is the optimal parameter. A pictorial representation is given in Figure 2. Additional discussion on the RWP function and its interpretations can be found in [6,5].

In the setting of the DRO formulation for (9) it is shown in [6], that  $\bar{\delta}_n = O(n^{-1})$  for (9) as  $n \rightarrow \infty$ . Intuitively, we expect that if the predictive variables possess a positive density supported in a lower dimensional manifold of dimension  $\bar{d} < d$ , then sketching  $\text{supp}(P_\infty)$  with  $O(n)$  data points will leave relatively large portions of the manifold unsampled (since, on average,  $O(n^{\bar{d}})$  sampled points are needed to be within distance  $O(1/n)$  of a given point in box of unit size in  $\bar{d}$  dimensions). The optimality criterion will recognize this type of discrepancy between  $\mathcal{X}_N$  and  $\text{supp}(P_\infty)$ . Therefore, we expect that  $\delta_{\gamma n, n}^*$  will converge to zero at a rate which might deteriorate slightly as  $\bar{d}$  increases.

This intuition is given rigorous support in Theorem 1 for linear regression with square loss function and  $L_2$  cost function for DRO. In turn, Theorem 1 follows as a corollary to the results in [5]. To make our paper self-contained, we have the detailed assumptions and a sketch of proof in the appendix.

**Theorem 1.** *1 Assume the linear regression model  $Y = \beta^* X + e$  with square loss function, i.e.  $l(X, X; \beta) = (Y - \beta^T X)^2$ , and transport cost*

$$c((x, y), (x', y')) = \|x - x'\|_2^2 I_{y=y'} + \infty I_{y \neq y'}.$$

*Assume  $N = \gamma n$  and under mild assumptions on  $(X, Y)$ , if we denote  $\tilde{Z} \sim \mathcal{N}(0, E[V_1])$ , we have:*

- *When  $d = 1$ ,  $nR_n(\beta_*) \Rightarrow \kappa_1 \chi_1^2$ .*
- *When  $d = 2$ ,  $nR_n(\beta_*) \Rightarrow F_2(\tilde{Z})$ , where  $F_2(\cdot)$  is a continuous function and  $F_2(z) = O(\|z\|_2^2)$  as  $\|z\|_2 \rightarrow \infty$ .*
- *When  $d \geq 3$ ,  $n^{1/2 + \frac{3}{2d+2}} R_n(\beta_*) \Rightarrow F_d(\tilde{Z})$ , where  $F_d(\cdot)$  is a continuous function (depending on  $d$ ) and  $F_d(z) = O(\|z\|_2^{d/2+1})$ .*

It is shown in Theorem 1 for SSL linear regression that when  $q = 2$ ,  $\delta_{\gamma n, n}^* = O(n^{-1/2 - 3/(2\bar{d}+2)})$  for  $\bar{d} \geq 3$ , and  $\delta_{\gamma n, n}^* = O(n^{-1})$  for  $\bar{d} = 1, 2$ . A similar argument can be made for logistic regression as well. We believe that this type of analysis and its interpretation is of significant interest and we expect to report a more complete picture in the future, including the case  $q \geq 1$  (which we believe should obey the same scaling).

## 7 Conclusions

We have shown that our SSL-DRO, as a semi-supervised method, is able to enhance the generalization predicting power versus its supervised counterpart. Our numerical experiments show superior performance of our SSL-DRO method when compared to state-of-the-art SSL algorithms such as ERLRL1 and STLRL1. We would like to emphasize that our SSL-DRO method is not restricted to linear and logistic regressions. As we can observe from the DRO formulation and the algorithm. If a learning algorithm has an accessible loss function and the loss gradient can be computed, we are able to formulate the SSL-DRO problem and benefit from unlabeled information. Finally, we discussed a stochastic gradient descent technique for solving DRO problems such as (1), which we believe can be applied to other settings in which the gradient is a non-linear function of easy-to-sample expectations.

## References

1. Akshay Balsubramani and Yoav Freund. Scalable semi-supervised aggregation of classifiers. In *NIPS*, pages 1351–1359, 2015.
2. Dimitris Bertsimas, David Brown, and Constantine Caramanis. Theory and applications of robust optimization. *SIAM review*, 53(3):464–501, 2011.
3. Dimitris Bertsimas, Vishal Gupta, and Nathan Kallus. Data-driven robust optimization. *arXiv preprint arXiv:1401.0212*, 2013.
4. Jose Blanchet and Peter Glynn. Unbiased Monte Carlo for optimization and functions of expectations via multi-level randomization. In *Proceedings of the 2015 Winter Simulation Conference*, pages 3656–3667. IEEE Press, 2015.
5. Jose Blanchet and Yang Kang. Sample out-of-sample inference based on wasserstein distance. *arXiv preprint arXiv:1605.01340*, 2016.
6. Jose Blanchet, Yang Kang, and Karthyek Murthy. Robust wasserstein profile inference and applications to machine learning. *arXiv preprint*, 2016.
7. Avrim Blum and Shuchi Chawla. Learning from labeled and unlabeled data using graph mincuts. 2001.
8. Stephen Boyd and Lieven Vandenberghe. *Convex optimization*. Cambridge university press, 2004.
9. Olivier Chapelle, Bernhard Scholkopf, and Alexander Zien. Semi-supervised learning. *IEEE Transactions on Neural Networks*, 20(3):542–542, 2009.
10. Michael Giles. Multilevel Monte Carlo path simulation. *Operations Research*, 56(3), 2008.
11. Yves Grandvalet and Yoshua Bengio. Semi-supervised learning by entropy minimization. In *Advances in NIPS*, pages 529–536, 2005.
12. Yuanqing Li, Cuntai Guan, Huiqi Li, and Zhengyang Chin. A self-training semi-supervised svm algorithm and its application in an eeg-based brain computer interface speller system. *Pattern Recognition Letters*, 29(9):1285–1294, 2008.
13. Moshe Lichman. UCI machine learning repository, 2013.
14. Marco Loog. Contrastive pessimistic likelihood estimation for semi-supervised classification. *IEEE transactions on pattern analysis and machine intelligence*, 38(3):462–475, 2016.
15. David G Luenberger. *Introduction to linear and nonlinear programming*, volume 28. Addison-Wesley Reading, MA, 1973.
16. Don McLeish. A general method for debiasing a Monte Carlo estimator. *Monte Carlo Meth. and Appl.*, 17(4):301–315, 2011.
17. Sundhar Ram, Angelia Nedić, and Venugopal Veeravalli. Distributed stochastic subgradient projection algorithms for convex optimization. *Journal of optimization theory and applications*, 147(3):516–545, 2010.
18. Chang-han Rhee and Peter Glynn. Unbiased estimation with square root convergence for SDE models. *Operations Research*, 63(5):1026–1043, 2015.
19. Yossi Rubner, Carlo Tomasi, and Leonidas Guibas. The earth mover’s distance as a metric for image retrieval. *International journal of computer vision*, 2000.
20. Soroosh Shafieezadeh-Abadeh, Peyman Mohajerin Esfahani, and Daniel Kuhn. Distributionally robust logistic regression. In *NIPS*, pages 1576–1584, 2015.
21. Alexander Shapiro, Darinka Dentcheva, et al. *Lectures on stochastic programming: modeling and theory*, volume 16. Siam, 2014.
22. Cédric Villani. *Optimal transport: old and new*, volume 338. Springer Science & Business Media, 2008.
23. Huan Xu, Constantine Caramanis, and Shie Mannor. Robust regression and lasso. In *Advances in Neural Information Processing Systems*, pages 1801–1808, 2009.
24. Xiaojin Zhu, John Lafferty, and Ronald Rosenfeld. *Semi-supervised learning with graphs*. Carnegie Mellon University, 2005.

## A Supplementary Material: Technical Details for Theorem 1

In this supplementary appendix, we first state the general assumptions to guarantee the validity of the asymptotically optimal selection for the distributional uncertainty size in Section A.1. In Section A.2 and A.3 we revisit Theorem 1 and provide a more detailed proof.

### A.1 Assumptions of Theorem 1

For linear regression model, let us assume we have a collection of labeled data  $\mathcal{D}_n = \{(X_i, Y_i)\}_{i=1}^n$  and a collection of unlabeled data  $\{X_i\}_{i=n+1}^N$ . We consider the set  $\mathcal{X}_N = \{X_i\}_{i=1}^N \times \{Y_i\}_{i=1}^n$ , to be the cross product of all the predictors from labeled and unlabeled data and the labeled responses. In order to have proper asymptotic results holds for the RWP function, we require some mild assumptions on the density and moments of  $(X, Y)$  and estimating equation  $\nabla_{\beta} l(X, Y; \beta) = (Y - \beta_*^T) X$ . We state them explicitly as follows:

**A)** We assume the predictors  $X_i$ 's for the labeled and unlabeled data are i.i.d. from the same distribution with positive differentiable density  $f_X(\cdot)$  with bounded bounded gradients.

**B)** We assume the  $\beta_* \in \mathbb{R}^d$  is the true parameter and under null hypothesis of the linear regression model satisfying  $Y = \beta_*^T X + e$ , where  $e$  is a random error independent of  $X$ .

**C)** We assume  $E[X^T X]$  exists and is positive definite and  $E[e^2] < \infty$ .

**D)** For the true model of labeled data, we have  $E_{P_*}[X(Y - \beta_*^T X)] = 0$  (where  $P_*$  denotes the actual population distribution which is unknown).

The first two assumptions, namely Assumption A and B, are elementary assumptions for linear regression model with an additive independent random error. The requirements for the differentiable positive density for the predictor  $X$ , is because when  $d \geq 3$ , the density function appears in the asymptotic distribution. Assumption C is a mild requirement on the moments exist for predictors and error, and Assumption D is to guarantee true parameter  $\beta_*$  could be characterized via first order optimality condition, i.e. the gradient of the square loss function. Due to the simple structure of the linear model, with the above four assumptions, we can prove Theorem 1 and we show a sketch in the following subsection.

### A.2 Revisit Theorem 1

In this section, we revisit the asymptotic result for optimally choosing uncertainty size for semi-supervised learning for the linear regression model. We assume that, under the null hypothesis,  $Y = \beta_*^T X + e$ , where  $X \in \mathbb{R}^d$  is the predictors,  $e$  is independent of  $X$  as random error, and  $\beta_* \in \mathbb{R}^d$  is the true parameter. We consider the square loss function and assume that  $\beta_*$  is the minimizer to the square loss function, i.e.

$$\beta_* = \arg \min_{\beta} E \left[ (Y - \beta^T X)^2 \right].$$

If we can assume the second-moment exists for  $X$  and  $e$ , then we can switch the order of expectation and derivative w.r.t.  $\beta$ , then optimal  $\beta$  could be uniquely characterized via the first order optimality condition,

$$E [X (Y - \beta_*^T X)] = 0.$$

As we discussed in Section 6, the optimal distributional uncertainty size  $\delta_{n,N}^*$  at confidence level  $1 - \alpha$ , is simply the  $1 - \alpha$  quantile of the RWP function defined in (12). In turn, the asymptotic limit of the RWP function is characterized in Theorem 1, which we restate more explicitly here.

**Theorem 1**[Restate of Theorem 1 in Section 6] For linear regression model we defined above and square loss function, if we take cost function for DRO formulation to be

$$c((x, y), (x', y')) = \|x - x'\|_2^2 I_{y=y'} + \infty I_{y \neq y'}.$$

If we assume Assumptions A,B, and D stated in Section A.1 to be true and number of unlabeled data satisfying  $N = \gamma n$ . Furthermore, let us denote:  $V_i = (e_i I - X_i \beta_*^T) (e_i I - \beta_*^T X_i^T)$ , where  $e_i = Y_i - \beta_*^T X_i$  being the residual under the null hypothesis. Then, we have:

- When  $d = 1$ ,

$$nR_n(\beta_*) \Rightarrow \frac{E [X_1^2 e_1^2]}{E [(e_1 - \beta_*^T X_1)^2]} \chi_1^2.$$

- When  $d = 2$ ,

$$nR_n(\beta_*) \Rightarrow 2\tilde{\zeta}(\tilde{Z})^T \tilde{Z} - \tilde{\zeta}(\tilde{Z})^T \tilde{G}_2(\tilde{\zeta}(\tilde{Z})) \tilde{\zeta}(\tilde{Z}),$$

where  $\tilde{Z} \sim \mathcal{N}(0, E[V_1])$ ,  $\tilde{G}_2 : \mathbb{R}^2 \rightarrow \mathbb{R}^2 \times \mathbb{R}^2$  is a continuous mapping defined as

$$\tilde{G}_2(\zeta) = E [V_1 \max(1 - \tau/(\zeta^T V_1 \zeta), 0)],$$

and  $\tilde{\zeta} : \mathbb{R}^2 \rightarrow \mathbb{R}^2$  is a continuous mapping, such that  $\tilde{\zeta}(\tilde{Z})$  is the unique solution to

$$\tilde{Z} = -E [V_1 I_{(\tau \leq \zeta^T V_1 \zeta)}] \zeta.$$

- When  $d \geq 3$ ,

$$n^{1/2 + \frac{3}{2d+2}} R_n(\beta_*) \Rightarrow -2\tilde{\zeta}(\tilde{Z})^T \tilde{Z} - \frac{2}{d+2} \tilde{G}_3(\tilde{\zeta}(\tilde{Z})),$$

where  $\tilde{Z} \sim \mathcal{N}(0, E[V_1])$ ,  $\tilde{G}_2 : \mathbb{R}^d \rightarrow \mathbb{R}$  is a deterministic continuous function defined as

$$\tilde{G}_2(\zeta) = E \left[ \frac{\pi^{d/2} \gamma f_X(X_1)}{\Gamma(d/2 + 1)} (\zeta^T V_1 \zeta)^{d/2+1} \right],$$

and  $\tilde{\zeta} : \mathbb{R}^d \rightarrow \mathbb{R}^d$  is a continuous mapping, such that  $\tilde{\zeta}(\tilde{Z})$  is the unique solution to

$$\tilde{Z} = -E \left[ V_1 \frac{\pi^{d/2} \gamma f_X(X_1)}{\Gamma(d/2 + 1)} (\zeta^T V_1 \zeta)^d \right] \zeta.$$

### A.3 Proof of Theorem 1

In this section, we provide a detailed proof for Theorem 1. As we discussed before, Theorem 1 could be treated as a non-trivial corollary of Theorem 3 in [5] and the proving techniques follow the 6-step proof for Sample-out-of-Sample (SoS) Theorem, namely Theorem 1 and Theorem 3 in [5].

*Proof (Proof of Theorem 1).* **Step 1.** For  $u \in \mathcal{D}_n$  and  $v \in \mathcal{X}_N$ , let us denote  $u_x, u_y$  and  $v_x, v_y$  to be its subvectors for the predictor and response. By the definition of RWP function as in (12), we can write it as a linear program (LP), given as

$$R_n(\beta_*) = \min_{\pi} \left\{ \sum_{u \in \mathcal{D}_n} \sum_{v \in \mathcal{X}_N} \pi(u, v) \left( \|u_x - v_x\|_2^2 I_{v_y = u_y} + \infty I_{v_y \neq u_y} \right) \right. \\ \text{s.t. } \pi \in \mathcal{P}(\mathcal{X}_N \times \mathcal{D}_n), \\ \sum_{u \in \mathcal{D}_n} \sum_{v \in \mathcal{X}_N} \pi(u, v) v_x (v_y - \beta_*^T v_x) = 0, \\ \left. \sum_{v \in \mathcal{X}_N} \pi(u, v) = 1/n, \forall u \in \mathcal{D}_n. \right\}$$

For as  $n$  large enough the LP is finite and feasible (because  $P_n$  approaches  $P_*$ , and  $P_*$  is feasible). Thus, for  $n$  large enough we can write

$$R_n(\beta_*) = \min_{\pi} \left\{ \sum_{u \in \mathcal{D}_n} \sum_{v_x \in \{X_i\}_{i=1}^N} \pi(u, v_x) \|u_x - v_x\|_2^2 \right. \\ \text{s.t. } \pi \in \mathcal{P}(\mathcal{X}_N \times \mathcal{D}_n) \\ \sum_{u \in \mathcal{D}_n} \sum_{v \in \mathcal{X}_N} \pi(u, v) v_x (u_y - \beta_*^T v_x) = 0, \\ \left. \sum_{v \in \mathcal{X}_N} \pi(u, v) = 1/n, \forall u \in \mathcal{D}_n. \right\}$$

We can apply strong duality theorem for LP, see [15], and write the RWP function in dual form:

$$R_n(\beta_*) = \max_{\lambda} \left\{ \frac{1}{n} \sum_{i=1}^n \min_{j=1, N} \left\{ -\lambda^T X_j (Y_i - \beta_*^T X_j) + \|X_i - X_j\|_2^2 \right\} \right\}, \\ = \max_{\lambda} \left\{ \frac{1}{n} \sum_{i=1}^n -\lambda^T X_i (Y_i - \beta_*^T X_i) \right. \\ \left. + \min_{j=1, N} \left\{ \lambda^T X_i (Y_i - \beta_*^T X_j) - \lambda^T X_j (Y_i - \beta_*^T X_j) + \|X_i - X_j\|_2^2 \right\} \right\}.$$

This finishes Step 1 as in the 6-step proving technique introduced in Section 3 of [5].

**Step 2 and Step 3,** When  $d = 1$  and  $2$ , we consider scaling the RWP function by  $n$  and let define  $\zeta = \sqrt{n}\lambda/2$  and denote  $W_n = n^{-1/2} \sum_{i=1}^n X_i e_i$ , we have the scaled RWP function becomes,

$$\begin{aligned} nR_n(\beta_*) &= \max_{\zeta} \{ -\zeta^T W_n \\ &+ \sum_{i=1}^n \min_{j=1, N} \{ -2 \frac{\zeta^T}{\sqrt{n}} X_j (Y_i - \beta_*^T X_j) + 2 \frac{\zeta^T}{\sqrt{n}} X_i (Y_i - \beta_*^T X_i) + \|X_i - X_j\|_2^2 \} \}. \end{aligned}$$

For each fixed  $i$ , let us consider the inner minimization problem,

$$\min_{j=1, N} \{ -2 \frac{\zeta^T}{\sqrt{n}} X_j (Y_i - \beta_*^T X_j) + 2 \frac{\zeta^T}{\sqrt{n}} X_i (Y_i - \beta_*^T X_i) + \|X_i - X_j\|_2^2 \}$$

Similar to Section 3 in [5], we would like to solve the minimization problem by first replacing  $X_j$  by  $a$ , which is a free variable without support constraint in  $\mathbb{R}^d$ , then quantify the gap. We then obtain a lower bound for the optimization problem via

$$\min_a \{ -2 \frac{\zeta^T}{\sqrt{n}} a (Y_i - \beta_*^T a) + 2 \frac{\zeta^T}{\sqrt{n}} X_i (Y_i - \beta_*^T X_i) + \|X_i - a\|_2^2 \}. \quad (13)$$

As we can observe in (13), the coefficient of second order of  $a$  is of order  $O(1/\sqrt{n})$  for any fixed  $\zeta$ , and the coefficients for the last term is always 1, it is easy to observe that, as  $n$  large enough, (13) has an optimizer in the interior.

We can solve for the optimizer  $a = \bar{a}_*(X_i, Y_i, \zeta)$  of the lower bound in (13) satisfying the first order optimality condition as

$$\begin{aligned} \bar{a}_*(X_i, Y_i, \zeta) - X_i &= (e_i I - \beta_*^T X_i) \frac{\zeta}{\sqrt{n}} \\ &+ (\beta_*^T (\bar{a}_*(X_i, Y_i, \zeta) - X_i) I - (\bar{a}_*(X_i, Y_i, \zeta) - X_i) \beta_*^T) \frac{\zeta}{\sqrt{n}}. \end{aligned} \quad (14)$$

Since the optimizer  $\bar{a}_*(X_i, Y_i, \zeta)$  is in the interior, it is easy to notice from (14) that  $\bar{a}_*(X_i, Y_i, \zeta) - X_i = O\left(\frac{\|\zeta\|_2}{\sqrt{n}}\right)$ . Plug in the estimate back into (14) obtain

$$\bar{a}_*(X_i, Y_i, \zeta) = X_i + (e_i I - \beta_*^T X_i) \frac{\zeta}{\sqrt{n}} + O\left(\frac{\|\zeta\|_2^2}{n}\right). \quad (15)$$

Let us define  $a_*(X_i, Y_i, \zeta) = X_i + (e_i I - \beta_*^T X_i) \frac{\zeta}{\sqrt{n}}$ . Using (15), we have

$$\|a_*(X_i, Y_i, \zeta) - \bar{a}_*(X_i, Y_i, \zeta)\|_2 = O\left(\frac{\|\zeta\|_2^2}{n}\right). \quad (16)$$

Then, for the optimal value function of lower bound of the inner optimization problem, we have:

$$\begin{aligned}
& -2\frac{\zeta^T}{\sqrt{n}}\bar{a}_*(X_i, Y_i, \zeta)(Y_i - \beta_*^T a) + 2\frac{\zeta^T}{\sqrt{n}}X_i(Y_i - \beta_*^T X_i) + \|X_i - \bar{a}_*(X_i, Y_i, \zeta)\|_2^2 \\
& = -2\frac{\zeta^T}{\sqrt{n}}a_*(X_i, Y_i, \zeta)(Y_i - \beta_*^T a) + 2\frac{\zeta^T}{\sqrt{n}}X_i(Y_i - \beta_*^T X_i) \\
& \quad + \|X_i - a_*(X_i, Y_i, \zeta)\|_2^2 + O\left(\frac{\|\zeta\|_2^3}{n^{3/2}}\right) \\
& = \frac{\zeta^T V_i \zeta}{n} + O\left(\frac{\|\zeta\|_2^3}{n^{3/2}}\right). \tag{17}
\end{aligned}$$

For the above equation, first equality is due to (16) and the second equality is by the estimation of  $\bar{a}_*(X_i, Y_i, \zeta)$  in (15).

Then for each fixed  $i$ , let us define a point process

$$N_n^{(i)}(t, \zeta) = \# \left\{ X_j : \|X_j - a_*(X_i, Y_i, \zeta)\|_2^2 \leq t^{2/d}/n^{2/d}, X_j \neq X_i \right\}.$$

We denote  $T_i(n)$  to be the first jump time of  $N_n^{(i)}(t, \zeta)$ , i.e.

$$T_i(n) = \inf \left\{ t \geq 0 : N_n^{(i)}(t, \zeta) \geq 1 \right\}.$$

It is easy to observe that, as  $n$  goes to infinity, we have

$$N_n^{(i)}(t, \zeta) | X_i \Rightarrow Poi(\Lambda(X_i, \zeta), t),$$

where  $Poi(\Lambda(X_i, \zeta), t)$  denotes a Poisson point process with rate

$$\Lambda(X_i, \zeta) = \gamma f_X \left( X_i + \frac{\zeta}{2\sqrt{\zeta}} \right) \frac{\pi^{d/2}}{\Gamma(d/2 + 1)}.$$

Then, the conditional survival function for  $T_i(n)$ , i.e.  $P(T_i(n) \geq t | X_i)$  is

$$P(T_i(n) \geq t | X_i) = \exp(-\Lambda(X_i, \zeta)t) \left( 1 + O\left(1/n^{1/d}\right) \right),$$

and we can define  $\tau_i$  to be the random variable with survival function being

$$P(\tau_i(n) \geq t | X_i) = \exp(-\Lambda(X_i, \zeta)t).$$

We can also integrate the dependence on  $X_i$  and define  $\tau$  satisfying

$$P(\tau \geq t) = E[\exp(-\Lambda(X_1, \zeta)t)].$$

Therefore, for  $d = 1$  by the definition of  $T_i(n)$  and the estimation in (17), we have the scaled RWP function becomes

$$nR_n(\beta_*) = \max_{\zeta} \left\{ -2\zeta W_n - \frac{1}{n} \sum_{i=1}^n \max \left( \zeta^T V_i \zeta - T_i(n)^2/n + O\left(\frac{\|\zeta\|_2^3}{n^{3/2}}\right), 0 \right) \right\}$$

The sequence of global optimizers is tight as  $n \rightarrow \infty$ , because according to Assumption C,  $E(V_i)$  is assumed to be strictly positive definite with probability one. In turn, from the previous expression we can apply Lemma 1 in [5] and use the fact that the variable  $\zeta$  can be restricted to compact sets for all  $n$  sufficiently large. We are then able to conclude

$$nR_n(\beta_*) = \max_{\zeta} \{ -2\zeta^T W_n - E[\max(\zeta^T V_i \zeta - T_i(n)^2/n, 0)] \} + o_p(1). \quad (18)$$

When  $d = 2$ , a similar estimation applies as for the case  $d = 1$ . the scaled RWP function becomes

$$nR_n(\beta_*) = \max_{\zeta} \{ -2\zeta^T W_n - E[\max(\zeta^T V_i \zeta - T_i(n)^2, 0)] \} + o_p(1). \quad (19)$$

For the case when  $d \geq 3$ , let us define  $\zeta = \lambda/(2n^{\frac{3}{2d+2}})$ . We follow a similar estimation procedure as in the cases  $d = 1, 2$ . We also define identical auxiliary Poisson point process, we can write the scaled RWP function to be

$$\begin{aligned} n^{\frac{1}{2} + \frac{3}{2d+2}} R_n(\beta_*) &= \max_{\zeta} \{ -2\zeta^T W_n \\ &\quad - n^{\frac{1}{2} + \frac{3}{2d+2} - \frac{2}{d}} E[\max(n^{\frac{2}{d} - \frac{6}{2d+2}} \zeta^T V_i \zeta - T_i(n)^{3/d}, 0)] \} + o_p(1). \end{aligned} \quad (20)$$

This addresses Step 2 and 3 in the proof.

**Step 4:** when  $d = 1$ , as  $n \rightarrow \infty$ , we have the scaled RWP function given in (18). Let us use  $G_1 : \mathbb{R} \rightarrow \mathbb{R}$  to denote a deterministic continuous function defined as

$$G_1(\zeta, n) = E[\max(\zeta^T V_i \zeta - T_i(n)^2/n, 0)].$$

By Assumption C, we know  $EV_i$  is positive, thus  $G_1$  as a function of  $\zeta$  is strictly convex. Thus the optimizer for the scaled RWP function could be uniquely characterized via the first order optimality condition, which is equivalent to

$$\zeta_n^* = -\frac{W_n}{E[V_i]} + o_p(1), \text{ as } n \rightarrow \infty. \quad (21)$$

We plug in (21) into (18) and let  $n \rightarrow \infty$ . Applying the CLT for  $W_n$  and the continuous mapping theorem, we have

$$\begin{aligned} nR_n(\beta_*) &= 2W_n^2/E[V_1] - G_1\left(-\frac{W_n}{E[V_1]}, n\right) + o_p(1) \\ &\Rightarrow \frac{\tilde{Z}^2}{E[V_1]} = \frac{E[X_1^2 e_1^2]}{E[(e_1 - \beta_* X_1)^2]} \chi_1^2, \end{aligned}$$

where  $W_n \Rightarrow \tilde{Z}$  and  $\tilde{Z} \sim \mathcal{N}\left(0, E[(e_1 - \beta_* X_1)^2]\right)$ .

We conclude the stated convergence for  $d = 1$ .

**Step 5:** when  $d = 2$ , as  $n \rightarrow \infty$ , we have the scaled RWP function given in (19). Let us use  $G_2 : \mathbb{R} \times \mathbb{N} \rightarrow \mathbb{R}$  to denote a deterministic continuous function defined as

$$G_2(\zeta, n) = E \left[ \max(\zeta^T V_i \zeta - T_i(n)^2, 0) \right].$$

Following the same discussion as in Step 4 for the case  $d = 1$ , we know that the optimizer  $\zeta_n^*$  can be uniquely characterized via first order optimality condition given as

$$W_n = -E \left[ V_1 I_{(\tau \leq \zeta^T V_1 \zeta)} \right] \zeta + o_p(1), \text{ as } n \rightarrow \infty.$$

Since we know that the objective function is strictly convex there exist a continuous mapping,  $\tilde{\zeta} : \mathbb{R}^2 \rightarrow \mathbb{R}^2$ , such that  $\tilde{\zeta}(W_n)$  is the unique solution to

$$W_n = -E \left[ V_1 I_{(\tau \leq \zeta^T V_1 \zeta)} \right] \zeta.$$

Then, we can plug-in the first order optimality condition to the value function, and the scaled RWP function becomes,

$$n\mathbb{R}_n(\beta_*) = 2\tilde{\zeta}(W_n)^T W_n - G_2(\tilde{\zeta}(W_n), n) + o_p(1).$$

Applying Lemma 2 of [5] we can show that as  $n \rightarrow \infty$ ,

$$n\mathbb{R}_n(\beta_*) \Rightarrow 2\tilde{\zeta}(\tilde{Z})^T \tilde{Z} - \tilde{\zeta}(\tilde{Z})^T \tilde{G}_2(\tilde{\zeta}(\tilde{Z})) \tilde{\zeta}(\tilde{Z})$$

where  $\tilde{G}_2 : \mathbb{R}^2 \rightarrow \mathbb{R}^2 \times \mathbb{R}^2$  is a continuous mapping defined as

$$\tilde{G}_2(\zeta) = E \left[ V_1 \max(1 - \tau / (\zeta^T V_1 \zeta), 0) \right].$$

This concludes the claim for  $d = 2$ .

**Step 6:** when  $d = 3$ , as  $n \rightarrow \infty$ , we have the scaled RWP function given in (20). Let us write  $G_3 : \mathbb{R} \times \mathbb{N} \rightarrow \mathbb{R}$  to denote a deterministic continuous function defined as

$$G_3(\zeta, n) = n^{\frac{1}{2} + \frac{3}{2d+2} - \frac{2}{d}} E \left[ \max(n^{\frac{2}{2} - \frac{6}{2d+2}} \zeta^T V_i \zeta - T_i(n)^{3/d}, 0) \right].$$

Same as discussed in Step 4 and 5, the objective function is strictly convex and the optimizer could be uniquely characterized via first order optimality condition, i.e.

$$W_n = -E \left[ V_1 \frac{\pi^{d/2} \gamma f_X(X_1)}{\Gamma(d/2 + 1)} (\zeta^T V_1 \zeta)^d \right] \zeta + o_p(1), \text{ as } n \rightarrow \infty.$$

Since we know that the objective function is strictly convex, there exist a continuous mapping,  $\tilde{\zeta} : \mathbb{R}^d \rightarrow \mathbb{R}^d$ , such that  $\tilde{\zeta}(W_n)$  is the unique solution to

$$W_n = -E \left[ V_1 \frac{\pi^{d/2} \gamma f_X(X_1)}{\Gamma(d/2 + 1)} (\zeta^T V_1 \zeta)^d \right] \zeta.$$

Let us plug-in the optimality condition and the scaled RWP function becomes

$$n^{\frac{1}{2} + \frac{3}{2d+2}} R_n(\beta_*) = -2\tilde{\zeta}(W_n)^T W_n - G_3\left(\tilde{\zeta}(W_n, n)\right) + o_p(1).$$

As  $n \rightarrow \infty$ , we can apply Lemma 2 in [5] to derive estimation for the RWP function and it leads to

$$n^{\frac{1}{2} + \frac{3}{2d+2}} R_n(\beta_*) \Rightarrow -2\tilde{\zeta}(\tilde{Z})^T \tilde{Z} - \frac{2}{d+2} \tilde{G}_3\left(\tilde{\zeta}(\tilde{Z})\right),$$

where  $\tilde{G}_2 : \mathbb{R}^d \rightarrow \mathbb{R}$  is a deterministic continuous function defined as

$$\tilde{G}_2(\zeta) = E \left[ \frac{\pi^{d/2} \gamma f_X(X_1)}{\Gamma(d/2 + 1)} (\zeta^T V_1 \zeta)^{d/2+1} \right].$$

This concludes the case when  $d \geq 3$  and for Theorem 1.



## A Supplementary Material: Technical Details for Theorem 1

In this supplementary appendix, we first state the general assumptions to guarantee the validity of the asymptotically optimal selection for the distributional uncertainty size in Section A.1. In Section A.2 and A.3 we revisit Theorem 1 and provide a more detailed proof.

### A.1 Assumptions of Theorem 1

For linear regression model, let us assume we have a collection of labeled data  $\mathcal{D}_n = \{(X_i, Y_i)\}_{i=1}^n$  and a collection of unlabeled data  $\{X_i\}_{i=n+1}^N$ . We consider the set  $\mathcal{X}_N = \{X_i\}_{i=1}^N \times \{Y_i\}_{i=1}^n$ , to be the cross product of all the predictors from labeled and unlabeled data and the labeled responses. In order to have proper asymptotic results holds for the RWP function, we require some mild assumptions on the density and moments of  $(X, Y)$  and estimating equation  $\nabla_{\beta} l(X, Y; \beta) = (Y - \beta_*^T) X$ . We state them explicitly as follows:

**A)** We assume the predictors  $X_i$ 's for the labeled and unlabeled data are i.i.d. from the same distribution with positive differentiable density  $f_X(\cdot)$  with bounded bounded gradients.

**B)** We assume the  $\beta_* \in \mathbb{R}^d$  is the true parameter and under null hypothesis of the linear regression model satisfying  $Y = \beta_*^T X + e$ , where  $e$  is a random error independent of  $X$ .

**C)** We assume  $E[X^T X]$  exists and is positive definite and  $E[e^2] < \infty$ .

**D)** For the true model of labeled data, we have  $E_{P_*}[X(Y - \beta_*^T X)] = 0$  (where  $P_*$  denotes the actual population distribution which is unknown).

The first two assumptions, namely Assumption A and B, are elementary assumptions for linear regression model with an additive independent random error. The requirements for the differentiable positive density for the predictor  $X$ , is because when  $d \geq 3$ , the density function appears in the asymptotic distribution. Assumption C is a mild requirement on the moments exist for predictors and error, and Assumption D is to guarantee true parameter  $\beta_*$  could be characterized via first order optimality condition, i.e. the gradient of the square loss function. Due to the simple structure of the linear model, with the above four assumptions, we can prove Theorem 1 and we show a sketch in the following subsection.

### A.2 Revisit Theorem 1

In this section, we revisit the asymptotic result for optimally choosing uncertainty size for semi-supervised learning for the linear regression model. We assume that, under the null hypothesis,  $Y = \beta_*^T X + e$ , where  $X \in \mathbb{R}^d$  is the predictors,  $e$  is independent of  $X$  as random error, and  $\beta_* \in \mathbb{R}^d$  is the true parameter. We consider the square loss function and assume that  $\beta_*$  is the minimizer to the square loss function, i.e.

$$\beta_* = \arg \min_{\beta} E \left[ (Y - \beta^T X)^2 \right].$$

If we can assume the second-moment exists for  $X$  and  $e$ , then we can switch the order of expectation and derivative w.r.t.  $\beta$ , then optimal  $\beta$  could be uniquely characterized via the first order optimality condition,

$$E [X (Y - \beta_*^T X)] = 0.$$

As we discussed in Section 6, the optimal distributional uncertainty size  $\delta_{n,N}^*$  at confidence level  $1 - \alpha$ , is simply the  $1 - \alpha$  quantile of the RWP function defined in (12). In turn, the asymptotic limit of the RWP function is characterized in Theorem 1, which we restate more explicitly here.

**Theorem 1**[Restate of Theorem 1 in Section 6] For linear regression model we defined above and square loss function, if we take cost function for DRO formulation to be

$$c((x, y), (x', y')) = \|x - x'\|_2^2 I_{y=y'} + \infty I_{y \neq y'}.$$

If we assume Assumptions A,B, and D stated in Section A.1 to be true and number of unlabeled data satisfying  $N = \gamma n$ . Furthermore, let us denote:  $V_i = (e_i I - X_i \beta_*^T) (e_i I - \beta_*^T X_i^T)$ , where  $e_i = Y_i - \beta_*^T X_i$  being the residual under the null hypothesis. Then, we have:

- When  $d = 1$ ,

$$nR_n(\beta_*) \Rightarrow \frac{E [X_1^2 e_1^2]}{E [(e_1 - \beta_*^T X_1)^2]} \chi_1^2.$$

- When  $d = 2$ ,

$$nR_n(\beta_*) \Rightarrow 2\tilde{\zeta}(\tilde{Z})^T \tilde{Z} - \tilde{\zeta}(\tilde{Z})^T \tilde{G}_2(\tilde{\zeta}(\tilde{Z})) \tilde{\zeta}(\tilde{Z}),$$

where  $\tilde{Z} \sim \mathcal{N}(0, E[V_1])$ ,  $\tilde{G}_2 : \mathbb{R}^2 \rightarrow \mathbb{R}^2 \times \mathbb{R}^2$  is a continuous mapping defined as

$$\tilde{G}_2(\zeta) = E [V_1 \max(1 - \tau/(\zeta^T V_1 \zeta), 0)],$$

and  $\tilde{\zeta} : \mathbb{R}^2 \rightarrow \mathbb{R}^2$  is a continuous mapping, such that  $\tilde{\zeta}(\tilde{Z})$  is the unique solution to

$$\tilde{Z} = -E [V_1 I_{(\tau \leq \zeta^T V_1 \zeta)}] \zeta.$$

- When  $d \geq 3$ ,

$$n^{1/2 + \frac{3}{2d+2}} R_n(\beta_*) \Rightarrow -2\tilde{\zeta}(\tilde{Z})^T \tilde{Z} - \frac{2}{d+2} \tilde{G}_3(\tilde{\zeta}(\tilde{Z})),$$

where  $\tilde{Z} \sim \mathcal{N}(0, E[V_1])$ ,  $\tilde{G}_2 : \mathbb{R}^d \rightarrow \mathbb{R}$  is a deterministic continuous function defined as

$$\tilde{G}_2(\zeta) = E \left[ \frac{\pi^{d/2} \gamma f_X(X_1)}{\Gamma(d/2 + 1)} (\zeta^T V_1 \zeta)^{d/2+1} \right],$$

and  $\tilde{\zeta} : \mathbb{R}^d \rightarrow \mathbb{R}^d$  is a continuous mapping, such that  $\tilde{\zeta}(\tilde{Z})$  is the unique solution to

$$\tilde{Z} = -E \left[ V_1 \frac{\pi^{d/2} \gamma f_X(X_1)}{\Gamma(d/2 + 1)} (\zeta^T V_1 \zeta)^d \right] \zeta.$$

### A.3 Proof of Theorem 1

In this section, we provide a detailed proof for Theorem 1. As we discussed before, Theorem 1 could be treated as a non-trivial corollary of Theorem 3 in [5] and the proving techniques follow the 6-step proof for Sample-out-of-Sample (SoS) Theorem, namely Theorem 1 and Theorem 3 in [5].

*Proof (Proof of Theorem 1).* **Step 1.** For  $u \in \mathcal{D}_n$  and  $v \in \mathcal{X}_N$ , let us denote  $u_x, u_y$  and  $v_x, v_y$  to be its subvectors for the predictor and response. By the definition of RWP function as in (12), we can write it as a linear program (LP), given as

$$R_n(\beta_*) = \min_{\pi} \left\{ \sum_{u \in \mathcal{D}_n} \sum_{v \in \mathcal{X}_N} \pi(u, v) \left( \|u_x - v_x\|_2^2 I_{v_y = u_y} + \infty I_{v_y \neq u_y} \right) \right. \\ \text{s.t. } \pi \in \mathcal{P}(\mathcal{X}_N \times \mathcal{D}_n), \\ \sum_{u \in \mathcal{D}_n} \sum_{v \in \mathcal{X}_N} \pi(u, v) v_x (v_y - \beta_*^T v_x) = 0, \\ \left. \sum_{v \in \mathcal{X}_N} \pi(u, v) = 1/n, \forall u \in \mathcal{D}_n. \right\}$$

For as  $n$  large enough the LP is finite and feasible (because  $P_n$  approaches  $P_*$ , and  $P_*$  is feasible). Thus, for  $n$  large enough we can write

$$R_n(\beta_*) = \min_{\pi} \left\{ \sum_{u \in \mathcal{D}_n} \sum_{v_x \in \{X_i\}_{i=1}^N} \pi(u, v_x) \|u_x - v_x\|_2^2 \right. \\ \text{s.t. } \pi \in \mathcal{P}(\mathcal{X}_N \times \mathcal{D}_n) \\ \sum_{u \in \mathcal{D}_n} \sum_{v \in \mathcal{X}_N} \pi(u, v) v_x (u_y - \beta_*^T v_x) = 0, \\ \left. \sum_{v \in \mathcal{X}_N} \pi(u, v) = 1/n, \forall u \in \mathcal{D}_n. \right\}$$

We can apply strong duality theorem for LP, see [15], and write the RWP function in dual form:

$$R_n(\beta_*) = \max_{\lambda} \left\{ \frac{1}{n} \sum_{i=1}^n \min_{j=1, N} \left\{ -\lambda^T X_j (Y_i - \beta_*^T X_j) + \|X_i - X_j\|_2^2 \right\} \right\}, \\ = \max_{\lambda} \left\{ \frac{1}{n} \sum_{i=1}^n -\lambda^T X_i (Y_i - \beta_*^T X_i) \right. \\ \left. + \min_{j=1, N} \left\{ \lambda^T X_i (Y_i - \beta_*^T X_j) - \lambda^T X_j (Y_i - \beta_*^T X_j) + \|X_i - X_j\|_2^2 \right\} \right\}.$$

This finishes Step 1 as in the 6-step proving technique introduced in Section 3 of [5].

**Step 2 and Step 3,** When  $d = 1$  and  $2$ , we consider scaling the RWP function by  $n$  and let define  $\zeta = \sqrt{n}\lambda/2$  and denote  $W_n = n^{-1/2} \sum_{i=1}^n X_i e_i$ , we have the scaled RWP function becomes,

$$\begin{aligned} nR_n(\beta_*) &= \max_{\zeta} \{ -\zeta^T W_n \\ &+ \sum_{i=1}^n \min_{j=1, N} \{ -2 \frac{\zeta^T}{\sqrt{n}} X_j (Y_i - \beta_*^T X_j) + 2 \frac{\zeta^T}{\sqrt{n}} X_i (Y_i - \beta_*^T X_i) + \|X_i - X_j\|_2^2 \} \}. \end{aligned}$$

For each fixed  $i$ , let us consider the inner minimization problem,

$$\min_{j=1, N} \{ -2 \frac{\zeta^T}{\sqrt{n}} X_j (Y_i - \beta_*^T X_j) + 2 \frac{\zeta^T}{\sqrt{n}} X_i (Y_i - \beta_*^T X_i) + \|X_i - X_j\|_2^2 \}$$

Similar to Section 3 in [5], we would like to solve the minimization problem by first replacing  $X_j$  by  $a$ , which is a free variable without support constraint in  $\mathbb{R}^d$ , then quantify the gap. We then obtain a lower bound for the optimization problem via

$$\min_a \{ -2 \frac{\zeta^T}{\sqrt{n}} a (Y_i - \beta_*^T a) + 2 \frac{\zeta^T}{\sqrt{n}} X_i (Y_i - \beta_*^T X_i) + \|X_i - a\|_2^2 \}. \quad (13)$$

As we can observe in (13), the coefficient of second order of  $a$  is of order  $O(1/\sqrt{n})$  for any fixed  $\zeta$ , and the coefficients for the last term is always 1, it is easy to observe that, as  $n$  large enough, (13) has an optimizer in the interior.

We can solve for the optimizer  $a = \bar{a}_*(X_i, Y_i, \zeta)$  of the lower bound in (13) satisfying the first order optimality condition as

$$\begin{aligned} \bar{a}_*(X_i, Y_i, \zeta) - X_i &= (e_i I - \beta_*^T X_i) \frac{\zeta}{\sqrt{n}} \\ &+ (\beta_*^T (\bar{a}_*(X_i, Y_i, \zeta) - X_i) I - (\bar{a}_*(X_i, Y_i, \zeta) - X_i) \beta_*^T) \frac{\zeta}{\sqrt{n}}. \end{aligned} \quad (14)$$

Since the optimizer  $\bar{a}_*(X_i, Y_i, \zeta)$  is in the interior, it is easy to notice from (14) that  $\bar{a}_*(X_i, Y_i, \zeta) - X_i = O\left(\frac{\|\zeta\|_2}{\sqrt{n}}\right)$ . Plug in the estimate back into (14) obtain

$$\bar{a}_*(X_i, Y_i, \zeta) = X_i + (e_i I - \beta_*^T X_i) \frac{\zeta}{\sqrt{n}} + O\left(\frac{\|\zeta\|_2^2}{n}\right). \quad (15)$$

Let us define  $a_*(X_i, Y_i, \zeta) = X_i + (e_i I - \beta_*^T X_i) \frac{\zeta}{\sqrt{n}}$ . Using (15), we have

$$\|a_*(X_i, Y_i, \zeta) - \bar{a}_*(X_i, Y_i, \zeta)\|_2 = O\left(\frac{\|\zeta\|_2^2}{n}\right). \quad (16)$$

Then, for the optimal value function of lower bound of the inner optimization problem, we have:

$$\begin{aligned}
& -2\frac{\zeta^T}{\sqrt{n}}\bar{a}_*(X_i, Y_i, \zeta)(Y_i - \beta_*^T a) + 2\frac{\zeta^T}{\sqrt{n}}X_i(Y_i - \beta_*^T X_i) + \|X_i - \bar{a}_*(X_i, Y_i, \zeta)\|_2^2 \\
& = -2\frac{\zeta^T}{\sqrt{n}}a_*(X_i, Y_i, \zeta)(Y_i - \beta_*^T a) + 2\frac{\zeta^T}{\sqrt{n}}X_i(Y_i - \beta_*^T X_i) \\
& \quad + \|X_i - a_*(X_i, Y_i, \zeta)\|_2^2 + O\left(\frac{\|\zeta\|_2^3}{n^{3/2}}\right) \\
& = \frac{\zeta^T V_i \zeta}{n} + O\left(\frac{\|\zeta\|_2^3}{n^{3/2}}\right). \tag{17}
\end{aligned}$$

For the above equation, first equality is due to (16) and the second equality is by the estimation of  $\bar{a}_*(X_i, Y_i, \zeta)$  in (15).

Then for each fixed  $i$ , let us define a point process

$$N_n^{(i)}(t, \zeta) = \#\left\{X_j : \|X_j - a_*(X_i, Y_i, \zeta)\|_2^2 \leq t^{2/d}/n^{2/d}, X_j \neq X_i\right\}.$$

We denote  $T_i(n)$  to be the first jump time of  $N_n^{(i)}(t, \zeta)$ , i.e.

$$T_i(n) = \inf\left\{t \geq 0 : N_n^{(i)}(t, \zeta) \geq 1\right\}.$$

It is easy to observe that, as  $n$  goes to infinity, we have

$$N_n^{(i)}(t, \zeta) | X_i \Rightarrow Poi(\Lambda(X_i, \zeta), t),$$

where  $Poi(\Lambda(X_i, \zeta), t)$  denotes a Poisson point process with rate

$$\Lambda(X_i, \zeta) = \gamma f_X\left(X_i + \frac{\zeta}{2\sqrt{\zeta}}\right) \frac{\pi^{d/2}}{\Gamma(d/2 + 1)}.$$

Then, the conditional survival function for  $T_i(n)$ , i.e.  $P(T_i(n) \geq t | X_i)$  is

$$P(T_i(n) \geq t | X_i) = \exp(-\Lambda(X_i, \zeta)t) \left(1 + O\left(1/n^{1/d}\right)\right),$$

and we can define  $\tau_i$  to be the random variable with survival function being

$$P(\tau_i(n) \geq t | X_i) = \exp(-\Lambda(X_i, \zeta)t).$$

We can also integrate the dependence on  $X_i$  and define  $\tau$  satisfying

$$P(\tau \geq t) = E[\exp(-\Lambda(X_1, \zeta)t)].$$

Therefore, for  $d = 1$  by the definition of  $T_i(n)$  and the estimation in (17), we have the scaled RWP function becomes

$$nR_n(\beta_*) = \max_{\zeta} \left\{ -2\zeta W_n - \frac{1}{n} \sum_{i=1}^n \max\left(\zeta^T V_i \zeta - T_i(n)^2/n + O\left(\frac{\|\zeta\|_2^3}{n^{3/2}}\right), 0\right) \right\}$$

The sequence of global optimizers is tight as  $n \rightarrow \infty$ , because according to Assumption C,  $E(V_i)$  is assumed to be strictly positive definite with probability one. In turn, from the previous expression we can apply Lemma 1 in [5] and use the fact that the variable  $\zeta$  can be restricted to compact sets for all  $n$  sufficiently large. We are then able to conclude

$$nR_n(\beta_*) = \max_{\zeta} \left\{ -2\zeta^T W_n - E \left[ \max \left( \zeta^T V_i \zeta - T_i(n)^2/n, 0 \right) \right] \right\} + o_p(1). \quad (18)$$

When  $d = 2$ , a similar estimation applies as for the case  $d = 1$ . the scaled RWP function becomes

$$nR_n(\beta_*) = \max_{\zeta} \left\{ -2\zeta^T W_n - E \left[ \max \left( \zeta^T V_i \zeta - T_i(n)^2, 0 \right) \right] \right\} + o_p(1). \quad (19)$$

For the case when  $d \geq 3$ , let us define  $\zeta = \lambda/(2n^{\frac{3}{2d+2}})$ . We follow a similar estimation procedure as in the cases  $d = 1, 2$ . We also define identical auxiliary Poisson point process, we can write the scaled RWP function to be

$$\begin{aligned} n^{\frac{1}{2} + \frac{3}{2d+2}} R_n(\beta_*) &= \max_{\zeta} \left\{ -2\zeta^T W_n \right. & (20) \\ &\left. - n^{\frac{1}{2} + \frac{3}{2d+2} - \frac{2}{d}} E \left[ \max \left( n^{\frac{2}{d} - \frac{6}{2d+2}} \zeta^T V_i \zeta - T_i(n)^{3/d}, 0 \right) \right] \right\} + o_p(1). \end{aligned}$$

This addresses Step 2 and 3 in the proof.

**Step 4:** when  $d = 1$ , as  $n \rightarrow \infty$ , we have the scaled RWP function given in (18). Let us use  $G_1 : \mathbb{R} \rightarrow \mathbb{R}$  to denote a deterministic continuous function defined as

$$G_1(\zeta, n) = E \left[ \max \left( \zeta^T V_i \zeta - T_i(n)^2/n, 0 \right) \right].$$

By Assumption C, we know  $EV_i$  is positive, thus  $G_1$  as a function of  $\zeta$  is strictly convex. Thus the optimizer for the scaled RWP function could be uniquely characterized via the first order optimality condition, which is equivalent to

$$\zeta_n^* = -\frac{W_n}{E[V_i]} + o_p(1), \text{ as } n \rightarrow \infty. \quad (21)$$

We plug in (21) into (18) and let  $n \rightarrow \infty$ . Applying the CLT for  $W_n$  and the continuous mapping theorem, we have

$$\begin{aligned} nR_n(\beta_*) &= 2W_n^2/E[V_1] - G_1 \left( -\frac{W_n}{E[V_1]}, n \right) + o_p(1) \\ &\Rightarrow \frac{\tilde{Z}^2}{E[V_1]} = \frac{E[X_1^2 e_1^2]}{E[(e_1 - \beta_* X_1)^2]} \chi_1^2, \end{aligned}$$

where  $W_n \Rightarrow \tilde{Z}$  and  $\tilde{Z} \sim \mathcal{N} \left( 0, E \left[ (e_1 - \beta_* X_1)^2 \right] \right)$ .

We conclude the stated convergence for  $d = 1$ .

**Step 5:** when  $d = 2$ , as  $n \rightarrow \infty$ , we have the scaled RWP function given in (19). Let us use  $G_2 : \mathbb{R} \times \mathbb{N} \rightarrow \mathbb{R}$  to denote a deterministic continuous function defined as

$$G_2(\zeta, n) = E \left[ \max(\zeta^T V_i \zeta - T_i(n)^2, 0) \right].$$

Following the same discussion as in Step 4 for the case  $d = 1$ , we know that the optimizer  $\zeta_n^*$  can be uniquely characterized via first order optimality condition given as

$$W_n = -E \left[ V_1 I_{(\tau \leq \zeta^T V_1 \zeta)} \right] \zeta + o_p(1), \text{ as } n \rightarrow \infty.$$

Since we know that the objective function is strictly convex there exist a continuous mapping,  $\tilde{\zeta} : \mathbb{R}^2 \rightarrow \mathbb{R}^2$ , such that  $\tilde{\zeta}(W_n)$  is the unique solution to

$$W_n = -E \left[ V_1 I_{(\tau \leq \zeta^T V_1 \zeta)} \right] \tilde{\zeta}.$$

Then, we can plug-in the first order optimality condition to the value function, and the scaled RWP function becomes,

$$n\mathbb{R}_n(\beta_*) = 2\tilde{\zeta}(W_n)^T W_n - G_2(\tilde{\zeta}(W_n), n) + o_p(1).$$

Applying Lemma 2 of [5] we can show that as  $n \rightarrow \infty$ ,

$$n\mathbb{R}_n(\beta_*) \Rightarrow 2\tilde{\zeta}(\tilde{Z})^T \tilde{Z} - \tilde{\zeta}(\tilde{Z})^T \tilde{G}_2(\tilde{\zeta}(\tilde{Z})) \tilde{\zeta}(\tilde{Z})$$

where  $\tilde{G}_2 : \mathbb{R}^2 \rightarrow \mathbb{R}^2 \times \mathbb{R}^2$  is a continuous mapping defined as

$$\tilde{G}_2(\zeta) = E \left[ V_1 \max(1 - \tau/(\zeta^T V_1 \zeta), 0) \right].$$

This concludes the claim for  $d = 2$ .

**Step 6:** when  $d = 3$ , as  $n \rightarrow \infty$ , we have the scaled RWP function given in (20). Let us write  $G_3 : \mathbb{R} \times \mathbb{N} \rightarrow \mathbb{R}$  to denote a deterministic continuous function defined as

$$G_3(\zeta, n) = n^{\frac{1}{2} + \frac{3}{2d+2} - \frac{2}{d}} E \left[ \max(n^{\frac{2}{2d+2} - \frac{6}{2d+2}} \zeta^T V_i \zeta - T_i(n)^{3/d}, 0) \right].$$

Same as discussed in Step 4 and 5, the objective function is strictly convex and the optimizer could be uniquely characterized via first order optimality condition, i.e.

$$W_n = -E \left[ V_1 \frac{\pi^{d/2} \gamma f_X(X_1)}{\Gamma(d/2 + 1)} (\zeta^T V_1 \zeta)^d \right] \zeta + o_p(1), \text{ as } n \rightarrow \infty.$$

Since we know that the objective function is strictly convex, there exist a continuous mapping,  $\tilde{\zeta} : \mathbb{R}^d \rightarrow \mathbb{R}^d$ , such that  $\tilde{\zeta}(W_n)$  is the unique solution to

$$W_n = -E \left[ V_1 \frac{\pi^{d/2} \gamma f_X(X_1)}{\Gamma(d/2 + 1)} (\zeta^T V_1 \zeta)^d \right] \tilde{\zeta}.$$

Let us plug-in the optimality condition and the scaled RWP function becomes

$$n^{\frac{1}{2} + \frac{3}{2d+2}} R_n(\beta_*) = -2\tilde{\zeta}(W_n)^T W_n - G_3\left(\tilde{\zeta}(W_n, n)\right) + o_p(1).$$

As  $n \rightarrow \infty$ , we can apply Lemma 2 in [5] to derive estimation for the RWP function and it leads to

$$n^{\frac{1}{2} + \frac{3}{2d+2}} R_n(\beta_*) \Rightarrow -2\tilde{\zeta}(\tilde{Z})^T \tilde{Z} - \frac{2}{d+2} \tilde{G}_3\left(\tilde{\zeta}(\tilde{Z})\right),$$

where  $\tilde{G}_2 : \mathbb{R}^d \rightarrow \mathbb{R}$  is a deterministic continuous function defined as

$$\tilde{G}_2(\zeta) = E \left[ \frac{\pi^{d/2} \gamma f_X(X_1)}{\Gamma(d/2 + 1)} (\zeta^T V_1 \zeta)^{d/2+1} \right].$$

This concludes the case when  $d \geq 3$  and for Theorem 1.

# Application of a power-exponential function based model to mortality rates forecasting

Andromachi Boulougari<sup>1c</sup>, Karl Lundengård<sup>1a</sup>, Milica Rančić<sup>1a</sup>, Sergei Silvestrov<sup>1a</sup>, Samya Suleiman<sup>1a</sup>, and Belinda Strass<sup>1b</sup>

<sup>a</sup> Department of Mathematics/Applied Mathematics, UKK, Mälardalen University, Västerås, Sweden,  
{karl.lundengård,milica.rančić,sergei.silvestrov,samya.suleiman}@mdh.se  
<sup>b</sup> belinda.strass@gmail.com, <sup>c</sup> a.boulougari@acg.edu

**Abstract.** Mortality rates of living organisms or equipment are modelled in different ways. Variation of mortality over a life span has different characteristics that put constraints and requirements on a model developed to represent it. A well-know problem that complicates modelling of human mortality rates is the "accident hump" occurring in early adulthood. The mortality rate model based on power-exponential functions, previously proposed by the authors, behaves as expected in that life period. Here, it will be compared to other models usually applied in practice and to empirical data. Models will be fitted to known data of measured death rates from many different countries using numerical techniques for curve-fitting with the non-linear least squares method. The properties of the model with respect to quality of fit and usefulness in applications such as insurance pricing or forecasting with the Lee-Carter method will be discussed.

**Keywords:** Mortality rates modelling, power-exponential function, non-linear curve fitting, Lee-Carter method.

## 1 Introduction

Understanding how the probability of surviving to or beyond a certain age is, can be an important question for insurers, actuaries, demographers and policies makers. For some purposes a simple mathematical model can be desirable. Consider an individual whose current age is  $x$  and whose age at time of death is denoted  $T_x$  then the survival function is defined as  $Pr[T_x > t] = S_x(t)$ . Often, this function is not analysed directly, instead the model is based on the mortality rate (also known as death rate or hazard rate)  $\mu(x) = -\ln(S_x(x+1))$ .

For most developed countries the observed behaviour of the mortality rate is  $\mu(x) \sim \frac{1}{x}$  for small  $x$  and  $\ln(\mu(x)) \propto x$  for large  $x$ , and a 'hump' for  $x$  that corresponds to early adolescence is typically most pronounced around age 25.

Modelling all the factors that can affect the lifespan of an individual is not feasible, so often a highly simplified models is used. For this paper we will consider only a few parametric models. Many of these have already been suggested, see Table 1. We will suggest two more and compare some of their properties to another pair of models.

For many applications it is also important to be able to forecast how the mortality rate will change in the future. There are several methods of producing the forecasts but the method proposed by Lee and Carter in 1992, [2] seems



Model	Mortality rate
Gompertz-Makeham [21]	$\mu(x) = a + be^{cx}$
Double Geometric [21]	$\mu(x) = a + b_1b_2^x + c_1c_2^x$
Thiele [1]	$\mu(x) = a_1e^{-b_1x} + a_2e^{-b_2\frac{(x-c)^2}{2}} + a_3e^{b_3x}$
Modified Perks [22]	$\mu(x) = \frac{a}{1 + e^{b-cx}} + d$
Gompertz-inverse Gaussian [22]	$\mu(x) = \frac{e^{a-bx}}{\sqrt{1 + e^{-c+bx}}}$
Weibull [19]	$\mu(x) = \frac{a}{b} \left(\frac{x}{b}\right)^{a-1}$
Heligman-Pollard HP1 [18]	$\mu(x) = a_1^{(x+a_2)^{a_3}} + b_1e^{-b_2\ln\left(\frac{x}{b_3}\right)^2} + c_1c_2^x$
Heligman-Pollard HP2 [18]	$\mu(x) = a_1^{(x+a_2)^{a_3}} + b_1e^{-b_2\ln\left(\frac{x}{b_3}\right)^2} + \frac{c_1c_2^x}{1 + c_1c_2^x}$
Heligman-Pollard HP3 [18]	$\mu(x) = a_1^{(x+a_2)^{a_3}} + b_1e^{-b_2\ln\left(\frac{x}{b_3}\right)^2} + \frac{c_1c_2^x}{1 + c_3c_1c_2^x}$
Heligman-Pollard HP4 [18]	$\mu(x) = a_1^{(x+a_2)^{a_3}} + b_1e^{-b_2\ln\left(\frac{x}{b_3}\right)^2} + \frac{c_1c_2^{x^{c_3}}}{1 + c_1c_2^{x^{c_3}}}$
Logistic [6]	$\mu(x) = \frac{ae^{bx}}{1 + \frac{ac}{b}(e^{bx} - 1)}$
Log-logistic [Pham, 2008]	$\mu(x) = \frac{abx^{a-1}}{1 + bx^a}$
Hannerz [20]	$\mu(x) = \frac{g(x)e^{G(x)}}{1 + e^{G(x)}}, g(x) = \frac{a_1}{x^2} + a_2x + a_3e^{cx}, G(x) = a_0 - \frac{a_1}{x} + \frac{a_2x^2}{2} + \frac{a_3}{c}e^{cx}$

**Table 1.** List of some models of mortality rate, note that references give a source that supplies a more detailed descriptions, not necessarily original source.

to be generally accepted, because it produces satisfactory fits and forecasts of mortality rates for various countries. Secondly, the structure of the Lee-Carter (L-C) model allows for easy computation of confidence intervals related to mortality projections.

The improved performance of the L-C model can be seen in the number and variety of mortality models that extended the original of L-C approach, see [4], [5], [6], [8] and [10] for examples of these extensions. These models extended the L-C approach by including additional period effects and in some cases cohort effects.

Lee and Carter developed their approach specifically for U.S. mortality data, 1900-1989 and forecasted (over a 50 year forecast horizon), 1990-2065. However, the method is now being applied to mortality data from many countries and time periods, all well beyond the application for which it was designed [3]. The LC model has been used for fitting and forecasting the mortality rates

for countries like: the United States [2], Chile [11], China [12], Japan [13], the seven most economically developed nations (G7) [15], India [14], [7], the Nordic countries [10], Sri Lanka [9] and [16].

In this paper we will fit several models to measured data and then use the fitted model to produce values for the L-C method and examine the differences in the predictions based on the different models.

## 2 Mortality rate modelled using power-exponential functions

Here we construct two phenomenological models with parameters that are easy to interpret in terms of the qualitative behaviour of the death rate. For more details, including full expressions for their survival functions, and a slightly more general version of these models see [23].

The models are based on what the authors have chosen to refer to as the power-exponential function  $f(x) = (xe^{1-x})^\beta$  that they have previously used for modelling of electrostatic discharges [24].

We will first construct a version of the model with 5 parameters that will be referred to as the *power-exponential model*

$$\mu(x) = \frac{c_1}{xe^{-c_2x}} + a_1 (xe^{-a_2x})^{a_3}. \quad (1)$$

The parameters  $c_1$ ,  $c_2$  and  $(a_1, a_2, a_3)$  can easily be interpreted in terms of qualitative properties of the curve.

To interpret the effects of  $c_1$  note that  $c_1 \mu(x) \rightarrow \frac{c_1}{x}$  when  $x \rightarrow 0$ . Looking at  $\ln(\mu(x))$  instead we can note that  $\frac{d}{dx} \ln(\mu(x)) \rightarrow c_2$  when  $x \rightarrow \infty$  so  $c_2$  gives the approximate slope of  $\ln(\mu(x))$  for large  $x$ .

In the simplest case where  $A = \{(a_1, a_2, a_3)\}$  we get the expected hump when  $a_i > 0$  for  $i = 1, 2, 3$ . In this case  $\frac{a_1}{a_3}$  gives the maximum height of the hump,  $\frac{1}{a_2}$  gives the time for the humps maximum and  $a_3$  determines the steepness of the hump (the larger  $a_3$  the steeper rise and the faster the decay).

In the power-exponential model the parameter  $c_1$  affects the shape of the curve both for high and low ages and  $a_3$  affects both the increasing and decreasing part of the hump.

To construct a model where this coupling is avoided we can split the two terms in the model at their respective local extreme points and adjust the values so that  $\mu(x)$  and  $\frac{d\mu}{dx}$  are continuous. We will refer to such a model as the *split power-exponential model* and it will give the following expression for the mortality rate.

$$\begin{aligned} \mu(x) = & \frac{c_1}{xe^{-\bar{c}x}} + a_1 (xe^{-a_2x})^{\bar{a}} + \Theta \left( x - \frac{1}{c_2} \right) \cdot c_1 \cdot c_2 \cdot \left( e - e^{\frac{c_3}{c_2}} \right) \\ & + \Theta \left( x - \frac{1}{a_2} \right) \cdot a_1 \cdot \left( \frac{e^{-a_3}}{a_1^{a_3}} - \frac{e^{-a_4}}{a_1^{a_4}} \right) \end{aligned}$$

where

$$\tilde{c} = \begin{cases} c_2, & x \leq \frac{1}{c_2} \\ c_3, & x > \frac{1}{c_2} \end{cases}, \quad \tilde{a} = \begin{cases} a_3, & x \leq \frac{1}{c_2} \\ a_4, & x > \frac{1}{c_2} \end{cases}, \quad \Theta(x) = \begin{cases} 0, & x \leq 0 \\ 1, & x > 0 \end{cases}.$$

This increases the total number of parameters from 5 to 7 but it can in certain cases give significant improvements to the fitting of the curve [23].

### 3 Lee–Carter method for forecasting

Lee and Carter assumed [2] that the mortality rate for a given age changes as a log-normal random walk with drift

$$\ln \mu(x, t) = a_x + b_x k_t + \varepsilon_{x,t}, \quad (2)$$

where  $\ln \mu(x, t)$  is the mortality rate at age  $x$  in year  $t$ ,  $a_x$  is the average pattern of mortality at age  $x$ ,  $b_x$  represents how mortality at each age varies when the general level of mortality changes,  $k_t$  is mortality index that captures the evolution of rates over time and  $\varepsilon_{x,t}$  an error term which causes the deviation of the model from the observed mortality rates, assumed to be normally distributed  $N(0, \sigma_t^2)$ .

The parametrization given in (2) is not unique. For example, if we have a solution  $a_x$ ,  $b_x$  and  $k_t$ , then there might exist any non-zero constant  $c \in \mathbb{R}$  which gives another solution of  $a_x - cb_x$ ,  $cb_x$  and  $k_t = c$ , for which these transformations might produce identical forecasts. In order to get a unique solution when fitting a L–C model, constraints must be imposed. Usually  $b_x$  is constrained to sum to 1 and  $k_t$  to sum to 0, which gives  $a_x$  to be as the average over time of the  $\ln(\mu(x, t))$ , as follows  $\sum_x b_x = 1$ ,  $\sum_t k_t = 0$  and

$$a_x = \frac{1}{T} \sum_x \ln(\mu(x, t)).$$

The parameters  $a_x$ ,  $b_x$  and the mortality indices  $k_t$  are found as follows:

Given a set of ages (or age ranges),  $\{x_i, i = 1, \dots, n\}$ , and a set of years,  $\{t_j, j = 1, \dots, n\}$ , first estimate  $\hat{a}_x = \frac{1}{T} \sum_x \ln(\mu(x, t))$ . Then construct the

matrix given by  $Z_{ij} = \ln(\mu(x_i, t_j)) - a_{x_i}$ . From the conditions imposed on  $b_x$  and  $k_t$  we now know that  $Z_{ij} = b_{x_i} k_{t_j}$  and thereby the values of  $b_x$  and  $k_t$  can be found using the singular value decomposition (SVD) of  $Z$ . Finding the standard SVD  $Z = USV^T$  gives  $\hat{b}_x$  as the first column of  $U$  and  $\hat{k}_t$  is given by the first singular value multiplied by the first column of  $V^T$ .

Forecasting future mortality indices can be done in different ways, but in practice the random walk with drift model (RWD) for  $\hat{k}_t$  is common because of its simplicity and straight forward interpretation, so we will also use the RWD model to estimate  $\hat{k}_t$  as follows:

$$\hat{k}_t = \hat{k}_{t-1} + \theta + \varepsilon_t$$

. In this specification,  $\theta$  is the drift term, and  $\hat{k}_t$  is forecast to decline linearly with increments of  $\theta$ , while deviations from this path,  $\varepsilon_t$ , are permanently

incorporated in the trajectory. The drift term  $\theta$  is estimated as below, which shows that  $\hat{\theta}$  only depends on the first and last values of  $\hat{k}_t$  estimates,

$$\hat{\theta} = \frac{\hat{k}_T - \hat{k}_1}{T - 1}.$$

In this paper, we will consider errors of forecasted mortality index,  $\varepsilon_t$ , which represent noise that causes deviation from the expected linear change. This term is normally distributed with mean 0 and variance  $\sigma_{error}^2$ . Note that the  $\hat{k}$ s are not independent, they have successive innovations that are independent and the variance of error between them is estimated as

$$(\text{see})^2 = \frac{1}{t-2} \sum_{t=2}^T (\hat{k}_t - \hat{k}_{t-1} - \hat{\theta})^2 \quad (3)$$

which is used to calculate the uncertainty in forecasting  $\hat{k}_t$  over any given horizon.

Then the associated error variance of forecasted values is given as

$$\text{var}(\hat{k}_t) = (\text{see})^2 \cdot \Delta t \quad (4)$$

and the square root of this gives the standard error estimate for the first forecast horizon

$$\text{SD}(\hat{k}_t) = \text{see} \cdot \sqrt{\Delta t},$$

where  $\Delta t$  is the forecast horizon which shows that standard deviation increases with the square root of the increasing distance to the forecast, and from standard deviation of  $\hat{k}_t$  we can calculate the confidence band using 95% confidence interval with t-factor of 1.96 as;

$$(\hat{k}_t) \pm 1.96(\text{SD}(\hat{k}_t)).$$

To forecast two period ahead, we just substitute for the definition of  $\hat{k}_{t-1}$  moved back in time one period and plug in the estimate of the drift parameter  $\hat{\theta}$

$$\hat{k}_{t-1} = \hat{k}_{t-2} + \hat{\theta} + \varepsilon_{t-1}$$

then  $\hat{k}_t$  becomes

$$\begin{aligned} \hat{k}_t &= \hat{k}_{t-1} + \hat{\theta} + \varepsilon_t \\ &= \hat{k}_{t-2} + \hat{\theta} + \varepsilon_{t-1} + (\hat{\theta} + \varepsilon_t) \\ &= \hat{k}_{t-2} + 2\hat{\theta} + (\varepsilon_{t-1} + \varepsilon_t). \end{aligned}$$

To forecast  $\hat{k}_t$  at time  $T + \Delta t$  with the data available up to  $T$ , we follow the same procedure iteratively  $\Delta t$  times and obtain

$$\begin{aligned} \hat{k}_{T+\Delta t} &= \hat{k}_T + \Delta t \hat{\theta} + \sum_{n=1}^{\Delta t} \varepsilon_{T+n} \\ &= \hat{k}_T + \Delta t \hat{\theta} + \sqrt{\Delta t} \varepsilon_t \end{aligned} \quad (5)$$

ignoring the error term since its mean is 0 and assumed to be independent with the same variance, we get forecast point estimates which follow a straight line as a function of  $\Delta t$  with slope  $\hat{\theta}$

$$\hat{k}_{T+\Delta t} = \hat{k}_T + \Delta t \hat{\theta}.$$

The forecast of the logarithm of the mortality rate can then be computed using the forecasted mortality index  $\ln(\hat{\mu}_{x,T+\Delta t}) = a_x + b_x \hat{k}_{T+\Delta t}$ .

In Figure 1 an example is shown where the L-C method was applied using three different models. A thirty year period (1970-2010) was used to compute mortality indices and a prediction was made 10 years in the future and compared to the measured mortality rate at that time.

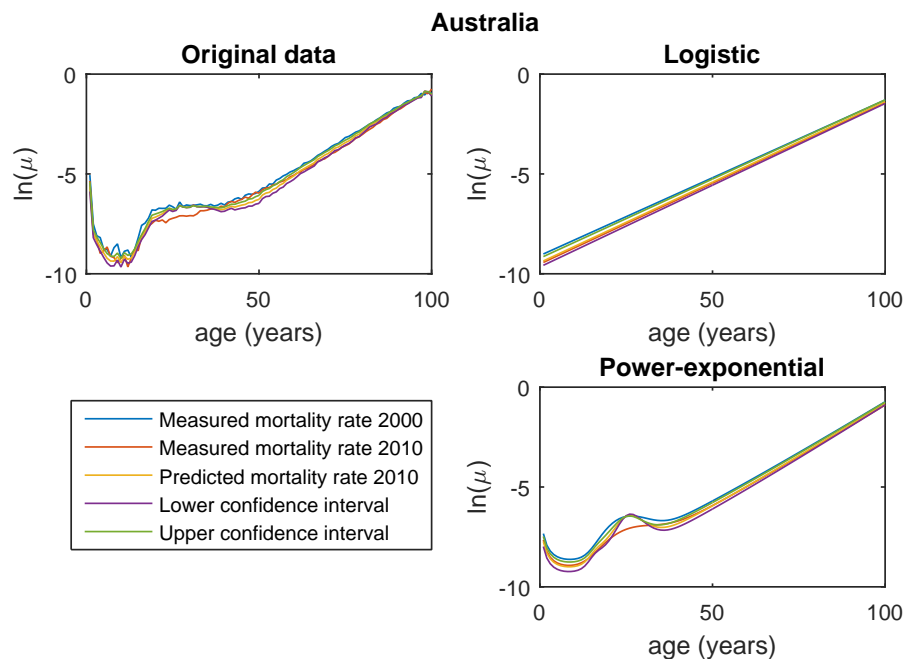


**Fig. 1.** Example of measured and forecasted mortality rates for Australia with three different models. The mortality indices were computed using data in the period (1970-2000) and the logarithm of the mortality was forecasted 10 years into the future. The forecasted result (predicted mortality rate 2010) is compared to the initial mortality rate (measured mortality rate 2000) and the measured value (measured mortality rate 2010).

## 4 Comparison of models

To compare the different models to each other the mortality indices will be computed over a period of time and then we will use the same RWD to forecast

$k_t$  in the interval  $t \in [1, T]$  and use the result to estimate the variance of  $\epsilon_t$  in (5). The variance of  $\epsilon_t$  will be estimated by computing the quantity  $\hat{l}_{\Delta t}$  that is found by removing the drift-term, constant term and the scaling of the stochastic term in (5),

$$\hat{l}_{\Delta t} = \frac{\hat{k}_{1+\Delta t} - \Delta t \hat{\theta}}{\sqrt{\Delta t}}.$$

We can then consider  $\hat{l}_{\Delta t}$  to be measurements of  $l_{\Delta t} = \epsilon_t \in \mathcal{N}(0, \text{var}(\epsilon_t))$  and then  $\text{var}(\epsilon_t)$  can be estimated using a standard maximum likelihood estimation of  $\hat{l}_t$ .

Since different models will give different  $k_t$  they will also give different  $\text{var}(\epsilon_t)$  and a lower variance indicates a more suitable model.

The second way to characterise the suitability of the model for forecasting is to compare the associated error variance of the forecasted values, by (4) this is characterized by the standard error estimate given by (3). Thus computing and comparing the standard error estimates also gives some idea of the comparative suitability for forecasting of different models. An example of how the mortality indices can change for different models is illustrated in Figure 2.

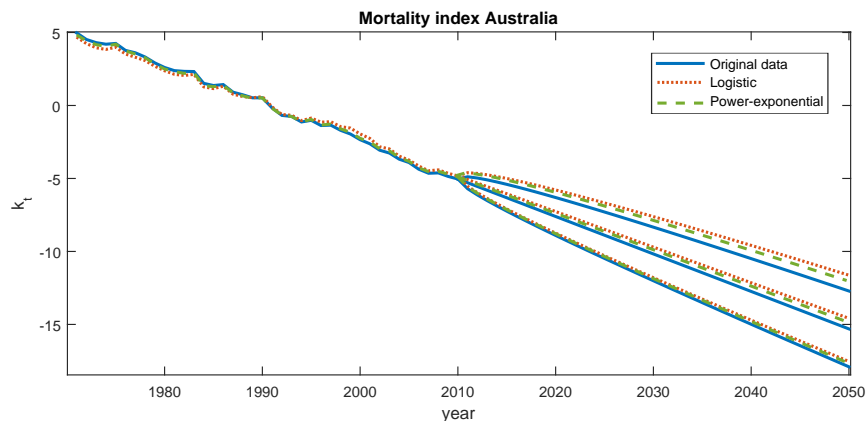


**Fig. 2.** Example of estimated and forecasted mortality indices for Australia with three different models. We hope to characterise both the reliability in the measured area (1970-2010) and the forecasted area (2011-2050).

## 5 Results, discussion and further work

Here we will present results of applying the methodology described in previous sections using five models and data from six countries. The models are the ones called Modified Perks, Logistic, Heligman–Pollard HP4 in Table 1 as well as the Power-exponential and Split power-exponential described in Section 2. The data is taken from the Human Mortality Database (HMD) [17], and gives the mortality rate for ages 1-100 in 1970-2010 for USA, Canada, Switzerland,

Japan, Taiwan and Australia. The choice of years and countries is primarily driven by practical consideration, we wanted a set of countries with varying properties with respect to geographical position, populations size and population density while also being developed enough to be qualitatively similar and have reliable data. The year range was chosen so that there would be no obvious major change in mortality in either of the countries. We also wanted a scenario where the fitting method worked efficiently and reliably and the assumptions behind L-C forecasting were relatively reasonable.

*Note:* For some of the countries data was missing for certain years and ages. In these cases the missing data was replaced with an average of neighbouring values.

The results are shown in Table 2 and 3. In both tables a lower value indicates a more reliable forecasting (assuming there are no major developments that significantly affect the mortality of certain population parts).

Estimated variance of $\epsilon_t$	Country					
	USA	Canada	Switzerland	Japan	Taiwan	Australia
Measured data	<b>0.111</b>	<b>0.123</b>	0.123	0.143	<b>0.113</b>	0.0607
Logistic	0.124	0.131	0.140	0.154	0.125	0.0704
Modified Perks	0.122	0.128	0.132	0.149	0.118	0.0695
Power-exponential	0.123	0.130	0.129	0.149	0.141	0.0615
Split power-exp.	0.115	0.125	<b>0.120</b>	0.143	0.135	<b>0.0602</b>
HP4	0.116	0.134	0.128	<b>0.142</b>	0.120	0.0647

**Table 2.** Estimated variance of  $\epsilon_t$  found in the way described on page 7.

Examining Table 2 we see that most of the time using the measured data for forecasting is the most desirable, the exception are Switzerland and Australia where the Split power-exponential model gives the best results (for Japan slightly better results are obtained by HP4). Note that using a simple parametrized model can bring advantages compared to using measured data so it is also interesting to only compare the different models with each other. Here the results vary significantly from country to country but usually estimated variance is lower for the more accurate models using more parameters.

Standard error estimate	Country					
	USA	Canada	Switzerland	Japan	Taiwan	Australia
Measured data	0.151	0.199	0.398	0.244	0.299	0.209
Logistic	0.158	0.201	0.345	0.239	0.277	0.238
Modified Perks	0.160	0.204	0.371	0.247	0.294	0.243
Power-exponential	0.157	0.210	0.359	0.235	0.308	0.226
Split power-exp.	0.156	0.209	0.385	0.244	0.297	0.222
HP4	0.152	0.209	0.356	0.245	0.298	0.216

**Table 3.** Standard error estimated of forecasted mortality indices.

Examining Table 3 we can see that for Switzerland and Taiwan the models tend to give a smaller standard error estimate than the measured data, but otherwise the measured data gives standard error estimates that are as good or better than the other models. There is also greater variation in what model seems to be the most reliable one with respect to forecasting compared to Table 2.

To understand if the variations here are indicative of trends for different classes of models a larger number of models should be applied to a larger number of datasets, note that more sophisticated fitting and forecasting method should probably also be employed to ensure that the comparison actually compares scenarios where each method is used in an appropriate way.

There are also other aspects and applications that require a different kind of analysis, for instance if we wanted to compare the models suitability for pricing life insurance or modelling pensions we would use different age ranges since life insurance is mostly intended for those who die at a relatively young age (but not children) while suitable pension planning requires understanding of how many individuals will live to a high age.

We have also only considered simple parametrized models and not taken the relative explanatory power of the models into account.

In other words, every aspect of the comparison could be improved but we believe that some sort of systematic comparison of these type of models on a easily available but relevant corpus of data could be a useful and informative tool for researchers and professionals.

## References

1. TN. Thiele. On a mathematical formula to express the rate of mortality throughout life. *Journal of the Institute of Actuaries*, 16:313–329, 1872.
2. Lee, R. D., and Carter, L. R. (1992). Modeling and Forecasting U.S. Mortality. *Journal of the American Statistical Association*, 87(419), 659–671. DOI:10.1080/01621459.1992.10475265.
3. Federico,G., and Gary,K. (2007). Understanding the Lee-Carter Mortality Forecasting Method.*Semi-Markov risk models for finance, insurance and reliability*, Harvard University, Cambridge MA 02138; (617) 495-2027).
4. O’Hare, C and Li, Y (2012). Explaining young mortality *Insurance: Mathematics and Economics*, 50, 12–25.
5. Lee, R. and Miller, T. (2000), Evaluating the L–C method for forecasting mortality, *Demography*, 38(4), 537–549.
6. Booth,H., and Tickle,L. (2008). Mortality modelling and forecasting: A review of methods *Probabilités, Analyse des Données et Statistique*,ADSRI Working Paper No. 3,2008.
7. Shinde, R. L., and Chavhan, R. N. (2016). Modeling and Forecasting Mortality Using the Lee-Carter Model for Indian Population Based on Decade-wise Data. Department of Statistics and Actuarial Science, School of Mathematical Sciences, North Maharashtra University,India, Jalgaon Jalgaon-425001, Sri Lankan Journal of Applied Statistics, Vol (17-1).
8. Li, N., Lee, R., and Tuljapurkar, S. (2004). Using the Lee-Carter Method to Forecast Mortality for Populations with Limited Data. *International Statistical Review*, 72(1), 1936. DOI:10.1111/j.1751-5823.2004.tb00221.

9. Aberathna, W., Alles, L., Wickremasinghe, W. N., and Hewapathirana, I. (2014). Modeling and Forecasting Mortality in Sri Lanka. *Sri Lankan Journal of Applied Statistics*, 15(3). DOI:10.4038/sljastats.v15i3.7794.
10. Koissi, M.-C., Shapiro, A. F., and Hgns, G. (2006). Evaluating and extending the LeeCarter model for mortality forecasting: Bootstrap confidence interval. *Insurance: Mathematics and Economics*, 38(1), 120. DOI:10.1016/j.insmatheco.2005.06.008.
11. Lee, R.D., and Rofman, R. (1994). Modeling and forecasting mortality in Chile. *Notas*, 22 (59), 182213.
12. Lin, J. (1995). Changing Kinship Structure and its Implications for Old-Age Support in Urban and Rural China. *Population Studies*, 49(1), 127145. DOI:10.1080/0032472031000148286.
13. Wilmoth, J.R., (1996). Mortality Projections for Japan: A Comparison of Four Methods. *Health and Mortality among Elderly Population*. In: Caselli, G., Lopez, A. (Eds.), Oxford University Press, New York.
14. Singh, A., and Ram, F. (2004). Forecasting mortality in India. Rawat Publications, Jaipur, *Population Health and Development*. Ed. TK Roy, M Guruswamy and P Arokiasamy.
15. Tuljapurkar, S., Nan, L., and Boe, C. (2000). A universal pattern of mortality decline in the G7 countries. *Nature*, 405, 789792.
16. Yasungnoen, N., and Sattayatham, P. (2016). Forecasting Thai Mortality by Using the Lee-Carter Model. *Asia-Pacific Journal of Risk and Insurance*, 10(1), 91-105. DOI:10.1515/apjri-2014-0042.
17. Human Mortality Database. Death rates. University of California, Berkeley (USA), and Max Planck Institute for Demographic Research (Germany). Available at [www.mortality.org](http://www.mortality.org) or [www.humanmortality.de](http://www.humanmortality.de) (data downloaded on 2017-06-14).
18. L. Heligman and J. H. Pollard. The age pattern of mortality. *Journal of the Institute of Actuaries*, 107:49–80, 1980.
19. Waloddi Weibull. A statistical distribution function of wide applicability. *Journal of Applied Mechanics*, 18:293–297, 1951.
20. Harald Hanmerz. An extension of relational methods in mortality estimation. *Demographic Research*, 4:337–368, June 2001.
21. Forfar, David O. *Mortality Laws*. Mathematical Formulae, 1-6. Encyclopedia of Actuarial Science, 2006.
22. Zoltan Butt and Steven Haberman. Application of frailty-based mortality models using generalized linear models. *Astin Bulletin*, 34(1):175–197, 2004.
- [Pham, 2008]Pham, Hoang. *Recent Advances in Reliability and Quality in Design*. Springer, 2008.
23. Lundengård, Karl, Rančić, Milica and Silvestrov, Sergei. *Modelling mortality rates using power exponential functions.*, to be published in the proceedings of the SPAS2017 conference.
24. Vesna Javor, Karl Lundengård, Milica Rancic, Sergei Silvestrov, *Analytical Representation of Measured Lightning Currents and Its Application to Electromagnetic Field Estimation*, IEEE Transactions on Electromagnetic Compatibility, Early Access Article, page 1–12.

# Men's Performance in Triple Jump: an approach with Extreme Value Theory

Frederico Caeiro<sup>1</sup>, Domingos Silva<sup>2</sup>, and Manuela Oliveira<sup>3</sup>

<sup>1</sup> Faculdade de Ciências e Tecnologia & Centro de Matemática e Aplicações (CMA), Universidade Nova de Lisboa, Portugal (E-mail: [fac@fct.unl.pt](mailto:fac@fct.unl.pt))

<sup>2</sup> Universidade de Évora, CIMA, Portugal (E-mail: [domingosjlsilva@gmail.com](mailto:domingosjlsilva@gmail.com))

<sup>3</sup> Universidade de Évora, CIMA, Portugal (E-mail: [mno@uevora.pt](mailto:mno@uevora.pt))

**Abstract.** Emil Gumbel was the first to use extreme value models in statistics applications. In the block method an Extreme Value distribution is fitted to the sample of block maxima obtained from non-overlapping blocks of a series of random variables. The block length is usually long (usually chosen as one year), to assure the independence of the block maxima sample. Although this method has proved to be useful in diversified situations, it has also been criticized since we are wasting information by using only the observed maxima from each block. To use more information about the tail of the model underlying the data, the block maxima method was more recently extended to the  $r$ -largest order statistics method. The choice of the number  $r \geq 1$  of largest order statistics taken from each block must be made with careful, due to the usual bias and variance trade-off. In this work we use the  $r$ -largest order statistical method to study the limit of men's performance in Triple Jump event. Our results indicate a negative extreme value index and thus a finite right endpoint for the extreme value model.

**Keywords:** Extreme value theory, Block maxima, Generalized extreme value distribution.

## 1 Introduction

The triple jump also called hop, step, and jump also called hop, step, and jump is an athletic event similar to the Long Jump, in which competitors attempt to jump as far as possible. This is one of the most complicated disciplines in athletics. The event starts with a sprint along a runway. After stepping the take-off board, athletes make a hop, then a step and finally a jump into a sandpit. Then, the distance travelled, from the edge of the take-off board to the nearest break in the sand, is measured. If any athlete steps beyond the take-off board, a foul is recorded and the jump is not measured. The runway velocity and power are important factors in the triple jump event. As in several other outdoor track events run in only one direction, wind speed can affect the athlete performance. In those events, wind speeds are recorded and rounded

---

<sup>5</sup>*th* SMTDA Conference Proceedings, 12-15 June 2018, Chania, Crete, Greece



up to the nearest tenth of a meter per second ( $m/s$ ). Only results associated to a (positive) wind reading of  $2.0 m/s$  or less are considered “legal” and may be used for records. The IAAF (International Amateur Athletic Federation until 2001 and International Association of Athletics Federations nowadays), created in 1912, is the authority for track and field athletic events and is responsible for collecting and ratify all official results.

In outdoor, the first triple jump men’s record is 12.95 meters and was obtained in 1826 by Andrew Beatti of GBI (Great Britain & Ireland). In 1896, at the first modern Olympic Games at Athens, the triple jump event was won by James Connolly of the United States of America (USA) with a jump of 13.71 meters. Jonathan Edwards was the first men to pass over 18m in triple jump event, with a jump of 18.16m at the Gothenburg World Championships in 1995. On his second jump, Jonathan Edwards reach an impressive distance of 18.29m and set the actual world record. The current Olympic record is 18.09m and was established by Kenny Harrison in 1996 in Atlanta. In the following years most athletes had to struggle to reach the 17.80m mark. This was possibly a consequence of the loss of popularity of the triple jump event. Only recently, a new generation of talented triple jumpers athletes, such as Christian Taylor and Pedro Pablo Pichardo, appeared and were able to come closer to Jonathan Edwards world record. So, it is possible that Jonathan Edwards record can be broken anytime soon. In Table 1 we present some triple jump records.

**Table 1.** Some world records.

Atleth	result	Year	Remarks
Andrew Beattie (GBI)	12.95m	1826	1st World Record
James Connolly (USA)	13.71m	1896	1st Olympic Games
Daniel Ahearn (GBI)	15.52m	1912	1st World Record by IAAF
Jonathan Edwards (GBR)	18.29m	1995	World Record
Kenny Harrison (USA)	18.09m	1996	Olympic Record

In this work we are interested in quantifying extreme events, such as a new world record, in men’s outdoor triple jump. The remainder of the paper is organized as follows: in section 2 we describe the triple jump event data under study. In section 3 we review the methodology used in the paper. Finally, in section 4 we apply the Extreme Value block maxima and  $r$ -largest order statistical models to the data and we provide some concluding remarks.

## 2 Data

The data studied in this work was obtained from the IAAF website (URL: <http://www.iaaf.org/>). Since triple jump technique has improved over time and triple jumpers population also changed over time, we restrict the data studied to the period that starts on January 1, 1990 and ends at December 31, 2017. This restricted period allow us to avoid problems with non-stationarity of the data and to exclude many (but not all) years where anti-doping control was

not sufficiently strict: out of competition testing was widely adopted in 1991; the IAAF only stores blood and urine samples since 2005. The year 1990 was included in the study because (apparently) it has no suspicious data. For each year we only collected the 10 best outdoor records. Each athlete appears only once in each year. Table 2 contains the data used in this study. The data is also presented in Figure 1. To check for the existence of non-randomness patterns such as trend or seasonal effects, the difference sign, the runs and Bartels rank test were applied ([8,15–17]). Due to the existence of several values obtained on the same day, the triple jump time series is not well-defined and only the annually maxima sample as tested for randomness. The null hypothesis of randomness was never rejected at the 5% significance level.

year	1	2	3	4	5	6	7	8	9	10
1990	17.93	17.90	17.75	17.74	17.56	17.47	17.43	17.34	17.33	17.31
1991	17.78	17.75	17.66	17.62	17.53	17.52	17.45	17.43	17.43	17.40
1992	17.72	17.60	17.48	17.41	17.36	17.34	17.34	17.32	17.31	17.28
1993	17.86	17.68	17.65	17.59	17.54	17.44	17.34	17.32	17.30	17.28
1994	17.68	17.62	17.61	17.55	17.43	17.43	17.41	17.39	17.38	17.35
1995	18.29	17.92	17.67	17.62	17.48	17.47	17.42	17.40	17.30	17.30
1996	18.09	17.88	17.75	17.70	17.57	17.36	17.31	17.30	17.19	17.18
1997	17.85	17.74	17.64	17.59	17.59	17.51	17.44	17.36	17.33	17.30
1998	18.01	17.65	17.53	17.44	17.42	17.41	17.34	17.27	17.27	17.24
1999	17.59	17.52	17.49	17.40	17.40	17.32	17.31	17.29	17.29	17.27
2000	17.71	17.60	17.47	17.46	17.45	17.41	17.37	17.30	17.30	17.26
2001	17.92	17.49	17.44	17.40	17.34	17.33	17.30	17.24	17.22	17.22
2002	17.86	17.68	17.64	17.63	17.59	17.50	17.43	17.42	17.34	17.33
2003	17.77	17.63	17.61	17.59	17.57	17.55	17.40	17.31	17.28	17.24
2004	17.79	17.78	17.72	17.68	17.63	17.58	17.55	17.53	17.47	17.41
2005	17.81	17.73	17.64	17.57	17.51	17.46	17.45	17.39	17.32	17.30
2006	17.71	17.67	17.63	17.56	17.55	17.54	17.50	17.42	17.40	17.38
2007	17.90	17.74	17.58	17.56	17.52	17.48	17.43	17.37	17.35	17.35
2008	17.67	17.62	17.59	17.52	17.50	17.49	17.48	17.46	17.43	17.43
2009	17.73	17.66	17.65	17.65	17.62	17.59	17.41	17.41	17.39	17.32
2010	17.98	17.81	17.55	17.51	17.49	17.41	17.29	17.29	17.22	17.22
2011	17.96	17.91	17.77	17.72	17.68	17.50	17.40	17.35	17.31	17.29
2012	17.81	17.62	17.53	17.53	17.49	17.47	17.39	17.38	17.35	17.31
2013	18.04	17.69	17.66	17.52	17.46	17.45	17.36	17.26	17.25	17.24
2014	17.76	17.75	17.58	17.51	17.48	17.35	17.30	17.29	17.27	17.24
2015	18.21	18.08	17.53	17.52	17.50	17.48	17.42	17.34	17.29	17.24
2016	17.86	17.76	17.58	17.30	17.21	17.20	17.18	17.18	17.16	17.16
2017	18.11	17.91	17.60	17.48	17.40	17.32	17.30	17.27	17.27	17.25

**Table 2.** Ten largest annual maxima men’s triple jump results, 1990–2017.

Only officially results considered to establish a record are considered. Therefore, distances with a wind speed of more than 2  $m/s$  were not considered. Since the wind speed can have a major role in the distance jumped by the athlete, in Figure 2 we present a scatter plot of the distance jumped versus the wind

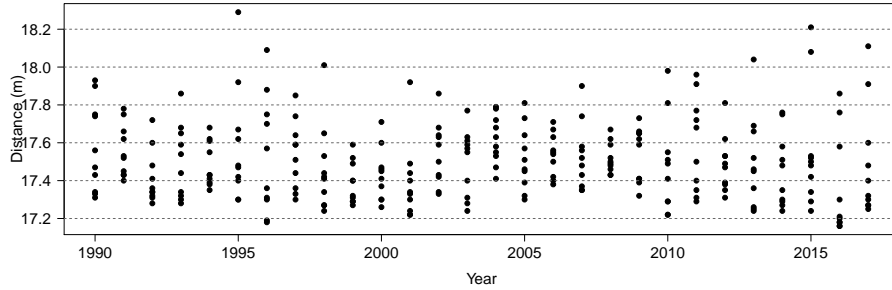


**Fig. 1.** Ten largest annual maxima men's triple jump results, 1990–2017.

speed. The proportion of jump distances obtained with a positive wind speed is approximately 80%.

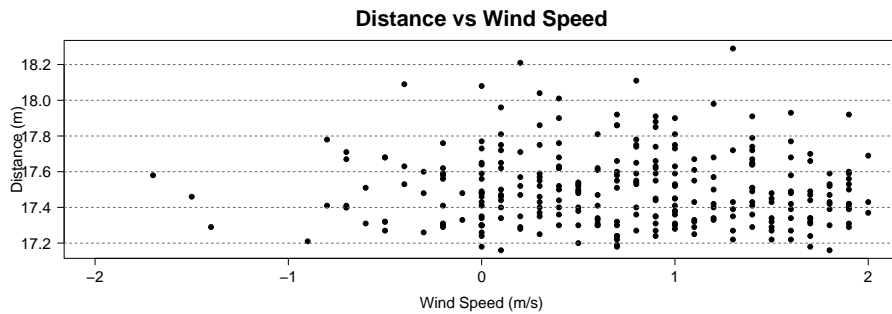


**Fig. 2.** Distance versus wind speed in the top 10 men's triple jump results, 1990–2017.

### 3 Methodology

The objective of extreme value theory (EVT) is to quantify the stochastic behaviour of extreme events, such as floods, droughts or a new world record. The domains of application of EVT are quite diverse and include fields such as hydrology, meteorology, geology, insurance, finance, structural engineering, telecommunications and sports. Thus EVT provides a framework to model the tail behaviour and is a useful tool to study athletic events, since a new world record is an extreme event.

#### 3.1 Main limit results

Let  $(X_1, \dots, X_n)$  be a sample of independent, identically distributed (iid) random variables from an underlying population with unknown distribution function (df)  $F$ . Here, and due to the nature of the athletic event under study, we

shall always deal with the right tail of  $F$ . Notice that since  $\min(X_1, \dots, X_n) = -\max(-X_1, \dots, -X_n)$ , results for the left tail can be easily derived from the analogous results for the right tail.

The first main result is due to Gnedenko [9] who fully characterized the possible non-degenerate limit distribution of the linearly normalised sample maximum of iid random variables (see also [6,7,18]). Let  $M_n = \max_{1 \leq i \leq n}(X_i)$  be the sample maximum. Let us also assume that there are normalizing constants  $a_n > 0$ ,  $b_n \in \mathbb{R}$  and some non-degenerate df  $G$  such that, for all  $x$ ,

$$\lim_{n \rightarrow \infty} P\left(\frac{M_n - b_n}{a_n} \leq x\right) = G(x). \quad (1)$$

With the appropriate choice of the normalizing constants,  $G$  is the generalized extreme value (GEV) distribution,

$$G(x) \equiv G(x|\xi) := \begin{cases} \exp(-(1 + \xi x)^{-1/\xi}), & 1 + \xi x > 0 & \text{if } \xi \neq 0 \\ \exp(-\exp(-x)), & x \in \mathbb{R} & \text{if } \xi = 0 \end{cases} \quad (2)$$

given here in the von Mises-Jenkinson form ([13,18]). When the non-degenerate limit in (1) exists, we say that  $F$  belongs to the max-domain of attraction of  $G$  and denote this by  $F \in \mathcal{D}(G)$ . The GEV model unifies the three possible limit max-stables distributions: Weibull ( $\xi < 0$ ), Gumbel ( $\xi = 0$ ) and Fréchet ( $\xi > 0$ ). The shape parameter  $\xi$  is related with the heaviness of the right-tail and it is often called the *extreme value index* (EVI).

Another important result in the field of EVT is the limiting distribution of the  $r$  largest order statistics (with  $r$  fixed). We shall assume that (1) holds, i.e., that  $(M_n - b_n)/a_n$  converges in distribution to  $G(x)$ , with adequate normalizing constants  $a_n > 0$  and  $b_n \in \mathbb{R}$ . Then, the limiting distribution of the normalized  $r$  largest order statistics

$$\left(\frac{X_{(1)} - b_n}{a_n}, \frac{X_{(2)} - b_n}{a_n}, \dots, \frac{X_{(r)} - b_n}{a_n}\right)$$

with  $X_{(1)} \geq X_{(2)} \geq \dots \geq X_{(r)}$ , is the multivariate GEV model (Dwass [5]), with an associated probability density function given by

$$h_r(x_1, x_2, \dots, x_r) = g(x_r) \prod_{j=1}^{r-1} \frac{g(x_j)}{G(x_j)} \quad \text{if } x_1 > x_2 > \dots > x_r, \quad (3)$$

where  $g(x) = \frac{dG(x)}{dx}$ , with  $G(x)$  the GEV distribution given in (2). Notice that for  $r = 1$ , (3) is the GEV distribution, as expected. Also, if we consider the extreme order statistic  $X_{(k)}$  for some fixed  $k$ , we have ([1])

$$\lim_{n \rightarrow \infty} P\left(\frac{X_{(k)} - b_n}{a_n} \leq x\right) = G(x) \sum_{i=0}^{k-1} \frac{(-\ln G(x))^i}{i!}. \quad (4)$$

If  $k = 1$ , (4) is the GEV distribution in (2). There is thus a strong relation between the asymptotic distribution of the sample maximum,  $X_{(1)}$ , and the

asymptotic distribution of the  $r$  largest order statistics and of the extreme order statistic  $X_{(k)}$ . Other important limit results outside the scope of this paper can be found in books [1,3,4,11,14]. For an overview of several topics in the field of EVT, see [2,10].

### 3.2 Block maxima method

We divide the sample in blocks of equal length and fit the GEV model in (2) to the sample of block maxima. The size of the block is important due to the usual trade-off between bias (small block size) and variance (large block size). When working with time series data it is usual to chose the block length as one year. This choice allow us to often assume that the block maxima is iid, even if the time series data is not exactly iid. Then, we fit the GEV model to the block maxima data. Since the normalizing constants  $a_n > 0$  and  $b_n \in \mathbb{R}$  are unknown, they are incorporated in the GEV distribution as location and scale parameters,  $\lambda$  and  $\delta$ , leading to the model

$$G(x|\xi, \lambda, \delta) := \begin{cases} \exp\left(-\left(1 + \xi \frac{x-\lambda}{\delta}\right)^{-1/\xi}\right), & 1 + \xi \frac{x-\lambda}{\delta} > 0 \text{ if } \xi \neq 0 \\ \exp(-\exp(-\frac{x-\lambda}{\delta})), & x \in \mathbb{R} \text{ if } \xi = 0 \end{cases} \quad (5)$$

The estimation of the parameters  $(\xi, \lambda, \delta)$  is usually performed using the Maximum Likelihood method [19] or the Probability Weighted Moment method [12]. Model checking can be done with a Histogram, a Probability Plot, a Quantile Plot or a with Return Level Plot (see Coles [3] for further details).

### 3.3 $r$ -largest order statistics method

When analysing extreme values, we often have samples with few observations and consequently, parameter estimators have a large variance. This problem has motivated researchers to use more data from the sample rather than the sample of block maxima. Smith [20] and Weissman [21] were the first to make inference with a model based on the  $r$ -largest order statistics from each block. Under this approach, data is divided in blocks and we select the  $r$  largest order statistics from each block. Then we fit model in (3) with additional location and scale parameters  $\lambda$  and  $\delta > 0$ . The estimation is usually performed by maximum likelihood. As with the choice of the block length, the choice of the parameter  $r$  accommodate a trade-off between bias (large  $r$ ) and variance (small  $r$ ). In practice it is advisable to chose  $r$  not too large ([20]).

*Remark 1.* Notice that both probabilistic models used in sections 3.2 and 3.3 share the same shape, location and scale parameters  $(\xi, \lambda, \delta)$ . Therefore it is usual to estimate those parameters, with increased precision, using the the  $r$ -largest order statistics method and then to incorporate those estimates in the GEV model in (5) to estimate other important parameters.

### 3.4 Estimation of other parameters of extreme and large events

An upper tail probability is the probability that the block maximum exceeds some high value  $y_p$  with probability  $p$  ( $p$  small). The tail probability can be estimated by  $1 - G(y_p | \hat{\gamma}, \hat{\lambda}, \hat{\delta})$  where  $G$  is the GEV df in (5).

Extreme quantiles exceeded with probability  $p$  of the block maximum can be obtained by inverting the GEV df in (5) and replacing the parameters by the corresponding estimates,

$$\hat{q}_{1-p} := G^{\leftarrow}(1 - p | \hat{\gamma}, \hat{\lambda}, \hat{\delta})$$

The quantile  $q_{1-p}$  is also the level expected to be exceeded on average once every  $1/p$  years. We usually say that  $q_{1-p}$  is the return level associated with the return period  $1/p$ . A plot of the return period (on a logarithmic scale) versus the return level is called a Return Level Plot.

If  $\xi < 0$ , the right endpoint of the GEV model is finite and it can be estimated by

$$\hat{y}^{GEV} = \hat{\lambda} - \frac{\hat{\delta}}{\hat{\xi}}.$$

## 4 Results and conclusions

The models presented in section 3 will now be applied to the triple jump data. The first step must be the choice of the number of  $r$  largest order statistics taken from each block. Table 3 shows the Maximized log-likelihood ( $ll_0$ ), parameters estimates and standard errors in parentheses of the multivariate GEV model for  $1 \leq r \leq 10$ .

$r$	$ll_0$	$\hat{\lambda}$	$\hat{\sigma}$	$\hat{\xi}$
1	-12.313	17.797 (0.029)	0.135 (0.021)	-0.034 (0.154)
2	-44.822	17.800 (0.028)	0.154 (0.016)	-0.133 (0.106)
3	-84.079	17.779 (0.027)	0.161 (0.015)	-0.113 (0.098)
4	-133.201	17.796 (0.027)	0.166 (0.012)	-0.202 (0.066)
5	-188.693	17.798 (0.026)	0.166 (0.012)	-0.214 (0.056)
6	-245.384	17.796 (0.026)	0.168 (0.012)	-0.212 (0.054)
7	-298.660	17.796 (0.027)	0.172 (0.012)	-0.225 (0.053)
8	-362.199	17.795 (0.026)	0.173 (0.012)	-0.223 (0.051)
9	-432.076	17.794 (0.026)	0.174 (0.012)	-0.216 (0.049)
10	-510.358	17.787 (0.026)	0.175 (0.014)	-0.189 (0.052)

**Table 3.** Maximized log-likelihood ( $ll_0$ ), parameters estimates and standard errors in parentheses of the multivariate GEV model for  $1 \leq r \leq 10$ .

Assuming the validity of the multivariate GEV model in (3) for a particular value of  $r$ , then we expect to get stability in the estimates of the shape, location and scale parameters. Comparing the results for different values of  $r$  we notice that both estimates and standard errors change substantially from  $r = 1$  until

$r = 4$ . Due to theoretical arguments, it is advisable to not let  $r$  be too large. Therefore, we choose  $r = 4$ . Since the parameters  $(\xi, \lambda, \delta)$  correspond exactly to the parameters of the (univariate) GEV model, in Figure 3 we present diagnostic plots of the GEV distribution. Those plots confirms that the accuracy of the fit is satisfactory.

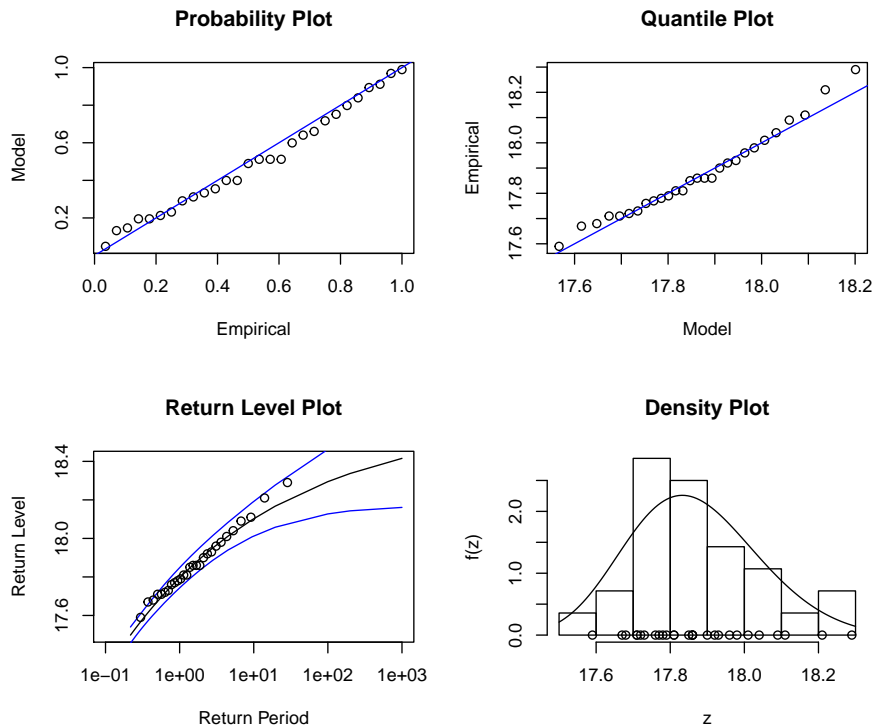


**Fig. 3.** Diagnostic Plots of the GEV model fit to the annual maxima men's triple jump results, 1990–2017.

The asymptotic 95% confidence intervals for the parameters  $\xi$ ,  $\lambda$  and  $\delta$  are respectively  $(-0.331, -0.073)$ ,  $(17.743, 17.848)$  and  $(0.142, 0.191)$ . The confidence interval for the shape parameter  $\xi$  confirms a negative shape parameter at the usual significance levels. Therefore the distribution of the annual maximum has a finite right endpoint which could be considered the ultimate world record for the men's triple jump (under the current conditions and rules). The maximum likelihood estimate of the right endpoint is 18.62m. Our results shows that the current world record cannot improve substantially. It can only improve 0.33m (about 1.8%). This results confirms that Jonathan Edwards world record is difficult (but not impossible) to improve in the near future. The estimated probability of an annual exceedance of the current world record is 0.011.

## References

1. B. C. Arnold, N. Balakrishnan and H. N. Nagaraja. *A first course in order statistics*, New York, Wiley, 1992.
2. J. Beirlant, F. Caeiro and M.I. Gomes, An overview and open research topics in statistics of univariate extremes, *Revstat* 10, 1, 1–31, 2012.
3. S. Coles. *An Introduction to Statistical Modeling of Extreme Values*. Springer-Verlag, London 2001.
4. H.A. David and H.N. Nagaraja. *Order Statistics*, 3rd ed. Hoboken, New Jersey: Wiley, 2003.
5. M. Dwass. Extremal processes. *Ann. Math. Statist.* 35, 1718–1725, 1964.
6. Fisher, R.A. and L.H.C. Tippett. Limiting forms of the frequency of the largest or smallest member of a sample, *Proc. Cambridge Phil. Soc.*, 24, 180–190, 1928.
7. M. Fréchet. Sur le loi de probabilité de l'écart maximum, *Ann. Soc. Polonaise Math.*, 6, 93–116, 1927.
8. J.D. Gibbons and S. Chakraborti. *Nonparametric Statistical Inference*. CRC Press, 2011.
9. B.V. Gnedenko. Sur la Distribution Limite du Terme Maximum d'une Série Aléatoire. *Ann. Math.*, 44, 423–453, 1943.
10. M.I. Gomes and A. Guillou, Extreme Value Theory and Statistics of Univariate Extremes: A Review. *International Statistical Review*, 83, 2, 263–292, 2015.
11. L. de Haan and A. Ferreira. *Extreme Value Theory: An Introduction*. New York: Springer Science+Business Media LLC, 2006.
12. J. Hosking, J. Wallis and E. Wood. Estimation of the generalized extreme value distribution by the method of probability-weighted moments. *Technometrics* 27(3), 251–261, 1985.
13. A.F. Jenkinson. The frequency distribution of the annual maximum (or minimum) values of meteorological elements, *Quart. J. R. Meteorol. Soc.*, 81, 158–171, 1955.
14. M.R. Leadbetter, G. Lindgren and H. Rootzn. *Extremes and Related Properties of Random Sequences and Processes*. New York - Berlin: Springer-Verlag, 1983.
15. A. Mateus and F. Caeiro. Comparing several tests of randomness based on the difference of observations. In T. Simos, G. Psihoyios and Ch. Tsitouras (eds.), *AIP Conf. Proc.* 1558, 809–812, 2013.
16. A. Mateus and F. Caeiro. An R implementation of several randomness tests. In T. E. Simos, Z. Kalogiratou and T. Monovasilis (eds.), *AIP Conf. Proc.* 1618, 531–534, 2014.
17. A. Mateus and F. Caeiro. The difference-sign randomness test: A review. In T.E. Simos, Z. Kalogiratou and T. Monovasilis, T. (eds.) *AIP Conference Proceedings* 1702, 030002, 2015.  
An R implementation of several randomness tests. In T. E. Simos, Z. Kalogiratou and T. Monovasilis (eds.), *AIP Conf. Proc.* 1618, 531–534, 2014.
18. R. von Mises. La distribution de la plus grande de n valeurs, *Revue Math. Union Interbalcanique*, 1, 141–160, 1936. Reprinted in *Selected Papers of Richard von Mises*, *Amer. Math. Soc.*, 2, 271–294, 1964.
19. R.L. Smith. Maximum likelihood estimation in a class of nonregular cases. *Biometrika*, 72, 1, 67–90, 1985.
20. R.L. Smith. Extreme Value Theory Based on the r largest Annual Events. *Journal of Hydrology*, 86, 27–43, 1986.
21. I. Weissman. Estimation of parameters and large quantiles based on the k largest observations. *J. Am. Statist. Assoc.*, 73, 812–815, 1978.



# On the behavior of alternative splitting criteria for CUB Model-based trees

Carmela Cappelli<sup>1</sup>, Rosaria Simone<sup>1</sup>, and Francesca di Iorio<sup>1</sup>

Department of Political Sciences via L. Rodinò, 22, Università Federico II, Napoli, Italy

(E-mail: [carcappe@unina.it](mailto:carcappe@unina.it), [rosaria.simone@unina.it](mailto:rosaria.simone@unina.it), [fdiorio@unina.it](mailto:fdiorio@unina.it))

**Abstract.** Ordinal responses in the form of ratings arise frequently in social sciences, marketing and business applications where preferences, opinions and perceptions play a major role and it is common to collect along with rater's evaluation, a set of covariates that characterize the respondent and/or the item/service. In this framework, the ordinal nature of the response has to be properly taken into account when the interest is in the understanding of different response patterns in terms of subjects' covariates. In this spirit, a model-based tree procedure for ordinal scores is illustrated: its structure is based on a class of mixture models for ordinal rating data that implies a twofold analysis in terms of feeling and uncertainty and effective graphical visualization of results. The chosen modelling framework entails that the splitting criterion can be customized according to the purposes of the study and the available data. Thus, the selection of variables yielding to the best partitioning results is driven by fitting measures or classical likelihood and deviance measurements, for instance. In order to illustrate the performances of the different splitting criterion for the CUBRE-MOT procedure, we consider data from the 5th European Working Condition Survey carried out by Eurofound in 2010, comparison with alternative approaches that grow trees for ordinal responses is also outlined.

**Keywords:** Ordinal Data, Model-based Trees, Splitting Criteria.

## 1 Introduction

Tree based methods are a non parametric approach to modelling the relationship between a response variable and a set of covariates. In the last decades they have proven to be useful tools for high dimensional data analysis, able to capture non-linear structures and interactions, leading to several methodological proposals and applications. The process of growing trees relies on a top-down partitioning algorithm that is known as recursive binary splitting, as it is based on a splitting criterion that allows to choose at each tree node (i.e. a subset of observations), the best split, i.e. binary division into two subgroups. All the covariates, irrespective of their original scale of measurements, are dichotomized to produce candidate splits in order to identify the optimal one that achieves the highest reduction in impurity when dividing the parent node into its child nodes. Impurity refers to the heterogeneity of the response

---

<sup>5</sup>*th* SMTDA Conference Proceedings, 12-15 June 2018, Chania, Crete, Greece



variable and the way it is practically measured depends on its nature. Recently, the case of ordinal responses has attracted the attention of the statistical community and procedures based on the definition of proper impurity functions for ordinal scores have been proposed [9] and implemented in the package `RpartScore` for the R environment.

In the spirit of the model-based partitioning approach [10], this issue has been addressed by [2,3] in a model based framework focussing on CUB models [4,8,5]. The acronym CUB derives from Combination of Uniform and shifted Binomial random variables in the mixture that define the model. Indeed, the rationale behind these models is that discrete choices arise from a psychological process that involves two components: a personal feeling and an inherent uncertainty in choosing the ordinal response. Feeling is usually related to subjects' motivations and it can be adequately represented by the shifted Binomial random variable since it provides a discrete version of a latent judgement process by mapping a continuous and unobserved evaluation into a discrete set of values. The discrete Uniform random variable is employed for describing the inherent uncertainty of a discrete choice process because it represents the model with maximum entropy on a finite discrete support and its weight in the mixture is thus a measure of heterogeneity. The model can be employed *per se* to estimate the expected distribution given a sample of  $n$  observed ordinal values. Nevertheless its usefulness and relevance are greatly improved by the introduction of covariates that can be related either to feeling or uncertainty. If we consider the model parameters as functions of subjects' covariates we get a CUB regression model, i.e., a regression model for an ordinal response in which the selection of the covariates for uncertainty and/or feeling, that mostly explain the response and improve the fitting, is a relevant issue.

The procedure for growing trees for ordinal responses in which every node is associated with a CUB regression model is known as CUBREMOT (CUB REGression MODEL Trees). So far, two splitting criteria for CUBREMOT have been implemented for node partitioning: the first considers the log-likelihood increment from the father node to the child nodes for each possible split, and then chooses the one that maximizes such deviance, the second focuses on the dissimilarity between child nodes, aiming at generating child nodes as far apart as possible with respect to the probability distributions estimated by CUB models. Both splitting criteria generate a model-based tree whose terminal nodes provide different profiles of respondents, which are classified into nodes according to levels of feeling and/or uncertainty conditional to the splitting covariates. In this way a twofold objective is achieved: the most explanatory covariates are automatically selected in the partitioning process and the terminal nodes in the tree provide alternative profiles of respondents based on the covariates values.

In what follows, we illustrate the structure of CUBREMOT and test the splitting criteria, then we present the results of an application to data on stress perception from the official European Working Condition Survey, also comparing our procedure with other tree methods for ordinal responses.

## 2 CUBREMOT

In CUBREMOT, the top-down partitioning algorithm that grows the tree is based on the estimation, at each tree node, of CUB models [4] whose paradigm designs the data generating process yielding to a discrete choice on a rating scale as the combination of a *feeling* and an *uncertainty* component. The resulting mixture prescribes a shifted Binomial distribution for feeling to account for substantial likes and agreement and assigns a discrete Uniform distribution for uncertainty to shape heterogeneity. Then, if  $R_i$  denotes the response of the  $i$ -th subject to a given item of a questionnaire collected on a  $m$  point scale,

$$Pr(R_i = r | \pi_i, \xi_i) = \pi_i \binom{m-1}{r-1} \xi_i^{m-r} (1-\xi_i)^{r-1} + (1-\pi_i) \frac{1}{m}, \quad r = 1, \dots, m,$$

where the model parameters  $\pi_i$  and  $\xi_i$  are called uncertainty and feeling parameter, respectively. Covariates are possibly specified in the model in order to relate feeling and/or uncertainty to respondents' profiles. Customarily, a logit link is considered:

$$\text{logit}(\pi_i) = \mathbf{y}_i \boldsymbol{\beta}; \quad \text{logit}(\xi_i) = \mathbf{w}_i \boldsymbol{\gamma}, \quad (1)$$

where  $\mathbf{y}_i, \mathbf{w}_i$  are the values of selected explanatory variables for the  $i$ -th subject. If no covariate is considered neither for feeling nor for uncertainty, then  $\pi_i = \pi$  and  $\xi_i = \xi$  are constant among subjects. Estimation of CUB models relies on likelihood methods and on the implementation of the Expectation-Maximization (EM) algorithm.

To grow a CUBREMOT, according to binary recursive partitioning, each of the available covariates is sequentially transformed into suitably splitting variables or binary questions which are Boolean condition on the value (or categories) of the covariate where the condition is either satisfied (“yes”) or not satisfied (“no”) by the observed value of that covariate (for details see [1]). Then, for a given node  $k \geq 1$  with size  $n_k$ , a CUB without covariates is fitted, whose log-likelihood at the final ML estimates  $(\hat{\pi}_k, \hat{\xi}_k)$  is denoted by  $\mathcal{L}_{n_k}(\hat{\pi}_k, \hat{\xi}_k)$ . For a splitting variable  $s$ , a CUB regression model is tested: if it is significant for at least one component, it implies a split into a left and a right child nodes that will be associated with the conditional distributions  $R|s = 0$  with parameter values  $(\hat{\pi}_{2k}, \hat{\xi}_{2k})$  and  $R|s = 1$  with parameter values  $(\hat{\pi}_{2k+1}, \hat{\xi}_{2k+1})$ , respectively. In this way a set of significant candidate splitting variables of node  $k$ ,  $\mathcal{S}_k = \{s_{k,1}, \dots, s_{k,l}\}$ , is identified. The best split in  $\mathcal{S}_k$  can be chosen according to two alternative *goodness of split* criteria.

- Log-likelihood splitting criterion: this criterion considers the improvement in log-likelihood yielded by the inclusion of the significant splitting variable and the best split, being associated with the maximum log-likelihood increment, provides the child nodes characterized by the most plausible values for CUB parameters. The best split maximizes the deviance:

$$\Delta \mathcal{L}_k = [\mathcal{L}_{n_{2k}}(\hat{\pi}_{2k}, \hat{\xi}_{2k}) + \mathcal{L}_{n_{2k+1}}(\hat{\pi}_{2k+1}, \hat{\xi}_{2k+1})] - \mathcal{L}_{n_k}(\hat{\pi}_k, \hat{\xi}_k). \quad (2)$$

- Dissimilarity measure splitting criterion: this criterion considers a proper version of the normalized index proposed by [7] that compares an estimated probability distribution with the observed relative frequencies and it is generally considered in the framework of CUB models as a goodness of fit measure. Specifically, aiming at the generation of child nodes that are the farthest apart from each other in terms of distribution of the responses, this criterion selects for the  $k$ -th node the split that maximizes the distance between the estimated CUB probability distributions  $\hat{p}^{(2k)}$  and  $\hat{p}^{(2k+1)}$  for the child nodes:

$$Diss(2k, 2k + 1) = \frac{1}{2} \sum_{r=1}^m |\hat{p}_r^{(2k)} - \hat{p}_r^{(2k+1)}|. \quad (3)$$

The choice of this normalized index entails that, as long as CUB models estimated at the child nodes provide an adequate fitting, the splitting variable generates an optimal partition of the father node in terms of the chosen distance. In particular, the resulting terminal nodes determine well-separated profiles of respondents, in terms of feeling (agreement, preferences, and so on) and/or uncertainty (indecision, heterogeneity).

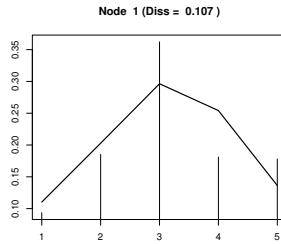
In both cases, the node partitioning process stops and a node is declared terminal if none of the available covariates is significant (neither for feeling nor for uncertainty), or if the sample size is too small to support a CUB model fit.

### 3 Application and comparison

In order to illustrate the classification performances of the different splitting criteria for the CUBREMOT procedure, we grown a tree, up to the 3rd level, considering data from the 5th European Working Condition Survey carried out by Eurofound in 2010, that allows to recover information on individuals about their working conditions for the EU28. The analysis of work-life balance indicators will focus on  $N = 972$  responses for Italy to the question ‘Do you experience stress in your work?’ measured on a  $m = 5$  wording-type scale: ‘Always’, ‘Most of the time’, ‘Sometimes’, ‘Rarely’, ‘Never’, coded from 1 to 5 for computational purposes. Thus, when testing CUB models, the feeling parameter  $\xi$  is a direct indicator of stress perception: Figure 1 displays observed (vertical bars) and fitted distributions.

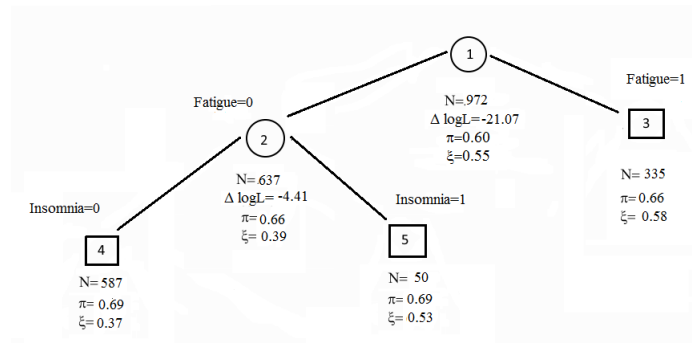
To avoid bias in favor of variables with many splits, we consider as covariates, dichotomous factors *Gender* (1 for women, 0 for men), experience of *Insomnia*, experience of *Fatigue*, experience of *Depression*, presence of *Risk* connected to the job stability. The only non dichotomous covariate is the size of the *Household* as number of components.

Figure 2 shows the CUBREMOT grown when applying the log-likelihood splitting criterion: for each split, the value of the deviance in log-likelihood is reported along with nodes sizes and parameter values; terminal nodes are squared. This method allows to disentangle that experience of *Fatigue* is the primary component of stress assessment, followed by *Insomnia*. These factors



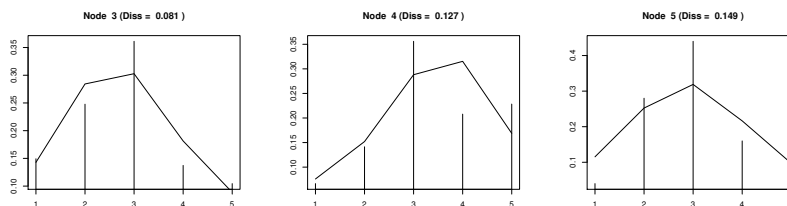
**Fig. 1.** Observed and fitted CUB distributions of work-related stress at the root node

induce higher level of stress experience but do not modify the level of heterogeneity and indecision (which is very moderate being  $1 - \pi < 0.5$  at each node).



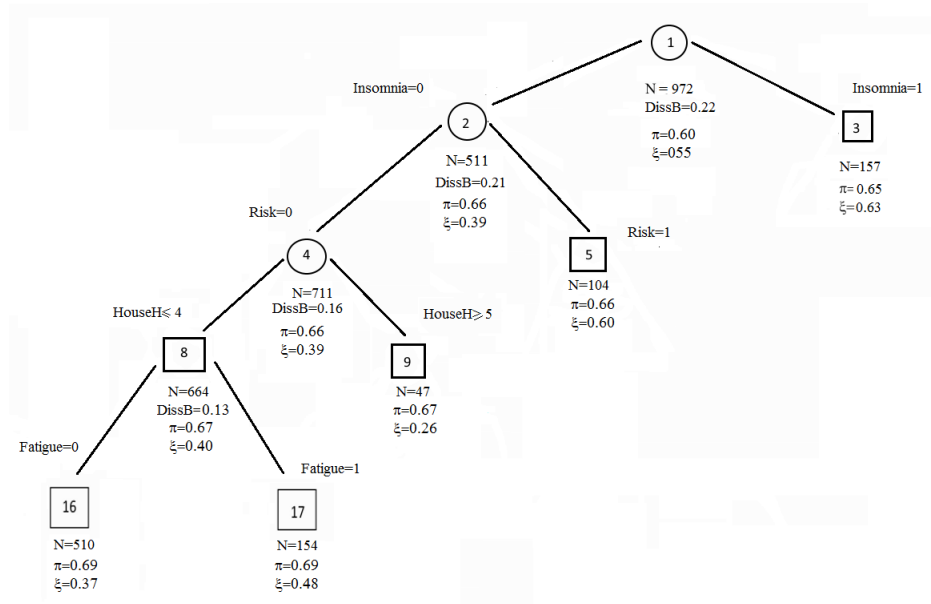
**Fig. 2.** CUBREMOT for Perceived Stress with application of the log-likelihood splitting criterion

Figure 5 shows observed (vertical lines) and estimated probability distributions for the root and the terminal nodes of the CUBREMOT tree grown up to the 3rd level with the log-likelihood splitting criterion. The dissimilarity between observed and fitted distributions is also noted.



**Fig. 3.** Terminal nodes distributions for the CUBREMOT with log-likelihood splitting

Figure 4 shows the CUBREMOT grown when applying the dissimilarity splitting criterion, instead: for each split, the value of the dissimilarity between estimated CUB distribution at nodes ( $DissB$ ) is reported along with nodes sizes and parameter values. From this perspective, it turns out that Insomnia is more crucial in discriminating responses according to stress perception: among people who do not suffer from Insomnia, risk perception intervenes in increasing stress experience. These factors induce higher level of stress experience but do not modify the level of heterogeneity and indecision (which is very moderate being  $1 - \pi < 0.5$  at each node). Among those not feeling at risk, having a large household (with more than 5 components) reduces work-related stress, whereas among those with smaller household sizes (less than 4 components), experiences of fatigue increases stress perception. As a result, we can state that in this case the dissimilarity splitting criterion offers a deeper understanding of the factors influencing work-related stress perception, reducing the dissimilarity between nodes from 22% down to 13%; the log-likelihood criterion, instead, despite being more natural, is more restrictive.



**Fig. 4.** CUBREMOT for Perceived Stress with application of the dissimilarity splitting criterion

Figure 5 shows observed (vertical lines) and estimated probability distributions for the root and the terminal nodes of the CUBREMOT tree grown up to the 3rd level with the log-likelihood splitting criterion. The dissimilarity between observed and fitted distribution is also noted.

The data set has been also analyzed with the MOdel-Based recursive partitioning (MOB) of [10] that first uses a parameter instability test to determine the splitting variable to be used before search all possible split points in that

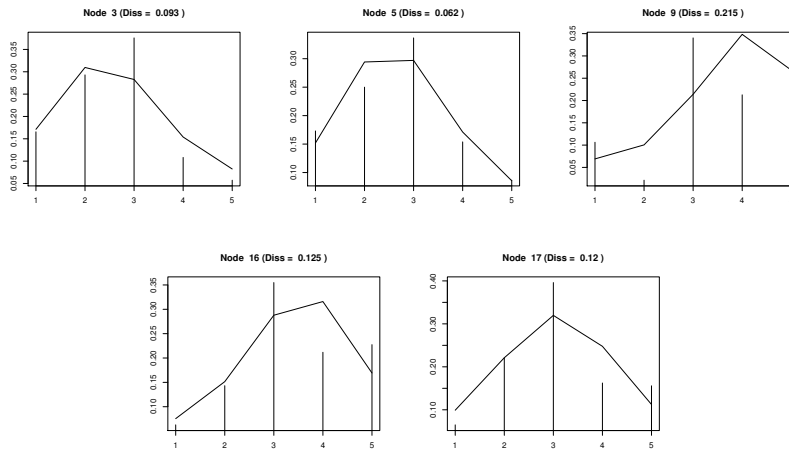


**Fig. 5.** Terminal nodes distributions for the CUBREMOT with dissimilarity splitting

variable, and with the functions in the R package `RpartScore` for building classification trees for ordinal responses within the CART framework, using the Generalized Gini impurity function. The corresponding trees are displayed in Figure 6 and Figure 7, respectively. Note that the upper splits of these trees are identical, but the tree built using `RpartScore` shows two further splits of lower level nodes. However, it is worth noticing that the `RpartScore` tree does not achieve any reduction of the estimated misclassification costs as shown by the associated plot. Moreover, both in MOB and `RpartScore` tree, after the split of the root node with factor Fatigue (as in CUBREMOT with the log-likelihood splitting criterion) the node with Fatigue = 0 (637 observations) is declared terminal and further splits are made on the other root node child. This finding suggests that CUBREMOT, being based on a different paradigm, helps to disentangle alternative drivers of the respondents opinions.

## 4 Further developments

The model-based approach to regression and classification trees comes with more advantageous discrimination performances: in light of this expectation, the CUBREMOT methodology has a wider outreach in flexibility and interpretation of results since it allows to integrate different goodness of fit measures with the partitioning algorithm while affording a twofold analysis of responses in terms of feeling and uncertainty. For the case study here analysed, uncertainty has been found overall constant when classifying respondents, namely, responses are homogeneous also when controlling for covariates values. In other circumstances, classification is needed also with respect to the latent uncertainty. In such cases, the implementation of a splitting criterion that selects, at each step, the partitioning variable for feeling that mostly reduces the overall uncertainty is eligible and it is under investigation. Furthermore, the CUBREMOT strategy could be easily extended to encompass CUB models extensions to

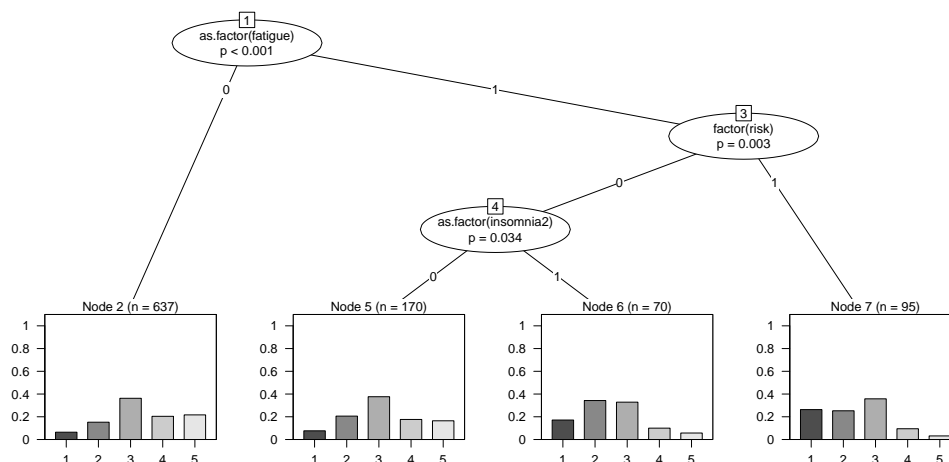


**Fig. 6.** Tree for Perceived Stress as implemented by the `partymob` package

incorporate (structural) inflated frequencies (like in the analyzed case study) and overdispersion: these ideas are under investigations as well.

## References

1. Breiman L., Friedman J.H., Olshen R.A, Stone C.J. *Classification and Regression Trees*. Wadsworth & Brooks: Monterey (CA), 1984.
2. Cappelli, M., Simone, R. and Di Iorio, F. Model-based trees to classify perception and uncertainty: analyzing trust in European institutions, *under review*, 2017.
3. Cappelli, C., Simone, R., Di Iorio, F. Growing happiness: a model-based tree. In SIS 2017. Statistics and Data Science: new challenges, new generations. Proceedings of the Conference of the Italian Statistical Society, Florence June 2017, 261-266, 2017.
4. D’Elia, A., Piccolo, D. A mixture model for preference data analysis. *Computational Statistics & Data Analysis*, 49, 917-934, 2005.
5. Iannario, M., Piccolo, D.: CUB models: Statistical methods and empirical evidence. In: R.S. Kenett and S. Salini (eds.), *Modern Analysis of Customer Surveys: with Applications Using R*, 231-258. Wiley, Chichester, 2012.
6. Galimberti, G., Soffritti, G. and Di Maso, M.: Classification Trees for Ordinal Responses in R: The RpartScore Package, *Journal of Statistical Software*, 47, 1-25, 2012.
7. Leti, G.: *Statistica descrittiva*. Il Mulino, Bologna, 1983.
8. Piccolo, D., D’Elia, A.: A new approach for modelling consumers’ preferences. *Food Quality & Preference*, 19, 47-259, 2008.
9. Piccarretta, R. Classification trees for ordinal variables, *Computational Statistics*, 23, 407-427, 2008.
10. Zeileis, A., Hothorn, T., Hornik, K., Model-Based Recursive Partitioning, *Journal of Computational and Graphical Statistics*, 17, 492-514, 2008.

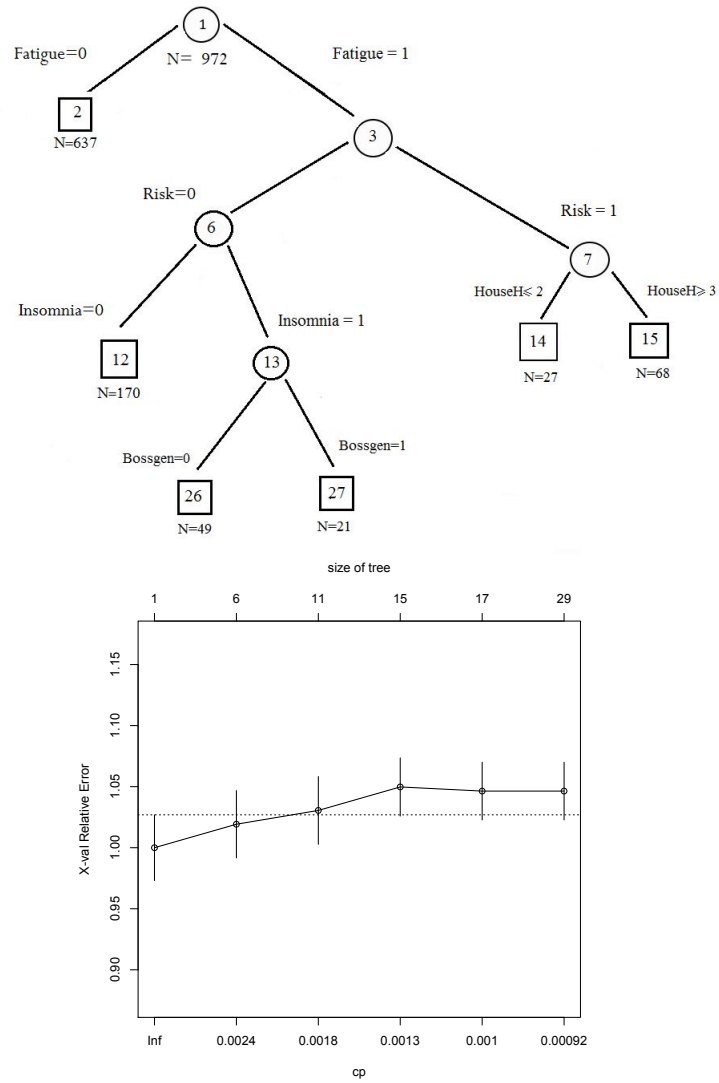


Fig. 7. Tree for Perceived Stress as implemented by the Rpartscore package



## Modeling of mortality in elderly by prostate diseases in Brazil

João Batista Carvalho<sup>1</sup> and Neir Antunes Paes<sup>2</sup>

- <sup>1</sup> Department of Statistics, Federal University of Campina Grande, PB, Brazil. PhD Candidate in Health and Decision Modeling Postgraduate Course, Federal University of Paraíba, João Pessoa, PB, Brazil.  
(E-mail: joaouaest@gmail.com)
- <sup>2</sup> Health and Decision Modeling Postgraduate Course. Federal University of Paraíba, João Pessoa, PB, Brazil.  
(E-mail: antunes@de.ufpb.br)

**Abstract:** Northeastern Brazil can be considered as one of the less developed regions of the country. With a population of 56 million inhabitants in 2015, it features deficient vital statistics, which hinders the ability of management and development of public health policies. Aiming at identifying explanatory factors of life conditions and vulnerability of one of the major causes of mortality in elderly, the prostate diseases, a cross-sectional ecological study to the year 2010, using micro-data information, was adopted to the 188 micro regions of the northeastern of Brazil. The following steps were performed: 1) The death data were corrected by underreporting, and ill defined causes as well garbage codes were redistributed to the corresponding prostate deaths by applying appropriate techniques; 2) The evolution of corrected mortality rates from 2010 to 2015 was performed; 3) The Structural Equations Modeling (SEM) was applied. The outcome mortality rates due to prostate disease were observed directly, and a set of life conditions and vulnerability indicators regarding to health, education, income and environmental conditions were used indirectly as latent variable. From the Health Ministry were extracted mortality data. This study traced a regional overview of the mortality due to prostate diseases among old men in the northeast of Brazil, pointing out distinct realities by using the micro-data of the late Census 2010. The SEM proved to be highly sensitive with significance in the measurement model for some relevant latent variables that can subsidize political planning. In view of the high rates observed and an aging process still rising in the Northeast, is expected that these levels should increase even more in the near future, aggravating an already worrying picture.

**Keywords:** prostate diseases, mortality in the elderly, structural equations modeling.



## 1 Introduction

Prostate cancer is one of the greater magnitude types of cancer in both incidence and mortality of men worldwide. For the year 2012, estimates of disease mortality rates produced by the Globocan project of the International Agency for Research on Cancer (IARC) showed a variation between 3 and 30 deaths per 100,000 men in the regions surveyed on all continents and an overall mortality rate of 7.8/100 thousand (Ferlay *et al.*[1]).

In Brazil, the number of cases has increased considerably in the last decades, partly due to the increase in life expectancy, since prostate cancer is rare in men under 40 years old and quite incident in men older than 60 years old (Howlader *et al.*[2]). A total of 68,220 new cases of the disease were estimated for each year of the 2018-2019 biennium. These values correspond to an estimated risk of 66.1 new cases per 100,000 men. For the Northeast region of the country, this value is 56.2/100 thousand (INCA[3]).

According to official statistics, prostate cancer occupies the first position among neoplasms in the mortality of brazilians in the age group of 60 years and over. In 2015, it was responsible for 13,755 deaths, which corresponded to 17.4% of the deaths of elderly men due to neoplasms. For the Northeast region, this percentage was 23.5% (Brazil[4]). With a population of 56 million in 2015 and an HDI of 0.69, classified as low, this region is considered to be one of the least developed in Latin America. It goes through a process of demographic and epidemiological transition that is late and unequal and faces the consequences of population aging without having reached reasonable levels of development.

In addition to age, clinical and genetic factors, mortality due to prostate cancer also varies according to socioeconomic and environmental factors (Howlader *et al.*[2]). On the one hand, the richer nations have already shown a downward trend in their rates, on the other, in developing and poor countries, rates are rising. In Brazil, an upward trend up to 2030 for the Northeast region was pointed out (Barbosa *et al.*[5]). Therefore, in this study, the objective was to identify life and vulnerability factors explaining the mortality of elderly people in the Brazilian Northeast for prostate cancer through the modeling of structural equations (SEM).

## 2 Methods

A cross-sectional ecological design was adopted in the years 2010 and 2015 having as units of observational analysis the 187 microregions that make up the nine states of the Northeast region of Brazil. Information on prostate cancer mortality and socioeconomic and demographic indicators for elderly men aged 60 and over in the microregions was used.

The census population of 2010 and the projected for 2015 of elderly men of the microregions were obtained from the Brazilian Institute of Geography and Statistics (IBGE). Information on deaths was extracted from the Mortality Information System of the Ministry of Health (SIM/MS). To reduce

the effect of random fluctuations in death data, the average of the deaths computed for the triennium 2009, 2010 and 2011 was used. The average of these years was used in the application of the SEM. Socioeconomic and demographic indicators were obtained from the System of Health Indicators and Follow-up of Policies for the Elderly (SISAP-Aged), managed by the Oswaldo Cruz Foundation (Fiocruz[6]).

The indicators referring to the elderly men used as explanatory and associated with prostate cancer mortality were: percentage of elderly people living in inadequate households, percentage of elderly people living in households with piped water, percentage of elderly people living in households with waste disposal service, percentage of elderly people living in households with sewage system, percentage of illiterate elderly people, percentage of elderly persons with a nominal income of up to one minimum wage, percentage of economically active elderly, percentage of elderly people living in poverty, percentage of elderly living alone and percentage of elderly people who are responsible for the household. The stages outlined for the development of the work are described below.

Stage 1: the method proposed by Ledermann[7] was used to redistribute between neoplasms and the other Chapters of the International Classification of Diseases (ICD-10) the deaths of elderly men from each microregion classified in the group of ill-defined (Chapter XVIII of ICD-10). This method uses simple linear regression (Vallin[8]). In its application, the proportion of deaths of elderly men due to neoplasms was considered as a response variable and the proportion of deaths of elderly men due to ill-defined causes was a covariate. Therefore, the absolute value of the coefficient of the estimated line provided the proportion of deaths due to ill-defined causes to be redistributed to the neoplasms in each microregion.

Stage 2: to reduce the impact of death coverage deficits, correction factors were estimated using the quotient between the deaths of elderly men due to neoplasms corrected according to Active Search Research and the ones registered at SIM. The product between the deaths corrected in the previous stage and the corresponding correction factors provided the total of deaths due to neoplasms corrected for underreporting in each microregion.

Stage 3: proportional redistribution of deaths due to neoplasms corrected for ill-defined causes and under-registration among types of neoplasms was carried out. In addition, the deaths related to the garbage codes were redistributed: malignant neoplasms from other poorly defined locations (C76) and malignant neoplasms with no location specification (C80). Thus, the deaths of elderly people due to poorly defined causes of prostate cancer, underreporting and garbage codes were obtained, which, proportionally, were redistributed among the five-year age groups of the elderly aged 60 and over.

Stage 4: The standardized rates of mortality of the elderly by prostate cancer were calculated for each microregion using as standard population the census population of Brazil in 2010, referring to the elderly of both sexes. Rates were expressed per 100,000 inhabitants.

Maps showing regional differentials for the standardized mortality rates of the elderly in the Northeastern microregions were constructed using TabWin software, version 3.6.

Stage 5: the structural equations modeling technique was used to test the validity of the association of socioeconomic factors with prostate cancer mortality.

The SEM consists of the simultaneous analysis of a series of casual, hypothetical relations between variables (Hair *et al.*[9]). This technique can be organized into two sub-templates according to the proposed relational structure for the study variables (Marôco[10]): the measurement sub-template (measurement equations), which establishes how exogenous constructs ( $\xi$ ) are measured by observable variables (X). This is,

$$X = \Lambda\xi + \varepsilon$$

Where  $\Lambda$  is the matrix of regression coefficients and  $\varepsilon$ , the vector of random errors; and the structural sub-template (structural equations), which represents the causal relationship between exogenous ( $\xi$ ) and endogenous ( $\eta$ ) variables. This sub-template has the following equation:

$$\eta = \Gamma\xi + B\eta + \delta$$

Where  $\Gamma$  and  $B$  are the regression coefficient matrices and  $\delta$ , the random error vector.

The proposed theoretical model involves the relation between the exogenous construct (living conditions and vulnerability), measured indirectly by the indicators obtained from the SISAP-Elderly, and the endogenous variable standardized rate of prostate cancer mortality. In the SEM application, the software AMOS - Analysis of Moment Structures, version 18 was used. The analysis provided the adjustment to the measurement sub-template using the standardized estimates or regression coefficients and the adjustment to the structural sub-template using the indexes of the quality of adjustment (Marôco[10]; Kline[11]).

### 3 Results

Among the stages of correction of deaths, under-reporting factor, redistribution of ill-defined causes and *garbage* codes, the first one was the one with the greatest impact for most of the microregions in the two years analyzed. Table 1 shows the contribution of each stage in the correction of prostate cancer deaths. In the Northeast, the original deaths observed were 1023 deaths in 2010 and 1040 in 2015. The states that gained the most recovered deaths were Maranhão and Bahia.

Table 1: Contribution of each stage of correction of prostate cancer deaths among the elderly in the microregions of the Northeast, 2010 and 2015.

State	Registered deaths	Corrected deaths	Stages of correction of deaths			Total
			Under-reporting	Ill-defined	Garbage codes	
<b>2010</b>						
Maranhão	270	390	77	33	10	120
Piauí	203	257	33	14	7	54
Ceará	545	687	88	31	22	142
Rio G. Norte	242	302	35	9	16	60
Paraíba	262	338	32	30	14	76
Pernambuco	615	742	49	48	31	127
Alagoas	128	169	11	22	8	41
Sergipe	149	177	10	13	5	28
Bahia	919	1294	121	210	44	375
Northeast	3333	4356	453	413	157	1023
<b>2015</b>						
Maranhão	349	478	94	26	9	129
Piauí	234	285	36	9	6	51
Ceará	593	743	94	34	22	150
Rio G. Norte	252	304	35	8	8	52
Paraíba	312	380	33	24	11	68
Pernambuco	683	797	52	34	29	114
Alagoas	154	184	12	12	6	30
Sergipe	175	209	12	16	6	34
Bahia	1124	1537	143	224	45	413
Northeast	3876	4916	511	388	141	1040

Figure 1 shows the spatial distribution, by microregions, of the standardized rates of prostate cancer mortality in 2010 and 2015. It is noted that the majority of microregions had higher rates in 2015. The range from 116 to 175 deaths/100 thousand included 47.6% of the microregions, being the most frequent in 2010. In 2015, most of the microregions (34.5%) presented their rates within the range of 175 to 235 deaths/100 thousand.

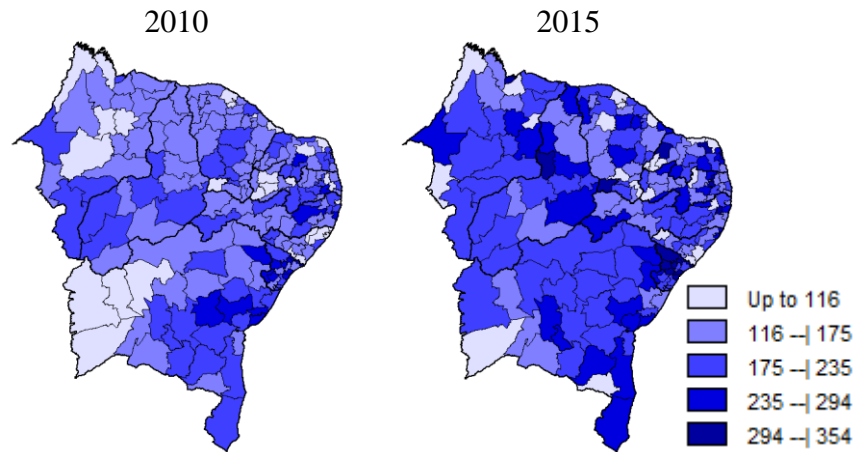


Fig. 1. Standardized mortality rates (per 100 thousand elderly) for prostate cancer for the microregions of the Northeast, 2010 and 2015.

Considering the standardized mortality rate by prostate cancer in Brazil in 2010 as a reference, whose value was 165.3 deaths per 100,000 elderly people, it was verified that, in 2010, 87 (46.5%) microregions presented rates above the rate national level, while in 2015 the percentage was 69.0%, corresponding to a total of 129 microregions.

Figure 2 illustrates the path diagram for the proposed re-specified theoretical model. Among the ten initial indicators used for analysis, three provided significance to the adjustment of the final model. The other indicators, because they showed multi-collinearity, were withdrawn. The results of the standardized SEM (correlations) solution for the final model were significant for the following indicators: percentage of illiterate elderly (0.66), percentage of elderly in poverty (0.71) and percentage of elderly living in inadequate households (0.87), meeting the criteria of convergent validity for the measurement model of the exogenous construct living conditions and vulnerability. It is emphasized that high values of these indicators reflect low living conditions of the elderly people. Thus, with a standardized coefficient of -0.44, the structural model had an inverse effect on the relation between indicators representing poor living conditions of the elderly and the standardized rates of prostate cancer mortality. That is, rates were higher in microregions where the magnitudes of these indicators were low. In addition, the criteria for a good adjustment of the model, established in Marôco[10] and Kline[11], were all satisfied, as shown in Table 2.

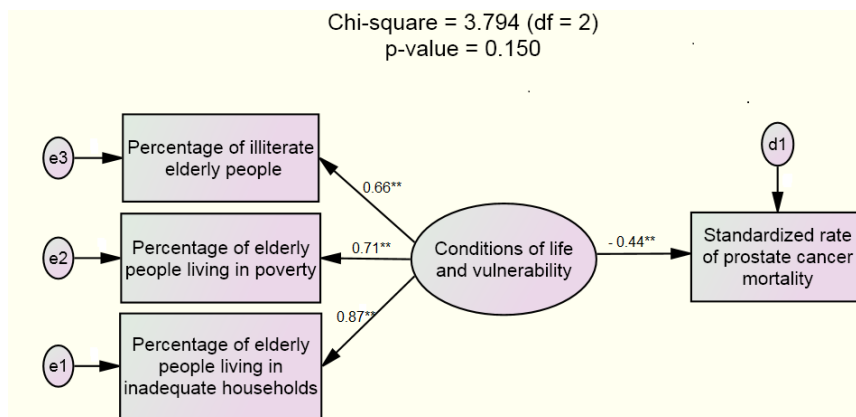


Fig. 2. Standardized estimates of the SEM for the final model.  
(\*\*significant correlations, p-value < 0,01)

Table 2. Adjustment indicators of the SEM for modeling the mortality of the elderly for prostate cancer in the microregions of the Brazilian Northeast.

Adjustment indicator	Criterion for a good fit of the model	Final model
Chi-square: $\chi^2$ (p-value)	-	3.794 (0.150*)
Normed chi-square ( $\chi^2/df$ )	between 1 and 2	1.897
Goodness of Fit Index (GFI)	above 0.90	0.989
Adjusted GFI (AGFI)	above 0.90	0.951
Normed Fit Index (NFI)	above 0.90	0.982
Tucker-Lewis Index (TLI)	above 0.90	0.991
Root Mean Square Error Approximation (RMSEA)	less than 0.08	0.069

(\*) p-value > 0.01 indicates overall adjustment of the model, at the 1% level of significance.

## 4 Discussion

Prostate cancer in the microregions of the Brazilian Northeast and of the country is the major cause of mortality of the male elderly among malignant neoplasms, highlighting the importance of investigating the association of mortality with indicators of living conditions and vulnerability of these populations.

A study about prostate cancer rates across the world found that incidence rates remain highest in regions with the highest incomes in the world, including North America, Oceania, and Europe. However, due to greater efficiency in health care and follow-up of patients with prostate disease in these regions, mortality rates presented declining trends. In low and middle-income regions, including parts of South America (Brazil), the Caribbean and sub-Saharan Africa, prostate cancer mortality follows an upward trend (Center *et al.*[12]).

The relationship between socioeconomic factors and cancer has been addressed in several researches (Ibfeft *et al.*[13]; Menvielle *et al.*[14]; Manser and Bauerfeind [15]; Pikala *et al.*[16]). Ribeiro and Nardocci[17] investigated associations between socioeconomic inequalities and cancer mortality and their types through the gathering of ecological studies conducted between 1998 and 2008 in several countries. Of the thirty-two eligible studies, eight refer to the populations of Brazil. In relation to prostate cancer, there was a positive association (risk of higher outcome in richer areas) with socioeconomic level of the area of residence.

These studies corroborate with the finding here, where SEM modeling indicated an inverse association between standardized rates of prostate cancer mortality and the exogenous construct measured by indicators that reflect the life conditions and vulnerability of the elderly in the northeastern microregions. In other words, the microregions with a lower percentage of elderly people living in inadequate households (for example households without running water, sewage networks or garbage collection services), lower percentage of elderly people living in poverty (household income per capita of up to half a minimum wage) and with lower illiteracy rates showed higher rates of prostate cancer mortality. This should be related to a higher rate of aging and a better quality of death data found in the more developed microregions.

As age is a factor that contributes to the elevation of mortality by prostate cancer, it is alerted to the states of the Northeast region that are in a stage of transition unconsolidated demographics with their elderly population on the rise. In this context, attention is drawn to the states of Sergipe and Alagoas, positioned among the states of Brazil with the lowest rates of aging in 2010.

According to data from the Atlas of Human Development, Paraíba had the highest rate of aging in the Northeast and the third highest in the Country in 2010 (ADH[18]). This year, the highest rate of aging in Brazil was observed in Rio Grande do Sul. This state is among the Brazilian states with the lowest fertility rates and the highest rates of prostate cancer mortality. In contrast, all the states of the Northeast had fertility rates above the value observed for Brazil. Thus, Rio Grande do Sul is a typical example of locality that completed the fourth phase of the demographic and epidemiological transition, whose characteristics are: low fecundity, high aging rate and high mortality rates due to chronic-degenerative diseases (Duarte and Barreto[19]). In this sense, the results pointed to a delay in the levels of development of the states of the Northeast in relation to the center-south of the Country, since in none of them was observed these three characteristics simultaneously.

## Conclusions

It is known that neoplasms have, by and large, a well-defined diagnosis in the midst of better follow-up of the patient throughout the treatment. This fact, consequently, provides a better quality in the recorded data of cancer compared to the registries of other causes of mortality. However, the results of this study indicate that the quality of cancer data in the Northeast still lacks improvements, since the variation in the number of deaths due to prostate cancer before and after the correction corresponded to 30.7% in 2010 and 26.8 % in 2015. Thus, the use of corrected deaths by underreporting, redistribution of ill-defined and non-specific causes of mortality meant important improvements. The considerable increases in the number of deaths after correction allowed a greater accuracy in the estimation of mortality rates at the level of microregions.

In the face of the high mortality rates due to this type of cancer presented by the microregions, which for an important amount of them surpassed the mortality rate of Brazil, coupled with an aging process still rising in the Northeast, it is speculated that these levels should still increase more in the near future, aggravating an already worrying picture. Furthermore, it is expected that rates will only begin to decline when the region reaches a certain level of the epidemiological transition as it has been in developed countries. However, given the serious problems of underdevelopment in the region, there will be a slow process. Health care and campaigns to raise the awareness of the importance of this pathology promoted by governmental institutions are useful, but they are not enough, considering the urgent challenges to be faced by the health system of the Brazilian Northeast.

## References

1. J. Ferlay *et al.* GLOBOCAN 2012 v1.0, Cancer Incidence and Mortality Worldwide: IARC CancerBase No. 11 [serial on the Internet] 2013 [cited 2018 feb 22]. Available from: <http://www.globocan.iarc.fr>.
2. N. Howlader *et al.* Seer Cancer Statistics Review, 1975-2014. Bethesda: National Cancer Institute, 2017 [cited 2018 mar 15]. Available from: <https://seer.cancer.gov/csr>.
3. National Cancer Institute José Alencar Gomes da Silva. Estimation of cancer incidence in Brazil 2018. Rio de Janeiro, 2017 [cited 2018 mar 16]. Available from: <http://www.inca.gov.br/estimativa/2018/index.asp>.
4. Brazil. Department of Informatics of SUS (DATASUS). Mortality Information System. Brasília: Ministry of Health, 2017 [cited 2018 fev 18]. Available from: <http://www.datasus.gov.br>.
5. I. Barbosa *et al.* Cancer mortality in Brazil: Temporal Trends and Predictions for the Year 2030. *Medicine (Baltimore)*, 94, 16, 2015.
6. Fundação Oswaldo Cruz (FIOCRUZ). System of Indicator of Health and Follow-up of Policies of the Elderly [cited 2018 jan 25]. Available from: <https://sisapidoso.icict.fiocruz.br/>
7. S. Ledermann. La repartition des décès de causes indéterminées. *Revue d'Institut International de Statistique*, v.23, n.I/3, 1955.
8. J. Vallin. Seminario sobre causas de muerte: Aplicación al caso de Francia. Instituto Nacional de Estudios Demográficos, Santiago-Chile, 1987.

9. Hair Jr. *et al.* Multivariate data analysis. 7. Ed. New York: Prentice Hall, 2010.
10. J. Marôco. Analysis of structural equations: theoretical foundations, software & applications. Pêro Pinheiro: Report Number, 2010.
11. R. Kline. Principles and practice of structural equation modeling. New York: Guilford press, 2011.
12. M. Center *et al.* International Variation in Prostate Cancer Incidence and Mortality Rates. *Eur Urol*, 2012.
13. E. Ibfelt *et al.* Socioeconomic position and survival after cervical cancer: influence of cancer stage, comorbidity and smoking among Danish women diagnosed between 2005 and 2010. *British Journal of Cancer*, 109, 9, 2489{2495, 2013.
14. G. Menvielle *et al.* Diverging trends in educational inequalities in cancer mortality between men and women in the 2000s in France. *BMC Public Health*, 13, 823, 2013.
15. C. Manser and P. Bauerfeind. Impact of socioeconomic status on incidence, mortality, and survival of colorectal cancer patients: a systematic review. *Gastrointestinal Endoscopy*, 80, 1, 42{60, 2014.
16. M. Pikala *et al.* Educational inequalities in premature mortality in Poland, 2002-2011: a population-based cross-sectional study. *BMJ Open*, 6, 9, 2016.
17. A. Ribeiro and A. Nardocci. Socioeconomic inequalities in cancer incidence and mortality: review of ecological studies, 1998-2008. *Health and society*, São Paulo, 22, 3, 878{891, 2013.
18. Atlas of Human Development in Brazil, 2013 [cited 2018 mar 18]. Available from: <http://atlasbrasil.org.br/2013/>.
19. E. Duarte and S. Barreto. Demographic and epidemiological transition: Epidemiology and Health Services revisits and updates the theme. *Epidemiology and Health Services*, 21, 4,529{532, 2012.

# Determining the Structure and Assessing the Psychometric Properties of Multidimensional Scales Constructed from Ordinal and Pseudo-Interval Items

Anastasia Charalampi<sup>1</sup>, Catherine Michalopoulou<sup>2</sup>, and Clive Richardson<sup>3</sup>

<sup>1</sup> Ph.D. Candidate, Department of Social Policy, Panteion University of Social and Political Sciences, Athens, Greece  
(E-mail: natashaharal@yahoo.gr)

<sup>2</sup> Professor of Statistics, Department of Social Policy, Panteion University of Social and Political Sciences, Athens, Greece  
(E-mail: kmichal@panteion.gr)

<sup>3</sup> Professor of Applied Statistics, Department of Economic and Regional Development, Panteion University of Social and Political Sciences, Athens, Greece  
(E-mail: crichard@panteion.gr)

**Abstract.** Determining the structure and assessing the psychometric properties of multidimensional scales before their application is a prerequisite of scaling theory. This involves splitting a sample of adequate size randomly into two halves and first performing Exploratory factor analysis (EFA) on one half-sample in order to assess the construct validity of the scale. Secondly, this structure is validated by carrying out Confirmatory factor analysis (CFA) on the second half. As in any statistical analysis — whether univariate, bivariate or multivariate — the first and most important consideration is to ascertain the level of measurement of the input variables, in this instance the defining items of the scale. This guides the correct choice of the methods to be used. In this paper, we carry out the investigation and assessment of the 2006 European Social Survey six-dimensional instrument of wellbeing for Germany and the Netherlands when items are considered as both ordinal and pseudo-interval.

**Keywords:** Exploratory factor analysis, Confirmatory factor analysis, Reliability, Construct validity, European Social Survey.

## 1 Introduction

Determining the structure and assessing the psychometric properties of multidimensional scales before their application is a prerequisite of scaling theory (Michalopoulou [15]). This involves splitting a sample of adequate size randomly into two halves and first performing Exploratory factor analysis (EFA) on one half-sample in order to investigate the theoretical model of latent factors underlying the observed variables (Bartholomew *et al.* [1]) and assess the construct validity of the scale. Then the structure indicated by EFA is

*5<sup>th</sup> SMTDA Conference Proceedings, 12-15 June 2018, Chania, Crete, Greece*

© 2018 ISAST



validated by carrying out Confirmatory factor analysis (CFA) on the second half-sample. Based on the full sample and the CFA results, the validity and reliability of the resulting subscales, i.e. their psychometric properties, are assessed. In performing these analyses, a sequence of theoretical and rule of thumb decisions is required (Charalampi *et al.* [5]; Michalopoulou [15]). However, as in any statistical analysis – whether univariate, bivariate or multivariate – the first and most important consideration is to ascertain the level of measurement of the input variables, in this instance the defining items of the scale. This guides the correct choice of the methods to be used.

The items of an attitude scale can be categorical or continuous (Tabachnick and Fidell [23]). Furthermore, following Stevens [22], we distinguish four levels of measurement: nominal, ordinal, interval and ratio. In all empirical research, nominal and ordinal items are considered as categorical and interval and ratio items as scale – treated in statistical analyses as continuous (Blalock [2]). In the literature, the level of measurement of the items of most attitude scales is ordinal. However, as we have noted in previous work (Charalampi *et al.* [5]; Michalopoulou [15]), when the number of response categories used for each item is at least five, ordinal categories can be treated as interval and standard statistical analyses may be performed using these pseudo-interval variables (Bartholomew *et al.* [1]).

In this paper, to demonstrate the importance of ascertaining the level of measurement of the items in choosing the methods to be used, we carry out the investigation and assessment of the 2006 European Social Survey (ESS) six-dimensional measurement of personal and social wellbeing. Because the ESS measurement of wellbeing is “a compromise between various theoretical models and the available data” (New Economics Foundation [17: p.59]), its items are assigned various numbers of response categories, in contrast to scaling theory in which responses should be on the same scale. Therefore the ESS items are considered as both ordinal and pseudo-interval. We present results for the European Social Survey Round 3 Data [10] using data from Germany and the Netherlands.

## 2 Method

The theoretical structure of the 2006 ESS measurement of wellbeing is comprised of 27 items defined in six key dimensions (European Social Survey [8, 9]; New Economics Foundation [17]): evaluative wellbeing (2 items), emotional wellbeing (6 items), functioning (8 items), vitality (4 items), community wellbeing (5 items) and supportive relationships (2 items). However, contrary to scaling theory, these items were assigned different number of response categories: 1-4 (11 items); 1-5 (9 Likert items); 1-2 (1 item); 0-6 (1 item); 0-10 (5 items). Therefore, the level of measurement was considered as both ordinal (1-4, 1-2) and pseudo-interval (1-5, 0-6, 0-10). Although this crucial methodological issue was dealt with in the statistical analyses, the

problem of using different definitions for the response categories remains unresolved.

In the first step of the analysis, the sample in each country was randomly split into two halves. EFA was performed on the first half in order to assess the construct validity of the scale. The structure suggested by EFA was subsequently validated by carrying out CFA on the second half. Statistical analyses were performed using Mplus Version 7.4 and IBM Statistics SPSS Version 20. Mplus was used for EFA and CFA because appropriate methods treating items considered as both ordinal and pseudo-interval are provided.

Tabachnick and Fidell [23] proposed that a sample size of 300 cases or more is adequate for performing factor analysis. Since the sample sizes were 2,916 (Germany) and 1,889 (Netherlands), the half-samples were 1,458 (Germany) and 944 (Netherlands) and were therefore considered large enough for carrying out factor analyses separately in each country.

Initially, missing data analysis and data screening for outliers and unengaged responses was performed (Charalampi *et al.* [5]; Michalopoulou [15]). Only cases with missing values on all items were excluded automatically from the analysis (Muthén and Muthén [16]). In addition, cases were eliminated if they exhibited low standard deviation ( $< 0.5$ ), i.e. no variance in the responses. Data screening for outliers was based on background variables e.g., gender (dichotomy), age (ratio) and education (pseudo-interval). Cases were eliminated if they were shown in the boxplots as outliers.

## 2.1 Exploratory Factor Analysis (EFA)

In performing EFA, as in our previous work (Charalampi *et al.* [5]; Michalopoulou [15]), the following sequence of decisions was required (Brown [4]; Tabachnick and Fidell [23]; Thompson [24]):

1. Initially, the items' frequency distributions were inspected for floor and ceiling effects, bearing in mind that percentages of responses in the range 1-15 are normally deemed acceptable. Next the items were rescaled into a 1-5 scale (see Section 2.3), univariate statistics were computed for each item and their distributional properties were inspected (testing for normality) to decide on the appropriateness of the methods to be used. The criterion of corrected item-total correlations  $< .30$  was used to decide which items to exclude from the analysis (Clark and Watson [6]; Nunnally and Bernstein [18]).

2. Decision on the matrix of association coefficients to analyze: as the items (before rescaling) were considered as both ordinal and pseudo-interval, the polychoric correlation matrix was employed as the appropriate matrix of associations (Brown [4]).

3. Factor extraction method: robust weighted least squares was applied as the appropriate method of factor extraction (Brown [4]) and also because it

“performs well ... for variables with floor or ceiling effects” (Brown 2015: p.355).

4. Decision on the number of factor to be extracted: considering the proposed theoretical structure of six key dimensions, the decision on the number of factors to be extracted was based on the performance of six models with one to six factors tested for each country. Model fit was considered adequate if  $\chi^2/df < 3$ , Comparative fit index (CFI) and Tucker-Lewis index (TLI) values were greater than or close to .95 and the Root-mean-square error approximation (RMSEA)  $\leq .06$  with the 90% Confidence interval (CI) upper limit  $\leq .06$  (Bollen [3]; Brown [4]; Hu and Bentler [12]; Schmitt [20] Tabachnick and Fidell [23]; Thompson [24]). Model fit was considered acceptable if  $\chi^2/df < 3$ , CFI and TLI values were  $> .90$  and RMSEA  $< .08$  with the 90% CI upper limit  $< .08$  (Hu and Bentler [12]; Marsh *et al.* [14]).

5. Factor rotation method: based on the correlations between factors and the simple structure criterion, geomin rotation was applied as the appropriate oblique factor rotation method (Brown [4]).

6. Items were considered salient if their factor loadings were  $> .30$  and therefore the meaning of each dimension was inferred from these items (Thompson [24]). Items with loadings  $> .30$  on one factor and  $> .22$  on another factor were considered as “cross-loading” items, i.e. items that loaded on multiple factors (Stevens [21]). Items with loadings  $< .30$  on all factors (i.e., low communalities) were excluded from the analysis. Also, factors with salient loadings for only two items were eliminated from the analysis as poorly defined (Brown [4]).

## 2.2 Confirmatory Factor Analysis (CFA)

In performing CFA, as in our previous work (Charalampi *et al.* [5]; Michalopoulou [15]), the following sequence of decisions was required (Brown [4]; Tabachnick and Fidell [23]; Thompson [24]):

1. The decision on the inclusion of items in the analysis was based on the results of the item analysis carried out on the first half-sample and those of EFA.

2. Model estimation: the model indicated as best by the EFA performed on the first half-sample was considered for testing. CFA of the polychoric correlation matrix was performed using robust weighted least squares.

3. Model evaluation: model fit was considered adequate or acceptable as in EFA, i.e. if  $\chi^2/df < 3$ , CFI and TLI values greater than or close to .95 and RMSEA  $\leq .06$  with the 90% CI upper limit  $\leq .06$ , or if  $\chi^2/df < 3$ , the CFI and TLI values were  $> .90$  and RMSEA  $< .08$  with the 90% CI upper limit  $< .08$ , respectively.

4. Model misspecification searches: searches for modification indices and further specifications were performed and, where necessary, correlations between error variances were introduced (Brown [4]; Thompson [24]).

### 2.3 Subscale Construction and Assessment

In order to resolve the issue of the varying number of response categories for the construction of the subscales, New Economics Foundation [17] proposed first computing standardized z-scores for each item and then, by a process of aggregation, transforming the recoded z-scores into scores for each predetermined wellbeing dimension. However, this approach fails to take into account that it is inappropriate to use standardization for ordinal items. Furthermore, it changes the scale and the meaning of its values since the difference of one unit is a difference of one standard deviation, rendering interpretation difficult. In this respect, taking into consideration what Kalmijn [13] proposed for the measurement of happiness, all items were rescaled into a 1-5 scale by applying the following simple transformation:

$$\left(\frac{max_{new} - min_{new}}{max_{old} - min_{old}}\right) \cdot (v - max_{old}) + max_{new}$$

Although this simple transformation in turn is not appropriate for ordinal items, it did produce scores that facilitated interpretation. The subscales were constructed for the full sample by averaging their rescaled defining items based on their factor loadings so that low and high scores would indicate low and high wellbeing values, respectively.

Descriptive statistics were computed for each subscale. Based on the CFA results for the full sample, as in our previous work (Charalampi *et al.* [5]; Michalopoulou [15]), the Average variance extracted (AVE) was computed for each subscale by averaging the sum of all squared standardized factor loadings in order to assess the convergent validity of the respective construct. Convergent validity was considered adequate if the AVE was above or around .50, i.e. a relaxed version of the Fornell and Larcker [11] criterion for  $AVE \geq .50$ . Average inter-item correlations in the recommended range of .15-.5 that cluster near their mean value were used as an indication of the unidimensionality of the subscales (Clark and Watson [6]). To demonstrate whether subscales are warranted or not, the condition of average correlation between items belonging to different subscales “significantly greater than zero but substantially less than the average within-subscale values (say, .20)” (Clark and Watson [6]: p.318) was used for justifying subscales. As Clark and Watson ([6]: 318) pointed out, “if this condition cannot be met, then the subscales should be abandoned in favor of a single overall score”. Evidence of discriminant validity was considered to be adequate if the squared correlations between subscales were less than their AVE estimates (Charalampi *et al.* [5]; Michalopoulou [15]). Furthermore, based on the CFA results for the full sample, composite reliability coefficients (Raykov [19]) were computed using the calculator provided by Colwell [7]; these are more appropriate than the commonly used Cronbach’s

alpha coefficient (Brown [4]; Raykov [19]). A subscale was considered reliable if the composite reliability coefficients were above or around .70, i.e. using a more relaxed version of the Nunnally and Bernstein [18] criterion for Cronbach's alpha coefficients  $\geq .70$ .

### 3 Results

The screening of both half-samples identified no unengaged responses in Germany and the Netherlands. In the German sample, 10 outlying cases with a Higher Education degree were detected and it was decided not to reject them from the analysis. There were no cases with missing values on all items in the sample of either country. Therefore, all cases were included in the analysis.

#### 3.1 EFA Results

Initial EFA resulted in the exclusion of one of the two items defining the supportive relationships dimension that was not defined as an opinion question and did not perform well in both cases. Consequently, models with up to five factors based on the remaining 26 items were considered for testing.

First, univariate statistics and the distributional properties of the items based on the first half-sample were inspected for Germany (Table 1.1) and the Netherlands (Table 1.2). The full range of possible responses was used for all items. However, in both cases, strong ceiling effects were detected for three items defining the emotional wellbeing dimension (Emwb1, Emwb2 and Emwb5), all the items defining the functioning (Fun1-Fun13) and vitality (Vi1-Vi4) dimensions and the surviving item of the supportive relationships dimension (Sur4). (Note that the numbering of the eight items defining functioning and the two items of the supportive relationships dimension is not consecutive, in order to maintain correspondence with the items defining these dimensions in the 2012 ESS measurement of wellbeing.)

As shown, in both cases, of Germany and the Netherlands, the proportion of missing values was negligible, exceeding 1.4% and 1.0% only for a single item Cowb4 (2.0% and 2.1%), respectively. Non-normality was not severe (skewness  $> 2$ ; kurtosis  $> 7$ ) or any item as the skewness and kurtosis values ranged from -2.44 to 0.04 (Germany) and -2.09 to -0.40 (Netherlands) and -0.57 to 6.89 (Germany) and 0.16 to 2.61 (Netherlands), respectively. Based on the criterion of corrected item-total correlations  $> .30$ , four (Cowb1, Cowb3, Cowb4 and Cowb5) of the five community wellbeing items were rejected from the analysis for Germany and all five were rejected for the Netherlands. Therefore, four theoretical dimensions (factors) were investigated with 22 (Germany) and 21 (Netherlands) items remaining in the analysis.

**Table 1.1** Item analysis of the 2006 European Social Survey measurement of wellbeing for Germany ( $n = 1,458$ )

Item	Mean	SD	95% CI	Frequency (%) of response categories												Skew.	Kurt.	CC
				0	1	2	3	4	5	6	7	8	9	10	NA			
Evwb1	3.71	0.88	3.66-3.76	1.9	1.3	2.4	4.0	4.9	11.5	10.8	16.8	25.9	12.2	8.0	0.2	-0.80	0.36	.568
Evwb2	3.82	0.77	3.78-3.86	0.5	0.8	1.9	3.2	3.2	11.2	11.4	20.0	27.3	11.5	8.7	0.3	-0.88	0.80	.604
Emwb1	4.38	0.83	4.33-4.42	-	1.3	4.0	37.7	56.4	-	-	-	-	-	-	0.6	-1.29	1.91	.579
Emwb2	4.32	0.91	4.27-4.37	-	2.4	5.3	35.7	55.9	-	-	-	-	-	-	0.8	-1.36	1.94	.592
Emwb3	3.17	1.11	3.11-3.23	-	8.4	35.5	40.0	15.6	-	-	-	-	-	-	0.6	-0.07	-0.57	.555
Emwb4	3.36	1.03	3.31-3.42	-	4.9	30.4	46.4	16.9	-	-	-	-	-	-	1.4	-0.19	-0.36	.578
Emwb5	4.71	0.64	4.67-4.74	-	0.8	1.7	17.4	79.6	-	-	-	-	-	-	0.5	-2.44	6.89	.352
Emwb6	3.44	1.02	3.39-3.50	-	5.1	24.8	52.9	16.6	-	-	-	-	-	-	0.5	-0.35	-0.12	.411
Fun1	3.80	0.86	3.76-3.85	-	1.7	8.4	17.2	54.9	17.4	-	-	-	-	-	0.4	-0.85	0.86	.449
Fun2	3.29	1.01	3.24-3.34	-	4.4	18.4	25.5	42.7	8.1	-	-	-	-	-	0.9	-0.43	-0.56	.413
Fun3	3.92	0.66	3.88-3.95	-	0.6	2.7	14.5	67.8	14.1	-	-	-	-	-	0.3	-0.88	2.32	.461
Fun7	3.84	0.77	3.80-3.88	-	1.0	3.8	18.8	60.4	14.7	-	-	-	-	-	1.2	-1.11	2.34	.310
Fun9	3.75	0.86	3.70-3.80	-	1.9	7.0	21.5	55.6	13.6	-	-	-	-	-	0.3	-1.00	1.39	.582
Fun11	4.03	0.66	4.00-4.07	-	0.3	3.1	9.8	66.1	20.2	-	-	-	-	-	0.5	-0.98	3.07	.452
Fun12	3.90	0.97	3.85-3.95	-	0.6	10.4	15.3	42.7	30.6	-	-	-	-	-	0.3	-0.62	-0.45	.426
Fun13	3.32	0.99	3.27-3.37	-	2.7	21.6	27.3	38.2	9.5	-	-	-	-	-	0.7	-0.28	-0.54	.385
Vi1	3.87	0.99	3.81-3.92	-	3.4	11.9	49.7	34.6	-	-	-	-	-	-	0.5	-0.74	0.51	.411
Vi2	3.98	1.07	3.93-4.04	-	4.0	10.0	42.5	43.1	-	-	-	-	-	-	0.4	-0.95	0.49	.414

**Table 1.1** (continued)

Item	Mean	SD	95% CI	Frequency (%) of response categories												Skew.	Kurt.	CC
				0	1	2	3	4	5	6	7	8	9	10	NA			
Vi3	4.35	0.89	4.30-4.40	-	1.8	4.7	32.9	59.7	-	-	-	-	-	-	0.9	-1.47	2.40	.447
Vi4	3.28	1.12	3.22-3.34	-	9.5	29.3	44.8	15.5	-	-	-	-	-	-	1.0	-0.19	-0.55	.544
Cowb1	2.88	0.92	2.83-2.93	5.8	3.4	8.0	13.4	11.8	19.9	11.6	14.9	7.1	2.1	1.9	0.1	-0.16	-0.46	.248
Cowb2	3.33	0.83	3.29-3.37	1.6	1.7	3.6	8.4	8.5	21.2	14.0	18.7	14.9	4.3	2.7	0.4	-0.36	-0.21	.302
Cowb3	3.00	0.85	2.96-3.05	2.7	2.3	6.4	14.3	13.8	23.5	12.0	12.4	7.7	2.9	1.9	0.2	0.04	-0.30	.273
Cowb4	3.34	1.05	3.28-3.39	4.7	5.6	12.2	22.6	24.2	20.4	8.4	-	-	-	-	2.0	-0.37	-0.51	.229
Cowb5	3.55	0.89	3.50-3.59	-	2.8	10.3	26.3	51.0	9.1	-	-	-	-	-	0.6	-0.69	0.40	.259
Sur4	4.53	0.85	4.48-4.57	-	1.7	4.4	23.9	69.5	-	-	-	-	-	-	0.5	-1.95	3.88	.514

SD = standard deviation; CI = confidence interval; NA = no answer (missing values); Skew. = skewness; Kurt. = kurtosis; CC = corrected item-total correlation. For the computation of univariate statistics items were rescaled into a 1-5 scale. Standard errors for skewness and kurtosis were 0.067 and 0.133, respectively.

**Table 1.2** Item analysis of the 2006 European Social Survey measurement of wellbeing for the Netherlands ( $n = 944$ )

Item	Mean	SD	95% CI	Frequency (%) of response categories												Skew.	Kurt.	CC
				0	1	2	3	4	5	6	7	8	9	10	NA			
Evwb1	4.04	0.63	4.00-4.08	0.2	0.3	1.0	2.2	2.1	4.2	6.7	22.7	38.6	14.9	7.0	0.1	-1.52	4.08	.537
Evwb2	4.09	0.57	4.05-4.13	0.1	0.3	0.3	1.5	1.4	3.6	5.7	24.5	39.1	16.5	6.7	0.3	-1.46	4.42	.488
Emwb1	4.31	0.85	4.25-4.37	-	0.8	4.0	40.9	54.1	-	-	-	-	-	-	0.1	-1.07	1.12	.528
Emwb2	4.48	0.84	4.43-4.54	-	1.3	3.0	28.6	66.6	-	-	-	-	-	-	0.5	-1.76	3.42	.585
Emwb3	3.68	1.04	3.61-3.75	-	4.6	19.4	48.5	27.3	-	-	-	-	-	-	0.2	-0.52	-0.05	.603
Emwb4	3.73	1.01	3.66-3.79	-	3.2	17.7	52.9	26.2	-	-	-	-	-	-	0.1	-0.64	0.38	.544
Emwb5	3.93	0.92	3.87-3.99	-	2.6	9.4	52.5	35.2	-	-	-	-	-	-	0.2	-0.67	0.72	.484
Emwb6	3.36	1.00	3.29-3.42	-	5.9	26.3	55.6	11.9	-	-	-	-	-	-	0.3	-0.40	0.02	.487
Fun1	4.08	0.79	4.02-4.13	-	0.5	3.9	10.7	54.2	30.2	-	-	-	-	-	0.4	-0.96	1.30	.352
Fun2	3.52	0.90	3.46-3.58	-	2.2	13.8	20.7	56.8	5.6	-	-	-	-	-	1.0	-0.84	0.16	.345
Fun3	3.66	0.75	3.61-3.71	-	0.6	9.5	21.4	60.9	7.1	-	-	-	-	-	0.4	-0.80	0.56	.416
Fun7	3.94	0.64	3.90-3.98	-	0.2	3.0	13.1	70.1	13.2	-	-	-	-	-	0.3	-0.98	2.61	.386
Fun9	3.65	0.87	3.59-3.70	-	0.8	11.2	21.3	55.4	11.0	-	-	-	-	-	0.2	-0.61	-0.04	.460
Fun11	3.74	0.75	3.69-3.79	-	0.4	7.9	19.5	62.8	9.1	-	-	-	-	-	0.2	-0.77	0.61	.384
Fun12	3.80	0.95	3.74-3.86	-	0.8	11.5	13.8	53.5	20.0	-	-	-	-	-	0.3	-0.83	0.24	.407
Fun13	3.31	0.94	3.25-3.37	-	3.5	19.5	22.5	50.5	3.5	-	-	-	-	-	0.5	-0.56	-0.61	.449
Vi1	4.26	0.95	4.19-4.32	-	2.2	7.3	35.2	55.2	-	-	-	-	-	-	0.1	-1.25	1.42	.566
Vi2	4.06	1.09	3.99-4.13	-	4.3	10.9	35.0	49.6	-	-	-	-	-	-	0.2	-1.05	0.51	.415

**Table 1.2** (continued)

Item	Mean	SD	95% CI	Frequency (%) of response categories												NA	Skew.	Kurt.	CC
				0	1	2	3	4	5	6	7	8	9	10					
Vi3	4.09	0.97	4.02-4.15	-	1.8	8.5	44.1	45.3	-	-	-	-	-	-	0.3	-0.93	0.69	.481	
Vi4	3.29	1.07	3.22-3.36	-	8.8	26.4	50.6	13.9	-	-	-	-	-	-	0.3	-0.47	-0.12	.523	
Cowb1	3.34	0.83	3.28-3.39	3.3	1.8	3.7	7.1	7.6	16.8	15.0	25.5	15.7	2.4	0.8	0.1	-0.87	0.52	.298	
Cowb2	3.53	0.71	3.48-3.57	0.8	0.6	3.2	4.8	5.0	15.5	15.8	28.6	20.1	3.3	2.0	0.3	-0.79	0.73	.288	
Cowb3	3.12	0.78	3.07-3.18	2.0	1.7	6.4	9.9	12.7	20.0	15.6	20.6	9.3	1.1	0.7	0.1	-0.34	-0.27	.213	
Cowb4	3.48	1.03	3.41-3.55	3.5	7.8	10.2	19.7	23.7	23.7	9.2	-	-	-	-	2.1	-0.54	-0.38	.193	
Cowb5	3.36	0.95	3.30-3.42	-	2.8	19.3	29.3	42.2	6.0	-	-	-	-	-	0.4	-0.44	-0.50	.193	
Sur4	4.58	.079	4.53-4.63	-	1.5	3.7	20.7	74.0	-	-	-	-	-	-	0.1	-2.09	4.64	.529	

SD = standard deviation; CI = confidence interval; NA = no answer (missing values); Skew. = skewness; Kurt. = kurtosis; CC = corrected item-total correlation. For the computation of univariate statistics items were rescaled into a 1-5 scale. Standard errors for skewness and kurtosis were 0.082 and 0.163, respectively.

EFA was performed with robust weighted least squares of the polychoric matrix of associations computed from the first half-samples of each country and geomin rotation was applied. Three different models were tested. Three items (Emwb6, Fun2 and Cowb2) were excluded from further analysis of the German half-sample and one item (Fun2) from the Netherlands, because factor loadings were  $< .30$  on all factors. Therefore, 19 (Germany) and 20 (Netherlands) items were retained in the analysis. Table 2 presents the results of testing the three models. The three-factor model provided the best interpretable solution in both countries, demonstrating acceptable model fit for both Germany ( $\chi^2/df = 5.76$ , CFI = .940, TLI = .913, RMSEA = .057 with the 90% CI upper limit = .061) and the Netherlands ( $\chi^2/df = 5.81$ , CFI = .926, TLI = .895, RMSEA = .071 with the 90% CI upper limit = .076).

**Table 2** Exploratory factor analysis of the 2006 European Social Survey wellbeing items performed with robust weighted least squares of the polychoric correlation matrix applying geomin rotation on the first half-samples: Goodness-of-fit indices

No. of factors tested	$\chi^2/df$	CFI	TLI	RMSEA (90% CI)
Germany ( $n = 1,458$ )				
1	12.40	.815	.792	.088 (.085-.092)
2	7.52	.907	.881	.067 (.063-.071)
3	5.76	.940	.913	.057 (.053-.061)
Netherlands ( $n = 944$ )				
1	9.90	.826	.805	.097 (.093-.101)
2	7.30	.890	.862	.082 (.077-.086)
3	5.81	.926	.895	.071 (.067-.076)

$df$  = degrees of freedom; CFI = comparative fit index; TLI = Tucker-Lewis index; RMSEA = root-mean-square error of approximation; CI = confidence interval. Model fit is considered adequate if  $\chi^2/df < 3$ , CFI and TLI values greater than or close to .95 and RMSEA  $\leq .06$  with the 90% CI upper limit  $\leq .06$ . Model fit is considered acceptable if  $\chi^2/df < 3$ , CFI  $> .90$ , TLI  $> .90$  and RMSEA  $< .08$  with the 90% CI upper limit  $< .08$ .

Tables 3.1 and 3.2 show the structure of the three-factor solution obtained by performing EFA with geomin rotation on the first half-samples of Germany and the Netherlands, respectively. In both cases, the correlations between factors I and II and between factors I and III were  $> .32$  implying that there was more

than a 10 percent overlap in the variance among factors, i.e. enough variance to justify the application of an oblique rotation (Michalopoulou [15]).

**Table 3.1** Exploratory factor analysis of the 2006 European Social Survey wellbeing items performed with robust weighted least squares of the polychoric correlation matrix applying geomin rotation on the first half-sample of Germany ( $n = 1,458$ )

Item	Factor I EMWB (+)	Factor II EMWB (-)	Factor III FUN
Evwb1	<b>.510</b>	.011	.159
Evwb2	<b>.538</b>	.052	.148
Emwb1	.176	<b>.688</b>	-.021
Emwb2	<b>.308</b>	<b>.567</b>	-.001
Emwb3	<b>.753</b>	-.004	.013
Emwb4	<b>.818</b>	-.006	-.028
Emwb5	-.090	<b>.634</b>	.207
Fun1	<b>.307</b>	-.070	<b>.321</b>
Fun3	<b>.254</b>	-.042	<b>.445</b>
Fun7	.090	-.023	<b>.353</b>
Fun9	<b>.309</b>	.030	<b>.459</b>
Fun11	-.005	.175	<b>.569</b>
Fun12	.034	.212	<b>.409</b>
Fun13	-.019	<b>.353</b>	<b>.246</b>
Vi1	.188	<b>.430</b>	-.033
Vi2	.185	<b>.409</b>	-.045
Vi3	.030	<b>.586</b>	.125
Vi4	<b>.362</b>	<b>.315</b>	.133
Sur4	<b>.229</b>	<b>.513</b>	.084
Factors	Correlations between factors		
EMWB (+)	—		
EMWB (-)	.541	—	
FUN	.434	.187	—

EMWB = emotional wellbeing; FUN = Functioning. Factor loadings > .22 are in boldface. Goodness of fit indices for this model:  $\chi^2/df = 5.76$ , CFI = .940, TLI = .913, RMSEA (90% CI) = .057 (.053-.061).

**Table 3.2** Exploratory factor analysis of the 2006 European Social Survey wellbeing items performed with robust weighted least squares of the polychoric correlation matrix applying geomin rotation on the first half-sample of Netherlands ( $n = 944$ )

Item	Factor I EMWB (+)	Factor II EMWB (-)	Factor III FUN
Evwb1	.078	<b>.343</b>	<b>.389</b>
Evwb2	-.017	<b>.431</b>	<b>.410</b>
Emwb1	<b>.846</b>	.035	-.162
Emwb2	<b>.869</b>	.002	-.091
Emwb3	<b>.455</b>	<b>.532</b>	.040
Emwb4	<b>.435</b>	<b>.613</b>	-.004
Emwb5	<b>.632</b>	-.010	.012
Emwb6	<b>.589</b>	.098	-.019
Fun1	.005	.049	<b>.429</b>
Fun3	.135	-.016	<b>.430</b>
Fun7	-.140	.010	<b>.650</b>
Fun9	.047	.110	<b>.520</b>
Fun11	.094	-.004	<b>.474</b>
Fun12	.212	-.033	<b>.356</b>
Fun13	<b>.451</b>	.004	.082
Vi1	<b>.785</b>	-.130	.062
Vi2	<b>.656</b>	-.042	-.147
Vi3	<b>.638</b>	-.211	.048
Vi4	<b>.450</b>	.077	.152
Sur4	<b>.646</b>	.189	-.044
Factors	Correlations between factors		
EMWB (+)	—		
EMWB (-)	.349	—	
FUN	.639	.298	—

EMWB = emotional wellbeing; FUN = Functioning. Factor loadings  $> .22$  are in boldface. Goodness of fit indices for this model:  $\chi^2/df = 5.81$ , CFI = .926, TLI = .895, RMSEA (90% CI) = .071 (.067-.076).

In the case of Germany (Table 3.1), all items exhibited strong factor loadings (greater than or close to .40) with the exception of three items originally defining the functioning dimension (Fun1, Fun7 and Fun13) and one item defining vitality (Vi4). A simple structure was achieved allowing seven cross-loading items: Emwb2 (factors I and II); Fun1 (factors I and III); Fun3 (factors I

and III) Fun9 (factors I and III); Fun13 (factors II and III); Vi4 (factors I and II); and Sur4 (factors I and II). The first factor was defined by five items — two items from the evaluative wellbeing dimension (Evwb1, Evwb2), two from the emotional wellbeing dimension (Emwb3, Emwb4) and one from the vitality dimension (Vi4). As the dominant items referred to positive emotional wellbeing, we gave this label to the underlying construct. The second factor was defined by eight items — three from the emotional wellbeing dimension (Emwb1, Emwb2, Emwb5), one from the functioning dimension (Fun13), three from the vitality dimension (Vi2, Vi3, Vi4) and one item from the supportive relationships dimension (Sur4). Based on the interpretation suggested by the dominant items, the underlying construct was labeled as negative emotional wellbeing. The third factor was defined by six items of the functioning dimension (Fun1, Fun3, Fun7, Fun9, Fun11 and Fun12) and therefore the underlying construct kept this name.

In the case of the Netherlands (Table 3.2), all items exhibited strong factor loadings (greater than or close to .40) with the exception of two items — one originally from the evaluative wellbeing dimension (Evwb1) and one from the functioning dimension (Fun12). A simple structure was achieved allowing four cross-loading items: Evwb1 (factors II and III); Evwb2 (factors II and III); Emwb3 (factors I and II); Emwb4 (factors I and II). The first factor was defined by 10 items — four from the emotional wellbeing dimension (Emwb1, Emwb2, Emwb5, Emwb6), one from the functioning dimension (Fun13), all four items from the vitality dimension (Vi1-Vi4) and one item of the supportive relationships dimension (Sur4). As the dominant items referred to positive emotional wellbeing, the underlying construct was given this label. The second factor was defined by three items — one from the evaluative wellbeing dimension (Evwb2) and two from the emotional wellbeing dimension (Emwb3, Emwb4). Based on the interpretation suggested by the dominant items, the underlying construct was labeled as negative emotional wellbeing. The third factor was defined by seven items — one from the evaluative wellbeing dimension (Evwb1) and six items from the functioning dimension (Fun1, Fun3, Fun7, Fun9, Fun11 and Fun12). As the dominant items referred to functioning, the underlying construct was labeled accordingly.

### 3.2 CFA Results

In both countries, the three-factor model indicated as best by the EFA results was tested by performing CFA of the polychoric correlation matrix using robust weighted least squares on the second half-samples. Modification searches were conducted and, where necessary, correlations between error variances were introduced.

The CFA results for Germany (Figure 1.1) showed adequate model fit for the solution with three first-order correlated factors:  $\chi^2/df = 3.86$ , CFI = .962,

TLI = .952, RMSEA (90% CI) = .044 (.040-.048). The CFA results for the Netherlands (Figure 1.2) also showed adequate model fit for the three first-order

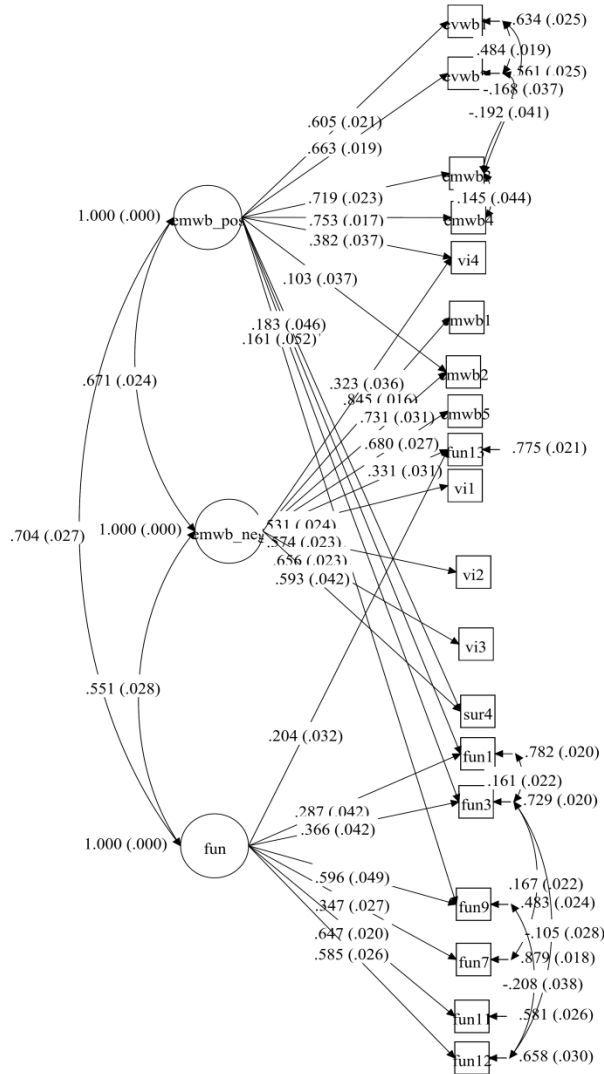


**Fig. 1.1** Standardized solution for the model with three first-order correlated factors and three cross-loading items based on CFA performed on the second half-sample of Germany ( $n = 1,458$ ). Observed variables are represented by squares and latent variables are enclosed in ellipses.

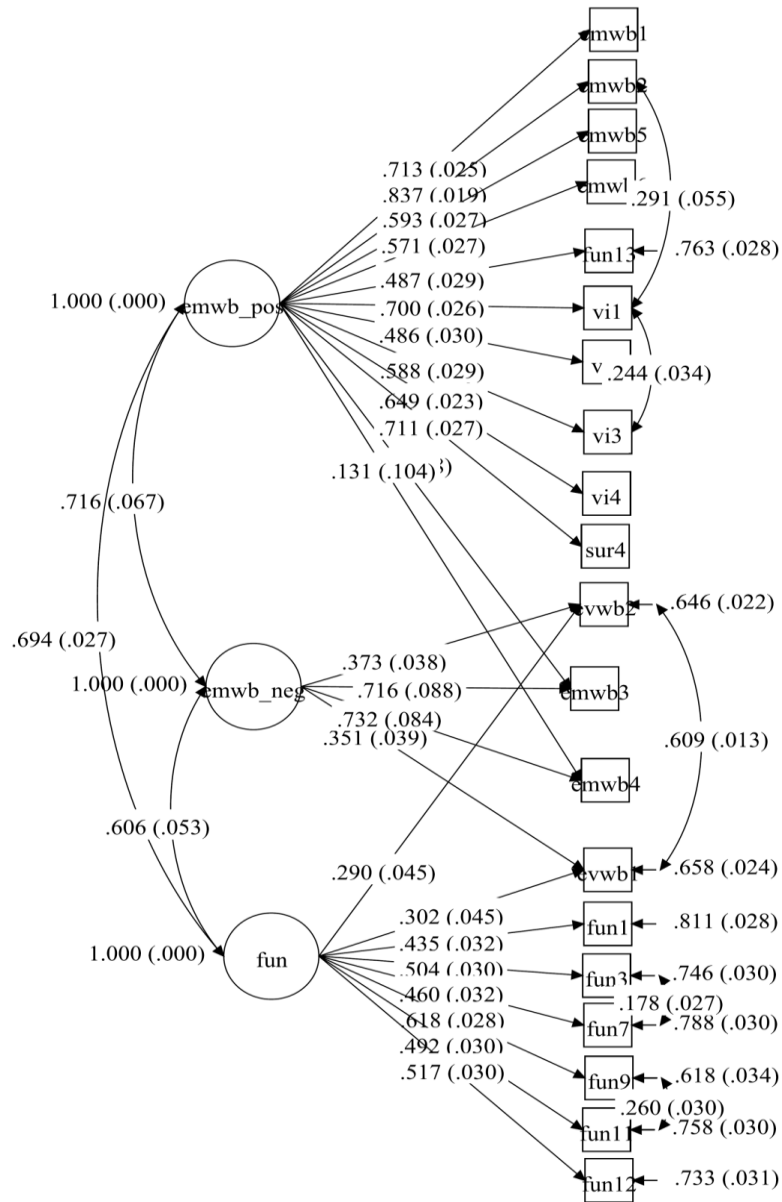


**Fig. 1.2** Standardized solution for the model with three first-order correlated factors and three cross-loading items based on CFA performed on the second half-sample of the Netherlands ( $n = 945$ ). Observed variables are represented by squares and latent variables are enclosed in ellipses.

correlated factors solution:  $\chi^2/df = 3.37$ , CFI = .956, TLI = .947, RMSEA (90% CI) = .050 (.045-.055). Therefore, the CFA findings supported the three-dimensional structure, confirming the solution suggested by EFA for Germany and the Netherlands.

### 3.3 Subscale Construction and Assessment

In Table 4, the wellbeing subscales and items of Germany and the Netherlands are presented according to their factor loadings. As shown, although the same labels were attached to the factors (subscales), the items comprising them differ between countries.

**Table 4** The wellbeing subscales and items presented according to their factor loadings: European Social Survey, 2006

Country	Wellbeing (WB) subscales	Items
DE	Emotional WB (positive)	Emwb4, Emwb3, Evwb2, Evwb1, Vi4
	Emotional WB (negative)	Emwb1, Emwb5, Vi3, Emwb2, Sur4, Vi1, Vi2, Fun13
NL	Functioning	Fun11, Fun9, Fun3, Fun12, Fun7, Fun1
	Emotional WB (negative)	Emwb2, Emwb1, Vi1, Vi2, Sur4, Vi3, Emwb5, Emwb6, Fun13, Vi4
	Emotional WB (positive) Functioning	Emwb4, Emwb3, Evwb2 Fun7, Fun9, Fun11, Fun3, Fun1, Evwb1, Fun12

Emwb = emotional wellbeing; Evwb = evaluative wellbeing; Fun = functioning; Vi = Vitality; Sur = Supportive relationships. Subscale items are presented according to their factor loadings.

Subscales were constructed by averaging their defining items after rescaling. In Tables 5.1 and 5.2, descriptive statistics, composite reliability, convergent and discriminant validity, and internal consistencies based on the full samples are presented for Germany and the Netherlands, respectively. The AVE was computed for each subscale based on the CFA analysis for the full sample of Germany (Figure 2.1:  $\chi^2/df = 5.19$ , CFI = .972, TLI = .963, RMSEA = .038 with the 90% CI = .035-.041) and the Netherlands (Figure 2.2:  $\chi^2/df = 4.24$ , CFI = .972, TLI = .964, RMSEA = .041 with the 90% CI = .038-.045). None of the subscales of Germany demonstrated adequate convergent validity (AVE above or around .50). The squared correlations between subscales were smaller than the AVE estimates, indicating adequate discriminant validity of all the subscales for both countries. The average inter-item correlations of all the subscales of

both countries were within the recommended range for unidimensionality (.15-.5). Also, in both cases, the individual inter-item correlations clustered well around their respective mean values as indicated by their range. As the average correlations between items from different subscales were less than the average correlations within-subscales, all subscales of both countries were justified.

**Table 5.1** Descriptive statistics, convergent and discriminant validity, composite reliability and internal consistencies of the 2006 European Social Survey wellbeing (WB) subscales: Germany ( $N = 2,916$ )

	Subscale		
	Emotional WB (+)	Emotional WB (-)	Functioning
Number of items	5	8	6
Mean (standard error)	3.47 (0.012)	4.18 (0.010)	3.88 (0.008)
95% Confidence interval	3.44-3.49	4.16-4.20	3.86-3.89
Standard deviation	0.630	0.515	0.429
Skewness	-0.406	-1.151	-0.511
Kurtosis	0.042	2.094	0.589
Convergent validity	.434	.370	.246
Composite Reliability	.789	.816	.645
Average inter-item correl.	.275	.245	.148
Min.-max. correlations	-.011-.668	.010-.527	-.018-.438
Range of correlations	.679	.518	.456
Average inter-item correlations between subscales			
Emotional WB (+)	—		
Emotional WB (-)	.223	—	
Functioning	.185	.172	—
Squared correlations between subscales			
Emotional WB (+)	—		
Emotional WB (-)	.050	—	
Functioning	.034	.030	—

Standard errors for skewness and kurtosis were 0.047 and 0.094, respectively.

Descriptive statistics, convergent and discriminant validity, composite reliability and internal consistencies of the 2006 European Social Survey wellbeing (WB) subscales: Netherlands ( $N = 1,889$ )

	Subscale		
	Emotional WB (+)	Emotional WB (-)	Functioning
Number of items	10	3	7
Mean (standard error)	3.94 (0.014)	3.79 (0.017)	3.82 (0.011)
95% Confidence interval	3.92-3.97	3.75-3.82	3.80-3.84
Standard deviation	0.594	0.724	0.473
Skewness	-1.052	-0.591	-0.679
Kurtosis	1.412	0.273	1.186
Convergent validity	.409	.402	.238
Composite Reliability	.871	.653	.681
Average inter-item correl.	.330	.502	.273
Min.-max. correlations	.243-.540	.421-.627	.213-.485
Range of correlations	.297	.206	.272
	<u>Average inter-item correlations between subscales</u>		
Emotional WB (+)	—		
Emotional WB (-)	.329	—	
Functioning	.262	.262	—
	<u>Squared correlations between subscales</u>		
Emotional WB (+)	—		
Emotional WB (-)	.108	—	
Functioning	.069	.069	—

Standard errors for skewness and kurtosis were 0.057 and 0.114, respectively.

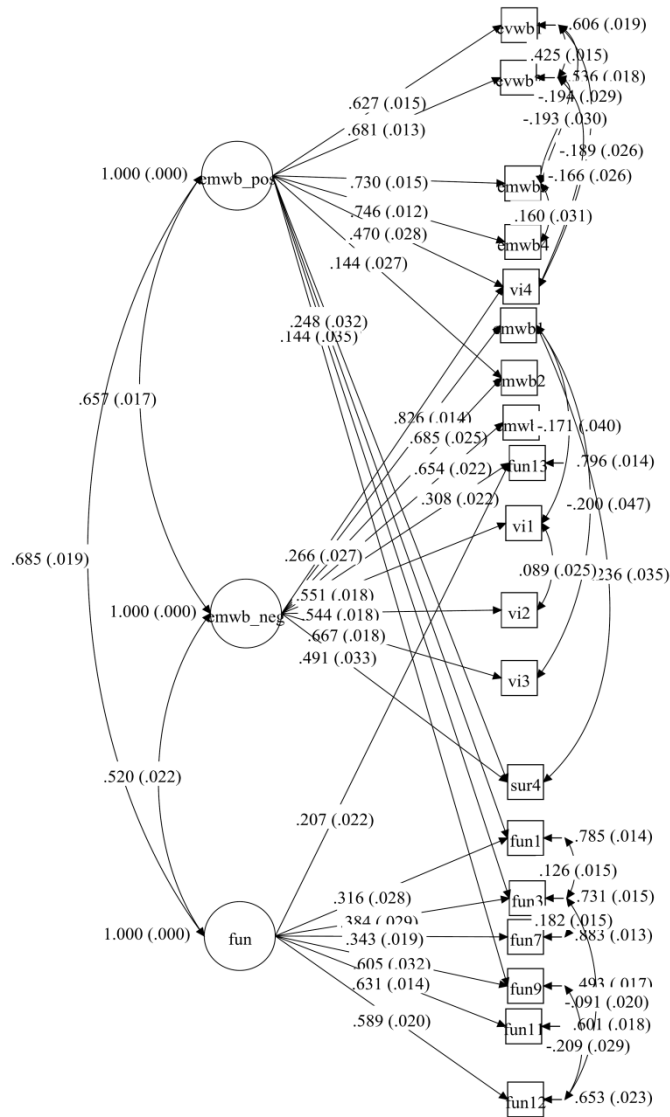


**Fig. 2.1** Standardized solution for the model with three first-order correlated factors and three cross-loading items based on CFA performed on the full sample of Germany ( $N = 2,916$ ). Observed variables are represented by squares and latent variables are enclosed in ellipses.



were reliable with composite reliability values ranging from .653 to .871. Thus the analysis in each country produced subscales that were reliable and valid but of problematic convergent validity.

## 4 Conclusion

In this paper, the importance of ascertaining the level of measurement of the items in the choice of the methods to be applied when validating multidimensional scales was demonstrated using the 2006 ESS six-dimensional measurement of personal and social wellbeing for Germany and the Netherlands, where items were considered as both ordinal and pseudo-interval.

The investigation of the structure (dimensionality) of the 2006 ESS measurement of personal and social wellbeing by applying the traditional approaches of EFA and CFA to randomly split half-samples resulted in both countries in a three-dimensional structure, different from the proposed theoretical one of six-dimensions (European Social Survey [8, 9]; New Economics Foundation [17]). However, the analysis produced reliable and valid subscales for each country.

The demonstration of the complex sequence of decisions required in performing EFA and CFA based on current theory and practice should be noted among the strengths of the study. In both countries, item analyses carried out on the first half-samples indicated that a number of items had first to be eliminated from further analysis. In each case, three models were tested. Models with three first-order correlated factors based on 19 items in Germany and 20 items in the Netherlands provided the best fit to the data. The fit was improved by considering cross-loadings: seven in Germany and four in the Netherlands. In both countries, the resulting three underlying dimensions were defined as positive emotional wellbeing, negative emotional wellbeing and functioning. None of the subscales demonstrated adequate convergent validity. However, every subscale exhibited adequate discriminant validity. Although the labeling of the subscales (factors) was the same for Germany and the Netherlands, it should be pointed out that they were comprised from different items in each country and therefore they should not be compared.

The ESS has included the wellbeing module in Round 3 (2006) and Round 6 (2012) and therefore this work could be extended to cover all participating countries in each round. In this way, researchers would be provided with valid and reliable subscales for their analyses.

## References

1. D. J. Bartholomew, F. Steele, I. Moustaki and J. Galbraith. Analysis of multivariate social science data, Chapman & Hall/CRC, London, 2008.
2. H. M. Blalock Jr. Social Statistics (revised second edition), McGraw-Hill, New York, 1979.

3. K.A. Bollen. Structural equations with latent variables, Wiley, New York, 1989.
4. T. A. Brown. Confirmatory factor analysis for applied research, The Guilford Press, New York, 2006.
5. A. Charalampi, C. Michalopoulou and C. Richardson. Investigating the structure of Schwartz's Human Values Scale. In J. R. Bozeman, T. Oliveira & C. H. Skiadas (Eds), Stochastic and data analysis methods and applications in statistics and demography (pp. 589-609), ISAST, 2016.
6. L. A. Clark and D. Watson. Constructing validity: Basic issues in objective scale development, *Psychological Assessment*, 7, 309-319, 1995.
7. S. R. Colwell. The composite reliability calculator, Technical Report (doi: 10.13140/RG.2.1.4298.088), 2016.
8. European Social Survey. Round 6 module on personal and social wellbeing – Final module in template, Centre for Comparative Social Surveys, City University London, 2013.
9. European Social Survey. Measuring and reporting on Europeans' wellbeing: Findings from the European Social Survey, ESS ERIC, London, 2015. Retrieved from: [https://www.europeansocialsurvey.org/docs/findings/ESS1-6\\_measuring\\_and\\_reporting\\_europeans\\_wellbeing.pdf](https://www.europeansocialsurvey.org/docs/findings/ESS1-6_measuring_and_reporting_europeans_wellbeing.pdf)
10. European Social Survey Round 3 Data. Data file edition 3.6. NSD - Norwegian Centre for Research Data, Norway – Data Archive and distributor of ESS data for ESS ERIC, 2006.
11. C. Fornell and D.F. Larcker. Evaluating structural equation models with unobservable variables and measurement error, *Journal of Marketing Research*, 18, 1, 39-50, 1981.
12. L. Hu and P. M. Bentler. Cutoff criteria for fit indexes in covariance structure analysis: Conventional criteria versus new alternatives, *Structural Equation Modeling*, 6, 1, 1-55, 1999.
13. W. Kalmijn. Conversion of measurement results. In R. Veenhoven (Ed.), *World database of happiness*, Erasmus University Rotterdam, 2015. [http://worlddatabaseofhappiness.eur.nl/hap\\_quer/hqi\\_fp.htm](http://worlddatabaseofhappiness.eur.nl/hap_quer/hqi_fp.htm).
14. H.W. Marsh, K. T. Hau and Z. Wen. In search of golden rules: Comment on hypotheses-testing approaches to setting cutoff values for fit indexes and dangers in overgeneralizing Hu and Bentler's (1999) findings, *Structural Equation Modeling*, 11, 3, 320-341, 2004.
15. C. Michalopoulou. Likert scales require validation before application – Another cautionary tale, *BMS Bulletin de Méthodologie Sociologique*, 134, 5-23, 2017.
16. L. K. Muthén and B. O. Muthén. *Mplus User's Guide* (7th edition), Muthén & Muthén, Los Angeles, California, 1998-2012.
17. New Economics Foundation. National accounts of well-being: Bringing real wealth onto the balance sheet, NEF, London, 2009. Retrieved from: [https://www.unicef.org/lac/National\\_Accounts\\_of\\_Well-being.pdf](https://www.unicef.org/lac/National_Accounts_of_Well-being.pdf)

18. J. C. Nunnally and I. H. Bernstein. *Psychometric theory*, McGraw-Hill, New York, 1994.
19. T. Raykov. Reliability if deleted, not “alpha if deleted”: Evaluation of scale reliability following component deletion, *British Journal of Mathematical and Statistical Psychology*, 60, 2, 201–216, 2007.
20. T. A. Schmitt. Current methodological considerations in exploratory and confirmatory factor analysis, *Journal of Psychoeducational Assessment*, 29, 304-322, 2011.
21. J. Stevens. *Applied multivariate statistics for the social sciences*, Lawrence Erlbaum Associates, New Jersey, 2002.
22. S. S. Stevens. On the theory of scales of measurement, *Science*, 103, 2684, 677-680, 1946.
23. B. G. Tabachnick and L. S. Fidell. *Using multivariate statistics*, Pearson Allyn & Bacon, Upper Saddle River, New Jersey, 2007.
24. B. Thompson. *Exploratory and confirmatory factor analysis: Understanding concepts and applications*, American Psychological Association, Washington DC, 2005.

# Some properties of the multivariate generalized hyperbolic laws

Stergios B. Fotopoulos\*, Venkata K. Jandhyala\*\*, Alex Paparas\*

\**Department of Finance and Management Science, Washington State University, Pullman, WA 99164-4746, USA*

\*\**Department of Mathematics & Statistics, Washington State University, Pullman, WA 99164-4113, USA*

## Abstract

The purpose of this study is to characterize multivariate generalized hyperbolic (MGH) distributions and their conditionals by considering the MGH as a subclass of the mean-variance mixing of the multivariate normal law. The essential contribution here lies in expressing multivariate generalized hyperbolic densities by utilizing various integral representations of the Bessel function. Moreover, in a more convenient form these modified density representations are more advantageous for deriving limiting results. The forms are also convenient for studying the transient as well as tail behavior of multivariate generalized hyperbolic distributions. The results include the normal distribution as a limiting form for the MGH distribution. This means the MGH model can be considered for modeling not only high frequency data but also for modeling low frequency data. This is against the currently prevailing notion that the MGH model is relevant for modeling only high frequency data.

*Keywords:* Scale mixture of multivariate distributions; generalized inverse Gaussian distributions; Non Gaussian; Conditional laws.

*AMS subject classification:* 60E10 60E07, 62H05, 60G15, 60F05.

## 1. Introduction

Generalized hyperbolic (GH) distributions have become quite popular in various areas of both theoretical and applied statistics. Originally, Barndorff-Nielsen (1977, 1978) employed this class of distributions to model wind-blown grain size distributions (see, e.g., Barndorff-Nielsen and Blaesild, 1981, Olbricht, 1981). Currently, GH distributions have proven to be standard models of statistical singularities in various characteristics of complex open systems in many fields (from turbulence to financial analysis). The literature on GH distributions is immense. Some of the pioneering investigations in the area of the GH family include: Barndorff-Nielsen (1977, 1978, and 1979), Madan and Seneta (1990), Eberlein and Keller (1995), Eberlein et al. (1998), Eberlein (2001) and Yu (2017), just to name a few. The high applicability of GH models can be attributed to the fact that many of its appropriately adjusted representations make it possible to fit these models to a wide variety of data. The class of GH distributions is very large and, in particular, contains symmetric and skewed student  $t$ -type distributions (including the Cauchy distribution), the variance gamma distributions (including symmetric and asymmetric Laplace distributions), normal inverse Gaussian distributions, among many others.

In applied probability, GH models were introduced as the distributions of randomly stopped Brownian motion with the stopping times having some generalized inverse Gaussian distribution (GIG) (see e.g., Fotopoulos et al. 2015a, Fotopoulos et al. 2015b). Although, the properties of the GH distributions are rather well studied, only recently, Korolev (2014), Korolev et al. (2016), and Korolev and Zeifman (2016)

*5<sup>th</sup> SMTDA Conference Proceedings, 12-15 June 2018, Chania, Crete, Greece*



showed that GH laws are limiting distributions of randomly stopped random walks. They also demonstrated that multivariate GH laws can be limiting not only for random sums but also for general statistics. Further, Korolev (2014) showed that special continuous random walks generated by double Poisson processes converge weakly to the GH distribution. Thus, just as the normal distribution is tied to the central limit theorem, the GH distribution can be seen as a weak convergence limit of many Poisson random sums. These sums have been shown to have vast theoretical interest apart from playing an important role in applied statistics.

Many tasks and problems arising in natural sciences and financial mathematics are inherently multivariate in nature. Consider for example a portfolio of assets or an option whose payoff depends on two or more underlings. In most of such multivariate situations, knowledge of the corresponding univariate marginals is by no means sufficient since they provide no information about the dependence structure that considerably influence the risks and returns of the portfolio and the value of the option. Many higher-dimensional models used in financial mathematics are still based on the multivariate normal distribution despite the fact that empirical investigations strongly reject the hypothesis of asset returns being multivariate normal: see for example Affeck-Graves and McDonald (1989), Richardson and Smith (1993) or McNeil et al. (2005, Chapter 3, pp. 70-73). Apart from the fact that the marginal log return-distributions deviate significantly from the normal law, a second reason for the rejection of the multivariate normal distribution is that it is a far too simplistic way of modeling dependence structure. Namely, the dependence structure among the components of the multivariate normal random vector is completely characterized by the corresponding covariance matrix, whereas financial data typically exhibit a much more complex dependence structure. In particular, the probability of joint extreme outcomes is severely underestimated by the normal distribution because it assigns too little weight to the joint tails. To overcome the deficiencies of the multivariate normal distribution, the multivariate GH distributions are considered more than adequate to fit financial data, and others. Prior to multivariate GH distributions becoming standard, various alternatives have been proposed in the literature. Here, we only mention the following examples (the list could surely be extended much further): the class of elliptical distributions (Owen and Rabinovitch 1983, Kring et al. 2009), multivariate  $t$ -distributions (Khan and Zhou 2006, Adcock 2010), multivariate variance gamma distributions (Luciano and Schoutens 2006, Semeraro 2008), and more recently symmetric Gaussian mixture with GGC scales (Fotopoulos, 2017). The more general multivariate GH distributions (Prause 1999, Chapter 4, Eberlein and Prause 2002, Sections 6 and 7, McNeil et al., 2005, Chapter 3.2) have been well-accepted to fit financial data. Thus, the success of the non-Gaussian mixture model based approaches to many applied sciences inspires this note to continue searching for more of their distributional properties.

The organization of this paper is as follows. Section 2 introduces the multivariate generalized hyperbolic distribution and provides many of its limiting forms by modifying various parameters. Section 3 considers a study of the conditional generalized hyperbolic distribution. In the conditional case also, various limiting results are obtained and exact expressions for the limiting density are derived.

## 2. The MGH family of distributions and their limiting forms.

Let  $Y$  be an  $\mathbb{R}^d$ -valued random variable satisfying the representation

$$Y = \mu + \beta\tau + \sqrt{\tau}X, \quad (2.1)$$

where  $\mu, \beta \in \mathbb{R}^d$  are fixed parameters and  $X \sim N_d(0, \Sigma)$  with  $\Sigma$  being a real-valued  $d \times d$  positive definite matrix. The real-valued, non-negative random variable  $\tau$  is assumed to be independent of  $X$ . Models that admit the form in (2.1) are defined as the multivariate normal mean-variance mixture. Note that the presence of the random variable  $\tau$  induces dependencies between all components of  $Y$ , even when the covariance matrix is diagonal (see, e.g., Hammerstein, 2010). In what follows, we let  $\langle x, y \rangle$  denote the inner product and  $\|x\|^2 = \langle x, x \rangle$  be the Euclidean norm, for  $x, y \in \mathbb{R}^d$ . For  $\Sigma \in \mathbb{R}^{d \times d}$ , we also set  $\|x\|_{\Sigma}^2 = \langle x, \Sigma x \rangle$ ,  $x \in \mathbb{R}^d$ . Now, since  $X$  and  $\tau$  are independent, it can be easily verified that the density of  $Y$  has the form

$$F_Y(dx) = f_Y(x)dx = \frac{|\Sigma|^{-1/2}}{(2\pi)^{d/2}} \int_0^{\infty} \xi^{-d/2} \exp\left(-\frac{1}{2\xi} \|x - \mu - \beta\xi\|_{\Sigma^{-1}}^2\right) F_{\tau}(d\xi) I(x \in \mathbb{R}^d) dx, \quad (2.2)$$

where  $F_{\tau}(d\xi)$  denotes the law of  $\tau$ , and  $I(\cdot)$  denotes the indicator variable.

Throughout this study, the following identity is utilized whenever it is convenient

$$\frac{1}{2\xi} \|x - \mu - \beta\xi\|_{\Sigma^{-1}}^2 = \frac{1}{2\xi} \|x - \mu\|_{\Sigma^{-1}}^2 - \langle x - \mu, \Sigma^{-1}\beta \rangle + \frac{\xi}{2} \|\beta\|_{\Sigma^{-1}}^2. \quad (2.3)$$

To comprehend the structure of the GH family, we first revisit some of its basic properties and then add some additional insights that were not put forth in previous studies. It is known that the multivariate GH (MGH) distribution satisfies expression (2.1), when the non-negative random variable  $\tau$  follows a generalized inverse Gaussian (GIG) distribution or  $N^-(\lambda, \delta, \gamma)$  with parameters  $\lambda, \delta, \gamma \in \mathbb{R}$ . For convenience, we state the form of the density of a GIG member as

$$f_{GIG(\lambda, \delta, \gamma)}(x) := \left(\frac{\gamma}{\delta}\right)^{\lambda} \frac{1}{2K_{\lambda}(\gamma\delta)} \exp\left\{-\frac{1}{2}(\delta^2 x^{-1} + \gamma^2 x)\right\} I(x \in (0, \infty)), \quad (2.4)$$

where  $K_\lambda(x)$  denotes the modified Bessel function of the third kind with index  $\lambda$ . Applying (2.2)-(2.4), the following alternative form of the MGH density with parameters  $\mu, \beta \in \mathbb{R}^d$ ,  $\lambda, \delta, \gamma \in \mathbb{R}$  and  $\Sigma \in \mathbb{R}^{d \times d}$  is obtained

$$f_Y(x) = \frac{|\Sigma|^{-1/2} e^{\langle x - \mu, \Sigma^{-1} \beta \rangle} \left(\frac{\gamma}{\delta}\right)^\lambda \left(\|x - \mu\|_{\Sigma^{-1}}^2 + \delta^2\right)^{(\lambda - \frac{d}{2})/2}}{(2\pi)^{d/2} \left(\|\beta\|_{\Sigma^{-1}}^2 + \gamma^2\right)^{(\lambda - \frac{d}{2})/2} K_\lambda(\delta\gamma)} K_{\lambda - \frac{d}{2}} \left\{ \delta\gamma \left(1 + \|x - \mu\|_{\Sigma^{-1}}^2 / \delta^2\right)^{1/2} \left(1 + \|\beta\|_{\Sigma^{-1}}^2 / \gamma^2\right)^{1/2} \right\} I(x \in \mathbb{R}^d). \quad (2.5)$$

It is noted that the GIG is a member of the generalized gamma convolution (GGC), which also implies that it is self-decomposable and infinitely divisible. Consequently, the random vectors satisfying (2.2) when  $\tau$  is GIG are also members of the GGC family (see, e.g., Hammerstein 2010) and, therefore, are self-decomposable and infinitely divisible. In this present work, we focus only on the MGH density and thus the relevant properties that can be derived viewing the MGH as a multivariate Lévy variable will be omitted.

For asymptotic purposes, the following integral representation of the density of  $Y$  is central.

**Proposition 2.1.** *Let  $\mu, \beta \in \mathbb{R}^d$  be fixed parameters. Then, for  $\lambda, \gamma, \delta \in \mathbb{R}$ , the MGH density has the following expression,*

$$f_Y(x) = \frac{|\Sigma|^{-1/2} e^{\langle x - \mu, \Sigma^{-1} \beta \rangle} \Gamma(\lambda - \frac{d-1}{2})}{(4\pi)^{d/2} \Gamma(\lambda + \frac{1}{2})} \frac{(\gamma^2)^{d/2}}{\left(1 + \frac{\|x - \mu\|_{\Sigma^{-1}}^2}{\delta^2}\right)^{1/2} \left(1 + \frac{\|\beta\|_{\Sigma^{-1}}^2}{\gamma^2}\right)^{\lambda - \frac{d-1}{2}}} \frac{\int_0^\infty \left\{ t^2 / \delta^2 \gamma^2 \left( \frac{\|x - \mu\|_{\Sigma^{-1}}^2}{\delta^2} + 1 \right) \left( \frac{\|\beta\|_{\Sigma^{-1}}^2}{\gamma^2} + 1 \right) \right\} + 1}{\int_0^\infty \left\{ t^2 / \delta^2 \gamma^2 \right\} + 1}^{-\lambda - \frac{d-1}{2}} \cos(t) dt}{\int_0^\infty \left\{ t^2 / \delta^2 \gamma^2 \right\} + 1}^{-\lambda - \frac{1}{2}} \cos(t) dt} I(x \in \mathbb{R}^d).$$

**Proof.** It can be seen that the following identity (Abramowitz and Stegun, 1998, 9.6.25) holds.

$$K_\nu(xz) = \frac{\Gamma\left(\nu + \frac{1}{2}\right) (2z)^\nu}{\sqrt{\pi} x^\nu} \int_0^\infty (t^2 + z^2)^{-\nu - \frac{1}{2}} \cos(xt) dt, \quad \nu > -\frac{1}{2}. \quad (2.6)$$

In light of (2.6), the representation of the density in (2.5) is modified as

$$\begin{aligned}
f_Y(x) &= \frac{|\Sigma|^{-1/2} e^{\langle x-\mu, \Sigma^{-1}\beta \rangle} \left(\frac{\gamma^2}{\delta^2}\right)^{d/4} \left(1 + \frac{\|x-\mu\|_{\Sigma^{-1}}^2}{\delta^2}\right)^{(\lambda-\frac{d}{2})/2}}{(2\pi)^{d/2} \left(1 + \frac{\|\beta\|_{\Sigma^{-1}}^2}{\gamma^2}\right)^{(\lambda-\frac{d}{2})/2}} \\
&= \frac{\Gamma(\lambda - \frac{d-1}{2})}{2^{d/2} (\gamma^2 \delta^2)^{d/4} \Gamma(\lambda + \frac{1}{2})} \left(1 + \frac{\|x-\mu\|_{\Sigma^{-1}}^2}{\delta^2}\right)^{(\lambda-\frac{d}{2})/2} \left(1 + \frac{\|\beta\|_{\Sigma^{-1}}^2}{\gamma^2}\right)^{(\lambda-\frac{d}{2})/2} \\
&\quad \frac{(\gamma^2 \delta^2)^{d/2} \int_0^\infty \left\{ t^2 / \delta^2 \gamma^2 \left( \frac{\|x-\mu\|_{\Sigma^{-1}}^2}{\delta^2} + 1 \right) \left( \frac{\|\beta\|_{\Sigma^{-1}}^2}{\gamma^2} + 1 \right) \right\} + 1}{\int_0^\infty \left\{ t^2 / \delta^2 \gamma^2 \right\} + 1}^{-\lambda + \frac{d-1}{2}} \cos(t) dt}{\left\{ \left(1 + \frac{\|x-\mu\|_{\Sigma^{-1}}^2}{\delta^2}\right) \left(1 + \frac{\|\beta\|_{\Sigma^{-1}}^2}{\gamma^2}\right) \right\}^{\lambda - \frac{d-1}{2}} \int_0^\infty \left\{ t^2 / \delta^2 \gamma^2 \right\} + 1}^{-\lambda - \frac{1}{2}} \cos(t) dt}.
\end{aligned}$$

After some algebraic simplifications, the alternative representation of the density as shown in Proposition 2.1 follows.  $\square$

The form of Proposition 2.1 is important for deriving various limiting results. Specifically, limit properties are derived assuming that the index  $\lambda$  is now related to either  $\delta$  or  $\gamma$  and then letting  $\lambda$  tend to infinity. Based on this, we first have the following theorem, remarks and corollary.

**Theorem 2.1.** *When  $\gamma^2 = \lambda v^2$  and  $\lambda \rightarrow \infty$ , the MGH density converges to the following proper density*

$$\lim_{\lambda \rightarrow \infty} f_{Y_\lambda}(x) = f_{Y_\infty}(x) = \frac{|\Sigma|^{-1/2}}{(4\pi/v^2)^{d/2}} e^{-\frac{v^2}{4} \left\| x - \mu - \frac{2\beta}{v^2} \right\|_{\Sigma^{-1}}^2} I(x \in \square^d),$$

where  $Y_\lambda \equiv Y = \mu + \beta\tau + \sqrt{\tau}X$  and  $\tau \sim GIG(\lambda, \delta, \gamma)$ .

In other words,  $Y_\lambda$  converges in distribution to a random vector admitting the following stochastic representation

$$Y_\lambda \rightarrow_D Y_\infty \equiv N_d \left( \mu + \frac{2\beta}{v^2}, \frac{2}{v^2} \Sigma \right).$$

**Proof.** To proceed with the proof, we note that the asymptotic representation of the gamma function for large values of  $\lambda$  is given by (see e.g., Gradshteyn and Ryzhik's (2000, 3.328))

$$\Gamma(\lambda) = \sqrt{2\pi} \lambda^{\lambda-1/2} e^{-\lambda} \left\{ 1 + \frac{1}{12\lambda} + O(\lambda^{-2}) \right\} = \sqrt{2\pi} \lambda^{\lambda-1/2} e^{-\lambda} \left\{ 1 + O(\lambda^{-1}) \right\}. \quad (2.7)$$

In what follows,  $\lambda$  tends to infinity. Thus, for purpose of obtaining the expression, the second representation in (2.7) is sufficient. Substituting  $\gamma^2 = \lambda v^2$  and (2.7) into Proposition 2.1, we have

$$f_Y(x) \square \frac{|\Sigma|^{-1/2} e^{\langle x-\mu, \Sigma^{-1}\beta \rangle}}{(4\pi)^{d/2}} \frac{(v^2)^{d/2} \lambda^{d/2} \left(\lambda - \frac{d-1}{2}\right)^{\lambda - \frac{d}{2}} e^{-(\lambda - \frac{d-1}{2})}}{\left(\lambda + \frac{1}{2}\right)^{\lambda - \frac{d}{2}} \left(\lambda + \frac{1}{2}\right)^{d/2} e^{-(\lambda + \frac{1}{2})} \left(1 + \frac{\|x - \mu\|_{\Sigma^{-1}}^2}{\delta^2}\right)^{1/2} \left(1 + \frac{\|\beta\|_{\Sigma^{-1}}^2}{\lambda v^2}\right)^{\lambda - \frac{d-1}{2}}} \frac{\int_0^\infty \left\{ \left\{ t^2 / \lambda \delta^2 v^2 \left( \frac{\|x - \mu\|_{\Sigma^{-1}}^2}{\delta^2} + 1 \right) \left( \frac{\|\beta\|_{\Sigma^{-1}}^2}{\lambda v^2} + 1 \right) \right\} + 1 \right)^{-\lambda + \frac{d-1}{2}} \cos(t) dt}{\int_0^\infty \left( \left\{ t^2 / \lambda \delta^2 v^2 \right\} + 1 \right)^{-\lambda - \frac{1}{2}} \cos(t) dt} I(x \in \square^d) \quad (2.8)$$

Next, letting  $\lambda \rightarrow \infty$ , and taking into the account the fact that  $\lim_{\lambda \rightarrow \infty} \left(1 \pm \frac{x}{\lambda(1 + O(\lambda^{-1}))}\right)^\lambda = e^{\pm x}$ , the

representation (2.8) becomes

$$\lim_{\lambda \rightarrow \infty} f_{Y_\lambda}(x) = \frac{|\Sigma|^{-1/2} e^{\langle x-\mu, \Sigma^{-1}\beta \rangle}}{(4\pi)^{d/2}} \frac{(v^2)^{d/2} e^{-d/2} e^{-\|\beta\|_{\Sigma^{-1}}^2/v^2} e^{d/2}}{\left(1 + \frac{\|x - \mu\|_{\Sigma^{-1}}^2}{\delta^2}\right)^{1/2}} \frac{\int_0^\infty e^{-t^2/\delta^2 v^2 \left(\frac{\|x - \mu\|_{\Sigma^{-1}}^2}{\delta^2} + 1\right)} \cos(t) dt}{\int_0^\infty e^{-t^2/\delta^2 v^2} \cos(t) dt} I(x \in \square^d) \quad (2.9)$$

Applying equation (2.10) (see, e.g., Gradshteyn and Ryzhik's, 2000, 3.896.4), below

$$\int_0^\infty e^{-\eta t^2} \cos b t dt = \frac{1}{2} \sqrt{\frac{\pi}{\eta}} e^{-b^2/4\eta}, \quad \eta > 0, \quad (2.10)$$

into (2.10), we finally obtain

$$\lim_{\lambda \rightarrow \infty} f_{Y_\lambda}(x) = \frac{|\Sigma|^{-1/2} e^{\langle x-\mu, \Sigma^{-1}\beta \rangle}}{(4\pi/v^2)^{d/2}} \frac{e^{-\|\beta\|_{\Sigma^{-1}}^2/v^2} \left(1 + \frac{\|x - \mu\|_{\Sigma^{-1}}^2}{\delta^2}\right)^{1/2}}{\left(1 + \frac{\|x - \mu\|_{\Sigma^{-1}}^2}{\delta^2}\right)^{1/2}} e^{-v^2 \|x - \mu\|_{\Sigma^{-1}}^2/4}. \quad (2.11)$$

Upon some algebraic manipulations, the proof of Theorem 2.1 follows.  $\square$

**Remark 1.1** Note that when  $\gamma^2 = \lambda \nu^2$ ,  $\lambda \rightarrow \infty$  and  $\tau$  is GIG, the skewness parameter  $\beta$  in (2.1) becomes a pure translation parameter vector weighted by  $2/\nu^2$ , as well as the dispersion matrix  $\Sigma$  is weighted by the same scale term.

**Remark 1.2** Note that the density in Theorem 2.1 is independent of the parameter  $\delta$ . Furthermore, when  $\gamma^2 = \lambda \nu^2$ ,  $\lambda \rightarrow \infty$ , the density of the random vector  $W$  is symmetric, while the original MGH  $Y$  was asymmetric. This suggests an MGH model with smaller fitted values of  $\lambda$  can be related to the presence of skewness in the data together with heavy tails. From applications point of view, this implies that the MGH model can be viewed as a good candidate for modeling high frequency log returns. However, as fitted values of  $\lambda$  become large, the MGH model captures the behavior of low frequency aggregated data that are stylistically well known to be Gaussian. Essentially, this means the MGH model can be considered for modeling both low frequency as well as high frequency data against the currently prevailing notion that the model is relevant for modeling only high frequency data. Thus, this observation makes Theorem 2.1 quite important from applications point of view.

**Remark 1.3** Surprisingly, when  $\delta = 0$ , one may observe that the mixing density  $GIG(\lambda, 0, \gamma)$  follows gamma distribution. Setting  $\gamma^2 = \lambda \nu^2$  in the  $GIG(\lambda, 0, \gamma)$  we have that the mean is  $2/\nu^2$  and the variance is  $2/\lambda \nu^2$ . Upon letting  $\lambda \rightarrow \infty$  the  $GIG(\lambda, 0, \gamma)$  tends to a degenerate random variable at  $\tau = 2/\nu^2$ . This then yields the same density as in Theorem 2.1.

On the other hand, when  $\delta^2 = \lambda \eta^2$  and  $\lambda \rightarrow \infty$ , the MGH converges to a degenerate distribution. Specifically, we have the following corollary.

**Corollary 2.1.** *When  $\delta^2 = \lambda \eta^2$  and  $\lambda \rightarrow \infty$ , the MGH distribution converges to a degenerate distribution, so that*

$$P(Y_\lambda \in A) \rightarrow I(\mu \in A), \text{ for any } A \text{ Borel set in } \mathcal{B}(\mathbb{R}^d).$$

**Proof.** It can be seen that the ratio of the two integrals in Proposition 2.1 is always constant. Thus, the remaining term of (2.5) can be expressed as

$$I = \lim_{\lambda \rightarrow \infty} c(x; \mu, \beta, \Sigma) \frac{\gamma^d \Gamma(\lambda - \frac{d}{2} - \frac{1}{2})}{\Gamma(\lambda + \frac{1}{2}) \left( \frac{\|x - \mu\|_{\Sigma^{-1}}^2}{\delta^2} + 1 \right)^{1/2} \left( \frac{\|\beta\|_{\Sigma^{-1}}^2}{\gamma^2} + 1 \right)^{\lambda - \frac{d}{2} + \frac{1}{2}}}$$

$$= \lim_{\lambda \rightarrow \infty} c(x; \mu, \beta, \Sigma) \frac{\left(1 - d/2 \left(\lambda + \frac{1}{2}\right)^{-1}\right)^{\lambda + \frac{1}{2}}}{\left(\lambda - \frac{d}{2} - \frac{1}{2}\right)^{d/2} \left(\frac{\|x - \mu\|_{\Sigma^{-1}}^2}{\delta^2} + 1\right)^{1/2} \left(\frac{\|\beta\|_{\Sigma^{-1}}^2}{\gamma^2} + 1\right)^{\lambda - \frac{d}{2} + \frac{1}{2}}} = 0$$

where  $c(x; \mu, \beta, \Sigma) = |\Sigma|^{-1/2} e^{\langle x - \mu, \Sigma^{-1} \beta \rangle} / (2\pi)^{d/2}$ . Further, from (2.2) the domain of  $\tau$  is strictly greater than zero and at  $\tau = 0$  the normal density is infinite. Thus, the density is always zero. In this case, the mass is focused on  $x = \mu$ .  $\square$

It is also worth mentioning that by using only expression (2.5), other limiting results can be derived assuming now that the parameters  $\delta$  or  $\gamma$ , or both, tend to infinity while allowing  $\lambda$  to be fixed. In all these cases, the MGH distribution leads to degenerate distributions. These results can be summarized in the following theorem.

**Theorem 2.2.** *As (i.)  $\gamma \rightarrow \infty$  and  $\delta, \lambda$  are fixed parameters, or (ii.)  $\delta \rightarrow \infty$  and  $\gamma, \lambda$  are fixed parameters or (iii.)  $\delta, \gamma \rightarrow \infty$  and  $\lambda$  is a fixed parameter then in all these cases the density of MGH converges to zero and we have*

$$P(Y_\lambda \in A) \rightarrow I(\mu \in A), \text{ for any } A \text{ Borel set in } \mathcal{B}(\mathbb{R}^d).$$

**Proof.** From Abramowitz and Stegun (1998, 9.7.2), the following approximation is adopted

$$K_\nu(x) \sim \sqrt{\frac{\pi}{2x}} e^{-x} \text{ as } x \rightarrow \infty. \quad (2.12)$$

In addition, the following approximations holds true

$$x^q e^{-cx} \rightarrow 0 \text{ as } x \rightarrow \infty \text{ for } q \in \mathbb{R} \text{ and } c > 0. \quad (2.13)$$

Assume that any of the three conditions in Theorem 2.2 hold. Then, applying (2.12) and (2.13) into the density form (2.5) of MGH, we have

$$f_Y(x) = c(x; \mu, \beta, \Sigma) \frac{\left(\frac{\gamma}{\delta}\right)^{d/2} \left(\frac{\|x - \mu\|_{\Sigma^{-1}}^2}{\delta^2} + 1\right)^{\left(\lambda - \frac{d}{2}\right)/2}}{\left(\frac{\|\beta\|_{\Sigma^{-1}}^2}{\gamma^2} + 1\right)^{\left(\lambda - \frac{d}{2}\right)/2}}$$

$$\frac{\exp \left\{ -|\gamma\delta| \left[ \left( \frac{\|x - \mu\|_{\Sigma^{-1}}^2}{\delta^2} + 1 \right)^{1/2} \left( \frac{\|\beta\|_{\Sigma^{-1}}^2}{\gamma^2} + 1 \right)^{1/2} - 1 \right] \right\}}{\sqrt{\left( \frac{\|x - \mu\|_{\Sigma^{-1}}^2}{\delta^2} + 1 \right)^{1/2} \left( \frac{\|\beta\|_{\Sigma^{-1}}^2}{\gamma^2} + 1 \right)^{1/2}}} I(x \in \square^d) \rightarrow 0$$

as  $\gamma \rightarrow \infty$  and  $\delta$  fixed or  $\delta \rightarrow \infty$  and  $\gamma$  fixed or both  $\delta, \gamma \rightarrow \infty$ . This completes the proof of Theorem 2.2.  $\square$

Finally, the behavior of MGH density is studied when the parameters  $\gamma, \delta$  tend to zero. To be consistent with the previous notations, set  $Y_{\lambda, \gamma, \delta} := Y$ . We begin with the following result.

**Theorem 2.3.** *As  $\delta \downarrow 0$ , the MGH density in (2,5) behaves as*

$$\lim_{\delta \rightarrow 0} \frac{f_{Y_{\lambda, \gamma, \delta}}(x)}{c(x; \mu, \beta, \Sigma) \frac{\gamma^{2\lambda} \|x - \mu\|_{\Sigma^{-1}}^{\lambda - d/2}}{2^{\lambda-1} \Gamma(\lambda) \left( \|\beta\|_{\Sigma^{-1}}^2 + \gamma^2 \right)^{(\lambda - d/2)/2}} K_{\lambda - d/2} \left\{ \|x - \mu\|_{\Sigma^{-1}} \left( \|\beta\|_{\Sigma^{-1}}^2 + \gamma^2 \right)^{1/2} \right\}} = 1,$$

where  $c(x; \mu, \beta, \Sigma) = |\Sigma|^{-1/2} e^{\langle x - \mu, \Sigma^{-1} \beta \rangle} / (2\pi)^{d/2}$ .

**Proof.** From Abramowitz and Stegun (1998, 9.6.9), the following identity is employed

$$K_\nu(x) \sim \frac{1}{2} \Gamma(|\nu|) \left( \frac{x}{2} \right)^{-|\nu|} \quad \text{as } x \downarrow 0. \quad (2.14)$$

Then, applying (2.14) the result follows.  $\square$

**Remark 2.** When  $\beta = 0$ , the expression in Theorem 2.3 simplifies into

$$\lim_{\delta \rightarrow 0} \frac{f_{Y_{\lambda, \gamma, \delta}}(x)}{|\Sigma|^{-1/2} \frac{\gamma^{\lambda + d/2} \|x - \mu\|_{\Sigma^{-1}}^{\lambda - d/2}}{2^{\lambda-1} (2\pi)^{d/2} \Gamma(\lambda)} K_{\lambda - d/2} \left\{ |\gamma| \|x - \mu\|_{\Sigma^{-1}} \right\}} = 1.$$

**Remark 3.** When  $\gamma \downarrow 0$  or when both the parameters  $\gamma, \delta \downarrow 0$  the MGH distribution converges to a degenerate distribution.

### 3. The conditional MGH distribution and its limits.

In this section we first introduce a few concepts for conditional densities and then formulate the conditional density for the multivariate GH. Next, we continue developing limiting results following similar ideas as in Section 2.

To obtain marginal and conditional distributions we partition the vector  $Y = \begin{pmatrix} Y_1 \\ Y_2 \end{pmatrix}$  with  $Y_1 \in \square^{d_1}$ ,

$1 \leq d_1 < d$  and  $Y_2 \in \square^{d-d_1}$ . Similar partitions for the vectors  $\mu, \beta$  and  $X \in \square^d$  in the model (2.1) can be made accordingly. Note that the variance covariance matrix  $\Sigma$  of the random vector  $X$  is correspondingly subdivided as  $\Sigma = \begin{pmatrix} \Sigma_{11} & \Sigma_{12} \\ \Sigma_{21} & \Sigma_{22} \end{pmatrix}$ , where  $\Sigma_{11} \in \square^{d_1 \times d_1}$ ,  $\Sigma_{12} \in \square^{d_1 \times (d-d_1)}$  and so on. In light of the above notation, the following Proposition is an analog of density in (2.5).

**Proposition 3.1.** *Let  $\mu, \beta \in \square^d$  be fixed parameters. Further, let the vectors  $Y, \mu, \beta$  and  $X \in \square^d$  be partitioned as indicated above. Then, for  $\lambda, \gamma, \delta \in \square$ , the conditional density of  $Y_2 | Y_1$  for a MGH vector  $Y$  with  $Y_1 \in \square^{d_1}$ ,  $1 \leq d_1 < d$ , has the following expression:*

$$f_{Y_2|Y_1}(x_2|x_1) = \frac{|\Sigma_{22.1}|^{-1/2} e^{\langle x_2 - \mu_{2.1}, \Sigma_{22.1}^{-1} \beta_{2.1} \rangle} \left( \frac{g_2^2}{g_1^2} \right)^{(d-d_1)/2} \left( \frac{1 + \frac{\|x_2 - \mu_{2.1}\|_{\Sigma_{22.1}^{-1}}^2}{g_1^2}}{1 + \frac{\|\beta_{2.1}\|_{\Sigma_{22.1}^{-1}}^2}{g_2^2}} \right)^{(\lambda - \frac{d}{2})/2}}{(2\pi)^{(d-d_1)/2}} \frac{K_{\lambda - \frac{d}{2}} \left\{ g_1 g_2 \left( 1 + \frac{\|x_2 - \mu_{2.1}\|_{\Sigma_{22.1}^{-1}}^2}{g_1^2} \right)^{1/2} \left( 1 + \frac{\|\beta_{2.1}\|_{\Sigma_{22.1}^{-1}}^2}{g_2^2} \right)^{1/2} \right\}}{K_{\lambda - \frac{d_1}{2}}(g_1 g_2)} I(x_2 \in \square^{d-d_1} | x_1 \in \square^{d_1}) \text{ a.e.,}$$

where  $\Sigma_{22.1} = \Sigma_{22} - \Sigma_{21} \Sigma_{11}^{-1} \Sigma_{12}$ ,  $\mu_{2.1} = \mu_2 + \Sigma_{21} \Sigma_{11}^{-1} (x_1 - \mu_1)$ ,  $\beta_{2.1} = \beta_2 - \Sigma_{21} \Sigma_{11}^{-1} \beta_1$ ,

$$g_1^2(x_2) := g_1(x_1, x_2; \mu_1, \mu_{2.1}, \Sigma_{11}, \Sigma_{22.1}, \delta)^2 = \|x_1 - \mu_1\|_{\Sigma_{11}^{-1}}^2 + \|x_2 - \mu_{2.1}\|_{\Sigma_{22.1}^{-1}}^2 + \delta^2,$$

$$g_2^2(\beta_2) := g_2(\beta_1, \beta_{2.1}, \Sigma_{11}, \Sigma_{22.1}, \gamma)^2 = \|\beta_1\|_{\Sigma_{11}^{-1}}^2 + \|\beta_{2.1}\|_{\Sigma_{22.1}^{-1}}^2 + \gamma^2,$$

$$g_1 := g_1(0) = \sqrt{\|x_1 - \mu_1\|_{\Sigma_{11}^{-1}}^2 + \delta^2}, \text{ and } g_2 := g_2(0) = \sqrt{\|\beta_1\|_{\Sigma_{11}^{-1}}^2 + \gamma^2} \equiv g_2.$$

**Proof.** Note that  $Y|\tau \sim N_d(\mu + \beta\tau, \tau\Sigma)$ . Then, it is not hard to see that the vectors  $Y_1|\tau \stackrel{D}{=} N_{d_1}(\mu_1 + \beta_1\tau, \tau\Sigma_{11})$  and  $Y_2|Y_1, \tau \stackrel{D}{=} N_{d-d_1}(\mu_{2.1} + \beta_{2.1}\tau, \tau\Sigma_{22.1})$  are independent. Applying the regular conditional density of  $Y_2|Y_1$ , it can be then seen that

$$f_{Y_2|Y_1}(x_2|x_1) = \frac{f_{Y_2, Y_1}(x_2, x_1)}{f_{Y_1}(x_1)} = \frac{\int_0^\infty f_{Y_2, Y_1|\tau}(x_2, x_1|\xi) f_\tau(\xi) d\xi}{f_{Y_1}(x_1)} I(x_2 \in \square^{d-d_1} | x_1 \in \square^{d_1}) \text{ a.e.}$$

Now, applying the conditional independence, the transition density becomes

$$f_{Y_2|Y_1}(x_2|x_1) = \frac{\int_0^\infty f_{Y_1|\tau}(x_1|\xi) f_{Y_2|Y_1,\tau}(x_2|x_1,\xi) f_\tau(\xi) d\xi}{\int_0^\infty f_{Y_1|\tau}(x_1|\xi) f_\tau(\xi) d\xi} I(x_2 \in \square^{d-d_1} | x_1 \in \square^{d_1}) \text{ a.e.}$$

In obtaining final expressions, we first decompose  $\|x_2 - \mu_{2.1} - \beta_{2.1}\xi\|_{\Sigma_{22.1}^{-1}}^2 / \xi$  as in (2.3) to have

$$\frac{1}{2\xi} \|x_2 - \mu_{2.1} - \beta_{2.1}\xi\|_{\Sigma_{22.1}^{-1}}^2 = \frac{1}{2\xi} \|x_2 - \mu_{2.1}\|_{\Sigma_{22.1}^{-1}}^2 - \langle x_2 - \mu_{2.1}, \Sigma_{22.1}^{-1} \beta_{2.1} \rangle + \frac{\xi}{2} \|\beta_{2.1}\|_{\Sigma_{22.1}^{-1}}^2, \quad (3.1)$$

for each fixed  $\xi > 0$ .

Substituting the known expressions for the densities of random variables  $Y_1|\tau$ ,  $Y_2|Y_1,\tau$  and  $\tau$ , the above conditional density is then formed as

$$f_{Y_2|Y_1}(x_2|x_1) = \frac{|\Sigma_{22.1}|^{-1/2} e^{\langle x_2 - \mu_{2.1}, \Sigma_{22.1}^{-1} \beta_{2.1} \rangle}}{(2\pi)^{(d-d_1)/2}} \frac{\int_0^\infty \xi^{\lambda - \frac{d}{2} - 1} \exp\left\{-\frac{1}{2} \left( \frac{g_1(x_2)^2}{\xi} + g_2(\beta_2)^2 \xi \right)\right\} d\xi}{\int_0^\infty \xi^{\lambda - \frac{d_1}{2} - 1} \exp\left\{-\frac{1}{2} \left( \frac{g_1^2}{\xi} + g_2^2 \xi \right)\right\} d\xi} I(x_2 \in \square^{d-d_1} | x_1 \in \square^{d_1}) \text{ a.e.}$$

Then, the theorem can be shown when one replaces the integrals with the Bessel functions.  $\square$

The next proposition is the conditional analogue of Proposition 2.1 that is used to obtain asymptotic results.

**Proposition 3.2.** *Let  $\mu, \beta \in \square^d$  be fixed parameters. Further, let the vectors  $Y, \mu, \beta$  and  $X \in \square^d$  be partitioned as indicated above. Then, for  $\lambda, \gamma, \delta \in \square$ , the conditional density of  $Y_2|Y_1$  for a MGH vector with  $Y_1 \in \square^{d_1}$ ,  $1 \leq d_1 < d$ , has the following expression:*

$$f_{Y_2|Y_1}(x_2|x_1) = \frac{(g_2^2)^{(d-d_1)/2} |\Sigma_{22.1}|^{-1/2} e^{\langle x_2 - \mu_{2.1}, \Sigma_{22.1}^{-1} \beta_{2.1} \rangle} \Gamma(\lambda - \frac{d}{2} + \frac{1}{2})}{(4\pi)^{(d-d_1)/2} \Gamma(\lambda - \frac{d_1}{2} + \frac{1}{2}) \left(1 + \frac{\|x_2 - \mu_{2.1}\|_{\Sigma_{22.1}^{-1}}^2}{g_1^2}\right)^{1/2} \left(1 + \frac{\|\beta_{2.1}\|_{\Sigma_{22.1}^{-1}}^2}{g_2^2}\right)^{(\lambda - \frac{d}{2}) + \frac{1}{2}}}$$

$$\frac{\int_0^\infty \left[1 + \left\{t^2 / g_1^2 g_2^2 \left(1 + \frac{\|x_2 - \mu_{2.1}\|_{\Sigma_{22.1}^{-1}}^2}{g_1^2}\right) \left(1 + \frac{\|\beta_{2.1}\|_{\Sigma_{22.1}^{-1}}^2}{g_2^2}\right)\right\}\right]^{-\lambda + \frac{d}{2} - \frac{1}{2}} \cos(t) dt}{\int_0^\infty \left\{1 + (t^2 / g_1^2 g_2^2)\right\}^{-\lambda + \frac{d_1}{2} - \frac{1}{2}} \cos(t) dt} I(x_2 \in \square^{d-d_1} | x_1 \in \square^{d_1}) \text{ a.e.,}$$

where  $\Sigma_{22.1} = \Sigma_{22} - \Sigma_{21}\Sigma_{11}^{-1}\Sigma_{12}$ ,  $\mu_{2.1} = \mu_2 + \Sigma_{21}\Sigma_{11}^{-1}(x_1 - \mu_1)$ ,  $\beta_{2.1} = \beta_2 - \Sigma_{21}\Sigma_{11}^{-1}\beta_1$ ,

$$g_1^2(x_2) := g_1(x_1, x_2; \mu_1, \mu_{2.1}, \Sigma_{11}, \Sigma_{22.1}, \delta)^2 = \|x_1 - \mu_1\|_{\Sigma_{11}^{-1}}^2 + \|x_2 - \mu_{2.1}\|_{\Sigma_{22.1}^{-1}}^2 + \delta^2,$$

$$g_2^2(\beta_2) := g_2(\beta_1, \beta_{2.1}, \Sigma_{11}, \Sigma_{22.1}, \gamma)^2 = \|\beta_1\|_{\Sigma_{11}^{-1}}^2 + \|\beta_{2.1}\|_{\Sigma_{22.1}^{-1}}^2 + \gamma^2,$$

$$g_1 := g_1(0) = \sqrt{\|x_1 - \mu_1\|_{\Sigma_{11}^{-1}}^2 + \delta^2}, \text{ and } g_2 := g_2(0) = \sqrt{\|\beta_1\|_{\Sigma_{11}^{-1}}^2 + \gamma^2} \equiv g_2.$$

**Proof.** Applying (3.1), and substituting expression (2.6) in both Bessel functions in Proposition 3.1, the ratio of the two Bessel functions now becomes

$$\begin{aligned} & \frac{K_{\lambda - \frac{d}{2}} \left\{ g_1 g_2 \left( 1 + \frac{\|x_2 - \mu_{2.1}\|_{\Sigma_{22.1}^{-1}}^2}{g_1^2} \right)^{1/2} \left( 1 + \frac{\|\beta_{2.1}\|_{\Sigma_{22.1}^{-1}}^2}{g_2^2} \right)^{1/2} \right\}}{K_{\lambda - \frac{d_1}{2}}(g_1 g_2)} \\ &= \frac{\Gamma\left(\lambda - \frac{d}{2} + \frac{1}{2}\right)(g_1 g_2)^{(d-d_1)/2}}{\Gamma\left(\lambda - \frac{d_1}{2} + \frac{1}{2}\right)2^{(d-d_1)/2}} \frac{1}{\left(1 + \frac{\|x_2 - \mu_{2.1}\|_{\Sigma_{22.1}^{-1}}^2}{g_1^2}\right)^{\frac{\lambda - \frac{d}{2} + \frac{1}{2}}{2} + \frac{1}{2}} \left(1 + \frac{\|\beta_{2.1}\|_{\Sigma_{22.1}^{-1}}^2}{g_2^2}\right)^{\frac{\lambda - \frac{d}{2} + \frac{1}{2}}{2} + \frac{1}{2}}} \\ & \frac{\int_0^\infty \left[ 1 + \left\{ t^2 / g_1^2 g_2^2 \left( 1 + \frac{\|x_2 - \mu_{2.1}\|_{\Sigma_{22.1}^{-1}}^2}{g_1^2} \right) \left( 1 + \frac{\|\beta_{2.1}\|_{\Sigma_{22.1}^{-1}}^2}{g_2^2} \right) \right\} \right]^{-\lambda + \frac{d}{2} - \frac{1}{2}} \cos(t) dt}{\int_0^\infty \left\{ 1 + \left( t^2 / g_1^2 g_2^2 \right) \right\}^{-\lambda + \frac{d_1}{2} - \frac{1}{2}} \cos(t) dt} \end{aligned}$$

Incorporating the remaining terms of Proposition 3.1, the proof follows upon applying several algebraic operations similar to Proposition 2.1.  $\square$

The next theorem is an analogue of Theorem 2.1.

**Theorem 3.1.** When  $\gamma^2 = \lambda v^2$  and  $\lambda \rightarrow \infty$ , the conditional density of  $Y_2|Y_1$  for a MGH vector with  $Y_1 \in \square^{d_1}$ ,  $1 \leq d_1 < d$ , converges to the following density:

$$\lim_{\lambda \rightarrow \infty} f_{Y_{2,\lambda}|Y_{1,\lambda}}(x_2|x_1) = \frac{|\Sigma_{22.1}|^{-1/2}}{(4\pi/v^2)^{(d-d_1)/2}} e^{-\frac{v^2}{4} \left\| x_2 - \mu_{2.1} - \frac{2\beta_{2.1}}{v^2} \right\|_{\Sigma_{22.1}^{-1}}^2} I\left(x_2 \in \square^{d-d_1} \mid x_1 \in \square^{d_1}\right) \text{ a.e.}$$

In other words,  $Y_{2,\lambda}|Y_{1,\lambda} \rightarrow_D Y_{2,\infty}|Y_{1,\infty} \sim N_{d-d_1}\left(\mu_{2.1} + \frac{2\beta_{2.1}}{v^2}, \frac{2}{v^2}\Sigma_{22.1}\right)$  a.s.

**Proof.** Since  $\gamma^2 = \lambda \nu^2$ ,  $\lambda \rightarrow \infty$ , from Stirling's formula and from Theorem 3.1, it can be seen as in Theorem 2.1 that

$$\begin{aligned}
& \lim_{\lambda \rightarrow \infty} \frac{(\gamma^2)^{(d-d_1)/2} \Gamma(\lambda - \frac{d}{2} + \frac{1}{2})}{\Gamma(\lambda - \frac{d_1}{2} + \frac{1}{2}) \left(1 + \frac{\|x - \mu\|_{\Sigma_{22,1}^{-1}}^2}{g_1^2}\right)^{1/2} \left(1 + \frac{\|\beta_{2,1}\|_{\Sigma_{22,1}^{-1}}^2}{\|\beta_1\|_{\Sigma_{11}^{-1}}^2 + \lambda \nu^2}\right)^{\lambda - \frac{d}{2} + \frac{1}{2}}} \\
&= \lim_{\lambda \rightarrow \infty} \frac{(\nu^2)^{d/2} \lambda^{(d-d_1)/2} \left(\lambda - \frac{d_1-1}{2} - \frac{d-d_1}{2}\right)^{\lambda - \frac{d}{2}} e^{-(\lambda - \frac{d_1-1}{2})} e^{(d-d_1)/2}}{\left(\lambda - \frac{d_1-1}{2}\right)^{\lambda - \frac{d}{2}} \left(\lambda - \frac{d_1-1}{2}\right)^{(d-d_1)/2} e^{-(\lambda - \frac{d_1-1}{2})} \left(1 + \frac{\|x - \mu\|_{\Sigma_{22,1}^{-1}}^2}{g_1^2}\right)^{1/2} \left(1 + \frac{\|\beta_{2,1}\|_{\Sigma_{22,1}^{-1}}^2}{\|\beta_1\|_{\Sigma_{11}^{-1}}^2 + \lambda \nu^2}\right)^{\lambda - \frac{d-1}{2}}} \\
&= \lim_{\lambda \rightarrow \infty} \frac{(\nu^2)^{(d-d_1)/2} e^{-(d-d_1)/2} e^{(d-d_1)/2}}{\left(1 + \frac{\|x - \mu\|_{\Sigma_{22,1}^{-1}}^2}{g_1^2}\right)^{1/2}} e^{-\|\beta_{2,1}\|_{\Sigma_{22,1}^{-1}}^2 / \nu^2}. \tag{3.2}
\end{aligned}$$

Also, imitating similar steps as earlier for the ratio of the two integrals, we conclude that

$$\begin{aligned}
& \lim_{\lambda \rightarrow \infty} \frac{\int_0^\infty \left[1 + \left\{t^2 / g_1^2 g_2^2 \left(1 + \frac{\|x_2 - \mu_{2,1}\|_{\Sigma_{22,1}^{-1}}^2}{g_1^2}\right) \left(1 + \frac{\|\beta_{2,1}\|_{\Sigma_{22,1}^{-1}}^2}{g_2^2}\right)\right\}\right]^{-\lambda + \frac{d_1}{2}} \cos(t) dt}{\int_0^\infty \left\{1 + \left(t^2 / g_1^2 g_2^2\right)\right\}^{-\lambda + \frac{d_1-1}{2}} \cos(t) dt} \\
&= \frac{\int_0^\infty e^{-t^2 / \nu^2 \left(\|x_1 - \mu_1\|_{\Sigma_{11}^{-1}}^2 + \|x_2 - \mu_{2,1}\|_{\Sigma_{22,1}^{-1}}^2 + \delta^2\right)} \cos(t) dt}{\int_0^\infty e^{-t^2 / \nu^2 \left(\|x_1 - \mu_1\|_{\Sigma_{11}^{-1}}^2 + \delta^2\right)} \cos(t) dt}. \tag{3.3}
\end{aligned}$$

Merging (3.2) and (3.3), Theorem 3.1 follows upon applying Gradshteyn and Ryzhik (2000, 3.896.4) equation.  $\square$

**Remark 4.** Note that the representation of the density in Proposition 3.2 is similar to that in Proposition 2.1, where the parameters  $\gamma$ ,  $\delta$ ,  $d$  are now replaced by  $g_2$ ,  $g_1$  and the dimensionality  $d - d_1$ , respectively. Upon this, the detailed proof of Theorem 3.2 may be omitted in showing the result.

**Remark 5.** Comparable observations to Remark 1 in Section 2 can also be extracted for Theorem 3.1.

It can be further shown that analogous results to Corollary 2.1, and Theorems 2.2-2.3 can be obtained for the conditional density. For reasons of brevity, these results will be omitted.

## References

- Abramowitz, M., Stegun I.A., 1968. Handbook of Mathematical Functions (5<sup>th</sup> Ed.). New York: Dover.
- Adcock, C.J., 2010. Asset pricing and portfolio selection based on the multivariate extended skew-Student-t distribution. *Ann. Oper. Res.* 176 (1), 221-234.
- Affleck-Graves, J., McDonald, B., 1989. Nonnormalities and tests of asset pricing theories. *J. Finance* 44 (4), 889-908.
- Barndorff-Nielsen, O.E., 1977. Exponentially decreasing distributions for the logarithm of particle size. *Proc. Roy. Soc. Lond. Ser. A* 353, 401-419.
- Barndorff-Nielsen, O.E., 1978. Hyperbolic distributions and distributions of hyperbolae. *Scand. J. Statist.* 5, 151–157.
- Barndorff-Nielsen, O.E., 1979. Models for non-Gaussian variation, with applications to turbulence. *Proc. Roy. Soc. Lond. Ser. A* 368, 501–520.
- Barndorff-Nielsen, O., Blaesild, P., 1981. Hyperbolic distributions and ramifications: contributions to theory and application. In *Statistical Distributions in Scientific Work, Vol 4*, C. Taillie et al. (eds.), pp. 19-44, D. Reidel, Dordrecht, Holland.
- Eberlein, E., Keller U., 1995. Hyperbolic distributions in finance. *Bernoulli* 1, 281-299.
- Eberlein, E., Keller, U., Prause, K., 1998. New insights into smile, mispricing, and value at risk: the hyperbolic model. *J. Business* 71, 371-405.
- Eberlein, E., Prause, K., 2002. The generalized hyperbolic model: financial derivatives and risk measures. In Geman, H., Madan, D., Pliska, S., Vorst T. (Eds.), *Mathematical Finance-Bachelier Congress 2000*, 245-267. Berlin-Springer.
- Eberlein, E., 2001. Application of generalized hyperbolic Lévy motions to finance. In Barndorff-Nielsen, O.E., Mikosch, T., Resnick, S. (Eds.), *Lévy Processes: Theory and Applications*, 319-336. Boston: Birkhäuser.
- Fotopoulos, S.B., Jandhyala, V.K., Luo, Y., 2015. Subordinated Brownian motion: last time the process reaches its supremum. *Sankhya Ser. A* 77, 46-64.
- Fotopoulos, S.B., Jandhyala, V.K., Wang, J., 2015. On the joint distribution of the supremum functional and its last occurrence for subordinated linear Brownian motion. *Statist. Prob. Lett.* 106, 149-156.
- Fotopoulos, S.B., 2017. Symmetric Gaussian mixture distributions with GGC scales. *J. Mult. Anal.* 160, 185-194.

- Gradshteyn, I.S., Ryzhik, I.M., 2000. Table of Integrals, Series, and Products, 6<sup>th</sup> Ed. Academic Press, San Diego, New York.
- Hammerstein, P., 2010. Generalized hyperbolic distributions: Theory and applications to CDO pricing. Ph.D. Thesis, Albert-Ludwigs-Universität Freiburg im Breisgau.
- Khan, R., Zhou, G., 2006. Modeling non-normality using multivariate t: Implications for asset pricing. Working paper, University of Toronto.
- Kring, S., Rachev, S.T., Höchstötter, M., Fabozzi, F.J., Bianchi, M.L., 2009. Multi-tail generalized elliptical distributions for asset returns. *Econometri. J.* 12, 272-291.
- Korolev, V. Yu., 2014. Generalized hyperbolic laws as limit distributions for random sums. *Theor. Prob. Appl.* 58, 63-75.
- Korolev, V. Yu., Chertok, A.V., Korchagin, A. Yu., Kossova, E.V. and Zeifman, A.I., 2016. A note on functional limit theorems for compound Cox processes. *J. Math. Scie.*, 218, 182-194.
- Korolev, V. Yu. And Zeifman, A.I., 2016. On normal variance-mean mixtures as limit laws for statistics with random sample sizes. *J. Stat. Plan. Inf.*, 2016, 169, 34-42.
- Luciano, E., Schoutens, W., 2006. A multivariate jump-driven financial asset model. *Quant. Finance* 6 (5), 385-402.
- Madan, D.B., Seneta, E., 1990. The variance gamma (V.G.) model for share market returns. *J. Business* 63, 511-524.
- McNeil, A., Frey, R., Embrechts, P., 2005. *Quantitative Risk Management*. Princeton: Princeton University Press.
- Olbricht, W., 1991. On mergers of distributions and distributions with exponential tails. *Comp. Stat. Data Anal.* 12, 315–326.
- Owen, J., Rabinovitch, R., 1983. On the class of elliptical distributions and their applications to the theory of portfolio choice. *J. Finance* 38 (3), 745-752.
- Prause, K., 1999. The generalized hyperbolic model: Estimation, financial derivatives, and risk measures. Ph.D. thesis, University of Freiburg.
- Richardson, M., Smith, T., 1993. A test for multivariate normality in stock returns. *J. Business* 66 (2), 295-321.
- Semeraro, P., 2008. A multivariate variance gamma model for financial applications. *Int. J. Theor. Appl. Finance* 11 (1), 1-18.
- Yu, Y., 2017. On normal variance-mean mixtures. *Stat. Prob. Lett.* 121, 45-50.



# On determining the value of online customer satisfaction ratings – a case-based appraisal

Jim Freeman<sup>1</sup>

<sup>1</sup> Alliance Manchester Business School, University of Manchester, Booth Street East, Manchester, UK  
(E-mail: [jim.freeman@manchester.ac.uk](mailto:jim.freeman@manchester.ac.uk))

**Abstract:** A positive online reputation is one of the most powerful marketing assets a business can possess. Thanks to ubiquitous electronic Word of Mouth (eWOM) the internet has become saturated with online ratings and rankings on consumer satisfaction as a plethora of review sites vie for dominance in the world of reputation marketing.

Disconcertingly, the survey design, data collection methods and analytical techniques employed for generating such ratings can vary markedly from review site to review site - not just in transparency but also in value and reliability.

This is especially so in the hospitality industry where hotel review postings, in particular, often attract debate, suspicion and disagreement. It is against this backdrop that a critical appraisal of the Which? Travel Large UK Hotel Chains 2016 survey operation was undertaken.

**Keywords:** Composite indicators, Customer satisfaction, Factor analysis, Ordinal scores, Voluntary response sampling.

## 1 Introduction

In a matter of relatively few years, the Internet has revolutionised business and communication beyond all imagination – fundamentally changing the way that buyers and sellers interact in the market place.

Today, the internet is inundated with reviews by customers - documenting their experiences and the quality of products and services they have purchased. No more is this true than in the hospitality industry where for example review sites such as Booking.com Tripadvisor.com, Expedia.com.... compete to service a tourist industry whose growth appears to be accelerating ever upwards. The sheer volume of reviews is staggering - the vast majority seemingly being offered for entirely altruistic reasons [1]. And such is consumer dependence on reviews that even in 2007, 52% of would-be customers would not book a hotel unless an online review was available. (So what the equivalent figure is now can hardly be imagined.)

As more people use the internet as an information source, for entertainment and as a tool of conducting business, online ratings [2] are likely to become even more the default for everyday purposes in the future.

The prevalence of online surveys owes much to their capability for reaching large audiences at low cost and high speed. [3]

However, biases and errors apart, online surveys can be especially susceptible to review fraud where individuals or companies manipulate the user-generated content for their own benefit [4]. Similarly the credibility of individual reviews can often be in question - forcing analysts to rely on the so-called “wisdom of the crowds” [5] – to dubiously justify the results of their aggregate assessment.

---

*5<sup>th</sup> SMTDA Conference Proceedings, 12-15 June 2018, Chania, Crete, Greece*

© 2018 ISAST



Despite most review sites making little or no attempt to verify the information provided for their reviews, the impact of ratings on consumer preferences and buying behaviour appears to grow unrelentingly. In fact, somewhat perversely, reviews - and the ratings generated from them - are often perceived nowadays as being more objective and independent than traditional commercial information [6], [7].

The hospitality industry - particularly the hotel sector - is especially influenced by review ratings [8], [9], [10], [11], [12] - often to the good but sometimes to their great detriment – as exemplified recently by consumer watchdog, Which?’s survey results for large hotel chains. Widely publicised in the British press the Which? assessment makes for compelling reading. But even on the most cursory of inspections, deficiencies in the consumer champion’s reported findings are clearly evident – raising real suspicions about not only the validity of the methodology employed but also the inferences drawn.

This is the motivation for the critical evaluation now undertaken. The paper is organized as follows: section 2 after a brief review of relevant survey methodology, investigates explicit anomalies and inconsistencies in Which? Travel’s published outputs. Section 3 examines the detrimental impact of Which? Travel’s use of highly variable sample sizes for deriving hotel chains’ customer scores. Section 4 focusses on the customer score criterion which from correlation and factor analyses appears to be a seriously compromised measure of ‘overall evaluation of the brand from a respondent perspective’. Section 5 looks into the non-standard scoring adopted by Which? for weighting its ratings data and shows how this markedly distorts resulting customer score comparisons. Section 6 provides background on the range of biases affecting survey exercises such as that of Which? Travel and describes how these progressively detract from the validity and credibility of corresponding results and inferences. Section 7 concludes with a summary of the principal outcomes of the research

## 2. Incomplete, inconsistent and contradictory results

Results for the large UK hotel chains In the Best and Worst UK Hotel chains – Which? article published on 15 December 2016 [13] are reproduced in Table 1:

Hotel Chain	Sample size	Average price paid (£)	Cleanliness	Quality of Bedrooms	Quality of Bathrooms	Value for money	Customer Score
Premier Inn	1462	70	★★★★	★★★★★	★★★★★	★★★★	83%
Hampton by Hilton	51	83	★★★★	★★★★★	★★★★★	★★★★	76%
Novotel	76	98	★★★★	★★★★★	★★★★	★★★★	75%
Hilton	154	126	★★★★★	★★★★★	★★★★★	★★★	72%
Double Tree by Hilton	64	113	★★★★★	★★★★★	★★★★★	★★★	71%
Best Western	296	96	★★★★	★★★★	★★★★	★★★★	70%
Marriot	109	125	★★★★	★★★★★	★★★★★	★★★	70%
Holiday Inn Express	230	76	★★★★	★★★★	★★★★	★★★	69%
Radisson Blu	64	120	★★★★★	★★★★★	★★★★★	★★★	69%
Crowne Plaza	75	114	★★★★	★★★★★	★★★★★	★★★	68%
Jury's Inn	56	87	★★★★	★★★★	★★★★	★★★	67%
Holiday Inn	252	96	★★★★	★★★★	★★★★	★★★	66%
Ibis	101	76	★★★★	★★★★	★★★★	★★★	66%
Ibis Styles	34	80	★★★★	★★★	★★★★	★★★★	66%

Park Inn by Radisson	30	85	★★★★	★★★★	★★★★★		66%
Ibis Budget	38	57	★★★★	★★★	★★★	★★★★	65%
Old English Inns	38	70	★★★	★★★	★★★	★★★★	65%
Travelodge	483	58	★★★	★★★	★★★	★★★★	65%
Days Inn	44	60	★★★★	★★★	★★★	★★★★	63%
MacDonald	80	139	★★★★	★★★★★	★★★★	★★	63%
Mercure	128	107	★★★★	★★★★	★★★★	★★★	63%
Copthorne	31	113	★★★★	★★★	★★★★	★★★	60%
Ramada	32	77	★★★★	★★★	★★★	★★★	55%
Britannia	50	80	★★★	★★	★★	★★	44%

**Table 1. Published Which? results, 2016**

The methodology used for obtaining these results - from the relevant Which? Methodology and Technical report - is summarised in Table 2:

<b>Survey form:</b>	A web-based survey form was posted on www.which.co.uk in July 2016.
<b>Invitations:</b>	E-mail invitations were sent to all members of Which? Connect (Which?'s online community)
<b>Response:</b>	From circa 39,000 panelists 4,283 Which? Connect Members completed the survey. This represents a response rate of 11%.
<b>Questions and Categories</b>	<p>Data were collected in two forms:</p> <p>To obtain the <b>customer score</b> (overall evaluation), responses were collected for the key <b>Satisfaction</b> and <b>Endorsement</b> questions – see Table 2.3 for details.</p> <p>In addition, customers were asked to rate the following <b>categories</b>:</p> <ul style="list-style-type: none"> <li>• Cleanliness;</li> <li>• Quality of Bedrooms;</li> <li>• Quality of Bathrooms;</li> <li>• Bed comfort;</li> <li>• Hotel Description;</li> <li>• Value for money</li> </ul> <p>using a five star scale – as described in Table 2.4.</p>
<b>Thresholds:</b>	<p>For the <b>customer score</b> evaluation, both <b>Satisfaction</b> and <b>Endorsement</b> questions had to be answered.</p> <p>For the <b>category</b> data, each brand (chain) had to have at least 30 valid responses.</p>
<b>Analysis:</b>	<p>For the <b>customer score</b>:</p> <p>Responses to the <b>Satisfaction</b> and <b>Endorsement</b> questions were first weighted (see Section 5 for details). Weights were then averaged and adjusted to fit with a scale from zero to 100%.</p> <p>For the <b>category</b> data:</p> <p>Analysis involved averaging responses across all hotels and then, using an undisclosed analysis of variance procedure, individual brand averages were converted back into a one to five star format.</p>

**Table 2: Which?'s survey methodology in overview**

★ Very poor	★★ Poor	★★★ Fair	★★★★ Good	★★★★★ Excellent
----------------	------------	-------------	--------------	--------------------

**Table 3: Scale used for category items**

<b>Satisfaction</b> (“Overall satisfaction with the brand”)				
★ Very dissatisfied	★★ Fairly dissatisfied	★★★ Neither satisfied or dissatisfied	★★★★ Fairly satisfied	★★★★★ Very satisfied
<b>Endorsement</b> (“Likelihood to recommend the brand to a friend/family member”)				
★ Definitely will not recommend	★★ Probably will not recommend	★★★ Not sure	★★★★ Probably will recommend	★★★★★ Definitely will recommend

**Table 4: Scales used for Satisfaction and Endorsement questions**

Checking the results in Table 1 for compliance with the methodology described in Tables 2 – 4, the following discrepancies quickly become evident:

- The total sample size reported in the Which? Technical Report is 4283, but the total number of respondents according to Table 1 is 3978 – a shortfall of more than 7%.
- Though star ratings were sought across six categories according to Table 2 only results for four categories are provided in Table 1. In particular, the evaluations for **Bed comfort** and **Hotel description** have been inexplicably omitted from the analysis?
- Another curious omission in Table 1 is that of a **Value for money** rating for the Park Inn by Radisson Hotel Chain. It is not clear whether this is due to a) non-response b) a typing error or c) some other cause?
- A more graphic anomaly arises in respect of the **average price paid (£)** for a Britannia room: this is recorded in Table 1 as £80. But according to the company’s owner, Alex Langsam, the average room rate in 2016 was much nearer £40 [14]. Section 4 reveals later, a misrepresentation of the Britannia’s average room rate to this degree would impact very negatively on the company’s **value for money** rating with very adverse consequences for its **customer score**.

### 3. Sample size volatility

From Table 1, sample sizes range from 30 (**Park Inn by Radisson**) to 1462 (**Premier Inn**) – with fifteen hotels having sample sizes of less than 100. This enormous range of variability is particularly evident from Figure 1:

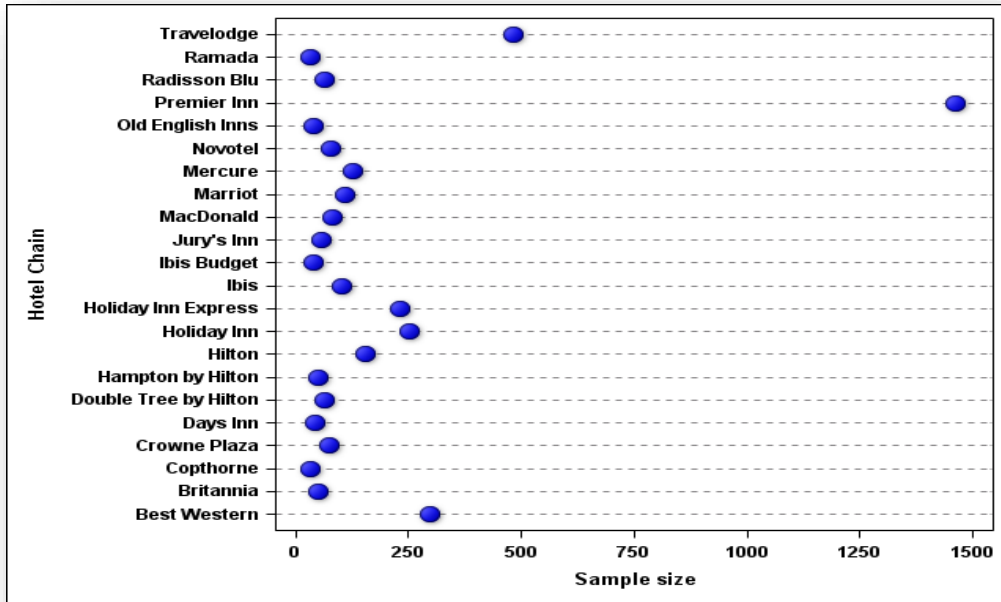


Fig 1. Sample size by hotel chain

The level of sample size volatility on display here unfortunately carries over to the corresponding precision of the satisfaction estimates involved - see Figure 2 below:

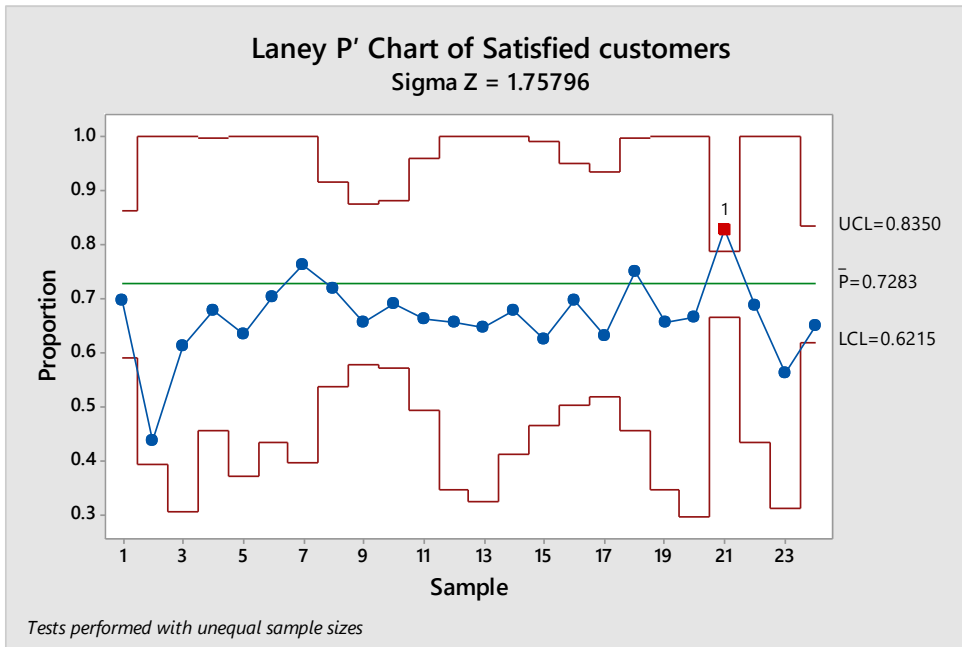


Fig 2. Laney P' chart of Customer Score by Hotel Chain

The Laney chart, a variant on the familiar quality control P chart, compensates for theoretical problems with the latter arising from the use of unequal sample sizes.

The UCL and LCL in the chart represent the upper and lower three sigma control limits respectively. Correspondingly, sample codes given equate to the hotel chain codes shown in Table 5:

Code number	Hotel chain	Code number	Hotel chain
1	Best Western	13	Ibis Styles
2	Britannia	14	Jury's Inn
3	Copthorne	15	MacDonald
4	Crown Plaza	16	Marriot
5	Days Inn/Hotel	17	Mercure
7	Hilton - Hampton by Hilton	18	Novotel
6	Hilton DoubleTree by Hilton	19	Old English Inns
8	Hilton Hotels	20	Park Inn by Radisson
9	Holiday Inn	21	Premier Inn
10	Holiday Inn Express	22	Radisson - Blu
11	Ibis	23	Ramada
12	Ibis Budget	24	Travelodge

**Table 5. Hotel Chain Codes used in Fig. 2**

Apart from the Premier Inn result, Figure 2 shows that all customer scores would be considered to be on target (Premier's would be deduced to be above-target).

#### 4. Technical inadequacies of the customer score criterion

Exploring possible inter-relationships between variables in the Which? Study, a Spearman's correlation analysis [15] of the data in Table 1 was undertaken – see Table 6 for details:

Spearman's rho		Sample size	Average price paid	Cleanliness	Quality of Bedrooms	Quality of Bathrooms	Value for money	Customer Score
Sample size	Correlation Coefficient	1	0.125	0.066	<b>.444*</b>	0.222	-0.012	<b>.455*</b>
	Sig. (2-tailed)	.	0.559	0.758	0.03	0.297	0.958	0.025
	N	24	24	24	24	24	23	24
Average price paid	Correlation Coefficient		1	<b>.560**</b>	<b>.643**</b>	<b>.602**</b>	<b>-.577**</b>	0.242
	Sig. (2-tailed)		.	0.004	0.001	0.002	0.004	0.255
	N		24	24	24	24	23	24
Cleanliness	Correlation Coefficient			1	<b>.622**</b>	<b>.673**</b>	-0.201	<b>.490*</b>
	Sig. (2-tailed)			.	0.001	0	0.358	0.015
	N			24	24	24	23	24
Quality of Bedrooms	Correlation Coefficient				1	<b>.849**</b>	-0.145	<b>.774**</b>
	Sig. (2-tailed)				.	0	0.509	0
	N				24	24	23	24
Quality of Bathrooms	Correlation Coefficient					1	-0.122	<b>.746**</b>
	Sig. (2-tailed)					.	0.58	0
	N					24	23	24
Value for money	Correlation Coefficient						1	0.32
	Sig. (2-tailed)						.	0.136
	N						23	23
Customer Score	Correlation Coefficient							1
	Sig. (2-tailed)							.
	N							24

\*. Correlation is significant at the 0.05 level (2-tailed).

\*\*.. Correlation is significant at the 0.01 level (2-tailed).

**Table 6. Spearman rank correlations**

From the latter significant positive relationships can be found to exist between:

- (1) cleanliness, quality of bedrooms, quality of bathrooms and customer score;
- (2) cleanliness and average price paid and
- (3) sample size and customer score

whilst a significant negative correlation holds between

- (4) average price paid and value for money

In support of (1) Radzi et al. [16] found that quality in the hotel industry was perceived as synonymous with clean, comfortable and well-maintained rooms. Similarly, the strong relationships between cleanliness, quality of bedrooms, quality of bathrooms and average price paid are in keeping with research results obtained by Arbelo-Perez et al. [17] and Shaked and Sutton [18] that higher quality translates into higher prices and vice versa

Oddly, result (3) suggests that large samples are associated with high customer scores and vice versa. This is a most extraordinary discovery - which as will be shown later - casts grave doubt on the credibility of the customer score criterion as an 'overall evaluation' measure.

Result (4) on the other hand, makes sense insofar as the value for money rating would be expected to go up if the average price paid rating went down and conversely.

The incidence of so many significant correlations in Table 6 suggests a factor analysis of the data may well prove productive. [19] – as is borne out by the selective output summarised in Figure 3.

Component	Initial Eigenvalues			Extraction Sums of Squared Loadings			Rotation Sums of Squared Loadings		
	Total	% of Variance	Cumulative %	Total	% of Variance	Cumulative %	Total	% of Variance	Cumulative %
1	3.484	49.774	49.774	3.484	49.774	49.774	3.477	49.676	49.676
2	2.057	29.381	79.155	2.057	29.381	79.155	2.064	29.479	79.155
3	.698	9.967	89.122						
4	.412	5.888	95.010						
5	.175	2.497	97.507						
6	.111	1.590	99.097						
7	.063	.903	100.000						

Extraction Method: Principal Component Analysis.

**Rotated Component Matrix<sup>a</sup>**

	Component	
	1	2
Sample size		.750
Average price paid	.776	
Cleanliness	.789	
Quality of Bedrooms	.928	
Quality of Bathrooms	.940	
Value for money		.800
Customer Score	.618	.738

Extraction Method: Principal Component Analysis.

Rotation Method: Varimax with Kaiser Normalization.

a. Rotation converged in 3 iterations.

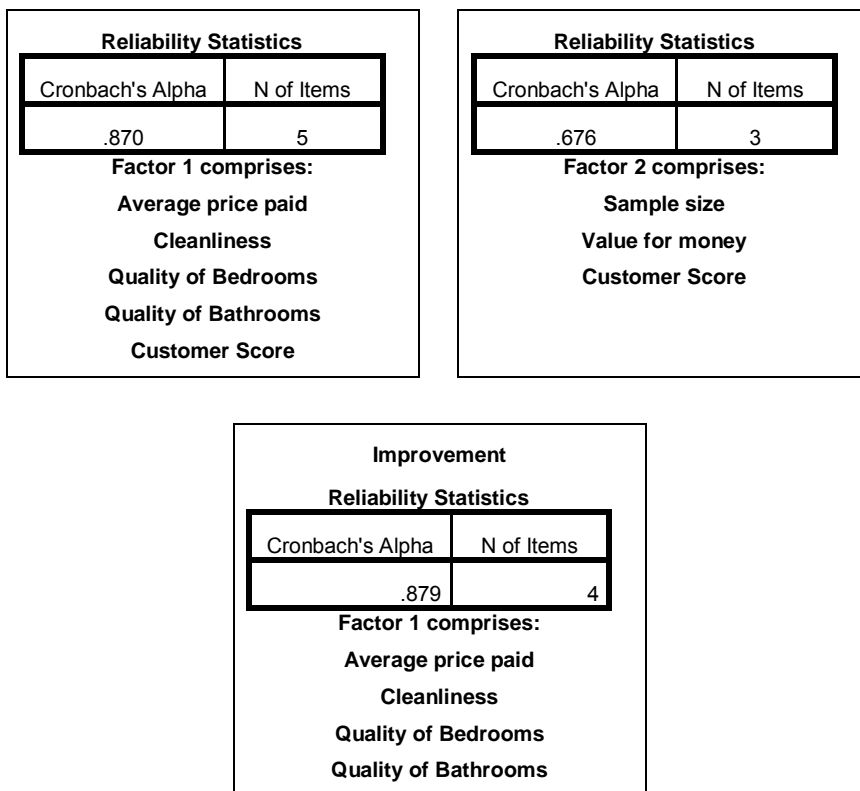


**Fig 3. Factor analysis – selective output**

From this output, it appears that two factors underlie the data. The first of these is associated with average price paid, cleanliness, quality of bedrooms and quality of bathrooms whereas the second links to sample size and value for money.

Both factors are found to have acceptable internal consistency based on Cronbach alpha values of 0.870 and 0.676 respectively. Unfortunately, cross-loading is clearly a problem with the analysis – particularly in respect of customer score.

If however customer score is treated as only loading on to factor 2. the new Cronbach alpha value of 0.879 for factor 1 is virtually the same as previously. From corresponding loadings, factor 1 for this model might well justify be labelled **Hotel quality** and factor 2, **Customer score credibility**.

## 5 Non-standard weighting of survey responses

To convert the ordinal categorical data [20] in Table 4 into interval data a score has been assigned to each option in the Which? Travel study as follows:

Satisfaction (“Overall satisfaction with the brand”)				
★	★ ★	★ ★ ★	★ ★ ★ ★	★ ★ ★ ★ ★
Very dissatisfied	Fairly dissatisfied	Neither satisfied or dissatisfied	Fairly satisfied	Very Satisfied
1	2	4	8	16

Endorsement (“Likelihood to recommend the brand to a friend/family member”)				
★	★ ★	★ ★ ★	★ ★ ★ ★	★ ★ ★ ★ ★
Definitely will not recommend	Probably will not recommend	Not sure	Probably will recommend	Definitely will recommend
1	2	4	8	16

**Table 7: Which?’s Scoring system for Satisfaction and Endorsement responses**

The (1, 2, 4, 8, 16) scoring method employed here is not a mainstream choice – by far the most popular option more generally being **equal spacing** e.g. (1, 2, 3, 4, 5). [21], [22], [23]

- To obtain the **customer score** (an example of a ‘composite’ or ‘indicator’ score), the **Satisfaction** and **Endorsement** scores were averaged for each respondent (both questions needed to be answered.) The average was then rescaled so that its values fell in the range 0-100%.
- But, the **Satisfaction** and **Endorsement** questions have completely different ordinal scales. For example, the same **customer score** of 5 can be obtained for the combination (Fairly satisfied, Probably will not recommend) as well as the combination (Fairly dissatisfied, Probably will recommend) which have quite different connotations.
- The **Satisfaction** and **Endorsement** scores are equally weighted in the **customer score** calculation but the scientific basis for this is not made clear. Why not a weighting ratio of 40:60 or 70:30 for example?
- Averaging the **Satisfaction** and **Endorsement** scores suggests they are being treated as independent measures. But what if - as is likely- they are correlated?
- The effect of the (1, 2, 4, 8, 16) scoring is to greatly exaggerate apparent differences between the chains listed in Table.1 – particularly between **Premier Inn** and **Britannia** – see Figure 4 for

details. Also Figure 5 which shows the equivalent results based on the equal spacing (1, 2, 3, 4, 5) scheme.



Fig 4. Published Which? Customer scores based on (1, 2, 4, 8, 16) scoring

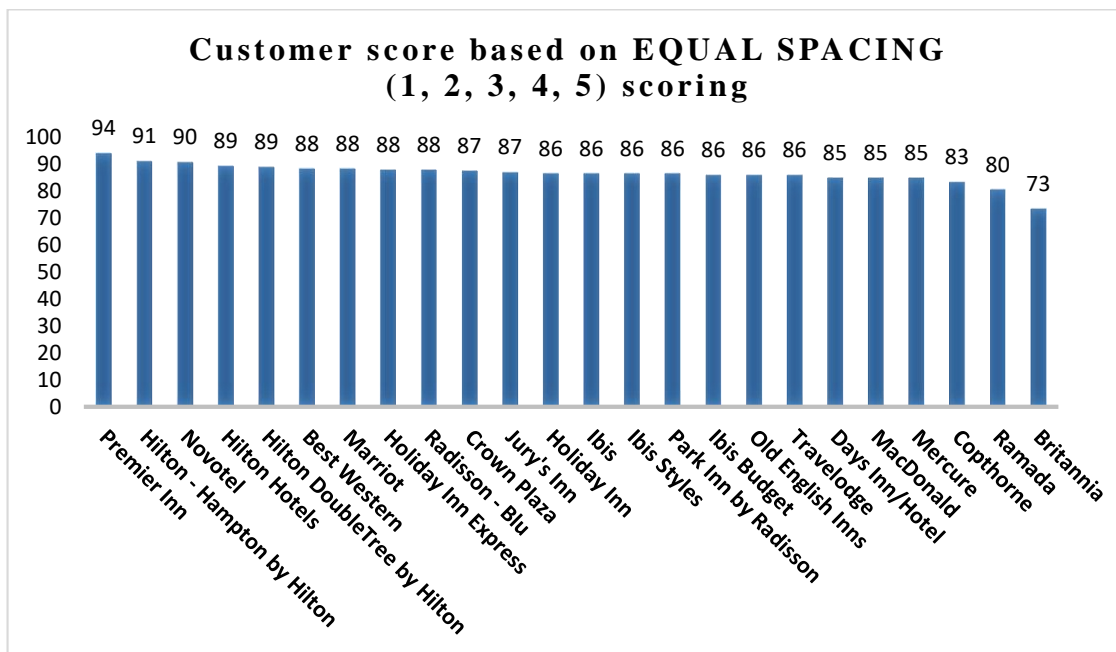


Fig 5. Alternative customer scores based on a (1, 2, 3, 4, 5) scoring scheme.

Clearly the contrast between the results graphed in the two Figures is quite striking. Under the (1, 2, 3, 4, 5) scheme, the Britannia now emerges with what appears to be a very respectable 73% **customer score** rating - 29% higher in value than its published 44% Which? rating. Premier Inn's **customer score** on the other hand is now 94% - up (but only by) 11% in value from its published 83% Which? rating.

## 6 Survey bias

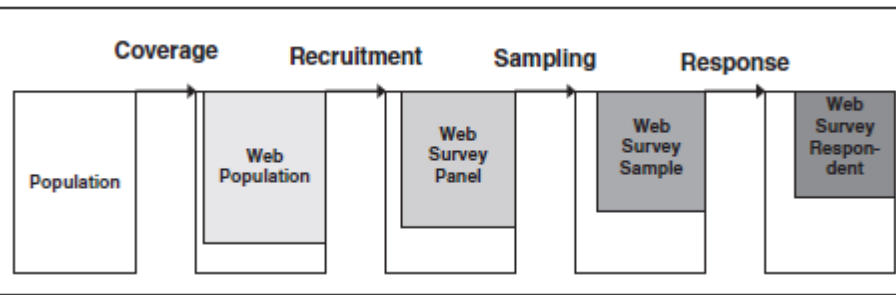


Fig 6. Volunteer panel web survey protocol Source: Lee and Valliant [25]

Figure 6 shows the various steps involved in a web survey and for each of these the different types of bias (coverage, recruitment, sampling and response) that can intrude if care is not taken. Note that the shadings signify that the people at each step are not necessarily representative of those in the steps beforehand. So by the time step 5 is reached, the respondents may bear very little resemblance to the ones originally targeted at step 1.

### 1. Population

From the Which Technical Report Hotel Chains Survey 2016, the population of interest would ostensibly be the set of all visitors who stayed at hotels in the chains listed in Table 5 for leisure purposes between 1 August 2015 and 31 July 2016.

### 2. Web population

However, the section of the population with web access is likely to be distinctly smaller than the target population primarily because of problems of coverage e.g. the elderly, poorly educated and non-indigenous parts of the population [26] are well-known to be much less disposed to using the internet. Similarly, continuing problems with broadband and wifi availability across the country have historically severely constrained internet usage. [27]

### 3. Web survey panel

Members of Which? Connect (Which?'s online research panel) were surveyed in July 2016. According to Which?, "The panel consists of a cross-section of subscribers to all Which? Products and services including Which? Magazine and which.co.uk. It includes Which? Members from all four nations of the UK and is reasonably representative of our members profile in terms of gender, age and location."

But what is meant by 'reasonably representative' here – is this statement based on expert judgment or scientific analysis of some kind? Clearly the reader has a lot to take on trust here.

### 4. Web survey sample

The sample generated for the Which? Hotel chains survey would be statistically classified as a **voluntary response** sample. Such samples arise from **self-selection** surveys for which selection probabilities are unknown. Unbiased estimates cannot therefore be computed for such surveys nor the accuracy of estimates determined.

Voluntary response samples are notorious for over-sampling individuals who have strong opinions whilst under-sampling those who do not – a property that can sometimes be cynically exploited by those seeking to project a loaded agenda. [28]

#### 5. Web survey non-response

The Which? Connect panel numbers some 39,000 members and responses were officially received from 4,283 of them. This represents a response rate of just 11% which is rather poor by normal panel survey standards (even when there are no incentives on offer). Poor response is intrinsically linked to estimate bias and unreliability. [29]

## 7. **Conclusions**

An in-depth evaluation of the Which? Travel 2016 survey methodology has been undertaken and significant deficiencies encountered at many different levels. In particular:

The markedly different sample sizes used in the Which? Study significantly impact on outcomes - to the detriment of chains with small samples but to the benefit of chains with large samples. When however sample size variability is statistically allowed for in the analysis, it appears there is no significant difference in customer score performance between any of the hotel chains – with the exception of Premier Inn.

Self-selection bias and under-coverage are major problems for online surveys such as that of Which? Travel. Because of such problems, conclusions from their survey are impossible to generalize to the population of interest. The high non-response rate (89%) and almost guaranteed non-representativeness of Which? Connect members to the population of interest only add to the unreliability of the results obtained.

Independently, the Which? **customer scores** give rise to real cause for concern in a number of different regards:

1. Though eight different pieces of rating information (re six categories and two questions) were collected by Which? the **customer score** only makes use of two of them?
2. The choice of the esoteric (1, 2, 4, 8, 16) system for coding answers to the **Satisfaction** and **Endorsement** questions in 1. has a markedly distorting effect on customer score calculations in the study.

3. **Customer score** was found to be significantly correlated with sample size. So, by adopting this criterion in their 'overall evaluation' methodology Which? has, in effect, systematically favoured hotel chains with large samples in their survey over those with small.

From the above, the 2016 Which? Travel survey / study would appear to be wanting in virtually every statistical respect.

## References

1. P. Resnick and R. Zeckhauser. Trust among strangers in internet transactions: Empirical analysis of eBay's reputation system, *The Economics of the Internet and E-commerce*. [online] Emeraldinsight.com. 2002. Available at: [http://www.emeraldinsight.com/doi/pdfplus/10.1016/S0278-0984\(02\)11030-3](http://www.emeraldinsight.com/doi/pdfplus/10.1016/S0278-0984(02)11030-3) [Accessed 26 Jul. 2017].
2. S. Aral. The Problem With Online Ratings, [online] MIT Sloan Management Review, 2013. Available at: <http://sloanreview.mit.edu/article/the-problem-with-online-ratings-2/> [Accessed 27 Jun. 2017].
3. D. Dillman, J. Smyth, J. and L. Christian. *Internet, mail, and mixed-mode surveys*. Hoboken, NJ: John Wiley. 2014.
4. A. Disney. Clamping down on review fraud - Cambridge Intelligence, 2015. [online] Cambridge Intelligence. Available at: <https://cambridge-intelligence.com/clamping-down-on-review-fraud/> [Accessed 27 Jun. 2017].
5. Minku, L. *The Wisdom of the Crowds in Software Engineering Predictive Modelling*, *Perspective on Data Science for Software Engineering*, Elsevier, 199{204, 2016.
6. F. Ricci and R. Wietsma. Product reviews in travel decision making. *Lausanne: Information and communication Technologies in Tourism*, 296{307, 2006. Available at: [http://dx.doi.org/10.1007/3-211-32710-X\\_41](http://dx.doi.org/10.1007/3-211-32710-X_41) [Accessed 31 Jul. 2017].
7. P. Blackshaw and M. Nazzaro. Consumer-generated media (CGM) 101: Word-of-mouth in the age of the web-fortified consumer, *A Nielsen Buzz Metrics white paper (2nd ed.)* Spring 2006.
8. G. Porto. Using survey data to assess the distributional effects of trade policy. *Journal of International Economics*, [online] 70, 1, 140{160, 2006. Available at: <http://dx.doi.org/10.1016/j.jinteco.2005.09.003> [Accessed 30 Jun. 2017].
9. J. Mellinas, S. Maria-Dolores, S. and J. Garcia. Effects of the Booking.com scoring system. *Tourism Management*, [online] 57, 80{83, 2016. Available at: <http://dx.doi.org/10.1016/j.tourman.2016.05.015> [Accessed 26 Jul. 2017].
10. D. Park, J. Lee and I. Han. The Effect of On-Line Consumer Reviews on Consumer Purchasing Intention: The Moderating Role of Involvement. *International Journal of Electronic Commerce*, [online] 11, 4, 125{148, 2007. Available at: <http://dx.doi.org/10.2753/jec1086-4415110405> [Accessed 26 Jul. 2017].
11. Reza Jalilvand and N. Samiei,. The impact of electronic word of mouth on a tourism destination choice. *Internet Research*, [online] 22, 5, 591{612. 2012. Available at: <http://dx.doi.org/10.1108/10662241211271563> [Accessed 26 Jul. 2017].
12. European Commission Study on online consumer reviews in the hotel sector. Report. 2014. [online] Publications.europa.eu. Available at: <https://publications.europa.eu/en/publication-detail/-/publication/7d0b5993-7a88-43ef-bfb5-7997101db6d5> [Accessed 5 Aug. 2017].
13. Which? Best and worst UK hotel chains. Available at: <http://www.which.co.uk/reviews/uk-hotel-chains/article/best-and-worst-uk-hotel-chains> [Accessed 29.4.2017].
14. J. Harmer. Britannia Hotels refutes results of Which? hotel survey *The Caterer*. Nov 2 2017. <https://www.thecaterer.com/articles/513979/britannia-hotels-refutes-results-of-which-hotel-survey> [Accessed 3 Apr. 2018].
15. B. Tabachnik and L. Fidell. *Experimental designs using ANOVA*. Belmont (Calif.): Thomson-Brooks/Cole. 2007.
16. S. Radzi, N. Sumarjan, C. Chik, M. Zahari, Z. Mohi, M. Bakhtiar. and F. Anuar. *Theory and practice in hospitality*

- and tourism research. 156{158, 2014.
17. M. Arbelo-Perez, A. Arbelo, A. and P. Perez-Gomez. Impact of quality on estimations of hotel efficiency. *Tourism Management*, [online] 61, 200{208. 2017.  
Available at: <http://dx.doi.org/10.1016/j.tourman.2017.02.011> [Accessed 18 Jul. 2017].
  18. A. Shaked, A. and J. Sutton, J. Product Differentiation and Industrial Structure. *The Journal of Industrial Economics*, [online] 36(2), 131. 1987. Available at: <http://dx.doi.org/10.2307/2098408> [Accessed 18 Jul. 2017].
  19. R.B. Cattell. (Factor analysis: an introduction and manual for the psychologist and social scientist. Harper. 1952.
  20. H-C. Chen, and N-S Wang. The Assignment of Scores Procedure for Ordinal Categorical Data. *The Scientific World Journal* 2014.
  21. W. Dai, G. Jin, J. Lee and m. Luca. Optimal Aggregation of Consumer Ratings: An Application to Yelp.com. *SSRN Electronic Journal*. 2012. [online] Available at: <http://dx.doi.org/10.2139/ssrn.2518998> [Accessed 28 Jul. 2017].
  22. I. Bross. How to Use Redit Analysis. *Biometrics*, 14, 1, 18, 1958. Available at: <http://dx.doi.org/10.2307/2527727> [Accessed 1 Aug. 2017].
  23. H. Liao, A. Zeng, M. Zhou, R. Mao, and B. Wang, Information mining in weighted complex networks with nonlinear rating projection. *Communications in Nonlinear Science and Numerical Simulation*, [online] 51, 115{123. 2017. Available at: <http://dx.doi.org/10.1016/j.cnsns.2017.03.018> [Accessed 26 Jul. 2017].
  24. J. Starkweather, How to Calculate Empirically Derived Composite or Indicator Scores. 2012.  
[https://it.unt.edu/sites/default/files/compositescores\\_jds\\_feb2012.pdf](https://it.unt.edu/sites/default/files/compositescores_jds_feb2012.pdf) [Accessed 29 Apr. 2017].
  25. S. Lee, and R. Valliant. Estimation for Volunteer Panel Web Surveys Using Propensity Score Adjustment and Calibration Adjustment. *Sociological Methods & Research*, [online] 37, 3, 319{343, 2009. Available at: <http://dx.doi.org/10.1177/0049124108329643> [Accessed 1 Aug. 2017].
  26. J. Bethlehem. Selection Bias in Web Surveys. *International Statistical Review*, [online] 78, 2, 161{188, 2010. Available at: <http://dx.doi.org/10.1111/j.1751-5823.2010.00112.x> [Accessed 24 Jul. 2017].
  27. ONS. Internet use in the UK: what are the facts? 2015. Available at: <http://visual.ons.gov.uk/internet-use/> [Accessed 28 Jul. 2017].
  28. University of Texas. Common mistakes in using statistics: spotting and avoiding them, 2012 Available at: <https://www.ma.utexas.edu/users/mks/statmistakes/biasedsampling.html> . [Accessed 1 Aug. 2017]
  29. D. A. Dillman. Mail and internet surveys - the tailored design method, 2nd ed. New York. Wiley. 2007.

# Credit Portfolio Risk Evaluation with non-Gaussian One-factor Merton Models and its Application to CDO Pricing

Takuya Fujii<sup>1</sup> and Takayuki Shiohama<sup>2</sup>

<sup>1</sup> Graduate School of Engineering, Tokyo University of Science  
(E-mail: 4417622@ed.tus.ac.jp)

<sup>2</sup> Department of Information and Computer Technology, Faculty of Engineering,  
Tokyo University of Science, 6-3-1 Nijuku, Katsushika Tokyo, 125-8585  
(E-mail: shiohama@rs.tus.ac.jp)

**Abstract** For measuring credit risks with structural modeling approach, it is often used one-factor Merton models which assume common single risk factor for all counterparties. We extend this model to have non-Gaussian and serially correlated asset returns for both single common risk and obligor's idiosyncratic factors. By using a standard Edgeworth expansion, we derive the approximate default rate distributions. Maximum likelihood estimators are introduced for estimating model parameters, and some credit risk measures are evaluated. Our empirical results illustrate that the proposed non-Gaussian models offer different credit risk evaluations compared with those obtained by Vasicek models. Applications for CDO pricing is also discussed.

**Keywords:** Credit risk model, CDO pricing, Edgeworth expansion, Cornish Fisher expansion, maximum likelihood estimation .

## 1 Introduction

Since the U.S. subprime mortgage crisis and the collapse of Lehman Brothers in 2008, financial institutions have paid more attention to the credit risk management. The need of assessment with credit risk model has become more essential for banks and financial institutions to manage and measure the credit risk of their portfolio loans. As noticed in Hull (2009) and Demanyk and van Hemert (2008), one of the reasons for the credit crush in 2008 is the lack of an easily updatable model of the credit risk of portfolios of loans.

The Basel accord, which is an international bank regulation, was enacted in 1988. Prior to this year, bank regulation had been done at the minimum level, such as the ratio of capital to total assets. Asset management varies from country to country, and the international competition of banks has intensified. This accord is aimed at stabilizing the financial system among the

---

*5<sup>th</sup> SMTDA Conference Proceedings, 12-15 June 2018, Chania, Crete, Greece*

international countries and correcting the inequality of competition among banks. Under the Basel II guideline, for the purpose of the calculating regulatory capital, banks are allowed to use their own estimated risk parameters and set default probabilities based on their own ratings. This is known as the internal ratings-based (IRB) approach to capital requirements for credit risk. For quantifying the credit risk, we consider default rate distribution in order to evaluate some credit risk measures.

There are mainly two types of models to quantify credit risk. One is the structural model and the other is the reduced form model. The former is based on Merton (1974) and is known as a balance sheet approach. This approach defines the event of default as the obligor's asset value process declines a certain threshold value. The reduced form models originated by Jarrow and Turnbull (1995), which treat an event of default as an unpredictable event governed by a hazard-rate process. For evaluating credit risk of the loan portfolio, the Vasicek single-factor model is widely used to measure the risk of a credit portfolio and to price collateralized debt obligations (CDO)s. Yet there are a number of models of the credit risk of portfolios, such as CreditMetrics by JP Morgan, CreditRisk+ by Credit Suisse Financial Products, CreditPortfolioView by McKinsey, and Moody's KMV and so on.

The Vasicek single-factor model assumes that the default events are driven by a latent common factor, which is assumed to follow the Gaussian distribution. However, it is well known that the Gaussian assumption for the asset return process is not valid as many empirical research suggests. Gordy (2002) provides a saddle point approximation to the default rate distribution in CreditRisk+ models. Hull et al. (2004) consider a jump diffusion model to explain the volatility skew in the credit default swap markets. In this study we evaluate the portfolio credit risk by using non-Gaussian distribution of the asset return process using the Vasicek single-factor model. Huand et al. (2007) investigate the saddle point approximations for the option premium evaluation and CDO pricing. Since pricing derivative products such as mortgage backed security (MBS) and other loan products like CDOs are mainly based on the Gaussian assumption, incorporating non-Gaussian portfolio credit risk models are beneficial for evaluating credit risks.

The rest of the paper is organized as follows. In Section 2 we introduce the Vasicek one-factor model with non-Gaussian and serially correlated obligor's asset returns. Section 3 reviews asymptotic evaluation of credit risk measures by using Edgeworth expansion. We show data analysis in Section 4 and numerical results of CDO pricing in Section 5. Section 6 concludes.

## 2 The Model and its Assumptions

In Merton's model, the asset value of obligor  $i$  is assumed to follow a geometric Brownian motion under the physical measure  $\mathbb{P}$ ,

$$dV_{i,t} = \mu V_{i,t} dt + \sigma V_{i,t} dW_{i,t},$$

where  $V_{i,t}$  denotes the asset value at time  $t$  of obligor  $i$ ,  $\mu$  is the drift, which means average growth rate of  $V_{i,t}$  and  $\sigma$  is the volatility parameter. We assume that these parameters are common every obligors. To model the obligor's asset correlation, the Brownian motion  $W_{i,t}$  is divided into two independent Brownian motions such that

$$dW_{i,t} = \sqrt{\rho} dX_{0,t} + \sqrt{1-\rho} dX_{i,t},$$

where  $X_{0,t}$  is a common systematic risk factor and  $X_{i,t}$  is a idiosyncratic risk factor. We also assume that two standard Brownian motions  $X_{0,t}$  and  $X_{i,t}$  are independent of each other. The  $\rho$  is the asset correlation coefficient between  $i$ -th and  $j$ -th obligor.

We consider the discretely observed asset process hereafter. Let the current time is 0 and we assume that the stochastic process  $\{V_{i,t}\}$  is discretely sampled with interval  $\Delta$  such that  $V_{i,j}$  is sampled at time  $0, \Delta, 2\Delta, \dots, n\Delta (\equiv t)$  over  $[0, t]$ . Then, the  $i$ -th obligor's asset value at time  $j\Delta$  is defined as follows:

$$\begin{aligned} \ln V_{i,j\Delta} &= \ln V_{i,(j-1)\Delta} + \mu\Delta + \sqrt{\Delta} W_{i,(j-1)\Delta}, \\ W_{i,(j-1)\Delta} &= \sqrt{\rho} X_{0,(j-1)\Delta} + \sqrt{1-\rho} X_{i,(j-1)\Delta}, \quad j = 1, \dots, n. \end{aligned} \quad (1)$$

Let  $c_{X_i}(u) = \text{Cov}(X_{i,t}, X_{i,t+u})$  be the lag  $u$  autocovariance function of  $X_{i,t}$ . In this paper, we consider that the process  $X_{i,j}$  is the stationary process with  $\mu_X = 0$  and  $\text{Var}(X_t) = \sum_{u=-\infty}^{\infty} c_{X_i}(u)$  which satisfies the following stationary conditions.

**Assumption 1** The processes  $\{X_{i,j}\}$  are fourth-order stationary in the sense that for each  $i \in \{0, 1, \dots, N\}$  and  $j, u_1, u_2, u_3 \in \mathbb{Z}$

1.  $E[X_{i,j}] = 0$ ,
2.  $\text{cum}(X_{i,j}, X_{i,j+u}) = c_{X_i}(u)$ ,
3.  $\text{cum}(X_{i,j}, X_{i,j+u_1}, X_{i,j+u_2}) = c_{X_i}(u_1, u_2)$ ,
4.  $\text{cum}(X_{i,j}, X_{i,j+u_1}, X_{i,j+u_2}, X_{i,j+u_3}) = c_{X_i}(u_1, u_2, u_3)$ .

The following absolutely summable conditions are satisfied for 2nd to 4th order cumulants.

**Assumption 2.** The  $k$ -th order cumulants  $c_{X_i}(u_1, \dots, u_{k-1})$  of  $\{X_i\}$ , for  $k = 2, 3, 4$  and  $i \in \{0, \dots, N\}$  satisfy

$$\sum_{u_1, \dots, u_{k-1} = -\infty}^{\infty} |c_{X_i}(u_1, \dots, u_{k-1})| < \infty.$$

From (1), the obligor's asset value at time  $t = n\Delta$  is expressed as

$$\ln V_{i,t} = \ln V_{i,0} + \mu n\Delta + \Delta^{1/2} \left( \sqrt{\rho} \sum_{j=1}^n X_{0,j} + \sqrt{1-\rho} \sum_{j=1}^n X_{i,j} \right).$$

We define  $Y_{0,n} = \frac{1}{\sqrt{n}} \sum_{j=1}^n X_{0,j}$  and  $Y_{i,n} = \frac{1}{\sqrt{n}} \sum_{j=1}^n X_{i,j}$ . Then we obtain the following cumulants for the processes  $Y_{i,n}$ . Recall that we have assumed that the random variables  $Y_{i,n}$  and  $Y_{j,n}$  are independent for all  $i, j = 0, \dots, N$  with  $i \neq j$ , all the joint cumulants of  $Y_{i,n}$  and  $Y_{j,n}$  are equal to zero.

**Lemma 1.** Under Assumptions 1 and 2, the cumulants of  $\{Y_{i,n}\}$  for  $i \in \{0, \dots, N\}$  are evaluated as follows:

1.  $E[Y_{i,n}] = 0$ ,
2.  $\text{cum}(Y_{i,n}, Y_{i,n}) = \sigma_{i,n}^2 + o(n^{-1})$ ,
3.  $\text{cum}(Y_{i,n}, Y_{i,n}, Y_{i,n}) = n^{-1/2} C_{Y_{i,3}}^{(n)} + o(n^{-1})$ ,
4.  $\text{cum}(Y_{i,n}, Y_{i,n}, Y_{i,n}, Y_{i,n}) = n^{-1} C_{Y_{i,4}}^{(n)} + o(n^{-1})$ ,

where  $\sigma_{i,n}^2$ ,  $C_{Y_{ijk,3}}^{(n)}$  and  $C_{Y_{ijkl,4}}^{(n)}$  are bounded for  $n$ .

To have the process  $\sqrt{\rho}Y_{0,n} + \sqrt{1-\rho}Y_{i,n}$  possess the unit variance and correlation coefficient  $\rho$  for different obligors, we consider the following standardized process. Let  $W_{i,n} = \sqrt{\rho}\sigma_{0,n}^{-1}Y_{0,n} + \sqrt{1-\rho}\sigma_{i,n}^{-1}Y_{i,n}$ . Then the asset value process  $V_{i,t}$  is expressed by

$$\begin{aligned} V_{i,t} &= V_{i,n\Delta} = V_{i,0} \exp\{\mu t + \sqrt{t}\sigma W_{i,n}\} \\ &= V_{i,0} \exp\left\{\mu t + \sqrt{t} \left( \sqrt{\rho}\sigma_{0,n}^{-1}Y_{0,n} + \sqrt{1-\rho}\sigma_{i,n}^{-1}Y_{i,n} \right)\right\}. \end{aligned} \quad (2)$$

The joint probability distribution function of  $\mathbf{W}_{N,n} = (W_{1,n}, \dots, W_{N,n})'$  can be obtained from the Edgeworth expansion below. To do this, we need to evaluate the joint cumulants of  $\mathbf{W}_{N,n}$ . Let  $\tilde{C}_{Y_{i,k}}^{(n)} = C_{Y_{i,k}}^{(n)} / \sigma_{i,n}^k$ , for  $k=3, 4$  and  $i \in \{0, \dots, N\}$

**Lemma 2.** Under Assumptions 1 and 2, the cumulants of  $\{\mathbf{W}_{N,n}\}$  are evaluated as follows:

1.  $E[\mathbf{W}_{N,n}] = \mathbf{0}_N$ ,

2.  $\text{Var}(\mathbf{W}_{N,n}) = \Sigma_{N,n} + o(1)$ , where the  $(i, j)$ th elements of  $\Sigma_{N,n}$  is  $\rho$  for  $i, j = 1, \dots, N$  and the diagonal elements are 1.

3. for  $i, j, k \in \{1, \dots, N\}$ ,  $\text{cum}(W_{i,n}, W_{j,n}, W_{k,n}) = \tilde{C}_{W,ijk}^{(n)} + o(1)$ , where

$$\tilde{C}_{W,ijk}^{(n)} = \begin{cases} n^{-1/2} \rho^{3/2} \tilde{C}_{Y_{0,3}}^{(n)} & (i \neq j \neq k), \\ n^{-1/2} (\rho^{3/2} \tilde{C}_{Y_{0,3}}^{(n)} + (1-\rho)^{3/2} \tilde{C}_{Y_{i,3}}^{(n)}) & (i = j = k). \end{cases}$$

4. for  $i, j, k, l \in \{1, \dots, N\}$ ,  $\text{cum}(W_{i,n}, W_{j,n}, W_{k,n}, W_{l,n}) = \tilde{C}_{W,ijkl}^{(n)} + o(1)$ , where

$$C_{W,ijkl}^{(n)} = \begin{cases} n^{-1} \rho^2 \tilde{C}_{Y_{0,4}}^{(n)} & (i \neq j \neq k \neq l), \\ n^{-1} (\rho^2 \tilde{C}_{Y_{0,4}}^{(n)} + (1-\rho)^2 \tilde{C}_{Y_{i,4}}^{(n)}) & (i = j = k = l). \end{cases}$$

Here we use the following rules for the cumulants with sum of independent random variables, namely the  $k$ -th order joint cumulant of  $X + Y$  is given by

$$\text{cum}^{(k)}(X + Y) = \sum_{j=0}^k \binom{n}{j} \text{cum}^{(k)}(\underbrace{X, \dots, X}_j, \underbrace{Y, \dots, Y}_{n-j}).$$

**Assumption 3.** The  $J$ -th order ( $J \geq 5$ ) cumulants of  $\{Y_{i,n}\}$  and  $\{\mathbf{W}_n\}$  are of order  $O(n^{-J/2+1})$ .

We then arrive at the following theorem. For more details and proofs, we refer Taniguchi and Kakizawa (2000).

**Theorem 1.** Under Assumptions 1–3, the third-order Edgeworth expansion of the density function of  $Y = Y_i / \sigma_{i,n}$  for  $i \in \{0, \dots, N\}$  is given by

$$g_{Y_i}(y) = \phi(y) \left\{ 1 + \frac{\tilde{C}_{Y_{i,3}}^{(n)}}{6\sqrt{n}} H_3(y) + \frac{\tilde{C}_{Y_{i,4}}^{(n)}}{24n} H_4(y) + \frac{(\tilde{C}_{Y_{i,3}}^{(n)})^2}{72n} H_6(y) \right\} + o(n^{-1}).$$

where  $\phi(\cdot)$  is the standard normal density function, and  $H_k(\cdot)$  is the  $k$ -th order Hermite polynomial.

The corresponding probability distribution function is of the form

$$G_{Y_i}(y) = \Phi(y) - \phi(y) \left\{ 1 + \frac{\tilde{C}_{Y_{i,3}}^{(n)}}{6\sqrt{n}} H_2(y) + \frac{\tilde{C}_{Y_{i,4}}^{(n)}}{24n} H_3(y) + \frac{(\tilde{C}_{Y_{i,3}}^{(n)})^2}{72n} H_5(y) \right\} + o(n^{-1}).$$

The Edgeworth expansion for the distribution function for  $\mathbf{W}_n$  is given by the following theorem. To do this, it is convenient notationally to adopt Einstein's summation convention, that is  $a_r Z^r$  denotes the linear combination  $a_1 Z^1 + \dots + a_N Z^N$  and  $a_{rs} Z^{rs}$  denotes  $a_{11} Z^{11} + a_{12} Z^{12} + \dots + a_{NN} Z^{NN}$ ,

and so on.

**Theorem 2.** Under Assumptions 1–3, the third-order Edgeworth expansion of the density function of  $\mathbf{W}_{N,n}$  is given by

$$g_{W_n}(y) = \phi_{\Sigma_{N,n}}(y) \left\{ 1 + \frac{1}{6\sqrt{n}} \tilde{C}_{W,ijk}^{(n)} H_{\Sigma_{N,n}}^{ijk}(y) \right. \\ \left. + \frac{1}{24n} \tilde{C}_{W,ijkl}^{(n)} H_{\Sigma_{N,n}}^{ijkl}(y) + \frac{1}{72n} \tilde{C}_{W,ijk}^{(n)} \tilde{C}_{W,i'j'k'}^{(n)} H_{\Sigma_{N,n}}^{ijk i'j'k'}(y) \right\} + o(n^{-1}).$$

where  $\phi_{\Sigma_{N,n}}(\mathbf{y})$  is the  $N$ -dimensional normal density function with mean  $\mathbf{0}_N$  and covariance matrix  $\Sigma_{N,n}$ .

To confirm (2) has expected return  $\mu$ , we define

$$m = \frac{\sigma^2}{2} + \frac{\sigma^3 \sqrt{t} (\rho^{3/2} \tilde{C}_{Y_{0,3}}^{(n)} + (1-\rho)^{3/2} \tilde{C}_{Y_{i,3}}^{(n)})}{6\sqrt{n}} + \frac{\sigma^4 t (\rho^2 \tilde{C}_{Y_{0,4}}^{(n)} + (1-\rho)^2 \tilde{C}_{Y_{i,4}}^{(n)})}{24n}.$$

With  $N = 1$  and Theorem 2, we obtain the expected value of  $\tilde{V}_{i,t} = V_{i,0} \exp \left\{ (\mu - m)t + \sqrt{t} \sigma W_{i,n} \right\}$  as follows,

$$E_0[\tilde{V}_{i,t}] = V_{i,0} e^{(\mu-m)t} \int_{-\infty}^{\infty} e^{\sigma \sqrt{t} y} g_{W_1}(y) dy = V_{i,0} e^{\mu t}.$$

Hereafter, we consider the process  $\tilde{V}_{i,t} = V_{i,0} \exp \left\{ (\mu - m)t + \sqrt{t} \sigma W_{i,n} \right\}$ .

### 3 Asymptotic Evaluation of Credit Risk Measures

Let  $PD_i$  be the probability of default and  $WCDR_i$  be the worst case default rate for the obligor  $i$ . In general, the worst case default rate are measured with a occurrence of probability 99%. The IRB approach for Basel II focuses on the credit risk measures such as expected loss (EL) and value at risk (VaR), which are defined by  $\sum_{i=1}^n PD_i \times LGD_i \times EAD_i$  and  $\sum_{i=1}^n WCDR_i \times LGD_i \times EAD_i$ , respectively. Here  $LGD_i$  is the obligor  $i$ 's loss given default, and  $EAD_i$  is the obligor  $i$ 's exposure at default. The economic capital (EC) is defined as  $VaR - EL$ .

We are interested in the default probabilities at time  $t$  of a portfolio within the same asset and liability structure. A credit portfolio is nothing but a collection of  $N$  transactions with certain counterparties. Since the portfolio would consist of  $N$  homogeneous obligors, the probability of default of obligor  $i$  and the initial asset value  $V_{i,0} = V_0$  are identical for every obligor. For the convenience of expression, we omit index  $i$ . For example,  $V_{i,t}$  and  $Y_{i,n}$  are denoted as  $V_t$  and  $Y_{1,n}$ , respectively for the sequel. To model the

defaults of the loan in a portfolio, we consider the case with  $\tilde{V}_t < D_t$ , where  $D_t$  is the amount of debt interest at time  $t$ . Then, the default time  $t$  can be expressed in terms of the random variable  $W_n$ :

$$\tilde{V}_t < D_t \iff W_n < K_t \iff Y_{1,n} < C_t,$$

$$K_t = \frac{\ln D_t / V_0 - (\mu - m)\sqrt{t}}{\sigma\sqrt{t}}, \quad C_t = \frac{K_t - \sqrt{\rho}\sigma_{0,n}^{-1}Y_{0,n}}{\sqrt{1 - \rho}\sigma_{1,n}^{-1}}.$$

Recall that we have assumed that all loans have the same cumulative probability distribution for the time to default, which are given in Theorem 2, and we denote this distribution as  $G_{W_1}$ . For notational convenience, we write the representative idiosyncratic random factor as  $Y_{1,n}$ . A representative obligor defaults when its asset value  $\tilde{V}_t$  falls below the default trigger  $K_t$ . Hence, the probability of default is stated in the following theorem.

**Theorem 4.** Assume that the assumptions 1–3 hold. Then the unconditional default probability is given by

$$PD = P(W_{1,n} < K_t) = p_t^{(1)} + p_t^{(2)} + p_t^{(3)} + p_t^{(4)} + o(n^{-1}),$$

where  $p_t^{(1)} = \Phi(K_t)$ ,

$$p_t^{(2)} = -\frac{1}{6\sqrt{n}} \left( \rho^{3/2}\tilde{C}_{Y_{0,3}}^{(n)} + (1 - \rho)^{3/2}\tilde{C}_{Y_{1,3}}^{(n)} \right) H_2(K_t)\phi(K_t),$$

$$p_t^{(3)} = -\frac{1}{24n} \left( \rho^2\tilde{C}_{Y_{0,4}}^{(n)} + (1 - \rho)^2\tilde{C}_{Y_{1,4}}^{(n)} \right) H_3(K_t)\phi(K_t),$$

$$p_t^{(4)} = -\frac{1}{72n} \left( \rho^3(\tilde{C}_{Y_{0,3}}^{(n)})^2 + 2(\rho(1 - \rho))^{3/2}\tilde{C}_{Y_{0,3}}^{(n)}\tilde{C}_{Y_{1,3}}^{(n)} + (1 - \rho)^3(\tilde{C}_{Y_{1,4}}^{(n)})^2 \right) \times H_5(K_t)\phi(K_t).$$

According to this theorem, the probability of default at time  $t$  depends on the value of the factor  $Y_0$ . This variable can be thought of as an index of the macroeconomic conditions. If  $Y_0$  is large, the macroeconomic conditions are good, and hence each  $W_{1,n}$  tends to be large so that the default probability reduces, and vice versa when  $Y_0$  is small. To explore this effect of the common factor  $Y_0$ , we consider the probability of default conditional on  $Y_0$ . The following results state about the conditional default probability given  $Y_0$ , and this conditional distribution is called default rate distribution.

**Corollary 1.** Under the same conditions on Theorem 4, conditional default rate is obtained for  $Y_{0,n} = y_0$ ,

$$DR = P(Y_{1,n} < C_t(Y_0) | Y_{0,n} = y_0)$$

$$= p_t(Y_0) = p_t^{(1)}(Y_0) + p_t^{(2)}(Y_0) + p_t^{(3)}(Y_0) + p_t^{(4)}(Y_0) + o(n^{-1}),$$

where

$$\begin{aligned}
p_t^{(1)}(Y_0) &= \Phi(C_t(Y_0)), \quad C_t(Y_0) = \frac{K_t - \sqrt{\rho}\sigma_{0,n}^{-1}Y_{0,n}}{\sqrt{1 - \rho}\sigma_{1,n}^{-1}}, \\
p_t^{(2)}(Y_0) &= -\frac{1}{6\sqrt{n}}\tilde{C}_{Y_{1,3}}^{(n)} \left( (C_t(Y_0)^2 - 1)\phi(C_t(Y_0)) \right), \\
p_t^{(3)}(Y_0) &= -\frac{1}{24n}\tilde{C}_{Y_{1,4}}^{(n)} \left( (C_t(Y_0)^3 + 3C_t(Y_0))\phi(C_t(Y_0)) \right), \\
p_t^{(4)}(Y_0) &= \frac{1}{72n}(\tilde{C}_{Y_{1,3}}^{(n)})^2 \left( (-C_t(Y_0)^5 + 10C_t(Y_0)^3 - 15C_t(Y_0))\phi(C_t(Y_0)) \right).
\end{aligned}$$

We refer to this probability as the default rate hereafter. Obviously, the default rate is a function that depends on the common risk factor  $Y_{0,n}$ , asset correlation and default trigger  $K_t$ . The default trigger  $K_t$  can be viewed as the following Cornish Fisher expansion.

**Corollary 2.** Since  $PD = G_{W_1}(K_t)$ , the default trigger  $K_t$  can be viewed as the following Cornish Fisher expansion:

$$\begin{aligned}
K_t &= G_{W_1}^{-1}(PD) \\
&= \Phi^{-1}(PD) + \frac{\rho^{3/2}\tilde{C}_{Y_{0,3}}^{(n)} + (1 - \rho)^{3/2}\tilde{C}_{Y_{1,3}}^{(n)}}{6\sqrt{n}} \left( (\Phi^{-1}(PD))^2 - 1 \right) \\
&\quad + \frac{\rho^2\tilde{C}_{Y_{0,4}}^{(n)} + (1 - \rho)^2\tilde{C}_{Y_{1,4}}^{(n)}}{24n} \left( (\Phi^{-1}(PD))^3 - 3\Phi^{-1}(PD) \right) \\
&\quad - \frac{\rho^3(\tilde{C}_{Y_{0,3}}^{(n)})^2 + (1 - \rho)^3(\tilde{C}_{Y_{1,3}}^{(n)})^2 + 2(\rho(1 - \rho))^{3/2}\tilde{C}_{Y_{0,3}}^{(n)}\tilde{C}_{Y_{1,3}}^{(n)}}{36n} \\
&\quad \times \left( 2(\Phi^{-1}(PD))^2 - 5\Phi^{-1}(PD) \right) + o(1).
\end{aligned}$$

According to Vasicek (2002), let  $L_i$  be the gross loss excluding recovery rate on the  $i$ -th loan, so that  $L_i = 1$  if the  $i$ -th obligor defaults and  $L_i = 0$  otherwise as a Bernoulli variable. The portfolio percentage loss  $L$  is  $N^{-1}\sum_{i=1}^N L_i$ . Generally, the default events of obligors in the portfolio are dependent with correlation among factors, which are macroeconomic factor, sector, and so on. We can see that the portfolio loss given by  $Y_0$  converges to the conditional default probability such that  $L^{(N)} = \sum_{i=1}^N w_i L_i \rightarrow p_t(Y_0)$  as  $N \rightarrow \infty$ , almost surely, where  $w_i$  is the weight of loan  $i$  satisfying  $\sum_{i=1}^N w_i = 1$  and  $w_i > 0$ . Therefore, the conditions of the central limit theorem are not satisfied and  $L$  is not asymptotically normal.

Then the approximate probability density functions of the default rate distributions are obtained as

$$h_{DR}(DR) = \sqrt{\frac{1-\rho}{\rho}} g_{Y_0} \left( \frac{\sqrt{1-\rho} G_{Y_1}^{-1}(DR) - G_{W_1}^{-1}(PD)}{\sqrt{\rho}} \right) \cdot \frac{1}{g_{Y_1}(G_{Y_1}^{-1}(DR))}.$$

Here the Edgeworth density functions  $g_{Y_0}(x)$ ,  $g_{Y_1}(x)$  and its corresponding distribution function  $G_{Y_1}(x)$  are given in Theorem 1. Under the Gaussian assumptions on the asset returns, the above density function reduces to that of Gaussian Merton model that is

$$f(DR) = \sqrt{\frac{1-\rho}{\rho}} \exp \left\{ \frac{1}{2} \left[ (N^{-1}(DR))^2 - \left( \frac{\sqrt{1-\rho} N^{-1}(DR) - N^{-1}(PD)}{\sqrt{\rho}} \right)^2 \right] \right\}.$$

#### 4 Data Analysis

We use default rate data of the U.S. default history record analyzed in Hull (2012). We formulate parameter estimation based on maximum likelihood method below. The model parameter vector  $\theta$  is denoted as  $\theta =$

$(PD, \rho, \tilde{C}_{Y_0,3}^{(n)}, \tilde{C}_{Y_0,4}^{(n)}, \tilde{C}_{Y_1,3}^{(n)}, \tilde{C}_{Y_1,4}^{(n)})^T$ . The observed default records are denoted as  $DR_t$  ( $t = 1, \dots, M$ ). Then the maximum likelihood estimator (MLE) of  $\theta$  is defined as

$$\hat{\theta}^{(ML)} = \operatorname{argmax}_{\theta} \sum_{t=1}^M \log h_{DR}(DR_t; \theta).$$

In order to avoid the negative values in density functions in Edgeworth expansions, we impose the following restrictions on the parameters in  $\theta$ , that is

$$C_{Y_i,3}^{(n)} - \frac{24\sqrt{n}H_3(F_{n,\min}^{-1}(C_{Y_i,4}^{(n)}))}{(3H_3(F_{n,\min}^{-1}(C_{Y_i,4}^{(n)})) \cdot H_2(F_{n,\min}^{-1}(C_{Y_i,4}^{(n)})) - 4H_3(F_{n,\min}^{-1}(C_{Y_i,4}^{(n)}))^2)} < 0$$

for  $C_{Y_i,3}^{(n)} \geq 0$ ,

$$C_{Y_i,3}^{(n)} - \frac{24\sqrt{n}H_3(F_{n,\max}^{-1}(C_{Y_i,4}^{(n)}))}{(3H_3(F_{n,\max}^{-1}(C_{Y_i,4}^{(n)})) \cdot H_2(F_{n,\max}^{-1}(C_{Y_i,4}^{(n)})) - 4H_3(F_{n,\max}^{-1}(C_{Y_i,4}^{(n)}))^2)} > 0,$$

for  $C_{Y_i,3}^{(n)} < 0$ , together with  $0 \leq \rho \leq 1$  and  $0 \leq PD \leq 1$ . Here the function  $F_n$  is defined as

$$F_n(x) = -72nH_2(x)/(3H_4(x) \cdot H_2(x) - 4H_3(x)^2)$$

and the values  $F_{n,\min}^{-1}(x)$  and  $F_{n,\max}^{-1}(x)$  are the roots of  $F_n(y) = x$ .

With above-mentioned constrained optimization, MLE are given in Table 1. We plotted default rate distributions with the estimated parameters and indicate credit risk measures including expected loss, unexpected loss, and economic capital in Figure 1 and Table 2.

**Table1.** the result of parameters estimation with maximum likelihood method

	$\hat{PD}$	$\hat{\rho}$	$\hat{C}_{Y_{0,3}}$	$\hat{C}_{Y_{0,4}}$	$\hat{C}_{Y_{1,3}}$	$\hat{C}_{Y_{1,4}}$	MLL
Gaussian	0.013	0.110					137.731
Y0:non-Gaussian	0.014	0.111	0.138	0.080			137.423
Y1:non-Gaussian	0.013	0.103			0.072	0.033	138.022

**Table2.** the result of credit risk measure under the assumption of parameters

	Expected Loss	Unexpected Loss	VaR(99%)	Economic Capital
Gaussian	1.345%	1.305%	6.340%	4.995%
Y0:non-Gaussian	1.353%	1.264%	6.050%	4.697%
Y1:non-Gaussian	1.316%	1.273%	6.200%	4.884%

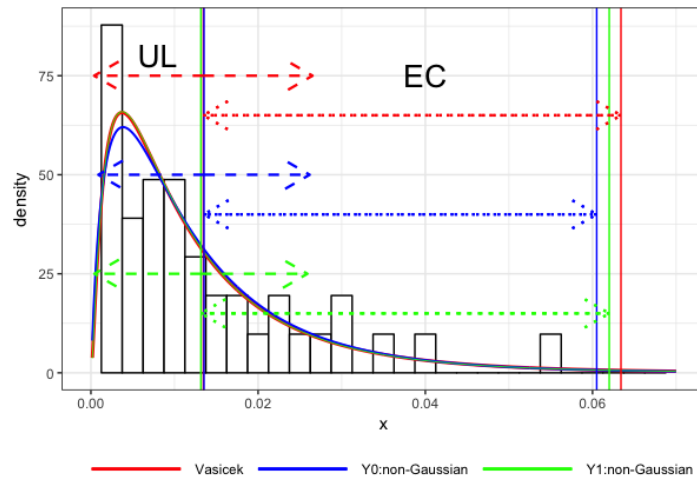


**Figure1.** The credit risk evaluation of non-Gaussian and Gaussian

## 5 CDO pricing

We assume that CDO portfolio is composed with  $m$  contractions of Credit Default Swap (CDS), which is the protection of the obligor  $i$ 's default. In pricing CDO, we need to consider loss distribution as well as to quantify the credit risk.

The number of names  $m$  is typically equal to 125. The notional  $N$  of the CDO is the total exposure of the portfolio. The contraction is conducted in each tranche for the amount of principal from the attachment point ( $AP$ ) to

detachment point ( $DP$ ).  $\{AP, DP\}$  of tranches are often defined as  $\{0\%, 3\%\}$ ,  $\{3\%, 6\%\}$ ,  $\{6\%, 9\%\}$ ,  $\{9\%, 12\%\}$ , and  $\{12\%, 22\%\}$ . The cumulative loss up to time  $t$  of the tranche  $\{AP, DP\}$  is  $L_t^{\{AP, DP\}} := (L_t - AP \cdot N)_+ - (L_t - DP \cdot N)_+$ . Default and premium payments can conveniently be expressed in terms of the cumulative loss process.

At a time  $\tau \leq T$  of the default of a name in the portfolio a default payment size

$$\Delta L_\tau^{\{AP, DP\}} := L_\tau^{\{AP, DP\}} - L_{\tau-}^{\{AP, DP\}}$$

is made. Assuming that the short term interest rate is  $(r(t))_{t \geq 0}$ , the initial value of all default payments up to time  $T$  is given by

$$V_{\{AP, DP\}}^{\text{def}} = E \left[ \int_0^T \exp \left( - \int_0^t r(s) ds \right) dL_t^{\{AP, DP\}} \right].$$

The value of the default payments can be expressed with the expected value of loss process by partial integration to keep our analysis simple below.

$$\begin{aligned} V_{\{AP, DP\}}^{\text{def}} &= \exp \left( - \int_0^T r(s) ds \right) E \left( L_T^{\{AP, DP\}} \right) \\ &+ \int_0^T r(t) \exp \left( - \int_0^t r(s) ds \right) E \left( L_t^{\{AP, DP\}} \right) dt. \end{aligned}$$

The premium payment leg consists of regular payments at fixed future dates

$$t_0 < t_1 < \dots < t_{T_n} = T$$

Given a spread  $x$  and  $t_0 = 0$ , the value of regular premium payments equals

$$\begin{aligned} V_{\{AP, DP\}}^{\text{prem}}(x) &= x \sum_{n=1}^{T_n} (t_n - t_{n-1}) \exp \left( - \int_0^{t_n} r(s) ds \right) \\ &\times \left[ (DP - AP)N - E \left( L_{t_n}^{\{AP, DP\}} \right) \right]. \end{aligned}$$

The fair tranche spread  $x^{\{AP, DP\}}$  is then determined by equating the value of default and premium payments,

$$V_{\{AP, DP\}}^{\text{def}} = V_{\{AP, DP\}}^{\text{prem}} \left( x^{\{AP, DP\}} \right).$$

In addition, we assume that default can only occur at the dates  $t_1 < \dots < t_N$  and  $L_{i,t} = PD_i \times LGD_i \times EAD_i$ , all we have to do to evaluate expected value of  $L_t$  is to focus on the default rate distribution. Then both sides of the equation can be expressed as functions of

$$\begin{aligned} E \left( L_t^{\{AP, DP\}} \right) &= E \left( (L_t - AP \cdot N)_+ - (L_t - DP \cdot N)_+ \right) \\ &= \frac{\int_{AP}^{DP} L_t \cdot h(L_t) dL_t}{P((AP < L_t) \cap (L_t < DP))}. \end{aligned}$$

For our numerical experiments, we choose the following parameters: identical probability of default  $PD(t) = 1 - e^{-\lambda t}$ ,  $EAD = 1$ ,  $LGD = 0.6$ , maturity  $T = 5$ , interest rate  $r = 0$ ,  $C_{Y_0,3} = 0.138$ ,  $C_{Y_0,4} = 0.08$ ,  $C_{Y_1,3} = 0.072$ ,  $C_{Y_1,4} = 0.033$ , and  $\rho$  represents the implied tranche correlation.  $\rho$  in each tranche is chosen from Hull and White (2004).

We show numerical results of CDO pricing in Table 3. Table 3 shows that the CDO-spread with Gaussian model is higher than  $Y_1$ : non-Gaussian model for all tranche. In addition, we find that for  $Y_0$  non-Gaussian cases, CDO-spreads for the [6, 9] and [12, 22] tranche have larger spreads than that of the other models.

**Table3.** the numerical results of CDO spread in each tranche

tranche	[0, 3] $\rho = 0.219$	[3, 6] $\rho = 0.042$	[6, 9] $\rho = 0.148$	[9, 12] $\rho = 0.223$	[12, 22] $\rho = 0.305$
Gaussian	55.22474%	11.61022%	3.768472%	2.180098%	0.4942221%
$Y_0$ :non-Gaussian	52.47056%	11.42896%	4.111445%	2.102742%	0.5278298%
$Y_1$ :non-Gaussian	54.88656%	11.55764%	3.558663%	2.07836%	0.4317376%

## 6 Conclusion

We have introduced non-Gaussian one-factor Merton model, which is one of credit risk modeling and its application to CDO pricing. By parameter estimation, we find that non-Gaussian model is more efficient than Gaussian model in terms of maximum log likelihood. In addition, we show that non-Gaussian model makes credit risk measurement, for example, EC, smaller than Gaussian model. Regarding with CDO pricing, overall non-Gaussian model makes CDO spread smaller than Gaussian model.

## Bibliography

- [1] Butler, R. W. (2007). *Saddlepoint Approximations with Application*, Cambridge University Press, New York.
- [2] Demyanyk Y. S., and van Hemert O. (2008). Understanding the subprime mortgage crisis. Available at SSRN: <https://ssrn.com/abstract=1020396>.
- [3] Gordy, M. (2002). Saddlepoint approximation of credit risk. *Journal of Banking and Finance*, 26, 1335 – 1353.
- [4] Jarrow, R. and Turnbull, S. (1995). Pricing derivatives on financial securities subject to credit risk. *Journal of Finance*, 50, 53 – 85.
- [5] Hull J. C. (2009). The credit crunch of 2007: what went wrong? Why? What lessons can be learnt? *Journal of Credit Risk*, 5, Number 2, 3 –18.
- [6] Hull, J. C. (2012). *Risk Management and Financial Institutions. Third Edition*, Wiley, New Jersey.
- [8] Huang, X., Oosterlee, C. W., and Weide, van der, J. A. M. (2007). Higher-order saddlepoint approximations in the Vasicek portfolio credit loss model, *Journal of Computational Finance*, 11, 93 – 113.
- [8] Huang, X. and Oosterlee, C. W. (2011). Saddlepoint approximations for expectations and application to CDO pricing, Society for Industrial and Applied Mathematics Journal on Financial Mathematics.
- [9] Taniguchi, M. and Kakizawa, Y., (2000). *Asymptotic theory of statistical inference for time series*. Springer, New York.
- [10] Vasicek, O. (2002). The Distribution of Loan Portfolio Value, *Risk*, December.



# Towards an improved Credit Scoring System with Alternative Data: the Greek case

Panagiota Giannouli and Christos E. Kountzakis

Department of Statistics and Actuarial-Financial Mathematics, School of Sciences,  
University of Aegean, Samos, Greece

(E-mail: [giannouli@aegean.gr](mailto:giannouli@aegean.gr) & [chr\\_koun@aegean.gr](mailto:chr_koun@aegean.gr) )

**Abstract.** During the development of credit risk assessment models, it is very important to find variables that allow the evaluation of a company's credit risk accurately, as the classification results depends on the appropriate characteristics for a selected data set. Many studies have been focused on the characteristics that should be used in credit scoring applications. The data that has been used in most of these studies are either financial data or credit behaviour data. But there other sources from which we can provide useful information as well and which have not been explored accordingly. Our main objective is to explore these alternative sources of information. To that end, we introduce alternative data to a predictive model which uses only traditional credit behaviour data in order to see if the first contribute to model's performance. In this paper, a new credit risk model tested on real data, which evaluate credit risk of Greek hotels is introduced. This model uses a combination of credit behaviour data and alternative data. The credit risk model, which is introduced in this paper does have some important additional advantages: a) it contains a relatively small number of variables, b) its stability is tested on samples after the time-period of the time-period of data-selection and for different population and c) the characterization of 'good' and 'bad' credit behaviour is strictly defined.

**Keywords:** alternative data, logistic regression, credit scoring, validation.

## 1 Introduction

Credit risk is one of the major threats that financial institutions face. Credit scoring is concerned with assessing credit risk and providing for informed decision making in the money lending business. (Hand and Jacka[7]) stated that the financial institution's process of modelling creditworthiness is referred as credit scoring. Given the importance of credit scoring, much research has been done around this area. Many studies have been focused on the characteristics that should be used in credit scoring applications (e.g. Pendharkar[12], Fletcher and Goss[5], Jo *et al.*[8], Desai *et al.*[3], Tam and Kiang[17], Salchenberger *et al.*[13], Leshno and Spector[9]). However, there are not many

---

*5<sup>th</sup> SMTDA Conference Proceedings, 12-15 June 2018, Chania, Crete, Greece*

© 2018 ISAST



studies that have been focused on alternative data's utility. The objective of this paper is to introduce alternative data to a model which uses only traditional credit behavior data like maximum percent credit utilization, worst payment status, etc. More specifically, we are interested in creating variables come from alternative sources concerning Greek hotels, introduce them to an already existing model for Greek hotels which uses only credit behavior variables and see if the alternative variables contribute to model's performance. Finally, we perform an out of time and out of sample validation for the logistic regression model which uses the combination of alternative and credit behavior variables in order to see if its performance remains stable over time and for different population.

## **2 Literature Review-Stages of Credit Scoring**

Applications of credit scoring have been widely used in various fields, including statistical techniques used in prediction purposes and classification problems. Particularly, in corporate credit scoring models a number of stages must be included, ranging from gathering and preparing relevant data to estimating a credit score using a formula induction algorithm, to developing, monitoring and recalibrating the scorecard. All stages have been explored in literature. For example, data gathering and preparation concern the handling of missing values (e.g. Florez-Lopez[6]) and the selection of predictive set of explanatory variables (e.g. Falangis and Glen[4], Liu and Schumann[10]). Once a data set is ready, a variety of prediction methods accommodate estimating different aspects of credit risk. Particularly, the Basel 2 Capital Accord requires financial institutions, who adopt an internal rating approach, to develop three forms of risk models to estimate the probability of default (PD), the exposure at default (EAD) and the loss given default (LGD). EAD and LGD prediction models have been explored in recent research (e.g. Bellotti and Crook[1], Loterman *et al.*[11], Somers and Whittaker[15]). Nevertheless, most studies concentrate on PD modelling using either classification or survival analysis. Survival analysis models are useful in estimating when a customer will default (e.g. Bellotti and Crook[2], Stepanova and Thomas[16], Tong *et al.*[18]). On the other hand, classification analysis benefits from an incomparable variety of modelling methods and represents the prevailing modelling approach in the literature.

## **3 Performance Definition**

There are two periods that are studied during the model's creation, the observation period and the performance period. In this work the period of 12 months (01/01/2016 to 31/12/2016) will be used as a performance period and 24

months (01/01/2014 to 31/12/2015) as an observation period, as it often occurs in creating similar models (for example in Siddiqi[14]). These models are intended to discriminate the 'bad' from 'good' behavior in the performance period. First of all, we have to specify what we mean by 'bad' and 'good' credit behavior of a company:

1. 'Good' are companies with no delinquency or companies with maximum delinquency in the last 12 months from 0 to 29 days past due or credit limit utilization over 102% from 0 to 29 days, concerning SME Overdrafts.
2. 'Bad' are companies showing 'severe delinquency', this means:
  - SME Contracts, not Overdrafts with maximum delinquency in the last 12 months greater or equal to 90 days past due or
  - SME Overdrafts with maximum delinquency in the last 12 months, greater or equal to 90 days past due or credit limit utilization over 102% for time period greater or equal to 90 days with over limit amount greater than 100€ or

In case where there is some Guarantor for the company, 'Bad' is the company which has the following credit behavior:

- SME Contracts, not Overdrafts with maximum delinquency in the last 12 months greater or equal to 150 days past due or
- SME Overdrafts with maximum delinquency in the last 12 months greater or equal to 150 days past due, or credit limit utilization over 102% for time period greater or equal to 90 days.

Also, a company is included in the ones with 'bad' credit behavior when there is a new DFO (loan denunciation), within performance period.

The term 'utilization' is the following ratio: Current Balance of the company/Credit Limit of it.

## **4 Data Description**

### ***4.1 Alternative Data in Credit Scoring***

The landscape of data is ever-changing, meaning analysts need to evolve both their thinking and data collection methods in order to stay ahead of the curve. In many cases, data that might have been considered unique, uncommon or unattainably expensive just a few years ago, is now widely used. The analysts who take advantage of these untapped data sources, can gain competitive advantage before the rest of their industry catch on. This type of data is often referred as alternative data and the ever-increasing levels of data available in the modern world comes the opportunity to gain unique insights and competitive industry advantage. Alternative data can also be described as data that has been delivered from non-traditional sources. Data that can be used to complement traditional data sources to produce improved analytical insights that would otherwise not have been achievable with traditional data alone. Put simple, it is

data that is not commonly being used within a specific industry, but can potentially be used to gain a competitive advantage over those that do not have access to it.

## ***4.2 Credit Scoring Data Set***

At this point it is important to note that for this research a real-world credit scoring data set was taken by the private database of Tiresias S.A. (a company founded by all banks in Greece) and contains data from business concerning loans and credit cards, information about the status of the credit, data concerning the credit behavior of individuals and companies and finally, data from mortgages. The set of hotels having credit transaction with banks (all 678 of them) was used throughout this analysis. The data set includes several independent variables to create a credit scorecard. These variables are associated with information from the application form (e.g. loan amount, etc.), the status of the credit (e.g. current balance, etc.) and the credit behavior of company (e.g. bankruptcies, etc.). In this data set we added the ‘alternative’ variables that we created using information from social media and customer reviews in order to analyze them together with the already existing variables. The alternative variables that took part in the analysis are: hotel’s registration in Facebook, twitter, Instagram, LinkedIn or YouTube, the number of hotel awards, hotel’s rating in TripAdvisor, the number of votes in TripAdvisor, hotel’s rating in Booking and the number of votes in Booking. Using the above alternative variables, we created two two-dimensional variables. The first one is the combination of hotel’s registration in twitter and Instagram. The second two-dimensional variable is the average rating of TripAdvisor and Booking combined with the sum of votes in TripAdvisor and Booking. In addition, this data set includes a binary response variable that indicates whether or not a default event was observed in a given period of time.

## ***4.3 Data Pre-Processing***

In this Section we employ some standard pre-processing operations to prepare the data for subsequent analysis. In particular, we grouped all the independent variables by creating dummy variables using weight-of-evidence (WOE) coding. Missing values were grouped separately. This process offers the following advantages:

1. It offers an easier way to deal with outliers with interval variables and rare classes.
2. Grouping makes it easier to understand relationships and therefore gain far more knowledge of the portfolio. A chart displaying the relationship between attributes of a characteristic and performance is a much more powerful tool than a simple variable strength statistic. It allows users to explain the nature of this relationship, in addition to the strength of the relationship.

3. Non-linear dependence can be modelled with linear models.

## 5 Models' Comparison

In this Section, we mention the independent credit behavior variables that are already used in the predictive model for Greek hotels as well as the K-S (Kolmogorov-Smirnov), Gini Index ( $=2 * AUC - 1$ ) and accuracy values of this model in order to compare them with the corresponding values of the 'alternative' model.

The already existing model for Greek hotels contains the independent variables: Sum occurrence delinquency one plus at last 24 months, utilization PJ (prim joint holders) update at last 12 months non-revolving, utilization PJ (prim joint holders) update at last 12 months revolving, worst payment status PJ last month vs 24 months. The K-S value for this model is 74,8%, Gini Index value is 0,88 and its accuracy is 91,4%.

Subsequently, we introduced into this model the two two-dimensional alternative variables (mentioned in Section 4.2), as they were stronger than the one-dimensional variables according to WOE and Information Value (IV). This resulted in the following 'alternative' model:

$$\ln(odds) = 1,55820 + 0,00610 * x_1 + 0,00587 * x_2 + 0,00750 * x_3 + 0,00494 * x_4 + 0,01191 * x_5 + 0,00932 * x_6$$

, where

x1= Sum occurrence delinquency one plus at last 24 months,

x2= Utilization PJ (prim joint holders) update at last 12 months non-revolving,

x3= Utilization PJ (prim joint holders) update at last 12 months revolving,

x4= Worst payment status PJ last month vs 24 months,

x5= Hotel's registration in twitter and Instagram,

x6= Average rating of TripAdvisor and Booking combined with the sum of votes in TripAdvisor and Booking.

Ln(odds) shows the possibility of a hotel to be 'good'. It takes values between 0 and 1 and the closer to 0 the better (closer to 'good' behavior) is the hotel.

Table 1: Classification table

Observed-Predicted	Bad	Good	Percentage Correct
Bad	104	28	78,8
Good	20	526	96,3
Overall Percentage	-	-	92,9

Table 1 is the Classification Table and it shows that the addition of independent variables increases the proportion of cases of the dependent variable that are correctly predicted by the model. In this case, the model correctly predicts

92,9% (accuracy) of the observations. This percentage is higher than the previous model's accuracy.

Table 2: K-S and Gini Index

Predicted probability	Bad	Good	Total	Bad Rate	K-S	Gini Index
≤ ,19102	64	3	67	95,5%	47,9%	-
,19103-,57739	42	26	68	61,8%	75,0%	0,02
,57740-,85966	16	55	71	22,5%	77,0%	0,03
,85967-,98958	9	193	202	4,5%	48,5%	0,05
,98959 +	1	269	270	0,4%	0,0%	0,01
Total	132	546	678	19,5%	77,0%	0,90

Table 2 contains K-S and Gini Index values which are 77,0% and 0,90 respectively and they are used in order to verify if the model is capable to distinguish two populations. We notice that both K-S and Gini Index values are higher than they were in the previous model.

At this point, it is important to note that this slight increase of accuracy, K-S and Gini Index is significant as we refer to real-world data set. Finally, based on the above results, we conclude that alternative data contribute to Greek hotel predictive model's performance.

## 6 Out of Time and out of Sample Validation

The following procedure verifies the alternative logistic regression model by running it in another time (04/2016 to 04/2017) in order to see if it is still efficient and stable, as it will be useful only if it can be used over time.

Table 3: Out of time validation K-S and Gini Index

Predicted probability	Bad	Good	Total	Bad Rate	K-S	Gini Index
≤ ,19102	54	6	60	90,0%	48,4%	-
,19103-,57739	37	24	61	60,7%	77,8%	0,02
,57740-,85966	11	46	57	19,3%	79,0%	0,02
,85967-,98958	5	193	198	2,5%	46,7%	0,03
,98959 +	2	254	256	0,8%	0,0%	0,03
Total	109	523	632	17,2%	79,0%	0,90

In Table 3 it appears that K-S (79,0%) is better than before (Section 5, Table 2) and Gini Index remains the same (0,90), so we can conclude that the model is still efficient and stable. Also, model's stability is confirmed once again in Table 4 as its stability value is 0,00.

Table 4: Stability

Score-Range	Development #	Validation #	Development %	Validation #	Stability Index- Validation
≤ ,19102	67	60	9,9%	9,5%	0,00
,19103-,57739	68	61	10,0%	9,7%	0,00
,57740-,85966	71	57	10,5%	9,0%	0,00
,85967-,98958	202	198	29,8%	31,3%	0,00
,98959 +	270	256	39,8%	40,5%	0,00
Total	678	632	100,0%	100,0%	0,00

Finally, we perform an out of sample validation by running this model for 122 new hotels.

Table 5: Out of sample validation K-S and Gini Index

Predicted probability	Bad	Good	Total	Bad Rate	K-S	Gini Index
≤ ,19102	22	1	23	95,7%	61,7%	-
,19103-,57739	5	5	10	50,0%	70,2%	0,01
,57740-,85966	5	6	11	45,5%	77,6%	0,03
,85967-,98958	3	32	35	8,6%	49,4%	0,06
,98959 +	0	43	43	0,0%	0,0%	0,00
Total	35	87	122	28,7%	77,6%	0,90.

In Table 5, it is observed that K-S (77,6%) and Gini Index (0,90) remain high providing that the model is also suitable for other population.

## Conclusions

We set out to explore the effectiveness of alternative data in credit scoring models. To that end, we created and introduced variables come from alternative sources, to an already existing predictive model for Greek hotels which uses only traditional credit behavior variables. For this purpose we used a real-world credit scoring data set of 678 Greek hotels. Comparing the ‘alternative’ model with the already existing one in terms of K-S, Gini Index and accuracy, we concluded that alternative data contribute to model’s performance. More specifically, we can see this contribution by observing the differences between the values of performance indicators for these two models (K-S: 77,0% >74,8%, accuracy: 92,9% >91,4%, Gini Index: 0,90 >0,88). By noticing this contribution

in model's performance for Greek hotels, we can say that it would be prudent to explore alternative data's utility in other industries as well.

Finally, we performed an out of time and out of sample validation for the logistic regression model with the alternative variables, that confirmed its efficiency and stability over time and for different population.

## References

1. T. Bellotti and J. Crook. Loss given default models incorporating macroeconomic variables for credit cards, *International Journal of Forecasting*, 28, 1, 171{182, 2012.
2. T. Bellotti and J. Crook. Credit scoring with macroeconomic variables using survival analysis, *Journal of the Operational Research Society*, 60, 1699{1707, 2009.
3. V.S. Desai, J.N. Crook and G.A. Overstreet. A Comparison of Neural Networks and Linear Scoring Models in the Credit Union Environment, *European Journal of Operational Research*, 95,1, 24{37, 1996.
4. K. Falangis and J.J. Glen. Heuristics for feature selection in mathematical programming discriminant analysis models, *Journal of the Operational Research Society*, 61, 5, 804{812, 2010.
5. D. Fletcher and E. Goss. Forecasting with neural networks: An application using bankruptcy data, *Information and Management*, 24, 3, 159{167, 1993.
6. R. Florez-Lopez. Effects of missing data in credit risk scoring. A comparative analysis of methods to achieve robustness in the absence of sufficient data, *Journal of the Operational Research Society*, 61, 3, 486{501, 2010.
7. D. J. Hand and S. D. Jacka. *Statistics in Finance*. Arnold Applications of Statistics, London, 1998.
8. H. Jo, I. Han and H. Lee. Bankruptcy prediction using case-based reasoning, neural networks and discriminant analysis, *Expert Systems with Applications*, 13, 2, 97{108, 1997.
9. M. Leshno and Y. Spector. Neural networks prediction analysis: The bankruptcy case, *Neurocomputing*, 10, 2, 125{147, 1996.
10. Y. Liu and M. Schumann. Data mining feature selection for credit scoring models, *Journal of the Operational Research Society*, 56, 9, 1099{1108, 2005.
11. G. Loterman, I. Brown, D. Martens, C. Mues and B. Baesens. Benchmarking regression algorithms for loss given default modelling, *International Journal of Forecasting*, 28, 1, 161{170, 2012.
12. P. C. Pendharkar. A threshold-varying artificial networks approach for classification and its application to bankruptcy prediction problems, *Computers and Operations Research*, 32, 10, 2561{2582, 2005.
13. L. M. Salchenberger, E. M. Cinar and N. A. Lash. Neural networks: A new tool for predicting thrift failures, *Decision Sciences*, 23, 4, 899{916, 1992.
14. N. Siddiqi. *Credit Risk Scorecard: Developing and Implementing Intelligent Credit Scoring*. John Wiley & Sons, Inc., New Jersey, 2006.
15. M. Somers and J. Whittaker. Quantile regression for modelling distributions of profit and loss, *European Journal of Operational Research*, 183, 3, 1477{1487, 2007.
16. M. Stepanova and L. Thomas. Survival analysis methods for personal loan data, *Operational Research*, 50, 2, 277{289, 2002.
17. K. Y. Tam and M. Y. Kiang. Managerial applications of neural networks: The case of bank failure predictions, *Management Science*, 38, 7, 926{947, 1992.

18. E. N. C. Tong, C. Mues and L. C. Thomas. Mixture sure models in credit scoring: if and when borrowers default, *European Journal of Operational Research*, 218, 1, 132{139, 2012.



# SIMILARITY BETWEEN STRAINS OF ZIKA FROM TROPICAL AND SUBTROPICAL REGIONS

JESÚS E. GARCÍA, V.A. GONZÁLEZ-LÓPEZ, S.L. MERCADO LONDOÑO,  
AND M.T.A. CORDEIRO

**ABSTRACT.** In this article we consider genomic data from tropical and subtropical regions and we identify in a robust way the strain which best represents the set. We analyze strains of the Zika virus obtained from the NCBI free source. Each sequence is identified with a finite-order Markov chain, on the alphabet  $\{a, c, g, t\}$ , and the proximity between pairs of sequences is established by the notion  $d$  (see García et al. (2018) [1]) based on the Bayesian information Criterion. Then, we use a  $d$ -based procedure to identify the most representative sequence and also the less representative sequence. With this methodology we can establish which strain can be considered as a reference in the study of Zika strains.

## 1. Introduction

The ease with which the Zika virus has developed in tropical and subtropical territories impose on the scientific world the task of deepening the understanding of its mechanisms of growth as well as the task of discover the implications of this virus in the public health. Zika has led many of these countries to borderline situations, since, for instance, the Zika virus is associated with an odd increase of cases of microcephaly and other neurological problems. For example, the high rates at which birth defects occurred in 2015 and 2016 lead to the prediction that Brazil has just a few years to develop specific inclusion policies for these children. Recent studies aim to map the genetic strains of this virus, Metsky et al. (2017)[4] reported genomic data from several countries, also analyzed the timing and patterns of introductions into distinct geographic regions. The evidence suggests a rapid expansion of the outbreak in Brazil and multiple introductions of outbreak strains into Puerto Rico, Honduras, Colombia, other Caribbean islands, and the continental United States. In the present article, we analyze genomic strains of the Zika virus from patients coming from different tropical

---

*Key words and phrases.* Markov Processes; Distance between Strings; Bayesian Information Criterion; Profile of Strains.

1

*5<sup>th</sup> SMTDA Conference Proceedings, 12-15 June 2018, Chania, Crete, Greece*

© 2018 ISAST



and subtropical regions and obtained from the NCBI source. The purpose of this article is to identify those sequences that can be considered as having a *standard* behavior, capable of representing the whole set of sequences. Such as sequences can be used as a profile of strains of Zika. In order to attain our goal we identify each genomic strain with a finite-order Markov chain, on the base alphabet  $\{a, c, g, t\}$ . Then, we quantify the distance between pairs of strains using a distance  $d$  (see García et al. (2018) [1]) based on the Bayesian information Criterion. In order to visualize which strains are near/distant we build clusters derived from  $d$ . We use a  $d$ -based notion:  $\delta$ , reported in Fernández et al. (2018) [2] to identify the most representative strains and also to identify the less representative strains. With this methodology we can establish which regions show a similar pattern.

When we refer to a standard behavior we are assuming that the sequences could show particularities, so we should use a robust procedure that operates minimizing great distortions, for that reason we use  $\delta$  (see Fernández et al. (2018) [2]).

In the section 2 we introduce the notation as well as the theoretical assumptions that we assume about the genomic data and also the notions of proximity that we will apply later. In section 3 we present the general characteristics as well as the source, of the data that we explored in this study. In section 4 we show the results and in section 5 we present the conclusions.

## 2. Preliminaries

Let  $X_t$  be a discrete time, order  $o$  (with  $o < \infty$ ) ergodic Markov chain on a finite alphabet  $A$ . Let us call  $\mathcal{S} = A^o$  the state space and, denote the string  $a_m a_{m+1} \dots a_n$  by  $a_m^n$  where  $a_i \in A$ ,  $m \leq i \leq n$ . For each  $a \in A$  and  $s \in \mathcal{S}$ ,  $P(a|s) = \text{Prob}(X_t = a | X_{t-o}^{t-1} = s)$ . In a given sample  $x_1^n$ , coming from the stochastic process, the number of occurrences of  $s$  in the sample  $x_1^n$  is denoted by  $N_n(s)$  and the number of occurrences of  $s$  followed by  $a$  in the sample  $x_1^n$  is denoted by  $N_n(s, a)$ . In this way  $\frac{N_n(s, a)}{N_n(s)}$  is the estimator of  $P(a|s)$ . We establish the notion of proximity between processes, through their samples in the next definition.

Consider two ergodic Markov chains  $X_{1,t}$  and  $X_{2,t}$ , of order  $o$ , arranged on a finite alphabet  $A$  with state space  $\mathcal{S}$ . Given  $s \in \mathcal{S}$  denote by  $\{P(a|s)\}_{a \in A}$  and  $\{Q(a|s)\}_{a \in A}$  the sets of conditional probabilities of  $X_{1,t}$  and  $X_{2,t}$  respectively. We introduce a local distance  $d_s$  that, when evaluated in a given string  $s$ , allows us to define how far or near the

processes locally are. Then, this notion can be extended to all the space  $\mathcal{S}$ .

**Definition 2.1.** Consider two ergodic Markov chains  $X_{1,t}$  and  $X_{2,t}$ , of order  $o$ , with finite alphabet  $A$ , state space  $\mathcal{S} = A^o$  and independent samples  $x_{1,1}^{n_1}, x_{2,1}^{n_2}$  respectively.

i. For a string  $s \in \mathcal{S}$

$$d_s(x_{1,1}^{n_1}, x_{2,1}^{n_2}) := \frac{\alpha}{(|A| - 1) \ln(n_1 + n_2)} \sum_{a \in A} \left\{ N_{n_1}(s, a) \ln \left( \frac{N_{n_1}(s, a)}{N_{n_1}(s)} \right) \right. \\ \left. + N_{n_2}(s, a) \ln \left( \frac{N_{n_2}(s, a)}{N_{n_2}(s)} \right) \right. \\ \left. - N_{n_1+n_2}(s, a) \ln \left( \frac{N_{n_1+n_2}(s, a)}{N_{n_1+n_2}(s)} \right) \right\}.$$

ii. For the state space  $\mathcal{S}$

$$d(x_{1,1}^{n_1}, x_{2,1}^{n_2}) := \max_{s \in \mathcal{S}} \{d_s(x_{1,1}^{n_1}, x_{2,1}^{n_2})\}.$$

With  $N_{n_1+n_2}(s, a) = N_{n_1}(s, a) + N_{n_2}(s, a)$ ,  $N_{n_1+n_2}(s) = N_{n_1}(s) + N_{n_2}(s)$ , where  $N_{n_1}$  and  $N_{n_2}$  are given as usual, computed from the samples  $x_{1,1}^{n_1}$  and  $x_{2,1}^{n_2}$  respectively. With  $\alpha$  a real and positive value.

The relevant properties of these concepts are listed below.

*Remark 2.2.* i. For a string  $s \in \mathcal{S}$

$$P(a|s) = Q(a|s) \forall a \in A \Leftrightarrow d_s(x_{1,1}^{n_1}, x_{2,1}^{n_2}) \xrightarrow{\min(n_1, n_2) \rightarrow \infty} 0, \\ \exists a \in A : P(a|s) \neq Q(a|s) \Leftrightarrow d_s(x_{1,1}^{n_1}, x_{2,1}^{n_2}) \xrightarrow{\min(n_1, n_2) \rightarrow \infty} \infty.$$

ii. From the properties of  $d_s(x_{1,1}^{n_1}, x_{2,1}^{n_2})$ , follows:

$$P(a|s) = Q(a|s) \forall a \in A, s \in \mathcal{S} \Leftrightarrow d(x_{1,1}^{n_1}, x_{2,1}^{n_2}) \xrightarrow{\min(n_1, n_2) \rightarrow \infty} 0, \\ \exists a \in A \text{ for } s \in \mathcal{S} : P(a|s) \neq Q(a|s) \Leftrightarrow d(x_{1,1}^{n_1}, x_{2,1}^{n_2}) \xrightarrow{\min(n_1, n_2) \rightarrow \infty} \infty.$$

The properties reported in the remark 2.2 ii show the consistency of the criterion  $d$  in being able to detect discrepancies between the samples. Since  $d$  takes arbitrarily small/big values, when the samples' laws are equal/different, we can use  $d$  for the comparison between the DNA samples. But we will go beyond this, we want to determine an order between the samples, indicating which samples are the most representative in the set and which samples are the least representative in the set. In order to attain our goal we incorporate two concepts.

**Definition 2.3.** Given  $m$  samples  $\{x_{i,1}^{n_i}\}_{i=1}^m$ , for each sample  $i$ , define

$$\delta(i) := \text{median}_{j \neq i} \{d(x_{i,1}^{n_i}, x_{j,1}^{n_j})\},$$

$$\beta(i) := \text{median}_{j \neq i} \{\text{mean}_{s \in \mathcal{S}} \{d_s(x_{i,1}^{n_i}, x_{j,1}^{n_j})\}\}.$$

The properties of  $d_s, d, \delta$  and  $\beta$  are widely studied in García et al. (2018) [1] and Fernández et al. (2018) [2].

Fernández et al. (2018) [2] introduces a procedure of selecting samples from a set of samples coming from Markovian processes of finite order and finite alphabet. This procedure is an ordering procedure which use the quantity  $\delta(\cdot)$  to establish a hierarchy between the samples. Under the assumption of the existence of a law that prevails in at least 50% of the samples of the collection,  $\delta(\cdot)$  allows to identify samples governed by the predominant law. This statement is proved in Fernández et al. (2018) [2]. The approach is based on the local metric  $d_s$  between samples, with the properties related in the remark 2.2.

That is to say that  $\delta(\cdot)$  allows to hierarchize samples using as criteria that those that receive lower values of  $\delta(\cdot)$  are generated by the predominant stochastic law in the whole set. Those that receive the highest values of  $\delta(\cdot)$  could belong to other laws, more rare and that do not command the set of samples.

In the next section we introduce the database and based on its structure we associate it with samples from stochastic processes.

### 3. Genomic Data

This section is devoted to describe the data used in this research. All the sequences are obtained from the source of the National Center for Biotechnology Information Support Center (NCBI), available in <https://www.ncbi.nlm.nih.gov/nuccore/>. Each sequence takes values in the alphabet  $\mathcal{A} = \{a,c,g,t\}$ , as illustrated in the case of the sequence KY817930.1, starting as

ctagcaacagtatcaacaggttttattttggatttga....

We consider each DNA sequence as a sample, that is to say that  $x_1^n$  is composed by the concatenation of elements of the alphabet  $\mathcal{A}$ . The complete list of sequences is given in the table 1, separated by country (a total of  $m = 153$  samples). We will assume that all genomic sequences behave as samples of stochastic processes and that at least 50% of them follow the same stochastic law. Under this assumption according to Fernández et al. (2018) [2], we can indicate the most representative samples and those less representative. This could be used to establish a profile about the Zika sequences. That is, if in another

research we want to compare genomic sequences of Zika, the recommendation would be to do it with the sequences (of this study) that show the lowest  $\delta$  values, since they would be the ones that show a behavior which represents the stochastic law of most of the samples in the set given by tabla 1.

The sequences of this database show sample sizes greater than or equal to  $n = 10807$ , which is the smallest size of all of them. Following the consensual rule that limits the maximum memory  $o$  to the relationship between the cardinal of the alphabet  $\mathcal{A}$ ,  $|\mathcal{A}|$  and the sample size  $n$ , as  $o < \lceil \log_{|\mathcal{A}|}(n) \rceil - 1 = 5$  and since we know that the bases of this alphabet are organized in triples, we adopt  $o = 3$ . According to the definitions previously introduced, see definitions 2.1, 2.3, we must establish a value for  $\alpha$ , which allows us to implement the computation of all these notions. Following Schwarz (1978) [5] we use  $\alpha = 2$ .

TABLE 1. Sequences of Zika by country: Brazil (BRA), Colombia (COL), Cuba (CUB), Dominican Republic (DOM), Honduras (HND), Jamaica (JAM), Martinique (MTQ), Mexico (MEX), Nicaragua (NIC), Puerto Rico (PRI), United States (USA), Venezuela (VEN).

Country	Sequences
Brazil (44)	KX197192.1, KY014296.2, KY014297.2, KY014301.2, KY014307.2 KY014308.2, KY014313.2, KY014317.2, KY014320.2, KY558999.1 KY559001.1, KY559003.1, KY559004.1, KY559005.1, KY559006.1 KY559007.1, KY559009.1, KY559010.1, KY559011.1, KY559012.1 KY559013.1, KY559014.1, KY559015.1, KY559017.1, KY559018.1 KY559019.1, KY559021.1, KY559023.1, KY559024.1, KY559027.1 KY559031.1, KY559032.1, KY785410.1, KY785426.1, KY785427.1 KY785429.1, KY785433.1, KY785437.1, KY785439.1, KY785450.1 KY785455.1, KY785456.1, KY785479.1, KY817930.1
US (34)	KX832731.1, KX842449.2, KX922703.1, KX922704.1, KX922705.1 KX922706.1, KX922707.1, KY014295.2, KY014298.1, KY014316.2 KY014325.2, KY014326.1, KY075932.1, KY075933.1, KY075934.1 KY075935.1, KY075936.1, KY325464.1, KY325465.1, KY325466.1 KY325467.1, KY325468.1, KY325469.1, KY325471.1, KY325472.1 KY325473.1, KY325476.1, KY325477.1, KY325479.1, KY785412.1 KY785445.1, KY785457.1, KY785459.1, KY785474.1
DOM (23)	KY014300.2, KY014302.3, KY014303.2, KY014304.2, KY014305.2 KY014314.2, KY014318.3, KY014321.2, KY785413.1, KY785415.1 KY785420.1, KY785423.1, KY785435.1, KY785441.1, KY785447.1 KY785449.1, KY785453.1, KY785463.1, KY785465.1, KY785470.1 KY785475.1, KY785476.1, KY785484.1
MEX (19)	MF801391.1, MF801395.1, MF801396.1, MF801398.1, MF801402.1 MF801403.1, MF801404.1, MF801406.1, MF801407.1, MF801408.1 MF801409.1, MF801410.1, MF801412.1, MF801413.1, MF801414.1 MF801417.1, MF801418.1, MF801420.1, MF801423.1
HND (13)	KY014306.2, KY014310.2, KY014312.2, KY014315.2, KY014319.2 KY014327.2, KY785414.1, KY785418.1, KY785442.1, KY785444.1 KY785448.1, KY785452.1, KY785461.1
NIC (7)	MF434516.1, MF434517.1, MF434518.1, MF434520.1, MF434521.1 MF434522.1, MF801426.1
JAM (4)	KY785419.1, KY785424.1, KY785430.1, KY785432.1
COL (3)	KY785417.1, KY785466.1, KY785469.1
PRI (2)	KY785462.1, KY785464.1
VEN (2)	KX702400.1, KX893855.1
CUB (1)	MF438286.1
MTQ (1)	KY785451.1

## 4. Results

We split the inspection of the results into three subsections, in the first two we inspect the samples from Brazil and the United States, respectively, since those are the largest databases, as shown in table 1. In the third subsection we compare all the samples. In each subsection we will consider a universe  $\mathcal{C}$  of samples to be compared. Given the set of samples  $\mathcal{C}$  we compute  $d(x_{i,1}^{n_i}, x_j^{n_j})$  - definition 2.1-ii between the pairs of samples  $i$  and  $j$  in  $\mathcal{C}$ , with them we built groups that allow us to identify which samples are closer and which are more distant. Also, by means of  $\delta$  we can hierarchize the samples in each set  $\mathcal{C}$ . That is, to each sample  $i$  in  $\mathcal{C}$ , we associate a value  $\delta(i)$  by definition 2.3. According to  $\delta(\cdot)$  the lowest values indicate the most representative samples and the largest values indicate the least representative samples, see Fernández et al. (2018) [2]. That is,

$$\operatorname{argmin}_{i \in \mathcal{C}} \{\delta(i)\}$$

is the most representative sample in  $\mathcal{C}$ , or it is governed by the law of the majority. And

$$\operatorname{argmax}_{i \in \mathcal{C}} \{\delta(i)\}$$

is the least representative sample in  $\mathcal{C}$ , or it can be governed by a odd stochastic law. In theoretical terms, and having seen the results of Fernández et al. (2018) [2], under the assumption that the law of the majority is shared by 50% of the samples in  $\mathcal{C}$ , all the samples associated with the 50% smaller  $\delta$  values, can be considered as referents of the law of the majority in  $\mathcal{C}$ .

**4.1. Brazilian Sequences.** In tables 2 and 3 we show the Brazilian sequences of zika and the values  $\delta$  and  $\beta$  computed for each one of them. We have ordered the list of sequences from top to bottom, according to the magnitude of  $\delta$  from the lowest to the highest value.

According to  $\delta$  values (tables 2 and 3) the sequence KY558999.1 is the most representative sequence of the Brazilian set, and the sequence KY785439.1 is the least representative in that universe as well. Then,

$$\text{KY558999.1} = \operatorname{argmin}_{i \in \mathcal{C}} \{\delta(i)\},$$

$$\text{KY785439.1} = \operatorname{argmax}_{i \in \mathcal{C}} \{\delta(i)\},$$

where  $\mathcal{C}$  is the collection of Brazilian samples. We see that the sequences near the top and bottom, according to column 2, receive  $\beta$  values also near the top and bottom of column 3.  $\delta$  takes values in the interval  $[0.01894, 0.19106]$  in the Brazilian case, with amplitude equal to 0.17212.

TABLE 2. 1 of 2: From left to right (a) Brazilian sequence of Zika, (b)  $\delta$  value, (c)  $\beta$  value (definition 2.3). Sequences ordered from top to bottom, according to the magnitude of  $\delta$ . In bold type, the lowest value per column.

Sequence	$\delta$	$\beta$
KY558999.1	<b>0.01894</b>	0.00434
KY559005.1	0.01919	0.00453
KY785450.1	0.01947	0.00444
KY559015.1	0.01987	<b>0.00432</b>
KY559007.1	0.02017	0.00470
KY559027.1	0.02025	0.00456
KY014307.2	0.02160	0.00536
KY785410.1	0.02180	0.00510
KY014320.2	0.02254	0.00523
KY014296.2	0.02277	0.00544
KY559013.1	0.02287	0.00516
KY785433.1	0.02335	0.00527
KY785479.1	0.02395	0.00539
KY785426.1	0.02471	0.00513
KY559012.1	0.02495	0.00591
KY559021.1	0.02519	0.00623
KY785455.1	0.02529	0.00540
KY785456.1	0.02576	0.00675
KY014317.2	0.02615	0.00539
KY785427.1	0.02615	0.00482
KY559023.1	0.02660	0.00705
KY014301.2	0.02725	0.00578

Tables 4 and 5 show the results of  $d$  (definition 2.1-ii) when we compare the most discrepant sequence (see table 3, column 2) with all the other Brazilian sequences. In column 1 we list the samples with which it is compared KY785439.1, in column 2 the  $\text{mean}_{s \in \mathcal{S}} \{d_s(x_{1,1}^{n_1}, x_{2,1}^{n_2})\}$  is computed, where sample 1 is KY785439.1 and sample 2 is shown to the left, column 3 gives the value of  $d$  and in the last column we report the string  $s^*$  where such a maximum occurs.

According to tables 4 and 5 the string most frequently indicated as responsible for the maximum value of  $d_s$  is  $s^* = \text{gtt}$ . This shows that the sequence KY785439.1 attributes transition probabilities of gtt for any other element of the alphabet, markedly different from those transition probabilities attributed by most of the sequences listed in tables 4 and

TABLE 3. 2 of 2 (continuation of table 2): From left to right (a) Brazilian sequence of Zika, (b)  $\delta$  value, (c)  $\beta$  value (definition 2.3). Sequences ordered from top to bottom, according to the magnitude of  $\delta$ . In bold type the highest value per column.

Sample	$\delta$	$\beta$
KX197192.1	0.02745	0.00598
KY014297.2	0.02847	0.00501
KY559024.1	0.02863	0.00756
KY559017.1	0.03005	0.00720
KY559003.1	0.03185	0.00656
KY785429.1	0.03450	0.00608
KY559006.1	0.03556	0.00896
KY559019.1	0.03623	0.00741
KY559018.1	0.03623	0.00751
KY014313.2	0.03878	0.00870
KY559031.1	0.04260	0.00959
KY559011.1	0.04423	0.00791
KY785437.1	0.04697	0.01029
KY559032.1	0.04830	0.01063
KY559010.1	0.05322	0.01133
KY559009.1	0.07372	0.01412
KY014308.2	0.07573	0.02532
KY559001.1	0.07797	0.01407
KY559014.1	0.09192	0.02303
KY559004.1	0.14313	0.02715
KY817930.1	0.14382	<b>0.04206</b>
KY785439.1	<b>0.19106</b>	0.02623

5.

In the figure 1 we build a dendrogram, using  $d$ , between all the Brazilian sequences. The figure 1 confirms the positions attributed to the Brazilian samples by  $\delta$ , registered in tables 2 and 3. We see the sequence KY785439.1 in the furthest cluster next to two other sequences: KY817930.1 and KY559004.1, also on bottom in table 3.

**4.2. North American Sequences.** We visualize in table 6 the values of  $\delta$  and  $\beta$  computed for this universe. In this case, the  $\delta$  values are in the interval  $[0.01045, 0.12153]$  with amplitude equal to 0.11108, that is, the sequences are relatively closer to each other, when compared with the Brazilian samples.

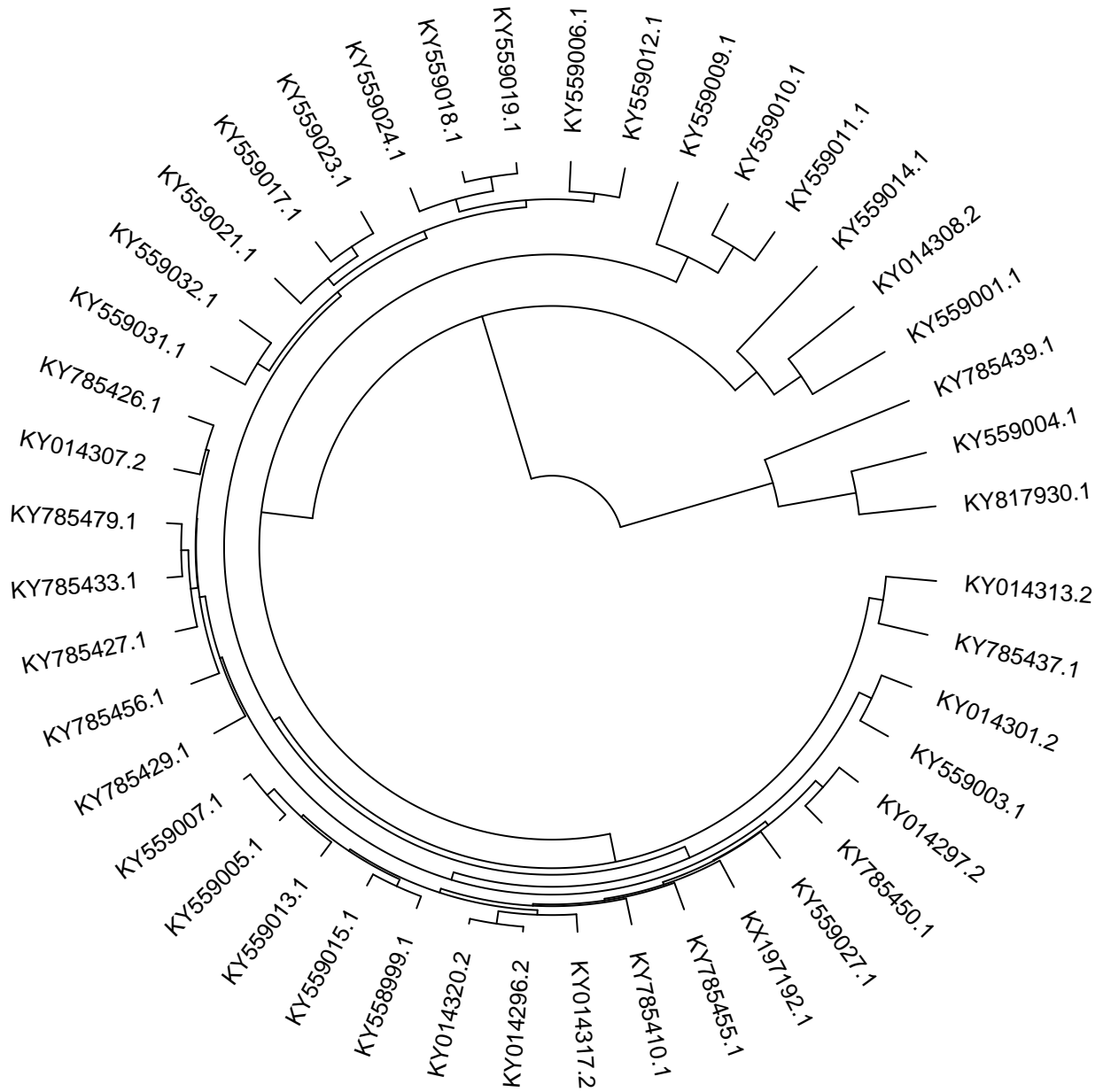


FIGURE 1. Clusters for the Brazilian sequences, built using  $d$  (definition (2.1) ii.) and the *average* criterion.

TABLE 4. 1 of 2 - From left to right: (a) Brazilian sequence, (b)  $\text{mean}_{s \in \mathcal{S}}\{d_s\}$ , (c)  $d$  value - definition 2.1 ii, (d)  $s^* = \text{argmax}_{s \in \mathcal{S}}\{d_s\}$ . (b) and (c) computed between the sequence KY785439.1 and each one of the Brazilian sequences (column 1). Sequences ordered from top to bottom according to the magnitude of  $d$ , in an increasing way.

Sequence	$\text{mean}_{s \in \mathcal{S}}\{d_s\}$	$d$	$s^*$
KY559014.1	0.02583	0.08814	acg
KY559001.1	0.01394	0.10743	gac
KY559004.1	0.02026	0.11981	gtt
KY559021.1	0.02417	0.12425	gtt
KY559023.1	0.02648	0.13573	gtt
KY559024.1	0.02622	0.13579	gtt
KY559011.1	0.02131	0.13885	gtt
KY559010.1	0.02217	0.14123	gtt
KY559019.1	0.02501	0.14256	gtt
KY014313.2	0.02334	0.14821	gtt
KY559018.1	0.02541	0.14971	gtt
KY559009.1	0.02469	0.15422	gtt
KY559017.1	0.02422	0.15687	gtt
KY014307.2	0.02511	0.16628	gtt
KY559027.1	0.02394	0.16667	gtt
KY785426.1	0.02480	0.16678	gtt
KY785456.1	0.02612	0.16719	gtt
KY817930.1	0.04588	0.16853	gtt
KY785455.1	0.02711	0.18165	gtt
KY559015.1	0.02673	0.18185	gtt
KY014317.2	0.02826	0.18302	gtt
KY559032.1	0.02222	0.18556	gtt

If  $\mathcal{C}$  is the set of USA sequences, we obtain

$$\text{KX922706.1 (or KY075936.1)} = \text{argmin}_{i \in \mathcal{C}} \{\delta(i)\},$$

and

$$\text{KY785457.1} = \text{argmax}_{i \in \mathcal{C}} \{\delta(i)\}.$$

That is to say that if we must indicate a sequence of standard behavior, in the universe of the sequences of the United States (listed in the table 1), KX922706.1 and KY075936.1 are the indicated. And the sequence with a more divergent behavior is the sequence KY785457.1, showing the highest  $\delta$  value in such a universe.

TABLE 5. 2 of 2 - (continuation of table 4) From left to right: (a) Brazilian sequence, (b)  $\text{mean}_{s \in \mathcal{S}}\{d_s\}$ , (c)  $d$  value - definition 2.1 ii, (d)  $s^* = \text{argmax}_{s \in \mathcal{S}}\{d_s\}$ . (b) and (c) computed between the sequence KY785439.1 and each one of the Brazilian sequences (column 1). Sequences ordered from top to bottom according to the magnitude of  $d$ , in an increasing way.

Sequence	$\text{mean}_{s \in \mathcal{S}}\{d_s\}$	$d$	$s^*$
KY559007.1	0.02653	0.19106	gtt
KY559031.1	0.02326	0.19358	gtt
KY559012.1	0.02710	0.19440	gtt
KY014297.2	0.02752	0.19811	gtt
KY558999.1	0.02752	0.19816	gtt
KY559005.1	0.02704	0.19819	gtt
KY559006.1	0.02845	0.19956	gtt
KY785429.1	0.02451	0.20219	gtt
KY014308.2	0.03823	0.20257	gtt
KY785427.1	0.02578	0.20538	gtt
KX197192.1	0.02957	0.20625	gtt
KY785450.1	0.02685	0.20657	gtt
KY785479.1	0.02656	0.20691	gtt
KY785437.1	0.02657	0.21218	gtt
KY014320.2	0.02827	0.21239	gtt
KY559013.1	0.02785	0.21357	gtt
KY785433.1	0.02460	0.21892	gtt
KY014296.2	0.02884	0.22096	gtt
KY785410.1	0.02663	0.22928	gtt
KY559003.1	0.02650	0.24205	gtt
KY014301.2	0.02576	0.24591	gtt

According to table 7, the string pointed as the one that provides the highest values of  $d_s$ , when we compare the sequence KY785457.1 with all the other USA sequences is  $s^* = \text{agt}$ .

Figure 2 shows the groups defined by  $d$ , when comparing the USA sequences among them. We see clearly the most distant groups, as well as indicated by the  $\delta$  values registered in table 6. The sequence KY785457.1 is, according to table 6 and figure 2 the most distant sequence in such a universe.

TABLE 6. From left to right: (a) USA sequence of Zika, (b)  $\delta$  value, (c)  $\beta$  value (definition 2.3). Sequences ordered from top to bottom, by the magnitude of  $\delta$ . In bold type, the lowest/highest value per column.

Sequence	$\delta$	$\beta$
KX922706.1	<b>0.01045</b>	0.00226
KY075936.1	<b>0.01045</b>	0.00229
KX922707.1	0.01075	0.00244
KX922705.1	0.01168	0.00250
KX922704.1	0.01241	0.00227
KY014325.2	0.01241	0.00232
KY325472.1	0.01286	0.00209
KY014295.2	0.01286	0.00206
KY325469.1	0.01286	0.00195
KX832731.1	0.01286	0.00263
KY325468.1	0.01286	<b>0.00176</b>
KY014316.2	0.01331	0.00248
KY325465.1	0.01337	0.00358
KY325467.1	0.01345	0.00267
KY325479.1	0.01347	0.00330
KY325473.1	0.01387	0.00275
KY075934.1	0.01589	0.00332
KY785445.1	0.01596	0.00325
KY325476.1	0.01601	0.00304
KY325477.1	0.01637	0.00316
KY075932.1	0.01761	0.00374
KY075935.1	0.01802	0.00356
KY325464.1	0.01848	0.00294
KX842449.2	0.01873	0.00295
KY075933.1	0.01873	0.00415
KX922703.1	0.01873	0.00330
KY785459.1	0.02110	0.00500
KY785412.1	0.03143	0.00734
KY014298.1	0.03558	0.00651
KY014326.1	0.04716	0.01064
KY325471.1	0.06538	0.01646
KY785474.1	0.09339	0.02002
KY325466.1	0.10675	<b>0.03223</b>
KY785457.1	<b>0.12153</b>	0.02514

TABLE 7. From left to right: (a) USA sequence, (b)  $\text{mean}_{s \in \mathcal{S}}\{d_s\}$ , (c)  $d$  value - definition 2.1 ii, (d)  $s^* = \text{argmax}_{s \in \mathcal{S}}\{d_s\}$ . (b) and (c) computed between the sequence KY785457.1 and each one of the USA sequences (column 1). Sequences ordered from top to bottom according to the magnitude of  $d$ , in an increasing way.

Sequence	$\text{mean}_{s \in \mathcal{S}}\{d_s\}$	$d$	$s^*$
KY785412.1	0.02460	0.08477	ata
KX922703.1	0.02384	0.09064	ata
KY075935.1	0.02435	0.09064	ata
KY785459.1	0.02090	0.09376	agt
KX842449.2	0.02387	0.09843	agt
KY014326.1	0.02148	0.09877	gag
KY075933.1	0.02406	0.09976	agt
KY014298.1	0.02015	0.10117	ata
KY785445.1	0.02427	0.10430	agt
KX922707.1	0.02482	0.11417	agt
KX922704.1	0.02514	0.11482	agt
KY075936.1	0.02501	0.11482	agt
KY014325.2	0.02513	0.11483	agt
KX832731.1	0.02477	0.11492	agt
KX922706.1	0.02576	0.11626	agt
KY325477.1	0.02482	0.12073	agt
KX922705.1	0.02414	0.12153	agt
KY075932.1	0.02462	0.12252	agt
KY075934.1	0.02525	0.12273	agt
KY325471.1	0.03394	0.12297	cta
KY014316.2	0.02607	0.13067	agt
KY325468.1	0.02622	0.13101	agt
KY325467.1	0.02653	0.13123	agt
KY325472.1	0.02619	0.13190	agt
KY014295.2	0.02614	0.13190	agt
KY325469.1	0.02610	0.13190	agt
KY325479.1	0.02687	0.13889	agt
KY325464.1	0.02607	0.13938	agt
KY325473.1	0.02584	0.13938	agt
KY325465.1	0.02713	0.14030	agt
KY325476.1	0.02706	0.14620	agt
KY785474.1	0.02810	0.15987	ctg
KY325466.1	0.04736	0.16180	agt



on the label of table 1.

Tables 8 to 10 record the 153 sequences and its  $\delta$  values. We note that the  $\delta$  values are in the interval  $[0.01456, 0.19644]$  with amplitude equal to 0.18188. The most representative sequence of the whole group of sequences corresponds to KY014318.3.DOM with  $\delta = 0.01456$ . If  $\mathcal{C}$  is the set of sequences described in table 1, we obtain

$$\text{KY014318.3.DOM} = \operatorname{argmin}_{i \in \mathcal{C}} \{\delta(i)\},$$

and

$$\text{KY785444.1.HND} = \operatorname{argmax}_{i \in \mathcal{C}} \{\delta(i)\}.$$

As can also be visualized in figure 3, the seven least representative sequences are at the end of the list declared in table 10 and they are together in a group in figure 3. Thus, relevant information on discrepancies is captured by  $\delta$  values and also visualized by dendrograms constructed using the notion  $d$ . We note that these seven sequences, with the highest values of  $\delta$ , could have been produced by different stochastic laws in comparison with the majority law operating in the set. With the purpose of inspecting aspects of these seven sequences in the most distant cluster, we collect some information in table 11.

Table 11 shows the values of  $d$  between the sequence KY014318.3.DOM and each one of the seven most distant sequences. Table 11 also gives which is the string  $s^*$  where the maximum value of  $d_s$  occurs in each comparison. The results show the variety of strings where the highest values of  $d_s$  can manifest. We also see that the Brazilian sequence KY785439.1.BRA considered most discrepant in subsection 4.1, is also included in this list (table 11), with a value  $d = 0.19038$ , which occurs in the same string  $gtt$  indicated as the main string that produces the highest values of  $d_s$ , according to tables 4 and 5.

Observing the figure 3 we do not see a clear separation between the countries, and regarding the representativeness of the sequences (low values of  $\delta$ ) according to table 8 is not verified the predominance of the same country, but the three most representative sequences are coming from Dominican Republic (DOM). Figure 3 allows us to identify some subgroups consisting of sequences from the same country. For example on the left and down of figure 3 we visualize concentrations of sequences from Brazil, also listed in table 12 - group 1, these sequences have in common at least another aspect, all are from the state of Rio de Janeiro. We also see groups of Brazilian sequences that are not coming from the same state, as is the case of the group 2 in table 12, visualized in figure 3 on the right and below. On this last case five of the sequences come from the state of Tocantins and three from the

TABLE 8. 1 of 3: Sequences of Zika ordered from top to bottom and from left to right, by the magnitude of  $\delta$ .

Sequence	$\delta$	Sequence	$\delta$
KY014318.3.DOM	<b>0.01456</b>	KY014320.2.BRA	0.01842
KY785435.1.DOM	0.01502	KX922705.1.USA	0.01851
KY785420.1.DOM	0.01543	KY014314.2.DOM	0.01859
KX922706.1.USA	0.01583	KY785475.1.DOM	0.01859
KY014302.3.DOM	0.01586	MF801391.1.MEX	0.01866
KY559005.1.BRA	0.01592	KY014310.2.HND	0.01867
KY075934.1.USA	0.01601	MF801414.1.MEX	0.01878
KY014306.2.HND	0.01604	KY785441.1.DOM	0.01890
KX922707.1.USA	0.01621	KY014307.2.BRA	0.01900
KY785464.1.PRI	0.01628	MF801413.1.MEX	0.01915
KY559007.1.BRA	0.01634	KY559027.1.BRA	0.01922
KX832731.1.USA	0.01649	MF434516.1.NIC	0.01924
MF801418.1.MEX	0.01660	MF801406.1.MEX	0.01936
KY075936.1.USA	0.01674	KY014303.2.DOM	0.01938
KY785450.1.BRA	0.01681	KY014321.2.DOM	0.01942
KY559015.1.BRA	0.01689	KY014312.2.HND	0.01942
KY014319.2.HND	0.01690	MF801410.1.MEX	0.01943
KY558999.1.BRA	0.01698	MF801417.1.MEX	0.01943
MF801426.1.NIC	0.01714	KY325473.1.USA	0.01949
MF801403.1.MEX	0.01750	KY785418.1.HND	0.01973
MF801395.1.MEX	0.01758	KY014317.2.BRA	0.01973
KY075932.1.USA	0.01761	KY785465.1.DOM	0.01980
KY559013.1.BRA	0.01762	KY325472.1.USA	0.01984
KY325465.1.USA	0.01777	KY014295.2.USA	0.01984
KY325479.1.USA	0.01777	KY325468.1.USA	0.01984
MF801412.1.MEX	0.01778	KY014316.2.USA	0.01985
KY785415.1.DOM	0.01814	MF801398.1.MEX	0.01992
KX922704.1.USA	0.01819	KY325469.1.USA	0.01996
KY014325.2.USA	0.01819	MF434521.1.NIC	0.01996
KY785455.1.BRA	0.01825	KX702400.1.VEN	0.02001
KY014297.2.BRA	0.01831	KX893855.1.VEN	0.02001
MF801396.1.MEX	0.01832	MF801402.1.MEX	0.02002
KY785476.1.DOM	0.01839	KY075933.1.USA	0.02005
KY785445.1.USA	0.01841	KY785410.1.BRA	0.02012
KY014296.2.BRA	0.01842	KY075935.1.USA	0.02017

state of São Paulo. See Faria et al. (2017) [3]. These agglomerations are not necessarily evident from the figure built only with the Brazilian

TABLE 9. 2 of 3: Sequences of Zika ordered from top to bottom and from left to right, by the magnitude of  $\delta$ .

Sequence	$\delta$	Sequence	$\delta$
KY785442.1.HND	0.02031	KY785462.1.PRI	0.02980
KY785484.1.DOM	0.02052	KY559024.1.BRA	0.03148
KX842449.2.USA	0.02059	KY559023.1.BRA	0.03148
KX922703.1.USA	0.02059	KY559017.1.BRA	0.03161
KY785452.1.HND	0.02060	MF801423.1.MEX	0.03262
KY785479.1.BRA	0.02062	KY559003.1.BRA	0.03262
KX197192.1.BRA	0.02064	KY559006.1.BRA	0.03409
KY014300.2.DOM	0.02074	KY785470.1.DOM	0.03432
KY785433.1.BRA	0.02102	KY785412.1.USA	0.03673
KY014304.2.DOM	0.02112	KY785463.1.DOM	0.03697
MF434522.1.NIC	0.02118	KY559019.1.BRA	0.03848
MF434517.1.NIC	0.02160	KY559018.1.BRA	0.03849
MF801408.1.MEX	0.02172	KY014298.1.USA	0.03968
KY325464.1.USA	0.02198	MF434518.1.NIC	0.03979
KY785419.1.JAM	0.02199	KY785414.1.HND	0.04050
KY325476.1.USA	0.02199	KY014313.2.BRA	0.04116
KY325477.1.USA	0.02232	KY785424.1.JAM	0.04167
KY325467.1.USA	0.02251	KY559031.1.BRA	0.04571
KY014315.2.HND	0.02297	KY785437.1.BRA	0.04642
KY785448.1.HND	0.02322	KY559032.1.BRA	0.05038
KY785427.1.BRA	0.02322	KY559011.1.BRA	0.05433
KY785426.1.BRA	0.02358	KY014326.1.USA	0.05496
KY014301.2.BRA	0.02403	KY785430.1.JAM	0.05648
KY014327.2.HND	0.02423	MF801404.1.MEX	0.05702
KY785469.1.COL	0.02438	KY785413.1.DOM	0.05936
KY785423.1.DOM	0.02447	KY559010.1.BRA	0.06237
KY785456.1.BRA	0.02500	KY325471.1.USA	0.06359
KY785453.1.DOM	0.02516	KY785451.1.MTQ	0.07057
KY559012.1.BRA	0.02570	KY014308.2.BRA	0.07579
KY785459.1.USA	0.02607	KY559009.1.BRA	0.07588
KY014305.2.DOM	0.02613	MF801407.1.MEX	0.07824
KY559021.1.BRA	0.02614	KY559001.1.BRA	0.08650
MF438286.1.CUB	0.02638	KY559014.1.BRA	0.09922
KY785466.1.COL	0.02674	KY785474.1.USA	0.10512
KY785429.1.BRA	0.02902	KY785417.1.COL	0.10523

sequences. Group 2 is identified in figure 1, above and to the center, group 1 maintains together 5 of its sequences to the left of figure 1.

TABLE 10. 3 of 3: Sequences of Zika ordered from top to bottom and from left to right, by the magnitude of  $\delta$ .

Sequence	$\delta$	Sequence	$\delta$
KY325466.1.USA	0.10613	KY817930.1.BRA	0.14631
KY785447.1.DOM	0.11085	KY559004.1.BRA	0.15752
MF801420.1.MEX	0.11465	MF801409.1.MEX	0.16916
KY785461.1.HND	0.11535	KY785449.1.DOM	0.17585
KY785457.1.USA	0.11971	KY785439.1.BRA	0.19191
KY785432.1.JAM	0.12871	KY785444.1.HND	<b>0.19644</b>
MF434520.1.NIC	0.13332		

TABLE 11. From left to right: (a) Sequence, (b)  $\delta$  value, (c)  $\text{mean}_{s \in \mathcal{S}}\{d_s\}$ , (d)  $d$  value - definition 2.1 ii, (e)  $s^* = \text{argmax}_{s \in \mathcal{S}}\{d_s\}$ . (c) and (d) computed between the sequence KY014318.3.DOM and each one of the sequences (in column 1). Sequences ordered from top to bottom according to the magnitude of  $\delta$ , in an increasing way.

Sequence	$\delta$	$\text{mean}_{s \in \mathcal{S}}\{d_s\}$	$d$	$s^*$
MF434520.1.NIC	0.13332	0.03943	0.14646	gca
KY817930.1.BRA	0.14631	0.04429	0.13496	tca
KY559004.1.BRA	0.15752	0.02897	0.17008	gac
MF801409.1.MEX	0.16916	0.04576	0.16816	gta
KY785449.1.DOM	0.17585	0.02958	0.16905	ttt
KY785439.1.BRA	0.19191	0.02784	0.19038	gtt
KY785444.1.HND	0.19644	0.03869	0.18435	cga

Table 13 (14) shows the  $d$  values computed between the sequences

TABLE 12. From left to right: (a) Group 1 of Brazilian sequences, (b) Group 2 of Brazilian sequences; see figure 3.

Group 1 (from Rio de Janeiro)	Group 2 (from Tocantins and São Paulo)
KY785450.1, KY014297.2, KY785456.1	KY559021.1, KY559017.2, KY559023.1
KY785429.1, KY785479.1, KY785433.1	KY559024.1, KY559018.1, KY559019.1
KY785427.1, KY785426.1	KY559006.1, KY559012.1

of group 1 (2). According to the table 13 we observe a tendency to indicate the string *gac* as the one that provides the highest values of



TABLE 13.  $d$  values (definition 2.1 - ii) between the Brazilian sequences of group 1 - table 12,  $s^* = \operatorname{argmax}_{s \in \mathcal{S}} \{d_s\}$ .

$d(\text{KY014297.2}, \text{KY}j)$			$d(\text{KY785426.1}, \text{KY}j)$		
$j$	$d$	$s^*$	$j$	$d$	$s^*$
785426.1	0.04213	gac	785427.1	0.00860	cta
785427.1	0.01897	gac	785429.1	0.01269	gag
785429.1	0.02847	gac	785433.1	0.01060	gtt
785433.1	0.01999	gac	785450.1	0.02926	gac
785450.1	0.00438	cta	785456.1	0.01707	tcc
785456.1	0.01826	gac	785479.1	0.00877	agc
785479.1	0.03207	gac			
$d(\text{KY785427.1}, \text{KY}j)$			$d(\text{KY785429.1}, \text{KY}j)$		
$j$	$d$	$s^*$	$j$	$d$	$s^*$
785429.1	0.01193	tac	785433.1	0.01596	ctg
785433.1	0.00968	ctt	785450.1	0.01747	gac
785450.1	0.01036	gac	785456.1	0.01092	ggt
785456.1	0.01173	ctt	785479.1	0.01641	gag
785479.1	0.01006	act			
$d(\text{KY785433.1}, \text{KY}j)$			$d(\text{KY785450.1}, \text{KY}j)$		
$j$	$d$	$s^*$	$j$	$d$	$s^*$
785450.1	0.01065	gac	785456.1	0.01603	agc
785456.1	0.01110	ctg	785479.1	0.01948	gac
785479.1	0.00726	ctg			
$d(\text{KY785456.1}, \text{KY}j)$					
$j$	$d$	$s^*$			
785479.1	0.02378	tcc			

$d_s$ . On the other hand, table 14 shows a huge variety of strings that cause the highest values of  $d_s$ .

TABLE 14.  $d$  values (definition 2.1 - ii) between the Brazilian sequences of group 2 - table 12,  $s^* = \operatorname{argmax}_{s \in \mathcal{S}} \{d_s\}$ .

$d(\text{KY559006.1, KY5590}j)$			$d(\text{KY559012.1, KY5590}j)$		
$j$	$d$	$s^*$	$j$	$d$	$s^*$
12	0.01975	tgt	17	0.02990	cgt
17	0.02562	tgg	18	0.01990	gta
18	0.01521	cgg	19	0.01719	atc
19	0.01689	ggc	21	0.05089	cga
21	0.05219	cga	23	0.01892	cga
23	0.02234	cga	24	0.01499	gta
24	0.01169	gtt			
$d(\text{KY559017.1, KY5590}j)$			$d(\text{KY559018.1, KY5590}j)$		
$j$	$d$	$s^*$	$j$	$d$	$s^*$
18	0.02052	cgg	19	0.00348	cgg
19	0.01739	gta	21	0.02007	ctg
21	0.01733	tta	23	0.01460	aga
23	0.01756	aag	24	0.00767	atc
24	0.02262	gta			
$d(\text{KY559019.1, KY5590}j)$			$d(\text{KY559021.1, KY5590}j)$		
$j$	$d$	$s^*$	$j$	$d$	$s^*$
21	0.02519	ctg	23	0.02185	ctg
23	0.01460	aga	24	0.02779	ctg
24	0.00767	atc			
$d(\text{KY559023.1, KY5590}j)$					
$j$	$d$	$s^*$			
24	0.00715	aga			

## 5. Conclusions

By means of the notion  $d$  we establish the proximity between the DNA sequences of Zika, reported in table 1. From theoretical properties of  $d$ , and if the smallest sample size  $n = 10807$  is large enough, we can confirm that all the sequences can be considered as coming from the same stochastic process, since  $d < 1$  in all the cases, see García et al. (2018) [1]. This result is natural, since all the sequences are DNA sequences of Zika. Even more, our results go further, through  $\delta(\cdot)$  we have been able to determine the sequences that best represent the set of sequences. We observed three different scenarios: (a) Brazilian sequences, (b) North American sequences and (c) the set of 153 sequences listed in table 1, coming from 12 countries. Based on

these different settings, we are able to identify those sequences that are locally more representative and also those sequences that are locally considered less representative. In (a) the sample that could be taken as standard (KY558999.1) shows a value of  $\delta = 0.01894$ . In (b) the standard samples (KX922706.1, KY075936.1) expose a value of  $\delta = 0.01045$ . In the global comparison, (c) the standard sequence (KY014318.3.DOM) presents a value of  $\delta = 0.01456$ . Also, through  $\delta(\cdot)$  we identify the sequences that best represent the entire set. For example, in table 15 we report the three most representative sequences (all from the Dominican Republic (DOM)). Under the assumption of the

TABLE 15. Top three sequences of Zika, to best representing the set reported in table 1.

Sequence	$\delta$
KY014318.3.DOM	0.01456
KY785435.1.DOM	0.01502
KY785420.1.DOM	0.01543

existence of a majority law, and if at least 50% of the sequences are coming from that law, those all selected sequences follow the majority law, and can be considered as standard, in each setting. About the less representative sequences in the whole comparison, figure 3 and table 10 point to the seven sequences listed in table 11. We see that the values of  $\delta$  belong to the interval  $[0.13332, 0.19644]$ . As expected, all greater than the ones associated to the standard sequences. We note that three of these seven sequences are Brazilian sequences.

In this work we use a range of consistent criteria coming from stochastic processes, which allow to identify sequences that can be considered standard (and other rare or less representative). With this analysis we intend to show how tools from stochastic processes are suited to the problem of classifying sequences, in this case to define the reference or standard sequence. Identifying a sequence as a reference sequence is itself already useful for the analysis of genomic data, but having a way to classify the sequences according to its representativeness allows to build robust models with the usual techniques, only stablishing a threshold in the values of  $\delta$ , that select which samples will be used to build the model.

## References

- [1] Jesús E. García, R. Gholizadeh & V. A. González-López (2018). *A BIC-based Consistent Metric between Markovian Processes*, Applied Stochastic Models in Business and Industry (<https://doi.org/10.1002/asmb.2346>)

- [2] M. Fernández, Jesús E. García, R. Gholizadeh & V. A. González-López (2018). *Sample Selection Procedure in Daily Trading Volume Processes* (submitted)
- [3] N. R. Faria et al. (2017). Establishment and cryptic transmission of Zika virus in Brazil and the Americas. *Nature* **546** (7658), 406.
- [4] H. C.Metsky et al. (2017). Zika virus evolution and spread in the Americas. *Nature* **546** (7658), 411.
- [5] G. Schwarz (1978), Estimating the dimension of a model, *The annals of statistics* **6**(2), 461-464.

JESÚS E. GARCÍA: DEPARTMENT OF STATISTICS, UNIVERSITY OF CAMPINAS, CAMPINAS, SP, CEP 13083-859, BRAZIL  
*Email address:* `jg@ime.unicamp.br`

V.A. GONZÁLEZ-LÓPEZ: DEPARTMENT OF STATISTICS, UNIVERSITY OF CAMPINAS, CAMPINAS, SP, CEP: 13083-859, BRAZIL  
*Email address:* `veronica@ime.unicamp.br`

S.L MERCADO LONDOÑO: UNIVERSITY OF CAMPINAS, CAMPINAS, SP, CEP: 13083-859, BRAZIL

M.T.A. CORDEIRO: UNIVERSITY OF CAMPINAS, CAMPINAS, SP, CEP: 13083-859, BRAZIL

# Resampling procedures for a more reliable extremal index estimation

Dora Prata Gomes<sup>1</sup> and M. Manuela Neves<sup>2</sup>

<sup>1</sup> Faculdade de Ciências e Tecnologia and CMA, Universidade Nova de Lisboa, Lisboa, Portugal

(E-mail: [dsrp@fct.unl.pt](mailto:dsrp@fct.unl.pt))

<sup>2</sup> Instituto Superior de Agronomia and CEAUL, Universidade de Lisboa, Lisboa, Portugal

(E-mail: [manela@isa.ulisboa.pt](mailto:manela@isa.ulisboa.pt))

**Abstract.** Extreme value theory (EVT) deals essentially with the estimation of parameters of extreme or rare events. Extreme events are usually described as observations that exceed a high threshold. In many environmental and financial applications clusters of exceedances of that high threshold are of practical concern. One important parameter in EVT, which measures the amount of clustering in the extremes of a stationary sequence, is the extremal index. It needs to be adequately estimated, not only by itself but because its influence on other parameters, such as a high quantile, the return period, the expected shortfall. Some classical estimators of the extremal index and their asymptotic properties are revisited. The challenges that appear for finite samples are illustrated. Resampling procedures, such as generalized jackknife methodology, followed by an ‘adequate’ block-bootstrap procedure, are discussed and applied to improve the extremal index estimation. An extensive simulation study was performed and an application to financial data is shown.

**Keywords:** Block-bootstrap, Extremal Index, Extreme Value Theory, Generalized-Jackknife, Semi-parametric estimation.

## 1 Introduction and Motivation

Extreme Value Theory (EVT) is an area of increasingly vast applications in environmental problems. Many authors have presenting research in several areas where disastrous extreme events can occur, such as sea levels (Smith[28] and Tawn[31]); river flows (Gumbel[13], Gomes[9] and Reiss and Thomas[26]); pollution levels (Buishand[2] and Carter and Challenor[3]); wind speeds (Walshaw and Anderson[32]); air temperatures (Smith *et al.*[30] and Coles *et al.*[4]); precipitation levels (Coles and Tawn[5]); burned areas (Delgado *et al.*[7] and Schoenberg *et al.*[27]) and earthquake thermodynamics (Lavenda and Cipollone[17]).

In many practical applications extreme conditions often persist over several consecutive observations. Inference regarding clusters of exceedances over a high threshold needs to be properly performed to control the risk for hazardous events.

---

<sup>5</sup>*th* SMTDA Conference Proceedings, 12-15 June 2018, Chania, Creete, Greece

© 2018 ISAST



Under adequate general local and asymptotic dependence conditions, the limiting point process of exceedances of a high level  $u_n$ , after a suitable normalization is a homogeneous compound Poisson process with intensity  $\theta\tau$  and limiting cluster size distribution  $\pi$  (Hsing *et al.*[16]). That constant  $\theta$  is the extremal index and has an important role in extreme value theory for weakly dependent processes, reflecting the effect of clustering of extremes observation on the limiting distribution of the maximum.

Suppose that  $\{X_n\}_{n \geq 1}$  is a strictly stationary sequence of random variables with marginal distribution function  $F$ . This sequence is said to have an extremal index  $\theta \in (0, 1]$  if, for each  $\tau > 0$ , there exists a sequence of levels  $(u_n(\tau))_{n \in \mathbb{N}}$ , such that  $n[1 - F(u_n(\tau))] \xrightarrow[n \rightarrow \infty]{} \tau$  and

$$P\{M_{1,n} \leq u_n(\tau)\} \xrightarrow[n \rightarrow \infty]{} \exp(-\theta\tau), \quad (1)$$

where  $M_{1,n} = \max\{X_1, \dots, X_n\}$  (Leadbetter *et al.*[19]). When  $\theta = 1$  the exceedances of high thresholds tend to occur isolated, as in the independent context. If  $\theta < 1$  we have groups of exceedances in the limit. The *extremal index* is the quantity that measures the amount of clustering of the extremes in a stationary sequence.

Different probabilistic characterizations of  $\theta$  led to the definition of different estimators for  $\theta$ . Let us present a brief review of some of them.

- Maxima Characterization (Leadbetter *et al.*[19])

Let us consider that the strictly stationary sequence  $\{X_n\}_{n \geq 1}$  satisfies the  $D(u_n)$  condition of Leadbetter *et al.*[19], and has a marginal distribution function  $F$ . That  $D(u_n)$  condition limits the long-range dependence in the sequence. For large  $n$  and  $u_n$ , is valid the asymptotic equivalence

$$P\{M_{1,n} \leq u_n\} \approx F^{n\theta}(u_n). \quad (2)$$

If there exist normalizing constants  $a_n (> 0)$  and  $b_n$  such that  $F^n(a_n x + b_n) \xrightarrow[n \rightarrow \infty]{} G(x)$ , then  $G(x)$  is the distribution function of a *GEV* distribution, and

$$P\{M_{1,n} \leq u_n\} \xrightarrow[n \rightarrow \infty]{} H(x) = G^\theta(x). \quad (3)$$

$\theta$  is the key parameter for extending extreme value theory from independent and identically distributed random variables to stationary processes.

- Down-Crossings Characterization (O'Brien[23])

An alternative characterization of  $\theta$ , in terms of down-crossings, is given by O'Brien[23], for sequences that satisfy a weak mixing condition that locally restricts the occurrence of clusters

$$P\{M_{2,r_n} \leq u_n | X_1 > u_n\} \xrightarrow[n \rightarrow \infty]{} \theta, \quad (4)$$

where  $M_{2,r_n} = \max\{X_2, \dots, X_{r_n}\}$  and  $r_n$  determines a partition of the sample of length  $n$  such that  $r_n \rightarrow \infty$  and  $r_n = o(n)$ .

- Mean Cluster Size Characterization (Hsing *et al.*[16])

Under a mixing condition which is slightly stronger than  $D(u_n)$  those authors showed that the point process of exceedances converge weakly to a compound Poisson process, provided that  $n[1 - F(u_n(\tau))] \xrightarrow[n \rightarrow \infty]{} \tau$ . The distribution  $\pi_n(j; u_n, r_n)$  of the cluster sizes is given by

$$\pi_n(j; u_n, r_n) = P \left\{ \sum_{i=1}^{r_n} I(X_i > u_n) = j \mid \sum_{i=1}^{r_n} I(X_i > u_n) > 0 \right\}, \quad (5)$$

for  $j = 1, \dots, r_n$ ,  $r_n \rightarrow \infty$  and  $r_n = o(n)$ , and  $I(\cdot)$  denoting the indicator function. Under additional summability conditions on the  $\pi_n$ ,

$$\sum_{j \geq 1} j \pi_n(j; u_n, r_n) \xrightarrow[n \rightarrow \infty]{} \theta^{-1}, \quad (6)$$

i.e., the limiting mean number of exceedances of  $u_n$  in an interval of length  $r_n$  corresponds to the arithmetic inverse of the extremal index. So, we can write,

$$\theta^{-1} = \sum_{j \geq 1} j \pi(j). \quad (7)$$

## 2 Properties and difficulties of classical estimators

The way of identifying clusters of exceedances above a high threshold gave rise to different estimators. Identifying clusters by the occurrence of downcrossings or upcrossings led to the classical up-crossing estimator (*UC*-estimator),  $\hat{\Theta}^{UC}$  of Nandagopalan[21] and Gomes[8,9], defined as

$$\hat{\Theta}^{UC} \equiv \hat{\Theta}^{UC}(u_n) := \frac{\sum_{i=1}^{n-1} I(X_i \leq u_n < X_{i+1})}{\sum_{i=1}^n I(X_i > u_n)}, \quad (8)$$

for a suitable threshold  $u_n$ , where  $I(A)$  denotes, as usual, the indicator function of  $A$ . Consistency of this estimator is obtained provided that the high level  $u_n$  is a normalized level, i.e. if with  $\tau \equiv \tau_n$  fixed, the underlying d.f.  $F$  verifies

$$F(u_n) = 1 - \tau/n + o(1/n), \quad n \rightarrow \infty \quad \text{and} \quad \tau/n \rightarrow 0.$$

Two classical methods to define clusters are the blocks method and the runs method, Hsing[14,15]. The *blocks estimator*, is derived by dividing the data into approximately  $k_n$  blocks of length  $r_n$ , where  $n \approx k_n \times r_n$ , i.e., considering  $k_n = \lfloor n/r_n \rfloor$ . Each block is treated as one cluster and the number of blocks in which there is at least one exceedance of the threshold  $u_n$  is counted. The *blocks estimator*,  $\hat{\Theta}_n^B(u_n)$ , is then defined as:

$$\hat{\Theta}_n^B(u_n) := \frac{\sum_{i=1}^{k_n} I(\max(X_{(i-1)r_n+1}, \dots, X_{ir_n}) > u_n)}{\sum_{i=1}^n I(X_i > u_n)}. \quad (9)$$

If we assume that a cluster consists of a run of observations between two exceedances, then the *runs estimator* is defined as:

$$\hat{\Theta}_n^R(u_n) := \frac{\sum_{i=1}^n I(X_i > u_n, \max(X_{i+1}, \dots, X_{i+r_n-1}) \leq u_n)}{\sum_{i=1}^n I(X_i > u_n)}. \quad (10)$$

Under mild conditions,  $\lim_{n \rightarrow \infty} \theta_n^B = \lim_{n \rightarrow \infty} \theta_n^R = \theta$ . Other properties of these estimators have been well studied by Smith and Weissman[29] and Weissman and Novak[33].

Although showing very nice properties, those estimators present several difficulties for finite samples. Indeed they present the usual drawback common to most semi-parametric estimators: they are strongly dependent on the threshold, with the usual bias-variance trade-off. To modify those estimators in order to obtain more stable and reliable path estimates became a topic of intense research. Here, some procedures based on resampling methods are reviewed and improved.

### 3 Resampling procedures in extremal index estimation. A simulation study

In this paper our attention will be focused on the *UC*-estimator, in (8). Given the sample  $\mathbf{X}_n := (X_1, \dots, X_n)$  and the associated ascending order statistics,  $X_{1:n} \leq \dots \leq X_{n:n}$ , we shall consider the level  $u_n$  as a deterministic level  $u \in [X_{n-k:n}, X_{n-k+1:n}]$ .

The *UC*-estimator, can now be written as a function of  $k$ , the number of top order statistics above the chosen threshold,

$$\hat{\Theta}^{UC} \equiv \hat{\Theta}^{UC}(k) := \frac{1}{k} \sum_{i=1}^{n-1} I(X_i \leq X_{n-k:n} < X_{i+1}). \quad (11)$$

For many dependent structures, the bias of  $\hat{\Theta}^{UC}(k)$  has two dominant components of orders  $k/n$  and  $1/k$ , see Gomes *et al.*[11],

$$\text{Bias}[\hat{\Theta}^{UC}(k)] = \varphi_1(\theta) \left(\frac{k}{n}\right) + \varphi_2(\theta) \left(\frac{1}{k}\right) + o\left(\frac{k}{n}\right) + o\left(\frac{1}{k}\right), \quad (12)$$

whenever  $n \rightarrow \infty$  and  $k \equiv k(n) \rightarrow \infty$ ,  $k = o(n)$ .

The Generalized Jackknife methodology, Gray and Schucany[12] has the properties of estimating the bias and the variance of any estimator, leading to the development of estimators with bias and mean squared error often smaller than those of an initial set of estimators.

The Generalized Jackknife methodology states that if the bias has two main terms that we would like to reduce, we need to have access to three estimators, with the same type of bias.

**Definition** (Gray and Schucany[12]) Given three biased estimators of  $\theta$ ,  $T_n^{(1)}$ ,  $T_n^{(2)}$  and  $T_n^{(3)}$  such that

$$E[T_n^{(i)} - \theta] = b_1(\theta)\varphi_1^{(i)}(n) + b_2(\theta)\varphi_2^{(i)}(n) \quad i = 1, 2, 3,$$

the generalized jackknife statistic (of order 2) is given by

$$T_n^{GJ} := \frac{\begin{vmatrix} T_n^{(1)} & T_n^{(2)} & T_n^{(3)} \\ \varphi_1^{(1)}(n) & \varphi_1^{(2)}(n) & \varphi_1^{(3)}(n) \\ \varphi_2^{(1)}(n) & \varphi_2^{(2)}(n) & \varphi_2^{(3)}(n) \end{vmatrix}}{\begin{vmatrix} 1 & 2 & 3 \\ \varphi_1^{(1)}(n) & \varphi_1^{(2)}(n) & \varphi_1^{(3)}(n) \\ \varphi_2^{(1)}(n) & \varphi_2^{(2)}(n) & \varphi_2^{(3)}(n) \end{vmatrix}}$$

Using the information obtained from (12) and based on the estimator  $\widehat{\Theta}^{UC}$  computed at the three levels,  $k$ ,  $[\delta k] + 1$  and  $[\delta^2 k] + 1$ , where  $[x]$  denotes, as usual, the integer part of  $x$ , Gomes *et al.*[11] proposed a class of Generalized Jackknife estimators, depending on a tuning parameter  $\delta$ ,  $0 < \delta < 1$ ,  $\widehat{\Theta}^{GJ(\delta)}$ , defined as

$$\widehat{\Theta}^{GJ(\delta)} \equiv \widehat{\Theta}^{GJ(\delta)}(k) := \frac{(\delta^2 + 1)\widehat{\Theta}^{UC}([\delta k] + 1) - \delta(\widehat{\Theta}^{UC}([\delta^2 k] + 1) + \widehat{\Theta}^{UC}(k))}{(1 - \delta)^2}. \quad (13)$$

This is an asymptotically unbiased estimator of  $\theta$ , in the sense that it can remove the two dominant components of bias referred to in (12). Under certain conditions, estimators  $\widehat{\Theta}^{UC}$  and  $\widehat{\Theta}^{GJ}$  are consistent and asymptotically normal if  $\theta < 1$ , see Nandagopalan[21] and Gomes *et al.*[11].

For illustrating the properties of the  $\widehat{\Theta}^{UC}$  and  $\widehat{\Theta}^{GJ(\delta)}$  estimators, let us consider the following max-autoregressive process:

- *Max-Autoregressive Process:* Let  $\{Z_n\}_{n \geq 1}$  be a sequence of independent, unit- Fréchet distributed random variables and  $Y_0$  a random variable with d.f.  $H_0(y) = \exp(-y^{-1}(\beta^{-1} - 1))$ . For  $0 < \beta < 1$ , let

$$Y_j = \beta \max\{Y_{j-1}, Z_j\}, \quad j = 1, 2, \dots \quad (14)$$

The extremal index of this process is  $\theta = 1 - \beta$ , Alpuim[1].

A Monte-Carlo simulation for the mean value and the mean squared error (MSE) of the *Up-Crossing estimator*,  $\widehat{\Theta}^{UC}$ , and the *Generalized Jackknife estimators*,  $\widehat{\Theta}^{GJ(\delta)}$ , for some values of  $\delta$  ( $\delta = 0.05$  (0.05) 0.95) and several values of  $\theta$  was performed. Some of results obtained are shown in Figures 1, 2 and 3. For this sample and also for other models considered the best values for mean values and mean squared error were obtained with  $\delta = 0.1$  and  $\delta = 0.25$ , depending on the level  $k$  chosen.

## 4 Some overall comments

- EVT is now a statistical domain that has revealing a great interest and a strong development, motivated for the challenges put by relevant and recent applications.

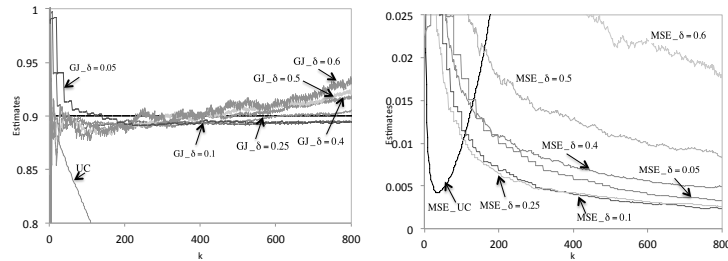


**Fig. 1.** Simulated of mean values and MSE of  $\hat{\Theta}^{UC}$  and  $\hat{\Theta}^{GJ(\delta)}$  with  $\delta = 0.05, 0.1, 0.25, 0.4, 0.5$  and  $0.6$  for max-autoregressive processes with  $\theta = 0.9$ , for samples of size  $n = 1000$  and 1000 replicates.

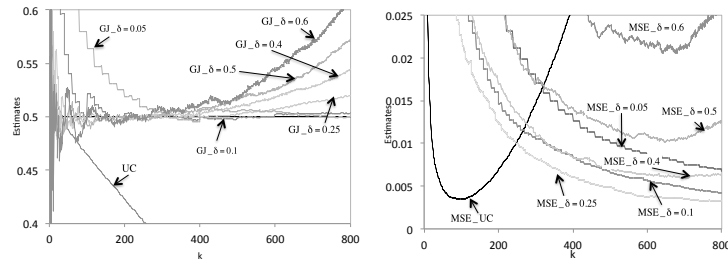


**Fig. 2.** Simulated of mean values and MSE of  $\hat{\Theta}^{UC}$  and  $\hat{\Theta}^{GJ(\delta)}$  with  $\delta = 0.05, 0.1, 0.25, 0.4, 0.5$  and  $0.6$  for max-autoregressive processes with  $\theta = 0.5$ , for samples of size  $n = 1000$  and 1000 replicates.

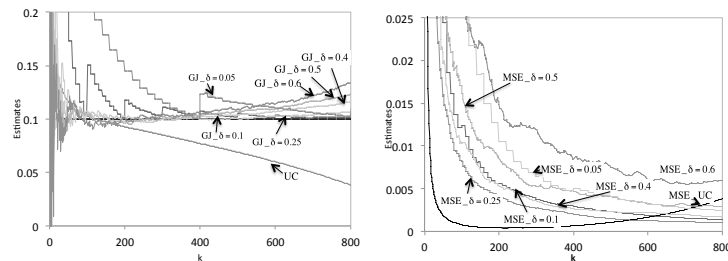


**Fig. 3.** Simulated of mean values and MSE of  $\hat{\Theta}^{UC}$  and  $\hat{\Theta}^{GJ(\delta)}$  with  $\delta = 0.05, 0.1, 0.25, 0.4, 0.5$  and  $0.6$  for max-autoregressive processes with  $\theta = 0.1$ , for samples of size  $n = 1000$  and 1000 replicates.

- In the semi-parametric approach, topics as the threshold selection and the bias reduction as well as the search for stable and reliable sample paths continue motivating intense research.
- Resampling methodologies, that need to be adapted when dealing with extremes are revealing promising results.
- To illustrate the application of the aforementioned resampling procedures an extensive simulation study, considering several models was performed.
- Those procedures were also applied to some real data sets.

- For a given sample, the choice of  $\delta$  was performed on basis of some stability criterion, as that one described in Neves *et al.*[22]. Once obtained the Generalized-Jackknife estimates a block-bootstrap procedure, as that one described in Prata Gomes and Neves[25] was applied to get a smoother path. In that work only the case  $\delta = 0.25$  was considered.

**Acknowledgement:** Research partially supported by National Funds through FCT – Fundação para a Ciência e a Tecnologia, projects PEst-OE/MAT/UI0006/2013 (CEAUL) and UID/MAT/00297/2013 (CMA).

## References

1. T. Alpuim. An extremal markovian sequence, *J. Appl. Probab.*, **26**, 219–232, 1989.
2. A. Buishand. *Statistics of extremes in climatology*, Statistica Neerlandica, **43**, 1-30, 1989.
3. T. Carter and G. Challenor. Estimating return values of environmental parameters, *Quarterly Journal of the Royal Meteorological Society*, **107**, 259-266, 1981.
4. S. Coles, J. Tawn, and R. Smith. A sazonal Markov model for extremely low temperatures, *Environmetrics*, **5**, 221-339, 1994.
5. S. Coles and J. Tawn. A Bayesian analysis of extreme rainfall data. *Appl. Stat.*, **45**, 463-478, 1996.
6. A. Davidson. *Statistics of Extremes*, Courses 2011–2012, École Polytechnique Fédérale de Lausanne (EPFL), 2011.
7. R. Díaz-Delgado, F. Lloret, X. Pons. Spatial patterns of fire occurrence in Catalonia, NE, Spain, *Landscape Ecol.*, **19**, **7**, 731-745, 2004.
8. M. I. Gomes. Statistical inference in an extremal markovian model, *COMPSTAT*, 257–262, 1990.
9. M. I. Gomes. On the estimation of parameters of rare events in environmental time series. *Statistics for the Environment (Barnett et. al. eds.)*, 226–241, 1993.
10. M. I. Gomes, A. Hall and C. Miranda. Subsampling techniques and the Jackknife methodology in the estimation of the extremal index. *J. Comput. Statist. and Data Analysis*, **52**, **4**, 2022-2041, 2008.
11. M. I. Gomes, M. J. Martins and M. Neves. Generalised Jackknife-based estimators for univariate extreme-value modeling, *Comm. Statist. Theory Methods*, **42**, **7**, 1227-1245, 2013.
12. H. Gray and W. Schucany. *The Generalized Jackknife Statistic*, Marcel Dekker. New York, 1972.
13. E. Gumbel. *Statistics of Extremes*, Columbia, University Press, New York, 1958.
14. T. Hsing. Estimating the parameters of rare events. *Stoch. Proces. Appl.*, **37**, 117–39, 1991.
15. T. Hsing. Extremal index estimation for a weekly dependent stationary sequence, *Ann. Statist.*, **21**, 2043–2071, 1993.
16. T. Hsing, J. Husler and M. Leadbetter. On exceedance point process for a stationary sequence, *Probab. Theory Related Fields*, **78**, 97-112, 1988.
17. B. Lavanda and E. Cipollone. Extreme value statistics and thermodynamics of earthquakes: aftershock sequences, *Annali di geofisica*, **43**, **5**, 967-982, 2000.
18. M. Leadbetter. Extremes and local dependence in stationary sequences. *Z. Wahrsch. Verw. Gebiete*, **65**, **2**, 291-306, 1983.
19. M. Leadbetter, G. Lindgren and H. Rootzén. *Extremes and related properties of random sequences and series*. Springer-Verlag, New York, 1983.

20. M. Leadbetter and L. Nandagopalan. *On exceedance point process for stationary sequences under mild oscillation restrictions*. In Extreme Value Theory: Proceedings, Oberwolfach 1987, ed J. Hüsler and R. D. Reiss, Lecture Notes in Statistics **51**, 69-80, Springer-Verlag, Berlin, 1989.
21. S. Nandagopalan. *Multivariate Extremes and Estimation of the Extremal Index*, PhD Thesis, University of North Carolina, Chapel Hill, 1990.
22. M. Neves, M. I. Gomes, F. Figueiredo and D. Prata Gomes. Modeling Extreme Events: Sample Fraction Adaptive Choice in Parameter Estimation. *J. Stat. Theory Pract.*, **9**, **1**, 184-199, 2015.
23. G. O'Brien. Extreme values for stationary and Markov sequences. *Ann. Probab.*, **15**, 281-291, 1987.
24. D. Prata Gomes and M. Neves. Bootstrap and other resampling methodologies in Statistics of Extremes, *Communications in Statistics-Simulation and Computation*, **44**, **10**, 2592-2607, 2015.
25. D. Prata Gomes and M. Neves. Revisiting resampling methods in the extremal index estimation: improving risk assessment", In T.A. Oliveira, C. Kitsos, A. Oliveira and L.M. Grilo (eds.), *Recent Studies on Risk Analysis and Statistical Modeling*, Springer International Publishing. *To appear*.
26. D. Reiss and M. Thomas. *Statistical Analysis of Extreme Values, with Application to Insurance, Finance, Hydrology and Other Fields*, Birkhäuser Verlag, 1997.
27. F. Schoenberg, R. Peng, Z. Huang and P. Rundel. Detection of nonlinearities in the dependence of burn area on fuel age and climatic variables. *Int. J. Wildland Fire*, **12**, **1**, 1-10, 2003.
28. R. Smith. Extreme value theory based on the  $r$  largest annual events. *J. Hydrol.*, **86**, 27-43, 1986.
29. R. Smith and I. Weissman. Estimating the extremal index, *J. R. Statist. Soc. B*, **56**, 515-528, 1994.
30. M. Smith, V. Malathy Devi, D. Benner and C. Rinsland. Temperature dependence of air-broadening and shift coefficients of  $O_3$  lines in the  $\nu_1$  band, *J. Mol. Spectrosc.*, **182**, 239-259, 1997.
31. J. Tawn. An extreme value theory model for dependent observations. *J. Hydrol.*, **101**, 227-250, 1988.
32. D. Walshaw and C. W. Anderson. A model for extreme wind gusts. *Journal of the Royal Statistical Society, Series C (Applied Statistics)*, **49**, 499-508, 2000.
33. I. Weissman and S. Novak. On blocks and runs estimators of the extremal index, *Journal of Statistical Planning and Inference*, **66**, 281-288, 1998.

# Generalizations of Poisson Process in The Modeling of Random Processes Related to Road Accidents

Franciszek Grabski

Polish Naval Academy, Department of Mathematics and Physics

e-mail: F.Grabski@amw.gdynia.pl

**Abstract.** The stochastic processes theory provides concepts and theorems that allow to build probabilistic models concerning accidents. So called counting process can be applied for modelling the number of road, sea and railway accidents in the given time intervals. A crucial role in construction of the models plays a Poisson process and its generalizations. The nonhomogeneous Poisson process and corresponding nonhomogeneous compound Poisson process are applied for modeling the road accidents number and number of injured and killed people in Polish road. To estimate model parameters were used data coming from the annual reports of the Polish police.

**Keywords:** Nonhomogeneous Poisson process, nonhomogeneous compound Poisson process

## 1 Introduction

A Poisson distribution is given by the rule:

$$p(k) = \frac{(\Lambda)^k}{k!} e^{-\Lambda}, \quad k \in S = \{0, 1, 2, \dots\}, \quad \Lambda > 0.$$

In 1837 Simeon-Denis Poisson derived this distribution to approximate the Binomial Distribution when a parameter  $p$ , determining the probability of success in a single experiment, is small. Application of this distribution was not found; when von Bortkiewitsch (1898) calculated from the data of the Prussian army the number of soldiers who died during the 20 consecutive years because of the kick by a horse. A random variable, say  $X$ , denoting the number of soldiers killed accidentally by the horse kick per year, turned out to have Poisson distribution

$$p(k) = P(X = k) = \frac{(\Lambda)^k}{k!} e^{-\Lambda}, \quad k \in S.$$

with parameter  $\Lambda = 0.61 \left[ \frac{1}{\text{year}} \right]$ .

Since then Poisson's distribution and its associated Poisson process have found use in various fields of science and technology. A Poisson process and its extensions are used in safety and reliability problems. They allow to construct the number of road, sea and railway accidents in the given time intervals. A nonhomogeneous Poisson process in modelling accidents number in Baltic Sea and Seaports was presented in the conference Summer Safety and Reliability Seminars 2017 and is published in Journal of Polish Safety and Reliability



Association [4]. The nonhomogenous compound Poisson process enables to anticipate to anticipate numbers of the injured people and fatalities. In the elaboration of the theoretical part of the paper, book [1] and papers [2], [4], [5] were used.

## 2 Nonhomogeneous Poisson process

Let

$$\tau_0 = \vartheta_0 = 0, \quad \tau_n = \vartheta_1 + \vartheta_2 + \dots + \vartheta_n, \quad n \in \mathbb{N}, \quad (1)$$

where  $\vartheta_1, \vartheta_2, \dots, \vartheta_n$  are positive independent and identical distributed random variables. Let

$$\tau_\infty = \lim_{n \rightarrow \infty} \tau_n = \sup\{\tau_n: n \in \mathbb{N}_0\}. \quad (2)$$

A stochastic process  $\{N(t): t \geq 0\}$  defined by the formula

$$N(t) = \sup\{n \in \mathbb{N}_0: \tau_n \leq t\} \quad (3)$$

is called a *counting process* corresponding to a random sequence  $\{\tau_n: n \in \mathbb{N}_0\}$ .

Let  $\{N(t): t \geq 0\}$  be a stochastic process taking values on  $S = \{0,1,2, \dots\}$ , value of which represents the number of events in a time interval  $[0, t]$ .

A *counting process*  $\{N(t): t \geq 0\}$  is said to be *nonhomogeneous Poisson process* (NPP) with an intensity function  $\lambda(t) \geq 0, t \geq 0$ , if

1.  $P(N(0) = 0) = 1$ ; (4)
2. The process  $\{N(t): t \geq 0\}$  is the stochastic process with independent increments, the right continuous and piecewise constant trajectories;

$$3. \quad P(N(t+h) - N(t) = k) = \frac{\left(\int_t^{t+h} \lambda(x) dx\right)^k}{k!} e^{-\int_t^{t+h} \lambda(x) dx}; \quad (5)$$

From this definition it follows that the one dimensional distribution of NPP is given by the rule

$$P(N(t) = k) = \frac{\left(\int_0^t \lambda(x) dx\right)^k}{k!} e^{-\int_0^t \lambda(x) dx}, \quad k = 0,1,2, \dots \quad (6)$$

The expectation and variance of NPP are the functions

$$\Lambda(t) = E[N(t)] = \int_0^t \lambda(x) dx, \quad V(t) = V[N(t)] = \int_0^t \lambda(x) dx, \quad t \geq 0. \quad (7)$$

The corresponding standard deviation is

$$D(t) = \sqrt{V[N(t)]} = \sqrt{\int_0^t \lambda(x) dx}, \quad t \geq 0. \quad (8)$$

The expected value of the increment  $N(t+h) - N(t)$  is

$$\Delta(t; h) = E(N(t + h) - N(t)) = \int_t^{t+h} \lambda(x) dx. \quad (9)$$

The corresponding standard deviation is

$$D(t; h) = D(N(t + h) - N(t)) = \sqrt{\int_t^{t+h} \lambda(x) dx} \quad (10)$$

An nonhomogeneous Poisson process with  $\lambda(t) = \lambda$ ,  $t \geq 0$  for each  $t \geq 0$ , is a regular Poisson process. The increments of an nonhomogeneous Poisson process are independent, but not necessarily stationary. A nonhomogeneous Poisson process is a Markov process.

### 3 Model of the road accidents number in Poland

Table 1 show the number of road accidents and their effects in Poland in years 2010-2016. The data coming from the annual Police's report [ 3 ].

Table 1. The number of road accidents and their effects in Poland in years 2010-2016

Year	Accidents number	Killed	Injured
2010	38 832	3 907	48 952
2011	40 065	4 189	49 501
2012	37 046	3 571	45 792
2013	35 046	3 357	44 059
2014	34 970	3 202	42 545
2015	32 967	2 938	39 778
2016	33 664	3 026	40 766

Let  $\{N(t); t \geq 0\}$  be a stochastic process taking values on  $S = \{0,1,2, \dots\}$ . A value of the process represents the number of the road accidents in Poland in a time interval  $[0, t]$ . Due to the nature of these events, pre-assumption that it is a nonhomogeneous Poisson process with some parameter  $\lambda(t) > 0$ , seems to be justified. The expected value of increment of this process is given by (9), while its one dimensional distribution is determined by (6). We can use practically these rules if will known the intensity function  $\lambda(t) > 0$ .

#### 3.1 Estimation of model parameters

Dividing the number of accidents in each year by 365 or 366 we get the intensity in units of  $[1 / \text{day}]$ . The results are shown in Table 2. Figure 1 shows the empirical intensity of the cars accidents.

Table 2. The road accidents in Poland in years 2010-2016

Year	Interval	Centres of interval	Number of accidents	Intensity [nb.ac./day]
2010	[0, 365)	182,5	38 832	106,38
2011	[365, 730)	547,5	40 065	109,77
2012	[730, 1096)	913	37 046	101,22
2013	[1096, 1461)	1278,5	35 046	93,02
2014	[1461, 1826)	1643,5	34 970	95,48
2015	[1826, 2201)	2008,5	32 967	90,32
2016	[2201, 2567)	2384	33 664	91,98

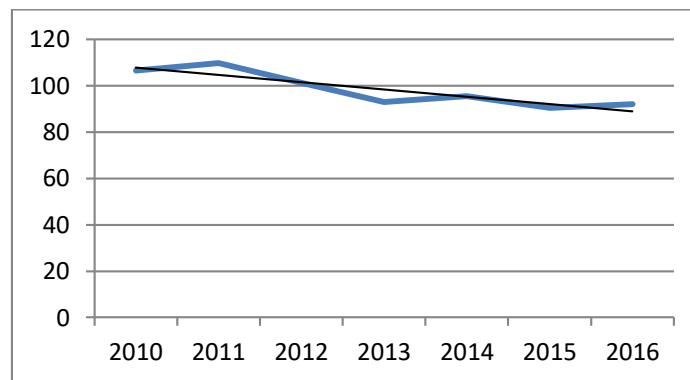


Fig. 1. The empirical intensity of the road accidents

To define the intensity function  $\lambda(t), t \geq 0$  we utilize information presented in table 2. The statistical analysis of the data shows that the empirical intensity can be approximated by the linear function  $\lambda(t) = at + b$ .

Using EXCEL system to find a linear regression function, we obtain the values of parameters  $a$  and  $b$  :

$$a = -0.00857, \quad b = 116.3167.$$

Therefore the linear intensity of accidents is

$$\lambda(x) = -0.00857x + 116.3167, \quad x \geq 0 \quad (11)$$

From (7) we have

$$\Lambda(t) = \int_0^t (-0.00857x + 116.3167) dx.$$

Hence we obtain

$$\Lambda(t) = -0.004285 t^2 + 116.3167t, \quad t \geq 0. \quad (12)$$

From (6) and (7) we obtain one dimensional distribution of NPP denoting the number of road accidents.

$$P(N(t) = k) = \frac{(\Lambda(t))^k}{k!} e^{-\Lambda(t)}, \quad k = 0, 1, 2, \dots \quad (13)$$

### 3.2 Anticipation of the accident number

Let us recall that

$$P(N(t+h) - N(t) = k) = \frac{[\Lambda(t+h) - \Lambda(t)]^k}{k!} e^{-[\Lambda(t+h) - \Lambda(t)]}. \quad (14)$$

It means that we can anticipate number of accidents at any time interval with a length of  $h$ . The expected value of an increment  $N(t+h) - N(t)$  is defined by (9). For the function  $\Lambda(t) = a \frac{t^2}{2} + b t$ ,  $t \geq 0$  we obtain the expected value of accidents in the time interval  $[t, t+h]$

$$E(N(t+h) - N(t)) = \Delta(t; h) = h \left( \frac{a h}{2} + b + a t \right). \quad (15)$$

The corresponding standard deviation is

$$D(t; h) = \sqrt{h \left( \frac{a h}{2} + b + a t \right)}. \quad (16)$$

#### Example 1

We want to anticipate the number of road accidents in Poland from June 1, 2017 to September 30, 2017. We also want to calculate the probability of a given number of that kind of accidents. Using the formula (15) we obtain the expected value of road accidents from June 1, 2017 to September 30, 2017. The intensity function  $\lambda(t) = -0,00857t + 116,3167$ , in year 2017 takes arguments from the interval  $[2567, 2932]$ . From January 1 of 2017 to June 1 of 2017 have passed 151 days. Hence  $t = 2567 + 151 = 2718$ . From June 1 to September 30 have passed  $h = 122$  days. For these parameters, using (15) and (16), we obtain

$$\Delta(t; h) = 11442,96, \quad D(t; h) = 106,97.$$

This means that the average predicted number of the road accidents between June 1, 2017 and September 30, 2017 will be about 11443 with a standard deviation about 107. For example, probability that the number of accidents in this time interval will be not greater than  $d=11600$  and not less than  $c=11200$  is

$$P_{9500 \leq k \leq 10000} = P(11200 \leq N(t+h) - N(t) \leq 11600) =$$

$$= \sum_{k=11200}^{k=11600} \frac{11442,96^k}{k!} e^{-11442,96}.$$

Applying approximation by the standard normal distribution we get

$$P_{11200 \leq k \leq 11600} \cong \Phi\left(\frac{11600-1144,96}{106,97}\right) - \Phi\left(\frac{11200-1144,96}{106,97}\right) \approx 0,9173 .$$

#### 4 Nonhomogeneous Compound Poisson Process

We assume that  $\{N(t): t \geq 0\}$  is a *nonhomogeneous Poisson process* (NPP) with an intensity function  $\lambda(t)$ ,  $t \geq 0$  such that  $\lambda(t) \geq 0$  for  $t \geq 0$ , and  $X_1, X_2, \dots$  is a sequence of the independent and identically distributed (i.i.d.) random variables independent of  $\{N(t): t \geq 0\}$ . A stochastic process

$$X(t) = X_1 + X_2 + \dots + X_{N(t)}, \quad t \geq 0 \quad (17)$$

is said to be a *nonhomogeneous compound Poisson process* (NCPP).

##### Proposition 1

Let  $\{X(t): t \geq 0\}$  be a *nonhomogeneous compound Poisson process* (NCPP).

If  $E(X_1^2) < \infty$ , then

$$1. \quad E[X(t)] = \Lambda(t) E(X_1) \quad (18)$$

$$2. \quad V[X(t)] = \Lambda(t) E(X_1^2), \quad (19)$$

where

$$\Lambda(t) = E[N(t)] = \int_0^t \lambda(x) dx.$$

**P r o o f:** Applying property of conditional expectation

$$E[X(t)] = E[E(X(t)|N(t))]$$

we have

$$E[E(X(t)|N(t))] = E\left(E(X_1 + X_2 + \dots + X_{N(t)}) \middle| N(t)\right) =$$

$$\sum_{n=0}^{\infty} E((X_1 + X_2 + \dots + X_n)P(N(t) = n)) = \sum_{n=0}^{\infty} E(X_1) n P(N(t) = n)$$

$$= E(X_1)E(N(t)) = \Lambda(t) E(X_1)$$

Using the formula

$$V[X(t)] = E[V(X(t)|N(t))] + V[E(X(t)|N(t))]$$

we get

$$\begin{aligned} E[V(X(t)|N(t))] &= E\left(V(X_1 + X_2 + \dots + X_{N(t)}) \middle| N(t)\right) = \\ &= \sum_{n=0}^{\infty} V(X_1 + X_2 + \dots + X_{N(t)} | N(t) = n) P(N(t) = n) = \\ &= \sum_{n=0}^{\infty} V(X_1 + X_2 + \dots + X_n) P(N(t) = n) = \\ &= \sum_{n=0}^{\infty} V(X_1) n P(N(t) = n) = V(X_1) E(N(t)) = V(X_1) \Lambda(t), \\ V[E(X(t)|N(t))] &= V\left(E(X_1 + X_2 + \dots + X_{N(t)}) \middle| N(t)\right) = \\ &= V(E(X_1)N(t)) = (E(X_1))^2 V(N(t)) = (E(X_1))^2 \Lambda(t). \end{aligned}$$

Therefore

$$\begin{aligned} V[X(t)] &= V(X_1) \Lambda(t) + (E(X_1))^2 \Lambda(t) = \Lambda(t) [E(X_1^2) - (E(X_1))^2 + (E(X_1))^2] = \\ &= \Lambda(t) E(X_1^2). \end{aligned}$$

### Corollary 1

Let  $\{X(t+h) - X(t): t \geq 0\}$  be an increment of *nonhomogeneous compound Poisson process* (NCP).

If  $E(X_1^2) < \infty$ , then

$$E[X(t+h) - X(t)] = \Delta(t; h) E(X_1), \quad (20)$$

$$V[X(t+h) - X(t)] = \Delta(t; h) E(X_1^2), \quad (21)$$

where

$$\Delta(t; h) = \int_t^{t+h} \lambda(x) dx. \quad (22)$$

### Proposition 2

If  $\{N(t): t \geq 0\}$  is a *nonhomogeneous Poisson process* (NPP) with an intensity function  $\lambda(t)$ ,  $t \geq 0$  such that  $\lambda(t) \geq 0$  for  $t \geq 0$ , then cumulative distribution function (CDF) of the *nonhomogeneous compound Poisson process* (NCP) is given by the rule

$$G(x, t) = I_{[0, \infty)}(x) e^{-\Lambda(t)} + \sum_{k=1}^{\infty} p(k; t) F_X^{(k)}(x), \quad (23)$$

where

$F_X^{(k)}(x)$  denotes the  $k$ -fold convolution of CDF of the random variables  $X_i$ ,  $i=1, 2, \dots$  and

$$p(k; t) = \frac{(\Lambda(t))^k}{k!} e^{-\Lambda(t)}, \quad t \geq 0, \quad k = 0, 1, \dots, \quad (24)$$

$$\Lambda(t) = E[N(t)] = \int_0^t \lambda(x) dx. \quad (25)$$

**P r o o f:** Using the total probability law we obtain cumulative distribution function (CDF) of NCPP.

$$\begin{aligned} G(x, t) &= P(X(t) \leq x) = P(X_1 + X_2 + \dots + X_{N(t)} \leq x) = \\ &= \sum_{k=0}^{\infty} P(X_1 + \dots + X_{N(t)} \leq x | N(t) = k) P(N(t) = k) = \\ &= \sum_{k=0}^{\infty} p(k; t) F_X^{(k)}(x) = I_{[0, \infty)}(x) e^{-\Lambda(t)} + \sum_{k=1}^{\infty} p(k; t) F_X^{(k)}(x). \end{aligned}$$

### Corollary 3

If the random variables  $X_i, i=1,2,\dots$  have a discrete probability function  $p_X(x) = P(X = x), x \in S$ , then the discrete distribution function of NCPP is given by the rule

$$g(x, t) = \sum_{k=1}^{\infty} p(k; t) p_X^{(k)}(x), \quad , \quad t > 0 \quad (26)$$

where  $p_X^{(k)}(x)$  denotes  $k$ -fold convolution of the discrete probability distribution  $p_X(x), x = 0, 1, 2, \dots$  of the random variable  $X$ .

### Illustrative example

We assume

$$p_X(x) = \frac{\mu^x}{x!} e^{-\mu}, \quad x = 0, 1, 2, \dots \quad \text{and} \quad p(k; t) = \frac{(\Lambda(t))^k}{k!} e^{-\Lambda(t)}, \quad k = 0, 1, 2, \dots,$$

where  $\Lambda(t) = -0.00000054 t^2 + 0,36t$  and  $\mu = 0,054$ . Using MATHEMATICA computer system, we get values of the probability ditribution of NCPP. Utilazing equality (26) for  $t = 4000$  we obtain resut that is shown in table 3 and figure 3.

Table 3. The values of the discrete probability ditribution of NCPP

$x$	0	1	2	3	4
$g(x, 4000)$	0,111263	0,23754	0,26022	0,194776	0,111938
$x$	5	6	7	8	9
$g(x, 4000)$	0,0526309	0,0210693	0,0073802	0,00230735	0,0006535

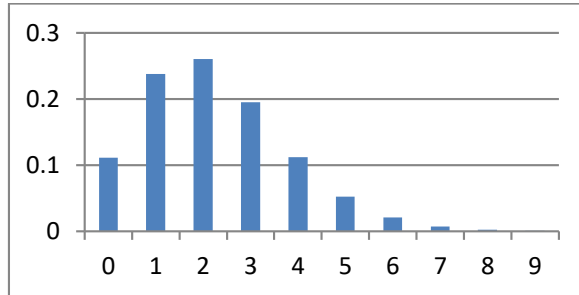


Figure 3. A discrete probability distribution of NCPP corresponding to Table 1

## 5 Data Analysis

In addition to the data presented in Table 1, Table 3 contain the frequency of fatalities and injured people with respect to the road accident in Poland in years 2010-2016. Figure 2 and Figure 3 show that the frequency of fatalities and injured people with respect to the road accident have a decreasing trend over time.

Table 3. Frequency of fatalities and injured people with respect to the accident

Year	Accidents number	Fatalities	Injured	Fatalities	Injured
				Accd.nb.	Accid.nb.
2010	38 832	3 907	48 952	0,1006	1,2606
2011	40 065	4 189	49 501	0,1045	1,2355
2012	37 046	3 571	45 792	0,0963	1,2360
2013	35 046	3 357	44 059	0,0957	1,2571
2014	34 970	3 202	42 545	0,0915	1,2166
2015	32 967	2 938	39 778	0,0891	1,2066
2016	33 664	3 026	40 766	0,0898	1,2109

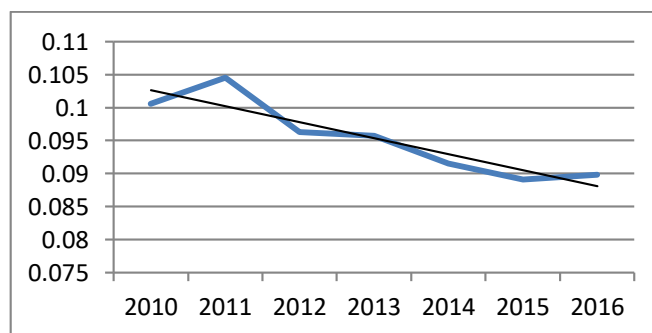


Fig. 2. Frequency of fatalities with respect to the number of accidents

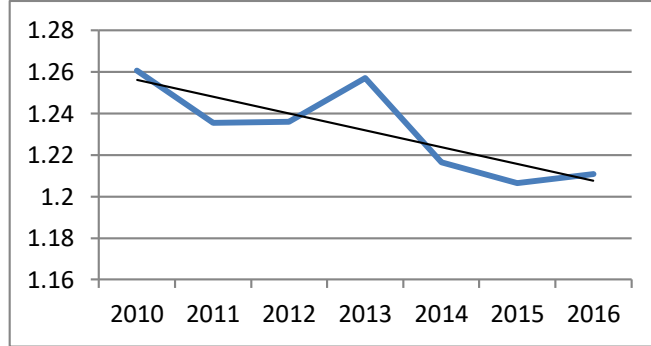


Fig. 3. Frequency of injured people with respect to the number of the road accidents

## 6 Anticipation of the accident consequences

We suppose that the random variables  $X_i, i = 1, 2, \dots$  have the Poisson distribution with parameters  $E(X_i) = V(X_i) = \mu, i = 1, 2, \dots, N(t)$ . From the data analysis it follows that the parameter  $\mu$  depend on time:  $\mu = \mu(t)$ . The function we approximate by linear function using date from table 2. Utilizing the EXCEL system to calculate the linear regression, we obtain the value of parameters

$$\tilde{a} = -0.000006627, \quad \tilde{b} = 0,10021139886.$$

Hence

$$\mu(t) = -0,000006627 t + 0,10021139886, \quad t \geq 0. \quad (27)$$

Note that the function in the time interval  $[t, t + h]$  is almost constant if the parameter  $h$  is not large. Therefore, to simplify the model we can assume that in the interval of prediction  $[t, t + h]$  for given  $t$  and small  $h$  the random variables  $X_i$  are i. i. d. with the constant expectation and variance

$$E(X_i) = V(X_i) = \tilde{\mu} = \frac{\mu(t) + \mu(t+h)}{2}. \quad (28)$$

From proposition 1 we have

$$E[X(t+h) - X(t)] = \Delta(t; h) \tilde{\mu} \quad (29)$$

$$V[X(t+h) - X(t)] = \Delta(t; h) (\tilde{\mu} + \tilde{\mu}^2) \quad (30)$$

$$D[X(t+h) - X(t)] = \sqrt{\Delta(t; h) (\tilde{\mu} + \tilde{\mu}^2)} \quad (31)$$

where

$$\Delta(t; h) = h\left(\frac{a h}{2} + b + a t\right),$$

### Example 2

Example 2 is a continuation of Example 1.

The expected number of fatalities at the time interval  $[t, t + h]$  is described by an increment  $X(t + h) - X(t)$ . Now we want to predict the number of fatalities in the road accidents in Poland from June 1, 2017 to September 30, 2017. Using results from Example 1 we have  $t = 2718$  and  $h = 122$ . For these parameters, using (15), we get

$$a = -0.00857, \quad b = 116.3167, \quad \Delta(t; h) = 11442.96, \quad D(t; h) = 106.97.$$

Applying the rule

$$E(X_i^2) = V(X_i) + [E(X_i)]^2 = \tilde{\mu} + \tilde{\mu}^2$$

for  $\tilde{\mu} = 0.08179315$  we get

$$E(X_i^2) = 0,08848326.$$

Applying (29) we obtain the predicted number of fatalities in the road accidents in Poland in considered period of time. Finally we obtain expected value of fatalities (**EFN**)

$$\mathbf{EFN=935.95}$$

Utilizing (31) we obtain the predicted standard deviation of fatalities number (DFN) in the road accidents in Poland in this time interval:

$$\mathbf{DFN=31,82}$$

In the same way we calculate the parameters of the model that allow to predict the number of *injured* people in the road accidents in Poland in this period.

To obtain the expectation (EIN) and standard deviation (DIN) of the injured people number we utilize the rules (29) and (31). For

$$\tilde{\mu} = 1,142378 \quad \text{and} \quad \Delta(t; h) = 11442,96$$

we get

$$\mathbf{EIN= 1307, 12}$$

$$\mathbf{DIN=167,34.}$$

## 4 Conclusions

The random processes theory deliver concepts and theorems that enable to construct stochastic models related to the road accidents. Counting processes

and processes with independent increments are the most appropriate for modelling number accidents in specified period of time. A crucial role in the models construction plays a nonhomogeneous Poisson process. Models of accidents number allow to anticipate number of accidents at any time interval. The identification of almost real parameters was possible thanks to the statistical data derived from the police report. The nonhomogeneous compound Poisson processes as the models of the road accidents consequences allow to anticipate numbers of the injured and killed people. Two examples are shown to explain presented models.

## References

1. F.Grabski. *Semi-Markov Processes: Application in System Reliability and Maintenance*. Elsevier, Amsterdam, Boston, Heidelberg, London, New York Oxford, Paris, San Diego, San Francisco, Sydney, Tokyo, 2015.
2. F.Grabski. Nonhomogeneous Poisson process in modelling accidents number in Baltic Sea waters and ports. *Journal of Polish Safety and Reliability Association; Summer Safety and Reliability Seminars*, Volume 8, Number 1, June 2017, p. 39-46.
3. E. Symon. *Wypadki drogowe w Polsce w roku 2016*. Komenda Główna Policji. Biuro ruchu drogowego. Warszawa, 2017.
4. A. Di Crescenzo, B. Martinucci, S. Zacks. Compound Poisson process with a Poisson subordinator. *Journal of Applied Probability*, Vol. 52, No. 2, p. 360-374 c 2015 by the Applied Probability Trust.
5. N. Zinchenko. Limit Theorems for Compound Renewal Processes: Theory and Application Proceedings ASMDA 2017 p. 1125-1136

# Regional Impacts of Future Climate Change on Health and Labor in Brazil

Gilvan R. Guedes<sup>a</sup>, Kenya Noronha<sup>b</sup>,  
Aline Magalhães<sup>b</sup>, Edson Domingues<sup>b</sup>, Kênia Souza<sup>b</sup>,  
Flaviane Santiago<sup>b</sup>, Débora Cardoso<sup>b</sup>

<sup>a</sup>*Department of Demography and Cedeplar - Universidade Federal de Minas Gerais - Brazil\**

<sup>b</sup>*Economics Department and Cedeplar - Universidade Federal de Minas Gerais - Brazil*

<sup>c</sup>*Center for Studies in Demography & Ecology - University of Washington*

March 27, 2018

## Abstract

Global climate and environmental change have increased in the last decades. Increased health stress is one of the most alarming consequences of these changes. Although many studies have tried to estimate the direct and indirect consequences of a warmer and drier environment for the economy, both at a global and local scale, a smaller number of studies have addressed the mid and long term health implications of these changes at a regional level. Building on their previous work, this study takes a multi-stage approach to estimate the climate-related consequences on cardiovascular/respiratory and infectious/vector-borne diseases, morbi/mortality, and labor supply in Brazil. Combining Spatial Bayes Smoothing, Spatial Econometrics, Global Burden of Disease data, and a Regional Computable General Equilibrium model, this study estimates the future development of climate-sensitive health disorders, their implications for morbi-mortality, and the consequences for labor supply and productivity for the Brazilian states and regions from 2010 to 2040. Our results suggest that partial effects of climate change on health and labor supply is higher than the total impact (from general equilibrium estimates). Increased morbi-mortality and labor loss would be higher for vector-borne and infectious than for non-communicable diseases, and mostly concentrated in less developed regions of the country.

*Keywords: Climate Change, Health, Labor Supply, Brazil, Computable General Equilibrium Model, Regional Impacts*

## 1 Introduction

Global climate and environmental change have aggravated in the last decades (Nordell, 2007). Increased health stress is one of the most alarming consequences of these changes. The impacts of climate change on human health is complex, ranging from more direct

---

\*Corresponding author. Email: grguedes@cedeplar.ufmg.br. Address: Av. Antônio Carlos, 6627, Pampulha, BH, MG, Brazil, 31270-901. Telephone: +55-31-34097165 - FAX: +55-31-34097203



consequences, such as increase in the prevalence of climate-sensitive diseases and in the demand for health care, to more indirect impacts, such as loss in labor supply (temporary through morbidity or permanent through deaths) and productivity (Pattanayak et al., 2009).

Although many studies have tried to estimate the direct and indirect consequences of a warmer and dryer environment for the economy, both at the global and the local scales, a smaller number of studies have addressed the mid and long term health implications of these changes at a regional level. Some studies are notable exceptions, such as the simulation of the economy-wide consequences of future climate change for human health conducted by Bosello et al. (2006). In Brazil, some studies have suggested climate-sensitive future scenarios of regional vulnerability (Barbieri et al., 2015), migration (Barbieri et al., 2010), agriculture productivity (Domingues et al., 2016), and infectious diseases (Barcellos et al., 2009). None of these studies, however, evaluates the health and wealth impacts of climate change as a dynamic process. Pattanayak et al. (2009) is one of the few exceptions, although their model do not compute the climate impact on labor supply through morbidity and mortality losses (gains) at a regional scale. Nor they recursively compute deaths due to climate in their population projection estimates.

Building on their previous work, this study takes a multi-stage approach to estimate the climate-related consequences on cardiovascular/respiratory and infectious/vector-borne diseases, morbi/mortality, and labor supply in Brazil. Combining Spatial Bayes Smoothing, Spatial Econometrics, data on the Global Burden of Disease, and a Regional Computable General Equilibrium (CGE) model, we estimate the future development of climate-sensitive health disorders, their implications for loss (gain) in morbidity and mortality, and the consequences for labor supply, family consumption, and economic growth for the Brazilian states and regions from 2010 to 2040. As far as we know, this is the only study estimating the impact of climate change on health and economic development at the regional level.

## 2 Materials and Methods

To evaluate the impact of climate change on the Brazilian economy as a result of its impacts on the labor supply through health, we combine different sources of data and analytical strategies. Population health was proxied by two groups of variables: *disease notifications* (dengue, malaria, and leishmaniosis) and *hospitalizations* (circulatory, respiratory, and infectious diseases). These health indicators were derived from administrative health records by municipality. Climate parameters were proxied by *precipitation* (total amount of rain within one year and its standard deviation) and *temperature* (12-month average). The climate scenario used in this analysis was the Representative Concentration Pathways 8.5.

The effect of climate change on the labor supply was obtained by a two-step strategy. The first step estimates the relationship between climate change and health. Building on Bosello et al. (2006) and Pattanayak et al. (2009), the second step analyses to what extent health losses due to climate change affects the labor supply based on the Global Burden of Disease parameters (WHO, 2016). The change in the number of cases estimated for the working age population (labor supply) was used in a computable general equilibrium model to verify the effect of climate change on the Brazilian economy by 2040. Our IMAGEM-B (Integrated Multiregional Applied General Equilibrium Model - Brazil) incorporates detailed data for the Brazilian economy, yielding the climate impact on the

main macroeconomic variables, such as Gross Domestic Product (GDP), employment, and family consumption. These impacts are reported at both national and state levels and are evaluated as the percentage cumulative deviation from a base scenario without considering the change in the climate parameters (*business-as-usual*).

## 2.1 Data and Variables

### 2.1.1 Climate Parameters

#### Historical Climate Data

In this study, we use data provided by the Center of Weather Forecast and Climate Studies (CPTEC), at the Brazilian Institute for Spatial Research (INPE). Measured on a daily basis by municipality from 1900 to 2010, the climate data were transformed into annual averages.

Precipitation data were classified as *precipitation intensity* and *precipitation dispersion*. Precipitation intensity was measured as the total amount of precipitation within a year. Precipitation dispersion was measured as the standard deviation of the monthly precipitation within a year. Although many studies use precipitation intensity only (Bosello et al., 2006), we included precipitation dispersion in order to capture the effect of the rainfall distribution throughout the year on climate-sensitive diseases (Hashizume et al., 2008; Pattanayak et al., 2009). Our temperature parameter represents the annual average temperature by municipality. For the econometric models testing the effect of these climate parameters on climate-sensitive health measures we use data for 2005 (base year). Figure 1 summarizes these measures and how they were applied to the econometric analysis.

Variable	Information available	Variable used in the econometric analysis	Measurement unit	Available years	Base year
Temperature	Monthly average temperature by year and municipality	<b>Annual average temperature:</b> average value of the monthly temperature averages within a year	°C	1900-2010	2005
Precipitation	Monthly cumulated precipitation by year and municipality	<b>Total annual precipitation:</b> sum of monthly precipitation over the year Standard deviation of precipitation within a year	mm		

Figure 1: Definition of climate variables used in the econometric models for health measures

#### Future Climate Scenarios

To simulate the impact of climate change on health, we use the Representative Concentration Pathways (RCP) 8.5 climate scenario provided by INPE. Based on the Model

for Energy Supply Strategy Alternatives and their General Environmental Impact (MESSAGE), the RCP 8.5 scenario assumes future economic growth, increased emission of greenhouse gases (GHG), and the absence of effective climate policies. Data for this scenario were based on the EtaHG2ES global circulation model with a spatial resolution of 0.2 degrees. In this scenario, the lack of effective climate mitigation policies leads to a considerable increase in GHG emissions over time, resulting in a radiative forcing of 8.5 W/m<sup>2</sup> by 2100 (Riahi et al., 2011).

Figure 2 shows the spatial distribution of annual average temperature for Brazil in 2010 and 2040, based on the RCP 8.5 climate scenario. Overall, municipalities experience a steady increase in temperature over time, with a larger number of municipalities scoring average temperatures above 24 degrees Celsius. Increase in temperature would be mostly concentrated in the Center-West, west of Minas Gerais, Maranhão, Piauí, and a large portion of the Eastern Brazilian Amazon. In contrast, the South region would have little variation, with some municipalities experiencing declining temperatures.

Figure 3 represents the spatial distribution of total annual precipitation over the same period. Along with increased temperature, most municipalities would experience a drier environment by 2040. The reduction in total rainfall would be mostly felt in a long corridor stretching from the Northeast *sertão* to the north part of Minas Gerais. São Paulo and large areas of the Brazilian Amazon would also be affected. In the South of Brazil, however, rainfall would increase.

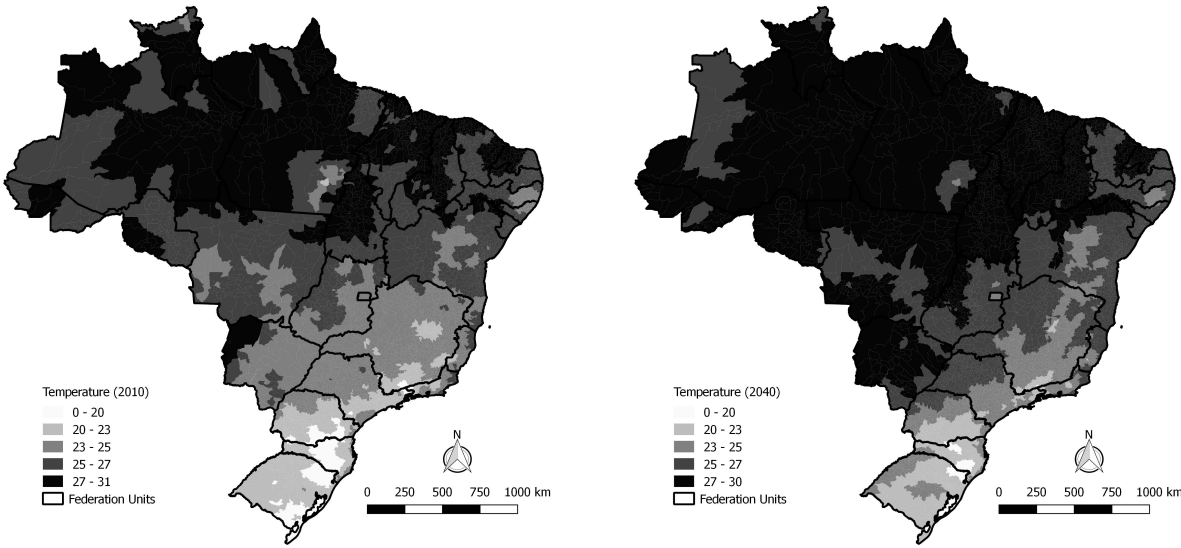


Figure 2: Spatial distribution of the annual average temperature from 2010 to 2040 - Brazil, RCP 8.5 Climate Scenario

**2.1.2 Population Health Measures**

We use two groups of climate-sensitive health indicators as summarized in Figure 4: indicators of hospitalizations by selected causes and disease notifications. Data on hospitalizations are provided by the Authorization Forms for Hospital Admittance. This information refers to in-patient care received in the Brazilian Public Health Care System, which responds for 66% of total hospitalizations in the country (IBGE, 2014). Data

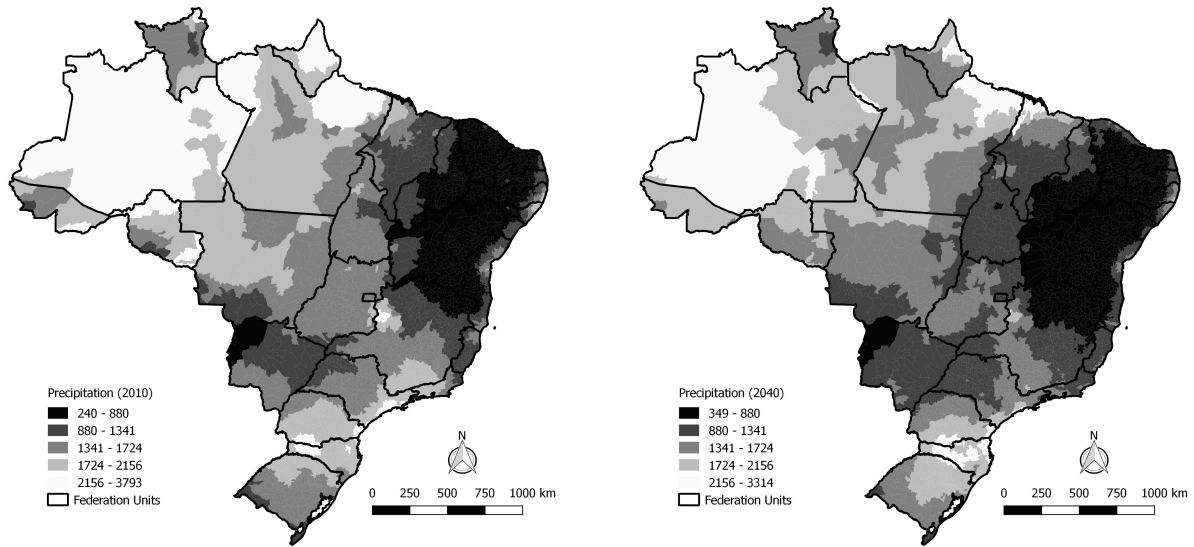


Figure 3: Spatial distribution of the total annual precipitation from 2010 to 2040 - Brazil, RCP 8.5 Climate Scenario

on disease notifications are provided by the Notifiable Disease Information System. All health data were obtained at the municipality level, using the municipality of residence instead of municipality of occurrence as the criterion of data selection.

Disease counts are based on a 5-year average centered in 2012. The population used to calculate the baseline rates of climate-sensitive diseases by municipality are the 2012 population estimates from the Brazilian Bureau of Statistics<sup>1</sup>. These rates represent number of cases by 1000 persons, and were corrected by the Spatial Empirical Bayes smoother to reduce potential small-area estimation bias (Anselin and Rey, 2014).

Population Health Indicator		Source
Number of Hospitalizations (per thousand persons)	Infectious and parasitic diseases (Ch. I ICD-10)	Health Ministry/Hospital Information System/ Authorization Forms for Hospital Admittance
	Diseases of the circulatory system (Ch. IX ICD-10)	
	Diseases of the respiratory system (Ch. X ICD-10)	
	Diarrhea and gastroenteritis of presumed infectious origin or other intestinal infectious diseases (ICD-10 codes A09; A02; A04-A05; A07-A08)	
Number of Disease Notifications (per thousand persons)	Dengue	Health Ministry/ Notifiable Diseases Information System
	Malaria	
	Visceral Leishmaniasis and American Cutaneous Leishmaniasis	

Figure 4: Population Health Indicators measured at the municipality level

<sup>1</sup>For dengue notifications, data were only available until 2012, so we used an average centered in 2010. Because of that, data on population used to estimate dengue prevalence was based on the 2010 Demographic Census.

### 2.1.3 Sociodemographic Measures

Health indicators are sensitive to key demographic and socioeconomic characteristics of the population (Dahlgren and Whitehead, 1991). To account for these confounding effects on the relation between climate and health, we include the following variables in our econometric analysis: proportion of individuals 0 to 14 years old, proportion of individuals 60 years old and above, proportion of women, proportion of individuals in urban areas, mean *per capita* household income, Gini Coefficient, and *per capita* health expenditures. All control variables are estimated at the municipality level. Data were obtained from the 2010 Demographic Census, except for the *per capita* health expenditures. The latter was provided by the Information System on health public budgets (SIOPS, in Portuguese).

## 2.2 Methods

### 2.2.1 Estimating the impact of climate change on labor supply through its impact on health

#### Model 1: Impact of climate on health

Assessing the relationship between climate change and health requires information on both indicators covering a sufficiently long time span. The Intergovernmental Panel on Climate Change (IPCC, 1990), for instance, defines climate change as a statistically significant variation in a climate parameter over a long period, typically measured in decades. Although we have reliable longitudinal data on climate, time series for health measures in Brazil are uncommon. The few longitudinal health data available in the country lack reliability, especially before the 1990's when the Brazilian Public Health System was created. A commonly used strategy to overcome this limitation is to estimate relations between health and other parameters (such as climate) using cross-sectional data at the municipality level. This strategy allows us to capture heterogeneity for the indicators used, since the Brazilian municipalities are highly diverse in their socioeconomic, health, and climate attributes (Barbieri et al., 2015).

In this study, we estimate the relation between climate and health using econometric analysis of cross-sectional data for all 5.565 Brazilian municipalities. The dependent variable is a measure of the average population health (log of the rates of hospitalization and disease notifications). Our key independent variables - the climate parameters - were measured in 2005 (our base year). The models control for socioeconomic and demographic characteristics, as explained in Section 2.1.3. The association between climate and health in this study is described by the following generic function:

$$\ln\Theta_{k,m} = f(R_m, \sigma(R_m), T_m, E_m) \quad (1)$$

where:

- $\ln\Theta_{k,m}$  = log of the  $k$ -th morbidity rate in municipality  $m$
- $R_m$  = annual total rainfall in municipality  $m$
- $\sigma(R_m)$  = standard deviation of rainfall in municipality  $m$
- $T_m$  = average temperature in municipality  $m$
- $E_m$  = vector of sociodemographic attributes of municipality  $m$

Ordinarily Least Square (OLS) models are routinely applied (Pattanayak et al., 2009). However, OLS estimators are biased in the presence of spatial dependence of error terms, violating the assumption of a diagonal error matrix. This is particularly true in the case of health and climate parameters. Vector-borne diseases, for instance, tend to cluster spatially due to vector mobility (Winters et al., 2010). Climate parameters and their variation are also similar in space (Khormi and Kumar, 2015). In this case, it is likely that the association between health and climate and unobserved factors affecting both will cause spatial dependency on the error term of the model (Anselin and Rey, 2014; Khormi and Kumar, 2015).

The main spatial econometric models for cross-sectional data are the Spatial Autoregressive Model (SAR) and the Spatial Error Model (SEM). While the SAR model includes the spatially lagged dependent variable as an independent variable, the SEM model includes the spatial dependence of unobserved influences in the error term only. The most common criterion to choose between the two specifications is the Robust Lagrange Multiplier (LM) statistics. If the LM statistics is significant for both specifications, Anselin and Rey (2014) suggest the use of the smaller value as the best model choice. This is the strategy used here. Models for dengue, malaria, and leishmaniosis were based on SAR estimates, while circulatory, respiratory, and infectious and parasitic diseases were modeled using the SEM specification. The spatial models were estimated in the GeoDaSpace software version 1.0 (GeoDa, 2016), using a Queen spatial weight matrix of order 1<sup>2</sup>.

## Model 2: Impact of health on labor supply

The first step to obtain the impact of health on labor supply due to climate change is to calculate counter-factual rates of diseases. The rates are based on predicted values from our spatial regressions. For the SEM model, predicted values are linear projections, as in a traditional OLS model. For the SAR models, the predicted value of  $k$ -th health indicator for the  $m$ -th municipality is given by:

$$\ln \hat{\Theta}_{k,m} = (I_n - \hat{\rho}W)^{-1} X_m \hat{\beta} \quad (2)$$

where  $I_n$  is a  $n \times n$  identity matrix,  $n$  is the number of municipalities,  $\hat{\rho}$  is the coefficient for the spatially lagged dependent variable,  $W$  is the Queen matrix for spatial weights,  $X_m$  is the matrix of covariates, and  $\hat{\beta} = (X_m X_m)^{-1} X_m (I_n - \hat{\rho}W) \ln \Theta_{k,m}$ .

Although the models were directly estimated by the GeoDaSpace software, values for Eq.(2) had to be estimated by a script developed by the authors in the R environment<sup>3</sup> (R Core Team, 2016). These values were exponentiated to get the predicted rates for the  $k$ -th morbidity. The predicted values of counter-factual rates of diseases ( $\Theta_{p,k,m}^{cf}$ ) were calculated by replacing the climate parameters (based on the year 2005) for their respective projections in 2010 and 2040<sup>4</sup>, as defined by the following equation:

$$\Theta_{t,k,m}^{cf} = \hat{\Theta}_{k,m} \times \left( \sum_C (\Delta C_{t,c,m} \times \hat{\beta}_{c,k}) + 1 \right) \quad (3)$$

<sup>2</sup>Two cases of islands were found among the 5,565 Brazilian municipalities. To avoid exclusion of these islands when using Queen matrices for spatial weights, we imputed their weights based on the 4-nearest neighbors.

<sup>3</sup>The script is available upon authors' request.

<sup>4</sup>We actually estimated all the results for quinquennial intervals. We decided to report results for 2010 and 2040 to avoid cluttering the text with excessive information. Results are available upon authors' request.

where  $\Delta C_{t,c,m} = C_{t,c,m} - C_{c,m}$  for  $t = 2010, 2040$ . The  $\Delta C_{t,c,m}$  represents the change in each of the climate parameters (temperature, precipitation level and dispersion) between the  $t$ -th and the base years.

The incidence of persons affected by the  $k$ -th morbidity in the  $t$ -th year can be obtained by multiplying the difference between the predicted prevalence rate at the base year and the counter-factual prevalence rate in year  $t$  by the projected population in the same year ( $P_{t,m}$ )<sup>5</sup>. The formula is given by:

$$\Gamma_{t,k,m} = \left( \Theta_{t,k,m}^{cf} - \hat{\Theta}_{k,m} \right) \times P_{t,m} \quad (4)$$

Eq.(4) provides the expected number of additional cases for the  $k$ -th morbidity in year  $t$  due to climate change. These additional cases can be decomposed into deaths (*permanent loss*) and disability (*temporary loss*) for the total population, using the following parameters from the Global Burden of Disease project: Disability-Adjusted Life Year (DALY) and its components (WHO, 2016). The DALY is the sum of the years of life lost (YLL) due to premature death and the years lost due to disability (YLD). The YLL is the product of the number of deaths and the life expectancy at the age of death. The YLD is the product of the number of incident cases, the mean duration of disability, and the weight of disability (Leite et al., 2015). These parameters are available by age, sex, country, and groups of morbidities, including the ones used in this study. The most recent estimates provided by the project for Brazil corresponds to 2015.

The first component of DALY (YLL) provides the permanent lives lost in the total population. In Eq.(5), factor **A** represents the total number of deaths from the  $k$ -th morbidity among the total population for each sex. Since we are interested in the labor loss only, this factor is weighted by the proportion of deaths ( $D$ ) among the working age population ( $\pi$ ) due to the  $k$ -th morbidity for each sex (factor **B**). The outer summation combines these permanent labor losses for each sex, given the final permanent labor loss for the working age population:

$$YLL_{t,k,u}^{\pi} = \sum_s \left( \underbrace{\sum_{a=0}^{80+} \left( \Gamma_{t,k,u} \times \frac{YLL_k^{a,s}}{DALY_k^{a,s}} \right)}_{\mathbf{A}} \times \underbrace{\zeta_{s,k,u}}_{\mathbf{B}} \right) \quad (5)$$

where  $a$  stands for age,  $s$  for sex,  $u$  for state, and  $\zeta_{s,k,u} = \frac{\sum_{a=15}^{69} D_{k,u}^{a,s}}{\sum_{a=0}^{80+} D_{k,u}^{a,s}}$ .

Data on mortality by age and sex was provided by the Latin American Human Mortality Database (Urdinola and Queiroz, 2013). The most updated data refers to 2010, available for the following morbidity groups used in this study: infectious and parasitic diseases, and diseases of the circulatory and respiratory system. Since information for dengue, malaria, and leishmaniosis is not available, we assume that the age profile of deaths for these morbidities is the same as the one for the infectious and parasitic diseases. We further assume that all age profiles of mortality by cause remain constant by

---

<sup>5</sup>The population projections for 2010 and 2040 by municipality are updated figures based on the small-area estimations provided by the Center for Development and Regional Planning at the Universidade Federal de Minas Gerais (CEDEPLAR, 2014). Since some individuals would die due to climate change between 2005 and the  $t$ -th year, the population exposed to reproduction changes. To incorporate this change in exposure, we recursively projected the population at each quinquennial time interval, excluding individuals aged 15 to 49 years old who would die from climate-sensitive morbidities. This updating will affect primarily the  $\Gamma_{t,k,u}$  parameter described in Eq.(4).

2040. The incidence parameter ( $\Gamma_{t,k,m}$ ) had to be aggregated at the state level due to lack of information by municipality<sup>6</sup>. This is why it is represented in Eq.(5) as  $\Gamma_{t,k,u}$ .

The second component of DALY (YLD) provides the temporary years of life lost in the total population due to disability. In Eq.(6), factor  $\mathbf{A}$  represents the total number of life years temporarily lost due to disability among the population for each sex. As in the first component, we need to restrict these figures to the labor force. We do so weighting factor  $\mathbf{A}$  by the proportion of hospitalizations / notifications ( $H$ ) among the working age population for each sex (factor  $\mathbf{B}$ ). The outer summation combines these temporary labor loss for each sex, given the final temporary labor loss for the working age population:

$$YLD_{t,k,u}^{\pi} = \sum_s \left( \underbrace{\sum_{a=0}^{80+} \left( \Gamma_{t,k,u} \times \frac{YLD_k^{a,s}}{DALY_k^{a,s}} \times w_k^{a,s} \times d_k^{a,s} \right)}_{\mathbf{A}} \times \underbrace{\varphi_{s,k,u}}_{\mathbf{B}} \right) \quad (6)$$

where  $w_k$  is the disability weight,  $d_k$  is the duration of disability, and  $\varphi_{s,k,u} = \frac{\sum_{a=15}^{69} H_{k,u}^{a,s}}{\sum_{a=0}^{80+} H_{k,u}^{a,s}}$ .

The percentage change in the labor force ( $\psi_{t,k,u}^{\pi}$ ) between the  $t$ -th and base year is given by:

$$\psi_{t,k,u}^{\pi} = \left( \frac{YLL^{\pi} + YLD^{\pi}}{\sum_{15}^{69} P_{k,u}} \right) \times 100 \quad (7)$$

### 2.2.2 The impact of climate induced change in labor supply on the Brazilian economy

The last step in our methodological strategy is to estimate the regional economic impact of changes in the labor supply due to climate change. To do that, we use the IMAGEM-B (Integrated Multi-regional Applied General Equilibrium Model - Brazil). IMAGEM-B is a computable general equilibrium (CGE) model of multiple regions for Brazil. The model follows the basic theoretical structure of the TERM model - The Enormous Regional Model - described in several other works (Horridge et al., 2005).

IMAGEM-B is a bottom-up CGE model that covers all 27 states in Brazil. Bottom-up models allow the simulation of policies with region-specific price effects, such as when wage labor increases in specific regions. They also allow us to model imperfect factor mobility between regions or between sectors. Thus, increased labor demand in one region may be both choked off by a local wage rise and accommodated by migration from other regions. Each regional CGE model is fairly conventional: producers choose a cost-minimizing combination of intermediate and primary factor inputs, subject to production functions structured by a series of constant elasticity of substitution (CES) “nesting” assumptions. Two high-level aggregates, of primary factors and of intermediate inputs, are each demanded in proportion to the industry output (Leontief assumption). The primary factor aggregate is a CES composite of capital, land, and a labor aggregate. The aggregate intermediate input is again a CES composite of different composite commodities, which are in turn CES composites of commodities from different sources (regions). Industry outputs are transformed into commodity outputs via a constant elasticity of transformation (CET) mechanism. The industries have constant-returns-to-scale technology and price at the marginal cost<sup>7</sup>.

<sup>6</sup>This aggregation does not cause loss of information, because it is a sum of number of cases.

<sup>7</sup>The use of increasing returns to scale in regional / structural CGE models is not a usual hypothesis,

Figure 5 illustrates the details of the IMAGEM-B system of demand sourcing for a single commodity (*Food*) by a single user (*Households*) in a single region (*Minas Gerais* state). The diagram depicts a series of ‘nests’, indicating the various substitution possibilities allowed by the model. The same diagram would apply to other commodities, users, and regions. At the top level, households choose between imported (from another country) and domestic food. A CES or Armington specification describes their choice. Demands are guided by user-specific purchasers’ prices with typical elasticity of substitution between domestic and imported composites. Demands for domestic food in a region are summed over users to yield its total value. The usage matrix is measured in “delivered” values, which include basic values and margins (trade and transport), but not the user-specific commodity taxes.

The second level treats the origin of the domestic compound across the various regions. A matrix shows how this compound is divided among the source regions (Minas Gerais, São Paulo, and Rio de Janeiro in the example). Again, a CES specification controls this allocation. The CES implies that regions with lower production costs will tend to increase their market share. The sourcing decision is made on the basis of delivered prices, which include transport and other margin costs. Hence, even with growers’ prices fixed, changes in transport costs will affect regional market shares. The variables at this level are not user specific, since the decision is made on an all-user basis as if wholesalers, not final users, decided where to source food products. The implication for our example using Minas Gerais is that the proportion of food which comes from São Paulo is the same for households, intermediate, and all other users. This feature is in agreement with the database available for the Brazilian interstate trade, which does not specify the use of flows by destination state.

The next level down shows how a “delivered” food product from Rio de Janeiro is a Leontief composite of basic food products and the various margin goods. The share of each margin in the delivered price is specific to a particular combination of origin, destination, commodity, and source. For example, we should expect transport costs to form a larger share for region pairs that are far apart, or for heavy or bulky goods. Under the Leontief specification we preclude substitution between Road and Retail Margins and incorporate a CES specification to accommodate Road/Rail switching.

The bottom part of the substitution hierarchy shows that margins on food passing from Rio de Janeiro to Minas Gerais could be produced in different regions. The figure shows the sourcing mechanism for the road and retail margins. We might expect this to be drawn more or less equally from the origin (Rio de Janeiro), the destination (Minas Gerais), and regions in between. There would be some scope for substitution (elasticity of  $\varepsilon = 0.5$ ), since trucking firms can relocate depots to cheaper regions. For retail margins, on the other hand, a larger share would be drawn from the destination region, yielding less scope for substitution ( $\varepsilon = 0.1$ ). Once again, this substitution decision takes place at

---

unlike the reduced econometric models of the New Economic Geography. Theoretically, the introduction of this hypothesis into a general equilibrium model can cause problems of existence or multiplicity of equilibria (Mas-Colell et al., 1995). A parametric approach to increasing returns in a regional CGE model for Brazil can be found in Haddad and Hewings (2005). In this work, however, only 8 economic sectors were specified and the return parameters were estimated in a cross-section for one Brazilian state. There are currently no econometric estimates for returns to scale at the sectoral and regional level for Brazil, justifying the theoretical and practical reasons for the hypothesis of constant returns used here. It can be considered at first that the results obtained from the simulations correspond to the lower results bound. Homogeneous returns in the regional sectors would tend to increase the positive impacts and minimize the negative impacts due to the hypotheses of fixed factors in the short or long term.

an aggregated level, implying that the share of, say, São Paulo, in providing Road margins on trips from Bahia to Santa Catarina is the same, whatever good is being transported. Parallel system of sourcing is also modeled for imported food products, tracing them back to port of entry instead of region of production.

The composition of household demand follows the linear expenditure system (LES). There is a set of representative families<sup>8</sup> in each region, consuming domestic goods (from the regions of the national economy) and imported goods. The treatment of household demand is based on a combined CES / Klein-Rubin preference system. The demand equations are derived from a utility maximization problem whose solution follows hierarchical steps. At the first level there is CES substitution between domestic and imported goods. At the subsequent level there is a Klein-Rubin aggregation of composite goods. Thus, utility derived from consumption is maximized by this utility function. This specification gives rise to the LES, in which the share of expenditure above the subsistence level for each good represents a constant proportion of the total subsistence expenditure of each household.

“Investors” are a category of use of the final demand, responsible for the production of new units of capital. These investors choose the inputs through a process of minimization of costs, subject to a hierarchical technology structure. As in production technology, capital goods are produced by domestic and imported inputs. Exports from each region’s port to the world face a constant elasticity of demand. The standard small country assumption is assumed, implying that Brazil is a price-taker in import markets. However, because the imported goods are differentiated from the domestically produced goods, the two varieties are aggregated using a CES function, based on the Armington assumption. Exports are linked to the demand curves negatively associated with domestic production costs and positively affected by an exogenous expansion of international income. Government consumption is typically exogenous and can be associated or not with household consumption or tax collection. Stocks accumulate, following the changes of production.

Our IMAGEM-B is a multi-period model with recursive-dynamic mechanisms. These mechanisms are: (i) a stock-flow relation between investment and capital stock, which assumes a one year gestation lag; (ii) a positive relation between investment and the rate of profit; and (iii) a relation between wage growth and regional employment, implying that unemployment rates vary, at least in the short run. The model is solved using the GEMPACK (Horridge et al., 2012), and contains a large database that tracks flows of interregional and international purchases of each commodity from each region of origin to each destination region. IMAGEM-B database is based on the 2005 Brazilian National Input-Output tables, along with other regional data sources. The database covers 55 sectors/products and the 27 Brazilian states. We use the model to construct a base forecast for future states of the economy, to which different policy scenarios can be compared. The new scenarios differ from the base only via shocks on labor force due to future climate change, which generate deviations from the base. These deviations can be directly interpreted as the effect of climate-induced change in labor supply through health on the main macroeconomic variables for the Brazilian economy and its states: Gross Domestic Product (GDP), labor, and household consumption.

---

<sup>8</sup>Families and households are used interchangeably.

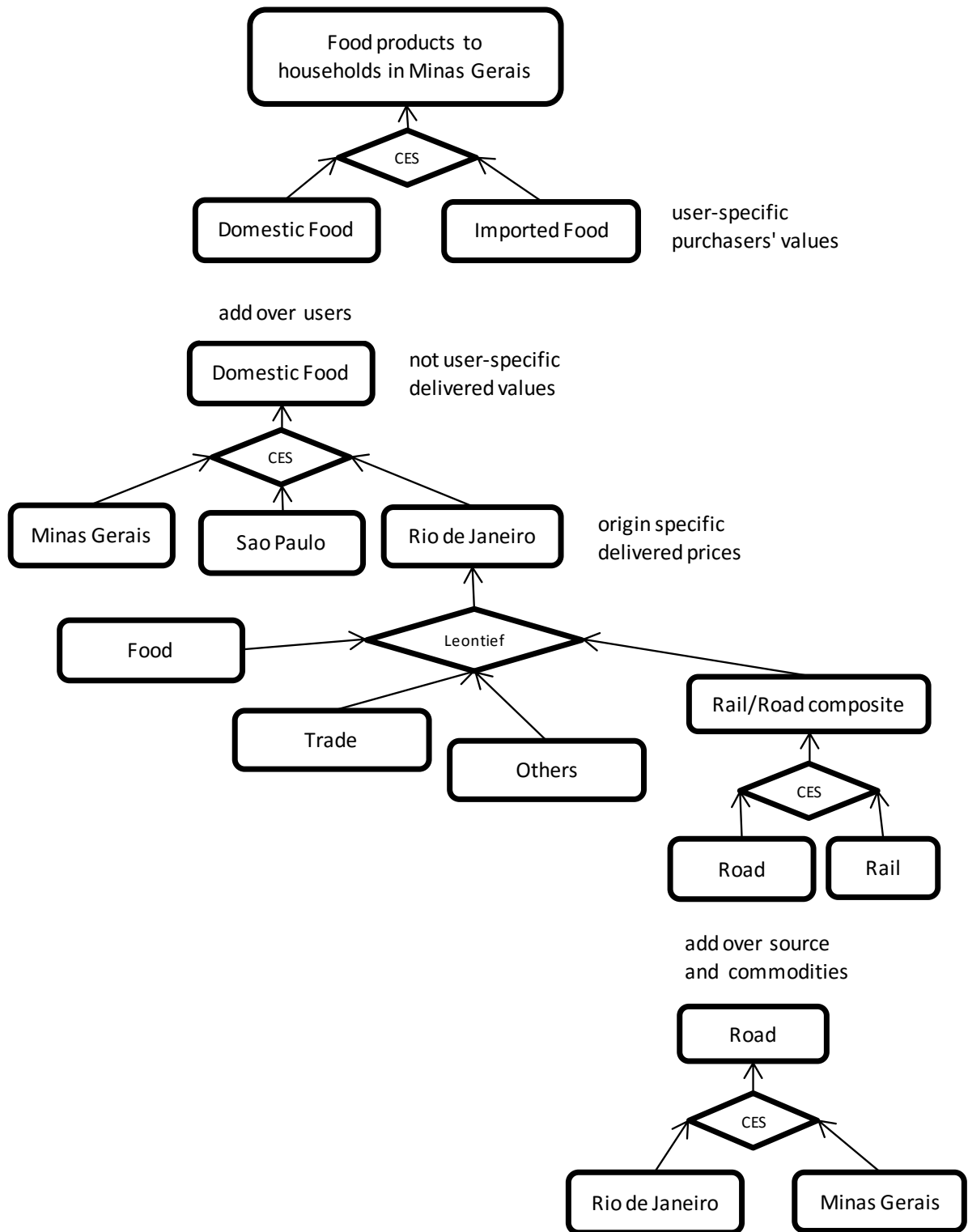


Figure 5: IMAGEM-B system of demand sourcing

### 3 Results

Figures 6 and 7 present the results from the expected partial impact of climate change on disease prevalence (Figure 6), morbi-mortality, and labor supply (Figure 7) by region and disease groups. Prevalence of circulatory diseases is expected to decline from 2005 to 2040

due to the projected increase in average temperature across most municipalities in Brazil (Figure 7 - Panel B). Consequently, the morbi-mortality rate from circulatory disease is expected to decline, yielding an increase in the labor supply by 2040. This pattern holds for all the Brazilian regions, with higher impacts in the South. Different from the circulatory diseases, prevalence of respiratory disease is expected to increase marginally, with a small increase in morbi-mortality and loss in the labor force across regions.

<i>Relative risk ratio of disease prevalence (2040/2005) - 95% Confidence Interval in brackets</i>						
<b>Region</b>	<b>Circulatory</b>	<b>Respiratory</b>	<b>Infectious</b>	<b>Diarrhea</b>	<b>Dengue</b>	<b>Leishmaniosis</b>
North	0.999 (0.991; 1.007)	1.059 (1.056; 1.063)	1.142 (1.137; 1.147)	1.372 (1.357; 1.387)	1.552 (1.495; 1.609)	0.971 (0.948; 0.993)
Northeast	0.982 (0.979; 0.985)	1.042 (1.039; 1.045)	1.09 (1.085; 1.094)	1.24 (1.230; 1.250)	1.128 (1.114; 1.143)	0.994 (0.983; 1.004)
Center-West	0.97 (0.962; 0.972)	1.058 (1.055; 1.061)	1.179 (1.174; 1.183)	1.495 (1.483; 1.507)	1.681 (1.668; 1.693)	1.133 (1.117; 1.150)
Southeast	0.982 (0.979; 0.984)	1.03 (1.028; 1.031)	1.109 (1.107; 1.111)	1.267 (1.265; 1.270)	1.533 (1.518; 1.549)	1.19 (1.184; 1.196)
South	0.896 (0.894; 0.898)	1.031 (1.029; 1.032)	1.107 (1.105; 1.110)	1.354 (1.340; 1.357)	0.915 (0.905; 0.925)	1.377 (1.372; 1.382)

Source: Author's own calculations. Based on simulated rates of diseases due to RCP 8.5 climate change scenario (INPE), WHO (2016), and regional economically active population projections for Brazil (Cedeplar, 2014). Estimates from counterfactual rates derived from spatial econometric models.

Figure 6: Impact of Climate Change (temperature and precipitation) on Disease Prevalence by Region and Disease - Brazil, 2040 (Base year = 2005)

The impact of future climate change on vector borne and infectious diseases is higher in magnitude when compared to the chronic conditions. Overall, prevalence of infectious diseases, and dengue is expected to increase across all regions, resulting in higher morbi-mortality rates and significant loss in the labor force by 2040. Change in the prevalence of all three diseases will be higher in the North (ranging from 14% for infectious diseases to 55% for dengue) and Center-West (ranging from 18% for infectious diseases to 68% for dengue). Despite the increase in the prevalence, rates themselves are low in magnitude (but high if compared to other countries). Therefore, additional morbi-mortality and loss in the labor force due to climate change would increase only marginally. Change in rates is the lowest for leishmaniosis.

Figures 8, 9, and 10 present the effect of climate change on employment, family consumption and economic growth, respectively, by the Brazilian states when partial and indirect effects through the economy are simultaneously considered (from the regional general equilibrium model). Different from the impacts suggested by Figures 6 and 7, these include change in production costs due to climate-induced loss (gain) in the labor supply. The regional impacts vary significantly, and is different by group of diseases.

Figure 8 shows the regional variation in the cumulated percentage change in employment by 2050. For the respiratory and circulatory disease, increase in unemployment due to the climate induced shocks on the labor supply would be mostly concentrated in the Southeast and parts of the Northeast. South, Center-West, and most of the North region would be benefited with increase in employment rates because of the expected increase in temperature, reducing the incidence of these chronic conditions. For the vector borne and infectious diseases, higher losses in job creation would concentrate in the South, Center-West, and North regions. Despite the large regional differences, the final impact on employment would be modest, and mostly due to change in the labor loss caused by the increased incidence of infectious and vector borne diseases.

*Panel A: Number and rate (%) of additional Deaths in 2040 by Region and Disease*

Region	Circulatory		Respiratory		Infectious		Diarrhea		Dengue		Leishmaniasis	
	N	Rate	N	Rate	N	Rate	N	Rate	N	Rate	N	Rate
North	-2,718	-0.12	22,782	1.00	84,614	3.70	69,456	3.04	54,565	2.39	-8,655	-0.38
Northeast	-27,119	-0.42	38,902	0.61	131,006	2.05	112,628	1.76	-7,121	-0.11	1,090	0.02
Center-West	-11,219	-0.70	19,036	1.18	58,246	3.62	45,509	2.83	149,083	9.26	1,756	0.11
Southeast	-74,910	-0.78	54,601	0.57	138,494	1.44	54,521	0.57	131,670	1.37	1,268	0.01
South	-157,019	-4.88	33,545	1.04	63,755	1.98	55,366	1.72	-352	-0.01	1,107	0.03

*Panel B: Number and rate (%) of additional Years of Life Diseased in 2040 by Region and Disease*

Region	Circulatory		Respiratory		Infectious		Diarrhea		Dengue		Leishmaniasis	
	N	Rate	N	Rate	N	Rate	N	Rate	N	Rate	N	Rate
North	-262	-0.01	19,596	0.86	13,519	0.59	36,213	1.58	37,853	1.66	-40	0.00
Northeast	-2,614	-0.04	33,461	0.52	20,932	0.33	58,722	0.92	-4,940	-0.08	5	0.00
Center-West	-1,081	-0.07	16,374	1.02	9,306	0.58	23,727	1.47	103,424	6.42	8	0.00
Southeast	-7,221	-0.08	46,964	0.49	22,128	0.23	28,426	0.30	91,344	0.95	6	0.00
South	-15,136	-0.47	28,853	0.90	10,187	0.32	28,867	0.90	-244	-0.01	5	0.00

*Panel C: Number and rate (%) of Labor Supply Loss due to Morbi-Mortality in 2040 by Region and Disease*

Region	Circulatory		Respiratory		Infectious		Diarrhea		Dengue		Leishmaniasis	
	N	Rate	N	Rate	N	Rate	N	Rate	N	Rate	N	Rate
North	-920	-0.06	7,381	0.45	47,742	2.88	39,565	2.39	28,671	1.73	-4,972	-0.30
Northeast	-7,630	-0.17	11,100	0.25	65,854	1.48	56,591	1.28	-640	-0.01	554	0.01
Center-West	-4,301	-0.38	5,679	0.51	30,148	2.69	23,693	2.12	78,174	6.99	1,027	0.09
Southeast	-26,667	-0.42	14,967	0.24	76,155	1.20	29,865	0.47	74,066	1.17	710	0.01
South	-46,780	-2.24	9,230	0.44	40,186	1.93	34,610	1.66	-276	-0.01	683	0.03

Source: Author's own calculations. Based on simulated rates of diseases due to RCP 8.5 climate change scenario (INPE), WHO (2016), and regional economically active population projections for Brazil (Cedeplar, 2014). Estimates from counterfactual rates derived from spatial econometric models.

Figure 7: Health impacts of climate change in Brazil by Region and Disease by 2040

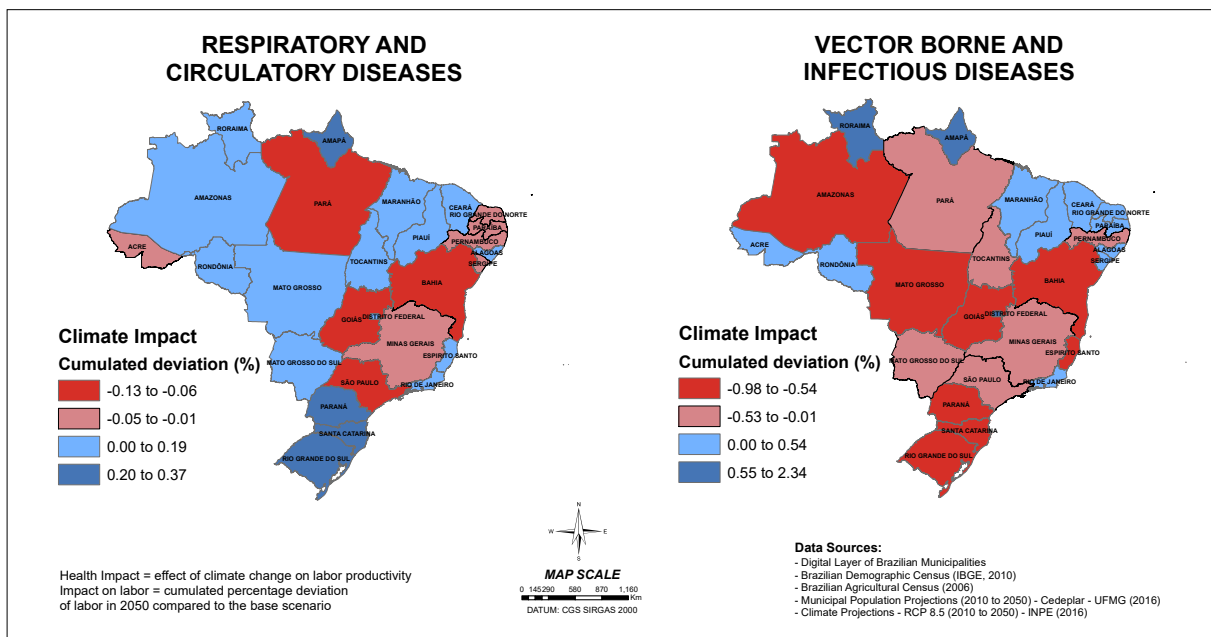


Figure 8: Change in State-level employment due to change in labor supply from climate-sensitive diseases - Brazil, 2015 to 2050

Figure 9 shows the regional variation in the accumulated percentage change in family consumption by 2050. Different from employment, family consumption would stay virtually unaltered if the climate-induced change in labor supply affected the economy only through the expected change in respiratory and circulatory disease. This trend would hold for all states, with expected increase in consumption due to the climate shock on respiratory and circulatory diseases ranging from 0.004% to 0.5% in 35 years. For the vector borne and infectious diseases, however, most states would experience reduction in family wellbeing. Most Northeastern states and four Northern states (Roraima, Amapá, Acre, and Rondônia) these impacts would be less felt. The most impacted states

would experience an average decline in family consumption of 2.5% by 2050 due to the expected labor loss in response to increased incident of vector-borne and infectious diseases only.

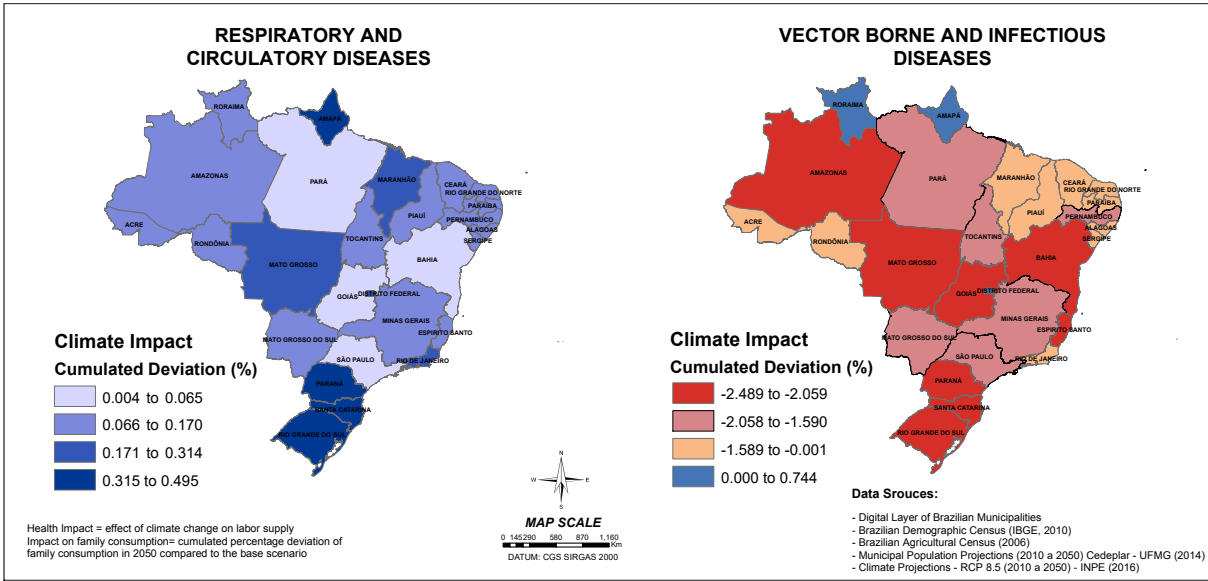


Figure 9: Change in State-level family consumption due to change in labor supply from climate-sensitive diseases - Brazil, 2015 to 2050

Figure 9 shows the regional variation in the accumulated percentage change in family consumption by 2050. Different from employment, family consumption would stay virtually unaltered if the climate-induced change in labor supply affected the economy only through the expected change in respiratory and circulatory disease. This trend would hold for all states, with expected increase in consumption due to the climate shock on respiratory and circulatory diseases ranging from 0.004% to 0.5% in 35 years. For the vector borne and infectious diseases, however, most states would experience reduction in family well-being. Most Northeastern states and four Northern states (Roraima, Amapá, Acre, and Rondônia) these impacts would be less felt. The most impacted states would experience an average decline in family consumption of 2.5% by 2050 due to the expected labor loss in response to increased incident of vector-borne and infectious diseases only.

The expected change in economic performance of the Brazilian states is similar to the regional trend found for employment (Figure 10). Growth in the regional GDP would be mostly due to expected labor shocks from vector-borne and infectious diseases. The most affected states would be the ones in the Brazilian agribusiness belt (Center-West), Bahia, and Amazonas. The South region would follow, with expected decline in economic growth of around 2% to 3% by 2050.

### 4 Concluding Remarks

Global climate and environmental change have increased in the last decades. Increased health stress is one of the most alarming consequences of these changes. Although many studies have tried to estimate the direct and indirect consequences of a warmer and drier environment for the economy, both at a global and local scale, a smaller number of studies have addressed the mid and long term health implications of these changes at

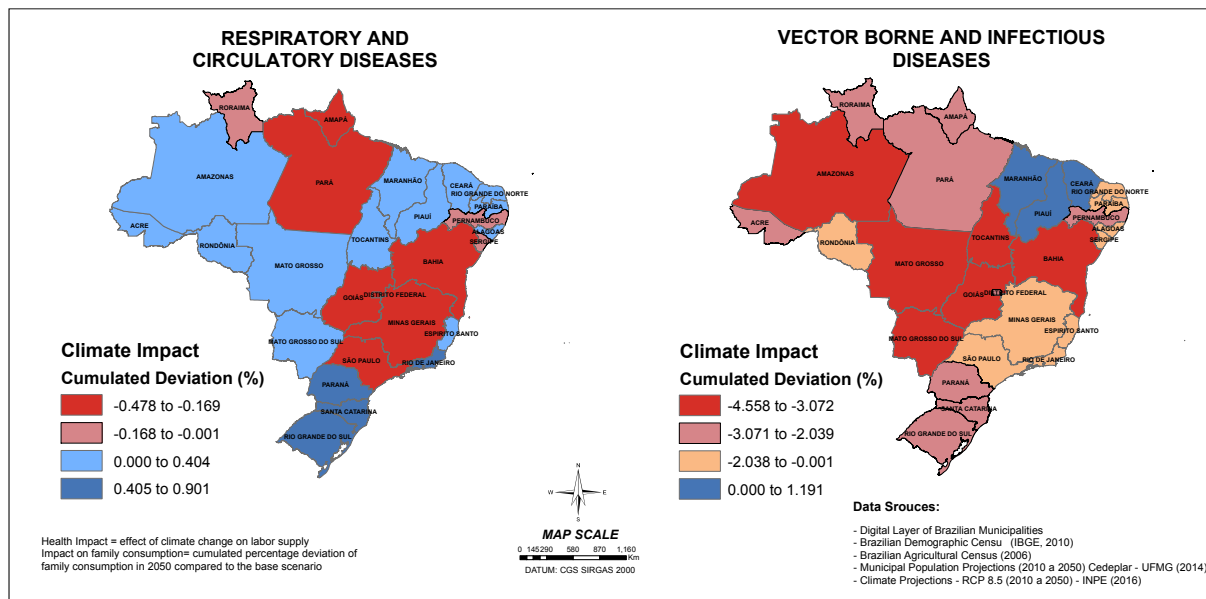


Figure 10: Change in State-level Gross Domestic Product due to change in labor supply from climate-sensitive diseases - Brazil, 2015 to 2050

a regional level and as a dynamic process. Pattanayak et al. (2009) is one of the few exceptions, although their model do not compute the climate impact on labor supply through morbidity and mortality losses (gains) at a regional scale. Nor they recursively compute deaths due to climate in their population projection estimates.

Building on their previous work, this study has taken a multi-stage approach to estimate the climate-related consequences on cardiovascular/respiratory and infectious/vector-borne diseases, morbi/mortality, and labor supply in Brazil. Combining Spatial Bayes Smoothing, Spatial Econometrics, Global Burden of Disease data, and a Regional Computable General Equilibrium model, this study estimated the future development of climate-sensitive health disorders, their implications for morbi-mortality, and the consequences for labor supply and productivity for the Brazilian states and regions from 2010 to 2040.

We found a link between between climate change and health, although this relation varies by disease and by region. The prevalence of circulatory diseases is expected to decline from 2005 to 2040 due to the projected increase in average temperature across most municipalities in Brazil. Consequently, the morbi-mortality rate from circulatory disease is expected to decline, yielding an increase in the labor supply by 2040. This effect is more pronounced in the South.

The impact of future climate change on vector borne and infectious diseases is higher in magnitude when compared to the chronic conditions. Overall, prevalence of infectious diseases, with large, and dengue more specifically, is expected to increase across all regions, resulting in higher morbimortality rates and significant loss in the labor force by 2040. Change in the prevalence of all three diseases will be higher in the North and in the Center-West. Despite the increase in the prevalence, rates themselves are low in magnitude (but high if compared to other countries). Therefore, additional morbi-mortality and loss in the labor force due to climate change would increase only marginally.

The impact of the projected climate change on labor (from the demographic model) is higher than its computed effect in the economy (from the computable regional general

equilibrium model). The CGE result shows that increased morbi-mortality and labor loss would be higher for vector-borne and infectious than for non-communicable diseases, and mostly concentrated in less developed regions of the country.

## References

- Anselin, L. and S. J. Rey (2014). *Modern spatial econometrics in practice: A guide to GeoDa, GeoDaSpace and PySAL*.
- Barbieri, A. F., E. Domingues, B. L. Queiroz, R. M. Ruiz, J. I. Rigotti, J. A. Carvalho, and M. F. Resende (2010). Climate change and population migration in brazil's northeast: scenarios for 2025–2050. *Population and environment* 31(5), 344–370.
- Barbieri, A. F., G. R. Guedes, K. Noronha, B. L. Queiroz, E. P. Domingues, J. I. R. Rigotti, G. P. d. Motta, F. Chein, F. Cortezzi, U. E. Confalonieri, et al. (2015). Population transitions and temperature change in Minas Gerais, Brazil: a multidimensional approach. *Revista Brasileira de Estudos de População* 32(3), 461–488.
- Barcellos, C., A. M. V. Monteiro, C. Corvalán, H. C. Gurgel, M. S. Carvalho, P. Artaxo, S. Hacon, and V. Ragoni (2009). Mudanças climáticas e ambientais e as doenças infecciosas: cenários e incertezas para o brasil. *Epidemiologia e Serviços de Saúde* 18(3), 285–304.
- Bosello, F., R. Roson, and R. S. Tol (2006). Economy-wide estimates of the implications of climate change: Human health. *Ecological Economics* 58(3), 579–591.
- CEDEPLAR (2014). Estimativas de população para o Brasil: total do país, unidades federativas e municípios, 2010-2030. Unpublished paper.
- Dahlgren, G. and M. Whitehead (1991). Policies and strategies to promote social equity in health. Technical report, Institute for Futures Studies.
- Domingues, E. P., A. S. Magalhães, and R. M. Ruiz (2016). Cenários de mudanças climáticas e agricultura no brasil: impactos econômicos na região nordeste. *Revista Econômica do Nordeste* 42(2), 229–246.
- Geoda Center (2016). GeoDaSpace 1.0 for Mac OS X. Downloaded from <https://geodacenter.github.io/GeoDaSpace/download.html>.
- Haddad, E. A. and G. J. Hewings (2005). Market imperfections in a spatial economy: some experimental results. *The Quarterly Review of Economics and Finance* 45(2), 476–496.
- Hashizume, M., B. Armstrong, S. Hajat, Y. Wagatsuma, A. S. Faruque, T. Hayashi, and D. A. Sack (2008). The effect of rainfall on the incidence of cholera in bangladesh. *Epidemiology* 19(1), 103–110.
- HorrIDGE, M., J. Madden, and G. Wittwer (2005). The impact of the 2002–2003 drought on australia. *Journal of Policy Modeling* 27(3), 285–308.

- Horridge, M., K. Pearson, A. Meeraus, and T. Rutherford (2012). Solution software for cge modeling. In P. Dixon and D. Jorgensen (Eds.), *Handbook of CGE modeling*, Chapter 20. Elsevier.
- IBGE (2014). Pesquisa Nacional de Saúde 2013: percepção do estado de saúde, estilos de vida e doenças crônicas.
- IPCC (1990). *Climate Change: The IPCC Scientific Assessment-Report of IPCC Working Group*. Cambridge, UK: Cambridge University Press.
- Khormi, H. M. and L. Kumar (2015). *Modelling interactions between vector-borne diseases and environment using GIS*. CRC Press.
- Leite, I. d. C., J. G. Valente, J. M. d. A. Schramm, R. P. Daumas, R. d. N. Rodrigues, M. d. F. Santos, A. F. d. Oliveira, R. S. d. Silva, M. R. Campos, and J. C. d. Mota (2015). Burden of disease in Brazil and its regions, 2008. *Cadernos de Saúde Pública* 31(7), 1551–1564.
- Mas-Colell, A., M. D. Whinston, J. R. Green, et al. (1995). *Microeconomic theory*, Volume 1. Oxford university press New York.
- Nordell, B. (2007). Global warming is large-scale thermal energy storage. In *Thermal Energy Storage for Sustainable Energy Consumption*, pp. 75–86. Springer.
- Pattanayak, S. K., M. T. Ross, B. M. Depro, S. C. Bauch, C. Timmins, K. J. Wendland, and K. Alger (2009). Climate change and conservation in brazil: Cge evaluation of health and wealth impacts. *BEJ Econom Anal Policy* 9, 6.
- R Core Team (2016). *R: A Language and Environment for Statistical Computing*. Vienna, Austria: R Foundation for Statistical Computing.
- Riahi, K., S. Rao, V. Krey, C. Cho, V. Chirkov, G. Fischer, G. Kindermann, N. Nakicenovic, and P. Rafaj (2011). Rcp 8.5a scenario of comparatively high greenhouse gas emissions. *Climatic Change* 109(1-2), 33.
- Urdinola, B. and B. Queiroz (2013). Latin American Human Mortality Database. Accessed on October, 2016. Available at [www.lamortalidad.org](http://www.lamortalidad.org).
- World Health Organization (2016). Global Burden of Disease Study 2015 (GBD 2015). Results. Data retrieved from the World Health Organization, <http://ghdx.healthdata.org/gbd-results-tool>.
- Winters, A. M., R. J. Eisen, M. J. Delorey, M. Fischer, R. S. Nasci, E. Zielinski-Gutierrez, C. G. Moore, W. J. Pape, and L. Eisen (2010). Spatial risk assessments based on vector-borne disease epidemiologic data: importance of scale for west nile virus disease in colorado. *The American journal of tropical medicine and hygiene* 82(5), 945–953.

# On Mixed PARMA Modeling of Epidemiological Time Series Data

Emmanouil-Nektarios Kalligeris<sup>1</sup>, Alex Karagrighoriou<sup>1</sup>, and Christina  
Parpoula<sup>1</sup>

Lab of Statistics and Data Analysis, Department of Mathematics,  
University of the Aegean, Karlovasi, 83200 Samos, Greece  
(E-mail: [sasm16009@aegean.gr](mailto:sasm16009@aegean.gr))

**Abstract.** A rich class of traditional statistical models and methods is currently available for the early detection of epidemic activity in epidemiological surveillance systems. Real time surveillance though, is often difficult to be fully achieved because of the seasonality involved in the series. Indeed, whenever the correlation structure of a series depends on the season, the time series involved fails to reach stationarity with all the associated modeling consequences. In such situations, a useful class of models is that of periodic auto-regressive moving average (PARMA) models allowing parameters that depend on season. In this work, for the modeling of influenza-like syndrome morbidity, the general form as well as special cases of PARMA models are considered, and via model selection identification and likelihood-based techniques, the optimal model is selected. Climatological and meteorological covariates associated with influenza-like syndrome are also incorporated into the model structure. The derived results are satisfactory since the selected model succeeds in identifying the epidemic waves, and in estimating accurately the influenza-like syndrome morbidity burden in the case of Greece (for the period 2014 – 2016).

**Keywords:** Statistical Modeling, Mixed Periodic Autoregressive Moving Average Models, Model Selection, Time Series, Influenza, Meteorological Covariates.

## 1 Introduction

Epidemiological surveillance constitutes a specific sector of biosurveillance related solely to the human population. It can be defined as “*the continuous, systematic collection, analysis and interpretation of health-related data needed for the planning, implementation, and evaluation of public health practice*” (32). By incorporating in the aforementioned definition aspects such as controlling the validity of data, analyzing data via advanced statistical methods as well as extracting safe conclusions with scientific and methodological adequacy, gives us the modern concept of epidemiological surveillance (6).

As seen from above, epidemiological surveillance is a dynamic scientific activity which continuously progresses and requires systematic monitoring in

---

<sup>1</sup>5<sup>th</sup> SMTDA Conference Proceedings, 12-15 June 2018, Chania, Creete, Greece

© 2018 ISAST

the field of health sciences and biostatistics. The need for timely and accurate prediction of an epidemic wave has led to the implementation of statistical routine methods to detect outbreaks in epidemiological surveillance systems in several European countries (10) and Centers for Disease Control and Prevention (CDC). The major challenges in epidemiological surveillance are the source of data, the statistical quality control, the monitoring (follow-up), the evaluation of statistical techniques used to detect outbreaks, anomalies and outliers in surveillance data, and extreme timeliness of detection (18).

Various statistical methodologies, discussed in the next section, are available for the early detection of epidemic activity in epidemiological surveillance systems. However, detailed recommendations as to which method is the “best” is not possible, since this depends critically on the specific details of the application and implementation, as well as its purpose and context. The main goals of this paper are firstly to develop novel regression approaches (within this framework, mixed periodic auto-regressive moving average regression (PARMA) models that work best for monitoring processes will be recommended), and secondly to compare and evaluate the developed methodologies via a retrospective analysis of time series of epidemiological data. The derived results are found to be satisfactory since the selected proposed model succeeds in identifying the epidemic waves, and outperforms typical cyclic regression models.

The rest of this paper is organized as follows. In Section 2, we discuss the motivation & scope of this paper. In Section 3, we describe the research methodology we follow. In Section 4, we conduct the detailed experimental study including model identification and evaluation. Finally, in Section 5, the obtained results are discussed and some concluding remarks are made.

## 2 Motivation & Scope

Perhaps the simplest regression model for outbreak detection is that described by Stroup et al. in (23) which ensures that seasonal effects are automatically adjusted for by design rather than explicit modeling, thus providing some element of robustness. This model though, does not incorporate time trends. A commonly used fully parametric regression model for outbreak detection is based on that of Serfling in (20). Serfling made use of a trigonometric function with linear trend, assuming Gaussian white noise errors, in order to model historical baselines. Costagliola et al. in (4) and (5), based on Serfling’s model, succeeded to detect the onset of epidemics of influenza. Additionally, Pelat et al. in (19) developed an automated version of the Serfling’s model with cubic trend and three trigonometric terms for prospective and retrospective surveillance, with model selection based both on ANOVA comparison and on Akaike Information Criterion (*AIC*) ((2), (21)).

During the past decade, a widespread implementation and use of several statistical modeling techniques for epidemiological surveillance purposes is observed. In the recent literature, detailed reviews of such modeling techniques (regression models, times series models, Bayesian and Markov models and spatio-temporal models) can be found in (27). Case counts of influenza-like

illness (ILI) exhibit a strong degree of seasonality, and typical approaches to modeling seasonal baseline commonly use cyclic regression models or variations on this approach. However, time series of infectious disease surveillance data and influenza data in particular, often exhibit high degrees of serial autocorrelation. The family of auto-regressive integrated moving average (ARIMA) models account for this auto-correlation explicitly, and these models have been used successfully in a variety of surveillance contexts (see (12), (16)). Some authors included auto-regressive terms in their models (as done in (30), (32)).

In this study, we develop an alternative approach in order to model seasonality of influenza, based on a periodic regression model which incorporates an additional auto-regressive and moving average component into Serfling's model including also climatological and meteorological covariates associated with ILI, with the ultimate aim of the early and accurate detection of outbreaks in an epidemiological surveillance system.

### **3 Research Methodology**

There are two types of statistical analysis for surveillance time series: retrospective and prospective analysis. The first one, locates and quantifies the impact of past epidemics, whereas the second one is useful when it comes to real time detection of epidemics. This study focuses on retrospective analysis, epidemic detection and quantification from time series data. Four steps are necessary to be followed in the case of detection of influenza epidemics in time series: (1) Determination of the training period; (2) Purge of the training period; (3) Estimation of the regression equation; (4) Epidemic alert notification.

#### **3.1 Determination of the Training Period**

Even if long time epidemiological time series are available, it is not typically the case that all data should be included in the training period (19). Over long time periods, possible changes in case reporting or/and demographics will likely be present, and this fact may affect how well the baseline model fits the data. Pelat et al. in (19) pointed out that a minimum of one year historical data is required to fit the models of influenza morbidity, whereas if one wants to obtain more reliable predictions, then at least two or even three year historical data is required. In this paper, the available two year historical data were included in the training period for conducting the experimental study in Section 4 (as done, for example, in (19), (22), (29) and (18)).

#### **3.2 Purge of the Training Period**

Model fitting on non-epidemic data enables modeling the truly non-epidemic baseline level. However, for seasonal diseases such as influenza, it is difficult to find long non-epidemic periods, since epidemics typically occur every year. There are two choices to make in order to deal with such an issue (19). The first choice (the less common one) requires explicit modeling of the epidemic periods.

The second choice is to identify epidemics, and then exclude the corresponding data from the series. Several rules have been suggested in the literature in this respect, such as excluding the 15% or 25% higher values from the training period (29), removing all data above a given threshold (5) or excluding whole periods known to be epidemic prone (for more details the reader may refer to (18) and (19)). In this work, following Pelat et al. in (19) we selected to exclude the 15% highest observations from the training period.

### 3.3 Estimation of the Regression Equation

The weekly estimated ILI rate, is a time series with specific characteristic properties, such as trend and seasonality. In the regression equation the trend is usually modeled using a linear term or a polynomial (of 2nd or 3rd degree) (19), while seasonality is usually modeled using sine and cosine terms with period of one year. However, refined models are found in literature, often with terms of period six months (5), 3 months (9), and smaller (13). In this work, we follow an exhaustive search process (based on periodic mixed regression models) in order to identify the optimal fit of the baseline model. Thus, linear, quadratic, cubic and quartic (for comparison purposes) trends are considered, and regarding the seasonal component, the most widely used periodicities are implemented, i.e. 12, 6, and 3 months. For a review of a general class of such models see (28).

Several other terms could be included in the regression equation. Some authors incorporated additional variables, such as day of the week, holiday, and post-holiday effects (15), sex and age (3), or climatological factors, for example temperature and humidity (30). Including all these terms simultaneously into the regression equation may offers more flexibility, but it will be more prone to result in unidentifiable models or other problems with model fit. In this work, we focus on the study of the possible impact of several climatological factors (*temperature, humidity, wind force, and wind direction*) on influenza morbidity.

Several authors have studied the climate changes and how these affect public health (see (8) and (11)), and it has already been observed that higher temperatures are likely to increase heat-related mortality worldwide. In addition, there is evidence that high temperatures are associated with mortality (1). The relationship between temperature and mortality may be confounded by a range of measured or unmeasured confounders. Confounding factors are present when a covariate is strongly associated with both the outcome and exposure of interest, but it is not a result of the exposure and may distort the association being studied between two other variables. As pointed out by Touloumi et al. in (25), a fundamental consideration in epidemiological modeling, is to properly control for all potential confounders. Such confounders may include meteorological indicators, such as relative humidity, seasonality and long-term trends. In addition, Tsangari et al. (26), concluded that high temperatures during warm months can result in increased mortality rates. Since influenza causes an estimated 290,000 – 650,000 deaths worldwide (31), it is considered reasonable to study the possible effect of climatological factors on ILI (see e.g. (30)) In this work, the additional climatological factors which were in-

corporated into the regression model were: minimum-maximum-median-mean temperature (temp), minimum-maximum-median-mean wind direction (wd), and minimum-maximum-median-mean wind force (wf). Moreover, first-second order auto-regressive terms and first-second order moving average terms, were also incorporated into the regression model.

Combining all the above components, the regression equation is defined by the following *mixed PARMA(2,2)* model:

$$\begin{aligned}
y_t = & \alpha_0 + \alpha_1 t + \alpha_2 t^2 + \alpha_3 t^3 + \alpha_4 t^4 + \gamma_1 \cos\left(\frac{2\pi t}{n}\right) + \delta_1 \sin\left(\frac{2\pi t}{n}\right) \\
& + \gamma_2 \cos\left(\frac{4\pi t}{n}\right) + \delta_2 \sin\left(\frac{4\pi t}{n}\right) + \gamma_3 \cos\left(\frac{8\pi t}{n}\right) + \delta_3 \sin\left(\frac{8\pi t}{n}\right) \\
& + \phi_1 y_{t-1} + \phi_2 y_{t-2} + \epsilon_t + \lambda_1 \epsilon_{t-1} + \lambda_2 \epsilon_{t-2} \\
& + \zeta_1 \text{minwd} + \zeta_2 \text{maxwd} + \zeta_3 \text{medianwd} + \zeta_4 \text{meanwd} \\
& + \theta_1 \text{minwf} + \theta_2 \text{maxwf} + \theta_3 \text{medianwf} + \theta_4 \text{meanwf} \\
& + \omega_1 \text{mintemp} + \omega_2 \text{maxtemp} + \omega_3 \text{mediantemp} + \omega_4 \text{meantemp}, \quad (1)
\end{aligned}$$

where  $\alpha_i, \gamma_i, \delta_i, \phi_i, \lambda_i, \zeta_i, \theta_i, \omega_i$ , are the appropriate coefficients of the relevant terms and  $\epsilon_t \sim WN(0, \sigma^2)$ .

Then, a thorough comparison was made, among all candidate periodic mixed models (e.g., *mixed PAR(1)*, *mixed PAR(2)*, *mixed PMA(1)*, *mixed PMA(2)*, *mixed PARMA(1, 1)*, *mixed PARMA(2, 1)*, *mixed PARMA(1, 2)*, *mixed PARMA(2, 1)*), with respect to the significance of the climatological factors. Note that all regression equations for the observed value  $y_t$  are special cases of equation (1).

The initial model selection process is described step by step as follows: We start from the simplest model labeled as *PAR(1)* by examining the significance of each of the climatological explanatory variables of the mixed model. If there is at least one significant, then we keep the model and go on to the next one (e.g. *PAR(2)*). The procedure goes on until the significance of the climatological factors for each model is examined. Finally, the models kept by the process, are being compared with respect to Modified Divergence Information Criterion (*MDIC*) criterion (see (14)). The model with the lowest *MDIC* value is being selected. Thus, *PARMA(2, 1)* mixed model with minimum temperature as a significant covariate ( $p$ -value < .001) was the model selected. For work see (24).

As a result, the time period and the minimum temperature are the explanatory variables, the observed time series values, weekly ILI rate (number of ILI cases per 1000 visits), is the dependent variable and all regression equations for the observed value  $y_t$  are special cases of the following *PARMA(2, 1)* mixed model:

$$\begin{aligned}
y_t = & \alpha_0 + \alpha_1 t + \alpha_2 t^2 + \alpha_3 t^3 + \alpha_4 t^4 + \gamma_1 \cos\left(\frac{2\pi t}{n}\right) + \delta_1 \sin\left(\frac{2\pi t}{n}\right) \\
& + \gamma_2 \cos\left(\frac{4\pi t}{n}\right) + \delta_2 \sin\left(\frac{4\pi t}{n}\right) + \gamma_3 \cos\left(\frac{8\pi t}{n}\right) + \delta_3 \sin\left(\frac{8\pi t}{n}\right)
\end{aligned}$$

$$+ \phi_1 y_{t-1} + \phi_2 y_{t-2} + \epsilon_t + \lambda_1 \epsilon_{t-1} + \omega_1 \text{mintemp}, \quad (2)$$

where  $\epsilon_t \sim WN(0, \sigma^2)$ ,  $n$  denotes the sample size, and parameter coefficients are estimated by least squares regression.

Selection of the best fitting model in terms of trend and seasonality is made possible by an exhaustive search among twelve candidate models (combining the four trends, namely, linear, quadratic, cubic and quartic, and the three seasonal periodicities, namely, 12, 6, and 3 months), and the selection process is relied on Analysis Of Variance (*ANOVA*) comparison (significance level  $\alpha$  is chosen to be 5%) to select between nested models, and on Akaike Information Criterion (*AIC*), or Modified Divergence Information Criterion (*MDIC*), or Bayesian Information Criterion (*BIC*) to select between non-nested models.

The latter process is described step by step as follows:

**Step 1:** The process starts comparing, by ANOVA, the simplest model labeled as *M11* (linear trend and 12-month seasonal periodicity), and defined as

$$\begin{aligned} M11: \quad y_t = & \alpha_0 + \alpha_1 t + \gamma_1 \cos\left(\frac{2\pi t}{n}\right) + \delta_1 \sin\left(\frac{2\pi t}{n}\right) + \phi_1 y_{t-1} \\ & + \phi_2 y_{t-2} + \epsilon_t + \lambda_1 \epsilon_{t-1} + \omega_1 \text{mintemp}, \end{aligned} \quad (3)$$

with the two models within which it is nested, labeled as *M12* (linear trend and 12- and 6-month seasonal periodicities) and *M21* (quadratic trend and 12-month seasonal periodicity), which are defined as

$$\begin{aligned} M12: \quad y_t = & \alpha_0 + \alpha_1 t + \gamma_1 \cos\left(\frac{2\pi t}{n}\right) + \delta_1 \sin\left(\frac{2\pi t}{n}\right) + \gamma_2 \cos\left(\frac{4\pi t}{n}\right) \\ & + \delta_2 \sin\left(\frac{4\pi t}{n}\right) + \phi_1 y_{t-1} + \phi_2 y_{t-2} + \epsilon_t + \lambda_1 \epsilon_{t-1} + \omega_1 \text{mintemp}, \end{aligned} \quad (4)$$

and

$$\begin{aligned} M21: \quad y_t = & \alpha_0 + \alpha_1 t + \alpha_2 t^2 + \gamma_1 \cos\left(\frac{2\pi t}{n}\right) + \delta_1 \sin\left(\frac{2\pi t}{n}\right) + \gamma_2 \cos\left(\frac{4\pi t}{n}\right) \\ & + \delta_2 \sin\left(\frac{4\pi t}{n}\right) + \gamma_3 \cos\left(\frac{8\pi t}{n}\right) + \delta_3 \sin\left(\frac{8\pi t}{n}\right) + \phi_1 y_{t-1} + \phi_2 y_{t-2} + \epsilon_t + \lambda_1 \epsilon_{t-1} \\ & + \omega_1 \text{mintemp}. \end{aligned} \quad (5)$$

**Step 2:** In the case that none of the alternative models (*M12* and *M21*) is significantly better than the initial one (*M11*), the process retains *M11* and stops.

**Step 3:** If one of the two alternative models is better than the initial one ( $p$ -value < 0.05), the algorithmic process keeps it and goes on.

**Step 4:** If both alternative models are better than the initial one, the algorithmic process keeps the one with the lowest *AIC*, *MDIC* or *BIC* respectively, and goes on.

The procedure is repeated until finding the “best overall” model over the twelve candidate models.

### 3.4 Epidemic Alert Notification

The epidemic thresholds which signal an unexpected change are typically obtained by taking an upper percentile for the prediction distribution (assumed to be normal), usually the upper 95<sup>th</sup> percentile (5), or upper 90<sup>th</sup> percentile (22). In addition, a minimum period above the epidemic threshold is also required. The latter step is important since in this way we avoid making alerts for isolated data points. In this paper, the rule was set to be “*a series of observations fall above the epidemic threshold during 2 weeks*” (see (19) and (29)). This way, the beginning of the epidemic is signaled the first time the series exceeds the threshold, and the end, the first time the series returns below the threshold.

## 4 Experimental Study

In Greece, since 1999, a sentinel system of epidemiological surveillance is operating. Through this system, the evolution of the frequency of certain diseases is recorded by selected reporting sites and health professionals report cases of the disease or syndrome under surveillance, based on clinical diagnoses. The sentinel medical doctors send weekly epidemiological data regarding the number of consultations for all causes and the number of consultations for each syndrome under surveillance, according to a specified clinical definition. This way, the Hellenic Center for Disease Control Prevention (HCDCP) estimates the weekly number of syndrome cases per 1000 visits, that is, the proportional morbidity, which reflects the activity of the syndrome under study (18).

After a reorganization of the sentinel system in Greece, during the period 2014-2015, the influenza-like illness (ILI) and gastroenteritis were established as syndromes of main interest. In this work, we focus on the study of weekly ILI rate data between September 29, 2014 and October 2, 2016. This data was used for analysis purposes, in order to determine the past two seasonal influenza outbreaks (signaled start and end weeks), establish optimal empirical epidemic thresholds, and detect early and accurately possible epidemics. Thus, we conducted a retrospective analysis for the period from 2014 to 2016, based on a model fit to two-season historical data (week40/2014 to week39/2016). It is worth to be noted here that recent sentinel surveillance system data are not considered comparable to those of the previous years (past influenza seasons until week39/2014) due to the aforementioned reorganization of the sentinel system in Greece.

### 4.1 Model Identification

We conducted a retrospective analysis; the whole time series with 105 observations was therefore included in the training period (as done for example in (18)). Then, we chose to exclude the top 15% observations from the training period (89 kept values from the total of 105). Based on ANOVA comparison, *AIC*, *BIC* and *MDIC* criteria values, the model selected was **M11** with a

linear trend, an annual periodic term (one year harmonics), first and second order auto-regressive terms, a first order moving average term, and the minimum temperature. The forecast interval was set to be 95%, that is the upper limit of the prediction interval which is used as a threshold to detect epidemics. The alert rule, was chosen to be “*an epidemic is declared when 2 weekly successive observations are above the estimated threshold*”.

The mathematical form of the selected model **M11** is described as follows:

$$y_t = \alpha_0 + \alpha_1 t + \gamma_1 \cos\left(\frac{2\pi t}{n}\right) + \delta_1 \sin\left(\frac{2\pi t}{n}\right) + \phi_1 y_{t-1} + \phi_2 y_{t-2} + \epsilon_t + \lambda_1 \epsilon_{t-1} + \omega_1 \text{mintemp.} \quad (6)$$

Table 1 presents the estimated parameters, the standard errors (sd), the test statistic values (t-value) and the associated p-values of the selected model. The twelve periodic regression mixed models are described in Table 2, in which the components included in each model are indicated by “\*”, along with *AIC*, *MDIC*, *BIC* and  $R_{GLLM(m)}^2$  (see (17)) values of each model. The model finally kept *M11* is in bold italics.

Figure 4.1 illustrate the model selection pathway using MDIC criterion. The model selection pathway for *ANOVA & AIC* and *ANOVA & BIC* respectively, is exactly the same as in Fig.4.1 and therefore is chosen not to be presented. In addition, Figure 4.2 illustrates the plots of the time series, the predicted baseline as well as the threshold. In Figure 4.2, the epidemics detected by the selected model (**M11**) appear in light red. Table 3 presents the dates and the results of the retrospective evaluation of the excess influenza morbidity in Greece for 2014 – 2016 along with excess percentages, using the *M11* periodic regression mixed model. The excess morbidity is defined as the cumulative difference between observations and baseline over the entire epidemic period. Excess percentages were calculated as the observed size divided by the sum of expected values throughout each epidemic.

**Table 1.** Selected Model M11

Parameter	Estimate	sd	t-value	p-value
$\alpha_0$	10.468	2.128	4.920	< .001
$\alpha_1$	-0.075	0.027	-2.789	0.007
$\gamma_1$	-10.315	1.444	-7.144	< .001
$\delta_1$	12.726	2.144	5.937	< .001
$\phi_1$	0.811	0.114	7.098	< .001
$\phi_2$	-0.234	0.090	-2.613	0.011
$\lambda_1$	0.261	0.135	-2.613	0.058
$\omega_1$	0.729	0.172	4.247	< .001

It is worth to be noted that we chose to present *MDIC*, along with the ANOVA comparisons, instead of *AIC* or *BIC*, because of the interesting characteristics that seems to appear and will be discussed in Section 4.

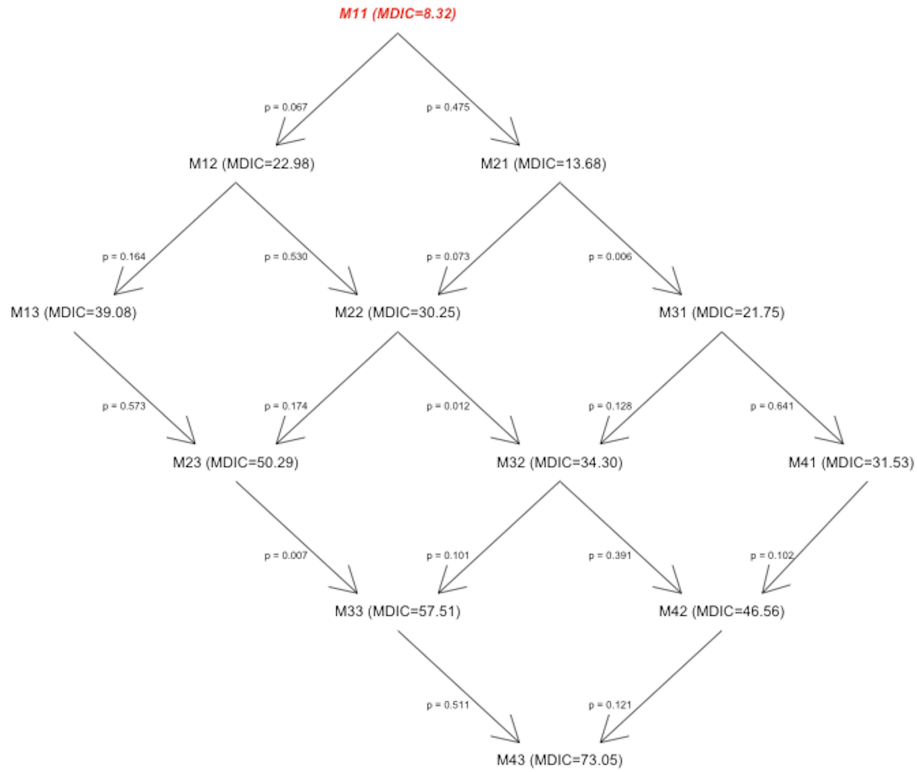


Fig. 1. Model selection pathway (ANOVA & MDIC).

Table 2. Models Selected Through the Algorithm Pathway

	T <sup>a</sup>				P <sup>b</sup>			ARMA			LV <sup>c</sup>	IC <sup>d</sup>			R <sup>2</sup>			
	t	t <sup>2</sup>	t <sup>3</sup>	t <sup>4</sup>	1	y <sup>f</sup>	6	m <sup>g</sup>	3	m	AR(1)	AR(2)	MA(1)	MT <sup>h</sup>	AIC	MDIC	BIC	R <sup>2</sup> <sub>GLMM(mar)</sub>
<b>M11</b>	*				*						*	*	*	*	409.31	8.32	429.29	0.927
M12	*				*		*				*	*	*	*	406.96	22.98	431.37	0.934
M13	*				*		*	*			*	*	*	*	406.56	39.08	435.42	0.928
M21	*	*			*						*	*	*	*	410.72	13.68	432.92	0.938
M22	*	*			*		*				*	*	*	*	408.49	30.25	435.11	0.934
M23	*	*			*		*	*			*	*	*	*	408.17	50.29	439.24	0.937
M31	*	*	*		*						*	*	*	*	403.82	21.75	428.23	0.938
M32	*	*	*		*		*				*	*	*	*	402.83	34.30	431.67	0.941
M33	*	*	*		*		*	*			*	*	*	*	401.04	57.51	434.33	0.937
M41	*	*	*	*	*						*	*	*	*	405.56	31.53	432.19	0.946
M42	*	*	*	*	*		*				*	*	*	*	403.90	46.56	434.97	0.942
M43	*	*	*	*	*		*	*			*	*	*	*	402.48	73.05	437.98	0.946

<sup>a</sup> "T" denotes trend; <sup>b</sup> "P" denotes periodicity; <sup>c</sup> "LV" denotes latent variable; <sup>d</sup> "IC" denotes information criterion; <sup>e</sup> "M" denotes model; <sup>f</sup> "y" denotes year; <sup>g</sup> "m" denotes months; <sup>h</sup> "MT" denotes minimum temperature.

**Table 3.** Retrospective Evaluation of the Excess Influenza Morbidity, Greece 2014-16

SW <sup>a</sup>	EW <sup>a</sup>	Cases	Expected cases	Excess cases	Excess percentage
201501	201512	1151	891	260	29%
201605	201608	316	225	91	40%

<sup>a</sup> SW and EW denote the signaled start and end weeks for epidemics, respectively.

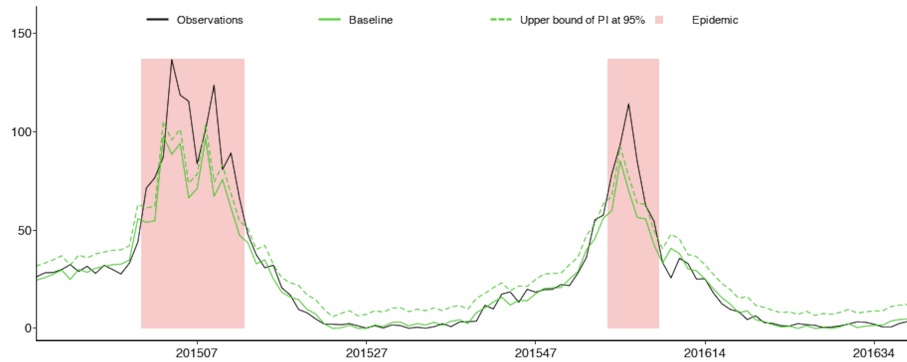


**Fig. 2.** Detected epidemics in Greece 2014 – 2016.

## 4.2 Model Performance Evaluation

In this section we evaluate the predictive performance of the selected model ( $M11$ ) in comparison with other significance models considered in this analysis. The selected periodic regression mixed model, identified as the optimal one, was  $M11$  defined in Eq. 3 (see also Table 2). However, one can easily observe from Fig.4.1, that the algorithm could have proceeded and stopped at  $M12$ , since the p-value is close to  $\alpha = 5\%$  (0.067). Moreover, the periodic regression mixed model  $M11$  was selected based on ANOVA comparison, and model selection criteria values (through the algorithm described in Section 3). It is worth to be noted that if we exclusively take into account the  $AIC$ ,  $BIC$  and  $R_{GLMM}^2(mar)$  values, then the “best overall” models would be  $M21$ ,  $M31$  and  $M33$ , respectively. Thus, one could make a comparison between the aforementioned models ( $M11$ ,  $M12$ ,  $M21$ ,  $M31$  and  $M33$ ) in order to ensure the selection of the “best overall” model with respect to several measures of prediction accuracy of a forecasting model, such as *Mean Error (ME)*, *Root Mean Squared Error (RMSE)*, *Mean Absolute Error (MAE)*, *Mean Percentage Error (MPE)*, *Mean Absolute Percentage Error (MAPE)* and *Mean Absolute Scaled Error (MASE)* (see (7)).

The results of the comparative study are presented in Table 4 where the full model ( $M43$ ) has also been included for the shake of completeness.

We observe from Table 4 that models  $M21$  and  $M31$  are not satisfactory, since their results are never the best for none of the accuracy measures examined. Although, the results for models  $M11$ ,  $M12$ , and  $M33$ , are similar,  $M11$  clearly outperforms the others in terms of  $MPE$  and  $MAPE$ . Even if model  $M33$  was better, we would choose again  $M11$ , since it has the advantage of less explanatory variables and a  $R_{GLMM}^2(mar)$  value very close to the value of  $M43$ . Thus,  $M11$  is the “best overall” model.

**Table 4.** Common Accuracy Measures

Model	ME	RMSE	MAE	MPE	MAPE	MASE
M11	-2.359224e-16	4.298974	3.040053	0.2782516	48.19166	0.230213
M12	2.179757e-16	4.10272	2.857186	-23.29906	75.60382	0.2163651
M21	4.937659e-17	4.280225	2.9915	7.396555	50.17105	0.2265362
M31	-3.469447e-17	4.009004	2.853861	22.26226	63.17711	0.2161133
M33	7.6736e-17	3.703522	2.757	-69.34156	127.622	0.2087783
M43	9.953614e-17	3.68828	2.783278	-69.73654	132.0232	0.2107683

It is worth to be noted that  $MDIC$ ,  $AIC$  and  $BIC$  values of the models are in full support of the above results. Indeed,  $MDIC$  is clearly in favor of model  $M11$  (smallest  $MDIC$  value). In respect to  $AIC$  and  $BIC$  values, we observe that  $M11$  is not the best; however, by choosing alternative models such as  $M12$ ,  $M33$  or  $M43$ , the gain is not significant enough to balance the complexity associated with these models. Moreover, the  $MDIC$  values tend to get bigger as more explanatory variables are included in the model. In fact, the penalty given by  $MDIC$  to the models is much bigger compared to the penalty given by  $AIC$ . Thus, the addition of explanatory variables makes  $MDIC$  a “somewhat stricter metric” in comparison with  $AIC$ , and nearly the exact opposite of  $R_{GLMM(mar)}^2$ .

## 5 Concluding Remarks

Conclusively, in this study, we conducted a retrospective analysis of epidemiological time series data (week40/2014 to week39/2016) for Greece. We developed an alternative approach in order to model seasonality of influenza, based on a periodic regression model which incorporates an additional auto-regressive and moving average component into Serfling’s model including additionally climatological and meteorological covariates associated with ILI, with the ultimate aim of the early and accurate outbreak detection. The model selected (via an exhaustive search process) as the optimal one succeeded in estimating accurately the influenza-like syndrome morbidity burden in Greece for the period 2014 – 2016 as well as the duration of the epidemic waves. Within this framework, the present work provided general recommendations to serve critical needs of Public Health for the very early and accurate detection of epidemic activity.

## Acknowledgements

The authors would like to thank the Hellenic National Meteorological Service (HNMS) for providing the real meteorological data as well as the Department of Epidemiological Surveillance and Intervention of the Hellenic Center for Disease Control and Prevention (HCDCP) for providing the influenza-like illness (ILI) rate data, collected weekly through the sentinel surveillance system. Finally, the work was carried out at the Lab of Statistics and Data Analysis of the University of the Aegean.

## Bibliography

- [1] Armstrong, B.: Models for the relationship between ambient temperature and daily mortality. *Epidemiology*, **17**, 624–631 (2006)
- [2] Bengtsson, T., Cavanaugh, J.E.: An improved Akaike information criterion for state-space model selection. *Computational Statistics and Data Analysis*, **50**, 2635–2654 (2006)
- [3] Brinkhof, M.W., Spoerri, A., Birrer, A., Hagman, R., Koch, D., Zwahlen, M.: Influenza-attributable mortality among the elderly in Switzerland. *Swiss Med Wkly*, **136(19–20)**, 302–309 (2006)
- [4] Costagliola, D., Flahault, A., Galinec, D., Garnerin, P., Menares, J., Valleron, A.-J.: When is the epidemic warning cut-off point exceeded? *Eur. J. Epidemiol.* **10**, 475–476 (1994)
- [5] Costagliola, D., Flahault, A., Galinec, D., Garnerin, P., Menares, J., Valleron, A.-J.: A routine tool for detection and assessment of epidemics of influenza-like syndromes in France. *American Journal of Public Health* **81**, 97–99 (1991)
- [6] Fleming, D.M., Rotar-Pavlic, D.: Information from primary care: its importance and value. A comparison of information from Slovenia and England and Wales, viewed from the "Health 21" perspective. *Eur. J. Public Health* **12**, 249–253 (2002)
- [7] Forecasting <<https://en.wikipedia.org/wiki/Forecasting>> as published in 11 February (2018)
- [8] Gosling, S.N., Lowe, J.A., McGregor, G.R., Pelling, M., Malamud, B.D.: Associations between elevated atmospheric temperature and human mortality: a critical review of the literature. *Clim. Change*, **92**, 299–341 (2009)
- [9] Housworth, J., Langmuir, A.D.: Excess mortality from epidemic influenza, 1957–1966. *Am. J. Epidemiol.*, **100**, 40–48 (1974)
- [10] Hulth, A., Andrews, N., Ethelberg, S., Dreesman, J., Faensen, D., van Pelt, W., Schnitzler, J.: Practical usage of computer-supported outbreak detection in five European countries. *Eurosurveillance* **15(36)**, 1–6 (2010). pii=19658
- [11] Kovats, R.S., Hajat, S.: Heat stress and public health: a critical review. *Ann. Rev. Public Health*, **29**, 41–55 (2008)
- [12] Lee, S., Oh, H.: Entropy test and residual empirical process for auto-regressive conditional duration models. *Computational Statistics and Data Analysis*, **86**, 1–12 (2015)
- [13] Lui, K.J., Kendal, A.P.: Impact of influenza epidemics on mortality in the United States from October 1972 to May 1985. *Am. J. Public Health*, **77**, 712–716 (1987)
- [14] Mantalos, P., Mattheou, K., Karagrigoriou, A.: An improved divergence information criterion for the determination of the order of an AR process. *Communications in Statistics – Simulation and Computation*, **39**, 865–879 (2010)
- [15] Mostashari, F., Fine, A., Das, D., Adams, J., Layton, M.: Use of ambulance dispatch data as an early warning system for community wide influenza-like illness, New York City. *J. Urban Health*, **80(2 Suppl 1)**, i43–49 (2003)
- [16] Müller, W., Stehlik, M.: Issues in the optimal design of computer simulation experiments. *Appl. Stochastic Models Bus. Ind.*, **25**, 163–177 (2009)
- [17] Nakagawa, S., Schielzeth, H.: A general and simple method for obtaining  $R^2$  from generalized linear mixed-effects models. *Methods in Ecology and Evolution*, **4**, 133–142 (2013)
- [18] Parpoula, C., Karagrigoriou, A., Lambrou, A.: Epidemic intelligence statistical modelling for biosurveillance. *J. Blömer et al. (Eds.): MACIS 2017, LNCS 10693*, 1–15 (2017)

- [19] Pelat, C., Boëlle, P.-Y., Cowling, B.J., Carrat, F., Flahault, A., Ansart, S., Valleron, A.-J.: Online detection and quantification of epidemics. *BMC Medical Informatics and Decision Making* **5**, 29 (2007)
- [20] Serfling, R.: Methods for current statistical analysis of excess pneumonia-influenza deaths. *Public Health Rep.* **78**, 494–506 (1963)
- [21] Shang, J., Cavanaugh, J.E.: Bootstrap variants of the Akaike information criterion for mixed model selection. *Computational Statistics and Data Analysis*, **52**, 2004–2021 (2008)
- [22] Simonsen, L., Reichert, T.A., Viboud, C., Blackwelder, W.C., Taylor, R.J., Miller, M.A.: Impact of influenza vaccination on seasonal mortality in the US elderly population. *Arch. Intern. Med.*, **165**, 265–272 (2005)
- [23] Stroup, D.F., Williamson, G.D., Herndon, J.L., Karon, J.M.: Detection of aberrations in the occurrence of notifiable diseases surveillance data. *Stat. Med.* **8**, 323–329 (1989)
- [24] Toma, A.: Model selection criteria using divergences. *Entropy*, **16(5)**, 2686–2698 (2014)
- [25] Touloumi, G., Atkinson, R., Tertre, L., Samoli, A.E., Schwartz, J., Schindler, C., Vonk, J.M., Rossi, G., Saez, M., Rabszenko, D., Katsouyanni, K.: Analysis of health outcome time series data in epidemiological studies. *Environmetrics*, **15**, 101–117 (2004)
- [26] Tsangari, H., Paschalidou, A., Vardoulakis, S., Heaviside, C., Konsoula, Z., Christou, S., Georgiou, K.E., Ioannou, K., Mesimeris, T., Kleanthous, S., Pashiardis, S., Pavlou, P., Kassomenos, P., Yamasaki, E.N.: Human mortality in Cyprus: the role of temperature and particulate air pollution. *Reg. Environ. Change*, **16**, 1905–1913 (2016)
- [27] Unkel, S., Farrington, C.P., Garthwaite, P.H., Robertson, C., Andrews, N.: Statistical methods for the prospective detection of infectious disease outbreaks: a review. *J. Royal Stat. Soc. Ser. A* **175**, 49–82 (2012)
- [28] Vasdekis, V.G.S, Rizopoulos, D., Moustaki, I.: Weighted composite likelihood estimation for a general class of random effects models. *Biostatistics*, **15(4)**, 677–689 (2014)
- [29] Viboud, C., Boelle, P.Y., Pakdaman, K., Carrat, F., Valleron, A.J., Flahault, A.: Influenza epidemics in the United States, France, and Australia, 1972–1997. *Emerg. Infect. Dis.*, **10**, 32–39 (2004)
- [30] Wong, C.M., Yang, L, Chan, K.P., Leung, G.M., Chan KH, Guan, Y., Lam, T.H., Hedley, A.J., Peiris, J.S.: Influenza-associated hospitalization in a subtropical city. *PLoS Med*, **3(4)**, e121 (2006)
- [31] World Health Organization <<http://www.who.int/mediacentre/factsheets/fs211/en/>> (2017)
- [32] World Health Organization <[http://www.who.int/topics/public\\_health\\_surveillance/en/](http://www.who.int/topics/public_health_surveillance/en/)> (2017)



## Dealing with limitations of empirical mortality data in small populations

Anastasia Kostaki<sup>1</sup> and Konstantinos N. Zafeiris<sup>2</sup>

<sup>1</sup>Professor of Statistics-Demography Laboratory of Stochastic Modeling and Applications Department of Statistics, School of Information Sciences and Technology Athens University of Economics and Business, Greece. E-mail: [kostaki@aueb.gr](mailto:kostaki@aueb.gr)

<sup>2</sup>Assistant Professor of Demography, Laboratory of Physical Anthropology, Department of History and Ethnology, Democritus University of Thrace, Greece. E-mail: [kzafiris@he.duth.gr](mailto:kzafiris@he.duth.gr)

### Abstract

It is fairly well established that empirical age-specific mortality data are often characterized by a number of limitations and deficiencies the most common of which is a pronounced tendency in age declaration to “round-off” to certain preferred digits. Another typical limitation of such data is that in many times they are only available aggregated in five-year age groups and/or they are incomplete. In addition to these problems, special limitations related to the efficiency and stability of the empirical death data also arise when these data refer to small populations. In such cases the age-specific death rates are inefficient estimators of the corresponding death probabilities as a result of the highest impact of randomness. However, for many purposes in both demographic analysis and actuarial practice, there is a need for both reliable and analytical estimation of age-specific mortality patterns. This paper provides a review of the typical problems and limitations affecting mortality data of small populations, discusses their consequences in estimating age-specific mortality patterns, and also proposes ways to deal with them. In that, a theoretically consistent though computationally simplest technique for minimizing random variations in age-specific death counts is proposed and demonstrated using empirical death counts of some chosen small populations.

**Key words:** age pattern of mortality, mortality estimation in small populations

---

*5<sup>th</sup> SMTDA Conference Proceedings, 12-15 June 2018, Chania, Crete, Greece*

© 2018 ISAST



## **1. Introduction**

Demographers and population geographers often deal with small populations of limited geographical areas. Biostatisticians, epidemiologists, regional planners, and actuaries typically work with small sized samples of target populations. For all this broad spectrum of disciplines analytical and reliable mortality estimation is a matter of great interest.

In demography, when dealing with limited populations of small geographical areas, age-specific mortality rates are required for a lot of purposes, as for constructing complete life tables, for providing population projections, for calculations of reproduction rates. In biomedical and epidemiological studies age-specific mortality rates are required for mortality estimations and comparisons, for constructing multiple decrement tables based on limited groups of patients. In addition, in actuarial practice, where the target exposed-to-risk populations are often too limited, age-specific mortality rates are required for designing life insurance and pension programs. Finally local authorities and regional planning services often require analytical and accurate mortality estimations for limited populations of small spatial units. However the empirical mortality data of small populations are often affected by problems, not allowing reliable and accurate age-specific mortality estimations. Many authors have contributed to the study of mortality estimations of small populations, e.g. Ahcan et al. (2014), Richards (2009), Wan et al. (2013), Williamson (2006).

This paper provides a description of the typical problems and limitations affecting mortality data of small populations, discusses their consequences in estimating age-specific mortality patterns, and also proposes simple ways to deal with them. In Section 2 the various problems and limitations affecting empirical mortality data of small

populations are presented and ways for overcoming them are proposed. In Section 3 a theoretically consistent though computationally simple technique for minimizing random variations in age-specific death counts is proposed and demonstrated.

## **2. Limitations and errors of empirical mortality data**

A typical limitation of empirical mortality data of small populations is that for several reasons death counts are almost always provided aggregated in five-year age groups, while for the later adult ages, usually 85+, these are provided as a single number. The reason for this grouping is twofold. Firstly, the age specific death counts of small populations exhibit substantial variability and highly irregular age patterns as they are severely affected by randomness while in some cases, especially for the younger ages, the empirical age-specific death counts often are zero and thus useless as a basis for estimating the underlying death probabilities. In addition these data are often affected by age heaping, i.e. a misclassification of deaths originated by a preference of the responder at age declaration to round off the age of the decedent in the nearest age which is multiple of five.

In order to overcome such limitations and inconsistencies, statistical offices usually group the empirical death counts in five-year age groups assuming that the inaccuracies in single ages offset each other into each five-year age group, while through grouping zero counts are often avoided. A way to overcome such a limitation is the expansion of the grouped death counts and rates in order to estimate the corresponding age-specific ones.

Thus the expansion of grouped mortality data should be for many reasons plausible and useful. Several methods have been presented for expanding death rates, e.g. the six-point Lagrangean interpolation formula applied to the survival probabilities of  $l(x)$  of the

abridged life table in order to provide estimations of these probabilities for ages that are missing from the abridged life table. Descriptions of this method are given in Elandt-Johnson and Johnson (1980), and Namboodiri (1991). Another technique for expanding an abridged life table was developed by Kostaki (1987, 1991) and also incorporated in the MORTPAK software package. This technique utilizes the Heligman-Pollard eight-parameter formula (Heligman-Pollard, 1980). Some years later Kostaki (2000) developed a nonparametric relational expanding technique which proved much simpler than all the above though at least equally successful as the previous ones. In addition for estimating age-specific death counts, from death counts given in five-year or wider age groups, Kostaki and Lanke (2000) developed a technique for degrouping death counts of the later adult ages. In that the classical Gompertz law of mortality is utilized.

In the following section a technique for minimizing random variations of the age-specific death counts, through degrouping of the five-year ones is proposed and demonstrated. This technique is based on the idea of Kostaki and Lanke (2000). This new technique can be applied not only to later adult ages but to the whole life span. It is nonparametric and it utilizes the relational technique of Kostaki (2000) instead of any parametric model. Thus the procedure becomes notably simpler and more flexible than the former, while it has the theoretical advantages of the technique of Kostaki and Lanke (2000) parametric one.

### **3. A technique for estimate age-specific death counts from data given in five-year age groups**

Consider the empirical death count for the five-year age interval  $[x, x+5)$ ,  ${}_5D_x$ ,  $x=0, 5, 10, \dots, w-5$ . Then the five-year death rates  ${}_5q_x$ ,  $x=0, 5, 10, \dots$  are calculated by

$${}_5q_x = {}_5d_x / \sum_{y \geq x} {}_5d_y \quad (3.1)$$

where the summation in the denominator of (3.1) is restricted to multiples of five. Obviously the consideration of the exposed-to-risk population of a given age as the sum of deaths after that age is precisely valid when the data concern a closed cohort. However, Kostaki and Lanke (2000) demonstrated that this procedure produces excellent results even when applied to period data.

The next step now is to expand the abridged  ${}_5q_x$  values as calculated by (3.1). For that we consider a set of one-year probabilities,  $q_x^{(S)}$  ( $S$  for Standard) of some available complete life table. Under the assumption that the force of mortality,  $\mu(x)$ , underlying the target abridged  ${}_5q_x$  values is, in each age of the five-year age interval  $[x, x+5)$ , a constant multiple of the one underlying the standard life table in the same age interval,  $\mu^{(S)}(x)$ , i.e.

$$\mu(x) = {}_5K_x \cdot \mu^{(S)}(x) \quad (3.2)$$

the one-year probabilities  $q_{x+i}$ ,  $i = 0, 1, \dots, 4$ , in each five-year age interval can be estimated using

$$\tilde{q}_{x+i} = 1 - (1 - q_{x+i}^{(S)})^{5K_x} \quad (3.3)$$

where

$${}_5K_x = \frac{\ln(1 - {}_5q_x)}{\sum_{i=0}^4 \ln(1 - q_{x+i}^{(S)})} \quad (3.4)$$

An inherent property of the results is that they fulfill the desired relation:

$$1 - \prod_{i=1}^4 (1 - \tilde{q}_{x+i}) = {}_5q_x \quad (3.5)$$

Now, using the estimated age-specific death probabilities, as calculated using (3.3), estimations of the age-specific death counts  $\tilde{d}_x$  can be calculated, for the ages that are multiples of five using

$$\tilde{d}_x = \tilde{q}_x \cdot \sum_{y \geq x} {}_5d_y \quad (3.6)$$

while for the rest of ages using

$$\tilde{d}_{x+i} = \prod_{j=0}^{i-1} (1 - \tilde{q}_{x+j}) \tilde{q}_{x+i} \cdot \sum_{y \geq x} {}_5d_y, \quad i = 1, 2, 3, 4 \quad (3.7)$$

It is interesting to observe that the resulting  $\tilde{d}_x$  fulfill the desirable property

$$\sum_{i=0}^4 \tilde{d}_{x+i} = {}_5d_x \quad (3.8)$$

#### 4. Evaluation

As a demonstration of the technique proposed, we apply it to empirical death data of the male and female populations of some chosen municipalities of Greece, for the year 2015.

For each population, we repeat the estimation procedure two times using two alternative

complete life tables as standards. These are the complete life tables of the total population of France and the total population of the US for the year 2015, both taken from the Human Mortality Database at <http://www.mortality.org>. The empirical age-specific death counts of males and females of Heraklion, Magnessia, and Ioannina for the year 2015 are taken from Hellenic Statistical Authority.

In order to estimate the age-specific death counts of each one of the target populations, we initially group the one-year death counts for each one of the six target populations in five-year age groups, while for the ages 85 and above we sum the death counts in a single number. Then using (3.1) we calculate the five-year death rates. Considering the grouped data as the basis of our calculations we firstly proceed considering as standard life table the complete ones of the total population of France and using (3.4) and (3.3) we provide estimates for the one-year death probabilities of each one of the six target populations. Then we repeat the same procedure using as standard life table the complete one of the total population of the US for the year 2015. Finally using (3.6) and (3.7) we provide estimates of the age-specific death counts of each one of the six target populations resulting using the two alternative standard populations. Figures 1-6 illustrate the empirical death counts (small circles), together with the resulting ones (small crosses and small rhombuses) by age. It is obvious that the estimates of the age-specific death counts are by far smoother than the corresponding empirical ones and therefore much less affected by random variations while importantly, they never become zero as far as there is at least a single event into each five-year age group. Comparing the results between the two applications in each target population we observe that they exhibit insignificant differences. In addition, independently of the standard life table used, their sums into each age group are equal to the empirical death count of this age group, a desired relation which is a property of our technique.

## 5. Remarks

In this paper errors and limitations of empirical death data of small populations are considered, and ways for overcoming these problems are discussed and proposed. Expanding techniques seems to be most useful for estimating age-specific mortality patterns when the empirical data are aggregated or/and when they suffer by inaccuracies such as erroneously age documentations especially when in addition to all the above, the empirical data refer to small populations. For the purpose of minimizing random variations of death counts but to also provide estimations of the age specific death counts of the higher adult ages 85+, a theoretically consistent though computational simplest technique is proposed. This technique is a modification of the degrouping technique proposed and evaluated by Kostaki and Lanke (2000), in which instead of using a parametric model for expanding the five-year death rates to one-year ones, the relational technique of Kostaki (2000) is utilized. This modification significantly simplifies the computations and allows estimation of the death curve for all ages, while the degrouping technique of Kostaki and Lanke (2000) is intended to estimate age-specific death counts only for the later adult ages. The new technique considerably minimizes random irregularities, while its results fulfill the desirable theoretical properties (3.5) and (3.8). It is impressive that the technique produces highly accurate estimations of the age-specific death counts for the ages 85+ based on a single aggregated death count for all these ages. As Kostaki (2000) has previously shown and the results of our calculations here also verify, the choice of the standard table does not affect the results. Finally the calculation procedure is very simple. No advance software is required, while it can be performed even by a plain pocket calculator.

Figure 1. Observed and estimated death counts of Heraklion males, 2015, using life tables of France and the USA.

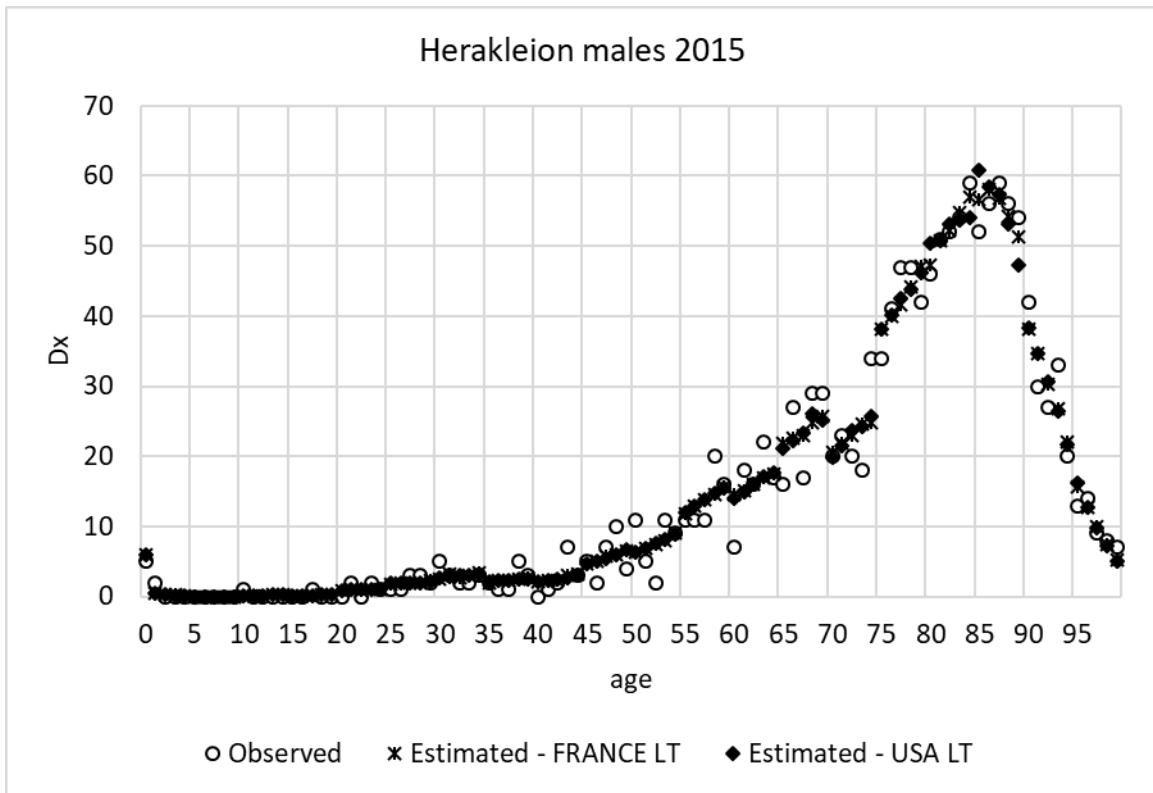


Figure 2. Observed and estimated death counts of Heraklion females, 2015, using life tables of France and the USA.

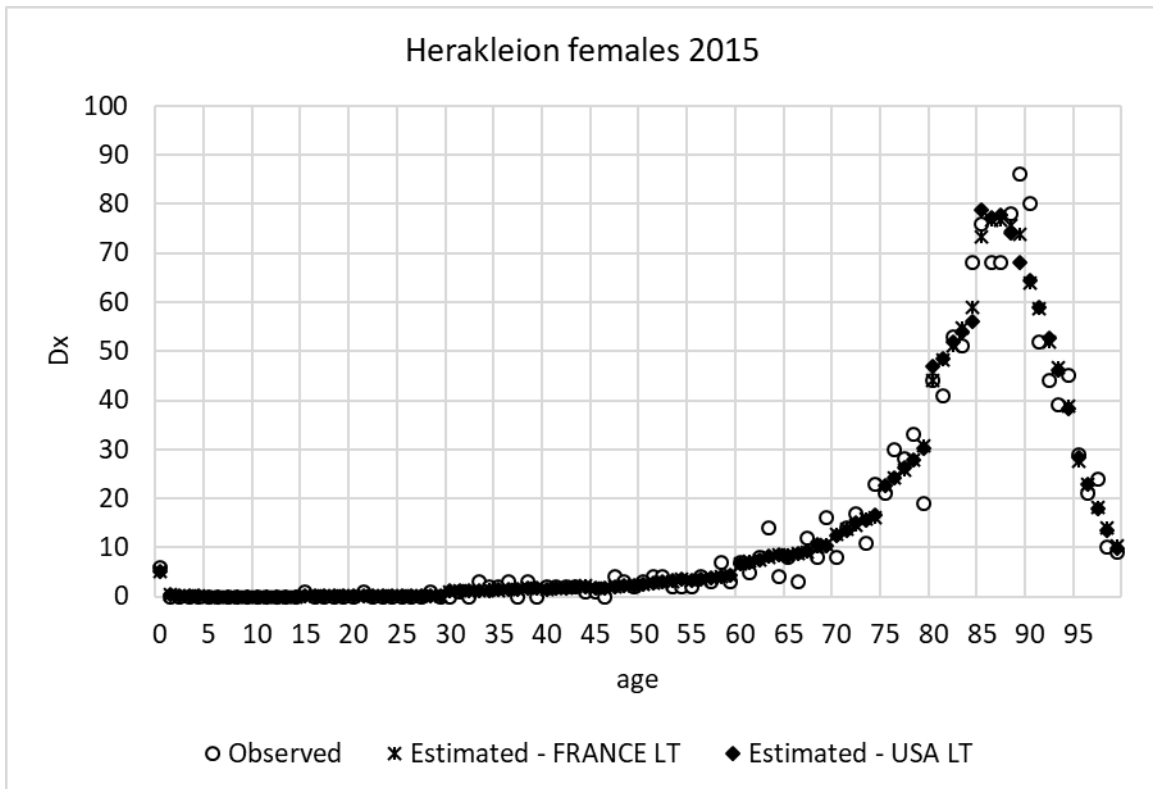


Figure 3. Observed and estimated death counts of Magnessia males, 2015, using life tables of France and the USA.

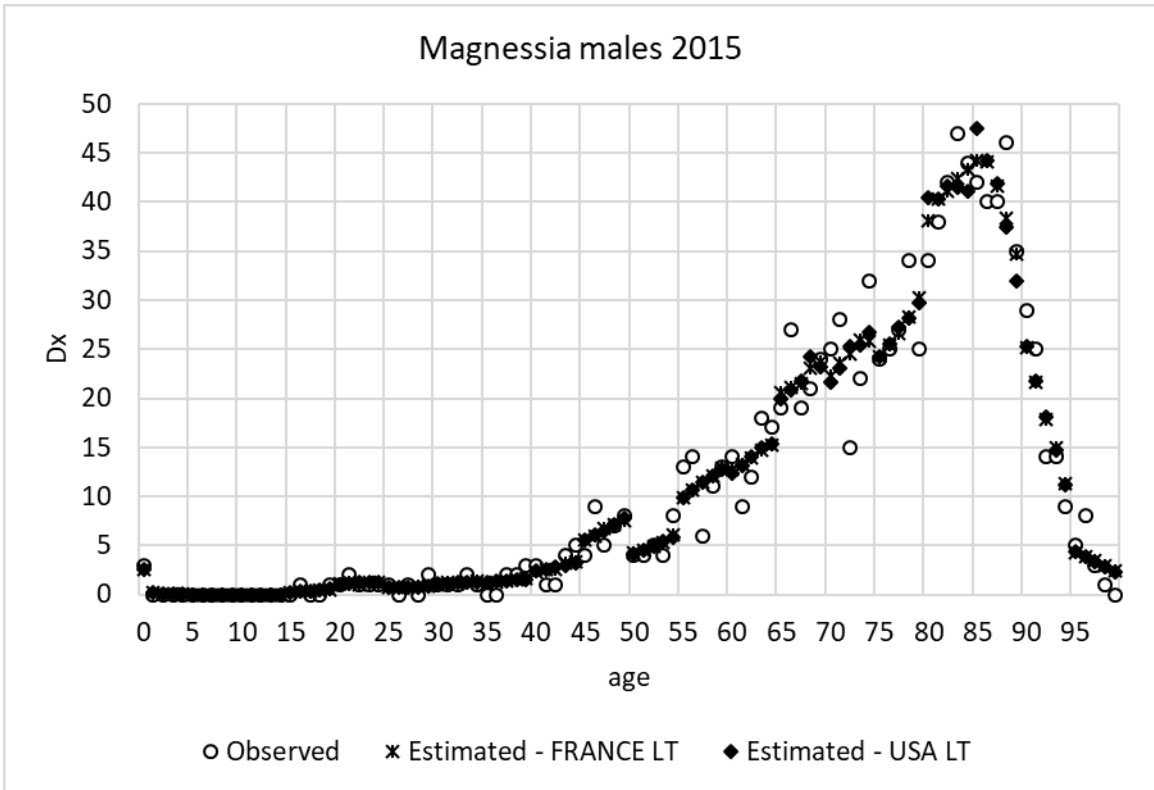


Figure 4. Observed and estimated death counts of Magnessia females, 2015, using life tables of France and the USA.

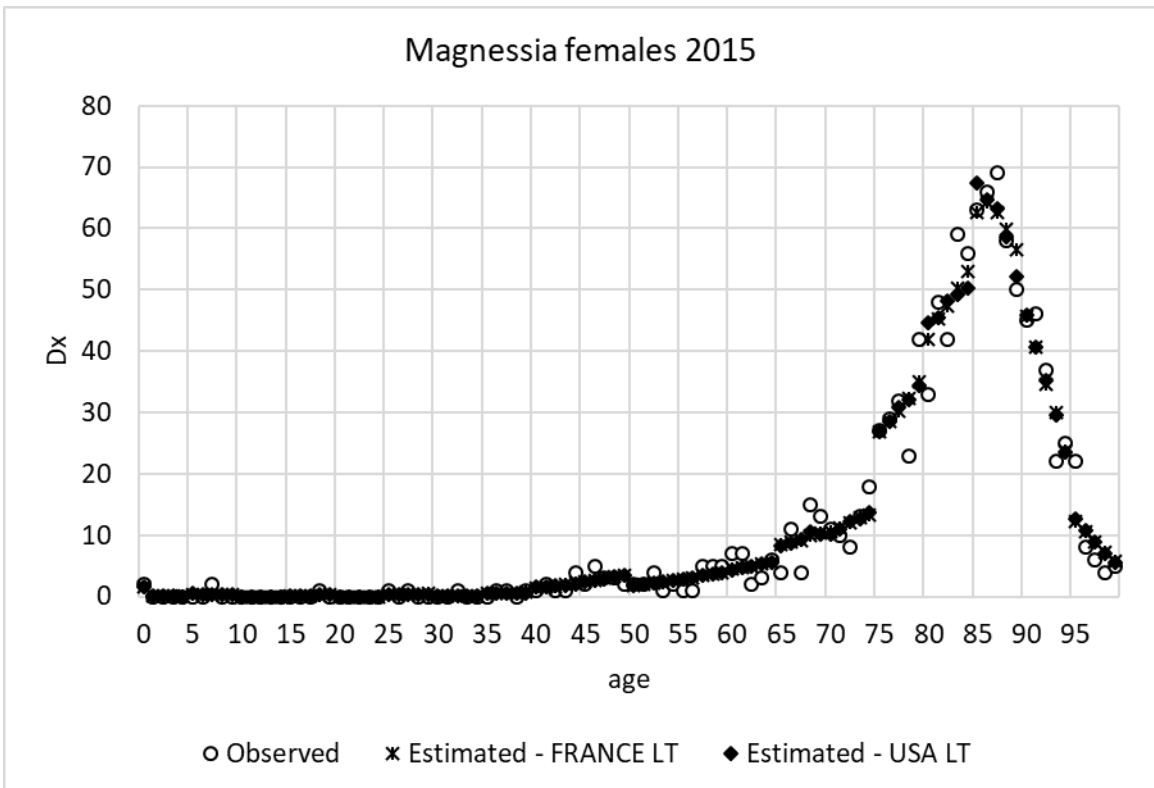


Figure 5. Observed and estimated death counts of Ioannina males, 2015, using life tables of France and the USA.

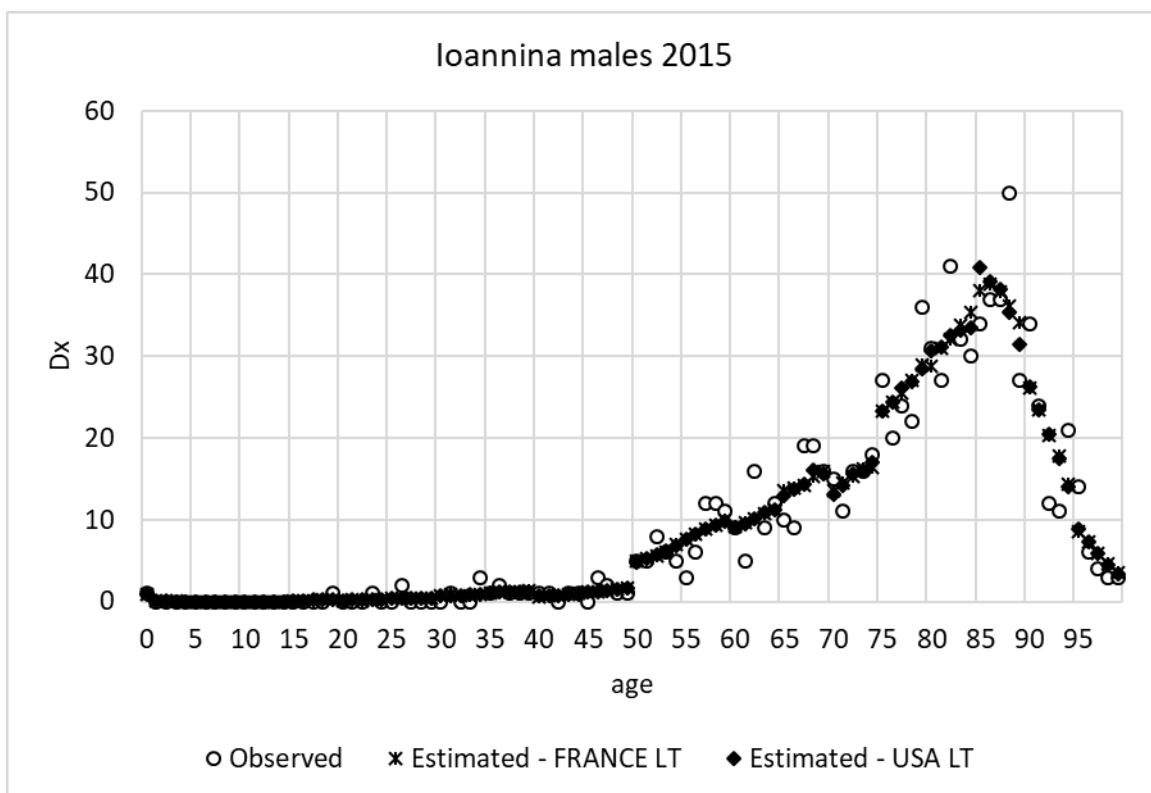
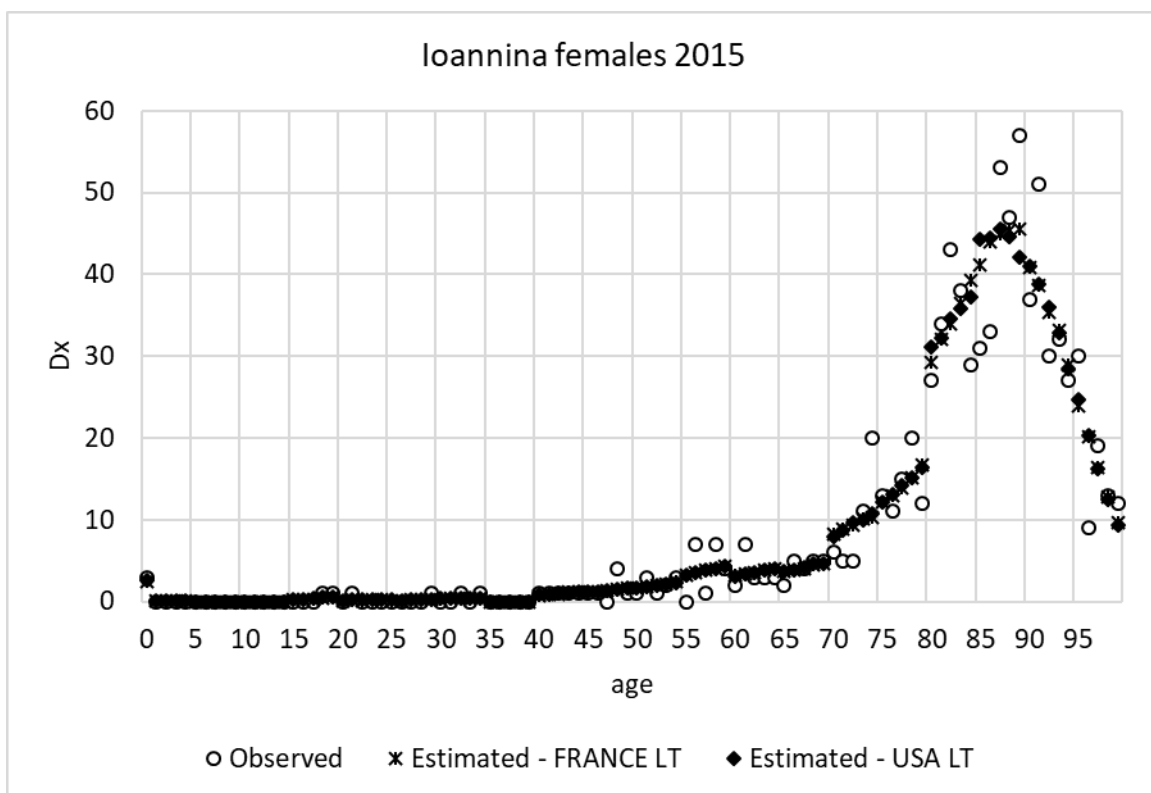


Figure 6. Observed and estimated death counts of Ioannina females, 2015, using life tables of France and the USA.



## References

- Ahcan, A., Medved, D., Olivieri, A., Pitacco E. 2014: Forecasting Mortality for Small Populations by Mixing Mortality Data. *Insurance: Mathematics and Economics*, 54: 12-27.
- Elandt-Johnson, R., Johnson, N. 1980: *Survival Models and Data Analysis*. New York, John Wiley.
- Heligman, L., Pollard, J. H. 1980: The Age Pattern of Mortality. *Journal of the Institute of Actuaries*, 107: 49-80.
- Kostaki, A. 1987: The Heligman-Pollard Formula as a Technique for Expanding an Abridged Life table. Technical report, Lusadgd-SAST-3116/1-15. Department of Statistics, University of Lund, Sweden.
- Kostaki, A. 1991: The Heligman-Pollard Formula as a Tool for Expanding an Abridged Life table. *Journal of Official Statistics*, 7(3): 311-323.
- Kostaki, A., 1992: A Nine-Parameter Version of the Heligman - Pollard Formula. *Mathematical Population Studies*, 3(4), 277-288.
- Kostaki A., Lanke J. 2000: Degrouping mortality data for the elderly. *Mathematical Population Studies*, 7(4), 331-341.
- Kostaki A. 2000: A relational technique for estimating the age-specific mortality pattern from grouped data. *Mathematical Population Studies*, (1), 83-95.
- Kostaki, A., Panousis, E. 2001: Methods of expanding abridged life tables: Evaluation and Comparisons. *Demographic Research*, 5(1), 1-15. <http://www.demographic-research.org/volumes/vol5/1/>.
- Kostaki, A., Moguerza, M.J., Olivares, A., Psarakis, 2011: Support Vector Machines as tools for Mortality Graduations. *Canadian Studies in Population* 38(3-4), 37-58. <http://www.canpopsoc.ca/CanPopSoc/assets/File/publications/journal/2011/CSPv38n3-4p37.pdf>
- Namboodiri N. K. 1991: *Demographic analysis: A stochastic approach*. Academic Press, San Diego.
- Richards, S. J. 2009: Selected issues in Modeling Mortality by cause and in small Populations, *British Actuarial Journal* 15, Supplement, 267-283
- Wan, C., Bertschi, L., Yang, Y. 2013: Coherent Mortality Forecasting for small Populations: an application to Swiss mortality data
- Williamson, L., 2006: *Developing Strategies for Deriving Small Population Mortality Rates*. CCSR Working Paper.

# Dependability and Performance Analysis for a Two Unit Multi-State System with Imperfect Switch

Vasilis P. Koutras<sup>1</sup>, Sonia Malefaki<sup>2</sup>, and Agapios N. Platis<sup>1</sup>

<sup>1</sup>Department of Financial and Management Engineering, School of Engineering, University of the Aegean, Chios, 82100, Greece.

(E-mail: [v.koutras@fme.aegean.gr](mailto:v.koutras@fme.aegean.gr); [platis@aegean.gr](mailto:platis@aegean.gr))

<sup>2</sup>Department of Mechanical Engineering & Aeronautics, University of Patras, Rio, Patras, 26504, Greece

(E-mail: [malefaki@upatras.gr](mailto:malefaki@upatras.gr))

**Abstract.** A two-unit multi-state deteriorating system under preventive conditioned based maintenance and imperfect switch among units is considered. The system consists of one operating and one unit in cold standby mode. System control is switched to the standby unit when the operational unit experiences a failure or enters in a maintenance state. The switching automated mechanism can experience failures either due to often use that incur aging and degradation effects, or even due to extended periods of being idle. In this case a manually switch is initiated. The operational unit is periodically inspected in order to distinguish if any maintenance action needs to be triggered. Moreover, maintenance can be imperfect, restoring the unit to a worse degraded state, or even to a total failure state, mainly due to external factors. The main aim of this work consists in studying the transient behaviour of the aforementioned two-unit system under a Markov framework and in examining how unit inspection intervals, as well as switching mechanism success probability, affect the entire system dependability and performance. Towards to this direction, system transient and asymptotic availability as well as total expected operational cost are derived. The endmost purpose of the current work is to determine an optimal inspection and thus maintenance policy that improves system dependability and performance measures.

**Keywords:** Multi-state system, redundancy, imperfect switch, maintenance, transient availability, dependability, total expected operational cost.

## 1. Introduction

The last decades the design of large scale and complexity technological systems is of great importance mainly due to the rapid development of technology and the increasing demand on various critical applications. The reliability and the availability of these systems are of great importance since their deterioration and/or failure may lead to serious economic and social losses [1]. Thus, in order to improve the operation of such a system and increase its availability and reliability, redundancy can be introduced. One of the most commonly used types of redundancy is the standby redundancy. In a standby redundant system, apart from the operational units, there are a number of standby units as backups, in order to replace any

*5<sup>th</sup> SMTDA Conference Proceedings, 12-15 June 2018, Chania, Crete, Greece*



component after a failure. The switching process from the failed unit to the standby unit is assigned to an automated mechanism, which is assumed that can fail with a positive probability ([21], [7], [16]). The automated restoration mechanism usually fails due to frequently use which results in aging and degradation, or due to the long period it is in standby mode. In the latter case, usually called imperfect switch, the switching process is operated manually ([6], [20]). The manual switch restores the system to an operational state again. However, more time is needed for manual than for automatic switch. After an automated mechanism failure, either maintenance or replacement actions are initiated.

For further improvement of the operational time and condition of a multi-state system, maintenance actions can be adopted [12], [15]. All necessary actions for keeping and/or restoring a system in an acceptable operating condition or even extending its lifetime are considered as system maintenance. These actions can be divided into corrective and preventive maintenance actions. Corrective maintenance occurs when the system fails, contrary to preventive maintenance that occurs during its operational period. Under normal circumstances, preventive maintenance is more effective than corrective, since its main aim is to keep the system available and avoid undesirable failures that incur considerably high cost [3], [2]. There are two main types of preventive maintenance, condition based and time based maintenance [10]. Time-based maintenance is carried out at specific time intervals independently of system's state. Condition based maintenance depends on system's state; the system is regularly inspected and depending on its state, either it is left without maintenance, if it works in an acceptable level, or minimal/major maintenance takes place, restoring the system in a previous deterioration level or in an as good as new state respectively, when the system operates in an inefficient deterioration level.

Although preventive maintenance has been adopted for improving the performance of a system, it incurs downtime and consequently implies a cost. Thus, preventive maintenance needs to be properly scheduled. An appropriate preventive maintenance policy that manages to reduce the total operational cost and improve the availability of the system is of critical importance. A lot of research effort has been paid to this direction (c.f. [14], [18], [19]). A recent review paper on optimal maintenance policies can be found in [5].

In the current work, a two identical unit cold standby system with imperfect switch is modeled. Each unit is functioning under multiple states of degradation, from their perfect state to their total failure [11]. The switching process between the two units is assigned to an automated mechanism, which is assumed that it can fail with a positive probability ([16]) and a manual switch is triggered to shift system control to the operating unit. Our aim is to compute the main dependability and performance measures for the proposed model in

transient as well as in its asymptotic phase, and to examine how unit inspection rate, switching mechanism success probability as well as the manual switch rate, affect the entire system dependability and performance in both phases.

The rest of the paper is organized as follows: In Section 2, the proposed model for the system under consideration is described analytically. In section 3, the main dependability and performance measures are defined in transient phase and in the steady state too. The optimization problems for detecting the optimal maintenance policy for system dependability and performance are presented in Section 4. In Section 5, some numerical results are presented to illustrate the theoretical framework provided and to examine also system behavior. The paper is concluding by providing a short discussion and mentions some points for further research.

## 2. Description of the system under maintenance and imperfect switch

In the current paper a two identical unit system which experiences deterioration is considered. One unit is operating and one is in a cold standby mode. It is assumed that initially both units are in their perfect state, thus the whole system is fully operational. The operational unit can be either in its perfect state (O), or in one of the deterioration states  $D_i$   $i = 1, 2, 3$  where  $D_i$  denotes the  $i^{\text{th}}$  deterioration level prior to the total failure (F). In order to delay or even to avoid a total failure, depending on the deterioration level of the operating unit, minimal (m) or major (M) maintenance actions are implemented. To identify the level of deterioration and thus decide on the type of maintenance to be triggered, periodical unit inspection takes place. In particular, from its perfect state or from each of the deterioration states, the operational unit may enter an inspection state  $I_k$ ,  $k = 0, 1, 2, 3$  respectively. Thus, the state space of the operational unit can be defined by

$$E^O = \{O, D_1, D_2, D_3, I_0, I_1, I_2, I_3, m, M, F\}.$$

As far as the standby unit is concerned, its operational states can be denoted by

- $O^S$ : if the standby unit is in its perfect state
- $D_i^S$ : if the standby unit is in the  $i^{\text{th}}$  deterioration level ( $i = 1, 2, 3$ )

When the operational unit enters a maintenance state (minimal or major) or experiences a failure, system control is switched to the standby unit either automatically with probability  $c$ , or manually, when the automated switch mechanism experiences a failure, with probability  $1 - c$ . Such failures are mainly due to either often use which incurs aging and degradation effects, or even due to extended periods of being idle. In case of manual switch

the operating unit enters a so-called manual switch state ( $MS^l, l = m, M, F$ ). Note that in this case the automated switch mechanism is replaced by a new identical one. During manual switch, either due to a failure or due to maintenance of the operating unit, the state of the standby unit does not change. It is important to note that system control will be switched to the standby unit after the completion of manual switch only if this is in an operational state. Taking into account the aforementioned description, the state space of each system unit, either in operational or in standby mode, is denoted by  $E$  ( $E^O \subset E$ ):

$$E = \{O, O^S, D_1, D_2, D_3, D_1^S, D_2^S, D_3^S, I_0, I_1, I_2, I_3, m, M, F, MS^m, MS^M, MS^F\}$$

In order to denote the state of the system, a pair  $(i, j)$  is used, where  $i, j \in E$  denote the condition of the primary and supplementary unit respectively. Initially, the system starts to operate in its perfect state, i.e. the primary and the standby units are both in their fully operational state  $(O, O^S)$ . From the perfect state the system may enter one of the next deterioration levels  $(D_i, O^S)$ ,  $i = 1, 2, 3$  or state  $(F, O)$  if system control is switched automatically from the failed unit to the standby unit, or even state  $(F, MS^F)$  if the automated switch mechanism experiences failure and the switching process is performed manually. Moreover, from state  $(O, O^S)$  the system may enter the inspection state  $(I_0, O^S)$ . From each of the deterioration states  $(D_i, j)$   $i = 1, 2, 3$ ,  $j \in \{O^S, D_1^S, D_2^S, D_3^S, m, M, F\}$ , the operational unit may enter an inspection state  $(I_i, j)$  respectively due to the assumption that during the inspection of the operating unit the state of the standby unit does not change. In case that unit deterioration occurs prior to inspection, the unit enters one of the next deterioration states (depending on the level of deterioration), or even the failure state in case of a sudden failure which can occur mainly due to external factors. If after the inspection the operating unit is detected in its perfect state, or in the first deterioration state  $(D_1)$ , no maintenance action takes place. On the other hand, if the unit is either in the second  $(D_2)$  or in the third  $(D_3)$  deterioration level, minimal or major maintenance action is triggered respectively, and the system control is switched to the standby unit, if this is allowed. Either minimal or major maintenance can be perfect, imperfect or failed. A perfect minimal maintenance restores the unit to its previous deterioration level (from state  $D_2$  to state  $D_1$ ), though an imperfect minimal maintenance restores the unit to the same deterioration level. Failed minimal maintenance leads the unit to a worse deterioration level or even to a total failure (from state  $D_2$  to state  $D_3$  or  $F$ ). On the other hand, perfect major maintenance restores the unit to its perfect state (as good as new), though imperfect major maintenance can restore the system to any of the previous deteriorations states  $(D_1$  or  $D_2)$  or even to the same deterioration level  $(D_3)$ , with different rates. Failed major maintenance leads the unit to the total failure state  $(F)$ .

The resulting system consists of 145 states in total. All states of the system as well as all possible transitions are presented in Table A1 in the Appendix.

Exponential distributions are assumed for all the sojourn times. Note that the failure rates for the deterioration process are state-dependent, i.e. the higher the deterioration level the more probable is for the system to enter a worse deterioration level [1]. Additionally, it is assumed that the inspection duration is negligible compared with any other sojourn time, thus there is not enough time for any other transition to occur during inspection [22]. The transition rates among unit possible states are presented in Table 1. Thus, the evolution of the system in time is described by a Markov process  $\{Z(t), t \geq 0\}$ .

Table. 1. Transition rates

Rate	Description	Rate	Description
$\lambda_1$	Deterioration rate from $O$ to $D_1$	$\mu_I$	Inspection response rate
$\lambda_{12}$	Deterioration rate from $O$ to $D_2$	$\lambda_n$	Minimal maintenance rate
$\lambda_{13}$	Deterioration rate from $O$ to $D_3$	$\lambda_{Im}$	Imperfect minimal maintenance rate
$\lambda_{f1}$	Sudden failure rate from $O$ to $F$	$\lambda_{fm}$	Failed minimal maintenance rate
$\lambda_2$	Deterioration rate from $D_1$ to $D_2$	$\lambda_{Fm}$	Failure rate due to minimal maintenance failure
$\lambda_{22}$	Deterioration rate from $D_1$ to $D_3$	$\lambda_M$	Major maintenance rate
$\lambda_{f2}$	Sudden failure rate from $D_1$ to $F$	$\lambda_{IM1}$	Imperfect major maintenance rate of level 1
$\lambda_3$	Deterioration rate from $D_2$ to $D_3$	$\lambda_{IM2}$	Imperfect major maintenance rate of level 2
$\lambda_{f3}$	Sudden failure rate from $D_2$ to $F$	$\lambda_{IM3}$	Imperfect major maintenance rate of level 3
$\lambda_4$	Deterioration rate from $D_3$ to $F$	$\lambda_{FM}$	Failure rate due to major maintenance failure
$\lambda_{IN}$	Inspection rate	$\lambda_R$	Repair rate

### 3. Dependability and performance measures

Initially, we intend to evaluate the dependability and performance of the proposed model for the two-unit multi state system under maintenance and imperfect switch aiming in examining the behavior of the system in terms of availability and operational cost. Let the entire system state space defined by  $E'$ . The elements of  $E'$  are shown in the 1<sup>st</sup> and the 3<sup>rd</sup> columns of Table A1 in the Appendix. Note that  $E'$  is divided in two subsets  $U$  and  $D$ . Subset  $U$  contains all system operational states, though subset  $D$  contains all states in which none of the system units is in an operational mode (down states) such as the following relationships hold true:  $E' = U \cup D, U \cap D = \emptyset$ .

Initially, the transient phase of the system is studied. However, since such systems are designed to operate continuously in time, its asymptotic behavior, in terms of dependability and performance, is also studied.

#### 3.1. Transient phase

In the transient phase (as well as in the asymptotic phase) system availability is used as a dependability measure though the total expected operational cost due to system downtime and due to any actions taken (inspection, maintenance, replacement of automated switch

mechanism, unit repair) is used as a system performance measure. To evaluate these measures at time  $t \geq 0$ , the probability transition matrix for the Markov process that describes systems' evolution in time needs to be derived.

For the homogeneous continuous time Markov process  $Z = \{Z(t), t \geq 0\}$  and the state space  $E'$  which have been already defined, let  $\mathbf{Q} = (q_{(i,j),(i',j')})_{(i,j),(i',j') \in E'}$  be the infinitesimal generator matrix with  $q_{(i,j),(i',j')} \geq 0, (i,j) \neq (i',j')$  and  $q_{(i,j),(i,j)} = -q_{(i,j)} = \sum_{(k,l) \in E', (k,l) \neq (i,j)} q_{(i,j),(k,l)}$ . Let also  $\boldsymbol{\alpha} = (\alpha(i,j))_{(i,j) \in E'}$  be the initial distribution of  $Z$  at time  $t = 0$  and  $\mathbf{P}(t) = (p_{(i,j),(i',j')}(t))_{(i,j),(i',j') \in E'}, t \geq 0$  its transition function with:

$$\begin{aligned} p_{(i,j),(i',j')}(t) &= \Pr(Z(t) = (i',j') | Z(0) = (i,j)) \\ &= \Pr(Z(t+h) = (i',j') | Z(h) = (i,j)), \forall h \geq 0. \end{aligned} \quad (1)$$

In this case, the solution of the Kolmogorov equation is:

$$\mathbf{P}(t) = e^{t \cdot \mathbf{Q}} \quad (2)$$

which is the probability transition matrix at  $t \geq 0$  with  $\mathbf{P}(0) = \mathbf{I}$  the identity matrix [17], [8].

### 3.1.1. Transient Availability

Based on the two-unit multistate deteriorating system model and the aforementioned assumptions, system instantaneous availability at time  $t \geq 0$  can be evaluated as follows [17]:

$$AV(t) = \Pr(Z(t) \in U) = \boldsymbol{\alpha} \cdot e^{t \cdot \mathbf{Q}} \cdot \mathbf{1}_{|E'|,|U|} \quad (3)$$

where  $\mathbf{1}_{|E'|,|U|}$  is a vector of dimensions  $|E'| \times 1$  containing ones in the entries that correspond to system operational states and zeros in the entries that correspond to the non operational states. Thus  $\mathbf{1}_{|E'|,|U|}$  contains  $|U|$  ones and  $|E'| - |U|$  zeros.

### 3.1.2. Total Expected Operational Availability

Minimal and major maintenance actions, repair/replacement along with other action schedules are usually designed for minimizing any system's downtime. As a consequence, system designers are usually interested in minimizing the total downtime. Taking also into account that for each unit, non operational time incurs a cost for the system, the total expected cost achieved when the system is in a non operational mode, should include also a cost per unit of downtime [9], [13]. In the proposed model, system downtime occurs when both units are non operational, when the operating unit is inspected and during manual switch among units. In order to define the total expected downtime cost let us define a reward function:

$$w^D(i, j) = \begin{cases} C_D, & \text{if } (i, j) \in D \\ 0, & \text{else} \end{cases} \quad (4)$$

where  $C_D$  is the cost per unit of downtime time that occurs when system is in a non operational state. Thereafter  $w^D(i, j)$  is used for evaluating the total expected downtime cost per unit time. In particular, let  $g(Z(t))$  be the downtime reward rate at time  $t$ :

$$g(Z(t)) = \sum_{(i,j) \in E'} w^D(i, j) \cdot I_{\{Z(t)=(i,j)\}} \quad (5)$$

where  $I_{\{Z(t)=(i,j)\}}$  is an indicator function. Then the total expected downtime cost can be expressed as the mean of the reward rate  $g(Z(t))$ :

$$\begin{aligned} TEDC(t) &= E[g(Z(t))] = E[\sum_{(i,j) \in E'} w^D(i, j) \cdot I_{\{Z(t)=(i,j)\}}] \\ &= \sum_{(i,j) \in E'} w^D(i, j) \cdot E[I_{\{Z(t)=(i,j)\}}] = \sum_{(i,j) \in E'} w^D(i, j) \cdot \Pr(Z(t) = (i, j)) \\ &= \sum_{(i,j) \in E'} w^D(i, j) \cdot \pi_{(i,j)}(t) \end{aligned} \quad (6)$$

where  $\pi_{(i,j)}(t)$  is the probability of state  $(i, j) \in E'$  and can be obtained using (2). Alternatively,  $TEDC(t)$  can be obtained according to the following equation:

$$TEDC(t) = C_D \left( \boldsymbol{\alpha} \cdot e^{t \cdot \mathbf{Q}} \cdot \mathbf{1}_{|E'|, |D|} \right) \quad (7)$$

where  $\mathbf{1}_{|E'|, |D|}$  is a vector of dimension  $|E'| \times 1$  containing ones in the entries that correspond to system down states and zeros in the entries that correspond to operational states. Thus  $\mathbf{1}_{|E'|, |D|}$  contains  $|D|$  ones and  $|E'| - |D|$  zeros.

Beyond downtime cost, whenever an action takes place, an additional action cost occurs. Thus, as already mentioned, inspection, minimal and major maintenance, unit repair as well as automated switch mechanism replacement after it experiences a failure incur cost. Similarly to  $TEDC(t)$ , for defining the total expected action cost  $TEAC(t)$ , the corresponding reward function is defined as follows:

$$w^A(i, j) = \begin{cases} C_I, & \text{if in state } (i, j) \text{ a unit is under inspection} \\ C_m, & \text{if in state } (i, j) \text{ a unit is under minimal maintenance} \\ C_M, & \text{if in state } (i, j) \text{ a unit is under major maintenance} \\ C_R, & \text{if in state } (i, j) \text{ a unit is under repair} \\ C_S, & \text{if in state } (i, j) \text{ the switched mechanism should be replaced} \\ 0, & \text{else} \end{cases} \quad (8)$$

where  $C_I$  is the cost per unit time for inspecting a unit,  $C_m$  is the cost per unit time for implementing minimal maintenance,  $C_M$  is the cost per unit time for implementing major maintenance,  $C_R$  is the cost per unit time for unit repair/replacement, while  $C_S$  is the cost for replacing the switch mechanism after a failure. Depending on their nature, let  $C_I < C_m < C_M < C_S < C_R$  since the cost of repairing/replacing a unit is higher than all other costs, while the cost of major maintenance is higher than the corresponding cost of minimal maintenance. Note that despite inspection's negligible duration compared with all the other actions, it incurs a cost which is the lowest among all others. Finally, it is assumed that the switch mechanism replacement cost is higher than maintenance costs but lower than unit repair cost. As far as the corresponding action reward rate, it can be defined as follows:

$$f(Z(t)) = \sum_{(i,j) \in E'} w^A(i,j) \cdot I_{\{Z(t)=(i,j)\}} \quad (9)$$

and then the total expected action cost can be defined similarly to equation (6). However, we will alternatively use equation (10) to define and evaluate this cost:

$$TEAC(t) = \alpha \cdot e^{t \cdot Q} \cdot w^A \quad (10)$$

where  $w^A$  is a vector with dimensions  $|E'| \times 1$  containing  $C_I, C_m, C_M, C_S, C_R$  in its entries that corresponds to system states that the aforementioned (costly) actions take place with respect to equation (9).

Finally, whenever a system similar to the one that is modelled in this paper is used, system designers are usually interested in evaluating a combined (downtime + action) cost. Let this cost be declared as Total Expected Operational Cost (*TEOC*). Then, the overall system cost at time  $t$  due to downtime and all actions taken can be defined as follows:

$$TEOC(t) = TEAC(t) + TEDC(t) \quad (11)$$

### 3.2. Asymptotic analysis

Since such systems are usually designed to operate continuously in time, we are also interested in evaluating the asymptotic behaviour of the system and consequently the limiting values of the defined dependability and performance measures.

In the way that availability as well as total operational cost have been defined in (3) and (11) respectively, it is not difficult to evaluate their limiting values by setting  $t \rightarrow \infty$ . Thus, the asymptotic availability and the total operational cost in steady state can be defined as follows:

$$AV = \lim_{t \rightarrow \infty} AV(t) \quad (12)$$

$$TEOC = \lim_{t \rightarrow \infty} TEOC(t) \quad (13)$$

Alternatively, the asymptotic availability and the total expected operational cost in steady state can be evaluated using equations:

$$AV = \sum_{(i,j) \in U} \pi_{(i,j)} \quad (14)$$

$$TEOC = \sum_{(i,j) \in E'} w^D(i,j) \cdot \pi_{(i,j)} + \sum_{(i,j) \in E'} w^A(i,j) \cdot \pi_{(i,j)} \quad (15)$$

where  $\boldsymbol{\pi} = (\pi_{(i,j)})_{(i,j) \in E'}$  is the steady state probability distribution vector. The steady state probability distribution for the proposed model can be derived by solving the following system of linear equations:  $\boldsymbol{\pi} \cdot \mathbf{Q} = \mathbf{0}$ ,  $\sum_{(i,j) \in E'} \pi_{(i,j)} = 1$ .

It is also worth mentioning that system designers are interested in determining the maintenance policies that optimise asymptotically the dependability and performance of a system. Thus equations (14) and (15) are used as objective functions in some optimization problems that are formulated in the following section, with the inspection rate  $\lambda_{IN}$  as the decision variable.

## 4. Optimal Maintenance Policy

Determining the optimal inspection policy is equivalent to determining the maintenance policy that optimizes either system dependability, or system performance, or even both of these measures. Although transient system behaviour is of prior interest in the current work, designing an optimal maintenance schedule would benefit the two-unit multistate system in the long-run. Thus, optimization problems for the dependability and performance measure using as objective functions the expressions derived in equations (14) and (15) are formulated. However, once the maintenance schedule that optimizes asymptotic availability and/or performance is derived, it would be implemented in the considered system from the beginning of its lifetime. Thus, the effects of the aforementioned optimal maintenance schedules on system's transient behaviour could be also observed.

### 4.1. Optimal maintenance policy for maximizing system availability

Depending on system characteristics, a lower ( $\lambda_{IN}^{LB}$ ) and an upper ( $\lambda_{IN}^{UB}$ ) bound can be settled for the inspection policy  $\lambda_{IN}$  which is the decision variable. Consequently the mathematical programming model for asymptotic system availability, with respect to the inspection policy is:

$$\begin{aligned} & \max AV \\ & s. t. \lambda_{IN}^{LB} \leq \lambda_{IN} \leq \lambda_{IN}^{UB} \end{aligned} \tag{16}$$

Solving (16) results in providing the optimal inspection policy that maximizes system asymptotic availability.

#### 4.2. Optimal maintenance policy for minimizing total expected operational cost

Depending on the system requirements, an inspection policy that minimizes the total operational cost could be also derived. Based on equation (14), the corresponding mathematical programming model that can be formulated for this case is:

$$\begin{aligned} & \min TEOC \\ & s. t. \lambda_{IN}^{LB} \leq \lambda_{IN} \leq \lambda_{IN}^{UB} \end{aligned} \tag{17}$$

Solving (17) results in providing the optimal inspection policy that minimizes system asymptotic total operational cost.

#### 4.3. Optimal maintenance policy for multi-objective optimization problems

Note that any inspection policy selected to be adopted for the system would have totally different effects on availability and overall cost. More specifically, performing inspections very often benefits the total expected operational cost since by inspection and thereafter maintenance the system is prevented from failures which incur a considerably high cost. On the other hand, since inspection states are considered as down states, such an inspection policy will provide lower availability. Contrarily, when inspection is performed less often, system availability is benefited because the system does not enter down states often. However, in the latter case, an increased overall cost would be achieved since when delaying inspection and hence maintenance, a total failure that incurs high cost is more probable for the system. Consequently, system designer should take into account these features in order to schedule the optimal maintenance policy that optimizes simultaneously both measures. This is usually achieved by formulating and solving multi-objective optimization problems. In the current work the multi-objective optimization problems is solved as an optimization problem with constraints. More specifically, the most important measure is considered as the objective function and the remaining measure participates in the optimization problem as a constraint.

Usually, especially in industrial applications, the designer is mainly interested in minimizing system operational cost. Thus, the optimization problem to be solved for the two-unit multistate system includes *TEOC* as the objective function, while availability (*AV*) is

included as constraint. In particular, a lower availability threshold ( $AV_0$ ) is settled and the optimization problem is solved by considering that system availability should be higher than this threshold. Note that  $AV_0$  depends on system characteristics and it can be decided by the designer:

$$\begin{aligned} & \min TEOC \\ & s. t. \quad AV \geq AV_0 \\ & \lambda_{IN}^{LB} \leq \lambda_{IN} \leq \lambda_{IN}^{UB} \end{aligned} \quad (18)$$

On the other hand, in cases of systems where availability is of prior importance, such as life-critical systems, asymptotic availability can be considered as the objective function. In this case, the optimization is implemented with respect to a higher cost threshold ( $TEOC_0$ ) which also depends on system characteristics and can be provided by the designer too.

## 5. Numerical Results

The proposed model can be further examined and illustrated through some numerical results based on experimental data provided in Table 2.

Table. 2. Experimental data

Parameter	Value	Parameter	Value	Parameter	Value
$\lambda_1$	$1/1200 \text{ h}^{-1}$	$\lambda_{IN}$	$0.05 \text{ h}^{-1}$	$\lambda_{FM}$	$1/10000 \text{ h}^{-1}$
$\lambda_{12}$	$1/2000 \text{ h}^{-1}$	$\mu_i$	$120 \text{ h}^{-1}$	$\lambda_R$	$0.025 \text{ h}^{-1}$
$\lambda_{13}$	$1/1500 \text{ h}^{-1}$	$\lambda_m$	$1 \text{ h}^{-1}$	$b$	$2 \text{ h}^{-1}$
$\lambda_{f1}$	$1/10000 \text{ h}^{-1}$	$\lambda_{im}$	$0.002 \text{ h}^{-1}$	$C_D$	$50 \text{ }^{\circ}\text{cu/h}$
$\lambda_2$	$1/1000 \text{ h}^{-1}$	$\lambda_{fm}$	$1/100 \text{ h}^{-1}$	$C_S$	$500 \text{ cu/h}$
$\lambda_{22}$	$1/1500 \text{ h}^{-1}$	$\lambda_{Fm}$	$1/10000 \text{ h}^{-1}$	$C_m$	$50 \text{ cu/h}$
$\lambda_{f2}$	$1/1000 \text{ h}^{-1}$	$\lambda_M$	$0.2 \text{ h}^{-1}$	$C_M$	$200 \text{ cu/h}$
$\lambda_3$	$1/800 \text{ h}^{-1}$	$\lambda_{IM1}$	$0.025 \text{ h}^{-1}$	$C_I$	$10 \text{ cu/h}$
$\lambda_{f3}$	$5/1000 \text{ h}^{-1}$	$\lambda_{IM2}$	$0.015 \text{ h}^{-1}$	$C_R$	$1000 \text{ cu/h}$
$\lambda_4$	$1/600 \text{ h}^{-1}$	$\lambda_{IM3}$	$0.01 \text{ h}^{-1}$	$c$	$0.9 -1$

### 5.1. Transient and asymptotic dependability and performance

Initially, let us set the probability of perfect switch among units in case of maintenance or in case of a total unit failure to be  $c = 0.95$ . Transient availability and total operational cost behavior for a time horizon of 10000 hours are presented in Figures 1 and 2 respectively. As expected, system availability decreases with time though the overall cost increases since, in the long run, the system will eventually experience failures.

Additionally, the convergence of  $AV(t)$  and  $TEOC(t)$  to  $AV$  and  $TEOC$  respectively, indicating how fast the system reaches steady state is also depicted in Figures 1 and 2. As it can be observed, the system needs about 4000 hours to reach steady state. This time interval is large enough highlighting hence the necessity of transient analysis.

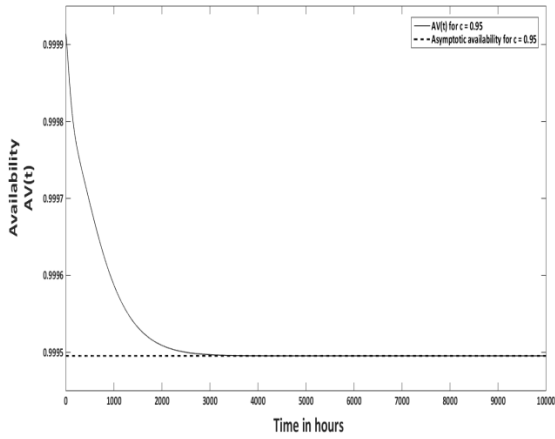


**Figure 1.** Transient availability in a time horizon of 10000 h

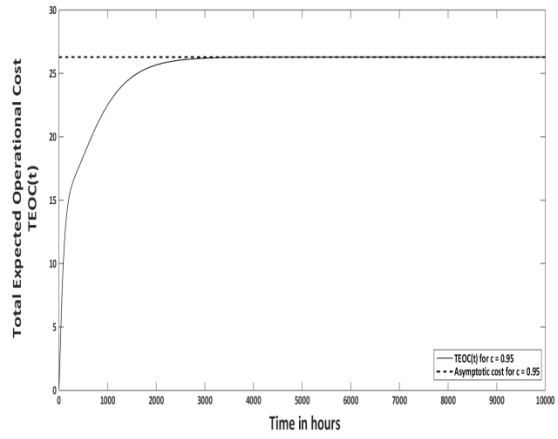


**Figure 2.** Transient total operational cost in a time horizon of 10000 h

However it is interesting to examine how the proposed model parameters affect the dependability and performance measures in the transient phase. Initially, the switch mechanism success probability  $c$  is examined, since it is one of the most critical parameters in a model that incorporates imperfect switch. As it can be observed in Figure 3, availability increases for higher success probability values, as expected, since a higher success probability prevents the system from entering the manual switch states which are down states. Correspondingly, as it is shown in Figure 4, the total expected operational cost seems not be significantly affected by the change on  $c$  values. Although an increased  $c$  slightly reduces  $TEOC(t)$  since it indicates that the switching mechanism operates properly with high probability and do not need to be replaced (avoid replacement cost), the improvement on the overall cost.

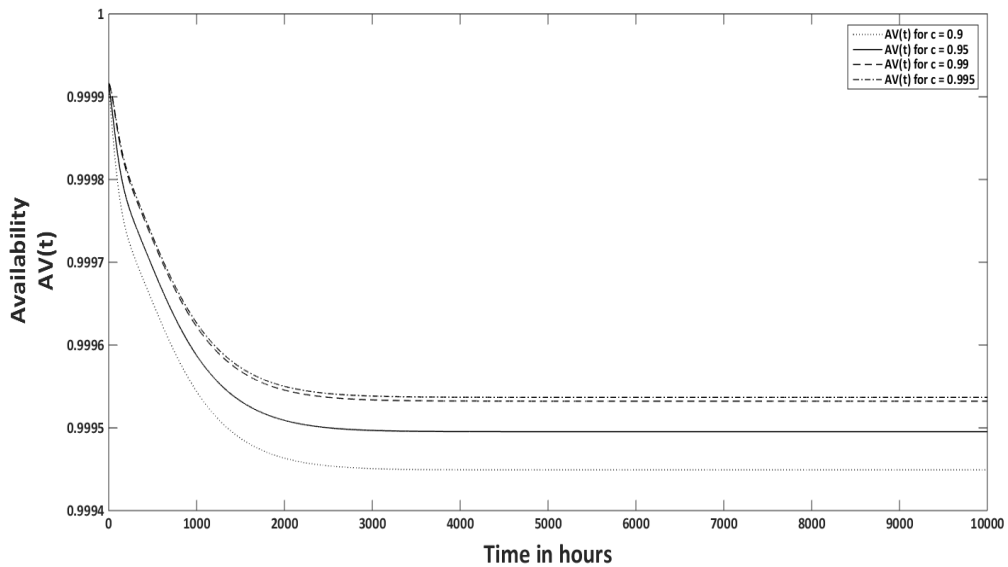


**Figure 3.** Transient availability with respect to success probability  $c$

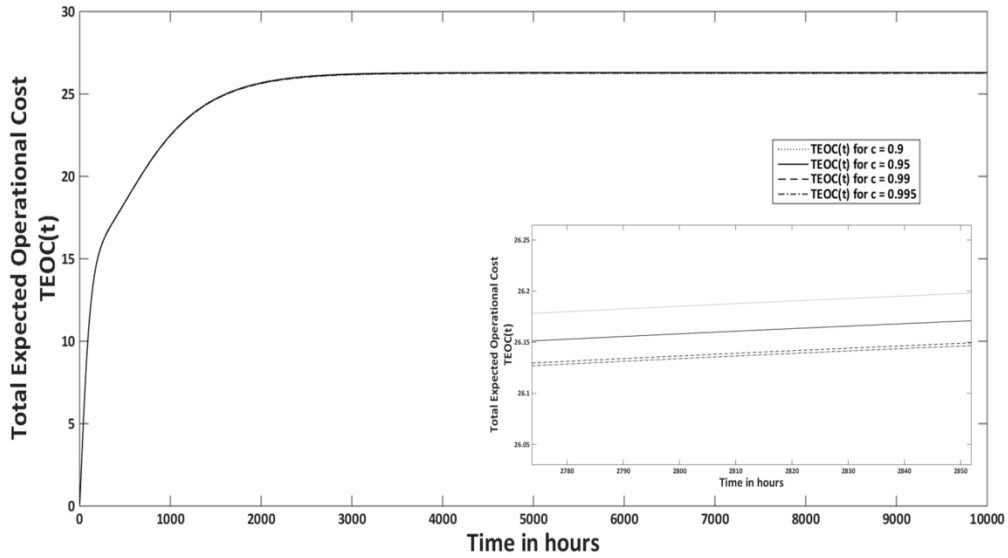


**Figure 4.** Transient total expected operational cost with respect to success probability  $c$

Moreover, the inspection rate  $\lambda_{IN}$  is of major importance too, since it indicates the inspection policy and thus the maintenance policy to be adopted for the two-unit multistate system. In Figure 5, the availability decreases with the increase of the inspection rate, since increasing  $\lambda_{IN}$  indicates more often inspection and thus maintenance actions which indicate that the system enters down states. Thus in this case, system's operational time decreases as well as availability does. Contrarily, as shown in Figure 6, the expected overall cost reduces with the increase of inspection frequency. Inspecting and consequently maintaining the system more often manages to delay future failures that incur considerably higher cost. Thus, the total expected operational cost is benefited by adopting a schedule which includes often maintenance actions.

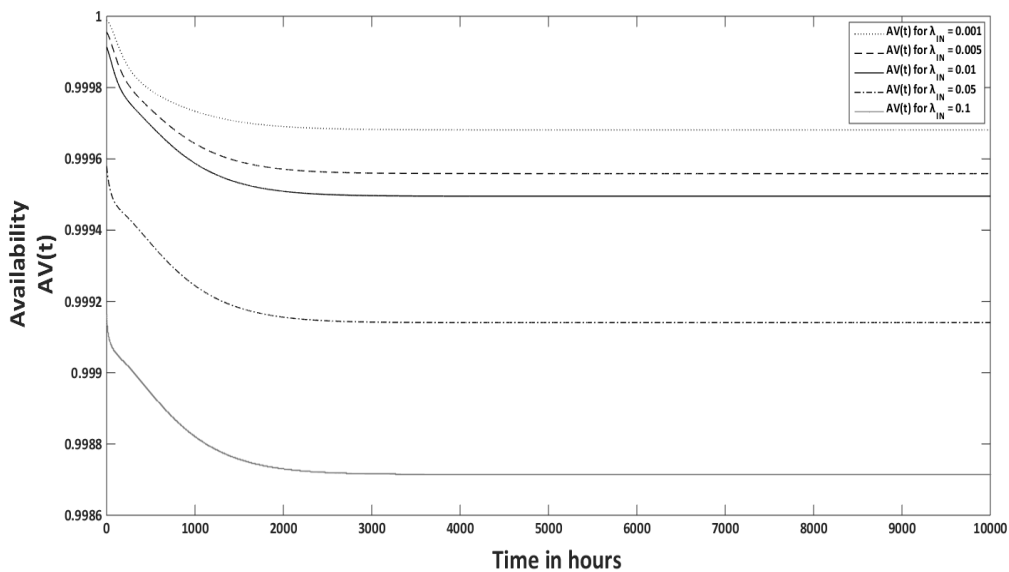


**Figure 5.** Transient availability with respect to the inspection rate  $\lambda_{IN}$

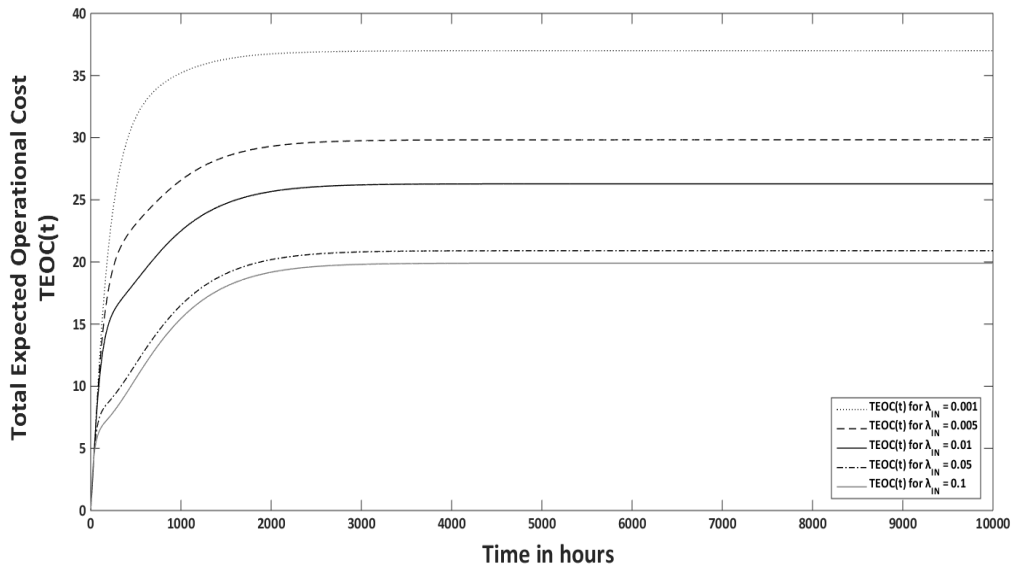


Figure 6. Transient total expect operational cost with respect to the inspection rate  $\lambda_{IN}$

Since, one of the innovative aspects of the proposed model for the system under consideration is the imperfect switch among its units, it is also interesting to examine how the time needed to switch system control manually, in case of a failure on the automated mechanism, affects the dependability and performance measures. This can be examined through the manual switch rate. In Figure 7, as expected, we observe that the increase of the manual switch rate results in increasing system availability. This is obvious since in this case the system spends less time in the non operation state of manual switch. However,  $b$  does not seem to affect importantly the  $TEOC(t)$  indicator. This is more or less reasonable because entering the manual switch state affects the cost (by triggering automation mechanism replacement cost) but the sojourn time in this state has no effect in the cost. Nevertheless, slight cost improvement can be obtained when  $b$  increases.

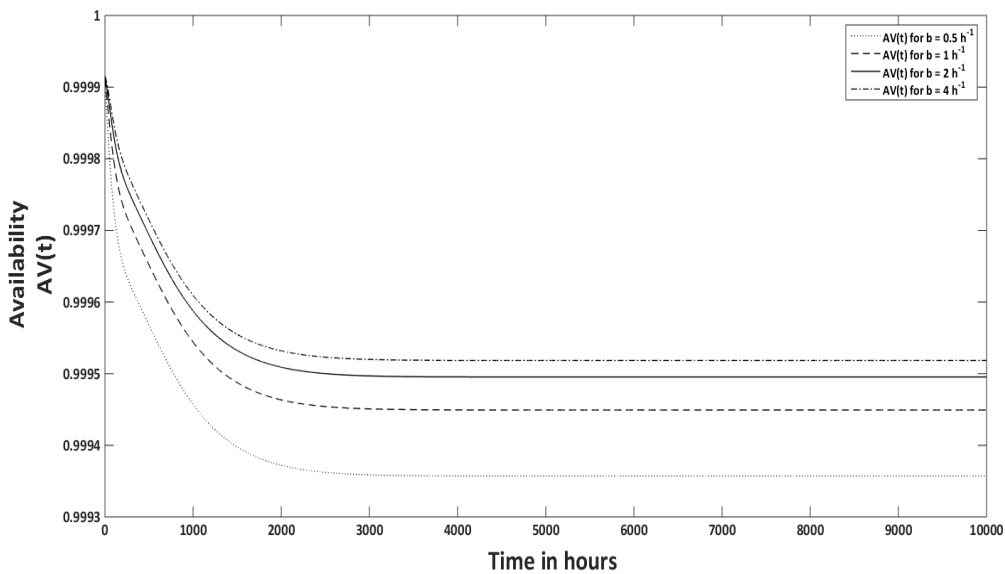
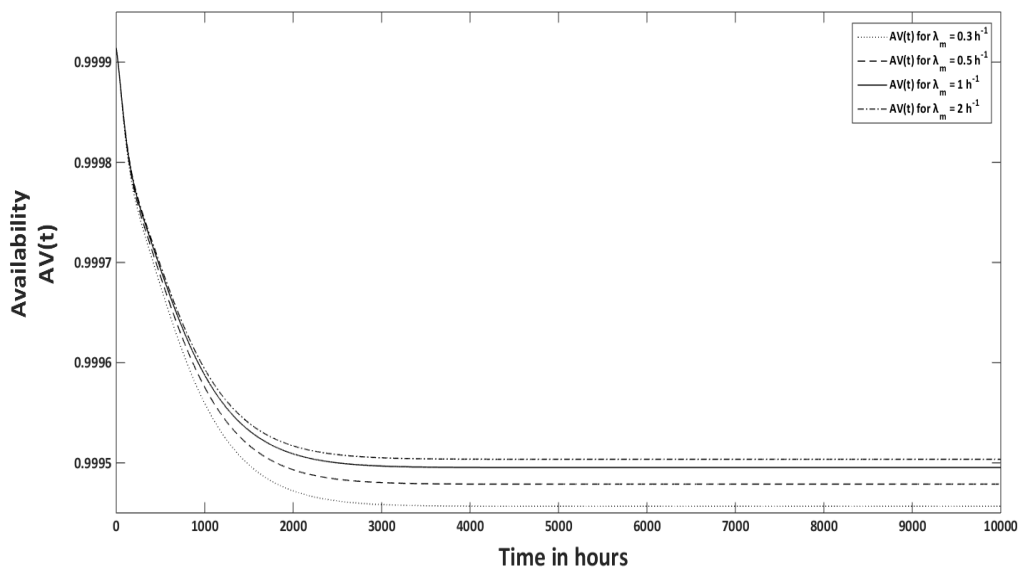


Figure 7. Transient availability with respect to the manual switch rate  $b$

The effect of the time needed for a unit to be restored to its previous deterioration level through minimal maintenance on dependability and performance is also examined in this section, through the minimal maintenance rate  $\lambda_m$  which represents the rate of minimal maintenance completion. As expected, when minimal maintenance lasts less time, transient availability increases since the system is restored faster to an operational state. However, similarly to the previous case, the total expected cost does not seem to be importantly affected by the duration of minimal maintenance rather than the fact that the system enters minimal maintenance state which incur cost, although that reduced minimal maintenance duration improves slightly the overall cost.



**Figure 8.** Transient availability with respect to the minimal maintenance rate  $\lambda_m$

The effects of the time needed for a unit to be restored to its fully operational state through major maintenance on dependability and performance is examined too through the major maintenance rate  $\lambda_M$ . Similarly to the minimal maintenance rate and due to exactly the same reason, transient system availability increases with the increase of  $\lambda_M$ , as shown in Figure 9. Contrarily though to minimal maintenance rate,  $\lambda_M$  seems to significantly affect  $TEOC(t)$ . As it can be observed in Figure 10,  $TEOC(t)$  reduces with the increase of  $\lambda_M$ . This is because major maintenance manages to restore the unit to its fully operational state causing thus an important delay on unit failures or even maintenance actions that incur cost. Thus, when the unit is restored to the perfect operating state through major maintenance faster, the need of maintaining this unit or repair it after a failure is delayed resulting in reducing the system overall cost at time  $t$ .

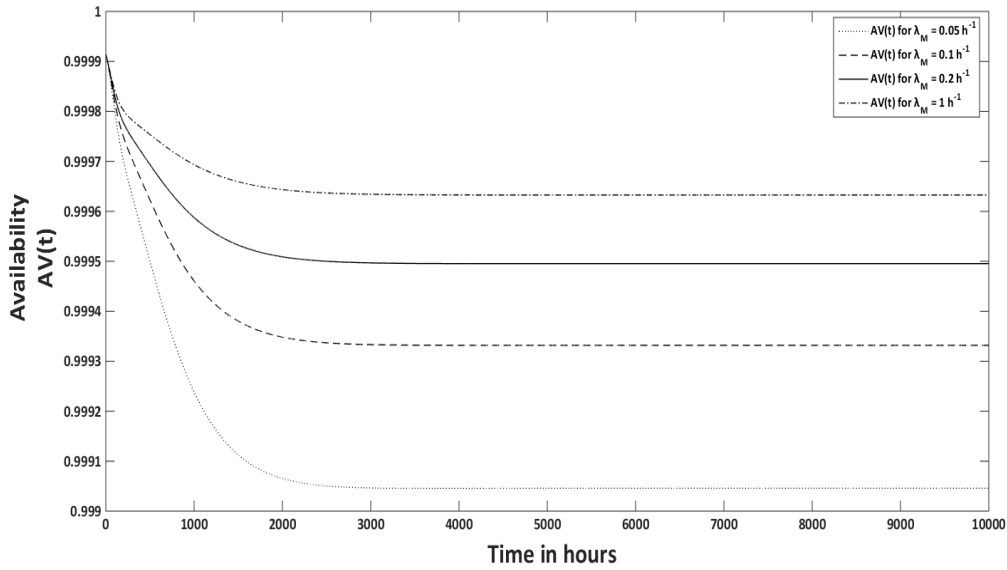


**Figure 9.** Transient availability with respect to the major maintenance rate  $\lambda_M$

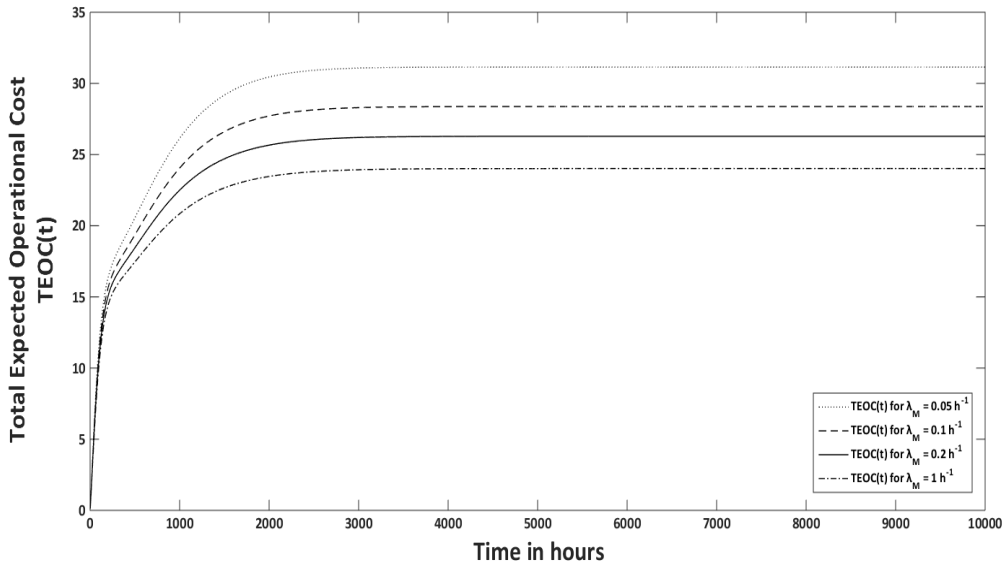


**Figure 10.** Transient total operational cost with respect to the major maintenance rate  $\lambda_M$

The rate of repairing/replacing a failed unit is also considered in analysis. In Figure 11 it can be observed that as faster unit repair/replacement is accomplished, restoring the system back to an operational state, as higher availability is achieved since the total system operational time increases. Respectively, as shown in Figure 12, the total expected operational cost reduces with fast unit repair/replacement since restoring the unit to its fully operational state (as good as new) indicates that its lifetime starts again and thus maintenance, repair or any other costly actions will be delayed for the unit.

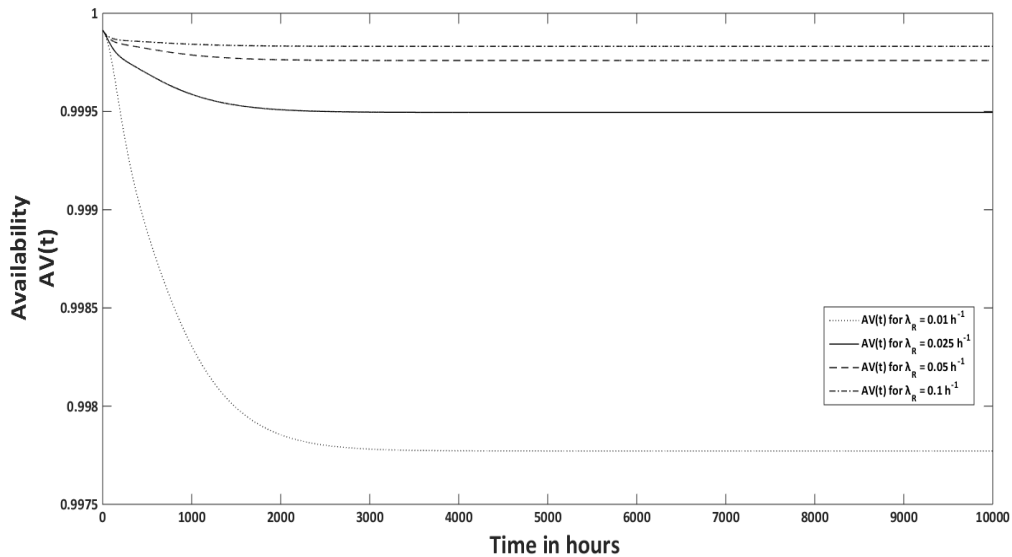


Figure 11. Transient availability with respect to the major maintenance rate  $\lambda_R$

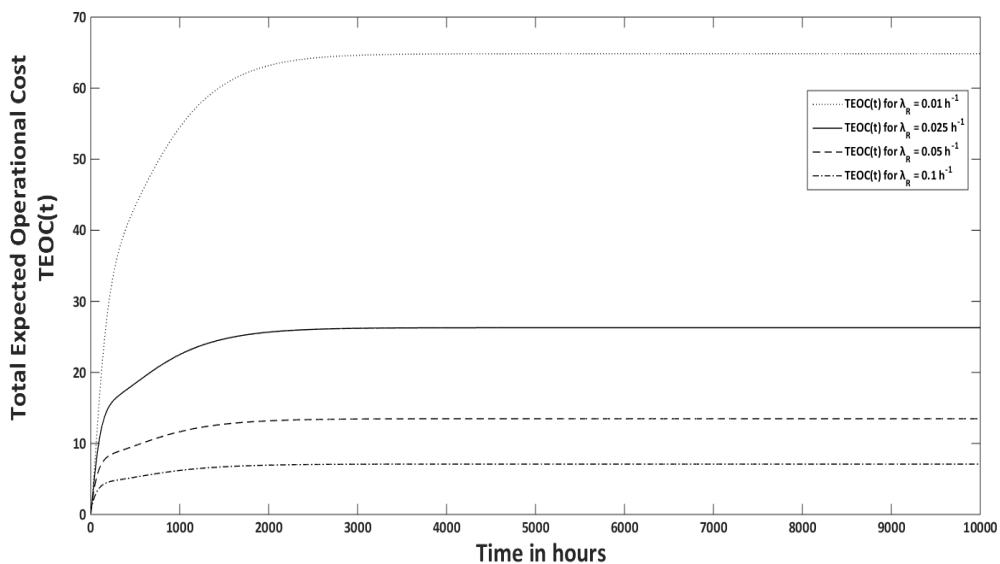


Figure 12. Transient total operational cost with respect to the major maintenance rate  $\lambda_R$

From the system designer point of view, it would be also interesting to examine how all of the actions costs as well as the downtime cost affect  $TEOC(t)$ . As shown in Figure 13, the inspection cost does not seem to critically affect  $TEOC(t)$  due to its small value compared to the rest of action costs. However, as expected there is a slight increase on  $TEOC(t)$  with the increase of  $C_I$ . Note that the same behavior holds true for the minimal maintenance cost  $C_m$ , the downtime cost  $C_D$  and the automated switch mechanism  $C_S$ . Note also that although  $C_S$  is much higher compared with the rest of the cost that does not affect  $TEOC(t)$  importantly, its changes seems not to cause any important change on  $TEOC(t)$ . On the other hand, major maintenance cost's  $C_M$  as well as unit repair/replacement cost's changes seem to have a notable effect on  $TEOC(t)$  (their increase results in total operational cost increase as expected) as shown in Figures 14 and 15 respectively.

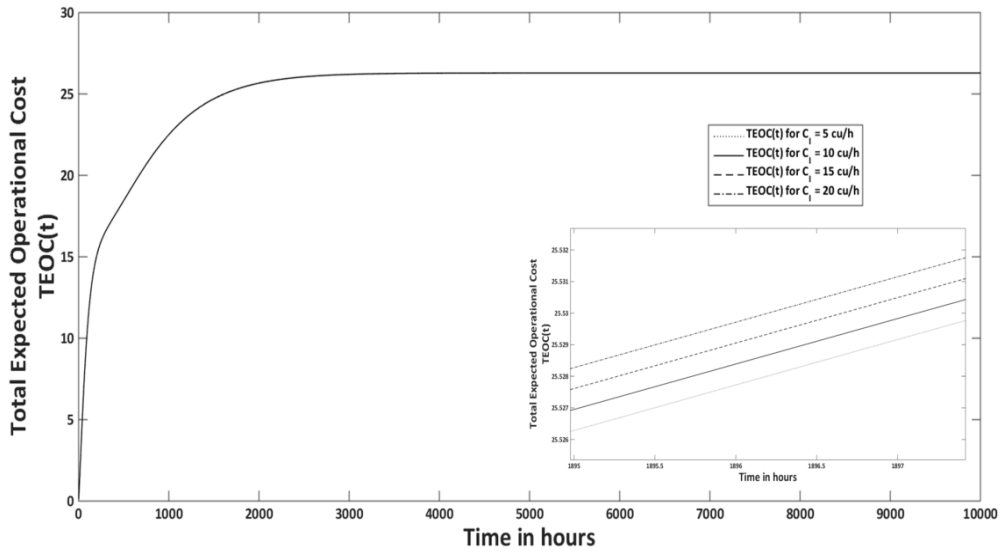


Figure 13. Transient total operational cost with respect to inspection cost  $C_I$

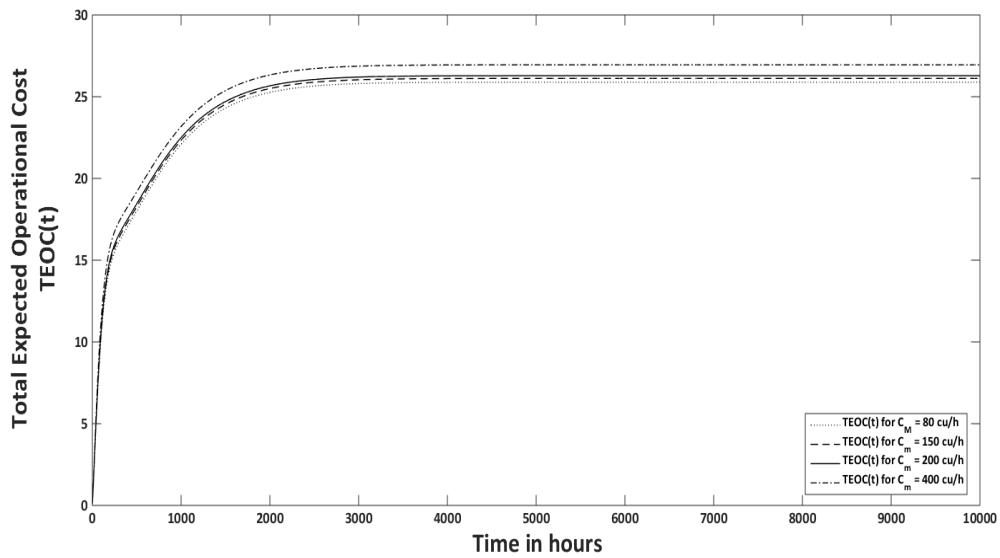


Figure 14. Transient total operational cost with respect to major maintenance cost  $C_M$

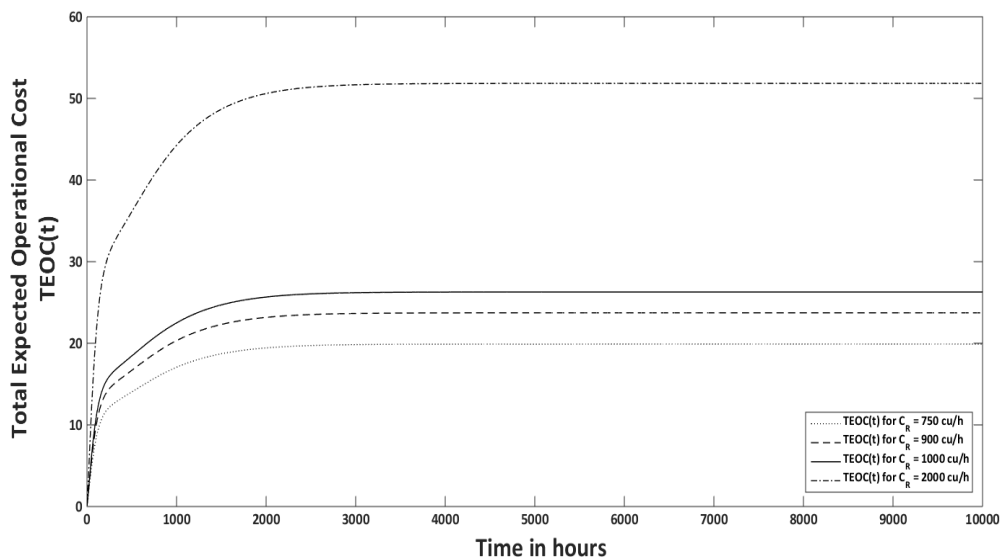


Figure 15. Transient total operational cost with respect to unit repair/replacement cost  $C_R$

## 5.2. Optimal asymptotic maintenance policies implemented in the transient phase

Taking into account that the maintenance schedule to be adopted is represented by the inspection schedule in the proposed model, the results of the optimization problems defined in equations (17), (18) and (19) are presented in Tables 3 and 4 respectively. For all the optimization problems we set  $\lambda_{IN}^{LB} = 0.001 h^{-1}$  and  $\lambda_{IN}^{UB} = 0.1 h^{-1}$ . Note that since we innovatively propose to model imperfect switch for the two-unit multistate deteriorating system with maintenance, we solve all of the optimization problems with respect to the success probability  $c$  too.

From the results (see Table 3) it can be obtained that the optimal inspection policy  $\lambda_{IN}^*$  that maximizes system asymptotic availability consists in inspecting the operating unit seldom (actually  $\lambda_{IN}^*$  is equal to the lowest possible value  $\lambda_{IN}^{LB}$ ) irrespectively of the success probability  $c$ . The result is obvious since often inspection leads the system to down states more frequently, reducing hence system availability. On the other hand, as shown also in Table 3, the total expected operational cost is minimized for often inspection and thus maintenance interval, irrespectively of the success probability  $c$ . The explanation lies on the fact that frequent inspection trigger maintenance actions avoiding or delaying hence operating unit failures that incur high cost. Finally, for the multi-objective optimization problem (see Table 4), we observe that the optimal inspection policy  $\lambda_{IN}^*$  depends mostly on the objective function. That is why  $\lambda_{IN}^*$  is closely to the optimal solution of problem (18). However, there are instances of problem (19), in particular when higher levels of availability are desired ( $AV_0 = 0.999$ ), for which the optimal inspection policy is slightly different from the optimal inspection schedule for problem (18).

<b>Table 3. Optimization results</b>					<b>Table 4. Multi-objective optimization results</b>				
$c$	$\lambda_{IN}^* (h^{-1})$	$AV^*$	$\lambda_{IN}^* (h^{-1})$	$TEOC^*$	$c$	$AV_0$	$\lambda_{IN}^* (h^{-1})$	$TEOC^*$	$AV^*$
0.900	0.001	0.999650	0.1	20.0075	0.900	0.990	0.100	19.8818	0.998661
0.950	0.001	0.999681	0.1	19.9430	0.900	0.995	0.100	19.8818	0.998661
0.990	0.001	0.999706	0.1	19.9108	0.900	0.999	0.060	20.5512	0.999002
0.995	0.001	0.999709	0.1	19.8850	0.950	0.990	0.100	19.8818	0.998714
					0.950	0.995	0.100	19.8818	0.998714
					0.950	0.999	0.066	20.3976	0.999004
					0.990	0.990	0.100	19.8818	0.998757
					0.990	0.995	0.100	19.8818	0.998757
					0.990	0.999	0.071	20.2921	0.999003
					0.995	0.99	0.100	19.8818	0.998763
					0.995	0.995	0.100	19.8818	0.998763
					0.995	0.999	0.072	20.2798	0.9990029

By adopting the policy that optimizes asymptotic availability or cost from the beginning of system operational time the dependability and performance measures would be benefited not only in the steady state phase but also at any time instant  $t$  of system's operational time. Since the multi-objective optimization problem provides optimal cost and

availability simultaneously, the behavior of  $AV(t)$  and  $TEOC(t)$  under the derived optimal policies from (19) shown in Table 4 is indicatively presented in Figures 16 and 17.

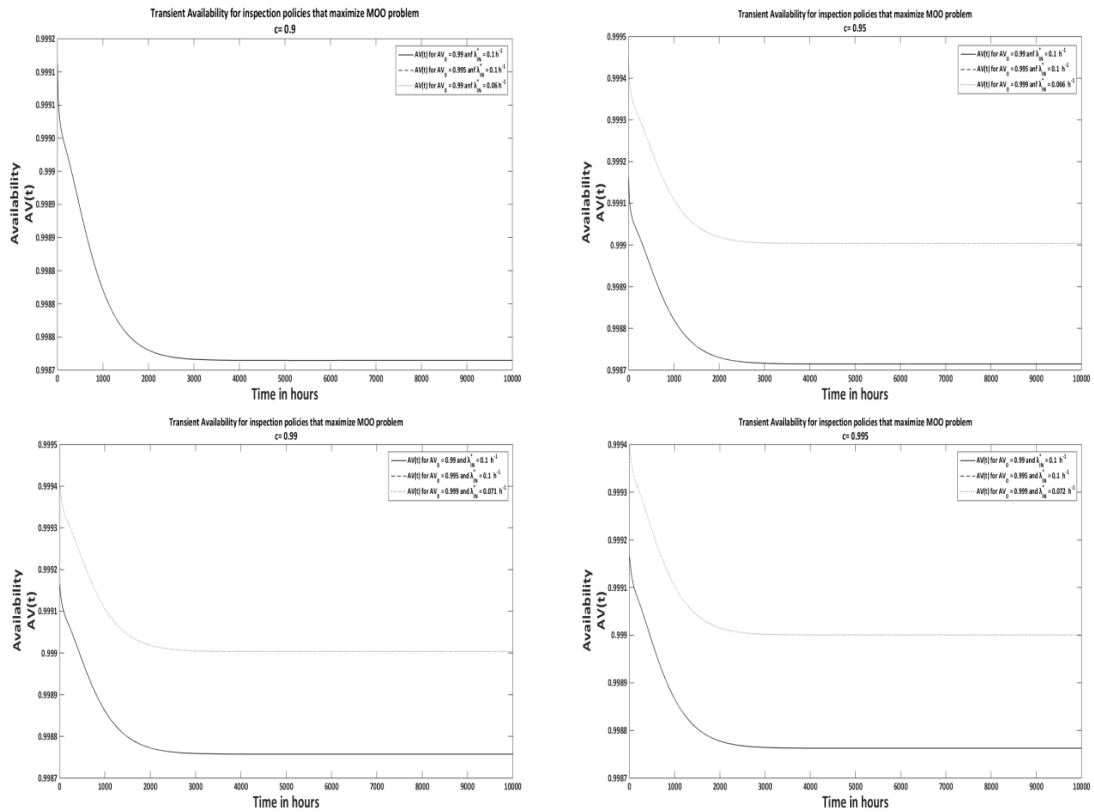


Figure 16. Transient availability for inspection policies for the multi-objective problem

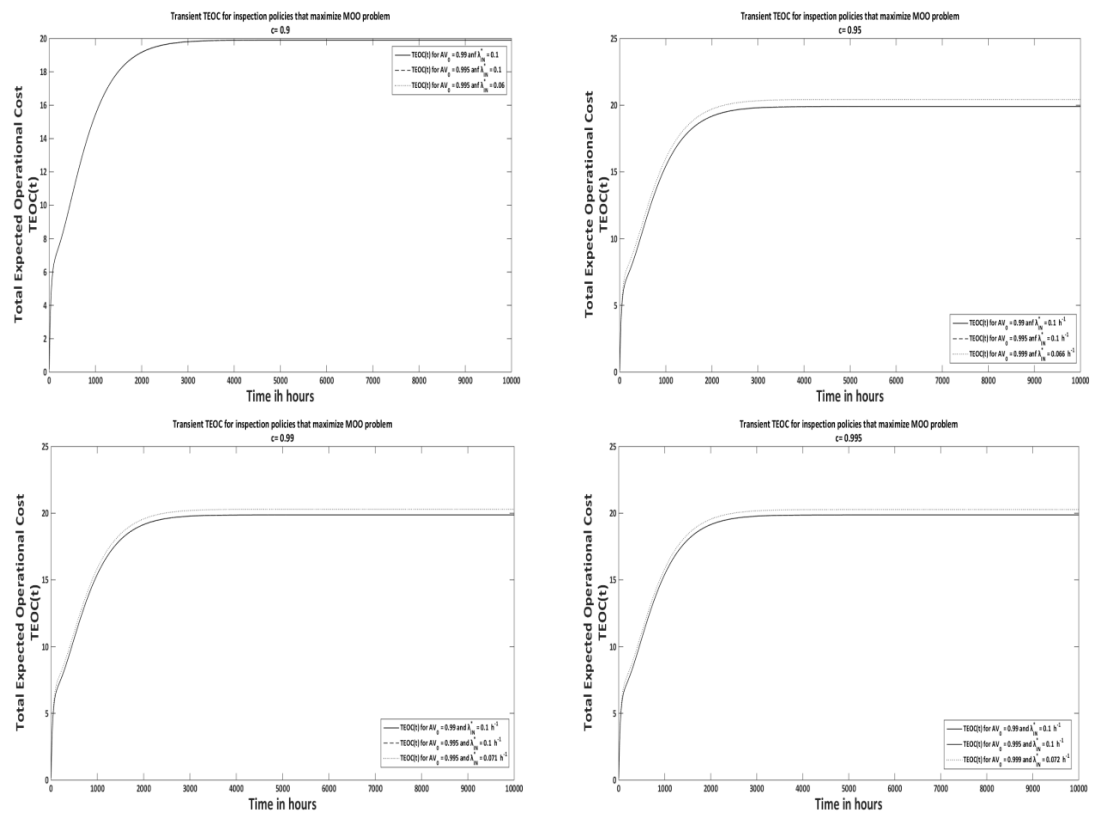


Figure 17. Transient total operational cost for inspection policies for the multi-objective problem

## 6. Conclusions and future work

In this paper, a two-unit multistate deteriorating system with minimal and major maintenance actions, triggered to prevent or delay unit failures is modeled, using a continuous time Markov process. Such systems can be met in many real-life applications. The innovative aspect of this paper consists in modeling the imperfect switch among the system units. Imperfect switch models the cases when the switch mechanism fails to operate whenever needed in order to switch the control from the operating to the standby unit.

The transient as well as the asymptotic behavior of the system under consideration in terms of dependability and performance, expressed by availability and total operational cost respectively, are analytically examined. Additionally, a sensitivity analysis with respect to model parameters is implemented through numerical results. Such an analysis is useful for system designers, since it provides knowledge on how the two-unit system should be designed in order to achieve the desired levels of availability or/and operational cost. To this direction, mathematical programming models for optimizing availability and cost are formulated and solved, in order to derive the optimal maintenance policies, expressed through the inspection rates. Consequently, we have provided the appropriate theoretical framework for designing efficient two-unit multistate deteriorating systems with maintenance and imperfect switch among units.

The proposed model can be extended in the future in two ways. Firstly, the exponentially distributed sojourn times in system states can be relaxed and more precise models like a semi-Markov model can be used to examine system's behavior in terms of dependability and performance, in the transient and/or asymptotic phase. Moreover, real-life system practices like for instance opportunistic maintenance actions can be also incorporated in the proposed model.

## References

- [1]. Aghezzaf E-H., Khatab A. and Phuoc Le Tam. 2016. "Optimizing production and imperfect preventive maintenance planning's integration in failure-prone manufacturing systems". *Reliability Engineering & System Safety*, 145: 190-198.
- [2]. Amari S.V., McLaughlin L. and Pham H. 2006. "Cost-effective condition-based maintenance using markov decision processes". *Reliability and Maintainability Symposium, 2006. RAMS '06. Annual: 464-469*, 23-26 Jan. 2006.
- [3]. Chen D., Cao Y., Trivedi K.S. and Hong Y. 2003. "Preventive maintenance of multi-state system with phase-type failure time distribution and non-zero inspection time". *International Journal Reliability of Quality and Safety Engineering*, 10(3):323-44.

- [4]. Chen D. and Trivedi K.S. 2002. "Closed-form analytical results for condition-based maintenance". *Reliability Engineering and System Safety*, 76(1): 43–51.
- [5]. Ding S.H. and Kamaruddin S. 2015. "Maintenance policy optimization-literature review and directions". *The international Journal of Advanced Manufacturing Technology*, 76(5): 1263-1283.
- [6]. Dugan J. B. and Trivedi K. S. 1989. "Coverage modelling for dependability analysis of fault-tolerant systems," *IEEE Trans. Computers*, 38(6): 775–787.
- [7]. Goel L. R., Gupta R. and Singh S.K. 1985. "Cost analysis of a two-unit priority standby system with imperfect switch and arbitrary distributions," *Microelectronics and Reliability*, 25, (1): 65–69.
- [8]. Kijima M. 1987. "Markov Processes for Stochastic Modeling", Boca Raton, FL, USA: CRC Press, 1997.
- [9]. Koutras V.P., Malefaki S. and Platis A.N. 2017. "Optimization of the dependability and performance measures of a generic model for multi-state deteriorating systems under maintenance", *Reliability Engineering and System Safety*, 166: 73-86.
- [10]. Lapa C.M.F., Pereira C.M.N.A and de Barros M.P. 2006. "A model for preventive maintenance planning by genetic algorithms based in cost and reliability". *Reliability Engineering and System Safety*, 91(2):233–240.
- [11]. Lisnianski A., Frenkel I. and Ding Y. 2010. "Multi-state System Reliability Analysis and Optimization for Engineers and Industrial Managers". Springer, London, 2010.
- [12]. Lisnianski A., Ding Y., Frenkel I. and Khvatskin L. 2007. "Maintenance optimization for multi-state aging systems". *Proc. of 5-th International Conference on Mathematical Methods in Reliability, Methodology and Practice*, Glasgo. United Kingdom.
- [13]. Malefaki S., Koutras V.P. and Platis A.N. 2017. "Optimizing availability and performance of a two-unit redundant multi-state deteriorating system", *Recent Advances in Multi-State Reliability, Springer Series in Reliability Engineering, Part of the Springer Series in Reliability Engineering book series (RELIABILITY)*, Springer, Berlin: 71-105.
- [14]. Naga P., Rao S. and Naikan V.N.A. 2006. "A condition-based preventive maintenance policy for Markov deteriorating systems", *International Journal of Performability Modeling*, 2(2): 175-189.
- [15]. Natvig B. 2011. "Probabilistic Modeling of Monitoring and Maintenance". In *Multi-state Systems Reliability Theory with Applications*, Chichester, UK.: John Wiley & Sons, Inc..
- [16]. Platis A., Drosakis E. 2009. "Coverage modeling and optimal maintenance frequency of an automated restoration mechanism", *IEEE Transactions on Reliability*, 58(3): 470-475.
- [17]. Sadek A., Limnios N. 2005. "Nonparametric estimation of reliability and survival function for continuous-time finite Markov processes", *Journal of Statistical Planning and Inference*, 133(1): 1-21.
- [18]. Sheu S-H., Chang C-C., Chen Y-L. and Zhang Z. G. 2015. "Optimal preventive maintenance and repair policies for multi-state systems", *Reliability Engineering and System Safety*, 140.
- [19]. Thein S., Chang Y.S. and Makatsoris C. 2012. "A study of condition based preventive maintenance model for repairable multi stage deteriorating system", *International Journal of Advanced Logistics*, 1(1): 83-102.
- [20]. Trivedi K. S. 2001. "Probability and Statistics with Reliability, Queuing, and Computer Science Applications", NY: John Wiley and Sons.
- [21]. Wang K.-H., Dong W.-L. and Ke J.-B. 2006. "Comparison of reliability and the availability between four systems with warm standby components and standby switching failures," *Applied Mathematics and Computation*, 183(2): 1310–1322.
- [22]. Xie X., Yiguang H. and Trivedi K.S. 2005. "Analysis of a two level software rejuvenation policy", *Reliability Engineering and System Safety*, 87(1): 13–22.

# Appendix A

**Table A1 : States and possible transitions for the proposed model**

From state	To state	From state	To state
(O, O <sup>5</sup> )	(D <sub>1</sub> , O <sup>5</sup> ), (D <sub>2</sub> , O <sup>5</sup> ), (D <sub>3</sub> , O <sup>5</sup> ), (F, O), (MS <sup>F</sup> , O <sup>5</sup> ), (I <sub>0</sub> , O <sup>5</sup> )	(M, M)	(O, M), (D <sub>1</sub> , M), (D <sub>2</sub> , M), (D <sub>3</sub> , M), (F, M), (M, O), (M, D <sub>1</sub> ), (M, D <sub>2</sub> ), (M, D <sub>3</sub> ), (M, F)
(D <sub>1</sub> , O <sup>5</sup> )	(D <sub>2</sub> , O <sup>5</sup> ), (D <sub>3</sub> , O <sup>5</sup> ), (F, O), (MS <sup>F</sup> , O <sup>5</sup> ), (I <sub>1</sub> , O <sup>5</sup> )	(O, F)	(I <sub>0</sub> , F), (D <sub>1</sub> , F), (D <sub>2</sub> , F), (D <sub>3</sub> , F), (F, F), (O, O <sup>5</sup> )
(D <sub>2</sub> , O <sup>5</sup> )	(D <sub>3</sub> , O <sup>5</sup> ), (F, O), (MS <sup>F</sup> , O <sup>5</sup> ), (I <sub>2</sub> , O <sup>5</sup> )	(D <sub>1</sub> , F)	(I <sub>1</sub> , F), (D <sub>2</sub> , F), (D <sub>3</sub> , F), (F, F), (D <sub>1</sub> , O <sup>5</sup> )
(D <sub>3</sub> , O <sup>5</sup> )	(F, O), (MS <sup>F</sup> , O <sup>5</sup> ), (I <sub>3</sub> , O <sup>5</sup> )	(D <sub>2</sub> , F)	(I <sub>2</sub> , F), (D <sub>3</sub> , F), (F, F), (D <sub>2</sub> , O <sup>5</sup> )
(I <sub>0</sub> , O <sup>5</sup> )	(O, O <sup>5</sup> )	(D <sub>3</sub> , F)	(I <sub>3</sub> , F), (F, F), (D <sub>3</sub> , O <sup>5</sup> )
(I <sub>1</sub> , O <sup>5</sup> )	(D <sub>1</sub> , O <sup>5</sup> )	(I <sub>0</sub> , F)	(O, F)
(I <sub>2</sub> , O <sup>5</sup> )	(m, O), (MS <sup>m</sup> , O <sup>5</sup> )	(I <sub>1</sub> , F)	(D <sub>1</sub> , F)
(I <sub>3</sub> , O <sup>5</sup> )	(M, O), (MS <sup>M</sup> , O <sup>5</sup> )	(I <sub>2</sub> , F)	(m, F)
(m, O)	(D <sub>1</sub> <sup>5</sup> , O), (D <sub>2</sub> <sup>5</sup> , O), (D <sub>3</sub> <sup>5</sup> , O), (F, O), (m, I <sub>0</sub> ), (m, D <sub>1</sub> ), (m, D <sub>2</sub> ), (m, D <sub>3</sub> ), (m, F)	(I <sub>3</sub> , F)	(M, F)
(M, O)	(O <sup>5</sup> , O), (D <sub>1</sub> <sup>5</sup> , O), (D <sub>2</sub> <sup>5</sup> , O), (D <sub>3</sub> <sup>5</sup> , O), (F, O), (M, I <sub>0</sub> ), (M, D <sub>1</sub> ), (M, D <sub>2</sub> ), (M, D <sub>3</sub> ), (M, F)	(m, F)	(D <sub>1</sub> , F), (D <sub>2</sub> , F), (D <sub>3</sub> , F), (F, F), (m, O)
(MS <sup>F</sup> , O <sup>5</sup> )	(F, O)	(M, F)	(O, F), (D <sub>1</sub> , F), (D <sub>2</sub> , F), (D <sub>3</sub> , F), (F, F), (M, O)
(F, O)	(F, I <sub>0</sub> ), (F, D <sub>1</sub> ), (F, D <sub>2</sub> ), (F, D <sub>3</sub> ), (F, F), (O <sup>5</sup> , O)	(F, M)	(F, O), (F, D <sub>1</sub> ), (F, D <sub>2</sub> ), (F, D <sub>3</sub> ), (F, F), (O, M)
(F, D <sub>1</sub> )	(F, I <sub>1</sub> ), (F, D <sub>2</sub> ), (F, D <sub>3</sub> ), (F, F), (O <sup>5</sup> , D <sub>1</sub> )	(m, I <sub>0</sub> )	(m, O)
(F, D <sub>2</sub> )	(F, I <sub>2</sub> ), (F, D <sub>3</sub> ), (F, F), (O <sup>5</sup> , D <sub>2</sub> )	(I <sub>1</sub> , m)	(D <sub>1</sub> , m)
(F, D <sub>3</sub> )	(F, I <sub>3</sub> ), (F, F), (O <sup>5</sup> , D <sub>3</sub> )	(m, I <sub>2</sub> )	(m, m)
(F, F)	(F, O), (O, F)	(m, I <sub>3</sub> )	(m, M)
(F, I <sub>0</sub> )	(F, O)	(M, I <sub>0</sub> )	(M, O)
(F, I <sub>1</sub> )	(F, D <sub>1</sub> )	(M, I <sub>1</sub> )	(M, D <sub>1</sub> )
(F, I <sub>2</sub> )	(F, m)	(M, I <sub>2</sub> )	(M, m)
(F, I <sub>3</sub> )	(F, M)	(M, I <sub>3</sub> )	(M, M)
(O, D <sub>1</sub> <sup>5</sup> )	(I <sub>0</sub> , D <sub>1</sub> <sup>5</sup> ), (D <sub>1</sub> , D <sub>1</sub> <sup>5</sup> ), (D <sub>2</sub> , D <sub>1</sub> <sup>5</sup> ), (D <sub>3</sub> , D <sub>1</sub> <sup>5</sup> ), (F, D <sub>1</sub> ), (MS <sup>F</sup> , D <sub>1</sub> <sup>5</sup> )	(O <sup>5</sup> , O)	(O <sup>5</sup> , I <sub>0</sub> ), (O <sup>5</sup> , D <sub>1</sub> ), (O <sup>5</sup> , D <sub>2</sub> ), (O <sup>5</sup> , D <sub>3</sub> ), (O, F), (O <sup>5</sup> , MS <sup>F</sup> )
(D <sub>1</sub> , D <sub>1</sub> <sup>5</sup> )	(I <sub>1</sub> , D <sub>1</sub> <sup>5</sup> ), (D <sub>2</sub> , D <sub>1</sub> <sup>5</sup> ), (D <sub>3</sub> , D <sub>1</sub> <sup>5</sup> ), (F, D <sub>1</sub> ), (MS <sup>F</sup> , D <sub>1</sub> <sup>5</sup> )	(O <sup>5</sup> , D <sub>1</sub> )	(O <sup>5</sup> , I <sub>1</sub> ), (O <sup>5</sup> , D <sub>2</sub> ), (O <sup>5</sup> , D <sub>3</sub> ), (O, F), (O <sup>5</sup> , MS <sup>F</sup> )
(D <sub>2</sub> , D <sub>1</sub> <sup>5</sup> )	(I <sub>2</sub> , D <sub>1</sub> <sup>5</sup> ), (D <sub>3</sub> , D <sub>1</sub> <sup>5</sup> ), (F, D <sub>1</sub> ), (MS <sup>F</sup> , D <sub>1</sub> <sup>5</sup> )	(O <sup>5</sup> , D <sub>2</sub> )	(O <sup>5</sup> , I <sub>2</sub> ), (O <sup>5</sup> , D <sub>3</sub> ), (O, F), (O <sup>5</sup> , MS <sup>F</sup> )
(D <sub>3</sub> , D <sub>1</sub> <sup>5</sup> )	(I <sub>3</sub> , D <sub>1</sub> <sup>5</sup> ), (F, D <sub>1</sub> ), (MS <sup>F</sup> , D <sub>1</sub> <sup>5</sup> )	(O <sup>5</sup> , D <sub>3</sub> )	(O <sup>5</sup> , I <sub>3</sub> ), (O, F), (O <sup>5</sup> , MS <sup>F</sup> )
(I <sub>0</sub> , D <sub>1</sub> <sup>5</sup> )	(O, D <sub>1</sub> <sup>5</sup> )	(O <sup>5</sup> , I <sub>0</sub> )	(O <sup>5</sup> , O)
(I <sub>1</sub> , D <sub>1</sub> <sup>5</sup> )	(D <sub>1</sub> , D <sub>1</sub> <sup>5</sup> )	(O <sup>5</sup> , I <sub>1</sub> )	(O <sup>5</sup> , D <sub>1</sub> )
(I <sub>2</sub> , D <sub>1</sub> <sup>5</sup> )	(m, D <sub>1</sub> ), (MS <sup>m</sup> , D <sub>1</sub> <sup>5</sup> )	(O <sup>5</sup> , I <sub>2</sub> )	(O, m), (O <sup>5</sup> , SM <sup>m</sup> )
(I <sub>3</sub> , D <sub>1</sub> <sup>5</sup> )	(M, D <sub>1</sub> ), (MS <sup>M</sup> , D <sub>1</sub> <sup>5</sup> )	(O <sup>5</sup> , I <sub>3</sub> )	(O, M), (O <sup>5</sup> , SM <sup>M</sup> )
(m, D <sub>1</sub> )	(m, I <sub>1</sub> ), (m, D <sub>2</sub> ), (m, D <sub>3</sub> ), (m, F), (D <sub>1</sub> <sup>5</sup> , D <sub>1</sub> ), (D <sub>2</sub> <sup>5</sup> , D <sub>1</sub> ), (D <sub>3</sub> <sup>5</sup> , D <sub>1</sub> ), (F, D <sub>1</sub> )	(O <sup>5</sup> , MS <sup>m</sup> )	(O, m)
(M, D <sub>1</sub> )	(M, I <sub>1</sub> ), (M, D <sub>2</sub> ), (M, D <sub>3</sub> ), (M, F), (O <sup>5</sup> , D <sub>1</sub> ), (D <sub>1</sub> <sup>5</sup> , D <sub>1</sub> ), (D <sub>2</sub> <sup>5</sup> , D <sub>1</sub> ), (D <sub>3</sub> <sup>5</sup> , D <sub>1</sub> ), (F, D <sub>1</sub> )	(O <sup>5</sup> , MS <sup>M</sup> )	(O, M)
(MS <sup>F</sup> , D <sub>1</sub> <sup>5</sup> )	(F, D <sub>1</sub> )	(O <sup>5</sup> , MS <sup>F</sup> )	(O, F)
(O, D <sub>2</sub> <sup>5</sup> )	(I <sub>0</sub> , D <sub>2</sub> <sup>5</sup> ), (D <sub>1</sub> , D <sub>2</sub> <sup>5</sup> ), (D <sub>2</sub> , D <sub>2</sub> <sup>5</sup> ), (D <sub>3</sub> , D <sub>2</sub> <sup>5</sup> ), (F, D <sub>2</sub> ), (MS <sup>F</sup> , D <sub>2</sub> <sup>5</sup> )	(D <sub>1</sub> <sup>5</sup> , O)	(D <sub>1</sub> <sup>5</sup> , I <sub>0</sub> ), (D <sub>1</sub> <sup>5</sup> , D <sub>1</sub> ), (D <sub>1</sub> <sup>5</sup> , D <sub>2</sub> ), (D <sub>1</sub> <sup>5</sup> , D <sub>3</sub> ), (D <sub>1</sub> , F), (D <sub>1</sub> <sup>5</sup> , MS <sup>F</sup> )
(D <sub>1</sub> , D <sub>2</sub> <sup>5</sup> )	(I <sub>1</sub> , D <sub>2</sub> <sup>5</sup> ), (D <sub>2</sub> , D <sub>2</sub> <sup>5</sup> ), (D <sub>3</sub> , D <sub>2</sub> <sup>5</sup> ), (F, D <sub>2</sub> ), (MS <sup>F</sup> , D <sub>2</sub> <sup>5</sup> )	(D <sub>1</sub> <sup>5</sup> , D <sub>1</sub> )	(D <sub>1</sub> <sup>5</sup> , I <sub>1</sub> ), (D <sub>1</sub> <sup>5</sup> , D <sub>2</sub> ), (D <sub>1</sub> <sup>5</sup> , D <sub>3</sub> ), (D <sub>1</sub> , F), (D <sub>1</sub> <sup>5</sup> , MS <sup>F</sup> )
(D <sub>2</sub> , D <sub>2</sub> <sup>5</sup> )	(I <sub>2</sub> , D <sub>2</sub> <sup>5</sup> ), (D <sub>3</sub> , D <sub>2</sub> <sup>5</sup> ), (F, D <sub>2</sub> ), (MS <sup>F</sup> , D <sub>2</sub> <sup>5</sup> )	(D <sub>1</sub> <sup>5</sup> , D <sub>2</sub> )	(D <sub>1</sub> <sup>5</sup> , I <sub>2</sub> ), (D <sub>1</sub> <sup>5</sup> , D <sub>3</sub> ), (D <sub>1</sub> , F), (D <sub>1</sub> <sup>5</sup> , MS <sup>F</sup> )
(D <sub>3</sub> , D <sub>2</sub> <sup>5</sup> )	(I <sub>3</sub> , D <sub>2</sub> <sup>5</sup> ), (F, D <sub>2</sub> ), (MS <sup>F</sup> , D <sub>2</sub> <sup>5</sup> )	(D <sub>1</sub> <sup>5</sup> , D <sub>3</sub> )	(D <sub>1</sub> <sup>5</sup> , I <sub>3</sub> ), (D <sub>1</sub> , F), (D <sub>1</sub> <sup>5</sup> , MS <sup>F</sup> )
(I <sub>0</sub> , D <sub>2</sub> <sup>5</sup> )	(O, D <sub>2</sub> <sup>5</sup> )	(D <sub>1</sub> <sup>5</sup> , I <sub>0</sub> )	(D <sub>1</sub> <sup>5</sup> , O)
(I <sub>1</sub> , D <sub>2</sub> <sup>5</sup> )	(D <sub>1</sub> , D <sub>2</sub> <sup>5</sup> )	(D <sub>1</sub> <sup>5</sup> , I <sub>1</sub> )	(D <sub>1</sub> <sup>5</sup> , D <sub>1</sub> )
(I <sub>2</sub> , D <sub>2</sub> <sup>5</sup> )	(m, D <sub>2</sub> ), (MS <sup>m</sup> , D <sub>2</sub> <sup>5</sup> )	(D <sub>1</sub> <sup>5</sup> , I <sub>2</sub> )	(D <sub>1</sub> , m), (D <sub>1</sub> <sup>5</sup> , MS <sup>m</sup> )
(I <sub>3</sub> , D <sub>2</sub> <sup>5</sup> )	(M, D <sub>2</sub> ), (MS <sup>M</sup> , D <sub>2</sub> <sup>5</sup> )	(D <sub>1</sub> <sup>5</sup> , I <sub>3</sub> )	(D <sub>1</sub> , M), (D <sub>1</sub> <sup>5</sup> , MS <sup>M</sup> )
(m, D <sub>2</sub> )	(m, I <sub>2</sub> ), (m, D <sub>3</sub> ), (m, F), (D <sub>1</sub> <sup>5</sup> , D <sub>2</sub> ), (D <sub>2</sub> <sup>5</sup> , D <sub>2</sub> ), (D <sub>3</sub> <sup>5</sup> , D <sub>2</sub> ), (F, D <sub>2</sub> )	(D <sub>1</sub> <sup>5</sup> , MS <sup>m</sup> )	(D <sub>1</sub> , m)
(M, D <sub>2</sub> )	(M, I <sub>2</sub> ), (M, D <sub>3</sub> ), (M, F), (O <sup>5</sup> , D <sub>2</sub> ), (D <sub>1</sub> <sup>5</sup> , D <sub>2</sub> ), (D <sub>2</sub> <sup>5</sup> , D <sub>2</sub> ), (D <sub>3</sub> <sup>5</sup> , D <sub>2</sub> ), (F, D <sub>2</sub> )	(D <sub>1</sub> <sup>5</sup> , MS <sup>M</sup> )	(D <sub>1</sub> , M)
(MS <sup>F</sup> , D <sub>2</sub> <sup>5</sup> )	(F, D <sub>2</sub> )	(D <sub>1</sub> <sup>5</sup> , MS <sup>F</sup> )	(D <sub>1</sub> , F)
(O, D <sub>3</sub> <sup>5</sup> )	(I <sub>0</sub> , D <sub>3</sub> <sup>5</sup> ), (D <sub>1</sub> , D <sub>3</sub> <sup>5</sup> ), (D <sub>2</sub> , D <sub>3</sub> <sup>5</sup> ), (D <sub>3</sub> , D <sub>3</sub> <sup>5</sup> ), (F, D <sub>3</sub> ), (MS <sup>F</sup> , D <sub>3</sub> <sup>5</sup> )	(D <sub>2</sub> <sup>5</sup> , O)	(D <sub>2</sub> <sup>5</sup> , I <sub>0</sub> ), (D <sub>2</sub> <sup>5</sup> , D <sub>1</sub> ), (D <sub>2</sub> <sup>5</sup> , D <sub>2</sub> ), (D <sub>2</sub> <sup>5</sup> , D <sub>3</sub> ), (D <sub>2</sub> , F), (D <sub>2</sub> <sup>5</sup> , MS <sup>F</sup> )
(D <sub>1</sub> , D <sub>3</sub> <sup>5</sup> )	(I <sub>1</sub> , D <sub>3</sub> <sup>5</sup> ), (D <sub>2</sub> , D <sub>3</sub> <sup>5</sup> ), (D <sub>3</sub> , D <sub>3</sub> <sup>5</sup> ), (F, D <sub>3</sub> ), (MS <sup>F</sup> , D <sub>3</sub> <sup>5</sup> )	(D <sub>2</sub> <sup>5</sup> , D <sub>1</sub> )	(D <sub>2</sub> <sup>5</sup> , I <sub>1</sub> ), (D <sub>2</sub> <sup>5</sup> , D <sub>2</sub> ), (D <sub>2</sub> <sup>5</sup> , D <sub>3</sub> ), (D <sub>2</sub> , F), (D <sub>2</sub> <sup>5</sup> , MS <sup>F</sup> )
(D <sub>2</sub> , D <sub>3</sub> <sup>5</sup> )	(I <sub>2</sub> , D <sub>3</sub> <sup>5</sup> ), (D <sub>3</sub> , D <sub>3</sub> <sup>5</sup> ), (F, D <sub>3</sub> ), (MS <sup>F</sup> , D <sub>3</sub> <sup>5</sup> )	(D <sub>2</sub> <sup>5</sup> , D <sub>2</sub> )	(D <sub>2</sub> <sup>5</sup> , I <sub>2</sub> ), (D <sub>2</sub> <sup>5</sup> , D <sub>3</sub> ), (D <sub>2</sub> , F), (D <sub>2</sub> <sup>5</sup> , MS <sup>F</sup> )
(D <sub>3</sub> , D <sub>3</sub> <sup>5</sup> )	(I <sub>3</sub> , D <sub>3</sub> <sup>5</sup> ), (F, D <sub>3</sub> ), (MS <sup>F</sup> , D <sub>3</sub> <sup>5</sup> )	(D <sub>2</sub> <sup>5</sup> , D <sub>3</sub> )	(D <sub>2</sub> <sup>5</sup> , I <sub>3</sub> ), (D <sub>2</sub> , F), (D <sub>2</sub> <sup>5</sup> , MS <sup>F</sup> )
(I <sub>0</sub> , D <sub>3</sub> <sup>5</sup> )	(O, D <sub>3</sub> <sup>5</sup> )	(D <sub>2</sub> <sup>5</sup> , I <sub>0</sub> )	(D <sub>2</sub> <sup>5</sup> , O)
(I <sub>1</sub> , D <sub>3</sub> <sup>5</sup> )	(D <sub>1</sub> , D <sub>3</sub> <sup>5</sup> )	(D <sub>2</sub> <sup>5</sup> , I <sub>1</sub> )	(D <sub>2</sub> <sup>5</sup> , D <sub>1</sub> )
(I <sub>2</sub> , D <sub>3</sub> <sup>5</sup> )	(m, D <sub>3</sub> ), (MS <sup>m</sup> , D <sub>3</sub> <sup>5</sup> )	(D <sub>2</sub> <sup>5</sup> , I <sub>2</sub> )	(D <sub>2</sub> , m), (D <sub>2</sub> <sup>5</sup> , MS <sup>m</sup> )
(I <sub>3</sub> , D <sub>3</sub> <sup>5</sup> )	(M, D <sub>3</sub> ), (MS <sup>M</sup> , D <sub>3</sub> <sup>5</sup> )	(D <sub>2</sub> <sup>5</sup> , I <sub>3</sub> )	(D <sub>2</sub> , M), (D <sub>2</sub> <sup>5</sup> , MS <sup>M</sup> )
(m, D <sub>3</sub> )	(m, I <sub>3</sub> ), (m, F), (D <sub>1</sub> <sup>5</sup> , D <sub>3</sub> ), (D <sub>2</sub> <sup>5</sup> , D <sub>3</sub> ), (D <sub>3</sub> <sup>5</sup> , D <sub>3</sub> ), (F, D <sub>3</sub> )	(D <sub>2</sub> <sup>5</sup> , MS <sup>m</sup> )	(D <sub>2</sub> , m)
(M, D <sub>3</sub> )	(M, I <sub>3</sub> ), (M, F), (O <sup>5</sup> , D <sub>3</sub> ), (D <sub>1</sub> <sup>5</sup> , D <sub>3</sub> ), (D <sub>2</sub> <sup>5</sup> , D <sub>3</sub> ), (D <sub>3</sub> <sup>5</sup> , D <sub>3</sub> ), (F, D <sub>3</sub> )	(D <sub>2</sub> <sup>5</sup> , MS <sup>M</sup> )	(D <sub>2</sub> , M)
(MS <sup>F</sup> , D <sub>3</sub> <sup>5</sup> )	(F, D <sub>3</sub> )	(D <sub>2</sub> <sup>5</sup> , MS <sup>F</sup> )	(D <sub>2</sub> , F)
(O, m)	(I <sub>0</sub> , m), (D <sub>1</sub> , m), (D <sub>2</sub> , m), (D <sub>3</sub> , m), (F, m), (O, D <sub>1</sub> <sup>5</sup> ), (O, D <sub>2</sub> <sup>5</sup> ), (O, D <sub>3</sub> <sup>5</sup> ), (O, F)	(D <sub>3</sub> <sup>5</sup> , O)	(D <sub>3</sub> <sup>5</sup> , I <sub>0</sub> ), (D <sub>3</sub> <sup>5</sup> , D <sub>1</sub> ), (D <sub>3</sub> <sup>5</sup> , D <sub>2</sub> ), (D <sub>3</sub> <sup>5</sup> , D <sub>3</sub> ), (D <sub>3</sub> , F), (D <sub>3</sub> <sup>5</sup> , MS <sup>F</sup> )
(D <sub>1</sub> , m)	(I <sub>1</sub> , m), (D <sub>2</sub> , m), (D <sub>3</sub> , m), (F, m), (D <sub>1</sub> , D <sub>1</sub> <sup>5</sup> ), (D <sub>1</sub> , D <sub>2</sub> <sup>5</sup> ), (D <sub>1</sub> , D <sub>3</sub> <sup>5</sup> ), (D <sub>1</sub> , F)	(D <sub>3</sub> <sup>5</sup> , D <sub>1</sub> )	(D <sub>3</sub> <sup>5</sup> , I <sub>1</sub> ), (D <sub>3</sub> <sup>5</sup> , D <sub>2</sub> ), (D <sub>3</sub> <sup>5</sup> , D <sub>3</sub> ), (D <sub>3</sub> , F), (D <sub>3</sub> <sup>5</sup> , MS <sup>F</sup> )
(D <sub>2</sub> , m)	(I <sub>2</sub> , m), (D <sub>3</sub> , m), (F, m), (D <sub>2</sub> , D <sub>1</sub> <sup>5</sup> ), (D <sub>2</sub> , D <sub>2</sub> <sup>5</sup> ), (D <sub>2</sub> , D <sub>3</sub> <sup>5</sup> ), (D <sub>2</sub> , F)	(D <sub>3</sub> <sup>5</sup> , D <sub>2</sub> )	(D <sub>3</sub> <sup>5</sup> , I <sub>2</sub> ), (D <sub>3</sub> <sup>5</sup> , D <sub>3</sub> ), (D <sub>3</sub> , F), (D <sub>3</sub> <sup>5</sup> , MS <sup>F</sup> )
(D <sub>3</sub> , m)	(I <sub>3</sub> , m), (F, m), (D <sub>3</sub> , D <sub>1</sub> <sup>5</sup> ), (D <sub>3</sub> , D <sub>2</sub> <sup>5</sup> ), (D <sub>3</sub> , D <sub>3</sub> <sup>5</sup> ), (D <sub>3</sub> , F)	(D <sub>3</sub> <sup>5</sup> , D <sub>3</sub> )	(D <sub>3</sub> <sup>5</sup> , I <sub>3</sub> ), (D <sub>3</sub> , F), (D <sub>3</sub> <sup>5</sup> , MS <sup>F</sup> )
(I <sub>0</sub> , m)	(O, m)	(D <sub>3</sub> <sup>5</sup> , I <sub>0</sub> )	(D <sub>3</sub> <sup>5</sup> , O)
(I <sub>1</sub> , m)	(D <sub>1</sub> , m)	(D <sub>3</sub> <sup>5</sup> , I <sub>1</sub> )	(D <sub>3</sub> <sup>5</sup> , D <sub>1</sub> )
(I <sub>2</sub> , m)	(m, m)	(D <sub>3</sub> <sup>5</sup> , I <sub>2</sub> )	(D <sub>3</sub> , m), (D <sub>3</sub> <sup>5</sup> , MS <sup>m</sup> )
(I <sub>3</sub> , m)	(M, m)	(D <sub>3</sub> <sup>5</sup> , I <sub>3</sub> )	(D <sub>3</sub> , M), (D <sub>3</sub> <sup>5</sup> , MS <sup>M</sup> )
(m, m)	(D <sub>1</sub> , m), (D <sub>2</sub> , m), (D <sub>3</sub> , m), (F, m), (m, D <sub>1</sub> ), (m, D <sub>2</sub> ), (m, D <sub>3</sub> ), (m, F)	(D <sub>3</sub> <sup>5</sup> , MS <sup>m</sup> )	(D <sub>3</sub> , m)
(M, m)	(O, m), (D <sub>1</sub> , m), (D <sub>2</sub> , m), (D <sub>3</sub> , m), (F, m), (M, D <sub>1</sub> ), (M, D <sub>2</sub> ), (M, D <sub>3</sub> ), (M, F)	(D <sub>3</sub> <sup>5</sup> , MS <sup>M</sup> )	(D <sub>3</sub> , M)
(F, m)	(O, m), (F, D <sub>1</sub> ), (F, D <sub>2</sub> ), (F, D <sub>3</sub> ), (F, F)	(D <sub>3</sub> <sup>5</sup> , MS <sup>F</sup> )	(D <sub>3</sub> , F)
(O, M)	(I <sub>0</sub> , M), (D <sub>1</sub> , M), (D <sub>2</sub> , M), (D <sub>3</sub> , M), (F, M), (O, O <sup>5</sup> ), (O, D <sub>1</sub> <sup>5</sup> ), (O, D <sub>2</sub> <sup>5</sup> ), (O, D <sub>3</sub> <sup>5</sup> ), (O, F)	(MS <sup>m</sup> , O <sup>5</sup> )	(m, O)
(D <sub>1</sub> , M)	(I <sub>1</sub> , M), (D <sub>2</sub> , M), (D <sub>3</sub> , M), (F, M), (D <sub>1</sub> , O <sup>5</sup> ), (D <sub>1</sub> , D <sub>1</sub> <sup>5</sup> ), (D <sub>1</sub> , D <sub>2</sub> <sup>5</sup> ), (D <sub>1</sub> , D <sub>3</sub> <sup>5</sup> ), (D <sub>1</sub> , F)	(MS <sup>m</sup> , D <sub>1</sub> <sup>5</sup> )	(m, D <sub>1</sub> )
(D <sub>2</sub> , M)	(I <sub>2</sub> , M), (D <sub>3</sub> , M), (F, M), (D <sub>2</sub> , O <sup>5</sup> ), (D <sub>2</sub> , D <sub>1</sub> <sup>5</sup> ), (D <sub>2</sub> , D <sub>2</sub> <sup>5</sup> ), (D <sub>2</sub> , D <sub>3</sub> <sup>5</sup> ), (D <sub>2</sub> , F)	(MS <sup>m</sup> , D <sub>2</sub> <sup>5</sup> )	(m, D <sub>2</sub> )
(D <sub>3</sub> , M)	(I <sub>3</sub> , M), (F, M), (D <sub>3</sub> , O <sup>5</sup> ), (D <sub>3</sub> , D <sub>1</sub> <sup>5</sup> ), (D <sub>3</sub> , D <sub>2</sub> <sup>5</sup> ), (D <sub>3</sub> , D <sub>3</sub> <sup>5</sup> ), (D <sub>3</sub> , F)	(MS <sup>m</sup> , D <sub>3</sub> <sup>5</sup> )	(m, D <sub>3</sub> )
(I <sub>0</sub> , M)	(O, M)	(MS <sup>M</sup> , O <sup>5</sup> )	(M, O)
(I <sub>1</sub> , M)	(D <sub>1</sub> , M)	(MS <sup>M</sup> , D <sub>1</sub> <sup>5</sup> )	(M, D <sub>1</sub> )
(I <sub>2</sub> , M)	(m, M)	(MS <sup>M</sup> , D <sub>2</sub> <sup>5</sup> )	(M, D <sub>2</sub> )
(I <sub>3</sub> , M)	(M, M)	(MS <sup>M</sup> , D <sub>3</sub> <sup>5</sup> )	(M, D <sub>3</sub> )
(m, M)	(D <sub>1</sub> , M), (D <sub>2</sub> , M), (D <sub>3</sub> , M), (F, M), (m, O), (m, D <sub>1</sub> ), (m, D <sub>2</sub> ), (m, D <sub>3</sub> ), (m, F)		



# Single-year Estimates in Developing Countries Mortality Database (DCMD)

Nan Li<sup>1</sup> and Hong Mi<sup>2</sup>

1. Population Division, Department of Economic and Social Affairs, United Nations, 2 UN Plaza, 233 East 44th Street, Room DC2-1938, New York, NY 10017, USA (Email: [li32@un.org](mailto:li32@un.org)). The views expressed in this paper are those of the author and do not necessarily reflect those of the United Nations.

2. Corresponding author, School of Public Affairs, Zhejiang University, Room 265#, Mengminwei Building, Zijing'gang Campus, Hangzhou, Zhejiang, P. R. China. (E-mail: [spsswork@163.com](mailto:spsswork@163.com)). The work on this paper was supported by the Nature Science Foundation of China (NSFC) project (NO.71490732), NSFC project (NO.71490733), Zhejiang Social Science Planning Project Key Program(NO.17NDJC029Z), and Nature Science Foundation of Zhejiang project (NO. LZ13G030001)

*In the earlier phases of Developing Countries Mortality Database (CDMD), the estimates of old-age mortality ( $45Q_{60}$  or  $Q_o$ ) and life tables used only census population at old ages. These estimates referred to the periods between successive censuses. This paper describes the method of converting period estimates into single-year estimates, using the relationship between period and single-year estimates and, when available, utilizing also the data on old-age deaths in census years collected from death registration or census.*

## (1) The method

### (1.1) Relationship estimates

In CDMD, the old-age mortality (the probability of dying between ages 60 and 75 years) for a multiple-year-period,  $Q_{op}$  (where subscript “o” and “p” stands for old age and period, respectively), is estimated using the numbers of old-age population enumerated in two successive censuses, the estimates of child mortality and adult mortality, and the two-input-parameter model life table (MLT) (Wilmoth, et al, 2012). After the  $Q_{op}$  is estimated, the corresponding life table can be calculated using the three-input-parameter MLT (Li, Mi, Gerland, Li, and Sun, 2017). The purpose of this paper is to indicate a method that converts  $Q_{op}$  into single-year old-age mortality,  $Q_o(t)$ , which lead to single-year life tables.

The three-input-parameter MLT is an extension of the two-input-parameter MLT that uses child mortality ( $Q_c(t)$ ) and adult mortality ( $Q_a(t)$ ) to produce a life table. Using this life table, old-age mortality,  $Q_{o_2}(t)$  (where subscript “2” stands for two-input-parameter MLT), is obtained. contains old-age mortality. The estimates of  $Q_{o_2}(t)$  are based on the  $Q_c(t)$  provided by the UNICEF ([www.childmortality.org](http://www.childmortality.org)) and the  $Q_a(t)$  estimated by the IHME (<http://www.healthdata.org/>). Thus, the over-time changes in  $Q_{o_2}(t)$  should contain the effects on  $Q_c(t)$  and  $Q_a(t)$  from socioeconomic developments and special events such as natural disasters, epidemics, and violent conflicts that have been taken into account by the UNICEF and IHME.

The basis of converting  $Q_{op}$  into  $Q_o(t)$  is the relationship between the over-time changes of  $Q_o(t)$  and that of  $Q_{o_2}(t)$ : the over-time changes of  $Q_o(t)$  and that of  $Q_{o_2}(t)$  should be similar. To be more specific, if there is a peak (or bottom) in  $Q_{o_2}(t)$ , there should also a peak (or bottom) in  $Q_o(t)$ . If  $Q_{o_2}(t)$  declines over time, so should  $Q_o(t)$ , and vice versa. To



establish this relationship, the multiple-year-period old-age mortality of the two-input-parameter MLT,  $Q_{o2p}$ , needs to be estimated.

In CDMD,  $Q_{o2p}$  can be defined using the period death rates  $M_p(60-64)$ ,  $M_p(65-69)$ , and  $M_p(70-74)$ , assuming the force of mortality to be constant within a age group:

$$Q_{o2p} = 1 - \exp[-5 \cdot \sum_x M_p(x)], \quad x = 60 - 64, \quad 65 - 69, \quad 70 - 74. \quad (1)$$

Further, the multiple-year-period death rates can be calculated approximately as the average of single-year death rates in the period, if the population change slowly over time:

$$M_p(x) = \frac{\sum_t d(x,t)}{\sum_t p(x,t)} = \sum_t M(x,t) \cdot \frac{p(x,t)}{\sum_t p(x,t)} \approx \sum_t M(x,t) / T, \quad (2)$$

where  $T$  is the number of years included in the period,  $d(x,t)$  and  $p(x,t)$  are the numbers of death and population in age group  $x$  and year  $t$ , and  $M(x,t)$  is the single-year death rate of age group  $x$  and year  $t$ . Furthermore, the sum of single-year death rates can be calculated as

$$\sum_x M(x,t) = -\frac{\text{Log}[1 - Q_{o2}(t)]}{5}. \quad (3)$$

Thus,  $Q_{o2p}$  can be calculated using (1)-(3).

Since  $Q_{o2}(t)$  is determined by child and adult mortality, the basic relationship can be expressed as that the over-time changes of  $Q_o(t)$  should be similar to that of  $Q_{o2}(t)$ , and can be written as

$$\frac{Q_{or}(t)}{Q_{op}} = \frac{Q_{o2}(t)}{Q_{o2p}}, \quad (4)$$

where  $Q_{or}(t)$  denotes the single-year old-age mortality estimated from the relationship, and subscript “r” stands for relationship. Eq(4) indicates that the shapes of  $Q_{or}(t)$  and  $Q_{o2}(t)$  are similar, and the levels of  $Q_o(t)$  and  $Q_{o2}(t)$  are determined by  $Q_{op}$  and  $Q_{o2p}$ . In other words, if there is a peak (or bottom) in  $Q_{o2}(t)$ , there will also be a peak (or bottom) in  $Q_{or}(t)$ . If  $Q_{o2}(t)$  declines over time, so will  $Q_o(t)$ , and vice versa. Using (4), the relationship estimate of old-age mortality is derived as

$$Q_{or}(t) = \frac{Q_{o2}(t)}{Q_{o2p}} Q_{op}. \quad (5)$$

### (1.2) Smoothing the relationship estimates

Since the values of the  $Q_{op}$  in two successive periods are often remarkably different, the changes in  $Q_{or}(t)$  at the boundary of two successive periods are often discontinuous.

These discontinuations can be eliminated using the local regression; and the smoothed estimates are denoted as  $Qos(t)$ , where “s” stands for smoothed.

**(1.3) Utilizing the numbers of death in census years**

For many developing countries, there are data on deaths collected from census (often within the 12 months before the census dates) or from vital registration in census years. By moving the census population  $t_0$  years forward, the census population can be adjusted to refer the middle point of the death registration or the death reported in census. To be specific,  $t_0$  is 0.5 minus the census date when using death registration, or is -0.5 when using data on death reported in census. Accordingly, death rates  $M_{odr}(x)$  (using data from death registration) or  $M_{odrc}(x)$  (using data from deaths reported in census) can be calculated as:

$$M_{odr}(x) = \frac{d(x)}{p(x) - t_0 \cdot d(x)}, \quad (6)$$

$$M_{odrc}(x) = \frac{d(x)}{p(x) + 0.5 \cdot d(x)},$$

where  $d(x)$  and  $p(x)$  are the numbers of death and population in age group  $x$  at the census year<sup>1</sup>. Subsequently, old-age mortality  $Q_{odr}$  (using data from death registration, DR) or  $Q_{odrc}$  (using data from deaths reported in census, DRC) are computed:

$$Q_{odr} = 1 - \exp[-5 \cdot \sum_x M_{odr}(x)],$$

$$Q_{odrc} = 1 - \exp[-5 \cdot \sum_x M_{odrc}(x)]. \quad (7)$$

**(1.4) Weights**

Using local regression, single-year  $Q_{odr}$  or  $Q_{odrc}$  are obtained as  $Q_{odr}(t)$  and  $Q_{odrc}(t)$ . Since the data on death registration or reported in census can be used to make the estimates more reliable, the final single-year estimates of old-age mortality is estimated as

$$Q_o(t) = w(t) \cdot Q_{os}(t) + (1 - w(t)) \cdot Q_{odr}(t),$$

$$Q_o(t) = w(t) \cdot Q_{os}(t) + (1 - w(t)) \cdot Q_{odrc}(t), \quad (8)$$

where  $w(t)$  are the weights.

The errors in  $Q_{os}$  are mainly caused by the underreporting of census population, and should be small when the underreporting rates of census population are small. On the other hand, besides the underreporting of census population, the errors in  $Q_{odr}$  or  $Q_{odrc}$  are also caused by the incompleteness of DR or DRC, because the numbers of death are required in calculating  $Q_{odr}$  or  $Q_{odrc}$  according to (6)-(7).

When the values of  $Q_{odr}$  (or  $Q_{odrc}$ ) are lower than that of  $Q_{os}$ , it implies that the DR or DRC is incomplete, even if there were no underreporting of census population. Because  $Q_{os}$  and  $Q_{odr}$  (or  $Q_{odrc}$ ) both depend on the data of census population, and because  $Q_{odr}$  (or

---

<sup>1</sup> Cohorts' fractions that move in or out the age range 60-75 years should also be adjusted in principle. But for many countries 75+ is the open age group, so that such an adjustment is not always doable.

Qodrc) depends in addition on data of DR (or DRC) that are known to be incomplete, the Qos should be more reliable than Qodr (or Qodrc). Subsequently, the weights of Qos should be bigger than that of Qodr (or Qodrc).

When the values of Qodr (or Qodrc) are higher than that of Qos, it implies that census population are underreported (or the underreporting of census population is more than the incompleteness of the DR (or (DRC))). Because the Qos depends only on the data of census population that are known to be underreported, and because the Qodr (or Qodrc) depends also on the data of DR or DRC that are known to be complete (or less incomplete than the underreporting of census population), the Qos should be less reliable than Qodr (or Qodrc). Subsequently, the weights of Qos should be smaller than that of Qodr (or Qodrc).

These analyses, however, still cannot determine the values of the weights. When arbitrary is inevitable, we choose the simplest arbitrary and set the default weights as

$$w(t) = 2/3, \text{ average}(Q_{os}(t)) > \text{average}(Q_{odr}(t), Q_{odrc}(t)), \quad (9)$$

$$w(t) = 1/3, \text{ otherwise.}$$

If there are no data on death for a census year  $t_1$ , it is nature to use  $Qodr(t_1)=Qodrc(t_1)=0$ ,  $w(t_1)=1$ , and  $Qo(t_1)=Qos(t_1)$ . However, when there are data on death at census year  $t_2$  that is successive to year  $t_1$ , there are  $w(t_1)=1$  and  $w(t_2)=2/3$ . To make  $w(t)$  change continuously between  $t_1$  and  $t_2$ , dummy  $Qodr(t_1)$  or  $Qodrc(t_1)$  are set using the same death rates at year  $t_2$ , and  $w(t)$  is set to change linearly from 1 at  $t_1$  to 2/3 or 1/3 at  $t_2$ . For other special situations, weights can also be different from the default ones.

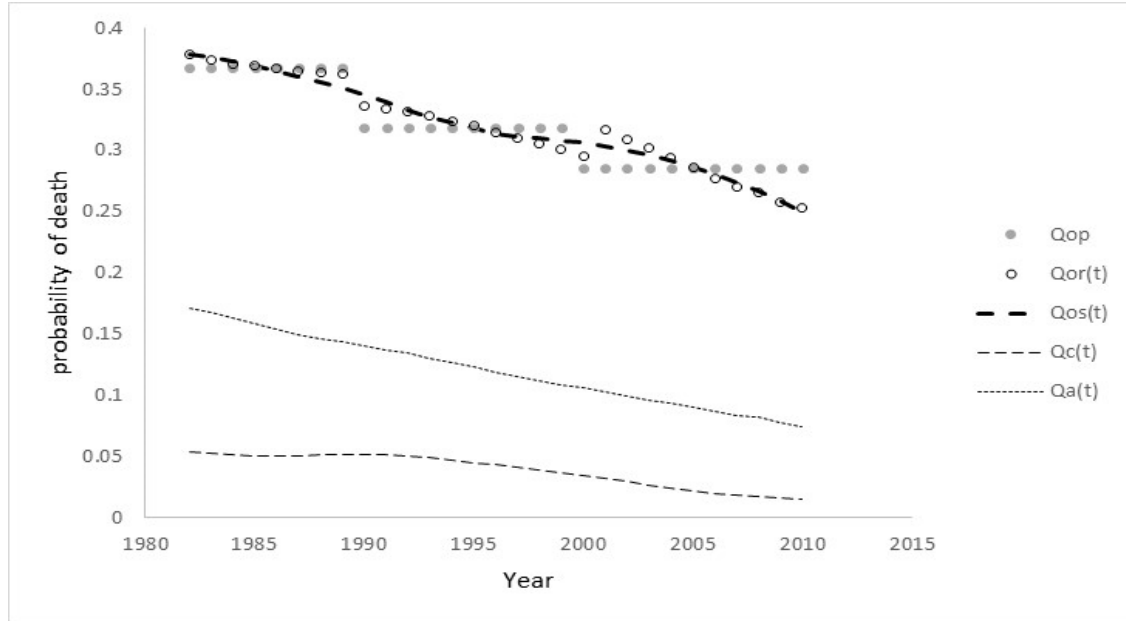
Finally, single-year life tables can be calculated using the three-input-parameter MLT.

## **(2) An example**

### **(2.1) Period, relationship, and smoothed estimates**

The estimates of Chinese women are chosen to provide below examples for illustration purpose. As can be seen in Figure 1, period old-age mortality (Qop) are displayed in grey circles, which are constant over time in the three periods between the censuses conducted in year 1982, 1990, 2000, and 2010. Relationship old-age mortality (Qor(t)) are shown in black-edged circles, which change over time slowly in 1982-1990 when the decline of child mortality (Qc(t)) was slow, and declines quickly in 1990-2010 when the declines of both  $Qa(t)$  and  $Qc(t)$  were faster.

Figure 1. Period, relationship, and smoothed estimates of old-age mortality, Chinese women



However, the changes in  $Qor(t)$  at the boundary of two successive periods, 1990 and 2000, are discontinuous. Local regression is used to eliminate the discontinuities and to produce the smoothed estimates  $Qos(t)$ , which is described by the dashed curve in Figure 1. If there were no data on deaths at census years,  $Qos(t)$  would serve as the final estimates.

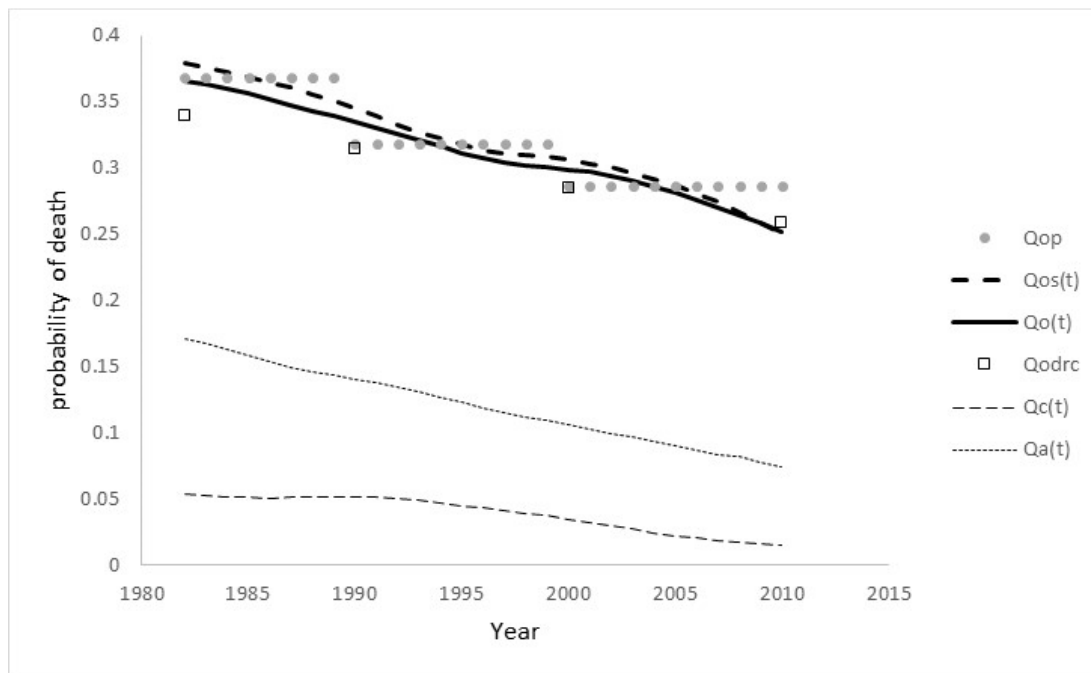
**(2.1) Data on deaths and final estimates**

The censuses conducted in China also collected the numbers of death occurred within 12 months<sup>2</sup> before the census dates, which should be used to improve the reliability of estimation. These data, together with the data on population at census years, provided the additional estimates of old-age mortality ( $Qodrc$ ), as are shown by the squares for the four census years in Figure 2.

Using (6)-(8), the final estimates,  $Qo(t)$ , are obtained and shown as the solid curve in Figure 2. The values of  $Qodrc$  are closer to that of  $Qos(t)$  in more recent years, and make the final estimates  $Qo(t)$  differ from  $Qos(t)$  notably in earlier years. Overall, the data on deaths improved the reliability of estimation.

Figure 2. Data on deaths and final estimates of old-age mortality, Chinese women

<sup>2</sup> The numbers of death collected during the 1982 census refer to the deaths occurred in 1981.



## References

Li N, Mi H, Gerland P, Li C, and Sun L. (2017) Establishing a developing countries mortality database (DCMD) on the basis of child, adult, and old-age mortality. *Xxx*

Wilmoth J, Zureick S, Canudas-Romo V, Inoue V, Sawyer C. (2012) A flexible two dimensional mortality model for use in indirect estimation. *Population Studies*: 661-28.

# Transition in health in people aged 65 in Europe

Justyna Majewska<sup>1</sup> and Grażyna Trzpiot<sup>2</sup>

<sup>1</sup> Department of Demography and Economic Statistics, University of Economics in Katowice, Poland

(E-mail: justyna.majewska@ue.katowice.pl)

<sup>2</sup> Department of Demography and Economic Statistics, University of Economics in Katowice, Poland

(E-mail: grazyna.trzpiot@ue.katowice.pl)

**Abstract.** Analysis of changes in the health of older people is an important issue for social policy and health protection. In the paper we present changes in morbidity for different cohorts (aged 65 and above) for selected 31 European countries. Using an approach called the general theory of aging of the population of Michel and Robine (2004) we confirm a cyclical movement of health transition process. Life expectancy and health-adjusted life expectancy are used in order to study the stages of health transition: the relative compression, relative expansion, and relative dynamic equilibrium.

**Keywords:** HALE, morbidity, health transition

## 1 Introduction

Three major potential scenarios have been proposed for future mortality and morbidity patterns. The ‘compression of morbidity’ scenario anticipates an increase in life expectancy and a decrease in the proportion of life spent with serious disease and disability. The ‘expansion of morbidity’ scenario anticipates an increase in the life expectancy and an increase in the proportion of life spent with underlying illness or disability. A third morbidity scenario ‘dynamic equilibrium’ hypothesizes a state of equilibrium where life expectancy increases, while a longer proportion of life spent living with diseases is counteracted by a decrease in the severity of these diseases, and resulting in a constant proportion of life spent in poor health.

Health expectancy (life expectancy in a defined state of health) and health expectancy is “health-adjusted life expectancy” (the average number of healthy years that a person would live under the mortality and morbidity prevailing at that time) are an important tool for monitoring trends in population health and for evaluating the evidence for morbidity scenarios. Existing in the literature analyses monitor these trends usually for one particular country (e.g. Eillen et al. 2011, Cutler et al. 2013, Steensma et al., 2017). It is commonly underline in the literature that comparison health of different countries is difficult because of cultural differences, differences in recording and classification practices, and different methodologies of data collecting. However in this study, the concept of using knowledge of existence of some common trends in mortality and longevity trends for closely related populations (Li and Lee 2005, Majewska

---

*5<sup>th</sup> SMTDA Conference Proceedings, 12-15 June 2018, Chania, Crete, Greece*

© 2018 ISAST



2017) is used in order to understand changes in health in European countries.

The aims of this study are two-fold: 1) present changes in morbidity for different cohorts, 2) using an approach called the general theory of aging of the population of Michel and Robine (2004) to confirm a cyclical movement of morbidity. As was pointed in Michel and Robine (2004) “first sicker people survive into old age and disability rises, then the number of years lived with disability decreases as new cohorts of healthier people enter old age, but finally, the number of years lived with disability rises again when the average age of death goes so high that many people spent their last years at an advanced old age burdened by multiple chronic diseases and frailty”.

In the first part of this study the ideas of morbidity scenarios and an approach called the general theory of aging of the population are presented. In the second part used data and methodology is described. Empirical analysis is conducted 31 European countries over the last three decades, and is presented in the third section. Conclusions end this paper.

## **2 Health transition models**

Three basic theories are known in the literature: compression of morbidity, expansion of morbidity and dynamic equilibrium theory, and a new approach called the general theory of aging of the population.

Theory of compression of morbidity (Fries 1980, Fries et al. 1989, Fries 2003) assumes the improvement of health in subsequent cohorts of the elderly and focusing on morbidity and disability in the oldest age groups. James F. Fries assumed that with the extension of life expectancy is clearly delayed when a serious disability occurs, indicating the possibility of coexistence of old age and good health. In the general model of health transition (WHO, 1984), this illustrates the shift of the survival curve without disease and disability along with the survival curve. In addition, the shift in the period of occurrence of diseases may be greater than changes in mortality, which in turn will shorten the period of disease burden, intensifying their occurrence in the last phase of life. The premise of this position is both the growing awareness of the impact of lifestyle on the state of their own health – manifested by the choice of diet, physical activity, decreasing consumption of drugs – as well as increasing knowledge of the impact of natural and social environment on the occurrence of activity restrictions.

The theory of disease expansion (also known as the pandemic theory of chronic diseases and disabilities) (Grunberg 1977, Kramer 1980) assumes that improving the survival of people with disability and burdened with diseases (as well as extending life expectancy for years, when diseases and disabilities occur naturally (biologically) more often), cause a general increase in fraction people in the population, especially in older age groups. The theory of morbidity expansion assumes a significant extension of life expectancy due to a decrease in mortality, with insignificant changes in the age of disability, which in turn results in an increase in the duration of life with disease burden and disability in

the population. According to this theory, the deterioration of the health of older people is the result of a combination of unfavorable factors affecting these people in the short and long term. The most important short-term factors include the expected – as a result of the co-occurrence of the population aging process and the extensive social security system – public finance crisis, which will probably lead both to reducing the disposable income of older people and limiting public expenditure on medical and care services. In turn, the key long-term factors include: the fact that future elderly practically all their lives were exposed to the accumulating in time action of environmental pollution and limitation due to the development of medical technology selection processes at previous stages of life, which makes it nowadays to all ages the individuals with a relatively weaker health condition live longer than their peers from previous generations, units that otherwise would have died long ago.

According to the theory of dynamic equilibrium (1982), a decrease in mortality may lead to an increase in the share and number of patients and with ailments, but only in terms of disease conditions of not very severe course, with a simultaneous decrease in the incidence of serious diseases and disabilities. According to Kenneth G. Manton, the changes taking place in mortality, which lead to life extension, are accompanied by multidirectional changes in the intensity of diseases and disabilities and their duration depending on the degree of disability and the type of disease. On the one hand, the period of life with moderate ailments and diseases, it is prolonged, that is, there is expansion of morbidity, and on the other hand there is compression in the field of severe diseases and serious limitations in fitness, that is, the duration of life with serious diseases is shortened. The effect of these changes is the state of equilibrium in the burden of diseases in the population, and the shift at the age of disability and life expectancy occurs in the same dimension.

The wider approach was made by Michel and Robine in 2004, proposing a general theory of the aging of the population. The authors emphasize that in order to understand the ongoing relationship between mortality trends and changes in disability and disease burden, it is necessary to take into account the stage of demographic and epidemiological transition on which the country is located, as well as socio-economic, geographical, cultural and medical conditions. The basis for the theory of population aging is the assumption of cyclic consecutive stages, the components of which are processes included in the model of health transition in their interrelationships. The first stage concerns the increase in the life expectancy due to the decrease in mortality in the oldest age groups. The increase in the survival of people at an advanced age burdened with various diseases and ailments results in an increase in the number of years lived with disability and the share of people in the population who are burdened with chronic diseases (expansion of morbidity). It is assumed that the stage of expansion of morbidity may be delayed in other regions of the world, especially in less developed countries, which are only entering the stage of decreasing mortality. The second stage corresponds to the theory of dynamic equilibrium. It is associated with further medical progress, which allows stopping or slowing down the development of many diseases and delaying the occurrence of severe

symptoms of the disease. An important element of this stage is adaptation to the existing demographic and epidemiological changes in the field of health policy, which was directed to the growing population of elderly people and diseases typical of this age. The third stage (compression of morbidity) occurs as a result of entering the aging process of the next generation. It is assumed that people from this cohort, thanks to pro-healthy behaviors and increasingly better living conditions, will enjoy better health compared to the previous generation. The improvement of health will be manifested in the delay in the occurrence of disability and chronic diseases, which will result in a shortening of years spent in poor health and the accumulation of diseases and disabilities in the late-old age. The authors of this theory suppose that the process may be continued and after the completion of one cycle, the first stage will be re-performed, albeit with a different quality.

It is worth to emphasize that each of these theoretical scenarios of changes in terms of morbidity and disability is associated with very important consequences, including economic ones, resulting from the need for medical and rehabilitation care. For example, the occurrence of the expansion of morbidity means the need to increase expenditure on health care and medical care of old-age persons.

### **3 Data and methodology**

Life expectancy and healthy adjusted life expectancy (HALE) were obtained from the Global Burden of Disease database (GBD, 2016). HALE summarizes the expected number of years to be lived in what might be termed the equivalent of full health. Some consider the HALE to provide the best available summary measure for measuring the overall level of health for populations (Mathers et al. 2001). Lost years of good health were calculated as a total life expectancy minus HALE. Both indicators (especially HALE calculated with different methodologies, see Zafeiris and Skiadas, 2015), when measured over time, are commonly used to in a verification of expansion and compression hypothesis (e.g. Steensma et al., 2017).

Data were collected for 31 European countries, separately for female and male, for the following age groups: 65-69, 70-74, 75-79, 80-84, 85-89, 90-94 and 95+. The analysis covers generational changes in life expectancy (two points in time i.e. 2016 in relation to 1990).

The discussion of the comparison results of HALE and disability life expectancy is provided within countries with similar characteristics related with health. Clustering was made by spatial analysis technique SKATER (Spatial 'K'luster Analysis by Tree Edge Removal) which is an alternative to other regionalization methods, based on minimum spanning trees (Assunção et al., 2006). SKATER first constructs a spatially contiguous graph by removing edges that do not connect geographic neighbors and then builds a minimum spanning tree from the graph (any tree built from this graph is spatially contiguous). The tree is then recursively partitioned to generate a given number of regions. Two important limitations of this algorithm are: (1) it uses contiguity constraints in a

static way, where the contiguity matrix is not dynamically updated during the clustering process and (2) minimum spanning tree has a well-known ‘chaining’ problem.

The spatial clustering algorithm involves some variables, representing the main indicators for similarities in the historic life expectancies of populations, or predictors for these similarities. Longer life (in health) is affected by many factors such as: socioeconomic status, the quality of the health system and the ability of people to access it, health behaviors such as tobacco and excessive alcohol consumption, nutrition, social factors, genetic factors, and environmental factors (WHO). Because understanding determinants of healthy life expectancy is very important, many analyses have been conducting in this area (Shaw et. al (2005), Lin et al. (2012)). However, such analysis limits from data access: although the economic factors are easy to derive, there is a little research on the health factors (e.g. nutrition, behavioral choice). Besides, indicators are often presented both for “self-reported” data (estimates from population-based health interview surveys) and “measured” data (precise estimates from health examinations). Thus, providing strict comparable (international) analyzes are difficult to conduct.

Having regard to the foregoing, in this empirical study, the following variables were used:

- Human Development Index – developed by the United Nations to measure and rank countries’ levels of social and economic development<sup>1</sup>,
- Air pollution – greenhouse gas emissions in tons per capita,
- Social protection expenditures measured as percentage of GDP,
- Doctors providing direct care to patients per 1000 inhabitants,
- Alcohol - annual sales of pure alcohol in liters per person aged 15 years and older,
- Cigarettes – a percentage of daily smokers of the population aged 15 years and over,
- Obesity – a percentage of obese inhabitants in population; obesity is measured by the body mass index.

Data were taken from Eurostat, OECD, UNDP databases and – in case of missing data – directly from national statistical offices, for 2014.

Albania, Belarus, Bosnia and Herzegovina, Moldavia, Macedonia, Montenegro, Serbia and Ukraine had to be excluded from the analysis due to lack of data.

## **4 Analysis**

### **Groups of countries**

The empirical analysis starts with obtaining homogenous spatial clusters of European countries according to the described above variables. As a result of

---

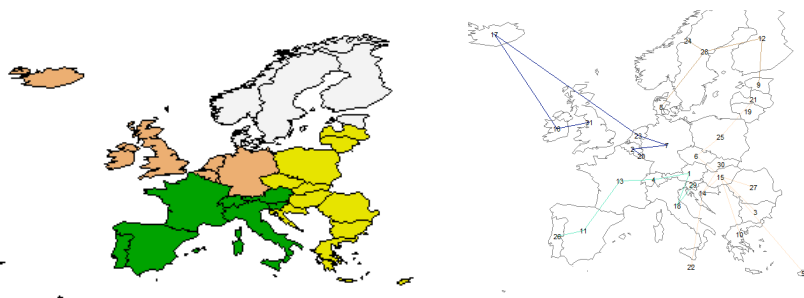
<sup>1</sup> The Human Development Index (HDI) is a composite statistic (composite index) of life expectancy, education, and per capita income indicators.

SKATER algorithm<sup>2</sup> four clusters were obtained:

- 1<sup>st</sup> cluster: Ireland, UK, Iceland, Netherlands, Luxembourg, Belgium, Germany
- 2<sup>nd</sup> cluster: Denmark, Sweden, Finland, Estonia, Norway
- 3<sup>rd</sup> cluster: France, Portugal, Spain, Italy, Austria, Switzerland, Slovenia, Malta
- 4<sup>th</sup> cluster: Czech Republic, Malta, Latvia, Lithuania, Poland, Slovakia, Croatia, Hungary, Romania, Bulgaria, Greece, Cyprus

The spatial diversification is shown in the figures 1 and 2. The results showed that this technique identifies regions that are considered homogeneous when regarding the variables connected strictly with determinants of healthy life and to geographical proximity. Differences between clusters result from geographical location that is related with socio-cultural behaviors, however inequalities in health and health care between clusters are clearly evident.

The first two clusters contain countries with very high HDI index. Even Estonia is in the group of thirty countries with the highest HDI (according to the UNDP, data from 2014 and 2015). Besides, Scandinavian influence on Estonian has determined that this country joined the cluster no. 2. Countries from cluster no. 1 were in a group of countries the most effective in reducing national smoking rates since 1985, with high HDI, and similar level of GHG emissions (exception is Luxembourg with the highest of emissions, but since 2004 the trend is decreasing). Countries from the third cluster have very high life expectancy. However, the presence of Slovenia may be surprising, but levels of other variables doesn't not allowed for joining this country for example to the fourth cluster. Slovenia has the lowest percentage of obesity among European countries (along with Switzerland), very low percentage of daily smokers, and a high position in the HDI ranking (25<sup>th</sup> place in 2014). The last cluster contains Eastern and Central European countries with the lowest social expenditures and the lowest HDI among analyzed countries in this study.



<sup>2</sup> A restriction to the procedure was added by establishing a minimum number of units in each cluster (minimum 3 countries). For each island – Iceland, Malta, Cyprus the nearest neighbour was found. All calculations were made in R environment (with spdep library).

Fig. 1. Spatial diversification of European countries in terms with variables in 2014

Fig. 2. A graph representation of the neighbor structure

### Changes in morbidity

Differences between LE and HALE indicate the life years that are lost due to ill health and are interpreted as unhealthy life expectancy or expected years lived with disability. Thus, the ratio HALE/LE is interpreted as the proportion of life expectancy spent in good health. It is desirable to distinguish here between absolute and relative compression/expansion of morbidity. Absolute compression occurs when unhealthy life expectancy decreases and absolute expansion occurs when unhealthy life expectancy increases. An absolute expansion of morbidity may lead to either an increase or a decrease in the proportion of life with disability/ill-health, and these situations are distinguished by referring to a relative compression of morbidity or relative expansion of morbidity.

Easy calculations (not shown here) demonstrate that over the last decades in the vast majority of European subpopulations we have been observing increase in the years spent in unhealthy state at old age 65+ (absolute expansion of morbidity). The exceptions are subpopulations in the oldest age: Croatia (male aged 90+), Greece (female aged 95+), Iceland (male and female aged 90+) and Malta (male aged 90+).

More interesting results come from verification the relative expansion/morbidity/balance hypotheses. Figures 3-12 present results of comparison HALE and lost years of good health, separately for female and male, and seven 5-year cohort groups. The difference between values of HALE/LE in 1990 and 2016 indicate substantial differentiation between populations. Thus, three stages of health transition are considered:

- A relative compression of morbidity:  
 $HALE_{2016}/LE_{2016} - HALE_{1990}/LE_{1990} > 0.3\%$ , where value 0.3% is a mean of all positive changes in proportion of years spent in good health,
- A relative expansion of morbidity:  
 $HALE_{2016}/LE_{2016} - HALE_{1990}/LE_{1990} < -1.0\%$ , where value -1.0% a mean of all negative changes in proportion of years spent in good health,
- A balance of morbidity:  $-1.0\% < HALE_{2016}/LE_{2016} - HALE_{1990}/LE_{1990} < 0.3\%$ .

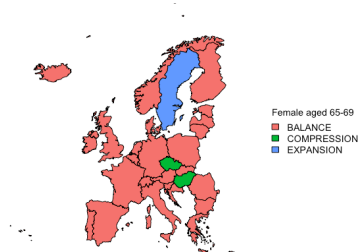


Fig. 3. Morbidity stages among female

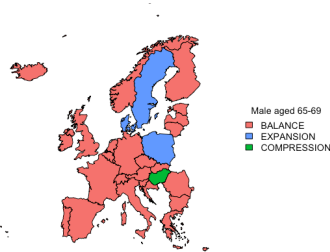


Fig. 4. Morbidity stages among male aged

aged 65-69

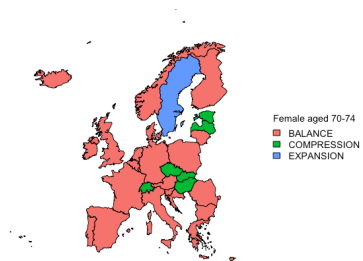


Fig. 5. Morbidity stages among female aged 70-74

65-69

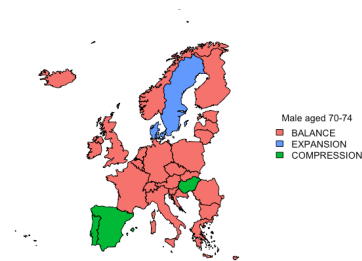


Fig. 6. Morbidity stages among male aged 70-74

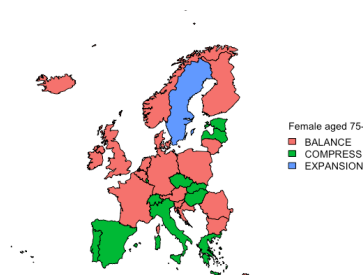


Fig. 7. Morbidity stages among female aged 75-79

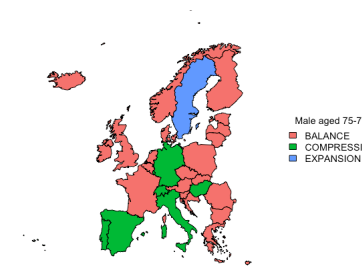


Fig. 8. Morbidity stages among male aged 75-79

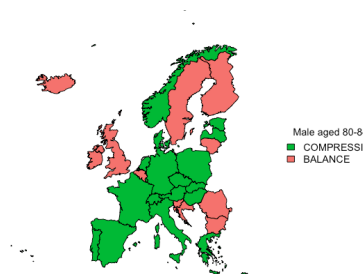


Fig. 9. Morbidity stages among female aged 80-84

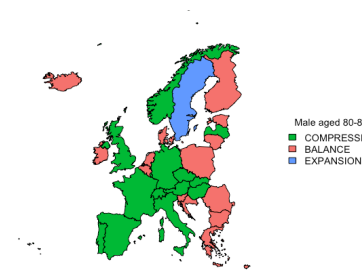


Fig. 10. Morbidity stages among male aged 80-84

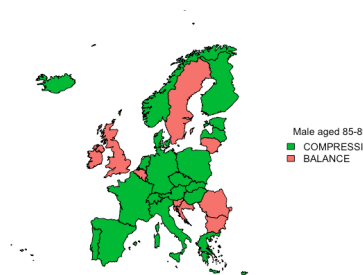


Fig. 11. Morbidity stages among female

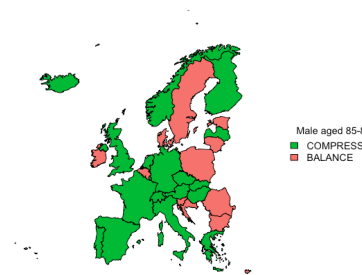


Fig. 12. Morbidity stages among male

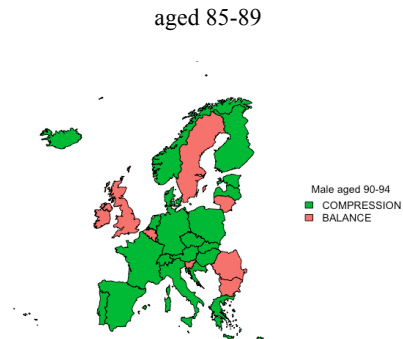


Fig. 11. Morbidity stages among female aged 90-94

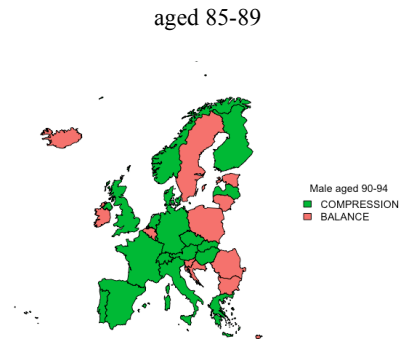


Fig. 12. Morbidity stages among male aged 90-94

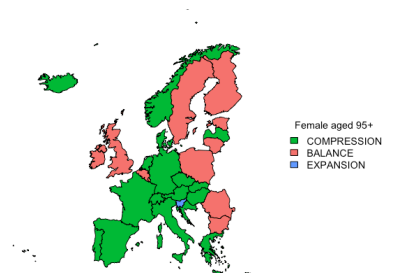


Fig. 11. Morbidity stages among female aged 95+

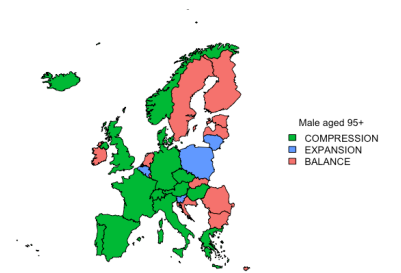


Fig. 12. Morbidity stages among male aged 95+

In Europe population aging is significantly diversified. Not surprisingly, age and sex are key factors in length of life spent in unhealthy state.

In most of European populations aged 80+ the proportion of life spent in an unhealthy state decreased which indicated a compression of morbidity – a key goal of healthy aging and longevity. To this group the following subpopulations belong:

- Germany (female) and UK male (cluster no. 1),
- Norway (regardless to sex and age), Denmark, Estonia and Netherland (female) (cluster no. 2),
- Austria, Portugal, Spain, Switzerland, Italy (regardless to sex and age) and France (female) (cluster no. 3),
- Slovakia and Hungary (regardless to sex and age), Greece, Latvia, Malta, Cyprus, Czech Republic (female) (cluster no. 4).

In the following countries compression of morbidity began among those in older age people, whereas those of lower age (but above 65) were still experiencing the balance of morbidity:

- Germany, Iceland (female), Luxembourg (female), Netherlands (female), UK (male) (cluster no. 1),

- Denmark (female), Norway (cluster no. 2),
- Austria, France, Italy, Malta (female), Portugal, Spain, Switzerland (cluster no. 3),
- Croatia (female), Cyprus (female), Czech Republic (male), Greece, Poland (female), Slovakia (cluster no. 4).

The balance of morbidity is demonstrated for subpopulations: Belgium (exception of male aged 95+), Bulgaria, Croatia (male), Cyprus (male), Estonia (male), Ireland, Lithuania (except of male 95+), Malta (male), Romania, Slovenia (except of 95+) and the UK (female).

From the perspective of general theory of aging population (Michel and Robine, 2004), the most interesting cases are subpopulations experiencing expansion of morbidity:

- Sweden (cluster no. 2): for female aged 65-79 and male 65-84,
- Denmark (cluster no. 2): only male aged 65-74,
- Belgium (cluster no. 1): only male aged 95+,
- Slovenia (cluster no. 3): female and male aged 95+,
- Lithuania (cluster no. 4): only male aged 95+,
- Poland (cluster no. 4): only male aged 65-69 and 95+.

Above results allow for a confirmation the hypothesis on the cycle of health transition process. It can be said that the young-old population from Sweden and Denmark experienced the 'new' expansion of morbidity.

Results for Denmark are consistent with conclusions made by Majewska and Trzpiot (2018). According to the analysis of Vallin and Meslé (2004), Denmark was a great example of country with perspectives on stepping to the third stage of health transition, however Majewska and Trzpiot (2018) showed that increasing disability seems to distance from entering the third phase of health transition.

## Conclusions

This study provides a comprehensive look into the public health scenarios of compression, expansion or balance of morbidity in most European countries by tracking trends in life expectancy and health-adjusted life expectancy in 2016 compared to 1990. Not surprisingly, both LE and HALE increased for majority female and male populations during the study period. The proportion of life spent in an unhealthy state differs from country to country. The following conclusions are made:

1. The cyclical movement of stages in an aging population model (Michel and Robine 2004) was confirmed. The 'new' expansion of morbidity (examples of subpopulations from Denmark and Sweden, from cluster no. 2) can be explained by common diseases affecting elderly. Denmark and Sweden are the only countries in Europe where musculoskeletal disorders have the largest share in YLDs among old people. However, further study is needed to assess which determinants of health may be influencing the changes observed in lost years of good health. Other countries from this cluster

experienced compression of morbidity in older age groups, preceded by balance of morbidity in younger groups.

2. The long life expectancy at birth or at age 65 is not a determinant of expansion of morbidity. Switzerland, Spain, Italy (from cluster no. 3) belong to the top countries with the highest life expectancy in Europe, and did not experience expansion of morbidity.
3. Rapid development of high technology treatment procedures, which followed the economic recovery of the Eastern and Central European countries, shrank the differences between these countries and the rest of Europe. Most subpopulations from Central and Eastern Europe (cluster no. 4) lived longer in positive health than their previous generations. An open area for further research is related with growing dominance of chronic diseases in Central and Eastern Europe. The financial costs associated with treating chronic diseases are extremely high, and given that the average age of populations is increasing, chronic diseases will continue to place an important pressure on national budgets (Brennan et al., 2017). Thus, will populations in older ages in Central and Eastern European countries have a chance to move to the next phase – compression of morbidity – when a trend is driven by rising levels of chronic diseases connected to alcohol use, poor diets, and smoking.

Obviously, estimates of LE and HALE, and conclusions about future scenarios – compression, expansion or balance of morbidity – should be made with great caution because of uncertainty with respect to future changes in disease epidemiology. Current changes in patterns of livelihood and living conditions mean changes in diseases and mortality patterns. Thus, as Robine and Michel (2004) suggested, this probably would lead the need of elaborating a new general theory on population aging.

## References

1. P. Brennan, M. Perola, G-J van Ommen, and E. Riboli. On behalf of the European Cohort Consortium. Chronic disease research in Europe and the need for integrated population cohorts. *European Journal of Epidemiology*, 32(9), 741-749, 2017.
2. J. Majewska and G. Trzpiot. The health transition and an ageing society – example of selected European countries. The 12th Professor Aleksander Zelias International Conference, on Modelling and Forecasting of Socio-Economic Phenomena. Conference Proceedings, 276-285, 2018.
3. C. Steensma, L. Loukine, and B.C. Choi. Evaluating compression or expansion of morbidity in Canada: trends in life expectancy and health-adjusted life expectancy from 1994 to 2010. *Health Promotion and Chronic Disease Prevention in Canada*, 37, 68-76, 2017.
4. R.M. Assunção, M.C. Neves, G. Camara, C.D.C. and Freitas. Efficient regionalization techniques for socio-economic geographical units using minimum spanning trees. *International Journal of Geographical Information Science*, 20, 797–811, 2006.
5. R.T Lin, Y-M Chen, L-C Chien and C-C Chan. Political and social determinants of life expectancy in less developed countries: a longitudinal study. *BMC Public Health*, 12:85, 2012.

6. CD Mathers, T. Vos, AD Lopez, JA. Salomon and M. Ezzati. National Burden of Disease Studies: A Practical Guide. 2nd ed. Global Program on Evidence for Health Policy. Geneva: World Health Organization, 2001.
7. J. W. Shaw, W.C. Horrace, R.J. Vogel. The determinants of life expectancy: an analysis of the OECD Health Data, *Southern Economic Journal* 71(4), 768-783, 2005.
8. K. Zafeiris and C.H. Skiadas. Some methods for the estimation of healthy life expectancy, *Conference Proceedings Reprodukce lidského kapitálu - vzájemné vazby a souvislosti*, 406-416, 2015.
9. J. Michel and J. Robine. A "New" General Theory of Population Ageing. *Geneva Papers on Risk and Insurance - Issues and Practice*, 29(4), 667-678, 2004.
10. J. Vallin and F. Meslé. Convergences and divergences in mortality. *Demographic Research*, Special 2, 11-44, 2004.
11. N. Li, R. Lee. Coherent mortality forecasts for a group of populations: an extension of the Lee-Carter method. *Demography*, 42(3), 575-594, 2005.
12. J. Majewska. An EU cross-country comparison study of life expectancy projection models. Selected papers from the 2016 Conference of European Statistics Stakeholders. Special Issue, Luxembourg: Publication Office of the European Union, 83-93, 2017.
13. M. Eileen, M. Crimmins, H. Beltrán-Sánchez. Mortality and Morbidity Trends: Is There Compression of Morbidity?, *The Journals of Gerontology: Series B*, Volume 66B, Issue 1, 1 January 2011, 75-86, 2011.
14. D.M. Cutler, K. Ghosh and M.B. Landrum. Evidence for Significant Compression of Morbidity in the Elderly U.S. Population, *Discoveries in the Economics of Aging*, 21-51, 2013.
15. JF. Fries, Aging, natural death, and the compression of morbidity. *Bull World Health Organ*, 80(3), 245-50, 2002.
16. JF. Fries Measuring and monitoring success in compressing morbidity. *Ann Intern Med.*, 139 (5 Part 2), 455-9, 2003.
17. Fries J, Green L, Levine S. Health promotion and the compression of morbidity. *The Lancet* 1989;333(8636): 481-3, 1989.
18. World Health Organization (1984). The uses of epidemiology in the study of the elderly: Report of a WHO Scientific Group on the Epidemiology of Aging. Geneva: WHO (Technical Report Series 706).
19. EM. Gruenberg. The failures of success. *Milbank Memorial Fund Q/Health Soc.* 55(1), 3-24, 1977.
20. Kramer M. The rising pandemic of mental disorders and associated chronic diseases and disabilities. *Acta Psychiatr Scand.* 1980;62(S285):382-97.
21. K.G. Manton. Changing concepts of morbidity and mortality in the elderly population, „*Milbank Memorial Fund Quarterly. Health and Society*” 60, 183-244, 1982.

# Construction of Mean Salary Lines by Generalization of Binomial Stochastic Process

Raimondo Manca

MEMOTEF

Università di Roma “La Sapienza”

---

*5<sup>th</sup> SMTDA Conference Proceedings, 12-15 June 2018, Chania, Crete, Greece*

© 2018 ISAST



# AGENDA

- Introduction to mean salary lines construction
- Automatic promotions
- Promotion by choice
- Recalling of some properties and some definitions of graphs
- Construction of binary graphs by binary trees
- Some conclusive remarks

# FORECASTING OF MEAN SALARY LINES I

Part of the man-power planning problem

- Evolution of salary of a cohort of workers
- Change of pyramidal organization of a company
- Future entrances and costs of pension funds
- Defined benefits
- Defined contributions

The salary depends on:

- I) Job seniority
- ii) The year
- iii)The rank
- IV)The rank seniority

(Usually only one seniority is considered depending on the rules of the company)

## THE STARTING MATRIX

First it is to construct a three dimensional array ( $\mathbf{A} = [a_{t,j,k}]$  matrix with three indices)

where  $t$  is the year,  $j$  the seniority,  $k$  the rank.

It is clear that at time  $t$   $a_{t,j,k}$  is known then we have:  $a_{t+n,j+n,k} = a_{t,j,k} * \prod_{h=t+1}^{t+n} (1 + r_h)$

$r_h$  is the forecasted increasing salary rate at time  $h$

In this way we obtain for each rank  $k$  a matrix in which the  $t, j$  give the related salary. The salary of a cohort will be the element of the diagonal of the sub-matrix. If there will not be rank promotion the salary line is obtained.

The promotion can be automatic or by choice. Taking into account the promotions from the starting matrix it will be obtained the three index matrix  $\mathbf{B}$

## **AUTOMATIC PROMOTION**

The automatic promotion happens when given a fixed seniority inside a rank a worker is promoted to the subsequent higher rank. All the workers of the same cohort will be promoted with the same seniority

In the rank promotion automatism it is possible the preserving of the work seniority or the partial or total loosing of the work seniority.

The construction of related mean salary line is really simple. Indeed, it is enough the merging of the salary lines to simulate the promotion in this case.

Generally, this kind of promotion is planned for low level ranks.

# AN EXAMPLE OF AUTOMATIC PROMOTION 1-I

Job Hiring at Rank 1: no promotion case																					
t	0	1	2	3	4	5	6	7	8	9	10	11	12	13	14	15	16	17	18	19	20
t	a(t,0,1)	a(t,1,1)	a(t,2,1)	a(t,3,1)	a(t,4,1)	a(t,5,1)	a(t,6,1)	a(t,7,1)	a(t,8,1)	a(t,9,1)	a(t,10,1)	a(t,11,1)	a(t,12,1)	a(t,13,1)	a(t,14,1)	a(t,15,1)	a(t,16,1)	a(t,17,1)	a(t,18,1)	a(t,19,1)	a(t,20,1)
t+1	a(t+1,0,1)	a(t+1,1,1)	a(t+1,2,1)	a(t+1,3,1)	a(t+1,4,1)	a(t+1,5,1)	a(t+1,6,1)	a(t+1,7,1)	a(t+1,8,1)	a(t+1,9,1)	a(t+1,10,1)	a(t+1,11,1)	a(t+1,12,1)	a(t+1,13,1)	a(t+1,14,1)	a(t+1,15,1)	a(t+1,16,1)	a(t+1,17,1)	a(t+1,18,1)	a(t+1,19,1)	a(t+1,20,1)
t+2	a(t+2,0,1)	a(t+2,1,1)	a(t+2,2,1)	a(t+2,3,1)	a(t+2,4,1)	a(t+2,5,1)	a(t+2,6,1)	a(t+2,7,1)	a(t+2,8,1)	a(t+2,9,1)	a(t+2,10,1)	a(t+2,11,1)	a(t+2,12,1)	a(t+2,13,1)	a(t+2,14,1)	a(t+2,15,1)	a(t+2,16,1)	a(t+2,17,1)	a(t+2,18,1)	a(t+2,19,1)	a(t+2,20,1)
t+3	a(t+3,0,1)	a(t+3,1,1)	a(t+3,2,1)	a(t+3,3,1)	a(t+3,4,1)	a(t+3,5,1)	a(t+3,6,1)	a(t+3,7,1)	a(t+3,8,1)	a(t+3,9,1)	a(t+3,10,1)	a(t+3,11,1)	a(t+3,12,1)	a(t+3,13,1)	a(t+3,14,1)	a(t+3,15,1)	a(t+3,16,1)	a(t+3,17,1)	a(t+3,18,1)	a(t+3,19,1)	a(t+3,20,1)
t+4	a(t+4,0,1)	a(t+4,1,1)	a(t+4,2,1)	a(t+4,3,1)	a(t+4,4,1)	a(t+4,5,1)	a(t+4,6,1)	a(t+4,7,1)	a(t+4,8,1)	a(t+4,9,1)	a(t+4,10,1)	a(t+4,11,1)	a(t+4,12,1)	a(t+4,13,1)	a(t+4,14,1)	a(t+4,15,1)	a(t+4,16,1)	a(t+4,17,1)	a(t+4,18,1)	a(t+4,19,1)	a(t+4,20,1)
t+5	a(t+5,0,1)	a(t+5,1,1)	a(t+5,2,1)	a(t+5,3,1)	a(t+5,4,1)	a(t+5,5,1)	a(t+5,6,1)	a(t+5,7,1)	a(t+5,8,1)	a(t+5,9,1)	a(t+5,10,1)	a(t+5,11,1)	a(t+5,12,1)	a(t+5,13,1)	a(t+5,14,1)	a(t+5,15,1)	a(t+5,16,1)	a(t+5,17,1)	a(t+5,18,1)	a(t+5,19,1)	a(t+5,20,1)
t+6	a(t+6,0,1)	a(t+6,1,1)	a(t+6,2,1)	a(t+6,3,1)	a(t+6,4,1)	a(t+6,5,1)	a(t+6,6,1)	a(t+6,7,1)	a(t+6,8,1)	a(t+6,9,1)	a(t+6,10,1)	a(t+6,11,1)	a(t+6,12,1)	a(t+6,13,1)	a(t+6,14,1)	a(t+6,15,1)	a(t+6,16,1)	a(t+6,17,1)	a(t+6,18,1)	a(t+6,19,1)	a(t+6,20,1)
t+7	a(t+7,0,1)	a(t+7,1,1)	a(t+7,2,1)	a(t+7,3,1)	a(t+7,4,1)	a(t+7,5,1)	a(t+7,6,1)	a(t+7,7,1)	a(t+7,8,1)	a(t+7,9,1)	a(t+7,10,1)	a(t+7,11,1)	a(t+7,12,1)	a(t+7,13,1)	a(t+7,14,1)	a(t+7,15,1)	a(t+7,16,1)	a(t+7,17,1)	a(t+7,18,1)	a(t+7,19,1)	a(t+7,20,1)
t+8	a(t+8,0,1)	a(t+8,1,1)	a(t+8,2,1)	a(t+8,3,1)	a(t+8,4,1)	a(t+8,5,1)	a(t+8,6,1)	a(t+8,7,1)	a(t+8,8,1)	a(t+8,9,1)	a(t+8,10,1)	a(t+8,11,1)	a(t+8,12,1)	a(t+8,13,1)	a(t+8,14,1)	a(t+8,15,1)	a(t+8,16,1)	a(t+8,17,1)	a(t+8,18,1)	a(t+8,19,1)	a(t+8,20,1)
t+9	a(t+9,0,1)	a(t+9,1,1)	a(t+9,2,1)	a(t+9,3,1)	a(t+9,4,1)	a(t+9,5,1)	a(t+9,6,1)	a(t+9,7,1)	a(t+9,8,1)	a(t+9,9,1)	a(t+9,10,1)	a(t+9,11,1)	a(t+9,12,1)	a(t+9,13,1)	a(t+9,14,1)	a(t+9,15,1)	a(t+9,16,1)	a(t+9,17,1)	a(t+9,18,1)	a(t+9,19,1)	a(t+9,20,1)
t+10	a(t+10,0,1)	a(t+10,1,1)	a(t+10,2,1)	a(t+10,3,1)	a(t+10,4,1)	a(t+10,5,1)	a(t+10,6,1)	a(t+10,7,1)	a(t+10,8,1)	a(t+10,9,1)	a(t+10,10,1)	a(t+10,11,1)	a(t+10,12,1)	a(t+10,13,1)	a(t+10,14,1)	a(t+10,15,1)	a(t+10,16,1)	a(t+10,17,1)	a(t+10,18,1)	a(t+10,19,1)	a(t+10,20,1)
t+11	a(t+11,0,1)	a(t+11,1,1)	a(t+11,2,1)	a(t+11,3,1)	a(t+11,4,1)	a(t+11,5,1)	a(t+11,6,1)	a(t+11,7,1)	a(t+11,8,1)	a(t+11,9,1)	a(t+11,10,1)	a(t+11,11,1)	a(t+11,12,1)	a(t+11,13,1)	a(t+11,14,1)	a(t+11,15,1)	a(t+11,16,1)	a(t+11,17,1)	a(t+11,18,1)	a(t+11,19,1)	a(t+11,20,1)
t+12	a(t+12,0,1)	a(t+12,1,1)	a(t+12,2,1)	a(t+12,3,1)	a(t+12,4,1)	a(t+12,5,1)	a(t+12,6,1)	a(t+12,7,1)	a(t+12,8,1)	a(t+12,9,1)	a(t+12,10,1)	a(t+12,11,1)	a(t+12,12,1)	a(t+12,13,1)	a(t+12,14,1)	a(t+12,15,1)	a(t+12,16,1)	a(t+12,17,1)	a(t+12,18,1)	a(t+12,19,1)	a(t+12,20,1)
t+13	a(t+13,0,1)	a(t+13,1,1)	a(t+13,2,1)	a(t+13,3,1)	a(t+13,4,1)	a(t+13,5,1)	a(t+13,6,1)	a(t+13,7,1)	a(t+13,8,1)	a(t+13,9,1)	a(t+13,10,1)	a(t+13,11,1)	a(t+13,12,1)	a(t+13,13,1)	a(t+13,14,1)	a(t+13,15,1)	a(t+13,16,1)	a(t+13,17,1)	a(t+13,18,1)	a(t+13,19,1)	a(t+13,20,1)
t+14	a(t+14,0,1)	a(t+14,1,1)	a(t+14,2,1)	a(t+14,3,1)	a(t+14,4,1)	a(t+14,5,1)	a(t+14,6,1)	a(t+14,7,1)	a(t+14,8,1)	a(t+14,9,1)	a(t+14,10,1)	a(t+14,11,1)	a(t+14,12,1)	a(t+14,13,1)	a(t+14,14,1)	a(t+14,15,1)	a(t+14,16,1)	a(t+14,17,1)	a(t+14,18,1)	a(t+14,19,1)	a(t+14,20,1)
t+15	a(t+15,0,1)	a(t+15,1,1)	a(t+15,2,1)	a(t+15,3,1)	a(t+15,4,1)	a(t+15,5,1)	a(t+15,6,1)	a(t+15,7,1)	a(t+15,8,1)	a(t+15,9,1)	a(t+15,10,1)	a(t+15,11,1)	a(t+15,12,1)	a(t+15,13,1)	a(t+15,14,1)	a(t+15,15,1)	a(t+15,16,1)	a(t+15,17,1)	a(t+15,18,1)	a(t+15,19,1)	a(t+15,20,1)
t+16	a(t+16,0,1)	a(t+16,1,1)	a(t+16,2,1)	a(t+16,3,1)	a(t+16,4,1)	a(t+16,5,1)	a(t+16,6,1)	a(t+16,7,1)	a(t+16,8,1)	a(t+16,9,1)	a(t+16,10,1)	a(t+16,11,1)	a(t+16,12,1)	a(t+16,13,1)	a(t+16,14,1)	a(t+16,15,1)	a(t+16,16,1)	a(t+16,17,1)	a(t+16,18,1)	a(t+16,19,1)	a(t+16,20,1)
t+17	a(t+17,0,1)	a(t+17,1,1)	a(t+17,2,1)	a(t+17,3,1)	a(t+17,4,1)	a(t+17,5,1)	a(t+17,6,1)	a(t+17,7,1)	a(t+17,8,1)	a(t+17,9,1)	a(t+17,10,1)	a(t+17,11,1)	a(t+17,12,1)	a(t+17,13,1)	a(t+17,14,1)	a(t+17,15,1)	a(t+17,16,1)	a(t+17,17,1)	a(t+17,18,1)	a(t+17,19,1)	a(t+17,20,1)
t+18	a(t+18,0,1)	a(t+18,1,1)	a(t+18,2,1)	a(t+18,3,1)	a(t+18,4,1)	a(t+18,5,1)	a(t+18,6,1)	a(t+18,7,1)	a(t+18,8,1)	a(t+18,9,1)	a(t+18,10,1)	a(t+18,11,1)	a(t+18,12,1)	a(t+18,13,1)	a(t+18,14,1)	a(t+18,15,1)	a(t+18,16,1)	a(t+18,17,1)	a(t+18,18,1)	a(t+18,19,1)	a(t+18,20,1)
t+19	a(t+19,0,1)	a(t+19,1,1)	a(t+19,2,1)	a(t+19,3,1)	a(t+19,4,1)	a(t+19,5,1)	a(t+19,6,1)	a(t+19,7,1)	a(t+19,8,1)	a(t+19,9,1)	a(t+19,10,1)	a(t+19,11,1)	a(t+19,12,1)	a(t+19,13,1)	a(t+19,14,1)	a(t+19,15,1)	a(t+19,16,1)	a(t+19,17,1)	a(t+19,18,1)	a(t+19,19,1)	a(t+19,20,1)
t+20	a(t+20,0,1)	a(t+20,1,1)	a(t+20,2,1)	a(t+20,3,1)	a(t+20,4,1)	a(t+20,5,1)	a(t+20,6,1)	a(t+20,7,1)	a(t+20,8,1)	a(t+20,9,1)	a(t+20,10,1)	a(t+20,11,1)	a(t+20,12,1)	a(t+20,13,1)	a(t+20,14,1)	a(t+20,15,1)	a(t+20,16,1)	a(t+20,17,1)	a(t+20,18,1)	a(t+20,19,1)	a(t+20,20,1)

# AN EXAMPLE OF AUTOMATIC PROMOTION 1-II

Job hiring at Rank 2 no promotion case																					
t	0	1	2	3	4	5	6	7	8	9	10	11	12	13	14	15	16	17	18	19	20
t	a(t,0,2)	a(t,1,2)	a(t,2,2)	a(t,3,2)	a(t,4,2)	a(t,5,2)	a(t,6,2)	a(t,7,2)	a(t,8,2)	a(t,9,2)	a(t,10,2)	a(t,11,2)	a(t,12,2)	a(t,13,2)	a(t,14,2)	a(t,15,2)	a(t,16,2)	a(t,17,2)	a(t,18,2)	a(t,19,2)	a(t,20,2)
t+1	a(t+1,0,2)	a(t+1,1,2)	a(t+1,2,2)	a(t+1,3,2)	a(t+1,4,2)	a(t+1,5,2)	a(t+1,6,2)	a(t+1,7,2)	a(t+1,8,2)	a(t+1,9,2)	a(t+1,10,2)	a(t+1,11,2)	a(t+1,12,2)	a(t+1,13,2)	a(t+1,14,2)	a(t+1,15,2)	a(t+1,16,2)	a(t+1,17,2)	a(t+1,18,2)	a(t+1,19,2)	a(t+1,20,2)
t+2	a(t+2,0,2)	a(t+2,1,2)	a(t+2,2,2)	a(t+2,3,2)	a(t+2,4,2)	a(t+2,5,2)	a(t+2,6,2)	a(t+2,7,2)	a(t+2,8,2)	a(t+2,9,2)	a(t+2,10,2)	a(t+2,11,2)	a(t+2,12,2)	a(t+2,13,2)	a(t+2,14,2)	a(t+2,15,2)	a(t+2,16,2)	a(t+2,17,2)	a(t+2,18,2)	a(t+2,19,2)	a(t+2,20,2)
t+3	a(t+3,0,2)	a(t+3,1,2)	a(t+3,2,2)	a(t+3,3,2)	a(t+3,4,2)	a(t+3,5,2)	a(t+3,6,2)	a(t+3,7,2)	a(t+3,8,2)	a(t+3,9,2)	a(t+3,10,2)	a(t+3,11,2)	a(t+3,12,2)	a(t+3,13,2)	a(t+3,14,2)	a(t+3,15,2)	a(t+3,16,2)	a(t+3,17,2)	a(t+3,18,2)	a(t+3,19,2)	a(t+3,20,2)
t+4	a(t+4,0,2)	a(t+4,1,2)	a(t+4,2,2)	a(t+4,3,2)	a(t+4,4,2)	a(t+4,5,2)	a(t+4,6,2)	a(t+4,7,2)	a(t+4,8,2)	a(t+4,9,2)	a(t+4,10,2)	a(t+4,11,2)	a(t+4,12,2)	a(t+4,13,2)	a(t+4,14,2)	a(t+4,15,2)	a(t+4,16,2)	a(t+4,17,2)	a(t+4,18,2)	a(t+4,19,2)	a(t+4,20,2)
t+5	a(t+5,0,2)	a(t+5,1,2)	a(t+5,2,2)	a(t+5,3,2)	a(t+5,4,2)	a(t+5,5,2)	a(t+5,6,2)	a(t+5,7,2)	a(t+5,8,2)	a(t+5,9,2)	a(t+5,10,2)	a(t+5,11,2)	a(t+5,12,2)	a(t+5,13,2)	a(t+5,14,2)	a(t+5,15,2)	a(t+5,16,2)	a(t+5,17,2)	a(t+5,18,2)	a(t+5,19,2)	a(t+5,20,2)
t+6	a(t+6,0,2)	a(t+6,1,2)	a(t+6,2,2)	a(t+6,3,2)	a(t+6,4,2)	a(t+6,5,2)	a(t+6,6,2)	a(t+6,7,2)	a(t+6,8,2)	a(t+6,9,2)	a(t+6,10,2)	a(t+6,11,2)	a(t+6,12,2)	a(t+6,13,2)	a(t+6,14,2)	a(t+6,15,2)	a(t+6,16,2)	a(t+6,17,2)	a(t+6,18,2)	a(t+6,19,2)	a(t+6,20,2)
t+7	a(t+7,0,2)	a(t+7,1,2)	a(t+7,2,2)	a(t+7,3,2)	a(t+7,4,2)	a(t+7,5,2)	a(t+7,6,2)	a(t+7,7,2)	a(t+7,8,2)	a(t+7,9,2)	a(t+7,10,2)	a(t+7,11,2)	a(t+7,12,2)	a(t+7,13,2)	a(t+7,14,2)	a(t+7,15,2)	a(t+7,16,2)	a(t+7,17,2)	a(t+7,18,2)	a(t+7,19,2)	a(t+7,20,2)
t+8	a(t+8,0,2)	a(t+8,1,2)	a(t+8,2,2)	a(t+8,3,2)	a(t+8,4,2)	a(t+8,5,2)	a(t+8,6,2)	a(t+8,7,2)	a(t+8,8,2)	a(t+8,9,2)	a(t+8,10,2)	a(t+8,11,2)	a(t+8,12,2)	a(t+8,13,2)	a(t+8,14,2)	a(t+8,15,2)	a(t+8,16,2)	a(t+8,17,2)	a(t+8,18,2)	a(t+8,19,2)	a(t+8,20,2)
t+9	a(t+9,0,2)	a(t+9,1,2)	a(t+9,2,2)	a(t+9,3,2)	a(t+9,4,2)	a(t+9,5,2)	a(t+9,6,2)	a(t+9,7,2)	a(t+9,8,2)	a(t+9,9,2)	a(t+9,10,2)	a(t+9,11,2)	a(t+9,12,2)	a(t+9,13,2)	a(t+9,14,2)	a(t+9,15,2)	a(t+9,16,2)	a(t+9,17,2)	a(t+9,18,2)	a(t+9,19,2)	a(t+9,20,2)
t+10	a(t+10,0,2)	a(t+10,1,2)	a(t+10,2,2)	a(t+10,3,2)	a(t+10,4,2)	a(t+10,5,2)	a(t+10,6,2)	a(t+10,7,2)	a(t+10,8,2)	a(t+10,9,2)	a(t+10,10,2)	a(t+10,11,2)	a(t+10,12,2)	a(t+10,13,2)	a(t+10,14,2)	a(t+10,15,2)	a(t+10,16,2)	a(t+10,17,2)	a(t+10,18,2)	a(t+10,19,2)	a(t+10,20,2)
t+11	a(t+11,0,2)	a(t+11,1,2)	a(t+11,2,2)	a(t+11,3,2)	a(t+11,4,2)	a(t+11,5,2)	a(t+11,6,2)	a(t+11,7,2)	a(t+11,8,2)	a(t+11,9,2)	a(t+11,10,2)	a(t+11,11,2)	a(t+11,12,2)	a(t+11,13,2)	a(t+11,14,2)	a(t+11,15,2)	a(t+11,16,2)	a(t+11,17,2)	a(t+11,18,2)	a(t+11,19,2)	a(t+11,20,2)
t+12	a(t+12,0,2)	a(t+12,1,2)	a(t+12,2,2)	a(t+12,3,2)	a(t+12,4,2)	a(t+12,5,2)	a(t+12,6,2)	a(t+12,7,2)	a(t+12,8,2)	a(t+12,9,2)	a(t+12,10,2)	a(t+12,11,2)	a(t+12,12,2)	a(t+12,13,2)	a(t+12,14,2)	a(t+12,15,2)	a(t+12,16,2)	a(t+12,17,2)	a(t+12,18,2)	a(t+12,19,2)	a(t+12,20,2)
t+13	a(t+13,0,2)	a(t+13,1,2)	a(t+13,2,2)	a(t+13,3,2)	a(t+13,4,2)	a(t+13,5,2)	a(t+13,6,2)	a(t+13,7,2)	a(t+13,8,2)	a(t+13,9,2)	a(t+13,10,2)	a(t+13,11,2)	a(t+13,12,2)	a(t+13,13,2)	a(t+13,14,2)	a(t+13,15,2)	a(t+13,16,2)	a(t+13,17,2)	a(t+13,18,2)	a(t+13,19,2)	a(t+13,20,2)
t+14	a(t+14,0,2)	a(t+14,1,2)	a(t+14,2,2)	a(t+14,3,2)	a(t+14,4,2)	a(t+14,5,2)	a(t+14,6,2)	a(t+14,7,2)	a(t+14,8,2)	a(t+14,9,2)	a(t+14,10,2)	a(t+14,11,2)	a(t+14,12,2)	a(t+14,13,2)	a(t+14,14,2)	a(t+14,15,2)	a(t+14,16,2)	a(t+14,17,2)	a(t+14,18,2)	a(t+14,19,2)	a(t+14,20,2)
t+15	a(t+15,0,2)	a(t+15,1,2)	a(t+15,2,2)	a(t+15,3,2)	a(t+15,4,2)	a(t+15,5,2)	a(t+15,6,2)	a(t+15,7,2)	a(t+15,8,2)	a(t+15,9,2)	a(t+15,10,2)	a(t+15,11,2)	a(t+15,12,2)	a(t+15,13,2)	a(t+15,14,2)	a(t+15,15,2)	a(t+15,16,2)	a(t+15,17,2)	a(t+15,18,2)	a(t+15,19,2)	a(t+15,20,2)
t+16	a(t+16,0,2)	a(t+16,1,2)	a(t+16,2,2)	a(t+16,3,2)	a(t+16,4,2)	a(t+16,5,2)	a(t+16,6,2)	a(t+16,7,2)	a(t+16,8,2)	a(t+16,9,2)	a(t+16,10,2)	a(t+16,11,2)	a(t+16,12,2)	a(t+16,13,2)	a(t+16,14,2)	a(t+16,15,2)	a(t+16,16,2)	a(t+16,17,2)	a(t+16,18,2)	a(t+16,19,2)	a(t+16,20,2)
t+17	a(t+17,0,2)	a(t+17,1,2)	a(t+17,2,2)	a(t+17,3,2)	a(t+17,4,2)	a(t+17,5,2)	a(t+17,6,2)	a(t+17,7,2)	a(t+17,8,2)	a(t+17,9,2)	a(t+17,10,2)	a(t+17,11,2)	a(t+17,12,2)	a(t+17,13,2)	a(t+17,14,2)	a(t+17,15,2)	a(t+17,16,2)	a(t+17,17,2)	a(t+17,18,2)	a(t+17,19,2)	a(t+17,20,2)
t+18	a(t+18,0,2)	a(t+18,1,2)	a(t+18,2,2)	a(t+18,3,2)	a(t+18,4,2)	a(t+18,5,2)	a(t+18,6,2)	a(t+18,7,2)	a(t+18,8,2)	a(t+18,9,2)	a(t+18,10,2)	a(t+18,11,2)	a(t+18,12,2)	a(t+18,13,2)	a(t+18,14,2)	a(t+18,15,2)	a(t+18,16,2)	a(t+18,17,2)	a(t+18,18,2)	a(t+18,19,2)	a(t+18,20,2)
t+19	a(t+19,0,2)	a(t+19,1,2)	a(t+19,2,2)	a(t+19,3,2)	a(t+19,4,2)	a(t+19,5,2)	a(t+19,6,2)	a(t+19,7,2)	a(t+19,8,2)	a(t+19,9,2)	a(t+19,10,2)	a(t+19,11,2)	a(t+19,12,2)	a(t+19,13,2)	a(t+19,14,2)	a(t+19,15,2)	a(t+19,16,2)	a(t+19,17,2)	a(t+19,18,2)	a(t+19,19,2)	a(t+19,20,2)
t+20	a(t+20,0,2)	a(t+20,1,2)	a(t+20,2,2)	a(t+20,3,2)	a(t+20,4,2)	a(t+20,5,2)	a(t+20,6,2)	a(t+20,7,2)	a(t+20,8,2)	a(t+20,9,2)	a(t+20,10,2)	a(t+20,11,2)	a(t+20,12,2)	a(t+20,13,2)	a(t+20,14,2)	a(t+20,15,2)	a(t+20,16,2)	a(t+20,17,2)	a(t+20,18,2)	a(t+20,19,2)	a(t+20,20,2)

# AN EXAMPLE OF AUTOMATIC PROMOTION 1-III

Job hiring at Rank 3																					
t	0	1	2	3	4	5	6	7	8	9	10	11	12	13	14	15	16	17	18	19	20
t	a(t,0,3)	a(t,1,3)	a(t,2,3)	a(t,3,3)	a(t,4,3)	a(t,5,3)	a(t,6,3)	a(t,7,3)	a(t,8,3)	a(t,9,3)	a(t,10,3)	a(t,11,3)	a(t,12,3)	a(t,13,3)	a(t,14,3)	a(t,15,3)	a(t,16,3)	a(t,17,3)	a(t,18,3)	a(t,19,3)	a(t,20,3)
t+1	a(t+1,0,3)	a(t+1,1,3)	a(t+1,2,3)	a(t+1,3,3)	a(t+1,4,3)	a(t+1,5,3)	a(t+1,6,3)	a(t+1,7,3)	a(t+1,8,3)	a(t+1,9,3)	a(t+1,10,3)	a(t+1,11,3)	a(t+1,12,3)	a(t+1,13,3)	a(t+1,14,3)	a(t+1,15,3)	a(t+1,16,3)	a(t+1,17,3)	a(t+1,18,3)	a(t+1,19,3)	a(t+1,20,3)
t+2	a(t+2,0,3)	a(t+2,1,3)	a(t+2,2,3)	a(t+2,3,3)	a(t+2,4,3)	a(t+2,5,3)	a(t+2,6,3)	a(t+2,7,3)	a(t+2,8,3)	a(t+2,9,3)	a(t+2,10,3)	a(t+2,11,3)	a(t+2,12,3)	a(t+2,13,3)	a(t+2,14,3)	a(t+2,15,3)	a(t+2,16,3)	a(t+2,17,3)	a(t+2,18,3)	a(t+2,19,3)	a(t+2,20,3)
t+3	a(t+3,0,3)	a(t+3,1,3)	a(t+3,2,3)	a(t+3,3,3)	a(t+3,4,3)	a(t+3,5,3)	a(t+3,6,3)	a(t+3,7,3)	a(t+3,8,3)	a(t+3,9,3)	a(t+3,10,3)	a(t+3,11,3)	a(t+3,12,3)	a(t+3,13,3)	a(t+3,14,3)	a(t+3,15,3)	a(t+3,16,3)	a(t+3,17,3)	a(t+3,18,3)	a(t+3,19,3)	a(t+3,20,3)
t+4	a(t+4,0,3)	a(t+4,1,3)	a(t+4,2,3)	a(t+4,3,3)	a(t+4,4,3)	a(t+4,5,3)	a(t+4,6,3)	a(t+4,7,3)	a(t+4,8,3)	a(t+4,9,3)	a(t+4,10,3)	a(t+4,11,3)	a(t+4,12,3)	a(t+4,13,3)	a(t+4,14,3)	a(t+4,15,3)	a(t+4,16,3)	a(t+4,17,3)	a(t+4,18,3)	a(t+4,19,3)	a(t+4,20,3)
t+5	a(t+5,0,3)	a(t+5,1,3)	a(t+5,2,3)	a(t+5,3,3)	a(t+5,4,3)	a(t+5,5,3)	a(t+5,6,3)	a(t+5,7,3)	a(t+5,8,3)	a(t+5,9,3)	a(t+5,10,3)	a(t+5,11,3)	a(t+5,12,3)	a(t+5,13,3)	a(t+5,14,3)	a(t+5,15,3)	a(t+5,16,3)	a(t+5,17,3)	a(t+5,18,3)	a(t+5,19,3)	a(t+5,20,3)
t+6	a(t+6,0,3)	a(t+6,1,3)	a(t+6,2,3)	a(t+6,3,3)	a(t+6,4,3)	a(t+6,5,3)	a(t+6,6,3)	a(t+6,7,3)	a(t+6,8,3)	a(t+6,9,3)	a(t+6,10,3)	a(t+6,11,3)	a(t+6,12,3)	a(t+6,13,3)	a(t+6,14,3)	a(t+6,15,3)	a(t+6,16,3)	a(t+6,17,3)	a(t+6,18,3)	a(t+6,19,3)	a(t+6,20,3)
t+7	a(t+7,0,3)	a(t+7,1,3)	a(t+7,2,3)	a(t+7,3,3)	a(t+7,4,3)	a(t+7,5,3)	a(t+7,6,3)	a(t+7,7,3)	a(t+7,8,3)	a(t+7,9,3)	a(t+7,10,3)	a(t+7,11,3)	a(t+7,12,3)	a(t+7,13,3)	a(t+7,14,3)	a(t+7,15,3)	a(t+7,16,3)	a(t+7,17,3)	a(t+7,18,3)	a(t+7,19,3)	a(t+7,20,3)
t+8	a(t+8,0,3)	a(t+8,1,3)	a(t+8,2,3)	a(t+8,3,3)	a(t+8,4,3)	a(t+8,5,3)	a(t+8,6,3)	a(t+8,7,3)	a(t+8,8,3)	a(t+8,9,3)	a(t+8,10,3)	a(t+8,11,3)	a(t+8,12,3)	a(t+8,13,3)	a(t+8,14,3)	a(t+8,15,3)	a(t+8,16,3)	a(t+8,17,3)	a(t+8,18,3)	a(t+8,19,3)	a(t+8,20,3)
t+9	a(t+9,0,3)	a(t+9,1,3)	a(t+9,2,3)	a(t+9,3,3)	a(t+9,4,3)	a(t+9,5,3)	a(t+9,6,3)	a(t+9,7,3)	a(t+9,8,3)	a(t+9,9,3)	a(t+9,10,3)	a(t+9,11,3)	a(t+9,12,3)	a(t+9,13,3)	a(t+9,14,3)	a(t+9,15,3)	a(t+9,16,3)	a(t+9,17,3)	a(t+9,18,3)	a(t+9,19,3)	a(t+9,20,3)
t+10	a(t+10,0,3)	a(t+10,1,3)	a(t+10,2,3)	a(t+10,3,3)	a(t+10,4,3)	a(t+10,5,3)	a(t+10,6,3)	a(t+10,7,3)	a(t+10,8,3)	a(t+10,9,3)	a(t+10,10,3)	a(t+10,11,3)	a(t+10,12,3)	a(t+10,13,3)	a(t+10,14,3)	a(t+10,15,3)	a(t+10,16,3)	a(t+10,17,3)	a(t+10,18,3)	a(t+10,19,3)	a(t+10,20,3)
t+11	a(t+11,0,3)	a(t+11,1,3)	a(t+11,2,3)	a(t+11,3,3)	a(t+11,4,3)	a(t+11,5,3)	a(t+11,6,3)	a(t+11,7,3)	a(t+11,8,3)	a(t+11,9,3)	a(t+11,10,3)	a(t+11,11,3)	a(t+11,12,3)	a(t+11,13,3)	a(t+11,14,3)	a(t+11,15,3)	a(t+11,16,3)	a(t+11,17,3)	a(t+11,18,3)	a(t+11,19,3)	a(t+11,20,3)
t+12	a(t+12,0,3)	a(t+12,1,3)	a(t+12,2,3)	a(t+12,3,3)	a(t+12,4,3)	a(t+12,5,3)	a(t+12,6,3)	a(t+12,7,3)	a(t+12,8,3)	a(t+12,9,3)	a(t+12,10,3)	a(t+12,11,3)	a(t+12,12,3)	a(t+12,13,3)	a(t+12,14,3)	a(t+12,15,3)	a(t+12,16,3)	a(t+12,17,3)	a(t+12,18,3)	a(t+12,19,3)	a(t+12,20,3)
t+13	a(t+13,0,3)	a(t+13,1,3)	a(t+13,2,3)	a(t+13,3,3)	a(t+13,4,3)	a(t+13,5,3)	a(t+13,6,3)	a(t+13,7,3)	a(t+13,8,3)	a(t+13,9,3)	a(t+13,10,3)	a(t+13,11,3)	a(t+13,12,3)	a(t+13,13,3)	a(t+13,14,3)	a(t+13,15,3)	a(t+13,16,3)	a(t+13,17,3)	a(t+13,18,3)	a(t+13,19,3)	a(t+13,20,3)
t+14	a(t+14,0,3)	a(t+14,1,3)	a(t+14,2,3)	a(t+14,3,3)	a(t+14,4,3)	a(t+14,5,3)	a(t+14,6,3)	a(t+14,7,3)	a(t+14,8,3)	a(t+14,9,3)	a(t+14,10,3)	a(t+14,11,3)	a(t+14,12,3)	a(t+14,13,3)	a(t+14,14,3)	a(t+14,15,3)	a(t+14,16,3)	a(t+14,17,3)	a(t+14,18,3)	a(t+14,19,3)	a(t+14,20,3)
t+15	a(t+15,0,3)	a(t+15,1,3)	a(t+15,2,3)	a(t+15,3,3)	a(t+15,4,3)	a(t+15,5,3)	a(t+15,6,3)	a(t+15,7,3)	a(t+15,8,3)	a(t+15,9,3)	a(t+15,10,3)	a(t+15,11,3)	a(t+15,12,3)	a(t+15,13,3)	a(t+15,14,3)	a(t+15,15,3)	a(t+15,16,3)	a(t+15,17,3)	a(t+15,18,3)	a(t+15,19,3)	a(t+15,20,3)
t+16	a(t+16,0,3)	a(t+16,1,3)	a(t+16,2,3)	a(t+16,3,3)	a(t+16,4,3)	a(t+16,5,3)	a(t+16,6,3)	a(t+16,7,3)	a(t+16,8,3)	a(t+16,9,3)	a(t+16,10,3)	a(t+16,11,3)	a(t+16,12,3)	a(t+16,13,3)	a(t+16,14,3)	a(t+16,15,3)	a(t+16,16,3)	a(t+16,17,3)	a(t+16,18,3)	a(t+16,19,3)	a(t+16,20,3)
t+17	a(t+17,0,3)	a(t+17,1,3)	a(t+17,2,3)	a(t+17,3,3)	a(t+17,4,3)	a(t+17,5,3)	a(t+17,6,3)	a(t+17,7,3)	a(t+17,8,3)	a(t+17,9,3)	a(t+17,10,3)	a(t+17,11,3)	a(t+17,12,3)	a(t+17,13,3)	a(t+17,14,3)	a(t+17,15,3)	a(t+17,16,3)	a(t+17,17,3)	a(t+17,18,3)	a(t+17,19,3)	a(t+17,20,3)
t+18	a(t+18,0,3)	a(t+18,1,3)	a(t+18,2,3)	a(t+18,3,3)	a(t+18,4,3)	a(t+18,5,3)	a(t+18,6,3)	a(t+18,7,3)	a(t+18,8,3)	a(t+18,9,3)	a(t+18,10,3)	a(t+18,11,3)	a(t+18,12,3)	a(t+18,13,3)	a(t+18,14,3)	a(t+18,15,3)	a(t+18,16,3)	a(t+18,17,3)	a(t+18,18,3)	a(t+18,19,3)	a(t+18,20,3)
t+19	a(t+19,0,3)	a(t+19,1,3)	a(t+19,2,3)	a(t+19,3,3)	a(t+19,4,3)	a(t+19,5,3)	a(t+19,6,3)	a(t+19,7,3)	a(t+19,8,3)	a(t+19,9,3)	a(t+19,10,3)	a(t+19,11,3)	a(t+19,12,3)	a(t+19,13,3)	a(t+19,14,3)	a(t+19,15,3)	a(t+19,16,3)	a(t+19,17,3)	a(t+19,18,3)	a(t+19,19,3)	a(t+19,20,3)
t+20	a(t+20,0,3)	a(t+20,1,3)	a(t+20,2,3)	a(t+20,3,3)	a(t+20,4,3)	a(t+20,5,3)	a(t+20,6,3)	a(t+20,7,3)	a(t+20,8,3)	a(t+20,9,3)	a(t+20,10,3)	a(t+20,11,3)	a(t+20,12,3)	a(t+20,13,3)	a(t+20,14,3)	a(t+20,15,3)	a(t+20,16,3)	a(t+20,17,3)	a(t+20,18,3)	a(t+20,19,3)	a(t+20,20,3)

# AN EXAMPLE OF AUTOMATIC PROMOTION 1-IV

Job hiring at rank 1, no loosening of seniority, promotion at rank 2 after 3 years, promotion at rank 3 after 5 years

t	0	1	2	3	4	5	6	7	8	9	10	11	12	13	14	15	16	17	18	19	20
t	b(t,0,1)	b(t,1,1)	b(t,2,1)	b(t,3,1)	b(t,4,1)	b(t,5,1)	b(t,6,1)	b(t,7,1)	b(t,8,1)	b(t,9,1)	b(t,10,1)	b(t,11,1)	b(t,12,1)	b(t,13,1)	b(t,14,1)	b(t,15,1)	b(t,16,1)	b(t,17,1)	b(t,18,1)	b(t,19,1)	b(t,20,1)
t+1	b(t+1,0,1)	b(t+1,1,1)	b(t+1,2,1)	b(t+1,3,1)	b(t+1,4,1)	b(t+1,5,1)	b(t+1,6,1)	b(t+1,7,1)	b(t+1,8,1)	b(t+1,9,1)	b(t+1,10,1)	b(t+1,11,1)	b(t+1,12,1)	b(t+1,13,1)	b(t+1,14,1)	b(t+1,15,1)	b(t+1,16,1)	b(t+1,17,1)	b(t+1,18,1)	b(t+1,19,1)	b(t+1,20,1)
t+2	b(t+2,0,1)	b(t+2,1,1)	b(t+2,2,1)	b(t+2,3,1)	b(t+2,4,1)	b(t+2,5,1)	b(t+2,6,1)	b(t+2,7,1)	b(t+2,8,1)	b(t+2,9,1)	b(t+2,10,1)	b(t+2,11,1)	b(t+2,12,1)	b(t+2,13,1)	b(t+2,14,1)	b(t+2,15,1)	b(t+2,16,1)	b(t+2,17,1)	b(t+2,18,1)	b(t+2,19,1)	b(t+2,20,1)
t+3	b(t+3,0,1)	b(t+3,1,1)	b(t+3,2,1)	b(t+3,3,1)	b(t+3,4,1)	b(t+3,5,1)	b(t+3,6,1)	b(t+3,7,1)	b(t+3,8,1)	b(t+3,9,1)	b(t+3,10,1)	b(t+3,11,1)	b(t+3,12,1)	b(t+3,13,1)	b(t+3,14,1)	b(t+3,15,1)	b(t+3,16,1)	b(t+3,17,1)	b(t+3,18,1)	b(t+3,19,1)	b(t+3,20,1)
t+4	b(t+4,0,1)	b(t+4,1,1)	b(t+4,2,1)	b(t+4,3,1)	b(t+4,4,1)	b(t+4,5,1)	b(t+4,6,1)	b(t+4,7,1)	b(t+4,8,1)	b(t+4,9,1)	b(t+4,10,1)	b(t+4,11,1)	b(t+4,12,1)	b(t+4,13,1)	b(t+4,14,1)	b(t+4,15,1)	b(t+4,16,1)	b(t+4,17,1)	b(t+4,18,1)	b(t+4,19,1)	b(t+4,20,1)
t+5	b(t+5,0,1)	b(t+5,1,1)	b(t+5,2,1)	b(t+5,3,1)	b(t+5,4,1)	b(t+5,5,1)	b(t+5,6,1)	b(t+5,7,1)	b(t+5,8,1)	b(t+5,9,1)	b(t+5,10,1)	b(t+5,11,1)	b(t+5,12,1)	b(t+5,13,1)	b(t+5,14,1)	b(t+5,15,1)	b(t+5,16,1)	b(t+5,17,1)	b(t+5,18,1)	b(t+5,19,1)	b(t+5,20,1)
t+6	b(t+6,0,1)	b(t+6,1,1)	b(t+6,2,1)	b(t+6,3,1)	b(t+6,4,1)	b(t+6,5,1)	b(t+6,6,1)	b(t+6,7,1)	b(t+6,8,1)	b(t+6,9,1)	b(t+6,10,1)	b(t+6,11,1)	b(t+6,12,1)	b(t+6,13,1)	b(t+6,14,1)	b(t+6,15,1)	b(t+6,16,1)	b(t+6,17,1)	b(t+6,18,1)	b(t+6,19,1)	b(t+6,20,1)
t+7	b(t+7,0,1)	b(t+7,1,1)	b(t+7,2,1)	b(t+7,3,1)	b(t+7,4,1)	b(t+7,5,1)	b(t+7,6,1)	b(t+7,7,1)	b(t+7,8,1)	b(t+7,9,1)	b(t+7,10,1)	b(t+7,11,1)	b(t+7,12,1)	b(t+7,13,1)	b(t+7,14,1)	b(t+7,15,1)	b(t+7,16,1)	b(t+7,17,1)	b(t+7,18,1)	b(t+7,19,1)	b(t+7,20,1)
t+8	b(t+8,0,1)	b(t+8,1,1)	b(t+8,2,1)	b(t+8,3,1)	b(t+8,4,1)	b(t+8,5,1)	b(t+8,6,1)	b(t+8,7,1)	b(t+8,8,1)	b(t+8,9,1)	b(t+8,10,1)	b(t+8,11,1)	b(t+8,12,1)	b(t+8,13,1)	b(t+8,14,1)	b(t+8,15,1)	b(t+8,16,1)	b(t+8,17,1)	b(t+8,18,1)	b(t+8,19,1)	b(t+8,20,1)
t+9	b(t+9,0,1)	b(t+9,1,1)	b(t+9,2,1)	b(t+9,3,1)	b(t+9,4,1)	b(t+9,5,1)	b(t+9,6,1)	b(t+9,7,1)	b(t+9,8,1)	b(t+9,9,1)	b(t+9,10,1)	b(t+9,11,1)	b(t+9,12,1)	b(t+9,13,1)	b(t+9,14,1)	b(t+9,15,1)	b(t+9,16,1)	b(t+9,17,1)	b(t+9,18,1)	b(t+9,19,1)	b(t+9,20,1)
t+10	b(t+10,0,1)	b(t+10,1,1)	b(t+10,2,1)	b(t+10,3,1)	b(t+10,4,1)	b(t+10,5,1)	b(t+10,6,1)	b(t+10,7,1)	b(t+10,8,1)	b(t+10,9,1)	b(t+10,10,1)	b(t+10,11,1)	b(t+10,12,1)	b(t+10,13,1)	b(t+10,14,1)	b(t+10,15,1)	b(t+10,16,1)	b(t+10,17,1)	b(t+10,18,1)	b(t+10,19,1)	b(t+10,20,1)
t+11	b(t+11,0,1)	b(t+11,1,1)	b(t+11,2,1)	b(t+11,3,1)	b(t+11,4,1)	b(t+11,5,1)	b(t+11,6,1)	b(t+11,7,1)	b(t+11,8,1)	b(t+11,9,1)	b(t+11,10,1)	b(t+11,11,1)	b(t+11,12,1)	b(t+11,13,1)	b(t+11,14,1)	b(t+11,15,1)	b(t+11,16,1)	b(t+11,17,1)	b(t+11,18,1)	b(t+11,19,1)	b(t+11,20,1)
t+12	b(t+12,0,1)	b(t+12,1,1)	b(t+12,2,1)	b(t+12,3,1)	b(t+12,4,1)	b(t+12,5,1)	b(t+12,6,1)	b(t+12,7,1)	b(t+12,8,1)	b(t+12,9,1)	b(t+12,10,1)	b(t+12,11,1)	b(t+12,12,1)	b(t+12,13,1)	b(t+12,14,1)	b(t+12,15,1)	b(t+12,16,1)	b(t+12,17,1)	b(t+12,18,1)	b(t+12,19,1)	b(t+12,20,1)
t+13	b(t+13,0,1)	b(t+13,1,1)	b(t+13,2,1)	b(t+13,3,1)	b(t+13,4,1)	b(t+13,5,1)	b(t+13,6,1)	b(t+13,7,1)	b(t+13,8,1)	b(t+13,9,1)	b(t+13,10,1)	b(t+13,11,1)	b(t+13,12,1)	b(t+13,13,1)	b(t+13,14,1)	b(t+13,15,1)	b(t+13,16,1)	b(t+13,17,1)	b(t+13,18,1)	b(t+13,19,1)	b(t+13,20,1)
t+14	b(t+14,0,1)	b(t+14,1,1)	b(t+14,2,1)	b(t+14,3,1)	b(t+14,4,1)	b(t+14,5,1)	b(t+14,6,1)	b(t+14,7,1)	b(t+14,8,1)	b(t+14,9,1)	b(t+14,10,1)	b(t+14,11,1)	b(t+14,12,1)	b(t+14,13,1)	b(t+14,14,1)	b(t+14,15,1)	b(t+14,16,1)	b(t+14,17,1)	b(t+14,18,1)	b(t+14,19,1)	b(t+14,20,1)
t+15	b(t+15,0,1)	b(t+15,1,1)	b(t+15,2,1)	b(t+15,3,1)	b(t+15,4,1)	b(t+15,5,1)	b(t+15,6,1)	b(t+15,7,1)	b(t+15,8,1)	b(t+15,9,1)	b(t+15,10,1)	b(t+15,11,1)	b(t+15,12,1)	b(t+15,13,1)	b(t+15,14,1)	b(t+15,15,1)	b(t+15,16,1)	b(t+15,17,1)	b(t+15,18,1)	b(t+15,19,1)	b(t+15,20,1)
t+16	b(t+16,0,1)	b(t+16,1,1)	b(t+16,2,1)	b(t+16,3,1)	b(t+16,4,1)	b(t+16,5,1)	b(t+16,6,1)	b(t+16,7,1)	b(t+16,8,1)	b(t+16,9,1)	b(t+16,10,1)	b(t+16,11,1)	b(t+16,12,1)	b(t+16,13,1)	b(t+16,14,1)	b(t+16,15,1)	b(t+16,16,1)	b(t+16,17,1)	b(t+16,18,1)	b(t+16,19,1)	b(t+16,20,1)
t+17	b(t+17,0,1)	b(t+17,1,1)	b(t+17,2,1)	b(t+17,3,1)	b(t+17,4,1)	b(t+17,5,1)	b(t+17,6,1)	b(t+17,7,1)	b(t+17,8,1)	b(t+17,9,1)	b(t+17,10,1)	b(t+17,11,1)	b(t+17,12,1)	b(t+17,13,1)	b(t+17,14,1)	b(t+17,15,1)	b(t+17,16,1)	b(t+17,17,1)	b(t+17,18,1)	b(t+17,19,1)	b(t+17,20,1)
t+18	b(t+18,0,1)	b(t+18,1,1)	b(t+18,2,1)	b(t+18,3,1)	b(t+18,4,1)	b(t+18,5,1)	b(t+18,6,1)	b(t+18,7,1)	b(t+18,8,1)	b(t+18,9,1)	b(t+18,10,1)	b(t+18,11,1)	b(t+18,12,1)	b(t+18,13,1)	b(t+18,14,1)	b(t+18,15,1)	b(t+18,16,1)	b(t+18,17,1)	b(t+18,18,1)	b(t+18,19,1)	b(t+18,20,1)
t+19	b(t+19,0,1)	b(t+19,1,1)	b(t+19,2,1)	b(t+19,3,1)	b(t+19,4,1)	b(t+19,5,1)	b(t+19,6,1)	b(t+19,7,1)	b(t+19,8,1)	b(t+19,9,1)	b(t+19,10,1)	b(t+19,11,1)	b(t+19,12,1)	b(t+19,13,1)	b(t+19,14,1)	b(t+19,15,1)	b(t+19,16,1)	b(t+19,17,1)	b(t+19,18,1)	b(t+19,19,1)	b(t+19,20,1)
t+20	b(t+20,0,1)	b(t+20,1,1)	b(t+20,2,1)	b(t+20,3,1)	b(t+20,4,1)	b(t+20,5,1)	b(t+20,6,1)	b(t+20,7,1)	b(t+20,8,1)	b(t+20,9,1)	b(t+20,10,1)	b(t+20,11,1)	b(t+20,12,1)	b(t+20,13,1)	b(t+20,14,1)	b(t+20,15,1)	b(t+20,16,1)	b(t+20,17,1)	b(t+20,18,1)	b(t+20,19,1)	b(t+20,20,1)

# AN EXAMPLE OF AUTOMATIC PROMOTION 1-V

Job hiring at rank 2, no loosing of seniority, promotion at rank 3 after 5 years

t	0	1	2	3	4	5	6	7	8	9	10	11	12	13	14	15	16	17	18	19	20
t	b(t,0,2)	b(t,1,2)	b(t,2,2)	b(t,3,2)	b(t,4,2)	b(t,5,2)	b(t,6,2)	b(t,7,2)	b(t,8,2)	b(t,9,2)	b(t,10,2)	b(t,11,2)	b(t,12,2)	b(t,13,2)	b(t,14,2)	b(t,15,2)	b(t,16,2)	b(t,17,2)	b(t,18,2)	b(t,19,2)	b(t,20,2)
t+1	b(t+1,0,2)	b(t+1,1,2)	b(t+1,2,2)	b(t+1,3,2)	b(t+1,4,2)	b(t+1,5,2)	b(t+1,6,2)	b(t+1,7,2)	b(t+1,8,2)	b(t+1,9,2)	b(t+1,10,2)	b(t+1,11,2)	b(t+1,12,2)	b(t+1,13,2)	b(t+1,14,2)	b(t+1,15,2)	b(t+1,16,2)	b(t+1,17,2)	b(t+1,18,2)	b(t+1,19,2)	b(t+1,20,2)
t+2	b(t+2,0,2)	b(t+2,1,2)	b(t+2,2,2)	b(t+2,3,2)	b(t+2,4,2)	b(t+2,5,2)	b(t+2,6,2)	b(t+2,7,2)	b(t+2,8,2)	b(t+2,9,2)	b(t+2,10,2)	b(t+2,11,2)	b(t+2,12,2)	b(t+2,13,2)	b(t+2,14,2)	b(t+2,15,2)	b(t+2,16,2)	b(t+2,17,2)	b(t+2,18,2)	b(t+2,19,2)	b(t+2,20,2)
t+3	b(t+3,0,2)	b(t+3,1,2)	b(t+3,2,2)	b(t+3,3,2)	b(t+3,4,2)	b(t+3,5,2)	b(t+3,6,2)	b(t+3,7,2)	b(t+3,8,2)	b(t+3,9,2)	b(t+3,10,2)	b(t+3,11,2)	b(t+3,12,2)	b(t+3,13,2)	b(t+3,14,2)	b(t+3,15,2)	b(t+3,16,2)	b(t+3,17,2)	b(t+3,18,2)	b(t+3,19,2)	b(t+3,20,2)
t+4	b(t+4,0,2)	b(t+4,1,2)	b(t+4,2,2)	b(t+4,3,2)	b(t+4,4,2)	b(t+4,5,2)	b(t+4,6,2)	b(t+4,7,2)	b(t+4,8,2)	b(t+4,9,2)	b(t+4,10,2)	b(t+4,11,2)	b(t+4,12,2)	b(t+4,13,2)	b(t+4,14,2)	b(t+4,15,2)	b(t+4,16,2)	b(t+4,17,2)	b(t+4,18,2)	b(t+4,19,2)	b(t+4,20,2)
t+5	b(t+5,0,2)	b(t+5,1,2)	b(t+5,2,2)	b(t+5,3,2)	b(t+5,4,2)	b(t+5,5,2)	b(t+5,6,2)	b(t+5,7,2)	b(t+5,8,2)	b(t+5,9,2)	b(t+5,10,2)	b(t+5,11,2)	b(t+5,12,2)	b(t+5,13,2)	b(t+5,14,2)	b(t+5,15,2)	b(t+5,16,2)	b(t+5,17,2)	b(t+5,18,2)	b(t+5,19,2)	b(t+5,20,2)
t+6	b(t+6,0,2)	b(t+6,1,2)	b(t+6,2,2)	b(t+6,3,2)	b(t+6,4,2)	b(t+6,5,2)	b(t+6,6,2)	b(t+6,7,2)	b(t+6,8,2)	b(t+6,9,2)	b(t+6,10,2)	b(t+6,11,2)	b(t+6,12,2)	b(t+6,13,2)	b(t+6,14,2)	b(t+6,15,2)	b(t+6,16,2)	b(t+6,17,2)	b(t+6,18,2)	b(t+6,19,2)	b(t+6,20,2)
t+7	b(t+7,0,2)	b(t+7,1,2)	b(t+7,2,2)	b(t+7,3,2)	b(t+7,4,2)	b(t+7,5,2)	b(t+7,6,2)	b(t+7,7,2)	b(t+7,8,2)	b(t+7,9,2)	b(t+7,10,2)	b(t+7,11,2)	b(t+7,12,2)	b(t+7,13,2)	b(t+7,14,2)	b(t+7,15,2)	b(t+7,16,2)	b(t+7,17,2)	b(t+7,18,2)	b(t+7,19,2)	b(t+7,20,2)
t+8	b(t+8,0,2)	b(t+8,1,2)	b(t+8,2,2)	b(t+8,3,2)	b(t+8,4,2)	b(t+8,5,2)	b(t+8,6,2)	b(t+8,7,2)	b(t+8,8,2)	b(t+8,9,2)	b(t+8,10,2)	b(t+8,11,2)	b(t+8,12,2)	b(t+8,13,2)	b(t+8,14,2)	b(t+8,15,2)	b(t+8,16,2)	b(t+8,17,2)	b(t+8,18,2)	b(t+8,19,2)	b(t+8,20,2)
t+9	b(t+9,0,2)	b(t+9,1,2)	b(t+9,2,2)	b(t+9,3,2)	b(t+9,4,2)	b(t+9,5,2)	b(t+9,6,2)	b(t+9,7,2)	b(t+9,8,2)	b(t+9,9,2)	b(t+9,10,2)	b(t+9,11,2)	b(t+9,12,2)	b(t+9,13,2)	b(t+9,14,2)	b(t+9,15,2)	b(t+9,16,2)	b(t+9,17,2)	b(t+9,18,2)	b(t+9,19,2)	b(t+9,20,2)
t+10	b(t+10,0,2)	b(t+10,1,2)	b(t+10,2,2)	b(t+10,3,2)	b(t+10,4,2)	b(t+10,5,2)	b(t+10,6,2)	b(t+10,7,2)	b(t+10,8,2)	b(t+10,9,2)	b(t+10,10,2)	b(t+10,11,2)	b(t+10,12,2)	b(t+10,13,2)	b(t+10,14,2)	b(t+10,15,2)	b(t+10,16,2)	b(t+10,17,2)	b(t+10,18,2)	b(t+10,19,2)	b(t+10,20,2)
t+11	b(t+11,0,2)	b(t+11,1,2)	b(t+11,2,2)	b(t+11,3,2)	b(t+11,4,2)	b(t+11,5,2)	b(t+11,6,2)	b(t+11,7,2)	b(t+11,8,2)	b(t+11,9,2)	b(t+11,10,2)	b(t+11,11,2)	b(t+11,12,2)	b(t+11,13,2)	b(t+11,14,2)	b(t+11,15,2)	b(t+11,16,2)	b(t+11,17,2)	b(t+11,18,2)	b(t+11,19,2)	b(t+11,20,2)
t+12	b(t+12,0,2)	b(t+12,1,2)	b(t+12,2,2)	b(t+12,3,2)	b(t+12,4,2)	b(t+12,5,2)	b(t+12,6,2)	b(t+12,7,2)	b(t+12,8,2)	b(t+12,9,2)	b(t+12,10,2)	b(t+12,11,2)	b(t+12,12,2)	b(t+12,13,2)	b(t+12,14,2)	b(t+12,15,2)	b(t+12,16,2)	b(t+12,17,2)	b(t+12,18,2)	b(t+12,19,2)	b(t+12,20,2)
t+13	b(t+13,0,2)	b(t+13,1,2)	b(t+13,2,2)	b(t+13,3,2)	b(t+13,4,2)	b(t+13,5,2)	b(t+13,6,2)	b(t+13,7,2)	b(t+13,8,2)	b(t+13,9,2)	b(t+13,10,2)	b(t+13,11,2)	b(t+13,12,2)	b(t+13,13,2)	b(t+13,14,2)	b(t+13,15,2)	b(t+13,16,2)	b(t+13,17,2)	b(t+13,18,2)	b(t+13,19,2)	b(t+13,20,2)
t+14	b(t+14,0,2)	b(t+14,1,2)	b(t+14,2,2)	b(t+14,3,2)	b(t+14,4,2)	b(t+14,5,2)	b(t+14,6,2)	b(t+14,7,2)	b(t+14,8,2)	b(t+14,9,2)	b(t+14,10,2)	b(t+14,11,2)	b(t+14,12,2)	b(t+14,13,2)	b(t+14,14,2)	b(t+14,15,2)	b(t+14,16,2)	b(t+14,17,2)	b(t+14,18,2)	b(t+14,19,2)	b(t+14,20,2)
t+15	b(t+15,0,2)	b(t+15,1,2)	b(t+15,2,2)	b(t+15,3,2)	b(t+15,4,2)	b(t+15,5,2)	b(t+15,6,2)	b(t+15,7,2)	b(t+15,8,2)	b(t+15,9,2)	b(t+15,10,2)	b(t+15,11,2)	b(t+15,12,2)	b(t+15,13,2)	b(t+15,14,2)	b(t+15,15,2)	b(t+15,16,2)	b(t+15,17,2)	b(t+15,18,2)	b(t+15,19,2)	b(t+15,20,2)
t+16	b(t+16,0,2)	b(t+16,1,2)	b(t+16,2,2)	b(t+16,3,2)	b(t+16,4,2)	b(t+16,5,2)	b(t+16,6,2)	b(t+16,7,2)	b(t+16,8,2)	b(t+16,9,2)	b(t+16,10,2)	b(t+16,11,2)	b(t+16,12,2)	b(t+16,13,2)	b(t+16,14,2)	b(t+16,15,2)	b(t+16,16,2)	b(t+16,17,2)	b(t+16,18,2)	b(t+16,19,2)	b(t+16,20,2)
t+17	b(t+17,0,2)	b(t+17,1,2)	b(t+17,2,2)	b(t+17,3,2)	b(t+17,4,2)	b(t+17,5,2)	b(t+17,6,2)	b(t+17,7,2)	b(t+17,8,2)	b(t+17,9,2)	b(t+17,10,2)	b(t+17,11,2)	b(t+17,12,2)	b(t+17,13,2)	b(t+17,14,2)	b(t+17,15,2)	b(t+17,16,2)	b(t+17,17,2)	b(t+17,18,2)	b(t+17,19,2)	b(t+17,20,2)
t+18	b(t+18,0,2)	b(t+18,1,2)	b(t+18,2,2)	b(t+18,3,2)	b(t+18,4,2)	b(t+18,5,2)	b(t+18,6,2)	b(t+18,7,2)	b(t+18,8,2)	b(t+18,9,2)	b(t+18,10,2)	b(t+18,11,2)	b(t+18,12,2)	b(t+18,13,2)	b(t+18,14,2)	b(t+18,15,2)	b(t+18,16,2)	b(t+18,17,2)	b(t+18,18,2)	b(t+18,19,2)	b(t+18,20,2)
t+19	b(t+19,0,2)	b(t+19,1,2)	b(t+19,2,2)	b(t+19,3,2)	b(t+19,4,2)	b(t+19,5,2)	b(t+19,6,2)	b(t+19,7,2)	b(t+19,8,2)	b(t+19,9,2)	b(t+19,10,2)	b(t+19,11,2)	b(t+19,12,2)	b(t+19,13,2)	b(t+19,14,2)	b(t+19,15,2)	b(t+19,16,2)	b(t+19,17,2)	b(t+19,18,2)	b(t+19,19,2)	b(t+19,20,2)
t+20	b(t+20,0,2)	b(t+20,1,2)	b(t+20,2,2)	b(t+20,3,2)	b(t+20,4,2)	b(t+20,5,2)	b(t+20,6,2)	b(t+20,7,2)	b(t+20,8,2)	b(t+20,9,2)	b(t+20,10,2)	b(t+20,11,2)	b(t+20,12,2)	b(t+20,13,2)	b(t+20,14,2)	b(t+20,15,2)	b(t+20,16,2)	b(t+20,17,2)	b(t+20,18,2)	b(t+20,19,2)	b(t+20,20,2)

# AN EXAMPLE OF AUTOMATIC PROMOTION 1-VI

Job hiring at rank 1, promotion at rank 2 after 3 years with loosing of 2 years of seniority, promotion at rank 3 after other 5 years loosing of 3 years of seniority

t	0	1	2	3	4	5	6	7	8	9	10	11	12	13	14	15	16	17	18	19	20
t	b(t,0,1)	b(t,1,1)	b(t,2,1)	b(t,3,1)	b(t,2,1)	b(t,3,1)	b(t,4,1)	b(t,5,1)	b(t,6,1)	b(t,4,1)	b(t,5,1)	b(t,6,1)	b(t,7,1)	b(t,8,1)	b(t,9,1)	b(t,10,1)	b(t,11,1)	b(t,12,1)	b(t,13,1)	b(t,14,1)	b(t,15,1)
t+1	b(t+1,0,1)	b(t+1,1,1)	b(t+1,2,1)	b(t+1,3,1)	b(t+1,2,1)	b(t+1,3,1)	b(t+1,4,1)	b(t+1,5,1)	b(t+1,6,1)	b(t+1,4,1)	b(t+1,5,1)	b(t+1,6,1)	b(t+1,7,1)	b(t+1,8,1)	b(t+1,9,1)	b(t+1,10,1)	b(t+1,11,1)	b(t+1,12,1)	b(t+1,13,1)	b(t+1,14,1)	b(t+1,15,1)
t+2	b(t+2,0,1)	b(t+2,1,1)	b(t+2,2,1)	b(t+2,3,1)	b(t+2,2,1)	b(t+2,3,1)	b(t+2,4,1)	b(t+2,5,1)	b(t+2,6,1)	b(t+2,4,1)	b(t+2,5,1)	b(t+2,6,1)	b(t+2,7,1)	b(t+2,8,1)	b(t+2,9,1)	b(t+2,10,1)	b(t+2,11,1)	b(t+2,12,1)	b(t+2,13,1)	b(t+2,14,1)	b(t+2,15,1)
t+3	b(t+3,0,1)	b(t+3,1,1)	b(t+3,2,1)	b(t+3,3,1)	b(t+3,2,1)	b(t+3,3,1)	b(t+3,4,1)	b(t+3,5,1)	b(t+3,6,1)	b(t+3,4,1)	b(t+3,5,1)	b(t+3,6,1)	b(t+3,7,1)	b(t+3,8,1)	b(t+3,9,1)	b(t+3,10,1)	b(t+3,11,1)	b(t+3,12,1)	b(t+3,13,1)	b(t+3,14,1)	b(t+3,15,1)
t+4	b(t+4,0,1)	b(t+4,1,1)	b(t+4,2,1)	b(t+4,3,1)	b(t+4,2,1)	b(t+4,3,1)	b(t+4,4,1)	b(t+4,5,1)	b(t+4,6,1)	b(t+4,4,1)	b(t+4,5,1)	b(t+4,6,1)	b(t+4,7,1)	b(t+4,8,1)	b(t+4,9,1)	b(t+4,10,1)	b(t+4,11,1)	b(t+4,12,1)	b(t+4,13,1)	b(t+4,14,1)	b(t+4,15,1)
t+5	b(t+5,0,1)	b(t+5,1,1)	b(t+5,2,1)	b(t+5,3,1)	b(t+5,2,1)	b(t+5,3,1)	b(t+5,4,1)	b(t+5,5,1)	b(t+5,6,1)	b(t+5,4,1)	b(t+5,5,1)	b(t+5,6,1)	b(t+5,7,1)	b(t+5,8,1)	b(t+5,9,1)	b(t+5,10,1)	b(t+5,11,1)	b(t+5,12,1)	b(t+5,13,1)	b(t+5,14,1)	b(t+5,15,1)
t+6	b(t+6,0,1)	b(t+6,1,1)	b(t+6,2,1)	b(t+6,3,1)	b(t+6,2,1)	b(t+6,3,1)	b(t+6,4,1)	b(t+6,5,1)	b(t+6,6,1)	b(t+6,4,1)	b(t+6,5,1)	b(t+6,6,1)	b(t+6,7,1)	b(t+6,8,1)	b(t+6,9,1)	b(t+6,10,1)	b(t+6,11,1)	b(t+6,12,1)	b(t+6,13,1)	b(t+6,14,1)	b(t+6,15,1)
t+7	b(t+7,0,1)	b(t+7,1,1)	b(t+7,2,1)	b(t+7,3,1)	b(t+7,2,1)	b(t+7,3,1)	b(t+7,4,1)	b(t+7,5,1)	b(t+7,6,1)	b(t+7,4,1)	b(t+7,5,1)	b(t+7,6,1)	b(t+7,7,1)	b(t+7,8,1)	b(t+7,9,1)	b(t+7,10,1)	b(t+7,11,1)	b(t+7,12,1)	b(t+7,13,1)	b(t+7,14,1)	b(t+7,15,1)
t+8	b(t+8,0,1)	b(t+8,1,1)	b(t+8,2,1)	b(t+8,3,1)	b(t+8,2,1)	b(t+8,3,1)	b(t+8,4,1)	b(t+8,5,1)	b(t+8,6,1)	b(t+8,4,1)	b(t+8,5,1)	b(t+8,6,1)	b(t+8,7,1)	b(t+8,8,1)	b(t+8,9,1)	b(t+8,10,1)	b(t+8,11,1)	b(t+8,12,1)	b(t+8,13,1)	b(t+8,14,1)	b(t+8,15,1)
t+9	b(t+9,0,1)	b(t+9,1,1)	b(t+9,2,1)	b(t+9,3,1)	b(t+9,2,1)	b(t+9,3,1)	b(t+9,4,1)	b(t+9,5,1)	b(t+9,6,1)	b(t+9,4,1)	b(t+9,5,1)	b(t+9,6,1)	b(t+9,7,1)	b(t+9,8,1)	b(t+9,9,1)	b(t+9,10,1)	b(t+9,11,1)	b(t+9,12,1)	b(t+9,13,1)	b(t+9,14,1)	b(t+9,15,1)
t+10	b(t+10,0,1)	b(t+10,1,1)	b(t+10,2,1)	b(t+10,3,1)	b(t+10,2,1)	b(t+10,3,1)	b(t+10,4,1)	b(t+10,5,1)	b(t+10,6,1)	b(t+10,4,1)	b(t+10,5,1)	b(t+10,6,1)	b(t+10,7,1)	b(t+10,8,1)	b(t+10,9,1)	b(t+10,10,1)	b(t+10,11,1)	b(t+10,12,1)	b(t+10,13,1)	b(t+10,14,1)	b(t+10,15,1)
t+11	b(t+11,0,1)	b(t+11,1,1)	b(t+11,2,1)	b(t+11,3,1)	b(t+11,2,1)	b(t+11,3,1)	b(t+11,4,1)	b(t+11,5,1)	b(t+11,6,1)	b(t+11,4,1)	b(t+11,5,1)	b(t+11,6,1)	b(t+11,7,1)	b(t+11,8,1)	b(t+11,9,1)	b(t+11,10,1)	b(t+11,11,1)	b(t+11,12,1)	b(t+11,13,1)	b(t+11,14,1)	b(t+11,15,1)
t+12	b(t+12,0,1)	b(t+12,1,1)	b(t+12,2,1)	b(t+12,3,1)	b(t+12,2,1)	b(t+12,3,1)	b(t+12,4,1)	b(t+12,5,1)	b(t+12,6,1)	b(t+12,4,1)	b(t+12,5,1)	b(t+12,6,1)	b(t+12,7,1)	b(t+12,8,1)	b(t+12,9,1)	b(t+12,10,1)	b(t+12,11,1)	b(t+12,12,1)	b(t+12,13,1)	b(t+12,14,1)	b(t+12,15,1)
t+13	b(t+13,0,1)	b(t+13,1,1)	b(t+13,2,1)	b(t+13,3,1)	b(t+13,2,1)	b(t+13,3,1)	b(t+13,4,1)	b(t+13,5,1)	b(t+13,6,1)	b(t+13,4,1)	b(t+13,5,1)	b(t+13,6,1)	b(t+13,7,1)	b(t+13,8,1)	b(t+13,9,1)	b(t+13,10,1)	b(t+13,11,1)	b(t+13,12,1)	b(t+13,13,1)	b(t+13,14,1)	b(t+13,15,1)
t+14	b(t+14,0,1)	b(t+14,1,1)	b(t+14,2,1)	b(t+14,3,1)	b(t+14,2,1)	b(t+14,3,1)	b(t+14,4,1)	b(t+14,5,1)	b(t+14,6,1)	b(t+14,4,1)	b(t+14,5,1)	b(t+14,6,1)	b(t+14,7,1)	b(t+14,8,1)	b(t+14,9,1)	b(t+14,10,1)	b(t+14,11,1)	b(t+14,12,1)	b(t+14,13,1)	b(t+14,14,1)	b(t+14,15,1)
t+15	b(t+15,0,1)	b(t+15,1,1)	b(t+15,2,1)	b(t+15,3,1)	b(t+15,2,1)	b(t+15,3,1)	b(t+15,4,1)	b(t+15,5,1)	b(t+15,6,1)	b(t+15,4,1)	b(t+15,5,1)	b(t+15,6,1)	b(t+15,7,1)	b(t+15,8,1)	b(t+15,9,1)	b(t+15,10,1)	b(t+15,11,1)	b(t+15,12,1)	b(t+15,13,1)	b(t+15,14,1)	b(t+15,15,1)
t+16	b(t+16,0,1)	b(t+16,1,1)	b(t+16,2,1)	b(t+16,3,1)	b(t+16,2,1)	b(t+16,3,1)	b(t+16,4,1)	b(t+16,5,1)	b(t+16,6,1)	b(t+16,4,1)	b(t+16,5,1)	b(t+16,6,1)	b(t+16,7,1)	b(t+16,8,1)	b(t+16,9,1)	b(t+16,10,1)	b(t+16,11,1)	b(t+16,12,1)	b(t+16,13,1)	b(t+16,14,1)	b(t+16,15,1)
t+17	b(t+17,0,1)	b(t+17,1,1)	b(t+17,2,1)	b(t+17,3,1)	b(t+17,2,1)	b(t+17,3,1)	b(t+17,4,1)	b(t+17,5,1)	b(t+17,6,1)	b(t+17,4,1)	b(t+17,5,1)	b(t+17,6,1)	b(t+17,7,1)	b(t+17,8,1)	b(t+17,9,1)	b(t+17,10,1)	b(t+17,11,1)	b(t+17,12,1)	b(t+17,13,1)	b(t+17,14,1)	b(t+17,15,1)
t+18	b(t+18,0,1)	b(t+18,1,1)	b(t+18,2,1)	b(t+18,3,1)	b(t+18,2,1)	b(t+18,3,1)	b(t+18,4,1)	b(t+18,5,1)	b(t+18,6,1)	b(t+18,4,1)	b(t+18,5,1)	b(t+18,6,1)	b(t+18,7,1)	b(t+18,8,1)	b(t+18,9,1)	b(t+18,10,1)	b(t+18,11,1)	b(t+18,12,1)	b(t+18,13,1)	b(t+18,14,1)	b(t+18,15,1)
t+19	b(t+19,0,1)	b(t+19,1,1)	b(t+19,2,1)	b(t+19,3,1)	b(t+19,2,1)	b(t+19,3,1)	b(t+19,4,1)	b(t+19,5,1)	b(t+19,6,1)	b(t+19,4,1)	b(t+19,5,1)	b(t+19,6,1)	b(t+19,7,1)	b(t+19,8,1)	b(t+19,9,1)	b(t+19,10,1)	b(t+19,11,1)	b(t+19,12,1)	b(t+19,13,1)	b(t+19,14,1)	b(t+19,15,1)
t+20	b(t+20,0,1)	b(t+20,1,1)	b(t+20,2,1)	b(t+20,3,1)	b(t+20,2,1)	b(t+20,3,1)	b(t+20,4,1)	b(t+20,5,1)	b(t+20,6,1)	b(t+20,4,1)	b(t+20,5,1)	b(t+20,6,1)	b(t+20,7,1)	b(t+20,8,1)	b(t+20,9,1)	b(t+20,10,1)	b(t+20,11,1)	b(t+20,12,1)	b(t+20,13,1)	b(t+20,14,1)	b(t+20,15,1)

# AN EXAMPLE OF AUTOMATIC PROMOTION 1-VII

Job hiring at rank 2, promotion at rank 3 after 5 years loosing 3 years of seniority																					
t	0	1	2	3	4	5	6	7	8	9	10	11	12	13	14	15	16	17	18	19	20
t	b(t,0,2)	b(t,1,2)	b(t,2,2)	b(t,3,2)	b(t,4,2)	b(t,5,2)	b(t,3,2)	b(t,4,2)	b(t,5,2)	b(t,6,2)	b(t,7,2)	b(t,8,2)	b(t,9,2)	b(t,10,2)	b(t,11,2)	b(t,12,2)	b(t,13,2)	b(t,14,2)	b(t,15,2)	b(t,16,2)	b(t,17,2)
t+1	b(+1,0,2)	b(+1,1,2)	b(+1,2,2)	b(+1,3,2)	b(+1,4,2)	b(+1,5,2)	b(+1,3,2)	b(+1,4,2)	b(+1,5,2)	b(+1,6,2)	b(+1,7,2)	b(+1,8,2)	b(+1,9,2)	b(+1,10,2)	b(+1,11,2)	b(+1,12,2)	b(+1,13,2)	b(+1,14,2)	b(+1,15,2)	b(+1,16,2)	b(+1,17,2)
t+2	b(+2,0,2)	b(+2,1,2)	b(+2,2,2)	b(+2,3,2)	b(+2,4,2)	b(+2,5,2)	b(+2,3,2)	b(+2,4,2)	b(+2,5,2)	b(+2,6,2)	b(+2,7,2)	b(+2,8,2)	b(+2,9,2)	b(+2,10,2)	b(+2,11,2)	b(+2,12,2)	b(+2,13,2)	b(+2,14,2)	b(+2,15,2)	b(+2,16,2)	b(+2,17,2)
t+3	b(+3,0,2)	b(+3,1,2)	b(+3,2,2)	b(+3,3,2)	b(+3,4,2)	b(+3,5,2)	b(+3,3,2)	b(+3,4,2)	b(+3,5,2)	b(+3,6,2)	b(+3,7,2)	b(+3,8,2)	b(+3,9,2)	b(+3,10,2)	b(+3,11,2)	b(+3,12,2)	b(+3,13,2)	b(+3,14,2)	b(+3,15,2)	b(+3,16,2)	b(+3,17,2)
t+4	b(+4,0,2)	b(+4,1,2)	b(+4,2,2)	b(+4,3,2)	b(+4,4,2)	b(+4,5,2)	b(+4,3,2)	b(+4,4,2)	b(+4,5,2)	b(+4,6,2)	b(+4,7,2)	b(+4,8,2)	b(+4,9,2)	b(+4,10,2)	b(+4,11,2)	b(+4,12,2)	b(+4,13,2)	b(+4,14,2)	b(+4,15,2)	b(+4,16,2)	b(+4,17,2)
t+5	b(+5,0,2)	b(+5,1,2)	b(+5,2,2)	b(+5,3,2)	b(+5,4,2)	b(+5,5,2)	b(+5,3,2)	b(+5,4,2)	b(+5,5,2)	b(+5,6,2)	b(+5,7,2)	b(+5,8,2)	b(+5,9,2)	b(+5,10,2)	b(+5,11,2)	b(+5,12,2)	b(+5,13,2)	b(+5,14,2)	b(+5,15,2)	b(+5,16,2)	b(+5,17,2)
t+6	b(+6,0,2)	b(+6,1,2)	b(+6,2,2)	b(+6,3,2)	b(+6,4,2)	b(+6,5,2)	b(+6,3,2)	b(+6,4,2)	b(+6,5,2)	b(+6,6,2)	b(+6,7,2)	b(+6,8,2)	b(+6,9,2)	b(+6,10,2)	b(+6,11,2)	b(+6,12,2)	b(+6,13,2)	b(+6,14,2)	b(+6,15,2)	b(+6,16,2)	b(+6,17,2)
t+7	b(+7,0,2)	b(+7,1,2)	b(+7,2,2)	b(+7,3,2)	b(+7,4,2)	b(+7,5,2)	b(+7,3,2)	b(+7,4,2)	b(+7,5,2)	b(+7,6,2)	b(+7,7,2)	b(+7,8,2)	b(+7,9,2)	b(+7,10,2)	b(+7,11,2)	b(+7,12,2)	b(+7,13,2)	b(+7,14,2)	b(+7,15,2)	b(+7,16,2)	b(+7,17,2)
t+8	b(+8,0,2)	b(+8,1,2)	b(+8,2,2)	b(+8,3,2)	b(+8,4,2)	b(+8,5,2)	b(+8,3,2)	b(+8,4,2)	b(+8,5,2)	b(+8,6,2)	b(+8,7,2)	b(+8,8,2)	b(+8,9,2)	b(+8,10,2)	b(+8,11,2)	b(+8,12,2)	b(+8,13,2)	b(+8,14,2)	b(+8,15,2)	b(+8,16,2)	b(+8,17,2)
t+9	b(+9,0,2)	b(+9,1,2)	b(+9,2,2)	b(+9,3,2)	b(+9,4,2)	b(+9,5,2)	b(+9,3,2)	b(+9,4,2)	b(+9,5,2)	b(+9,6,2)	b(+9,7,2)	b(+9,8,2)	b(+9,9,2)	b(+9,10,2)	b(+9,11,2)	b(+9,12,2)	b(+9,13,2)	b(+9,14,2)	b(+9,15,2)	b(+9,16,2)	b(+9,17,2)
t+10	b(+10,0,2)	b(+10,1,2)	b(+10,2,2)	b(+10,3,2)	b(+10,4,2)	b(+10,5,2)	b(+10,3,2)	b(+10,4,2)	b(+10,5,2)	b(+10,6,2)	b(+10,7,2)	b(+10,8,2)	b(+10,9,2)	b(+10,10,2)	b(+10,11,2)	b(+10,12,2)	b(+10,13,2)	b(+10,14,2)	b(+10,15,2)	b(+10,16,2)	b(+10,17,2)
t+11	b(+11,0,2)	b(+11,1,2)	b(+11,2,2)	b(+11,3,2)	b(+11,4,2)	b(+11,5,2)	b(+11,3,2)	b(+11,4,2)	b(+11,5,2)	b(+11,6,2)	b(+11,7,2)	b(+11,8,2)	b(+11,9,2)	b(+11,10,2)	b(+11,11,2)	b(+11,12,2)	b(+11,13,2)	b(+11,14,2)	b(+11,15,2)	b(+11,16,2)	b(+11,17,2)
t+12	b(+12,0,2)	b(+12,1,2)	b(+12,2,2)	b(+12,3,2)	b(+12,4,2)	b(+12,5,2)	b(+12,3,2)	b(+12,4,2)	b(+12,5,2)	b(+12,6,2)	b(+12,7,2)	b(+12,8,2)	b(+12,9,2)	b(+12,10,2)	b(+12,11,2)	b(+12,12,2)	b(+12,13,2)	b(+12,14,2)	b(+12,15,2)	b(+12,16,2)	b(+12,17,2)
t+13	b(+13,0,2)	b(+13,1,2)	b(+13,2,2)	b(+13,3,2)	b(+13,4,2)	b(+13,5,2)	b(+13,3,2)	b(+13,4,2)	b(+13,5,2)	b(+13,6,2)	b(+13,7,2)	b(+13,8,2)	b(+13,9,2)	b(+13,10,2)	b(+13,11,2)	b(+13,12,2)	b(+13,13,2)	b(+13,14,2)	b(+13,15,2)	b(+13,16,2)	b(+13,17,2)
t+14	b(+14,0,2)	b(+14,1,2)	b(+14,2,2)	b(+14,3,2)	b(+14,4,2)	b(+14,5,2)	b(+14,3,2)	b(+14,4,2)	b(+14,5,2)	b(+14,6,2)	b(+14,7,2)	b(+14,8,2)	b(+14,9,2)	b(+14,10,2)	b(+14,11,2)	b(+14,12,2)	b(+14,13,2)	b(+14,14,2)	b(+14,15,2)	b(+14,16,2)	b(+14,17,2)
t+15	b(+15,0,2)	b(+15,1,2)	b(+15,2,2)	b(+15,3,2)	b(+15,4,2)	b(+15,5,2)	b(+15,3,2)	b(+15,4,2)	b(+15,5,2)	b(+15,6,2)	b(+15,7,2)	b(+15,8,2)	b(+15,9,2)	b(+15,10,2)	b(+15,11,2)	b(+15,12,2)	b(+15,13,2)	b(+15,14,2)	b(+15,15,2)	b(+15,16,2)	b(+15,17,2)
t+16	b(+16,0,2)	b(+16,1,2)	b(+16,2,2)	b(+16,3,2)	b(+16,4,2)	b(+16,5,2)	b(+16,3,2)	b(+16,4,2)	b(+16,5,2)	b(+16,6,2)	b(+16,7,2)	b(+16,8,2)	b(+16,9,2)	b(+16,10,2)	b(+16,11,2)	b(+16,12,2)	b(+16,13,2)	b(+16,14,2)	b(+16,15,2)	b(+16,16,2)	b(+16,17,2)
t+17	b(+17,0,2)	b(+17,1,2)	b(+17,2,2)	b(+17,3,2)	b(+17,4,2)	b(+17,5,2)	b(+17,3,2)	b(+17,4,2)	b(+17,5,2)	b(+17,6,2)	b(+17,7,2)	b(+17,8,2)	b(+17,9,2)	b(+17,10,2)	b(+17,11,2)	b(+17,12,2)	b(+17,13,2)	b(+17,14,2)	b(+17,15,2)	b(+17,16,2)	b(+17,17,2)
t+18	b(+18,0,2)	b(+18,1,2)	b(+18,2,2)	b(+18,3,2)	b(+18,4,2)	b(+18,5,2)	b(+18,3,2)	b(+18,4,2)	b(+18,5,2)	b(+18,6,2)	b(+18,7,2)	b(+18,8,2)	b(+18,9,2)	b(+18,10,2)	b(+18,11,2)	b(+18,12,2)	b(+18,13,2)	b(+18,14,2)	b(+18,15,2)	b(+18,16,2)	b(+18,17,2)
t+19	b(+19,0,2)	b(+19,1,2)	b(+19,2,2)	b(+19,3,2)	b(+19,4,2)	b(+19,5,2)	b(+19,3,2)	b(+19,4,2)	b(+19,5,2)	b(+19,6,2)	b(+19,7,2)	b(+19,8,2)	b(+19,9,2)	b(+19,10,2)	b(+19,11,2)	b(+19,12,2)	b(+19,13,2)	b(+19,14,2)	b(+19,15,2)	b(+19,16,2)	b(+19,17,2)
t+20	b(+20,0,2)	b(+20,1,2)	b(+20,2,2)	b(+20,3,2)	b(+20,4,2)	b(+20,5,2)	b(+20,3,2)	b(+20,4,2)	b(+20,5,2)	b(+20,6,2)	b(+20,7,2)	b(+20,8,2)	b(+20,9,2)	b(+20,10,2)	b(+20,11,2)	b(+20,12,2)	b(+20,13,2)	b(+20,14,2)	b(+20,15,2)	b(+20,16,2)	b(+20,17,2)

# AN EXAMPLE OF AUTOMATIC PROMOTION 1-VIII

Job hiring at rank 1, loosing of seniority, promotion at rank 2 after 3 years, promotion at rank 3 after 5 years

t	0	1	2	3	4	5	6	7	8	9	10	11	12	13	14	15	16	17	18	19	20
t	b(t,0,1)	b(t,1,1)	b(t,2,1)	b(t,3,1)	b(t,0,1)	b(t,1,1)	b(t,2,1)	b(t,3,1)	b(t,4,1)	b(t,0,1)	b(t,1,1)	b(t,2,1)	b(t,3,1)	b(t,4,1)	b(t,5,1)	b(t,6,1)	b(t,7,1)	b(t,8,1)	b(t,9,1)	b(t,10,1)	b(t,11,1)
t+1	b(t+1,0,1)	b(t+1,1,1)	b(t+1,2,1)	b(t+1,3,1)	b(t+1,0,1)	b(t+1,1,1)	b(t+1,2,1)	b(t+1,3,1)	b(t+1,4,1)	b(t+1,0,1)	b(t+1,1,1)	b(t+1,2,1)	b(t+1,3,1)	b(t+1,4,1)	b(t+1,5,1)	b(t+1,6,1)	b(t+1,7,1)	b(t+1,8,1)	b(t+1,9,1)	b(t+1,10,1)	b(t+1,11,1)
t+2	b(t+2,0,1)	b(t+2,1,1)	b(t+2,2,1)	b(t+2,3,1)	b(t+2,0,1)	b(t+2,1,1)	b(t+2,2,1)	b(t+2,3,1)	b(t+2,4,1)	b(t+2,0,1)	b(t+2,1,1)	b(t+2,2,1)	b(t+2,3,1)	b(t+2,4,1)	b(t+2,5,1)	b(t+2,6,1)	b(t+2,7,1)	b(t+2,8,1)	b(t+2,9,1)	b(t+2,10,1)	b(t+2,11,1)
t+3	b(t+3,0,1)	b(t+3,1,1)	b(t+3,2,1)	b(t+3,3,1)	b(t+3,0,1)	b(t+3,1,1)	b(t+3,2,1)	b(t+3,3,1)	b(t+3,4,1)	b(t+3,0,1)	b(t+3,1,1)	b(t+3,2,1)	b(t+3,3,1)	b(t+3,4,1)	b(t+3,5,1)	b(t+3,6,1)	b(t+3,7,1)	b(t+3,8,1)	b(t+3,9,1)	b(t+3,10,1)	b(t+3,11,1)
t+4	b(t+4,0,1)	b(t+4,1,1)	b(t+4,2,1)	b(t+4,3,1)	b(t+4,0,1)	b(t+4,1,1)	b(t+4,2,1)	b(t+4,3,1)	b(t+4,4,1)	b(t+4,0,1)	b(t+4,1,1)	b(t+4,2,1)	b(t+4,3,1)	b(t+4,4,1)	b(t+4,5,1)	b(t+4,6,1)	b(t+4,7,1)	b(t+4,8,1)	b(t+4,9,1)	b(t+4,10,1)	b(t+4,11,1)
t+5	b(t+5,0,1)	b(t+5,1,1)	b(t+5,2,1)	b(t+5,3,1)	b(t+5,0,1)	b(t+5,1,1)	b(t+5,2,1)	b(t+5,3,1)	b(t+5,4,1)	b(t+5,0,1)	b(t+5,1,1)	b(t+5,2,1)	b(t+5,3,1)	b(t+5,4,1)	b(t+5,5,1)	b(t+5,6,1)	b(t+5,7,1)	b(t+5,8,1)	b(t+5,9,1)	b(t+5,10,1)	b(t+5,11,1)
t+6	b(t+6,0,1)	b(t+6,1,1)	b(t+6,2,1)	b(t+6,3,1)	b(t+6,0,1)	b(t+6,1,1)	b(t+6,2,1)	b(t+6,3,1)	b(t+6,4,1)	b(t+6,0,1)	b(t+6,1,1)	b(t+6,2,1)	b(t+6,3,1)	b(t+6,4,1)	b(t+6,5,1)	b(t+6,6,1)	b(t+6,7,1)	b(t+6,8,1)	b(t+6,9,1)	b(t+6,10,1)	b(t+6,11,1)
t+7	b(t+7,0,1)	b(t+7,1,1)	b(t+7,2,1)	b(t+7,3,1)	b(t+7,0,1)	b(t+7,1,1)	b(t+7,2,1)	b(t+7,3,1)	b(t+7,4,1)	b(t+7,0,1)	b(t+7,1,1)	b(t+7,2,1)	b(t+7,3,1)	b(t+7,4,1)	b(t+7,5,1)	b(t+7,6,1)	b(t+7,7,1)	b(t+7,8,1)	b(t+7,9,1)	b(t+7,10,1)	b(t+7,11,1)
t+8	b(t+8,0,1)	b(t+8,1,1)	b(t+8,2,1)	b(t+8,3,1)	b(t+8,0,1)	b(t+8,1,1)	b(t+8,2,1)	b(t+8,3,1)	b(t+8,4,1)	b(t+8,0,1)	b(t+8,1,1)	b(t+8,2,1)	b(t+8,3,1)	b(t+8,4,1)	b(t+8,5,1)	b(t+8,6,1)	b(t+8,7,1)	b(t+8,8,1)	b(t+8,9,1)	b(t+8,10,1)	b(t+8,11,1)
t+9	b(t+9,0,1)	b(t+9,1,1)	b(t+9,2,1)	b(t+9,3,1)	b(t+9,0,1)	b(t+9,1,1)	b(t+9,2,1)	b(t+9,3,1)	b(t+9,4,1)	b(t+9,0,1)	b(t+9,1,1)	b(t+9,2,1)	b(t+9,3,1)	b(t+9,4,1)	b(t+9,5,1)	b(t+9,6,1)	b(t+9,7,1)	b(t+9,8,1)	b(t+9,9,1)	b(t+9,10,1)	b(t+9,11,1)
t+10	b(t+10,0,1)	b(t+10,1,1)	b(t+10,2,1)	b(t+10,3,1)	b(t+10,0,1)	b(t+10,1,1)	b(t+10,2,1)	b(t+10,3,1)	b(t+10,4,1)	b(t+10,0,1)	b(t+10,1,1)	b(t+10,2,1)	b(t+10,3,1)	b(t+10,4,1)	b(t+10,5,1)	b(t+10,6,1)	b(t+10,7,1)	b(t+10,8,1)	b(t+10,9,1)	b(t+10,10,1)	b(t+10,11,1)
t+11	b(t+11,0,1)	b(t+11,1,1)	b(t+11,2,1)	b(t+11,3,1)	b(t+11,0,1)	b(t+11,1,1)	b(t+11,2,1)	b(t+11,3,1)	b(t+11,4,1)	b(t+11,0,1)	b(t+11,1,1)	b(t+11,2,1)	b(t+11,3,1)	b(t+11,4,1)	b(t+11,5,1)	b(t+11,6,1)	b(t+11,7,1)	b(t+11,8,1)	b(t+11,9,1)	b(t+11,10,1)	b(t+11,11,1)
t+12	b(t+12,0,1)	b(t+12,1,1)	b(t+12,2,1)	b(t+12,3,1)	b(t+12,0,1)	b(t+12,1,1)	b(t+12,2,1)	b(t+12,3,1)	b(t+12,4,1)	b(t+12,0,1)	b(t+12,1,1)	b(t+12,2,1)	b(t+12,3,1)	b(t+12,4,1)	b(t+12,5,1)	b(t+12,6,1)	b(t+12,7,1)	b(t+12,8,1)	b(t+12,9,1)	b(t+12,10,1)	b(t+12,11,1)
t+13	b(t+13,0,1)	b(t+13,1,1)	b(t+13,2,1)	b(t+13,3,1)	b(t+13,0,1)	b(t+13,1,1)	b(t+13,2,1)	b(t+13,3,1)	b(t+13,4,1)	b(t+13,0,1)	b(t+13,1,1)	b(t+13,2,1)	b(t+13,3,1)	b(t+13,4,1)	b(t+13,5,1)	b(t+13,6,1)	b(t+13,7,1)	b(t+13,8,1)	b(t+13,9,1)	b(t+13,10,1)	b(t+13,11,1)
t+14	b(t+14,0,1)	b(t+14,1,1)	b(t+14,2,1)	b(t+14,3,1)	b(t+14,0,1)	b(t+14,1,1)	b(t+14,2,1)	b(t+14,3,1)	b(t+14,4,1)	b(t+14,0,1)	b(t+14,1,1)	b(t+14,2,1)	b(t+14,3,1)	b(t+14,4,1)	b(t+14,5,1)	b(t+14,6,1)	b(t+14,7,1)	b(t+14,8,1)	b(t+14,9,1)	b(t+14,10,1)	b(t+14,11,1)
t+15	b(t+15,0,1)	b(t+15,1,1)	b(t+15,2,1)	b(t+15,3,1)	b(t+15,0,1)	b(t+15,1,1)	b(t+15,2,1)	b(t+15,3,1)	b(t+15,4,1)	b(t+15,0,1)	b(t+15,1,1)	b(t+15,2,1)	b(t+15,3,1)	b(t+15,4,1)	b(t+15,5,1)	b(t+15,6,1)	b(t+15,7,1)	b(t+15,8,1)	b(t+15,9,1)	b(t+15,10,1)	b(t+15,11,1)
t+16	b(t+16,0,1)	b(t+16,1,1)	b(t+16,2,1)	b(t+16,3,1)	b(t+16,0,1)	b(t+16,1,1)	b(t+16,2,1)	b(t+16,3,1)	b(t+16,4,1)	b(t+16,0,1)	b(t+16,1,1)	b(t+16,2,1)	b(t+16,3,1)	b(t+16,4,1)	b(t+16,5,1)	b(t+16,6,1)	b(t+16,7,1)	b(t+16,8,1)	b(t+16,9,1)	b(t+16,10,1)	b(t+16,11,1)
t+17	b(t+17,0,1)	b(t+17,1,1)	b(t+17,2,1)	b(t+17,3,1)	b(t+17,0,1)	b(t+17,1,1)	b(t+17,2,1)	b(t+17,3,1)	b(t+17,4,1)	b(t+17,0,1)	b(t+17,1,1)	b(t+17,2,1)	b(t+17,3,1)	b(t+17,4,1)	b(t+17,5,1)	b(t+17,6,1)	b(t+17,7,1)	b(t+17,8,1)	b(t+17,9,1)	b(t+17,10,1)	b(t+17,11,1)
t+18	b(t+18,0,1)	b(t+18,1,1)	b(t+18,2,1)	b(t+18,3,1)	b(t+18,0,1)	b(t+18,1,1)	b(t+18,2,1)	b(t+18,3,1)	b(t+18,4,1)	b(t+18,0,1)	b(t+18,1,1)	b(t+18,2,1)	b(t+18,3,1)	b(t+18,4,1)	b(t+18,5,1)	b(t+18,6,1)	b(t+18,7,1)	b(t+18,8,1)	b(t+18,9,1)	b(t+18,10,1)	b(t+18,11,1)
t+19	b(t+19,0,1)	b(t+19,1,1)	b(t+19,2,1)	b(t+19,3,1)	b(t+19,0,1)	b(t+19,1,1)	b(t+19,2,1)	b(t+19,3,1)	b(t+19,4,1)	b(t+19,0,1)	b(t+19,1,1)	b(t+19,2,1)	b(t+19,3,1)	b(t+19,4,1)	b(t+19,5,1)	b(t+19,6,1)	b(t+19,7,1)	b(t+19,8,1)	b(t+19,9,1)	b(t+19,10,1)	b(t+19,11,1)
t+20	b(t+20,0,1)	b(t+20,1,1)	b(t+20,2,1)	b(t+20,3,1)	b(t+20,0,1)	b(t+20,1,1)	b(t+20,2,1)	b(t+20,3,1)	b(t+20,4,1)	b(t+20,0,1)	b(t+20,1,1)	b(t+20,2,1)	b(t+20,3,1)	b(t+20,4,1)	b(t+20,5,1)	b(t+20,6,1)	b(t+20,7,1)	b(t+20,8,1)	b(t+20,9,1)	b(t+20,10,1)	b(t+20,11,1)

# AN EXAMPLE OF AUTOMATIC PROMOTION 1-IX

Job hiring at rank 2, promotion at rank 3 after 5 years loosing of seniority																					
t	0	1	2	3	4	5	6	7	8	9	10	11	12	13	14	15	16	17	18	19	20
t	b(t,0,2)	b(t,1,2)	b(t,2,2)	b(t,3,2)	b(t,4,2)	b(t,5,2)	b(t,0,2)	b(t,1,2)	b(t,2,2)	b(t,3,2)	b(t,4,2)	b(t,5,2)	b(t,6,2)	b(t,7,2)	b(t,8,2)	b(t,9,2)	b(t,10,2)	b(t,11,2)	b(t,12,2)	b(t,13,2)	b(t,14,2)
t+1	b(+1,0,2)	b(+1,1,2)	b(+1,2,2)	b(+1,3,2)	b(+1,4,2)	b(+1,5,2)	b(+1,0,2)	b(+1,1,2)	b(+1,2,2)	b(+1,3,2)	b(+1,4,2)	b(+1,5,2)	b(+1,6,2)	b(+1,7,2)	b(+1,8,2)	b(+1,9,2)	b(+1,10,2)	b(+1,11,2)	b(+1,12,2)	b(+1,13,2)	b(+1,14,2)
t+2	b(+2,0,2)	b(+2,1,2)	b(+2,2,2)	b(+2,3,2)	b(+2,4,2)	b(+2,5,2)	b(+2,0,2)	b(+2,1,2)	b(+2,2,2)	b(+2,3,2)	b(+2,4,2)	b(+2,5,2)	b(+2,6,2)	b(+2,7,2)	b(+2,8,2)	b(+2,9,2)	b(+2,10,2)	b(+2,11,2)	b(+2,12,2)	b(+2,13,2)	b(+2,14,2)
t+3	b(+3,0,2)	b(+3,1,2)	b(+3,2,2)	b(+3,3,2)	b(+3,4,2)	b(+3,5,2)	b(+3,0,2)	b(+3,1,2)	b(+3,2,2)	b(+3,3,2)	b(+3,4,2)	b(+3,5,2)	b(+3,6,2)	b(+3,7,2)	b(+3,8,2)	b(+3,9,2)	b(+3,10,2)	b(+3,11,2)	b(+3,12,2)	b(+3,13,2)	b(+3,14,2)
t+4	b(+4,0,2)	b(+4,1,2)	b(+4,2,2)	b(+4,3,2)	b(+4,4,2)	b(+4,5,2)	b(+4,0,2)	b(+4,1,2)	b(+4,2,2)	b(+4,3,2)	b(+4,4,2)	b(+4,5,2)	b(+4,6,2)	b(+4,7,2)	b(+4,8,2)	b(+4,9,2)	b(+4,10,2)	b(+4,11,2)	b(+4,12,2)	b(+4,13,2)	b(+4,14,2)
t+5	b(+5,0,2)	b(+5,1,2)	b(+5,2,2)	b(+5,3,2)	b(+5,4,2)	b(+5,5,2)	b(+5,0,2)	b(+5,1,2)	b(+5,2,2)	b(+5,3,2)	b(+5,4,2)	b(+5,5,2)	b(+5,6,2)	b(+5,7,2)	b(+5,8,2)	b(+5,9,2)	b(+5,10,2)	b(+5,11,2)	b(+5,12,2)	b(+5,13,2)	b(+5,14,2)
t+6	b(+6,0,2)	b(+6,1,2)	b(+6,2,2)	b(+6,3,2)	b(+6,4,2)	b(+6,5,2)	b(+6,0,2)	b(+6,1,2)	b(+6,2,2)	b(+6,3,2)	b(+6,4,2)	b(+6,5,2)	b(+6,6,2)	b(+6,7,2)	b(+6,8,2)	b(+6,9,2)	b(+6,10,2)	b(+6,11,2)	b(+6,12,2)	b(+6,13,2)	b(+6,14,2)
t+7	b(+7,0,2)	b(+7,1,2)	b(+7,2,2)	b(+7,3,2)	b(+7,4,2)	b(+7,5,2)	b(+7,0,2)	b(+7,1,2)	b(+7,2,2)	b(+7,3,2)	b(+7,4,2)	b(+7,5,2)	b(+7,6,2)	b(+7,7,2)	b(+7,8,2)	b(+7,9,2)	b(+7,10,2)	b(+7,11,2)	b(+7,12,2)	b(+7,13,2)	b(+7,14,2)
t+8	b(+8,0,2)	b(+8,1,2)	b(+8,2,2)	b(+8,3,2)	b(+8,4,2)	b(+8,5,2)	b(+8,0,2)	b(+8,1,2)	b(+8,2,2)	b(+8,3,2)	b(+8,4,2)	b(+8,5,2)	b(+8,6,2)	b(+8,7,2)	b(+8,8,2)	b(+8,9,2)	b(+8,10,2)	b(+8,11,2)	b(+8,12,2)	b(+8,13,2)	b(+8,14,2)
t+9	b(+9,0,2)	b(+9,1,2)	b(+9,2,2)	b(+9,3,2)	b(+9,4,2)	b(+9,5,2)	b(+9,0,2)	b(+9,1,2)	b(+9,2,2)	b(+9,3,2)	b(+9,4,2)	b(+9,5,2)	b(+9,6,2)	b(+9,7,2)	b(+9,8,2)	b(+9,9,2)	b(+9,10,2)	b(+9,11,2)	b(+9,12,2)	b(+9,13,2)	b(+9,14,2)
t+10	b(+10,0,2)	b(+10,1,2)	b(+10,2,2)	b(+10,3,2)	b(+10,4,2)	b(+10,5,2)	b(+10,0,2)	b(+10,1,2)	b(+10,2,2)	b(+10,3,2)	b(+10,4,2)	b(+10,5,2)	b(+10,6,2)	b(+10,7,2)	b(+10,8,2)	b(+10,9,2)	b(+10,10,2)	b(+10,11,2)	b(+10,12,2)	b(+10,13,2)	b(+10,14,2)
t+11	b(+11,0,2)	b(+11,1,2)	b(+11,2,2)	b(+11,3,2)	b(+11,4,2)	b(+11,5,2)	b(+11,0,2)	b(+11,1,2)	b(+11,2,2)	b(+11,3,2)	b(+11,4,2)	b(+11,5,2)	b(+11,6,2)	b(+11,7,2)	b(+11,8,2)	b(+11,9,2)	b(+11,10,2)	b(+11,11,2)	b(+11,12,2)	b(+11,13,2)	b(+11,14,2)
t+12	b(+12,0,2)	b(+12,1,2)	b(+12,2,2)	b(+12,3,2)	b(+12,4,2)	b(+12,5,2)	b(+12,0,2)	b(+12,1,2)	b(+12,2,2)	b(+12,3,2)	b(+12,4,2)	b(+12,5,2)	b(+12,6,2)	b(+12,7,2)	b(+12,8,2)	b(+12,9,2)	b(+12,10,2)	b(+12,11,2)	b(+12,12,2)	b(+12,13,2)	b(+12,14,2)
t+13	b(+13,0,2)	b(+13,1,2)	b(+13,2,2)	b(+13,3,2)	b(+13,4,2)	b(+13,5,2)	b(+13,0,2)	b(+13,1,2)	b(+13,2,2)	b(+13,3,2)	b(+13,4,2)	b(+13,5,2)	b(+13,6,2)	b(+13,7,2)	b(+13,8,2)	b(+13,9,2)	b(+13,10,2)	b(+13,11,2)	b(+13,12,2)	b(+13,13,2)	b(+13,14,2)
t+14	b(+14,0,2)	b(+14,1,2)	b(+14,2,2)	b(+14,3,2)	b(+14,4,2)	b(+14,5,2)	b(+14,0,2)	b(+14,1,2)	b(+14,2,2)	b(+14,3,2)	b(+14,4,2)	b(+14,5,2)	b(+14,6,2)	b(+14,7,2)	b(+14,8,2)	b(+14,9,2)	b(+14,10,2)	b(+14,11,2)	b(+14,12,2)	b(+14,13,2)	b(+14,14,2)
t+15	b(+15,0,2)	b(+15,1,2)	b(+15,2,2)	b(+15,3,2)	b(+15,4,2)	b(+15,5,2)	b(+15,0,2)	b(+15,1,2)	b(+15,2,2)	b(+15,3,2)	b(+15,4,2)	b(+15,5,2)	b(+15,6,2)	b(+15,7,2)	b(+15,8,2)	b(+15,9,2)	b(+15,10,2)	b(+15,11,2)	b(+15,12,2)	b(+15,13,2)	b(+15,14,2)
t+16	b(+16,0,2)	b(+16,1,2)	b(+16,2,2)	b(+16,3,2)	b(+16,4,2)	b(+16,5,2)	b(+16,0,2)	b(+16,1,2)	b(+16,2,2)	b(+16,3,2)	b(+16,4,2)	b(+16,5,2)	b(+16,6,2)	b(+16,7,2)	b(+16,8,2)	b(+16,9,2)	b(+16,10,2)	b(+16,11,2)	b(+16,12,2)	b(+16,13,2)	b(+16,14,2)
t+17	b(+17,0,2)	b(+17,1,2)	b(+17,2,2)	b(+17,3,2)	b(+17,4,2)	b(+17,5,2)	b(+17,0,2)	b(+17,1,2)	b(+17,2,2)	b(+17,3,2)	b(+17,4,2)	b(+17,5,2)	b(+17,6,2)	b(+17,7,2)	b(+17,8,2)	b(+17,9,2)	b(+17,10,2)	b(+17,11,2)	b(+17,12,2)	b(+17,13,2)	b(+17,14,2)
t+18	b(+18,0,2)	b(+18,1,2)	b(+18,2,2)	b(+18,3,2)	b(+18,4,2)	b(+18,5,2)	b(+18,0,2)	b(+18,1,2)	b(+18,2,2)	b(+18,3,2)	b(+18,4,2)	b(+18,5,2)	b(+18,6,2)	b(+18,7,2)	b(+18,8,2)	b(+18,9,2)	b(+18,10,2)	b(+18,11,2)	b(+18,12,2)	b(+18,13,2)	b(+18,14,2)
t+19	b(+19,0,2)	b(+19,1,2)	b(+19,2,2)	b(+19,3,2)	b(+19,4,2)	b(+19,5,2)	b(+19,0,2)	b(+19,1,2)	b(+19,2,2)	b(+19,3,2)	b(+19,4,2)	b(+19,5,2)	b(+19,6,2)	b(+19,7,2)	b(+19,8,2)	b(+19,9,2)	b(+19,10,2)	b(+19,11,2)	b(+19,12,2)	b(+19,13,2)	b(+19,14,2)
t+20	b(+20,0,2)	b(+20,1,2)	b(+20,2,2)	b(+20,3,2)	b(+20,4,2)	b(+20,5,2)	b(+20,0,2)	b(+20,1,2)	b(+20,2,2)	b(+20,3,2)	b(+20,4,2)	b(+20,5,2)	b(+20,6,2)	b(+20,7,2)	b(+20,8,2)	b(+20,9,2)	b(+20,10,2)	b(+20,11,2)	b(+20,12,2)	b(+20,13,2)	b(+20,14,2)

## THE MATRIX ELEMENTS

Up to now the elements of **A** and **B** are monetary values they could be also index numbers. We think that indices work better because the rank and the seniority are the most important issues of the salary, but it is possible that there are some salary differences among workers with the same rank and seniority, for example because of a different composition of family. Working with indices it is possible taking into account these differences.

Posing the initial index=  $b_{t,j,k}$ , the initial salary=  $S_{t,j,k}$  the index after  $n$  years=  $b_{t+n,j+n,k}$

$$S_{t+n,j+n,k} = S_{t,j,k} * \frac{b_{t+n,j+n,k}}{b_{t,j,k}}$$

## PROMOTION BY CHOICE

We must consider the rank change because of a promotion to a higher rank  
Calculation of the probabilities, for each year of the time horizon and for each possible cohort, to be promoted in a higher rank with a given seniority.

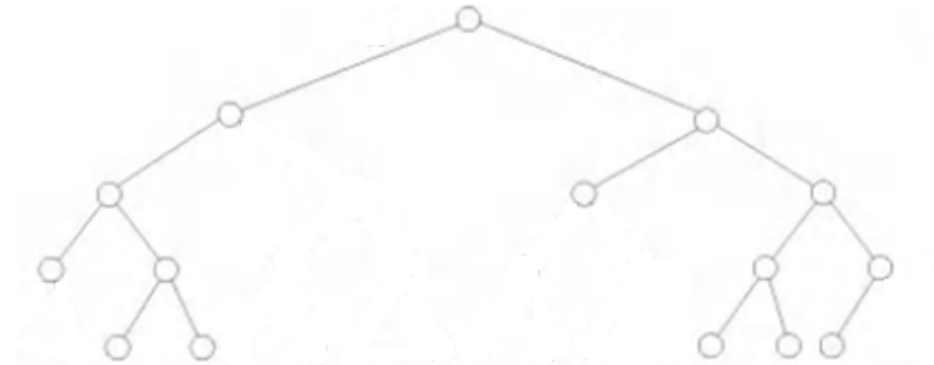
Given a cohort for each considered year, it will be calculated a probability distribution. These probabilities will be computed taking into account the company rank change rules and the observed data of the promotions among the ranks.

The basis data are the calculated probabilities and the three dimensional array **A**. For each year, seniority and rank is constructed a probability distribution. The probability to stay in a rank with a given seniority at a give year will be multiplied by the corresponding salary or index value, in this way the mean salary at each year of the studied horizon year will be calculated. Starting from the matrix **A** it will be calculated the **B** matrix

## DEFINITIONS I

Tree a connected graph with  $n+1$  nodes and  $n$  edges

A binary tree is a tree in which each node has at most two sons (left and right sons)



**Leaf:** node without sons

**Root:** node without father

**Edge:** segment that connects two nodes

**Path:** sequence of nodes that are connected by edges

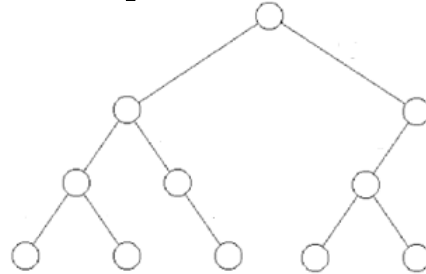
**Path:** sequence of edge in which the second node of the previous edge is equal to the first node of the subsequent edge

**Simple path:** a path in which each node appears only once

**Level of a node:** Max number of edges of a simple path that connects the root to the node

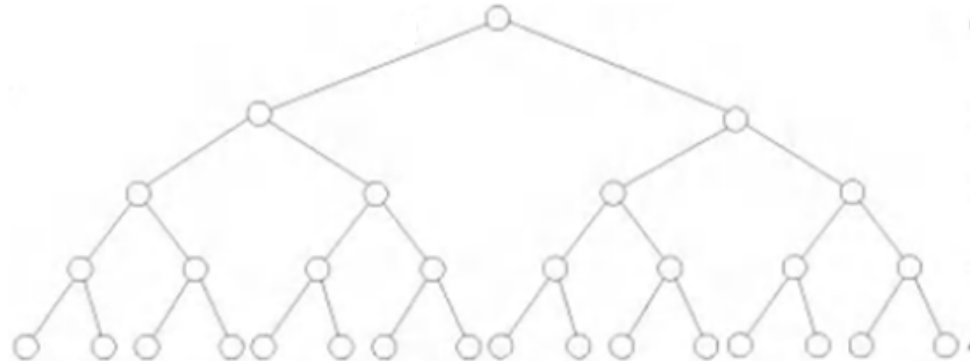
## DEFINITIONS II

**A n-level binary tree  $\Gamma^n$**  : binary tree in which each leaf is a n-level node.



$\Gamma_i^k$  represents the i-th node (starting from the left) of the k-th level and  ${}^r\gamma_i^k, {}^l\gamma_i^k$  respectively its right and left subgraphs;  ${}^l\beta_i^k, {}^r\beta_i^k \in \mathbb{R}$  are respectively the values given to the left and the right edges if the related subgraphs are not empty

**n-level complete binary tree:** n-level binary tree with  $2^n$  leaves



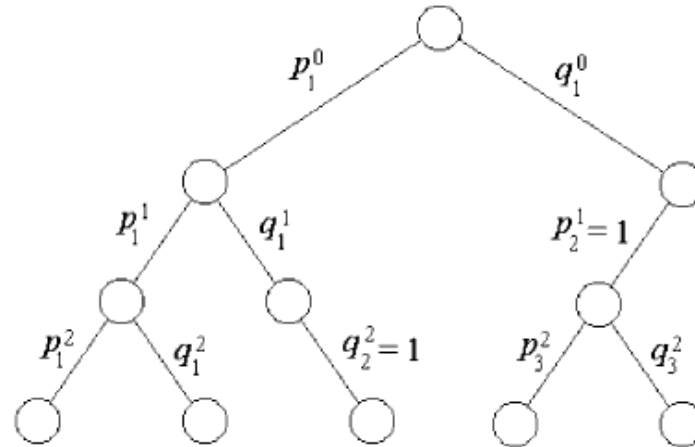
It is easy to prove that the number of n-level binary trees is  $2^{(2^n)} - 1$

### DEFINITIONS III

A **weighted n-level binary tree**  $B^n$ : n-level binary tree in which to each edge is assigned a real number the  ${}^l\beta_i^k, {}^r\beta_i^k$ .

A **weighted n-level binary trial tree**  $P^n$ : weighted n-level binary tree in which left and right weights are respectively:  $p_i^k, q_i^k, 0 \leq p_i^k, q_i^k \leq 1, p_i^k + q_i^k = 1$

$$\Pr\{\Gamma_i^k\} = \prod_{j=0}^{k-1} {}^s\pi_{i_j}^j; \text{ where } \pi = p \text{ if it is a left edge and } \pi = q \text{ if it is a right edge and } s \in \{l, r\}.$$



Given  $\Gamma_1^k, \Gamma_2^k, \dots, \Gamma_{m_k}^k$  the nodes of level k of  $P^n$  then  $\sum_{i=1}^{m_k} \Pr\{\Gamma_i^k\} = 1$

## DEFINITIONS IV

**n-level binary graph**  $G^n$ : graph to which a hierarchical structure is associated it can either have only a 0-level node (0 level binary graph) or be constituted by one or two (n-1)-level binary subgraphs (n-level binary graph) and each node of level k can have one or two (n-k-1)-level binary subgraphs.

A n-level binary tree is particular case of a n-level binary graph

$\mathbf{T}^k = \{T_1^k, T_2^k, \dots, T_{r_k}^k\}$ : Set of all the simple path from the root to the k-level nodes.

$i_k \in \{1, \dots, m_k\}$ ,  $m_k$  number of nodes of level k,  $G_{i_k}^k$  is a node of level k.

$G_{i_k}^k$  is **hierarchical attainable** from the node  $G_{i_h}^h$  if exists a simple path

$$\left\{ G_{i_h}^h, G_{i_{h+1}}^{h+1}, \dots, G_{i_k}^k \right\}, h < k \quad \left( \left\{ {}^s\beta_{i_h}^h, {}^s\beta_{i_{h+1}}^{h+1}, \dots, {}^s\beta_{i_{k-1}}^{k-1} \right\}, s \in \{l, r\} \right).$$

The path can also be described by the edges that links the nodes

## DEFINITIONS V

$u \in \{1, \dots, m_u\}$ ,  $\mathbf{T}_u^k = \left\{ T_j^k : T_j^k = {}^s \beta_{j, i_0}^0, \dots, {}^s \beta_{j, i_{k-1}}^{k-1} \right\}$ ,  $s \in \{l, r\}$  where  ${}^s \beta_{j, i_{k-1}}^{k-1}$  connect  $i_{k-1}$  to  $u$

$\mathbf{T}_u^k$  set of simple paths from the root to the  $u$ -th node of the  $k$ -th level

**A weighted n-level binary graph:** n-level binary graph in which to each edge is assigned a real number.

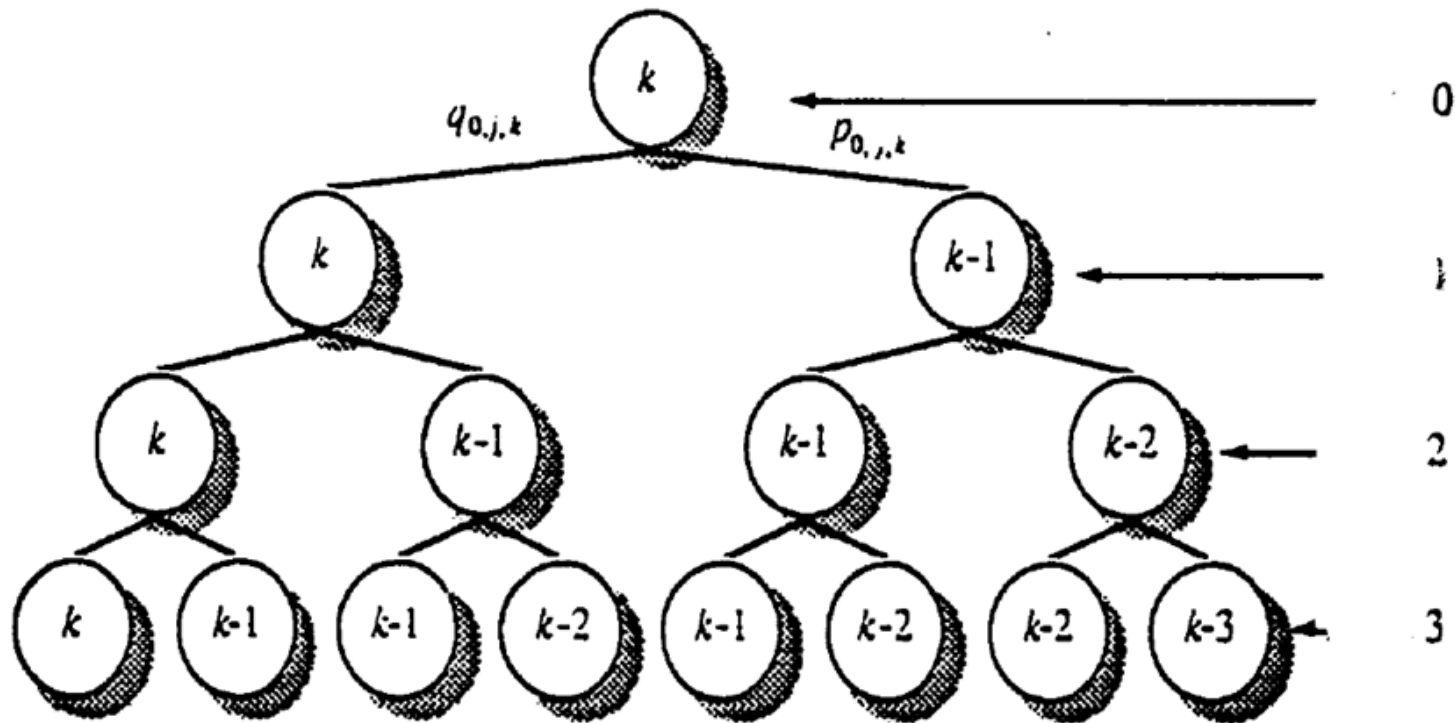
**A weighted n-level binary trial graph:** weighted n-level binary graph in which left and right weights are respectively:  $p_i^k, q_i^k$ ,  $0 \leq p_i^k \leq 1$ ,  $q_i^k, p_i^k + q_i^k = 1$

$G^n$  weighted n-level binary trial graph,  $G_u^k, k \in \{1, \dots, n\}$  its probability is given by:

$$\Pr \left\{ G_u^k \right\} = \sum_{h \in \mathbf{T}_u^k} \prod_{j=0}^{k-1} {}^s \pi_{h, i_j}^j, s \in \{l, r\}$$

Although a n level binary tree is a particular case of a n-level binary graph a n-level binary graph can be obtained from a n-level binary tree

# THE CONSTRUCTION OF A BINARY TREE



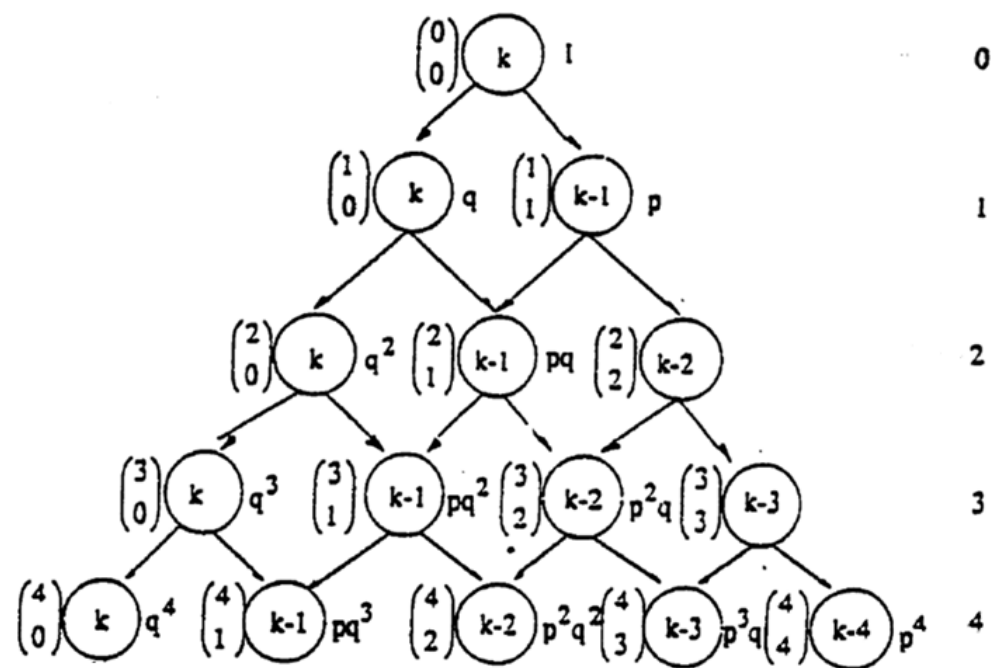
## PROPOSITION

Let  $P^n$  be a complete weighted  $n$ -level binary trial tree. Suppose that the events  $E_1, \dots, E_n$  are equally likely, with probability  $p$ , independent events. It is possible  $\forall n \in \mathbb{N}$  grouping this tree as a weighted  $n$ -level Bernoulli trial graph in which the probability of nodes of the  $n$ -th level correspond to the binomial distribution  $Bi(n, p)$

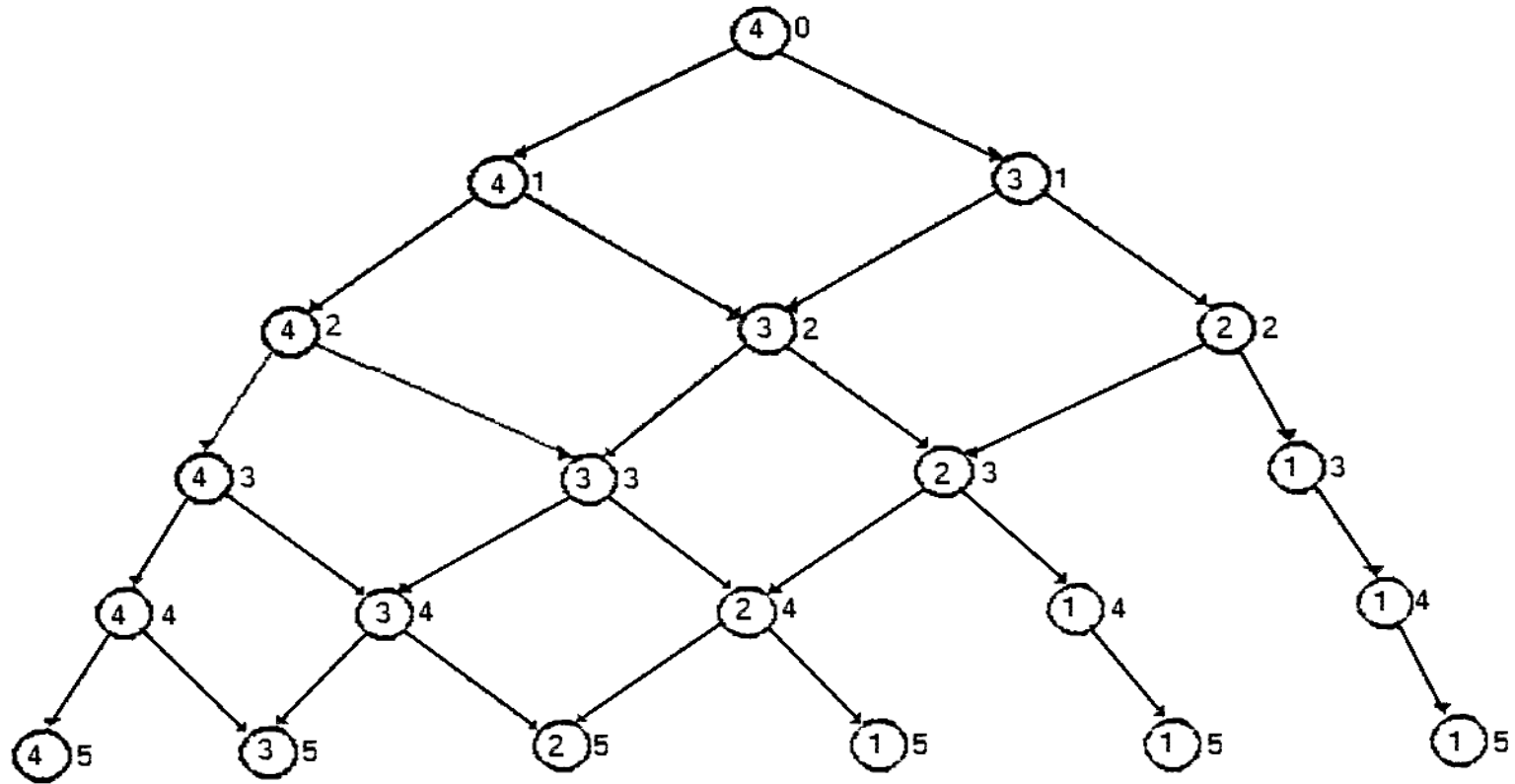
The proof can be done easily by induction



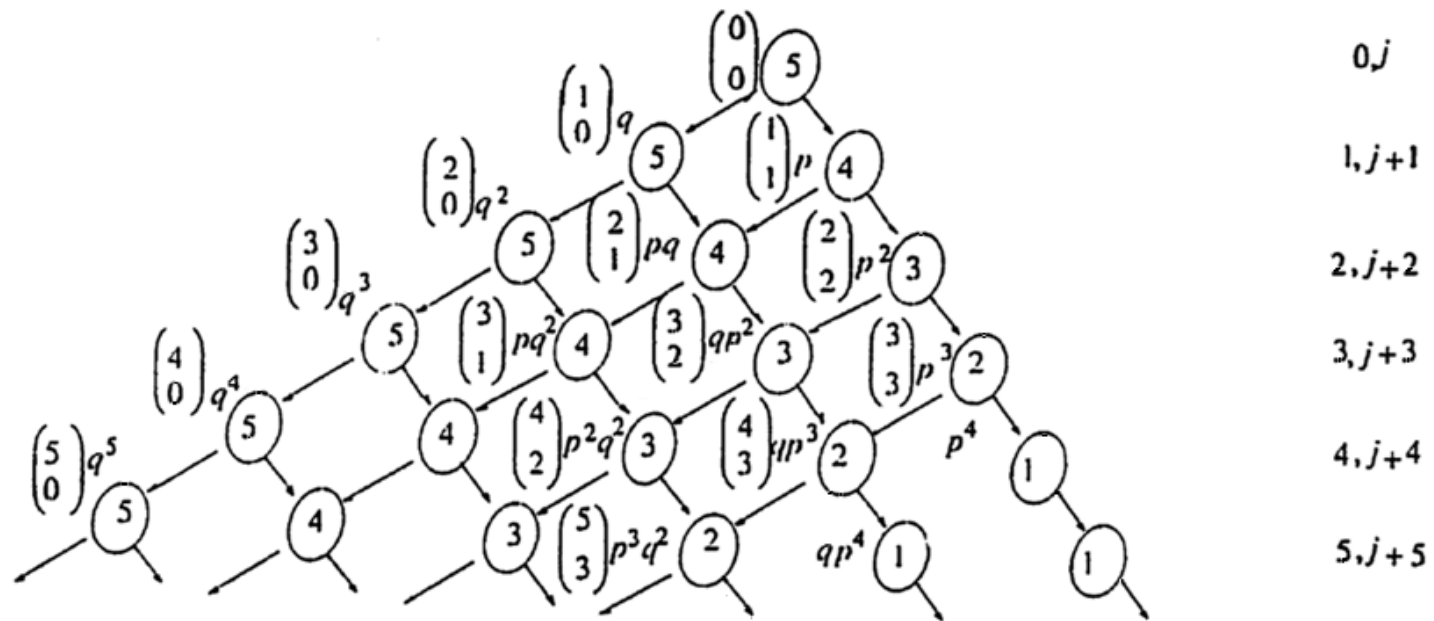
# THE BINOMIAL DISTRIBUTION II



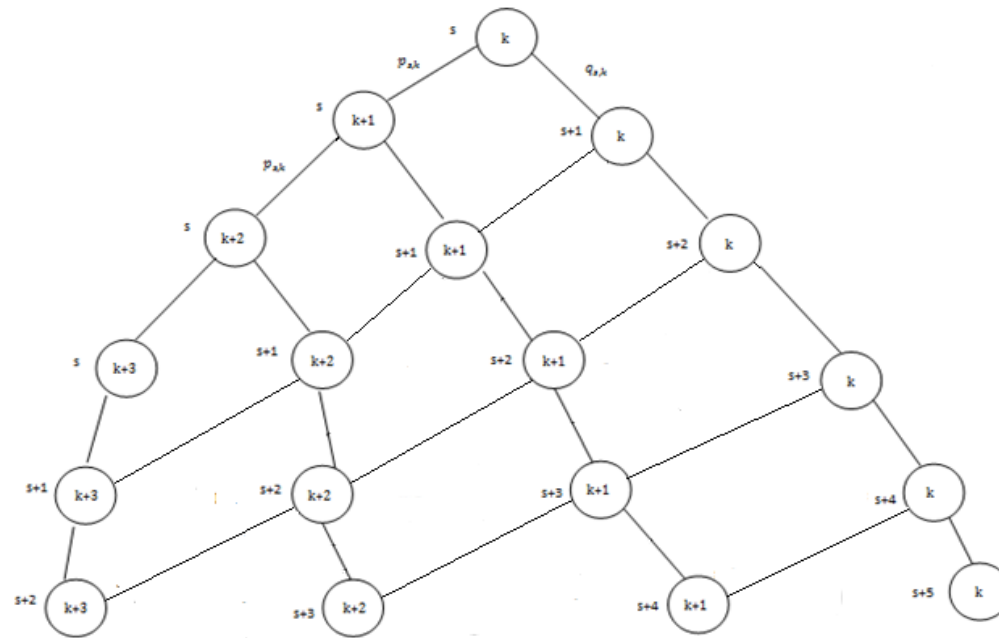
# I CASE WITH MAXIMUM RANK



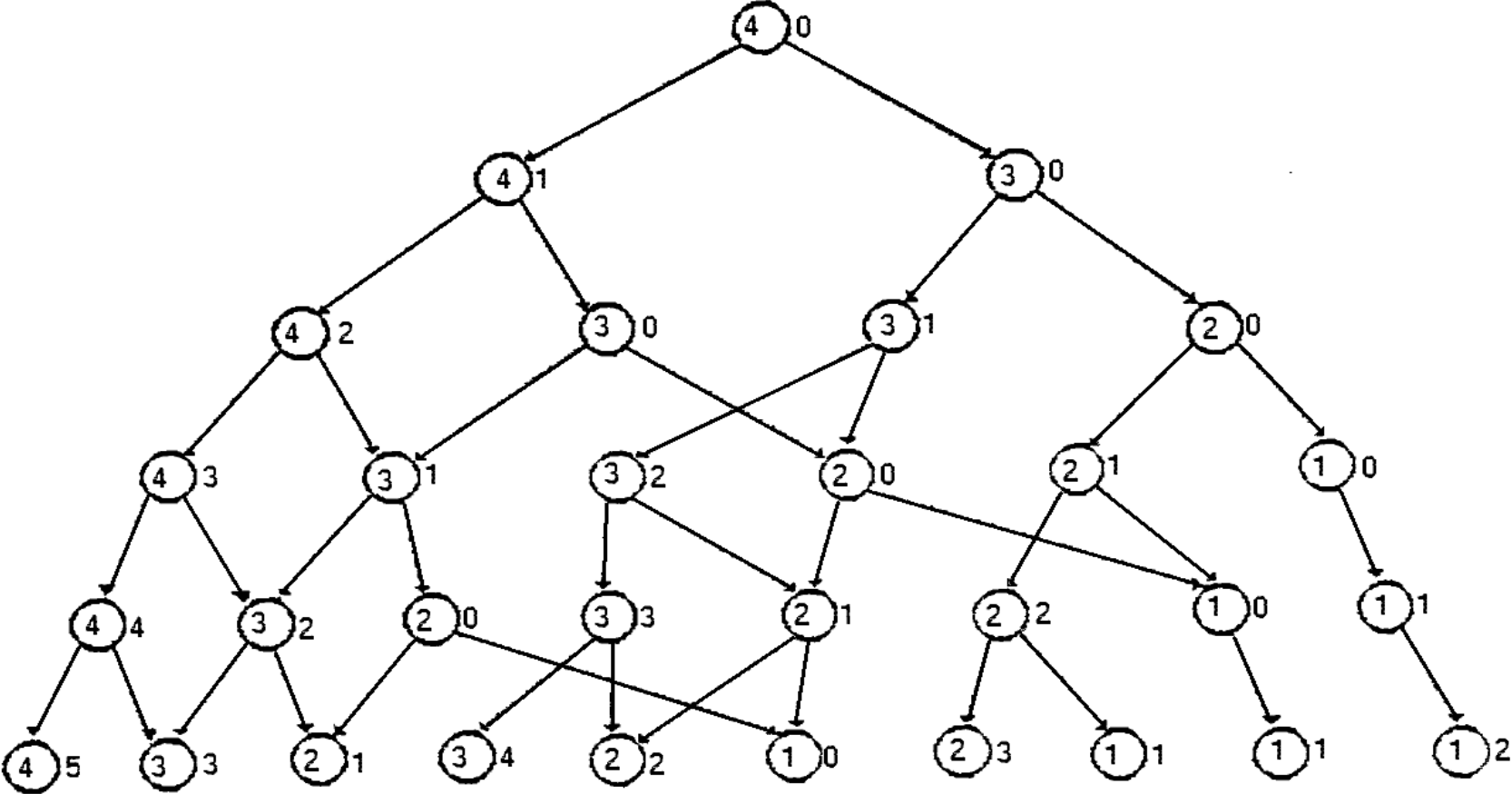
# I CASE: NO CONSTRAINTS



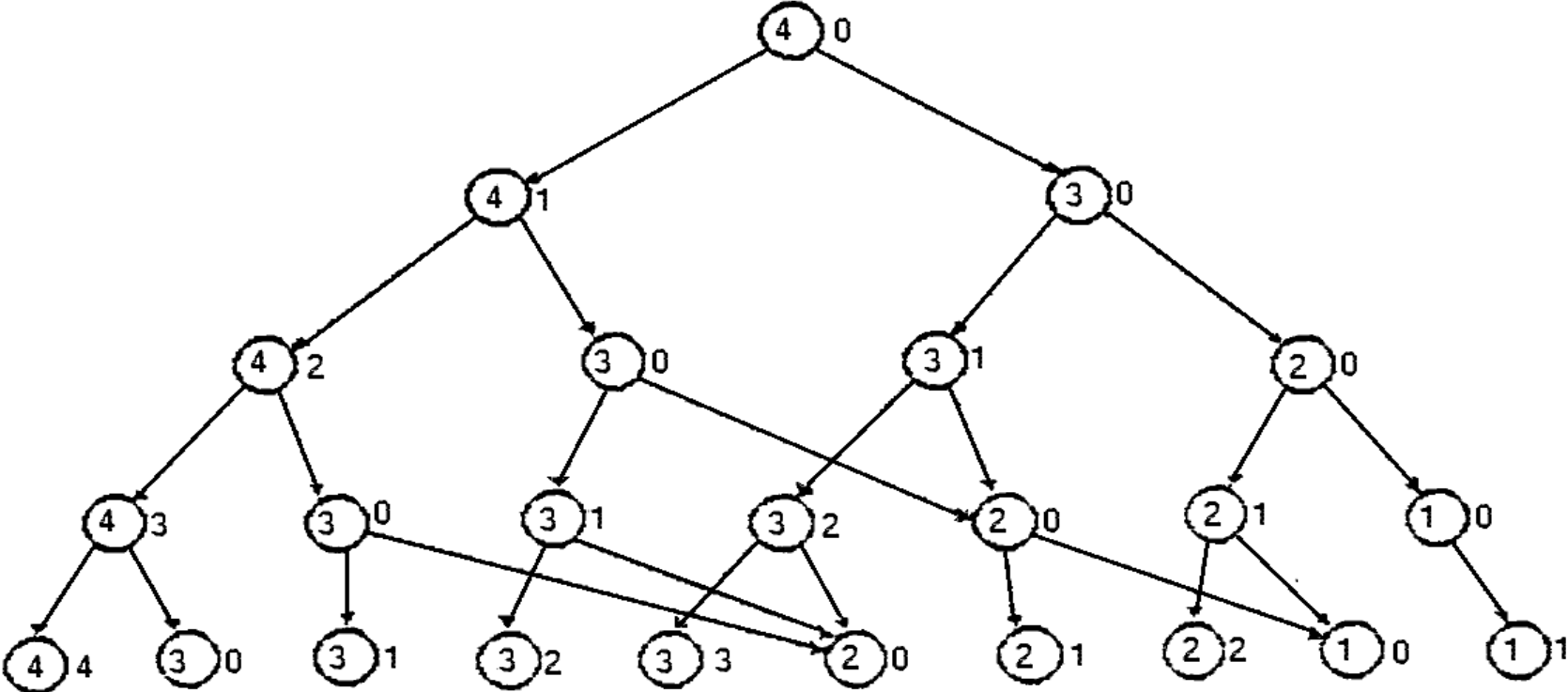
# IICASE WITH PROMOTION LOOSING OF 1 SENIORITY YEAR



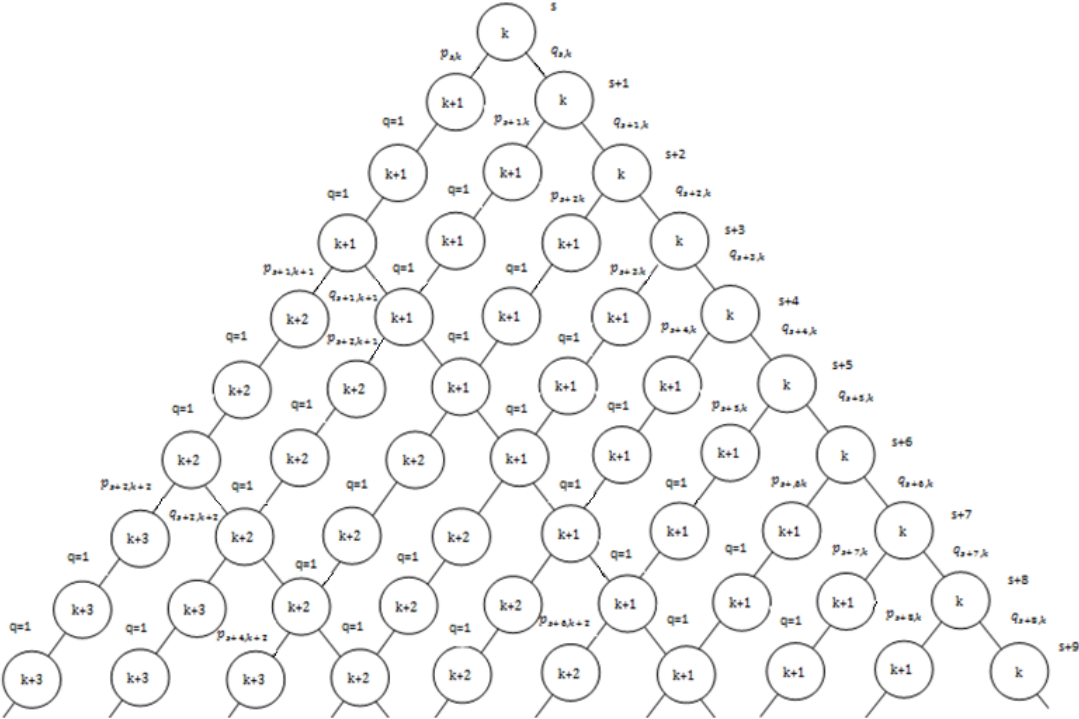
# III CASE WITH PROMOTION LOOSING OF 2 SENIORITY YEARS



# IV CASE WITH PROMOTION LOOSING OF ALL THE SENIORITY



# V SENIORITY IS PRESERVED: AFTER PROMOTION 3 YEARS WITHOUT PROMOTION



# **FUTURE APPLICATION**

Comparison with the usual method of the salary cost calculation

Construction of salary lines in NDC settings with transformation coefficients calculated by direct method for Italy and Sweden and comparison with the coefficients calculated by the public authorities

## SOME REFERENCES

- Blasi A., G. Di Biase & R. Manca. (2003)- A systematic derivation of finite probability distribution by graph theoretic consideration. *Far East Journal of Applied Mathematics*. **13**, 145-164,
- Bartholomew D. J. (1982) *Stochastic processes for social models*, John Wiley.
- Bartholomew D. J., A.F. Forbes, S.I. McClean. (1991). *Statistical Techniques for Man Power Planning*, Wiley
- D'Amico G., Di Biase G., Gismondi F. & Manca R. (2010). Generalized Non-Homogeneous Semi-Markov and Bernoulli Processes for Salary Lines Construction. *SMTDA 2010*
- D'Amico G., Di Biase G., Gismondi F. & Manca R. (2013). The Evaluation of Generalized Bernoulli Processes for Salary Lines Construction by Means of Continuous Time Generalized Non-Homogeneous Semi-Markov Processes, *Communications in Statistics - Theory and Methods*, **42**:16, 2889-2901
- Di Biase G. & Manca R. (2001). Generation and enumeration of atoms in the presence of logical constraints through binary trees *Far East Journal of Mathematical Science*.
- Di Biase G. & Manca R. (2006) Atoms, Binary Trees and dichotomic non Markovian Processes. *Far East Journal of Applied Mathematics*. **22**, 1-16.
- Janssen J. & Manca R. (2002). Salary cost evaluation by means of non-homogeneous semi-Markov processes. *Stochastic Models*, **18**, 7-23.
- Gismondi F., R. Manca & Swishchuk A. V. (2010). Salary lines forecasting by means of generalized binomial processes. *International Journal of Management Science and Engineering Management*, vol 4, 309- 320,-
- J. Janssen & R. Manca .(1997). Mean salary lines construction, a stochastic approach. *Scritti in onore di Giuseppe Ottaviani*, Roma
- Vajda S. (1978) *Mathematics of manpower management*. John Wiley

I THANK YOU

# Optimal scaling and contingency tables reveal the mismatch between patients' attitude and perception towards their asthma medications and complaints during the I-MUR service provision

Andrea Manfrin<sup>1</sup>, Cecilio Mar Molinero<sup>2</sup>, Janet Krska<sup>3</sup>

<sup>1</sup> Senior Lecturer in Pharmacy Practice at Sussex School of Pharmacy, School of Life Sciences, University of Sussex, Brighton, UK (a.manfrin@sussex.ac.uk)

<sup>2</sup> Emeritus Professor at Kent Business School, University of Kent, UK (C.Mar-Molinero@kent.ac.uk)

<sup>3</sup> Professor of Clinical and Professional Practice at Medway School of Pharmacy, University of Greenwich and Kent, UK (J.Krska@kent.ac.uk)

## Abstract

Asthma prevalence is increasing and the economic loss due to lack of asthma control is €72 billion in EU 28. Pharmacists have a role to play, and a bespoke novel pharmacist-led intervention for asthma patients, called Italian Medicines Use Review (I-MUR), has shown both effectiveness and cost-effectiveness. The I-MUR intervention enables asthma patients to optimise the effect of their medications. This study aimed at assessing the mismatch between patients' attitude-perception towards their medications and their complaints during the I-MUR service provision. The I-MUR was provided in four different Italian locations; data were collected and analysed using descriptive statistics, optimal scaling and contingency tables. The number of pharmacists and asthma patients involved in the study was 74 and 895 respectively. The majority of patients (72%) did not believe that they had problems with their medications, 78% confirmed that they had full knowledge and understanding of their medications, 75% said that their medications were working and 45% confirmed that they missed a dose. The number of patients who raised complaints was 683 (76%) and the number of complaints raised by each patient ranged between 1 to 5. Only 18% of the patient population reported having neither medicine-related problems nor asthma-related complaints. The use of optimal scaling and contingency tables unveiled the mismatch between patients' attitude-perception towards their medicines and the type and number of complaints raised by them during the I-MUR service provision.

**Keywords:** optimal scaling, contingency tables, asthma, patients, attitude, perception, complaints, Italian Medicines Use Review, community pharmacy



## 1. Introduction

### What is asthma?

Asthma is a very old word. In modern medical texts, the word "asthma" first originated from the Greek word derived from the verb *Aazein* (breath hard), meaning to exhale with an open mouth or to pant (Asthma History – Through The Ages). Homer mentioned it in some of his books (*Iliad* and *Odyssey*). Originally, asthma did not mean wheeze, but rather noisy breathing, making a blowing nose, panting or even groaning.

Asthma is a chronic pulmonary inflammatory disease that can result in the narrowing of the airways and reversible airflow obstruction when triggered by a variety of stimuli. The narrowing of the airways in the lungs can be caused by one, or a combination, of the following changes (GINA, 2015) [1]:

- swelling of the airways;
- tightening of the muscles surrounding the airways (known as bronchoconstriction);
- production of excess mucus, which can obstruct the airways; and
- long-term damage to the walls of the airways, which prevents them from opening as widely as normal.

### Epidemiology and economic burden of asthma

The prevalence of asthma has been increasing since the late 1990's and it has been estimated that about 400 million people will suffer from asthma by 2025 [2, 3]. Currently, the number of disability-adjusted life years (DALYs) lost to lack of control of asthma worldwide translates into a global loss of 15 million DALYs per year and an estimated one in every 250 deaths worldwide is caused by asthma. Asthma accounts for an economic loss of €72 billion annually in the 28 countries of the EU [4]; this includes the annual costs of health care (about €20 billion), the loss of productivity for patients (€14 billion), and a monetised value of DALYs loss of €38 billion.

### Role of pharmacists in asthma management

Many studies have been published showing the role of pharmacists in asthma management.[5-20] A recent systematic review and meta-analysis of randomised controlled trials of medication review (pharmacist-led consultation) suggested that an isolated medication review has minimal effect on clinical outcomes, no effect on quality of life, and lacks evidence of economic outcomes; although studies have shown a decrease in the number of drug-related problems, more changes in medication, more drugs with dosage decrease and a greater decrease or smaller increase of the number of drugs used. [21]

A recent publication [22] has demonstrated that a novel bespoke pharmacist-led intervention for asthma patients provided effectiveness and cost-effectiveness; this intervention is called Italian Medicines Use review (I-MUR). This novel intervention is a face to face consultation provided by community pharmacists to asthma patients. The I-MUR consisted of a systematic, structured interview with 22 closed answer questions, conducted in a private room within the pharmacy, which covered asthma symptoms, medicines used, attitudes towards medicines and adherence.

Amongst the key success factors of I-MUR, there are some questions tailored to reveal the possible mismatch between patients' attitude and perception about their medicines and their complaints about asthma symptoms, if any.

These types of information were extremely important because they prompted the pharmacists not only to be proactive but also to make the best and most appropriate recommendations during the consultation. This was deemed to be a crucial factor in the success of this pharmacist-led intervention.

## 2. Aim

This paper aimed at assessing the mismatch between patients' attitude and perception towards their medications and their complaints during the I-MUR service provision, using optimal scaling and contingency tables.

## 3. Method

The development of I-MUR was guided by the Medical Research (MRC) Framework for the development of complex intervention, and retrospectively mapped to it. The justification of this approach relies on the fact that I-MUR is a complex intervention.

Full details of the I-MUR development process, data gathering during the study, inclusion, exclusion criteria, patient recruitment, I-MUR provision and data collection have been published elsewhere [23].

### **Data analysis**

Data were analysed using descriptive statistics, contingency tables (cross-tabulation) for categorical data; Goodman and Kruskal's gamma was used for non-parametric data when they had many tied ranks. The questions relative to patients' attitude and perceptions were analysed using an optimal scaling technique called correspondence analysis.

### **Optimal scaling**

Meulman (1998) in her SPSS white paper entitled "Optimal scaling methods for multivariate categorical data analysis" suggested that the aim of the optimal scaling procedure is to turn qualitative variables into quantitative one. This aspect is extremely important in particular for researchers working in social and behavioural science, because they are often required to use data which are non-numerical, where the recorded measurements are recorded on a scale and therefore have an uncertain unit of measurement. [24] Categories procedures use optimal scaling to analyse data that are difficult or impossible for standard statistical procedures to analyse. These procedures and their implementation were developed for IBM SPSS Statistics by the Data Theory Scaling System Group (DTSS), consisting of members of the Department of Education and Psychology, Faculty of social Behavioural Science at Leiden University in the Netherland. The approach adopted by optimal scaling is to assign numerical quantification to the categories of each variable, thus allowing standard procedures to be used to obtain a solution on the quantified variable. [25]

The optimal scaling procedure used for our analysis was correspondence analysis, because it was recognised as the best statistical approach in our case.

### **Correspondence analysis**

Correspondence analysis (CA) was applied to explore the correlation between two sets of variables (contingency table) producing a visual map which highlighted the correspondence between rows and columns. CA can suggest unexpected dimensions and relationships between categorical data, and the results can be seen analytically and visually.[26]

The CA methodology was initially proposed by Hirschfeld in 1935, [27] it was further developed in France in 1973 by Benzécri et al. [28]; then Greenacre introduced the "Theory and Applications of Correspondence Analysis" in 1984. [29]

The principle of CA is conceptually similar to principal component (PC) analysis, but CA is applied to categorical data, while PC is applied to continuous data. It is possible to use CA for the analysis of cases-by-variables categories matrices for non-negative data. CA is also a multivariate descriptive data analytic technique. As already mentioned, the results and information provided by CA are very similar to the ones provided by PC and factor analysis (FA).[30] The graphical representation provided by CA shows the relationships between column and row categories simplifying complex data and providing detailed descriptions of nearly every single piece of information encapsulated in the data set, yielding a simple but exhaustive analysis.[31-32]

## **4. Results**

The number of pharmacists who completed the study providing the I-MUR service was 74, the number of patients who received the service was 895. The pharmacists were deliberately divided between the four Italian locations, Brescia, Pistoia, Torino, and Treviso.

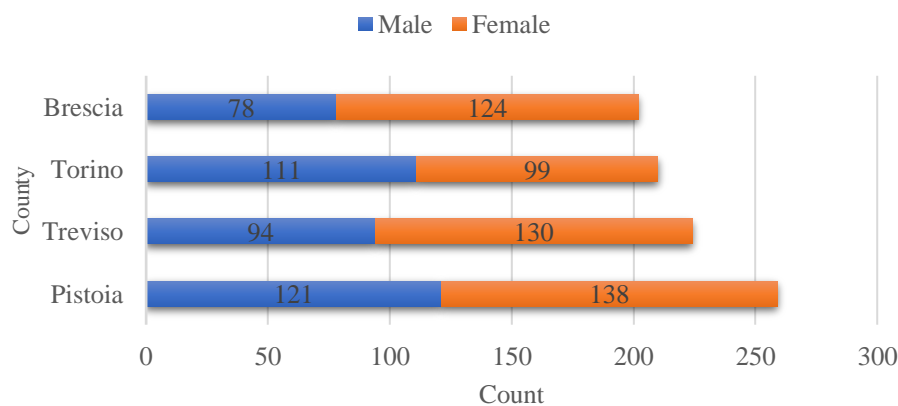
### **Patients' demographic data**

Patients were unevenly split by gender, 45.13% (n=404) were male and 54.86% (n=491) female, their ages are shown in Table 1 and the distribution across the four Italian counties in Figure 2.

**Table 1 Age range of patients receiving I-MURs**

Patients' age	N	%
Between 18 and 30 years old	87	9.70
Between 31 and 40 years old	83	9.30
Between 41 and 50 years old	128	14.30
Between 51 and 60 years old	146	16.30
Between 61 and 70 years old	185	20.70
Between 71 and 80 years old	185	20.70
Over 81 years old	78	8.70
Total	892	99.70
Missing data	3	0.30
Total	895	

**Figure 2 Patients' distribution according to gender and county**



**Patient attitudes towards their medications and adherence to treatment**

The majority of patients confirmed they did not believe they had problems with their medications 72.20% (n=640), while only 25.60% (n=227) indicated they did have some problems and 2.10% (n=19) believed they had lots of problems. Hence there were 27.80% (n=246) patients with self-reported problems. The vast majority of patients 77.80% (n=689) confirmed that they had full knowledge and understanding of their medicines, 21.10% (n=187) only partially and 1.10% (n=10) did not know how to take their medications. In order to visualise the relations between these two sets of responses, correspondence analysis was used.

Figure 3 Matching problems with knowledge and understanding

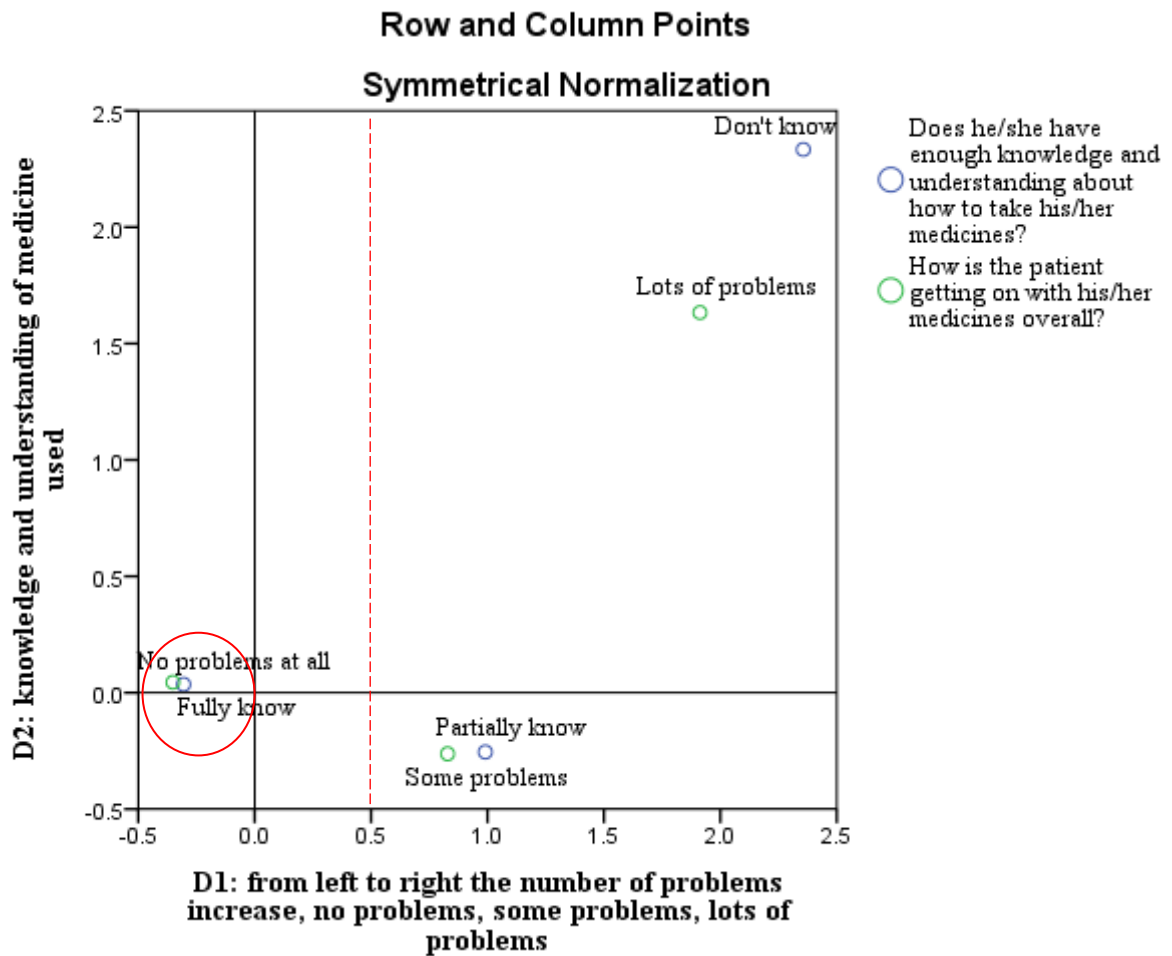


Figure 3 gives a clear representation of the relation that was found between patients' knowledge and how they get on with their medication: Dimension 2 (D2) is related to patients' knowledge and understanding of their medications and dimension 1 (D1) is showing whether or not patients report having problems with their medications. It appears clear that patients who have a full understanding of their medication do not have problems; patients who have only partial knowledge of their medications have some problems, meanwhile the ones who do not know much about their medication have lots of problems. The dotted red line represents a division of the figure in two parts: left-hand side and right-hand side. The left-hand side of D1 represents patients who did not have problems, they confirmed that they knew and understood their medication fully (>70%) meanwhile the right-hand side represents the percentage (<30%) of patients who were having some/lots of problems and confirmed either knowing their medicines only partially or not knowing at all. A positive linear correlation was found between these variables ( $\gamma = 0.649$ ,  $p < 0.01$ ).

A similar analysis between believing medicines are working and expected efficacy was conducted. The proportion of patients (n=882) who thought that all their medicines were working was 74.70% (n=659), 20.40% (n=180) confirmed that some are working, 0.70% (n=6) none are working and 4.20% (n=37) did not know. The proportion (n=882) who thought their medicines were as effective as he/she was expecting were 75.60% (n=667), the ones who did not 14.70% (n=130) and 9.60% (n=85) did not know.

**Figure 4 Patterns between patients' expectation and are medicines working**

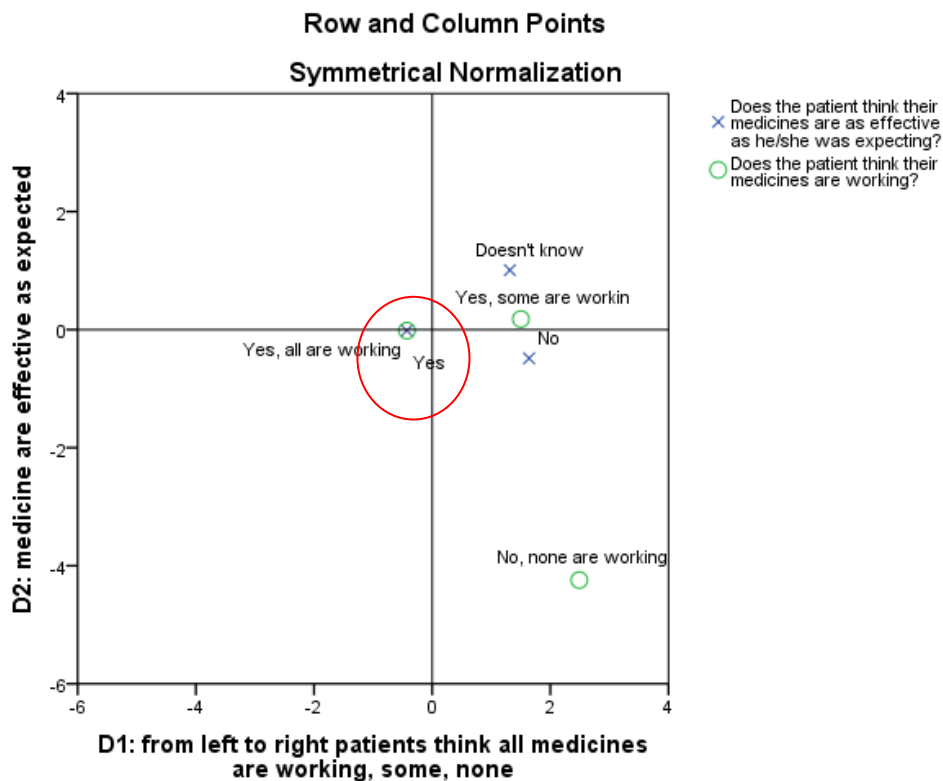


Figure 4 represents patients' perceptions about their medications. D1 explains, from left to right, the way in which patients perceive how their medicines were working, and this value decrease moving from the left side to the right side of the X-axis. D2 shows if patients believe that their medications were effective as they were expecting. D2 is not clearly interpreted as D1. The statement "No, none are working" stands alone only, five patients chose this option. Patients who have chosen "yes some are working" is placed between the other two statements "does/t know and "No". In this figure, the red circle shows patients who confirm that all the medicines they used were working according to their expectation. A strong positive linear correlation was found between the two questions ( $r = 0.88, p < 0.01$ ).

#### Patients' self-reported adherence to asthma medications

Adherence to treatment was assessed using two questions adapted from the MMAS 8-items. [33] Of the 895 cases, the question: "Does the patient miss any doses of his/her medicines or change when he/she takes them?" was completed in 882 cases. Of these, 44.58% (n=399) patients confirmed that they miss a dose or change when they take their medications, 51.40% (n=453) did not and 3.40% (n=30) did not know. In the entire sample population, 50.50% (n=202) of male patients were potentially non-adherent to treatments compared to 40.90% (n=197) of females. The last time the patient missed a dose was reported for 623 cases. This showed that 54.50% (339) patients did not remember when was the last time they missed a dose, 12.40% (n=77) last week, 11.90% (n= 74) this week and last month, 9.30% (n=58) yesterday.

### Problems and complaints

After the initial question about problems with medicines, the I-MUR template included a list of specific complaints relating to asthma, about which patients were asked. The responses are summarized in Table 2.

**Table 2 Self-reported complaints identified by patients during I-MUR interviews**

Complaints	N	% of incidence of each complaint
Daytime symptoms such as shortness of breath, tightness in the chest, coughing, wheezing, or exacerbations	470	35.91
Limitation on activity, including exercise	357	27.27
Need for rescue medication	237	18.11
Night time awakening	180	13.75
Other	65	4.97
Total number of complaints	1309	

The number of patients who indicated they had one or more complaints was 683 (76.3%). The total number of different complaints identified by patients was 1309 (Table 3) with a mean of 1.9 per patient; patients could select multiple options, therefore, the percentages do not sum to 100%. Complaints related to daytime symptoms were most frequently identified by 470 (35.91%); 9.5% (65) were classified as others such as hands shaking, muscle pain, heat, dizziness, tachycardia, fatigue. Positive correlations were found between age and number of complaints ( $\rho=0.12$ ,  $p<0.001$ ), number of active ingredients and number of complaints ( $\rho=0.25$ ,  $p<0.01$ )

**Table 3 Number of complaints made by patients**

No of complaints	No of patients	%
1	289	42.31
2	218	31.92
3	122	17.86
4	50	7.32
5	4	0.59
Total	683	

A cross-tabulation of the two questions was conducted to find out if patients who did not indicate any problems with medicines subsequently confirmed not having asthma-related complaints, when specific questioning was used (Table 4).

**Table 4 Cross-tabulation of multiple response sets: Complaints versus problems**

Does the patient complain.....	Problems		Total
	(no problems)	(some/lots)	
Daytime symptoms such as shortness of breath, tightness in the chest, coughing, wheezing, or exacerbations	291	175	466
Night time awakening	105	74	179
Need for rescue medication	141	96	237
Limitation on activity, including exercise	217	137	354
No complaints	144	10	154
Total	575	232	807

Comparison of responses to these two questions indicated that 10 patients out of the 807 (90.2%=802/895) who replied to both questions had no complaints, but did have medicine-related problems. However, of the 575 who indicated that they did not have medicine-related problems, only 144 (25.04%) also had no asthma-related complaints. Overall only 144 (17.84% =144/807) patients reported having neither medicine-related problems nor asthma-related complaints.

## 5. Conclusions

The use of correspondence analysis enabled the visualisation of patients' attitude towards their medication indicating that the vast majority of patients were happy with their medications. Nevertheless, different results were highlighted by tables showing patients' complaints. The results are showing a clear mismatch between patients' attitude and perception and the reality. In fact, data gathered during the I-MUR service showed that of 575 patients who initially indicated they did not have any medicine-related problems, the majority, in fact, had at least one asthma-related complaint.

The combination of CA and cross-tabulation allowed acquiring a clear picture regarding the mismatch between patients' attitude-perception and the type and number of complaints raised by the patients.

This project is the first project ever conducted in Italian community pharmacy testing whether pharmacists were able to undertake the process of completing an I-MUR with asthma patients and uploading the data onto the platform. The results have shown one of the first application of CA to analyse the results obtained during a pharmacist-led intervention. These results need to be confirmed by a larger study.

This analysis provided a clear insight into patients' attitude-perception and the mismatch between these two domains and the type and numbers of complaints raised by the patients as well. This mismatch prompted the pharmacist to act pro-actively making suggestions and recommendations to asthma patients. [22]

### **Acknowledgments**

The authors thank the Italian pharmacists, general practitioners, and consultants, patients and all other people who have been involved in the studies.

### **Financial support**

The authors are grateful to the Italian Pharmacists' Federation (FOFI) to Ordine dei farmacisti di Brescia, Pistoia, Torino and Farmarca Treviso who founded the project.

### **Conflict(s) of Interest**

None.

### **Ethical Standard**

The authors assert that all procedures contributing to this work comply with the ethical standards of the relevant national and institutional guidelines on human experimentation and with the Helsinki Declaration of 1975, as revised in 2008. The study was approved by the University of Kent Ethics Advisory Group for Human Participants on September 19<sup>th</sup>, 2012 (ref. No 020S11/12).

### **Informed consent**

Informed consent was obtained from all individual participants included in the study. Participants consented to the study after full explanation of what was involved was given. Signed consent forms from pharmacists were retained in the University. Signed consent forms from patients were retained by pharmacists in the pharmacies.

### **Anonymity and data storage**

Data obtained during I-MUR consultations were coded and stored electronically on a computer system at the University of Kent, in a directory which is password protected. Hard copies of any patient data, if any were collected during the I-MUR, were the responsibility of the participating Italian pharmacists to store in a secure filing cabinet in their pharmacies. All electronic data regarding this study have been password protected and are accessible only by the researcher.

## **References**

1. Global Initiative for Asthma. Pocket guide for asthma management and prevention – Global Initiative for asthma - GINA. 2015. Available from: <http://ginasthma.org/2016-pocket-guide-for-asthma-management-and-prevention/> [Accessed 23rd September 2016].
2. De Marco R, Cappa V, Accordini S, Rava M, Antonicelli L, Bortolami O, et al. Trends in the prevalence of asthma and allergic rhinitis in Italy between 1991 and 2010. *Eur Respir J.* 2012;39:883–92.
3. Masoli M, Fabian D, Holt S, Beasley R. Global Burden of Asthma. The global burden of asthma: executive summary of the GINA Dissemination Committee Report. *Allergy.* 2004;59(5):469-78. Available from: [http://ginasthma.org/local/uploads/files/GINABurdenSummary\\_1.pdf](http://ginasthma.org/local/uploads/files/GINABurdenSummary_1.pdf) (2003). (Accessed 20th October 2015).
4. European Respiratory Society. European Lung White book. The economic burden of lung disease. <http://www.erswhitebook.org/chapters/the-economic-burden-of-lung-disease/> (2016). [Accessed 10th Sept 2015].
5. Barbanel D, Eldridge S, Griffiths C. Can a self-management programme delivered by a community pharmacist improve asthma control? A randomised trial. *Thorax.* 2003;58(10):851–4.
6. Bunting BA, Cranor CW. The Asheville project: long-term clinical, humanistic, and economic outcomes of a community-based medication therapy management program for asthma. *J Am Pharm Assoc.* 2006;46(2):133–47.
7. Emmerton L, Shaw J, Kheir N. Asthma management by New Zealand pharmacists: a pharmaceutical care demonstration project. *J Clin Pharm Ther.* 2003;28(5):395–402.
8. McLean W, Gillis J, Waller R. The BC community pharmacy asthma study: a study of clinical, economic and holistic outcomes influenced by an asthma care protocol provided by specially trained community pharmacists in British Columbia. *Can Respir J.* 2003;10:195–202
9. Mehuys E, Van Bortel L, De Bolle L et al. Effectiveness of pharmacist intervention for asthma control improvement. *Eur Respir J.* 2008;31(4):790–9.

10. García-Cárdenas V, Sabater-Hernández D, Kenny P, et al. Effect of a pharmacist intervention on asthma control. A cluster randomised trial. *Respir Med.* 2013;107(9):1346–55.
11. García-Cardenas V, Armour C, Benrimoj SI et al. Pharmacists' interventions on clinical asthma outcomes: a systematic review. *Eur Respir J.* 2016;47:1043–1046. doi: 10.1183/13993003.01497-2015
12. Herborg HB, Soendergaard B, Jorgensen T et al. Improving drug therapy for patients with asthma-part 2: Use of antiasthma medications. *J Am Pharm Assoc.* 2001;41(4):551-559.
13. Schulz M, Verheyen F, Mühlig S et al. Pharmaceutical care services for asthma patients: A controlled intervention study. *J Clin Pharmacol.* 2001;41(6):668-76.
14. Saini B, Krass I, Armour C. Development, implementation, and evaluation of a community pharmacy-based asthma care model. *Ann Pharmacother.* 2004;38:1954–60.
15. Armour C, Bosnic-Anticevich S, Brillant M et al. Pharmacy asthma care program (PACP) improves outcomes for patients in the community. *Thorax.* 2007;62:496–502.
16. Narhi U, Airaksinen M, Tanskanen P, Erlund H. Therapeutic outcomes monitoring by community pharmacists for improving clinical outcomes in asthma. *J Clin Pharm Ther.* 2000;25:177–83.
17. Haathela T, Toumisto LE, Pietinalho A et al. A 10 year asthma programme in Finland: major change for the better. *Thorax.* 2006;61(8):663:670.
18. Mangiapane S, Schulz M, Mühlig S et al. Community pharmacy-based pharmaceutical care for asthma patients. *Ann Pharmacother.* 2005;39(11):1817–22.
19. Cordina M, McElnay JC, Hughes CM. Assessment of a community pharmacy-based program for patients with asthma. *Pharmacotherapy.* 2001;21(10):1196–203
20. Armour CL, Reddel HK, LeMay KS et al. Feasibility and effectiveness of an evidence-based asthma service in Australian community pharmacies: a pragmatic cluster randomized trial. *J Asthma.* 2013;50(3):302-9. doi: 10.3109/02770903.2012.754463
21. Huiskes VJB, Burger DM, van den Ende CHM et al. Effectiveness of medication review: a systematic review and meta-analysis of randomized controlled trials. *BMC Fam Pract.* 2017;18(1):5. <https://doi.org/10.1186/s12875-016-0577-x>.
22. Manfrin A, Tinelli M, Thomas T, Krska J. A cluster randomised control trial to evaluate the effectiveness and cost-effectiveness of the Italian medicines use review (I-MUR) for asthma patients. *BMC Health Serv Res.* 2017. <https://doi.org/10.1186/s12913-017-2245-9>.
23. Manfrin A, Thomas T, Krska J. Randomised evaluation of the Italian medicines use review provided by community pharmacists using asthma as a model (RE I-MUR). *BMC Health Serv Res.* 2015. <http://dx.doi.org/10.1186/s12913-015-0791-6>
24. Meulman J.J. Optimal scaling methods for multivariate categorical data analysis. Data Theory Group Faculty of Social and Behavioural Sciences Leiden University (The Netherlands). SPSS white paper. 1998;1-12. Available from: <http://citeseerx.ist.psu.edu/viewdoc/download?doi=10.1.1.476.904&rep=rep1&type=pdf>. [Accessed 15<sup>th</sup> December 2017]
25. IBM SPSS categories 22, Available from: [http://www.sussex.ac.uk/its/pdfs/SPSS\\_Categories\\_22.pdf](http://www.sussex.ac.uk/its/pdfs/SPSS_Categories_22.pdf) (Accessed 14 December 2017)
26. Ayele, D., Zewotir, T. and Mwambi, H. Multiple correspondence analysis as a tool for analysis of large health surveys in African settings. *African Health Sciences.* 2015;14(4):1036
27. Hirschfeld, H.O. "A connection between correlation and contingency", *Proc. Cambridge Philosophical Society.* 1935;31:520–524
28. Benzécri J-P. *Analyse des Donneés.* 1 and 2. Dunod; 1973. (Fre).
29. Greenacre MJ. *Theory and Applications of Correspondence Analysis.* Academic Press; 1984.
30. Hill MO. Correspondence Analysis: A Neglected Multivariate Method. *Journal of the Royal Statistical Society.* 1974;23(3):340–354.
31. Greenacre MJ, Blasius J. *Multiple correspondence analysis and related methods.* Boca Raton: Chapman & Hall/CRC; 2006.
32. Johnson RA, Wichern DW. *Applied multivariate statistical analysis.* Vol. 6. New Jersey: Pearson/Prentice Hall; 2007.
33. Morisky DE, Alfonso A, Krousel-Wood M, Ward HJ. Predictive validity of a medication adherence measure in outpatient setting. *J Clin Hypertens.* 2008;10(5):348–54.

# Advanced Monte Carlo pricing of European options in a market model with two stochastic volatilities

Anatoliy Malyarenko<sup>1</sup>, Ying Ni<sup>1</sup>, Betuel Canhanga<sup>2</sup>, and Sergei Silvestrov<sup>1</sup>

<sup>1</sup> Division of Applied Mathematics, School of Education, Culture and Communication, Mälardalen University, Box 883, SE-721 23 Västerås, Sweden (E-mail: [anatoliy.malyarenko@mdh.se](mailto:anatoliy.malyarenko@mdh.se), [ying.ni@mdh.se](mailto:ying.ni@mdh.se), [sergei.silvestrov@mdh.se](mailto:sergei.silvestrov@mdh.se))

<sup>2</sup> Faculty of Sciences, Department of Mathematics and Computer Sciences, Eduardo Mondlane University, Box 257, Maputo, Mozambique (E-mail: [betuel.canhanga@mdh.se](mailto:betuel.canhanga@mdh.se))

**Abstract.** We consider a market model with four correlated factors and two stochastic volatilities, one of which is rapid-changing, while another one is slow-changing in time. An advanced Monte Carlo methods based on the theory of cubature in Wiener space, is used to find the no-arbitrage price of the European call option in the above model.

**Keywords:** Stochastic volatility, market model, Monte Carlo method.

## 1 Introduction

Consider a market model

$$\begin{aligned}d\mathbf{X}(t) &= \mu(t, \mathbf{X}(t)) dt + \sum_{i=1}^d \mathbf{V}_i(t, \mathbf{X}(t)) d\mathbf{W}_i^*(t), \\ \mathbf{X}(0) &= \mathbf{X}_0,\end{aligned}\tag{1}$$

where  $\mathbf{X}(t): [0, T] \rightarrow \mathbb{R}^m$  is a stochastic process,  $\mu: [0, T] \times \mathbb{R}^m \rightarrow \mathbb{R}^m$  is the drift,  $\mathbf{V}_i: [0, T] \times \mathbb{R}^m \rightarrow \mathbb{R}^m$  are the diffusion coefficients and  $\mathbf{W}^*(t)$  is the standard  $d$ -dimensional Brownian motion under the risk-neutral probability measure  $\mathbb{P}^*$  defined on a measurable space  $(\Omega, \mathfrak{F})$ . Currently, two general methods of pricing contingent claims in such a model are available: the Feynman–Kac theorem and Monte Carlo simulation.

Using the former method, Canhanga *et al.* [1]–[5] priced a European call option in the model with stochastic security price  $S$ , two stochastic volatilities

---

<sup>5</sup>*th* SMTDA Conference Proceedings, 12–15 June 2018, Chania, Crete, Greece



$V_1$  and  $V_2$  and four factors:

$$\begin{aligned} dS &= (r - q)S dt + \sqrt{V_1}S dW_1^* + \sqrt{V_2}S dW_2^*, \\ dV_1 &= \left( \frac{1}{\varepsilon}(\theta_1 - V_1) - \lambda_1 V_1 \right) dt + \frac{1}{\sqrt{\varepsilon}}\xi_1 \sqrt{V_1}\rho_{13} dW_1^* + \frac{1}{\sqrt{\varepsilon}}\xi_1 \sqrt{V_1(1 - \rho_{13}^2)} dW_3^*, \\ dV_2 &= (\delta(\theta_2 - V_2) - \lambda_2 V_2) dt + \sqrt{\delta}\xi_2 \sqrt{V_2}\rho_{24} dW_2^* + \sqrt{\delta}\xi_2 \sqrt{V_2(1 - \rho_{24}^2)} dW_4^*. \end{aligned} \quad (2)$$

Here  $r$  is the spot risk-free interest rate,  $q$  is the continuously compounded dividend rate,  $\lambda_1, \lambda_2$  are two constants determining market prices of variance risks, the processes  $V_1, V_2$  are mean-reverting variance processes with reversion rates of  $\frac{1}{\varepsilon}, \delta$ , volatilities  $\sqrt{\frac{1}{\varepsilon}}\xi_1$  and  $\sqrt{\delta}\xi_2$ , and long run averages of  $\theta_1, \theta_2$  respectively. The processes  $W_i^*$  are independent Brownian motions. Note that model (2) is a particular case of model (1) for  $m = 3, d = 4$ . In Canhanga *et al.* [13], they used the latter method and compared the answers.

We would like also to refer to the comprehensive books on Monte Carlo based on Glasserman [9] and other stochastic approximation methods by Silvestrov [16,17] for pricing processes, where readers also can find extended bibliographies of works in the area.

In this paper, we apply an advanced numerical Monte Carlo scheme, based on the theory of cubature in Wiener space, to the system (2) and discuss advantages and properties of the scheme.

The rest of the paper is organised as follows. In Section 2 we give a quick introduction to the advanced Monte Carlo simulation scheme using theory of cubature in Wiener space. The simulation algorithm is described in details in Section 3. The results of simulation are presented in Section 4. Section 5 concludes. Necessary results from tensor algebra are described in Appendix A.

## 2 Stochastic cubature formulae

To introduce the subject, consider the one-dimensional Itô stochastic differential equation in integral form:

$$X(t) = X(0) + \int_0^t \mu(X(s)) ds + \int_0^t \sigma(X(s)) dW^*(s), \quad (3)$$

and assume that the functions  $\mu$  and  $\sigma$  are infinitely differentiable and satisfy the linear growth bound. For any twice continuously differentiable function  $f$ , the Itô formula gives

$$f(X(t)) = f(X(0)) + \int_0^t \mathcal{L}^0 f(X(s)) ds + \int_0^t \mathcal{L}^1 f(X(s)) dW^*(s), \quad (4)$$

where

$$\mathcal{L}^0 = \mu \frac{\partial}{\partial x} + \frac{1}{2} \sigma^2 \frac{\partial^2}{\partial x^2}, \quad \mathcal{L}^1 = \sigma \frac{\partial}{\partial x}.$$

Apply the Itô formula (4) to the functions  $f = \mu$  and  $f = \sigma$  in (3). We obtain the simplest non-trivial *Taylor–Itô expansion*

$$X(t) = X(0) + \mu(X(0)) \int_0^t ds + \sigma(X(0)) \int_0^t dW(s) + R$$

with remainder

$$\begin{aligned} R = & \int_0^t \int_0^s \mathcal{L}^0 \mu(X(u)) du ds + \int_0^t \int_0^s \mathcal{L}^1 \mu(X(u)) dW^*(u) ds \\ & + \int_0^t \int_0^s \mathcal{L}^0 \sigma(X(u)) du dW^*(s) + \int_0^t \int_0^s \mathcal{L}^1 \sigma(X(u)) dW^*(u) dW^*(s), \end{aligned}$$

see Kloeden and Platen [11]. One can continue the above process to arbitrarily high order. The result by Kloeden and Platen [11, Section 5.5] is complicated, because the differential operator  $\mathcal{L}^0$  contains the second derivative.

To overcome this difficulty, replace Equation (3) with the equivalent one-dimensional *Stratonovich* stochastic differential equation in integral form:

$$X(t) = X(0) + \int_0^t \tilde{\mu}(X(s)) ds + \int_0^t \sigma(X(s)) \circ dW^*(s),$$

where the second integral is the Stratonovich stochastic integral and the coefficients  $\tilde{\mu}$  and  $\mu$  are connected with the *Stratonovich correction*

$$\tilde{\mu} = \mu - \frac{1}{2} \sigma \sigma'.$$

The solution of a Stratonovich stochastic differential equation transforms according to the deterministic chain rule, so Equation (4) becomes

$$f(X(t)) = f(X(0)) + \int_0^t \tilde{\mathcal{L}}^0 f(X(s)) ds + \int_0^t \mathcal{L}^1 f(X(s)) \circ dW^*(s),$$

where

$$\tilde{\mathcal{L}}^0 = \tilde{\mu} \frac{\partial}{\partial x}.$$

The simplest nontrivial *Stratonovich–Itô expansion* takes the form

$$X(t) = X(0) + \tilde{\mu}(X(0)) \int_0^t ds + \sigma(X(0)) \int_0^t \circ dW(s) + R$$

with remainder

$$\begin{aligned} R = & \int_0^t \int_0^s \tilde{\mathcal{L}}^0 \tilde{\mu}(X(u)) du ds + \int_0^t \int_0^s \mathcal{L}^1 \tilde{\mu}(X(u)) \circ dW^*(u) ds \\ & + \int_0^t \int_0^s \tilde{\mathcal{L}}^0 \sigma(X(u)) du \circ dW^*(s) + \int_0^t \int_0^s \mathcal{L}^1 \sigma(X(u)) \circ dW^*(u) \circ dW^*(s). \end{aligned}$$

Write down the market model (1) in the Stratonovich form

$$\mathbf{X}(t) = \mathbf{X}(0) + \sum_{i=0}^d \int_0^t \mathbf{V}_i(\mathbf{X}(s)) \circ dW_i^*(s), \quad (5)$$

where the Stratonovich correction takes the form

$$V_0^j(\mathbf{y}) = \mu^j(\mathbf{y}) - \frac{1}{2} \sum_{i=1}^d \sum_{k=1}^m V_i^k(\mathbf{y}) \frac{\partial V_i^j}{\partial y_k}(\mathbf{y}), \quad 1 \leq j \leq m. \quad (6)$$

Define the action of the vector field  $\mathbf{V}_i$  on the set of infinitely differentiable functions  $f(\mathbf{y})$  by

$$(\mathbf{V}_i f)(\mathbf{y}) = \sum_{k=1}^m V_i^k(\mathbf{y}) \frac{\partial f}{\partial y_k}(\mathbf{y}).$$

Let  $k$  be a nonnegative integer, and let  $\alpha$  be either the empty set if  $k = 0$  or a multi-index  $\alpha = (\alpha_1, \dots, \alpha_k)$  with integer components  $0 \leq \alpha_i \leq d$ . Define the number  $\|\alpha\|$  as  $k$  plus the number of zeroes among the  $\alpha_i$ 's and call it the *degree* of  $\alpha$ . Let  $I(t, \emptyset, \circ d\mathbf{W}^*)$  be the identity operator, and let

$$I(t, \alpha, \circ d\mathbf{W}^*) = \int_0^t \cdots \int_0^{t_{k-2}} \int_0^{t_{k-1}} \circ dW_{\alpha_k}^*(t_k) \circ \cdots \circ dW_{\alpha_1}^*(t_1)$$

be the multiple Stratonovich integral. The Stratonovich–Itô expansion takes the form

$$f(\mathbf{X}(t)) = \sum_{\|\alpha\| \leq n} I(t, \alpha, \circ d\mathbf{W}^*)(\mathbf{V}_{\alpha_k} \cdots \mathbf{V}_{\alpha_1} f)(\mathbf{x}) + R_n,$$

where  $n$  is a positive integer, and where the remainder  $R_n$  contains multiple Stratonovich integrals of degrees greater than  $n$ .

Let  $C_{\mathbf{0}, \text{BV}}([0, 1]; \mathbb{R}^{d+1})$  be the Banach space of  $\mathbb{R}^{d+1}$ -valued continuous functions of bounded variation in  $[0, 1]$  which start at  $\mathbf{0} \in \mathbb{R}^{d+1}$  with norm

$$\|\mathbf{g}\| = \left( \sum_{i=0}^d (\text{Var}([0, 1]; g_i))^2 \right)^{1/2},$$

where  $\text{Var}([0, 1]; g_i)$  is the total variation of the  $i$ th component  $g_i$  of a function  $\mathbf{g} \in C_{\mathbf{0}, \text{BV}}([0, 1]; \mathbb{R}^{d+1})$ . Let  $\mathfrak{B}$  be the  $\sigma$ -field of the Borel sets of the above space. A *random path* is a measurable map  $\omega: \Omega \rightarrow C_{\mathbf{0}, \text{BV}}([0, 1]; \mathbb{R}^{d+1})$ .

Along with the system (5), consider the following system of *random* ordinary differential equations in the integral form:

$$\tilde{\mathbf{X}}(t) = \mathbf{X}(0) + \sum_{i=0}^d \int_0^t \mathbf{V}_i(\tilde{\mathbf{X}}(s)) d\omega_i(s). \quad (7)$$

Let  $\tilde{\mathbf{X}}_\omega(t)$  be its solution.

Define the time-scaled random path  $\omega[t](s): \Omega \rightarrow C_{\mathbf{0}, \text{BV}}([0, t]; \mathbb{R}^{d+1})$  by

$$\omega_i[t](s) = \begin{cases} t\omega_0(s/t), & \text{if } i = 0, \\ \sqrt{t}\omega_i(s/t), & \text{if } 1 \leq i \leq d, \end{cases}$$

and the probability measure  $\mu$  on  $\mathfrak{B}$  by

$$\mu(A) = \mathbf{P}^*(\omega^{-1}(A)), \quad A \in \mathfrak{B}.$$

Let  $f(\mathbf{y})$  be the discounted payoff of a financial instrument. We would like to estimate the *weak approximation error*

$$\begin{aligned} & |\mathbf{E}^*[f(\mathbf{X}(t))] - \mathbf{E}[f(\tilde{\mathbf{X}}_{\omega[t]}(t))]| \\ &= \left| \int_{\Omega} f(\mathbf{X}(t)) \, d\mathbf{P}^*(\omega) - \int_{C_{\mathbf{0}, \text{BV}}([0, t]; \mathbb{R}^{d+1})} f(\tilde{\mathbf{X}}_{\omega[t]}(t)) \, d\mu(\omega) \right|, \end{aligned}$$

when we replace the true price  $\mathbf{E}^*[f(\mathbf{X}(t))]$  of the financial instrument with its approximate value  $\mathbf{E}[f(\tilde{\mathbf{X}}_{\omega[t]}(t))]$ . The deterministic Taylor formula for  $f(\tilde{\mathbf{X}}_{\omega[t]}(t))$  has the form

$$f(\tilde{\mathbf{X}}_{\omega[t]}(t)) = \sum_{\|\alpha\| \leq n} I(t, \alpha, d\omega[t]) (\mathbf{V}_{\alpha_k} \cdots \mathbf{V}_{\alpha_1} f)(\mathbf{x}) + \tilde{R}_n,$$

where

$$I(t, \alpha, d\omega[t]) = \int_0^t \cdots \int_0^{t_{k-2}} \int_0^{t_{k-1}} d\omega_{\alpha_k}(t_k) \cdots d\omega_{\alpha_1}(t_1).$$

The following definition was proposed by Kusuoka [12].

**Definition 1 (The moment matching condition).** The measure  $\mu$  satisfies the *moment matching condition* of order  $n$  and is called a *cubature formula* of degree  $n$ , if

$$|\mathbf{E}^*[I(t, \alpha, \text{od}\mathbf{W}^*)] - \mathbf{E}[I(t, \alpha, d\omega)]|, \quad \|\alpha\| \leq n.$$

For such a measure  $\mu$  we obtain

$$|\mathbf{E}^*[f(\mathbf{X}(t))] - \mathbf{E}[f(\tilde{\mathbf{X}}_{\omega[t]}(t))]| = |R_n - \tilde{R}_n|,$$

and we expect that this difference is small. Indeed, we have

**Theorem 1 (Tanaka, [18]).** *Let  $\mu$  satisfies the moment matching condition. If  $f$  is infinitely differentiable with bounded derivatives of all orders, then there exists a constant  $C = C(n, f)$  such that*

$$|\mathbf{E}^*[f(\mathbf{X}(t))] - \mathbf{E}[f(\tilde{\mathbf{X}}_{\omega[t]}(t))]| \leq Ct^{(n+1)/2}.$$

If  $t$  is not small, create  $N$  independent copies  $\omega^{(i)}$  of the random path  $\omega$  and define a new random path  $\bar{\omega}$  in  $[0, 1]$  by

$$\bar{\omega}(t) = \omega^{(i)}[1/N](t - (i-1)/N),$$

if  $(i-1)/N \leq t < i/N$ .

**Theorem 2 (Tanaka, [18]).** *If  $f$  is infinitely differentiable with bounded derivatives of all orders, then there exists a constant  $C = C(n, f)$  such that*

$$|\mathbf{E}^*[f(\mathbf{X}(1))] - \mathbf{E}[f(\tilde{\mathbf{X}}_{\bar{\omega}}(1))]| \leq \frac{C}{N^{(n-1)/2}}.$$

Using the results in Kusuoka [12], one can show the convergence for the case of only Lipschitz continuous  $f$  under mild conditions on the vector fields  $V_i$ . We will not consider these generalisations here.

**Definition 2 (Lyons and Victoir, [10]).** A measure  $\mu$  is called a *classical cubature formula* of degree  $n$  if it satisfies the moment matching condition of order  $n$  and is supported on a finite set.

In the case of a classical cubature formula the approximation  $\mathbf{E}[f(\tilde{\mathbf{X}}_{\bar{\omega}}(1))]$  can be computed exactly (without integration error!) by solving the system (7). Lyons and Victoir [10] proved the existence of classical cubature formulae and gave explicit but complicated examples for arbitrary  $d$  and degrees  $n = 3$  and  $n = 5$ . Gyurkó and Lyons [8] found even more sophisticated classical cubature formulae in some cases of  $n \geq 7$  for  $d = 1, 2$ .

In calculations, we will use a simple *non-classical* cubature formula of degree 5 proposed by Ninomiya and Victoir [14].

*Example 1 (The Ninomiya–Victoir scheme).* Let  $A$  be a Bernoulli random variable independent of  $\mathbf{W}(t)$  and taking values  $\pm 1$  with probability  $1/2$ . The random path is

$$d\omega_i(t) = \begin{cases} (d+2)dt, & \text{if } i = 0, t \in [0, \frac{1}{d+2}) \cup [\frac{d+1}{d+2}, 1), \\ (d+2)W_i(1) dt, & \text{if } 1 \leq i \leq d, A = 1, t \in [\frac{i}{d+2}, \frac{i+1}{d+2}), \\ (d+2)W_i(1) dt, & \text{if } 1 \leq i \leq d, A = -1, t \in [\frac{d+1-i}{d+2}, \frac{d+2-i}{d+2}), \\ 0, & \text{otherwise.} \end{cases} \quad (8)$$

This non-classical cubature formula is of degree 5.

### 3 The simulation algorithm

As a first step, apply the Stratonovich correction (6) to the system (2). We obtain the system (5) with

$$\mathbf{V}_0 = \begin{pmatrix} \left( r - q - \frac{1}{2}(V_1 + V_2) - \frac{1}{4} \left( \frac{1}{\sqrt{\varepsilon}} \xi_1 \rho_{13} + \sqrt{\delta} \xi_2 \rho_{24} \right) \right) S \\ \frac{1}{\varepsilon} (\theta_1 - V_1 - \frac{1}{4} \xi_1^2) - \lambda_1 V_1 \\ \delta (\theta_2 - V_2 - \frac{1}{4} \xi_2^2) - \lambda_2 V_2 \end{pmatrix}$$

and

$$\begin{aligned} \mathbf{V}_1 &= (\sqrt{V_1} S, \frac{1}{\sqrt{\varepsilon}} \xi_1 \sqrt{V_1} \rho_{13}, 0)^\top, \\ \mathbf{V}_2 &= (\sqrt{V_2} S, 0, \sqrt{\delta} \xi_2 \sqrt{V_2} \rho_{24})^\top, \\ \mathbf{V}_3 &= (0, \frac{1}{\sqrt{\varepsilon}} \xi_1 \sqrt{V_1 (1 - \rho_{13}^2)}, 0)^\top, \\ \mathbf{V}_4 &= (0, 0, \sqrt{\delta} \xi_2 \sqrt{V_2 (1 - \rho_{24}^2)})^\top. \end{aligned}$$

Next, we write down the system (7), using the Ninomiya–Victoir scheme (8). Following Ninomiya and Victoir [14], denote by  $\exp(\mathbf{V}_i)\mathbf{x}$  the solution at time 1 of the boundary value problem

$$\frac{d\mathbf{z}(t)}{dt} = \mathbf{V}_i(\mathbf{z}(t)), \quad \mathbf{z}(0) = \mathbf{x}. \quad (9)$$

Let  $T$  be the maturity and  $K$  be the strike price of the European call option with Lipschitz continuous payoff  $f(S(T)) = \max\{S(T) - K, 0\}$ . Divide the interval  $[0, T]$  into  $N$  intervals of equal length. Let  $\mathbf{Z}^i$ ,  $0 \leq i \leq N - 1$  be the independent standard normal 4-dimensional random vectors, let  $A_i$ ,  $0 \leq i \leq N - 1$  be the Bernoulli random variables of Example 1, and assume all of them are independent. Define the set of random vectors  $\mathbf{X}^{i/N}$ ,  $0 \leq i \leq N - 1$  by

$$\begin{aligned} \mathbf{X}^0 &= \mathbf{X}(0), \\ \mathbf{X}^{(i+1)/N} &= \begin{cases} \exp(\frac{T}{2N}\mathbf{V}_0) \exp(\frac{\sqrt{T}Z_1^i}{\sqrt{N}}\mathbf{V}_1) \cdots \exp(\frac{\sqrt{T}Z_4^i}{\sqrt{N}}\mathbf{V}_4) \exp(\frac{T}{2N}\mathbf{V}_0)\mathbf{X}^{i/N}, \\ \exp(\frac{T}{2N}\mathbf{V}_0) \exp(\frac{\sqrt{T}Z_4^i}{\sqrt{N}}\mathbf{V}_4) \cdots \exp(\frac{\sqrt{T}Z_1^i}{\sqrt{N}}\mathbf{V}_1) \exp(\frac{T}{2N}\mathbf{V}_0)\mathbf{X}^{i/N}, \end{cases} \end{aligned}$$

where the upper formula is used whenever  $A_i = 1$ , while the lower formula is used whenever  $A_i = -1$ . By [14, Theorem 2.1], for an arbitrary Lipschitz continuous function  $f$  we have

$$|\mathbb{E}^*[f(\mathbf{X}(T))] - \mathbb{E}[f(\mathbf{X}^1)]| \leq \frac{C}{N^2},$$

where  $C$  is a constant.

The solution to systems (9) has the form

$$\begin{aligned} \exp(s\mathbf{V}_1)\mathbf{x} &= \left( x_1 \exp\left(\frac{\xi_1 \rho_{13}}{2\sqrt{\varepsilon}} s + \sqrt{x_2}\right)^2 - x_2, \left(\frac{\xi_1 \rho_{13}}{2\sqrt{\varepsilon}} s + \sqrt{x_2}\right)^2, x_3 \right)^\top, \\ \exp(s\mathbf{V}_2)\mathbf{x} &= \left( x_1 \exp\left(\frac{\left(\frac{1}{2}\xi_2 \rho_{24} \sqrt{\delta} s + \sqrt{x_3}\right)^2 - x_3}{\xi_2 \rho_{24} \sqrt{\delta}}\right), x_2, \left(\frac{1}{2}\xi_2 \rho_{24} \sqrt{\delta} s + \sqrt{x_3}\right)^2 \right)^\top, \\ \exp(s\mathbf{V}_3)\mathbf{x} &= \left( x_1, \left(\frac{\xi_1 \sqrt{1 - \rho_{13}^2}}{2\sqrt{\varepsilon}} s + \sqrt{x_2}\right)^2, x_3 \right)^\top, \\ \exp(s\mathbf{V}_4)\mathbf{x} &= \left( x_1, x_2, \left(\frac{1}{2}\xi_2 \sqrt{\delta(1 - \rho_{24}^2)} s + \sqrt{x_3}\right)^2 \right)^\top. \end{aligned}$$

and

$$\exp(s\mathbf{V}_0)\mathbf{x} = \begin{pmatrix} x_1 \exp\left(\left[r - q - \frac{1}{4}\left(\frac{1}{\sqrt{\varepsilon}}\xi_1 \rho_{13} + \sqrt{\delta}\xi_2 \rho_{24}\right) - (J_2 + J_3)/2\right]s\right) \\ + \frac{1}{2}\left(\frac{x_2 - J_2}{\varepsilon^{-1} + \lambda_1}(e^{-(\varepsilon^{-1} + \lambda_1)s} - 1) + \frac{x_3 - J_3}{\delta + \lambda_2}(e^{-(\delta + \lambda_2)s} - 1)\right) \\ (x_2 - J_2)e^{-(\varepsilon^{-1} + \lambda_1)s} + J_2 \\ (x_3 - J_3)e^{-(\delta + \lambda_2)s} + J_3 \end{pmatrix},$$

where

$$J_2 = \frac{\theta_1 - \xi_1^2/4}{1 + \lambda_1 \varepsilon},$$

$$J_3 = \frac{\delta(\theta_2 - \xi_2^2/4)}{\delta + \lambda_2}.$$

We can implement this second-order algorithm/scheme using Monte-Carlo technique to obtain  $E[f(\mathbf{X}^1)]$ . For convenience we refer to this scheme hereafter as “advanced MC” scheme.

## 4 Numerical results

We implement advanced MC scheme using MATLAB in a PC with Intel i5-5200U CPU and 16 GB RAM. We consider European option pricing in model (2) under the set of parameters in Table 1 unless stated otherwise. The initial values are  $S_0 = 100, V_1 = 0.03, V_2 = 0.03$  and the day convention is assumed to be 252 trading days per year. The problem is to compute the option price as a discounted expectation i.e.  $C = e^{-rT} E[f(S_T)]$ .

**Table 1.** Model parameters (shortened as param) used in numerical experiments

	Param Value	$V_1$ param Value	$V_2$ param Value
$S_0$	100	$\varepsilon$	0.001, 0.01, ..., 0.5
$K$	70, 80, ..., 120	$\theta_1$	0.04
$r$	0.05	$\lambda_1$	0.1
$q$	0	$\xi_1$	0.1
$T$	90/252 years	$\rho_{13}$	0.5
			$\delta$
			$\theta_2$
			$\lambda_2$
			$\xi_2$
			$\rho_{24}$

We use  $N$  time steps on the time interval  $[0, T]$  and simulate  $M = 100,000$  sample paths which follow our scheme. In this way we generate  $M$  independent realizations of the random variable  $S_T, S_{i,T}, i = 1, \dots, M$ , and approximating

$$C = e^{-rT} E[f(S_T)] \approx \hat{C} := e^{-rT} \frac{1}{M} \sum_{i=1}^M f(S_{T,i}).$$

Note that  $\hat{C}$  is a random variable with mean  $C$  (only approximately due to the discretization error) and standard deviation  $\sigma_C$  of order  $O(\sqrt{M})$  by the central limit theorem. We do an experiment of 50 trails and obtain  $\hat{C}_i, i = 1, \dots, 50$ . We compute the mean and standard deviation of these 50 draws of  $\hat{C}$ , denote it as  $\hat{C}_{avg}$  and  $s_{\hat{C}}$  respectively. The quantity  $\hat{C}_{avg}$  is our approximation price. Note that  $\hat{C}_{avg} \approx E[\hat{C}] \approx C$  and  $s_{\hat{C}} \approx \sigma_C$ .

Most of the experiments have been performed using both the traditional order-one Euler-Maruyama scheme and the order-two advanced MC scheme. For both schemes, while fixing  $M$ , increasing  $N$  will reduce the discretization

error and improve accuracy of  $\hat{C}_{avg}$ , reducing the value of  $\sigma_C$  is mainly achieved by increasing the number of sample paths  $M$  (or using variance-reduction techniques). For the same  $M$  and  $N$ , both schemes have similar values for standard error  $s_{\hat{C}}$ , hence we focus on the effect of  $N$  on the accuracy of  $\hat{C}_{avg}$ . A reference price  $C_{CZ}$  is calculated for each experiment using the approach by Chiarella and Ziveyi [7]. For small values of model parameters  $\varepsilon$  and  $\delta$ , i.e. when the variance processes are fast mean-reverting and show mean-reverting respectively, price  $C_{CZ}$  is very close to the approximated price using an asymptotic approach in Canhanga *et al.* [2] and [5]. For other values of  $\varepsilon$  and  $\delta$  we have run Monte-Carlo simulations using the traditional Euler–Maruyama scheme and confirmed that  $C_{CZ}$  is accurate enough as a reference price. We refer to Canhanga et al [13] for an option pricing formula adapted to model (2) using the Chiarella and Ziveyi approach.

#### 4.1 Rate of Convergence

To save computation time we use  $T = 30/252$  in this section. An inspection of formulas in the advanced MC scheme indicates that, for the same number of time steps, i.e. for same  $N$ , the traditional Euler–Maruyama scheme involves simpler computation and hence should run faster. It should be possible to improve the performance of the advanced MC scheme and hence reduce its execution time without altering the problem/algorithm but our main concern is on comparing rate of convergence. As a order-two scheme, the advanced MC scheme has its relative errors decreasing faster with respect to  $N$  in many cases. We found the clearest evidence under a large mean-reversion rate e.g.  $\varepsilon = 0.001$ , as illustrated in Table 2. Experiments in Table 2 use  $K = 90$ . Similar pattern in the rate of convergence can be observed for other values of  $K$  under large mean-reversion rates.

**Table 2.** Relative errors under Advanced MC and Euler–Maruyama scheme

N	Advanced MC	Euler–Maruyama
5	0.0338	0.2196
10	0.0156	0.1795
30	0.0038	0.0410
100	$9.3780 \times 10^{-4}$	$9.7907 \times 10^{-4}$

As we are pricing a plain vanilla European option, the traditional Euler–Maruyama scheme is sufficiently accurate with a moderate large  $N$ . A larger  $N$  might be needed if we use Euler–Maruyama scheme in pricing for example an Asian option. In the above example, let  $N \geq 100$ , both schemes perform well and in general generate relative errors of similar magnitude for same values of  $M$  and  $N$ . Therefore our discussions hereafter concentrate on the properties of the advanced MC scheme by itself.

## 4.2 The effect of mean-reversion rates

As the model was proposed in Canhanga *et al.* [1]–[5] as having a fast mean-reverting variance process and a slow mean-reverting process. It is interesting to study how the mean-reversion rates  $1/\varepsilon$  and  $\delta$  affect the accuracy of  $\hat{C}_{avg}$ . We fix the number of sample path  $M = 100,000$  and let the number of time steps be  $N = 5$ . Note that  $T = \frac{90}{252}$  here so  $N = 5$  is relatively small. The parameters are as shown in Table 1 with  $K = 100$ , i.e. we price an at-the-money(ATM) option. The relative error (**Rel error**) is defined as  $|\hat{C}_{avg} - C_{CZ}|/C_{CZ}$ .

**Table 3.** Relative errors for ATM call options under various  $\varepsilon$

$\varepsilon$	<b>Rel error</b>	$s_{\hat{C}}$
0.5	$1.6613 \times 10^{-4}$	0.0379
0.4	$4.6014 \times 10^{-4}$	0.0338
0.2	$4.9700 \times 10^{-4}$	0.0311
0.15	$8.9606 \times 10^{-4}$	0.0327
0.10	0.0010	0.0338
0.05	0.0056	0.0325
0.01	0.0490	0.0412
0.005	0.1121	0.0404
0.001	0.5562	0.0651

As  $\hat{C}_{avg}$  is a random variable, the values of relative errors will be slightly different in another experiment but the pattern is similar. Table 3 indicates that, under these value of  $M$  and  $N$ , the approximations are poor when  $\varepsilon$  is too small ( $\varepsilon \leq 0.01$ ) i.e. the mean-reversion rate for  $V_1$  process is too large. Similar things happen if  $V_2$  process has a large mean-reversion rate for example if  $\delta = 1000$ .

Increasing  $M$  reduces  $s_{\hat{C}}$  but does not help much with reducing **Rel error**. As shown in Table 3, when the mean-reversion rate  $\frac{1}{\varepsilon}$  is too large, a small value of  $N = 5$  is not sufficient. The problem can be fixed by increasing  $N$ . Figure 1 shows how the relative error decreases as one increases  $N$  under  $\varepsilon = 0.001$ . To save time, the experiments behind this figure were carried out for smaller  $M (= 50000)$ . In particular, the relative error reduced from 55.54% to 0.31% when we increase  $N$  from  $N = 5$  to  $N = 320$ .

## 4.3 The effect of moneyness

In this section we consider various strike prices  $K$ . The effect of mean-reversion rate e.g.  $\varepsilon$  is similar to the at-the-money case studied above. We fix therefore  $\varepsilon = 0.1$  in all experiments. Also  $T = \frac{90}{252}$ ,  $N = 5$ . The values of  $s_{\hat{C}}$  of these experiments are in the range of 0.012 – 0.017. Table 4 lists out the reference prices, our approximation prices and the relative errors. It suggests that the accuracy of  $\hat{C}_{avg}$  is good for deep in-the-money, in-the-money, at-the-money and moderately out-of-the-money options with relative error of order  $10^{-4}$  or

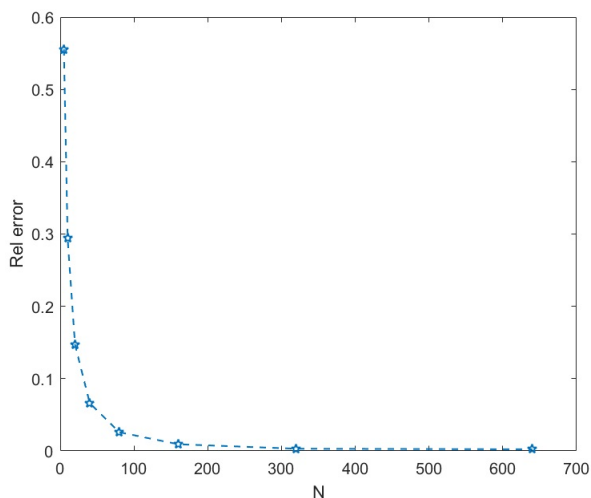


**Fig. 1.** Increasing  $N$  improves the accuracy under large mean-reversion rate ( $\varepsilon = 0.0001$ )

$10^{-3}$ . For deep out-of-the-money options, i.e., when  $K \geq 120$ , the relative error is of  $10^{-2}$ . Increasing  $N$  from 5 to 100 yields only a slight improvement in reducing **Rel error** (0.0275) and increasing  $M$  simultaneously (from 100000 to 500000) reduces  $s_{\hat{C}}$  to 0.0037 but does not reduce **Rel error**. On the other hand, the Euler–Maruyama scheme gives approximations very consistent with our algorithm even under large  $N = 500$  and  $M = 500000$ . It is therefore natural to question whether the reference price itself works perfectly for deep out-of-the money options.

**Table 4.** Relative errors under various strike price  $K$

$K$	$C_{CZ}$	$\hat{C}_{avg}$	<b>Rel error</b>
70	31.2430	31.2586	0.0005
80	21.6904	21.7017	0.0005
90	13.2286	13.2489	0.0015
105	4.7854	4.8029	0.0036
110	3.1855	3.2040	0.0058
120	1.2967	1.3186	0.0169
130	0.4778	0.5016	0.0498

## 5 Conclusions and further remarks

We obtained an advanced Monte-Carlo algorithm/scheme with explicit expressions using Ninomiya-Victoir scheme. The numerical results show that this algorithm in general gives accurate approximation for European option pricing under the parameters studied. A larger number of time steps, i.e. a larger  $N$ , is required when the mean-reversion rate is too high for example if  $\varepsilon = 0.001$ . Some caution should be paid when one prices a deep out-of-the-money option. If the mean-reversion rate is large, it is clear that the advanced Monte-Carlo scheme has a better order of convergence than the first-order Euler-Maruyama scheme. Further studies may involve exotic option pricing with comparison to the traditional Euler-Maruyama scheme.

## A Cubature on a tensor algebra

Let  $\{\mathbf{e}_i: 0 \leq i \leq d\}$  be the standard basis of the space  $\mathbb{R}^{1+d}$ . Define  $\mathbf{e}_\emptyset = 1$  and

$$\mathbf{e}_\alpha = \mathbf{e}_{\alpha_1} \otimes \cdots \otimes \mathbf{e}_{\alpha_k}$$

for any multi-index  $\alpha = (\alpha_1, \dots, \alpha_k)$ . Let  $U_k(\mathbb{R}^{1+d})$  be the linear space of rank  $k$  tensors with the basis  $\{\mathbf{e}_\alpha: \|\alpha\| = k\}$ . Denote by  $T(\mathbb{R}^{1+d})$  the direct sum of the spaces  $U_k(\mathbb{R}^{1+d})$  over all nonnegative  $k$ , and let  $\mathbf{a}_0 \in U_0(\mathbb{R}^{1+d}), \dots, \mathbf{a}_k \in U_k(\mathbb{R}^{1+d}), \dots$  be the components of an element  $\mathbf{a} \in T(\mathbb{R}^{1+d})$ . Define the sum, tensor product, the action of scalars by

$$\begin{aligned} (\mathbf{a} + \mathbf{b})_k &= \mathbf{a}_k + \mathbf{b}_k, \\ (\mathbf{a} \otimes \mathbf{b})_k &= \sum_{l=0}^k \mathbf{a}_l \otimes \mathbf{b}_{k-l}, \\ (\lambda \mathbf{a})_k &= \lambda \mathbf{a}_k. \end{aligned}$$

With this operations,  $T(\mathbb{R}^{1+d})$  becomes an associative algebra. Define the exponent and logarithm on  $T(\mathbb{R}^{1+d})$  by

$$\begin{aligned} \exp(\mathbf{a}) &= \sum_{k=0}^{\infty} \frac{\mathbf{a}^{\otimes k}}{k!}, \\ \ln(\mathbf{a}) &= \ln(\mathbf{a}_0) + \sum_{k=1}^{\infty} \frac{(-1)^{k-1}}{k} (\mathbf{a}_0^{-1} \mathbf{a} - 1)^{\otimes k}, \quad \mathbf{a}_0 > 0, \end{aligned}$$

where the series converge coordinate-wise. The *truncated tensor algebra of degree  $n$* ,  $T^{(n)}(\mathbb{R}^{1+d})$ , is the direct sum of the linear spaces  $U_k(\mathbb{R}^{1+d})$ ,  $0 \leq k \leq n$ . Let  $\pi_n$  be the natural projection of  $T(\mathbb{R}^{1+d})$  to  $T^{(n)}(\mathbb{R}^{1+d})$ . Finally, the operation  $[\mathbf{a}, \mathbf{b}] = \mathbf{a} \otimes \mathbf{b} - \mathbf{b} \otimes \mathbf{a}$  defines a Lie bracket on both  $T(\mathbb{R}^{1+d})$  and  $T^{(n)}(\mathbb{R}^{1+d})$ . Let  $\mathcal{U}$  be the space of linear combinations of finite sequences of Lie brackets of elements of  $\mathbb{R}^{1+d}$ . Then  $\mathcal{U}$  is the free Lie algebra generated by  $\mathbb{R}^{1+d}$ , see [15]. An element of the set  $\pi_n(\mathcal{U})$  is called a *Lie polynomial of*

degree  $n$ , and an element  $\mathbf{a} \in T(\mathbb{R}^{1+d})$  is called a *Lie series* if all  $\pi_n \mathbf{a}$  are Lie polynomials.

Define a map  $\mathcal{S}: C_{\mathbf{0},\text{BV}}([0, T]; \mathbb{R}^{d+1}) \rightarrow T(\mathbb{R}^{1+d})$  by

$$\mathcal{S}(\omega) = \sum_{\alpha} I(T, \alpha, d\omega[T]) \mathbf{e}_{\alpha},$$

and call  $\mathcal{S}(\omega)$  the *signature* of the path  $\omega$ . Not all elements in  $T(\mathbb{R}^{1+d})$  represent a signature. However, Chen [6] proved the following result. The *truncated logarithmic signature*  $\pi_n \ln \mathcal{S}(\omega)$  of any path  $\omega \in C_{\mathbf{0},\text{BV}}([0, T]; \mathbb{R}^{d+1})$  is a Lie polynomial. Conversely, for any Lie polynomial  $\mathcal{L} \in \pi_n \mathcal{U}$  there is a path  $\omega \in C_{\mathbf{0},\text{BV}}([0, T]; \mathbb{R}^{1+d})$  with  $\pi_n \ln \mathcal{S}(\omega) = \mathcal{L}$ .

Similarly, define the *Wiener signature* by

$$\mathcal{S}(\mathbf{W}_{[0,T]}^*) = \sum_{\alpha} I(T, \alpha, \circ d\mathbf{W}^*) \mathbf{e}_{\alpha}.$$

It is easy to see the following. A measure  $\mu$  is a classical cubature formula of degree  $n$  if and only if there are Lie polynomials  $\mathcal{L}_1, \dots, \mathcal{L}_m$  and positive weights  $\lambda_1, \dots, \lambda_m$  such that

$$\pi_n \mathbf{E}[\mathcal{S}(\mathbf{W}_{[0,1]}^*)] = \sum_{j=1}^m \lambda_j \pi_n \exp(\mathcal{L}_j).$$

The expectation in the left hand side of this equation was calculated by Lyons and Victoir in [10]. They obtained the following result:

$$\mathbf{E}[\mathcal{S}(\mathbf{W}_{[0,1]}^*)] = \exp\left(\mathbf{e}_0 + \frac{1}{2} \sum_{i=1}^d \mathbf{e}_i \otimes \mathbf{e}_i\right).$$

In order to find a classical cubature formula of degree  $n$ , one has to find Lie polynomials  $\mathcal{L}_1, \dots, \mathcal{L}_m \in \pi_n \mathcal{U}$  and positive weights  $\lambda_1, \dots, \lambda_m$  with  $\lambda_1 + \dots + \lambda_m = 1$  such that

$$\pi_n \exp\left(\mathbf{e}_0 + \frac{1}{2} \sum_{i=1}^d \mathbf{e}_i \otimes \mathbf{e}_i\right) = \sum_{j=1}^m \lambda_j \pi_n \exp(\mathcal{L}_j).$$

Given the solution, we need to construct the paths  $\omega_j$  of bounded variation on  $[0, T]$  satisfying  $\pi_n \ln \mathcal{S}(\omega_j) = \mathcal{L}_j$ . To perform these tasks, Gyurkó, Lyons, and Victoir use methods based on technical tools from the theory of free Lie algebras like the Lyndon words basis, the Philip Hall basis, Poincaré–Birkhoff–Witt theorem and Baker–Campbell–Hausdorff formula, see [8,10,15].

## References

1. Canhanga, B., Malyarenko, A., Ni, Y. and Silvestrov, S. Perturbation methods for pricing European options in a model with two stochastic volatilities. In: R. Manca, S. McClean, C. H. Skiadas (Eds.), *New Trends in Stochastic Modelling and Data Analysis*. ISAST (2015), 199–210.

2. Canhanga, B., Malyarenko, A., Murara, J.-P., Ni, Y. and Silvestrov, S. Numerical studies on asymptotic of European option under multiscale stochastic volatility. In C. H. Skiadas (Ed.), *16th ASMDA Conference Proceedings*. 30 June –04 July 2015, Piraeus, Greece (2015), 53–66.
3. Canhanga, B., Malyarenko, A., Ni, Y. and Silvestrov, S. Second order asymptotic expansion for pricing European options in a model with two stochastic volatilities. In C. H. Skiadas (Ed.), *16th ASMDA Conference Proceedings*. 30 June –04 July 2015, Piraeus, Greece (2015), 37–52.
4. Canhanga, B., Malyarenko, A., Murara, J.-P. and Silvestrov, S. Pricing European options under stochastic volatilities models. In: Silvestrov S., Rančić M. (Eds.), *Engineering Mathematics I. Electromagnetics, Fluid mechanics, Material physics and Financial engineering*, Springer, Heidelberg (2016), 23–44.
5. Canhanga, B., Malyarenko, A., Ni, Y., Rančić, M., and Silvestrov, S. Numerical methods on European options second order asymptotic expansions for multiscale stochastic volatility. In S. Sivasundaram (Ed.), 11th International Conference on Mathematical problems in Engineering, Aerospace, and Sciences ICNPAA 2016, volume **1798** (2017) of *AIP Conf. Proc.*, pages 020035-1–10, La Rochelle, France, 05–08 July 2016.
6. Chen, K.T. Integration of paths, geometric invariant and a generalized Campbell–Hausdorff formula. *Ann. Math. (2)* **65** (1957), 163–178.
7. Chiarella, C., and Ziveyi, J. Pricing American options written on two underlying assets. *Quant. Finance* **14**, no. 3 (2014), 409–426.
8. Gyurkó, L. G. and Lyons, T. J. Efficient and practical implementations of cubature on Wiener space. In D. Crisan (Ed.), *Stochastic analysis 2010*, Springer, Heidelberg (2011), 73–111.
9. Glasserman, P. Monte Carlo Methods in Financial Engineering. Applications of Mathematics, 53, Stochastic Modelling and Applied Probability, Springer, Berlin, 2003.
10. Lyons, T. J., and Victoir, N. Cubature on Wiener space. *Proc. R. Soc. Lond. A* **460**, no. 2041 (2004), 169–198.
11. Kloeden, P. E. and Platen, E. *Numerical solution of stochastic differential equations*, Applications of Mathematics (New York), **23**, Springer-Verlag, Berlin, 1992.
12. Kusuoka, S. Approximation of expectation of diffusion process and mathematical finance. In *Taniguchi Conference on Mathematics Nara '98*, volume **31** of *Adv. Stud. Pure Math.*, pages 147–165. Math. Soc. Japan, Tokyo, 2001.
13. Ni, Y., Canhanga, B., Malyarenko, A., and Silvestrov, S. Approximation methods of European option pricing in multiscale stochastic volatility model. In S. Sivasundaram (Ed.), 11th International Conference on Mathematical problems in Engineering, Aerospace, and Sciences ICNPAA 2016, volume **1798** (2017) of *AIP Conf. Proc.*, pages 020112-1–10, La Rochelle, France, 05–08 July 2016.
14. Ninomiya, S., and Victoir, N. Weak approximation of stochastic differential equations and application to derivative pricing. *Appl. Math. Finance* **15** (2008), 107–121.
15. Reutenauer, C. *Free Lie algebras*. London Mathematical Society Monographs **7**, Oxford Science Publications, Oxford, 1993.
16. Silvestrov, D.S. American-Type Options. Stochastic Approximation Methods, Volume 1. De Gruyter Studies in Mathematics, 56, Walter de Gruyter, Berlin, 2014.
17. Silvestrov, D.S. American-Type Options. Stochastic Approximation Methods, Volume 2. De Gruyter Studies in Mathematics, 57, Walter de Gruyter, Berlin, 2015.
18. Tanaka, H. Cubature formula on Wiener space from the viewpoint of splitting methods. *RIMS Kôkuûroku* **1844** (2013), 50–59.

# Conjoint Analysis of Gross Annual Salary re-evaluation: evidence from Lombardy Electus data

Paolo Mariani<sup>1</sup>, Andrea Marletta<sup>2</sup>, and Mariangela Zenga<sup>3</sup>

<sup>1</sup> Department of Economics Management and Statistics, University of  
Milano-Bicocca, Piazza dell'Ateneo Nuovo, 1 , Milano, Italy  
(E-mail: [paolo.mariani@unimib.it](mailto:paolo.mariani@unimib.it))

<sup>2</sup> Department of Economics Management and Statistics, University of  
Milano-Bicocca, Piazza dell'Ateneo Nuovo, 1 , Milano, Italy  
(E-mail: [andrea.marletta@unimib.it](mailto:andrea.marletta@unimib.it))

<sup>3</sup> Department of Statistics and Quantitative Methods, University of  
Milano-Bicocca, Via Bicocca degli Arcimboldi, 8, Milano, Italy  
(E-mail: [mariangela.zenga@unimib.it](mailto:mariangela.zenga@unimib.it))

**Abstract.** This paper discusses annual salary enhancements for newly hired employees in companies taking on new graduates. The decision process for selecting candidates with the best skill-sets seems to be one of the most difficult obstacles to overcome. In particular, the analysis is based on an Education-for-Labour Elicitation from Companies' Attitudes towards University Studies Project involving 471 enterprises, with 15 or more employees, operating in Lombardy. The recruiters' preference analysis was carried out using Conjoint Analysis (CA). Starting from CA part-worth utilities, an index of economic revaluation was used to compare different salary profiles for five job vacancies.

**Keywords:** Conjoint Analysis, Economic re-evaluation, Electus, Job Market, New-Graduates.

## 1 Introduction

In recent decades, tertiary-level Education has expanded rapidly across many countries, as well as in Italy. In general, the expectation is that higher education should prepare young people to become highly productive and successful in the labour market. Sometimes, the skills required of the graduates for the job do not coincide with the skills offered by the graduates applying, creating a mismatch between education and the labour market. In general, the mismatch occurs when:

”...there is a difference between the skills a worker provides and the skills necessary for the job. In particular, working in a job below an individual's level of skills limits individual productivity and leads to underutilization of education.” [7].

---

*5<sup>th</sup> SMTDA Conference Proceedings, 12-15 June 2018, Chania, Creete, Greece*

© 2018 ISAST



The mismatch in Italy has been well described by ISTAT data from an Italian Survey on University Graduates' Vocational Integration [12]. In fact, in 2015 the transition into the labour market was rather difficult for Humanities graduates (with 61.7% of the bachelor's degree graduates and 73.4% of the master's degree graduates being employed) and Earth Sciences graduates (with 58.6% of the bachelor's degree and 76.5% of the master's degree graduates being employed). On the other hand, the master's degree graduates in Defence and Security, Medicine and Engineering had the highest employment levels (99.4%, 96.5% and 93.9% respectively). Moreover, 52.8% of the bachelor's graduates and 41.9% of master's graduates found employment in "non-stable" jobs. Of course, this information has to be considered in light of the worldwide economic crisis, which wreaked severe consequence on the employment situation in the labour market in general. Looking at the Italian situation in 2015, while the overall unemployment rate was at 11.9%, the unemployment rate among young people (15-24 years old) increased dramatically to 40.3%. Moreover, unemployment in the service sector hit 16% [8].

This research concerns labour market comprehension policies for new graduates and the relationships among enterprises and universities. The study is based on the multi-centre research project, Education-for-Labour Elicitation from Companies' Attitudes towards University Studies [9], which involved several Italian universities. This work has three main objectives. First, it focuses on the identification of an ideal graduate profile for several job positions. Second, it is seeking recommendations of some across-the-board skills, universally recognized as "best practices" for graduates. Finally, the analysis is attempting to give a comparative view of the differences between and the assessments of wages and skill-sets for new graduates.

The paper is structured as follows: Section 1 serves as an introductory preface. Section 2 introduces the methodology of Conjoint Analysis and the Coefficient of Economic Valuation, Section 3 presents the results from the Eelectus research and Section 4 gives the conclusions.

## 2 Methodology

Conjoint Analysis (CA) is among the methods most used to analyse consumer choices and to assign consumers utility drawn from the properties of single characteristics of goods, services or, as in this application, jobs being offered on the market.

Different models that have been used to measure the economic value derived from CA are described in the literature. In [3], the monetary value of a utility unit is computed as the ratio of the difference between its maximum price and its minimum price compared to related utilities.

The quantification of the monetary value of the utility, of a given attribute, is obtained by multiplying the monetary value for the utility perceived by customers with the better or worse level of the attribute.

Hu et al. [11] introduced some measures of customers' willingness to pay (WTP) following an interpretation of part-worth utilities and the offer of monetary values for various attributes. The *ratio* is created if a change in attribute

increases welfare. Therefore, an individual will pay more to have that change in attribute and *vice versa* [6]. Following Louviere [13], these measures of WTP are calculated as the part-worth utility for the various attribute levels divided by the negative of the marginal utility of income.

In this paper, the conjoint rating response format is used to gather and use additional information about respondent's preferences. This preference model uses a part-worth utility linear function. Part-worth utilities are also assumed for each level of the various attributes estimated by using OLS multiple regression. In this formulation, attention is focused on a rating scale, opting for a very general preference model used in traditional CA.

In fact, of all the attribute levels that describe the graduate, the information contained in the conjoint rating format is exploited by regressing individual responses on a piece-wise linear function. A non-metric estimation procedure such as MONANOVA might be more appropriate than OLS, since the conjoint data are collected on a non-metric scale. However, as demonstrated in Carmone [4] and Cattin [5], OLS regression provides similar parameter estimates for both ranking and rating scales. Hence, OLS seems to be an appropriately reliable estimation procedure. The function is defined as follows:

$$U_k = \sum_{i=0}^n \beta_i x_{ik} \quad (1)$$

where  $x_0$  is equal to 1 and  $n$  is the number of all levels of the attributes which define the combination of a given good. Each  $x_{ij}$  variable is a dichotomous variable, which refers to a specific attribute level. This variable equals 1 if the corresponding attribute level is present in the combination of attributes that describes the alternative  $k$ . Otherwise, that variable will be 0. As a result, the utility associated with the alternative  $k$  ( $U_k$ ) is obtained by summing the terms  $\beta_i x_{ik}$  over all attribute levels, where  $\beta_i$  is the partial change in  $U_k$  for the presence of the attribute level  $i$ , with all other variables remaining constant. In this paper, it refers to this piece-wise linear function as a part-worth function model that gives a specific utility value for each level of the considered attributes, usually referred to as part-worth utility. Consequently, the number of parameters estimated by assuming the part-worth specification is greater than what is required by alternative preference model specifications such as the vector model form and the ideal model.

## 2.1 Coefficient of Economic Valuation

A coefficient based on part-worth utilities can determine the monetary variation associated with any change in the combination of the attributes assigned to a good, service, or in this case a job, compared to the actual revenue generated by that job.

Having chosen the preference model (and the rating scale), a coefficient of economic valuation is developed for a hypothetical change that may occurs in the combination of attribute levels-as described by Mariani and Mussini [14].

Total utility variation is computed by replacing one attribute level of *status quo*  $b$ , where  $b$  is the current profile of the job, with attribute level  $i$  (with

$i = 1, \dots, n$ ) which is different from  $b$ .  $M_i$  is given by the ratio of the difference between the total utility of alternative  $i$  and the *status quo*  $b$  over the total utility of the *status quo*  $b$ ; formally:

$$M_i = \frac{U_i - U_b}{U_b} \quad (2)$$

where  $U_i$  denotes the sum of the utility scores associated with alternative profile  $i$  and  $U_b$  (assumed to be different from 0), which denotes the sum of the part-worth utilities associated with the *status quo*  $b$  of the job. Equation (2) indicates whether the *status quo*  $b$  modification gives a loss or a gain. If  $M_i = 0$ , there is no loss or gain in terms of total utility. However, the utility change arising from an attribute-level modification can be considered more or less important by respondents. Hence, this change may have a more important economic impact with respect to a changed utility, which has a similar intensity but involves a less relevant attribute. As a solution, the relative importance of the modified attribute is used as a weighting [10].

The range of the utility values for each attribute from highest to lowest, provides an indicator of how important the attribute is compared to the others. The larger the utility ranges the more important is the role that the attributes play. This applies in the same manner to smaller ranges. For any attribute  $j$ , the relative importance can be computed by dividing its utility range by the sum of all utility ranges as follows:

$$I_j = \frac{\max(W_j) - \min(W_j)}{\sum_{j=1}^J [\max(W_j) - \min(W_j)]}, \quad (3)$$

where  $J$  is the number of attributes and  $W_j$  is the set of part-worth utilities referring to the various levels of attribute  $j$ . Usually, importance values are represented as percentages with a total score of one hundred. Otherwise, these importance values may be expressed in terms of decimals whose sum is one. If this is the case, entering the importance of the modified attribute in equation 2, the coefficient formulation becomes the following:

$$MI_{ij} = M_i * I_j. \quad (4)$$

Assuming a change in the *status quo* profile, the formula (1) will be used to estimate the variation of the total revenue generated. Given the Gross Annual Salary ( $GAS$ ) associated with the *status quo* profile, the coefficient of economic valuation (CEV) is expressed as follows:

$$V_{ij} = MI_{ij} * GAS \quad (5)$$

where  $V_{ij}$  denotes the amount of the salary variation. The variation  $V_{ij}$  is obtained by supposing that the job's monetary attribute will vary in proportion to the change in total utility. This assumption may seem restrictive. However,

it is possible to argue that the monetary amount asked for an employer for a job reflects how that user values the combination of attributes of the job in terms of its utility. Under this hypothesis, it is credible to assess the economic value of a change in the combination of attributes as a function of the utility and importance of the modified attribute. In addition, CA serves to approximate the real structure of preferences, given that only a partial knowledge of preferences can be known. Therefore it is possible to use the CEV as a monetary indicator that approximates the impact of a given utility change in monetary terms.

The proposed coefficient was then applied to the Electus survey. First, an ideal profile was obtained by maximizing part-worth utilities. Then, economic variations on the proposed Gross Annual Salary for graduates were computed by using the coefficient.

### 3 Application and results

The survey was conducted in 2015 using Computer-Assisted Web Interviewing (CAWI). Data were collected using a software program called Sawtooth [15]. Data manipulation and Conjoint Analysis were performed using *R* software and *Conjoint* package [1].

The questionnaire contained two sections: the first concerned the conjoint experiment for the five job positions and the second contained general information about the company (demographic data). The five job positions considered for the new graduates, were Administration clerk, HR assistant, Marketing assistant, ICT professional and CRM assistant. Six attributes were used to specify the candidates' profile:

- *Field of Study* with 10 levels (Philosophy and Literature, Educational Sciences, Political Sciences/ Sociology, Economics, Law, Statistics, Industrial Engineering, Mathematics/Computer sciences, Psychology, Foreign Languages);
- *Degree Mark* with 3 levels (Low, Medium, High);
- *Degree Level* with 2 levels (Bachelor's, Master's);
- *English Knowledge* with 2 levels (Suitable for communication with foreigners, Inadequate for communication with foreigners);
- *Relevant Work Experience* with 4 levels (No experience at all, Internship during or after completion of university studies, Discontinuous or occasional employment during university studies, One year or more of regular employment);
- *Willingness to Travel on Business* with 3 levels (Unwilling to travel on business, Willing to travel on business only for short periods, Willing to travel on business even for long periods).

After having rated the selected profile and chosen the best one, the entrepreneurs were asked to propose a Gross Annual Salary for the chosen profile to measure WTP [2].

As far as the Milano-Bicocca research unit was concerned, the interviewees were representatives of companies registered on the Portal of Almalaurea for

recruitment and linkage, limited to the university site. There were 471 final respondents. The company profiles showed that most of the respondents had 20-49 employees (52%), followed by business with 50-249 employees enterprises (25.6%) and then enterprises with at least 250 companies (22.4%). The activity sectors most represented were industry services (62.1%), individual services (16.2%) and manufacturing (14.9%). The majority of the companies (89.4%) operated fully or partially in the domestic market. Moreover, they were mainly under the management of the entrepreneur (64.2%). Frequency distributions for Electus' data are found in Table 1.

**Table 1.** Basic features of Electus' companies

Company supervisor	Employees	Activity sectors	Activity market
Entrepreneur 64.2%	0 – 19 37.5%	Services industry 62.1%	International 45.7%
Manager 23.2%	20 – 49 14.5%	Personal services 16.2%	National 43.8%
Other 12.6%	50 – 249 25.6%	Manufacturing 14.9%	Both 10.6%
	250+ 22.4%	Other 6.8%	

Source: Electus data (2015)

Five CAs were achieved, corresponding to the different job positions in order to measure the entrepreneurs' preferences. The results for part-worth utilities are presented in table 2.

It was deemed necessary to introduce and define cross competencies or specialized skills. A cross competence is defined as having part-worth utilities that are independently higher than required for the chosen vacancy. On the other hand, if the level of the attribute changes due to the job position, that competence is defined as specialized.

It is important to recall that, since the definition of the sum of utilities for all levels of an attribute will equal 0, less desirable attributes may generate negative utilities.

In the application, the part-worth utilities seemed to be similar for all the attributes, except for *Field of Study*. This means that other competencies have some levels that are universally identified as 'best practices' for graduates.

The *Relevant work experience* and *English Knowledge* attributes always generated the highest utilities for the same level for each vacancy. Fluent communication with foreigners and one or more years of regular employment experience are recognized as preferred.

*Degree Mark* and *Willingness to travel on business* variables were competencies where the top two levels were consistently preferred. Hence, candidates holding a degree earned with medium to high marks and who expressed their willingness to travel on business for short or long periods were preferred.

Utility scores for the *Degree level* variable were very close to 0 for each position. This means that for the respondents there was no significant difference

**Table 2.** Competencies part-worth utilities for job positions

<b>Competencies</b>	AC	HR	ICT	MKT	CRM
<i>Field of study</i>					
Philosophy and Literature	-0.8312	0.1561	-0.6792	-0.1247	-0.5629
Educational Sciences	-0.5959	0.8598	-0.0759	-0.2299	-0.2086
Political Sciences	0.3031	0.1876	-0.7714	0.0313	0.1996
Economics	1.8811	0.3210	0.2981	1.3350	1.0165
Law	0.0737	0.5498	4.8612	-0.5211	-0.0909
Statistics	0.4506	-0.6956	0.3956	-0.0129	-0.1686
Engineering	-0.5488	-1.5581	0.8889	-0.4019	0.0469
Computer Sciences	0.4444	2.9842	2.9842	-0.4163	0.0252
Psychology	-1.0678	1.5375	-1.0325	0.0974	-0.1557
Foreign Languages	-0.1091	-0.2371	-1.1121	0.2431	-0.1015
<i>Degree Mark</i>					
Bachelor	0.0485	0.0251	-0.0483	-0.0092	-0.0586
Master	-0.0485	-0.0251	0.0483	0.0092	0.0586
<i>Degree Level</i>					
Low	-0.3960	-0.2497	-0.1047	-0.1407	-0.2299
Medium	0.2169	0.0950	-0.0431	0.0203	0.1401
High	0.1790	0.1547	0.1478	0.1204	0.0898
<i>English Knowledge</i>					
Suitable	0.4608	0.2699	0.0969	0.3145	0.2998
Inadequate	-0.4608	-0.2699	-0.0969	-0.3145	-0.2998
<i>Relevant Work Experience</i>					
No experience	-0.3169	-0.1666	0.0303	-0.3177	-0.1619
Internship	-0.0045	-0.0019	-0.0182	-0.0464	-0.1313
Occasional	-0.1219	-0.1383	-0.1300	0.1736	0.1014
Regular	0.4433	0.3068	0.1179	0.1905	0.1918
<i>Willingness to Travel on Business</i>					
Unwilling to travel	-0.0793	-0.3530	-0.0768	-0.0862	-0.4198
Short period	-0.0279	0.0698	-0.0295	0.0610	0.2353
Long period	0.1072	0.2832	0.1063	0.0252	0.1845

Source: Electus data (2015)

AC = Administration Clerk

HR = Human Resource assistant

ICT = Information Communication Technology professionals

MKT = Marketing assistant

CRM = Customer Relationship Management

between a bachelor's and a master's degree. This was due to the fact that all the positions analysed were very basic not requiring specialized skills.

The *Field of Study* attribute required a more complex analysis since it is less wide-ranging and a degree in one field could be the best for one position and the less good for an other.

Table 3, shows the ideal profiles for each job vacancy. As can be noted, these profiles were similar to one another except for *Field of Study*. This confirms the theory of the existence of some transversal or specialized competencies.

As concerns the *Field of Study* variable, Economics was preferred for three position (AC, MKT, CRM) out of the five. A degree in Psychology was desirable for the HR assistant post, while for a more technical position such as ICT professional the field of study with the largest part-worth utility was Computer Sciences/Mathematics. For this reason, according the previous definition *Field of study* is a specialized competence.

The *Relevant work experience* and *English Knowledge* attributes show that the best level perceived does not depend on the duties to be performed, which means they could be considered cross competencies. After all, it is easy to imagine that companies would prefer to employ a candidate with one year or more of regular work experience and who is capable of communicating with foreigners.

Two levels are recognized as 'best practices' for *Degree Mark* and *Willingness to travel on business* the attributes, they could be defined as being nearly cross competencies.

Finally, since part-worth utilities for the *Degree level* variable were very close to 0 and there was no difference between these levels, meaning that this could be defined as a non-binding attribute.

**Table 3.** Competencies attributes and ideal levels for job vacancies

<b>Competencies</b>	AC	HR	ICT	MKT	CRM
Field of Study	Economic	Psychology	Comp.Sci	Economic	Economic
Degree level	Bachelor's	Bachelor's	Master's	Master's	Master's
Degree Mark	Medium	High	High	High	Medium
English Knowledge	Suitable	Suitable	Suitable	Suitable	Suitable
Relevant work experience	Regular	Regular	Regular	Regular	Regular
Willingness to travel	Long	Long	Long	Short	Short

Source: Electus data (2015)

Table 4 shows the percentage of the importance index for the five CAs computed using equation 3. It is important to remember that higher values for the index corresponds with a more important competence for the respondents.

For each profile, the attribute with the highest values for the index was *Field of Study*. This percentage reached a maximum of 80.54% for ICT professionals. The only other position where this values was not over 50% was CRM Assistant. Another high percentage is for this post was *Willingness to Travel*, which was nearly 20%.

*English Knowledge* appeared to be the most important competence after *Field of Study*. Except for ICT professionals, it was always over 10% with a peak of 17.83% for MKT assistant.

Third, on the same level, there were *Degree Mark*, *Relevant Work Experience* and *Willingness to Travel* with an average importance of about 10%. Finally, because of all part-worth utilities were close to 0, the index of importance for *Degree Level* was very low for each job position.

**Table 4.** Importance indexes of competence attributes for job vacancies

<b>Competence</b>	<b>AC</b>	<b>HR</b>	<b>ICT</b>	<b>MKT</b>	<b>CRM</b>
Field of Study	53.35%	59.39%	80.54%	54.27%	42.98%
Degree level	1.75%	1.04%	1.91%	0.54%	3.19%
Degree Mark	11.09%	7.67%	4.98%	7.63%	10.07%
English Knowledge	16.67%	10.55%	3.82%	18.39%	16.32%
Relevant work experience	13.75%	9.12%	4.89%	14.86%	9.62%
Willingness to travel	3.37%	12.23%	3.61%	4.30%	17.83%

Source: Electus data (2015)

The last step of the analysis done for this research consisted in the computation of the CEVs  $M_{ij}$ . To obtain these figures, the part-worth utilities in Table 2 were used combined with the importance indexes in Table 4.

As seen in the previous section, one of the limits of using this methodology is at the variations can only be extrapolated by evaluating changes in utility for a unique attribute. The attribute considering variable in this case study was *Field of Study*. Therefore, the utilities were computed, with other attributes remaining constant. In particular, in this application, the *status quo* profile was the worst profile because it minimized total utilit. So  $U_b$  is the sum of the lowest part-worth utilities (plus an intercept) for each attribute  $j$ . This means that all  $MI_{ij}$  coefficients and all variations  $V_{ij}$  are positive.

Table 5 shows  $M_{ij}$  CEVs for *Field of Study*, as expected each  $M_{ij} \geq 0$  and  $M_{ij} = 0$  only in correspondence of the Field of Study with the minimum of part-worth utilities. Comparing the job positions, ICT professionals showed higher variations. This is due to the fact the  $I_j$  was very high: a degree in Mathematics or Computer Sciences was fully specialized for this position. The biggest CEV is for a degree in Mathematics or Computer sciences for ICT professionals, in comparison to a graduate in Foreign Languages, the former earn a twice the Gross Annual Salary.

It seems pretty clear that Economics graduates can expect higher re-evaluation percentage coefficients. In comparison with the lowest utility values, the  $M_{ij}$  coefficients were close to 25% for Administration Clerk (against Psychology) and 20% for HR (against Industrial Engineering) and MKT assistant (against Law). A degree in Psychology was very favourable for HR assistant but for other vacancies its CEV was very low. Statistics and Industrial engineering had good coefficients only for ICT professionals. Finally for CRM assistant all wages were very close one another, in comparison with the worst (Philosophy and Literature), with the only post that went over 10% being Economics.

**Table 5.**  $M_{ij}$  coefficients for Field of Study by job vacancies

<b>Field of Study</b>	AC	HR	ICT	MKT	CRM
Philosophy and literature	102	118	111	104	<b>100</b>
Educational sciences	104	126	127	103	103
Political science/ Sociology	112	118	109	106	106
Economics	125	120	136	119	112
Law	110	122	106	<b>100</b>	104
Statistics	113	109	139	105	103
Industrial engineering	104	<b>100</b>	152	101	105
Mathematics/ Computer sciences	113	104	206	101	105
Psychology	<b>100</b>	133	102	106	103
Foreign languages	108	114	<b>100</b>	108	104
Minimum <i>GAS</i>	19230 €	19600 €	11420 €	21070 €	24960 €

Source: Electus data (2015)

## 4 Conclusions

This paper proposed the use of the Mariani-Mussini index in combination with CA utilities. The aim was to give a monetary assessment of the competencies for Gross Annual Salary for five different job positions. This monetary evaluation was found to be changeable according to some competencies maintained by new graduates. Data referring to the Electus project applied in Lombardy, showed the existence of different kinds of attributes declared as cross, specialized or non-binding. In particular, *Relevant work experience* and *English Knowledge* appeared to be cross competencies, while *Field of Study* seemed to indicate a specialized skill. For this reason, it was possible to create different ideal profiles on the basis of the required job position.

Using Conjoint Analysis, the competencies were measured according to the perceived importance. *Field of Study* was proven to be the most relevant, especially when the job vacancy was more specialized. The high importance of *Field of Study* resulted in taking into consideration the monetary variation according to different academic fields. Economics were preferred for the role of Administration Clerk, Marketing Assistant and Customer Relationship Management. The Gross Annual Salary for these positions was 25%, 19%, 12% respectively higher than the degree course with the lowest utilities. When the position concern Human Resources, a degree in Psychology was preferred by companies. Its post's salary was 33% higher than posts requiring a degree in Engineering. Because Information and Communications Technology is a specialized field, the CEVs are higher. Therefore, the salary for a graduate in Mathematics or Computer sciences was twice that of a graduate in Foreign Languages.

Future research aim to focus attention in two directions. First, the results coming from stratified CA based on socio-demographic features of companies responding in the Electus project could be discussed. Second, it would clearly be advantageous to extend of the Mariani-Mussini economic re-evaluation coef-

ficient to more than one attribute, in order to jointly analyse more competencies as well as possible interactions.

## References

1. Bak, A. and Bartlomowicz, T. (2012). Conjoint analysis method and its implementation in conjoint R package, 239–248. *Data analysis methods and its applications*.
2. Breidert, C. (2006). *Estimation of Willingness-to-Pay. Theory, Measurement, Application*. Deutscher Universitäts-Verlag, Wiesbaden.
3. Busacca, B., Costabile, M., and Ancarani, F. (2004). *Prezzo e valore per il cliente. Tecniche di misurazione e applicazioni manageriali*. Etas, Perugia.
4. Carmone, F., Green, P.E., and Jain, A.K. (1978). Robustness of conjoint analysis: Some monte carlo results. In *Journal of Marketing Research*, 15: 300–303.
5. Cattin, P. and Wittink, D. (1982). Commercial use of conjoint analysis: A survey. In *Journal of Marketing*, 46: 44–53.
6. Darby, K., Batte, M.T., Ernst, S., and Roe, B. (2008). Decomposing local: A conjoint analysis of locally produced foods. In *American Journal of Agricultural Economics*, 90 (2): 476–486.
7. EC (2008). Commission staff working paper accompanying new skills for new jobs. anticipating and matching labour market and skills need. In COM, 868.
8. EUROSTAT (2017), <http://ec.europa.eu/eurostat/data/database>.
9. Fabbris, L. and Scioni, M. (2015). Dimensionality of scores obtained with a paired-comparison tournament system of questionnaire item. In A. Meerman and T. Kliewe, eds., *Academic Proceedings of the 2015 University-Industry Interaction Conference: Challenges and Solutions for Fostering Entrepreneurial Universities and Collaborative Innovation*. Amsterdam.
10. Garavaglia, C. and Mariani, P. (2017). How much do consumers value protected designation of origin certifications? Estimates of willingness to pay for pdo dry-cured ham in italy. In *Agribusiness*.
11. Hu, W., Batte, M.T., Woods, T., and Ernst, S. (2012). Consumer preferences for local production and other value-added label claims for a processed food product. In *European Review of Agricultural Economics*, 39 (3): 489–510.
12. ISTAT (2017), <http://www.istat.it/en/archive/190700>.
13. Louviere, J.J., Hensher, D.A., and Swait, J.D. (2000). *Stated Choice Methods: Analysis and Application*. Cambridge University Press.
14. Mariani, P. and Mussini, M. (2013). A new coefficient of economic valuation based on utility scores. In *Argumenta Oeconomica*, 2: 33–46.
15. Sawtooth, S. (2017). <http://www.sawtoothsoftware.com>.



# Quantile estimation for Pareto distribution

Ayana Mateus<sup>1</sup> and Frederico Caeiro<sup>2</sup>

<sup>1</sup> Faculdade de Ciências e Tecnologia, Universidade Nova de Lisboa, Portugal and  
Centro de Matemática e Aplicações (CMA)

(E-mail: [amf@fct.unl.pt](mailto:amf@fct.unl.pt))

<sup>2</sup> Faculdade de Ciências e Tecnologia, Universidade Nova de Lisboa, Portugal and  
Centro de Matemática e Aplicações (CMA)

(E-mail: [fac@fct.unl.pt](mailto:fac@fct.unl.pt))

**Abstract.** The Pareto distribution was created by the economist Vilfredo Pareto (1848-1923) who introduced it while studying distributions for modeling large incomes. Since then, the Pareto distribution has been widely used in various applications including economics, engineering and environmental studies. In this work, we compare the finite sample behaviour of several quantile estimators for a Pareto type I distribution. Quantile estimators are obtained by replacing the scale and shape parameters in the quantile expression by their estimates. For the estimation of this distribution, we shall consider several classic methods such as: the moments, the maximum likelihood and the probability weighted moments.

**Keywords:** Pareto distribution, Monte Carlo method, quantile, maximum likelihood, probability weighted moments.

## 1 Introduction

The Pareto distribution was first introduced as a model for large incomes (Pareto[11]) and nowadays has been widely used in various applications including economics, engineering and environmental studies. Its importance has been recently extended to financial risk management and insurance as it often provides adequate descriptions of the extreme tail events of financial and insurance loss datasets (Kim[2]). Although there are several variants of this distribution, in this work we shall consider the classic Pareto distribution also known as Pareto type I. A random variable  $X$  has a Pareto type I distribution if its distribution function (d.f.) is

$$F_X(x) = P(X \leq x) = 1 - \left(\frac{c}{x}\right)^a, \quad x > c, \quad c > 0, \quad a > 0, \quad (1)$$

where  $a$  and  $c$  are shape and scale parameters, respectively. In this work we shall consider both parameters  $a$  and  $c$  unknown. Estimation of the parameters  $a$  and  $c$  has already been extensively addressed in the literature (see (Arnold, [1], Johnson[9], Quandt[12] and references therein). The parameter  $a$  measures the heaviness of the right tail and in the literature it is also known as the tail

---

5<sup>th</sup> SMTDA Conference Proceedings, 12-15 June 2018, Chania, Crete, Greece

© 2018 ISAST



index. The associated quantile function of  $X$  is obtained by inverting the d.f. in (1) and given by:

$$Q_X(p) = F_X^{\leftarrow}(p) = c(1-p)^{-1/a}, \quad 0 < p < 1, \quad c > 0, \quad a > 0, \quad (2)$$

where  $p$  denotes the lower tail probability. In this paper, we compare the finite sample behaviour of several quantile estimators for the classic Pareto distribution. Other works related with the quantiles estimation of the Pareto distribution can be seen in Caeiro and Gomes[5], Caeiro *et al.*[6] and references therein. Quantile estimators are obtained by replacing the scale and shape parameters in the quantile function by their estimates. For the estimation of this distribution, we shall consider several classic methods such as: the moments, the maximum likelihood and the probability weighted moments. In the next section, we briefly describe the estimation methods above mentioned. In section 3 we present the simulation studies for quartiles estimators and some concluding remarks.

## 2 Estimation methods for the parameters of the Pareto distribution

In this section, we review the most usual methods used to estimate the Pareto distribution. In the following, we shall assume that  $X_1, X_2, \dots, X_n$  is a sample of independent and identically distributed random variables, with a Pareto distribution given in (1). The corresponding sample of non-decreasing order statistics are denoted by  $X_{1:n}, X_{2:n}, \dots, X_{n:n}$ .

The maximum likelihood estimators (ML) are given by:

$$\hat{a}^{ML} = \left( \frac{1}{n} \sum_{i=1}^n \ln X_i - \ln X_{1:n} \right)^{-1}, \quad \hat{c}^{ML} = X_{1:n}.$$

The maximum likelihood estimators is the standard method for estimating parameters for a given distribution as it is known to be consistent, asymptotically normal and efficient. However, for small sample sizes, its performance deteriorates and other alternative estimators may perform better in terms of the mean squared error (Kim[2]).

By equating the two moments to the corresponding sample moments and solving the system of equations in order to the parameters, Quandt[12] in 1966 obtained the moment estimators (M):

$$\hat{a}^M = \frac{n\bar{X} - X_{1:n}}{n(\bar{X} - X_{1:n})}, \quad \hat{c}^M = \left( 1 - \frac{1}{n\hat{a}^M} \right) X_{1:n}, \quad (3)$$

where  $\bar{X}$  denotes the arithmetic sample mean. Since the first non central moment only exists for  $a > 1$ , the estimators in (3) are only consistent for  $a > 1$ .

We also consider the estimators based on the probability weighted moment method (PWM) introduced in Greenwood *et al.*[7]. The probability weighted

moments of a continuous random variable  $X$  with distribution function  $F$  are defined as

$$M_{p,r,s} = E(X^p(F(X))^r(1 - F(X))^s)$$

with  $p, r$  and  $s$  any real numbers. The PWM estimators are obtained by equating  $M_{p,r,s}$  with their corresponding sample moments, and then solving those equations in order of the parameters. This method is a generalization of the classic method of moments. Hosking *et al.*[8] advise the use of  $M_{1,r,s}$ , because the relations between parameters and moments have usually a much simpler form. Also, when  $r$  and  $s$  are integers  $F(X)^r(1 - F(X))^s$  can be written as a linear combination of powers of  $F(X)$  or  $1 - F(X)$ . So it is usual to work with one of the two special cases:

$$\alpha_r = M_{1,0,r} = E(X(1 - F(X))^r) \quad \text{or} \quad \beta_r = M_{1,r,0} = E(X(F(X))^r). \quad (4)$$

The unbiased estimators of  $\alpha_r$  and  $\beta_r$  in (4) are, respectively,

$$\hat{\alpha}_r = \frac{1}{n} \sum_{i=1}^{n-r} \frac{\binom{n-i}{r}}{\binom{n-1}{r}} X_{i:n}, \quad \text{and} \quad \hat{\beta}_r = \frac{1}{n} \sum_{i=r+1}^n \frac{\binom{i-1}{r}}{\binom{n-1}{r}} X_{i:n}.$$

Caeiro and Gomes[3] and Caeiro *et al.*[4] considered the moments  $\alpha_0$  and  $\alpha_1$  and derived the corresponding PWM estimators for the shape and scale parameters of the classic Pareto distribution. Those estimators are:

$$\hat{a}^{PWM} = \frac{1}{1 - \left(\frac{\hat{\alpha}_1}{\hat{\alpha}_0 - \hat{\alpha}_1}\right)} \quad \text{and} \quad \hat{c}^{PWM} = \hat{\alpha}_0 \left(\frac{\hat{\alpha}_1}{\hat{\alpha}_0 - \hat{\alpha}_1}\right)$$

Since the PWM estimators use the sample mean, they are only consistent if  $a > 1$ . In order to have consistent estimators for  $a > 0$ , Caeiro and Mateus[10] considered the log probability weighted moments,

$$l_r = E((\ln X)(1 - F(X))^r),$$

and derived the corresponding moments for the Pareto distribution,

$$l_r = \ln(C)/(1 + r) + 1/a(1 + r)^2.$$

For non-negative integer  $r$ , the unbiased estimator of  $l_r$  is:

$$\hat{l}_r = \frac{1}{n} \sum_{i=1}^{n-r} \frac{\binom{n-i}{r}}{\binom{n-1}{r}} \ln X_{i:n}. \quad (5)$$

Considering the moments  $l_0$  and  $l_1$ , Caeiro and Mateus[10] obtained the log probability weighted moment estimators (LPWM):

$$\hat{a}^{LPWM} = \frac{1}{2\hat{l}_0 - 4\hat{l}_1} \quad \text{and} \quad \hat{c}^{LPWM} = \exp(4\hat{l}_1 - \hat{l}_0)$$

where  $\hat{l}_0$  and  $\hat{l}_1$  are given in (5).

### 3 Finite Sample behaviour of the quartiles estimators

In this section, we have implemented a Monte-Carlo simulation experiment in R software environment (R Development Core Team [13]), with 20,000 samples of sizes  $n = 10, 15, 20, 30, 40, 50, 75$  and 100 from the Pareto distribution with parameters  $(a, c) = (0.5, 1)$  and  $(a, c) = (2, 2)$ .

The simulation was design to evaluate the performance of the quartiles estimators. Quartiles estimators were obtained by replacing the scale and shape parameters in the quantile function in (2) by the corresponding estimator and considering  $p = 0.25, 0.5$  and  $0.75$ . The Pareto distribution was estimated by the M, ML, PWM and LPWM methods. For the sake of simplicity, we present the ratio between the estimated and true quartile,  $\hat{Q}(p)/Q(p)$ ,  $p = 0.25, 0.5, 0.75$ .

In Tables 1–6 we present the simulated mean values and the root mean squared error (RMSE), up to four decimal places, of the the ratio between the estimated and true quartile. In both tables the “best” mean value and RMSE, for each sample size, are underlined. In figures 1–3 we present the simulated values of the ratio between the estimated and true quartile, with 20,000 samples of sizes  $n = 30, 100$  for a Pareto with  $(a, c) = (2, 2)$ . For a better visualization of the results a horizontal line was marked in the optimal racio.

On the basis of the simulation study, we drawn the following conclusions:

- According to the theory the M and PWM estimators are not consistent for  $a \leq 1$  and the simulated mean values and the root mean squared error presented in Tables 1–3 for these estimators confirms it.
- The LPWM quartiles estimators provide good results essentially for the estimation of the first and second quartile. In those cases, the LPWM estimator has the smallest bias.
- Regarding bias, the best results, for the estimation of the third quartile were obtained by the ML quartiles estimators.
- For large sample sizes, the ML quartiles estimators were always the best estimator regarding minimum RMSE. This can be partially explained by the optimal properties of the regular maximum likelihood estimators.
- In terms of precision, the best results for estimation of the first quartile for moderate and large sample sizes were obtained by the ML and M estimation methods (see figure 1).
- There are no significance differences in terms of precision in the estimation the second and third quartile for moderate and large sample sizes (see figure 2 and 3).
- Regarding the different estimation methods, we conclude that there is no an competitive estimator. But the results here presented allow us to conclude that the LPWM estimators have a very attractive behavior.

### References

1. B.C. Arnold. Pareto and Generalized Pareto Distributions. *In D. Chotikapanich (ed.) Modeling Income Distributions and Lorenz Curves*, Springer, New York, 119–145 (2008)

**Table 1.** Simulated mean value / RMSE of the ratio between the estimated and true quartile estimator with  $p = 0.25$ , for the Pareto model with  $(a, c) = (0.5, 1)$ .

$n$	ML	M	PWM	LPWM
	$\hat{Q}(p)/Q(p)$			
10	1.1982 / 0.4296	0.8330 / <u>0.2694</u>	6.9340 / 141.1994	<u>1.0658</u> / 0.4597
15	1.1226 / 0.2724	0.8002 / <u>0.2355</u>	7.5666 / 243.6303	<u>1.0403</u> / 0.3215
20	1.0882 / <u>0.2078</u>	0.7855 / 0.2319	6.2652 / 51.3711	<u>1.0286</u> / 0.2658
30	1.0566 / <u>0.1465</u>	0.7726 / 0.2341	6.4768 / 73.5933	<u>1.0182</u> / 0.2057
40	1.0426 / <u>0.1184</u>	0.7668 / 0.2367	6.6328 / 90.1173	<u>1.0136</u> / 0.1718
50	1.0337 / <u>0.1001</u>	0.7632 / 0.2389	6.5373 / 63.0567	<u>1.0109</u> / 0.1518
75	1.0225 / <u>0.0769</u>	0.7587 / 0.2422	6.3086 / 39.9115	<u>1.0070</u> / 0.1217
100	1.0170 / <u>0.0643</u>	0.7564 / 0.2441	8.6612 / 255.7352	<u>1.0055</u> / 0.1045

**Table 2.** Simulated mean value / RMSE of the ratio between the estimated and true quartile estimator with  $p = 0.5$ , for the Pareto model with  $(a, c) = (0.5, 1)$ .

$n$	ML	M	PWM	LPWM
	$\hat{Q}(p)/Q(p)$			
10	1.1990 / 0.7284	0.5419 / <u>0.4789</u>	4.5225 / 92.5043	<u>1.1255</u> / 0.6747
15	1.1223 / 0.4924	0.5249 / 0.4824	4.9668 / 161.3528	<u>1.0782</u> / <u>0.4701</u>
20	1.0878 / 0.3954	0.5172 / 0.4864	4.1163 / 33.9924	<u>1.0562</u> / <u>0.3851</u>
30	1.0559 / 0.2952	0.5108 / 0.4906	4.2707 / 48.8753	<u>1.0359</u> / <u>0.2945</u>
40	1.0426 / <u>0.2464</u>	0.5080 / 0.4928	4.3824 / 59.9523	<u>1.0277</u> / 0.2470
50	1.0338 / <u>0.2139</u>	0.5062 / 0.4942	4.3244 / 41.9493	<u>1.0221</u> / 0.2163
75	1.0230 / <u>0.1699</u>	0.5041 / 0.4961	4.1797 / 26.5366	<u>1.0151</u> / 0.1729
100	1.0178 / <u>0.1452</u>	0.5030 / 0.4971	5.7500 / 170.1910	<u>1.0119</u> / 0.1484

**Table 3.** Simulated mean value / RMSE of the ratio between the estimated and true quartile estimator with  $p = 0.75$ , for the Pareto model with  $(a, c) = (0.5, 1)$ .

$n$	ML	M	PWM	LPWM
	$\hat{Q}(p)/Q(p)$			
10	<u>1.4523</u> / 2.3865	0.2605 / <u>0.7429</u>	2.1818 / 44.9050	1.6411 / 3.0936
15	<u>1.2595</u> / 1.2860	0.2555 / <u>0.7458</u>	2.4208 / 79.7696	1.3532 / 1.4855
20	<u>1.1832</u> / 0.9718	0.2533 / <u>0.7473</u>	2.0092 / 16.7717	1.2454 / 1.0804
30	<u>1.1129</u> / <u>0.6727</u>	0.2519 / 0.7484	2.0967 / 24.2714	1.1490 / 0.7202
40	<u>1.0849</u> / <u>0.5402</u>	0.2513 / 0.7488	2.1586 / 29.8623	1.1110 / 0.5717
50	<u>1.0667</u> / <u>0.4602</u>	0.2510 / 0.7491	2.1342 / 20.8901	1.0866 / 0.4813
75	<u>1.0452</u> / <u>0.3556</u>	0.2506 / 0.7494	2.0681 / 13.1939	1.0582 / 0.3685
100	<u>1.0350</u> / <u>0.3016</u>	0.2504 / 0.7496	2.8547 / 84.8362	1.0445 / 0.3106

2. J.H.T.Kim, S. Ahn and S.Ahn, Parameter estimation of the Pareto distribution using pivotal quantity, *Journal of the Korean Statistical Society* **46**, 438–450 (2017)
3. F. Caeiro and M. I. Gomes. Semi-parametric tail inference through probability-weighted moments. *Journal of Statistical Planning and Inference*, 141, 937–950, (2011)
4. F. Caeiro, M.I. Gomes and B. Vandewalle, Semi-Parametric Probability-Weighted Moments Estimation Revisited. *Methodol Comput Appl Probab*, 16, 1–29, (2014)
5. F. Caeiro and D. Prata Gomes. A Log Probability Weighted Moment Estimator of Extreme Quantiles. *Theory and Practice of Risk Assessment – Springer Pro-*

**Table 4.** Simulated mean value / RMSE of the ratio between the estimated and true quartile estimator with  $p = 0.25$ , for the Pareto model with  $(a, c) = (2, 2)$ .

$n$	ML	M	PWM	LPWM
$\hat{Q}(p)/Q(p)$				
10	1.0385 / 0.0809	0.9912 / <u>0.0580</u>	1.0198 / 0.1126	<u>1.0035</u> / 0.0891
15	1.0254 / 0.0572	0.9924 / <u>0.0433</u>	1.0158 / 0.0902	<u>1.0024</u> / 0.0699
20	1.0188 / 0.0456	0.9933 / <u>0.0363</u>	1.0133 / 0.0784	<u>1.0016</u> / 0.0596
30	1.0124 / 0.0337	0.9946 / <u>0.0290</u>	1.0103 / 0.0643	<u>1.0010</u> / 0.0479
40	1.0095 / 0.0278	0.9957 / <u>0.0253</u>	1.0087 / 0.0562	<u>1.0008</u> / 0.0409
50	1.0075 / 0.0238	0.9963 / <u>0.0227</u>	1.0076 / 0.0508	<u>1.0007</u> / 0.0365
75	1.0051 / <u>0.0186</u>	0.9972 / 0.0192	1.0058 / 0.0427	<u>1.0004</u> / 0.0297
100	1.0039 / <u>0.0157</u>	0.9978 / 0.0172	1.0049 / 0.0378	<u>1.0004</u> / 0.0256

**Table 5.** Simulated mean value / RMSE of the ratio between the estimated and true quartile estimator with  $p = 0.5$ , for the Pareto model with  $(a, c) = (2, 2)$ .

$n$	ML	M	PWM	LPWM
$\hat{Q}(p)/Q(p)$				
10	1.0229 / 0.1253	0.9750 / <u>0.0968</u>	<u>0.9935</u> / 0.1205	1.0070 / 0.1205
15	1.0150 / 0.0976	0.9804 / <u>0.0821</u>	0.9949 / 0.0966	<u>1.0047</u> / 0.0961
20	1.0110 / 0.0828	0.9835 / <u>0.0740</u>	0.9955 / 0.0831	<u>1.0033</u> / 0.0824
30	1.0072 / 0.0658	0.9872 / <u>0.0635</u>	0.9964 / 0.0671	<u>1.0021</u> / 0.0665
40	1.0057 / <u>0.0566</u>	0.9899 / 0.0573	0.9973 / 0.0579	<u>1.0019</u> / 0.0573
50	1.0046 / <u>0.0500</u>	0.9913 / 0.0524	0.9977 / 0.0515	<u>1.0015</u> / 0.0510
75	1.0032 / <u>0.0406</u>	0.9937 / 0.0454	0.9984 / 0.0421	<u>1.0012</u> / 0.0416
100	1.0026 / <u>0.0351</u>	0.9950 / 0.0410	0.9988 / 0.0364	<u>1.0010</u> / 0.0360

**Table 6.** Simulated mean value / RMSE of the ratio between the estimated and true quartile estimator with  $p = 0.75$ , for the Pareto model with  $(a, c) = (2, 2)$ .

$n$	ML	M	PWM	LPWM
$\hat{Q}(p)/Q(p)$				
10	<u>1.0058</u> / 0.2340	0.9547 / <u>0.1839</u>	0.9576 / 0.1872	1.0277 / 0.2517
15	<u>1.0038</u> / 0.1862	0.9652 / 0.1611	0.9663 / <u>0.1577</u>	1.0179 / 0.1960
20	<u>1.0026</u> / 0.1597	0.9712 / 0.1472	0.9711 / <u>0.1403</u>	1.0130 / 0.1666
30	<u>1.0015</u> / 0.1285	0.9779 / 0.1277	0.9772 / <u>0.1182</u>	1.0083 / 0.1325
40	<u>1.0017</u> / 0.1109	0.9826 / 0.1159	0.9815 / <u>0.1053</u>	1.0068 / 0.1140
50	<u>1.0014</u> / 0.0985	0.9851 / 0.1063	0.9841 / <u>0.0954</u>	1.0055 / 0.1008
75	<u>1.0013</u> / <u>0.0804</u>	0.9893 / 0.0923	0.9881 / 0.0810	1.0041 / 0.0820
100	<u>1.0013</u> / <u>0.0696</u>	0.9916 / 0.0837	0.9904 / 0.0721	1.0034 / 0.0709

ceedings in Mathematics & Statistics, **136**, 293–303, (2015)

6. F. Caeiro, A.P. Martins and I.J. Sequeira. Finite sample behaviour of Classical and Quantile Regression Estimators for the Pareto distribution. In T.E. Simos and C. Tsitouras (eds.), AIP Conf. Proc. **1648**, 540007 (2015)
7. J.A. Greenwood, J.M. Landwehr, N.C. Matalas and J.R. Wallis. Probability Weighted Moments: definition and relation to parameters of several distributions expressible in inverse form. *Water Resources Research*, **15**(5), 1049–1054 (1979)

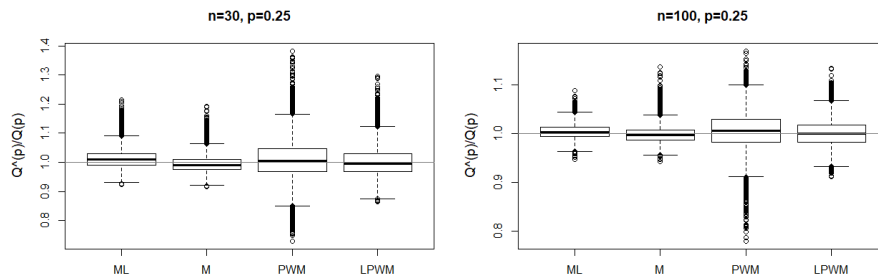


**Fig. 1.** Simulated ratio between the estimated and true quartile, for the Pareto model with  $(a, c) = (2, 2)$ ,  $p = 0.25$ ,  $n = 30$ (left),  $n = 100$ (right).

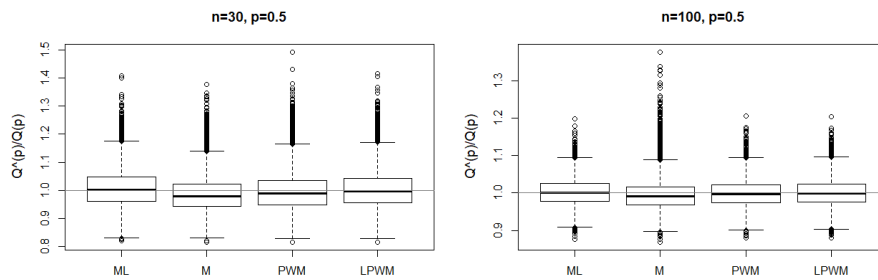


**Fig. 2.** Simulated ratio between the estimated and true quartile, for the Pareto model with  $(a, c) = (2, 2)$ ,  $p = 0.5$ ,  $n = 30$ (left),  $n = 100$ (right).

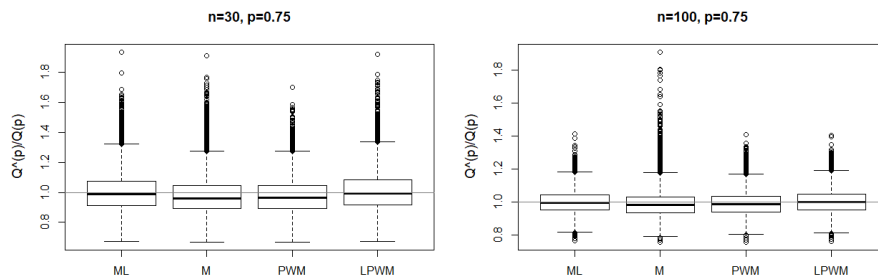


**Fig. 3.** Simulated ratio between the estimated and true quartile, for the Pareto model with  $(a, c) = (2, 2)$ ,  $p = 0.75$ ,  $n = 30$ (left),  $n = 100$ (right).

8. J. Hosking, J. Wallis and E. Wood. Estimation of the generalized extreme value distribution by the method of probability-weighted moments. *Technometrics*, **27**(3), 251–261 (1985)

9. N.L. Johnson, S. Kotz and N. Balakrishnan. *Continuous Univariate Distributions*, Wiley, New York, Vol.1, 2nd Ed. (1994)

10. F. Caeiro and A. Mateus. Log Probability Weighted Moments Method for Pareto distribution. In Skiadas, C.H. (ed.) 17th ASMDA Conference Proceedings, 211–218 (2017)
11. V. Pareto. Cours d'Economie Politique, Vol. 2, Lausanne (1897)
12. R. E. Quandt. Old and new Methods of Estimation and the Pareto Distribution. *Metrika*, 10, 55–82 (1966)
13. R Development Core Team, R: A language and environment for statistical computing. R Foundation for Statistical Computing, Vienna, Austria (2018) URL: <http://www.R-project.org/>

# The Generalized Vandermonde Interpolation Polynomial Based on Divided Differences

Asaph Keikara Muhumuza<sup>1,2</sup>, Karl Lundengård<sup>2</sup>, Jonas Österberg<sup>2</sup>, Sergei Silvestrov<sup>2</sup>, John Magero Mango<sup>3</sup>, and Godwin Kakuba<sup>3</sup>

- <sup>1</sup> Department of Mathematics, Busitema University, Box 238 Tororo, Kampala, Uganda, East Africa.  
(E-mail: [asaph.keikara.muhumuza@mdh.se](mailto:asaph.keikara.muhumuza@mdh.se))
- <sup>2</sup> Division of Applied Mathematics, Mälardalen University, Box 883, Högscoleplan 1, SE 721 23 Västerås, Sweden  
(E-mail: {[karl.lundengard](mailto:karl.lundengard@mdh.se), [jonas.osterberg](mailto:jonas.osterberg@mdh.se), [sergei.silvestrov](mailto:sergei.silvestrov@mdh.se)}@mdh.se)
- <sup>3</sup> Department of Mathematics, College of Natural Sciences, Makerere University, Box 7062, Kampala, Uganda, East Africa.  
(E-mail: {[mango](mailto:mango@cns.mak.ac.ug), [kakuba](mailto:kakuba@cns.mak.ac.ug)}@cns.mak.ac.ug)

**Abstract.** In this article, we will construct the divided differences interpolation polynomial based on the generalized Vandermonde determinant approach. Some results regarding the appropriateness for this method for curve-fitting and approximation will be discussed. The proposed interpolation technique will be tested by construction of approximative models based on experimental data.

**Keywords:** Generalized Vandermonde determinant, Divided Differences interpolating polynomial, Approximative models..

## 1 The Interpolation Problem and the Vandermonde Determinant

Given the values of the function  $f(x)$  at  $n + 1$  distinct points  $x_0, x_1, \dots, x_n$  which may not be necessarily equally spaced or even arranged in increasing order, the only restriction being that they must be distinct [30]. We want to construct a polynomial  $P_n \in \mathbb{P}_n$ , a family of polynomials of degree at most  $n + 1$ , which take on the same values as  $f$  at the  $n + 1$  points  $x_0, x_1, \dots, x_n$ . Thus as an alternative approach to the interpolation problem by considering directly a polynomial of the form [38]:

$$P_n(x) = a_0 + a_1x + a_2x^2 + \dots + a_nx^n = \sum_{n=0}^n a_nx^n$$

and we would require that the following interpolation conditions are satisfied  $P_n(x_j) = f(x_j), \quad j = 0, 1, 2, \dots, n$ .

These interpolation conditions, imply that

$$a_0 + a_1x_j + \dots + a_nx_j^n = f(x_j), j = 0, \dots, n. \quad (1)$$



In matrix form (1) can be expressed as

$$\begin{pmatrix} 1 & x_0 & x_0^2 & \cdots & x_0^n \\ 1 & x_1 & x_1^2 & \cdots & x_1^n \\ \vdots & \vdots & \vdots & \ddots & \vdots \\ 1 & x_n & x_n^2 & \cdots & x_n^n \end{pmatrix} \begin{pmatrix} a_0 \\ a_1 \\ \vdots \\ a_n \end{pmatrix} = \begin{pmatrix} f(x_0) \\ f(x_1) \\ \vdots \\ f(x_n) \end{pmatrix} \quad (2)$$

In order for the system (2) to have a unique solution, it has to be nonsingular. This means, for example, that the determinant of its coefficients matrix must not vanish [31], that is,

$$\begin{vmatrix} 1 & x_0 & x_0^2 & \cdots & x_0^n \\ 1 & x_1 & x_1^2 & \cdots & x_1^n \\ \vdots & \vdots & \vdots & \ddots & \vdots \\ 1 & x_n & x_n^2 & \cdots & x_n^n \end{vmatrix} \neq 0. \quad (3)$$

The coefficient matrix in the system (2) is called the Vandermonde matrix and its determinant in (3), is known as the Vandermonde determinant. The Vandermonde determinant equals to the product of terms of the form  $|x_i - x_j|$  for  $i > j$  [17], that is,

**Theorem 1.** *The expression for the determinant of the Vandermonde matrix is well-known [17]:*

$$\begin{vmatrix} 1 & x_0 & x_0^2 & \cdots & x_0^n \\ 1 & x_1 & x_1^2 & \cdots & x_1^n \\ \vdots & \vdots & \vdots & \ddots & \vdots \\ 1 & x_n & x_n^2 & \cdots & x_n^n \end{vmatrix} = \prod_{\substack{i=0 \\ i \neq j}}^n (x_i - x_j).$$

The simplified proof of this proof can be got from [26]. Since we assume that the points  $x_0, \dots, x_n$  are distinct, the determinant in (3) is indeed non zero. Hence, the system (2) has a solution that is also unique.

Instead of using the monomials  $1, x, x^2, \dots, x^n$  as a basis for the polynomials of degree at most  $n$ , we now use the fundamental polynomials  $L_0, L_1, \dots, L_n$ , where

$$P_n(x) = L_0(x)f(x_0) + L_1(x)f(x_1) + \cdots + L_n(x)f(x_n) \quad (4)$$

where each  $L_i \in \mathbb{P}_n$ . The polynomial  $P_n$  will have the same values as  $f(x)$  at  $x = x_0, x_1, \dots, x_n$  if

$$L_i(x_j) = \delta_{ij} \quad 0 \leq i \leq n. \quad (5)$$

In (5) we write the  $\delta_{ij}$  to denote the *Kronecker delta* function, which takes on the value 0 when  $i \neq j$  and the value 1 when  $i = j$ . For general value of  $i, 0 \leq i \leq n$ , we have

$$L_i(x) = \prod_{\substack{i=0 \\ i \neq j}}^n \left( \frac{x - x_j}{x_i - x_j} \right). \quad (6)$$

From (6) we notice immediately that  $L_i$  is zero at all values  $x = x_0, x_1, \dots, x_n$ , except for  $x = x_i$  when  $L_i$  takes the value 1. This agrees with the requirement (5) and therefore the interpolation polynomial can be written in the form  $P_n(x) = \sum_{i=0}^n f(x_i)L_i(x)$ . This is famously known as the Lagrange form of the interpolating polynomial as elaborately discussed in [8,38].

## 2 Generalized Divided Differences

Divided differences are important in connection with polynomial interpolation, (for example see, [30,31]. Let  $x_0, x_1, \dots, x_n$  to be any  $n + 1$  distinct numbers and attempt to write  $P_n(x)$ , the interpolation polynomial for  $f(x)$  at the points, as

$$\begin{aligned} P_n(x) &= a_0 + (x - x_0)a_1 + (x - x_0)(x - x_1)a_2 + \dots \\ &= (x - x_0)(x - x_1) \dots (x - x_{n-2})(x - x_{n-1})a_n. \end{aligned} \quad (7)$$

Substituting  $x = x_0, x_1, \dots, x_n$  in turn into (7) we obtain the following set of simultaneous equation

$$\begin{aligned} f(x_0) &= a_0 \\ f(x_1) &= a_0 + (x_1 - x_0)a_1 \\ f(x_2) &= a_0 + (x_2 - x_0)a_1 + (x_2 - x_0)(x_2 - x_1)a_2 \\ &\vdots \\ f(x_n) &= a_0 + (x_n - x_0)a_1 + \dots + (x_n - x_0) \dots (x_n - x_{n-1})a_n. \end{aligned}$$

We see that these triangular equations determine values for  $a_0, a_1, \dots, a_n$  uniquely. Thus, the constant coefficients  $a_j$  involves  $f(x_0), f(x_1), \dots, f(x_j)$  only which can be rewritten as  $a_j = f[x_0, x_1, \dots, x_j]$  to emphasize its dependence on these suffixes. At this level, it is instructive to compare (7) with the Lagrange form (4). By equating the coefficients of  $x^n$ , we obtain [38]:

$$f[x_0, x_1, \dots, x_n] = \sum_{i=0}^n \frac{f(x_i)}{\prod_{\substack{i=0 \\ i \neq j}}^n (x_i - x_j)}. \quad (8)$$

This leads to leads to the recurrence expression called *divided differences*, which is given by

$$f[x_0, x_1, \dots, x_n] = \frac{f[x_1, \dots, x_n] - f[x_0, \dots, x_{n-1}]}{x_n - x_0}. \quad (9)$$

Applying this scheme to (7), we can write the interpolating polynomial in the Newton form

$$\begin{aligned} P_n(x) &= f[x_0] + (x - x_0)f[x_0, x_1] + \dots \\ &= (x - x_0)(x - x_1) \dots (x - x_{n-1})f[x_0, x_1, \dots, x_n] \end{aligned} \quad (10)$$

Basing on the recurrence formula in Equation (9) the explicit formula representation of divided differences is given by [31]:

$$[x_0, \dots, x_n | f] = \frac{V \left( \begin{array}{c} p_0, \dots, p_{n-1}, f \\ x_0, \dots, x_{n-1}, x_n \end{array} \right)}{V \left( \begin{array}{c} p_0, \dots, p_{n-1}, p_n \\ x_0, \dots, x_{n-1}, x_n \end{array} \right)} \quad (11)$$

where the right-hand side is quotient of two determinants of the form

$$V \left( \begin{array}{c} p_0, \dots, p_{n-1}, p_n \\ x_0, \dots, x_{n-1}, x_n \end{array} \right) = \det p_i(x_k) = \begin{vmatrix} p_0(x_0) & \dots & p_0(x_n) \\ \vdots & \vdots & \vdots \\ p_n(x_0) & \dots & p_n(x_n) \end{vmatrix}$$

and  $p_i(x) = x^i$  ( $i = 0, 1, \dots, n$ ) are the simple “monomials” or “power-functions”.

The basic characteristic of these “ordinary” divided differences is the classical complete Tchebychev (CT) system [30],  $(p_0, p_1, \dots, p_n)$ . We obtain the *generalized divided differences* of a function  $f$ , if we replace this system by an arbitrary Tchebychev-system  $(f_0, f_1, \dots, f_m)$  (complete or not) using (11) as definition we have

$$\left[ \begin{array}{c} f_0, f_1, \dots, f_m \\ x_0, x_1, \dots, x_m \end{array} \middle| f \right] = \frac{V \left( \begin{array}{c} f_0, \dots, f_{m-1}, f \\ x_0, \dots, x_{m-1}, x_m \end{array} \right)}{V \left( \begin{array}{c} f_0, \dots, f_{m-1}, f_m \\ x_0, \dots, x_{m-1}, x_m \end{array} \right)} \quad (12)$$

Be we give a theorem that verifies that divided differences (12) satisfy a recurrence formula in analogy to (11) which simplifies computation, we first give some basic definitions of complete Tchebychev (CT)-system and extended complete Tchebychev (ECT)- system [30,46].

**Definition 1.** Let  $f_0, \dots, f_m$  denote continuous real-valued functions defined on a closed finite interval  $[a, b]$ . The functions will be called a Tchebychev system over  $[a, b]$ , abbreviated  $T$ - system (with reference to the interval  $[a, b]$  if no ambiguity arises) provided the  $n + 1$ st order determinants

$$V \left( \begin{array}{c} f_0, \dots, f_m \\ x_0, \dots, x_m \end{array} \right) = \begin{vmatrix} f_0(x_0) & \dots & f_0(x_m) \\ \vdots & \vdots & \vdots \\ f_m(x_0) & \dots & f_m(x_m) \end{vmatrix} \quad (13)$$

are strictly positive whenever  $a \leq x_0 < x_1 < \dots < x_m \leq b$ .

The functions  $(f_0, \dots, f_m)$ ,  $f_i \in C^{m-1}[a, b]$ , will be referred to as an Extended Complete Tchebychev (ECT) system if  $\{f_0, \dots, f_k\}$  is a  $T$ -system for each  $k = 0, 1, \dots, m$ .

The set of monomials  $f(x_i) = x^i, i = 0, 1, \dots, n$ , defined on any finite interval  $[a, b]$ , is a classical example of an ECT-system. In this case the determinant in (13) reduces to the familiar Vandermonde determinant with values

$$v_n(x) = \prod_{0 \leq i < j \leq n} (x_j - x_i).$$

**Theorem 2.** Let  $I \subseteq \mathbb{R}$  be an interval and  $m \geq 1$ . Let  $(f_0, \dots, f_m)$ ,  $(f_0, \dots, f_{m-1})$  and (in the case  $m \geq 2$  also)  $(f_0, \dots, f_{m-2})$  be Tchebychev-systems over  $I$ . Consider  $m + 1$ st different knots  $x_i \in I (i = 0, 1, \dots, m)$ . Then,

$$\left[ \begin{array}{c} f_0, f_1, \dots, f_m \\ x_0, x_1, \dots, x_m \end{array} \middle| f \right] = \frac{\left[ \begin{array}{c} f_0, f_1, \dots, f_{m-1} \\ x_1, x_2, \dots, x_m \end{array} \middle| f \right] - \left[ \begin{array}{c} f_0, f_1, \dots, f_{m-1} \\ x_0, x_1, \dots, x_{m-1} \end{array} \middle| f \right]}{\left[ \begin{array}{c} f_0, f_1, \dots, f_{m-1} \\ x_1, x_2, \dots, x_m \end{array} \middle| f_m \right] - \left[ \begin{array}{c} f_0, f_1, \dots, f_{m-1} \\ x_0, x_1, \dots, x_{m-1} \end{array} \middle| f_m \right]}. \quad (14)$$

**Theorem 3.** Let  $x_0, x_1, \dots, x_j, x_{j+1}, \dots, x_k$  and  $y_0, y_1, \dots, y_j, y_{j+1}, \dots, y_k$  with  $x_{j+1} = x_{j+1}, \dots, x_k = y_k$  be  $k + j + 2$  distinct points of an interval  $I$  ( $0 \leq j \leq k$ ). Suppose also that  $(f_0, f_1, \dots, f_{k+1})$  is a complete Tchebychev system over  $I$  and set for  $i = 0, 1, \dots, j$  such that

$$a_{ik}(f) = \left[ \begin{array}{c} f_0, f_1, \dots, f_k \\ x_0, x_1, \dots, x_i, y_{i+1}, \dots, y_k \end{array} \middle| f \right] - \left[ \begin{array}{c} f_0, f_1, \dots, f_k \\ x_0, x_1, \dots, x_{i-1}, y_i, \dots, y_k \end{array} \middle| f \right]$$

Then, we have

$$\left[ \begin{array}{c} f_0, f_1, \dots, f_k \\ x_0, x_1, \dots, x_k \end{array} \middle| f \right] - \left[ \begin{array}{c} f_0, f_1, \dots, f_k \\ y_0, x_1, \dots, y_k \end{array} \middle| f \right] = \sum_{i=0}^j a_{ik}(f_{k+1}) \left[ \begin{array}{c} f_0, f_1, \dots, f_k \\ x_0, x_1, \dots, x_{i-1}, y_i, \dots, y_k \end{array} \middle| f \right] \quad (15)$$

The equation (15) generalizes the formula for divided differences in (14).

The following resulting Corollary is a direct application of Theorem 2.

**Corollary 1.** If the divided differences of  $f$  with respect to  $(f_0, f_1, \dots, f_{k+1})$  are bounded on  $I$  and the divided differences of  $f_{k+1}$  with respect to  $(f_0, f_1, \dots, f_k)$ , then the divided differences of  $f$  with respect to  $(f_0, f_1, \dots, f_k)$  are bounded on  $I$ .

### 3 The Error in Polynomial Interpolation

Our goal here is to provide estimates on the “error” we make when interpolating data that is taken from sampling an underlying function  $f(x)$ . While the interpolant and the function agree with each other at the interpolation points, there is, in general, no reason to expect them to be close to each other elsewhere. Nevertheless, we can estimate the difference between them, a difference which we refer to as the interpolation error, for more details see [24–26,35–37]. We let  $\Pi_n$  denote the space of polynomials of degree  $\leq n$ , and let  $C^{n+1}[a, b]$  denote the space of functions that have  $n + 1$  continuous derivatives on the interval  $[a, b]$ .

**Theorem 4.** Let  $f(x) \in C^{n+1}[a, b]$  and  $Q_n(x) \in \Pi_n$  such that it interpolates  $f(x)$  at the  $n + 1$  distinct points  $x_0, \dots, x_n \in [a, b]$ . Then for all  $x \in [a, b]$ , there

exists  $\xi_n \in (a, b)$  such that

$$f(x) - Q(x) = \frac{1}{(n+1)!} f^{(n+1)}(\xi_n) \prod_{j=0}^n (x - x_j). \quad (16)$$

This is a well-known theorem, see for example [38] for proof.

### 3.1 Lebesgue Function and Lebesgue Constants

Given  $X = \{x_j, j = 0, 1, 2, \dots, n; \in \mathbb{R}\}$  be a set of  $n+1$  distinct interpolation points (or nodes) on the real interval  $[-1, 1]$  such that  $-1 \leq x_0 < x_1 < \dots < x_n \leq 1$ . We define a  $f \in C[-1, 1]$  such that when approximating  $f$  from a finite-dimensional  $\mathcal{V}_n = \text{span}\{\phi_0, \phi_1, \dots, \phi_n\}$  with  $\phi_i \in C[-1, 1]$  for  $0 \leq i \leq n$ , then there exists at least one element  $p_n^* \in \mathcal{V}_n$  that is closet to  $f$ . When using the  $\|f\|_\infty = \max_{x \in [-1, 1]} |f(x)|$  approximation criteria, for example see [15,51], the element  $p_n^*$  is the closest one if the  $\phi_0, \phi_1, \dots, \phi_n$  are a Tchebychev system.

We are interested in the interpolation points  $x_j$  that make the interpolation error [38]

$$\left\| f(x) - \sum_{i=0}^n \alpha_i \phi_i(x_i) \right\| = \max_{x \in [-1, 1]} \left| f(x) - \sum_{i=0}^n \alpha_i \phi_i(x_i) \right|$$

as small as possible. In other words, there is an interest in using the interpolating polynomials that are near best approximants [30].

When for instance, we consider the monomials  $\phi_i(x) = x^i$  and  $f$  to be sufficiently differentiable say  $f \in C^{n+1}[-1, 1]$ , then the interpolant

$$p_n(x) = \sum_{i=0}^n \alpha_i x^i \text{ satisfying } p_n(x_j) = f(x_j), \quad 0 \leq j \leq n,$$

the error  $\|f - p_n\|$  is bounded such that from (16), we have

$$\|f - p_n\|_\infty \leq \max_{x \in [-1, 1]} \left( \frac{|f^{(n+1)}(x)|}{(n+1)!} \right) \max_{x \in [-1, 1]} \prod_{j=0}^n |x - x_j|. \quad (17)$$

Throughout this study, we will refer to the inequality (17) the first interpolating error formula [30,38]. It is well known that  $\|(x - x_0)(x - x_1) \dots (x - x_n)\|_\infty$  is minimal on  $[-1, 1]$  if the  $x_j$  are the zeroes of the  $(n+1)$ th-degree Tchebychev polynomial  $T_{n+1}(x) = \cos((n+1) \arccos x)$ .

The operator that associates with  $f$  its interpolant  $p_n$  is linear and given by

$$P_n[x_0, \dots, x_n] : C([-1, 1]) \rightarrow \mathcal{V}_n : f(x) \rightarrow p_n(x) = \sum_{i=0}^n f(x_i) l_i(x), \quad (18)$$

where the basic Lagrange polynomial [41,42]:

$$l_i(x) = \prod_{\substack{j=0 \\ j \neq i}}^n \frac{x - x_j}{x_i - x_j}$$

satisfy  $l_i(x_j) = \delta_{ij}$ . So another bound for the interpolation error is given by

$$\|f - p_n\|_\infty \leq (1 + \|P_n\|) \|f - p_n^*\|_\infty \|P_n\| = \max_{x \in [-1,1]} \sum_{i=0}^n |l_i(x)|$$

where  $P_n := P_n[x_0, \dots, x_n]$  is the linear operator defined by (18), and  $p_n^*$  is the best uniform polynomial approximation to  $f$ .

**Definition 2.** For a fixed  $n \in \mathbb{R}$  and a given  $x_0, \dots, x_n$ , the Lebesgue function [27,28] is defined by:

$$L_n(x) = L_n(x_0, \dots, x_n; x) = \sum_{i=1}^n |l_i(x)|,$$

and the Lebesgue constant [6,7,44,45] is defined by:

$$\Lambda_n = \Lambda_n(x_0, \dots, x_n) = \max_{-1 \leq x \leq 1} \sum_{i=1}^n |l_i(x)|.$$

It can be clearly seen that both  $L_n(x)$  and  $\Lambda_n$  depend on the location of the interpolation points  $x_j$  as well as on the degree  $n$  but not necessarily on the function values  $f(x_i)$ . It should also be noted that the operator norm of  $P_n$  defined in (18) is equal to the infinity norm of the Lebesgue function [47,50,51]:

$$\|P_n\|_\infty = \lambda_n = \max_{-1 \leq x \leq 1} L_n(x).$$

In the general setting, we consider  $\Omega \subset \mathbb{R}^d$  (or  $\mathbb{C}^d$ ) a compact set or manifold [9]. For example,  $\Omega = [-1, 1]^2 \subset \mathbb{R}^2$  or  $\Omega = [-1, 1]^3 \subset \mathbb{R}^3$ , as in the case of triangle and spheres respectively. Let  $\xi_1, \dots, \xi_N \subset \Omega$  be the interpolating points. The monomials  $\phi_i = \phi(\xi_i) = \phi(\xi_1, \dots, \xi_N) = \xi_1^{\alpha_1(i)}, \dots, \xi_N^{\alpha_n(i)} = x^{\alpha(i)}$ ,  $N = \dim(\mathcal{P}_n^N(\Omega))$  in a certain order  $(\xi, \alpha \in \mathbb{R}^n$  (or  $\mathbb{C}^d$ )). We construct the Vandermonde matrix  $V(\xi, \phi) = [\phi_j(\xi_i)]$  and  $\det(V) \neq 0$ . We define the

determinantal Lagrange formula by  $H_n f(x) = \sum_{j=1}^N f(\xi_j) l_j(x)$ , where

$$l_j(x_j) = \frac{\det[V(\xi_1, \dots, \xi_{j-1}, x, \xi_{j+1}, \dots, \xi_N)]}{\det[V(\xi_1, \dots, \xi_{j-1}, \xi_j, \xi_{j+1}, \dots, \xi_N)]}, \quad l_j(\xi_i) = \sigma_{ij}.$$

**Definition 3.** The Lebesgue function  $L_N(x)$  and Lebesgue constant  $\Lambda_N$  associated with the set of points  $\{x_i\}_{i=1}^N$  is defined by [16,21,29,40]

$$L_N(x) = \sum_{j=1}^N |l_j(x)|, \text{ and } \Lambda_N = \max_{x \in \Omega} L_N(x) \text{ respectively.}$$

Considering the compact domain  $\Omega \subset \mathbb{R}^d$  (or  $\mathbb{C}^d$ ), it should be noted that the determinant of the Vandermonde matrix constructed with respect to the polynomial basis  $\{\phi_k\}$  is key in determining a set for good interpolation points called the Fekete points deeply discussed in [19,20,23,43,48,49].

**Definition 4.** The *Fekete Points* are classical optimal interpolating points that maximize the absolute value of the Vandermonde determinant, that is,  $\max |V(\xi_1, \dots, \xi_N)|$  over the compact subset or manifold  $\Omega \subset \mathbb{R}^d$  (or  $\mathbb{C}^d$ ). Thus, as a result, the Lebesgue constant

$$A_N = \max_{x \in \Omega} \sum_{j=1}^N |l_j(x)| \leq N \text{ since } |l_j(x)| \leq 1.$$

The Fekete points (and Lebesgue constant) are independent of the choice of the basis.

To compute the Lebesgue constant [41,42], we discretize the subset  $\Omega \in \mathbb{R}^n$  with “grid”  $G \subset \Omega$  containing  $K$  well spaced points such that

$$A = \max_{x \in \Omega} \sum_{i=1}^N |l_i(x)| \rightarrow A \approx \max_{x \in G} \sum_{i=1}^N |l_i(x)|$$

The above results can be summarized in the following theorem [33]:

**Theorem 5.** *Let  $x_0, x_1, \dots, x_n$  be  $n + 1$  distinct points on  $[a, b]$ . The linear polynomial  $P_n$  which in is  $C[a, b]$  associates with any function  $f$  the polynomial  $P_n f \in P_n$  interpolates  $f$  between the  $x_k$ 's has the form*

$$\|P_n\| = A_n = \max_{x \in [a, b]} \sum_{k=0}^n |l_k(x)|$$

## 4 Weighted Fekete Points, Transfinite Diameter and Fekete Polynomials

We start with the definition of an admissible weight function [5,14,47] over a space  $\Sigma \subset \mathbb{R}$  (or)  $\mathbb{C}$ .

**Definition 5.** Let  $\omega : \mathbb{R} \rightarrow \infty$ . We say that  $\omega$  is a Freud (type) admissible weight (function), if  $Q(x) = \log(1/\omega(x))$ , is an even, that is  $\omega(x) = \omega(-x)$ , convex function on  $\mathbb{R}$ ,  $Q$  is twice continuously differentiable on  $(0, \infty)$ , and there are constants  $c_1$  and  $c_2$  such that  $0 < c_1 \leq \frac{xQ''(x)}{Q'(x)} \leq c_2 < \infty$  for all  $x \in (0, \infty)$

For example, if  $\omega(x) = \exp(-\frac{1}{2}x^2)$  qualifies as a Gaussian type weight function.

Fekete's idea was to look for points in the compact set  $\Sigma \subset \mathbb{C}$  that are as far apart as possible in the sense of the geometric mean of the distances between the points. Thus considering the Vandermonde determinant [1,14,26]:

$$v_n(\mathbf{x}) = \prod_{1 \leq i < j \leq n} (x_i - x_j), \quad \mathbf{x} = (x_1, \dots, x_n)$$

and any system of points  $\{x_1, \dots, x_n\} \subset \Sigma$  maximizing  $|v_n(\mathbf{x})|$  is called an  $n$ -th (unweighted) Fekete set for  $\Sigma$  and the points  $x_i$  in the set is called Fekete points. If the  $n(n-1)/2$ -th roots of this maximum is denoted by  $\delta_n$ , then the sequence  $\{\delta_n\}_2^\infty$  has a limit  $\delta(\Sigma)$  which is called the transfinite diameter of  $\Sigma$ .

A remarkable theorem of Fekete asserts that the transfinite diameter [12] of any compact set coincides with the logarithmic capacity. For example, if  $\Sigma$  is the unit disk or unit circle, then the  $n$ -th roots of unity form  $n$ -th roots of unity form  $n$ -th Fekete set and in this case  $\delta_n = n^{1/(n-1)}$ , which tends to 1, the capacity of  $\Sigma$ .

It easily follows from this definition that Fekete points are “almost ideal” points for Lagrange interpolation. In fact, each basic interpolating polynomial

$$L_{n-1,k}(z) = \prod_{j=1, j \neq k}^n (z - x_j) / \prod_{j=1, j \neq k}^n (x_k - x_j)$$

satisfies  $|L_{n-1,k}(z)| \leq 1$  for all  $z \in \Sigma$  by choice of the Fekete points  $\{x_j\}$ ; hence the Lebesgue constant is at most  $n$ : In particular, if  $P$  is a polynomial of degree at most  $n$ :

$$L = \sup_{z \in \Sigma} \sum_{k=1}^n |L_{n-1,k}(z)| \leq n.$$

In particular, if  $P$  is a polynomial of degree at most  $n - 1$ , then, for the sum norm:  $\|P\|_{\Sigma} \leq n\|P\|_{\{x_k\}_{k=1}^n}$

The weighted analogue of Fekete points is defined as the points whose expression is given by:

$$\prod_{1 \leq j < k \leq n} |x_i - x_j| \omega(z_i) \omega(z_j)$$

which attains its maximum value at all possible choices of the  $z_i, z_j \in \Sigma$ . Here  $\omega$  is referred to as the quasi-admissible weight on the closed set  $\Sigma$ , that is  $\omega \geq 0$  is upper semicontinuous (usc) and  $|z|\omega(z) \rightarrow 0$  as  $|z| \rightarrow \infty, z \in \Sigma$ , if  $\Sigma$  is unbounded [5]. For any integer  $n \geq 2$  we obtain

$$\delta_n^\omega = \sup_{z \in \Sigma} \left\{ \prod_{1 \leq i \leq j \leq n} |z_i - z_j| \omega(z_i) \omega(z_j) \right\}^{2/n(n-1)}. \quad (19)$$

The supremum definition [22] of  $\delta_n^\omega$  in (19) is obviously attained for some set  $\mathcal{F}_n = \{z_1, z_2, \dots, z_n\} \subseteq \Sigma$ . These  $\mathcal{F}_n$  are called weighted-Fekete sets associated with  $\omega$ , or more briefly  $\omega$ -Fekete sets, and the points  $z_1, z_2, \dots, z_n$  in  $\mathcal{F}_n$  are called weighted Fekete points. It should be noted that the sequence  $\{\delta_n^\omega\}_{n=2}^\infty$  are closely related to the weighted capacity which can be anticipated from the fact that  $Q = \log(1/\delta_n^\omega)$  is a sort of substitute for the “discrete minimal energy.”

## 5 Weighted Lebesgue Constant and Lebesgue Function

Lagrange interpolation at the zeros of orthogonal polynomials is probably the most studied of all approximation processes associated with exponential weights [14] of the type,  $\omega(x) = \exp(-Q)$ . Denoting the zeros of  $P_n$ , the  $n$ th orthogonal polynomial for the weight  $W^2$  by  $-\infty < x_{nn} < x_{n-1,n} < \dots < x_{2n} < x_{1n} < \infty$ . Given a function  $f$ , we define the  $n$ th Lagrange interpolation polynomial to  $f$  at  $\{x_{jn}\}_{j=1}^n$  to be the unique polynomial of degree  $\leq n - 1$  that satisfies

$$L_n[f](x_{jn}) = f(x_{jn}), \quad 1 \leq j \leq n. \text{ One formula for } L_n[f] \text{ is } L_n[f] = \sum_{j=1}^n f(x_{jn}) l_{jn}$$

where  $\{l_{jn}\}_{j=1}^n$  are fundamental polynomials of Lagrange interpolation satisfy-

$$\text{ing } l_{jn}(x_{kn}) = \delta_{jk}. \text{ The } \{l_{jn}\} \text{ admits the expression } l_{jn}(x) = \prod_{k=1, k \neq j}^n \frac{x - x_{kn}}{x_{jn} - x_{kn}},$$

but because we are using zeros of orthogonal polynomials [17], there are others like  $l_{jn}(x) = \frac{K_n(x, x_{kn})}{K_n(x_{jn}, x_{kn})}$ , which is constructed basing on the Christoffel-Darboux formula [32,47].

Another advantage of interpolating at zeros of orthogonal polynomials is the ease of analysis, largely because we have the Gauss quadrature formula

[38]. For polynomial  $P$  of degree  $\leq 2n - 1$ ,

$$\int_{-\infty}^{\infty} PW^2 = \sum_{j=1}^n \lambda_{ij} P(x_{jn}), \text{ where } \lambda_{ij} = \lambda_n(W^2, x_{jn}) = 1/K_n(x_{jn}, x_{jn})$$

are called Christoffel numbers. Since  $L_n[f]^2$  has degree  $\leq 2n - 2$  and agrees with  $f$  at  $\{x_{jn}\}$  we see that

$$\int_{-\infty}^{\infty} L_n[f]^2 W^2 = \sum_{j=1}^n \lambda_{jn} f^2(x_{jn}).$$

Thus convergence and boundedness of  $\{L_n[f]\}$  is closely associated with convergence of Gauss quadrature [11].

### 5.1 Mean Convergence

Just as  $\{S_n[f]\}$  converges in  $L^2$  so do the  $\{L_n[f]\}$ , a famous theorem of Erdős-Tuán [36,37]. Indeed, we may think of  $L_n[f]$  as a discretization of  $S_n[f]$  as:

$$\begin{aligned} L_n[f](x) &= \sum_{j=1}^n \lambda_{jn} f(x_{jn}) K_n(x, x_{jn}) \approx \int_{-\infty}^{\infty} W^2(t) f(t) K_n(x, t) dt \\ &= S_n[f](x). \end{aligned}$$

**Theorem 6.** *Let  $f$  be continuous on the real line. Let  $W(x) = \exp\{-\frac{1}{2}x^2\}$  be the Hermite weight, and assume that  $\lim_{|x| \rightarrow \infty} \|(1 + |x|)W(x)\|_p(\mathbb{R}) = 0$ . Let  $\{L_n[f]\}$  denote the Lagrange interpolation polynomials to  $f(x)$  at the zeros of Hermite polynomials. Then, for  $p > 1$ ,  $\lim_{n \rightarrow \infty} \|(f - L_n[f])W\|_p(\mathbb{R}) = 0$ .*

### 5.2 Lebesgue Function and Pointwise Convergence

Since  $L_n[P] = P$  for any polynomial  $P$  of degree  $\leq n - 1$ , the convergence of  $\{L_n\}$  in almost any norm is equivalent to the norms of these operators being bounded independent of  $n$ . The Lebesgue function is the weighted norm [10]  $L_n[f]$  at the given point when working on infinite intervals, it makes more sense to investigate weighted versions of these. The idea is as follows:

$$\begin{aligned} |L_n[f](x)W(x)| &\leq \sum_{j=1}^n |f(x_{jn})| |l_{jn}(x)| W(x) \\ &\leq \|fW\|_{L_\infty(\mathbb{R})} W(x) \sum_{j=1}^n |l_{jn}(x)| W^{-1}(x_{jn}) \\ &= \|fW\|_{L_\infty(\mathbb{R})} A_n(x). \end{aligned}$$

It can be easily seen that by suitable choice of  $f$  that  $A_n(x) = \sup\{|L_n[f](x)W(x)| : \|fW\|_{L_\infty(\mathbb{R})} \leq 1\}$ .

Thus the weighted Lebesgue function,  $A_n(x)$ , is indeed a norm. The weighted Lebesgue constant of  $L_n$  is

$$A_n = \|A_n(x)\|_{L_\infty(\mathbb{R})}.$$

We observe that for any function  $f$ , there is a pointwise error estimate

$$\begin{aligned} W(x)|f - L_n[f]|(x) &\leq (1 + A_n(x)) \inf_{\deg(P) \leq n-1} \|(f - P)W\|_{L_\infty(\mathbb{R})} \\ &= (1 + A_n(x))E_n[f, W]_\infty \end{aligned}$$

and hence the weighted global estimate

$$\|W(f - L_n[f])\|_{L_\infty} \leq (1 + A_n(x))E_n[f, W]_\infty.$$

Therefore the error in weighted approximation [11] of  $f$  by polynomials of degree  $\leq n$  in the  $L_p$  norm is  $E_n[f, W]_p \leq \inf_{\deg(P) \leq n} \|(f - P)W\|_{L_p(\mathbb{R})}$ .

## 6 The Optimization of Wishart Ensembles as Weighted Fekete Points

Here we will briefly discuss an example of an application weighted Fekete points in probability distributions and data analysis based on density optimization of Wishart density as Gaussian orthogonal ensembles [18,46].

We notice that if  $\lambda_1, \lambda_2, \dots, \lambda_N$  are eigenvalues of a large Wishart matrix [34,39,52],  $X \subset \mathbb{R}(\text{or } \mathbb{C})$ , such that  $\lambda_1 \geq \lambda_2 \geq \dots \geq \lambda_N$ , then  $\lambda_i, i = 1, \dots, N$  have a multivariate distribution also referred to a  $\beta$  ensemble:

$$\mathbb{P}^{(\beta)}(\lambda) = C_N \prod_{i < j} (\lambda_j - \lambda_i)^\beta \exp\left(-\frac{\beta}{4} \sum_{i=1}^N \lambda_i^2\right)$$

where  $C_N$  is a normalizing constant.

The cases  $\beta = 2$  is most well-known and called the Gaussian Orthogonal Ensemble (GOE) [39]. For the case  $\beta = 2$  in (20), which is an applicable case in electrostatics, the distribution becomes

$$\mathbb{P}^{(\beta)}(\lambda) = C_N \prod_{i < j} |\lambda_j - \lambda_i|^2 \exp\left(-\frac{1}{2} \sum_{i=1}^N \lambda_i^2\right) \quad (20)$$

The distribution (20) can be expressed as the squared Weighted Fekete points with weight  $\omega(x) = \exp(-\frac{1}{2}x^2)$  [14] and squared transfinite diameter  $\delta_n^\omega$  as defined in (19). It can be shown that the eigenvalues  $\lambda_i$  will be real and lie on a sphere whose radius can be computed from  $X$ . Finding the transfinite diameter can be shown to be equal to maximizing the Vandermonde determinant [2].

### 6.1 Fitting Interpolating Polynomial to Experimental Data

Let  $\omega(x)$  be a nonnegative integrable function  $[a, b]$  such that  $\omega(x) > 0$  on  $(a, b)$ . For each set of  $n + 1$  points  $x_0, x_1, \dots, x_n$  in the interval  $[a, b]$ , let  $p_\nu(x), \nu = 0, 1, \dots, n$  denote  $n$  polynomials in  $x$  of arbitrary degree such that  $\omega(x_i)p_\nu(x_i) = \delta_{i\nu}, i, \nu = 0, 1, \dots, n$ . The emphasis here is that we permit  $p_\nu$  to be of arbitrary degree while the polynomials  $r_\nu$  are of minimal degree. Then,

the system  $\{\omega(x)p_\nu(x)\}_{\nu=0}^n$  is called a *stable interpolating system* if whenever  $y_\nu \geq 0, \nu = 0, 1, \dots, n$ , we have  $0 \leq \sum_{\nu=0}^n y_\nu w(x)p_\nu(x) \leq \max_\nu y_\nu(x)$ . Note that the function  $\sum_{\nu} y_\nu w(x)p_\nu(x)$  takes on the values  $y_\nu$  at  $x_\nu$ . A stable interpolation system is called *most economical* provided  $\sum_{\nu} \deg p_\nu(x)$  is minimum.

**Theorem 7.** [46] If  $r_\nu(x) = \omega^{-\frac{1}{2}}(x) \frac{l(x)}{l'(x_\nu)(x - x_\nu)}$  where  $l(x) = \prod_{\nu=0}^n (x - x_\nu)$ ,

then, in the three cases:

- (i)  $w(x) = (1 - x)^{\alpha+1}(1 + x)^{\beta+1}$  on  $[-1, 1], \alpha > -1, \beta > -1$ ,
- (ii)  $x^{\alpha+1}e^{-x}$  on  $[0, \infty), \alpha > -1$  and
- (iii)  $e^{-x^2}$  on  $(-\infty, \infty)$ .

the system  $\{\omega(x)p_\nu(x)\}$  is a most economical stable interpolating system if and only if  $p_\nu(x) = r_\nu^2(x)$  and  $x_0, x_1, \dots, x_n$  are respectively, the zeros of

- (i)  $P_{n+1}^{(\alpha, \beta)}(x) = 0$  (Jacobi polynomials),
- (ii)  $L_{n+1}^{(\alpha)}(x) = 0$  (Laguerre polynomials) and
- (iii)  $H_{n+1}(x) = 0$  (Hermite Polynomials).

This will provide a reliable, stable and economic interpolation system for numerical solution of Black-Scholes type partial differential equations in financial mathematics [4] based on large dimension observational and experimental data.

### Acknowledgement

We acknowledge the financial support for this research by the Swedish International Development Agency, (Sida), Grant No.316, International Science Program, (ISP) in Mathematical Sciences, (IPMS). We are also grateful to the Division of Applied Mathematics, Mälardalen University for providing an excellent and inspiring environment for research education and research.

### References

1. A. K., Muhumuza, K., Lundengård, J., Österberg, S., Silvestrov, J. M., Mango, G., Kakuba. Notes on the extreme points of the Vandermonde determinant on surfaces implicitly determined by a univariate polynomial. *To appear in the proceedings of the SPAS2017 conference.*
2. A. K., Muhumuza, K., Lundengård, J., Österberg, S., Silvestrov, J. M., Mango, G., Kakuba. The Multivariate Wishart Distribution Based on Generalized Vandermonde Determinant. *Presented at the IWAP2018 conference.*
3. A. K., Muhumuza, K., Lundengård, J., Österberg, S., Silvestrov, J. M., Mango, G., Kakuba. Critical points of the Vandermonde determinant on spheres defined by various norms. *Presented at the SMTDA2018 conference.*
4. A. K., Muhumuza, K., A., Malyalenko, S., Silvestrov. Lie Symmetries of the Black-Scholes Type Equations in Financial Mathematics. *To appear in the proceedings of the ASMDA2017 London conference.*

5. B-O., Turesson. *Nonlinear Potential Theory and Weighted Sobolev Spaces*. Springer-Verlag Berlin Heidelberg. 2000.
6. B., Sündermann. *Lebesgue constants in Lagrangian interpolation at the Fekete points*. Mitt. Math. Ges. Hamb. **11**(2), 204–211, 1983.
7. B., Sündermann. *On projection constants of polynomial space on the unit ball in several variables*. Math. Z. **188**(1), 111–117 (1984).
8. C., De Boor, A. Pinkus. *Proof of the conjectures of Bernstein and Erdős concerning the optimal nodes for polynomial interpolation*. Bull. J. Approx. Theory **24**(4), 289–303, 1978.
9. C. K., Qu and R., Wong. *Szegős conjecture on Lebesgue constants for Legendre series*. Pacific J. Math. **135**, 157–188, 1988.
10. D. M., Matijla. *Bounds for Lebesgue Functions for Freud Weights*. Journal of Approximation Theory. **79**, 385–406, 1994.
11. D. S., Lubinsky. *A Survey of Weighted Polynomial Approximation with Exponential Weights*. 1 January, 2007.
12. E. B., Saff. *Logarithmic Potential Theory with Applications to Approximation Theory*. Survey in Approximation Theory. Vol. **5**, pp. 165–200, 2010.
13. F. J., Dyson. *A Brownian-motion Model for the Eigenvalues of a Random Matrix*. J. Math. Phys. **3**, N0.6, 31–60, 1962.
14. G., Freud (Budapest). *On Polynomial Approximation with Weights  $\exp\{-\frac{1}{2}x^{2k}\}$ ,  $k \geq 1$* . Acta Mathematica Academiae Scientiarum Hungaricae Tomus **24** (3–4), pp. 363–371, 1973.
15. G. M., Phillips. *Interpolation and Approximation by Polynomials*. CMS Books in Mathematics [Ouvrages de Mathématiques de la SMC], vol. **14**, p. xiv+312. Springer, New York, 2003.
16. G. N., Watson. *The constants of Landau and Lebesgue*. Quart. J. Math. **1**, 310–318, 1930.
17. G., Szegő. *Orthogonal Polynomials*. American Mathematics Society, 1939.
18. G. W., Anderson, A., Guionnet, and O. Zeitouni. *An Introduction to Random Matrices*. Cambridge University Press.
19. H. J., Rack. *An example of optimal nodes for interpolation*. Int. J. Math. Educ. Sci. Technol. **15**(3), 355–357, 1984.
20. H. J., Rack. *An example of optimal nodes for interpolation revisited*. In: Advances in Applied Mathematics and Approximation Theory. Springer Proc. Math. Stat., vol. **41**, pp. 117–120. Springer, New York, 2013.
21. H., Lebesgue. *Sur la représentation trigonométrique approchée des fonctions satisfaisant à une condition de Lipschitz*. Bull. Soc. Math. France, **38** 184–210, 1910; also in Oeuvres Scientifiques, v. 3, L'Enseignement Math., pp. 363–389, 1972.
22. H. N., Mhaskar, and E. B., Saff. *Weighted Analogues of Capacity, Transfinite Diameter and Chebyshev Constant*. Springer-Verlag New York, 1992.
23. J. R., Angelos, E. H., Kaufman, M. S., Henry, T. D., Lenker. *Optimal nodes for polynomial interpolation*. In: Chui, CK, Schumaker, LL, Ward, JD (eds.) Approximation Theory. VI, pp. 17–20. Academic Press, New York, 1989.
24. J. S., Hesthaven. *From electrostatics to almost optimal nodal sets for polynomial interpolation in a simplex*. SIAM J. Numer. Anal. **35**(2), 655–676, 1998.
25. J., Szabados, P., Vértesi. *Interpolation of Functions*. World Scientific, Teaneck, 1990.
26. K., Lundengård, J., Österberg, S., Silvestrov. *Extreme points of the Vandermonde determinant on the sphere and some limits involving the generalized Vandermonde determinant*. *arXiv*, eprint arXiv:1312.6193.
27. L., Brutman. *Lebesgue functions for polynomial interpolation - a survey*. Ann. Numer. Math. **4**(1–4), 111–127, 1997.

28. L., Brutman. *On the Lebesgue function for polynomial interpolation*. SIAM J. Numer. Anal. **15**(4), 694–704, 1978.
29. L., Carlitz. *Note on Lebesgue's constants*. Proc. Amer. Math. Soc. **12**, 932–935, 1961.
30. L. L., Schumaker. *Spline Functions: Basic Theory*. Cambridge University Press, 3rd Edition, 2007.
31. L. M., Milne–Thomson. *The Calculus of Finite Differences*. MacMillan and Co Limited, London, 1933.
32. M., Abramowitz and I., Stegun. *Handbook of Mathematical Functions with Formulas, Graphs, and Mathematical Tables*. Dover, New York, 1964.
33. M. A., Taylor, B. A., Wingate, and R. E., Vincent. *An Algorithm for Computing Fekete Points in the Triangle*. SIAM Journal of Numerical Analysis Vol. **38**, No. 5, pp 1707–1720, 2000.
34. M. L., Mehta. *Random Matrices and the Statistical Theory of Energy Levels*. Academic Press, New York, London, 1967.
35. M. J. D., Powell. *On the maximum errors of polynomial approximations defined by interpolation and by least squares criteria*. Comput. J., **9**, pp. 404–407, 1967.
36. P., Erdős. *Problems and results on the theory of interpolation*. I. Acta Math. Acad. Sci. Hung. **9**, 381–388, 1958.
37. P., Erdős. *Some remarks on the theory of graphs*. Bull. Am. Math. Soc. **53**, 292–294, 1947.
38. P. J., Davis. *Interpolation and Approximation*. Blaisdell, New York, 1963.
39. P. J., Forester. *Log-Gases and Random Matrices*. London Mathematical Society Monographs, Princeton University Press, London, 2010.
40. P. V., Galkin. *Estimates for Lebesgue constants (in Russian)*. Trudy Mat. Inst. Steklov. **109**, 3–5, 1971; Engl. transl. in Proc. Steklov Inst. Math. **109**, 1–4, 1971.
41. P., Vértesi. *On the optimal Lebesgue constants for polynomial interpolation*. Acta Math. Hung. **47**(1-2), 165–178, 1986.
42. P., Vértesi. *Optimal Lebesgue constant for Lagrange interpolation*. SIAM J. Numer. Anal. **27**(5), 1322–1331, 1990.
43. Q., Chen, I., Babuska. *Approximate optimal points for polynomial interpolation of real functions in an interval and in a triangle*. Comput. Methods Appl. Mech. Eng. **128**(3-4), 405–417, 1995.
44. R., Günttner. *Evaluation of Lebesgue constants*. SIAM J. Numer. Anal. **17**(4), 512–520, 1980.
45. R., Günttner. *Note on the lower estimate of optimal Lebesgue constants*. Acta Math. Hung. **65**(4), 313–317, 1994.
46. S., Karlin, and W. J., Studden., (1966) *Tchebycheff System: With applications in Analysis and Statistics*. Interscience Publishers, John Wiley & Sons.
47. S. R., Finch. *Mathematical Constants*. Encyclopedia of Mathematics and its Applications Vol. **94**, Cambridge University Press, 2003.
48. T. A., Kilgore. *Optimization of the norm of the Lagrange interpolation operator*. Bull. Am. Math. Soc. **83**(5), 1069–1071, 1977.
49. T. A., Kilgore. *A characterization of the Lagrange interpolating projection with minimal Tchebycheff norm*. Bull. J. Approx. Theory **24**(4), 273–288, 1978.
50. T. J., Rivlin. *The Lebesgue constants for polynomial interpolation, Functional Analysis and Its Application*. Int. Conf.; Madras, 1973, H. G. Garnir et al., eds., Springer-Verlag, Berlin, 1974.
51. T. M., Mills, S. J., Smith. *The Lebesgue constant for Lagrange interpolation on equidistant nodes*. Numer. Math. **61**(1), 111–115, 1992.
52. W., König. *Orthogonal Polynomial Ensembles in Probability Theory*. Probability Surveys Vol. **2**, 385–447, 2005.

# Social application of multivariate regression chain graph models

Federica Nicolussi and Manuela Cazzaro

Department of Statistics and Quantitative Methods, via Bicocca degli Arcimboldi 8,  
University of Milano Bicocca, Milano, Italy

(E-mail: [federica.nicolussi@unimib.it](mailto:federica.nicolussi@unimib.it); [manuela.cazzaro@unimib.it](mailto:manuela.cazzaro@unimib.it))

**Abstract.** In this work we focus on the study of relationships among a set of categorical variables. Beyond the conditional and marginal relationships we also consider the context-specific independencies that are particular conditional independencies holding only for certain values of the conditioning variables. At this aim we use an improve of chain graphical models combined with the hierarchical multinomial marginal models. A social application on the life satisfaction is provide.

**Keywords:** Chain Regression Model, Multivariate Regression Model, Context-specific independence.

## 1 Introduction

This work studies how the satisfaction of the interviewees' life can be affected by individual characteristics and personal achievement and, at the same time, how the personal aspects can affect the educational level and the working position. We propose to describe this kind of relationships through a multivariate logistic regression model based on the Chain Graph model. By following the approach of Marchetti and Lupparelli, [4], in fact, we take advantage of a particular case of Chain Graph model, called "of type IV", in order to express variables as *purely explicative*, *purely response* or *mixed* variables. In addition, we also study the relationships under the context-specific independence point of view. This means that we study if there are conditional independencies that hold only for a subset of categories of the conditioning variables. Formally, a context-specific independence (CSI) has the form  $A \perp B|C = i_C$  where  $A$ ,  $B$  and  $C$  are three sets of variables and  $i_C$  is the vector of certain values of the variables in  $C$ . Nyman et al. [6] handle with the context-specific independencies in graphical models, through the so-called *strata* added to the graphs. We improved their approach by implementing the *strata* also in the Chain Graph models, see [5]. This work is finalized in showing the multiple aspects that it is possible to highlight by implementing these models, in both graphical and parametric point of views.

This work follows this structure. In Section 2 is presented the graphical models

---

5<sup>th</sup> SMTDA Conference Proceedings, 12-15 June 2018, Chania, Creete, Greece

© 2018 ISAST



and the parametrization that we adopted. In Section 3 we analysed the ISTAT dataset on the “*aspects of everyday life*”, [3]. Interesting results were showed.

## 2 Methodology

Graphical models take advantage of graphs to represent system of (conditional and/or marginal) independencies among a set of variables. In a graphical model, each vertex of the graph represents a variable and any missing arc is a symptom of independence. In this work we consider chain graph where the arcs between two vertices can be both directed or undirected. In a Chain Regression Graph Models (CRGM), variables linked by undirected arcs have a symmetric relationship (as two covariates or two response variables for instance). Each directed arc links a covariate to its dependent variable. The rules to extract a list of independencies from a graph are called Markov properties. In this work we take advantage of the so-called multivariate regression Markov properties, see [4]. In order to consider also the CSIs we improve the graphical models through labelled arcs. The label on the arcs reports the list of categories of the conditioning variables according to the arc vanishes. These labels are exactly the values of the conditioning variables for which the CSI holds. We refer to this new graphical model as Stratified Chain Regression Graph Model (SCRGM). Figure 1 reports examples of CRGM and SCRGM. Note that the independencies represented by these kinds of graphical models

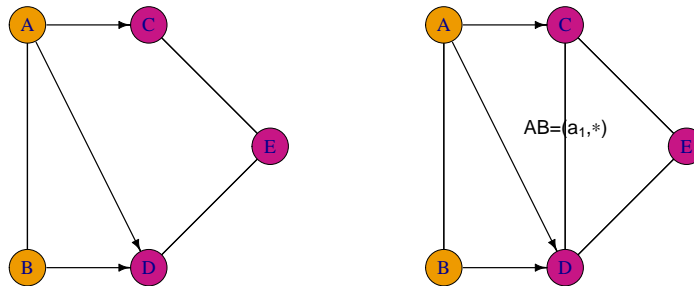


**Fig. 1.** On the left, a CRGM representing  $C \perp D|AB$ ,  $B \perp C|A$  and  $AB \perp E$ . On the right, a SCRGM representing  $C \perp D|AB = (a_1, *)$ ,  $B \perp C|A$  and  $AB \perp E$ . Note that the response variables are displayed in purple and the covariates in orange.

are to be understood marginally with respect to the other response variables. As mentioned before, we can split the variables in “responses” and “covariates”. We adopt the Hierarchical Multinomial Marginal (HMM) parameters, denoted with the symbol  $\eta$ , see [1], to model the dependence among these variables. The HMM parameters are sum of logarithms of probabilities defined on

marginal and joint distributions according to certain properties of hierarchy and completeness. For this reason, each parameter is denoted by the marginal distribution where it is evaluated  $\mathcal{M}$ , by the set of the variables involved by the parameter  $\mathcal{L}$  and by the values of variables in  $\mathcal{L}$  which it refers  $i_{\mathcal{L}}$ :  $\eta_{\mathcal{L}}^{\mathcal{M}}(i_{\mathcal{L}})$ . Note that, when  $\mathcal{L}$  is composed of only one variable, the HMM parameter is a logit. In correspondence of each subset of response variables we can build a regression model. For instance, by considering the SCRGM in Figure 1 (right side), with regard to the dependent variable  $D$ , we have:

$$\eta_D^{ABD}(i_D|i_{AB}) = \beta_{\emptyset}^D + \beta_A^D(i_A) + \beta_B^D(i_B) + \beta_{AB}^D(i_{AB}) \quad (1)$$

Similar regression models can be built for the other response variables or for combination of these.

Each marginal or conditional independence on the data corresponds to certain zero constraints on these parameters. Quite similar situation is obtained when we consider the CSIs, see [5]. In particular, by looking to the SCRGM in Figure 1 (right side), in addition to the model in formula (1), we have that the model with response variable  $C$ , due to the independence  $B \perp C|A$  becomes:

$$\eta_C^{ABC}(i_C|i_{AB}) = \beta_{\emptyset}^C + \beta_A^C(i_A).$$

The response variables  $C$  and  $D$  together can be represented by the following model, by taking into account the CSI  $C \perp D|AB = (a_1, *)$ , when  $AB \neq (a_1, *)$ :

$$\eta_{CD}^{ABCD}(i_{CD}|i_{AB} \neq (a_1, *)) = \beta_{\emptyset}^{CD} + \beta_A^{CD}(i_A) + \beta_B^{CD}(i_B) + \beta_{AB}^{CD}(i_{AB})$$

and it is equal to zero when  $AB = (a_1, *)$ . Note that the other parameters  $\eta_E^{ABE}(i_E|i_{AB})$ ,  $\eta_{CE}^{ABCE}(i_{CE}|i_{AB})$ ,  $\eta_{DE}^{ABDE}(i_{DE}|i_{AB})$  and  $\eta_{CDE}^{ABCDE}(i_{CDE}|i_{AB})$  are all equal to zero according to the independence  $AB \perp E$ . Thus, given a graph, we have a list of independencies among the variables. These independencies correspond to certain constraints on the HMM parameters. The unconstrained parameters describe the dependence.

### 3 Application

In this section we present an application on a real dataset in order to highlight the relationships that are among a set of variables. At first we identify the best fitting SCRGM. Each model is tested by evaluating the likelihood ratio test  $G^2$ . The selection is done through a three step algorithm explained below.

*Step 1:* We test all the plausible pairwise independencies (involving only two variables at time) in the complete graph. From this step we select the models with a *p-value* greater than 0.01.

*Step 2:* We further investigate all possible CSIs concerning the independence discarded in step 1, by applying, to the graph labelled arcs (one at time) with all possible labels. We take advantage also of mosaic plots. In this step we take into account the models with a *p-value* greater than 0.1.

*Step 3:* From all admissible models selected in the previous two steps, we test all possible combinations of marginal, conditional and CSIs and we maintain

the one with lower AIC (Akaike Information Criterion) between the models with a  $p$ -value higher than 0.05.

All the analysis are carried out with the statistical software R [7], and the package `hmmm`, [2].

### 3.1 Survey on multiple aims analysis

From the survey on the every day aspects of life, [3], we select 5 variables: Gender ( $G$ ) ( $male=1$ ,  $female=2$ ), Age ( $A$ ) ( $25 - 34=1$ ,  $35 - 44=2$ ,  $45 - 54=3$ ,  $55 - 59=4$ ,  $60 - 64=5$ ), Educational level ( $E$ ) ( $less\ than\ high\ school=1$ ,  $high\ school,\ no\ college =2$ ,  $bachelor\ degree =3$ ,  $doctoral\ degree=4$ ), Working condition ( $W$ ) ( $looking\ for\ a\ job=1$ ,  $unemployed=2$ ,  $employed=3$ ) and Life satisfaction ( $S$ ) ( $0 - 4$ : low satisfaction= $1$ ,  $5 - 7$ : medium satisfaction= $2$ ,  $8 - 10$ : high satisfaction= $3$ ). The survey covers 23880 interviewers, collected in a contingency table of 360 cells of which only 8 cells are null.

The aim of the analysis is to investigate how gender and age affect the educational level and the working condition; at the same time we want to study how all these variables affect the life satisfaction. Thus, we select different marginal distributions where to study the dependencies in order to satisfy these aim. First of all, we consider the smallest  $(G, A)$  for studying the symmetrical relationship between the *personal* characteristics. Then we add, one at time and then together, the *achievement* variables ( $E$  and  $W$ ) in order to investigate how the *personal* characteristics affect these dependent variables. Finally, we consider the joint distribution for the study of the life satisfaction. Thus, the class of marginal distributions is  $\{(G, A); (G, A, E); (G, A, W); (G, A, E, W); (G, A, E, W, S)\}$ .

With the selected marginal distributions, the list of all possible pairwise marginal/conditional independencies is (a)  $G \perp A$ , (b)  $G \perp E|A$ , (c)  $A \perp E|G$ , (d)  $G \perp W|A$ , (e)  $A \perp W|G$ , (f)  $E \perp W|AG$ , (g)  $G \perp S|AEW$ , (h)  $A \perp S|GEW$ , (i)  $E \perp S|GAW$ , (j)  $W \perp S|GAE$ . Among this list of independencies only the first present the empirical evidence. Thus, only the undirected arc between the variables  $G$  and  $A$  should be missed from the CRGM ( $G^2 = 10.74$ ,  $df=4$ ,  $p$ -value= 0.03). Getting to the second step at the procedure, the study of the CSI leads to several plausible models. In figure 2 are depicted the mosaic plots concerning the variables  $W$  and  $S$  in two different conditional distributions in order to have an idea of the independencies that hold only in particular conditioning distributions. In particular, in the plot on the left, where the squares of the mosaic form a quite regular grid, there is high evidence of independence between  $W$  and  $S$ . On the other hand, the plot on the right shows evidence of strong dependence among the two variables because their "irregular" lines. By testing all possible combinations of the plausible models we select the one reported in Figure 3. The SCRGM in Figure 3 represents a system of relationships where the gender  $G$  and the age  $A$  are marginally independent (missing undirected arc between  $G$  and  $A$ ); where the gender  $G$  does not affect the life satisfaction  $S$  when the age  $A$  is among 45–54, the educational level is doctoral degree and the working condition  $W$  is employed (labelled directed arc between  $G$  and  $S$ ); where the educational level  $E$  does not affect  $S$  for male among 35

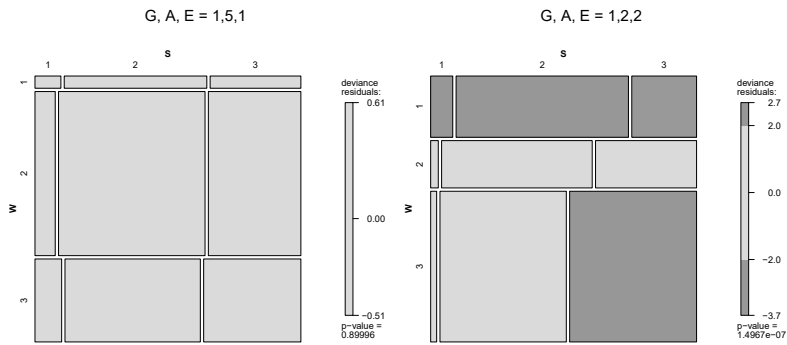


**Fig. 2.** Mosaic plots concerning the variables  $W$  and  $S$  in two conditional distributions. On the left,  $G$  male,  $A=60 - 64$  and  $E=less\ than\ high\ school$ . On the right,  $G= male$ ,  $A=35 - 44$  and  $E=high\ school$ .

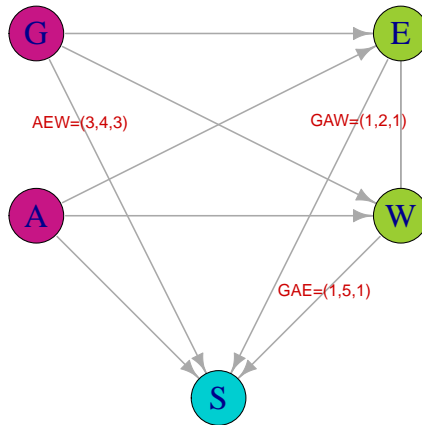


**Fig. 3.** Best fitting SCRGM.  $G^2 = 25.68$ ,  $df=16$ ,  $p\text{-value}=0.06$ ,  $AIC=-658.32$ .

and 44 years old that are looking for a job; where the working condition  $W$  does not affect  $S$  for old male with the lowest educational level. The undirected arc with no label shows the strongest dependence because any independence holds among all possible conditioning distributions.

The dependence structure is described by the regression models. For brevity we report only the model with  $S$  as dependent variables in Tables 1. In Table 1 the

**Table 1.** Regression parameters  $\eta_S^{GAEWS}(i_S|i_{GAEW})$  of dependent variable  $S$  for all possible values of covariates  $G, A, E$  and  $W$

GAEW	S=2	S=3	GAEW	S=2	S=3	GAEW	S=2	S=3	GAEW	S=2	S=3
(1111)	1,204	-0,405	(2441)	34,897	33,981	(1342)	1,792	0,693	(2313)	2,159	1,099
(2111)	24,569	23,653	(1541)	23,288	23,47	(2342)	1,705	1,253	(1413)	2,241	1,569
(1211)	1,256	0,34	(2541)	0,693	-0,693	(1442)	1,386	0	(2413)	1,312	0,887
(2211)	0,511	-0,693	(1112)	0,693	0,693	(2442)	1,872	1,946	(1513)	1,72	1,085
(1311)	0,93	-1,099	(2112)	2,303	2,197	(1542)	1,658	1,658	(2513)	2,639	1,099
(2311)	0,754	-0,288	(1212)	0,511	-30,445	(2542)	2,457	2,485	(1123)	2,163	1,887
(1411)	0,262	-0,916	(2212)	1,856	0,875	(1113)	1,846	0,693	(2123)	2,52	2,165
(2411)	35,234	34,674	(1312)	-0,47	-1,674	(2113)	25,039	24,058	(1223)	2,117	1,638
(1511)	1,72	1,085	(2312)	0,981	-0,105	(1213)	3,02	1,504	(2223)	2,09	1,771
(2511)	1,386	0,693	(1412)	1,386	0,223	(2213)	1,386	0,511	(1323)	2,359	1,899
(1121)	1,285	0,28	(2412)	1,353	0,502	(1313)	1,992	1,269	(2323)	2,318	1,836
(2121)	2,022	1,022	(1512)	1,72	1,085	(2313)	2,159	1,099	(1423)	2,206	1,593
(1221)	1,256	0,34	(2512)	1,483	0,853	(1413)	2,241	1,569	(2423)	2,106	1,692
(2221)	1,418	0,853	(1122)	0,134	-0,847	(2413)	1,312	0,887	(1523)	2,09	1,705
(1321)	0,991	-0,089	(2122)	1,492	0,894	(1513)	1,72	1,085	(2523)	2,327	2,225
(2321)	1,187	0,159	(1222)	0,747	-0,811	(2513)	2,639	1,099	(1133)	2,632	2,367
(1421)	0,719	0,1	(2222)	1,638	1,172	(1123)	2,163	1,887	(2133)	2,355	2,001
(2421)	0,847	0	(1322)	1,073	0,074	(2123)	2,52	2,165	(1233)	2,42	2,197
(1521)	0,802	-0,619	(2322)	1,776	1,105	(1223)	2,117	1,638	(2233)	2,592	2,285
(2521)	1,735	1,099	(1422)	2,132	1,488	(2223)	2,09	1,771	(1333)	2,38	2,126
(1131)	1,996	0,986	(2422)	2,227	1,514	(1323)	2,359	1,899	(2333)	2,363	1,842
(2131)	1,738	0,838	(1522)	2,639	2,303	(2532)	1,979	1,52	(1433)	2,398	1,756
(1231)	1,256	0,34	(2522)	1,648	1,304	(1142)	3,689	3,497	(2433)	1,98	1,445
(2231)	1,471	0,83	(1132)	1,405	0,731	(2142)	2,983	2,584	(1533)	2,655	2,147
(1331)	1,292	-0,223	(2132)	2,865	2,325	(1242)	0,405	0	(2533)	1,624	1,293
(2331)	1,306	0,353	(1232)	-0,486	-0,773	(2242)	2,159	2,12	(1143)	2,803	2,733
(1431)	0,871	-0,492	(2232)	2,215	1,843	(1342)	1,792	0,693	(2143)	3,049	3,054
(2431)	0,452	0	(1332)	1,299	0,606	(2342)	1,705	1,253	(1243)	3,016	2,958
(1531)	1,012	-0,134	(2332)	2,075	1,504	(1442)	1,386	0	(2243)	2,862	2,875
(2531)	1,705	1,253	(1432)	2,277	1,386	(2442)	1,872	1,946	(1343)	2,413	2,244
(1141)	1,73	0,857	(2432)	2,534	2,104	(1542)	1,658	1,658	(2343)	2,413	2,244
(2141)	2,054	1,076	(1532)	1,67	1,792	(2542)	2,457	2,485	(1443)	2,28	2,335
(1241)	1,256	0,34	(2532)	1,979	1,52	(1113)	1,846	0,693	(2443)	3,517	2,979
(2241)	2,979	2,457	(1142)	3,689	3,497	(2113)	25,039	24,058	(1543)	4,007	4,159
(1341)	1,658	0,811	(2142)	2,983	2,584	(1213)	3,02	1,504	(2543)	2,833	2,639
(2341)	2,12	1,386	(1242)	0,405	0	(2213)	1,386	0,511			
(1441)	24,611	0	(2242)	2,159	2,12	(1313)	1,992	1,269			

positive parameters refers to situations where the frequency of subjects with life

satisfaction  $S$  neutral or high is greater than the frequency of low life satisfaction. From the table it is possible to deduce that, only for male among 45 and 54 years old with the lowest educational level and unemployed, the frequency of unsatisfied is greater than the neutral category ( $\eta_S^{GAEW}(2|1312) = -0.47$ ). In the same categories, also the frequency of high satisfied people is lower than the unsatisfied ( $\eta_S^{GAEW}(3|1312) = -1.674$ ). We can find a similar trend among the categories male between 35 and 44 years old with a bachelor degree and unemployed ( $\eta_S^{GAEW}(2|1232) = -0.486$  and  $\eta_S^{GAEW}(3|1232) = -0.773$ ). On the other hand, in correspondence of female among 55 and 59 years old with lower educational level that are looking for a job we have very few number of unsatisfied with respect to the other categories ( $\eta_S^{GAEW}(2|2411) = 35.234$  and  $\eta_S^{GAEW}(3|2411) = 34.674$ ).

## 4 Conclusion

The SCRGMs presented in this work are a useful tool to explore and represent the system of relationships among a set of categorical variables. In particular, the labelled arcs in the graph suggest which dependence relationships are weak. The regression parameters, in addition, quantifies the dependence relationships. These results are presented through an application to a life satisfaction. Here, for brevity, few comments and partial results are presented. However, it is possible to deep the analysis and the study of unconstrained parameters.

## References

1. Bartolucci, Francesco, Colombi, Roberto, & Forcina, Antonio. *An extended class of marginal link functions for modelling contingency tables by equality and inequality constraints*. *Statistica Sinica*, **17**, 691-711 (2007).
2. Colombi, Roberto, Giordano, Sabrina & Cazzaro, Manuela. *hmmm: An R Package for Hierarchical Multinomial Marginal Models*. *Journal of Statistical Software*, **59**(11), 1-25, (2014).
3. Istat. Multiscopo ISTAT - *Aspetti della vita quotidiana*. *UniData - Bicocca Data Archive*, Milano. Codice indagine SN167. Versione del file di dati 1.0 (2015)
4. Marchetti, Giovanni M., & Lupparelli, Monia. *Chain graph models of multivariate regression type for categorical data*. *Bernoulli*, **17**(3), 827-844, (2011).
5. Nicolussi, Federica & Cazzaro, Manuela. *Context-specific independencies for ordinal variables in chain regression models*. arXiv:1712.05229, (2017).
6. Nyman, Henrik, Pensar, Johan, Koski, Timo, & Corander, Jukka. *Context specific independence in graphical log-linear models*. *Computational Statistics*, **31**(4), 1493-1512, 2016.
7. R Core Team. *R: A Language and Environment for Statistical Computing*. R Foundation for Statistical Computing, Vienna, Austria, 2014.



# Subjective survival: an assessment of accuracy according to individual social profile

Apostolos Papachristos<sup>1</sup> FIA CERA, Georgia Verropoulou<sup>2</sup>

<sup>1</sup> Department of Statistics and Insurance Science, University of Piraeus, Greece

(E-mail: [apapachristos@webmail.unipi.gr](mailto:apapachristos@webmail.unipi.gr))

<sup>2</sup> Department of Statistics and Insurance Science, University of Piraeus, Greece

(E-mail: [gverrop@unipi.gr](mailto:gverrop@unipi.gr))

## Abstract

Past literature suggests that personal views on subjective survival vary according to an individual's characteristics. The present study aims at identifying traits that relate to the underestimation or the overestimation of survival, using information from an especially rich dataset, the Survey of Health Ageing and Retirement in Europe (SHARE wave 6, 2015) and the Human Mortality Database. The statistical analysis is based on generalized linear regression models.

The findings indicate that better cognitive function and higher educational attainment are linked to more accurate predictions. On the other hand, female gender, smoking, poor health and memory, lower income and higher depression levels seem associated with the under-estimation of future life expectancy. Further, persons who consume less frequently fruits or vegetables and eggs or legumes, also tend to under-estimate future life expectancy. By contrast, older age, better quality of life, being in paid employment and having more children are related to the over-estimation of survival. Furthermore, widowed, divorced, never married and financially distressed individuals also tend to over-estimate future life expectancy.

Hence, the study indicates, in line with past research, that accuracy of predictions diversifies across individuals with different characteristics. Grouping of traits can be of particular interest for life insurers and pension funds to be incorporated in their benefits' structure and policies.

**Keywords:** Subjective survival probabilities, SHARE, HMD, Social profile, Flexible pension benefits, Longevity risk

*This work has been partly supported by the University of Piraeus Research Center.*



## 1. Introduction

It is a fact that some people are more optimistic than others. (Lyubomirsky [1]). This is generally reflected in their expectations, including their future survival. Prior studies have noted that individuals take into account their own experiences, history and environmental influences when forming survival expectations (Griffin et al. [2]). Individual-specific judgment is the main reason that subjective survival probabilities exhibit greater variability compared to actual survival probabilities (Hamermesh [3]).

Nevertheless, there are common factors influencing subjective survival expectations. One explanation is that people may have similar awareness and understanding about the factors affecting future life expectancy through media, health campaigns, and their own experiences (Griffin et al. [2]). For example, the fact that smoking reduces life expectancy is well known (Doll et al. [4]).

Grouping these common factors in homogeneous groups will allow us to identify individuals who are more or less optimistic about their own survival. Furthermore, earlier research has shown that subjective survival probabilities predict future longevity improvements (Perozek [5]). Therefore, this grouping would allow us to extract credible information about future longevity improvements, associated with homogeneous groups of people.

### *Homogeneous groups of survival predictions*

In this study we define three homogeneous groups, based on the comparison of the objective expected survival and the individuals' views on subjective survival. The first group consists of common features found in individuals who over-estimate survival. The second group consists of common features found in individuals who predict accurately survival; and the third group consists of common features found in individuals who under-estimate survival. The objective of this study is twofold. Firstly, we investigate the common factors driving subjective survival probabilities. Secondly, we classify these factors into three homogeneous groups, according to the predictive accuracy of subjective survival probabilities.

Our main hypotheses are:

**Hypothesis 1** Demographic variables such as age, gender, country of residence the number of children and marital status could differentiate the predictive ability of individuals. Arpino et al. [6] argued that males overestimate survival compared to females. They also found that older people tend to overestimate survival. Furthermore, Rappange et al. [7] found significant variation in the subjective survival probabilities for countries across Europe. In addition, Liu et al. [8] and Mirowski [9] estimated that respondents who live with children report higher survival expectations.

**Hypothesis 2** Socio-economic factors such as education, income, financial distress and current job situation could differentiate the predictive ability of individuals. There is a wider agreement in the literature that those who are not well educated; earn less income and they are financially distressed, under-estimate subjective life expectancy (Balía [10], Liu et al. [8], Mirowski [9], Arpino et al. [6] and Rappange et al. [7]).

**Hypothesis 3** Physical health variables such as the existence of chronic diseases; limitations with Activities of Daily Living (ADLs), and the self-rated health status, could differentiate the predictive ability of individuals. There is a wider agreement in the literature that poorer health is associated with lower survival expectations. (Liu et al. [8], Rappange et al. [7], Balía [10], Hurd & McGarry [11], and Van Solinge et al. [12]).

Cognitive function and mental health variables such as depression, numeracy, writing skills, memory and orientation in time could differentiate the predictive ability of individuals. Elder [13]; Balía [10]; Rappange et al. [7]; and Griffin et al. [2] estimated significant associations between cognitive skills and subjective survival probabilities. We expect better cognitive skills to be associated with more accurate predictions.

**Hypothesis 4** Lifestyle variables representing behavioral risk factors such as physical inactivity, smoking, Body Mass Index and diet habits could differentiate the predictive ability of individuals. Rappange et al. [7], Griffin et al. [2] and Liu et al. [8] estimated that physical activity is positively associated with subjective survival expectations. Furthermore,

Khwaja et al. [14] argued that current smokers are relatively optimistic whereas never smokers are relatively pessimistic in their survival predictions. Griffin et al. [2], show that the total number of servings of fruits or vegetables per day, is positively associated with subjective life expectancy. We expect better lifestyle and diet to be associated with survival overestimation.

**Hypothesis 5** Quality of life and Social support could differentiate the predictive ability of individuals. Griffin et al. [2] as well as Ross & Mirowsky [15] argued that there is a positive association between social connectedness, family support, optimism and subjective life expectancy.

## 2 Methods

### Data

We used data from the 6<sup>th</sup> Wave of the Survey of Health, Ageing and Retirement in Europe (SHARE). SHARE (Börsch-Supan et al. [16]) is a cross-national and multidisciplinary panel database with information on health, socio-economic status, and social and family networks. Its format is analogous to the US Health and Retirement Study (HRS) and the English Longitudinal Study of Ageing (ELSA). SHARE has been mainly funded by the European Commission and is coordinated centrally at the Mannheim Research Institute for the Economics of Ageing. The data collection of the 6<sup>th</sup> Wave was completed in November 2015 (Börsch-Supan [17]) and the sampling was carried out in 18 countries (Austria, Belgium, Croatia, Czech Republic, Denmark, Estonia, France, Germany, Greece, Israel, Italy, Luxembourg, Poland, Portugal, Spain, Sweden, Switzerland and Slovenia). More documentation and information on SHARE can be found at <http://www.share-project.org>.

The original sample covered 67346 individuals aged 50 or higher. Due to SHARE rules, information about future life expectancy was not collected for 2906 individuals (4.3%), for whom proxy interviews were conducted. In addition, there were 596 individuals with missing values in the variables of interest (less than 1%). Hence, the sample used in the analysis includes 63844 individuals.

#### *Life tables*

The objective survival probabilities were obtained from the Human Mortality Database (HMD [18]). The estimated life tables refer to the 5-year period 2010-2014. SHARE Wave 6 was undertaken in 2015; therefore we consider these life tables relevant for our study (Post and Hanewald [19]; Balia [10]).

### Variables

#### *Subjective survival probabilities (SSPs)*

In the 'Expectations' module of the SHARE questionnaire, respondents were asked to state their survival expectations on a scale from 0 to 100 as follows:

*What are the chances that you will live to be age [T] or more?*

The target age T (75, 80, 85, etc.) was defined dependent on the age of the respondent at the interview.

#### *Objective survival probabilities (OSPs)*

The cumulative OSPs, calculated from the HMD life tables, are compared subsequently to the SSPs. The reported SSPs correspond to a specific prediction interval, starting from current age up to the target age. Therefore, the OSPs should cover the same time horizon (Peracchi and Perotti [20]). Hence,

$$OSP_{x,N} = \prod_{t=1}^N OSP_{x+t}$$

where 'x' is the age of the respondent and 'N' is the prediction interval.

## Dependent variables

The first dependent variable, deviation, is in continuous form and represents the difference between subjective and objective cumulative survival probabilities:

$$Deviation_{x,N} = SSP_{x,N} - OSP_{x,N}$$

The second dependent variable is in continuous form and provides an alternative estimate of the distance between subjective and objective survival probabilities.

$$Absolute\ Deviation_{x,N} = |SSP_{x,N} - OSP_{x,N}|$$

## Explanatory variables

### *Demographic characteristics*

This group of variables includes age (in years), gender, marital status (widowed, divorced, never married, separated, married, in partnership), the number of children of the respondent as well as country of residence. In addition, age squared /100 is also included in order to capture the non-linear shape of survival probabilities.

### *Socio-economic factors*

This group of variables includes total household income in quartiles, whether the household is able to make ends meet (1=with great difficulty to 4=easily), education level in 4 categories based on the ISCED-97 classification, including Primary (code 1), Lower Secondary (code 2), Upper Secondary (codes 3 & 4) Tertiary (codes 5 & 6), and the current employment status (retired, employed, unemployed, permanently disabled, homemaker and other).

### *Physical & Mental Health*

This group of variables includes the number of chronic conditions (out of a list of 13), the number of limitations in Activities of Daily Living (out of a list of 6 basic, everyday tasks) and self-rated health (ranging from 1=excellent to 5=poor). In addition, the EURO-D depression scale is included (ranging from 0 to 12 symptoms), the score of a memory test (1=excellent to 5=poor), the score of a numeracy test (1=bad to 5=good), the self-rated writing skills (1=excellent to 5=poor), and the score of orientation in time test (0=bad to 4=good). Biomarkers such as the grip strength and the peak flow were also included to check the robustness of the models' estimates.

### *Lifestyle & Behavioral risk factors*

This group of variables includes the BMI in four categories (underweight, normal weight, overweight and obese), whether the respondent does vigorous or moderate physical activity, whether the respondent ever smoked daily and the frequency of eating meat or chicken, fruits or vegetables, legumes and eggs and dairy products (1 = almost daily to 5 = less than once a week).

### *Quality of life & Social support*

This group of variables includes the quality of life (CASP index, ranging from 12 to 48), the life satisfaction score (ranging from 0 to 10), and the number of times the respondent received help from others (ranging from 0 to 3).

Finally, the prediction interval in years is also included as an explanatory variable.

### Statistical modeling

In the analysis we use a Generalised Linear Model (GLM) with a linear link function, including  $Deviation_{x,N}$  as dependent variable, and another GLM with a log link function, including  $Absolute\ Deviation_{x,N}$ . The dependent variables are assumed to be normally distributed.

## 3. Results

### Sample

The sample characteristics are presented in Table 1. The mean of subjective survival probabilities is 64%, 5 percentage points higher than the mean of objective survival probabilities (59%). The average respondent is 68 years old, males represent 44% of the sample and seven out of ten respondents are married. Luxemburg represents 2% whereas Belgium represents 9% of the total sample. The average respondent has 2 children as well as 2 chronic diseases. Furthermore, three out of ten respondents are overweight or obese and 65% of the respondents report a fair and good health.

Nine out of ten respondents do some sort of physical activity. Respondents eat almost every day fruits or vegetables as well as dairy products. On the other hand, they eat meat or chicken 3 – 6 times per week and eggs or legumes twice a week. Six out of ten households are able to make ends meet easily and fairly easily. Furthermore, six out of ten respondents are retired and they have post-secondary and tertiary education. The average prediction interval is 14 years.

**Table 1** Sample characteristics (n = 63 844)

Variable	%
<b>Dependent Variables</b>	
Subjective survival probabilities (mean [SD])	64% [28%]
Objective survival probabilities (mean [SD])	59% [26%]
Deviation of SSPs – OSPs (mean [SD])	5% [29%]
<b>Independent Variables</b>	
Prediction interval (years) (mean [SD])	14 [3.6]
<b>Demographic Characteristics</b>	
Age (mean [SD])	68 [10]
Male	44%
Marital Status	
Widowed	15%
Divorced	9%
Never married	6%
Separated	1%
Partnership	2%
Married	68%
Country of residence	
Slovenia	6%
Sweden	6%
Portugal	2%
Poland	3%
Luxembourg	2%
Israel	3%
Italy	8%
Croatia	4%
Greece	7%
France	6%
Spain	8%

Estonia	8%
Denmark	6%
Germany	7%
Switzerland	4%
Czech Republic	7%
Belgium	9%
Austria	5%
Number of children (mean [SD])	2.1 [1.3]
<b>Socio-economic Status</b>	
Household is able to meet ends	
With great difficulty	12%
With some difficulty	27%
Fairly easily	27%
Easily	34%
Education level	
ISCED-97 code 0 & 1 (Primary)	22%
ISCED-97 code 2 (Lower secondary)	18%
ISCED-97 codes 3 & 4 (Upper secondary)	37%
ISCED-97 codes 5 & 6 (Tertiary)	23%
Employment Status	
Other	2%
Homemaker	9%
Permanently Disabled	3%
Unemployed	3%
Employed	25%
Retired	59%
Income	
Income Q1 (mean [SD] in €)	7,212 [2,746]
Income Q2 (mean [SD] in €)	15,241 [2,549]
Income Q3 (mean [SD] in €)	27,508 [4,806]
Income Q4 (mean [SD] in €)	84,080 [95,627]
<b>Physical and Mental Health</b>	
Chronic conditions (mean [SD])	1.8 [1.6]
Number of ADLs (mean [SD])	0.3 [0.9]
Self-rated health	
Excellent	7%
Very good	18%
Good	36%
Fair	29%
Poor	10%
Depression (mean [SD])	2.4 [2.2]
Numeracy (mean [SD])	3.4 [1.03]
Writing skills (mean [SD])	2.4 [1.14]
Orientation in time (mean [SD])	3.8 [0.51]
Memory (mean [SD])	3 [0.95]
<b>Lifestyle and behavioral risk factors</b>	
BMI	
Underweight	1%
Normal	29%
Overweight	45%
Obese	25%
Physically active	90%
Ever smoked daily	44.7%
Dietary habits	
Meat or chicken (mean [SD])	1.9 [0.9]
Fruits or vegetables (mean [SD])	1.3 [0.7]
Legumes and eggs (mean [SD])	2.9 [1.13]
Dairy products (mean [SD])	1.6 [1.03]
<b>Quality of Life &amp; Social Support</b>	
Quality of life (mean [SD])	34 [11.1]

Life satisfaction (mean [SD])	7.6 [1.7]
Times received help (mean [SD])	0.37 [0.7]

## Multivariable analyses

### *Demographic characteristics*

Age is positively associated with survival overestimation as well as less accurate survival predictions. The regression coefficients, presented in Table 2, are positive for both models. Widowed, divorced and never married persons tend to over-estimate survival compared to married persons. The coefficients of the country of residence as well as the gap of SSPs to OSPs vary considerably (ANOVA,  $F=76.7$ ); countries are ranked based on the degree of overestimation compared to the residents of Austria. For example, residents in France underestimate survival whereas residents in Estonia overestimate survival compared to the residents of Austria. Our regression results show that individuals with more children are optimistic concerning their survival and they predict less accurately survival.

### *Socio-economic status*

Our regression results suggest that low and medium income earners underestimate survival compared to high income earners. Furthermore, low and medium income earners predict less accurately survival compared to high income earners. Financially distressed individuals tend to overestimate survival. In other words, individuals who are not financially distressed predict survival more accurately. Respondents at lower and intermediary education levels tend to overestimate survival compared to those who have completed tertiary education; hence, persons in the latter category predict survival more accurately. Employed and unemployed overestimate survival compared to retired individuals whereas homemakers tend to under-estimate survival. Furthermore, employed tend to provide more accurate survival predictions compared to retired. Permanently sick or disabled persons report inaccurate survival predictions compared to retired individuals.

### *Physical & Mental Health*

The number of chronic diseases is associated with survival underestimation. Respondents who report excellent, very good, good and fair health overestimate survival compared to those who report poor health. The regression results show that individuals with ADLs and depression tend to under-estimate survival. Better numeracy, memory, orientation in time and writing skills are associated with a more accurate predictive ability as well as with a marginal under-estimation of survival.

### *Lifestyle & Behavioural Risk Factors*

Persons of normal weight are more likely to predict more accurately their survival compared to the obese. This also holds for underweight and overweight persons. Respondents in these groups are also marginally under-estimate survival. Hence, obese overestimate their survival compared to normal weight persons and the other groups. Physically active individuals over-estimate survival compared to those who never do vigorous nor moderate physical activity and are less likely to underestimate survival. Our regression results suggest that respondents who never smoked are more likely to overestimate survival compared to smokers.

Respondents who consume less frequently (e.g. less than once a week (=5) fruits or vegetables and eggs or legumes tend to underestimate survival. On the other hand, the consumption of dairy products as well as meat or chicken does not have a material impact on predictive ability.

### *Quality of life & Social Support*

Respondents who are more satisfied with their lives, have a better quality of life receive help frequently tend to overestimate survival. Furthermore, better quality of life and life satisfaction are associated with lower survival prediction accuracy.

Finally our regression results show that the longer the time horizon the greater the chances of survival overestimation; and the larger the scope for survival prediction error.

**Table 2** Coefficients based on generalised linear and log-linear models.

Independent variables	Deviation linear model <sup>a</sup>	Absolute deviation log-linear model <sup>b</sup>
Constant	-2.241**	-4.537**
Prediction Interval	0.025**	0.042**
<i>Demographic characteristics</i>		
Age	0.026**	0.034**
Age Squared/100	-0.003*	-0.003
<b>Gender (reference: Female)</b>		
Male	0.108**	0.118**
<b>Country of residence (reference: Austria)</b>		
France	-0.069**	-0.027
Switzerland	-0.069**	-0.019
Sweden	-0.061**	-0.115**
Belgium	-0.041**	-0.038*
Germany	-0.018**	0.017
Czech Republic	-0.008	0.032
Luxembourg	-0.007	0.111**
Israel	-0.002	-0.066*
Spain	0.002	-0.031
Greece	0.001	-0.031
Croatia	0.006	0.069**
Poland	0.01	0.033
Italy	0.011*	0.102**
Slovenia	0.012*	0.052*
Portugal	0.04**	0.1**
Denmark	0.053**	0.131**
Estonia	0.091**	0.131**
<b>Marital status (reference: Married)</b>		
Widowed	0.001	-0.014
Divorced	0.017**	0.042**
Never married	0.011*	0.012
Separated	-0.001	0.033
Married/Partnership	0.003	0.038
Number of children	0.002*	0.007**
<i>Socio-economic status</i>		
<b>Household is able to meet ends (reference: Easily)</b>		
With great difficulty	0.016**	0.121**
With some difficulty	0.009	0.041**
Fairly easily	0.003	-0.004
<b>Education (reference: Tertiary education)</b>		
Primary	0.013**	0.076**
Lower Secondary	0.004	0.056**
Upper secondary	0.005	0.055**
<b>Current job situation (reference: Retired)</b>		
Other	0.018*	-0.037
Homemaker	-0.013**	0.013
Permanently Disabled	0.015*	0.196**
Unemployed	0.023**	0.01
Employed	0.027**	-0.119**
<b>Income quartiles (reference: Q4)</b>		
Income Q1	-0.023**	0.026*
Income Q2	-0.019**	0.05**
Income Q3	-0.016**	0.027**

<b><i>Physical &amp; Mental Health</i></b>		
Chronic diseases	-0.007**	0.001
ADLs	-0.002	-0.014**
<b>Self-rated health (reference: Poor)</b>		
Excellent	0.153**	0.143**
Very good	0.129**	0.071**
Good	0.095**	0.051**
Fair	0.057**	0.034**
Depression	-0.007**	0.014**
Numeracy	-0.003**	-0.019**
Writing skills	-0.002*	-0.01**
Orientation	-0.006**	-0.004
Memory	-0.007**	-0.008*
<b><i>Lifestyle &amp; Behavioural Risk Factors</i></b>		
<b>BMI (reference: Obese)</b>		
Underweight	-0.01	-0.043
Normal	-0.007*	-0.024**
Overweight	-0.002	-0.031**
<b>Physical activity (reference: Physically Inactive)</b>		
Physically Active	0.017**	0.011
<b>Ever smoked daily (reference: Yes)</b>		
Never smoked daily	0.006**	-0.03**
<b>Dietary habits</b>		
Meat or chicken	-0.000079	0.001
Dairy	0	0.012**
Egg or legumes	-0.005**	-0.016**
Fruit or vegetables	-0.007**	0.011
<b><i>Quality of life and Social Support</i></b>		
Quality of Life	0.003**	0.004**
Times received help	0.008**	-0.002
Life satisfaction	0.02**	0.012**

---

### 3 Discussion

The study has two main objectives: firstly, to explore the main factors driving subjective survival probabilities and secondly, to classify these factors to three homogeneous groups, dependent on the predictive accuracy of respondents. To achieve that aim data from Wave 6 of the SHARE study was used, including 63844 respondents from 18 countries. We estimated two generalised linear and log-linear models, using the deviation and the absolute deviation between subjective and objective survival probabilities as dependent variables. The results of these models, allow us to assess the validity of our hypotheses.

#### *Over-estimation of survival expectations*

Males overestimate survival compared to females. Liu et al. [8], Arpino et al. [6] confirmed this finding. Furthermore, Mirowski [9] suggests that males usually have on average a higher socioeconomic status, level of education, income and tend to report a better health status. As the number of children increases, the chances of overestimating survival increase. Liu et al. [8] and Mirowski [9] estimated that respondents who live with children report higher survival expectations. They have also explained that living with children increases individuals' emotional well-being, and therefore respondents may be more optimistic about future longevity. Furthermore, Ross and Mirowsky [15] concluded that the number of adult children is associated with longer subjective life expectancy. Older people tend to either overestimate survival compared to younger. Misowski [9] concluded also that people become more optimistic with age. Moreover, Griffin et al. [2] as well as Ross & Mirowsky [15] estimated a positive association between age and subjective life expectancy.

The impact of marital status on subjective life expectancy is not fully understood. On the one hand, Balia [10] estimated also that widows report higher SSPs., Liu et al. [8] and Rappange et al. [7] estimated that living alone is negatively associated with subjective survival. On the other hand, van Solinge et al. [12] estimated that partner status is not associated with subjective life expectancy. Ross and Mirowsky [15] argued that there is a 3-way interaction between marital status, age and gender. Their results suggest that marriage may increase life expectancy for older men but not for older women. Our results suggest that widowed, divorced and never married over-estimate survival compared to those who are married and living together with their spouse. Overall, we find significant evidence showing that demographic factors differentiate the predictive accuracy of SSPs. This supports our first hypothesis.

Physically active individuals overestimate survival. Rappange et al. [7], Griffin et al. [2] and Liu et al. [8] estimated also that physical activity is positively associated with subjective survival expectations. Obese people overestimate survival compare to those who maintain a normal weight. Rappange et al. [7] and Liu et al. [8] estimated also that obesity is negatively associated with survival expectations. Furthermore, Ross & Mirowsky [15] argued that obese do not accurately estimate their survival expectations compared to those who maintain a normal weight. These findings suggest that certain lifestyle factors are associated with survival overestimation. This supports our third hypothesis.

Better quality of life, greater life satisfaction and receiving help from others increase the chances of over-estimating survival. Van Solinge et al. [12] found a positive relationship between self-efficacy, life satisfaction and subjective life expectations. They conclude that individuals take psychological variables into account when predicting longevity. Furthermore, Griffin e. al. [2] found that optimism and social connectedness are predictors of life expectancy overestimation. Ross and Mirowsky [15] also estimated that emotional support increases subjective life expectancy. These findings clearly support our fifth hypothesis.

The current job situation is the only socio-economic variable which is not clearly associated with more accurate survival predictions. In particular, employed, unemployed and permanently disabled overestimate survival compared to retired. Coe et al. [21] estimated that retirement is associated with worse health outcomes. This could explain why retired underestimate their survival.

#### *Under-estimation of survival expectations*

Poor self-rated health, the existence of limitations in Activities of Daily living and a larger number of chronic diseases are associated with survival under-estimation. This is broadly consistent with the literature. Liu et al. [8], Rappange et al.

[7], Balia [10], Hurd & McGarry [11] and Van Solinge et al. [12] concluded that poorer health is associated with lower survival expectations.

Respondents who have poor memory and are depressed tend to under-estimate survival. Griffin et al. [2] confirmed that psychological distress is a significant predictor of survival under-estimation. Rappange et al. [7] estimated that depression is negatively associated with survival expectations. Overall, we find significant evidence showing that poor physical and mental health predict survival under-estimation. This supports our second hypothesis.

Smokers underestimate survival compared to never smokers. On the one hand, Rappange et al. [7] estimated that current smokers report lower survival expectations whereas those who stopped smoking report higher survival expectations. Furthermore, Hurd & McGarry [11] also estimated that current smokers report lower survival expectations. On the other hand, Liu et al. [8] and Balia [10] concluded that current smokers over-estimate survival. Our results suggest that smokers take into account the negative impact of smoking, when reporting subjective survival probabilities.

The infrequent consumption of fruits or vegetables and eggs or legumes indicates survival under-estimation. This is in line with the results of Griffin et al. [2], which show that the total number of servings of fruits or vegetables per day is positively associated with subjective life expectancy. Furthermore, Knuops et al. [22] concluded that elderly people, who adopted Mediterranean diet and healthy lifestyle, reduced by more than 50% their actual mortality rates. These findings suggest that certain lifestyle factors are associated with survival under-estimation and support our third hypothesis.

#### *Accurate prediction of survival*

The main finding is that socio-economic status is associated with more accurate survival predictions. In particular, individuals with higher education attainment, higher income and not financially distressed, are able to predict survival accurately. Rappange et al. [7], Hurd & McGarry [11], Liu et al. [8], Kutlu-Koc et al. [23] concluded that higher income and wealth are associated with higher subjective life expectancy. Furthermore, Griffin et al. [2] and Arpino et al. [6] argue that higher education leads to more accurate predictions of subjective life expectancy.

Better numeracy score is also associated with more accurate subjective predictions. However, orientation in time and self-rated writing skills are not clearly associated with the accuracy of survival predictions. Elder [13] suggested that those with better cognitive functioning may form more accurate probability assessments. Our results confirm better cognitive skills are associated with accurate predictions. Overall, we find significant evidence showing that socio-economic status and cognitive skills differentiate the predictive accuracy of SSPs. These findings support our second and fourth hypotheses.

## **5. Limitations**

Some limitations of the study should be taken into account when considering the findings. Firstly, SHARE includes only one SSP question. This does not allow us to estimate the whole distribution of SSPs for each individual. However, the impact of this limitation is reduced due to the significant number of individuals, included in Wave 6 dataset, who report SSPs. Secondly; we did not examine interactions among explanatory variables. For example, Rappange et al. [7] examined the interaction of alcohol consumption with gender and physical inactivity with age. In all six regression models we included 28 statistically significant independent variables. This reduces the impact of not investigating interactions. Finally, we have used the HMD life tables, which are estimated from the whole population. On the one hand this choice reduces parameter error, because the estimation of the mortality rates is robust. On the other hand, these life tables reflect the average population mortality and they do not vary with socio-economic and health status.

## **6. Conclusion**

This study shows that individuals tend to assess their future survival based on common factors. The consistent grouping of these factors would allow Governments and pension schemes to understand the profile of individuals who share similar views on subjective survival. Furthermore, Governments could use our results to set or adjust “pension flexibility rules” in order to reduce the financial burden of pension schemes and to ensure that pension savings would suffice over the individuals’ lifetime.

The risk of individuals “selecting against their pension schemes”, can be also mitigated. In particular, our social profile classification can be considered in the design stage of new flexible pension benefits. For example, for individuals who under-estimate survival, additional restrictions can be imposed on the total amount and the timing of lump sum payments. On the other hand, for individuals who over-estimate survival, restrictions can be imposed on the maximum retirement age. This would ensure that individuals who over-estimate survival will receive a fair proportion of their total pension savings during their lifetime.

Finally, Governments could introduce policies aiming to increase the overall accuracy of survival predictions for the whole population. For example, Governments could make higher education available to all individuals aged above 50. Furthermore, additional funding could be available to financially distressed and low income households. The next steps involve the more detailed examination of differences by country of residence, marital status, employment status as well as exploring the importance of interactions between the predictors. It will be also important to evaluate the subjective survival probabilities using a panel dataset, which would include data from previous SHARE waves.

### Acknowledgements

This paper uses data from SHARE Wave 6 (DOI: 10.6103/SHARE.w6.600), see Börsch-Supan et al. (2013) for methodological details. The SHARE data collection has been primarily funded by the European Commission through FP5 (QLK6-CT-2001-00360), FP6 (SHARE-I3: RII-CT-2006-062193, COMPARE: CIT5-CT-2005-028857, SHARELIFE: CIT4-CT-2006-028812) and FP7 (SHARE-PREP: N°211909, SHARE-LEAP: N°227822, SHARE M4: N°261982). Additional funding from the German Ministry of Education and Research, the Max Planck Society for the Advancement of Science, the U.S. National Institute on Aging (U01\_AG09740-13S2, P01\_AG005842, P01\_AG08291, P30\_AG12815, R21\_AG025169, Y1-AG-4553-01, IAG\_BSR06-11, OGHA\_04-064, HHSN271201300071C) and from various national funding sources is gratefully acknowledged (see [www.share-project.org](http://www.share-project.org)).

### References

1. Lyubomirsky S. (2001) Why are some people happier than others? The role of cognitive and motivational processes in well-being. *American psychologist*, 56(3), 239.
2. Griffin, B., Loh, V., & Hesketh, B. (2013) A mental model of factors associated with subjective life expectancy. *Social science & medicine*, 82, 79-86.
3. Hamermesh D. S. (1985) Expectations, life expectancy, and economic behavior. *The Quarterly Journal of Economics*, 100(2), 389-408.
4. Doll R., Peto R., Wheatley K., Gray R., & Sutherland I. (1994) Mortality in relation to smoking: 40 years' observations on male British doctors. *Bmj*, 309(6959), 901-911.
5. Perozek M. (2008) Using subjective expectations to forecast longevity: Do survey respondents know something we don't know? *Demography*, 45(1), 95-113.
6. Arpino B., Bordone V., & Scherbov S. (2017) Smoking, Education and the Ability to Predict Own Survival Probabilities: An Observational Study on US Data.
7. Rappange D. R., Brouwer W. B., & Exel J. (2016) Rational expectations? An explorative study of subjective survival probabilities and lifestyle across Europe. *Health Expectations*, 19(1), 121-137
8. Liu J. T., Tsou M. W., & Hammitt J. K. (2007) Health information and subjective survival probability: Evidence from Taiwan. *Journal of Risk Research*, 10(2), 149-175.
9. Mirowsky J. (1999) Subjective life expectancy in the US: correspondence to actuarial estimates by age, sex and race. *Social science & medicine*, 49(7), 967-979.
10. Balia S. (2011) Survival expectations, subjective health and smoking: Evidence from European countries. University of York, Centre for Health Economics.
11. Hurd M.D., McGarry K., (1995) Evaluation of the subjective probabilities of survival in the health and retirement study. *The Journal of Human Resources* 30, S268-S292
12. Van Solinge H., & Henkens K. (2017) Subjective life expectancy and actual mortality: results of a 10-year panel study among older workers. *European Journal of Ageing*, 1-10
13. Elder T. E., (2007) Subjective Survival Probabilities in the Health and Retirement Study: Systematic Biases and Predictive Validity, *Michigan Retirement Research Center Research Paper No. WP 2007-159*. Available at SSRN: <https://ssrn.com/abstract=1083823> or <http://dx.doi.org/10.2139/ssrn.1083823>
14. Khwaja, A., Sloan, F. A., & Chung S. (2007) The relationship between individual expectations and behaviors: Evidence on mortality expectations and smoking decisions. *Journal of Risk and Uncertainty*, 35(2), 179-201.

15. Ross C. E., & Mirowsky J. (2002) Family relationships, social support and subjective life expectancy. *Journal of health and social behavior*, 469-489.
16. Börsch-Supan A., Brandt M., Hunkler C., Kneip T., Korbmacher J., Malter F., Schaan B., Stuck S. & Zuber S. (2013) Data resource profile: the Survey of Health, Ageing and Retirement in Europe (SHARE). *International journal of epidemiology*, 42(4), 992-1001. DOI: 10.1093/ije/dyt088
17. Börsch-Supan A. (2017) Survey of Health, Ageing and Retirement in Europe (SHARE) Wave 6. Release version: 6.0.0. SHARE-ERIC. Data set. DOI: 10.6103/SHARE.w6.600
18. Human Mortality Database. *University of California, Berkeley (USA), and Max Planck Institute for Demographic Research (Germany)*. Available at [www.mortality.org](http://www.mortality.org) (data downloaded on 2/10/2017).
19. Post, T., & Hanewald, K. (2010) Stochastic Mortality, Subjective Survival Expectations, and Individual Saving Behavior (No. SFB649DP2010-040). Humboldt University, Collaborative Research Center 649.
20. Peracchi, F., & Perotti, V. (2010). Subjective survival probabilities and life tables: evidence from Europe. *Einaudi Institute for Economics and Finance (EIEF) Working Paper*, 10, 16.
21. Coe N. B., & Lindeboom M. (2008) Does retirement kill you? Evidence from early retirement windows.
22. Knoop K. T., de Groot L. C., Kromhout D., Perrin A. E., Moreiras-Varela O., Menotti A., & Van Staveren W. A. (2004) Mediterranean diet, lifestyle factors, and 10-year mortality in elderly European men and women: the HALE project. *Jama*, 292(12), 1433-1439.
23. Kutlu-Koc V., & Kalwij A. (2017) Individual survival expectations and actual mortality: Evidence from Dutch survey and administrative data. *European Journal of Population*, 33(4), 509-532.



# Sampling in Special Kinds of Nets

Papageorgiou Myrto<sup>1</sup>, Farmakis Nikolaos<sup>2</sup>

<sup>1</sup> School of Mathematics, Aristotle University of Thessaloniki (Email: myrtomp@hotmail.gr)

<sup>2</sup> School of Mathematics, Aristotle University of Thessaloniki (Email: farmakis@math.auth.gr)

**Abstract:** In many cases of sampling applications the (target) Population has the form of a net. In this case we face some problems especially with the bias of estimators, as we use classic sampling procedures, like simple random sampling (srs), systematic sampling, etc. In the present paper we try srs in nets, providing unbiased estimators of the mean value of some random variables. This result is reached by adoption of some axioms for the nets. A set of five axioms is associated with the net. These suitable nets are taken to have the form of the graphos presented by a matrix or, at least, by a part of the mentioned matrix. A theoretic proof for the unbiasedness of the estimators is given in a graphos with size the nature number:  $N=4,5,\dots$ . The graphos constituted by the above axioms is working as a kind of finite geometry. We could define some kind of parallelism in a structure like this geometry. Some examples are given to illustrate the above ideas of sampling in nets with the structure of finite geometry and show that the estimators of the parameters (mean value at least) are unbiased.

**Keywords:** Net, graphos, sampling, unbiased,

**MCS2010:** 62D05, 97K20, 05A19, 05B20.

## 1 Introduction

The tendency of Science to see the solution of several problems on many topics, through the prism and the logic of the networks, is observed to be increasing continuously. Thus, we have different kinds of networks to be the framework and the tool for studying various subjects of Economics, Biology, Medicine, Informatics and Mathematics. Mathematical tools are of course the graphos and the matrix used by all the above disciplines (as tools) for their studies.

Suppose now that there is a non-empty set  $V$ . This set is considered to have  $N$  elements (usually called *vertices*) that we usually symbolize with their representatives natural numbers 1,2,3, ... or the elements of an alphabet A, B, C, ... etc. Let (e.g.) be  $V=\{1,2,3,4,5,6\}$  where the element 1 represents one of the 6 ( $= N$ ) elements of the set  $V$ . The 6 elements can be 6 students or 6 firms of enterprises for which study is taking place. We then consider the Cartesian product  $V \times V = \{(x, y), x, y \in V\} = V^2$  and its non-empty subset  $E \subseteq V \times V$ . The elements of the  $E$  are usually called *edges*. Sometimes it is  $E = V \times V$ .

**Definition 1:** The structure  $G=(V,E)$  is called graphos or graph (Γράφος ή Γράφημα).

For some application the structure  $G_1=(V_1,E_1)$  is taken and used as a graphos, where  $V_1 \subseteq V$ ,  $E_1 \subseteq E$ . It depends on the needs of the study.

A graphos can be symbolized as a matrix and also be represented by this matrix.

In this paper the reference set is  $V$ , even if we are referring the structure  $G$  (graphos). We use to attach to the structure  $G$  a set of axioms  $A$ . So a new structure is produced, the  $\Gamma=(V,E,A)$ . As we see the set of axioms  $A$  we ask to meet certain conditions. At least three conditions have to be met: *Consistency, Completeness, Independence*

**Definition 2:** The structure  $\Gamma=(V,E,A)$  is called *Axiomatic Geometry*. When the set  $V$  is finite the structure  $\Gamma$  is called *Finite (axiomatic) Geometry*.

For some applications  $V, E$  can be substituted by  $V_1, E_1$ .

Even if the reference set is finite, it may be very large. So any research on it becomes difficult or impossible. So we need to use a suitable part of the structure. We have to make a sampling on the graph. Sampling on graphs (networks) is not a proper decision for the majority of the cases. In most of cases the estimators coming out of a sampling process are not unbiased. So we have to be careful and we have to connect the graphs with suitable techniques of sampling. **In the present paper we try to find the form of graphs permitting unbiased sampling estimators to be derived. We can say that: This work tries to achieve the conjugation of network theory (in the form of graphs in particular) and sampling with its techniques, with unbiased estimators for the involved parameters.**

<sup>5</sup>*th* SMTDA Conference Proceedings, 12-15 June 2018, Chania, Crete, Greece



## Axiomatic Geometries

Suppose we have the structure  $G=(V,E)$ . We adopt the next five axioms:

**Axiom 1:** Every pair of elements of  $V$  (vertices) has at least 1 connecting element.

**Axiom 2:** Every pair of elements of  $V$  (vertices) has at most 1 connecting element.

**Axiom 3:** Every elements of  $E$  (edge) connects at least in 2 elements of  $V$ .

**Axiom 4:** Every elements of  $E$  (edge) connects at most in 2 elements of  $V$ .

**Axiom 5:** The set  $V$  of vertices has exactly  $M$  elements.

We take the above 5 axioms as a set  $A$  and so we have constructed the structure  $\Gamma=(V,E,A)$ . This is a Finite Geometry with five axioms, called also axiomatic, Artemiadis (1977). Two questions arise now:

*What is the form of the elements of the structure  $\Gamma=(V,E,A)$ ?*

*How could we present the shape of this structure?*

We will try for a representation of the Geometry  $\Gamma=(V,E,A)$  an its elements. First of all the proof of some theorems will take place.

**Theorem 1:** Every pair of elements of  $V$  (vertices) has exactly 1 connecting element.

**Proof:** Obvious from axioms 1 and 2.

**Theorem 2:** Every elements of  $E$  (edge) belongs exactly in 2 elements of  $V$ .

**Proof:** Obvious from axioms 3 and 4.

**Theorem 3:** The elements of  $E$  (edge) are  $M \cdot (M - 1) / 2$ .

**Proof:** In the set  $V$  there are  $M$  elements. Every pair of elements of  $V$  corresponds (and defines) an element of  $E$  (edge). The pairs of elements of  $V$  are as many as the combinations of all the elements of

$V$  by 2, i.e.  $\binom{M}{2} = M \cdot (M - 1) / 2$ .

**Theorem 4:** For every element of  $V$  can be defined  $M-1$  elements of  $E$  (edges).

**Proof:** In the set  $V$  there are  $M$  elements. Every pair of elements of  $V$  defines and corresponds to an element of  $E$  (edge). Let us see the element (e.g.)  $\zeta$  of  $V$  and the pairs  $(\zeta, \theta) = (\theta, \zeta)$ . The element  $\theta$  represents the  $M - 1$  elements of  $V$ , which are different of  $\zeta$ . So there are  $M - 1$  pairs and  $M - 1$  elements of  $E$ .

**Definition 3:** Two elements of  $E$  are *parallel* if and only if are defined by different elements of  $V$ , i.e.  $(\xi, \theta), (\psi, \tau) \in E$  are parallel elements, if and only if it is  $\{\xi, \theta\} \cap \{\psi, \tau\} = \emptyset$ .

**Theorem 5:** In  $E$  there are  $(M - 2) \cdot (M - 3) / 2$  parallel elements to every element  $(\zeta, \nu)$  of  $E$ .

**Proof:** Suppose  $(\zeta, \nu) \in E$ . See the set  $V - \{\zeta, \nu\}$ . This set has  $M-2$  elements. That  $M-2$  elements taken by 2 (in pairs) define  $(M - 2) \cdot (M - 3) / 2$  elements of  $E$ , like the  $(\xi, \theta)$  e.g. It is of course  $\{\xi, \theta\} \cap \{\zeta, \nu\} = \emptyset$ . Thus, the element  $(\xi, \theta)$  of  $E$  is parallel to the element  $(\zeta, \nu)$  of  $E$ , among the  $(M - 2) \cdot (M - 3) / 2$  totally.

**Example 1:** Let us see the Axiomatic Geometry  $\Gamma=(V,E,A)$ . The set  $V$  contains 4 elements. The set of axioms  $A$  contains the 5 axioms above mentioned. What is the image of set  $E$ ?

**Answer:** We write the set  $V=\{1,2,3,4\}$ . The symbols 1,2,3,4 are the representatives of the 4 elements of  $V$ , for our convenience. They are not in general the natural numbers 1,2,3,4. The set of edges is the set of pairs (unordered) of element of  $V$ . So we have the set of 6 edges:

$E=\{(1,2),(1,3),(1,4),(2,3),(2,4),(3,4)\}$  (Theorems 1,2,3).

According to the Theorem 4 and for the element 3, e.g., we have the 3 edges (1,3),(2,3),(4,3), since for  $M=4$  the forecast is  $M-1=3$ . For the element 1 we have the 3 edges (1,2),(1,3),1,4), and so on.

According to the parallelism of definition 3, let us see the element  $(\zeta, \nu) = (2, 3) \in E$  e.g. In the set  $V - \{2,3\} = \{1,4\}$  we have 2 vertices. They give only 1 edge (Theorem 1), the (1,4). This edge is parallel to (2,3) and it is unique. This result reminds us the Euclidean Geometry with a related property (axiom) for the straight lines.

We symbolize as a=(1,2), b=(1,3), c=(1,4), d=(2,3), e=(2,4) and f=(3,4). In the next 4x4 matrix:

$$\Gamma = \begin{bmatrix} - & a & b & c \\ - & - & d & e \\ - & - & - & f \\ - & - & - & - \end{bmatrix}.$$

We see a way of symbolizing the set of edges  $E$ . It is the upper right region of the matrix  $\Gamma$ .

**Example 2:** Let us study the Axiomatic Geometry  $\Gamma=(V,E,A)$ , with  $M=5$  elements in  $V$ . The set of axioms  $A$  contains the 5 axioms above mentioned.

Study: It is now  $V= \{1,2,3,4,5\}$ . The suitable set  $E=\{(1,2),(1,3),(1,4),\dots,(3,5),(4,5)\}$  contains 10 elements. There are  $M-1=4$  edges connecting the element (e.g.) 2 with all the other in  $V$ . They are  $(1,2),(2,3),(2,4),(2,5)$ . The same is running with all the other elements.

For the parallels we meet the next situation: Without any lose of generality choosing the edge  $(\zeta, \nu) = (2, 5) \in E$  we have in the remaining set (difference)  $V-\{2,5\}=\{1,3,4\}$  three vertices. From this set 3 pairs are coming out, the edges  $(1,3),(1,4),(3,4)$ . These edges are parallel to the chosen edge  $(2,5)$ . This is in accordance with theorem 5 saying that there are  $(M-2) \cdot (M-3) / 2 = 3$  parallel edges to anyone edge  $(\zeta, \nu) \in E$ .

For an image of the set  $E$  we need a similar matrix  $\Gamma$  with dimension  $5 \times 5$ . The upper right region (trigonal again) of  $\Gamma$  is the image of the set of edges  $E$ .

## 2 Sampling in Nets. Unbiasedness of Estimators

**Random variable  $X$ :** A function from a set  $V=\{1,2,3,\dots,N\}$  to the set of real numbers. It is taken its values randomly (Abbreviation: rv). This means that  $X(i) = X_i \in R, i \in V$ .

A definition set may be also the  $V \times V = E$ , i.e. we have a rv  $Y(i, j) = Y_{ij} = X_i + X_j$  or more generally  $Y(i, j) = Y_{ij} = \lambda_1 \cdot X_i + \lambda_2 \cdot X_j, \lambda_1, \lambda_2 \in R$ , etc.

It is used to call the definition set  $V$  or the set  $V \times V = E$  population, symbolized  $\Pi$ , Farmakis (2009). In general, the population  $\Pi$  is a reference set. We draw a subset from  $\Pi$ , called sample. The process to draw samples is the sampling (technique). Usually used sampling techniques are the simple random sampling (srs), the systematic sampling (sys), the stratified sampling (sts), etc., Farmakis (2015, 2016), Cochran (1977). With definition set  $V \times V = E$  and values set the  $R \times R = R^2$  some useful rv are:

$$\begin{aligned} U(i, j) &= X_i + X_j, \quad i, j = 1, 2, 3, \dots, N \\ Z(i, i) &= X_i + X_i = 2 \cdot X_i, \quad i = 1, 2, 3, \dots, N \\ W(i, j) &= X_i + X_j, \quad i < j = 2, 3, 4, \dots, N \\ R(i, j) &= Y_i + Y_j, \quad j < i = 2, 3, 4, \dots, N. \end{aligned} \tag{1}$$

The next matrix  $M$  is a presentation of the definition set  $V \times V = E$ . The pair  $(i, j)$  stands for  $(X_i, X_j)$  or for  $X_i + X_j, i, j \in \{1, 2, 3, \dots, N\}$ . It depends on the needs of the study.

$$M = \begin{bmatrix} (1,1) & (1,2) & (1,3) & \dots & (1,N-2) & (1,N-1) & (1,N) \\ (2,1) & (2,2) & (2,3) & \dots & (2,N-2) & (2,N-1) & (2,N) \\ (3,1) & (3,2) & (3,3) & \dots & (3,N-2) & (3,N-1) & (3,N) \\ \dots & \dots & \dots & \dots & \dots & \dots & \dots \\ (N-2,1) & (N-2,2) & (N-2,3) & \dots & (N-2,N-2) & (N-2,N-1) & (N-2,N) \\ (N-1,1) & (N-1,2) & (N-1,3) & \dots & (N-1,N-2) & (N-1,N-1) & (N-1,N) \\ (N,1) & (N,2) & (N,3) & \dots & (N,N-2) & (N,N-1) & (N,N) \end{bmatrix}$$

Matrix  $M$  is definition set of  $U$  and of the rv  $Z, W, R$  some parts of it.

In general from a population  $\Pi$  size  $N$  we draw sample of size  $n < N$ . We study the rv  $X$  using only the sample data and we take estimators for several parameters of the rv  $X$ . For the parameter  $G$  of  $X$ , let  $\bar{g}$  the estimator. For every sample we have a value of the estimator.

**Definition 4:** The estimator  $\bar{g}$  of the parameter  $G$  is unbiased if  $E\bar{g} = G$ . Cochran (1977), Farmakis (2015, 2016)

**Example 3:** Let  $\Pi=V=\{1,2,3,\dots,N\}$ . Take all the samples of size  $n < N$ , by srs. How many samples are there? For the rv  $X(i)=X_i=i$ ,  $i=1,2,3,\dots,N$  we take the (parameter) mean value as

$$EX = \bar{X} = \frac{1}{N} \sum_{i=1}^N X_i \text{ and the estimator } \bar{x} = \frac{1}{n} \sum_{i=1}^n x_i \text{ where the set } \delta = \{x_1, x_2, \dots, x_n\} \text{ is the drawn}$$

sample. Is the estimator unbiased?

**Answer:** From the literature Farmakis (2015, 2016), Cochran (1977) we have that with srs without

replacement we have  $\binom{N}{n}$  samples of size  $n$ . With replacement the samples are  $N^n$ . In both the processes the unbiasedness of the estimator can be proved, i.e.

$$E\bar{x} = \bar{X} = EX. \quad (2)$$

Proof is given in Farmakis (2015, 2016) and in Cochran (1977).

Since it is  $Z(i,i) = X_i + X_i = 2 \cdot X_i$ ,  $i=1,2,3,\dots,N$ , obviously it is  $EZ = E2X = 2EX$  and for the

suitable estimator by an srs  $z = \hat{Z}$  we get  $E\bar{z} = E2\bar{x} = 2 \cdot EX = EZ$ .

Also for the rv  $W$  we have its mean value:

$$EW = \frac{\sum_{i=1}^{N-1} \sum_{j>i}^N (X_i + X_j)}{\binom{N}{2}} = \frac{\sum_{m=1}^N (N-1) \cdot X_m}{\binom{N}{2}} = 2 \frac{\sum_{m=1}^N X_m}{N} = 2EX \quad (3)$$

Also it is  $ER = 2 \cdot EX$  if we change the role of indices  $i$  and  $j$  as it is done in (1).

The definition set of the rv  $W$  is the upper right region of the matrix  $M$  and the suitable for the rv  $R$  is the down left region of  $M$ .

Note that for the above rv  $X(i)=X_i=i$ ,  $i=1,2,3,\dots,N$  we have

$$EX = (N+1)/2$$

and so it is

$$EZ = EW = ER = 2 \cdot EX = N+1. \quad (4)$$

**Example 4:** Let  $\Pi=V=\{1,2,3,\dots,N\}$ . Take all the samples of size  $n < N$ , by srs. How many samples are there? For the rv  $X(i)=X_i=a_i$ ,  $i=1,2,3,\dots,N$  we take the mean value and its estimator from drawn by srs

sample  $\delta = \{x_1, x_2, \dots, x_n\} = \{a_{(1)}, a_{(2)}, \dots, a_{(n)}\}$ . The mean and its estimator is

$$EX = \bar{X} = \frac{1}{N} \sum_{i=1}^N X_i = \frac{1}{N} \sum_{i=1}^N a_i \text{ and } \bar{x} = \frac{1}{n} \sum_{i=1}^n x_i. \text{ Is the estimator unbiased? What we can say}$$

about the related estimators of the mean values  $EZ, EW, ER$ ?

**Answer:** From the literature Farmakis (2015, 2016), Cochran (1977) we have the answer given before by the relation (2).

Also, this result can be extended for  $EZ, EW$  and  $ER$  as in (3). This is because the thoughts in (3) they are based on values of the rv  $X$  not only equal to  $X(i)=i$  but real values in general.

Let us see a special sampling design on the structure  $\Gamma=(V,E,A)$ .  $V=\{1,2,3,\dots,N\}$  stands for population (frame). From this population we draw a sample  $\delta = \{i_1, i_2, i_3, \dots, i_n\}$  by srs and of size  $n$ . Without any limitation of generality, suppose that the sizes in  $\delta$  are growing up, with the indices. As we said before there are  $\binom{N}{n}$  samples like  $\delta$ . We adopt now the concept of the "implemented sample"  $\delta_{im}$ , where

$$\delta_{im} = \{(i, j) \text{ or } (j, i) \in \text{urr of } M, i \neq j = 1, 2, 3, \dots, N, \forall i \in \delta\}$$

and urr= "upper right region". Obviously, the sample  $\delta_{im}$  is a sample drawn from the urr, if we see urr as a population. In  $\delta_{im}$  the elements (pairs) are  $n \cdot (N-1)$ , i.e.  $N-1$  values of  $j$  for any value of  $i$  in  $\delta$ . In urr of  $M$  and for the rv  $W$  in (1) the relation (3) holds. Also, in  $\delta_{im}$  we have the (sample) mean for  $W$ , the next one

$$\bar{w} = \frac{\sum_{i=i_1}^{i_n} \sum_{i \neq j=1}^N (X_i + X_j)}{n \cdot (N-1)}. \quad (5)$$

**Theorem 6:** The mean value in (5) is an unbiased estimator of  $EW$  in (3), i.e.  $E\bar{w} = EW$ .

**Proof:** In the double summation of the nominator in (5) any value of  $X_{i_\lambda}, \lambda = 1, 2, 3, \dots, n$  comes in  $N-1$  times as first added number and  $n-1$  times as second one. So in the above nominator there are  $(N+n-2)$  participations for every  $X_{i_\lambda}, \lambda = 1, 2, 3, \dots, n$  and also for every index (say  $j$ ) in the set  $\{1, 2, 3, \dots, N\} - \delta = J$  we see  $n$  times the value  $X_j$ . So the samples  $\delta$  and  $\delta_{im}$  give nominator of  $\bar{w}$  in (5) the quantity  $(N+n-2) \cdot \sum_{\lambda=1}^n X_{i_\lambda} + n \cdot \sum_{m=1}^{N-n} X_{j_m}$ . Running over all the pairs of samples  $\delta$  and  $\delta_{im}$  we calculate the mean of all the sample means in (5). This mean is the one

$$E\bar{w} = \frac{\sum_{m=1}^r \bar{w}_m}{r}, \quad r = \binom{N}{n} \quad (6)$$

In the nominator of the ratio in (6) there are all the nominators in (5). This is equal to imagine the value  $X_{i_\lambda}, \lambda = 1, 2, 3, \dots, N$  with  $(N+n-2)$  participation multiplied by the number of samples including the index  $i_\lambda, \lambda = 1, 2, 3, \dots, N$ . The number of those samples is  $\binom{N-1}{n-1}$ , Cochran (1977), Farmakis (2015, 2016). Corresponding to the above mentioned for every  $j \in J$  the value  $X_j$  participates in the nominator in (6)  $n$  times multiplied by the number of pairs of samples  $\delta$  and  $\delta_{im}$  for which  $j \notin \delta$ . The number of those samples is  $\binom{N}{n} - \binom{N-1}{n-1}$  obviously.

Finally all the values of the rv  $X$ , the  $X_m, m = 1, 2, 3, \dots, N$ , participate in the nominator of the quantity  $\sum_{m=1}^r \bar{w}_m, r = \binom{N}{n}$  with the same multiplicity, due to the definition of random sample, Cochran (1977), Farmakis (2015, 2016). The value  $X_m, m = 1, 2, 3, \dots, N$  participates as value with index in the sample (for all the samples)  $\binom{N-1}{n-1} \cdot (N+n-2)$  times and as a value with its index out of the sample (for all the samples too)  $n \cdot \left( \binom{N}{n} - \binom{N-1}{n-1} \right)$  times. Summarizing we get that the nominator of the quantity

$$\sum_{m=1}^r \bar{w}_m, r = \binom{N}{n} \text{ is equal to the quantity} \\ S_r = \left\{ \binom{N-1}{n-1} \cdot (N+n-2) + \left\{ \binom{N}{n} - \binom{N-1}{n-1} \right\} \cdot n \right\} \cdot \sum_{m=1}^N X_m \quad (7)$$

and therefore, the relation (6) becomes

$$E\bar{w} = \frac{S_r}{n \cdot (N-1) \cdot \binom{N}{n}} = \frac{2 \cdot \binom{N-1}{n-1}}{n \cdot \binom{N}{n}} \cdot \sum_{r=1}^N X_r = 2 \cdot EX = EW \quad (8)$$

and the theorem is proved.

It is easy to extend this proof for the rv  $U$  and  $R$  too.

### 3 Results and discussion

Using the rv  $X$  defined in the set  $\{1, 2, 3, \dots, N\}$  and taking a random sample  $\delta$  from this definition field of the rv  $X$  we used the matrix-graphos  $\mathbf{M}$  and its areas as definition fields for the rv  $U, W, R$  and  $Z$  in (1) to get a product of  $\delta$  the implemented (randomly) sample  $\delta_{im}$ . After this by using the data in the sample  $\delta_{im}$  we proved the unbiasedness of the estimators of the means of the rv  $U, W, R$  and  $Z$  in (1).

Since the unbiasedness of estimators for the parameters of a rv  $X$  with definition field a graphos (net, etc.) is a very rare case the above results seem to be a quite important one.

## References

1. Artemiadis N. (1977) "*Elementary Geometry from an upper point of view*", Publications of Hellenic Mathematical Society, Athens (in Greek).
2. Cochran W. (1977) "*Sampling Techniques*", John Wiley & Sons, Inc, New York, Toronto.
3. Farmakis N. (2009) "*Surveys and Ethics*", 2<sup>nd</sup> Edition, A & P Christodoulidi, Thessaloniki (in Greek).
4. Farmakis N. (2015) "*Sampling and Applications*" Hellenic Academic e-Books, Athens, ISBN: 978-960-603-093-2 (in Greek).
5. Farmakis N. (2016) "*Introduction to Sampling*", Kyriakidis Bros Editing S.A, Thessaloniki (in Greek).

# A STUDY ON PROBABILITY DENSITY FUNCTIONS WITH NEGATIVE EXPONENT

*Papatsouma Ioanna, Farmakis Nikolaos*

*Department of Mathematics*

*Aristotle University of Thessaloniki*

*54124, Thessaloniki, Greece*

[ioannapapatsouma@gmail.com](mailto:ioannapapatsouma@gmail.com), [farmakis@math.auth.gr](mailto:farmakis@math.auth.gr)

## Abstract

Sampling can help researchers to study the distributions of the various random variables and produce very satisfying results in terms of accuracy and speed. The probability density function (pdf) of a random variable (rv)  $X$  can be estimated via sampling and various parameters of the rv  $X$ , e.g. the mean, the variance, the coefficient of variation, the range, etc. and then with knowledge of the pdf, further statistical problems can be tackled. This procedure is both theoretical and empirical, based on sample data. In applied statistics, an initial hypothesis is made upon for a particular situation about the form of the pdf of  $X$  or an approximation of this pdf, that can be efficient and easy to be managed by researchers. The choice of the type of the suitable pdf and the time it takes to process the data in order to construct the pdf is vital. In the present paper we study how to get the suitable estimator from the sample, when the pdf has a polynomial form with a negative exponent. Illustrative examples are given to highlight the basic results of the theoretical approach.

**Key words:** Sampling, Probability density function, Coefficient of variation, Mean, Variance, Range.

**MSC2010 Classification:** 62D05, 62E17

## 1. Introduction

The probability density function (pdf), a concept known from the literature, refers to a random variable  $X$  (rv  $X$ ). The pdf is a very useful for the proper study of the rv  $X$ . It gives us a good and complete picture of the behavior of  $X$ , in general.

In the present work, sampling gives us enough initial data useful to exploit the rest of the information in the data. For the present work the key element is the distribution range  $R$  of the rv  $X$  which is estimated by difference between the maximum value of the sample data  $X_{max}$  and the minimum value of the rv  $X$ . The pdf of the rv  $X$  is denoted and defined by the relation  $f(x) = P(X = x)$  and has two basic properties:

$$f(x) \geq 0 \tag{1}$$

and



$$\int_{-\infty}^{\infty} f(x)dx = 1 \quad (2)$$

The forms of pdf are infinitely numbered. In the present paper we study only the pdf with the form of a mononym with negative exponent, i.e.

$$f(x) = \begin{cases} x^{-\nu}, & x \in [\varepsilon, \beta] \\ 0, & x \notin [\varepsilon, \beta] \end{cases}, \quad 0 < \varepsilon < \beta, \quad \nu = 1, 2, 3, \dots \quad (3)$$

The parameter  $\beta$  is suitably determined by sample  $\delta$  and is always  $\beta \geq X_{\max} \in \delta$ . The limit  $\varepsilon$  is suitably defined as a function of  $\beta$  and the exponent  $\nu$ , such as the relations (1) and (2) are valid.

We will examine some cases of the exponent  $\nu$ , e.g.  $\nu=1, 2$  as well as the general case for all the possible values of  $\nu$ .

### $\nu=1$

From the equation (3) we get:

$$f(x) = \begin{cases} x^{-1}, & x \in [\varepsilon, \beta] \\ 0, & x \notin [\varepsilon, \beta] \end{cases}, \quad 0 < \varepsilon < \beta \quad (1.1)$$

The validity of (1) is obvious as it is  $0 < \varepsilon \leq x \leq \beta$ .

Of course, from (2) is easy to reach the value of  $\varepsilon$ , as:

$$1 = \int_{-\infty}^{+\infty} f(x)dx = \int_{\varepsilon}^{\beta} x^{-1} dx = \ln \frac{\beta}{\varepsilon} \Leftrightarrow \varepsilon = \frac{\beta}{e} \quad (1.2)$$

The basic parameters of the rv  $X$  are easily calculated from well-known relations:

The mean value is given by:

$$EX = \mu = \int_{\varepsilon}^{\beta} x \cdot f(x)dx = \beta - \varepsilon = \beta \cdot \left( \frac{e-1}{e} \right) \quad (1.3)$$

or  $\mu=0.6321\beta$  (to four decimal digits accuracy).

The variance is given by:

$$VarX = \sigma^2 = EX^2 - (EX)^2 = \frac{\beta^2(e^2-1)}{2 \cdot e^2} - \beta^2 \cdot \left( \frac{e-1}{e} \right)^2 = \dots = \frac{\beta^2}{2 \cdot e^2} \cdot \{1 - (e-2)^2\} \quad (1.4)$$

where  $EX^2$  is:

$$EX^2 = \int_{\varepsilon}^{\beta} x^2 \cdot f(x)dx = \int_{\varepsilon}^{\beta} x dx = \frac{\beta^2 - \varepsilon^2}{2} = \dots = \frac{\beta^2(e^2-1)}{2 \cdot e^2}$$

or equivalently:  $\sigma^2 = 0.0328 \cdot \beta^2$ .

The standard deviation (SD) is given by:

$$\sigma = \sqrt{VarX} = \frac{\beta}{2e} \cdot \sqrt{2 \cdot \{1 - (e-2)^2\}} \quad (1.5)$$

or  $SD = \sigma = 0.1810 \cdot \beta$ .

The Coefficient of variation ( $Cv$ )

$$Cv = \frac{\sqrt{VarX}}{EX} = \dots = \frac{\sqrt{2 \cdot \{1 - (e-2)^2\}}}{2 \cdot (e-1)} \quad (1.6)$$

or  $Cv = 0.2863$ , i.e.  $Cv$  is independent of the range  $\beta$ , or better units free.

The Squared Inverse of Coefficient of variation ( $ICv^2=q$ ) is given by:

$$ICv^2 = \frac{(EX)^2}{VarX} = \dots = \frac{2 \cdot (e-1)^2}{1 - (e-2)^2} = q \quad (1.7)$$

or  $q = ICv^2 = Cv^{-2} = 12.1999$ , independent of the range  $\beta$ , or better units free at all.

## v=2

From the function in (3) we have:

$$f(x) = \begin{cases} x^{-2}, & x \in [\varepsilon, \beta] \\ 0, & x \notin [\varepsilon, \beta] \end{cases}, \quad 0 < \varepsilon < \beta \quad (2.1)$$

Since it is  $0 < \varepsilon \leq x \leq \beta$ , we have that (1) holds and also it follows that:

$$1 = \int_{-\infty}^{+\infty} f(x) dx = \int_{\varepsilon}^{\beta} x^{-2} dx = -x^{-1} \Big|_{\varepsilon}^{\beta} = \frac{\beta - \varepsilon}{\beta \cdot \varepsilon} = 1 \Leftrightarrow \varepsilon = \frac{\beta}{\beta + 1} \quad (2.2)$$

The parameters of the rv  $X$  are resulting from the calculations as follows:

The mean value is given by:

$$EX = \mu = \int_{\varepsilon}^{\beta} x \cdot f(x) dx = \int_{\varepsilon}^{\beta} \frac{dx}{x} = \ln x \Big|_{\varepsilon}^{\beta} = \ln \frac{\beta}{\varepsilon} = \ln(\beta + 1) \quad (2.3)$$

The variance is given by:

$$VarX = \sigma^2 = EX^2 - (EX)^2 = \frac{\beta^2}{\beta + 1} - \{\ln(\beta + 1)\}^2 = \dots = \frac{\beta^2 - \{\ln(\beta + 1)\}^2}{\beta + 1}$$

where  $EX^2$  is:

$$EX^2 = \int_{\varepsilon}^{\beta} x^2 \cdot f(x) dx = \int_{\varepsilon}^{\beta} 1 dx = \beta - \varepsilon = \dots = \frac{\beta^2}{\beta + 1}$$

or, equivalently by:

$$VarX = \sigma^2 = \frac{\beta^2 - \{\ln(\beta + 1)\}^2}{\beta + 1} \quad (2.4)$$

The standard deviation is given by:

$$\sigma = SD = \sqrt{VarX} = \sqrt{\frac{\beta^2 - \left\{ \ln(\beta+1) \right\}^{\sqrt{\beta+1}}}{\beta+1}}. \quad (2.5)$$

The Coefficient of variation (Cv) is given by:

$$Cv = \frac{\sqrt{VarX}}{EX} = \dots = \frac{\sqrt{\frac{\beta^2 - \left\{ \ln(\beta+1) \right\}^{\sqrt{\beta+1}}}{\beta+1}}}{\ln(\beta+1)} = \frac{\sqrt{\beta^2 - \left\{ \ln(\beta+1) \right\}^{\sqrt{\beta+1}}}}{\ln(\beta+1)^{\sqrt{\beta+1}}}$$

or, equivalently by:

$$Cv = \sqrt{\frac{\beta^2}{\left\{ \ln(\beta+1) \right\}^{\sqrt{\beta+1}}} - 1}. \quad (2.6)$$

The inverse of the Coefficient of variation squared is given by:

$$q = ICv^2 = \frac{(EX)^2}{VarX} = \dots = \frac{\left\{ \ln(\beta+1) \right\}^{\sqrt{\beta+1}}}{\beta^2 - \left\{ \ln(\beta+1) \right\}^{\sqrt{\beta+1}}} = Cv^{-2}. \quad (2.7)$$

## v>2

Suppose we have the pdf in relation (3).

Since it is  $0 < \varepsilon \leq x \leq \beta$ , then the (1) is valid and of course it is also

$$1 = \int_{-\infty}^{+\infty} f(x)dx = \int_{\varepsilon}^{\beta} x^{-n} dx = -\frac{x^{-n+1}}{n-1} \Big|_{\varepsilon}^{\beta} = \dots = \frac{\beta^{v-1} - \varepsilon^{v-1}}{(v-1) \cdot \beta^{v-1} \cdot \varepsilon^{v-1}} \Leftrightarrow \varepsilon^{v-1} = \frac{\beta^{v-1}}{(v-1) \cdot \beta^{v-1} + 1}.$$

Finally, it is:

$$\varepsilon = \frac{\beta}{\sqrt[v-1]{(v-1) \cdot \beta^{v-1} + 1}} = \frac{1}{\sqrt[v-1]{(v-1) + \frac{1}{\beta^{v-1}}}}. \quad (3.1)$$

We can consider the parameter  $\varepsilon$  as the  $v^{\text{th}}$  element of a sequence  $\varepsilon_v$  we adopt the formula (3.2)

instead of (3.1)

$$\varepsilon_v = \frac{\beta}{\sqrt[v-1]{(v-1) \cdot \beta^{v-1} + 1}} = \frac{1}{\sqrt[v-1]{(v-1) + \frac{1}{\beta^{v-1}}}} \quad (3.2)$$

i.e. it is valid that  $0 < \varepsilon_v < 1$ .

It is also well-known from the literature that  $\lim_{v \rightarrow \infty} \varepsilon_v = 1$ .

The parameters of the rv  $X$  are calculated as follows:

The mean value is given by:

$$EX = \mu = \int_{\varepsilon}^{\beta} x \cdot f(x) dx = \int_{\varepsilon}^{\beta} x^{-\nu+1} dx = -\frac{1}{\nu-2} \cdot x^{-\nu+2} \Big|_{\varepsilon}^{\beta} = \dots = \frac{1}{\nu-2} \cdot \frac{\beta^{\nu-2} - \varepsilon^{\nu-2}}{\beta^{\nu-2} \cdot \varepsilon^{\nu-2}} \quad (3.3)$$

The variance is given by:

$$VarX = \sigma^2 = EX^2 - (EX)^2 = \frac{\beta^{\nu-3} - \varepsilon^{\nu-3}}{(\nu-3) \cdot \beta^{\nu-3} \cdot \varepsilon^{\nu-3}} - \frac{(\beta^{\nu-2} - \varepsilon^{\nu-2})^2}{(\nu-2)^2 \cdot \beta^{2\nu-4} \cdot \varepsilon^{2\nu-4}}$$

where  $EX^2$  is:

$$EX^2 = \int_{\varepsilon}^{\beta} x^2 \cdot f(x) dx = \int_{\varepsilon}^{\beta} x^{-\nu+2} dx = \dots = \frac{\beta^{\nu-3} - \varepsilon^{\nu-3}}{(\nu-3) \cdot \beta^{\nu-3} \cdot \varepsilon^{\nu-3}}$$

or, equivalently by:

$$VarX = \sigma^2 = \frac{\beta^{2\nu-4} \cdot \left\{ (\nu-2)^2 \cdot \varepsilon^{\nu-1} - \nu + 3 \right\} - \varepsilon^{2\nu-4} \cdot \left\{ (\nu-2)^2 \cdot \beta^{\nu-1} - \nu + 3 \right\} + 2(\nu-3) \cdot (\beta\varepsilon)^{\nu-2}}{(\nu-2)^2 \cdot (\nu-3) \cdot (\beta\varepsilon)^{2\nu-4}} \quad (3.4)$$

The Standard Deviation is given by:

$$\sigma = \sqrt{\frac{\beta^{2\nu-4} \cdot \left\{ (\nu-2)^2 \cdot \varepsilon^{\nu-1} - \nu + 3 \right\} - \varepsilon^{2\nu-4} \cdot \left\{ (\nu-2)^2 \cdot \beta^{\nu-1} - \nu + 3 \right\} + 2(\nu-3) \cdot (\beta\varepsilon)^{\nu-2}}{(\nu-2)^2 \cdot (\nu-3) \cdot (\beta\varepsilon)^{2\nu-4}}} \quad (3.5)$$

The Coefficient of variation (CV) is given by:

$$Cv = \frac{\sigma}{\mu} = \frac{\sqrt{\frac{\beta^{2\nu-4} \cdot \left\{ (\nu-2)^2 \cdot \varepsilon^{\nu-1} - \nu + 3 \right\} - \varepsilon^{2\nu-4} \cdot \left\{ (\nu-2)^2 \cdot \beta^{\nu-1} - \nu + 3 \right\} + 2(\nu-3) \cdot (\beta\varepsilon)^{\nu-2}}{(\nu-2)^2 \cdot (\nu-3) \cdot (\beta\varepsilon)^{2\nu-4}}}}{\frac{1}{\nu-2} \cdot \frac{\beta^{\nu-2} - \varepsilon^{\nu-2}}{\beta^{\nu-2} \cdot \varepsilon^{\nu-2}}}$$

or, equivalently by:

$$Cv = \sqrt{\frac{\beta^{2\nu-4} \cdot \left\{ (\nu-2)^2 \cdot \varepsilon^{\nu-1} - \nu + 3 \right\} - \varepsilon^{2\nu-4} \cdot \left\{ (\nu-2)^2 \cdot \beta^{\nu-1} - \nu + 3 \right\} + 2(\nu-3) \cdot (\beta\varepsilon)^{\nu-2}}{(\nu-3) \cdot (\beta^{\nu-2} - \varepsilon^{\nu-2})^2}} \quad (3.6)$$

Finally, the inverse of the Coefficient of variation squared is given by:

$$q = ICv^2 = \frac{(\nu-3) \cdot (\beta^{\nu-2} - \varepsilon^{\nu-2})^2}{\beta^{2\nu-4} \cdot \left\{ (\nu-2)^2 \cdot \varepsilon^{\nu-1} - \nu + 3 \right\} - \varepsilon^{2\nu-4} \cdot \left\{ (\nu-2)^2 \cdot \beta^{\nu-1} - \nu + 3 \right\} + 2(\nu-3) \cdot (\beta\varepsilon)^{\nu-2}} \quad (3.7)$$

## 2. Examples

Some examples are given in order to examine if the theoretic and the sample estimated values are similar when the data seem to follow the law of the negative exponent. We start from the low limit of the price field of the rv  $X$  and we follow on with mean value, variance, standard deviation, coefficient of variation and parameter  $q$  (=inverse of the Coefficient of variation squared). An analysis with the use of pdf and the coefficient of variation is taken place. Also a Chi-Squared test is used, in order to certify a good fitting between theoretic and observed values of frequency.

**Example 1:** A relatively simple problem on probabilities was given to  $n=360$  students of Agriculture of Aristotle University of Thessaloniki (AUTH). Everybody gave his (her) answer. The maximum time for the solution was  $X_{\max}=\beta=11$  minutes and the minimum one was  $X_{\min}=3.8$  minutes. The pdf must be descending, since the problem is simple. We adopt the space  $A=[3.8, 11]$  as the field of values of the rv  $X$ =time for the answer and we make and a division of  $A$  into 6 subspaces (classes) of length  $w=1.2$  minutes each one, in Table 1.

Table 1

Classes	Centers $x_i$	Frequency $n_i$	$x'_i$	$nx'$	$nx^2$	$\theta_i$
3.8 – 5.0	4.4	79	-2	-158	316	76,2
5.0 – 6.2	5.6	71	-1	-71	71	77,4
6.2 – 7.4	<b>6.8</b>	63	0	0	0	63,7
7.4 – 8.6	8.0	55	1	55	55	54,1
8.6 – 9.8	9.2	49	2	98	196	47,0
9.8 – 11.0	10.4	43	3	129	387	41,6
TOTALS		<b><math>n=360</math></b>		<b><math>T_1=53</math></b>	<b><math>T_2=1025</math></b>	<b>360.0</b>

As temporary mean value ( $m=6.8$ ) the center of the 3<sup>rd</sup> class is taken. So the 4<sup>th</sup>, 5<sup>th</sup> and 6<sup>th</sup> column are obtained. The 7<sup>th</sup> column is the one in which figure the theoretic frequencies in accordance with the relation (3) with exponent -1 (or  $v=1$ ). Accuracy level: 1 decimal digit after the point. See that the total is always equal to  $n=360$  as it is in 3<sup>rd</sup> column too. We can apply the Chi-squared test between observed and theoretic frequencies.

The question that arises is: *Can the pdf of the rv  $X$ =time needed to answer, be expressed by the formula (3), with  $v=1$ ?*

*Answer:* First of all, we use the  $X_{\max}$  and (1.2) to calculate  $\varepsilon=4.0467$ . As the  $X_{\min}=3.8$  seems to be a value near to the theoretic  $\varepsilon=4.0467$ . This is an initial step giving a chance to follow on comparing the other parameters (=theoretic values) with the statistics (=sample values). The mean value from the sample is

$$\bar{x} = m + w \cdot T_1 / n = 6.8 + 1.2 \cdot 53 / 360 = 6.9767$$

and the theoretic one from (1.3) is

$$EX=6.9533$$

From Table 1 we calculate the variance of the rvX as

$$s^2 = \frac{w^2}{n-1} \cdot \left( T_2 - \frac{T_1^2}{n} \right) = \frac{1.2^2}{359} \cdot \left( 1025 - \frac{53^2}{360} \right) = 4.0801$$

And from (1.4) the theoretic value of variance is resulting

$$VarX = \sigma^2 = EX^2 - (EX)^2 = \dots = \frac{\beta^2}{2 \cdot e^2} \cdot \{1 - (e-2)^2\} = 0.0328 \cdot \beta^2 = 3.9688.$$

Also, from (1.6) we get the value for CvX (it is independent from the range  $\beta$  and free of units)

$$CvX = \frac{\sqrt{VarX}}{EX} = \dots = \frac{\sqrt{2 \cdot \{1 - (e-2)^2\}}}{2 \cdot (e-1)} = 0.2863$$

and the corresponding sample value is

$$\hat{CvX} = \frac{\sqrt{4.0801}}{6.9531} = 0.2905.$$

The corresponding value for the inverse of the Coefficient of variation squared resulting from (1.7) is  $q=ICv^2=12.1814$  and from the sample we have

$$q = IC\hat{v}^2 = \frac{\bar{x}^2}{s^2} = \frac{6.9767^2}{4.0801} = 11.9297.$$

All the above the sample results and the theoretic ones are figuring in the next Table 2 helping for a direct comparison:

**Table 2**

	Mean value	Variance	SD	Cv	ICv <sup>2</sup> =q
<b>Sample</b>	6.9767	4.0801	2.0199	0.2905	11.9297
<b>Theoretic</b>	6.9533	3.9688	1.9922	0.2863	12.1814

Only little variations between experimental (sample) and theoretical values are observed in this Table. Even in this case we need a test of good fitness to accept or not the  $H_0$ : "The sample data are from a distribution described by (3) with exponent -1.

A Chi-squared test took place with Hypothesis  $H_0$  and  $H_1$  as follows:

$H_0$ : "The observed values (sample) have a good fitting with the theoretic ones"

$H_1$ : "Non the  $H_0$ "

The observed values are in the 3<sup>rd</sup> column and the theoretic ones are in the 7<sup>th</sup> column of Table

1. Degrees of freedom  $\kappa-1=5$  and the critical value of the test is  $X_{5;0.05}^2 = 11.0705$ .

The experimental value of  $X^2=1.9720 < 11.0705$ .

So, there is not sufficient information to reject the null Hypothesis,  $H_0$ .  $H_0$  remains valid.

**Example 2:** A sample of  $n=280$  students faced a question to be answered after a Web searching of some minutes. All the students answered in a period of, at most, 17 minutes. The minimum time for the answer was 56 seconds.

The question was considered easy and the pdf of the rv  $X$ = time of running on web searching is expected to be descending. With a step of  $w=2.3$  minutes and seven classes we created the next Table 3 of frequencies fill up with the suitable data of processing data.

The arising question was: ‘*Is it possible the data of Table 3 to come out of a distribution described by (2.1) or by (3) for an exponent bigger than 2?*’

**Table 3**

classes	centers $x_i$	frequencies $n_i$	$x'_i$	$nx'$	$nx^2$	$\theta_i$
0.9 – 3.2	2.05	203	-3	-609	1827	209
3.2 – 5.5	4.35	38	-2	-76	152	37
5.5 – 7.8	6.65	16	-1	-16	16	15
7.8 – 10.1	<b>8.95</b>	11	0	0	0	8
10.1 – 12.4	11.25	5	1	5	5	5
12.4 – 14.7	13.55	4	2	8	16	4
14.7 – 17.0	15.85	3	3	9	27	3
TOTALS		<b><math>n=280</math></b>		<b><math>T_1=-679</math></b>	<b><math>T_2=2043</math></b>	<b>280</b>

As temporary mean value ( $m=8.95$ ) the center of the 4<sup>th</sup> class is taken. So the 4<sup>th</sup>, 5<sup>th</sup> and 6<sup>th</sup> column are obtained. The 7<sup>th</sup> column is the one in which figure the theoretic frequencies in accordance with the relation (3) with exponent -2 (or  $v=2$ ). Accuracy level the integer unit. See that the total is always equal to  $n=280$  as it is in 3<sup>rd</sup> column too. We can apply the Chi-squared test between observed and theoretic frequencies.

The question is now: The pdf of the rv  $X$ =time needed to answer, can be expressed by the formula (3), with  $v=2$  or  $v>2$  say 3,4?

*Answer:* First of all we examine the least possible value of the rv  $X$ = time of running on web searching. For  $v=2$  it is  $\varepsilon=\beta/(\beta+1)=0.9444$  minutes. This value is very near to the observed  $X_{\min}=56/60=0.9333$  minutes. So Table 3 begins with its 1<sup>st</sup> class limited from 0.9 to 3.2, step= $w=2.3$  minutes.

The mean value from the sample is:

$$\bar{x} = m + w \cdot T_1 / n = 8.95 + 2.3 \cdot (-679) / 280 = 3.3725$$

The theoretic mean value is

$$EX=2.8904$$

From Table 3 the experimental variance is resulting as:

$$s^2 = \frac{w^2}{n-1} \left( T_2 - \frac{T_1^2}{n} \right) = \frac{2.3^2}{279} \cdot \left( 2043 - \frac{(-679)^2}{280} \right) = 7.5164$$

Since from (2.4) we yield

$$VarX = \sigma^2 = \frac{\beta^2 - \left\{ \ln(\beta+1)^{\sqrt{\beta+1}} \right\}^2}{\beta+1} = \frac{289 - \left\{ \ln 18^{\sqrt{18}} \right\}^2}{18} = 7.7013.$$

Thus it is theoretic value

$$Cv = \frac{\sqrt{VarX}}{EX} = 0.9601$$

And sample value the

$$\hat{Cv} = \frac{\sqrt{7.5164}}{3.3725} = 0.8129.$$

The calculation based on (2.7) gives for the parameter  $q=ICv^2=1.5132$  and the sample is giving the experimental value

$$q = I\hat{Cv}^2 = \frac{\bar{x}^2}{s^2} = \frac{3.3725^2}{7.5164} = 1.5132.$$

All the above, the sample results and the theoretic ones, are figuring in the next Table 4 helping for a direct comparison:

Table4

	Mean value	Variance	SD	Cv	ICv <sup>2</sup> =q
<b>Sample</b>	3.3725	7.5164	2.7416	0.8129	1.5132
<b>Theoretic</b>	2.8904	7.7013	2.7751	0.9601	1.0848

Only little variations between experimental (sample) and theoretical values are observed in this Table. Even in this case we need a test of good fitness to accept or not the  $H_0$ : "The sample data are from a distribution described by (3) with exponent -1.

A Chi-squared test took place with hypothesis  $H_0$  and  $H_1$  as follows:

$H_0$ : "The observed values (sample) have a good fitting with the theoretic ones"

$H_1$ : "Non the  $H_0$ "

The observed values are in the 3<sup>rd</sup> column and the theoretic ones are in the 7<sup>th</sup> column of Table

3. Degrees of freedom  $\kappa-1-1=5^{(*)}$  and the critical value of the test is  $X_{5,0.05}^2 = 11.0705$ .

The experimental value of  $X^2=1.4000 < 11.0705$ .

So, there is not sufficient information to reject the null Hypothesis,  $H_0$ .  $H_0$  remains valid.

(\*) Since  $\theta_6, \theta_7 < 5$  the classes 6<sup>th</sup> and 7<sup>th</sup> merged into one and the degrees of freedom (df) are resulting from the remaining 6 classes, instead of the initial 7 ones. So we have  $6-1=5$  df.

A trial to check if a pdf (3) with  $\nu=3$  can describe the frequencies in the 3<sup>rd</sup> column of Table 3 gives the next findings:

- The value for the low boundary of the range is  $\varepsilon_2=0.7065<56/60=0.9333<0.9444$ .
- The 95% of the observations is demanded to figure in the 1<sup>st</sup> class of the distribution, i.e. about 265 observations among the 280. This is big enough for the 203 observed cases.
- For the 2<sup>nd</sup> class the foreseen frequency is about 10 cases, very little in relation with the 38 observed cases.
- For the 3<sup>rd</sup> class the foreseen frequency is about  $3<5$ .
- The above mean that for the next four classes only 2 observations are remaining, instead of the 23 observed cases. Also the Chi-Squared test is forbidden by these frequencies.
- We tried to merge the 5 last classes into one for a Chi-squared test. So we have had only 3 classes, i.e. 2 df. The experimental value of  $X^2$  was some hundreds rejecting the null hypothesis.

$H_0$ : “The observed values (sample) have a good fitting with the theoretic ones”

And the alternative one

$H_1$ : “Non the  $H_0$ ”

Is valid, i.e. the exponent of the pdf in (3) is not -3 or less. We remain to the result “the exponent is -2”.

### 3. Theorems

The following theorems have been used in the present paper:

**Theorem 1:** *The sequence of real numbers  $(\alpha_n)_{n \in \mathbb{N}}$ , where  $\alpha_n = \sqrt[n]{n+\lambda}$ ,  $\lambda > 0$ , is given.*

*Prove that its limit is 1.*

**Proof:** (a) Let us think of the set of the non-zero natural numbers  $\mathbb{N}^* = \{1, 2, 3, \dots, n, \dots\}$  and the obvious inequality

$$n + \lambda \geq 1, n \in \mathbb{N}^*$$

This leads to the next two equivalent inequalities:

$$\sqrt[n]{n+\lambda} \geq 1 \iff \sqrt[n]{n+\lambda} - 1 \geq 0 \iff \alpha_n - 1 \geq 0. \quad (4.1)$$

(b) We define the sequence

$$\theta_n = \alpha_n - 1 = \sqrt[n]{n+\lambda} - 1 \geq 0, \forall n \in \mathbb{N}^* \quad (4.2)$$

It is sufficient to be proved that  $\theta_n \rightarrow 0$ .

We are able to get the series of the following relations:

$$1 + \theta_n = \sqrt[n]{n + \lambda} \quad \text{and} \quad n + \lambda = (1 + \theta_n)^n \geq 1 + n \cdot \theta_n + \binom{n}{2} \cdot \theta_n^2 > \frac{n \cdot (n-1)}{2} \cdot \theta_n^2. \quad \text{So, it is valid}$$

$$\forall n \geq 2, n + \lambda > \frac{n \cdot (n-1)}{2} \cdot \theta_n^2 \quad \text{or after some simplifications we get the } 0 \leq \theta_n^2 < \frac{2 \cdot (n + \lambda)}{n \cdot (n-1)}.$$

Finally results that

$$0 \leq \theta_n < \sqrt{\frac{2 \cdot (n + \lambda)}{n \cdot (n-1)}} \quad (4.3)$$

Adopting the symbols of the zero sequences the  $(\gamma_n = 0)_{n \in \mathbb{N}}$ ,  $\left( \beta_n = \sqrt{\frac{2 \cdot (n + \lambda)}{n \cdot (n-1)}} \right)_{n \in \mathbb{N}}$ , the

$$(4.3) \text{ can be written as } 0 = \gamma_n \leq \theta_n < \beta_n = \sqrt{\frac{2 \cdot (n + \lambda)}{n \cdot (n-1)}} \rightarrow 0.$$

This last relation leads to the conclusion that  $\theta_n \rightarrow 0$  and  $\alpha_n = \sqrt[n]{n + \lambda} \rightarrow 1$  ■

**Theorem 2:** The limit of the sequence of real numbers  $(\alpha_n)_{n \in \mathbb{N}}$ , where  $\alpha_n = \sqrt[n]{n + 1}$  is 1.

**Proof:** Obvious, if we apply theorem 1 with  $\lambda=1>0$ . ■

**Theorem 3:** The sequence of real numbers  $(A_n)_{n \in \mathbb{N}}$ ,  $A_n = \sqrt[n]{n + \lambda^n}$ ,  $\lambda \in [0, 1]$  is given. Prove that this sequence tends to 1.

**Proof:** (a) See the set of the non-zero natural numbers  $\mathbb{N}^* = \{1, 2, 3, \dots, n, \dots\}$  and the obvious inequality:

$$n + \lambda^n \geq 1, \quad n \in \mathbb{N}^*$$

This leads to the next two equivalent inequalities:

$$\sqrt[n]{n + \lambda^n} \geq 1 \quad \text{and} \quad \sqrt[n]{n + \lambda^n} - 1 \geq 0 \quad \text{or} \quad \theta_n = A_n - 1 \geq 0, \quad A_n = \sqrt[n]{n + \lambda^n} \quad (4.4)$$

(b) We adopt the symbols of the two zero sequences as:

$$(\gamma_n = 0)_{n \in \mathbb{N}} \quad \text{and} \quad \left( \beta_n = \sqrt[n]{n + 1} - 1 \right)_{n \in \mathbb{N}}$$

From  $\lambda \in [0, 1]$  and theorem 2, it is valid that  $0 = \gamma_n \leq \theta_n < \beta_n = \sqrt[n]{n + 1} - 1 \rightarrow 0$ . This leads

to the conclusion that  $\theta_n \rightarrow 0$  and therefore  $A_n = \sqrt[n]{n + \lambda^n} \rightarrow 1$ . ■

#### 4. Conclusions

In this paper, we have examined the pdf, of a rv  $X$  taking values between  $\varepsilon$  and  $\beta$ , having a form of a mononym with negative exponent and its parameters. Sampling is the key that gives us enough initial data useful to exploit the rest of the information in the data. The parameter  $\beta$  is suitably determined by sample  $\delta$  and is always  $\beta \geq X_{\max} \in \delta$ . The limit  $\varepsilon$  is suitably defined as a function of  $\beta$  and the exponent  $\nu$ . It is found that for value of the exponent more 3 it is possible to expect a value of  $\varepsilon$  tending to 1 from the left, i.e.  $\varepsilon_n \rightarrow 1^-$ , e.g. for a range  $\beta=10$  and for exponent  $\nu=3$  it is  $\varepsilon_3 = 0.7053$  and for  $\nu=5$   $\varepsilon_5 = 0.7071$  and so on. We proposed a simple and easy-to-remember method to examine whether sample data can be described by the pdf given in equation (3) and we concluded, through goodness-of-fit tests, that there is a good fitting between theoretic and sample values. The proposed method can be characterised as a high-budget sampling, because of the large sample size.

#### REFERENCES

- Farmakis N. (2001).** *Statistics, Theory in brief, Exercise.* A & P Christodoulidi, Thessaloniki (In Greek).
- Farmakis N. (2015).** *Sampling and Applications.* e-Book, Repository of Greek Academic Libraries, Athens, ISBN: 978-960-603-093-2 (in Greek) .
- Farmakis N. (2016).** *Introduction to Sampling.* Kyriakidis Bros Editing S.A., Thessaloniki (In Greek).
- Moysiadis P. (2000).** *Advanced Mathematics.* A & P Christodoulidi, Thessaloniki (In Greek).

# Modeling the Reliability and Performance of a Wind Farm Using the Universal Generating Function Technique

Panagiotis M. Psomas, Agapios N. Platis, Vasilis P. Koutras  
Department of Financial and Management Engineering, School of Engineering, University of the Aegean, Chios, 82100, Greece,  
[fme10117@fme.aegean.gr](mailto:fme10117@fme.aegean.gr); [platis@aegean.gr](mailto:platis@aegean.gr); [v.koutras@fme.aegean.gr](mailto:v.koutras@fme.aegean.gr)

## SPECIAL INVITED SESSION: Statistical, Stochastic and Data Analysis Methods and Applications, Part I & II (SSDAMA)

**Abstract.** The objective of this paper is to assess the dependability of a wind farm power system and particularly the overall ability of the system to generate and supply electrical energy by means of the Universal Generating Function Technique (UGF). There are two major factors affecting the general performance and thus the wind farm output: the wind intensity and the wind turbine failures. For the wind intensity, a power curve is used to determine the monthly energy output for a given wind turbine in a given location. However, the energy output depends also on the different wind turbine degraded states due to a variety of failures. Combining the wind intensity categories with the power output of a wind farm consisting of 20 wind turbines, we have developed a multi-state system model, characterizing all the different levels of energy output through a formally composition operator, to obtain the final system dependability measures, such as availability and output performance. The data were provided by the Hellenic National Meteorological Service (HNMS). The availability as well as the output performance of a wind farm are calculated using different types of repair and failure rates. The main aim of this work is to compare these approaches and find out how they affect the availability and the performance of our system.

**Keywords:** Wind Energy, Reliability, Weibull Distribution, Homogeneous Markov Chains, Universal Generating Function(UGF).

## 1 Introduction

Renewable energy sources currently supply approximately 15% - 20% of world's total energy demand. Several studies investigate the potential contribution of renewables to global energy supplies indicating that in the second half of the 21<sup>st</sup> century their contribution might range from 20% to more than 50% with the appropriate policies in place.

---

*5<sup>th</sup> SMTDA Conference Proceedings, 12-15 June 2018, Chania, Crete, Greece*

© 2018 ISAST



Wind energy has been the fastest growing renewable energy resource over the last decade mainly due to very significant improvements in wind energy technology and is one of the most efficient and affordable energy technologies. A benefit which makes wind energy to become fully competitive with conventional fossil-fuel electricity generation is that the wind industry continuously improves the cost and performance of wind turbines. A wind turbine consists of several critical components such as gearbox, generator and electrical system, each of them characterized by different failure frequencies and effects. These components seem to require important maintenance and repair attempts. On the other hand, weather conditions can affect the reliability of wind turbines substantially. At very low temperature sites, wind turbines suffer from icing problems, which manage to reduce power generation. Lightning strikes can also cause serious damage to blades. Additionally, the performance of a wind farm depends on the intensity of the wind blowing in the area where the wind farm is intended to be, or it is actually installed and the failure and repair rate of wind turbines.

In this paper we evaluate the reliability of a wind farm considering the weather data provided by the Hellenic National Meteorological Service (HNMS) for Stephani Korinthias. The data refer to March 2012. For this time period, wind speed data, measured daily every 3 hours, was available. In order to have an overall view of the wind speed during a day, it would be better to use the sum of the wind speed for every day individually. Due to the nature of wind and the different intensities over time, the model is based on the categorization of wind intensity in 4 categories (Gouveia and Matos [1]). Combining wind intensity categories with the power output of 20 wind turbines, we develop two models. The first model consists of four states of wind speed, where every state represents the power output of the 20 wind turbines based on the percentage of energy production for the corresponding wind speed. The categorization of wind intensity is the following: state A is the case where there is no wind (0%), states B and C are intermediate states, in which there is partial wind production (30%) and strong wind production (70%) respectively and finally, state D is the case where wind can provide maximum electricity generation with rated wind production of 100%. The above-mentioned percentage values in every state express the electricity production of the wind turbines for the corresponding wind speed. The wind turbine generators model consists of the 20 wind turbines with 21 states in total. Every state expresses the power output of the operational wind turbines.

The remainder of this paper is organized as follows: In section 2 the wind turbines generation model is described as well as the Maximum Likelihood Method which is applied for the estimation of the Weibull parameters and according to bibliography Maximum likelihood method is a more accurate and robust approach and is a more suitable computer-based method for estimating the Weibull parameters. The Universal Generating Function Technique which is known to be a very efficient way of evaluating the availability of different types of MSSs as it reduces the computational complexity of MSS reliability assessment and is briefly summarized in section 3. In section 4 we present an example followed by the conclusions.

## 2 Model descriptions

The proposed wind turbine generation model consists of two concepts: wind speed modeling and wind turbine generation operation. The wind turbines contain two different sources that can affect their overall performances, an external and an internal. The external is the wind speed and the internal is the failure and repair behavior. The generalized model proposed in this paper is a system consisting of 20 wind turbines that are able to operate under different wind intensities. Due to the nature of wind, its intensity ranges between 4 different categories (Gouveia and Matos): no-wind state, partial-wind production state, strong-wind production state and the last one describes a state in which there is a rated-wind production.

In our approach we will consider wind variation through a month. We observed the fluctuations of the wind for an ordinary month of spring and in particular of March. The entire work is based on meteorological data provided by the National Meteorological Service. The state space of the wind speed model is  $E_2=\{1,2,3,4\}$ . Fig. 1 shows the Markov model for all the possible transitions between the four states of wind.

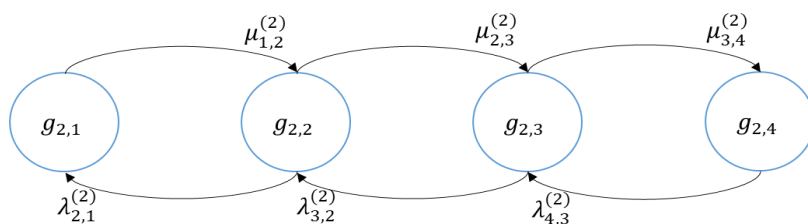


Fig.1 Markov chain model for the 4 states of the wind

The state transition diagram of Fig.1 consists of four states. Each state consists of a different performance. Each performance can be expressed as  $g_{i,j}$ ,  $i=2$ ,  $j=1,2,3,4$ , where  $i$  is the second element and  $j$  expresses the states of the model and shows the power output for each state of the 20 wind turbines based on the percentage of electricity production that the wind is able to provide. We assume that in every state, all of the 20 wind turbines are operational. Every transition rate shows how often the wind speed changes in a month. Transition rate  $\mu_{ij}$  shows how wind increases, whereas  $\lambda_{ij}$  shows how wind decreases. A transition from one state to another takes place when a change of wind intensity occurs.

For an operational wind farm, we consider the number of wind turbines in operation as well as the failure rates  $\lambda$  and repair rates  $\mu$  of wind turbines. In this work the wind farm is a group of wind turbines in the same location which consist of 20 individual wind turbines. Any future state of the system depends only on the current state and not the previous ones. In every state, the overall output of the operational wind turbines, is of interest. The state space of the wind turbine generators model is  $E_1=\{0,1,2,3,\dots,20\}$ . In Fig.2, the state transition diagram of a Markov model used to describe the evolution of a wind farm consisting of 20 wind turbines is presented. The state transition diagram consists

of 21 different states, where every state represents the power output for the corresponding operational wind turbines with different performance rate. A transition occurs in two possible ways. Either when a mechanical failure of a wind turbine occurs or when a repair of a wind turbine is performed.

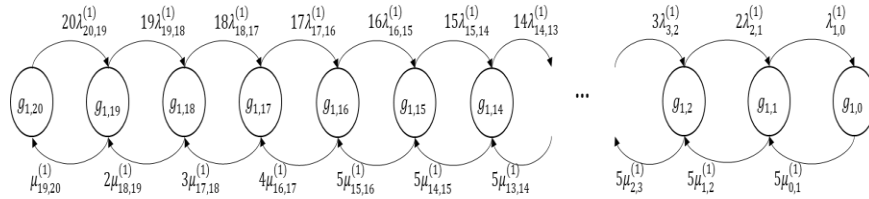


Fig.2 Markov model of a wind farm consisting of 20 wind turbines

For the generation system we set  $k_1=21$  (1: generation system) states, where every state expresses the performance of the operational wind turbines and  $k_2=4$  (2: generation source) states for the generation source, where every state represents the performance of the 20 wind turbines for the corresponding percentage of energy production.  $g_{ij}$  and  $p_{ij}$  express the performance output and the state probabilities for the two models, where  $i=1$  expresses the first element which is the wind turbines and  $j=0,1,2,\dots,20$  represents the states of this element and for the wind speed  $i=2$  represents the second element with  $j=1,2,3,4$  showing the states of this element. The performance  $g$  in every state of the wind turbine generators diagram in Fig.2 is measured by the output of the turbines that are functioning. A state where the turbine generators are not functioning, and the wind speed is equal to zero corresponds to a total failure and an output performance of 0 in our system.

The main aim of our work is to evaluate the dependability measures of the wind farm such as the availability and the output performance, using the Universal Generating Function Technique (UGF) which reduces the computational complexity of Multi-State System (MSS) reliability assessment and through the UGF technique we can find the entire MSS performance distribution based on the performance distribution of its elements using algebraic procedures (Lisnianski et al. [7]). The UGF technique is used for the individual element multi-state modeling and through the multiplication composition operator we combine the individual UGFs into the UGF renewable generator power output. The overall system UGF is then created and dependability measures are computed from the UGFs. Initially the wind turbines start at an operational state, and therefore they can convert all the wind power to electricity.

The Weibull distribution has been used to model the wind speed randomness. In recent years the Weibull distribution has successfully been applied to the wind speed distribution. Weibull distribution fits well to the observed long-term distribution of mean wind speeds for a range of sites, is very flexible and fortunately the wind data behaves almost in similar fashion as Weibull does (Seguro and Lambert [2]): In equation (1) the pdf of Weibull distribution with respect to wind speed  $v$  is given:

$$f(v) = \frac{k}{c} \left(\frac{v}{c}\right)^{k-1} \exp\left[-\left(\frac{v}{c}\right)^k\right], (k > 0, v > 0, c > 1) \quad (1)$$

where  $k$  is the shape parameter and  $c$  the scale parameter.

There are several ways to estimate a Weibull pdf to fit a wind speed distribution. The common method to calculate the Weibull parameters is the Maximum Likelihood Method (MLM) (Seguro and Lambert [2]) which is widely used. Weibull parameters  $k$  and  $c$  are used for the estimation of the power output formula (4) of the wind turbine generator. According to (Dokur and Kurban [3]) the shape parameter  $k$  and the scale parameter  $c$  can be found by the following equations:

$$k^{-1} = \frac{\sum_{i=1}^n v_i^k \ln(v_i)}{\sum_{i=1}^n v_i^k} - \frac{\sum_{i=1}^n \ln(v_i)}{n} \quad (2)$$

$$c = \left(\frac{\sum_{i=1}^n v_i^k}{n}\right)^{1/k} \quad (3)$$

where  $v_i$  is the wind speed in time step  $i$  and  $n$  is the number of nonzero wind speed data points.

In order to estimate the power output of the wind turbine generator alongside the wind speed which is discretized into multiple states, the output of the one wind turbine can be modeled by the following function (Hetzer et al. [4], Ghali et al. [5], Gavanidou [6])

$$P_w(v) = \begin{cases} P_R [(v^k - v_c^k)/v_R^k - v_c^k], & (v_c \leq v \leq v_R) \\ P_R, & (v_R \leq v \leq v_F) \\ 0, & (v \leq v_c \text{ and } v \geq v_F) \end{cases} \quad (4)$$

where  $P_R$  is the rated electrical power,  $v_c$  is the cut-in wind speed,  $v_R$  is the rated wind speed,  $v_F$  is the cut-off wind speed,  $k$  is the Weibull shape parameter. At the cut-in wind speed, the blades start to turn, and the wind turbine starts generating electricity. At the rated wind speed, the turbine can generate electricity at its maximum, or rated capacity. The cut-off wind speed denotes how fast the turbine can go before wind speeds get so fast that it risks damage from further operation (Hetzer et al. [4], Ghali et al. [5]).

### 3 Universal Generating Function Method

A specific approach called the Universal Generating Function (UGF) method has been widely applied to Multi-State System (MSS) reliability analysis. In our work, the UGF technique is used to model the power output of a generation source and a generation system. The universal generating function modeling the generation source and the generation system are combined by a multiplication operator to obtain the final u-function of the generator power output.

The UGF of a discrete random variable  $x$  is defined as a polynomial:

$$z\{x\} = u_x(z) = \sum_{i=1}^k p_i z^{x_i} \quad (5)$$

In order to obtain the u-function of a system containing a number of elements, composition operators are introduced. These operators determine the system u-function expressed as a polynomial  $U(z)$  for a group of elements using simple algebraic operators over individual u-functions of elements (Lisnianski et al. [7]). For a system with  $n$  elements, the resulting UGF of the whole system with the arbitrary structure function can be obtained based on the individual u-functions of the elements.

The Universal Generating Operator, for a random variable  $Y = f(X_1, X_2)$  is defined by:

$$u_Y(z) = \Omega_f\{u_{X_1}(z), u_{X_2}(z)\} = \sum_{j_1=1}^{k_1} \sum_{j_2=1}^{k_2} p_{1j_1} p_{2j_2} z^{f(x_{1j_1}, x_{2j_2})} \quad (6)$$

where  $j_1$  and  $j_2$  determine the corresponding value of the random variable  $Y$ . The function  $\Omega_f$  in composition operators expresses the entire performance of a subsystem consisting of different elements in terms of the individual performance of the elements.

In our approach, the connection of the  $n$  generating elements can be represented as the series structure. The wind speed affects directly the power output of the wind turbines so, with lower wind speed the production from the wind turbines will be lower too. The power output depends on the wind speed and therefore these two elements are connected in series. When the elements are connected in series, the element with the lower performance becomes the bottleneck of the system. This unit therefore defines the total system productivity. To calculate the UGF for the whole system the series composition operator  $\Omega_{f_{ser}}$  is applied. The structure function for such a system takes the form:

$$\Omega_{f_{ser}}(u_1(z), u_2(z)) = \Omega_{f_{ser}}\left(\sum_{j_1=1}^{k_1} p_{1j_1} z^{x_{1j_1}}, \sum_{j_2=1}^{k_2} p_{2j_2} z^{x_{2j_2}}\right) = \sum_{j_1=1}^{k_1} \sum_{j_2=1}^{k_2} p_{1j_1} p_{2j_2} z^{\min(x_{1j_1}, x_{2j_2})} \quad (7)$$

where parameters  $k_1$  and  $k_2$  are the performance levels for the elements,  $x_{1j_1}$  and  $x_{2j_2}$  denote the performance of the two elements,  $p_{1j_1}$  and  $p_{2j_2}$  are the steady-state probabilities of the above mentioned two elements respectively.

In our approach, we express the u-function of the wind turbines and the u-function of the wind speed and then through the operator we obtain the u-function of the system. Let  $p_1 = \{p_{1,0}, p_{1,1}, \dots, p_{1,20}\}$  and  $p_2 = \{p_{2,0}, p_{2,1}, p_{2,2}, p_{2,3}\}$  denote the state probability distribution of wind turbines and wind speed respectively. Let  $g_1 = \{g_{1,0}, g_{1,1}, \dots, g_{1,20}\}$  and  $g_2 = \{g_{2,0}, g_{2,1}, g_{2,2}, g_{2,3}\}$  denote the state values of the wind turbines and wind speed respectively. The u-function of the wind turbine state is:

$$\begin{aligned}
u_1(z) = & p_{1,0}z^{g_{1,0}} + p_{1,1}z^{g_{1,1}} + p_{1,2}z^{g_{1,2}} + p_{1,3}z^{g_{1,3}} + p_{1,4}z^{g_{1,4}} + p_{1,5}z^{g_{1,5}} \\
& + p_{1,6}z^{g_{1,6}} + p_{1,7}z^{g_{1,7}} + p_{1,8}z^{g_{1,8}} + p_{1,9}z^{g_{1,9}} + p_{1,10}z^{g_{1,10}} + p_{1,11}z^{g_{1,11}} \\
& + p_{1,12}z^{g_{1,12}} + p_{1,13}z^{g_{1,13}} + p_{1,14}z^{g_{1,14}} + p_{1,15}z^{g_{1,15}} + p_{1,16}z^{g_{1,16}} \\
& + p_{1,17}z^{g_{1,17}} + p_{1,18}z^{g_{1,18}} + p_{1,19}z^{g_{1,19}} + p_{1,20}z^{g_{1,20}} \quad (8)
\end{aligned}$$

The u-function of the wind speed is:

$$u_2(z) = p_{2,1}z^{g_{2,1}} + p_{2,2}z^{g_{2,2}} + p_{2,3}z^{g_{2,3}} + p_{2,4}z^{g_{2,4}} \quad (9)$$

The overall u-function of the system is:

$$\begin{aligned}
U(z) = & \Omega_{f_{ser}}(u_1(z), u_2(z)) \\
= & \Omega_{f_{ser}}(p_{1,0}z^{g_{1,0}} + p_{1,1}z^{g_{1,1}} + p_{1,2}z^{g_{1,2}} + p_{1,3}z^{g_{1,3}} + p_{1,4}z^{g_{1,4}} \\
& + p_{1,5}z^{g_{1,5}} + p_{1,6}z^{g_{1,6}} + p_{1,7}z^{g_{1,7}} + p_{1,8}z^{g_{1,8}} + p_{1,9}z^{g_{1,9}} \\
& + p_{1,10}z^{g_{1,10}} + p_{1,11}z^{g_{1,11}}p_{1,12}z^{g_{1,12}} + p_{1,13}z^{g_{1,13}} + p_{1,14}z^{g_{1,14}} \\
& + p_{1,15}z^{g_{1,15}} + p_{1,16}z^{g_{1,16}} + p_{1,17}z^{g_{1,17}} + p_{1,18}z^{g_{1,18}} + p_{1,19}z^{g_{1,19}} \\
& + p_{1,20}z^{g_{1,20}}, p_{2,1}z^{g_{2,1}} + p_{2,2}z^{g_{2,2}} + p_{2,3}z^{g_{2,3}} + p_{2,4}z^{g_{2,4}}
\end{aligned}$$

Taking also into account that  $\sum_{j=0}^{20} p_{i,j} = 1, i = 1$  for the wind turbines model and  $\sum_{j=1}^4 p_{i,j} = 1, i = 2$  for the wind speed model we can simplify the last expression for  $U(z)$  and obtain the resulting UGF associated with the output performance and the state probabilities  $g, p$  of the entire system in the following form:

$$U(z) = \sum_{i=1}^{21} p_i z^{g_i} \quad (10)$$

### 3.1 Reliability Assessment Indices Using UGF

In MSS modeling, reliability is in general defined as the probability that the MSS lies in the states with capacity levels greater than or equal to the demand  $w$  (Lisnianski et al. [7]). Since the UGF represents the performance distribution of the MSS, it can be used for evaluating the MSS reliability measures which are MSS availability, MSS expected output performance and unsupplied energy

We define the MSS availability  $A(t)$  as the probability that the system is in states with performance level greater than or equal to demand  $w$ . We can obtain the system availability for a constant demand  $w$  using the following operator  $\delta_A$ :

$$A(t) = \delta_A(U(z), w) = \delta_A(\sum_{i=1}^K p_i z^{g_i}, w) = \sum_{i=1}^K p_i 1(F(g_i, w) \geq 0) \quad (11)$$

where  $k$  is the number of states of the MSS, and  $g_i$  is the output of the MSS at state  $i$  and  $F(g_i, w)$  is an acceptability function where

$$1_{(F(g_i, w) \geq 0)} = \begin{cases} 1, & \text{if } F(g_i, w) \geq 0 \\ 0, & \text{if } F(g_i, w) < 0 \end{cases}$$

This means that operator  $\delta_A$  summarizes all the probabilities of acceptable states.

The MSS expected output performance can be defined as:

$$E = \delta_E(U(z)) = \delta_E(\sum_{i=1}^K p_i z^{g_i}) = \sum_{i=1}^K p_i g_i, \quad (12)$$

In (12) we can obtain that the expected output performance does not depend on demand  $w$ . Therefore,  $E$  defines the mean output performance of the power system.

We obtain the unsupplied performance for the given  $U(z)$  and constant demand  $w$  using the following equation:

$$D(w) = \delta_D(U(z), w) = \delta_D(\sum_{i=1}^K p_i z^{g_i}, w) = \sum_{i=1}^K p_i \cdot \max(w - g_i, 0) \quad (13)$$

The UGF approach is used to evaluate the different dependability measures of the power system. In this section the UGF technique is used to model the output performance of the generation system which consists of the wind turbines and the wind speed. Through their connection in series and the composition operator we obtain the final UGF of the system, which is then solved to calculate the dependability measures.

## 4 Numerical Application

Considering the area Stephani as an example, the average monthly wind speed is 6,5m/s at 37m above the ground level as obtained from the weather data recorded by the Peloponnese observatory.

Table 1 provides the daily averages over a 31 days' period. Each entry represents an average wind speed. The Maximum Likelihood Method is applied to the sample data set that is shown in Table I. From the recorded wind data, using  $n = 31$  with successive applications of Eq (4) to the data in Table 1 the shape parameter  $k$  is estimated to be 1.61 and the scale  $c$  estimation is 5.26.

**Table 1: Wind speeds for a typical spring month**

Day	Wind speed(m/s)	Day	Wind speed(m/s)
1	7	17	1
2	4	18	2
3	3	19	2
4	4	20	2
5	2	21	4
6	2	22	4
7	1	23	5
8	2	24	2
9	3	25	1
10	7	26	1
11	5	27	5
12	4	28	2
13	9	29	2
14	5	30	2
15	1	31	2
16	5		

The output of a wind turbine depends on what kind of wind speed is rated for. This is the most important parameter concerning how well a wind turbine performs. To analyze the wind turbine’s power output, a wind turbine of 900kW is selected. All 20 wind turbines are identical as each one generates rated electrical power  $P_R = 900kW$  at rated wind speed 8m/s and hub height 55m. The cut-in speed is 2m/s and the cut-off is 12m/s. According to the above-mentioned data and by Eq (4) we calculate  $P_w(v) = 612kW$  for  $(2m/s \leq v \leq 8m/s)$  at hub height 55m.

In order to find the state probabilities of the wind speed Markov model we calculated its transition rates. Table 2 represents how often the wind speed changes in a month.

**Table 2: Transition rates for the wind speed Markov model**

$\mu_{1,2}^{(2)} = 17month^{-1}$	$\mu_{2,3}^{(2)} = 11month^{-1}$	$\mu_{3,4}^{(2)} = 2month^{-1}$
$\lambda_{2,1}^{(2)} = 19month^{-1}$	$\lambda_{3,2}^{(2)} = 12month^{-1}$	$\lambda_{4,3}^{(2)} = 2month^{-1}$

The distribution of wind speed has been divided into 4 states, with the associated state probabilities and power outputs (Table 3). We were able to find the state probabilities from the balance equations from Fig.1. According to the percentage of production for the corresponding wind speed and the power output of the wind turbine we were able to find the overall power output of the 20 wind turbines for the 4 categories of the wind intensity.

**Table 3: Four-state wind model**

State No	Wind speed(m/s)	Probability	Power output(kW)
1	0-3	0.29	0
2	3-6	0.26	3672
3	6-9	0.23	8568
4	9-12	0.22	12240

The wind farm will supply energy to a residential area for a constant demand level  $w = 720\text{kW}$ . By obtaining wind speed data and the power output of the wind turbine we can calculate the mean production of the examined system. The individual wind turbine is modeled with two states: failure and functioning. In order for the system to achieve the best performance and to analyze how the reliability measures change according to the failure and repair rates we were able to estimate the dependability measures through a range of different experimental values of failure and repair rates (Table 4) for the wind turbines Markov model.

**Table 4:** The experimental values of failure and repair rates

$\lambda$ (in $\text{h}^{-1}$ )	$\mu$ (in $\text{h}^{-1}$ )
0,00005	0,001
0,0001	0,002
0,00015	0,003
0,0002	0,004
0,00025	0,005
0,0003	0,006
0,00035	0,007
0,0004	0,008
0,00045	0,009
0,0005	0,01
0,00055	0,011
0,0006	0,012
0,00065	0,013
0,0007	0,014
0,00075	0,015
0,0008	0,016
0,00085	0,017
0,0009	0,018
0,00095	0,019
0,001	0,02
0,00105	
0,0011	
0,00115	
0,0012	
0,00125	

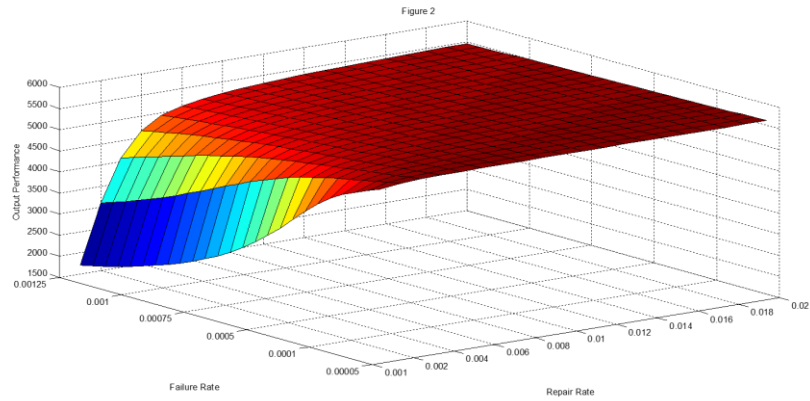


Fig.3 Comparison of the Output Performance for different values of the failure and repair rates

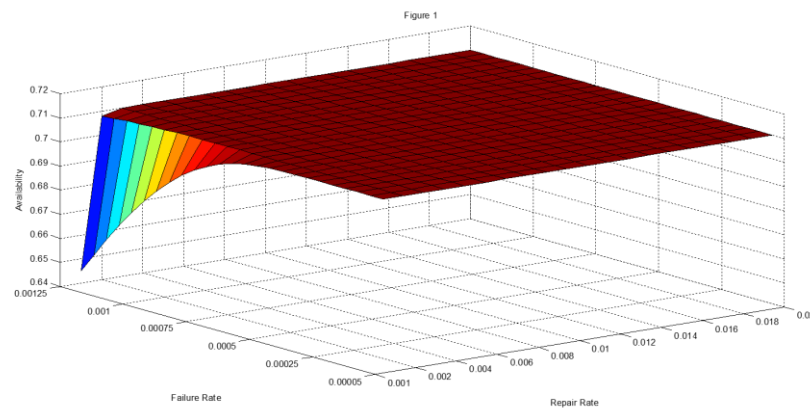


Fig.4 Comparison of the Availability for different values of the failure and repair rates

As we can observe from the Fig.3 for the output performance, as expected, when the failure rate increases the output performance of the system decreases resulting in a decrease of power production. This occurs because any damage or failure to the components of wind turbines may slow down the operation of the system or even to shut down the whole system. The output performance of the system increases with the increase of the repair rate. Maintenance keeps the system to a sustained state of operation and so it performs better and for a longer period of time. Reliable components and effective preventive maintenance procedure can reduce failures and as a result the power production will be higher.

Similarly, in Fig.4, as expected, an increased repair rate results in an improved availability for lower repair rates. However, this effect becomes extinct very fast. Due to the repair, it is possible to increase the availability by reducing

technical failures of the wind turbines. By reducing the failures due to the components, the availability can be increased. On the other hand, by increasing the failure rate, the availability of the system decreases due to the mechanical failure of the wind turbines.

## Conclusions

In this paper, we have calculated the dependability measures of a wind park using the wind intensity and wind turbine generators Markov models and the Universal Generating Function. The UGF is utilized to mathematically represent the wind speed model and the wind turbines model and combine their states through a composition operator, to obtain the final system model which allows computing the dependability measures. Our main purpose was to calculate the reliability measures Availability and Output Performance of the wind farm using different experimental values of failure and repair rates for the wind turbine generators model and compare the results through the Fig. 3 and Fig. 4 in order to determine how the failure and repair rates affect the reliability of the system.

According to the results, as the failure rate decreases the output performance of the system increases resulting in an increase of power production. On the contrary by reducing the repair rate the output performance of the system decreases. Additionally, an increased repair rate results in an improved availability. However, the system cannot perform at its maximum performance with an increased failure rate and as a result the availability decreases.

In the future we could obtain more wind categories, we could also study how by optimizing the MSS maintenance policy we can achieve the desired level of system reliability requiring minimal cost. The major costs for this kind of systems are operational and maintenance costs. Financial losses could also be evaluated for different operational, maintenance and failure conditions.

## References

1. E. M. Gouveia, M. A. Matos. Evaluating operational risk in a power system with a large amount of wind power, *Electric Power Systems Research*, 79, pp. 734-739, (2009)
2. J.V. Seguro, T.W. Lambert. Modern estimation of the parameters of the Weibull wind speed distribution for wind energy analysis. *Journal of Wind Engineering and Industrial Aerodynamics* 85, 74-84, (2000)
3. Dokur E. and Kurban M. Wind Speed Potential Analysis Based on Weibull Distribution, *JOURNAL OF ELECTRICAL AND COMPUTER ENGINEERING*, Vol. 3. No. 4, pp. 231-235, (2015).
4. Hetzer J., Yu D. C., Bhattarai K. *IEEE Transactions on Energy Conversion*, 23(2), 603-611, (2008)
5. Ghali FMA, Abd el Aziz MM, Syam FA. Simulation and analysis of hybrid systems using probabilistic techniques. In: *Power Conversion Conference*, Nagaoka, 2:831-5, (1997).
6. Gavanidou ES, Bakirtzis AG. Design of a standalone system with renewable energy sources using trade off methods. *IEEE Trans. Energy Conversion* 7(1):42-8, (1992).
7. Lisnianski A., Frenkel I., and Ding Y. *Multi-state System Reliability Analysis and Optimization for Engineers and Industrial Managers*, Springer, London (2010).

# EM Algorithm for Estimating the Parameters of the Multivariate Stable Distribution

Leonidas Sakalauskas<sup>1</sup>, Ingrida Vaiciulyte<sup>2</sup>

<sup>1</sup> Siauliai University, P. Visinskio st. 38, LT-76352 Siauliai, Lithuania  
(leonidas.sakalauskas@mii.vu.lt)

<sup>2</sup> Faculty of Business and Technologies, Siauliai State College, Ausros av. 40, LT-76241  
Siauliai, Lithuania  
(i.vaiciulyte@svako.lt)

**Abstract.** Research of  $\alpha$ -stable distributions is especially important nowadays, because they often occur in the analysis of financial data and information flows along computer networks. It has been found that financial data are often leptokurtic with a heavy-tailed distributions; many authors, e.g., Rachev, Mittnik (2000), Kabasinskas *et al.* (2012), Sakalauskas *et al.* (2013) have proved that the most often used normal distribution is not the most suitable way to analysis economic indicators and suggested to replace it with more general, for example, stable distributions. Since Rachev, Mittnik (2000), Kabasinskas *et al.* (2012), Sakalauskas *et al.* (2013) have estimated one-dimensional  $\alpha$ -stable distributions a problem arises how to estimate multidimensional data. Maximum likelihood method for the estimation of multivariate  $\alpha$ -stable distributions by using EM algorithm is presented in this work. Integrals included in the expressions of the estimates have been calculated using the Gaussian and Gauss-Laguerre quadrature formulas. The constructed model can be used in stock market data analysis.

**Keywords:** Gaussian and  $\alpha$ -stable model, EM algorithm, Likelihood ratio test, Quadrature formulas.

## 1 Introduction

Stochastic processes can be modeled, estimated and predicted by probabilistic statistical methods, using the data that describes the course of the process. A number of empirical studies confirm that real commercial data are often characterized by skewness, kurtosis and heavy-tail (Janicki, Weron, 1993; Rachev, Mittnik, 2000; Samorodnitsky, Taqqu, 1994; etc.). Therefore, a well-known normal distribution does not always fit – for example, returns of stocks or risk factors are badly fitted by the normal distribution (Kabasinskas *et al.*, 2009; Belovas *et al.*, 2006). In this case, normal distributions are replaced with more general, for example, stable distributions, which allow to model both leptokurtic and asymmetric (Fielitz, Smith, 1972; Rachev, Mittnik, 2000; Kabasinskas *et al.*, 2012; Sakalauskas *et al.*, 2013). So stable distributions are the most often used in business and economics data analysis. Following to some experts, the  $\alpha$ -stable distribution offers a reasonable improvement if not

---

5<sup>th</sup> SMTDA Conference Proceedings, 12-15 June 2018, Chania, Crete, Greece

© 2018 ISAST



the best choice among the alternative distributions that have been proposed in the literature over the past four decades (e.g., Bertocchi *et al.*, 2005; Hoehstoetter *et al.*, 2005). However, a practical application of stable distributions is limited by the fact that their distribution and density functions are not expressed through elementary functions, except for a few special cases (Janicki, Weron, 1993; Rachev, Mittnik, 2000; Belovas *et al.*, 2006). By the way, stable distributions have infinite variance (except for the normal case, when parameter of stability  $\alpha = 2$ ). In this work the stable multivariate variables expression through normal multivariate vector with random variance, changing by a particular stable law, are used for the simulation.

Although the estimation of parameters of multivariate stable distributions has been discussed long time ago, the problem is not solved to the end yet (Press, 1972; Rachev, Xin, 1993; Nolan, 1998; Davydov, Paulauskas, 1999; Kring *et al.*, 2009; Ogata, 2013). Maximum likelihood approach for the estimation of multivariate  $\alpha$ -stable distribution by using EM algorithm is presented in this work.

In one-dimension case, random stable value is described by four parameters: stability  $\alpha \in (0; 2]$ , skewness  $\beta \in [-1; 1]$ , scale  $\sigma > 0$  and position  $\mu \in \mathfrak{R}^1$ . Stable parameter  $\alpha$  is the most important, which is essential for characterizing financial data, and parameter of scale  $\sigma$  can be also used to measure risk. Random variables, that are stable for a fixed number of random elements with respect to the composition, are called  $\alpha$ -stable.

In one-dimension case, it is known that  $s = \sqrt{s_1 \cdot s_2}$ , where:

$s_1$  – random stable variable with skewness parameter  $\beta = 1$  and shape parameter  $\alpha_1 < 1$ ;

$s_2$  – another random stable variable, independent of  $s_1$ , with skewness parameter  $\beta = 0$  and shape parameter  $\alpha_2$ ;

$s$  – random stable variable with skewness parameter  $\beta = 0$  and shape parameter  $\alpha = \alpha_1 \cdot \alpha_2$  (Rachev, Mittnik, 1993; Samorodnitsky, Taqqu, 1994; Ravishanker, Qiou, 1999).

While applying this method, it is usually chosen that  $s_2$  be a random variable,

which is normally distributed, i.e.,  $\alpha_1 = \frac{\alpha}{2}$  and  $\alpha_2 = 2$ . Random stable variable

when  $\alpha_1 < 1$  and  $\beta = 1$  is called stable subordinator, and always obtains only positive values (Rachev, Mittnik, 1993; Ravishanker, Qiou, 1999).

This approach produces multidimensional random vector with dependent components, in which the heavy tailed data can be modeled (Nolan, 2007; Sakalauskas, Vaičiulytė, 2014). In this way, the multivariate stable symmetric vector can be expressed through normally distributed random vector, and  $\alpha$ -stable variables (Ravishanker, Qiou, 1999; Rachev, Mittnik, 1993):

$$X = \mu + \sqrt{s_1} \cdot s_2, \quad (1)$$

where

$s_1$  – subordinator with parameter  $\alpha$ ,

$s_2$  – random vector, distributed by  $d$ -variate normal law  $N(0, \Omega)$ ,

$\mu$  – random vector of mean.

## 2 Estimators of maximum likelihood approach

Maximum likelihood (ML) approach allows us to obtain the values of parameter sets of model, which maximize the likelihood function for fixed independent uniformly distributed model data sample (Sakalauskas, 2010; Kabasinskas *et al.*, 2009; Ravishanker, Qiou, 1999). The higher the size is the higher is probability to obtain estimators, which will almost not differ from the actual parameter values.

Let's consider probability density of random vector created according to (1). Indeed, the density of the multivariate vector  $N(\mu, s \cdot \Omega)$  is as follows:

$$f(x|\mu, s, \Omega) = \frac{s^{-\frac{d}{2}}}{(2\pi)^{\frac{d}{2}} \cdot |\Omega|^{\frac{1}{2}}} \cdot \exp\left[-\frac{(x-\mu)^T \cdot \Omega^{-1} \cdot (x-\mu)}{2 \cdot s}\right]. \quad (2)$$

Let us write down the probability density of  $\alpha$ -stable subordinator (Rachev, Mittnik, 2000; Bogdan *et al.*, 2009):

$$f(s|\alpha) = \frac{\alpha \cdot s^{\frac{2}{\alpha}-2}}{2 \cdot |2-\alpha|} \int_{-1}^1 (U_\alpha(y))^{\frac{\alpha}{2-\alpha}} \cdot \exp\left[-\left(\frac{U_\alpha(y)}{s}\right)^{\frac{\alpha}{2-\alpha}}\right] dy, \quad (3)$$

where,  $s \geq 0$ , and

$$U_\alpha(y) = \frac{\sin\left(\frac{\pi}{4} \cdot \alpha \cdot (y+1)\right) \cdot \cos\left(\frac{\pi}{4} \cdot (\alpha - (2-\alpha) \cdot y)\right)^{\frac{2-\alpha}{\alpha}}}{\cos\left(\pi \cdot \frac{y}{2}\right)^{\frac{2}{\alpha}} \cdot \cos\left(\frac{\pi \cdot \alpha}{4}\right)^{\frac{2}{\alpha}}}. \quad (4)$$

Thus, probability density of random vector under given parameters  $\mu, \Omega, \alpha$  is expressed as bivariate integral

$$f(x|\mu, \Omega, \alpha) = \frac{\left(\frac{\alpha}{2-\alpha}\right)}{2 \cdot (2\pi)^{\frac{d}{2}} \cdot |\Omega|^{\frac{1}{2}}} \cdot \int_0^1 \int_{-1}^1 \exp\left[-\frac{1}{2}(x-\mu)^T \frac{\Omega^{-1}}{s}(x-\mu) - \frac{U_\alpha(y)}{s^{2-\alpha}}\right] \times \frac{U_\alpha(y)}{s^{\frac{\alpha}{2-\alpha} + \frac{d}{2}}} dy ds. \quad (5)$$

Let's consider the sample  $X = (X^1, X^2, \dots, X^K)$  consisting of independent  $d$ -variate stable vectors. The likelihood function by virtue of (5) is

$$\tilde{L}(X, \mu, \Omega, \alpha) = \prod_{i=1}^K f(X^i | \mu, \Omega, \alpha) = \frac{\left(\frac{\alpha}{2-\alpha}\right)^K}{2^K \cdot (2\pi)^{\frac{K \cdot d}{2}} \cdot |\Omega|^{\frac{K}{2}}} \times \prod_{i=1}^K \int_0^1 \int_{-1}^1 \exp\left[-\frac{1}{2}(X^i - \mu)^T \frac{\Omega^{-1}}{s_i}(X^i - \mu) - s_i^{\frac{\alpha}{2-\alpha}} \cdot U_\alpha(y_i)\right] \cdot \frac{U_\alpha(y_i)}{s_i^{\frac{d}{2} + \frac{2-\alpha}{2}}} dy_i ds_i. \quad (6)$$

Denote

$$z_i = s_i^{\frac{\alpha}{2-\alpha}} \cdot U_\alpha(y_i). \quad (7)$$

The log-likelihood function now is as follows

$$L(X, \mu, \Omega, \alpha) = -\sum_{i=1}^K \ln(f(X^i | \mu, \Omega, \alpha)) = -\sum_{i=1}^K \ln\left(\int_0^\infty \exp\{-z_i\} \int_{-1}^1 B(X^i, y_i, z_i, \mu, \Omega, \alpha) dy_i dz_i\right), \quad (8)$$

where

$$B(X^i, y_i, z_i, \mu, \Omega, \alpha) = \frac{1}{2 \cdot (2\pi)^{\frac{d}{2}} \cdot |\Omega|^{\frac{1}{2}} \cdot U_\alpha(y_i)} \cdot z_i^{\frac{d(2-\alpha)}{2\alpha}} \times \exp\left\{-\frac{(X^i - \mu)^T \Omega^{-1} (X^i - \mu)}{2 \cdot U_\alpha(y_i)} \cdot z_i^{\frac{2-\alpha}{\alpha}}\right\}. \quad (9)$$

Maximum likelihood estimators of multivariate  $\alpha$ -stable distribution parameters  $\mu, \Omega$  for a given and fixed  $\alpha$  are calculated by equating the likelihood function derivatives of optimized parameters to zero and solving the system of received equations:

$$\begin{cases} \frac{\partial L(X, \mu, \Omega, \alpha)}{\partial \mu} = -\sum_{i=1}^K \frac{\partial f(X^i | \mu, \Omega, \alpha)}{\partial \mu} \cdot \frac{1}{f(X^i | \mu, \Omega, \alpha)} = 0, \\ \frac{\partial L(X, \mu, \Omega, \alpha)}{\partial \Omega} = -\sum_{i=1}^K \frac{\partial f(X^i | \mu, \Omega, \alpha)}{\partial \Omega} \cdot \frac{1}{f(X^i | \mu, \Omega, \alpha)} = 0. \end{cases} \quad (10)$$

Let us denote the derivatives

$$\begin{aligned} \frac{\partial B(X^i, y_i, z_i, \mu, \Omega, \alpha)}{\partial \mu} &= -\frac{1}{2 \cdot (2\pi)^{\frac{d}{2}} \cdot |\Omega|^{\frac{1}{2}} \cdot U_\alpha(y_i)} \cdot z_i^{\frac{(d+2)(2-\alpha)}{2\alpha}} \times \\ &\times \Omega^{-1}(X^i - \mu) \cdot \exp\left\{-\frac{(X^i - \mu)^T \Omega^{-1}(X^i - \mu)}{2 \cdot U_\alpha(y_i)} \cdot z_i^{\frac{2-\alpha}{\alpha}}\right\} = \end{aligned} \quad (11)$$

$$\begin{aligned} &= \frac{\Omega^{-1}(X^i - \mu)}{U_\alpha(y_i)} \cdot z_i^{\frac{(2-\alpha)}{\alpha}} \cdot B(X^i, y_i, z_i, \mu, \Omega, \alpha), \\ \frac{\partial B(X^i, y_i, z_i, \mu, \Omega, \alpha)}{\partial \Omega} &= -\frac{1}{2 \cdot (2\pi)^{\frac{d}{2}} \cdot |\Omega|^{\frac{1}{2}} \cdot U_\alpha(y_i)} \cdot z_i^{\frac{(d+2)(2-\alpha)}{2\alpha}} \times \\ &\times \left(-\Omega^{-1} + \Omega^{-1} \cdot (x - \mu) \cdot (x - \mu)^T \cdot \Omega^{-1}\right) \cdot \exp\left\{-\frac{(X^i - \mu)^T \Omega^{-1}(X^i - \mu)}{2 \cdot U_\alpha(y_i)} \cdot z_i^{\frac{2-\alpha}{\alpha}}\right\} = \end{aligned} \quad (12)$$

$$= \left(-\Omega^{-1} + \frac{\Omega^{-1} \cdot (x - \mu) \cdot (x - \mu)^T \cdot \Omega^{-1}}{U_\alpha(y_i)} \cdot z_i^{\frac{(2-\alpha)}{\alpha}}\right) \cdot B(X^i, y_i, z_i, \mu, \Omega, \alpha)$$

Differentiating integrals by the parameters these derivatives are obtained:

$$h(X, \mu, \Omega, \alpha) = \frac{\sum_{i=1}^K \frac{X^i \cdot g_i}{f_i}}{\sum_{i=1}^K \frac{g_i}{f_i}}, \quad (13)$$

$$w(X, \mu, \Omega, \alpha) = \sum_{i=1}^K \frac{(X^i - \hat{\mu})(X^i - \hat{\mu})^T g_i}{f_i}. \quad (14)$$

The derivatives of log-likelihood function we can denote in this way:

$$\frac{\partial L}{\partial \mu} = (h(X, \mu, \Omega, \alpha) - \mu) \cdot \sum_{i=1}^K \frac{g_i}{f_i}, \quad (15)$$

$$\frac{\partial L}{\partial \Omega} = -K \cdot \Omega^{-1} + \Omega^{-1} \cdot w(X, \mu, \Omega, \alpha) \cdot \Omega^{-1}. \quad (16)$$

where

$$g(X, \mu, \Omega, \alpha) = \int_{0-1}^{\infty} \int_{-1}^1 \frac{z^{2-\alpha}}{U_{\alpha}(y)} \cdot B(X^i, y, z, \mu, \Omega, \alpha) \cdot \exp\{-z\} dy dz, \quad (17)$$

$$f(X, \mu, \Omega, \alpha) = \int_{0-1}^{\infty} \int_{-1}^1 B(X^i, y, z, \mu, \Omega, \alpha) \cdot \exp\{-z\} dy dz. \quad (18)$$

Estimators of parameters satisfy equations of the fixed-point method:

$$\hat{\mu} = \frac{\sum_{i=1}^K X^i \cdot g_i}{\sum_{i=1}^K \frac{g_i}{f_i}}, \quad (19)$$

$$\hat{\Omega} = \frac{1}{K} \cdot \sum_{i=1}^K \frac{(X^i - \hat{\mu})(X^i - \hat{\mu})^T g_i}{f_i}, \quad (20)$$

The shape parameter  $\alpha$  estimate is obtained by solving the minimization problem of one-dimensional likelihood function:  $\hat{\alpha} = \arg \max_{0 \leq \alpha \leq 1} L(X, \hat{\mu}, \hat{\Omega}, \alpha)$ .

Golden section search method can be applied to the minimization.

### 3 Quadrature formulas

Integrals included in the expressions of the estimates can be calculated by integral calculation subprograms in mathematical systems MathCad, Maple and etc., or using the Gaussian and Gauss-Laguerre quadrature formulas (Ehrich, 2002; Stoer, Bulirsch, 2002; Kovvali, 2012; Casio Computer co., 2015).

Gauss-Laguerre quadrature formulas:

$$\int_0^{\infty} x^{\alpha} e^{-x} f(x) dx \cong \sum_{i=1}^n \omega_i f(x_i), \quad (21)$$

where  $f(x_i)$  – integrated function,  $n$  – number of nodes,  $x_i$  – integration nodes,  $\omega_i$  – fixed weights.

Gaussian quadrature formulas:

$$\int_{-1}^1 f(\chi) d\chi \cong \sum_{i=1}^m \vartheta_i f(\chi_i), \quad (22)$$

where  $f(\chi_i)$  – integrated function,  $m$  – number of nodes,  $\chi_i$  – integration nodes,  $\vartheta_i$  – fixed weights.

#### 4 Computer modeling

Maximum likelihood parameters estimation by EM algorithm is an iterative process needing to choose initial values and perform a certain number of iterations while values in adjacent steps differ insignificantly. In order to test the behaviour of created algorithm, the experiments were made with financial statements – Total Current Assets, Total Assets, Total Current Liabilities, Total Liabilities – of 124 companies in the USA. According to the much shorter computing time (error of the likelihood function is only in the sixth sign), integrals were calculated using the Gaussian (22) and Gauss-Laguerre (21) quadrature formulas.

In this experiment, data consisted of 124 fourth-dimensional vectors with these sampling means and sampling covariances matrix:

$$\alpha = 1.5, \quad \mu = \begin{pmatrix} 1.044 \\ 2.046 \\ 0.37 \\ 0.873 \end{pmatrix}, \quad \Omega = \begin{pmatrix} 1.175 & 2.024 & 0.486 & 0.911 \\ 2.024 & 5.225 & 1.038 & 2.572 \\ 0.486 & 1.038 & 0.418 & 0.667 \\ 0.911 & 2.572 & 0.667 & 1.953 \end{pmatrix}. \quad (23)$$

We have developed an algorithm, where alpha is minimized in each iteration. Fig. 1 shows that likelihood function is unimodal. Therefore, it can be applied to the minimization by the golden section search method.

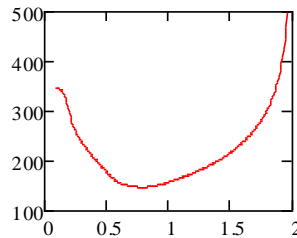


Fig. 1. Likelihood function dependence on alpha

Total 100 iterations by the described EM algorithm were performed. Fig. 2 shows the obtained parameters of  $\alpha$ -stable law in dependence on the number of iterations. We see that the value of the likelihood function and the parameters estimates in a few iterations converge to the values, calculated with MathCad minimization subprogram.

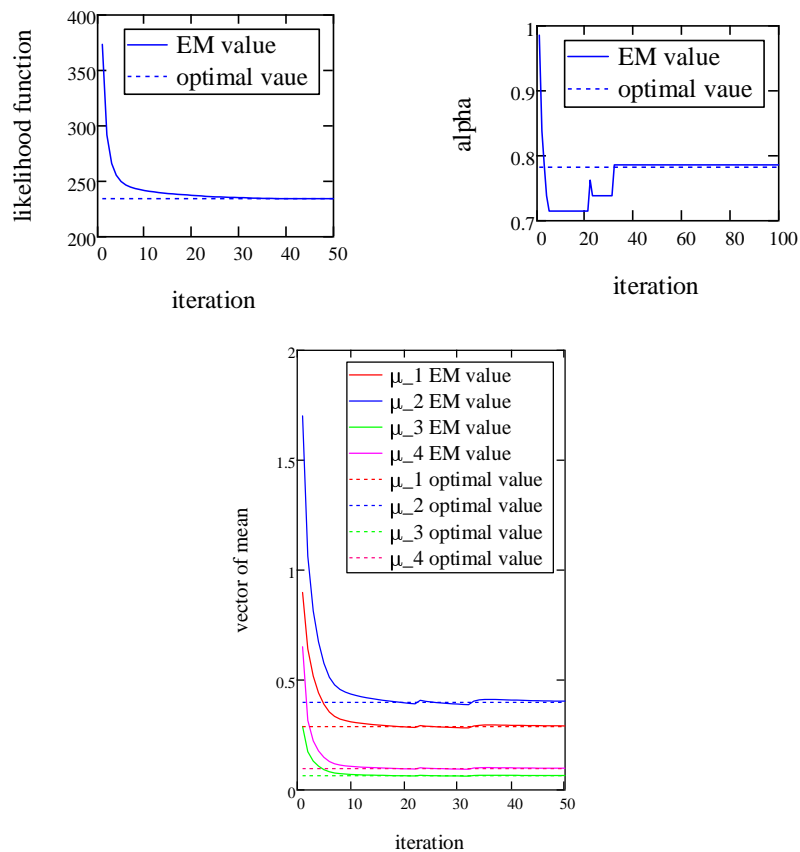


Fig. 2. Parameters dependence on the number of iterations

Further were generated  $K = 100$  four-dimensional random  $\alpha$ -stable law values with obtained parameters estimates and was performed a likelihood ratio test:

- Parameters of the model were estimated by maximum likelihood method using practical data.
- Then were generated a new sample by stable model whose parameters correspond to obtained estimates.

- Further were calculated the empirical likelihood function and the likelihood function values of this sample, derived from practical data, empirical probability. If this probability is in the interval  $\left(\frac{\alpha}{2}, 1 - \frac{\alpha}{2}\right)$ , this is not a reason to reject the hypothesis about the data matching to the analyzed probability model, in a given case, to the  $\alpha$ -stable law with reliability  $\alpha$ .
- Thus, the empirical probability of the test with financial balance data was 21.47 % (see, Fig. 3).

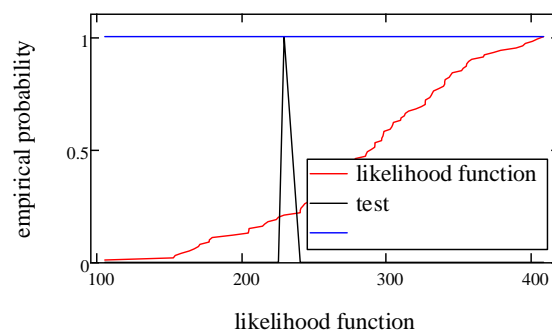


Fig. 3. Likelihood function test

## Conclusions

1. The maximum likelihood method for the multivariate  $\alpha$ -stable distribution was created in this work, which allows to estimate parameters of this distributions using EM algorithm.
2.  $\alpha$ -stable distribution parameters estimators obtained by numerical simulation method are statistically adequate, because after a certain number of iterations, values of likelihood function and parameters convergent to the maximum likelihood values.
3. It was shown that this method realizes log-likelihood function golden section search, implementing it with EM algorithm.
4. This algorithm was applied for creation of model of balance data of USA companies. And it can be used creating financial models in stock market data analysis. Also algorithm can be used to test the systems of stochastic type and to solve other statistical tasks by using EM algorithm.

## References

1. I. Belovas, A. Kabasinkas, L. Sakalauskas. A Study of Stable Models of Stock Markets. *Information Technology and Control*, 35(1), 34–56, 2006.
2. M. Bertocchi, R. Giacometti, S. Ortobelli, S. Rachev. The impact of different distributional hypothesis on returns in asset allocation. *Finance Letters*, 3(1), 17–27, 2005.

3. K. Bogdan, T. Byczkowski, T. Kulczycki, M. Ryznar, R. Song, Z. Vondracek. *Potential Analysis of Stable Processes and its Extensions*. Springer Science & Business Media, 2009.
4. Casio Computer co. [online]. Available from Internet [2016-09-02]: <http://keisan.casio.com/exec/system/1281279441>
5. Yu. Davydov, V. Paulauskas. On the Estimation of the Parameters of Multivariate Stable Distributions. *Acta Applicandae Mathematica*, Vol. 58. No. 1., 107–124, 1999.
6. S. Ehrlich. On stratified extensions of Gauss-Laguerre and Gauss-Hermite quadrature formulas. *Journal of Computational and Applied Mathematics*. 140 (1-2), 291–299, 2002.
7. B. D. Fielitz, E. W. Smith. Asymmetric stable distributions of stock price changes. *Journal of American Statistical Association*, 67(340), 331–338, 1972.
8. M. Hoehstoetter, S. Z. Rachev, F. J. Fabozzi. Distributional analysis of the stocks comprising the DAX 30. *Probability and Mathematical Statistics*, 25(1) 363–383, 2005.
9. A. Janicki, A. Weron. *Simulation and Chaotic Behavior of  $\alpha$ -Stable Stochastic Processes*. New York: Marcel Dekker, 1993.
10. A. Kabasinskas, S. Rachev, L. Sakalauskas, W. Sun, I. Belovas. Stable Paradigm in Financial Markets. *Journal of Computational Analysis and Applications*, 11(3), 642–688, 2009.
11. A. Kabasinskas, L. Sakalauskas, E. W. Sun, I. Belovas. Mixed-Stable Models for Analyzing High-Frequency Financial Data. *Journal of Computational Analysis and Applications*, 14(7), 1210–1226, 2012.
12. N. Kovvali. *Theory and Applications of Gaussian Quadrature Methods*. Morgan & Claypool Publishers, 2012.
13. S. Kring, S. T. Rachev, M. Hochstotter, F. J. Fabozzi. Estimation of  $\alpha$ -Stable Sub-Gaussian Distributions for Asset Returns. *Risk Assessment: Decisions in Banking and Finance*, 111–152, 2009.
14. J. P. Nolan. Multivariate stable distributions: approximation, estimation, simulation and identification. *A practical guide to heavy tails*, 509–525, 1998.
15. J. P. Nolan. *Stable Distributions – Models for Heavy Tailed Data*. Boston: Birkhauser, 2007.
16. H. Ogata. Estimation for multivariate stable distributions with generalized empirical likelihood. *Journal of Econometrics*, Vol. 172. No. 2., 248–254, 2013.
17. S. J. Press. Estimation in Univariate and Multivariate Stable Distributions. *Journal of the American Statistical Association*, 67(340), 842–846, 1972.
18. S. T. Rachev, S. Mittnik. Modeling Asset Returns with Alternative Stable Distributions. *Econometric Reviews*, 12(3), 261–330, 1993.
19. S. T. Rachev, S. Mittnik. *Stable Paretian Models in Finance*. New York: Wiley, 2000.
20. S. T. Rachev, H. Xin. Test for Association of Random Variables in the Domain of Attraction of Multivariate Stable Law. *Probability and Mathematical Statistics*, 14(1), 125–141, 1993.
21. N. Ravishanker, Z. Qiou. Monte Carlo EM Estimation for Multivariate Stable Distributions. *Statistics & Probability Letters*, 45(4), 335–340, 1999.
22. L. Sakalauskas. On the Empirical Bayesian Approach for the Poisson-Gaussian Model. *Methodology and Computing in Applied Probability*, 12(2), 247–259, 2010.
23. G. Samorodnitsky, M. S. Taqqu. *Stable Non-Gaussian Random Processes. Stochastic Models with Infinite Variance*. New York: Chapman & Hall, 1994.
24. L. Sakalauskas, Z. Kalsyte, I. Vaiciulyte, I. Kupciunas. The application of stable and skew  $t$ -distributions in predicting the change in accounting and governance risk

- ratings. *Proceedings of the 8th International Conference „Electrical and Control Technologies“*, 53–58, 2013.
25. L. Sakalauskas, I. Vaičiulytė. Sub-gausinio vektoriaus skirstinio parametru vertinimas Monte-Karlo Markovo grandinės metodu. *Jaunųjų mokslininkų darbai*, 1(41), 104–107, 2014.
26. J. Stoer, R. Bulirsch. *Introduction to Numerical Analysis*. Springer Science & Business Media, 2002.



# A Projection Pursuit Clustering Algorithm for preference data

Mariangela Sciandra<sup>1</sup>, Antonio D'Ambrosio<sup>2</sup>, and Antonella Plaia<sup>1</sup>

<sup>1</sup> Department of Economics, Business and Statistics, viale delle Scienze, Edificio 13, University of Palermo, Palermo, Italy

(E-mail: [mariangela.sciandra@unipa.it](mailto:mariangela.sciandra@unipa.it) , [antonella.plaia@unipa.it](mailto:antonella.plaia@unipa.it))

<sup>2</sup> Department of Economics and Statistics, University of Naples Federico II , Via Cinthia, M.te S. Angelo, Napoli, Italy

(E-mail: [antdambr@unina.it](mailto:antdambr@unina.it))

**Abstract.** In the framework of preference rankings, the interest can lie in clustering individuals or items in order to reduce the complexity of the preference space for an easier interpretation of collected data. The last years have seen a remarkable flowering of works about the use of decision tree for clustering preference vectors. As a matter of fact, decision trees are useful and intuitive, but they are very unstable: small perturbations bring big changes. This is the reason why it could be necessary to use more stable procedures in order to clustering ranking data. In this work, a Projection Clustering Unfolding (PCU) algorithm for preference data will be proposed in order to extract useful information in a low-dimensional subspace by starting from a high but mostly empty dimensional space. Comparison between unfolding configurations and PCU solutions will be carried out through Procrustes analysis.

**Keywords:** Projection pursuit, Preference data, Clustering rankings.

## 1 Introduction

Projection pursuit includes a lot of techniques for finding interesting projections of multivariate data in low dimensional spaces [16]. One particular structure is that of clusters in the data. Projection Pursuit Clustering (PPC) is a synthesis of projection pursuit and nonhierarchical clustering methods that simultaneously attempt to cluster the data and to find a low-dimensional representation of this cluster structure. As introduced by Huber [24], a PP algorithm consists of two components: an index function  $I(\alpha)$  that measures the “usefulness” of projection and a search algorithm that varies the projection direction so as to find the optimal projections, given the index function  $I(\alpha)$  and the data set  $X$ . In this work we propose an iterative strategy that combines suitable clustering methods for preference rankings with Multidimensional unfolding techniques. We call our proposal *Projection Clustering Unfolding*. All the methodology is illustrated and evaluated on a real and well known dataset.

---

<sup>5</sup>*th* SMTDA Conference Proceedings, 12-15 June 2018, Chania, Creete, Greece

© 2018 ISAST



## 2 Preference data

In every day life ranking and classification are basic cognitive skills that people use in order to graduate everything that they experience. Grouping and ordering a set of elements is considered easy and communicative, so often it happens to observe rankings of sport-teams, universities, countries and so on. A particular case of ranking data is represented by preference data, in which individuals show their preferences over a set of alternatives, items from now on. Since preference rankings can be considered as indicators of individual behaviours, when subject-specific characteristics are available, an important issue relies on the identification of profiles of respondents giving same/similar rankings.

Ranking data arise when a group of judges is asked to rank a fixed set of objects (*items*) according to their preferences. When ranking  $k$  items, labeled  $1, \dots, k$ , a ranking  $\pi$  is a mapping function from the set of items  $\{1, \dots, k\}$  to the set of ranks  $\{1, \dots, k\}$ , endowed with the natural ordering of integers, where  $\pi(i)$  is the rank given by the judge to item  $i$ . When all  $k$  items are ranked in  $k$  distinct ranks, we observe a complete ranking or *linear ordering* [7]. Yet, it is also possible that a judge fails to distinguish between two or more objects and assigns them equally, thus resulting in a tied ranking or *weak ordering*. Besides complete and tied rankings, *partial* and *incomplete rankings* exist: the first occurs when only a specific subset of  $q < k$  objects are ranked by judges, while incomplete ranking occurs when judges are free to rank different subsets of  $k$  objects [7]. Obviously, different types of ordering will generate different sample space of ranking data. With  $k$  objects there are  $k!$  possible complete rankings; this number gets even larger when ties are allowed (for the cardinality of the universe when ties are allowed refer to [18] and [32]). From a methodological point of view, preference analysis often models the probability for certain preference structures, finally providing the probabilities for choosing one single object. Many models have been proposed over the years, such as order statistics models, distance-based models and Bradley-Terry models. Moreover, in order to incorporate subject specific covariates, extension of the above mentioned models have been proposed, such as distance based tree models [31], decision tree models with ad-hoc impurity functions ([43],[37]), distance-based multivariate trees for rankings [10] and some log-linear version of standard Bradley-Terry models [13]. Recently, model-based clustering algorithms to analyse and explore ranking data have been proposed in literature ([26], [1]). Yet, it is important to note that the classical cluster algorithm not always can be extended to preference data, because the concept of clustering for this type of data is not unique: in presence of preference data, clustering can be done over the individuals or over the objects. Often rank data can reveal simultaneous clusters of both individuals and items.

---

Preference rankings can be represented through either rank vectors (as in this paper) or order vectors [9].

### 3 Projection pursuit

Projection pursuit includes a lot of techniques for finding interesting projections of multivariate data in low dimensional projections [16]. One particular structure is that of clusters in the data. Projection Pursuit Clustering (PPC) is a synthesis of projection pursuit and nonhierarchical clustering methods that simultaneously attempts to cluster the data and to find a low-dimensional representation of this cluster structure.

One of the most important features of PP is that it is one of the few multivariate methods able to bypass the “curse of dimensionality” problem. Many of the methods of classical multivariate analysis turn out to be special cases of PP, for example principal components and discriminant analysis.

How does PP work? When PP is performed on a small number of dimensions, it is possible to examine essentially all such projections to select those of interest: the appearance of the projected data set does not change abruptly as the projection direction changes, and the space of projection directions will be of low dimensionality. When the projection is made up in higher dimensions, the appearance of the projected data will still smoothly change, but it becomes increasingly impractical to explore possible projections exhaustively [39].

Projection pursuit works by associating a function value to each and every low-dimensional projection. This function value must be a measure of “interestingness” so it should be large for projections revealing interesting structure, and small for uninteresting ones. Then, PP could be defined as the process of making such selections by the local optimisation over projection directions of some index of “interestingness”. The notion of “interesting projection” has usually been defined referring to departure from normality [24], but several alternatives have been proposed also looking for multimodality [36] or clustering. Once an objective function  $I$ , called *projection index* and depending on a normalized projection vector  $\alpha$ , is assigned to every projection characterizing the structure present in the projection, interesting projection are then automatically picked up through a numerical optimization of the projection index. One of the most common problems in PP is the oscillating behaviour of the projection indices: often procedures looking for the most interesting projection stop at the nearest local optimum from the starting point. So several authors devoted their works to avoid the local property of the optimization algorithm [20,38]. A way for catching all and only all significantly interesting projections is to extract them in a monotonic way from the most structured projection to the least but still useful solution. In its classical notation a PP can be summarized as follows. Let  $X$  be either a  $P$ -dimensional random vector (distributional) or some  $P \times N$  data matrix (sample). To form a univariate linear projection of  $X$  onto the real line we require a  $P$ -vector  $a$ . This vector might as well be of unit length, since it is only the direction of projection that is of interest. The projected data,  $Z$ , are formed by  $Z = a^T X$ . For a linear projection onto  $K$  ( $K < P$ ) dimensions we require a  $P \times K$  matrix  $A$ , and the projected data,  $Z$ , are formed by  $Z = A^T X$ . If the columns of  $A$  form an orthonormal set then the projection will be orthogonal.

The measure of “interestingness” evaluated by the projection index  $I$ , then will

be expressed as

$$I(Z) = I(A^\top X) = I(A).$$

These interesting projections will be evidence of structure within the multivariate set and may form the basis of hypotheses which may be confirmed by more traditional statistical methods.

### 3.1 Projection Indexes

The aim of projection pursuit is to reveal possible non-linear and therefore interesting structures hidden in high-dimensional data. As introduced before, to what extent these structures are “interesting” is measured by an index. Principal components analysis, for example, can be seen as a projection pursuit method in which the index of “interestingness”  $I(a)$  is the proportion of the total variance accounted for by a linear combination  $a^\top X$  subject to the normalizing constraint  $a^\top a = 1$ . In this particular case, this projection index is simple to maximize and has an algebraic solution; however this is the exception rather than the rule. Most projection indexes require an algorithm that will calculate  $I$  at values of  $a$  and maximize  $I$  according to some numerical optimization routine.

Several projection indexes have been proposed in literature. Since the work of Huber [24], the notion of an “interesting projection” has been clearly defined as one exhibiting departure from normality. Consequently, test for non-normality were thought as suitable projection indexes. But it has also been shown that in order a projection index to be considered efficient, must satisfy basic requirements, namely affine invariance [24], consistency [20], simplicity and sensitivity to departure from normality in the core rather than in the tails of the distribution. Friedman and Tukey [16] developed a hill-climbing optimization methods to find interesting projections. The index they used for 1-dimensional projection pursuit can be written as a combination of two components  $I(a) = s(a)d(a)$ , where  $s(a)$  measures the general spread of the data, and  $d(a)$  measures the local density of the data after projection onto a projection vector  $a$ . As an alternative, Jones and Sibson [27] defined a measure of un-interesting projections and attempted to maximise divergence away from it. Other projection indexes were based on some measure of entropy [42]; Jones and Sibson (1987) developed an approximation to the entropy index, called the moment index, which is based on summary statistics of the data (more precisely the third and fourth outer product tensors). Very few projection pursuit indices incorporate class or group information in the calculation. Hence, they cannot be adequately applied in *supervised* classification problems to provide low dimensional projections revealing class differences in the data. Aim of the projection Pursuit Clustering (PPC) is to recover clusters in lower dimensional subspaces of the data by simultaneously performing dimension reduction and clustering. Therefore, results from a PPC algorithm could make possible to use them as a first step of *unsupervised* classification problems.

## 4 Projection pursuit clustering

Bolton and Krzanowski [3] define Projection Pursuit Clustering as the synthesis of a projection pursuit algorithm and nonhierarchical clustering methods that simultaneously attempt to cluster the data and to find a low-dimensional representation of this cluster structure. Aim of the PPC is to seek, in high dimensional data, a few interesting low-dimensional projections that reveal differences between classes. PPC works as follows: iteratively it finds both an optimal clustering for a subspace of given dimension and an optimal subspace for this clustering. Some author has already associated PP with clustering; for example [15] proposed the use in a PP algorithm of projection indexes with class information able to uncover low-dimensional cluster structure; Lee, Cook, Klinke, and Lumley (2005) [29] proposed the LDA (linear discriminant analysis) projection pursuit index using class information through an extension of the linear discriminant analysis idea. Lee and Cook (2010) [30] developed a Penalized Discriminant Analysis (PDA) index useful when data exhibit high correlation data or for situations with a small number of observations over a large number of variables.

Other contributions looked at MDS (multidimensional scaling) in terms of projection pursuit by identifying the *stress* function with the projection index and constrain the multidimensional configuration to orthogonal projections of the data [5]. In a more recent work Lee *et al.* [31] developed a projection pursuit classification tree, a new approach to build a classification tree using projection pursuit indices with class information. A PP step is performed at each node so that the best projection is used to separate two groups of classes using various projection pursuit indices with class information. One class is assigned to only one final node and the depth of the projection pursuit classification tree cannot be greater than the number of classes. The projection coefficients of each node can be interpreted as the importance of the variables to the class separation of each node; then the way in which these coefficients change should be useful to explore how classes are separated in a tree.

## 5 Clustering preference data

In dealing with preference rankings, one of the main issues is to identify homogeneous sub-populations of judges when heterogeneity among them is assumed. This is exactly the goal of clustering methods. Projection pursuit-based clustering methods have been proposed over the years in order to deal with a large variety of data ([16], [2], [23], [34]). As a matter of fact, there is no proposal that allows to deal with preference data. Preference rankings are characterized by a set of items, or objects, and a set of judges, or individuals, that have to rank the items according to their preference. Clustering methods for preference rankings can be done over the individuals [35], [26], or over the objects [33]. Often rank data can reveal simultaneous clusters of both individuals and items. Multidimensional unfolding techniques can graphically show such a situation [12]. Here we combine suitable clustering methods for preference

rankings with Multidimensional unfolding techniques. Our approach is similar to the Cluster Differences Unfolding (CDU) [41], which can be considered as the natural extension to Unfolding of the Cluster Difference Scaling (CDS) [22]. The main difference is that CDU, which is devoted to metric Unfolding, performs a cluster analysis over both the sets of individuals and objects, producing a configuration plot that shows the baricenter of the sets retaining their preference relationship.

Here we propose an iterative strategy that performs a non-hierarchical cluster analysis on only one set, typically the individuals, leaving the other set free to be configured in the reduced geometrical space in such a way that the relationships between the preference order of the individuals with respect to the items remain unchanged. We call our proposal *Projection Clustering Unfolding* (PCU).

### 5.1 The *Projection Clustering Unfolding* (PCU)

Unfolding can be seen as a particular Multidimensional Scaling technique for rectangular data, in general showing preference of  $n$  persons for  $m$  objects. The most accepted formulation of the problem in terms of a badness-of-fit function is given in a least squares framework by the minimization of the *stress* function [28], defined as

$$\sigma^2(\mathbf{A}, \mathbf{B}, \hat{\Delta}) = \sum_{i=1}^n \sum_{j=1}^m (\hat{\delta}_{ij} - d_{ij})^2, \quad (1)$$

where  $\hat{\Delta}$  is a  $n \times m$  matrix in which each entry  $\hat{\delta}_{ij}$  represents the disparity or monotonically transformed dissimilarity between the  $i$ th individual and the  $j$ th item, and  $d_{ij} = d_{ij}(\mathbf{A}, \mathbf{B})$  represents the Euclidean distance between the individuals' ( $\mathbf{A}$ ) and items ( $\mathbf{B}$ ) configuration points in  $P$ -dimensional space,  $i = 1, \dots, n$ ,  $j = 1 \dots, m$  [5].

Here we assume that  $\mathbf{A} = \mathbf{G}\mathbf{X}$ , where  $\mathbf{G}$  is a  $n \times K$  indicator matrix whose elements  $g_{ik}$ ,  $k = 1, \dots, K$ , are equal to one if the  $i$ th individual belongs to the  $k$ th cluster, and zero otherwise. We assume that  $g_{ik} \cap g_{il} = \emptyset$  for  $k \neq l = 1, \dots, K$   $\forall i = 1, \dots, n$ .  $\mathbf{X}$  is the  $K \times P$  matrix of the baricenter of the  $K$  clusters, where  $P$  indicates the dimension of the Unfolding solution.

We propose an alternating optimization strategy that, given a configuration of both the individuals and the items, searches the optimal partition of the individuals in  $K$  clusters. Then, given the optimal partition of the individuals, the configuration of both individuals and items are updated. The first step consists in a first unfolding configuration with a random assignment of the individuals to the  $K$  clusters. As Unfolding model, we use the PREFSCAL algorithm [6], which is particularly feasible when dealing with ordinal Unfolding, that penalizes the stress function and uses the SMACOF-3 algorithm [21] as optimization engine.

### 5.2 The *Projection Clustering Unfolding*: a real example

As an example, we analyse the well-known breakfast data set [19]. Breakfast data contains the preferences of 42 individuals towards 15 breakfast items from

the most preferred (1) to the least preferred (15). We set  $K = 4$  clusters and the “primary approach to ties” [11]. As the final solution is sensitive to the random choice of the clusters at the first step, we repeated the analysis 20 times, obtaining the configuration shown in Figure 1.

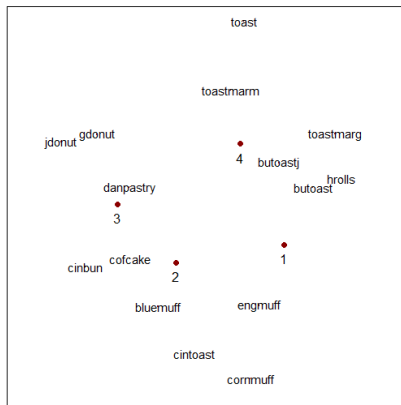


**Fig. 1.** Projection Clustering Unfolding solution. Items are coded as: toast=toast pop-up; butoast=buttered toast; engmuff=English muffin and margarine; jdonut=jelly donut; cintoast=cinnamon toast; bluemuff=blueberry muffin and margarine; hrolls=hard rolls and butter; toastmarm=toast and marmalade; butoastj=buttered toast and jelly; toastmarg=toast and margarine; cinbun=cinnamon bun; danpastry=Danish pastry; gdonut=glazed donut; cofcake=coffee cake; corrmuff=corn muffin and butter.

Fig. 1 shows the configuration of the 4 cluster centers in the 2-dimensional solution. We expect that the closer the baricenter are to the items, the higher is the preference of that cluster to that items. We ran the Unfolding analysis without any restriction on the same data, and then we performed a Procrustes analysis [4] by considering the unrestricted solution as target configuration. Procrustes analysis allows to evaluate the ability to reproduce the configurations both graphically and with the  $L$ -statistic, which is the sum of the squared differences between the true and the fitted configuration after that both are set into optimal correspondence through Procrustean transformation. The lower the Procrustes statistic, the better the fitted configuration. We used a normalized version of the Procrustes statistic as suggested by [40]:

$$L(\mathbf{X}, \hat{\mathbf{X}}) = \frac{\text{tr}((\mathbf{X} - \hat{\mathbf{X}})^T(\mathbf{X} - \hat{\mathbf{X}}))}{\text{tr}(\mathbf{X}^T \mathbf{X})}, \quad (2)$$

where  $\mathbf{X}$  is the true configuration and  $\hat{\mathbf{X}}$  is the fitted one.

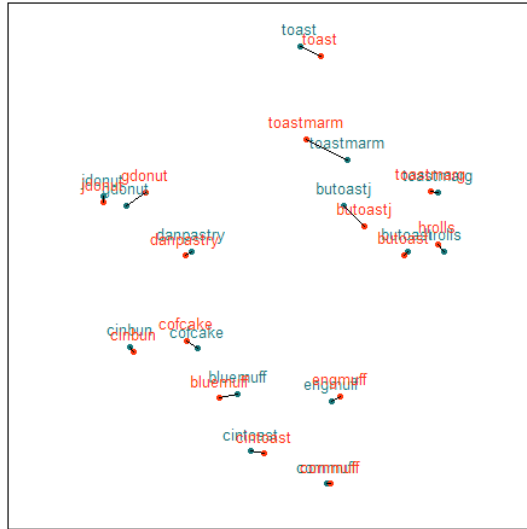


**Fig. 2.** Procrustes configuration plot: objects' points unfolding configuration (green) vs objects' points PCU solution (red).

Figure 2 shows the Procrustes configuration plot limited to only the objects points. The recovery is excellent, also confirmed by a value of  $L = 0.013$ .

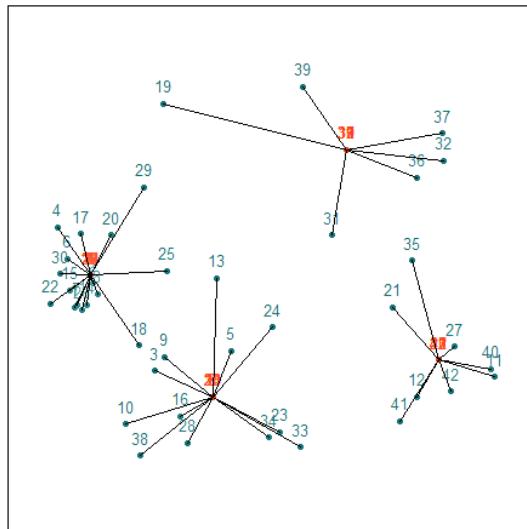


**Fig. 3.** Procrustes configuration plot: individuals' points unfolding configuration (green) vs individuals' points PCU solution (red).



In order to check the homogeneity of the analysis in terms of preference rankings, we computed the median ranking within each cluster. We obtained the results shown in Table 1. These median rankings can be interpreted as the baricenter in terms of preference rankings. We noticed that the results are consistent with the graphical solution. Last row shows the averaged  $\tau_X$  rank correlation coefficient [14] within cluster, which informs about the goodness of the solution of the median ranking problem. The last column shows the median ranking of the entire data set. It can be noticed that the homogeneity in terms of  $\tau_X$  rank correlation coefficient is much larger within each cluster.

**Table 1.** Median ranking within cluster

Item	Cluster 1	Cluster 2	Cluster 3	Cluster 4	Median ranking	Breakfast data
toast	13	13	15	7		15
butoast	1	10	11	1		11
engmuff	2	3	7	8		6
jdonut	15	12	3	6		7
cintoast	5	5	8	13		8
bluemuff	6	2	6	9		3
hrolls	4	9	14	2		12
toastmarm	8	8	10	2		10
butoastj	7	7	9	2		9
toastmarg	3	11	12	3		13
cinbun	12	4	5	10		4
danpastry	10	4	1	4		1
gdonut	14	6	4	5		5
cofcake	9	1	2	11		2
cornmuff	11	6	13	12		14
$\tau_X$	0.554	0.520	0.647	0.514		0.306

As a global homogeneity measure of the PCU, we can compute the quantity  $H = \sum_{k=1}^K \tau_{X_k} \pi_k$ , where  $\pi_k$  is the proportion of cases in the  $k$ th cluster. The shown configuration returns  $H = 0.575$ , which is about 1.877 times larger than the homogeneity of the entire data set.

## Conclusions

In dealing with preference rankings, one of the main issues is to identify homogeneous sub-populations of judges when heterogeneity among them is assumed. In this work a Projection pursuit-based clustering method has been proposed in order to deal with preference data. The *Projection Clustering Unfolding* algorithm combines suitable clustering methods for preference rankings with Multidimensional unfolding techniques. The strengths of the proposed algorithm have been shown through an application to a real dataset: a Procrustes analysis, used to perform a comparison between the PCU and the Unfolding without restriction configurations, gives excellent results.

## References

1. C. Biernacki and J. Jacques, A generative model for rank data based on sorting algorithm, *Computational Statistics & Data Analysis*, 58, 162-176, 2013
2. H. H. Bock, *On the interface between cluster analysis, principal component analysis, and multidimensional scaling*, In Multivariate statistical modeling and data analysis, Springer, Dordrecht, 17-34, 1987.
3. R. J. Bolton and W. J. Krzanowski, Projection Pursuit Clustering for Exploratory Data Analysis, *Journal of Computational and Graphical Statistics*, 12, 1, 121-142, 2003.
4. I. Borg and J. Lingoes, *Multidimensional similarity structure analysis*, Springer-Verlag New York, 1987.
5. I. Borg and P.J.F. Groenen, *Modern Multidimensional Scaling: Theory and Applications*, Springer, New York, 1997. Statistics Series.
6. F. M. T. A. Busing, P.J.F. Groenen and W. J. Heiser, W. J., Avoiding degeneracy in the multidimensional unfolding by penalizing on the coefficient of variation, *Psychometrika*, 70, 71-98, 2005.
7. W. Cook, M. Kress, and L. M. Seiford, An axiomatic approach to distance on partial orderings, *Revue Franaise d'Automatique, d'Informatique et De Recherche Oprationnelle. Recherche Oprationnelle*, 20, 2, 115-122, 1986.
8. D. Cook, A. Buja, and J. Cabrera, Projection pursuit indices based on expansions with orthonormal functions, *Journal of Computational and Graphical Statistics*, 2, 3, 225-250, 1993.
9. A. D'Ambrosio, S. Amodio, and C. Iorio, Two algorithms for finding optimal solutions of the kemeny rank aggregation problem for full rank, *Electronic Journal of Applied Statistical Analysis*, 8, 2, 2015.
10. A. D'Ambrosio and W.J Heiser, A recursive partitioning method for the prediction of preference rankings based upon Kemeny distances, *Psychometrika*, 81, 3, 774-94, 2016.
11. J. De Leeuw, Correctness of Kruscal's algorithms for monotone regression with ties. *Psychometrika*, 42, 1, 141-144, 1977.
12. G. De Soete, and W. J. Heiser, A latent class unfolding model for analyzing single stimulus preference ratings, *Psychometrika*, 58, 4, 545-565, 1993.
13. R. Dittrich, R. Hatzinger, W. Katzenbeisser, Modelling the effect of subject-specific covariates in paired comparison studies with an application to university rankings, *Journal of the Royal Statistical Society: Series C (Applied Statistics)*, 47, 4, 511-525, 1998.
14. E. Emond and D. Mason, A new rank correlation coefficient with application to the consensus ranking problem. *Journal of Multi-Criteria Decision Analysis*, 11, 1, 17-28, 2002.
15. G. Eslava and F.H.C. Marriott, Some criteria for projection pursuit, *Statistics and Computing*, 4, 13-20, 1994.
16. J.H. Friedman and J.W Tukey, A projection pursuit algorithm for exploratory data analysis, *IEEE Transactions on Computers*, 23, 881-889, 1974.
17. J. H. Friedman, Exploratory Projection Pursuit, *Journal of the American Statistical Association*, 82, 249-266, 1987.
18. I. J. Good, The number of orderings of n candidates when ties and omissions are both allowed, *Journal of Statistical Computation and Simulation*, 10, 2, 159-160, 1980.
19. P. E. Green and V. Rao, *Applied multidimensional scaling*. Hinsdale, IL: Dryden, 1972.

20. P. Hall, Estimating the direction in which a data set is most interesting, *Probability Theory and Related Fields*, 80, 1, pp 51-77, 1988.
21. W.J. Heiser, *Unfolding Analysis of Proximity Data*, unpublished doctoral dissertation, University of Leiden, The Netherlands, 1981.
22. W. J. Heiser, *Clustering in low-dimensional space*. In O. Opitz, B. Lausen, and R. Klar (Eds.), *Information and classification: Concepts, methods and applications*, 162-173, Heidelberg: Springer Verlag, 1993.
23. W. J. Heiser and P. J. Groenen, Cluster differences scaling with a within-clusters loss component and a fuzzy successive approximation strategy to avoid local minima, *Psychometrika*, 62, 1, 63-83, 1997.
24. P. J. Huber, Projection Pursuit, *Ann. Statist.*, 13, 2, 435-475, 1985.
25. J. Jacques and C. Biernacki, Model-based clustering for multivariate partial ranking data, *Project-Teams MDAL, Research Report n 8113*, 2012.
26. J. Jacques and C. Biernacki, Model-based clustering for multivariate partial ranking data, *Journal of Statistical Planning and Inference*, 149, 201-217, 2014.
27. M. C. Jones and R. Sibson, What is projection pursuit? (with discussion), *J. R. Statist. Soc. A*, 150, 1-36, 1987.
28. J. B. Kruskal, Multidimensional scaling by optimizing goodness of fit to a non-metric hypothesis, *Psychometrika*, 29, 1, 1-27, 1964.
29. E. Lee, D. Cook, S. Klinke, and T. Lumley, Projection pursuit for exploratory supervised classification, *Journal of Computational and Graphical Statistics*, 14, 4, 831-846, 2005.
30. E. K. Lee and D. Cook, A projection pursuit index for large p small n data, *Statistics and Computing*, 20, 3, 381-392, 2010.
31. P. H. Lee, and P.L. Yu, Distance-based tree models for ranking data, *Computational Statistics & Data Analysis*, 54, 6, 1672-1682, 2010.
32. P. Marcus, Comparison of heterogeneous probability models for ranking data. *Master thesis*. <http://www.math.leidenuniv.nl/scripties/MasterMarcus.pdf>, 2013.
33. J. I. Marden, *Analyzing and modeling rank data*, Chapman and Hall/CRC, 2014.
34. A. D. Miasnikov, J. E. Rome and R. M. Haralick, *A hierarchical projection pursuit clustering algorithm*, in Pattern Recognition, 2004. ICPR 2004. Proceedings of the 17th International Conference, 1, 268-271, 2004.
35. T. B. Murphy and D. Martin, Mixtures of distance-based models for ranking data, *Computational statistics and data analysis*, 41, 3, 645-655, 2003.
36. G. P. Nason and R. Sibson, Measuring multimodality, *Statistics and Computing*, 2, 3, pp 153-160, 1992.
37. A. Plaia and M. Sciandra, Weighted distance-based trees for ranking data, *Advances in Data Analysis and Classification*, 1-18, 2017.
38. C. Posse, Tools for Two-Dimensional Exploratory Projection Pursuit, *Journal of Computational and Graphical Statistics*, 4, 2, pp. 83-100, 1995.
39. P. A. Tukey and J. W. Tukey, *Preparation; prechosen sequences of views*. In V. Barnett, editor, *Interpreting Multivariate Data*, 189-213. Wiley, 1981.
40. K. Van Deun, W. J. Heiser, and L. Delbeke, Multidimensional unfolding by non-metric multidimensional scaling of spearman distances in the extended permutation polytope, *Multivariate Behavioral Research*, 42, 1, 103-132, 2007.
41. J. F. Vera, R. Macías and W. J. Heiser, Cluster differences unfolding for two-way two-mode preference rating data, *Journal of classification*, 30, 3, 370-396, 2013.
42. I. S. Yenyukov, *Indices for projection pursuit*. In Diday, editor, *Data Analysis Learning Symbolic and Numeric Knowledge*, 181-188. Nova Science Publishers, New York, 1989.
43. P. L. Yu, W. M. Wan, P. H. Lee, *Decision tree modeling for ranking data*. In: *Preference Learning*. Springer, 83-106, 2010.

# Exploring the factors that determine depression among 50+ Europeans since childhood: the role of adverse experiences as mediators

Eleni Serafetinidou<sup>1</sup> and Georgia Verropoulou<sup>1</sup>,

<sup>1</sup> Department of Statistics and Insurance Science, University of Piraeus, Piraeus, Greece

(e-mails: [elen\\_sta@outlook.com.gr](mailto:elen_sta@outlook.com.gr), [gverrop@unipi.gr](mailto:gverrop@unipi.gr))

**Abstract.** Depression is a mental health condition causing major issues to individuals, families and society as a whole and may affect different periods of life. The present study aims to explore factors and predictors leading to depression in later life for both genders in a sample of 23816 Europeans aged 50 and higher in 2008. Observations were collected from the database of the Survey of Health and Retirement in Europe (SHARE). More specifically, the analysis includes respondents participating both at wave 3 (SHARELIFE), which contains retrospective information from childhood and adulthood, and at wave 2 which contains information pertaining to the present. For the purposes of the analysis binary logistic regression models were applied using Stata software, version 13. Further, health and socioeconomic status in later life are decomposed in direct and indirect effects and factors causing adverse experiences to persons from different periods of life are examined as mediators, allowing comparisons for both sexes. Results showed that all conditions included in the model were significant, since childhood, over the life course and current life, and predict depression in older ages, both for men and women. Regarding most childhood circumstances men are more vulnerable than women with the exception of adverse experiences (parents drinking heavily) which has a greater impact in older ages for women. Regarding adulthood conditions there is a predominance of ‘period of stress’ which causes higher levels in later life depression for women compared to men. Finally, among current life predictors, health factors covering symptoms and self-perceived health levels seem to be of equal importance for both genders while financial difficulties affect men to a greater extent. The role of education seems to be unimportant only for European men while age does not affect the European women included in our sample. Taking into consideration the findings of the mediation analysis the factor of whether the household is able to make ends meet is mediated stronger through adverse experiences for both sexes. Conclusions will inform policy makers to focus on modifiable depression risk factors in order to take appropriate action dealing with mental health issues for men and women.

**Key words:** depression, later life, adverse experiences, mediation, genders.

**Acknowledgement:** “This work was fully supported from the General Secretariat for Research and Technology (GSRT) and the Hellenic Foundation for Research and Innovation (HFRI)”.

## 1. Introduction

Depression is a mental health condition that can cause major issues on individuals, families and society as a whole (WHO[52]; Rockville[42]). It is evident there is a strong bond between depression and morbidity as well as mortality from medical conditions (Farrokhi *et al.*[24]; Nuyen *et al.*[37]) while other results show that it is connected with a decline in quality of life (D’Alisa *et al.*[21]; Frühwald *et al.*[26]).

Many studies have explored paths between childhood circumstances and later life conditions leading to the onset of depression disorders (Pakpahan *et al.*[38]; Brandt *et al.*[9]; Colman and Atallahjan[17]). Childhood conditions such as health in a development phase and cognitive function play a dominant role in later development of mental health (Pakpahan[39]). Furthermore, childhood health influences health status in adulthood and early mental health problems may predict future health (Currie *et al.*[20]): physical abuse in early ages is a strong predictor of mental disorders during adulthood (Goodwin *et al.*[30]). Finally, studies of adverse experiences in childhood are of particular interest for tracing the origin of depression in older ages (Anda *et al.*[2]). In particular, living with a parent who drinks heavily is negatively associated with childhood health (Angelini and Mierau[4]).

Regarding socioeconomic status in childhood it is supported that it is associated with an increased risk of mid-life disorders even in a weak manner (Stansfeld *et al.*[46]). In the present study socioeconomic position can be determined by the number of books the respondent had access to at age ten. Increasing number of books indicate a higher level of education and a better financial status of the parents. Low childhood socioeconomic status has a long effect on the onset of depression in later life (Tani *et al.*[50]; Angelini *et al.*[3]).

*5<sup>th</sup> SMTDA Conference Proceedings, 12-15 June 2018, Chania, Crete, Greece*

© 2018 ISAST



Concerning adverse experiences over the life course, previous research has shown that adverse life events may increase the levels of depression in later life (Semeijn *et al.*[43]). Experiencing a period of financial hardship, which in most cases may be connected with unemployment or underemployment, seems to be responsible for later life mental health disorders (Crowe and Butterworth[19]). Moreover, findings suggest that current financial hardship is strongly associated with depression (Gallagher *et al.*[27]; Butterworth *et al.*[14]). Going further, financial difficulties can be associated with experiencing a period of hunger; the latter directly affects mental health of individuals in later life (Halmdienst and Winter-Ebmer[31]). It is also supported that nutrition intake may cause depression in older adults (Bulut[13]). The above mentioned characteristics can combine and up to a point contribute to a period of poor health the respondents may experience in their lives. Poor health may include physical health problems or psychological wellbeing which both affect survival at older ages. The role of diseases is very important in predicting later life depression. Suffering from illnesses such as coronary heart disease, arthritis and chronic lung disease may raise depressed mood in older people and this is bidirectional with subjective wellbeing and potential stressful events (Steptoe *et al.*[48]; Jeon and Dunkle[33]; Blazer and Hybels[6]; Fiske *et al.*[25]).

The potential negative outcome of the above predictors may be moderated by sociodemographic and socioeconomic factors playing an important protective role in later life against depression disorders. These factors include education and financial status; higher education level and higher socioeconomic status are associated with lower levels of poor mental health in later life (Buber and Engelhardt[11]; Fiske *et al.*[25]; Buber and Engelhardt[12]). Findings support that an extra year of education decreases the probability of suffering from depression by 6.5 percentage points (Crespo *et al.*[18]).

Researchers have given emphasis in differentiations between genders regarding prevalence of depression in older ages. Past research studies showed that depression is more dominant in girls than boys, an expanding conclusion among women and men in their middle-late adulthood (De Velde *et al.*[23]; Hankin[32]). In most cases, this is due to differences in temperament among the sexes and in part because of the way males and females handle emotionally adverse and stressful life events such as a divorce or the loss of a person they love. Concerning childhood, studies indicate that emotional characteristics in sexes' behaviour are associated with depressive symptoms in both genders, while only girls are vulnerable with respect to proximal negative life events related to depressive symptoms (St Clair *et al.*[47]). Moreover, at older ages, females usually experience more stressful events and more childhood adversity compared to males. They insist to hold a more negative self-view of life events and they tend to explore and explain the cause and consequence of these events in a more negative manner than males (Hankin[32]). Depression in adulthood and later life is not a sole disease but often coexists with other health and mental conditions that afflict patients such as eating, anxiety disorders, multiple sclerosis and obesity, mostly in women (Silverstein and Lynch[44]). Further, the reverse holds i.e. bad health in young ages and successively in later life has a strong effect on depression outcome for both genders (Kamiya *et al.*[34]). Finally, the presence of socioeconomic factors such as having a good socioeconomic position is associated with lower risk of depression for men and women as well (De Velde *et al.*[23]).

The present study aims to explore factors and predictors that may cause depression in later life. The main objectives are: a) to investigate the importance of childhood predictors, adulthood circumstances and later life conditions for both genders b) to identify the mediating role of adverse experiences in different life periods in health and socioeconomic position for men and women. For the purposes of the analysis, logistic regression models have been run and cross-sectional as well retrospective data from the Survey of Health, Ageing and Retirement in Europe (SHARE) have been used.

## 2. Data and Methods

Data have been derived from the Survey of Health, Ageing and Retirement in Europe (SHARE). SHARE is an electronic database of micro data that collects information for respondents' lives regarding health, demographic and socioeconomic characteristics. Individuals participating at the survey are 50 years old or higher and come from several European countries (Börsch-Supan *et al.*[7]). The sample analyzed in this study includes cross-sectional data from the second wave of the survey, carried out in 2006-2007, combined with information concerning childhood from the third wave of the survey (SHARELIFE) which was carried out in 2008-2009. The total sample includes 23816 individuals participating at both waves, who originate in 14 countries that cover all geographical areas

of Europe: Greece, Germany, Sweden, Netherlands, Spain, Italy, France, Denmark, Austria, Switzerland, Belgium, Czech Republic, Poland and Ireland.

#### Dependent variable

The outcome variable is depression in binary form. It is used to compare respondents having 4 or more depressive symptoms to those having reported 0-3 symptoms (the reference category is the second: no depression). According to European standards, depression is measured with the EURO-D psychometric scale, including 12 items. EURO-D was constructed and established by Prince *et al.*[40,41] and since then it has been used widely by scientists worldwide as an indicator of depression levels (Beekman *et al.*[5]; Borch-Supan *et al.*[8]).

#### Independent variables

The independent variables include childhood conditions, events occurring in adulthood and later life controls and predictors.

Regarding childhood, predictors of health, socioeconomic position and adverse experiences have been considered, all in binary form. In particular, subjective health was reported as excellent, good and very good (reference category) and fair and poor. The procedure of merging categories with small frequencies is considered acceptable (De Vaus[22]) and often increases reliability of the analysis (Stone and Wright[49]; Linacre[35]). Concerning socioeconomic position, it is based on the number of books the respondent had access to at the age of ten. It is distinguished in two categories: none or very few including 0-10 books and more than 10 books which is reference category. Past research suggests that this factor is associated with educational attainment of parents, good cognitive function of the child and economic well-being of the family (Cavapozzi *et al.*[16]; Verropoulou and Zakythinou[51]). Finally, adverse experience is represented by whether the respondent had parents drinking heavily or not (reference category).

In the next step, events occurring in adulthood have been included in the model. Adverse events such as indicators of whether the respondent had ever experienced a period of stress, a period of poor health and a period of financial hardship have been examined. Furthermore, educational attainment of the respondents has been included in two categories: 0-9 years and 10 years or more which is reference category.

Finally, predictors referring to later life and related to health, socioeconomic status and demographic factors were taken into consideration. More specifically, concurrent health status is represented by two indicators showing the number of symptoms the respondent suffered (less than two symptoms is the reference category) and SPH expressing the respondents' subjective health (good, very good or excellent is the reference category and fair and poor is the other one). Socioeconomic position is represented by a variable on whether the household is able to make ends meet in binary form: easily or fairly easily, which is the reference category, and facing great or some difficulty. Lastly, as variables of demographic interest, age of the respondent and the country that he/she comes from have been included in the model.

#### Statistical analysis

The analysis included logistic regression models, carried out with STATA 13 separately for men and women. Furthermore, a technique to assess mediation was applied in order to decompose the total effect of later life predictors through adverse experiences as mediators. This technique provides robust estimates under the sequential ignorability assumption (Breen *et al.*[10]) There was no indication of multicollinearity as standard errors were below two (Agresti[1]). The goodness of fit of the models was tested on the basis of pseudo-R<sup>2</sup> showing the predictive ability of the model. High scores of pseudo-R<sup>2</sup> indicate a better fit of the model although in general, this parameter has low scores when logistic regression models are applied.

### 3. Results

#### Descriptive analysis

Table 1 shows descriptive characteristics for the respondents. The total sample consists of 10514 men and 13302 women 50 years and over from different European countries participating in the analysis. The median age for men is 65 years while for women it is 64. According to the results, it is obvious that females present higher levels of depression (30.3%) compared to males (14.9%).

Regarding childhood conditions, for both genders differences are not remarkable. In their vast majority men and women denoted that they had very good or excellent health status as children. Further, the percentage of men having access to none or very few books is a little higher compared to women. The adverse experience of having parents drinking heavily seems to be equivalent for both sexes with a corresponding relative frequency of 8.5%. With respect to adulthood circumstances women exhibit higher proportions than men relating to all factors included in the study. Looking at the table results it is evident that, compared to men, more women have experienced a period of stress in their life (54.5%) as also a period of poor health (42.5%) and financial hardship (34.5%). Educational attainment is higher for men as 63.5% of males have been educated for more than 10 years compared to 56.5% for females. Concerning later life predictors, women suffer more from symptoms (48%) compared to men (33.2%) and they denote higher percentages of poor and fair health (34.8%). Finally, according to socioeconomic status, it is easier for males to make ends meet (63.4%) while they deal with financial issues with some or great difficulty at 36.6% compared to females who face difficulties in financial issues at a percentage of 41.8%.

Table 1. Descriptive statistics for men and women in the sample: childhood predictors, over the life course conditions and later life events.

	<b>Males</b>	<b>Females</b>
<b>Childhood conditions</b>		
Childhood self-perceived health		
excellent, very good and good	92.8%	91.1%
fair and poor	7.2%	8.9%
Number of books at the age of 10		
access to at least 10 books	55.4%	57%
none or very few books	44.6%	43%
Parents drank heavily		
no	91.5%	91.6%
yes	8.5%	8.4%
<b>Factors over the life course</b>		
Period of stress		
no	53.1%	45.5%
yes	46.9%	54.5%
Period of poor health		
no	60.8%	57.5%
yes	39.2%	42.5%
Period of financial hardship		
no	69.3%	65.5%
yes	30.7%	34.5%
Educational attainment		
10 years or more	63.5%	56.5%
0-9 years	36.5%	43.5%
<b>Later life predictors</b>		
Symptoms		
less than 2 symptoms	66.8%	52%
2+ symptoms	33.2%	48%
Self-Perceived Health (SPH)		
good, very good or excellent health	70.5%	65.2%
fair and poor	29.5%	34.8%
Household able to make ends meet		
fairly easily or easily	63.4%	58.2%
great or some difficulty	36.6%	41.8%

Age at interview	65	64
<b>Total Sample</b>	<b>10514</b>	<b>13302</b>
Depression (based on EUROD)		
no	85.1%	69.7%
yes	14.9%	30.3%

#### Logistic regression analysis

Table 2 shows the results of the comprehensive logistic regression model that was applied and the corresponding levels of significance for both sexes. It is evident that almost all factors included in the model were significant at level 1%.

Regarding conditions in childhood, males have higher relative chances of having depression in later life if they reported fair or poor health (30.9%) as children compared to others having good, very good or excellent health. Similarly, if they had access to very few or no books they show an increasing relative percentage of 24% compared in those having more than 10 books in their house. Corresponding percentages for women indicate an increase in depression in older ages to a lesser extent, equally to 17.6% and 17.4% respectively. The result is opposite when adverse experience of parents drinking heavily is taken considered. This factor seems to affect especially women (odds ratio = 1.516) contrasted to men (odds ratio = 1.249). Moving in the next period of life and examining adulthood events, apparently they cause a higher increase in the relative chances of depression in older ages compared with childhood factors. Not surprisingly, experiencing a period of stress increases the relative chances of depression by 49.5% for women and by 35.1% for men. On the other hand, men who had lived a period of poor health have 41.7% higher relative chances of depression in later life while women only 32.4%. Period of financial hardship is proved the only adverse experience in middle ages that causes the lowest increase in depression levels in older people, 27.6% for males and 15% for females. Finally, education seems unimportant for men. The conclusion is not the same for women; those with low educational attainment have 20.8% higher relative chances of depression prevalence in later life in comparison to those having high educational skills. Inclusion of later life circumstances and predictors is important in tracing the factors associated with depression in older ages. The presence of two or more symptoms indicate a remarkable increase in the depression burden for both genders and to the same extent (odds ratio equal to 3.590 for men and 3.487 for women) proving the importance of somatic symptoms and the fact that they are strongly associated with mental health. In parallel, self-perceived health is associated with the potential of depression in old ages. Men with fair or poor health have 2.165 times higher odds of having this mental disorder compared to men having good, very good or excellent health and respectively, women have 2.025 higher odds. The last predictor, whether household is able to make ends meet, raises the relative chances of bad mental health in later life by 64.4% for men having to deal with economic difficulties and, correspondingly, by 49% for women.

Pseudo-R<sup>2</sup>, showing the amount of variance of the response factor that is interpretable by the independent variables indicates slightly greater explanatory power of the model referring to women (R<sup>2</sup> = 0.1728) instead of men (R<sup>2</sup> = 0.1673). Furthermore, the probability in deviance difference is equal to zero for both sexes, showing that the model is significant with the predictors that have been added.

Table 2. Odds ratios and 95% confidence intervals for childhood predictors, over the life course conditions and later life events for both sexes based on logistic regression models.

	<b>Males</b>	<b>Females</b>
<b>Childhood conditions</b>		
Childhood self-perceived health		
excellent, good and very good (ref. cat.)	1	1
fair and poor	1.309*	1.176*
	(1.151 1.488)	(1.074 1.286)
Number of books at the age of 10		
access to at least 10 books (ref. cat.)	1	1
none or very few books	1.240*	1.174*
	(1.085 1.417)	(1.066 1.291)

Parents drank heavily		
no (ref. cat.)	1	1
yes	1.249**	1.516*
	(1.035 1.508)	(1.314 1.749)
<b>Factors over the life course</b>		
Period of stress		
no (ref. cat.)	1	1
yes	1.351*	1.495*
	(1.191 1.533)	(1.365 1.639)
Period of poor health		
no (ref. cat.)	1	1
yes	1.417*	1.324*
	(1.252 1.605)	(1.212 1.446)
Period of financial hardship		
no (ref. cat.)	1	1
yes	1.276*	1.150*
	(1.125 1.448)	(1.050 1.260)
Educational attainment		
10 years or more (ref. cat.)	1	1
0-9 years	1.050 n.s	1.208*
	(0.909 1.213)	(1.094 1.335)
<b>Later life predictors</b>		
Symptoms		
less than 2 symptoms (ref. cat.)	1	1
2+ symptoms	3.590*	3.487*
	(3.164 4.073)	(3.184 3.819)
Self-Perceived Health (SPH)		
good, very good or excellent health (ref. cat.)	1	1
fair and poor	2.165*	2.025*
	(1.792 2.615)	(1.792 2.288)
Household able to make ends meet		
fairly easily or easily (ref. cat.)	1	1
great or some difficulty	1.644*	1.490*
	(1.438 1.880)	(1.357 1.637)
Age at interview	1.009*	0.998 n.s
	(1.002 1.016)	(0.993 1.003)
<b>LR chi2(24)</b>	1480.79	2818.78
<b>Prob &gt; chi2</b>	0.0000	0.0000
<b>Pseudo R2</b>	0.1673	0.1728

\* p-value<0.01 \*\* p-value<0.05 n.s non significant

#### Mediation analysis

Table 3 shows the decomposition of the total effect of later life predictors on depression into their direct and indirect parts considering adverse experiences in life time as mediators. The fact that having three key variables guides to decompose each one of them controlling for the others. So when we have symptoms as a key variable, the other two are supposed to be controls in both the full and the reduced models.

We observe that in men, all predictors have higher coefficients compared to women. In particular, the presence of more than two symptoms in male respondents increases the log odds of later life depression by 1.394. Controlling for all adverse experiences included in the model, the effect of symptoms is reduced to 1.278, leaving an indirect effect of 0.116. The conclusion is similar for women too although the values for the individual parts are lower. Furthermore, fair or poor SPH for males increases the log

odds of depression in older ages by 0.839. Controlling for adverse experiences, the effect of SPH is reduced to 0.772, leaving an indirect effect of 0.067. Regarding females the coefficients for all parts are lower with a higher divergence in values among males. Finally, whether household was able to make ends meet, having great or some difficulty increases the log odds of depression in later life by 0.560. Controlling for all adverse experiences, the effect of this factor is reduced to 0.497, leaving an indirect effect of 0.063. As regards women, whether having economic hardships does not affect them in equal or higher manner than men.

The table also informs us about the confounding ratio and confounding percentage. Concerning males, the total effect of symptoms is 1.091 times larger than the direct effect whereas the total effect of SPH is 1.087 times larger than the direct effect. Further, the 8.34% of the total effect of symptoms is due to adverse experiences while the corresponding percentage for SPH is 7.99%. The highest value of confounding percentage refers to the household ability to make ends meet for both sexes (11.22%). In other words, it is evident that the effect of this factor is more strongly mediated by adverse experiences compared to symptoms and SPH for both males and females.

Table 3. Decomposition of the total effects of later life predictors mediated by adverse experiences over the life course for males and females.

	<b>Males</b>	<b>Females</b>
<b>Later life predictors</b>		
	Coefficients	Coefficients
<b>Symptoms</b>		
Reduced Model (Total effect)	1.394	1.358
Full (Direct effect)	1.278	1.249
Difference (Indirect effect)	0.116	0.109
Confounding ratio	1.091	1.087
Confounding percentage	8.34%	8.04%
<b>Self-Perceived Health (SPH)</b>		
Reduced (Total effect)	0.839	0.747
Full (Direct effect)	0.772	0.705
Difference (Indirect effect)	0.067	0.042
Confounding ratio	1.087	1.059
Confounding percentage	7.99%	5.58%
<b>Household able to make ends meet</b>		
Reduced (Total effect)	0.560	0.449
Full (Direct effect)	0.497	0.399
Difference (Indirect effect)	0.063	0.050
Confounding ratio	1.126	1.126
Confounding percentage	11.21%	11.22%

Tables 4 and 5 show the contribution of each mediator to the indirect effect as well as the contribution of the respective mediator to the total confounding percentage separately for later life predictor for both sexes. The last column sums up to the overall confounding percentages as they are calculated in the Table 3. Decomposing the factor of symptoms for men it is evident that experiencing a period of poor health and a period of stress in adulthood or middle life cover most of the indirect effect. This is verified looking at the contribution of these mediators to the total effect in the next column. Regarding SPH in men, the result is the same as before. For the last predictor relating to financial hardship it is apparent that men are affected more from an adverse period of financial hardship or a period of poor health over the life course that makes them unable to handle financial obligations and at a lesser extent by the fact that their parents drank heavily.

Table 4. Relative contribution of the mediators to the indirect effects: males.

<b>Mediators for males</b>	<b>Contribution of each mediator to the indirect effect</b>	<b>Contribution of the confounding of the respective mediator to the total effect</b>
<b>Symptoms (key variable)</b>		
Parents drank heavily	7.00%	0.58%
Period of stress	22.11%	1.84%
Period of poor health	55.44%	4.63%
Period of financial hardship	15.45%	1.29%
		Sum=8.34%
<b>SPH (key variable)</b>		
Parents drank heavily	-1.71%	-0.13%
Period of stress	15.58%	1.24%
Period of poor health	82.19%	6.56%
Period of financial hardship	3.94%	0.32%
		Sum=7.99%
<b>Household able to make ends meet (key variable)</b>		
Parents drank heavily	12.40%	1.39%
Period of stress	1.24%	0.14%
Period of poor health	24.67%	2.76%
Period of financial hardship	61.69%	6.91%
		Sum=11.2%

Concerning women, the decomposition analysis showed that poor health and stress in adulthood contribute more to the indirect effect of symptoms. Moreover, SPH as it is reported by the respondents seems to be determined mostly by having experienced a period of poor health over the life course. Finally, dealing with financial hardship with great difficulty is indirectly affected more strongly by having experienced a period of financial hardship, stress and poor health in adulthood rather than adverse experiences in childhood.

Table 5. Relative contribution of the mediators to the indirect effects: females.

<b>Mediators for females</b>	<b>Contribution of each mediator to the indirect effect</b>	<b>Contribution of the confounding of the respective mediator to the total effect</b>
<b>Symptoms (key variable)</b>		
Parents drank heavily	11.06%	0.89%
Period of stress	35.48%	2.85%
Period of poor health	44.04%	3.54%
Period of financial hardship	9.42%	0.76%
		Sum=8.04%
<b>SPH (key variable)</b>		
Parents drank heavily	-1.43%	-0.08%
Period of stress	2.07%	0.12%
Period of poor health	98.67%	5.50%
Period of financial hardship	0.69%	0.04%
		Sum=5.58%
<b>Household able to make ends meet (key variable)</b>		
Parents drank heavily	1.93%	0.22%
Period of stress	26.91%	3.02%

Period of poor health	23.98%	2.69%
Period of financial hardship	47.18%	5.29%
		Sum=11.22%

#### 4. Discussion

The present study aimed at exploring factors and conditions through different life periods which determine depression levels in older ages. The main purpose of the study was to detect the significance of childhood factors, events in middle life and current circumstances in order to forecast later life depression for both genders. To achieve this aim cross-sectional and retrospective data were combined from SHARE database (waves 2 and 3) and logistic regression models were applied. At a later stage, factors of childhood and adulthood representing adverse experiences were analyzed with a mediation analysis technique in order to trace their direct and indirect impact on later life predictors, separately for men and women. The analysis was conducted using software of STATA, version 13.

The descriptive statistics help us shape a picture of the samples considered. More specifically, males and females have low percentages with poor health in childhood or parents drinking excessively. Further, more than half of the sample had access to 10 or more books when they were children. Moving on to adulthood, men have experienced mostly a period of stress and a period of poor health rather than a period of financial hardship while women seem to have higher percentages in all these adverse experiences compared to men. Taking into consideration concurrent factors, it is evident that women have worse health and face more financial difficulties compared to men.

The findings based on logistic regression models indicate that all factors included in the models are significant for the forecasting of later life depression for both sexes but childhood factors are the least ones. Poor childhood health and number of books at age ten affects males more than females. On the other hand, whether parents drank heavily is a condition that affects more females during their life. These results are consistent with internationally literature. For example, “number of books at the age of ten” are a measure of childhood SES (Cavapozzi *et al.*[16]; Verropoulou and Zakythinou[51]). Further, other scientists have marked the importance of childhood health as a strong predictor of poor mental health in later life (Gilman *et al.*[29]; Case *et al.*[15]; Luo and Waite[36]). Moreover, “parents drinking heavily” has been an experience of predicting bad mental health in childhood and later on (Anda *et al.*[2]; Gilman *et al.*[28]; Springer *et al.*[45]).

Conditions over the life course are very important and more significant than childhood circumstances. Experiencing a period of stress is more threatening for females regarding depression in older ages while periods of poor health and financial hardship seem to increase more the relative chances for the depression outcome regarding males. The specific conclusion does not conflict with other studies having proved that, concerning adverse experiences over the life course, they may increase the levels of depression in later life (Semeijn *et al.*[43]).

Circumstances related to concurrent events such as SPH, symptoms and economic hardships exhibit the strongest associations with depression in older ages for both genders. Previous results have shown that current financial difficulties are strongly associated with depression (Gallagher *et al.*[27]; Butterworth *et al.*[14]). Furthermore, diseases leading to poor health in later life are capable of increasing the burden of later life poor mental health (Steptoe *et al.*[48]; Jeon and Dunkle[33]).

The results of the mediation analysis indicate the extent that adverse experiences in lifetime mediate the effect of the later life predictors. It is proved that the indirect effect of concurrent socioeconomic circumstances (i.e. whether household was able to make ends meet with difficulty) is stronger than other indirect effects both for males and females. The indirect effects regarding “symptoms” and SPH through mediators of adverse experiences revealed to have higher values for men compared to women. Trying to specify which mediator causes the highest contribution to the indirect effect for each later life factor, we conclude that childhood mediators, such as whether parents drank heavily, affects mostly men regarding their ability to handle economic hardship and women regarding symptoms they suffer. Similarly, mediators in adulthood such as experiencing a period of stress, poor health and financial hardship contribute the most in various fluctuations for both genders.

## Conclusions

The present study aimed at exploring the significance of factors from different periods of life, childhood, adulthood and current life for both sexes in depression in older ages. The results indicated that childhood circumstances are the least important factors, especially for women, though they retain some significance in older ages. Adverse experiences over the life course seem to have a greater impact to the depression outcome, mainly period of stress. Period of financial hardship in women is the predictor with the smallest effect on later life depression. Current health status, represented by symptoms and SPH, is the factor that contributes the most to the presence of depressive disorder in later life for both sexes. Further, current financial hardship proves to matter mostly among the male population, though it increases the relative chances of depression to a lesser extent compared to health predictors. Regarding all factors included in the model, men in general tend to be more affected than women except for whether the respondents' parents drank heavily and having experienced a period of stress in adulthood. Taking into consideration the results from adverse experiences as mediators, it is observed that the highest percentage of the total effect for both genders is due to current financial hardship. Finally, the decomposition method for later life predictors revealed that for both sexes, experiencing a period of poor health and a period of financial hardship are the mediating factors that contribute the most to indirect effects.

## References

1. A. Agresti. *An Introduction to Categorical Data Analysis*. Wiley, New York, 1996.
2. R.F. Anda, C.L. Whitfield, V.J. Felitti, D. Chapman, V.J. Edwards, S.R. Dube, and D.F. Williamson. Adverse Childhood Experiences, Alcoholic Parents, and Later Risk of Alcoholism and Depression. *Psychiatric Services*, 53, 8, 1001{1009, 2002.
3. V. Angelini, B. Klijs, N. Smidt and J.O. Mierau. Associations between Childhood Parental Mental Health Difficulties and Depressive Symptoms in Late Adulthood: The Influence of Life-Course Socioeconomic. Health and Lifestyle Factors, *PloS One*, 2016.
4. V. Angelini and J.O. Mierau. Social and economic aspects of childhood health. *IDEAS*, 2012.
5. A.T. Beekman, J.R. Copeland and M.J. Prince. 1999. Review of community prevalence of depression in later life. *The British Journal of Psychiatry*, 174, 4, 307{311, 1999.
6. DG Blazer and CF Hybels. Origins of depression in later life. *Psychological Medicine*, 35, 9, 1241{1252, 2005.
7. A. Börsch-Supan, M. Brandt, C. Hunkler, T. Kneip, J. Korbmacher, F. Malter, B. Schaan, S. Stuck and S. Zuber. Data Resource Profile: The Survey of Health, Ageing and Retirement in Europe (SHARE). *Int J Epidemiol*, 42, 4, 992{1001, 2013.
8. A. Börsch-Supan and H. Jürges. *The Survey of Health, Ageing and Retirement in Europe*. Methodology. Mannheim Research Institute for the Economics of Ageing, Mannheim, Germany, 2005.
9. M. Brandt, C. Deindl and K. Hank. Tracing the origins of successful aging: The role of childhood conditions and social inequality in explaining later life health. *Social Science & Medicine*, 74, 9, 1418{1425, 2011.
10. R. Breen, K.B. Karlson and A. Holm. Total, direct and indirect effects in logit and probit models. *Sociological Methods & Research*, 42, 2, 164{191, 2013.
11. I. Buber and H. Engelhardt. The Association between Age and Depressive Symptoms among Older Men and Women in Europe. Findings from SHARE. *Comparative Population Studies*, 36, 1, 2011.
12. I. Buber and H. Engelhardt. Children's impact on the mental health of their older mothers and fathers: findings from the Survey of Health, Ageing and Retirement in Europe. *European Journal of Ageing*, 5, 1, 31{45, 2008.
13. S. Bulut. LATE LIFE DEPRESSION: A LITERATURE REVIEW OF LATE-LIFE DEPRESSION AND CONTRIBUTING FACTORS. *Annals of Psychology*, 25, 1, 21{26, 2009.
14. P. Butterworth, B. Rodgers and T.D. Windsor. Financial hardship, socio-economic position and depression: Results from the PATH Through Life Survey. *Social Science & Medicine*, 69, 2, 229{237, 2009.
15. A. Case, A. Fertig and C. Paxson. The lasting impact of childhood health and circumstance. *Journal of health economics*, 24, 2, 365{389, 2005.
16. D. Cavapozzi, C. Garrouste and O. Paccagnela. Childhood, schooling and income inequality. In Börsch-Supan, A., Brandt, M., Hank, K. & Schröder, M. (eds) *The Individual and the Welfare State*. Life Histories in Europe. Springer, Berlin, 31{43, 2011.
17. I. Colman and A. Ataullahjan. Life Course Perspectives on the Epidemiology of Depression. *The Canadian Journal of Psychiatry*, 55, 10, 622{632, 2010.
18. L. Crespo, B. López-Noval and P. Mira. Compulsory schooling, education and mental health: New evidence from SHARELIFE. *Economics of Education Review*, 43, 36{46, 2014.
19. L. Crowe and P. Butterworth. The role of financial hardship, mastery and social support in the association between employment status and depression: results from an Australian longitudinal cohort study. *BMJ Open*, 2016.
20. J. Currie, P. Manivong, L.L. Roos and M. Stabile. Child Health and Young Adult Outcomes. *Journal of Human Resources*, 45, 3, 517{548, 2010.

21. S. D'Alisa, G. Miscio, S. Baudo, A. Simone, L. Tesio and A. Mauro. Depression is the main determinant of quality of life in multiple sclerosis: A classification-regression (CART) study. *Disability and Rehabilitation*, 28, 5, 2006.
22. D De Vaus. *Analyzing social science data: 50 key problems in data analysis*. Sage Publications: London, 2002.
23. S V De Velde, P. Bracke and K. Levecque. Gender differences in depression in 23 European countries. Cross-national variation in the gender gap in depression. *Social Science & Medicine*, 71, 2, 305{313, 2010.
24. F. Farrokhi, N. Abedi, J. Beyene, P. Kurdyak and S. V. Jassal. Association Between Depression and Mortality in Patients Receiving Long-term Dialysis: A Systematic Review and Meta-analysis. *American Journal of Kidney Diseases*, 63, 4, 623{635, 2014.
25. A. Fiske, J.L. Wetherell and M. Gatz. Depression in Older Adults. *Annual Review of Clinical Psychology*, 5, 1, 363{389, 2009.
26. S. Frühwald, H. Löffler, R. Eher, B. Saletu and U. Baumhackl. Relationship between Depression, Anxiety and Quality of Life: A Study of Stroke Patients Compared to Chronic Low Back Pain and Myocardial Ischemia Patients. *Psychopathology*, 34, 50{56, 2001.
27. D. Gallagher, G.M. Sawa, R. Kenny and B.A. Lawlor. What predicts persistent depression in older adults across Europe? Utility of clinical and neuropsychological predictors from the SHARE study. *Journal of Affective Disorders*, 147, 192{197, 2013.
28. S.E. Gilman, I. Kawachi, G.M. Fitzmaurice and S.L. Buka. Socio-economic status, family disruption and residential stability in childhood: relation to onset, recurrence and remission of major depression. *Psychological Medicine*, 33, 8, 1341{1355, 2003.
29. S.E. Gilman, I. Kawachi, G.M. Fitzmaurice and S.L. Buka. Socioeconomic status in childhood and the lifetime risk of major depression. *International journal of epidemiology*, 31, 2, 359{367, 2002.
30. R.D. Goodwin, C.W. Hoven, R. Murison and M. Hotopf. Association Between Childhood Physical Abuse and Gastrointestinal Disorders and Migraine in Adulthood. *American Journal of Public Health*, 93, 7, 1065{1067, 2003.
31. N. Halmdienst and R. Winter-Ebmer. Long-run relations between childhood shocks and health in late adulthood - evidence from the Survey of Health, Ageing, and Retirement in Europe. *CESifo Economic Studies*, 60, 2, 402{434, 2014.
32. Hankin. *Gender Differences in Depression From Childhood Through Adulthood: A Review of Course, Causes, and Treatment*. Primary Psychiatry, 2002.
33. H.S. Jeon and R.E. Dunkle. Stress and Depression Among the Oldest-Old: A Longitudinal Analysis. *Research on Aging*, 31, 6, 661{687, 2009.
34. Y. Kamiya, M. Doyle, J.C. Henretta and V. Timonen. Depressive symptoms among older adults: The impact of early and later life circumstances and marital status. *Aging & Mental Health*, 17, 3, 349{357, 2013.
35. J. M. Linacre. Optimizing rating scale category effectiveness. *J Appl Meas*, 3, 1, 85{106, 2002.
36. Y. Luo and L.J. Waite. The impact of childhood and adult SES on physical, mental, and cognitive well-being in later life. *The Journals of Gerontology Series B: Psychological Sciences and Social Science*, 60, 2, S93{S101, 2005.
37. J. Nuyen, A.C. Volkers, P.F.M. Verhaak, F.G. Schellevis, P.P Groenewegen and G.A.M. van de Bos. Accuracy of diagnosing depression in primary care: the impact of chronic somatic and psychiatric co-morbidity. *Psychological Medicine*, 35, 8, 1185{1195, 2005.
38. E. Pakpahan, R. Hoffmann and H. Kröger. The long arm of childhood circumstances on health in old age: Evidence from SHARELIFE. *Advances in Life Course Research*, 31, 1{10, 2017.
39. E. Pakpahan, R. Hoffmann and H. Kröger. Retrospective life course data from European countries on how early life experiences determine health in old age and possible mid-life mediators. *Data in Brief*, 10, 277{282, 2017.
40. M.J. Prince, F. Reischies, A.T.F. Beekman, R. Fuhrer, C. Jonker, S.L. Kivela, B.A. Lawlor, A. Lobo, H. Magnusson, M. Fichter, H. Van Oyen, M. Roelands, I. Skoog, C. Turrina and J.R.M. Copeland. Development of the EURO-D scale-a European, Union initiative to compare symptoms of depression in 14 European centres. *The British Journal of Psychiatry*, 174, 4, 330{338, 1999a.
41. M.J. Prince, A.T.F. Beekman, DJ Deeg, R. Fuhrer, S.L. Kivela, B.A. Lawlor, A. Lobo, H. Magnusson, I. Meller, H. Van Oyen, F. Reischies, M. Roelands, I. Skoog, C. Turrina and J.R. Copeland. Depression symptoms in late life assessed using the EURO-D scale. Effect of age, gender and marital status in 14 European centres. *The British Journal of Psychiatry*, 174, 4, 339{345, 1999b.
42. Rockville. *Mental health: A report of the surgeon general*. U.S. Department of Health and Human Services, 1999.
43. E.J. Semeijn, H.C. Comijs, J.J. Kooij, M. Michielsen, A.T.F. Beekman and D.J.H. Deeg. The role of adverse life events on depression in older adults with ADHD. *Journal of Affective Disorders*, 174, 574{579, 2015.
44. B. Silverstein and A.D. Lynch. Gender Differences in Depression: The Role Played by Paternal Attitudes of Male Superiority and Maternal Modeling of Gender-Related Limitations. *Sex Roles*, 38, 7{8, 539{555, 1998.
45. K.W. Springer, J. Sheridan, D. Kuo and M. Carnes. Long-term physical and mental health consequences of childhood physical abuse: Results from a large population-based sample of men and women. *Child abuse & neglect*, 31, 5, 517{530, 2007.
46. S.A. Stansfeld, C. Clark, B. Rodgers, T. Caldwell and C. Power. Repeated exposure to socioeconomic disadvantage and health selection as life course pathways to mid-life depressive and anxiety disorders. *Social Psychiatry and Psychiatric Epidemiology*, 46, 7, 549{558, 2011.

47. M. St Clair, T. Croudace, V.J. Dunn, P.B. Jones, J. Herbert and I. M. Goodyer. Childhood adversity subtypes and depressive symptoms in early and late adolescence. *Development and Psychopathology*, 27, 3, 885{899, 2015.
48. A. Steptoe, A. Deaton and A.A Stone. Psychological wellbeing, health, and ageing. *The Lancet*, 385, 9968, 640{648, 2015.
49. M.H. Stone and B.D Wright. Maximizing rating scale information. *Rasch Measurement Transactions*, 8, 3, 386, 1994.
50. Y. Tani, T. Fujiwara, N. Kondo , H. Noma, Y. Sasaki and K. Kondo. Childhood Socioeconomic Status and Onset of Depression among Japanese Older Adults: The JAGES Prospective Cohort Study. *The American Journal of Geriatric Psychiatry*, 24, 9, 717{726, 2016.
51. G. Verropoulou and M. Zakynthinou. Contrasting concurrent and childhood socioeconomic predictors of self-rated health among older european men and women. *Journal of biosocial science*, 1{20, 2016.
52. World Health Organization. *Prevention and promotion in mental health*, Geneva, 2002.

# CHANGE TO FORWARD PROBABILITY MEASURE IN NON-HOMOGENEOUS SEMI-MARKOV CHAINS APPLIED TO CREDIT RISK

P.-C.G. VASSILIOU

*Department of Statistical Sciences University College London; Mathematics Department,  
AUTH.*

## 1. INTRODUCTORY NOTES

The various aspects of the model and most of the techniques presented in this paper are applicable to the valuation of general corporate liabilities, corporate loans etc. However, merely for presentation purposes we choose to limit the discussion to defaultable corporate bonds. A *defaultable risk* is the possibility that a counter party in a financial contract will not fulfill a contractual commitment to meet their stated obligations. We shall use the term *defaultable bond* for any kind of bond with the possibility of default. With the term *credit risk* we mean the risk associated with any kind of credit-linked event. For example, a change in the credit quality, a variation of credit spread, or the default event. *Corporate bonds* are debt instruments issued by corporations, while *State bonds* are bonds issued by states. We shall concentrate on discount bonds, that is, we assume that the bonds pay no coupons.

Assume, that the credit quality of a corporate bond is quantified and categorized into a finite number of disjoint credit rating classes. Each credit class is represented by an element of a finite set, denoted by  $\mathbb{K} = \{1, 2, \dots, k, k + 1\}$ . It is natural to distinguish a particular element  $k + 1$  of the set  $\mathbb{K}$  as formally corresponding to the default event, and to assume that credit quality 1 is the highest. The main issue of the credit migrations approach is the modelling of the transition probabilities/intensities of the migration process, under the risk-neutral, the forward and the real world probabilities. The classical way of modelling the evolution of credit migrations is in terms of either a discrete-or continuous-time homogeneous Markov chain (or conditionally homogeneous Markov chain).

In the study by Carty and Fons (1994) *J. Fixed Income* 4, 27-41, drawn from the Moody's Investors Service proprietary database, with data span from 1976 to 1993, it was established, that the duration of stay in a specific credit rating class followed the Weibull distribution. The estimation of the parameters of the particular Weibull distribution varied for each credit rating class. Thus, Carty and Fons (1994) in fact established, without stating it, that the appropriate model was not a simple Markov chain - in which case the duration of stay in each credit rating class would follow

---

*Date:* June 20, 2016.

*2000 Mathematics Subject Classification.* Primary 05C38, 15A15; Secondary 05A15, 15A18.

*Key words and phrases.* Keyword one, keyword two, keyword three.

1

---

*5<sup>th</sup> SMTDA Conference Proceedings, 12-15 June 2018, Chania, Crete, Greece*

© 2018 ISAST



the exponential distribution (or the geometric distribution in the discrete case) - but rather was a semi-Markov process.

In Vasileiou and Vassiliou (2006) *Advances in Applied Probability* 38, 171-198,  $\mathbb{G}$ -inhomogeneous discrete time semi-Markov process have been introduced to model the migration process and to study the term structure of credit risk spreads. Various stochastic aspects of semi-Markov processes related to credit risk were studied in Vassiliou et al (2013) *Linear Algebra and its Applications* 438, 2880-2903; Vassiliou (2013) *Fuzzy Sets and Systems* 223, 39-58; Vassiliou (2014) *Linear Algebra and its Applications* 450, 13-43; D' Amico et al (2010) *Methodol. Comput. Appl. Prob.* 12, 215-225; D' Amico et al (2011) *Comp. Econom.* 38, 465-481. The detailed mathematical foundation of the market theory exists in the book Vassiliou (2010) J. Wiley.

## 2. A GENERAL DISCRETE-TIME MARKET MODEL

We assume a fixed probability space  $(\Omega, \mathcal{F}, \mathbb{P})$  to model all "possible states of the market". Fix a time set  $\mathbb{T} = \{0, 1, 2, \dots, T\}$ , where  $T$  is the *trading horizon* and represents the terminal date of the economic activity being modeled, and the points of  $\mathbb{T}$  are the admissible *trading dates*. In what follows we assume, that on a general state space  $\Omega$ , the  $\sigma$ -algebra  $\mathcal{F}$  in question is finitely generated, that is, there is a finite partition of  $\Omega$  into mutually disjoint sets  $A_1, A_2, \dots, A_n$ , whose union is  $\Omega$ . Also, we demand that the probability measure  $\mathbb{P}$  on  $\mathcal{F}$  satisfies  $\mathbb{P}(A_i) > 0$  for all  $i$ . We will refer to  $\mathbb{P}$  as the *real-world probability measure*, since it is the one that represents the actual probability of events in the probability space  $(\Omega, \mathcal{F}, \mathbb{P})$ .

### The Market $M_d$ .

Assume, that the stochastic process  $\{r_t\}_{t=0}^{\infty}$  represents the interest rate of the savings account in the market and that it is adapted to the filtration  $F_t$ . The market consists of the savings account, who's value at time  $t$  we denote by

$$(2.1) \quad B_t = \prod_{u=0}^{t-1} (1 + r_u), \text{ with } B_0 = 1;$$

the default free zero-coupon bond with price process  $B(t, T)$  for  $t = 0, 1, \dots, T$ ; the  $k$  defaultable zero-coupon bonds, where  $k$  is the number of grades distinguished for defaultable bonds with price process  $D_i(t, T)$  for specific  $T \in \mathbb{T}$  and  $t = 0, 1, \dots, T$ ,  $i = 1, 2, \dots, k$ . We call the market just described the market  $M_d$  and we assume that it is perfect, i.e., all assets in market  $M_d$  are perfectly divisible and the market is frictionless.

The price process of the assets in market  $M_d$  is represented by the column vector of stochastic processes, or the  $k + 2$ -dimensional stochastic process

$$(2.2) \quad \mathbf{D}(t, T) = \left[ B_t^{(0)}, B^{(1)}(t, T), D_1^{(2)}(t, T), D_2^{(3)}(t, T), \dots, D_k^{(k+1)}(t, T) \right]^T.$$

We will use as numéraire the savings account. Then the  $k+2$ -dimensional stochastic process  $\tilde{\mathbf{D}}(t, T)$  is defined as

$$(2.3) \quad \tilde{\mathbf{D}}(t, T) = \left[ 1, \beta_t B^{(1)}(t, T), \beta_t D_1^{(2)}(t, T), \beta_t D_2^{(3)}(t, T), \dots, \beta_t D_k^{(k+1)}(t, T) \right],$$

with  $\beta_t = 1/B_t^{(0)}$ , and is called the discounted price process of the market. In the present market where the assets are  $k + 2$  we are to decide how many units of each

asset, we are to hold at each time instant. We define by

$$(2.4) \quad \boldsymbol{\delta}_t = \left[ \delta_t^{(0)}, \delta_t^{(1)}, \dots, \delta_t^{(k+1)} \right] \quad \text{for } t = 0, 1, \dots, T;$$

to be the  $k + 2$  stochastic process, with components the stochastic processes  $\delta_t^{(m)}$  representing the number of units of the asset  $m$  ( $m = 0, 1, \dots, k+2$ ), held at the time instant  $t$ . We call the stochastic process  $\boldsymbol{\delta}_t$  the *dynamic portfolio or the trading strategy* at time  $t$ . We assume that  $\boldsymbol{\delta}_t$  is *predictable*. At time  $t - 1$  the investor takes the position  $\boldsymbol{\delta}_t$ . At time instant  $t$ , the position will not be  $\boldsymbol{\delta}_t$ , due to the fact that the number of defaultable bonds held in each grade will change due to transitions in the various grades. However, at time  $t$  we know all the possible transitions, and let that the position the investor has found himself at time  $t$  is  $\hat{\boldsymbol{\delta}}_t$ . The value of the portfolio held by the investor at time  $t$  will be

$$(2.5) \quad V_t(\boldsymbol{\delta}) = \hat{\boldsymbol{\delta}}_t \mathbf{D}(t, T).$$

Now, at time  $t$  after the transitions have taken place and the new prices are known, the investor will take a new position  $\boldsymbol{\delta}_{t+1}$ . In the market  $M_d$  we provide the following definition of *self financing strategy*:

**Definition 1.** *Let the market  $M_d$  of default free bonds, defaultable bonds and a savings account. We call a trading strategy  $\boldsymbol{\delta}_t$  self financing if and only if*

$$(2.6) \quad \hat{\boldsymbol{\delta}}_t \mathbf{D}(t, T) = \boldsymbol{\delta}_{t+1} \mathbf{D}(t, T).$$

For a self financing strategy  $\boldsymbol{\delta}_t$  we have that

$$\begin{aligned} \Delta V_t(\boldsymbol{\delta}) &= \hat{\boldsymbol{\delta}}_t \mathbf{D}(t, T) - \hat{\boldsymbol{\delta}}_{t-1} \mathbf{D}(t-1, T) \\ &= \hat{\boldsymbol{\delta}}_t \mathbf{D}(t, T) - \boldsymbol{\delta}_t \mathbf{D}(t-1, T) \\ &= \boldsymbol{\delta}_{t+1} \mathbf{D}(t, T) - \boldsymbol{\delta}_t \mathbf{D}(t-1, T). \end{aligned} \quad (2.7)$$

We now provide the following definition.

**Definition 2.** *Let the market  $M_d$  of default free bonds, defaultable bonds and a savings account. We define as the gain process:*

$$(2.8) \quad G_0(\boldsymbol{\delta}) = 0 \quad \text{and} \quad G_t(\boldsymbol{\delta}) = \sum_{s=1}^t \Delta V_s(\boldsymbol{\delta}).$$

Now, using (2.7) and following the steps of the proof of Proposition 6.13 in Vassiliou (2010) we could easily show that,

**Proposition 1.** *Let the market  $M_d$  of default free bonds, defaultable bonds and a savings account. Then the trading strategy  $\boldsymbol{\delta}_t$  is self financing if and only if the following is true*

$$(2.9) \quad V_t(\boldsymbol{\delta}) = V_0(\boldsymbol{\delta}) + G_t(\boldsymbol{\delta}).$$

or for the respective discounted processes

$$(2.10) \quad \tilde{V}_t(\boldsymbol{\delta}) = V_0(\boldsymbol{\delta}) + \tilde{G}_t(\boldsymbol{\delta}).$$

We will call *admissible* strategies, the trading strategies  $\boldsymbol{\delta}_t \in \Delta$ - the set of all possible trading strategies- that are such that  $V_t(\boldsymbol{\delta}) \geq 0$  for all  $t \in \mathbb{T}$ . We will denote by  $\Delta_a$  the class of all admissible strategies for the market  $M_d$ . The physical meaning of the restrictions  $V_t(\boldsymbol{\delta}) \geq 0$  for all  $t \in \mathbb{T}$  is that certain types of short sales are not permitted, i.e., although we can still borrow certain of our assets

(have  $\delta_t^{(i)} < 0$  for some values of  $i = 1, 2, \dots, k$ ), the overall value process must remain nonnegative for each  $t$ . We are now in a position to provide two equivalent definitions of an arbitrage opportunity in the present context, see also Vassiliou (2010).

**Definition 3.** *Let the market  $M_d$  of default free bonds, defaultable bonds and a savings account. An arbitrage opportunity is an admissible strategy  $\delta_t \in \Delta_a$  such that*

$$(2.11) \quad V_0(\delta) = 0, V_t(\delta) \geq 0, \text{ for all } t \in \mathbb{T} \text{ and } \mathbb{E}_{\mathbb{P}}[V_T(\delta)] > 0.$$

**Definition 4.** *Let the market  $M_d$  of default free bonds, defaultable bonds and a savings account. An arbitrage opportunity is a self-financing strategy  $\delta_t \in \Delta$  such that*

$$(2.12) \quad \text{If } \mathbb{P}\{V_0(\delta) = 0\} = 1 \text{ and } \mathbb{P}\{V_T(\delta) \geq 0\} = 1 \text{ then } \mathbb{P}\{V_T(\delta) > 0\} > 0.$$

The market  $M_d$  is called *viable or arbitrage free* if it does not contain any arbitrage opportunities, i.e.,

$$(2.13) \quad \text{If } \delta_t \in \Delta_a \text{ with } V_0(\delta) = 0 \text{ then } V_T(\delta) = 0 \text{ almost surely.}$$

Suppose now that we are able to find on our filtered probability space  $(\Omega, \mathcal{F}, \mathbb{P})$ , the filtration of which is generated by our finite market  $M_d$ , a probability measure  $\mathbb{Q}$  equivalent with  $\mathbb{P}$ , which is such that the discounted bond price process  $\tilde{B}(t, T) = B(t, T)/B_t$ , for  $0 \leq t \leq T$  and all maturities  $T$  is a martingale under  $\mathbb{Q}$  and in relation with the filtration  $\mathcal{F}_t$ . Then we call  $\mathbb{Q}$  an equivalent martingale measure for the discounted bond price  $\tilde{B}(t, T)$ . How to construct such equivalent martingale measures is known and could be found in Pliska (1997), Elliot and Kopp (1999), Bingham and Kiesel (1998), Musiela and Rutkowski (2000) and Vassiliou (2010). The next step is to introduce the notion of an equivalent martingale measure for the market  $M_d$ . An equivalent with  $\mathbb{P}$  probability measure  $\mathbb{Q}$  is an equivalent martingale measure for the market  $M_d$ , if for any admissible strategy, i.e.,  $\delta_t \in \Delta_a$  the discounted process  $\tilde{V}_t(\delta)$  follows a martingale under the equivalent martingale measure  $\mathbb{Q}$ , with respect to the filtration  $\mathcal{F}_t$ . From Vassiliou (2010, p.214) we get the following two theorems:

**Theorem 1.** *A probability measure  $\mathbb{Q}$  on  $(\Omega, \mathcal{F}, \mathbb{P})$  equivalent with  $\mathbb{P}$  is called an equivalent martingale measure for the market  $M$  if and only if it is an equivalent martingale for the discounted asset price process  $\tilde{S}_t$ .*

**Theorem 2.** *Consider a probability space  $(\Omega, \mathcal{F}, \mathbb{P})$  and a market  $M$  with  $d$  assets and a numéraire. Also, let  $\mathcal{V}_T \in \mathfrak{B}$  be any European contingent claim in  $M$ , and consequently, since  $T$  is the settling time the filtration  $\mathcal{F}_t$  is such that  $\mathcal{F} = \mathcal{F}_T$ . If the class of all equivalent martingale measures for the discounted asset price process  $\tilde{S}_t$ , is not empty, then the market  $M$  is viable, that is, it is arbitrage-free.*

We will now prove the following theorem:

**Theorem 3.** *Let the probability space  $(\Omega, \mathcal{F}, \mathbb{P})$  and the market  $M_d$ . (i). A martingale measure  $\mathbb{Q}$  on  $(\Omega, \mathcal{F}, \mathbb{P})$  equivalent with  $\mathbb{P}$  is called an equivalent martingale measure for the market  $M_d$ , given that the default time  $\tau$  is a random variable independent of the default-free interest rate process  $r$ , conditionally upon the filtration  $\mathcal{F}$  under the martingale measure  $\mathbb{Q}$ , **if and only if** it is an equivalent martingale measure for the discounted bond price  $\tilde{B}(t, T)$ . In addition if the class of all*

equivalent martingale measures for the discounted bond price process is not empty then the market  $M_d$  is viable, that is, it is arbitrage free. (ii). If the class of all equivalent martingale measures for the discounted bond price process is not empty, then there exists the forward martingale measure which is an equivalent martingale measure for the market  $M_d$ , **if and only if** it is an equivalent forward martingale measure for the discounted bond price  $\tilde{B}(t, T)$  and then the market  $M_d$  is viable.

In here in the second part the independence assumption for  $\tau_i$ , is relaxed. Define the forward probability measure by the Randon-Nikodým derivative

$$(2.14) \quad \frac{d\mathbb{Q}_T}{d\mathbb{Q}} = \frac{1}{B(0, T) B_T} = \eta_T, \quad \mathbb{Q}\text{-almost surely,}$$

where  $\eta_T$  the  $\mathcal{F}_T$ -measurable random variable is strictly positive  $\mathbb{Q}$ -almost surely. Notice that the above Randon-Nikodým derivative, when restricted to the  $\sigma$ -algebra  $\mathcal{F}_t$  satisfies,

$$(2.15) \quad \eta_t := \frac{d\mathbb{Q}_T}{d\mathbb{Q}} \Big|_{\mathcal{F}_t} = \mathbb{E}_{\mathbb{Q}} \left( \frac{1}{B(0, T) B_T} \Big|_{\mathcal{F}_t} \right) = \frac{B(t, T)}{B(0, T) B_T}.$$

The power in the applications of the condition of equivalent martingale measures lies in the fact, that it is more convenient mathematically to search for equivalent measures, under which the given process  $\tilde{B}(t, T)$  is a martingale, than having to show that no arbitrage opportunities exist for market  $M_d$ . However, as we shall see in the following theorem, the condition of the existence of an equivalent martingale measure for the discounted asset price, is far more important since it is also necessary. The following theorem could be proved following the steps of the proof of Theorem 6.26 in Vassiliou (2010) J. Wiley p.217.

**Theorem 4.** *Let the probability space  $(\Omega, \mathcal{F}, \mathbb{P})$  and the market  $M_d$ . (i). The market  $M_d$  is viable **if and only if** there exists an equivalent martingale measure for the discounted bond price  $\tilde{B}(t, T)$ , given that the default time  $\tau$  is a random variable independent of the default-free interest rate process  $r$ , conditionally upon the filtration  $\mathcal{F}$  under the martingale measure  $\mathbb{Q}$ . (ii). The market  $M_d$  is viable **if and only if** there exists an equivalent martingale measure from which we construct the forward probability measure and under which the discounted bond price  $\tilde{B}(t, T)$  is a martingale.*



# Models for time series whose trend has local maximum and minimum values

Norio Watanabe<sup>1</sup>

Department of Industrial and Systems Engineering, Chuo University, Tokyo, Japan  
(E-mail: watanabe@indsys.chuo-u.ac.jp)

**Abstract.** Economical time series includes a trend usually and it becomes important to capture a trend adequately. Typical examples are series of stock prices or stock indices. In many cases trends show repeated up-and-down behavior. For such time series it is expected to predict time points of local maxima or minima and values themselves, and some prediction methods have been proposed. However, it is not clear whether those methods are appropriate or not. In this study we propose two kinds of models for time series whose trend has local maximum and minimum values. The first is a trend stationary model. The second is a random walk type model. Proposed models provide a basis for discussion about appropriateness of estimation and prediction methods. Simulation studies suggest that estimation and prediction is meaningless in some cases when time series includes a stochastic trend even though the mean value function has local maximum and minimum values. A procedure for estimating points of local maxima and minima is also proposed based on a piecewise linear regression by using a fuzzy trend model.

**Keywords:** Stock index, Peak and trough, Random walk, Piecewise linear regression, Fuzzy trend model.

## 1 Introduction

It is important to capture a trend adequately when time series includes it. One of typical patterns of trends is a repeated up-and-down movement. Examples are series of stock prices or stock indices. In this note we consider the problem on local maximum and minimum in such a trend. Some methods have been proposed for estimation of local maximum and minimum values (see [5], for example). However, it is not clear whether those methods are appropriate or not, since the property or model of time series is not stated clearly. In this study we propose two kinds of models for time series whose trend has local maximum and minimum values. The first is a trend stationary model and the second is a random walk type model. In both model we assume that the mean value function is continuous piecewise linear. We can discuss the problem on estimation of local maximum and minimum values based on proposed models.

From simulation studies we can say that a basis of estimation for random walk type models is weak usually, since there is no direct relationship between up-and-down behavior of time series and local maximum and minimum values

---

<sup>1</sup>*5<sup>th</sup> SMTDA Conference Proceedings, 12-15 June 2018, Chania, Crete, Greece*

of the mean value function. On the other hand it is reasonable to estimate local maximum and minimum values of trends for trend stationary models. A procedure for estimating points of local maxima and minima is also proposed based on a piecewise linear regression by applying a fuzzy trend model. The piecewise linear function can be used for approximation in many cases, though it has a restricted form. One advantage of the usage of the piecewise linear function is that an estimation result shows point of peaks and troughs directly.

## 2 Models

Let  $\{x_n|n = 1, \dots, N\}$  be an observed time series, whose trend has local maximum and minimum values. We consider two models for  $\{x_n\}$ . The first is a mean stationary or trend stationary model and the second is a random walk type model.

**Model 1** (Trend stationary model).

$$x_n = \mu_n + v_n, \quad (1)$$

where  $\{v_n\}$  is a zero mean stationary process, and  $\{\mu_n\}$  is the mean value function of  $\{x_n\}$  given by the recursion:

$$\mu_n = \mu_{n-1} + d_n, \quad (n = 1, \dots, N) \quad (2)$$

with the initial value  $\mu_0 = d_0$ . The series of constants  $\{d_n\}$  is defined as follows.

Let  $\{u(k)|k = 1, 2, \dots\}$  be a given series satisfying

$$u(k)u(k-1) < 0, \quad (3)$$

and  $S_n = (s_{1n}, s_{2n})$  be a state variable determined stochastically by the equation:

$$S_n = \begin{cases} S_{n-1} & \text{with prob. } g(n - s_{2,n-1}) \\ (1 + s_{1n}, n) & \text{with prob. } 1 - g(n - s_{2,n-1}) \end{cases} \quad (4)$$

for  $n \geq 2$ , where  $S_1 = (1, 0)$ , and  $g(t)$  is a monotonically decreasing function such that  $g(1) = 1$ ,  $g(t) \geq 0$  for  $t \geq 1$ . Then  $d_n$  is given by

$$d_n = u(s_{1n}). \quad (5)$$

The series  $\{d_n\}$  is stochastic but we consider under the condition that  $\{d_n\}$  is given. The process  $\{u(k)\}$  can also be stochastic as shown in an example in Section 3. In this model the mean value function  $\mu_n$  is the trend, and the trend is continuous piecewise linear. The assumption (3) means that the local maximum and minimum values appear by turns. In other words, the trend shows the up and down behavior. Note that the assumption (3) can be weakened or removed.

The first component of the state variable,  $s_{1n}$ , means the number of local linear trends. That is,  $\mu_n$  is on the  $s_{1n}$ -th straight line. The second component

$s_{2n}$  is the time point when the  $s_{1n}$ -th local linear trend begins. The time point of local maximum or minimum values is given by

$$T_k = \min_{n \in \{n | s_{1n} = k\}} n - 1, \quad (k = 1, 2, \dots) \quad (6)$$

and we put  $T_0 = 0$ .

An alternative approach for modeling drift term  $\{d_n\}$  is to introduce stochastic structure on duration of drift term. However, this is not natural, since the events in future have to be predetermined.

**Model 2** (Random walk type model).

$$x_n = x_{n-1} + d_n + e_n, \quad (n = 1, 2, \dots) \quad (7)$$

where  $d_n$  is a series of constants defined in Model 1, and  $\{e_n\}$  is a zero mean i.i.d. process with the variance  $\sigma^2$ . We assume that the initial value  $x_0$  is zero for simplicity.

In Model 2 the expectation of  $x_n$  is identical to  $\mu_n$  in Model 1 under the condition that  $\{d_n\}$  is given. That is,  $E(x_n | \{d_m\}) = \mu_n$ .

We show two examples of monotone function  $g(t)$  ( $t \geq 1$ ), where  $1 - g(t)$  is the probability of occurrence of the structural change in local linear trends. The first example is the exponential function:

$$g(t) = \rho^{t-1} \quad (8)$$

where  $\rho < 1$ . The second is the cosine type function:

$$g(t) = 1 / \left( 1 + \left( \frac{t-1}{m} \right)^{2b} \right), \quad (9)$$

where  $m$  is a positive constant and  $b$  is a positive integer. We call (9) the cosine type probability, since we can show the relation:

$$1 / \left( 1 + \left( \frac{t-1}{m} \right)^{2b} \right) = \left( 1 + \cos \left( 2 \tan^{-1} \left( \frac{t-1}{m} \right)^b \right) \right) / 2. \quad (10)$$

Examples of the cosine type probability are illustrated in Fig. 1 for  $b = 1, 2, \dots, 9$  and  $m = 10, 15, 20, \dots, 40$ . The most left curve is for  $m = 10$  and the most right is for  $m = 40$  in each graph.

### 3 Simulation

In this section we show examples of two models.

The same sequence  $d_n$  is used in these examples. Let  $y(k)$  be independently distributed to the chi-square distribution with the degree of freedom  $d_F$ . We

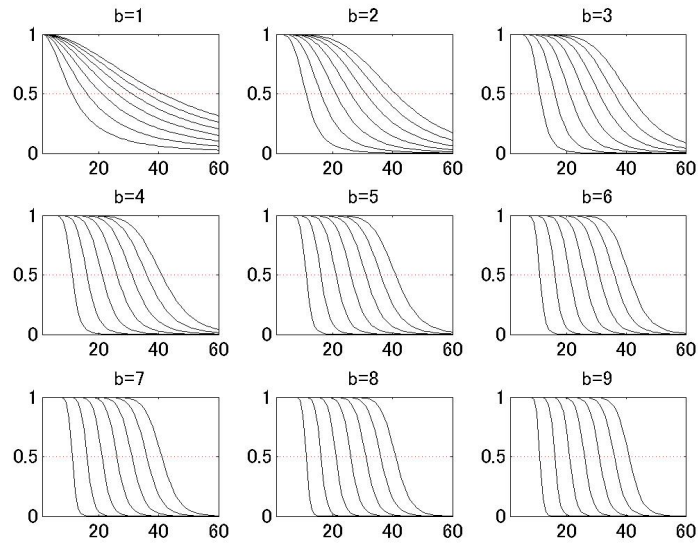


**Fig. 1.** Examples of  $g$ .

set  $u(k) = \pm 0.1y(k)/d_F$  where  $d_F = 10$ . As the monotone function  $g$  we adopt the cosine type probability with  $m = 20$  and  $b = 2$ .

In Model 1 we assume that the stationary process  $\{v_n\}$  is the Gaussian white noise with the variance  $0.4^2$ . Fig. 2 demonstrates an example of time series generated by Model 1, where  $N = 200$ . The trend  $\mu_n$  is shown by the bold piecewise linear line.

In Model 2 we assume that white noise  $\{e_n\}$  is Gaussian with the variance  $0.4^2$ . An example of time series obtained by Model 2 is shown in Fig. 3. The mean value function shown by the bold piecewise linear line is the same as the trend in Fig. 2.

For Model 1 it is reasonable to estimate local maximum and minimum values of the trend, since these values are local maxima and minima of the mean value function.

On the other hand validity of estimation for random walk type models is weak, since there is no direct relationship between up-and-down behavior of time series and local maximum and minimum values of the mean value function usually as Fig. 3 shows. The estimated peaks and troughs have no meaning, unless the variance of the white noise is relatively small compared with the range of fluctuation of  $d_n$ . As a result it is difficult to show validity of prediction methods for peaks and troughs in some cases when a stochastic trend is included in time series. It is another problem whether a peak detection method for time series from Model 2 is useful or not in practical analysis apart from the theoretical aspect.

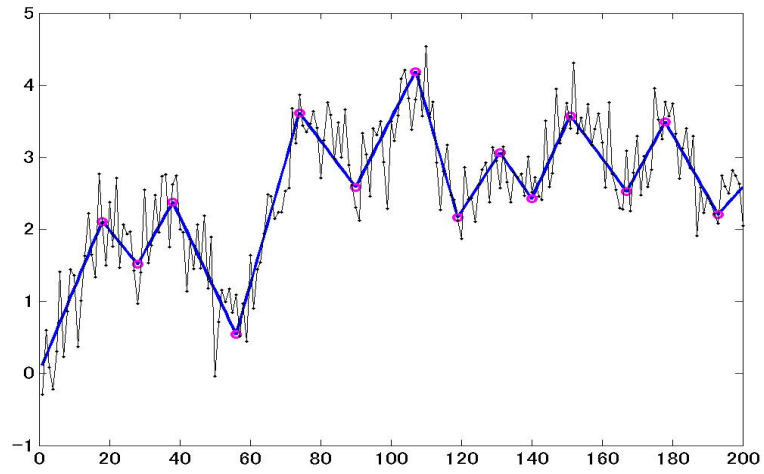


**Fig. 2.** Example of trend stationary model.

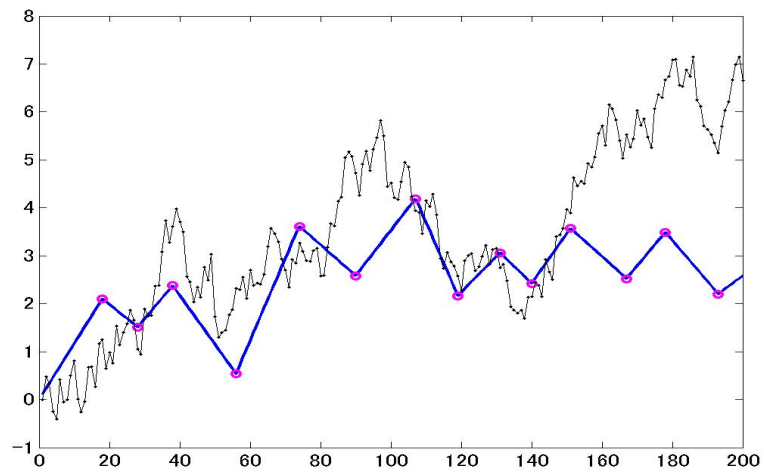


**Fig. 3.** Example of random walk type model.

## 4 Estimation

In this section we propose a procedure for identification and estimation of a trend in Model 1 for the case when no information on kink points is available. The kink point means the point where a structural change occurs in local linear trends. This procedure can be applied to time series from Model 2. However, it is difficult to evaluate the validity of the procedure for Model 2 as was stated in Section 3.

We apply the piecewise linear regression, since the trend is assumed to be continuous piecewise linear. However, it is not easy to identify the piecewise linear function, when the number of segments is unknown. The piecewise linear regression can be achieved by the  $\ell_1$  trend filtering method ([3]) without information on kink points, but it is not clear how to choose the regularization parameter. Thus we adopt another approach and introduce an identification procedure by applying the simple fuzzy trend model for pre-estimation. General fuzzy trend models are discussed by Watanabe and Watanabe ([6]), for example.

The outline of our procedure is as follows:

**Identification procedure.**

- Step 1. fitting of a fuzzy trend model
- Step 2. detection of peaks and troughs
- Step 3. continuous piecewise linear regression
- Step 4. modification of kink points

The fuzzy trend model used here is a one-parameter model for scalar time series based on the fuzzy if-then rule:

$$R_\ell : \text{ If } n \text{ is } A_\ell, \text{ then } \mu_n(\ell) = \alpha_\ell,$$

for  $\ell = 1, 2, \dots, L$ , where the number of rules  $L$  is determined by the width parameter of the membership function of  $A_\ell$ . We use the membership functions illustrated in Fig. 4. In Fig. 4 the width parameter is 12. The width parameter of  $A_\ell$  have to be set smaller for applying to the piecewise linear regression.

Let  $\{\hat{\alpha}_\ell | \ell = 1, \dots, L\}$  be the estimate of the latent process  $\{\alpha_\ell\}$  in the fuzzy trend model. In Step 2, peaks and troughs are detected by checking the change of  $\hat{\alpha}_\ell$ . We judge that the change occurs if  $|\hat{\alpha}_\ell - \hat{\alpha}_{\ell-1}| > t_\alpha S_\alpha$ , where  $t_\alpha$  is a given positive constant and  $S_\alpha$  is the sample standard deviation of  $\{\hat{\alpha}_\ell\}$ . Then the time of kink points in the piecewise linear function is pre-estimated.

The piecewise linear regression is easy, if the time of kink points in the piecewise linear function are given (cf. [1], [2]).

Finally time points are determined among the neighborhood of pre-estimated points by minimizing the mean squared error of piecewise linear regression. Minimization is achieved sequentially, since it is difficult to re-estimate for all combination of time points.

Figs. 5-6 show an example of the estimated trend by applying the proposed method. In this example we use the value 6 as the width parameter in the fuzzy trend model. Moreover we set  $t_\alpha = 0.2$  in Step 2. The estimated trend is shown by the bold line in Fig. 5, where time series is the same as Fig. 2. The pre-estimated, re-estimated, and true trends are illustrated in Fig. 6

## 5 Concluding remarks

We proposed two models whose mean value functions are piecewise linear. We can discuss validity of estimation methods for peaks and troughs based on

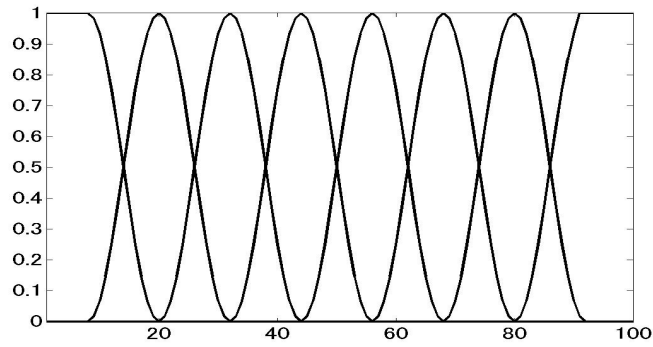


**Fig. 4.** Membership functions in fuzzy trend model.

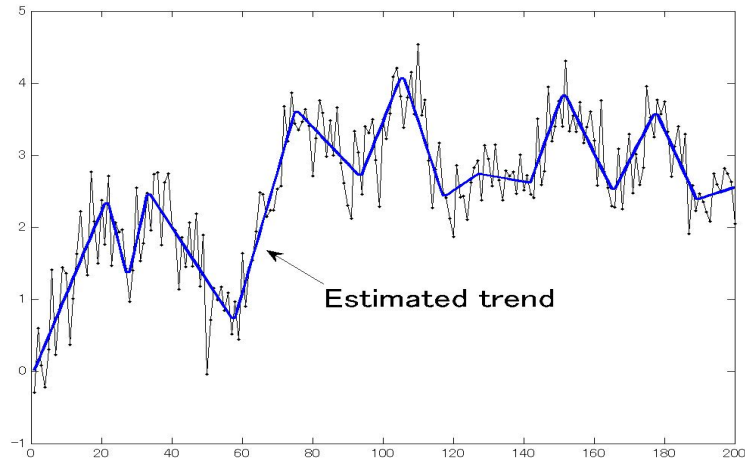


**Fig. 5.** Example of estimated trend.

the proposed models. As a result the validity is doubtful in some cases when stochastic trends are included. Thus it is important to investigate the property of observed time series in practical analysis. This is a problem of statistical hypothesis test or model selection.

Moreover we proposed an identification method for peaks and troughs in the trend. The example in Section 4 shows that the proposed method is applicable. When the constant  $t_\alpha$  should be selected by data, it can be determined by an information criterion if some candidates of  $t_\alpha$  are given. However, further simulation studies are required for verification.

After peaks and troughs are estimated, inference on  $\{d_n\}$  and  $\{u(k)\}$ , from which a trend is generated, becomes possible. For example, prediction of the time point and height of the next peak can be considered.

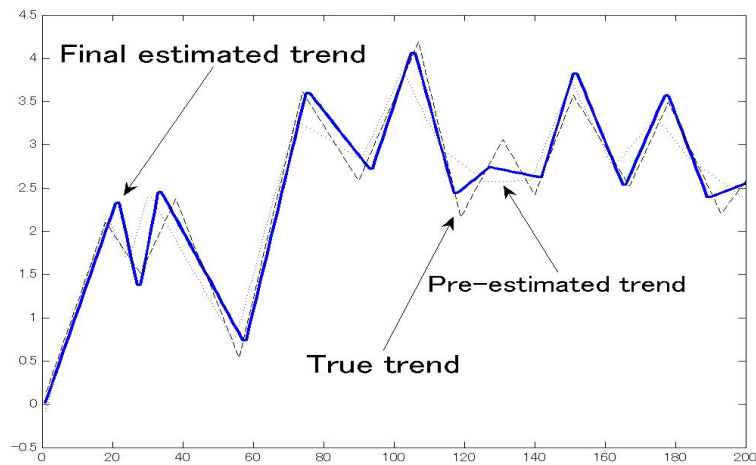


Fig. 6. True and estimated trends.

## References

1. N. R. Draper and H. Smith. *Applied Regression Analysis*. (3rd ed.) Wiley, 1998.
2. A. R. Gallant and Wayne A. Fuller. Fitting segmented polynomial regression models whose join points have to be estimated. *JASA*, 68, 341, 144–147, 1973.
3. S.-J. Kim et al.  $\ell_1$  trend filtering. *SIAM Review*, 51, 2, 339–360.
4. M. Kuwabara and N. Watanabe. Financial time series analysis based on a fuzzy trend model. (in Japanese) *J. of Japan Society for Fuzzy Theory and Intelligent Informatics*, 20, 2, 244–254, 2008.
5. T. Suzuki and M. Ota. Nonlinear prediction for top and bottom values of time series. (in Japanese) *The Information Processing Society of Japan, Transactions on Mathematical Modeling and its Applications*, 2, 1, 123–132, 2009.
6. E. Watanabe and N. Watanabe. Weighted multivariate fuzzy trend model for seasonal time series. in *Stochastic Modeling, Data Snalysis and Statistical Applications* (L. Filus et al. eds.) 443–450, ISAST, 2015.

# The Impact of Definitions in Classifying the Employed, Unemployed and Inactive when Comparing Measurements from Different Sources

Aggeliki Yfanti<sup>1</sup>, Catherine Michalopoulou<sup>2</sup>, and Stelios Zachariou<sup>3</sup>

<sup>1</sup> Ph.D. Candidate, Department of Social Policy, Panteion University of Social and Political Sciences, Athens, Greece

(E-mail: [aggelikiyfanti@panteion.gr](mailto:aggelikiyfanti@panteion.gr))

<sup>2</sup> Professor of Statistics, Department of Social Policy, Panteion University of Social and Political Sciences, Athens, Greece

(E-mail: [kmichal@panteion.gr](mailto:kmichal@panteion.gr))

<sup>3</sup> Head of the Labour Force Division, Hellenic Statistical Authority, Greece

(E-mail: [s.zachariou@statistics.gr](mailto:s.zachariou@statistics.gr))

**Abstract.** In all large-scale sample surveys and the census, gender, age, marital status, educational and occupational variables are included as background variables to provide information necessary for defining subpopulations and “contexts in which respondents’ opinions, attitudes, and behavior are socio-economically embedded”. Because these background variables play such a central role in social research, establishing their measurement’s cross-national and overtime comparability is essential and consequently, international classifications have been developed. However, in the case of the employment status, i.e. one of the occupational variables, all large-scale sample surveys and the census use a perception question for its measurement whereas the European Union Labour Force Survey (EU-LFS) is using a synthesized economic construct according to the International Labour Organization (ILO) conventional definitions of the employed, unemployed and inactive. In this paper, we investigate the classification issues arising from these two different measurements. The analysis is based on the 2008-2014 EU-LFS annual datasets and the 2001 and 2011 Integrated Public Use Microdata Series (IPUMS)-International census datasets for Eastern (Hungary, Poland, Romania) and Southern (Greece, Portugal and Spain) Europe. The results are reported for the age group 15-74 so as to allow for comparability with the ILO conventional definition of unemployment.

**Keywords:** Employment status, ILO, EU-LFS, IPUMS-International, Eastern Europe, Southern Europe.

## 1 Introduction

In all social large-scale sample surveys and the census, gender, age, marital status, educational and occupational variables are included as background variables to provide information necessary for defining subpopulations and

---

*5<sup>th</sup> SMTDA Conference Proceedings, 12-15 June 2018, Chania, Crete, Greece*

© 2018 ISAST



“contexts in which respondents’ opinions, attitudes, and behavior are socio-economically embedded” (Braun and Mohler [1: 115]; see also Hoffmeyer-Zlotnik [10, 11]; Wolf and Hoffmeyer-Zlotnik [14]). Background variables are considered “to provide the backbone of statistical analyses” (Braun and Mohler [1: 114]) in national and cross-national sample surveys. Because these background variables play such a central role in social research, establishing their measurement’s cross-national and overtime comparability is essential and consequently, international classifications have been developed. In social sample survey research, the most widely used such classifications are the International Standard Classification of Education (ISCED) developed by UNESCO, the International Standard Industrial Classification of All Economic Activities (ISIC) developed by the United Nations Statistics Division and the International Standard Classification of Occupations (ISCO) developed by the International Labour Organization (ILO). However, in the case of the employment status, i.e. one of the occupational background variables, all social large-scale sample surveys and the census use a perception question for its measurement whereas the European Union Labour Force Survey (EU-LFS) is using a synthesized economic construct according to the ILO conventional definitions of the employed, unemployed and inactive. As we have mentioned in previous work (Yfanti *et al.* [15]), since 2006, Eurostat has included in the annual EU-LFS datasets such a perception question but in 2008 changed the reference period for this measurement. In this paper, we investigate the classification issues arising from these two different measurements when comparing data from different sources.

The EU-LFS is a set of independent national multipurpose surveys conducted by the respective statistical offices of the member countries. The EU-LFS is designed centrally to comply with the demanding prerequisites for cross-national comparability. The Integrated Public Use Microdata Series (IPUMS)-International (Minnesota Population Center [13]) provide harmonised census data by “the creation of a desired degree of comparability between statistics of different countries” (Ehling [3: 17]). However, if we were to compare data from these two data sets, we need first to investigate their comparability.

In 1994, Kish [12: 168] defined the following seven major aspects of the sample survey design that should be considered for comparability: definition of concepts, variables and populations; survey design and methods of measurements; substantive analysis; weighting procedures; statistical analysis; sample design and selection; sizes (and fractions) of samples, also of the population. According to Kish [12], similarity and standardization of the survey aspects (definition of concepts, variables, populations, methods of measurement and data collection) are essential to avoid biases in comparisons, though admittedly difficult. In contrast, flexibility in sampling designs and sizes, to reduce variances, is permissible as long as a probability selection method is assumed (Kish [12]).

Both the EU-LFS and the IPUMS-International use the same broad survey population definition and implement a probability selection method (Eurostat [4, 5, 7]; Minnesota Population Center [13]) and in this respect the prerequisites for comparability are satisfied. However, as mentioned before, because different definitions are used for the employment status the comparability of these measurements needs to be thoroughly investigated. The analysis is based on the 2008-2014 EU-LFS annual datasets and the 2001 and 2011 Integrated Public Use Microdata Series (IPUMS)-International census datasets (Minnesota Population Center [13]) for Eastern (Hungary, Poland, Romania) and Southern (Greece, Portugal and Spain) Europe. The results are reported for the age group 15-74 so as to allow for comparability with the ILO conventional definition of unemployment.

## 2 Method

### 2.1 The comparability of definitions

In the EU-LFS datasets (Eurostat [6]), as mentioned in previous work (Yfanti *et al.* [15]), the employment-activity status (labelled as ILOSTAT) is a variable derived from a synthesized economic construct according to the ILO conventional definitions of the employed, unemployed and inactive. For its measurement, the EU-LFS distinguishes the population into two major categories, the economically active and inactive. The economically active population is comprised by the employed and the unemployed. According to Eurostat [7], as employed are defined “persons aged 15 years and over who, during the reference week performed work, even for just one hour a week, for pay, profit or family gain or who were not at work but had a job or business from which they were temporarily absent because of something like, illness, holiday, industrial dispute or education and training”. As unemployed are considered “persons aged 15-74 who were without work during the reference week, but who are currently available for work and were either actively seeking work in the past four weeks or had already found a job to start within the next three months”. Inactive are “those classified neither as employed nor as unemployed” (Eurostat, [7]). It should be noted that, the EU-LFS definitions of the employment status allow the use as an extra, separate category the compulsory military service.

Furthermore, in the annual EU-LFS datasets (Eurostat [6]), a perception question is used for the measurement of the employment status (labelled as MAINSTAT) with eight response categories which may be classified as follows: “Carries out a job or profession, including unpaid work for a family business or holding, including an apprenticeship or paid traineeship, etc.” (employed); unemployed; “pupil, student, further training, unpaid work experience” (inactive); “In retirement or early retirement or has given up business” (inactive); “Permanently disabled” (inactive); “In compulsory military

service” (separate category); “Fulfilling domestic tasks” (inactive); “Other inactive person” (inactive). The reference period for this variable is the previous week.

The EU-LFS provide cross-nationally and overtime comparable measurements of these two variables. It should be mentioned, that in the samples of the six countries under investigation, there is no data for the extra category of compulsory military service.

The IPUMS-International datasets provide the general version of the harmonised employment status measurement (labelled as EMPSTAT) which is compiled from the respective perception question with three response categories: employed, unemployed and inactive. There is no category in the IPUMS-International datasets for compulsory military service. Also, information for the comparability of this measurement is presented for each country. The definitions used for the microdata of 2001 and 2011 are comparable for Hungary. In the case of Poland (2002), the persons who were classified as economically inactive yet farming on one's own farm or plot of land (with no agriculture production or in subsistence farming) were considered as inactive. In the cases of Romania (2002, 2011) and Greece (2001, 2011), the reference period for this variable is the previous week. In the case of Portugal (2001, 2011), all samples consider labour force participation as one hour of paid work or 15 hours of unpaid work. Also, the 2011 sample includes a category for persons at work on a family holding, working at least 15 hours per week and omits a category for military service. In the case of Spain (2001, 2011), the data is largely comparable, with some category availability differences (Minnesota Population Center [13]).

Although the same labelling is used for the response categories of these three variables classifying the respondents into the three categories of the employed, unemployed and inactive, it should be kept in mind that as indicated by their definitions they are not strictly comparable according to the prerequisite for comparability of standardized measurements [Kish, 12]. Furthermore, in order to allow for comparability with the ILO conventional definition of unemployment, the results would be reported for the age group 15-74.

## **2.2 Statistical analyses**

The analysis was based on the 2008-2014 EU-LFS annual datasets and the 2001 and 2011 IPUMS-International census datasets for Eastern (Hungary, Poland, Romania) and Southern (Greece, Portugal and Spain) Europe. In the cases of Poland and Romania, the IPUMS-International provided data of the 2002 censuses. In the case of Poland, because there were no available data from IPUMS-International for 2011, census data were used instead which is provided online by Eurostat [8].

The three variables used for the analyses were the ILOSTAT (EU-LFS), the recoded MAINSTAT (EU-LFS) and the EMPSTAT (IPUMS-International). In

the first step of the analysis, the frequency distributions of these measurements were investigated in great detail. Then the analysis focused on obtaining the social and demographic “profile” of these three different measurements of the employment status. The “profiling” was based on the following social and demographic characteristics: gender (male-female); age (15-24, 25-34, 35-44, 45-54, 55-64 and 65-74); marital status (single, married, and other, i.e. widowed, divorced or legally separated); and highest level of educational attainment (primary, secondary and tertiary). For the measurement of the highest level of educational attainment, the recoded version of the variable HATLEVEL was used from the EU-LFS (Eurostat [6]). The definition of this variable is based on the ISCED97 up to 2013 and according to ISCED2011 from 2014 onwards. As for the education, in the EU-LFS, a recoded variable of HATLEVEL (level of educational attainment) was used, which is based on ISCED97 up to 2013 and ISCED2011 from 2014 onwards. Also, the recoded variable EDATTAIN (educational attainment, international recode – general version) from IPUMS-International was used, which is defined in the following four response categories: less than primary education completed; primary education completed; secondary education completed; university education completed.

### 3 Results

In Figures 1 to 6, the IPUMS-International and EU-LFS self-received measurement of their employment status as they compare to the ILO conventional definitions (EU-LFS) is presented for Eastern (Hungary, Poland and Romania) and Southern (Greece, Portugal and Spain) Europe, respectively.

As shown in Figure 1, the IPUMS-International (2001) and EU-LFS (2008-2010) and IPUMS-International (2011) and EU-LFS (2011-2014) frequency distributions of Hungarians’ perceptions of their employment status differ only slightly. However, both perception measurements differ by a 2.0 to 3.0% increase in the measurement of the unemployed as compared to the ILO conventional definition.

In the case of Poland (Figure 2), the IPUMS-International (2002) frequency distribution of the self-perceived employment status differs markedly from the respective EU-LFS (2008-2010) frequency distributions (by more than a 7.8% for the employed) and the ILO conventional definitions. However, the Census (2011) and EU-LFS (2011-2014) frequency distributions of Polish perceptions of their employment status differ only very slightly. The EU-LFS perception measurement of the unemployed is increased by 1.5 to 1.9% as compared to the ILO conventional definition.

In the case of Romania (Figure 3), the IPUMS-International (2002) frequency distribution of the self-perceived employment status differs – but not as markedly as in the case of Poland – from the respective EU-LFS (2008-

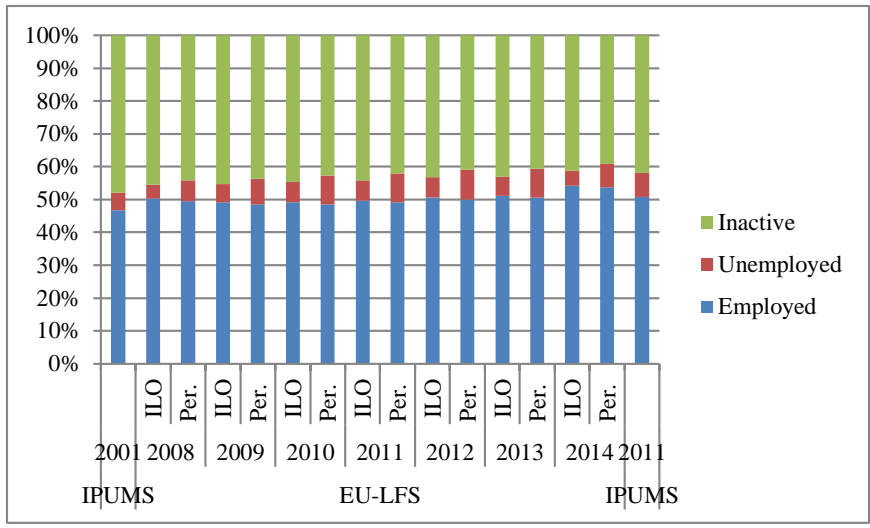


Fig. 1. Employment status according to IPUMS-International and the EU-LFS ILO and perception question: Hungary

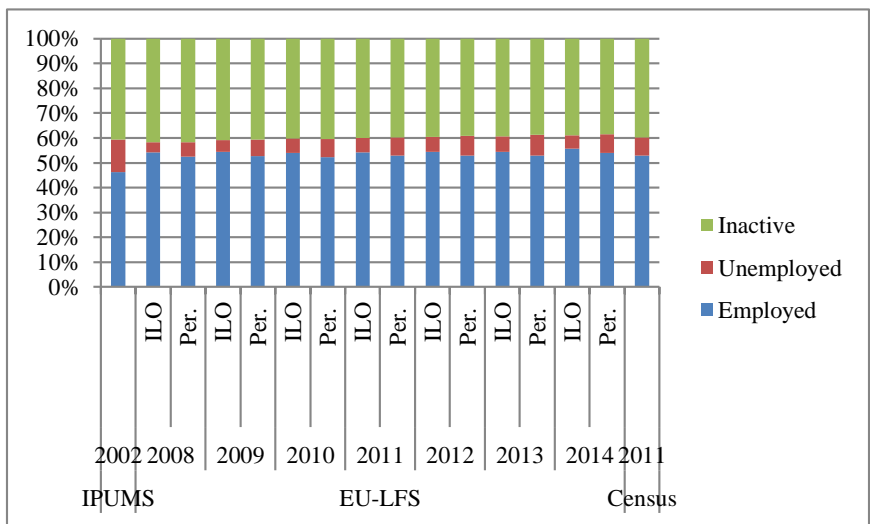


Fig. 2. Employment status according to IPUMS-International and the EU-LFS ILO and perception question: Poland

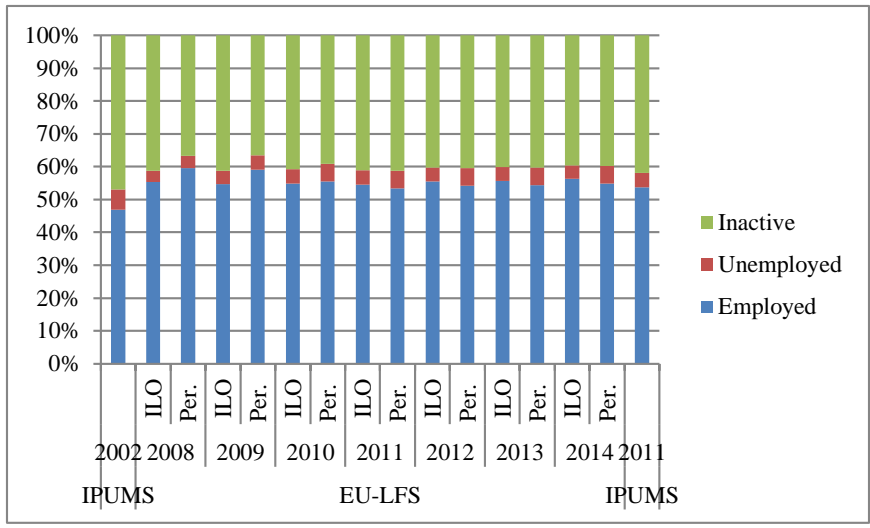


Fig. 3. Employment status according to IPUMS-International and the EU-LFS ILO and perception question: Romania

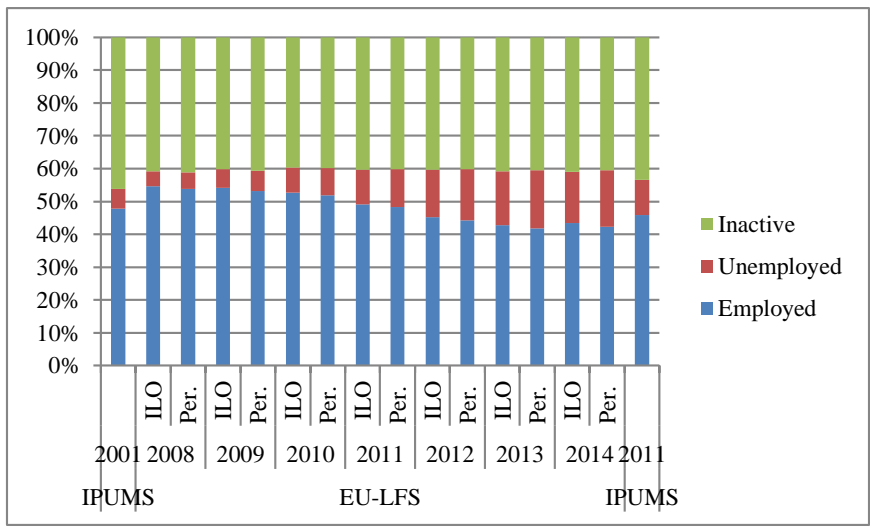


Fig. 4. Employment status according to IPUMS-International and the EU-LFS ILO and perception question: Greece

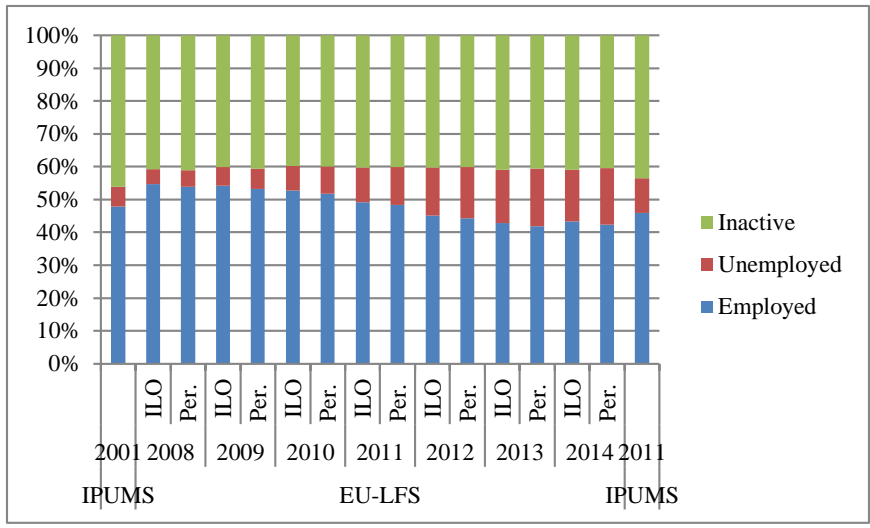


Fig. 5. Employment status according to IPUMS-International and the EU-LFS ILO and perception question: Portugal

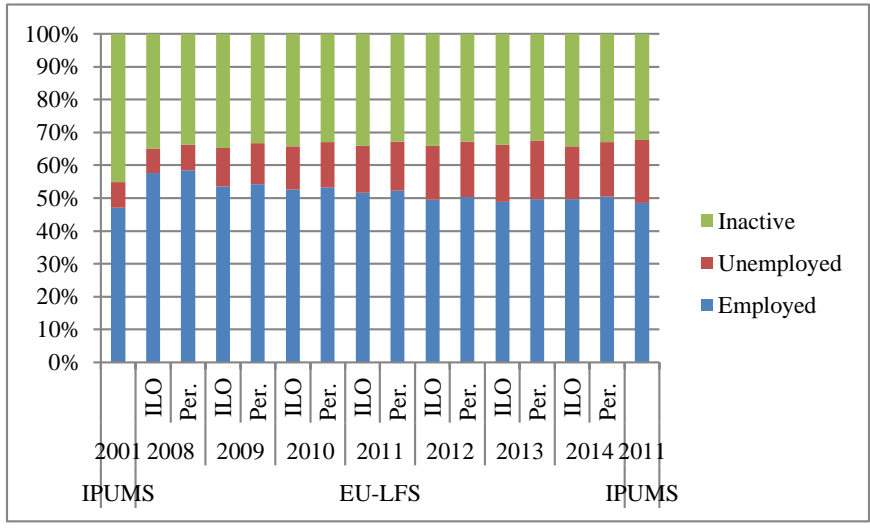


Fig. 6. Employment status according to IPUMS-International and the EU-LFS ILO and perception question: Spain

2010) frequency distributions and the ILO conventional definitions. However, the IPUMS-International (2011) and EU-LFS (2011-2014) frequency distributions of Romanian perceptions of their employment status differ only very slightly. The EU-LFS perception measurement of the unemployed is increased by 0.3 to 1.3% as compared to the ILO conventional definition. Furthermore, an increase of 4.3 to 4.4% is noted in the EU-LFS perception measurement of the employed for 2008 and 2009 as compared to the respective ILO conventional definition.

As shown in Figure 4, the IPUMS-International (2001) and EU-LFS (2008-2010) and IPUMS-International (2011) and EU-LFS (2011-2014) frequency distributions of Greeks' perceptions of their employment status differ. The differences for the employed ranged from 3.9 to 5.9% for the IPUMS-International (2001) and EU-LFS (2008-2010) and 1.7 to 3.6% for the IPUMS-International (2011) and EU-LFS (2011-2014). Slight differences are indicated for the unemployed ranging from 0.3 to 0.7% for the IPUMS-International (2001) and EU-LFS (2008-2010). However, these differences are more marked for the IPUMS-International (2011) and EU-LFS (2011-2014) ranging from 1.0 to 7.4%. Furthermore, both perception measurements increase slightly by a 0.3 to 1.7% the measurement of the unemployed as compared to the ILO conventional definition.

In the case of Portugal (Figure 5), the IPUMS-International (2001) and EU-LFS (2008-2010) and IPUMS-International (2011) and EU-LFS (2011-2014) frequency distributions of Portuguese people perceptions of their employment status differ. The differences for the employed ranged from 0.7 to 2.2% for the IPUMS-International (2001) and EU-LFS (2008-2010) and 0.2 to 4.2% for the IPUMS-International (2011) and EU-LFS (2011-2014). More marked are the differences for the unemployed ranging from 3.0 to 5.3 for the IPUMS-International (2001) and EU-LFS (2008-2010) and 3.8 to 6.7% for the IPUMS-International (2011) and EU-LFS (2011-2014). Both perception measurements increase the unemployed by a 2.1 to 6.7% as compared to the ILO conventional definition.

In the case of Spain (Figure 6), the IPUMS-International (2001) and EU-LFS (2008-2010) and IPUMS-International (2011) and EU-LFS (2011-2014) frequency distributions of Portuguese people perceptions of their employment status differ only slightly. More marked are the differences for the employed ranging from 6.2 to 11.4% for the IPUMS-International (2001) and EU-LFS (2008-2010) and 1.3 to 2.0% for the IPUMS-International (2011) and EU-LFS (2011-2014). The differences for the unemployed are ranging from 0.0 to 6.0% for the IPUMS-International (2001) and EU-LFS (2008-2010) and 1.4 to 4.3% for the IPUMS-International (2011) and EU-LFS (2011-2014). Both perception measurements slightly increase by a 0.4 to 0.6% the measurement of the unemployed as compared to the ILO conventional definition.

In Figures 7 to 12, the demographic and the social "profile" of the employed, unemployed and inactive according to the IPUMS-International, the EU-LFS

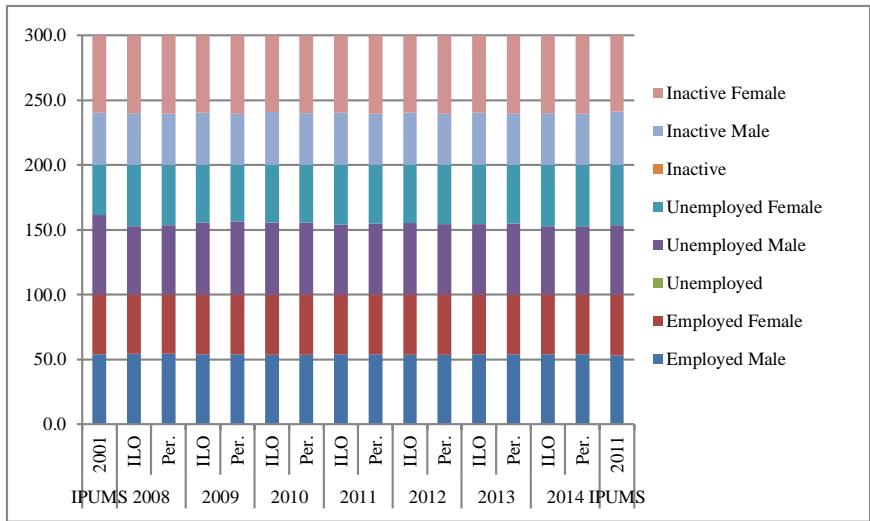


Fig. 7.1. The gender of the employment status according to IPUMS-International and the EU-LFS ILO and perception question: Hungary

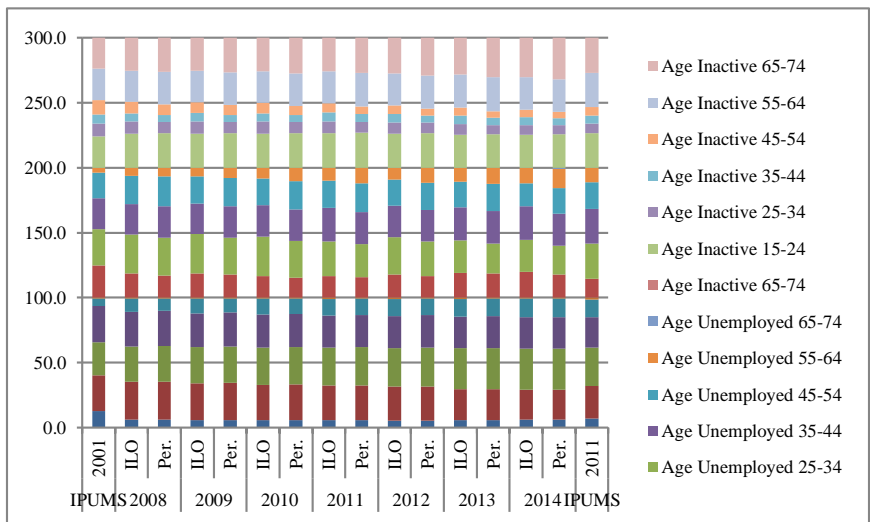


Fig. 7.2. The age of the employment status according to IPUMS-International and the EU-LFS ILO and perception question: Hungary

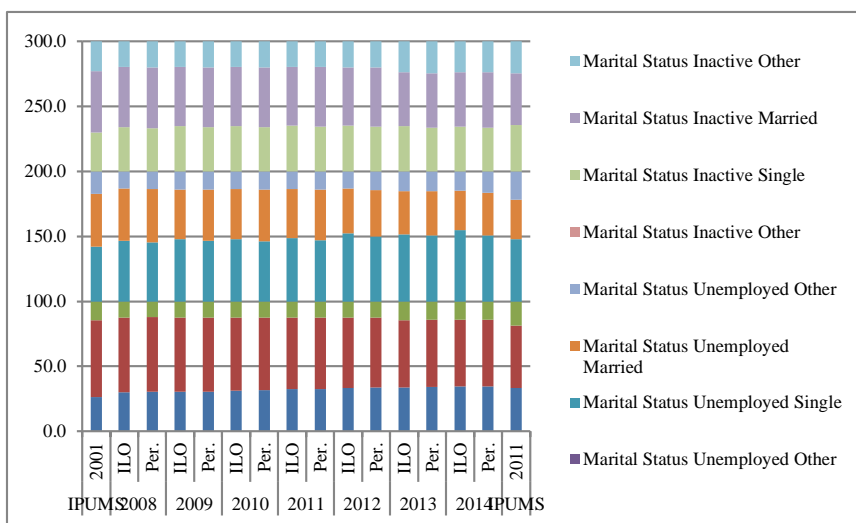


Fig. 7.3. The marital status of the employment status according to IPUMS-International and the EU-LFS ILO and perception question: Hungary

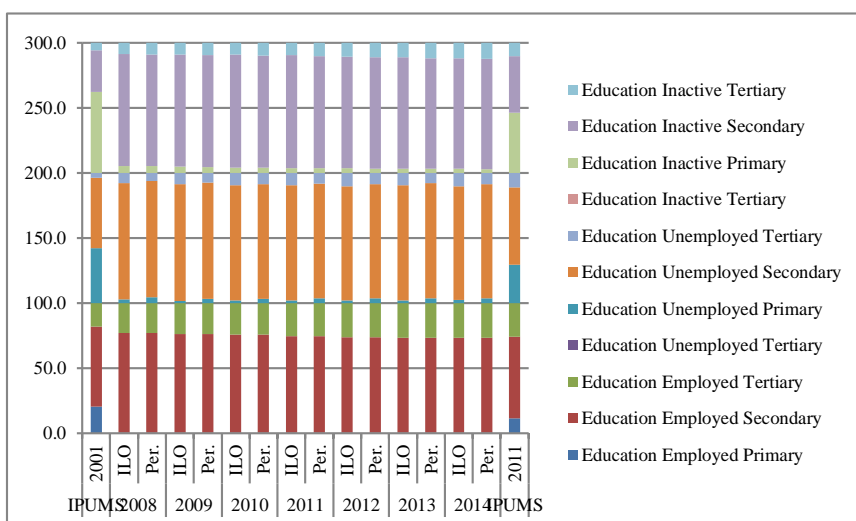


Fig. 7.4. The level of educational attainment of the employment status according to IPUMS-International and the EU-LFS ILO and perception question: Hungary

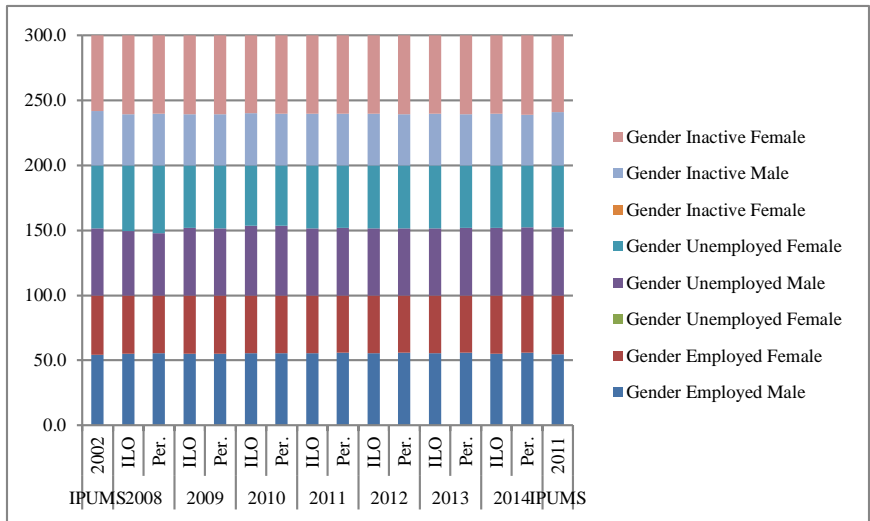


Fig. 8.1. The gender of the employment status according to IPUMS-International and the EU-LFS ILO and perception question: Poland

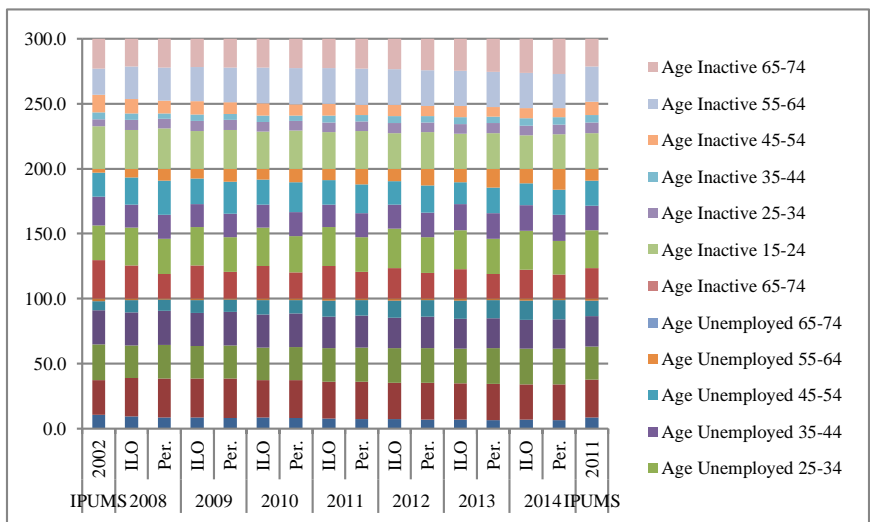


Fig. 8.2. The age of the employment status according to IPUMS-International and the EU-LFS ILO and perception question: Poland

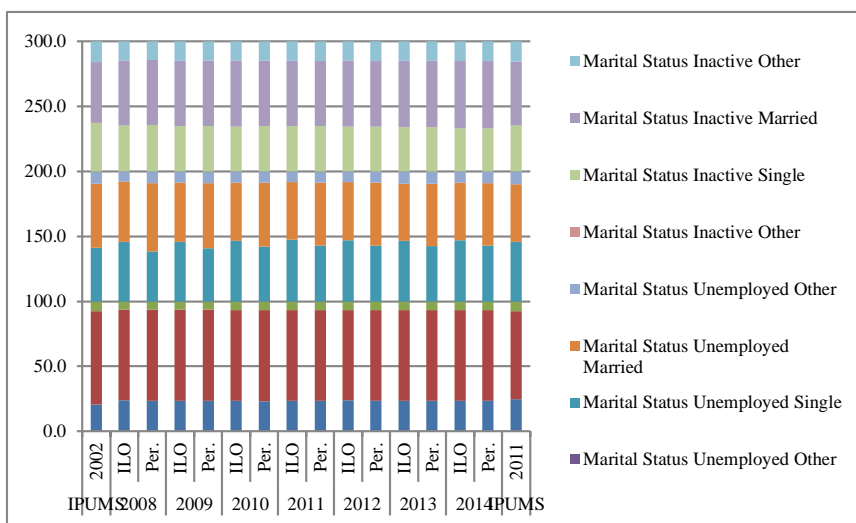


Fig. 8.3. The marital status of the employment status according to IPUMS-International and the EU-LFS ILO and perception question: Poland

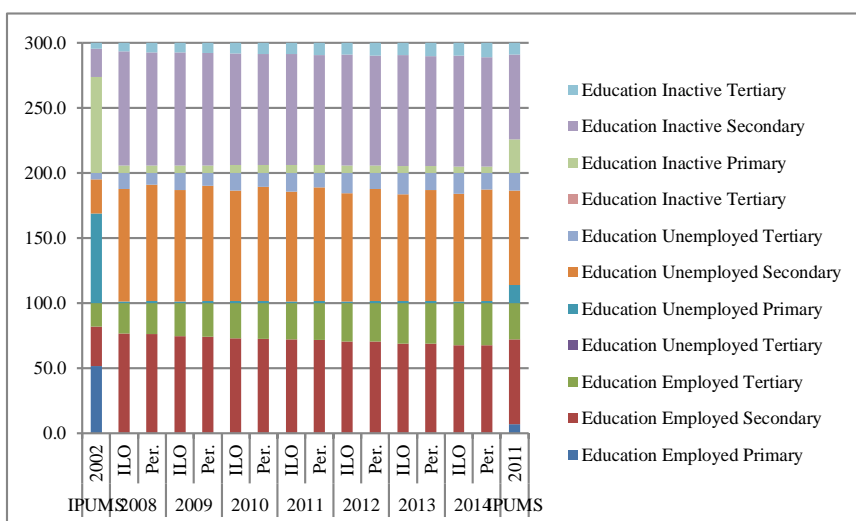


Fig. 8.4. The level of educational attainment of the employment status according to IPUMS-International and the EU-LFS ILO and perception question: Poland

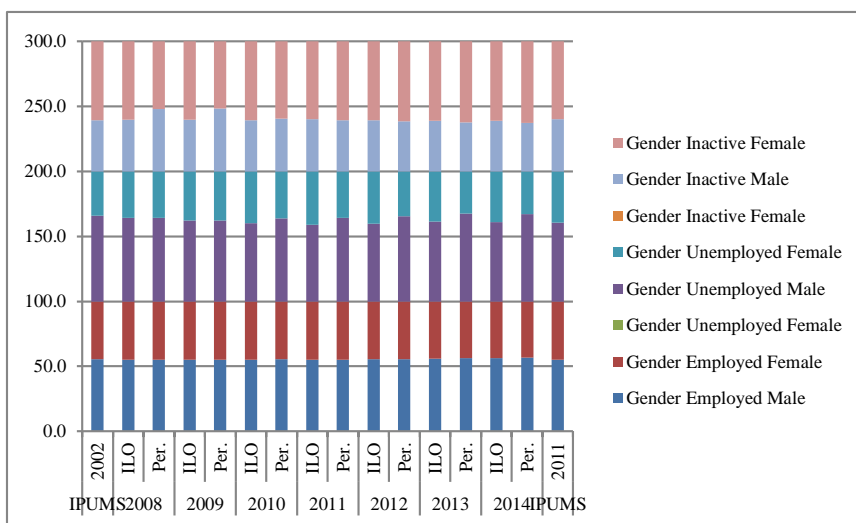


Fig. 9.1. The gender of the employment status according to IPUMS-International and the EU-LFS ILO and perception question: Romania

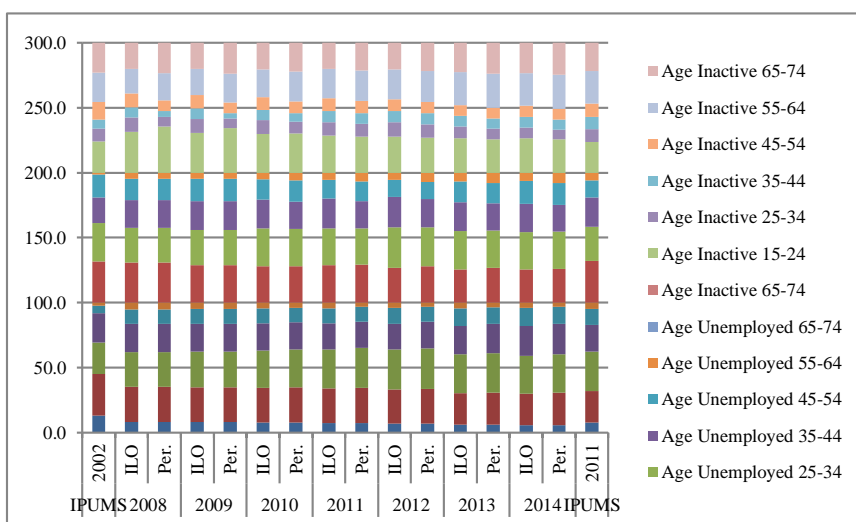


Fig. 9.2. The age of the employment status according to IPUMS-International and the EU-LFS ILO and perception question: Romania

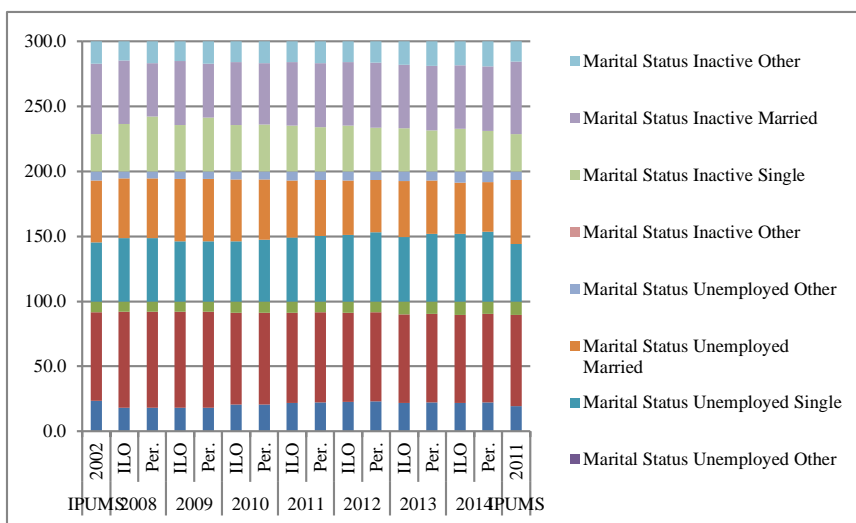


Fig. 9.3. The marital status of the employment status according to IPUMS-International and the EU-LFS ILO and perception question: Romania

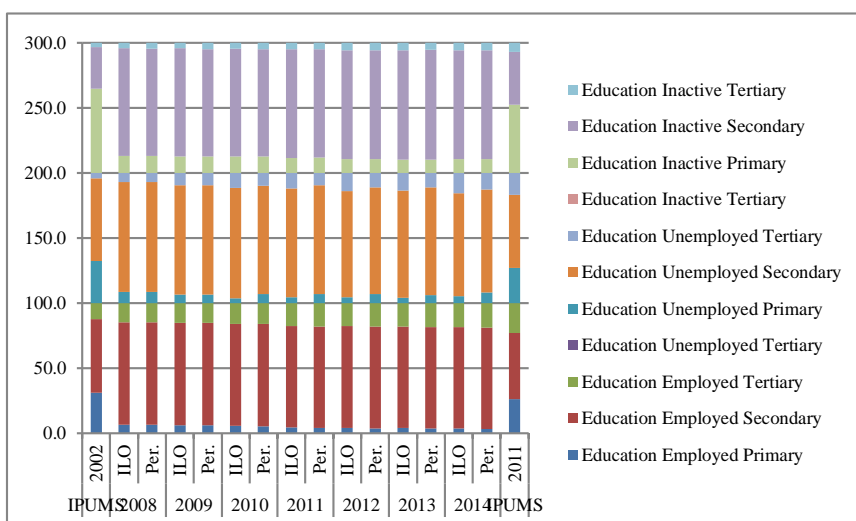


Fig. 9.4. The level of educational attainment of the employment status according to IPUMS-International and the EU-LFS ILO and perception question: Romania

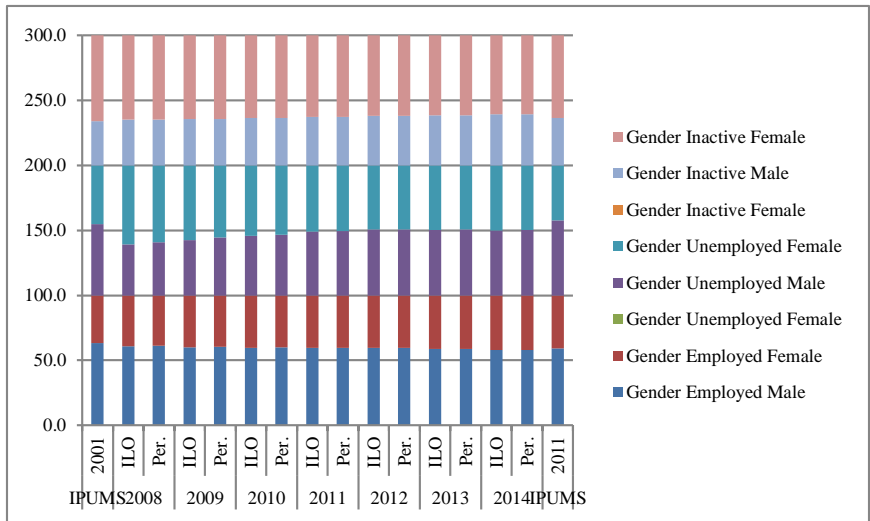


Fig. 10.1. The gender of the employment status according to IPUMS-International and the EU-LFS ILO and perception question: Greece

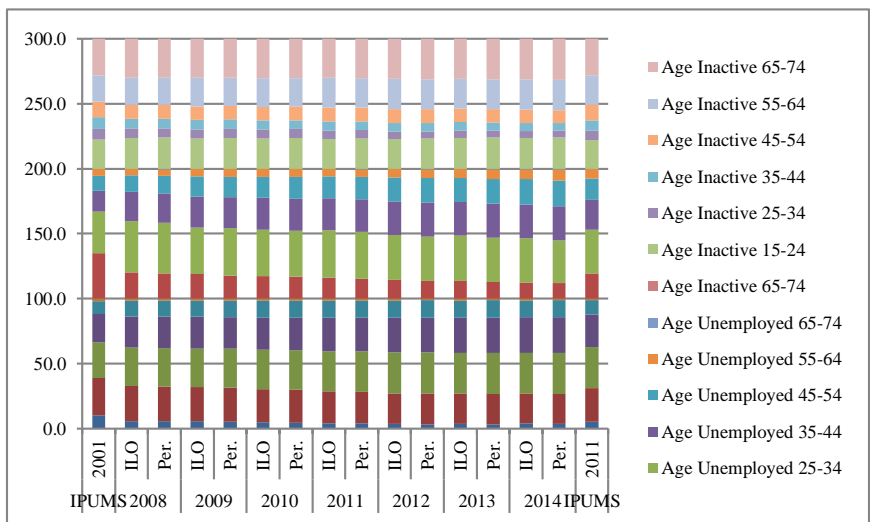


Fig. 10.2. The age of the employment status according to IPUMS-International and the EU-LFS ILO and perception question: Greece

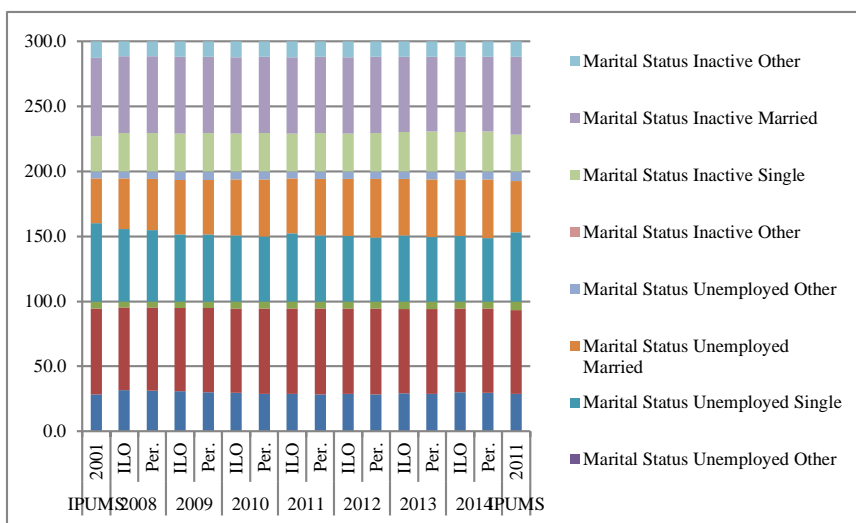


Fig. 10.3. The marital status of the employment status according to IPUMS-International and the EU-LFS ILO and perception question: Greece

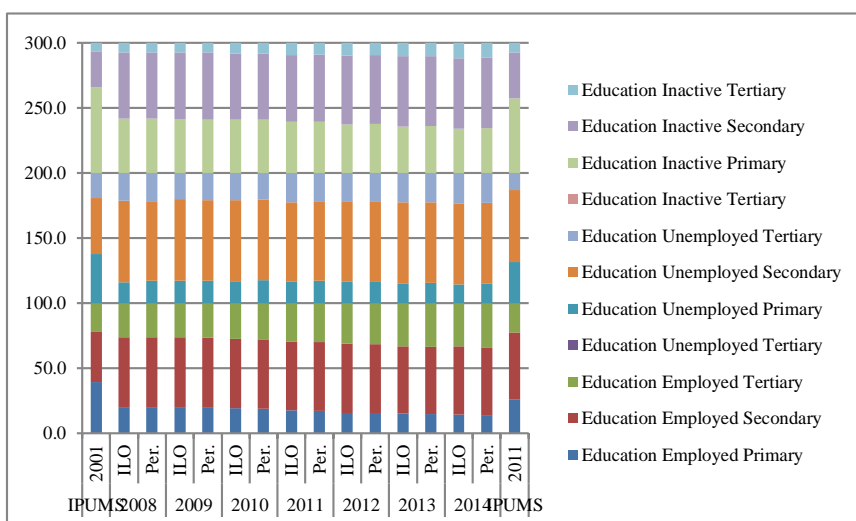


Fig. 10.4. The level of educational attainment of the employment status according to IPUMS-International and the EU-LFS ILO and perception question: Greece

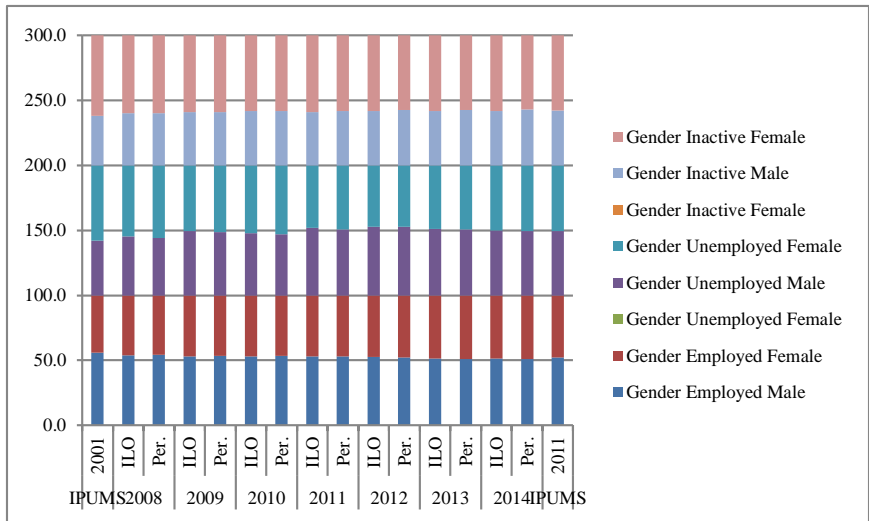


Fig. 11.1. The gender of the employment status according to IPUMS-International and the EU-LFS ILO and perception question: Portugal

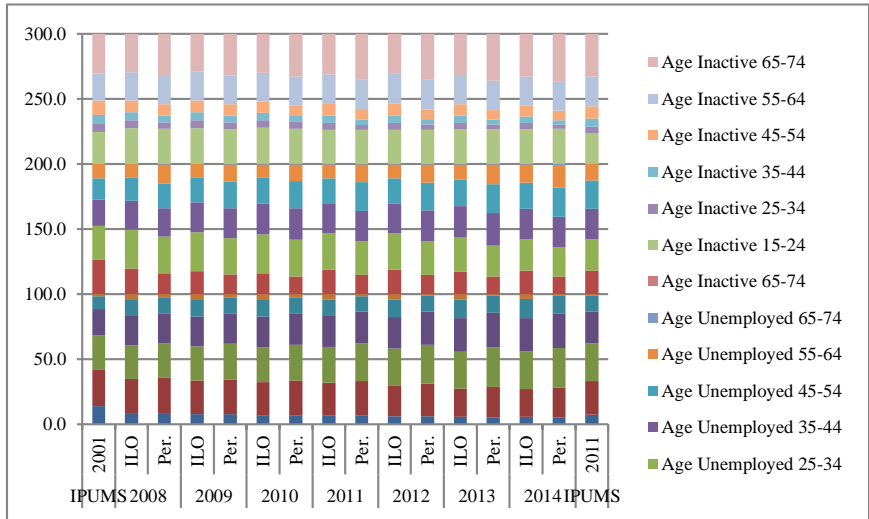


Fig. 11.2. The age of the employment status according to IPUMS-International and the EU-LFS ILO and perception question: Portugal

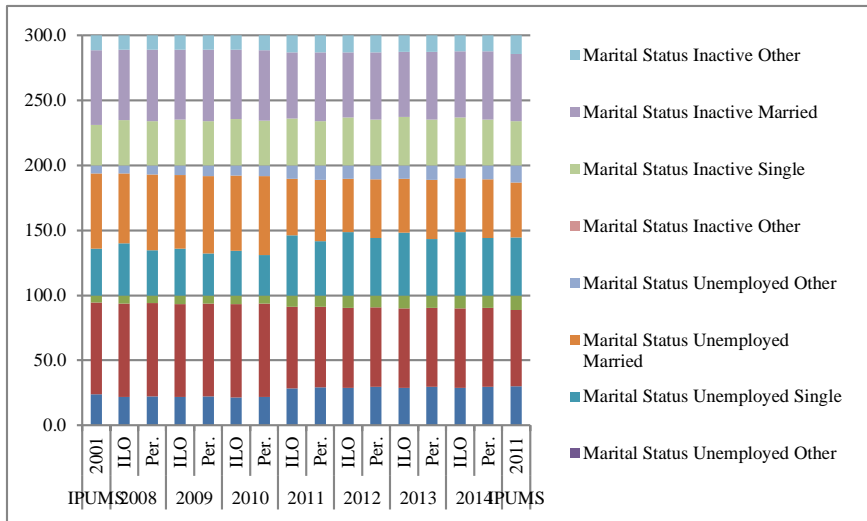


Fig. 11.3. The marital status of the employment status according to IPUMS-International and the EU-LFS ILO and perception question: Portugal

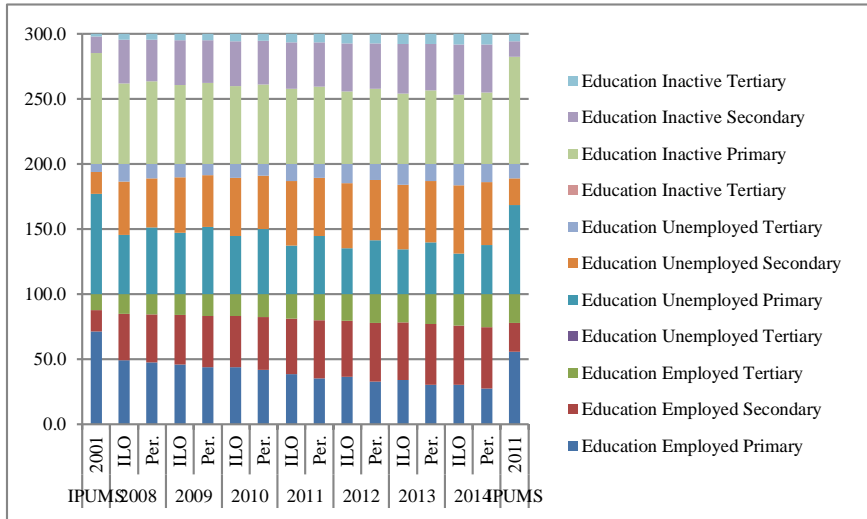


Fig. 11.4. The level of educational attainment of the employment status according to IPUMS-International and the EU-LFS ILO and perception question: Portugal

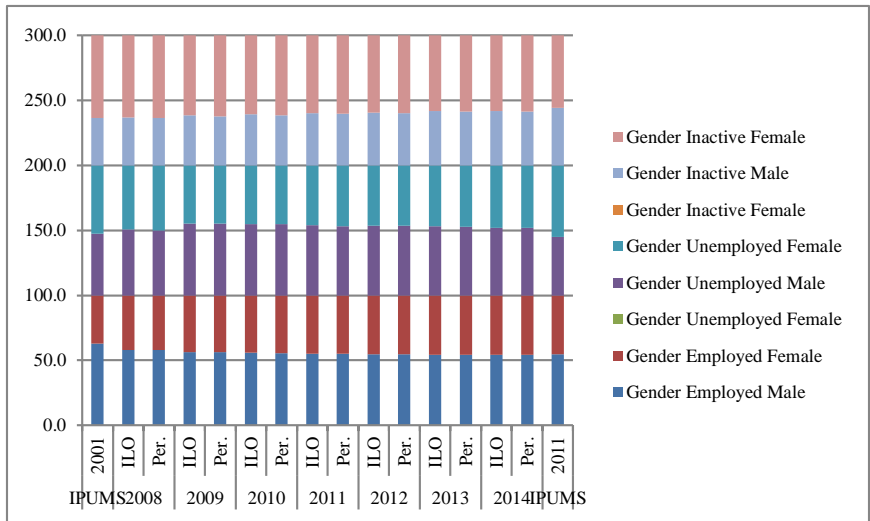


Fig. 12.1. The gender of the employment status according to IPUMS-International and the EU-LFS ILO and perception question: Spain

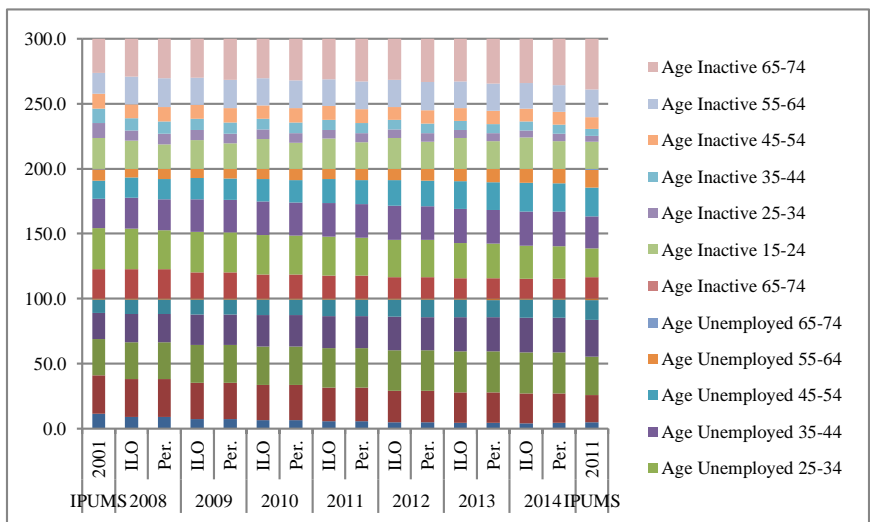


Fig. 12.2. The age of the employment status according to IPUMS-International and the EU-LFS ILO and perception question: Spain

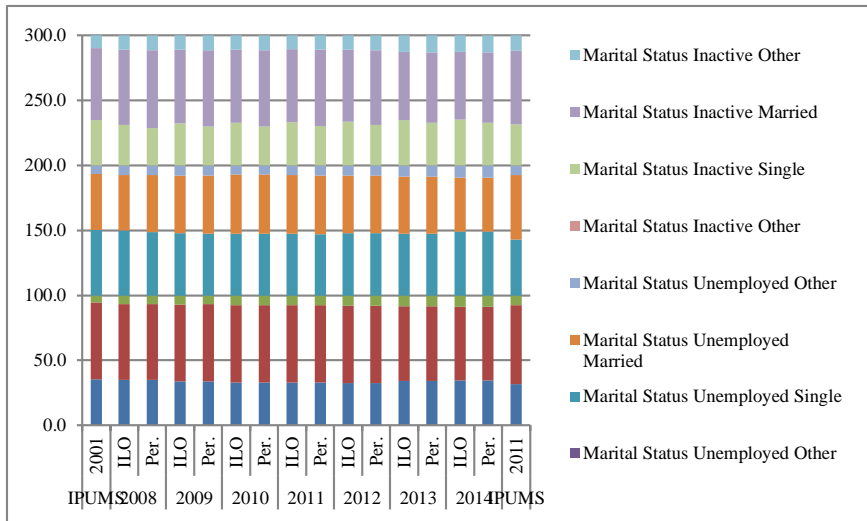


Fig. 12.3. The marital status of the employment status according to IPUMS-International and the EU-LFS ILO and perception question: Spain

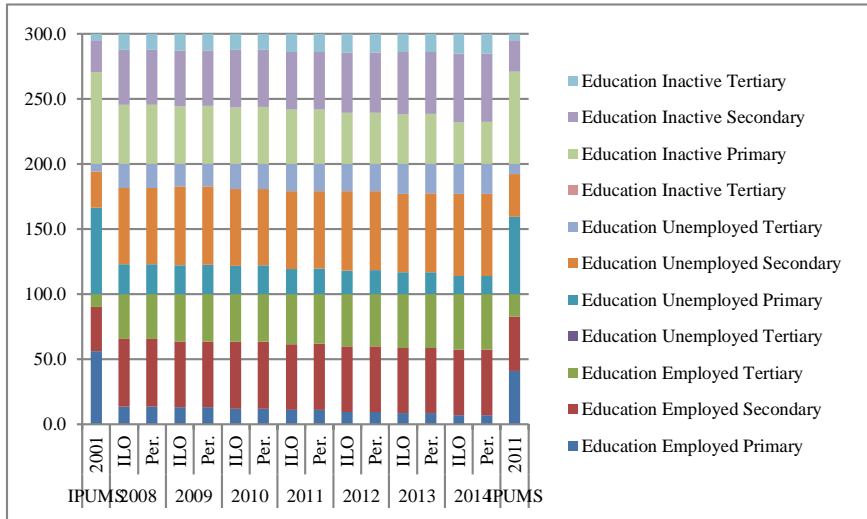


Fig. 12.4. The level of educational attainment of the employment status according to IPUMS-International and the EU-LFS ILO and perception question: Spain

ILO conventional definitions and the EU-LFS self-perceived measurement definitions are presented for each country. The detailed investigation of the three classification categories distributions — employed, unemployed and inactive — based on IPUMS-International and EU-LFS perception measurements and the ILO conventional definitions showed that they do differ in terms of their demographic and social “profile”.

In the case of Hungary (Figures 7.1-7.4), the differences between the definitions are slight for gender and only the IPUMS-International (2001) differs markedly for the unemployed men by 5.0 to 8.5% as compared to the EU-LFS perception measurement and the ILO conventional definition. In terms of age, although there are only slight differences for the employed and inactive, the two perception measurements result in an increase for the unemployed aged 25-34 and 35-44 as compared to the ILO conventional definition. There are only slight differences when considering the marital status. However, the IPUMS-International (2011) results in a consistent underestimation of the married in all three categories. In the case of education, although no significant differences are detected between the two EU-LFS measurements, the IPUMS-International measurement differs markedly in all three categories by more than 20%.

In the case of Poland (Figures 8.1-8.4), there are only slight differences between the measurements in the definitions by gender and marital status. However, there are differences when considering age, especially for the unemployed aged 45-54 and 55-64 where the EU-LFS perception measurement indicated a considerable increase as compared to the ILO conventional definitions. For instance, for the unemployed aged 55-64, the IPUMS-International (2002) and Census (2011) show that the size of this age group was 2.9% and 9.0%, respectively. The respective range for EU-LFS perception measurement is from 9.0 to 15.9% and for the ILO conventional definition is from 6.6 to 10.8%. In terms of education, although there are differences between the two EU-LFS measurements, the IPUMS-International measurement differs markedly in all three categories. For example, the size for employed of primary education in IPUMS-International of 2002 and 2011 is 51.4% and 6.9%, respectively, where for both EU-LFS measurements is about 0.3%. Furthermore, the size for the unemployed of primary education in IPUMS-International of 2002 and 2011 is 68.8% and 13.7%, respectively, where for both EU-LFS measurements it ranges from 1.2 to 1.7%.

In the case of Romanian (Figures 9.1-9.4), there are only slight differences between the measurements in the definitions of the employed and inactive by gender. However, the IPUMS-International of 2011 results in an underestimation of the unemployed men. Differences of more than 4.9% and 5.5% are detected for the employed aged 15-24 and 25-34, respectively, when comparing the IPUMS-International measure of 2002 to both EU-LFS measurements of 2008-2010. Furthermore, differences of more than 6.6% are detected for the unemployed aged 15-24 when comparing the IPUMS-International measure of 2011 to both EU-LFS measurements of 2011-2014.

There are only slight differences between the three measurements in all three categories by marital status. In terms of education, although there are differences between the two EU-LFS measurements, the IPUMS-International measurement differs markedly in all three categories. For example, the size for employed of secondary education in IPUMS-International of 2002 and 2011 is 56.7% and 51.0%, respectively, where for both EU-LFS measurements is about 78.0%. Furthermore, the size for the unemployed of secondary education in IPUMS-International of 2002 and 2011 is 63.8% and 56.1%, respectively, where for both EU-LFS measurements it is over 79.3%.

In the case of Greece (Figures 10.1-10.4), there are only slight differences between the measurements in the definitions by gender. However, the IPUMS-International of 2001 overestimates the size of the employed and unemployed men. Although the differences between the two EU-LFS measurements are not large, both IPUMS-International measures overestimate the size of the employed and unemployed aged 15-24. There are only slight differences between the three measurements in all three categories by marital status. In terms of education, although there are differences between the two EU-LFS measurements, the IPUMS-International measurement differs markedly in all three categories. For example, the size for employed of primary education in IPUMS-International of 2002 and 2011 is 39.2% and 25.5%, respectively, which differs by 19.2% (2008-2010) and 8.5% (2011-2014) for both EU-LFS measurements. Furthermore, the size for the unemployed of primary education in IPUMS-International of 2002 and 2011 is 37.7% and 31.4%, respectively, which differs by 20.2% (2008-2010) and 14.1% (2011-2014) for both EU-LFS measurements.

In the case of Portugal (Figures 11.1-11.4), there are only slight differences between the measurements in the definitions by gender. Although the differences between the two EU-LFS measurements are not large, the IPUMS-International measure of 2001 overestimate the size of the employed aged 15-24 and 55-64 by over 5.4% and 3.1%, respectively, as well as that of the unemployed aged 15-24 and 35-44 by over 7.2% and 4.3%, respectively. Although there are differences between the measurements when considering the marital status, the IPUMS-International measure of 2001 underestimates the size of the employed the single by 3.9%. In terms of education, although there are differences between the two EU-LFS measurements, the IPUMS-International measurement differs markedly in all three categories. For example, the size for employed of primary education in IPUMS-International of 2001 and 2011 is 71.3% and 55.5%, respectively, which differs by 22.3% (2008-2010) and 19.3% (2011-2014) for both EU-LFS measurements. Furthermore, the size for the unemployed of primary education in IPUMS-International of 2001 and 2011 is 77.2% and 68.2%, respectively, which differs by 25.9% (2008-2010) and 23.5% (2011-2014) for both EU-LFS measurements.

In the case of Spain (Figures 12.1-12.4), there are only slight differences between the measurements in the definitions by gender, age and marital status.

As far as education is concerned, although there are differences between the two EU-LFS measurements, the IPUMS-International measurement differs markedly in all three categories. For example, the size for employed of primary education in IPUMS-International of 2001 and 2011 is 56.1% and 40.9%, respectively, which differs by 42.6% (2008-2010) and 30.0% (2011-2014) for both EU-LFS measurements. Furthermore, the size for the unemployed of primary education in IPUMS-International of 2001 and 2011 is 66.5% and 59.5%, respectively, which differs by 43.6% (2008-2010) and 40.0% (2011-2014) for both EU-LFS measurements.

## Conclusions

In this paper, the impact of asking a single question for classifying the respondents as employed, unemployed and inactive as is the case in most large-scale social sample surveys was assessed by comparing the IPUMS-International and EU-LFS perception single-question measurements to the EU-LFS synthesized economic construct measured according to the ILO conventional definitions. The findings showed that only in the cases of Hungary and Spain the IPUMS-International (2001) and EU-LFS (2008-2010) and IPUMS-International (2011) and EU-LFS (2011-2014) perception measurements differed only slightly. In all other countries, differences were detected between these measurements. In the case of Poland, the IPUMS-International (2002) and EU-LFS (2008-2010) perception measurements differed markedly but less so in the case on Romania for the same measurements under consideration. Furthermore, differences between these measurements were detected for Greece – IPUMS-International (2011) and EU-LFS (2011-2014) – and Spain – IPUMS-International (2001) and EU-LFS (2008-2010). In most cases, these perception measurements increased the unemployed as compared to the respective ILO conventional definition. The detailed investigation of the demographic and social “profile” of the three different measurements revealed only slight differences by gender (Poland, Greece, Portugal and Spain) and marital status (Hungary, Poland, Romania, Greece and Spain). Marked differences were detected in all samples when considering age and the highest level of educational attainment.

These findings exhibited the great divide between people’s perceptions of their employment status and that resulting from applying the ILO conventional definitions; a result in line with Gauckler and Körner [9]. Therefore, the differences that ensued are the result of comparing differently defined measurements. This study demonstrates the importance of the measurements’ definitions and the complexity of classifying key variables used in social research by discussing as Connelly [2: 2] pointed out “a range of issues related to the inclusion of these measures in sociological analyses”.

## References

1. M. Braun and P.Ph. Mohler. Background variables. In J.A. Harkness, F.J.R. Van de Vijver and P.Ph. Mohler (Eds), *Cross-cultural survey methods*, Wiley, New York, 101-115, 2003.
2. R. Connelly, V. Gayle and P. S. Lambert. A Review of occupation-based social classifications for social survey research, *Methodological Innovations*, 9, 1-14, 2016.
3. M. Ehling. Harmonising data in official statistics. In J.H.P. Hoffmeyer-Zlotnik, and C. Wolf (Eds.), *Advances in cross-national comparison: A European working book for demographic and socio-economic variables*, Kluger Academic-Plenum, New York, 17-31, 2003.
4. Eurostat. Labour Force Survey revised explanatory notes (to be applied from 2008Q1 onwards), European Commission, 2008.
5. Eurostat. Task Force on the quality of the Labour Force Survey: Final report, European Commission, 2009.
6. Eurostat. EU Labour Force Survey database user guide, European Commission, 2016.
7. Eurostat The European Union labour force survey: Methods and definitions, European Commission, 2001.
8. Eurostat. Your key to European statistics. 2011 Census. Available at: <http://ec.europa.eu/eurostat/web/population-and-housing-census/census-data/2011-census>
9. B. Gauckler and T. Körner. Measuring the employment status in the Labour Force Survey and the German Census 2011: Insights from recent research at Destatis, *Methoden –Daten–Analysen*, 5, 2, 181-205, 2011.
10. J.H.P. Hoffmeyer-Zlotnik. Harmonisation of demographic and socio-economic variables in cross-national survey research. *Bulletin of Sociological Methodology*, 98, 2, 5-24, 2008.
11. J.H.P. Hoffmeyer-Zlotnik and C. Wolf, (Eds.). *Advances in cross-national comparison: A European working book for demographic and socio-economic variables*, Kluwer Academic-Plenum, New York, 2003.
12. L. Kish. Multipopulation survey designs: Five types with seven shared aspects, *International Statistical Review*, 62, 2, 167-186, 1994.
13. Minnesota Population Center. Integrated public use microdata series, international: Version 6.4 [Machine-readable database]. Minneapolis: University of Minnesota, 2015.
14. C. Wolf and J.H.P. Hoffmeyer-Zlotnik. Measuring demographic and socio-economic variables in cross-national research: An overview. In J.H.P. Hoffmeyer-Zlotnik and C. Wolf (Eds), *Advances in cross-national comparison: A European working book for demographic and socio-economic variables*, Kluwer Academic-Plenum, New York, 1-13, 2003.
15. A. Yfanti, C. Michalopoulou, A. Mimis and S. Zachariou. Investigating Southern Europeans' perceptions of their employment status. In C.H. Skiadas and C. Skiadas (Eds), *Demographic and health issues - population aging, mortality and data analysis*, Springer, in print.



## **Mortality differentials among the Euro-zone countries: an analysis based on the most recent available data**

Konstantinos N. Zafeiris

Laboratory of Physical Anthropology, Department of History and Ethnology,  
Democritus University of Thrace. P. Tsaldari 1, 69100 Komotini. E-mail:

[kzafiris@he.duth.gr](mailto:kzafiris@he.duth.gr)

Euro-zone is consisting by 19 countries with different developmental and economic characteristics. During the first years of the 21<sup>st</sup> century several of them underwent a rapid economic and social crisis while others, like Germany, exhibited steadily economic and social growth. The scope of this paper is to compare the mortality experience of these countries using the last available data which correspond to the years 2016 and 2015. The method used is a combination of a modified Heligman-Pollard procedure in addition with three cubic splines for the smoothing of the  $q(x)$  life tables distribution and the estimation of several parameters. Among them is modal age at death, Kannisto's indicators and others in order to find some important features of a life table's  $dx$  curve. Also, life expectancy at birth and other ages and the causes of death were studied. A cluster analysis was applied at last. Results indicate the existence of significant differences among the countries studied.

### **Introduction**

In 1992 Economic and Monetary Union (EMU) was launched by the European Union countries involving the coordination of economic and fiscal policies, a common monetary policy and a common currency, the (Euro). Even all 28 European Union members take part in the economic union only 19 of them have adopted the Euro as their official currency (Map 1). These countries are Austria (AT), Belgium (BE), Cyprus (CY), Estonia (EE), Finland (FI), France (FR), Germany (DE), Greece (EL), Ireland (IE), Italy (IT), Latvia (LV), Lithuania (LT), Luxembourg (LU), Malta (MT), the Netherlands (NL), Portugal (PT), Slovakia (SK), Slovenia (SL) and Spain (ES) (see [https://europa.eu/european-union/about-eu/money/euro\\_en](https://europa.eu/european-union/about-eu/money/euro_en)).

However, these countries have quite a different recent political, economic and social history. Lithuania (LT), Latvia (LV) and Estonia (EE), the Baltic democracies, were formed after the dissolution of the former Soviet Union in 1991.



## **MAP 1 about here**

It is well known that these countries originally faced significant social and economic problems in their effort to adapt to the new circumstances but afterwards they followed a rapid developmental course. Also, Slovakia came into existence after the dissolution of Czechoslovakia, the famous “velvet divorce” which took effect on January 1993. Slovenia, finally, gained its independence from Yugoslavia in 1991.

Of the other countries of the Eurozone area some, like Germany, maintained steady economic growth until today, though even they faced some problems in the past. Others like Greece (EL), Portugal (PT), Ireland (IE) and Cyprus (CY) faced a severe economic crisis. Greece (EL) actually faced a vast economic and fiscal crisis which holds until today. Overall, the Eurozone area is characterized by a significant heterogeneity concerning its recent history and the economic, social cultural and even environmental regimes in each of the countries being part of it.

There is an undoubted relationship between mortality and the economic, social and political situation of a country (see for example Brenner and Moone, 1983; Catalano and Dooley, 1983; Catalano, 1997; Cutler et al., 2002; Falagas et al., 2009; Granados, 2005; Hill and Palloni, 1994; Laporte, 2004). Thus, the question that will be addressed in this paper is the current mortality situation in the Eurozone countries and the similarities and differences they have not only by taking into consideration mortality levels but also the causes of death and their effects on populations' longevity.

Therefore, besides the introduction session of this paper, in the Data and Methods session data and methods used will be described analytically. In the results session the probabilities of death, life expectancy at various ages, several findings of the death curve of a life table, and the effects of the causes of death on life expectancy will be

presented. The relationships among the countries will be revealed with the aid of cluster analysis by taking into consideration all the variables discussed previously. Finally, in the conclusions session all the findings of the paper will be summed up.

### **Data and methods**

Data come from the Eurostat database (<http://ec.europa.eu/eurostat/data/database>). The population by one-year age classes and gender for the 1<sup>st</sup> of January of 2016 and 2017 was used for the calculation of the average population of year 2016. The relevant number of deaths was used in order for the full life tables to be constructed. The Chiang method (1984) was used for the calculation of the probabilities of death  $q_x$  and subsequently the other elements of the full life tables. All the calculations refer to Eurozone countries described in the introductory session of this paper as well as the whole population by gender of the European Union, which will be used for comparative reasons. The probabilities of deaths by age and gender for the countries studied and EU will be the first group of variables studied in this paper.

The second group of variables is related to the longevity. Thus, life expectancy at birth and at various ages (15, 45 and 65 years) as average measures of longevity in these ages will be studied (see Acsádi and Nemeskéri, 1970; for the method used in the calculations see Preston et al., 2001, pp. 38-70).

### **Figure 1 about here**

The other group of variables used deals with the bimodality of human death curve firstly described by Lexis (1878; Figure 1). The first mode corresponds to infant mortality, and afterwards despite an elevation of deaths in the accident hump (between ages 15 and 30), deaths remain low until the age heap at old ages. The death curve at the old age heap reaches a maximum at a particular age which is denoted in the literature as the

“modal age at death”. Thus, this measurement corresponds to the age at which most of deaths occur at the old age heap. In comparison to life expectancy at birth it has the advantage that modal age at death is not affected by infant, child, young and middle-age adult mortality. In that way, it has been widely used as a measure of longevity, taking into consideration that the probability of deaths of the infants has declined to very low levels today (see Canudas-Romo, 2008; Cheung and Robine, 2007; Cheung et al., 2009; Horiuchi et al., 2013 etc.).

The width of the old age heap seen in Figure 1 can be described with the Kannisto’s C-family indicators (see Kannisto, 2000, where also the formulas for the calculation; for review of the several methods used for this purpose see Robine, 2001). Of them the C50 indicator will be used in this paper, defined as the narrowest age interval in which 50% of all deaths occur. The height of the old age heap can simply be described by the numbers of deaths in the modal age at death. This analysis is equivalent to the rectangularization hypothesis, according to which the human survival curve becomes more rectangular as mortality levels decrease (see Wilmoth and Horiuchi, 1999; Robine, 2001; see also Cheung et al., 2009). This is because the survival curve is the direct product of the death curve  $dx$  in a life table. If the death curve is wide enough then the rectangularization is smaller than in the opposite situation, i.e. the death curve is narrow.

However, these measurements require some kind of fitting in the death or probability curves of a life table, as chance fluctuations can be observed among the age classes for several reasons, for example because the small population sizes. Of the several methods used for this purpose (see for example Gompertz, 1825; Makeham, 1860; Weibull, 1951; Peristera and Kostaki, 2005; Bongaarts, 2005; Ouellette and Bourbeau, 2011 etc).

In this paper, the method used in a previous one of Zafeiris and Kostaki (2018) will be applied. This method consists of a combination of the Heligman-Pollard (1980) method as modified by Kostaki (1992) along with three cubic splines. The Heligman-Pollard method (1980) is a parametric one, having three components and including 8 parameters which describe these components. Kostaki (1992) added later a 9<sup>th</sup> parameter in order to enhance the accuracy of the method. This procedure was used because it had the advantage of combining the ability of the Heligman-Pollard approach to describe mortality with the flexibility of cubic splines. The mathematical formulas for the calculations of the procedure are discussed in Zafeiris and Kostaki (2018), where this method was firstly developed and effectively used for the examination of mortality trends in Greece.

The rest of the analysis deals with the causes of death in each of the countries studied. Data come from the Eurostat database (<http://ec.europa.eu/eurostat/data/database>). However, the most recent available data refer to the year 2015. Also, there are no adequate data for analysis for the countries Luxembourg (LU), Slovenia (SL), Cyprus (CY) and Malta (MT); so these countries were omitted from the cluster analysis that will follow. Seven groups, i.e. the most important, causes of death were used in the analysis: diseases of the circulatory, respiratory, digestive systems, neoplasms, external causes of morbidity and mortality and infectious and parasitic diseases. The rest of the causes of death were studied as a separate group. However, instead of discussing the relative frequencies of these diseases in each of the population studied a different procedure was used here. The population of each gender and country was compared with the relevant population of the European Union in order to estimate the effect of each cause of death to the observed mortality. The method used is that described in Andreev and Shkolnikov (2012; see also Andreev et al., 2002) according to which “*a*

*general algorithm for the decomposition of differences between two values of an aggregate demographic measure of age and other dimensions is realized as Excel/VBA. It assumes that the aggregate measure is computed from similar matrices of discrete demographic data for two populations under comparison. The algorithm estimates the effects of replacement for each elementary cell of one matrix by the respective cell of another matrix. The replacement runs from young to old ages".* In practice, the abridged life tables of the European Union per gender were compared with the relevant populations of each country and the effect for each cause of death on life expectancy at birth was estimated. This procedure allowed the easy categorization of the countries according the effects of each cause of death on observed mortality in relationship to the population of the European Union which was used as some kind of a "standard" one for each of the two genders. In this procedure, if this effect is positive then mortality caused by a group of diseases is lower than the European Union. The opposite happens when it is negative. For convenience the relevant effects will be called "positive" and "negative" in this paper.

The final step of the analysis deals with the clustering of populations in homogeneous groups. In statistical exploratory studies a multivariate set of data is used in order for a correlation matrix to be produced. Based on that matrix, various methods of grouping variables, according to the magnitudes and interrelationships among their correlations have been developed. These methods are generally known as cluster analysis (Sokal and Rohlf, 1995), and they are aimed at identifying relatively homogenous groups of cases (or even variables) in a data set, based on selected characteristics of these cases. Hierarchical cluster analysis methods form the final classes (clusters), i.e. the final grouping of the different cases or variables, either by hierarchically grouping sub-clusters or by splitting parent clusters (Hand, 1981). In theory, the agglomerative

clustering method used here begins with a few sub-clusters consisting of one point each, then these are combined to form larger sub-clusters, and then these are combined to form even larger ones, and so on until the desired number of clusters has been achieved. At each step more similar sub-clusters are combined (Hand, 1981). Of the various clustering methods, we have used that of Average Linking, combined with Euclidean distances (see Hand, 1981, p.p.153-185) because it gave the best results. This is a fairly robust method in which the distance between two clusters is calculated as the average distance between all pairs of subjects in the two clusters.

The final result of hierarchical cluster analysis is the production of a dendrogram, which is the graphical summary of cluster solution. In a dendrogram cases are listed along the left vertical axis, the horizontal axis shows the distance between clusters when they are joined. We have to note that because of the “scaling differences” of the variables used in the analysis they were standardized into z-scores. In that way all the standardized variables have a mean of 0 and a standard deviation of 1. All the variables described so far were used in the analysis,

## **Results**

### **1. The probabilities of death**

The probabilities of death by age of 19 countries are very difficult to visualize in a figure. Therefore, because of the space limitations of this paper, it was decided that only the countries with the lowest and highest mortality, as well as the probabilities of death of the European Union would be visualized in Figure 2. All the other countries are located – taking of course into consideration some considerable fluctuations - somewhere between the extreme values denoted by the relevant ones of Italy (IT) and

Lithuania (LT) for males and Spain (ES) and Latvia (LV) for females. However, in the cluster analysis that will be carried out later data from all countries will be used.

### **Figure 2 about here**

As seen in Figure 2 the differences of the probabilities of death are significant in both genders among the countries. In males, these differences become larger from the age of 10 until the age of 45 and smaller afterwards comparing Italy (IT) and Lithuania (LT). Italy (IT) is closer to the European Union (EU) than Lithuania (LT). The probabilities of death of Latvia (LV), Estonia (EE) and Slovakia (SK) are between those of European Union (EU) and Lithuania (LT). The probabilities of death of the rest of the countries are below those of the European Union. A similar situation is found for females; however in them the differences among the three populations of Figure 2 are smaller. Of course, - as seen in all of the human populations and in both genders - the probabilities of death increase from the beginning of the accident hump around the age of 15 until the end of human life. Before, the probabilities of death decrease from the infants until childhood.

## **2. Life expectancy at birth and various ages**

The scatter plot of male and female life expectancy at birth (**Figure 3**) is indicative of the variability existing in the Eurozone countries concerning mortality levels. Three zones of countries are formed according to this characteristic. The most separated group, named “Group A” in figure 3, lies quite apart from the others. Two countries are included in this group, namely Lithuania (LT) and Latvia (LV).

### **Figure 3 about here**

The second group (Group B) is formed by Estonia (EE) and Slovakia (SK). Though it must be noted that both groups are formed by countries of ex-Soviet Union and Slovakia, the Group C is formed by all the other countries of the Eurozone. Actually, even if these countries are in a better situation concerning their mortality levels in comparison to the other two groups and the European Union (EU), variability among them is significant. At the lower edge of this group countries like Slovenia (SL), Greece (EL) and Germany are located. At the other edge, those of very small mortality, Spain (ES), Cyprus (CY) and Italy (IT) are cited.

An analogous situation is observed by examining the scatter plots of the ages 15 and 45 years. Therefore and because of the space limitation of this paper these scatter plots are not cited here. However, at the age of 65 a different grouping of the countries occurs because of the mortality differences observed among them in these ages and above (Figure 4).

**Figure 4 about here**

At this age Latvia (LV) and Lithuania (SK) have partially converged with Slovakia (SK) and Estonia (EE) noting that the heterogeneity of the average length of life is significant among them. In general, people there are expected to live fewer years than the other Eurozone countries. At the same time males in Slovakia (SK) and Estonia (EE) live much longer than those of Latvia (LV) and Lithuania (LT). The same is the case for females in Estonia (EE).

The heterogeneity still exists in the other group. A number of countries cluster together relatively tightly close to the EU. Only Germany (DE) and Slovenia (SL) have lower e65 in males. Greece (EL), Portugal (PT), Finland (FI), Netherlands (NL), Ireland (IE), Austria (AT) and Belgium (BE) are the other countries of this group, while some of

them have lower life expectancy in females. Luxemburg (LU) is somewhat further located, as happens with Malta (MT), in that case because of the higher male life expectancy. The remaining countries, Cyprus (CY), Italy (IT), Spain (ES) and France (FR) are clearly differentiated from each other because of their high life expectancy in both genders.

### **3. The dx curve**

The age at which most of the deaths occur in the old age heap in both genders is seen in figure 5, denoted as “modal age at death”. Obviously in females, in which mortality transition has moved well ahead (see Figures 3 and 4), this age is higher. Also, because of being in a lower mortality regime, the differences among the populations are not of the same magnitude as they are in males.

#### **Figure 5 about here**

The more advanced age concerning modal age at death in females is found in France (FR) one of the countries with the longest life expectancy at birth along with Portugal (PT), Spain (ES), Italy (IT) and Cyprus (CY). On the other edge Slovakia (SK) where the lower modal age is found is followed by Latvia (LV), and Lithuania (LT). All the other countries cluster together with the European Union (EU). The range between the maximum and minimum values is about 5 years.

In males this range is more than 9 years. The minimum value is found in Latvia (LV) and the maximum in France (FR), while the clustering of the countries in three separate groups, as found for life expectancy at birth, is obvious.

#### **Figure 6 about here**

The second question, which needs to be addressed, relates to the width of the old age death heap described by the C50 indicator (seen in relationship to the modal age at death in Figure 6). In females the width of the old age heap is smaller than males. The range between minimum and maximum value is about 2 years in females comparing with more 8 years in males. As mortality has decreased considerably in the female population of the Eurozone countries the width of the old age heap tends to fluctuate between 12 and 14 years, meaning that 50% of the deaths of the female population are concentrated around a small number of years around the modal age at death. Also, in them the relationship between modal age at death and the C50 indicator can be described adequately with any linear regression lines. On the contrary in males the linear regression line among the two variables gives an  $R^2$  of about 67%. Thus, it seems that among the males of the Eurozone countries, where mortality levels are higher than females, the higher the modal age at death the shorter is the width of the old age death heap even if this relationship is not perfect. Quite expectedly, if mortality continues to decline in the male population then an analogous situation to the females will arise. Also, the differences among the countries in both genders reveal the differences in the health status of the older people resulting from the socio-economic differentials, the social security and health system and the other factors which affect health in these ages.

The last question that will be addressed concerning the dx curve of the life tables of the populations studied deals with the height of this curve in the old age heap (Figure 7). In females besides the fact that the width of this curve is smaller it is also steeper. Among the countries the differences are small, about 500-600 deaths and their classification is not that obvious. The linear regression among modal age at death and deaths at his age gave very poor results ( $R^2=2\%$ ), thus it cannot be described that way. In males the differences among the countries are greater, and a similar classification

with life expectancy at birth holds. The peak of the death curve is lower in the populations where the modal age at death is also low and the death curve tends to become steeper as modal age at death increases. In fact, there is a linear relationship between modal age at death and the relevant number of deaths, which has a coefficient of determination  $R^2=77\%$ , which is very good but not perfect.

**Figure 7 about here**

#### **4. Causes of death**

In Figure 8 the countries were ranked according to the effect each group of causes of death had on the male population. Only the most important findings will be discussed, as the scope of this analysis is to provide data evidence for the forthcoming clustering of the countries in the last part of this session and not the epidemiology of the diseases.

**Figure 8 about here**

The most important group of diseases affecting mortality levels are of circulatory system. In males the most serious problem is found in the Baltic countries (Latvia LV, Lithuania LT and Estonia EE) along with Slovakia (SK). In a number of countries (Austria AT, Greece EL, Finland FI and Germany DE) the effect is small. On the contrary, in the rest of the countries, the effect of those diseases is positive, which means that mortality is not aggravated by this group of diseases to the same degree as in the whole European Union because their prevalence is smaller. France (FR) and Spain (ES) are facing the smaller problem.

A similar picture emerges for females, however in Slovakia (SK) a strong positive effect is found, the opposite of what happens in males. It seems that -besides the biological agents which are responsible for this group of diseases - behavioral factors also act and operate differently in the two genders and are responsible for this

phenomenon. At the same time, the existing differences among the Eurozone countries signal the necessity of several interventions and social policies probably on public health and life style in order to diminish the effect of these diseases on mortality on the most aggravated populations.

The same is the case for the external causes of morbidity and mortality which have a tremendous negative effect in the males of the Baltic countries and a more moderate in Slovakia (SK), Austria (AT), Finland (FI), Belgium (BE), and France (FR). Greece (EL) is very close to the European Union, while in the other counties a positive effect is found because of the smaller prevalence of this group of causes of death. Spain (ES) and Italy (IT) face the smaller problem. In females, on the contrary, the effects are minor in comparison to males due to the small effect of car and industrial accidents and in general of life style. However, it must be stressed that also other causes like violent deaths and suicides are included in this category, thus any improvements in mortality for these causes of death must be connected with integrated policies covering the whole range of human activities.

Neoplasms are the third most important cause of death in the Eurozone. In the males living in the Baltic countries and in Slovakia (SK) the effect of this group of diseases is more significant than the others. On the other side of this classification the effect reaches 0.37 years in Ireland (IE) and 0.84 in Finland (FI). Females, however, do not have the same ranking as males and the more burdened countries are Netherlands (NL), Latvia (LV), Lithuania (LT), Ireland (IE) and Estonia (EE). Spain (ES), Portugal (PT) and Slovakia (SK) face the smaller problem. Obviously gender related factors are responsible for these differences.

The diseases of digestive system are of lesser importance. Once again, in the male population, the Baltic countries are clearly distinguished. Finland (FI) may be included in this category, despite the fact that it was classified in a better position in the previously studied causes of death. Netherland (NL), Greece (EL) and Ireland (IE) face the smaller problem. The classification is somewhat different in the female populations, for example in the females of Slovakia (SK) a small positive effect is found while in males a more important aggravation of mortality levels is evident.

The infectious and parasitic diseases have an even smaller impact; however their effect is not negligible ranging from almost -0.3 years in the males of Lithuania (LT) and reaching +0.15 years in Finland (FI). In females their effect is from -0.2 years in Greece up to 0.15 in Finland (FI).

In the diseases of the respiratory system, the classification of the more burdened countries is different than the other causes of death. In males, Portugal (PT), Slovakia (SK), Spain (ES), Ireland (IE), Belgium (BE), and Greece (EL) are distinguished from the others. It seems that life style factors like heavy smoking, affect the prevalence and the significance of these diseases on mortality. In females, Ireland (IE), Greece (EL), Slovakia (SK), Portugal (PT) and Belgium face the most significant problem. The final group of causes of death studied is an overall measurement of the rest of the diseases affect mortality in the Eurozone area. In males this group of diseases has a negative effect in France (FR), Germany (DE), Portugal (PT) and Latvia (LV). This effect becomes positive gradually up to Austria (AT). In females, more countries face a negative effect. However, the Baltic countries have a positive effect.

The effect of these causes of death by age was also studied in the two genders and the countries of Figure 8 with the method described in the Data and Methods session of this

paper. However, because of the space limitation of this paper the results for 4 countries, those with the higher mortality Lithuania (LT) and Latvia (LV) and two of the countries with lower mortality France (FR) and Spain (ES) will be indicatively and briefly discussed here (Figure 9). However, the findings for all the countries studied will be included in the forthcoming cluster analysis.

### **Figure 9 about here**

These examples are indicative of the differences existing among the Eurozone countries concerning the effects of the causes of death studied in different ages. In the males from France (FR) a positive effect is found because of the smaller prevalence of the diseases of the circulatory system in comparison to the European Union (EU) in all ages. A smaller positive effect is also found because of the diseases of the respiratory system. However, the neoplasms have a small negative effect up to an age and a positive one afterwards. The category of diseases “all others” have a steady negative effect which becomes larger in the last age group of 85+. A similar situation is observed in females though in them the effects of the causes of death studied come later in life. Especially the diseases of the circulatory system show a steady increase by age.

In males from Spain (ES) also the positive effect of the circulatory diseases increases by age. However, in the younger-middle ages a significant effect is also found for the external causes of morbidity and mortality and to a lesser degree for “all others”. The diseases of the respiratory system contribute negatively in the older ages. Neoplasms play a minor role. The picture in females is significantly differentiated. First of all neoplasms contributed positively and to a greater degree in comparison with males to the observed longevity of the population after the age of 50. The same is the case for

the diseases of the circulatory system. In the very old ages and infants the groups of diseases named “all others” play a significant role too.

In Latvia, one of the countries of higher mortality, there is a steady negative effect of the external causes of morbidity and mortality in the ages 15-65 years in males. Neoplasms act negatively in the ages 45-74 years while there is an increasing negative effect of the diseases of the circulatory system even from the age of 25-29 years. The effects of this group of diseases decrease in the last years of human life, though they remain negative. Only the diseases of the respiratory system act positively in the old ages. The same is the case for the “all other”, even if in infants they cause an increase of mortality in comparison to the European Union. In females the most important effect is after the age of 35-39 years are the diseases of the circulatory system. The diseases of the respiratory system burden mortality in the older ages and the group “all others” in the age 85+.

The picture in the males of Lithuania is very similar to the males of Latvia. The same is the case for females.

## **5. The clustering of the countries**

In males, the cluster analysis revealed the division of Europe into two groups of countries. The first group is consisting of the Baltic democracies and Slovakia (SK) and is “divided” into two smaller groups lying quite apart from each other. Latvia (LV) and Lithuania (LT) cluster - though not that tightly – together. The same is the case for Estonia (EE) and Slovakia (SK).

### **Figure 10 about here**

The other group of countries is quite a heterogeneous one concerning mortality. Italy (IT), Spain (ES) and Netherlands (NL) cluster closely together and this group is closely

connected with the group of Belgium (BE) and Germany (DE). These groups are connected more remotely with Portugal (PT) and subsequently the similarities in mortality become smaller towards the group of Greece (EL) and France (FR), Ireland (IE) and the group of Austria (AT) and Finland (FI). It seems then that besides the original division of the Eurozone into two areas, the existing heterogeneity concerning the mortality regimes among these areas must be considered as significant.

The same is the case with females, in which mortality transition has moved ahead to a greater degree. Two countries of the European South, Italy (IT) and Spain (ES) cluster closely together, thus they have many similarities in their mortality regime. These countries bear more similarities with another country of the European South, which is Greece (EL) and continuously with the group of Portugal (PT) and Slovakia (SK) and the three neighboring countries: Germany (DE), Netherlands (NL) and Belgium (BE) and the group of Austria (AT) and France (FR). Ireland (IE) and Finland (FI) are more remote located. All these countries, in their turn, furtherly and remotely cluster with Estonia (EE). The most remote group is formed by two countries: Latvia (LV) and Lithuania (LT). It seems then that the heterogeneity is also significant in the female population. At the same time clustering bears many dissimilarities with the male population as a result of the differences found in the existing mortality regime of the two genders. Also, there is an observed tendency of neighboring countries to cluster together. This finding must further be examined in terms of the environmental, sociopolitical and economic characteristics of these areas. Finally, we have to note that the countries for which data for the causes of death is absent or problematic and judging from the other variables studied, may cluster somewhere near the countries of western Europe and of course far apart from the Baltic democracies.

## **Conclusions**

The probabilities of death by age are very heterogeneous among the populations studied. Baltic countries and Slovakia have more similarities. The other countries of the Eurozone, even if the variability is significant, tend to bear more similarities together than with the previous group of countries.

The examination of life expectancy by gender among the Eurozone countries revealed the existence of significant differences among them. The most differentiated are the Baltic countries and Slovakia. However, the heterogeneity is also significant among the other countries of the Eurozone area. It has to be added that the average length of life in the age of 65 is variable among the countries studied. Taking into consideration that these people are already pensioners or very close to getting their pension the existing heterogeneity suggests that the Eurozone countries need to apply special policies and interventions among them in order for the fully convergence among these countries to take place. That is of course the case considering also the existing differences in mortality levels in the other ages.

Concerning modal age at death, the differences found not only between the Eurozone countries, but also between the two genders within these countries are significant expressing the different stages of demographic transition among them. The lower mortality populations tend to have higher modal age at death than the others. In females the width of the old age heap is smaller than males. The range between minimum and maximum value is about 2 years in females compared with more than 8 years in males. In females, besides the fact that the width of death curve at the old age heap is smaller it is also steeper. Among the countries the differences are small. In males the differences among the countries are greater, and a similar classification with life expectancy at birth holds. The peak of the death curve is lower in the populations where the modal age at death is also low and the death curve tends to become steeper as modal age at death

increases. The differences among the countries in the death curves in both genders reveal the differences in the health status of the older people resulting from the socio-economic differentials, the social security and health system and the other factors which affect health in these ages.

There is also a differential effect of all the groups of causes of death discussed in this paper on gender and country grounds. However, it seems that in the majority of the causes studied the Baltic countries and Slovakia (SK) are facing the greater problems. Also, differences were found among the two genders. On one hand these differences must be attributed to biological agents, but on the other hand to social, environmental, ethological, life style and other reasons.

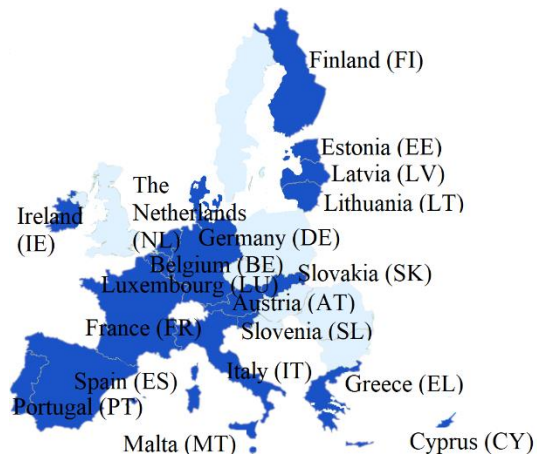
Finally, cluster analysis revealed the existing variability in the mortality regimes of the Eurozone countries. The Baltic Democracies and Slovakia are clearly differentiated than the others except for Slovakia in females. The other countries of the Eurozone era besides their closer clustering are characterized by a great variability. Thus, besides the fact of the monetary union in which these countries are members greater effort should be made for their social, political and economic integration.

## References

- Acsádi, G. and J. Nemeskéri. 1970. History of human life span and mortality. Budapest: Akadémiai Kiadó.
- Andreev E. M. and V. M. Shkolnikov. 2012. An Excel spreadsheet for the decomposition of a difference between two values of an aggregate demographic measure by stepwise replacement running from young to old ages. *MPIDR TECHNICAL REPORT* 2012-002. APRIL 2012
- Andreev, E.M., V.M. Shkolnikov, and A. Z. Begun. (2002). Algorithm for decomposition of differences between aggregate demographic measures and its application healthy life expectancies, parity-progression ratios and total fertility rates. *Demographic Research* 7: 499–522.
- Bongaarts, J. 2005. Long-range trends in adult mortality: Models and projection methods. *Demography* 42(1): 23–49.

- Brenner, M.H. and A. Mooney. 1983. Unemployment and health in the context of economic change. *Social Science & Medicine* 17(16):1125-1138.
- Canudas-Romo, V. 2008. The modal age at death and the shifting mortality hypothesis. *Demographic Research*, 19(30): 1179-1204.
- Catalano, R. 1997. The effect of deviations from trends in national income on mortality: the Danish and USA data revisited. *Eur J Epidemiol* 13(7):737-743.
- Catalano, R. and D. Dooley. 1983. Health Effects of Economic Instability: A Test of Economic Stress Hypothesis. *Journal of Health and Social Behavior* 24(1):46-60.
- Cheung, S. L. K., and J-M. Robine. 2007. Increase in common longevity and the compression of mortality: the case of Japan. *Population Studies* 61(1): 85–97.
- Cheung, S. L. K., Robine, J. M., Paccaud, F., and A. Marazzi. 2009. Dissecting the compression of mortality in Switzerland, 1876-2005. *Demographic Research* 21(19): 569-598.
- Cheung, S. L. K., Robine, J-M., Paccaud, F. and A. Marazzi. 2009. Dissecting the compression of mortality in Switzerland, 1876-2005. *Demographic Research* 21(19), 569-598.
- Chiang, C. L. 1984. *The Life Table and Its Applications.*, Malabar: Robert E. Krieger Publishing Company.
- Cutler, D.M., Knaul, F., Lozano, R., Méndez, O., and B. Zurita. 2002. Financial crisis, health outcomes and ageing: Mexico in the 1980s and 1990s. *Journal of Public Economics* 84(2):279-303.
- Falagas, M.E., Vouloumanou, E.K., Mavros, M.N. and D.E. Karageorgopoulos. 2009. Economic crises and mortality: a review of the literature. *International Journal of Clinical Practice* 63(8):1128-1135.
- Gompertz, B. 1825. On the Nature of the Function Expressive of the Law of Human Mortality, and on a New Mode of Determining the Value of Life Contingencies. *Philosophical Transactions of the Royal Society of London* 123: 513-583.
- Granados, J.T. 2005. Recessions and Mortality in Spain, 1980–1997. *European Journal of Population / Revue européenne de Démographie* 21(4):393-422.
- Hand, D. J. 1981. *Discrimination and Classification.* New York: John Wiley and Sons.
- Heligman, L. and J. H. Pollard. 1980. The age pattern of mortality. *Journal of the Institute of Actuaries* 107:47-80.
- Hill, K. and A. Palloni. 1994. Demographic responses to economic shocks: the case of Latin America. *Research in human capital and development* 8:197-223.
- Horiuchi, S., Ouellette, N., Cheung S. L. K. and J-M Robine. 2013. Modal age at death: lifespan indicator in the era of longevity extension. *Vienna Yearbook of Population Research* 11: 37-69.

- Kannisto V. 2000. Measuring the compression of Mortality. *Demographic Research* 3(6).
- Kostaki, A. 1992. A nine parameter version of the Heligman-Pollard formula. *Mathematical Population Studies* 3(4): 277-288.
- Laporte, A. 2004. Do economic cycles have a permanent effect on population health? Revisiting the Brenner hypothesis. *Health Economics* 13(8):767-779.
- Lexis, W. 1878. Sur la durée normale de la vie humaine et sur la théorie de la stabilité des rapports statistiques. *Annales de Démographie Internationale* 2(5): 447-460.
- Makeham, W.M. 1860. On the law of mortality and the construction of annuity tables. *The Assurance Magazine and Journal of the Institute of Actuaries* 8: 301–310.
- Ouellette, N. and R. Bourbeau. 2011. Changes in the age-at-death distribution in four low mortality countries: A non-parametric approach. *Demographic Research* 25(19): 595-628.
- Peristera, P. and A. Kostaki. 2005. An evaluation of the performance of kernel estimators for graduating mortality data. *Journal of population Research* 22(2): 85-197.
- Preston, S. H., Heuveline, P. and M. Guillot. 2001. *Demography. Measuring and modeling population processes*. Malden Massachusetts: Blackwell Publishers Inc.
- Robine, J-M. 2001. Redefining the stages of epidemiological transition by a study of dispersion of life spans: the case of France. *Population: an English Selection*, 13(1): 173-194.
- Sokal, R. R. and F. J. Rohlf. 1995. *Biometry*. 3rd edition. New York: W. H. Freeman and Company.
- Weibull, W. 1951. A statistical distribution function of wide applicability. *Journal of applied mechanics* 18(3): 293-297.
- Wilmoth, R. J. and S. Horiuchi. 1999. Rectangularization revisited: variability of age at death with in human population. *Demography* 36(4): 475-495.
- Zafeiris, K. N. and A. Kostaki, 2018. Recent mortality trends in Greece. *Communication in Statistics - Theory and Methods*.  
<https://doi.org/10.1080/03610926.2017.1353625>



**Map 1.** The European Union. In dark blue the Eurozone countries.

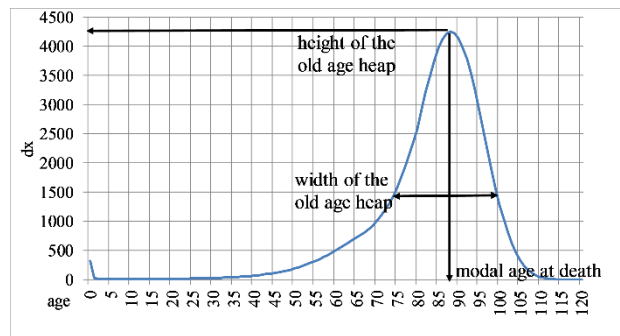


**Figure 1.** The death curve ( $dx$ ) of a life table. Germany, females, 2016. The calculation of  $dx$  values was based on fitted values of the probabilities of death.

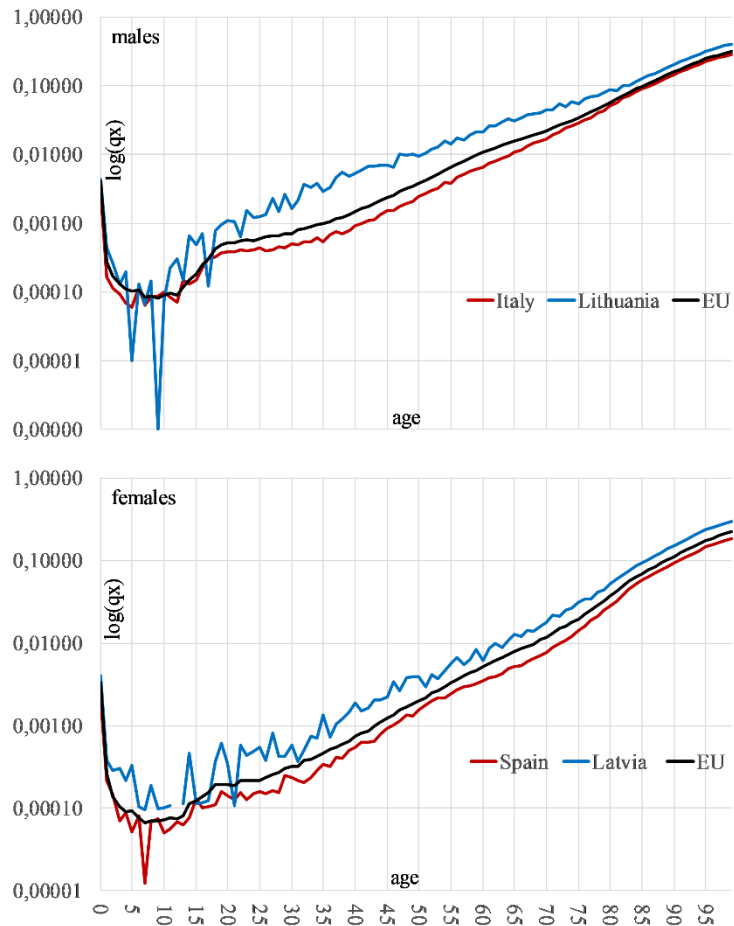


**Figure 2.** The observed probabilities of death in selected countries by gender. 2016.

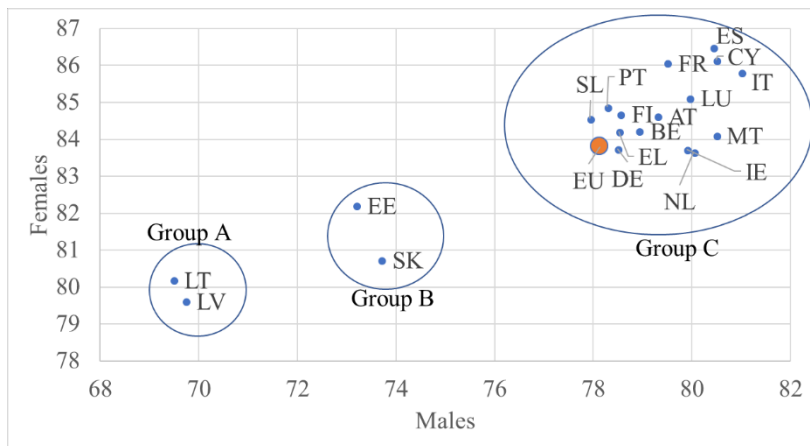


**Figure 3.** Scatterplot of male and female life expectancy at birth. Eurozone, 2016

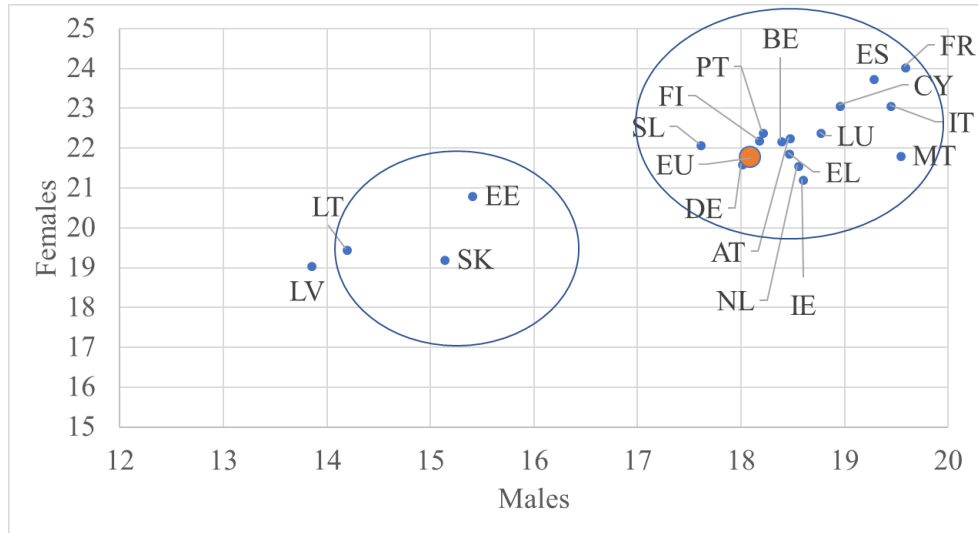


**Figure 4.** Scatterplot of male and female life expectancy at age 65 (e65). Eurozone, 2016

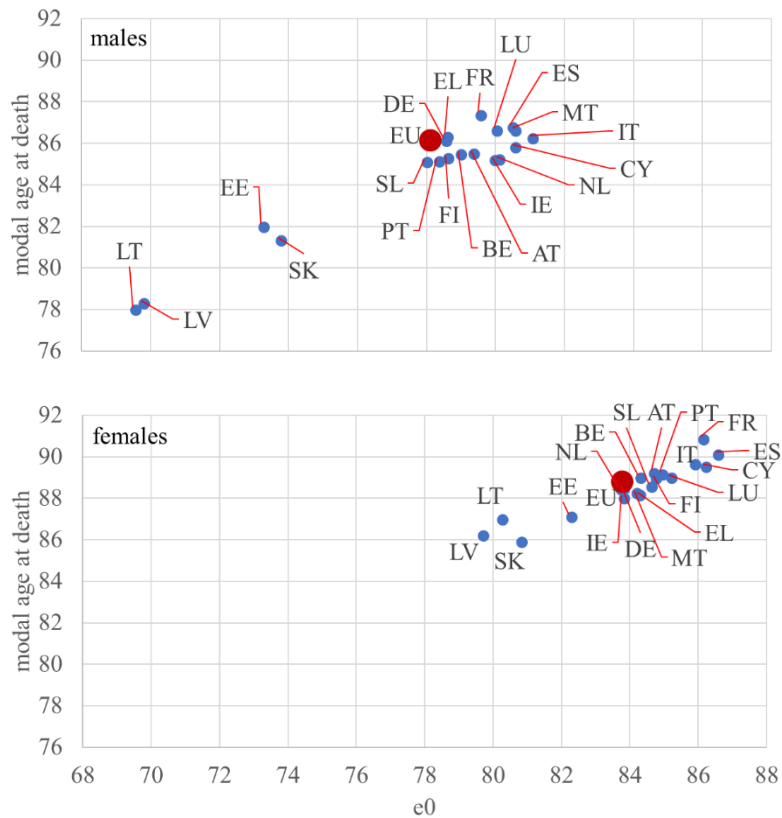


**Figure 5.** Scatterplot of male and female modal age at death in relationship to life expectancy at birth. Eurozone, 2016

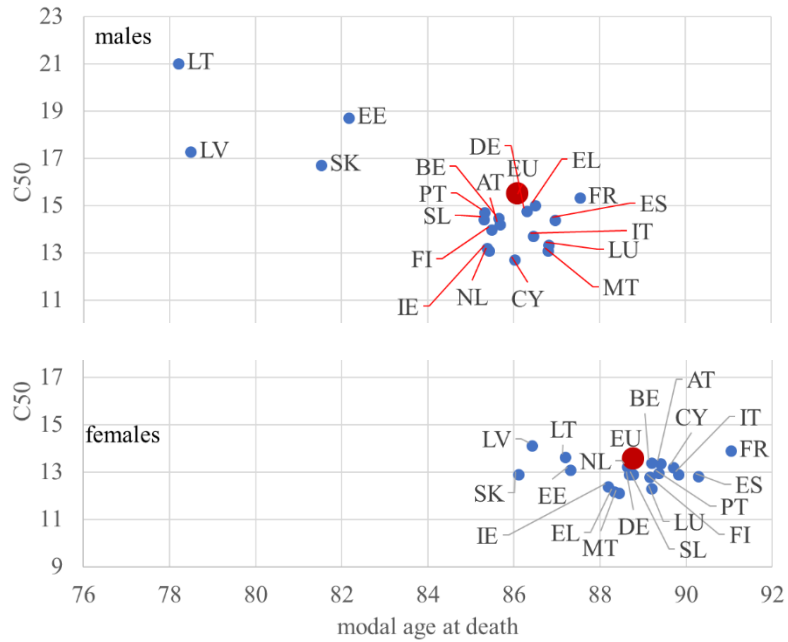


**Figure 6.** Scatterplot of male and female C50 indicator in relationship to modal age at death. Eurozone, 2016

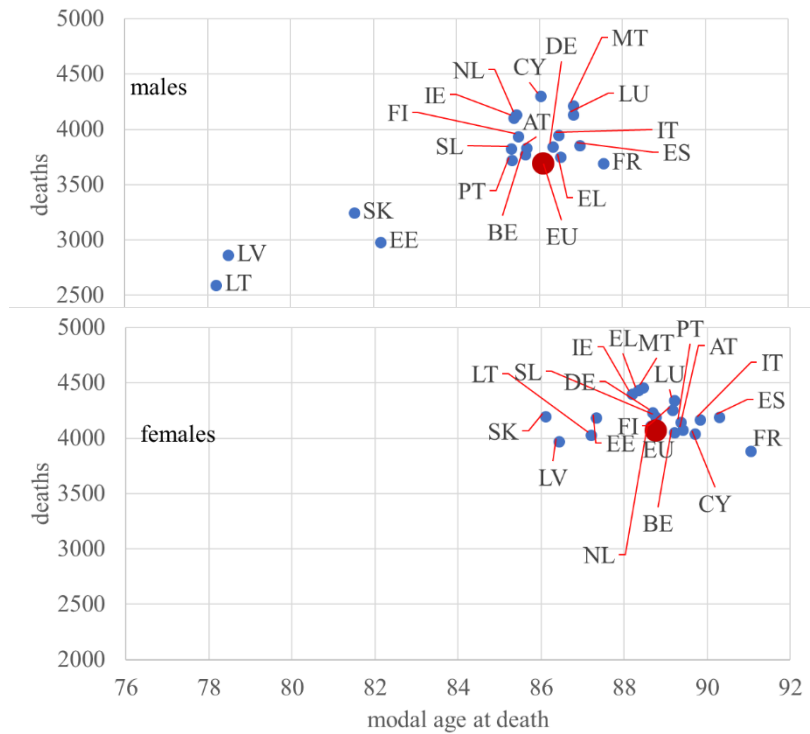
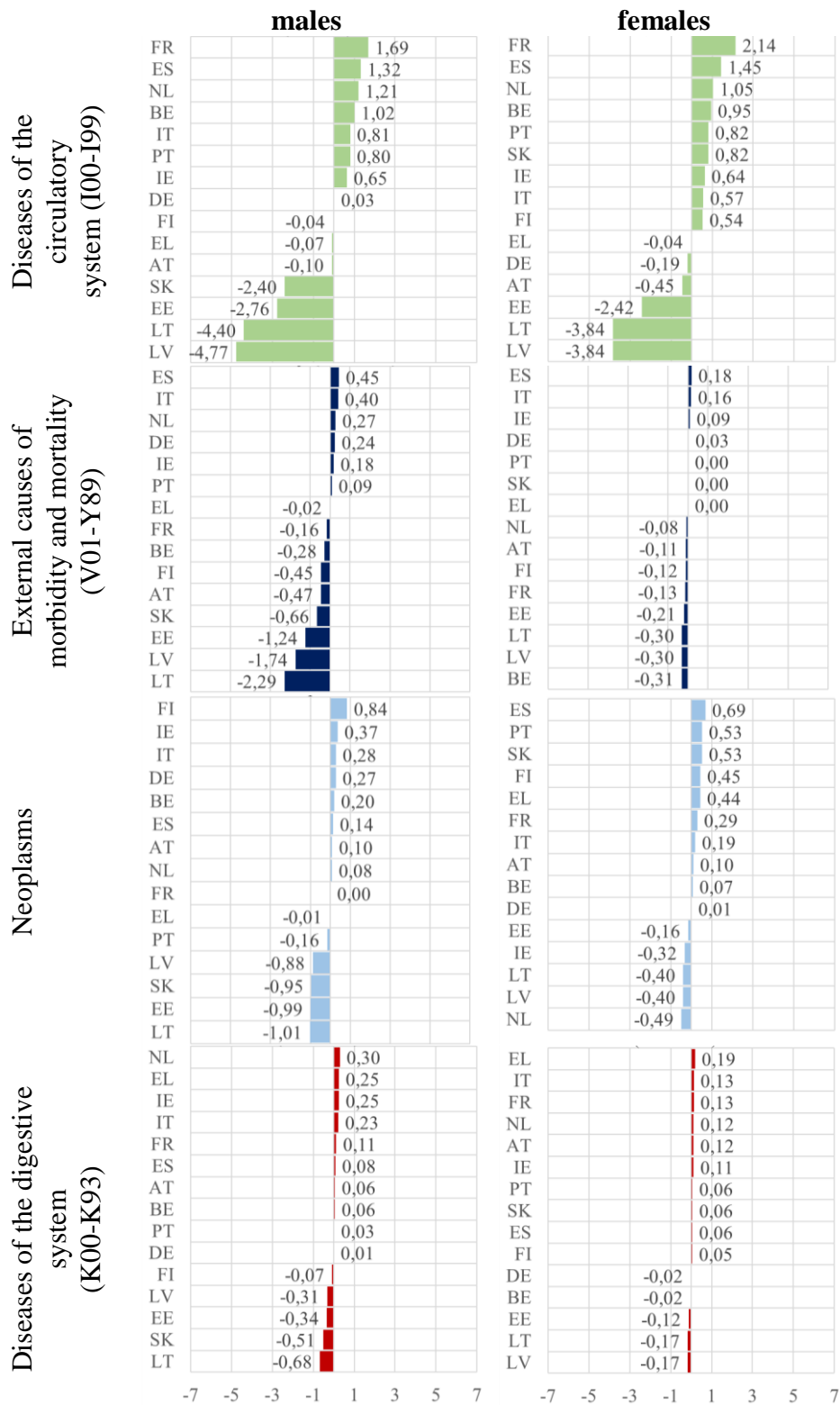
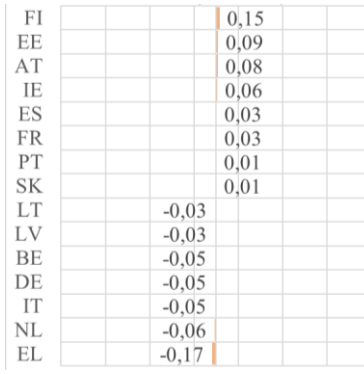
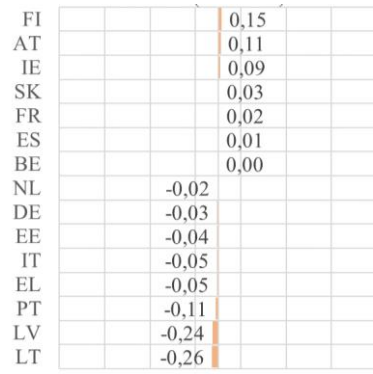


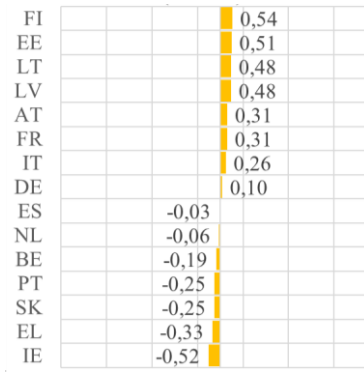
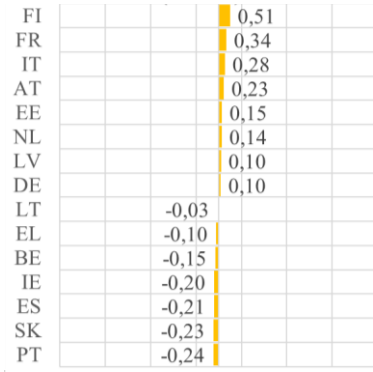
**Figure 7.** Scatterplot of number of deaths in the modal age at death versus modal age at death. Eurozone, 2016



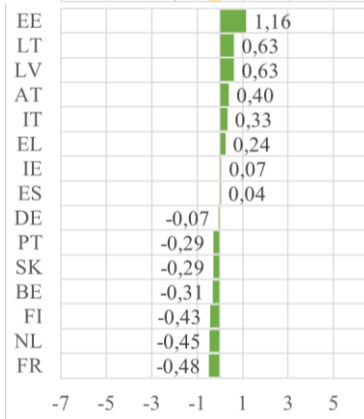
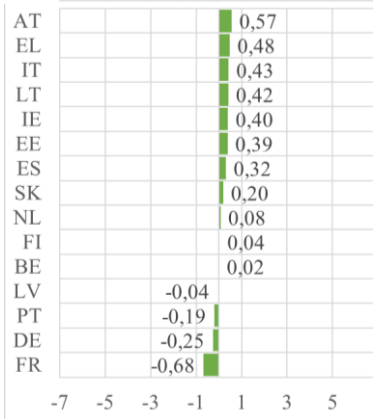
Certain infectious and parasitic diseases (A00-B99)



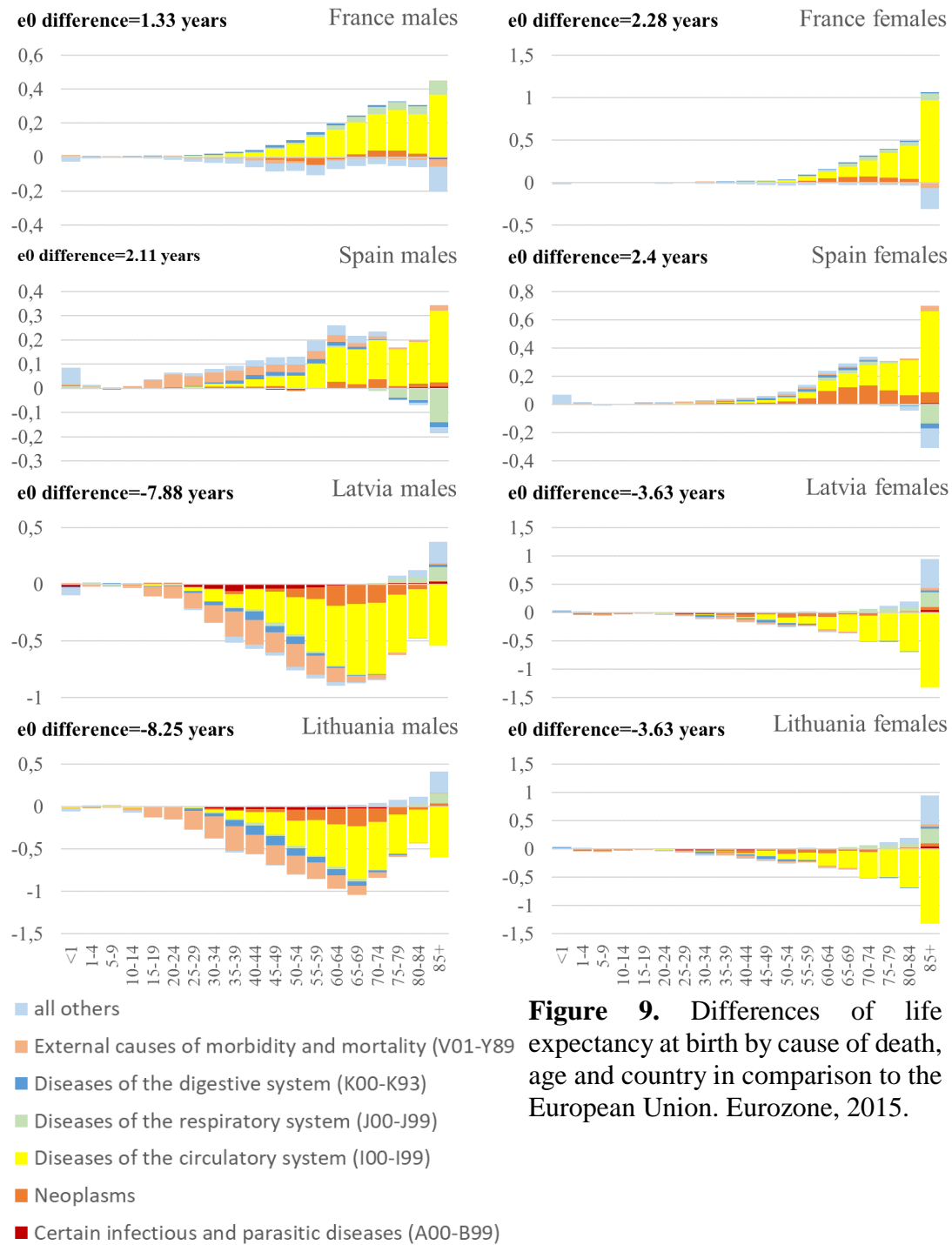
Diseases of the respiratory system (J00-J99)



All others



**Figure 8.** Differences of life expectancy at birth by cause of death and country in comparison to the European Union. Eurozone, 2015.



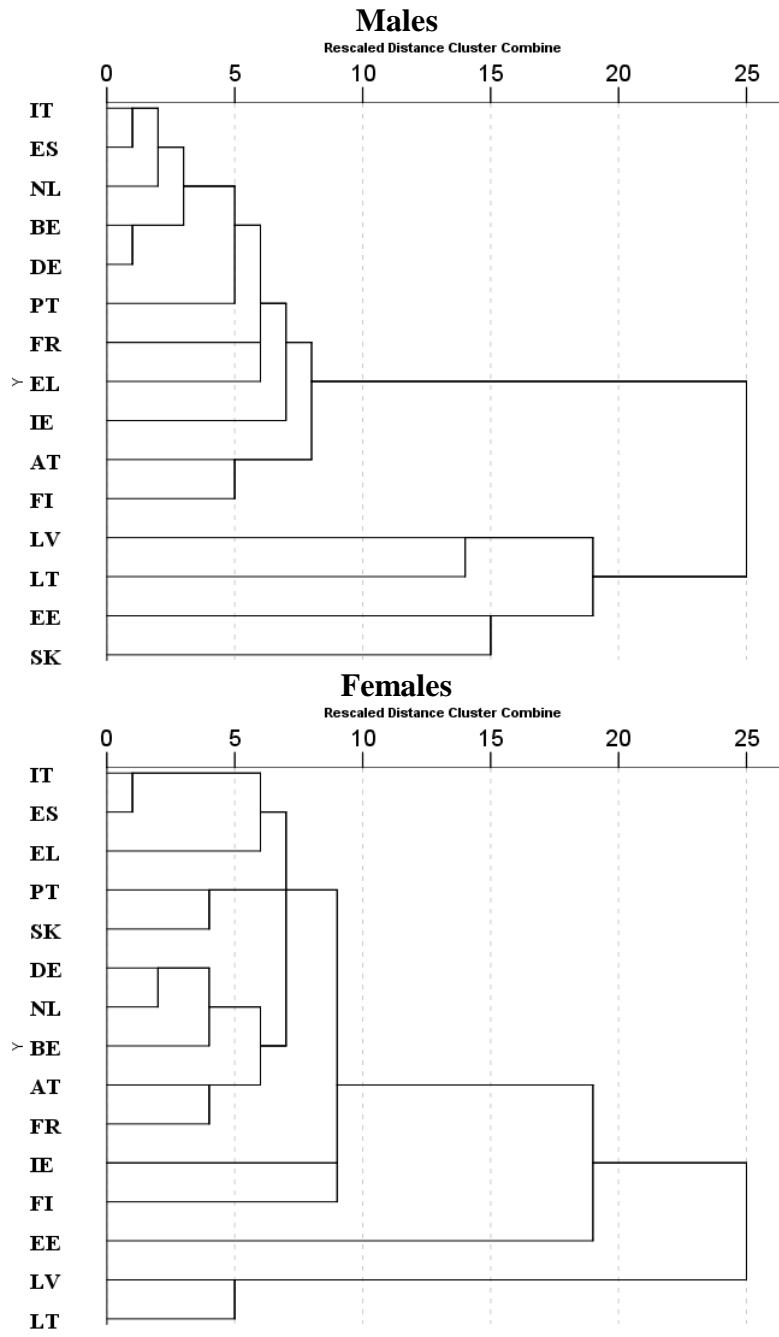


**Figure 10.** The clustering of the countries by gender according to the average linkage method (between groups)

